

Altair AcuSolve 2021.2

Altair AcuSolve Validation Manual

Updated: 08/03/2021

Intellectual Property Rights Notice

Copyright © 1986-2021 Altair Engineering Inc. All Rights Reserved.

This Intellectual Property Rights Notice is exemplary, and therefore not exhaustive, of intellectual property rights held by Altair Engineering Inc. or its affiliates. Software, other products, and materials of Altair Engineering Inc. or its affiliates are protected under laws of the United States and laws of other jurisdictions. In addition to intellectual property rights indicated herein, such software, other products, and materials of Altair Engineering Inc. or its affiliates may be further protected by patents, additional copyrights, additional trademarks, trade secrets, and additional other intellectual property rights. For avoidance of doubt, copyright notice does not imply publication. Copyrights in the below are held by Altair Engineering Inc. except where otherwise explicitly stated. Additionally, all non-Altair marks are the property of their respective owners.

This Intellectual Property Rights Notice does not give you any right to any product, such as software, or underlying intellectual property rights of Altair Engineering Inc. or its affiliates. Usage, for example, of software of Altair Engineering Inc. or its affiliates is governed by and dependent on a valid license agreement.

Altair Simulation Products

Altair® AcuConsole® ©2006-2021

Altair® AcuSolve® ©1997-2021

Altair Activate® ©1989-2021

Altair Compose® ©2007-2021

Altair® ConnectMe™ ©2014-2021

Altair® EDEM™ ©2005-2021 Altair Engineering Limited, ©2019-2021 Altair Engineering Inc.

Altair® ElectroFlo™ ©1992-2021

Altair Embed® ©1989-2021

Altair Embed® SE ©1989-2021

Altair Embed®/Digital Power Designer ©2012-2021

Altair Embed® Viewer ©1996-2021

Altair® ESAComp® ©1992-2021

Altair® Feko® ©1999-2021 Altair Development S.A. (Pty) Ltd., ©1999-2021 Altair Engineering Inc.

Altair® Flow Simulator™ ©2016-2021

Altair® Flux® ©1983-2021

Altair® FluxMotor® ©2017-2021

Altair® HyperCrash® ©2001-2021

Altair® HyperGraph® ©1995-2021

Altair® HyperLife® ©1990-2021

Altair® HyperMesh® ©1990-2021

Altair® HyperStudy® ©1999-2021

Altair® HyperView® ©1999-2021

Altair® HyperWorks® ©1990-2021

Altair® HyperXtrude® ©1999-2021

Altair® Inspire™ ©2009-2021

Altair® Inspire™ Cast ©2011-2021

Altair® Inspire™ Extrude Metal ©1996-2021

Altair® Inspire™ Extrude Polymer ©1996-2021

Altair® Inspire™ Form ©1998-2021

Altair® Inspire™ Friction Stir Welding ©1996-2021

Altair® Inspire™ Mold ©2009-2021

Altair® Inspire™ PolyFoam ©2009-2021

Altair® Inspire™ Play ©2009-2021

Altair® Inspire™ Print3D ©2021

Altair® Inspire™ Render ©1993-2016 Solid Iris Technologies Software Development One PLLC, ©2016-2021 Altair Engineering Inc

Altair® Inspire™ Resin Transfer Molding ©1990-2021

Altair® Inspire™ Studio ©1993-2021

Altair® Material Data Center™ ©2019-2021

Altair® MotionSolve® ©2002-2021

Altair® MotionView® ©1993-2021

Altair® Multiscale Designer® ©2011-2021

Altair® nanoFluidX® ©2013-2018 FluiDyna GmbH, ©2018-2021 Altair Engineering Inc.

Altair® OptiStruct® ©1996-2021

Altair® PollEx™ ©2003-2021

Altair® Radioss® ©1986-2021

Altair® SEAM® ©1985-2019 Cambridge Collaborative, Inc., ©2019-2021 Altair Engineering Inc.

Altair® SimLab® ©2004-2021

Altair® SimSolid® ©2015-2021

Altair® ultraFluidX® ©2010-2018 FluiDyna GmbH, ©2018-2021 Altair Engineering Inc.

Altair® Virtual Wind Tunnel™ ©2012-2021

Altair® WinProp™ ©2000-2021

Altair® WRAP™ ©1998-2021 Altair Engineering AB

Altair Packaged Solution Offerings (PSOs)

Altair® Automated Reporting Director™ ©2008-2021

Altair® Geomechanics Director™ ©2011-2021

Altair® Impact Simulation Director™ ©2010-2021

Altair® Model Mesher Director™ ©2010-2021

Altair® NVH Director™ ©2010-2021

Altair® Squeak and Rattle Director™ ©2012-2021

Altair® Virtual Gauge Director™ ©2012-2021

Altair® Weld Certification Director™ ©2014-2021

Altair® Multi-Disciplinary Optimization Director™ ©2012-2021

Altair HPC & Cloud Products

Altair® PBS Professional® ©1994-2021

Altair® Control™ ©2008-2021

Altair ®Access™ ©2008-2021

Altair® Accelerator™ ©1995-2021

Altair® Accelerator™ Plus©1995-2021

Altair® FlowTracer™ ©1995-2021

Altair® Allocator™ ©1995-2021

Altair® Monitor™ ©1995-2021

Altair® Hero™ ©1995-2021

Altair® Software Asset Optimization (SAO) ©2007-2021

Altair Mistral™ ©2021

Altair Drive ©2021

Altair® Grid Engine® ©2001, 2011-2021

Altair® DesignAI™ ©2021

Altair Breeze™ ©2021

Altair Data Analytics Products

Altair® Knowledge Studio® ©1994-2020 Angoss Software Corporation, ©2020-2021 Altair Engineering Inc.

Altair® Knowledge Studio® for Apache Spark ©1994-2020 Angoss Software Corporation, ©2020-2021 Altair Engineering Inc.

Altair® Knowledge Seeker™ ©1994-2020 Angoss Software Corporation, ©2020-2021 Altair Engineering Inc.

Altair® Knowledge Hub™ ©2017-2020 Datawatch Corporation, ©2020-2021 Altair Engineering Inc.

Altair® Monarch® ©1996-2020 Datawatch Corporation, ©2020-2021 Altair Engineering Inc.

Altair® Panopticon™ ©2004-2020 Datawatch Corporation, ©2020-2021 Altair Engineering Inc.

Altair® SmartWorks™ ©2021

Altair SmartCore™ ©2011-2021

Altair SmartEdge™ ©2011-2021

Altair SmartSight™ ©2011-2021

Altair One™ ©1994-2021

2021.2

July 07, 2021

Technical Support

Altair provides comprehensive software support via web FAQs, tutorials, training classes, telephone, and e-mail.

Altair One Customer Portal

Altair One (https://altairone.com/Dashboard/) is Altair's customer portal giving you access to product downloads, a Knowledge Base, and customer support. We recommend that all users create an Altair One account and use it as their primary portal for everything Altair.

When your Altair One account is set up, you can access the Altair support page via this link: www.altair.com/customer-support/

Altair Community

Participate in an online community where you can share insights, collaborate with colleagues and peers, and find more ways to take full advantage of Altair's products.

Visit the Altair Community (https://community.altair.com/community) where you can access online discussions, a knowledge base of product information, and an online form to contact Support. These valuable resources help you discover, learn and grow, all while having the opportunity to network with fellow explorers like yourself.

Altair Training Classes

Altair's in-person, online, and self-paced trainings provide hands-on introduction to our products, focusing on overall functionality. Trainings are conducted at our corporate and regional offices or at your facility.

For more information visit: https://learn.altair.com/

If you are interested in training at your facility, contact your account manager for more details. If you do not know who your account manager is, contact your local support office and they will connect you with your account manager.

Telephone and E-mail

If you are unable to contact Altair support via the customer portal, you may reach out to technical support via phone or e-mail. Use the following table as a reference to locate the support office for your region.

When contacting Altair support, specify the product and version number you are using along with a detailed description of the problem. It is beneficial for the support engineer to know what type of workstation, operating system, RAM, and graphics board you have, so please include that in your communication.

Location	Telephone	E-mail
Australia	+61 3 9866 5557	anzsupport@altair.com
Brazil	+55 113 884 0414	br_support@altair.com

Location	Telephone	E-mail
Canada	+1 416 447 6463	support@altairengineering.ca
China	+86 400 619 6186	support@altair.com.cn
France	+33 141 33 0992	francesupport@altair.com
Germany	+49 703 162 0822	hwsupport@altair.de
Greece	+30 231 047 3311	eesupport@altair.com
India	+91 806 629 4500 +1 800 425 0234 (toll free)	support@india.altair.com
Israel		israelsupport@altair.com
Italy	+39 800 905 595	support@altairengineering.it
Japan	+81 3 6225 5830	support@altairjp.co.jp
Malaysia	+60 32 742 7890	aseansupport@altair.com
Mexico	+52 55 5658 6808	mx-support@altair.com
New Zealand	+64 9 413 7981	anzsupport@altair.com
South Africa	+27 21 831 1500	support@altair.co.za
South Korea	+82 704 050 9200	support@altair.co.kr
Spain	+34 910 810 080	support-spain@altair.com
Sweden	+46 46 460 2828	support@altair.se
United Kingdom	+44 192 646 8600	support@uk.altair.com
United States	+1 248 614 2425	hwsupport@altair.com

If your company is being serviced by an Altair partner, you can find that information on our web site at https://www.altair.com/PartnerSearch/.

See www.altair.com for complete information on Altair, our team, and our products.

Contents

Intellectual Property Rights Notice ii
Technical Support vi

AcuSolve Validation Manual 13

Turbulent Flow 16

Multiphase Flow Within a Sloshing Tank 17
Single-Phase Nucleate Boiling in a Rectangular Channel 24
Turbulent Flow Through a Pipe 29
Turbulent Flow Behind an Open-Slit V 33
Turbulent Flow Through a Wavy Channel 40
Turbulent Flow with Separation in an Asymmetric Diffuser 48
Turbulent Flow Past a Wall-Mounted Hump 56
Turbulent Flow Over a Backward-Facing Step 64
Turbulent Flow with Separation in an Axisymmetric Diffuser 71
Turbulent Flow Past a Convex Curve in a Channel 79
Turbulent Natural Convection Inside a Tall Cavity 86
Turbulent Flow Over a NACA 0012 Airfoil 94
Turbulent Flow Over an Oscillating Rigid Body Assembly 102
Turbulent Flow Through a 180 Degree Curved Channel 110
Turbulent Mixing Layers in an Open Channel 116
Turbulent Flow Through a Heated Periodic Channel 121
Two-Phase Nucleate Boiling in a Cylindrical Pipe 127
Supersonic Flow Through a Converging-Diverging Nozzle 131

Steady Flow 136

Flow Between Concentric Cylinders 137
Laminar Flow Through a Pipe With Imposed Heat Flux 143
Turbulent Flow Through a Pipe 148
Laminar Couette Flow with Imposed Pressure Gradient 152
Laminar Couette Flow with Imposed Pressure Gradient and Heated Walls 158
Laminar Poiseuille Flow Through a Pipe 164
Laminar Flow Through a Pipe with Species Transport 168
Flow Inside a Rotating Cavity 174
Natural Convection in a Concentric Annulus 182
Laminar Flow Past a 90° T-Junction 188
Turbulent Flow Through a Wavy Channel 193
Laminar Flow Through a Channel with Heated Walls 201
Turbulent Flow Behind an Open-Slit V 206

Turbulent Flow Over a NACA 0012 Airfoil....213
Turbulent Natural Convection Inside a Tall Cavity.... 221
Viscous Heating Inside a Rotating Annulus.... 229
Separated Laminar Flow Over a Blunt Plate.... 236
Laminar Flow Through a Pipe with Constant Wall Temperature.... 243
Turbulent Flow with Separation in an Asymmetric Diffuser.... 248
Turbulent Flow with Separation in an Axisymmetric Diffuser....256
Turbulent Flow Over a Backward-Facing Step.... 264
Turbulent Flow Past a Convex Curve in a Channel.... 271
Turbulent Flow Past a Wall-Mounted Hump.... 278
Heat Transfer Between Radiating Concentric Cylinders....286
Turbulent Mixing Layers in an Open Channel....292
Laminar to Turbulent Transition Over an Airfoil....297
Turbulent Flow Through a 180 Degree Curved Channel.... 302
Turbulent Flow Through a Heated Periodic Channel....308
Heat Transfer Between Radiating Concentric Spheres.... 314
Radiation Heat Transfer Through a Cube with a Specular Interface....319
Single-Phase Nucleate Boiling in a Rectangular Channel.... 326

Laminar Flow.... 331

Circumferential Flow in a Cylinder Induced by a Rotating Solid....332
Laminar Flow Through a Pipe With Imposed Heat Flux....338
Laminar Couette Flow with Imposed Pressure Gradient.... 343
Laminar Couette Flow with Imposed Pressure Gradient and Heated Walls....349
Laminar Flow Through a Pipe with Species Transport.... 355
Flow Inside a Rotating Cavity.... 361
Laminar Flow Past a 90° T-Junction....369
Laminar Flow Through a Channel with Heated Walls.... 374
Viscous Heating Inside a Rotating Annulus.... 379
Oscillating Laminar Flow Around a Circular Cylinder....386
Ideal Gas Compression in an Actuating Piston....391
Separated Laminar Flow Over a Blunt Plate.... 398
Laminar Flow Through a Pipe with Constant Wall Temperature.... 405
Laminar Free Surface Flow Inside a Rotating Cavity....410
Natural Convection in a Concentric Annulus.... 416
Flow Between Concentric Cylinders....422
Laminar Poiseuille Flow Through a Pipe....428
Heat Transfer Between Radiating Concentric Cylinders....432

Internal Flow....438

Flow Between Concentric Cylinders....440
Laminar Flow Through a Pipe With Imposed Heat Flux.... 446
Turbulent Flow Through a Pipe....451
Laminar Couette Flow with Imposed Pressure Gradient.... 455

Laminar Couette Flow with Imposed Pressure Gradient and Heated Walls 461
Laminar Poiseuille Flow Through a Pipe 467
Laminar Flow Through a Pipe with Species Transport 471
Flow Inside a Rotating Cavity 477
Natural Convection in a Concentric Annulus 485
Laminar Flow Past a 90° T-Junction 491
Turbulent Flow Through a Wavy Channel 496
Laminar Flow Through a Channel with Heated Walls 504
Turbulent Natural Convection Inside a Tall Cavity 509
Viscous Heating Inside a Rotating Annulus 517
Ideal Gas Compression in an Actuating Piston 524
Laminar Flow Through a Pipe with Constant Wall Temperature 531
Turbulent Flow with Separation in an Asymmetric Diffuser 536
Turbulent Flow with Separation in an Axisymmetric Diffuser 544
Turbulent Flow Over a Backward-Facing Step 552
Turbulent Flow Past a Convex Curve in a Channel 559
Turbulent Flow Past a Wall-Mounted Hump 566
Laminar Free Surface Flow Inside a Rotating Cavity 574
Heat Transfer Between Radiating Concentric Cylinders 580
Turbulent Flow Through a 180 Degree Curved Channel 586
Circumferential Flow in a Cylinder Induced by a Rotating Solid 592
Turbulent Flow Through a Heated Periodic Channel 598
Multiphase Flow Within a Sloshing Tank 604
Heat Transfer Between Radiating Concentric Spheres 611
Radiation Heat Transfer Through a Cube with a Specular Interface 616
Two-Phase Nucleate Boiling in a Cylindrical Pipe 623
Single-Phase Nucleate Boiling in a Rectangular Channel 627
Supersonic Flow Through a Converging-Diverging Nozzle 632

External Flow 637

Turbulent Flow Behind an Open-Slit V 638
Turbulent Flow Over a NACA 0012 Airfoil 645
Oscillating Laminar Flow Around a Circular Cylinder 653
Separated Laminar Flow Over a Blunt Plate 658
Turbulent Mixing Layers in an Open Channel 665
Turbulent Flow Over an Oscillating Rigid Body Assembly 670
Laminar to Turbulent Transition Over an Airfoil 678

Transitional Flow 683

Laminar to Turbulent Transition Over an Airfoil 684

Transient Flow 689

Oscillating Laminar Flow Around a Circular Cylinder 690

Ideal Gas Compression in an Actuating Piston....695
Laminar Free Surface Flow Inside a Rotating Cavity....702
Turbulent Flow Over an Oscillating Rigid Body Assembly....708
Circumferential Flow in a Cylinder Induced by a Rotating Solid....716
Multiphase Flow Within a Sloshing Tank....722
Two-Phase Nucleate Boiling in a Cylindrical Pipe....729
Supersonic Flow Through a Converging-Diverging Nozzle....733

Heat Transfer/Radiation....738

Laminar Flow Through a Pipe With Imposed Heat Flux....739
Laminar Couette Flow with Imposed Pressure Gradient and Heated Walls....744
Natural Convection in a Concentric Annulus....750
Laminar Flow Through a Channel with Heated Walls....756
Turbulent Natural Convection Inside a Tall Cavity....761
Viscous Heating Inside a Rotating Annulus....769
Ideal Gas Compression in an Actuating Piston....776
Laminar Flow Through a Pipe with Constant Wall Temperature....783
Heat Transfer Between Radiating Concentric Cylinders....788
Turbulent Flow Through a Heated Periodic Channel....794
Heat Transfer Between Concentric Cylinders with Heat Source....800
Heat Transfer Between Radiating Concentric Spheres....805
Radiation Heat Transfer Through a Cube with a Specular Interface....810
Two-Phase Nucleate Boiling in a Cylindrical Pipe....817
Single-Phase Nucleate Boiling in a Rectangular Channel....821
Supersonic Flow Through a Converging-Diverging Nozzle....826

Moving Mesh....831

Ideal Gas Compression in an Actuating Piston....832
Laminar Free Surface Flow Inside a Rotating Cavity....839
Turbulent Flow Over an Oscillating Rigid Body Assembly....845
Circumferential Flow in a Cylinder Induced by a Rotating Solid....853
Multiphase Flow Within a Sloshing Tank....859

Reference Frame....866

Flow Between Concentric Cylinders....867
Flow Inside a Rotating Cavity....873
Viscous Heating Inside a Rotating Annulus....881

Species Transport....888

Laminar Flow Through a Pipe with Species Transport....889

Multiphase 895

Multiphase Flow of a 2D Dam Break 896
Multiphase Flow Within a Sloshing Tank 900
Two-Phase Nucleate Boiling in a Cylindrical Pipe 907

Compressible 911

Supersonic Flow Through a Converging-Diverging Nozzle 912
Ideal Gas Compression in an Actuating Piston 917

Index 924

AcuSolve Validation Manual

1

Collection of AcuSolve simulation cases for which results are compared against analytical or experimental results to demonstrate the accuracy of AcuSolve results.

The accuracy of the solutions presented in this document validates the capability of AcuSolve to simulate complex flow for a variety of problems. The goal is to provide accurate results for each validation case. Grid sensitivity studies have been performed, however, the simulation settings have not been optimized to minimize computation time. Instead, the cases presented are intended to portray settings that show a good trade off between accuracy and compute time.

Supporting database files (`*.acs` and `*.hm` for AcuConsole and HyperMesh, respectively) are available for the validation cases in a compressed `.zip` archive, `validation.zip`, in the `\model_files \validation` directory of your AcuSolve installation. Copy `validation.zip` to a working directory, then expand it for access to individual database files. These can be used to recreate the results for a particular validation case or can be examined to see the AcuSolve settings in detail.

Each validation contains information in the following sections:

Problem Description	A description of the geometry, physical properties, and specific AcuSolve modeling strategy.
AcuSolve Results	Results obtained from the AcuSolve simulation compared against theoretical or experimental results.
Summary	A summary of the validation case.
Simulation Settings	AcuSolve settings for the specific validation case and the name and location of the associated database file.
References	Sources of theoretical equations or experimental results.

AcuSolve Results Presentation

Results for each validation case are presented with one or more contour plots that represent the converged CFD solution. A consistent set of contour colormapping has been adopted to represent each scalar quantity. The following image illustrates the colormap conventions for contours of velocity magnitude, pressure, temperature and vorticity magnitude.

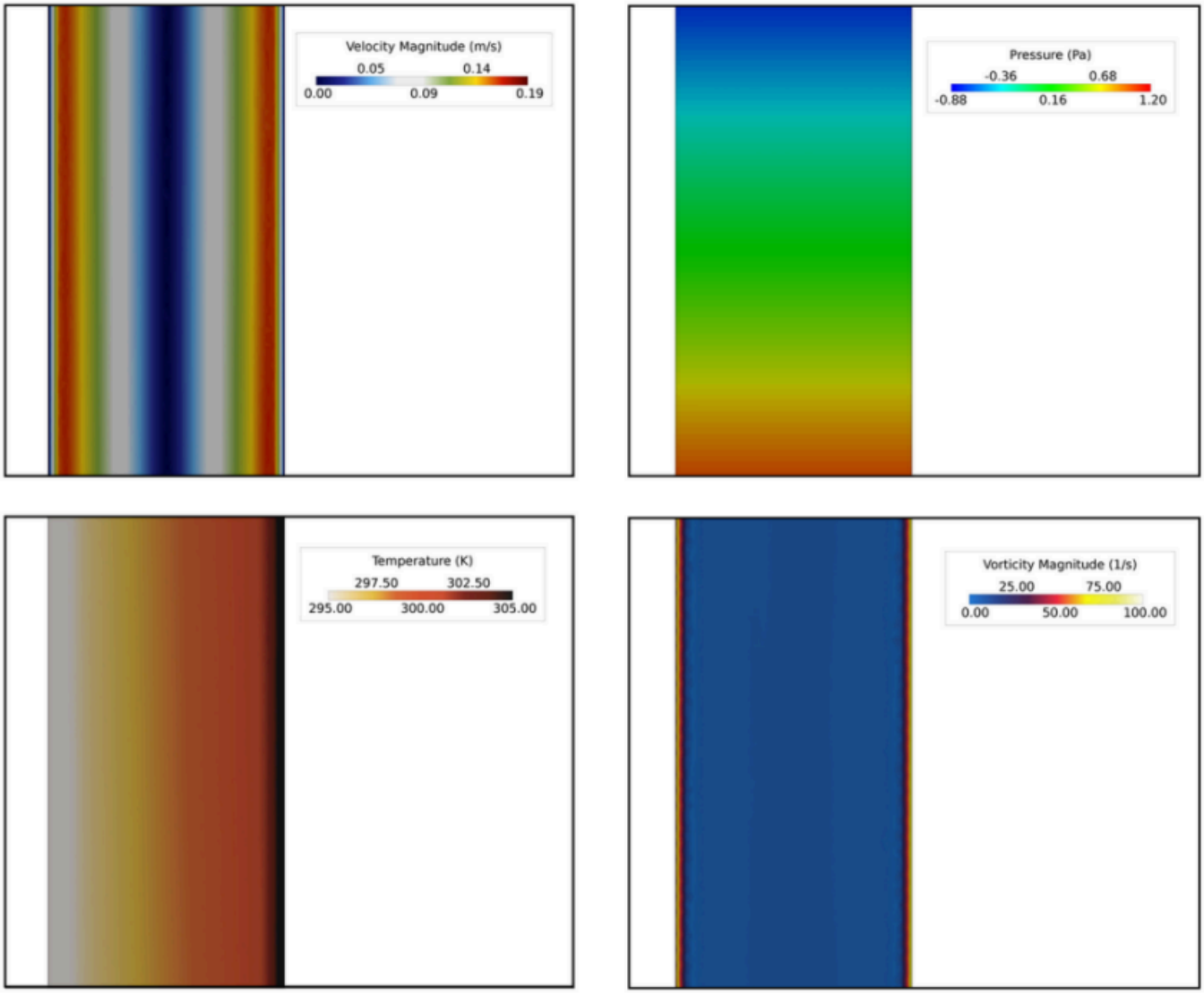


Figure 1:

Recreating the Results

You can recreate the AcuSolve results by using the database files provided. The general process to recreate the results is as follows:

1. Start AcuConsole or HyperMesh and open the database file (`*.acs` or `*.hm`) for a particular validation case.
2. Launch AcuSolve to generate a solution.
3. Post-process results with AcuProbe, AcuTrans or AcuFieldView.

Typographical Conventions

Simulation settings are presented so that you can recreate the simulation case. The presentation of the simulation settings reflects the AcuSolve commands that are modified from default values. Labels in the GUI are indicated with highlighting, for example, Problem Description. Tree items that can be renamed

are presented in normal font. Settings selected from a list are indicated after a dash. Settings that are entered directly into a field are indicated by courier font.

As an example, the following would indicate that the Global settings tree item was expanded, the Problem Description panel was opened, the Analysis type was set to Steady State, and the Turbulence equation set to Laminar.

Global	Problem Description
Analysis type	Steady State
Turbulence equation	Laminar

The following would indicate that Global in the tree was expanded, Material Model was also expanded, Gas is a branch that can be renamed and the material properties panel is opened, and the Density is entered as `1.808` with the units of kg/m3.

Global	Material Model
Gas	Material Type - Fluid
	Density `1.808` kg/m3

Turbulent Flow

2

This section includes validation cases containing flow conditions that will cause turbulence to form, requiring that a turbulence model is used.

This chapter covers the following:

- Multiphase Flow Within a Sloshing Tank (p. 17)
- Single-Phase Nucleate Boiling in a Rectangular Channel (p. 24)
- Turbulent Flow Through a Pipe (p. 29)
- Turbulent Flow Behind an Open-Slit V (p. 33)
- Turbulent Flow Through a Wavy Channel (p. 40)
- Turbulent Flow with Separation in an Asymmetric Diffuser (p. 48)
- Turbulent Flow Past a Wall-Mounted Hump (p. 56)
- Turbulent Flow Over a Backward-Facing Step (p. 64)
- Turbulent Flow with Separation in an Axisymmetric Diffuser (p. 71)
- Turbulent Flow Past a Convex Curve in a Channel (p. 79)
- Turbulent Natural Convection Inside a Tall Cavity (p. 86)
- Turbulent Flow Over a NACA 0012 Airfoil (p. 94)
- Turbulent Flow Over an Oscillating Rigid Body Assembly (p. 102)
- Turbulent Flow Through a 180 Degree Curved Channel (p. 110)
- Turbulent Mixing Layers in an Open Channel (p. 116)
- Turbulent Flow Through a Heated Periodic Channel (p. 121)
- Two-Phase Nucleate Boiling in a Cylindrical Pipe (p. 127)
- Supersonic Flow Through a Converging-Diverging Nozzle (p. 131)

Multiphase Flow Within a Sloshing Tank

In this application, AcuSolve is used to simulate water and the time-dependent interface of air-water within a tank subject to a prescribed sloshing motion. AcuSolve results are compared with experimental pressure measurements as reported by Tankaka, et al. (2000) and Rhee (2005). The close agreement of AcuSolve results with experimental results validates the ability of AcuSolve to model multiphase flow problems with user-defined motion.

Problem Description

The problem consists of a tank filled to 20 percent capacity with water that is rotated or translated according to a user-defined function, as shown in the following image, which is not drawn to scale, where three monitoring locations, P1, P2 and P3, are denoted. The motion of the tank causes the fluid to begin sloshing rapidly, creating a time-dependent pressure field due to the height of the local water column. Non-slip boundary conditions for the top, bottom, left and right sides are applied with slip boundary conditions on the front and back faces. The SST turbulence model along with a global time-step of 0.001 seconds is used for the simulation. The pressure at each of the monitoring locations is compared against the experimental measurements as described in Tankaka, et al. (2000). It should be noted that the pressure computed and presented in the images represent the time-dependent dynamic pressure, static pressure is subtracted to be consistent with the measurements, at the specified point. Roll-Short is the case provided with the Validation Manual. The results for this case as well as Sway - Short are presented within this overview. In each case, the motion profile is defined with the following function and coefficients as defined in the table below.

$$x = A\sin(\omega t) \tag{1}$$

Where A = amplitude of oscillation, ω = frequency of oscillation = 2 π/T, t = time (sec) and T = Time period of oscillation (sec).

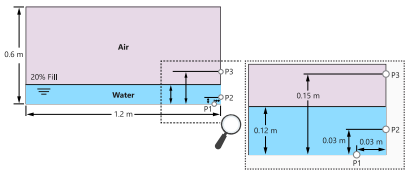


Figure 2: Critical Dimensions and Parameters for Simulating a 2D Tank Slosh with Mesh Motion

Table 1: Sine Function Scaling Parameters for Tank Motion Profile

Cases	Mesh Motion	Amplitude (A)	Time Periods (T)	Tank Filling Level
Sway – Base	Sway motion	0.06 m	1.94 sec	20% height

Cases	Mesh Motion	Amplitude (A)	Time Periods (T)	Tank Filling Level
Sway – Short	Sway motion	0.06 m	1.74 sec	20% height
Roll – Base	Rolling motion	10 degrees	2.25 sec	20% height
Roll – Short	Rolling motion	10 degrees	1.85 sec	20% height

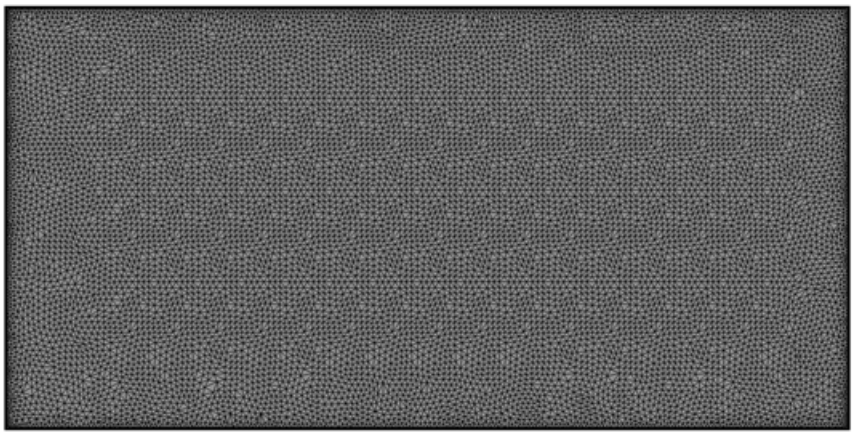


Figure 3: Mesh Used for Simulating Multiphase Sloshing Within a 2D Tank

AcuSolve Results

The AcuSolve solution is run for a time of t/T=5.0, 9.25 sec for Roll - Short, and the results presented reflect the transient motion of the water within the tank. The experimental values of pressure (kPa) and normalized simulation time are presented with the corresponding AcuSolve results at three measurement locations. The AcuSolve results show good agreement with the experimental results for pressure magnitude, the local water column height, as well as accurate timing of the peaks, indicating that the air-water interface is properly captured. Additional motion cases, as well as comparisons between two dimensional versus three dimensional simulations have been simulated with AcuSolve. The accuracy and solution requirements of these simulations are omitted for brevity but are available upon request. It was found that the differences between 2D and 3D simulations may be of interest for engineers, however the 2D results are shown to be adequate and less computationally expensive than 3D in the cases studied.

User-Defined Multiplier Function

This validation case relies on defining the motion of the elements within the tank, leading to the water sloshing in the presence of air. The motion is defined using an AcuSolve User-Defined Function (UDF) to specify the time-dependent multiplier function applied to the mesh motion command. The mesh motion is assigned to the Fluid element set, causing all of the elements to move according to the specified sine function. For the Roll - Short case, the mesh motion command is specified as rotation with the rotation multiplier function specified as rotation. If you are interested in simulating one of the other motion profiles, for example Sway - Base/Short, the type of mesh motion command would be changed to translation with the translation multiplier function assigned with the same UDF. The function name is designated at usrMotion and is contained within the source file `motion.c`. The source file, along with

pre-compiled binaries for Linux64 and Windows64 are provided with the validation case. Depending on your architecture it may be necessary to re-compile the source on the local system. Please refer to the *Programs Reference Manual* for details on using AcuMakeLib or AcuMakeDll for Linux and Windows, respectively.

Summary

The AcuSolve solution compares well with experimental results for tank sloshing simulations. In this application, the time dependent motion of the tank and the multiphase flow solution are simulated with AcuSolve using the level-set formulation and the SST turbulence model. The experimental values for instantaneous pressure at three locations and for two motion profiles are presented with the corresponding AcuSolve results. A good agreement of simulation results with the experiment validates the ability to solve time-dependent/accurate sloshing cases using the multiphase capabilities of AcuSolve.

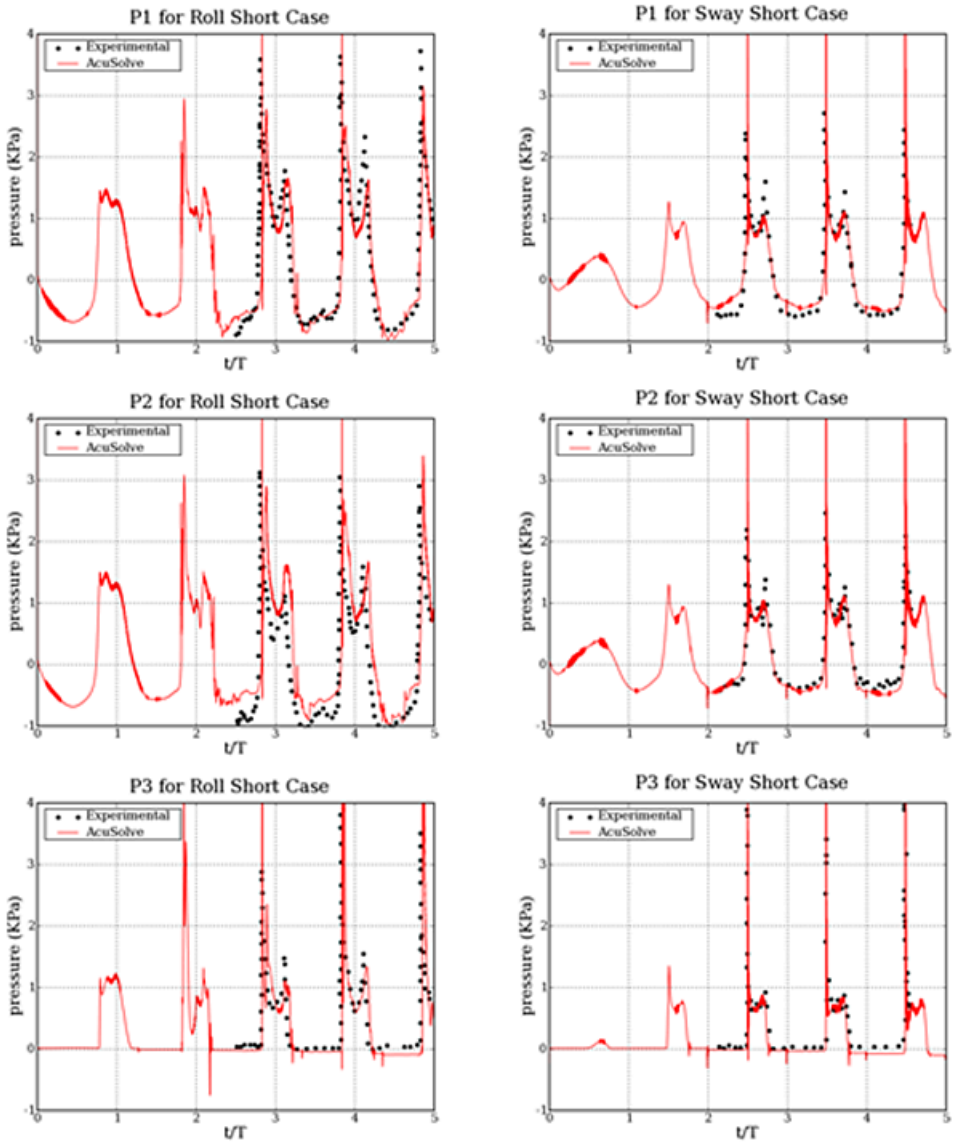


Figure 4: Time Dependent Pressure at Three Monitoring Locations Within the Sloshing Tank for Two Motion Profiles (Roll-Short, Left and Sway-Short, Right)

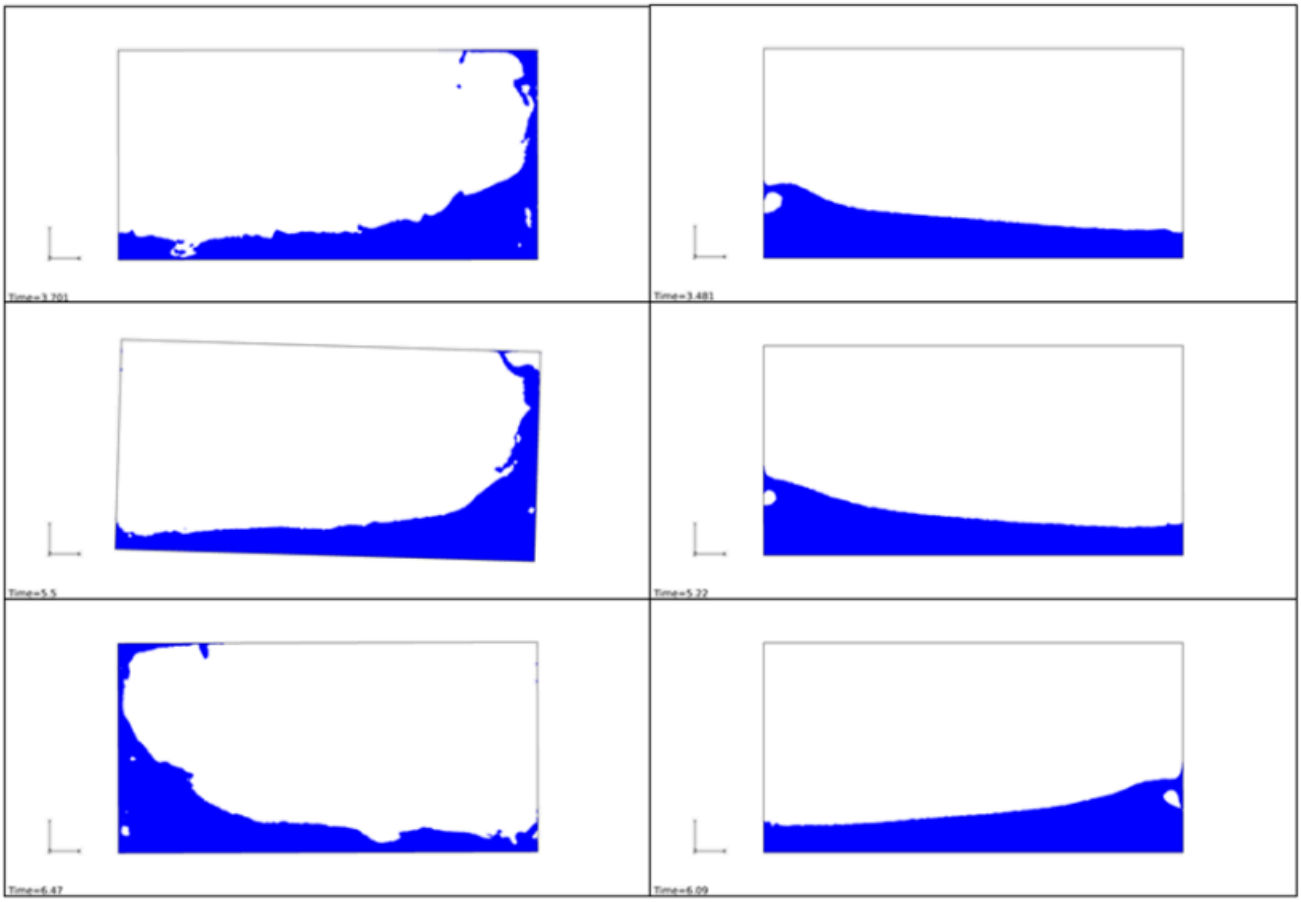


Figure 5: Instantaneous Volume Fraction Contour (Blue Showing Water) at Three Moments in Time (t/T=2.0, 3.0 and 3.5) for Two Motion Profiles (Roll-Short, Left and Sway-Short, Right)

Simulation Settings for Multiphase Flow Within a Sloshing Tank

AcuConsole database file: `<your working directory>\tank_sloshing_multiphase \tank_sloshing.acs`

Global

- Problem Description
  - Analysis type - Transient
  - Turbulence equation - SST
  - Multiphase equation – Level Set
- Auto Solution Strategy
  - Final time - `9.5` sec
  - Initial time increment - `0.001` sec
  - Min stagger iterations - `2`
  - Max stagger iterations - `10`
  - Fluid 1 - Water
  - Fluid 2 - Air

- Multiplier Function
  - rotation
    - Type - User Function
    - User function name - UsrMotion
    - User function values - `10.0`, `1.85`, `0.0`
- Material Model
  - Air
    - Type - Constant
    - Density - `1.225` kg/m^3
    - Velocity - `1.781e-5` kg/m-sec
  - Water
    - Type - Constant
    - Density - `1000` kg/m^3
    - Velocity - `0.001` kg/m-sec
- Mesh motion
  - rotation
    - Type - Rotation
    - Rotation center – `0.0`, `0.0`, `0.0`
    - Angular velocity – `0.0`, `0.0`, `0.0174533` (1.0 deg/sec)
    - Rotation variable – Multiplier Function
    - Rotation multiplier function – rotation

  Model
  - Volumes
    - Fluid
      1. Element Set
         1. Medium – Multiphase
         2. Multi field model – Water-Air
         3. Body force – Gravity
         4. Mesh motion – rotation
- Surfaces
  - x+
    - Simple Boundary Condition – Wall
  - x-
    - Simple Boundary Condition – Wall
  - y+
    - Simple Boundary Condition – Wall
  - y-
    - Simple Boundary Condition – Wall

- z+
  - Simple Boundary Condition – Slip
- z-
  - Simple Boundary Condition – Slip

References

Shin Hyung Rhee, 2005, "Unstructured Grid Based Reynolds-Averaged Navier-Stokes Method for Liquid Tank Sloshing", Journal of Fluids Engineering, Vol 127, pp. 572- 582.

Tanaka, Y., Ando, T., and Miyamoto, T., 2000, "Experimental Study on Sloshing Load Measured by Panel-Type Pressure Gauge," Proc. 74th. General Meeting of Ship Research Institute, Ship Research Institute, Tokyo, Japan, pp. 137-142.

Single-Phase Nucleate Boiling in a Rectangular Channel

In this application, AcuSolve is used to simulate the wall heat flux due to nucleate boiling at a heated wall inside a rectangular channel with water flow. Results are compared with experimental heat flux measurements as reported by Steiner, et al. (2005). The close agreement of AcuSolve results with experimental results validates the ability of AcuSolve to model single phase nucleate boiling problems.

Problem Description

The problem consists of a channel with a heated wall at the bottom. The temperature of the wall is selected to onset the nucleate boiling at the heated wall. The dimensions of the inlet are 0.03 x 0.04 m; the inlet velocity (v) is 0.39 m/s and the temperature (T) of the fluid entering the inlets is varied from 373.15 K (100 C) to 406.15 (133 C)), while the atmospheric pressure is specified to be 2 bar. The pre-heated water enters the inlets and heat is transferred into the fluid from the heated walls. The heat causes sub-cooled boiling to occur in the region close to the wall and leads to the formation of bubbles at nucleation sites. The surface tension and vapor phase models are specified to emulate the physical process of water changing state to water vapor.

The heat transfer in this regime is dominated by two effects, the macro convection due to the motion of the bulk liquid and the latent heat transport associated with the evaporation of the liquid micro-layer between the bubble and the heated wall. Each of these effects are modeled with AcuSolve and the prediction of their processes is demonstrated in the following results.

The AcuSolve simulation is prepared as a steady state heat transfer simulation to determine the temperature and heat flux on the heated walls of the model. AcuSolve computes the single-phase nucleate boiling by employing Chen’s model for two-phase boiling flow described in Chen (1966). The heat flux values for different wall temperatures are compared against the experimental measurements, as described in Steiner, et al. (2005).

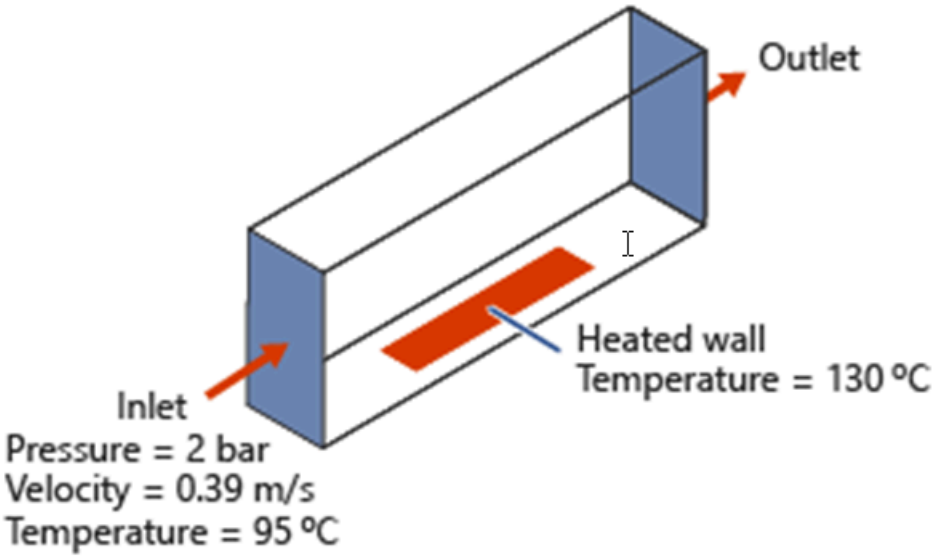


Figure 6: Critical Dimensions and Parameters for Simulating a Single-Phase Nucleate Boiling in a Rectangular Channel

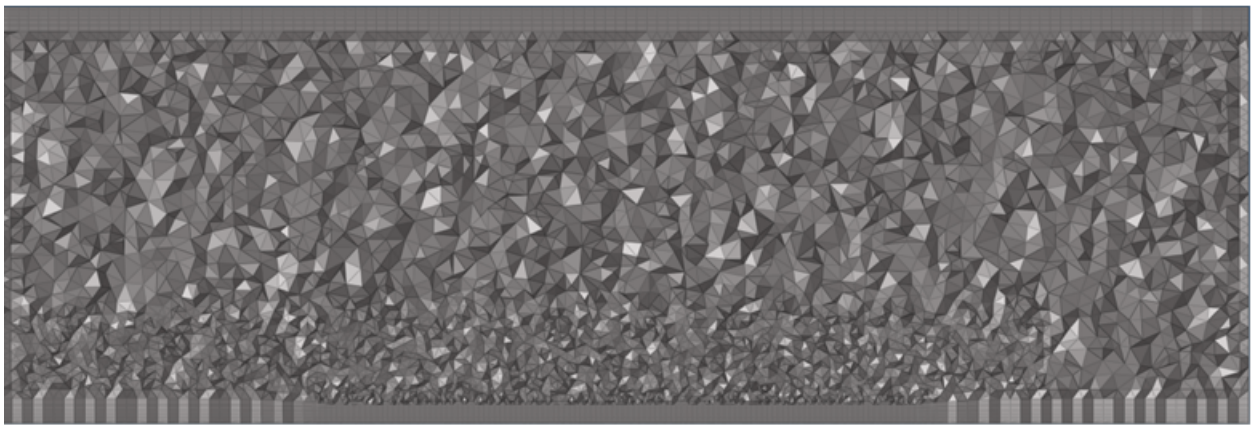


Figure 7: Mesh Used for Simulating a Single-Phase Nucleate Boiling in a Rectangular Channel

AcuSolve Results

The AcuSolve solution is run for heated wall temperature values of 100 C, 105 C, 110 C, 115 C, 120 C, 125 C, 130 C, 133 C and the results presented reflect the heat flux from the wall as the temperature nears the saturation temperature. The experimental values of heat flux (MW/m2) and wall temperature are presented with the corresponding AcuSolve results at seven temperature values. The AcuSolve results show good agreement with the experimental results for the heat flux, indicating that the single-phase nucleate boiling is properly captured.

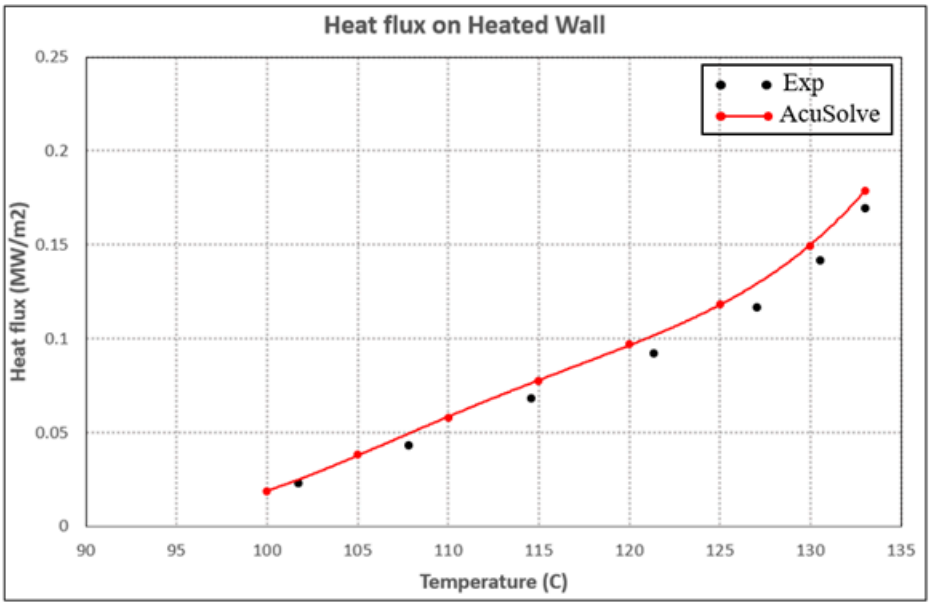


Figure 8: Heat Flux Values for Varying Wall Temperatures Compared to Experimental Data

Summary

The AcuSolve solution compares well with experimental results for single-phase nucleate boiling simulations. In this application, heat flux generated by the wall as the onset of boiling approaches are simulated with AcuSolve using the nucleate boiling feature and the RKE turbulence model. The experimental values of heat flux for the wall temperature range are presented with the corresponding AcuSolve results. A good agreement of simulation results with the experiment validates the ability to solve single-phase nucleate boiling using the nucleate boiling capabilities of AcuSolve.

Simulation Settings for Single-Phase Nucleate Boiling in a Rectangular Channel

HyperWorks CFD database file: `<your working directory>\channel_single_phase_boiling \channel_single_phase_boiling.hm`.

Global

- Problem Description
  - Analysis type – Steady
  - Turbulence equation – RKE
  - Temperature equation – Advective Diffusive
  - Nucleate Boiling Single Phase – On
- Auto Solution Strategy
  - Convergence Tolerance – `0.001` sec
  - Relaxation factor – `0.4`
- Surface Tension Model (“Water-srfTns”)
  - Type – Constant
  - Surface Tension – `0.07`

- Material Model
  - Vapor
    - Type – Constant
    - Density – `1.128` kg/m^3
    - Viscosity – `1.29e-5` kg/m-sec
    - Specific Heat – `2174.59` J/kg-K
    - Latent Heat – `2256000`
    - Latent Heat Temperature – `393.45` K
    - Conductivity – `0.02749` W/m-K
    - Turbulent Prandtl number – `1.0`
  - Water
    - Type – Constant
    - Density – `965.36` kg/m^3
    - Viscosity – `0.000314` kg/m-sec
    - Specific Heat – `4204.8` J/kg-K
    - Conductivity – `0.675` W/m-K
    - Turbulent Prandtl number – `0.91`
    - Vapor phase model – Vapor
    - Surface Tension model – Water-srfTns

Model

- Volumes
  - Fluid
    - Material– Water
- Surfaces
  - Inflow
    - Simple Boundary Condition – Inflow
    - Inflow type – Average Velocity
    - Average Velocity – `0.39` m/sec
    - Temperature – `368.15` K
  - Outflow
    - Simple Boundary Condition – Outflow
    - Back flow condition – On
    - Temperature back flow type – Mass flux average
    - Kinetic energy back flow type – Mass flux average
    - Dissipation rate back flow type – Mass flux average
  - Bottom
    - Simple Boundary Condition – Wall
  - Top

        - Simple Boundary Condition – Wall
    - Side_MinY
        - Simple Boundary Condition – Wall
    - Side_MaxY
        - Simple Boundary Condition – Wall
    - Heated Wall
        - Simple Boundary Condition – Wall
        - Temperature type – Value
        - Temperature – [373.15, 378.15, 383.15, 388.15, 393.15, 398.15, 403.15, 406.15] K

References

Helfried Steiner, Alexander Kobor, Ludwig Gebhard, 2005, "A wall heat transfer model for subcooled boiling flow", International Journal of Heat and Mass Transfer, Vol 48, pp. 4161- 4173.

Chen, J.C., 1966, "Correlation for Boiling Heat Transfer to Saturated Fluids in Convective Flow", United States: N. p., 1962. Web. doi:10.2172/4636495.

Turbulent Flow Through a Pipe

In this application, turbulent flow of air through a pipe is simulated. AcuSolve results are compared with experimental results as described in White (1991) and extracted from the Moody chart. The close agreement of AcuSolve results with experimental results validates the ability of AcuSolve to model turbulent flow within pipes.

Problem Description

The problem consists of air flowing through a pipe 0.004 m in diameter and 0.02 m long, as shown in the following image, which is not drawn to scale. The AcuSolve simulation utilizes periodic boundary conditions to obtain the fully developed profile within the pipe. The defined pressure drop, applied as a body force on the fluid volume, offsets the change in pressure due to the friction created by the no-slip walls of the pipe. The Reynolds number for this problem is approximately 8,250.

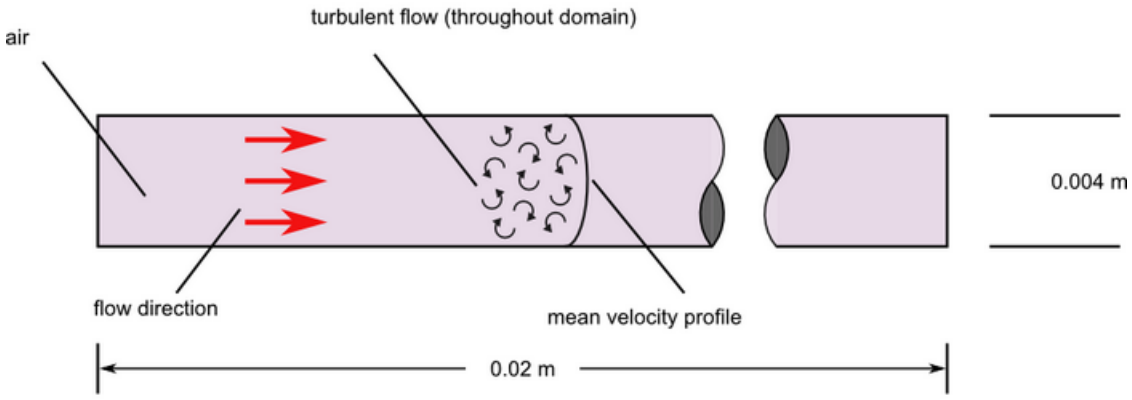


Figure 9: Critical Dimensions and Parameters for Simulating Turbulent Flow Through a Pipe

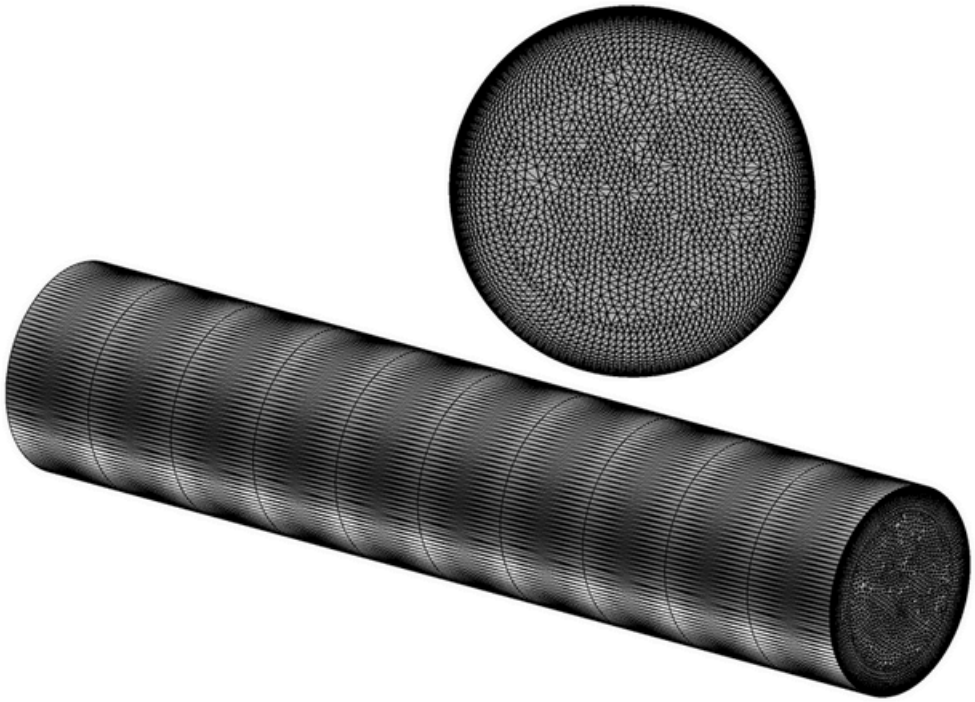


Figure 10: Mesh of a Periodic Segment Used for Simulating Turbulent Flow Through a Pipe

AcuSolve Results

The AcuSolve solution converged to a steady state and the results reflect the mean flow conditions with a turbulent velocity profile that is fully developed. The simulation was performed using the Spalart-Allmaras single-equation turbulence model. The velocity and eddy viscosity profiles are constant along the length of the pipe.

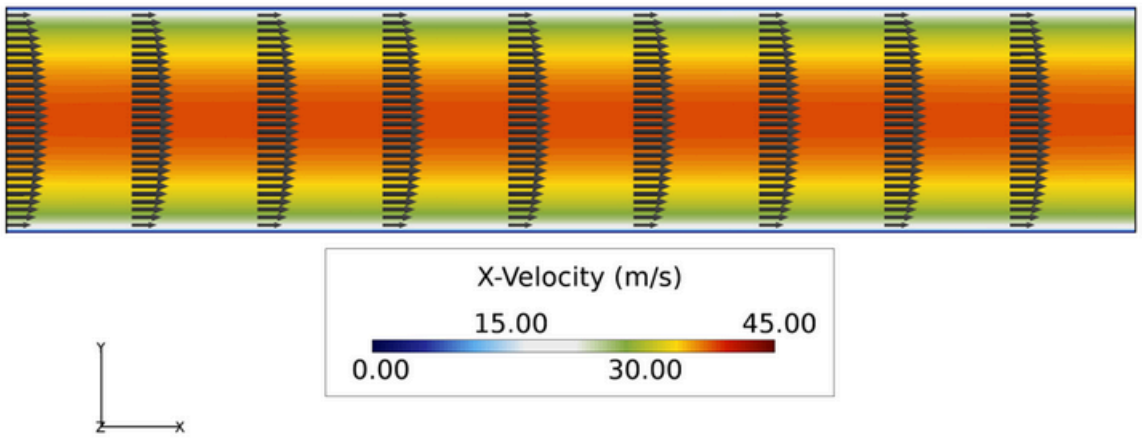


Figure 11: Velocity Contours and Periodic Velocity Vectors for the Averaged Turbulent Flow

The experimental result for average velocity at the inlet is presented with the corresponding AcuSolve prediction in the following table.

Table 2:

	Experimental result	AcuSolve prediction	Percent deviation from experimental
Average inlet velocity	30.0	29.71	0.971

Summary

The AcuSolve solution compares well with the experimental result for average inlet velocity for turbulent flow through a pipe. In this application, the applied body force counteracts the change in pressure due to the viscous stresses near the pipe wall. The resulting friction factor for a smooth wall pipe and the specified Reynolds number is approximately 0.0326. With the imposed pressure drop defining the flow, the AcuSolve prediction of average inlet velocity is within 1.0 percent of the Darcy-Weisbach approximation.

Simulation Settings for Turbulent Flow Through a Pipe

AcuConsole database file: `<your working directory >\pipe_turbulent\pipe_turbulent.acs`.

Global

- Problem Description
  - Analysis type - Steady State
  - Turbulence equation - Spalart Allmaras
- Auto Solution Strategy

    - Relaxation factor - `0.4`
- Material Model
    - Air
        - Density - `1.225` kg/m3
        - Viscosity - `1.781e-05` kg/m-sec
- Body Force
    - dpdx
        - Gravity
            1. X-component - `3739.98` m/s2

  Model
- Volumes
    - Fluid
        - Element Set
            1. Material model - Air
            2. Body force - dpdx
- Surfaces
    - Inlet
        - Simple Boundary Condition - (disabled to allow for periodic conditions to be set)
    - Outlet
        - Simple Boundary Condition - (disabled to allow for periodic conditions to be set)
    - Wall
        - Simple Boundary Condition
            1. Type - Wall
            2. Roughness height - `0.0` mm
- Periodics
    - Periodic 1
        - Periodic Boundary Condition
            1. Type - Periodic

References

F. M. White. "Viscous Fluid Flow". Section 3-2.1. McGraw-Hill Book Co., Inc.. New York. 1991.

Experimental solution adapted from Darcy-Weisbach equation based on friction factor taken from the Moody chart with a Reynolds number of approximately 8,250.

Turbulent Flow Behind an Open-Slit V

In this application, AcuSolve is used to simulate turbulent flow of air through and behind a two dimensional open-slit V. AcuSolve results are compared with experimental results adapted from Yang and Tsai (1993). The close agreement of AcuSolve results with experimental results validates the ability of AcuSolve to model the Coandă effect.

Problem Description

The problem consists of air flowing through and past an open-slit V positioned within a flow domain, as shown in the following image, which is not drawn to scale. The flow domain is 0.3 m long and 0.1 m high. The narrow end of the V is positioned 0.05 m from the domain inlet. The slit in the V is 0.002 m high. The V widens to 0.022 m at 0.075 m from the domain inlet. Air enters the domain with a constant velocity of 20 m/s. The upper and lower limits of the domain are defined as no-slip boundary conditions.

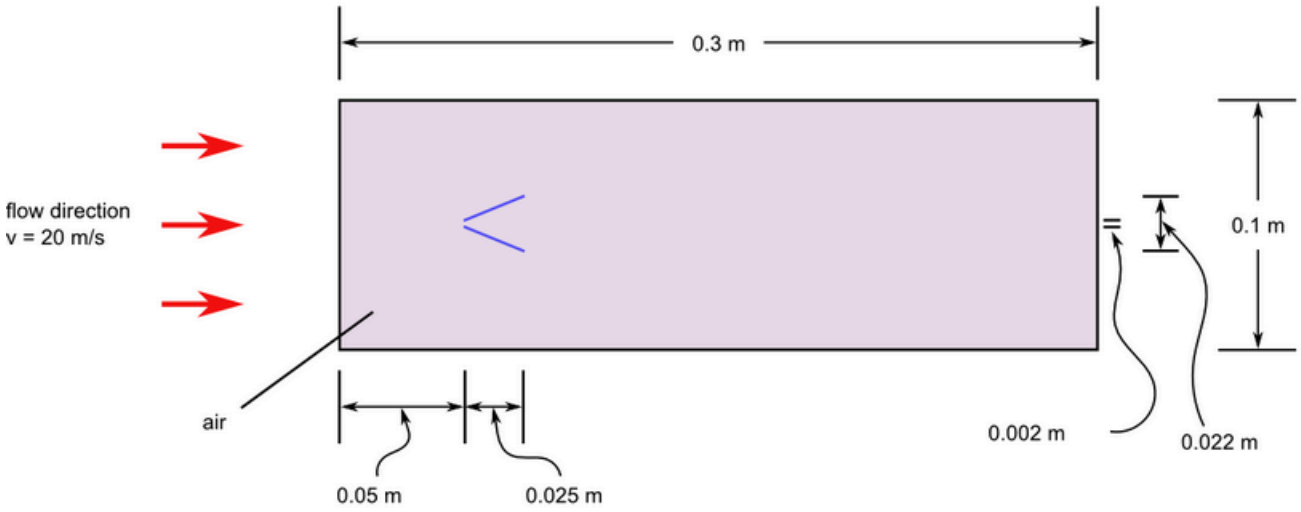


Figure 12: Critical Dimensions and Parameters for Simulating Turbulent Flow Behind an Open-Slit V

The simulation was performed as a two dimensional problem by restricting flow in the out-of-plane direction through the use of a mesh that is one element thick. A coarse mesh is used throughout much of the domain, with mesh refinement closer to the V.

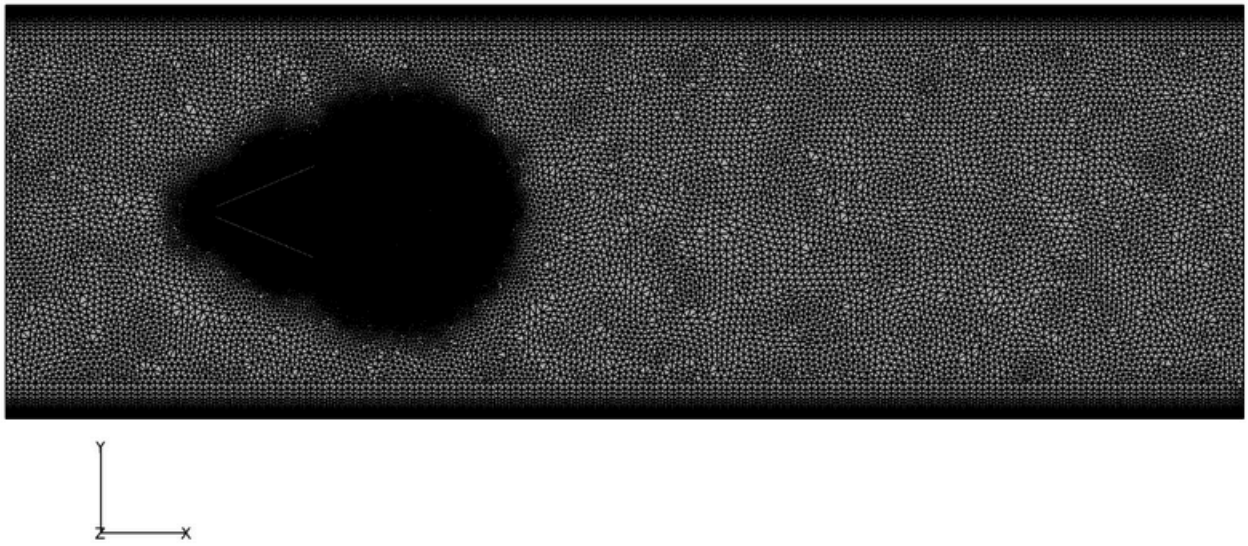


Figure 13: Mesh used for Simulating Turbulent Flow Behind an Open-Slit V (the V Lies Within the Dense Area of the Mesh)

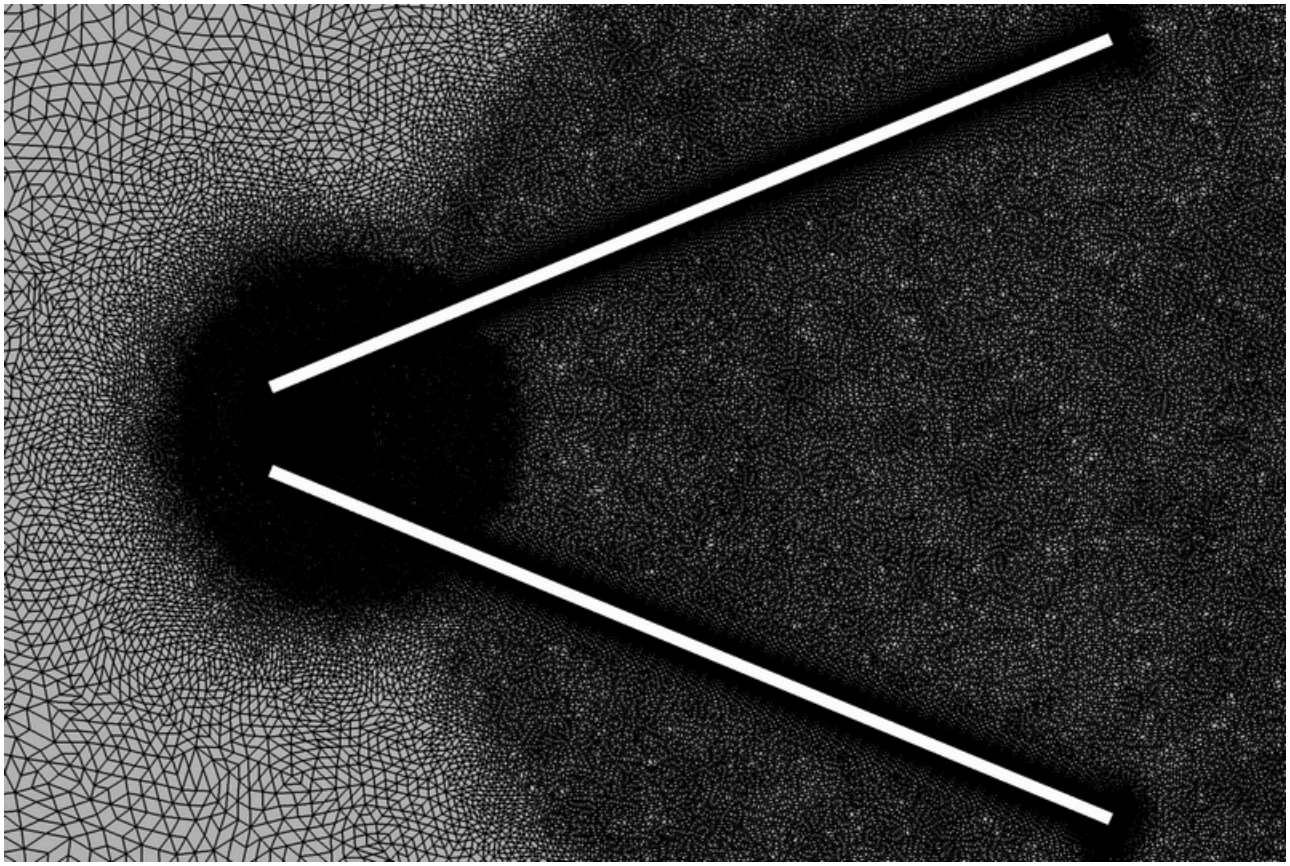


Figure 14: Mesh Surrounding the Open-Slit V

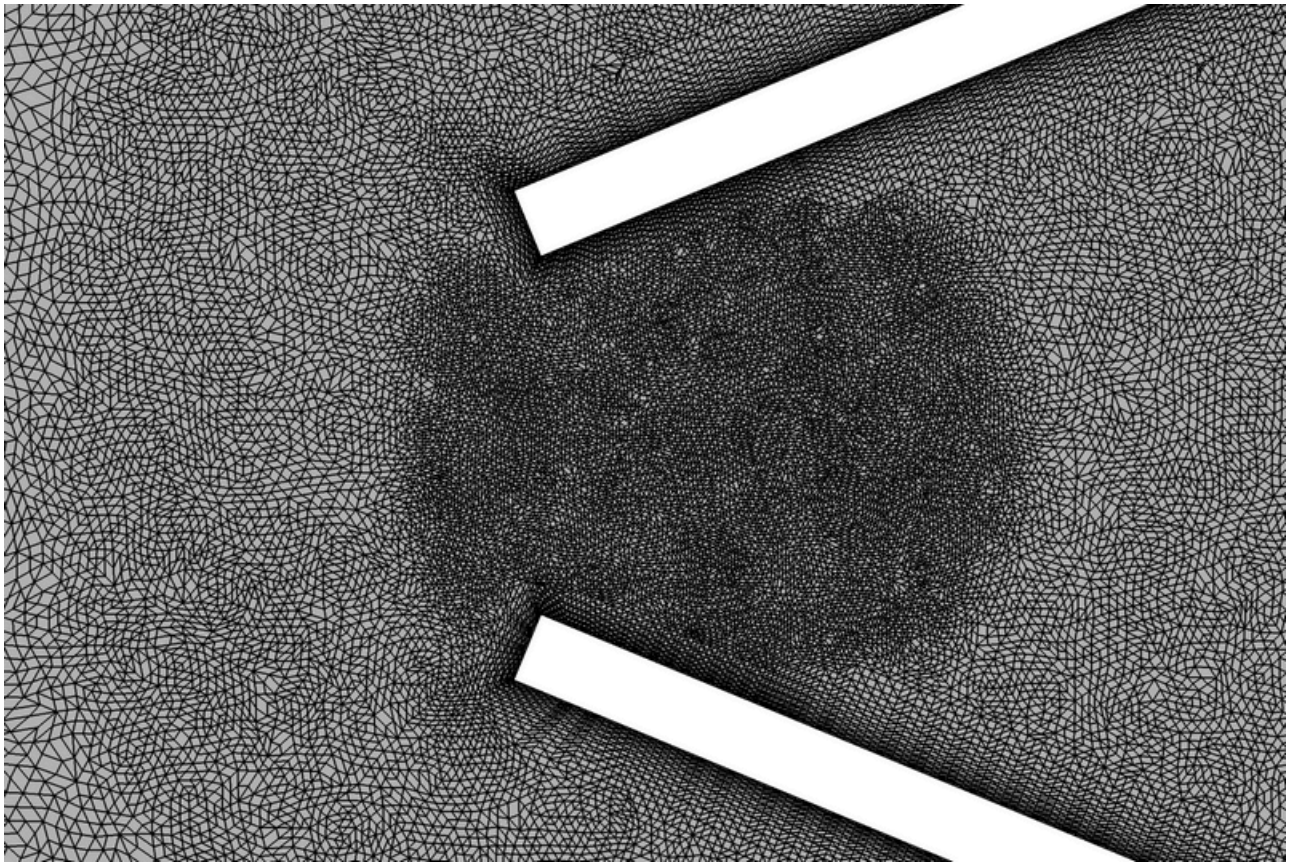


Figure 15: Mesh Near the Open Slit

AcuSolve Results

The AcuSolve solution converged to a steady state and the results reflect the mean flow conditions. Air flows through the open slit in the V and accelerates while being forced to one side due to the Coandă effect. As air encounters the exterior of the widening gutter, velocity increases and the wake induces recirculation near the exit of the V. The recirculation zone extends downstream of the V gutter.

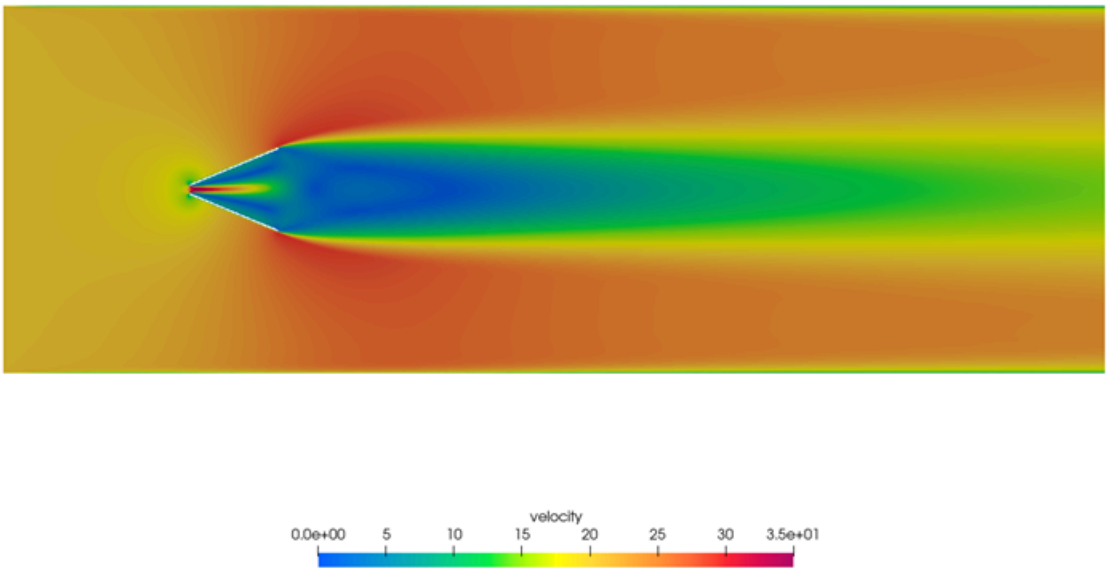


Figure 16: Contours of X-Velocity of Flow Through and Around an Open-Slit V (the Vertical Line Represents the Location, 0.022 m Downstream from the V exit, at Which Experimental Data is Compared to AcuSolve Results)

AcuSolve results were compared to experimental results at different heights 0.022 m behind the V exit. X-velocity is near zero at the bottom of the domain (height = -0.05 m), rising steeply with distance from the wall. The velocity gradient decreases until approximately 0.018 m below the center line of the domain, which is slightly below the bottom of the V exit. The velocity behind the V drops sharply with an increase in height, due to the blockage caused by the presence of the slanted walls. The lowest velocity is just above the center line of the domain.

The slight asymmetry in the velocity profile in the wake of the V is expected due to the Coandă effect.

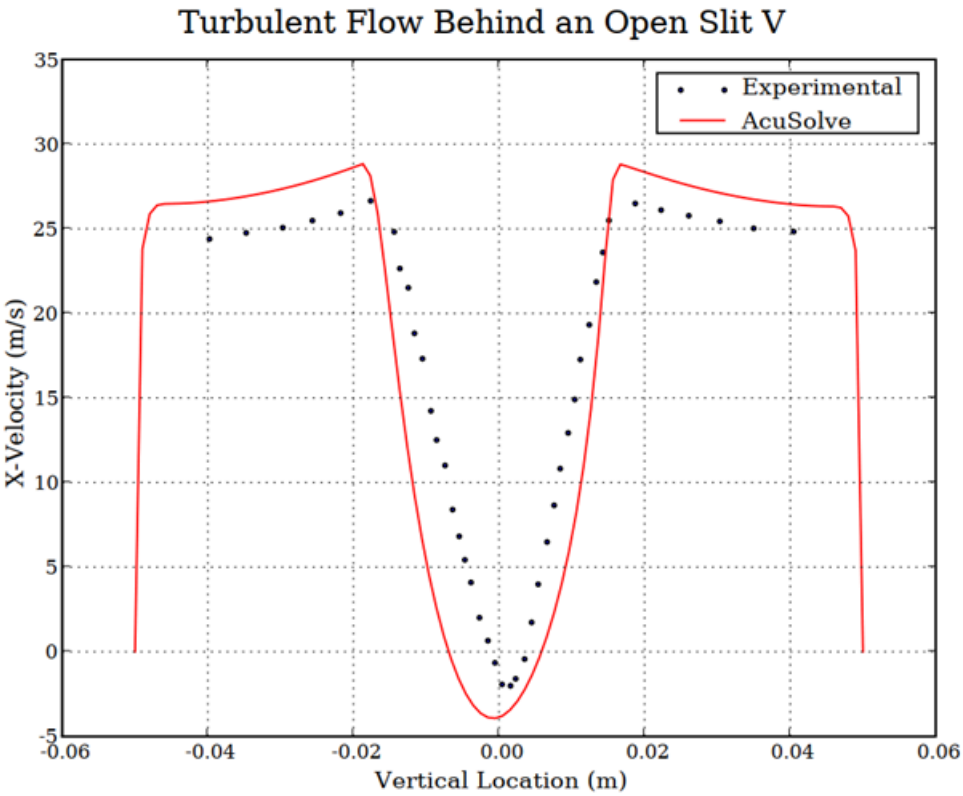


Figure 17: X-Velocity Plotted Against Vertical Location 0.0022 m Downstream of the V Exit

Summary

The AcuSolve results compare well with the experimental results for flow through and around an open-slit V. In this application, the V-shaped geometry diverts flow towards the side walls of the channel and also creates a high-velocity jet through the slit. The low pressure associated with the jet causes a deflection towards the walls of the V, resulting in an asymmetric flow field within the V shape. This application illustrates the ability of AcuSolve to accurately predict the Coandă effect. The acceleration of the flow due to the deflection along the V-shaped walls and the momentum deficit in the wake of the V is captured accurately.

Simulation Settings for Turbulent Flow Behind an Open-Slit V

HyperWorks CFD database file: `<your working directory>\v_gutter_turbulent\v_gutter_turbulent.hm`

Global

- Problem Description
  - Analysis type - Steady State
  - Turbulence equation - Spalart Allmaras
- Auto Solution Strategy
  - Relaxation factor - `0.5`
- Material Model

- Air
  - Density - `1.0` kg/m3
  - Viscosity - `1.8333e-05` kg/m-sec

Model

- Volumes
  - Fluid
    - Element Set
      1. Material model - Air
- Surfaces
  - Inlet
    - Simple Boundary Condition
      1. Type - Inflow
      2. Inflow type - Velocity
      3. X velocity - `20.0` m/sec
      4. Eddy viscosity - `0.000800426` m2/sec
  - LE_TE
    - Simple Boundary Condition
      1. Type - Wall
  - Outlet
    - Simple Boundary Condition
      1. Type - Outflow
  - Symm_MaxZ
    - Simple Boundary Condition
      1. Type - Slip
  - Symm_MinZ
    - Simple Boundary Condition
      1. Type - Slip
  - V_Walls
    - Simple Boundary Condition
      1. Type - Wall
  - Walls
    - Simple Boundary Condition
      1. Type - Wall

References

J.-T. Yang and G.-L. Tsai. "Near-wake flow of a v-gutter with slit bleed". Journal of Fluid Engineering. 115:13-20. March, 1993.

Turbulent Flow Through a Wavy Channel

In this application, AcuSolve is used to simulate turbulent flow through a channel with a lower wall shaped as a sinusoidal wave. AcuSolve results are compared with experimental results adapted from Kuzan (1986). The close agreement of AcuSolve results with experimental results validates the ability of AcuSolve to model cases with internal flow through a channel with wavy walls.

Problem Description

The problem consists of air flowing through a channel with a wavy bottom wall. The channel is 1.1 m high, 1.0 m wide, and is modeled as a section 1.0 m in length, as shown in the following image, which is not drawn to scale. The bottom wall wave shape has an amplitude of 0.1 m and a wavelength of 1 m. The mass flow rate through the channel is set to a constant value of 0.816 kg/s. The flow field develops as a result of the non-planar bottom wall and viscous stresses acting near the top and bottom walls. Collision of air with the peak of the wave on the channel floor causes an acceleration of the flow, followed by recirculation as the flow area expands into the valley.

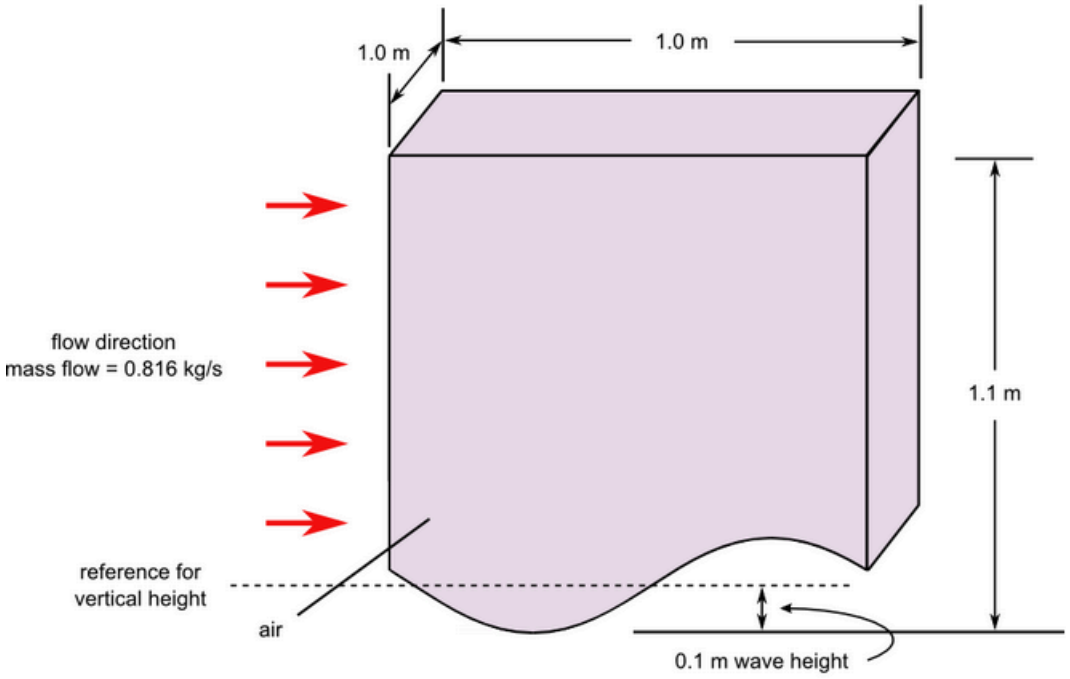


Figure 18: Critical Dimensions and Parameters for Simulating Turbulent Flow Through a Wavy Channel

The simulation was performed as a two dimensional problem by restricting flow in the out-of-plane direction through the use of a mesh that is one element thick. The elements were extruded to the width of the channel.

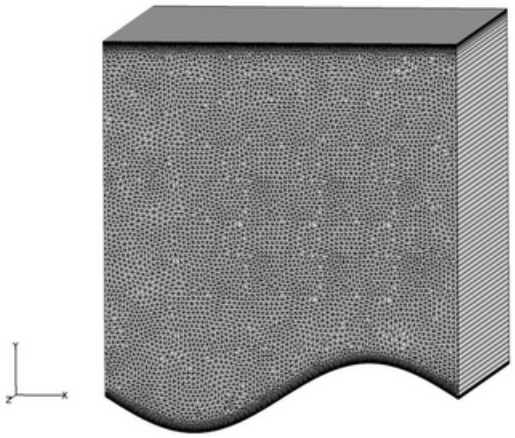


Figure 19: Mesh Used for Simulating Turbulent Flow Through a Wavy Channel

AcuSolve Results

The AcuSolve solution converged to a steady state and the results reflect the mean flow conditions. The expansion of the cross section as the air passes the trough in the wave causes an adverse pressure gradient to form. This results in separation of the flow along the downward-slanting walls of the wavy surfaces. The recirculation zone establishes itself within the troughs of the wave. The remaining flow above the troughs maintains its velocity in the streamwise direction and distributes throughout the channel. The flow accelerates as it travels over the wave peak and the velocity continues to increase as a function of distance from the wall until it reaches a maximum velocity approximately 0.3 m away from the upper wall.

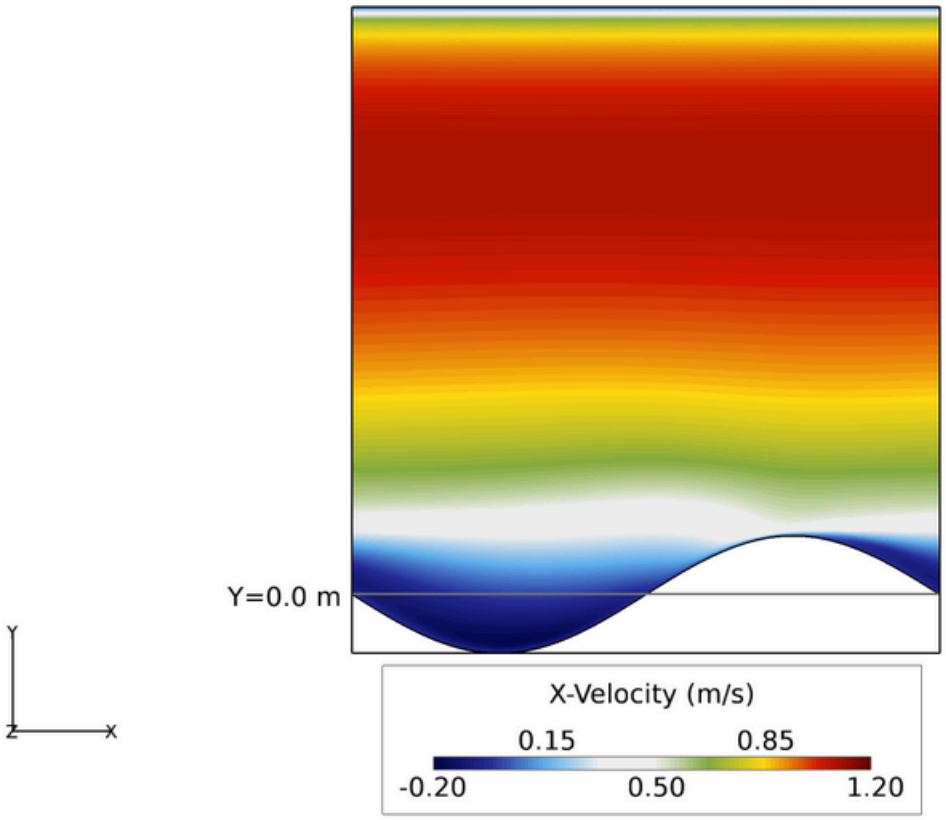


Figure 20: Velocity Contours in the X-Y Plane in a Wavy Channel (the Horizontal Line Represents the Reference for Wave Height - the Wave Crest is 0.1 m Above The Reference Height, and the Wave Valley is 0.1 m Below the Reference Height)

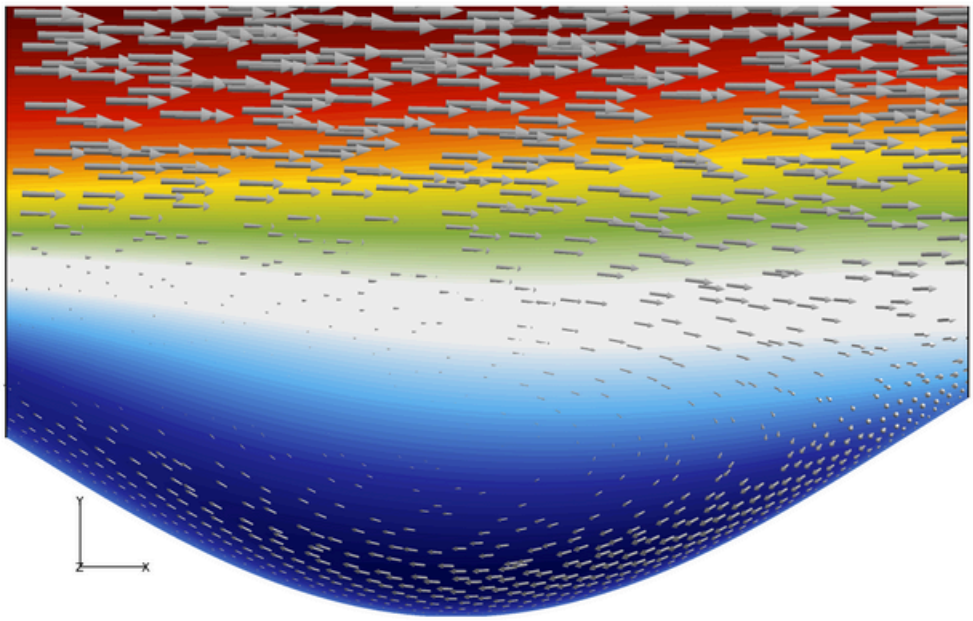


Figure 21: Close-Up View of Velocity Contours and Velocity Vectors in the X-Y Plane Near the Valley of a Wave

The X-velocity directly over the center of the wave valley initially decreases (backflow) as distance away from the bottom wall increases, with a maximum velocity in the -X direction at approximately 0.03 m above the valley floor. The X-velocity then increases to zero m/sec at 0.1 m above the valley, reflecting an end of the recirculation.

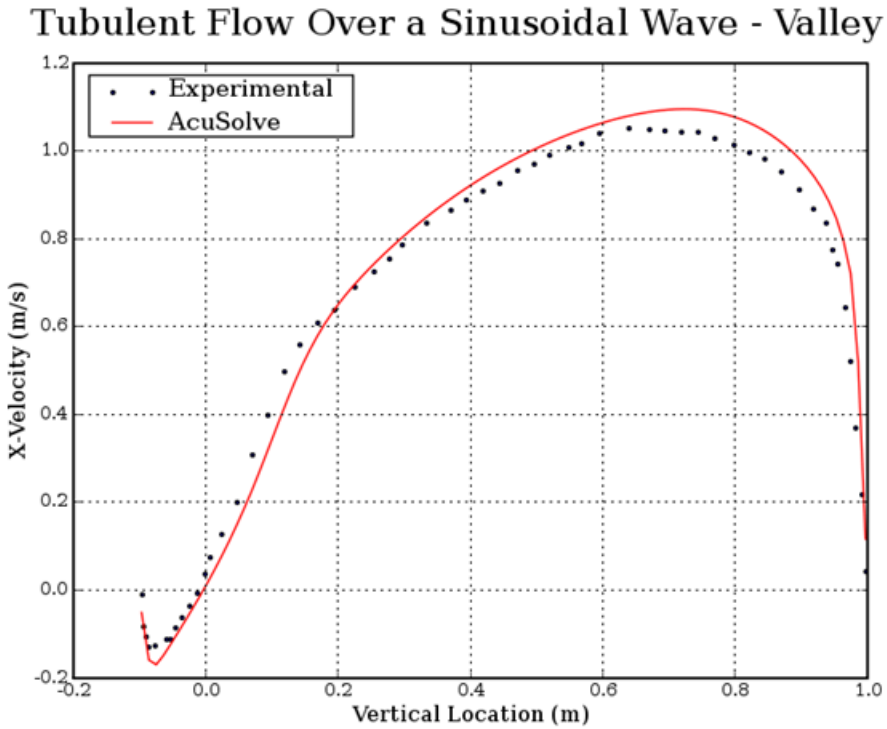


Figure 22: X-Velocity Plotted Against Vertical Location in the Channel Above the Valley Center (the Valley Floor is 0.1 m Below the Reference Height)

The X-velocity directly over the wave peak has different behavior due to the lack of recirculation. The velocity above the peak increases as distance away from the bottom wall increases, with a maximum velocity in the X direction at approximately 0.75 m. The velocity then decreases to zero at the top wall.

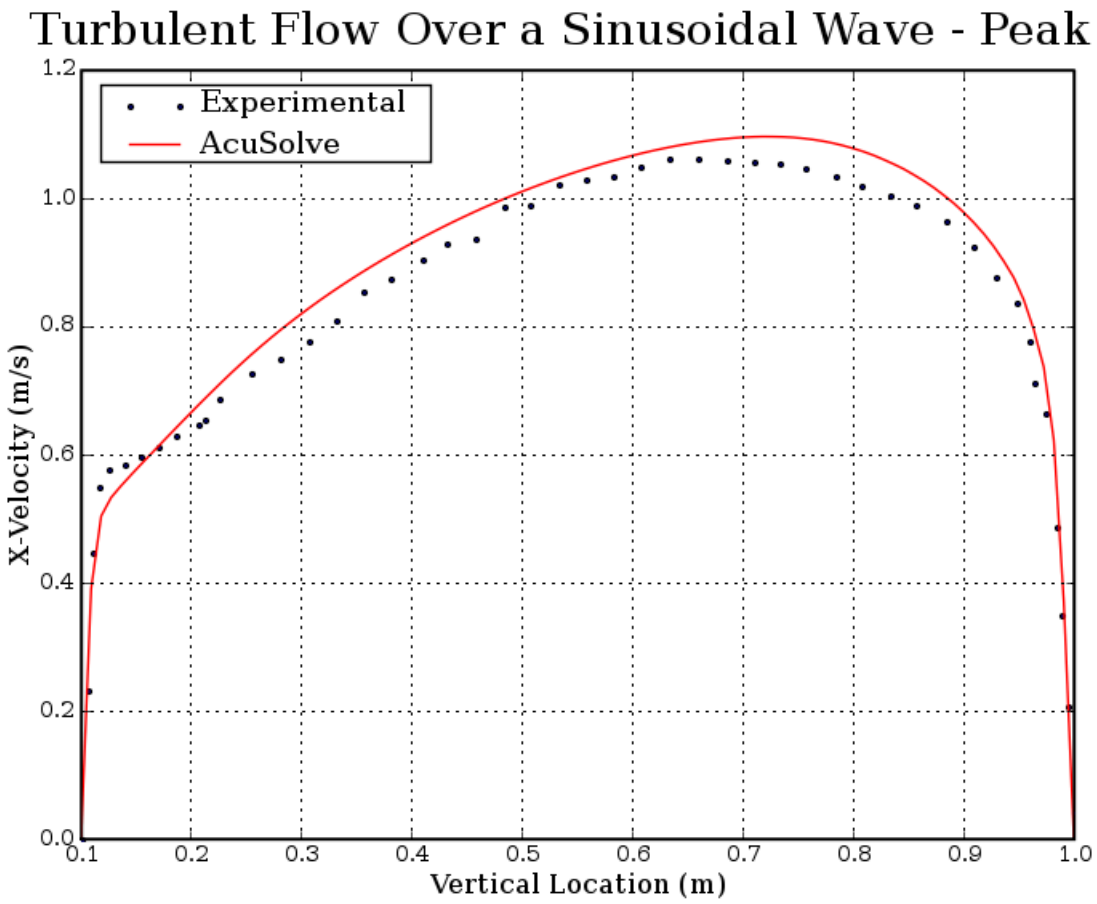


Figure 23: X-Velocity Plotted Against Vertical Location in the Channel Above the Wave Peak (the Wave Peak is 0.1 m Above the Reference Height)

Summary

The AcuSolve results compare well with the experimental data for X-velocity in a channel with a wavy floor. In this application, the flow is driven with a constant mass flow rate and periodic constraints are used to model a repeating array of channel segments with a wavy bottom wall. Separation of the flow occurs as a result of the adverse pressure gradient created by the changes in area. This leads to recirculation within the wave valleys. The flow separation occurs along the smoothly tapered wave wall, illustrating the ability of AcuSolve to accurately predict the separation point in this type of application. The X-velocity predicted by AcuSolve matches the experimental results with an overall coefficient of determination (R2) of 0.99 for each location shown in the plots.

Simulation Settings for Turbulent Flow Through a Wavy Channel

AcuConsole database file: `<your working directory>\wavy_channel_turbulent\wavy_channel_turbulent.acs`

Global

- Problem Description

- Analysis type - Steady State
- Turbulence equation - Spalart Allmaras

- Auto Solution Strategy
  - Relaxation factor - `0.4`
- Material Model
  - Air
    - Density - `1.0` kg/m3
    - Viscosity - `0.0001` kg/m-sec

  Model
- Volumes
  - Fluid
    - Element Set
      1. Material model - Air
- Surfaces
  - Max_X
    - Simple Boundary Condition - (disabled to allow for periodic conditions to be set)
  - Max_Y
    - Simple Boundary Condition
      1. Type - Wall
  - Max_Z
    - Simple Boundary Condition - (disabled to allow for periodic conditions to be set)
  - Min_X
    - Simple Boundary Condition - (disabled to allow for periodic conditions to be set)
    - Advanced Options
      1. Integrated Boundary Conditions
         1. Mass Flux
            1. Type - Constant
            2. Constant value - `-0.816` kg/sec
  - Min_Y
    - Simple Boundary Condition
      1. Type - Wall
  - Min_Z
    - Simple Boundary Condition - (disabled to allow for periodic conditions to be set)
- Periodics
  - Periodic-Crossflow
    - Periodic Boundary Condition
      1. Type - Periodic

- Periodic-Streamwise
  - Periodic Boundary Condition
    1. Type - Periodic
  - Individual Periodic BCs
    1. Velocity
       1. Type - Periodic
    2. Pressure
       1. Type - Single Unknown Offset
    3. Eddy Viscosity
       1. Type - Periodic

References

J. D. Kuzan."Velocity Measurements for Turbulent Separated and Near-Separated Flows Over Solid Waves". Ph.D. thesis. Deptartment of Chemical Engineering. University of Illinois. University of Illinois. Urbana, IL. 1986

Turbulent Flow with Separation in an Asymmetric Diffuser

In this application, AcuSolve is used to simulate fully developed turbulent flow through an asymmetric diffuser with a divergent lower wall and a straight upper wall. AcuSolve results are compared with experimental results as described in Buice and Eaton (2000). The close agreement of AcuSolve results with experimental results validates the ability of AcuSolve to model cases with internal turbulent flow with flow separation and reattachment in an asymmetric diffuser.

Problem Description

The problem consists of air flowing through an asymmetric diffuser with a divergent lower wall and a straight upper wall, as shown in the following image, which is not drawn to scale. The diffuser inlet has a height of 1.5 cm (H) and extends 9 cm (6H) to the divergent section. The lower wall of the diffuser diverges at an angle of 10° and expands to 7.05 cm (4.7H). The divergent section has a horizontal length of 31.5 cm (21H). The expanded section of the diffuser extends 84 cm (56H) to the outlet. Air, with a density of 1.225 kg/m^3 and a viscosity of 1.8325 X 10^{-5} kg/m-s enters the diffuser through the inlet of the diffuser with a fully developed turbulent profile at a Reynolds's number of 20,000. The simulation was conducted with the Reynolds Averaged Navier-Stokes equations using four turbulence models, Spalart Allmaras, Shear Stress Transport (SST), K-ω and Realizable K-ε.

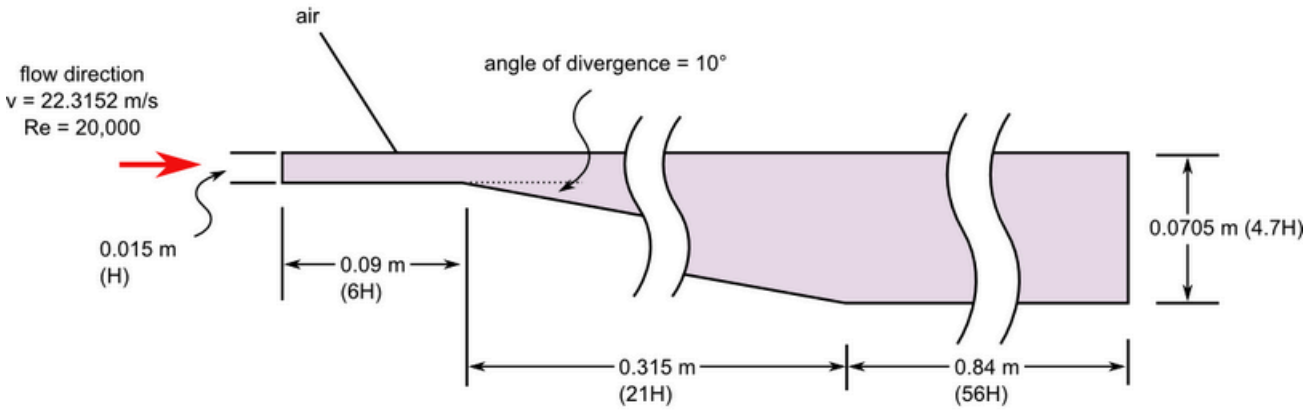


Figure 24: Critical Dimensions and Parameters for Simulating Turbulent Flow with Separation in an Asymmetric Diffuser

The simulation was performed as a two dimensional problem by constructing a volume mesh that contains a single layer of elements extruded in the cross stream direction (perpendicular to the flow plane) and by imposing symmetry boundary conditions on the extruded planes.



Figure 25: Mesh Details Near the Inlet and Divergent Section of Diffuser

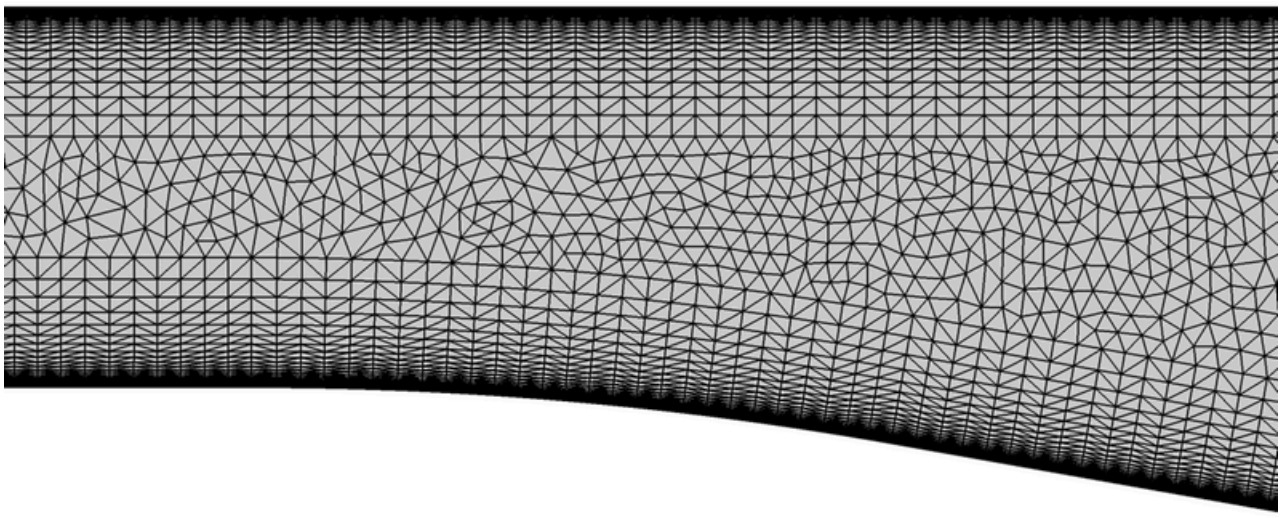


Figure 26: Mesh Details at the Beginning of the Divergence of the Lower Wall in the Diffuser

AcuSolve Results

The AcuSolve solution converged to a steady state and the results reflect the mean flow conditions. As the fully developed turbulent flow enters the divergent section, the peak velocity is maintained until the expansion of the cross-sectional height, forms an adverse pressure gradient. After the flow enters the divergent section, the velocity decreases significantly, due to the expansion of the cross-section height. This causes separation of the flow along the divergent wall and results in an area of recirculation.
The bulk of the flow above the divergent wall maintains its streamwise direction, while a portion of it reverses direction before reattaching further downstream of the divergent section. The following images show the steady state flow solution for flow within the diffuser.

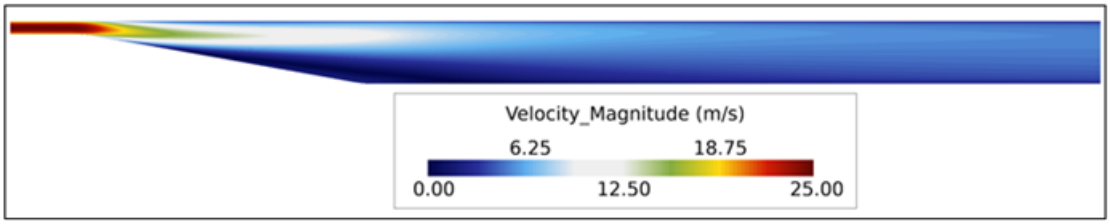


Figure 27: Velocity Contours Within the Diffuser

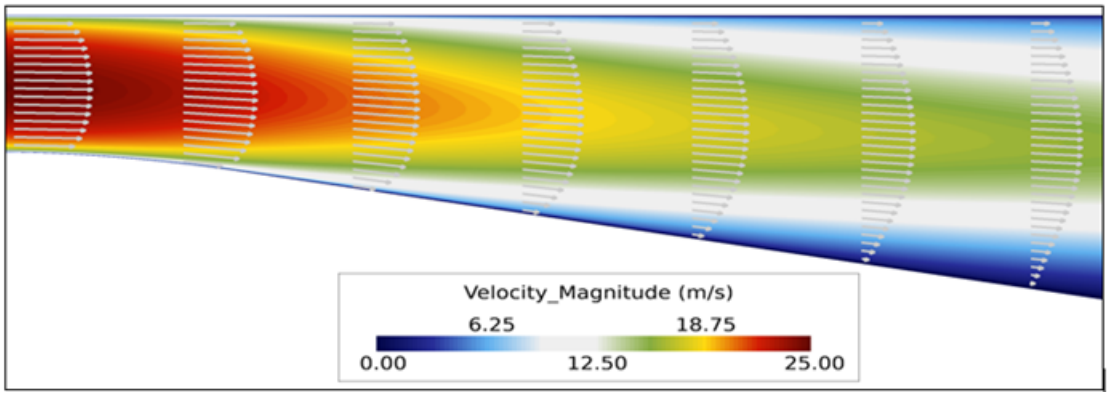


Figure 28: Close up View of Velocity Vectors and Contours of Velocity Magnitude in the Diffuser

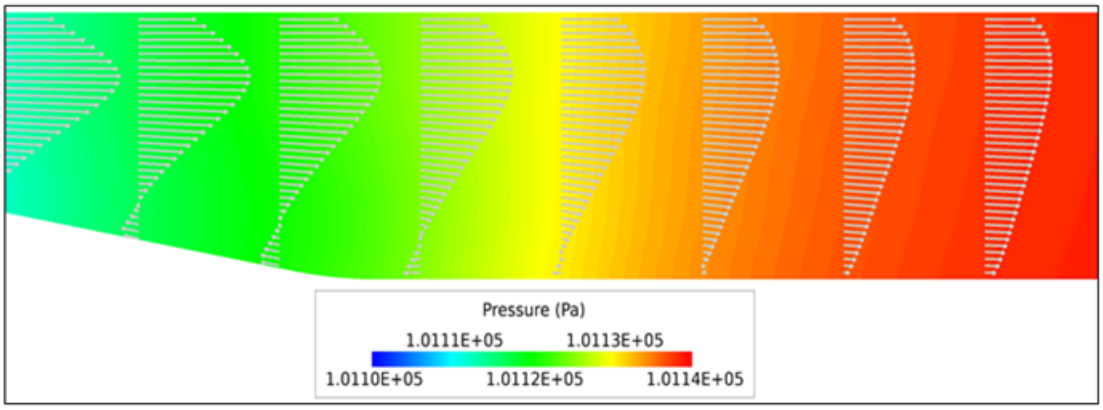


Figure 29: Close up View of Velocity Vectors and Contours of Pressure to Show Recirculation as it Approaches the Reattachment Point

Upstream of the diffuser section, the streamline velocity increases as the distance from the lower wall increases until it reaches the maximum velocity at the center of the channel. As the flow enters the divergent section of the channel, the streamwise velocity decreases near the bottom wall. The images below show the velocity profiles at three locations as measured from the midpoint of the curve where the bottom wall begins to diverge (X=0.0) for each of the tested turbulence models. The first location, where X/H = -5.944, is close to the inlet. The second location, where X/H = 13.468, is approximately 0.2 m downstream of the divergent section (~ 0.1 m from the fully expanded section). The third location, where X/H = 24.066, is approximately 0.16 m downstream of the point where the diffuser has reached the maximum height. In these plots the black circles represent the experimental measurements (Buice and Eaton 2000), the solid red lines for the prediction for the Spalart Allmaras model, solid blue lines for the prediction for the SST model, solid green lines for the prediction for the K-ω model and solid cyan lines for the K-ε model, representing the AcuSolve results. The non-dimensional height is represented by the fraction of the vertical height (Y) divided by the inlet height (H) and the velocity is normalized by the inlet velocity (Uref).

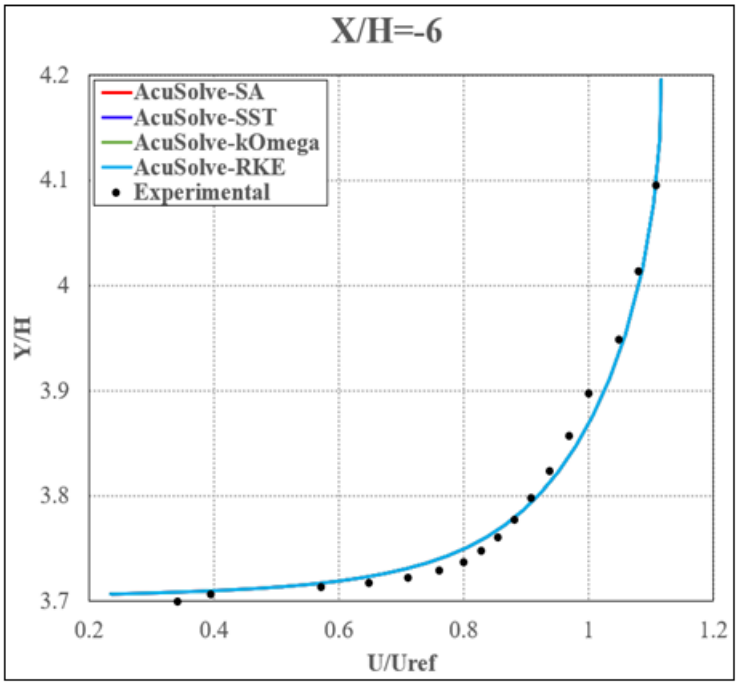


Figure 30: Non-Dimensional Streamwise Velocity Plotted Against Vertical Location Near the Inlet (X/H=-5.9442, Where the Reference Point is 6H Downstream of the Inlet)

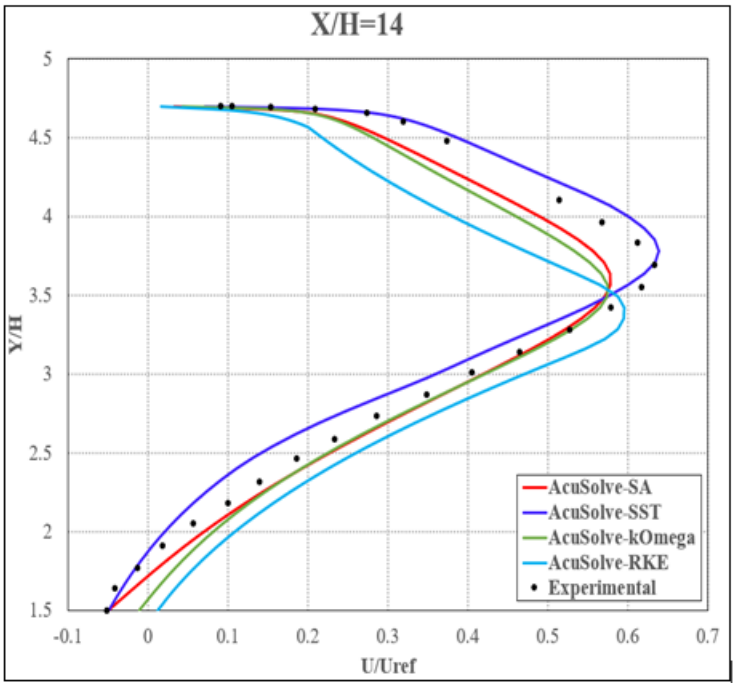


Figure 31: Non-Dimensional Streamwise Velocity Plotted Against Vertical Location Approximately 0.2 m Downstream of the Divergence (X/H = 13.468, Where the Reference Point is 6H Downstream of the Inlet)

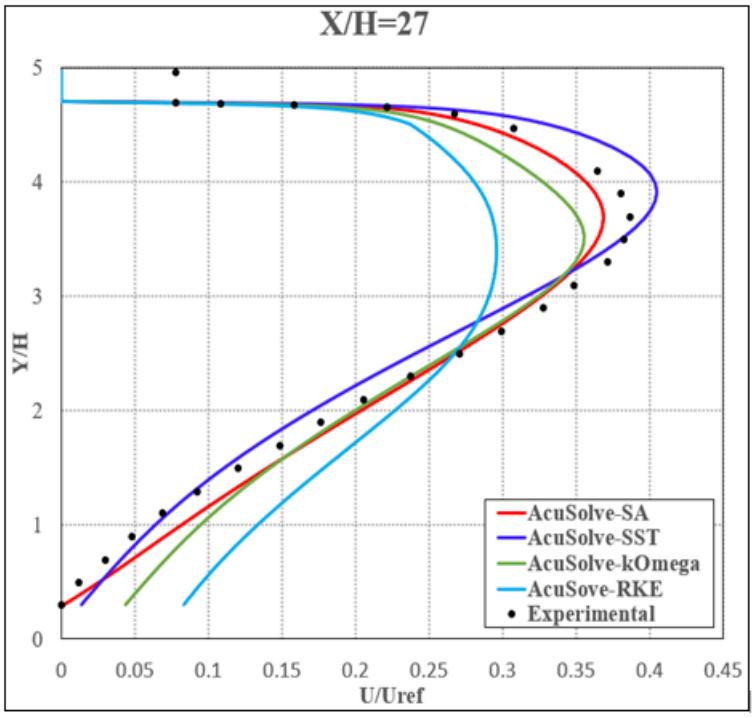


Figure 32: Non-Dimensional Streamwise Velocity Plotted Against Vertical Location Approximately 0.2 m Downstream of the Transition to the Fully Divergent Section (X/H = 27.066, Where the Reference Point is 6H Downstream of the Inlet)

The non-dimensional pressure coefficient (Cp), defined by the integrated inlet pressure and Uref predicted by AcuSolve along the bottom of the diffuser is compared to experimental results. The figure below shows Cp, along a constant vertical height, as a function of the streamwise distance from the inlet of the channel. The results demonstrate that AcuSolve is capable of accurately predicting the pressure within the diffuser within the expected range based on the type of turbulence model used. The performance of the three turbulence models were found to be consistent with previously published results for flow through the diffuser as published by Buice and Eaton (2000), with the SST model predicting the pressure distribution most accurately. Note that the inlet of the experimental duct was 6H longer than that modeled - AcuSolve values where X/H < -6 are reported as the inlet value.

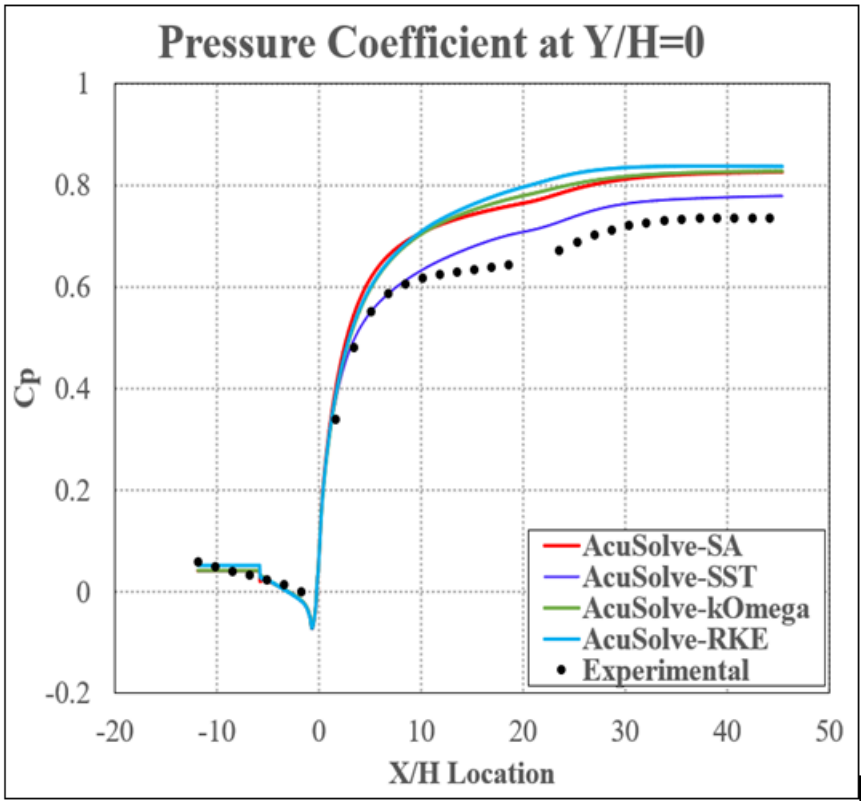


Figure 33: Non-Dimensional Pressure Coefficient (Cp) Plotted Against Relative Distance Along the Diffuser at a Constant Height Equal to the Bottom of the Inlet

Summary

In this application, a fully developed turbulent flow at a Reynolds number of 20,000 is studied. Due to the adverse pressure gradient, separation of flow occurs and causes recirculation in the divergent section of the diffuser. The results were found to be consistent with previously published computational studies and experimental data. The results of this validation demonstrate the ability of AcuSolve to accurately predict the separation point, the recirculation that occurs along the divergent wall, and the reattachment point in the straight section of the diffuser.

Simulation Settings for Turbulent Flow with Separation in an Asymmetric Diffuser

HyperWorks CFD database file: `<your working directory>\asymmetric_diffuser_turbulent\asymmetric_diffuser_turbulent.hm`

Global

- Problem Description
  - Analysis type - Steady State
  - Turbulence equation - Spalart Allmaras
- Auto Solution Strategy
  - Max time steps - `150`
  - Relaxation Factor - `0.2`
- Material Model
  - Air
    - Density - `1.225.0` kg/m3
    - Viscosity - `1.8325e-5` kg/m-sec

  Model
- Volume
  - Volume
    - Element Set
      1. Material model - Air
- Surfaces
  - Bottom
    - Simple Boundary Condition
      1. Type - Wall
  - Inlet
    - Simple Boundary Condition (disabled to allow for nodal boundary conditions to be set)
    - Advanced Options
      1. Nodal Boundary Conditions
         1. X-Velocity
            1. Type - Linear
            2. Precedence - `2`
            3. Curve fit variable - Y coordinate
            4. Curve fit values (included in database)
         2. Y-Velocity
            1. Type - Linear
            2. Precedence - `2`
            3. Curve fit variable - Y coordinate
            4. Curve fit values (included in database)
         3. Eddy Viscosity
            1. Type - Linear
            2. Precedence - `2`

3 Curve fit variable - Y coordinate
4 Curve fit values (included in database)

- Outlet
  - Simple Boundary Condition
    1 Type - Outflow - 101139.0 Pa
- Side 1
  - Simple Boundary Condition
    1 Type - Symmetry
- Side 2
  - Simple Boundary Condition
    1 Type - Symmetry
- Top
  - Simple Boundary Condition
    1 Type - Wall

References

C.U. Buice, and J.K., Eaton. "Experimental Investigation of Flow Through an Asymmetric Plane Diffuser". Journal of Fluids Engineering 122:433-435. June 2000.

S. Obi, K. Aoki and S. Masuda. "Experimental and Computational Study of Turbulent Separating Flow in an Asymmetric Plane Diffuser". Ninth Symposium on Turbulent Shear Flows. p. 305. Kyoto, Japan. August 16-19, 1993.

Turbulent Flow Past a Wall-Mounted Hump

In this application, AcuSolve is used to simulate fully developed turbulent flow past a smooth hump on the lower wall of a flow domain. AcuSolve results are compared with experimental results as described in Seifert and Pack (2002) and on the NASA Langley Research Center Turbulence Modeling Resource web page. The close agreement of AcuSolve results with experimental data and reference turbulence model performance validates the ability of AcuSolve to model cases with turbulent flow moving past a wall protrusion resulting in flow separation and recovery.

Problem Description

The problem consists of a fluid with material properties close to air flowing through a flow domain containing a well-defined smooth hump with a slit opening at approximately 65 percent of the hump chord. The inlet of the domain is defined with an inflow velocity in the streamwise direction that develops into fully turbulent flow at a Reynolds number (Re) of 936,000, based on the hump chord length of 1.0 m. The density of the flow medium is 1.0 kg/m^3 and the dynamic viscosity is 1.0684 X 10^{-6} kg/m-s. The simulation is conducted with the Reynolds Averaged Navier-Stokes equations using the Spalart Allmaras turbulence model, shear stress transport (SST) model, the K-ω model and Realizable K-ε model to evaluate the performance of the turbulence models. The flow predictions from AcuSolve are compared against experimental data and previously published turbulence model performance for pressure and friction coefficients within the domain.

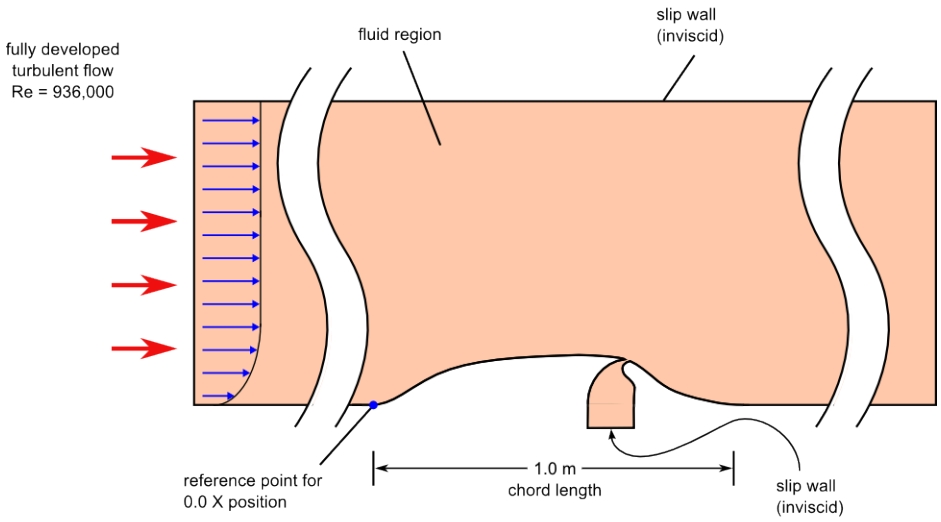


Figure 34: Critical Dimensions and Parameters for Simulating Turbulent Flow Through a Domain with a Wall-Mounted Hump

The upper walls of the domain are specified as slip (inviscid) and the lower walls are specified as no-slip. The inlet velocity and appropriate turbulence parameters are specified in the streamwise direction to match the desired Reynolds Number of 936,000. The outflow pressure is set to zero, and the lower wall on cavity below the hump is set to slip. The problem is simulated as two dimensional with a single layer of elements extruded in the cross stream direction and by defining the side walls as slip.

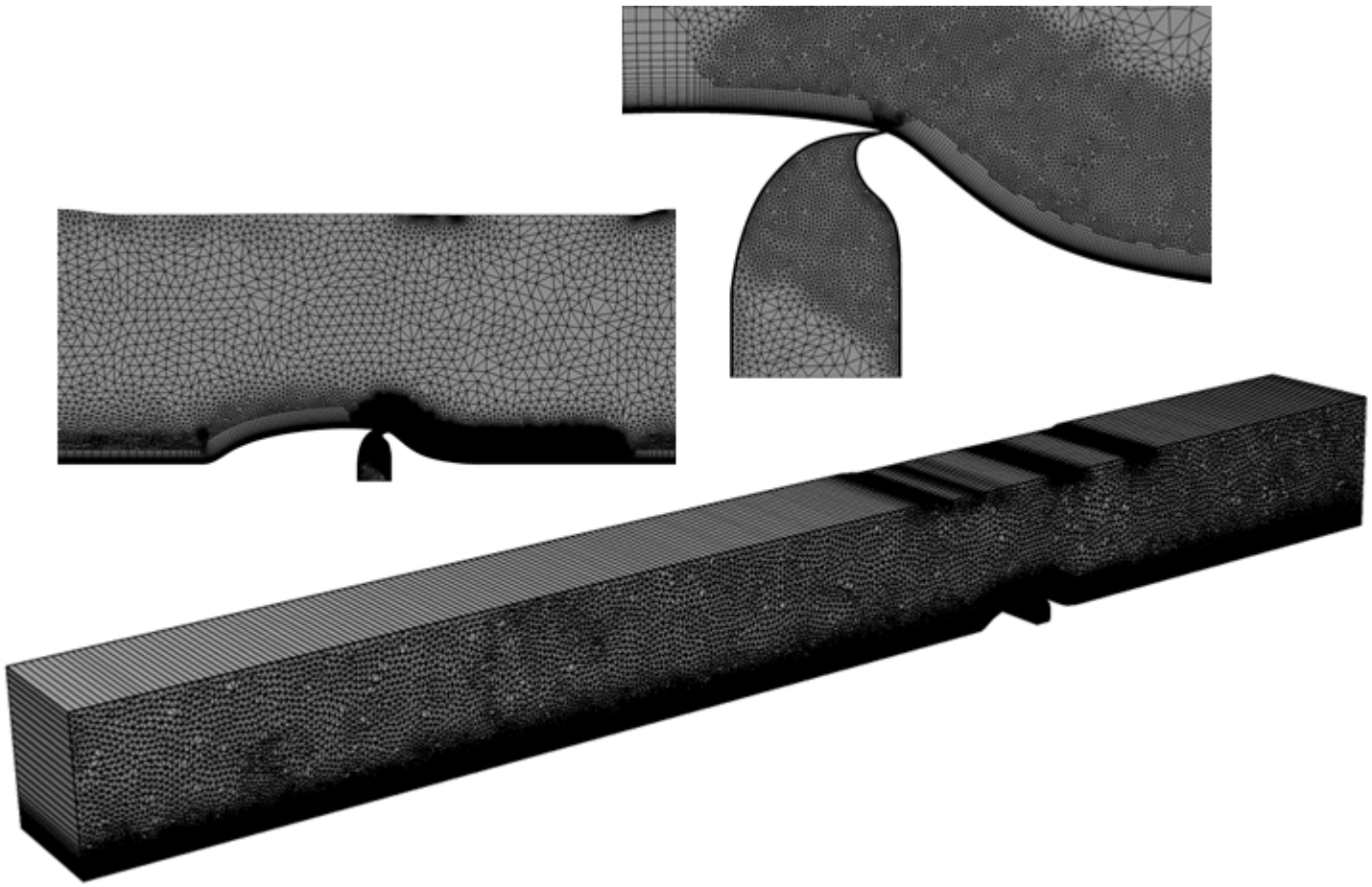


Figure 35: Three Views of the Mesh Used for Simulating Turbulent Flow over a Wall-Mounted Hump (Full Mesh is Shown on the Bottom, with Increased Resolution in Clockwise Views)

AcuSolve Results

The AcuSolve solution converged to a steady state and the results reflect the mean flow conditions within the domain. The images below show contours of velocity within the domain as well as the recirculation region directly downstream of the hump. As the flow enters the domain with a bulk velocity, it begins to develop a turbulent boundary layer near the lower wall prior to reaching the hump. As the flow approaches the hump section, the velocity near the lower wall decreases, but does not recirculate in front of the hump. It then accelerates over the top of the hump and separates immediately after reaching the cavity opening. The recirculation region propagates downstream, before the flow recovers and reattaches to the lower wall.

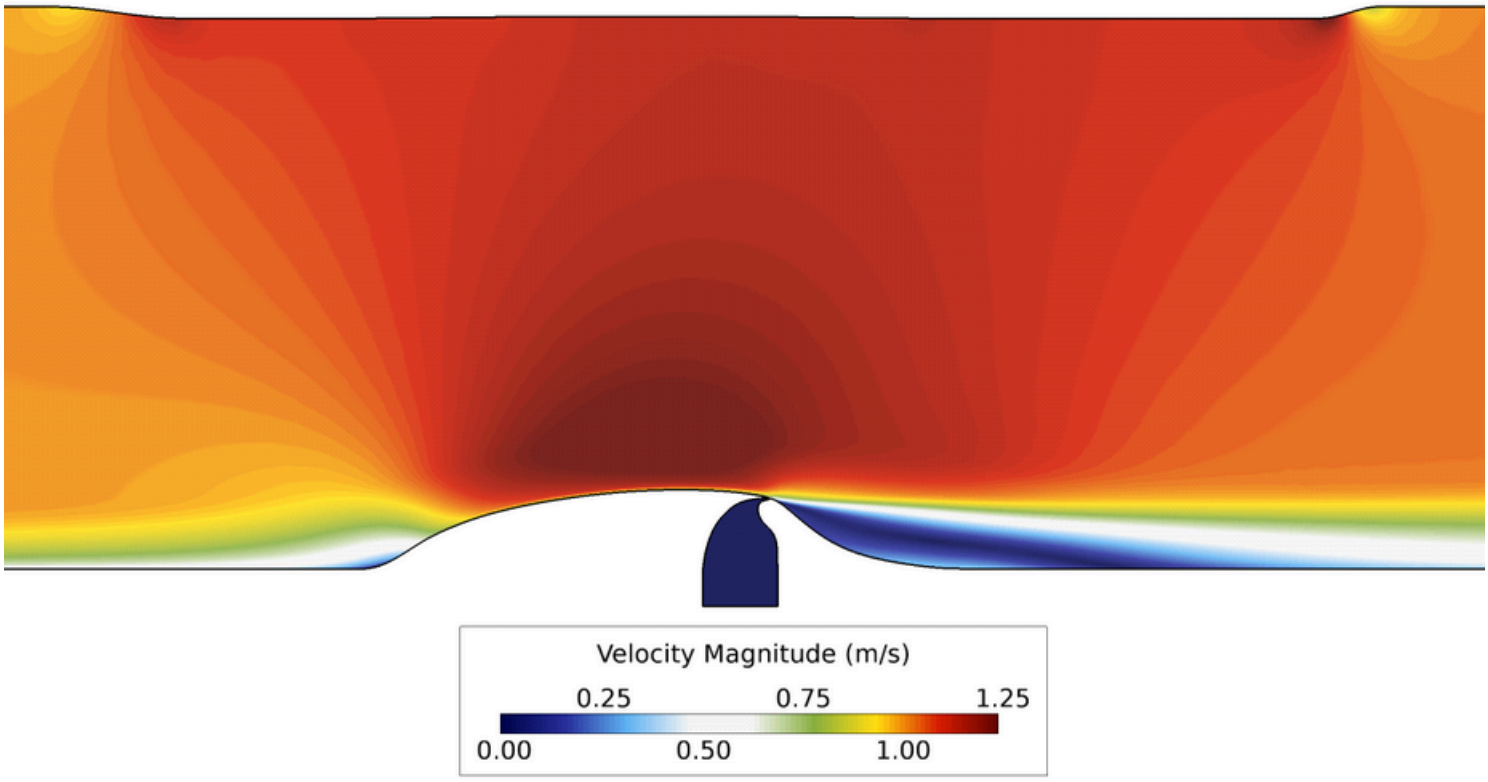


Figure 36: Velocity Contours on the Boundaries of the Domain, Showing Velocity Magnitude

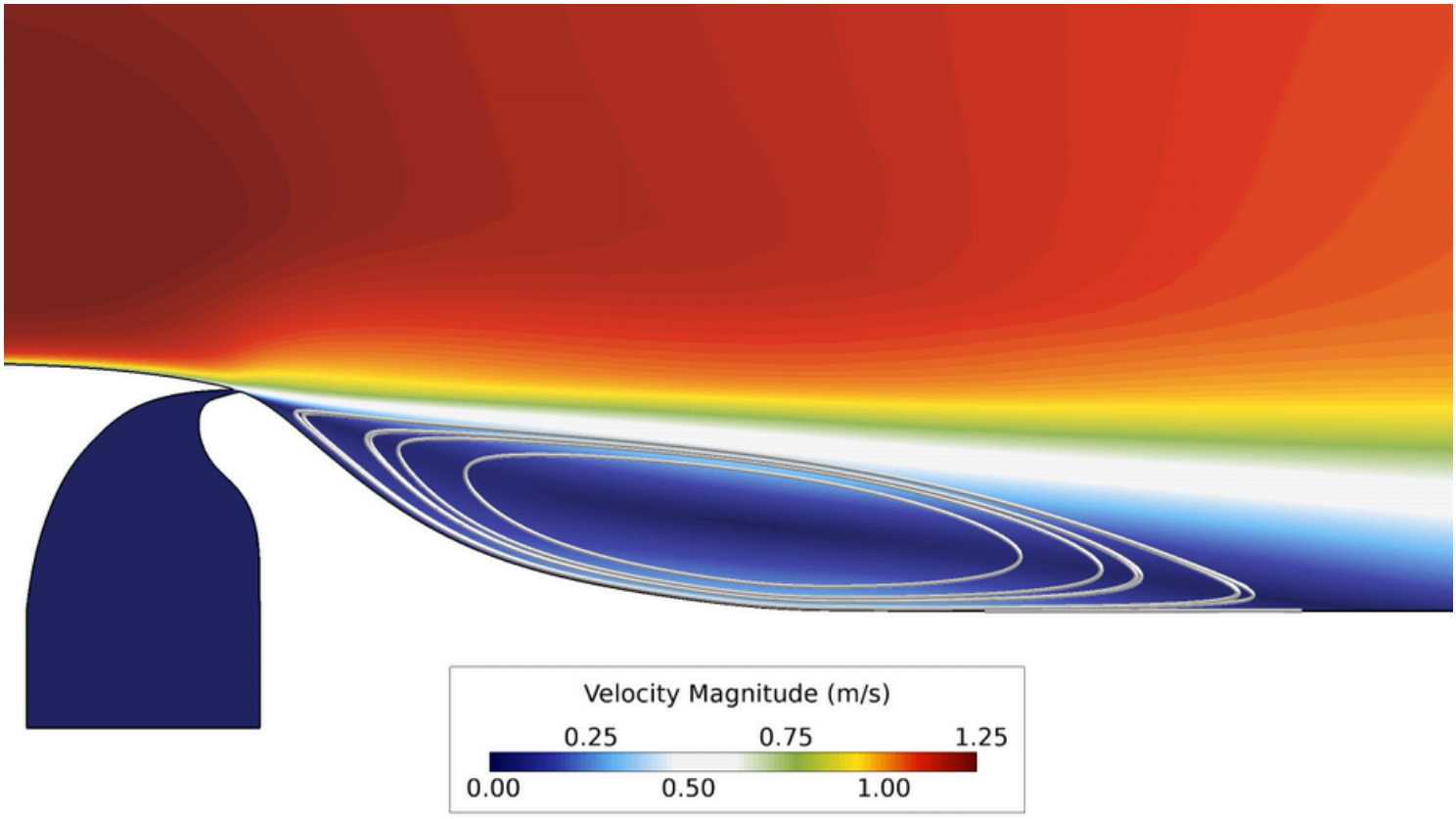


Figure 37: Close up View of Velocity Contours Showing the Recirculation Region with Streamlines (White Lines) Representing the Region of Backflow

The images below show the coefficient of pressure and coefficient of skin friction along the lower wall of the flow domain plotted with experimental results. The non-dimensional values are defined by the integrated inlet pressure and the magnitude of the inlet velocity. The images show black circles representing the experimental measurements (Seifert and Pack 2002), solid red lines for the SA model, solid blue lines for the SST model, solid green lines for the K-ω model and solid cyan lines for the K-ε model, representing the AcuSolve results. The resulting pressure coefficient within the domain demonstrates that there are minor differences between the three turbulence models. All three models are shown to perform accurately in predicting the increase in surface pressure on the front of the hump, but tend to over predict the skin friction in the wake of the hump, leading to an over prediction of the reattachment location. The SA model predicts a slightly larger recirculation region, and does not meet the expected recovery pressure compared to SST, K- ω and K-ε. This performance was found to be consistent with comparisons to other one equation models (NASA 2015).

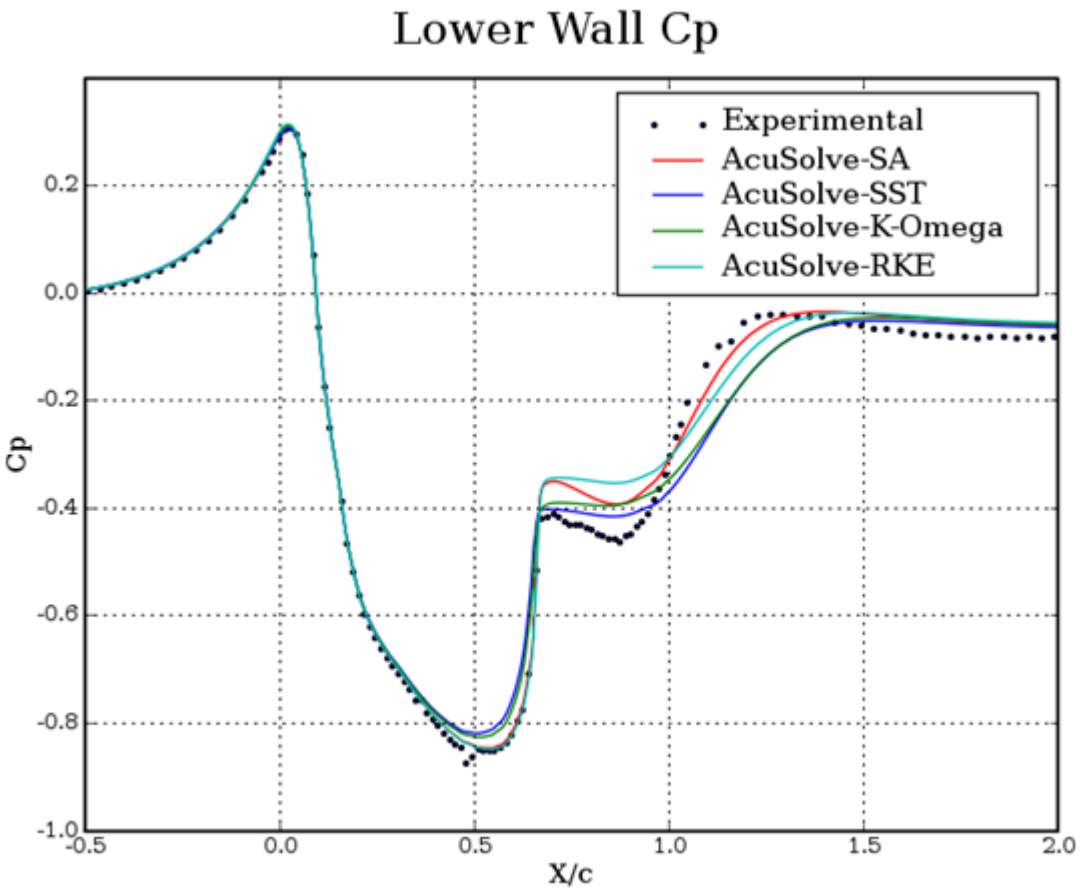


Figure 38: Coefficient of Pressure Along the Lower Wall as the Flow Moves Past the Hump, Where c is the Hump Chord Length and 0.0 is the Reference Location at the Front of the Hump in the X-Direction (Streamwise)

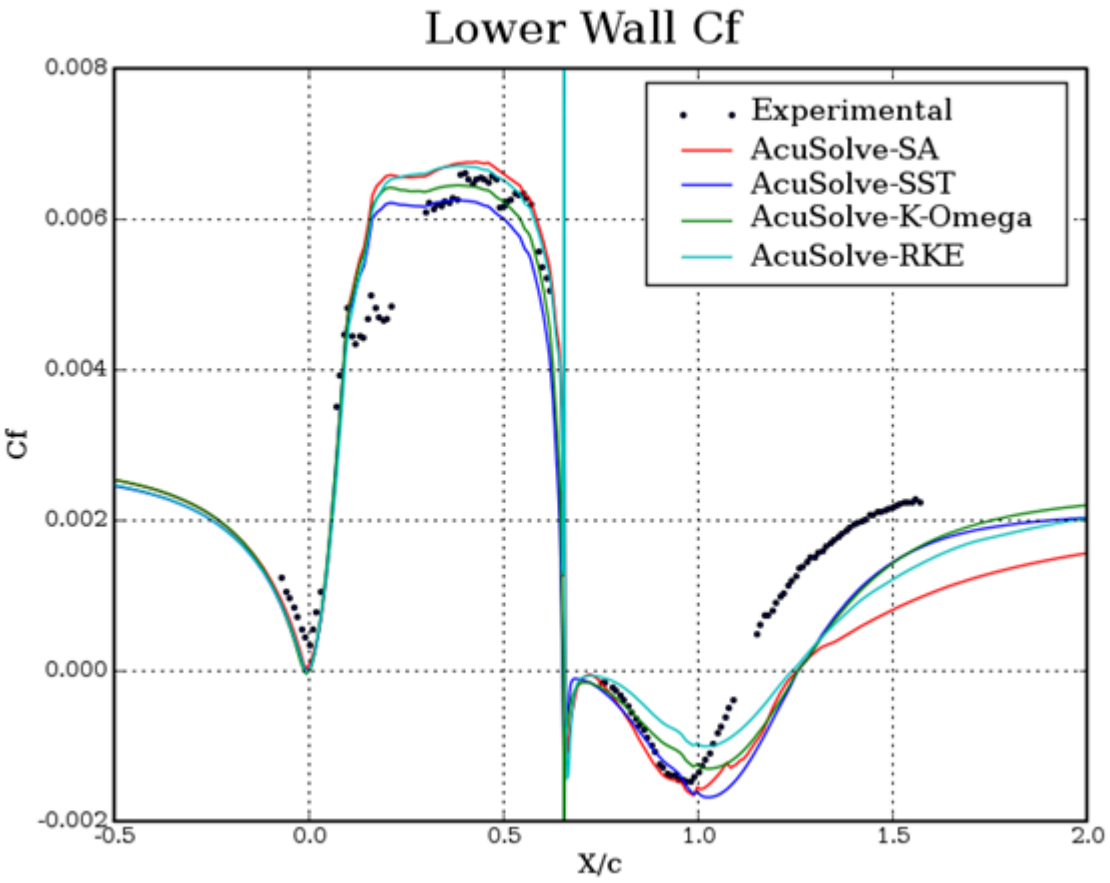


Figure 39: Skin Friction Coefficient Along the Lower Wall as the Flow Moves Past the Hump, Where c is the Hump Chord Length and 0.0 is the Reference Location at the Front of the Hump in the X-Direction (Streamwise)

Summary

In this application, a bulk turbulent flow at a Reynolds number of 936,000 within a flow domain containing a wall-mounted hump is studied and compared against experimental data. The AcuSolve results compare well with the experimental data for pressure coefficient and skin friction coefficient near the hump and downstream. The performance of the three turbulence models were found to be consistent with previously published results for flow over a wall-mounted hump (NASA 2015). For this application, the two equation models appear to outperform the one equation turbulence model, with better agreement for the downstream pressure on the wall. This application demonstrates AcuSolve's ability to predict the distribution of pressure and shear stress on protruding bodies within a turbulent flow field and serves to validate current turbulence modeling capabilities.

Simulation Settings for Turbulent Flow past a Wall-Mounted Hump

AcuConsole database file: `<your working directory>\wall_mounted_hump_turbulent\wall_mounted_hump_turbulent.acs`

Global

- Problem Description

- Analysis type - Steady State
- Turbulence equation - Spalart Allmaras

- Auto Solution Strategy
  - Max time steps - `100`
  - Convergence tolerance - `0.001`
  - Relaxation factor - `0.4`
- Material Model
  - Fluid
    - Density - `1.0` kg/m3
    - Viscosity - `1.0684e-6` kg/m-sec

  Model
- Volumes
  - Fluid
    - Element Set
      1. Material model - Fluid
- Surfaces
  - +Y
    - Simple Boundary Condition
      1. Type - Slip
  - -Y
    - Simple Boundary Condition
      1. Type - Slip
  - Cavity walls
    - Simple Boundary Condition
      1. Type - Wall
      2. Turbulence wall type - Wall Function
  - Hump walls
    - Simple Boundary Condition
      1. Type - Wall
      2. Turbulence wall type - Wall Function
  - Hump walls - downstream
    - Simple Boundary Condition
      1. Type - Wall
      2. Turbulence wall type - Wall Function
  - Inlet
    - Simple Boundary Condition
      1. Type - Inflow

2. Inflow type - Velocity
3. Inflow velocity type - Cartesian
4. X Velocity - `1.0` m/sec
5. Turbulence input type - Direct
6. Eddy viscosity - `3.205128e-6` m2/sec

- Lower slip
  - Simple Boundary Condition
    1. Type - Slip
- Lower wall
  - Simple Boundary Condition
    1. Type - Wall
    2. Turbulence wall type - Wall Function
- Nozzle walls
  - Simple Boundary Condition
    1. Type - Wall
    2. Turbulence wall type - Wall Function

- Outlet
  - Simple Boundary Condition
    - Type - Outflow
- Slip
  - Simple Boundary Condition
    - Type - Slip

References

A Seifert and L.G. Pack. "Active Flow Separation Control on Wall-Mounted Hump at High Reynolds Numbers". AIAA Journal. 40(7). 2002.

NASA Langley Research Center Turbulence Modeling Resource web page. http://turbmodels.larc.nasa.gov/nasahump_val.html. Accessed June 2015.

Turbulent Flow Over a Backward-Facing Step

In this application, AcuSolve is used to simulate fully developed turbulent flow over a backward-facing step. AcuSolve results are compared with experimental results as described in Driver (1985) and on the NASA Langley Research Center Turbulence Modeling Resource web page. The close agreement of AcuSolve results with experimental data and reference turbulence model performance validates the ability of AcuSolve to model cases with turbulent flow that forms a shear layer, recirculates and then reattaches downstream of the divergent step.

Problem Description

The problem consists of a fluid with material properties close to air flowing through a channel containing a sharp expansion, as shown in the following image, which is not drawn to scale. The step causes the flow to recirculate before reattaching downstream of the step. The inlet height of the channel is 8.0 m and expands as a step function to 9.0 m at a distance 20.0 m downstream of the inlet. This expanded section of the channel extends 50 m downstream of the step. The inflow of the channel is defined as fully developed at a Reynolds number (Re) of 36,000, based on the step height to match the experimental conditions. The density of the flow medium is 1.1837 kg/m^3 and the dynamic viscosity is 1.457 X 10^{-3} kg/m-s. The simulation was conducted with the Reynolds Averaged Navier-Stokes equations using four turbulence models, Spalart Allmaras, Shear Stress Transport (SST), K-ω and K-ε.

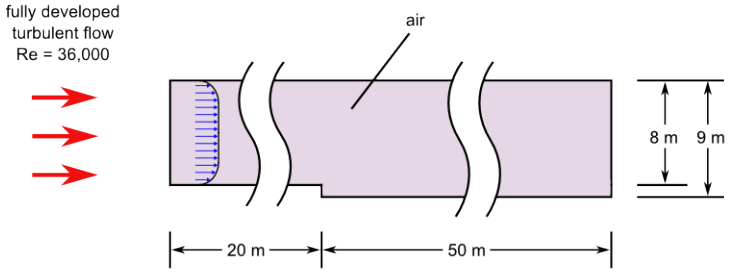


Figure 40: Critical Dimensions and Parameters for Simulating Turbulent Flow Through a Channel with a Backward-Facing Step

The simulation was performed as a two-dimensional problem by constructing a volume mesh that contains a single layer of elements extruded in the cross-stream direction, normal to the flow plane and by imposing symmetry boundary conditions on the extruded planes. The upper and lower walls are specified as no-slip, the inlet velocity and eddy viscosity are specified to match the conditions in the experiment (Driver 1985) at a distance of 20 m upstream of the step.

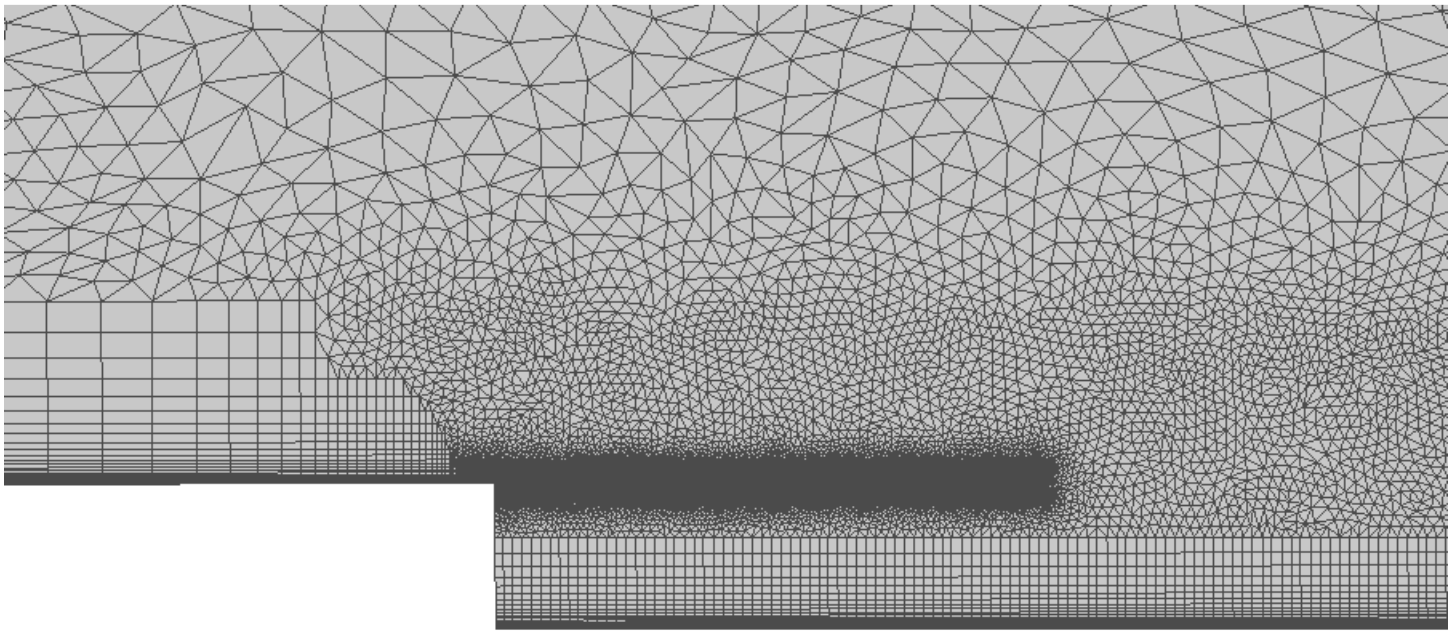


Figure 41: Detail of Mesh Near the Backward-Facing Step

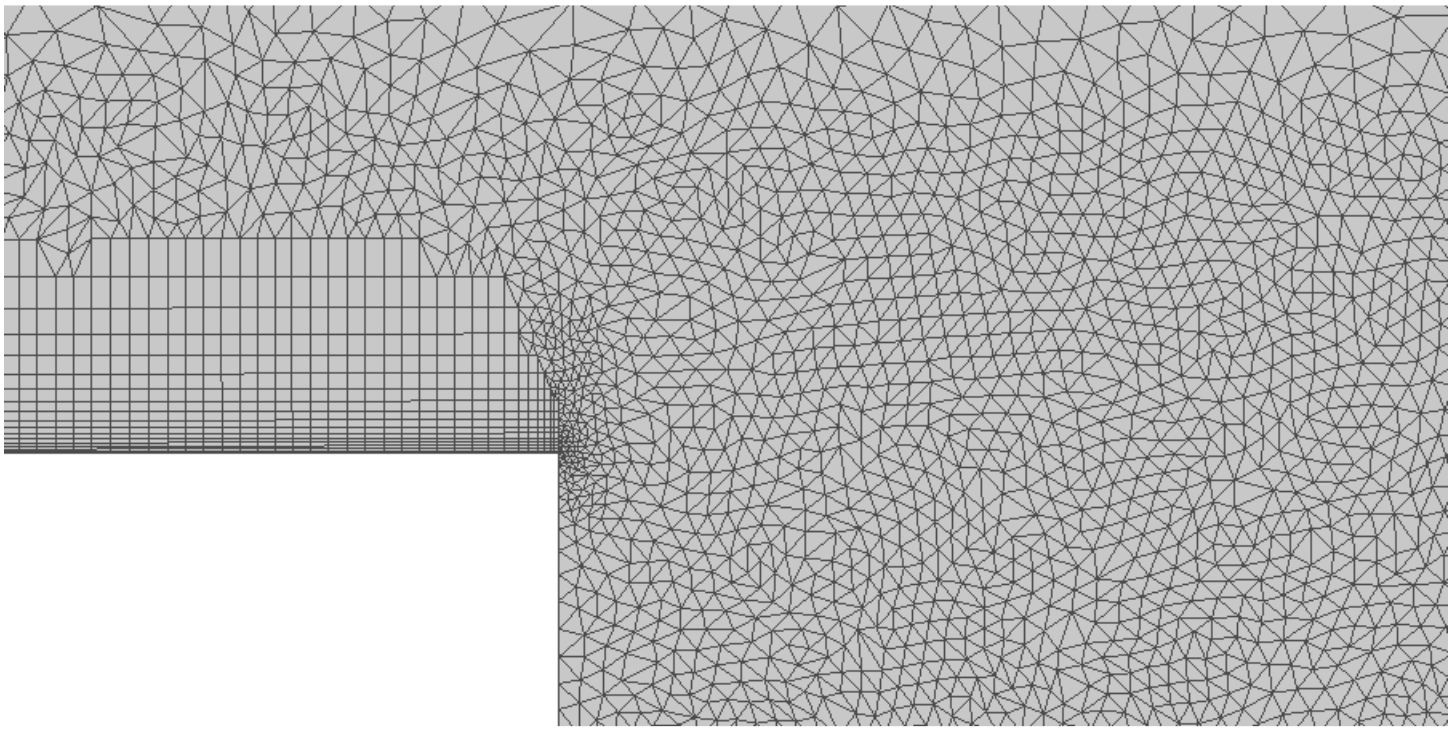


Figure 42: Finer Detail of Mesh Near the Backward-Facing Step

AcuSolve Results

The AcuSolve solution converged to a steady state and the results reflect the mean flow conditions. As the fully developed turbulent flow enters the divergent section, the expansion of the cross-sectional height causes a shear layer to develop above the lower wall. The expansion causes two recirculation zones; one immediately near the step wall and one that extends further downstream near the lower wall. The recirculation region eventually recovers downstream and the flow reattaches. The following images show the flow solution within the channel, demonstrating the recirculation region and reattachment point.

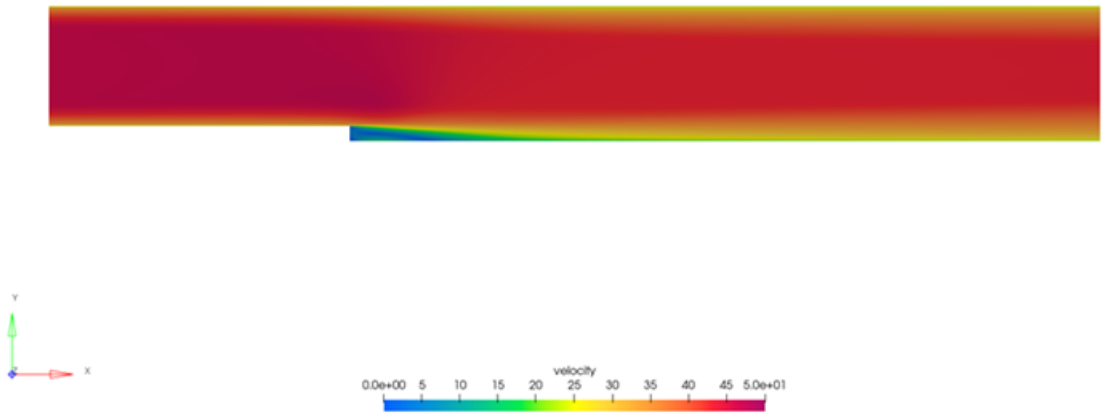


Figure 43: Velocity Contours Showing Low Velocity Near the Step Wall

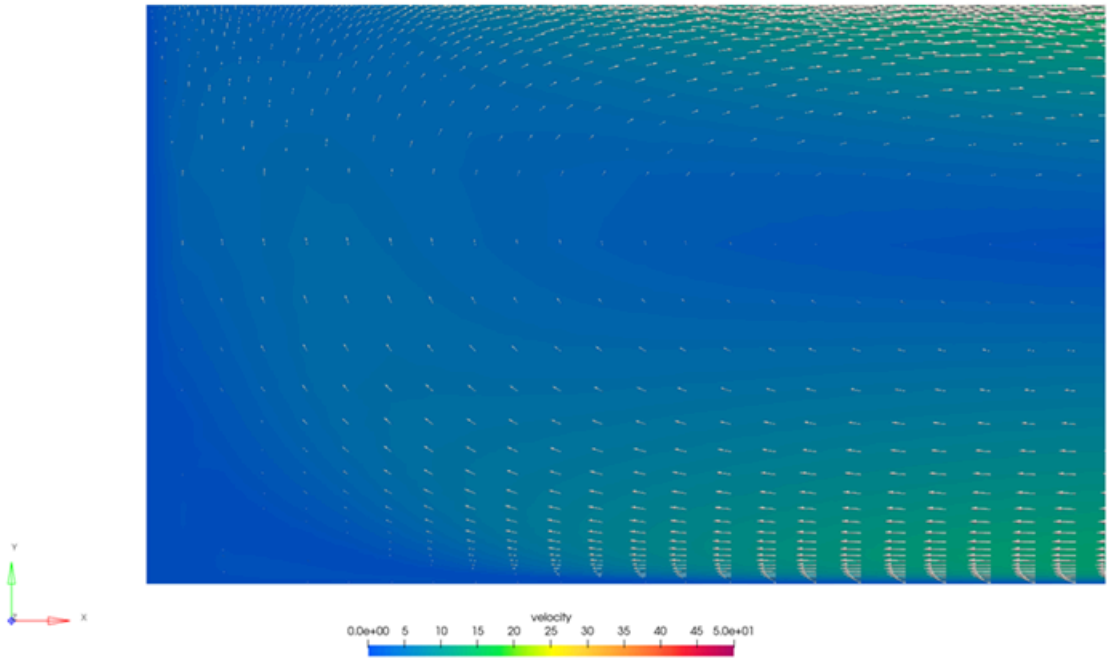


Figure 44: Close-Up View of Velocity Vectors and Contours in the Cross-Stream Plane Directly After the Step

Upstream of the expansion section, the streamwise velocity increases as the distance from the lower wall increases until it reaches the centerline of the channel and then begins decreasing until it reaches zero at the top wall. As the flow passes the step, it expands into the region directly downstream of the step wall, separating from the wall and recirculating until it recovers further downstream. The image below shows the coefficient of pressure along the lower wall of the step compared against experimental results. The non-dimensional values are defined by the integrated inlet pressure and the magnitude of the inlet velocity. The image shows black circles representing the experimental measurements (Driver 1985), a solid red line for the SA model, a solid blue line for the SST model, a solid green line for the K-ω model and a solid cyan line for the K-ε model, representing the AcuSolve results. The resulting pressure coefficient within the channel demonstrates minor differences between the three turbulence models. The SA model predicts a slightly larger recirculation region and does not reach the peak pressure in the wake of the step, compared to the SST model.

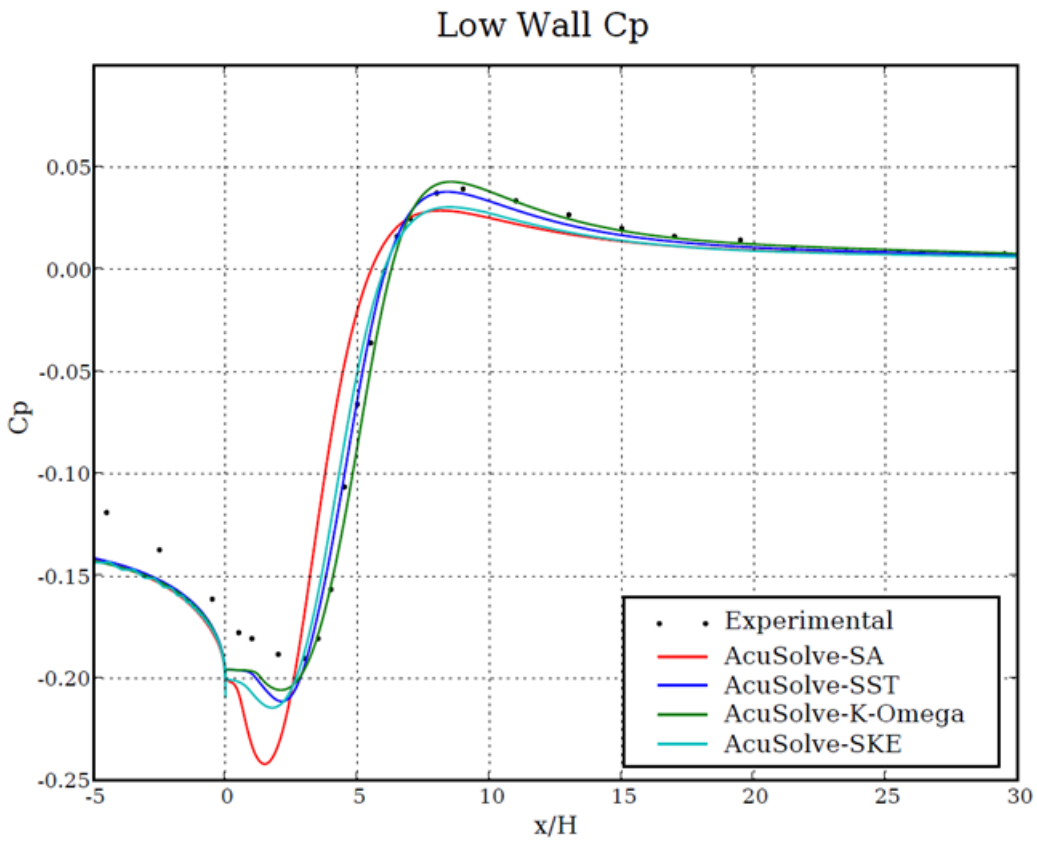


Figure 45: Coefficient of Pressure Plotted Against Location Along the Lower Wall Before and After the Step

Summary

In this application, a fully developed turbulent flow at a Reynolds number of 36,000 is studied and compared against experimental data. The AcuSolve results compare well with the experimental data for pressure coefficient. The performance of the Spalart Allmaras turbulence model was found to be consistent with previously published results for flow over a backward facing step (NASA 2015). The K-ω model appears to perform the best out of the three, predicting the reattachment and pressure distribution most accurately. AcuSolve demonstrates the ability to predict the shear layer in this type of application, the recirculation that occurs downstream of the step, as well as the reattachment point within the channel.

Simulation Settings for Turbulent Flow over a Backward-Facing Step

HyperWorks CFD database file: `<your working directory>\backstep_turbulent\backstep_turbulent.hm`

Global

- Problem Description
  - Analysis type - Steady State
  - Turbulence equation - Shear Stress Transport
- Auto Solution Strategy

    - Max time steps - `100`
    - Relaxation Factor - `0.5`
- Material Model
    - Air
        - Density - `1.183` kg/m3
        - Viscosity - `1.4575e-3` kg/m-sec

  Model
- Volume
    - Fluid
        - Element Set
            1. Material model - Air
- Surfaces
    - +Z
        - Simple Boundary Condition
            1. Type - Slip
    - -Z
        - Simple Boundary Condition
            1. Type - Slip
    - Inlet
        - Simple Boundary Condition - (disabled to allow for nodal boundary conditions to be set)
        - Advanced Options
            1. Nodal Boundary Conditions
                1. X-Velocity
                    1. Type - Linear
                    2. Precedence - Always
                    3. Curve fit variable - Y reference coordinate
                    4. Curve fit values - (included in database)
                2. Y-Velocity
                    1. Type - Linear
                    2. Precedence - Always
                    3. Curve fit variable - Y reference coordinate
                    4. Curve fit values - (included in database)
                3. Z-Velocity
                    1. Type - Zero
                4. Kinetic Energy
                    1. Type - Linear
                    2. Precedence - Always

3 Curve fit variable - Y reference coordinate
4 Curve fit values - (included in database)
5 Eddy Frequency
1 Type - Linear
2 Precedence - Always
3 Curve fit variable - Y reference coordinate
4 Curve fit values - (included in database)

- Outlet
  - Simple Boundary Condition
    1 Type - Outflow
- Wall - Lower - Downstream
  - Simple Boundary Condition
    1 Type - Wall
    2 Turbulence wall type - Low Reynolds Number
- Wall - Lower - Upstream
  - Simple Boundary Condition
    1 Type - Wall
    2 Turbulence wall type - Low Reynolds Number
- Wall - Step
  - Simple Boundary Condition
    1 Type - Wall
    2 Turbulence wall type - Wall Function
- Wall - Upper
  - Simple Boundary Condition
    1 Type - Wall
    2 Turbulence wall type - Low Reynolds Number

References

D. M. Driver and H. L. Seegmiller. "Features of Reattaching Turbulent Shear Layer in Divergent Channel Flow". AIAA Journal, 23(2): 163-171. Feb 1985.

NASA Langley Research Center Turbulence Modeling Resource webpage. http://turbmodels.larc.nasa.gov/backstep_val.html. Accessed June 2021.

Turbulent Flow with Separation in an Axisymmetric Diffuser

In this application, AcuSolve is used to simulate fully developed turbulent flow through an axisymmetric diffuser with a divergent upper wall and a straight lower wall. AcuSolve results are compared with experimental results as described in Driver (1991) and on the NASA Langley Research Center Turbulence Modeling Resource webpage. The close agreement of AcuSolve results with experimental data and reference turbulence model performance validates the ability of AcuSolve to model cases with turbulent flow with separation due to an adverse pressure gradient within an axisymmetric geometry.

Problem Description

The problem consists of a fluid with material properties close to air flowing around a cylinder through an axisymmetric diffuser, as shown in the following image, which is not drawn to scale. The diffuser has a divergent section designed to generate an adverse pressure gradient. The inlet height between the cylinder and the upper section of the diffuser is 0.0355 m. The diffuser is constructed such that the section is axisymmetric around a cylinder with a diameter of 0.14 m. The inflow of the diffuser is set to produce a fully developed turbulent flow profile at a Reynolds number (Re) of 2,000,000. The upper section is modeled with a slip boundary condition, in order to match experimental conditions. The density of the fluid is 1.0 kg/m^3 and with a dynamic viscosity of 1.5 X 10-5 kg/m-s. The simulation was conducted with the Reynolds Averaged Navier-Stokes equations using four turbulence models, Spalart Allmaras, Shear Stress Transport (SST), K-ω and Realizable K-ε.

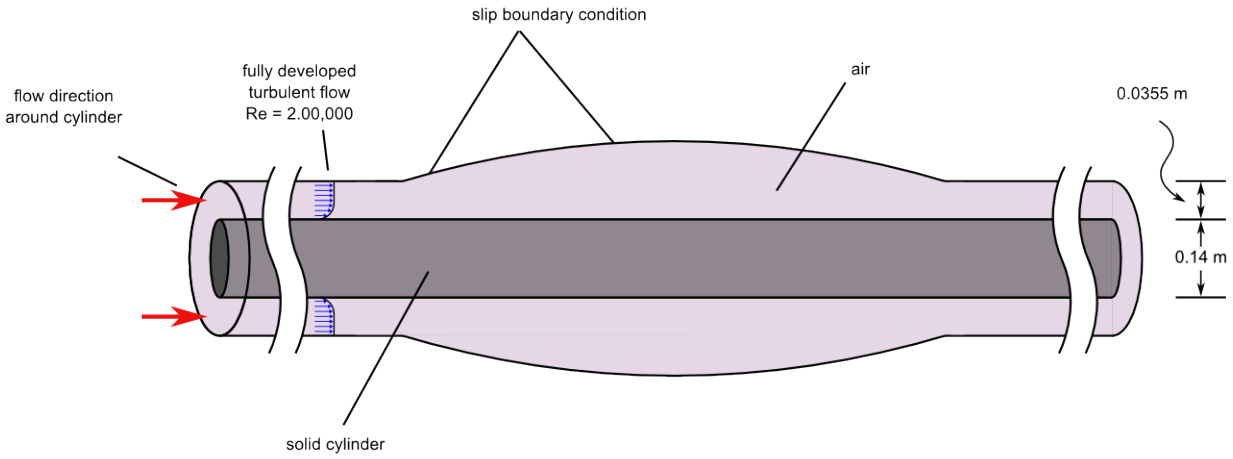


Figure 46: Critical Dimensions and Parameters for Simulating Turbulent Flow Through an Axisymmetric Diffuser

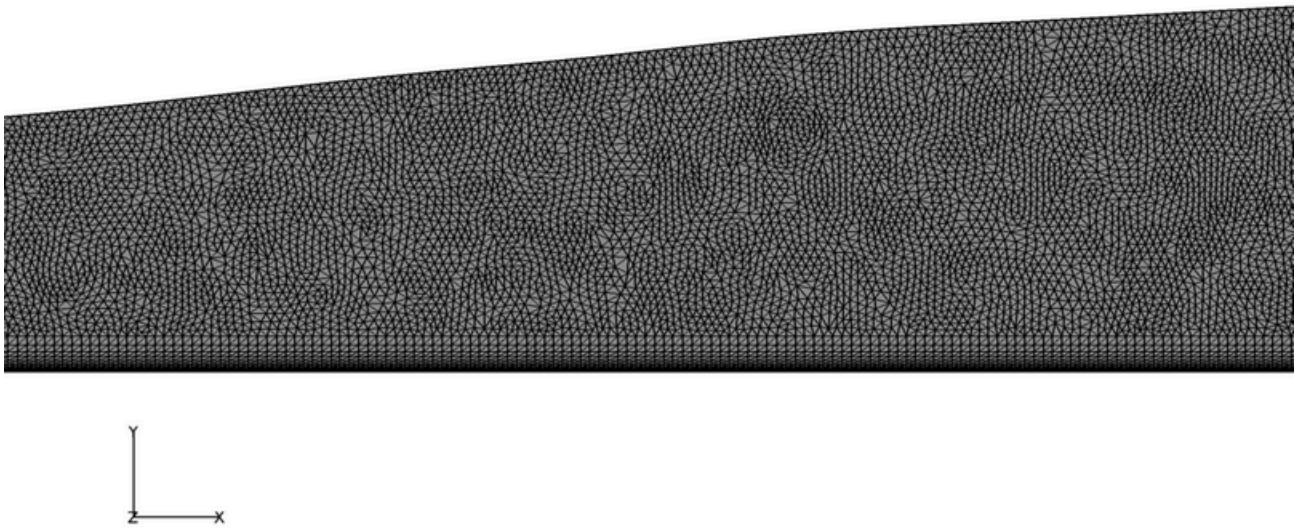


Figure 47: Mesh Detail Near the Divergence of the Walls in the Mesh used for Simulating Turbulent Flow Through an Axisymmetric Diffuser

The problem is simulated as axisymmetric by considering a 1 degree portion of the diffuser with the axisymmetric boundary condition applied on the cross-stream surfaces. The mesh elements were extruded in the axisymmetric direction to create a mesh with two elements spanning the simulated section.



Figure 48: Cross Section (Perpendicular to Flow) of Mesh used for Simulating Turbulent Flow Through an Axisymmetric Diffuser

AcuSolve Results

The AcuSolve solution converged to a steady state and the results reflect the mean flow conditions. As the fully developed turbulent flow enters the divergent section, the expansion of the cross-sectional height causes the streamwise velocity to decrease. This causes separation of the flow along the cylinder wall and results in an area of recirculation that eventually recovers downstream. After the flow enters the diffuser, the velocity decreases significantly from the inlet velocity, due to the rapid expansion of the cross section height in the divergent section. A separation bubble forms within the diffuser, with decreased flow velocity and increased pressure near the lower wall.

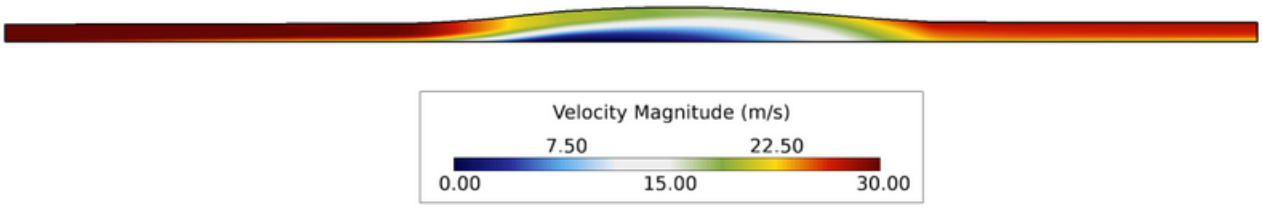


Figure 49: Velocity Contours Within the Diffuser

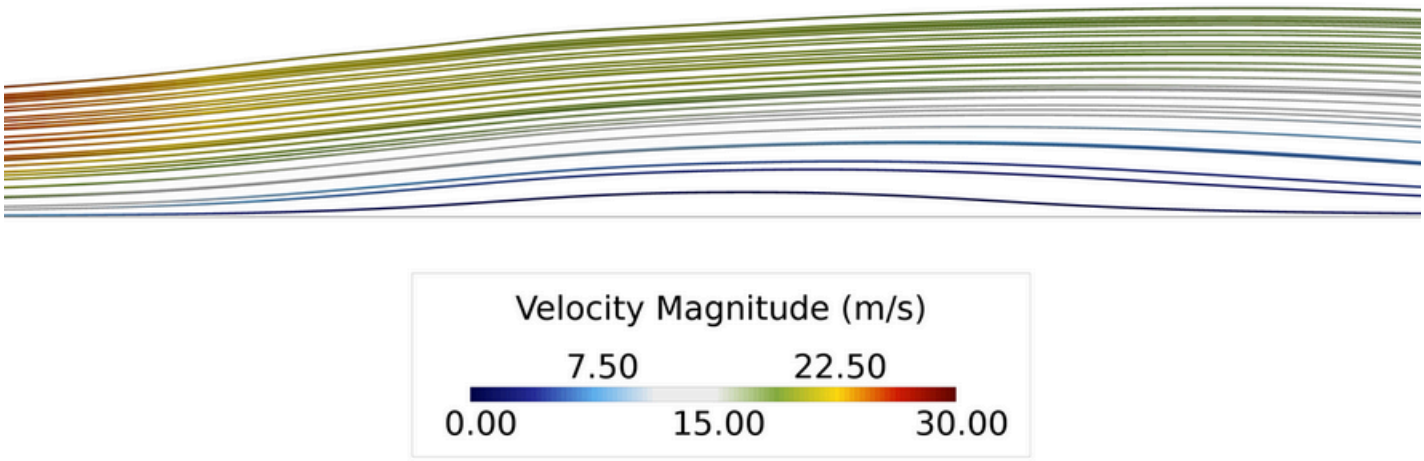


Figure 50:

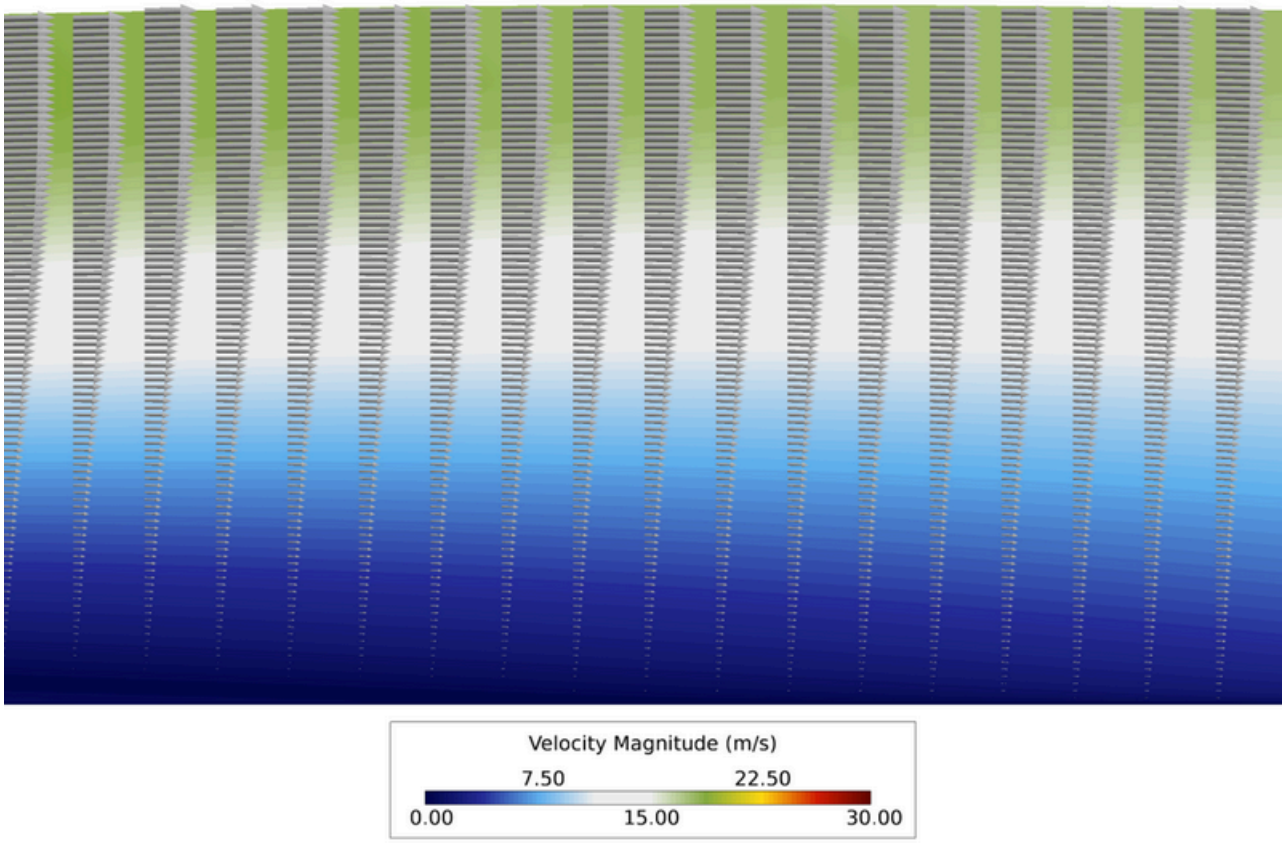


Figure 51: Close up View of Velocity Vectors and Contours in the Streamwise Plane Near the Reattachment Point

Upstream of the diffuser section, the streamwise velocity increases as the distance from the cylinder wall increases, with no influence from the top wall of the diffuser. As the flow enters into the divergent section, the streamwise velocity decreases near the cylinder wall and changes direction in the

recirculation region. Within the recirculation region, the reduced speed of the streamwise flow causes the wall shear stress to decrease and eventually change direction for a short distance along the cylinder surface. The images below show the coefficient of pressure (Cp) and coefficient of skin friction (Cf) along the cylinder wall in the diffuser compared against experimental results. The non-dimensional values are defined by the integrated inlet pressure and the magnitude of the inlet velocity. In the images black circles represent the experimental measurements (Driver 1991), solid red lines represent the prediction for the SA model, solid blue lines represent the prediction for the SST model, solid green lines represent the prediction for the K-ω model and solid cyan lines for the K-ε model, representing the AcuSolve results. There are minor differences in the prediction of the pressure coefficient within the diffuser between the three turbulence models. The SA model predicts a slightly higher value of pressure as the flow separates from the cylinder wall compared to both SST and K- ω. The shearing on the cylinder wall shows similar behavior, with the SA model predicting a slightly longer recirculation region and with the K- ω model predicting the separation further upstream. It was found that all three turbulence models predict the separation point further upstream than what is shown in the experiment. This is shown to be consistent with previous studies for each of the turbulence models used (NASA 2014).

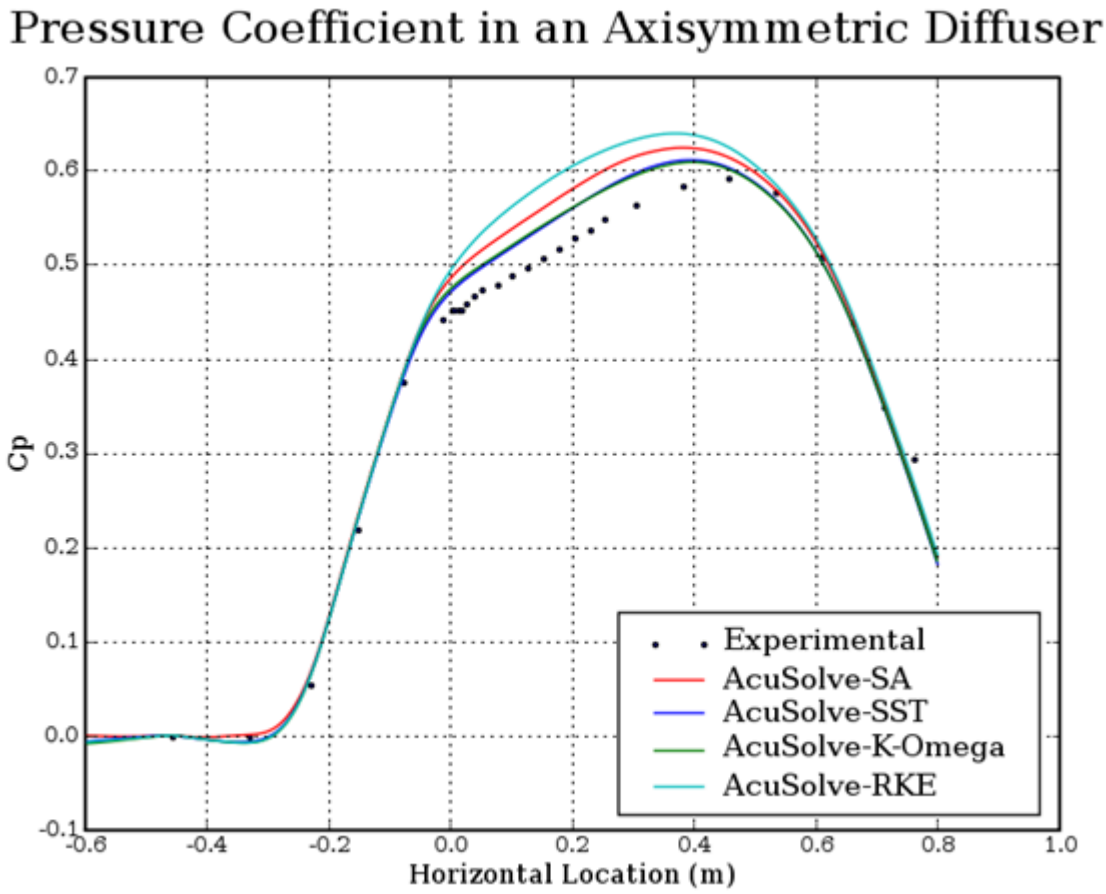


Figure 52: Coefficient of Pressure Along the Cylinder Wall Within the Diffuser Section (Horizontal Location = ~ 2.7m at the Midpoint of the Expanded Region of the Diffuser)

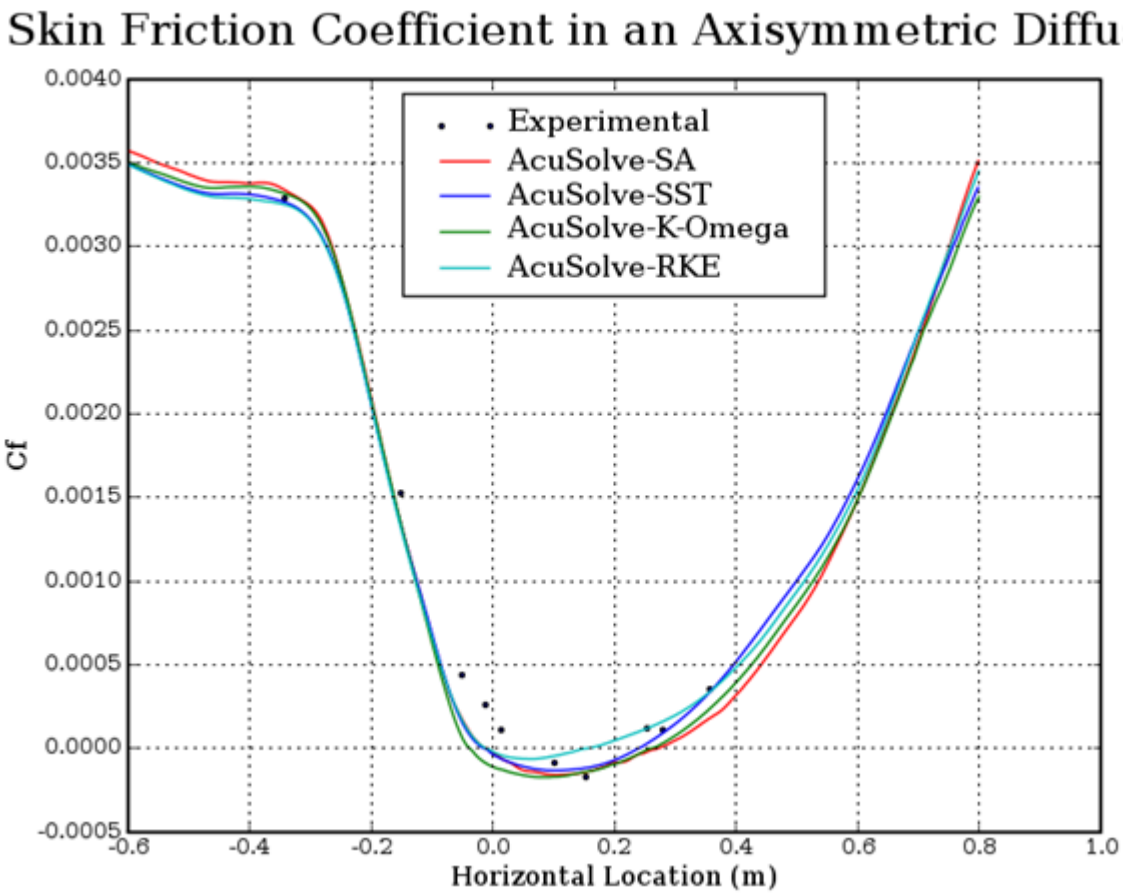


Figure 53: Skin Friction Coefficient Along the Cylinder Wall Within the Diffuser Section (Horizontal Location = 0 at the Point Where Flow Separation is Expected to Begin)

Summary

In this application, a fully developed turbulent flow at a Reynolds number of 2,000,000 is studied and compared against experimental data. The AcuSolve results compare well with the experimental data for pressure coefficient and skin friction coefficient. The recirculation region is slightly over predicted by the turbulence models studied, but the results still show a reasonable trend compared to experimental results. The performance of the three turbulence models was found to be consistent with previously published results for flow within an axisymmetric diffuser (NASA 2014). The results of this validation demonstrate the ability of AcuSolve to accurately predict flow recirculation with axisymmetric boundary conditions.

Simulation Settings for Turbulent Flow with Separation in an Axisymmetric Diffuser

AcuConsole database file: `<your working directory>\axisymmetric_diffuser_turbulent\axisymmetric_diffuser_turbulent.acs`

Global

- Problem Description
  - Analysis type - Steady State

    - Turbulence equation - Spalart Allmaras
- Auto Solution Strategy
    - Max time steps - `150`
    - Relaxation Factor - `0.4`
- Material Model
    - Fluid
        - Density - `1.0` kg/m3
        - Viscosity - `1.5e-5` kg/m-sec

  Model
- Volume
    - Fluid
        - Element Set
            1. Material model - Fluid
- Surfaces
    - Axisymmetric_maxZ
        - Simple Boundary Condition - (disabled to allow for periodic conditions to be set)
    - Axisymmetric_minZ
        - Simple Boundary Condition - (disabled to allow for periodic conditions to be set)
    - Inlet
        - Simple Boundary Condition
            1. Type - Inflow
            2. Inflow type - Velocity
            3. X velocity - `30.0` m/sec
            4. Turbulence input type - Direct
            5. Eddy viscosity - `1.5e-5` m2/sec
    - Outlet
        - Simple Boundary Condition
            1. Type - Outflow
    - Slip_maxY
        - Simple Boundary Condition
            1. Type - Slip
    - Wall_minY
        - Simple Boundary Condition
            1. Type - Wall
- Periodics
    - Axisymmetric
        - Periodic Boundary Condition

1 Type - Axisymmetric
2 Rotation Axis
    1 Point 1
        1 x-coordinate - `1.4` m
        2 y-coordinate - `0.0` m
        3 z-coordinate - `0.0` m
    2 Point 2
        1 x-coordinate - `-1.5` m
        2 y-coordinate - `0.0` m
        3 z-coordinate - `0.0` m

References

D. M. Driver. "Reynolds Shear Stress Measurements in a Separated Boundary Layer Flow". AIAA Paper 91-1787 from the AIAA 22nd Fluid Dynamics, Plasma Dynamics, and Lasers Conference. Honolulu, HI. June 1991.

NASA Langley Research Center Turbulence Modeling Resource webpage, http://turbmodels.larc.nasa.gov/driver_val.html. Accessed December 2014.

Turbulent Flow Past a Convex Curve in a Channel

In this application, AcuSolve is used to simulate fully developed turbulent flow through a channel containing a convex curve in the lower wall. AcuSolve results are compared with experimental results as described in Smits (1979) and on the NASA Langley Research Center Turbulence Modeling Resource webpage. The close agreement of AcuSolve results with experimental data and reference turbulence model performance validates the ability of AcuSolve to model cases with turbulent flow moving past a convex curved wall.

Problem Description

The problem consists of a fluid with material properties close to air flowing through a channel containing a 30° swept wall, with a lower convex wall. The inlet channel height and remaining duct height is 0.127 m. The bulk velocity (v) normal to the inlet is 31.9 m/s and an integrated outflow pressure is specified to allow the flow to pass through the channel. The flow develops into fully turbulent flow at a Reynolds's number (Re) of 2,100,000. The density of the flow medium is 1.225 kg/m3 and the dynamic viscosity is 1.8608 X 10-5 kg/m-s. The simulation is conducted with the Reynolds Averaged Navier-Stokes equations using the Spalart Allmaras, Shear Stress Transport (SST), K-ω and Realizable K-ε turbulence models. The flow conditions are compared against experimental data and the current state-of-the-art performance for coefficient of pressure and coefficient of friction.

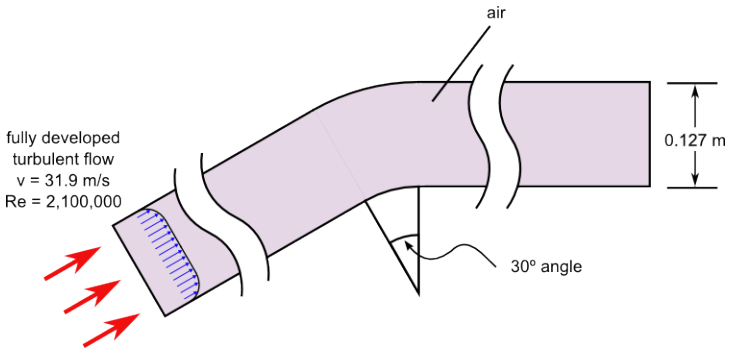


Figure 54: Critical Dimensions and Parameters for Simulating Turbulent Flow Through a Convex Channel

The simulation was performed as a two dimensional problem by restricting flow in the out-of-plane direction through the use of a mesh that is one element thick. The upper and lower walls are specified as no-slip, the inlet velocity and eddy viscosity are specified normal to the inlet face to match the experimental Reynolds Number.

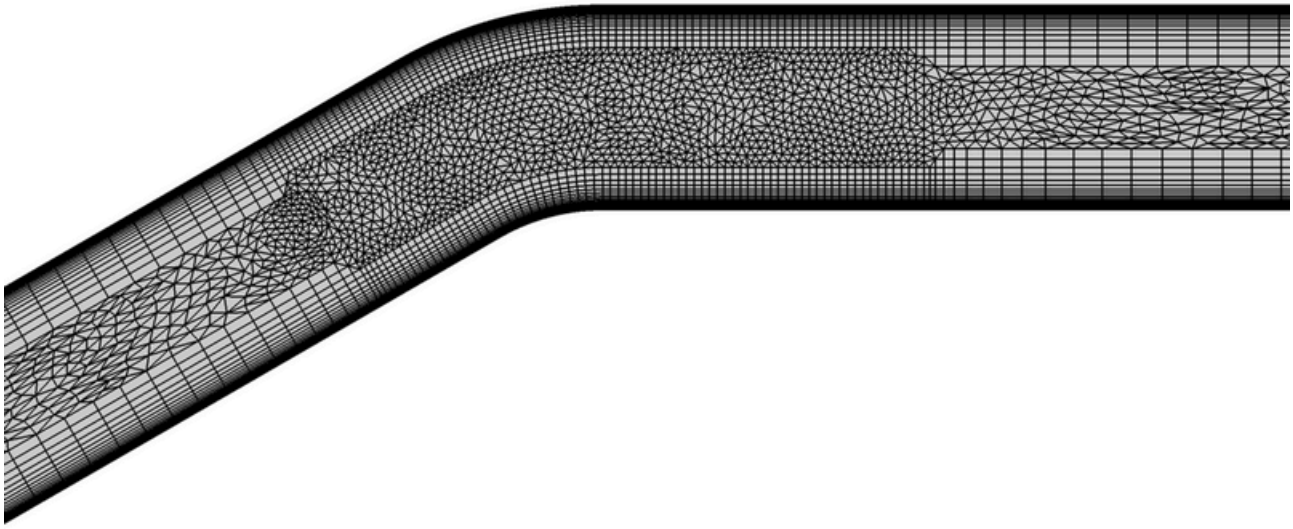


Figure 55: Detail of the Mesh used for Simulating Turbulent Flow Through a Convex Channel

AcuSolve Results

The AcuSolve solution converged to a steady state and the results reflect the mean flow conditions within the channel. As the fluid enters the channel it develops into fully turbulent flow exhibiting a steep parabolic velocity profile across the width of the channel. The flow begins to accelerate near the lower wall and decelerate near the top wall as it approaches the 30° bend. The results show that the upper (concave) wall destabilizes the boundary layer, increasing the eddy viscosity and forcing the flow velocity to decrease. The following figures show the flow conditions within the channel.

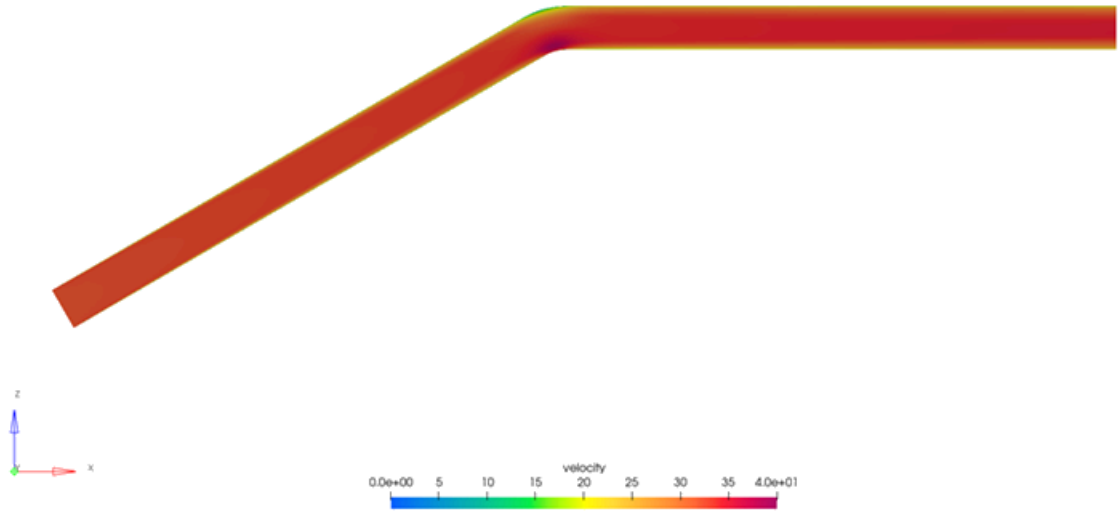


Figure 56: Velocity Contours in the Streamwise Plane

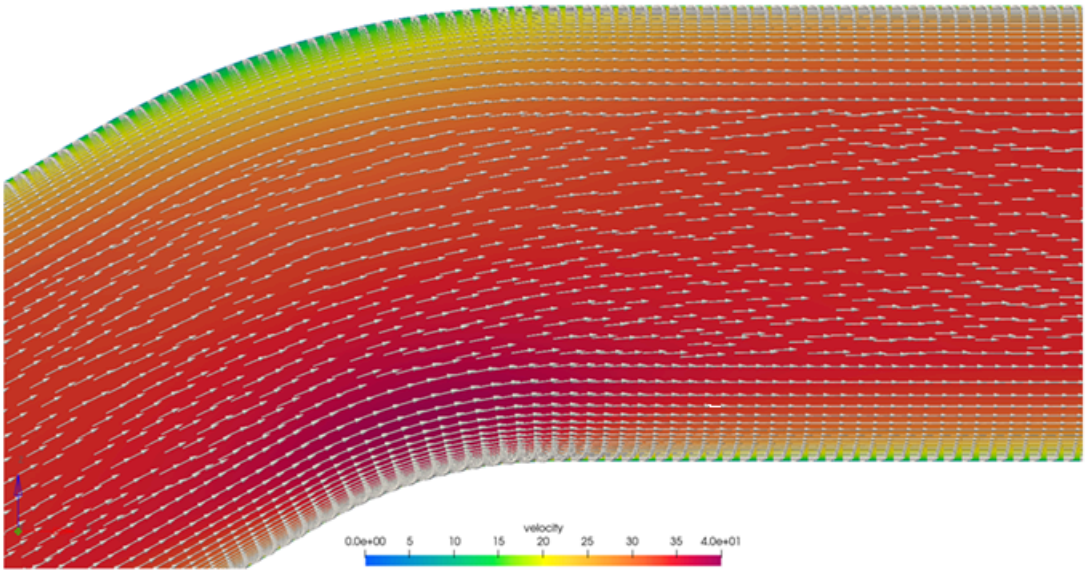


Figure 57: Close up View of Velocity Vectors and Velocity Contours at the 30° Bend

Upstream of the curved section of the channel, the flow normal to the channel opening increases as the distance from the lower wall increases until it reaches the centerline of the channel and then begins decreasing until it reaches zero at the top wall. As the flow approaches the curved section, it begins to accelerate, requiring that the flow velocity near the upper wall decrease to conserve momentum. The relatively low angle of curvature in the channel does not cause the accelerated fluid to recirculate. The images below show the coefficient of pressure (Cp) and coefficient of skin friction (Cf) along the lower wall of the channel. The images show black circles representing the experimental measurements (Smiths 1979), solid red lines for the SA model, solid blue lines for the SST model, solid green lines for the K-ω model and a solid cyan line for the K-ε model, representing the AcuSolve results. The coefficient of pressure within the channel is predicted nearly identically compared to the experiment for each of the turbulence models. It appears that the SST and K-ε models capture the low velocity region with the best accuracy, demonstrating that the flow velocity decreases significantly, but does not recirculate within the channel. This is shown in the friction coefficient plot, where the coefficient of friction, and subsequently the wall shear stress, does not decrease below zero.

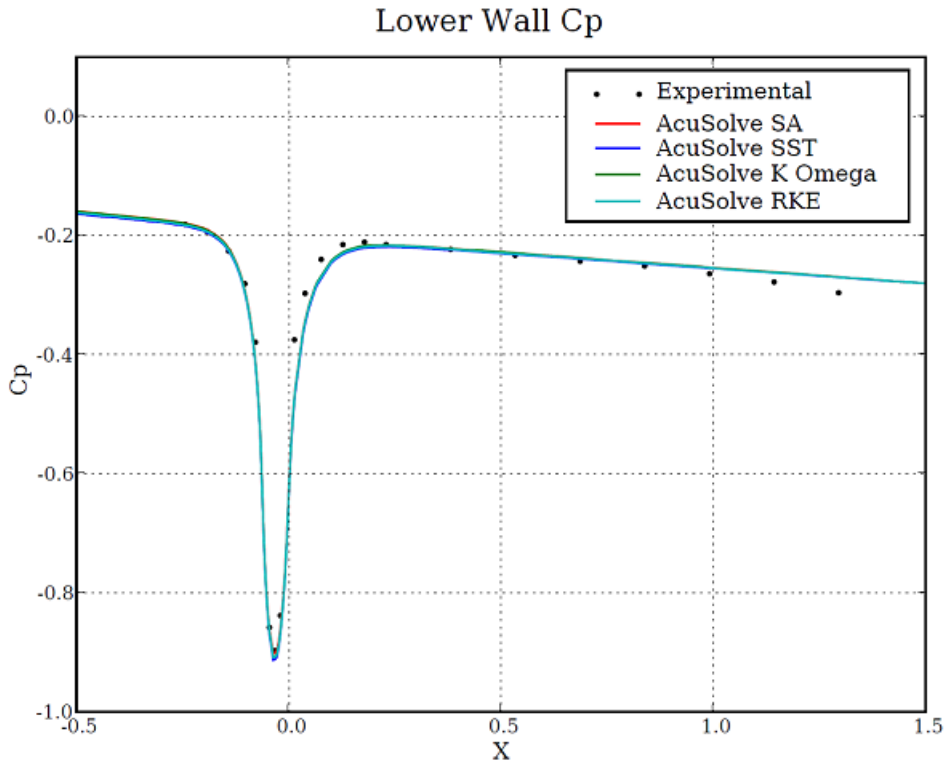


Figure 58: Coefficient of Pressure Plotted Against Relative Distance Along the Lower Wall from the Curve

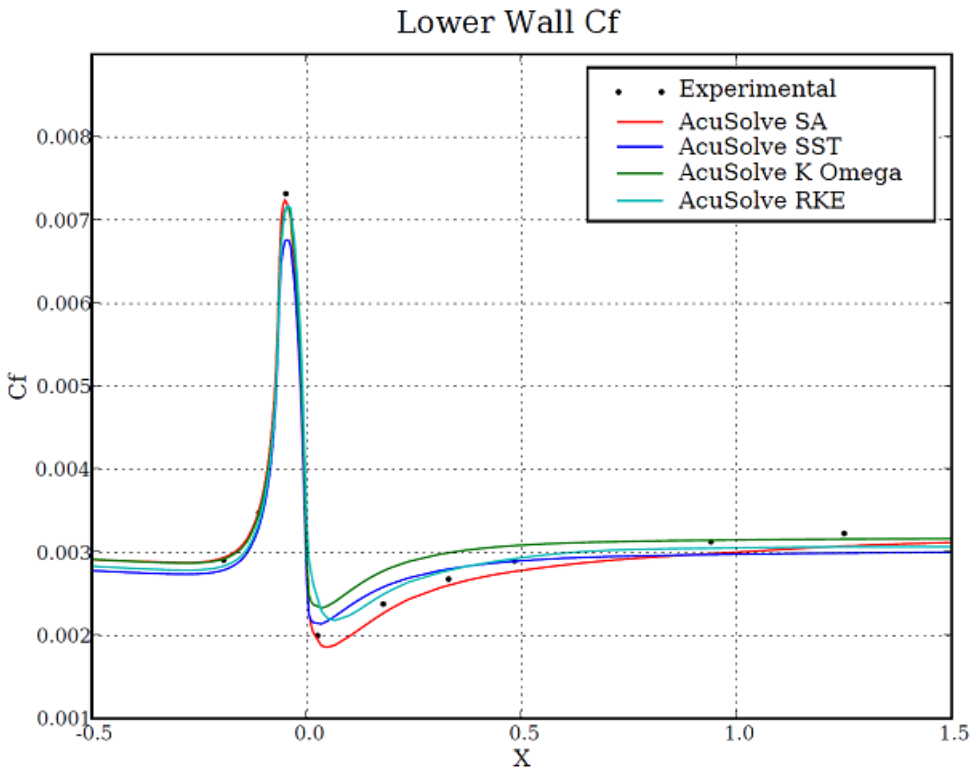


Figure 59: Skin Friction Coefficient Plotted Against Relative Distance Along the Lower Wall from the Curve

Summary

In this application, a turbulent flow through a curved channel at a Reynolds number of 2,100,000 is simulated and compared against experimental data. The AcuSolve results compare well with the experimental data for pressure coefficient and skin friction coefficient within the channel. The performance of the Spalart Allmaras turbulence model was found to be consistent with previously published results for flow through a convex-curved channel (NASA 2015) and the SST turbulence model appears to predict the shear stress on the lower wall most accurately. AcuSolve demonstrates the ability to predict the complex boundary layers resulting from the curvature of the channel and accurately predicts the propagation of the flow further downstream.

Simulation Settings for Turbulent Flow past a Convex Curve in a Channel

HyperWorks CFD database file: `<your working directory>\convex_curvature_turbulent \convex_curvature_turbulent.hm`

Global

- Problem Description
  - Analysis type - Steady State
  - Turbulence equation - Spalart Allmaras
- Auto Solution Strategy
  - Max time steps - `100`
  - Convergence tolerance - `0.0001`

    - Relaxation factor - `0.4`
- Material Model
    - Fluid
        - Density - `1.225` kg/m3
        - Viscosity - `1.8603e-5` kg/m-sec

  Model
- Volumes
    - Fluid - elbow
        - Element Set
            1. Material model - Fluid
    - Fluid - inlet
        - Element Set
            1. Material model - Fluid
    - Fluid - outlet
        - Element Set
            1. Material model - Fluid
- Surfaces
    - -Y
        - Simple Boundary Condition
            1. Type - Slip
    - +Y
        - 1. Type - Slip
    - Inlet
        - Simple Boundary Condition
            1. Type - Inflow
            2. Inflow type - Velocity
            3. Inflow velocity type - Normal
            4. Normal velocity - `31.9` m/sec
            5. Turbulence input type - Direct
            6. Eddy viscosity - `1.3671e-7` m2/sec
- Internal
    - Simple Boundary Condition - (disabled)
- Lower Wall
    - Simple Boundary Condition
        - Type - Wall
        - Turbulence wall type - Low Reynolds Number
- Outlet

    - Simple Boundary Condition
        - Type - Outflow
- Upper Wall
    - Simple Boundary Condition
        - Type - Wall
        - Turbulence wall type - Low Reynolds Number

References

A. J. Smits, S. T. B. Young, and P. Bradshaw. "The Effect of Short Regions of High Surface Curvature on Turbulent Boundary Layers". Journal of Fluid Mechanics. 94(2):209-242. 1979

NASA Langley Research Center Turbulence Modeling Resource webpage. http://turbmodels.larc.nasa.gov/smitscurve_val.html. Accessed May 2021.

Turbulent Natural Convection Inside a Tall Cavity

In this application, AcuSolve is used to simulate the natural convection of a turbulent flow field within a tall rectangular cavity. AcuSolve results are compared with experimental results as described in Betts and Bokhari (2000). The close agreement of AcuSolve results with experimental results validates the ability of AcuSolve to model cases with natural convection of turbulent flow within a tall cavity.

Problem Description

The problem consists of air within a tall cavity with a hot wall and a cold wall, as shown in the following image, which is not drawn to scale. The cavity is 2.18 m tall, 0.0762 m wide, and 0.52 m deep. The cavity's vertical walls differ in temperature, causing the fluid to transfer the heat, leading to natural convection. The temperature of the hot wall is 307.85 K, while the temperature of the cold wall is 288.25 K. The horizontal walls of the cavity are adiabatic. The length-to-width ratio of 28.6 and temperature difference of 19.6 K produce a turbulent flow field within the cavity with a Rayleigh number of $8.6X10^{5}$ (Betts and Bokhari 2000). The flow medium is air, with a Boussinesq approximation for density, a specific heat of 1005 J/kg-K, and a viscosity of $1.781 X 10^{-5}$ kg/m-s. Gravity is applied globally to the volume of air.

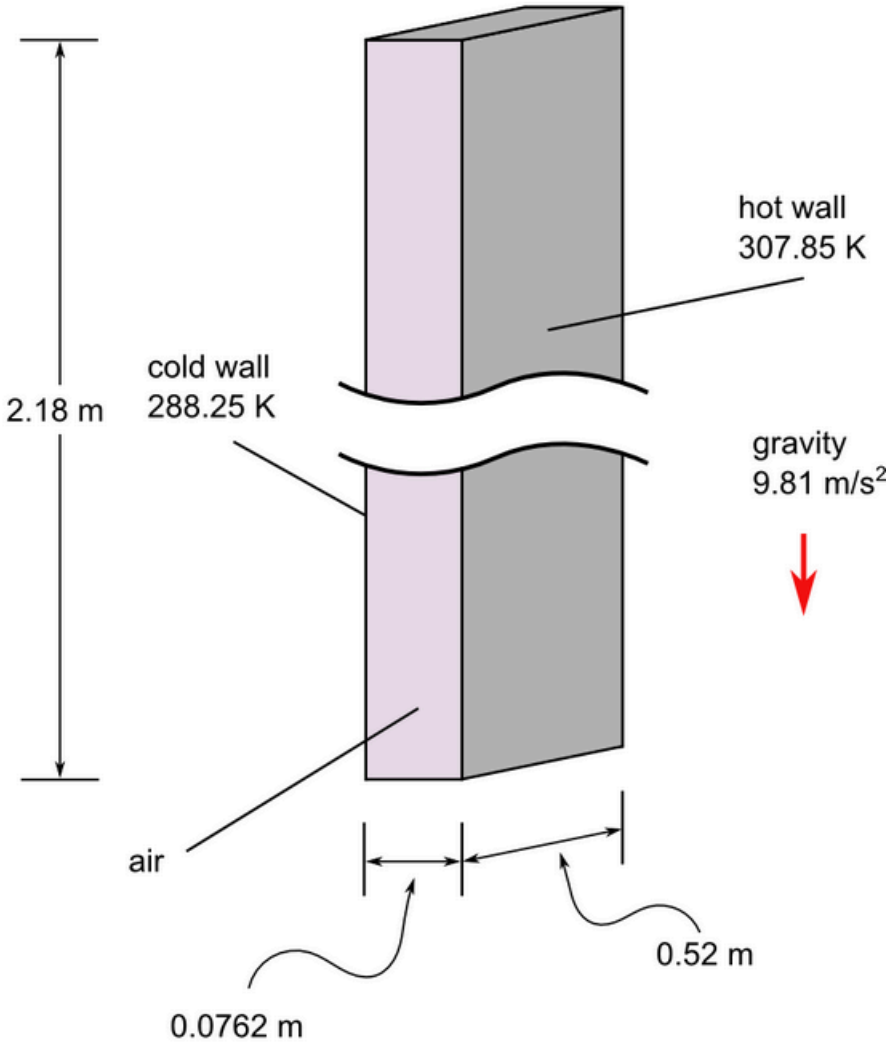


Figure 60: Critical Dimensions and Parameters for Simulating Turbulent Natural Convection in a Tall Cavity

The simulation was performed as a two dimensional problem by constructing a volume mesh that contains a single layer of elements in the extruded direction, normal to the flow plane and by imposing symmetry boundary conditions on the extruded planes.

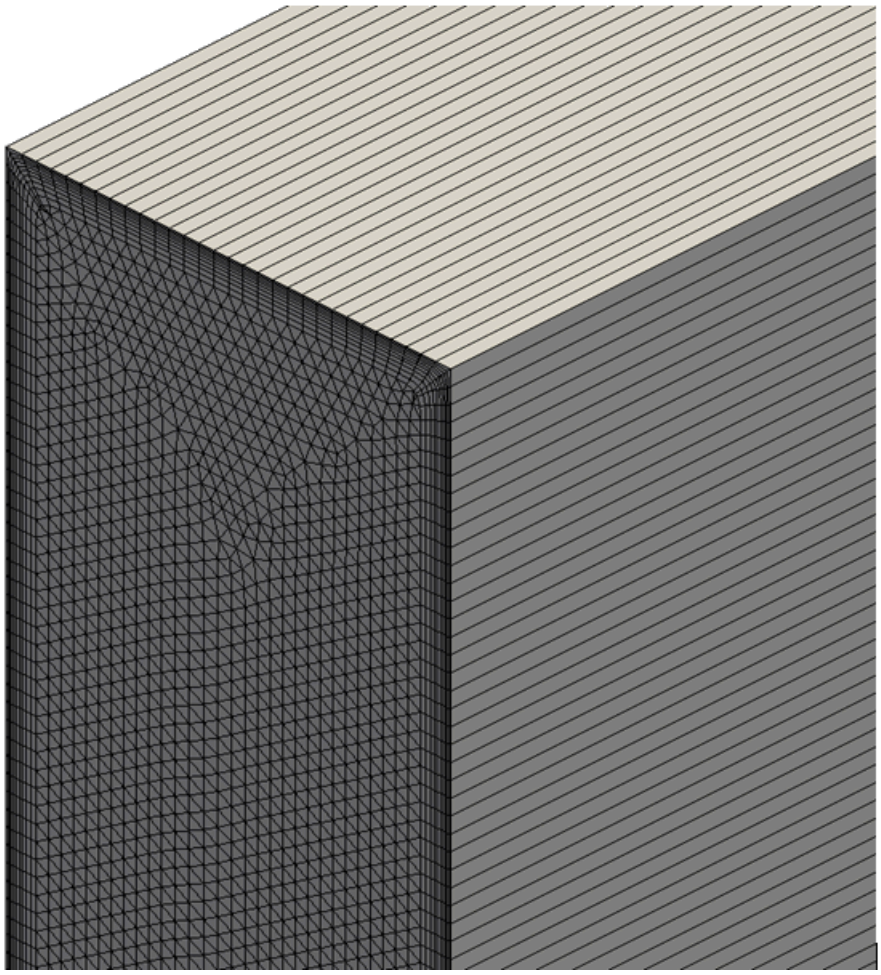


Figure 61: Mesh used for Simulating the Natural Convection of Turbulent Flow in a Tall Cavity

AcuSolve Results

The AcuSolve solution converged to a steady state and the results reflect the mean flow conditions. The natural convection of the flow is generated by heat transfer from the vertical walls to the fluid in the cavity. The temperature gradients created by this heat transfer cause differing densities within the flow region. The warmer air rises to the top of the cavity due to its lower density while the colder air sinks to the bottom of the cavity due to its higher density. This produces flow near the hot vertical wall in the positive vertical direction and flow near the cold wall in the negative vertical direction.

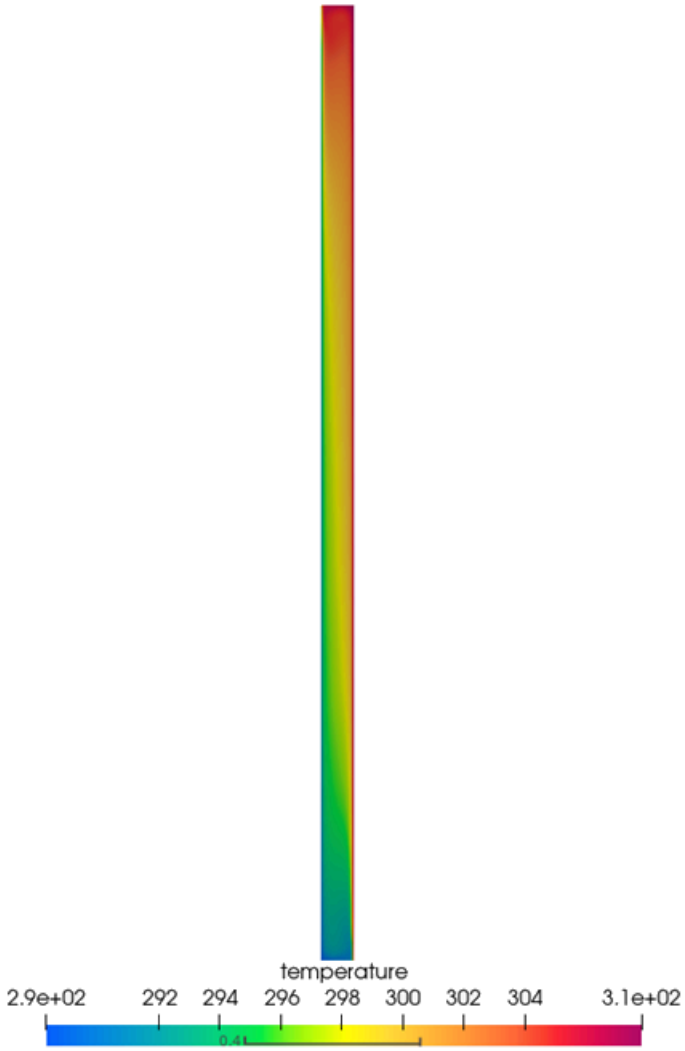


Figure 62: Temperature Contours Throughout Tall Cavity in the X-Y Plane

The AcuSolve results of the temperature and vertical velocity within the cavity are compared to the corresponding experimental values in the plots shown below. The temperature of the air is lowest near the cold vertical wall, remains relatively steady in the middle of the cavity, and then peaks near the hot vertical wall. Following a similar trend, the AcuSolve results show that the velocity is lowest near the cold vertical wall, due to the air sinking, and then steadily increases as the air begins to rise near the hot vertical wall. The velocity at the walls is zero due to the no-slip boundary condition. Additional comparisons are made to evaluate the performance of four turbulence models, Spalart-Allmaras (SA), shear stress transport (SST), K-Omega and K-ε.

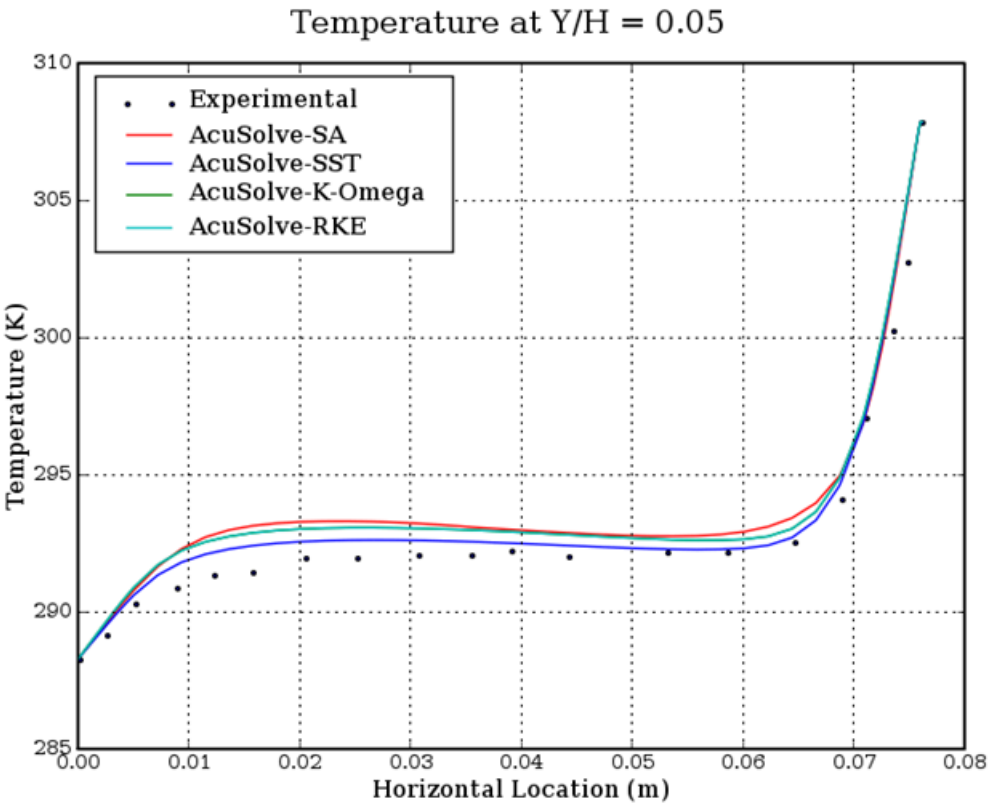


Figure 63: Temperature Plotted against Location along Horizontal at a Position of y/H=0.05 in the Cavity, where H is the Cavity Height and y is the Distance from the Bottom Wall

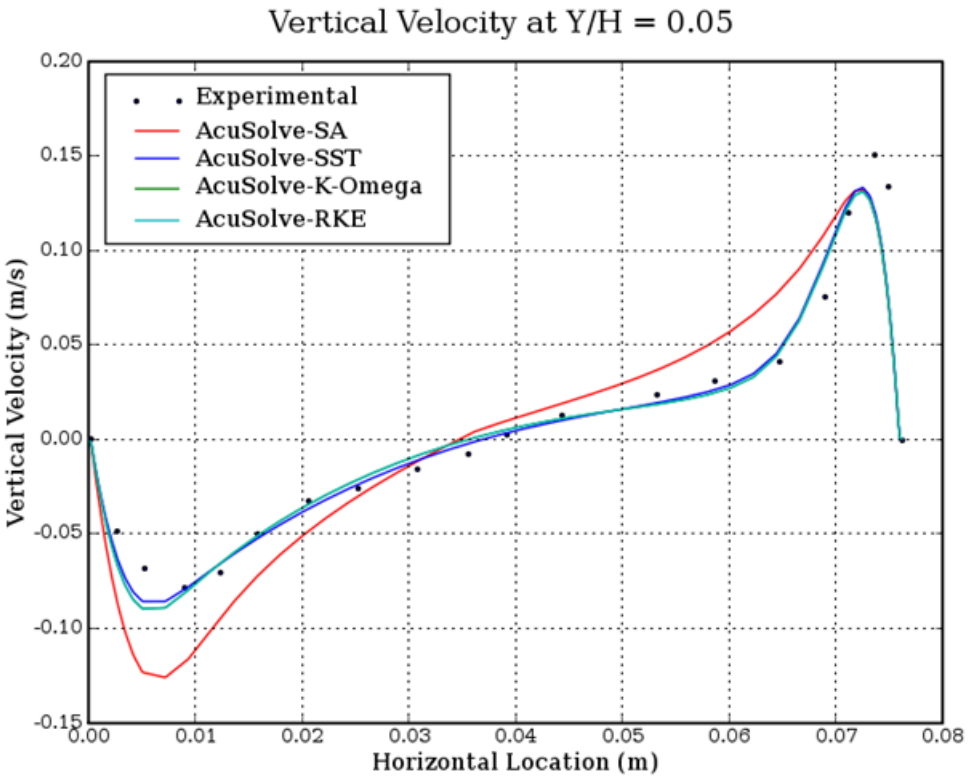


Figure 64: Vertical Velocity Plotted against Location along Horizontal at a Position of y/H=0.05 in the Cavity, where H is the Cavity Height and y is the Distance from the Bottom Wall

Summary

In this application, turbulent flow developed by natural convection, at a Rayleigh number of 8.6X105, is studied within a tall cavity. The AcuSolve results compare well with the experimental data for temperature and vertical velocity along a horizontal line at a location of y/H=0.05 in the tall cavity, with the two-equation models capturing the velocity gradient with greater accuracy. A temperature difference occurs within the flow region due to the heat transfer from the vertical walls of the cavity. The hotter, less-dense air rises to the top of the cavity while the colder, denser air sinks to the bottom, giving rise to recirculation. AcuSolve demonstrates the ability to accurately predict the natural convection of turbulent flow within a tall cavity.

Simulation Settings for Turbulent Natural Convection Inside a Tall Cavity

HyperWorks CFD database file: `<your working directory\cavity_turbulent_heat\cavity_turbulent_heat.hm`

Global

- Problem Description
  - Analysis type - Steady State
  - Turbulence equation - SST
- Auto Solution Strategy
  - Relaxation factor - `0.5`

- Convergence tolerance - `0.005`

- Material Model
  - Air
    - Type - Boussinesq
    - Density - `1.225` kg/m3
    - Specific Heat - `1005` J/kg-K
    - Viscosity - `1.781e-5` kg/m-sec

  Model
- Volumes
  - Volume
    - Element Set
      1. Material model - Air
- Surfaces
  - Back
    - Simple Boundary Condition
      1. Type - Symmetry
  - Bottom
    - **Simple Boundary Condition**
      1. Type - Wall
      2. Temperature BC type - Flux
      3. Heat Flux - `0.0` W/m2
  - Cold
    - **Simple Boundary Condition**
      1. Type - Wall
      2. Temperature BC type - Value
      3. Temperature - `288.25` K
  - Front
    - Simple Boundary Condition
      1. Type - Symmetry
  - Hot
    - Simple Boundary Condition
      1. Type - Wall
      2. Temperature BC type - Value
      3. Temperature - `307.85` K
  - Top
    - Simple Boundary Condition
      1. Type - Wall

2 Temperature BC type - Flux

3 Heat Flux - `0.0` W/m2

References

P.L. Betts and I.H. Bokhari. "Experiments on Turbulent Natural Convection in an Enclosed Tall Cavity". International Journal of Heat and Fluid Flow 21:675-683. 2000.

Turbulent Flow Over a NACA 0012 Airfoil

In this application, AcuSolve is used to simulate turbulent flow of a fluid over a NACA 0012 airfoil at 3 angles of attack, 0 degrees, 10 degrees, and 15 degrees. AcuSolve results are compared with experimental results for coefficients of pressure, lift, and drag reported by NASA. The close agreement of AcuSolve results with experimental results validates the ability of AcuSolve to model external aerodynamics.

Problem Description

The problem consists of a NACA 0012 airfoil located in the center of a cylindrical domain, as shown in the following image, which is not drawn to scale. Fluid enters the domain with a velocity of 1.0 m/s. The domain edges are distant, 500 chord lengths, from the airfoil to minimize any far field effects. The problem is set up to simulate high Reynolds number flow, with Re = 6,000,000.

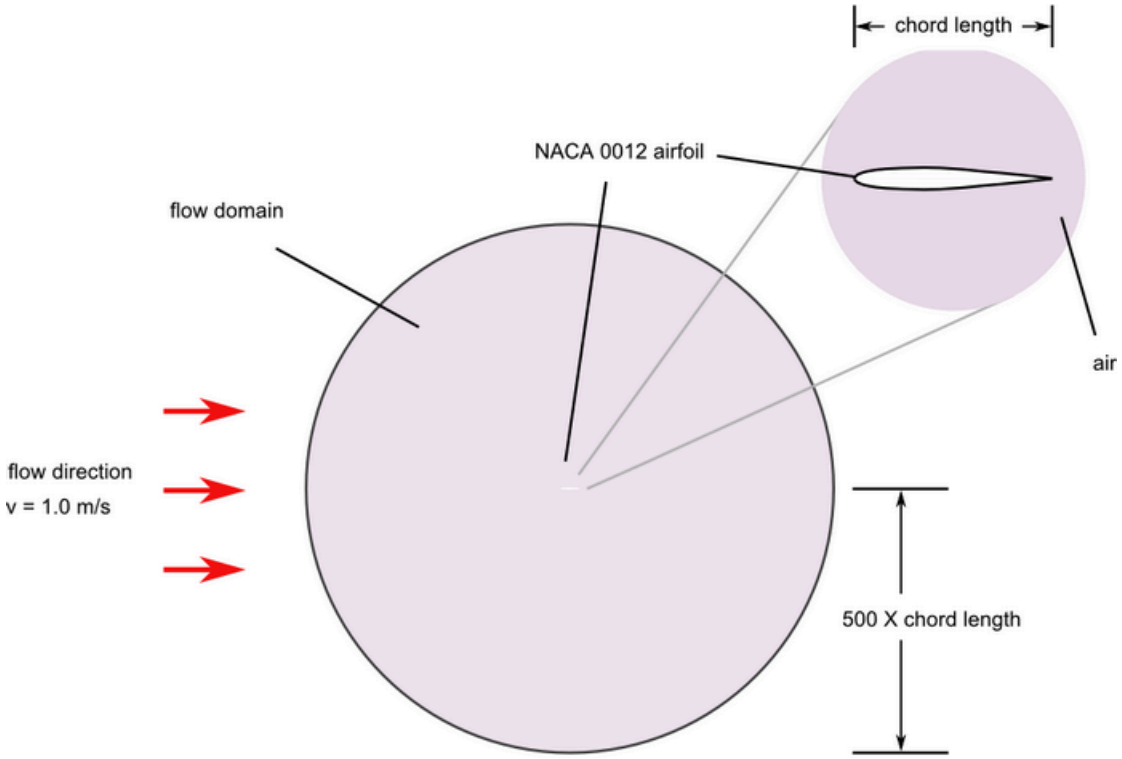


Figure 65: Critical Dimensions and Parameters for Simulating Turbulent Flow over a NACA 0012 Airfoil

The simulation was performed as a two dimensional problem by restricting flow in the out-of-plane direction through the use of a mesh that is one element thick.

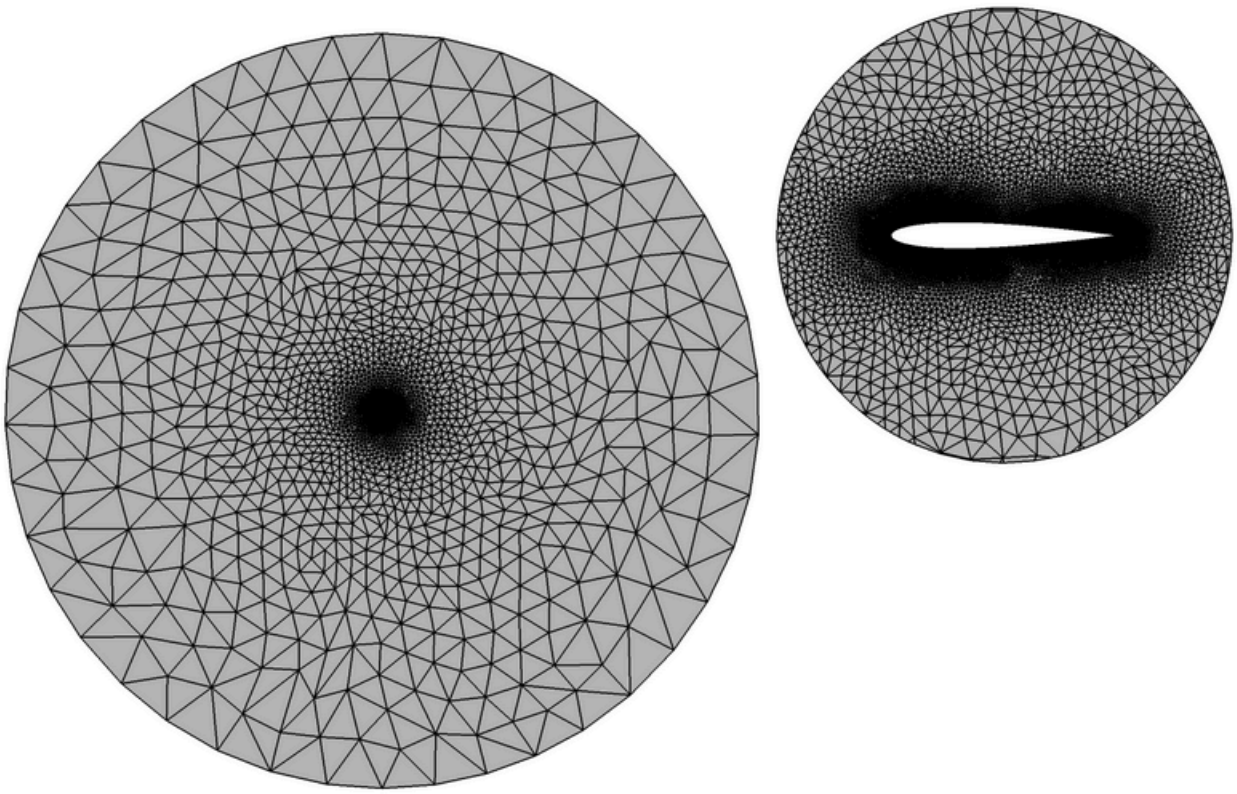


Figure 66: Mesh Used for Simulating Turbulent Flow over a NACA 0012 Airfoil (the Image on the Left Represents the Full Mesh, the Image on the Right Represents Mesh Details near the Airfoil)

AcuSolve Results

The AcuSolve solution converged to a steady state and the results reflect the mean flow conditions for each of the three angles of attack, 0 degrees, 10 degrees, and 15 degrees. For each case, the angle of attack was varied by changing the angle of the incident flow. Note that this enables the use of a single mesh for all of the simulations.

With a 0 degree angle of attack, the flow field is symmetric as the fluid flows over and under the airfoil. The airfoil impedes the flow, causing stagnation at the leading edge. As the fluid passes over and under the airfoil, velocity increases. As the fluid passes over the blunt trailing edge, a minor amount of flow separation occurs. The flow reattaches shortly after it passes the trailing edge and recovers the mean velocity in the distant far field.

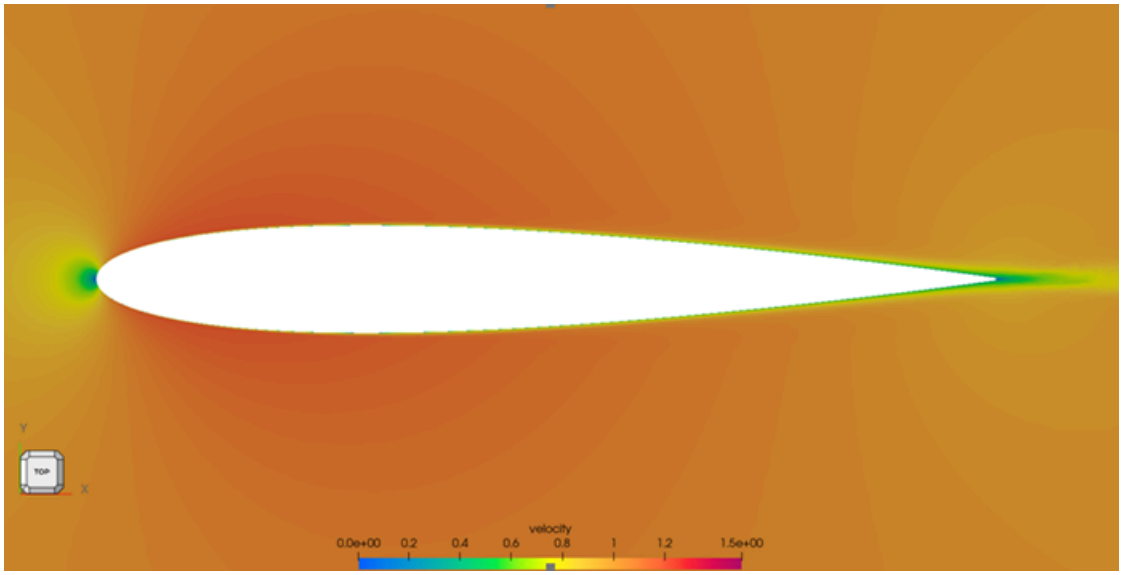


Figure 67: Contours of Velocity Magnitude Where Angle of Attack = 0 Degrees

With a 10 degree angle of attack, the stagnation point is shifted downward (relative to the airfoil), reflective of the shifted angle of attack. Fluid velocity above the airfoil is markedly different than that below the airfoil. A small low-velocity region is evident on the suction side of the airfoil, indicating some separation toward the trailing edge.

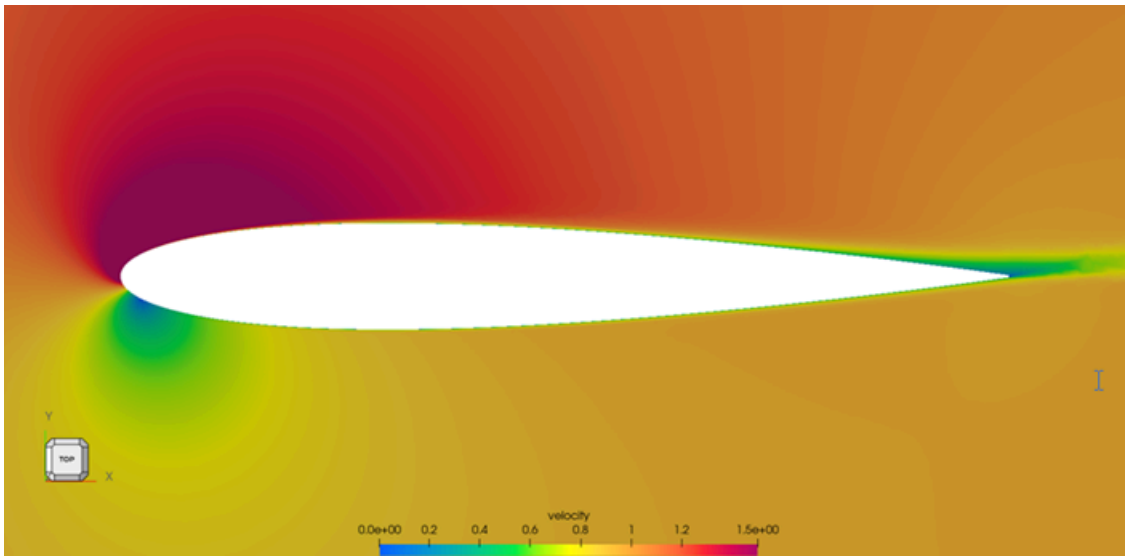


Figure 68: Contours of Velocity Magnitude Where Angle of Attack = 10 degrees

With a 15 degree angle of attack, the stagnation at the front of the airfoil is shifted even farther downward (relative to the airfoil), reflective of the shifted angle of attack. Additionally, the low-velocity wake increases in size, reflecting separation along the suction surface of the airfoil.

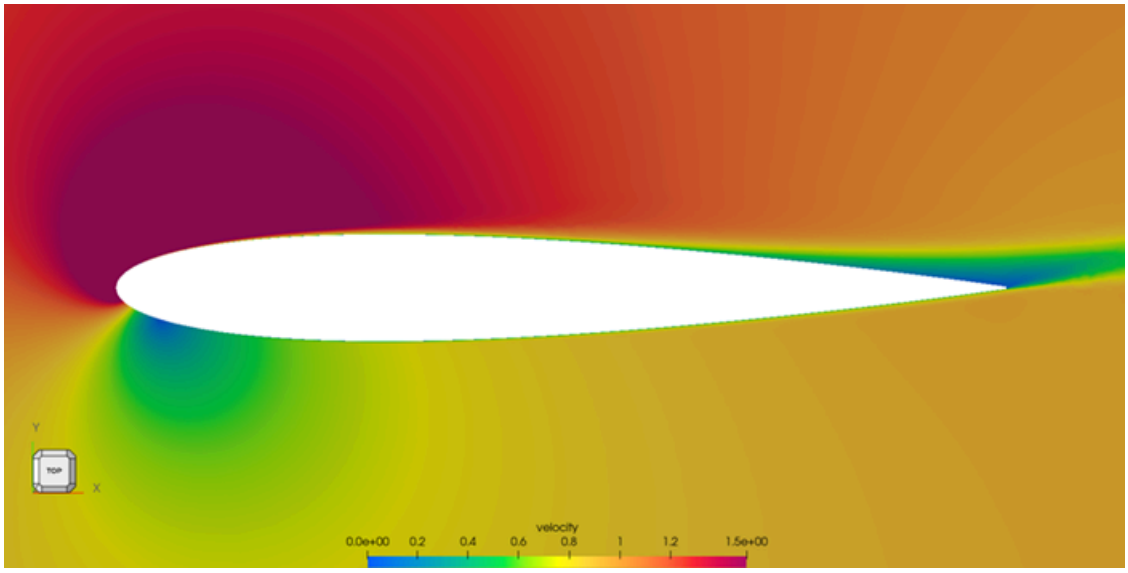


Figure 69: Contours of Velocity Magnitude Where Angle of Attack = 15 Degrees

Experimental values of coefficient of lift (CL) at angles of attack (α) of 10 degrees and 15 degrees and values of drag coefficient (cd) at angles of attack (α) of 0 degrees,10 degrees, and 15 degrees are presented with the corresponding AcuSolve results in the following table.

Table 3:

	CL (α=10)	**CL (α=15)**	**cd (α=0)**	**cd (α=10)**	**cd (α=15)**
Experimental	1.0941	1.5576	0.0082	0.0123	0.0207
AcuSolve	1.0905	1.5428	0.0081	0.0124	0.0208
Percent deviation from experimental	0.33	0.95	1.22	0.81	0.48

AcuSolve values for coefficient of pressure are plotted against experimental results for angles of attack (α) of 0 degrees, 10 degrees, and 15 degrees in the following plots. The results are presented for normalized distance along the airfoil, given by x/c, where x is the distance from the leading edge and c is the chord length.

For each case, AcuSolve is able to predict the flow characteristics at each point along the airfoil surface.

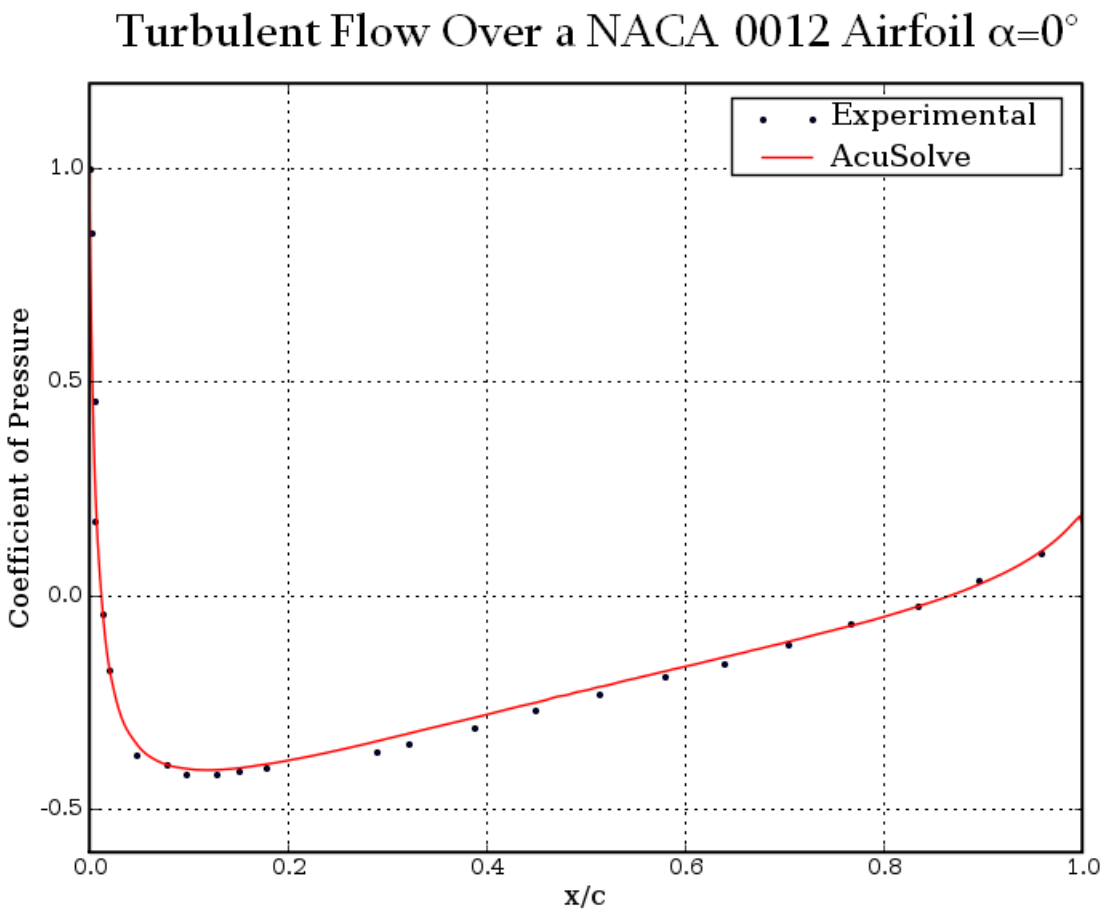


Figure 70: Coefficient of Pressure Plotted Against Normalized Distance Along the Airfoil for Angle of Attack (a) = 0 Degrees

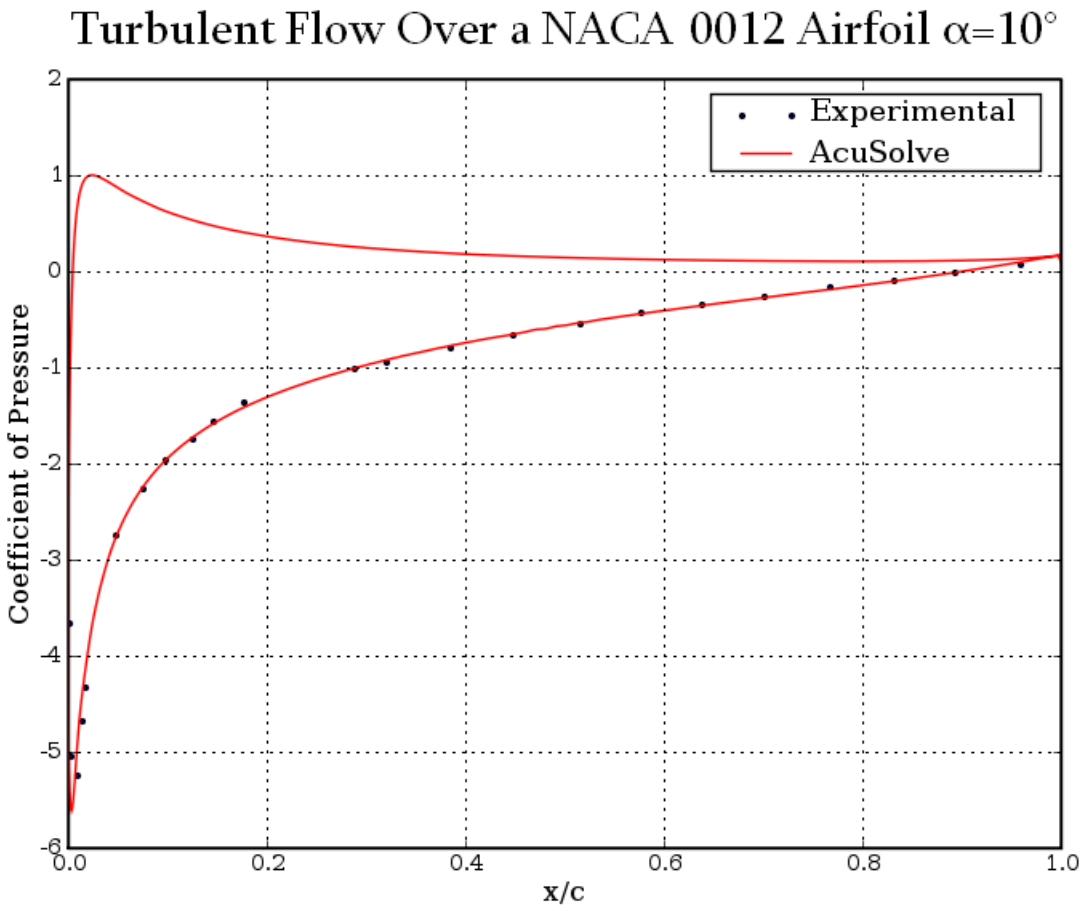


Figure 71: Coefficient of Pressure Plotted Against Normalized Distance Along the Airfoil For Angle of Attack (α) = 10 Degrees

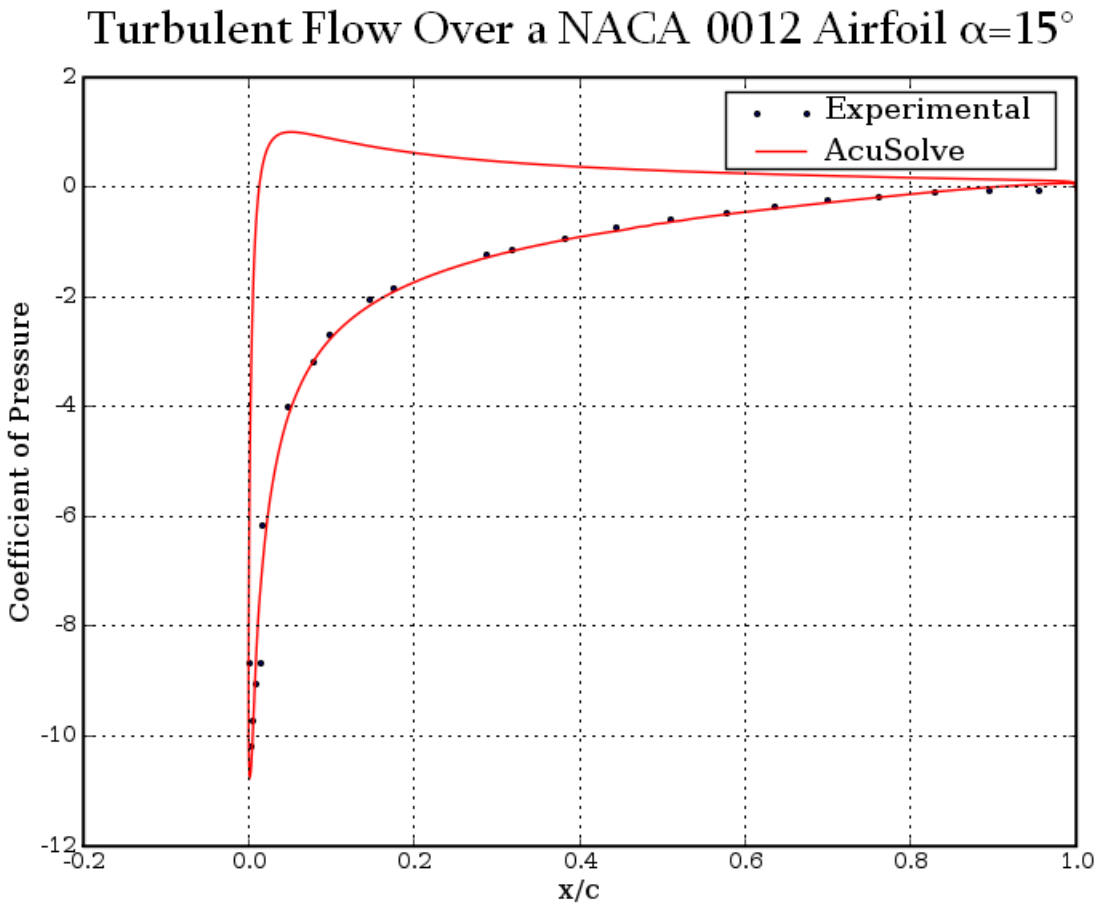


Figure 72: Coefficient of Pressure Plotted Against Normalized Distance Along the Airfoil for Angle of Attack (a) = 15 Degrees

Summary

The AcuSolve results compare well with the experimental results for flow over a NACA 0012 airfoil. In this application, a constant-velocity flow field impinges on the airfoil surface. As the flow convects in the streamwise direction along the airfoil surface, a boundary layer develops. The rate at which the boundary layer develops has significant impact on the viscous stresses present on the airfoil surface. At low angles of attack these stresses dominate the drag on the airfoil. As the angle of attack increases, the flow over the airfoil is no longer symmetric, which leads to the generation of lift. For non-zero angles of attack, the asymmetric pressure distribution on the airfoil creates another source of drag that is combined with the viscous stresses to determine the total drag on the airfoil. The AcuSolve results for coefficients of lift and drag at the 15 percent angle of attack are within 0.91 percent and 0.5 percent of experimental values, respectively. AcuSolve results for coefficient of pressure closely agree with experimental results along the length of the airfoil for all three angles of attack that were investigated.

Simulation Settings for Turbulent Flow Over a NACA0012 Airfoil

HyperWorks CFD database file: `<your working directory>\airfoil_turbulent\airfoil_turbulent.hm`

Global

- Problem Description
  - Analysis type - Steady State
  - Turbulence equation - Spalart Allmaras
- Auto Solution Strategy
  - Convergence tolerance - `0.0001`
  - Relaxation factor - `0.4`
- Material Model
  - Fluid
    - Density - `1.0` kg/m3
    - Viscosity - `1.667e-7` kg/m-sec

  Model
- Volumes
  - Fluid
    - Element Set
      1. Material model - Fluid
- Surfaces
  - +z slip
    - Simple Boundary Condition
      1. Type - Slip
  - -z slip
    - Simple Boundary Condition
      1. Type - Slip
  - airfoil surface
    - Simple Boundary Condition
      1. Type - Wall
  - farfield
    - Simple Boundary Condition
      1. Type - Far Field
      2. X velocity - cos(α) m/sec
      3. Y velocity - sin(α) m/sec
- Eddy viscosity - `1.0e-9` m2/sec

References

NASA - Langley Research Center. http://turbmodels.larc.nasa.gov/naca0012_val_sa.html

Turbulent Flow Over an Oscillating Rigid Body Assembly

In this application, AcuSolve is used to simulate the fluid-structure interaction of a fluid moving over a cylinder/plate assembly. AcuSolve results are compared with experimental results as described in Gomes and Lienhart (2009). The close agreement of AcuSolve results with the experimental results validates the ability of AcuSolve to model cases in which the fluid forces lead to structural motions.

Problem Description

The problem consists of a fluid having material properties of standard water with density of 998 kg / m^3 and kinematic viscosity of 0.97e-6 m^2/sec through a two dimensional channel over a cylinder and plate assembly. The diameter of the cylinder is 0.022 m and the plate length is 0.042 m, while the inlet velocity is specified to match experimental conditions with a max velocity of 1.07 m/sec, as is shown in the following image, which is not drawn to scale. The model is simulated as transient with constant inflow conditions, allowing an oscillatory motion of the assembly to develop. The Shear Stress Transport (SST) turbulence model is used to model the turbulent portion of the flow and AcuSolve's internal rigid body motion is used to capture the motion of the oscillating assembly.

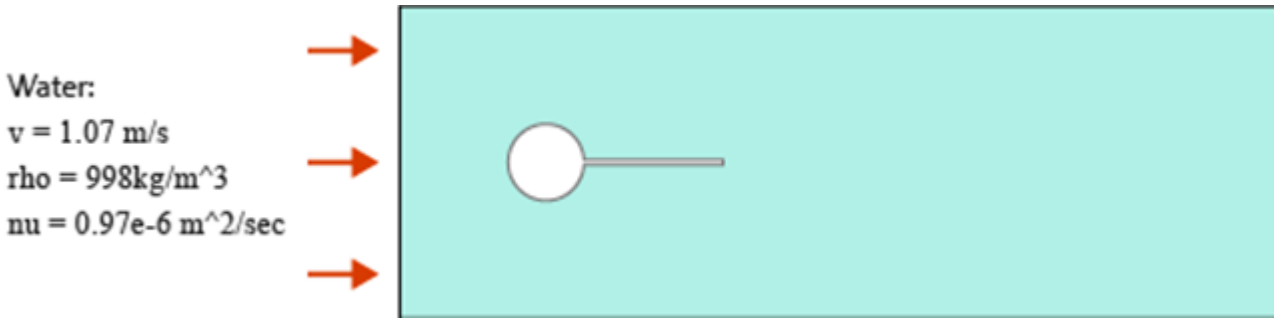


Figure 73: Critical Dimensions and Parameters used for Simulating Rigid Body Motion of Flow Past a Cylinder/Plate Assembly

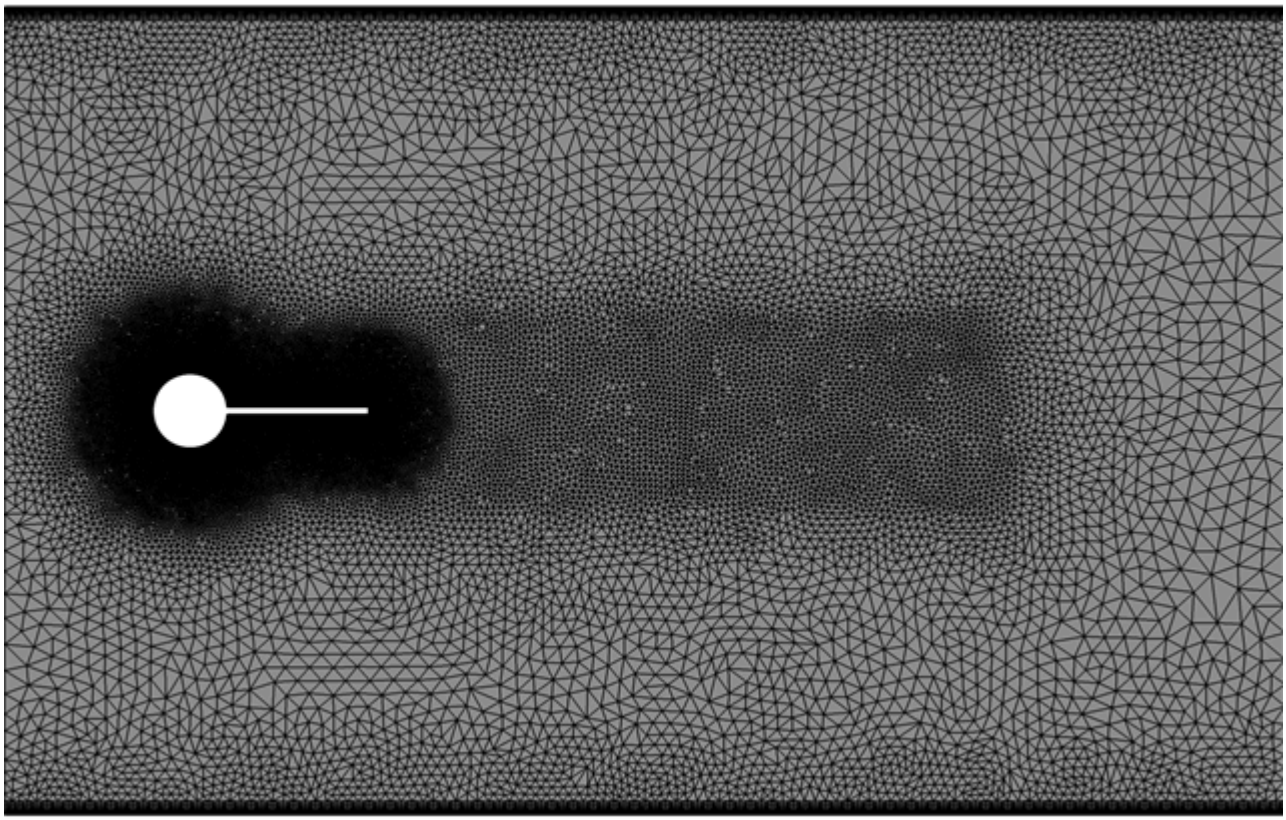


Figure 74: Mesh used for Simulating Rigid Body Motion of Flow Past a Cylinder/Plate Assembly

The simulation was performed as a two dimensional problem by constructing a volume mesh that contains a single layer of elements extruded in the cross stream direction, normal to the flow plane and by imposing symmetry boundary conditions on the extruded planes. The upper and lower walls are specified as no-slip and the inlet velocity is specified to match the conditions of the experiment (Gomes and Lienhart 2009).

AcuSolve Results

The AcuSolve solution reached a regularly repeating oscillatory state and the simulation was allowed to proceed for 10 seconds of physical time to obtain a sufficient number of cycles for statistical analysis. The motion of the cylinder/plate assembly is directly attributed to the vortices shedding in its wake. The fluctuating loads on the assembly that result from the vortex shedding lead to a repeating cycle of structural rotation. The dominant oscillation frequency from the simulation was found to match well with the experimental measurements, within approximately 3.5 percent. The images below show the rigid body displacement of the assembly as it oscillates within the flow. Contours of velocity magnitude demonstrate the forcing on the assembly, while the mesh motion around the structure is captured and plotted for a single time step. Two dimensional plots showing the angular displacement demonstrate the motion, showing a single red line for the AcuSolve results.

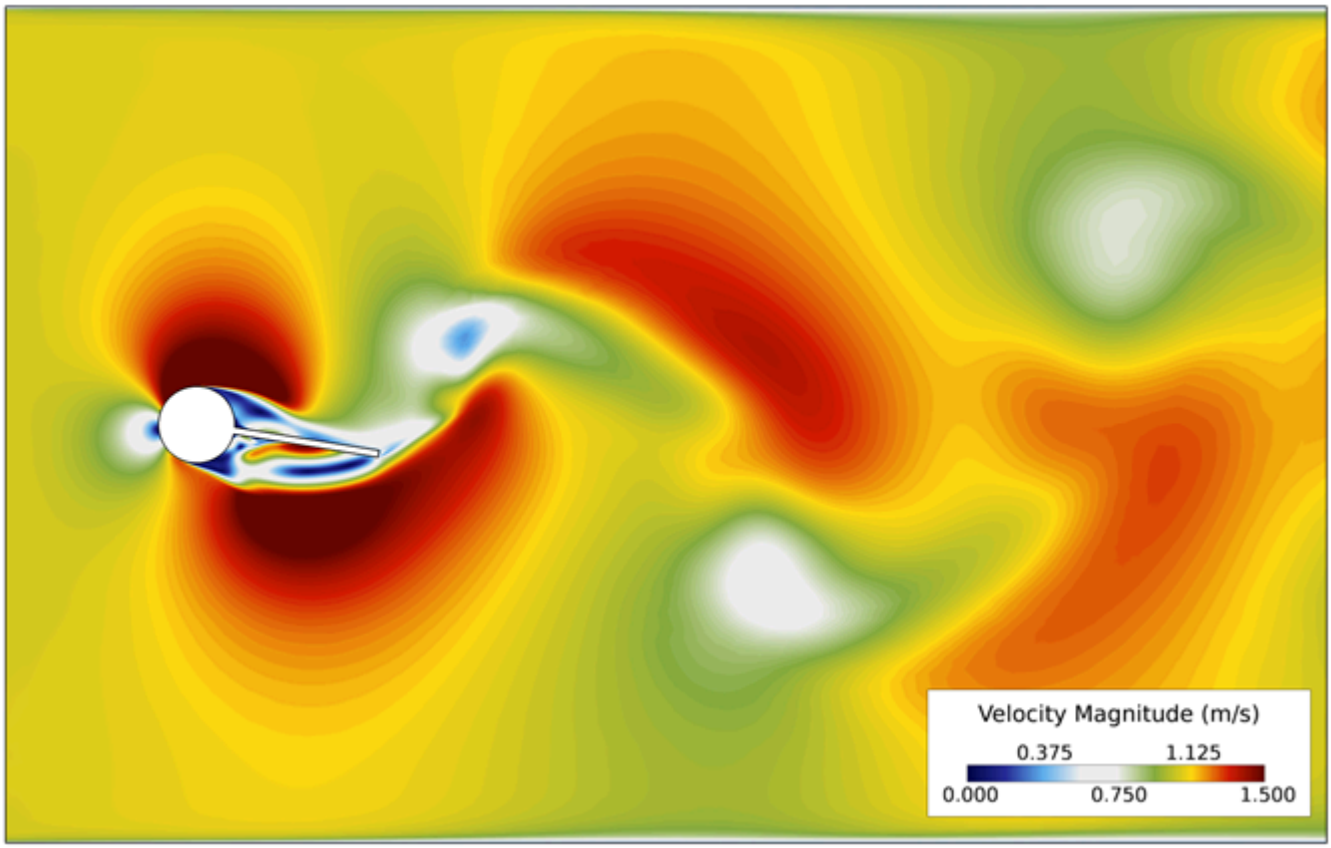


Figure 75: Velocity Contours Near the Assembly for a Single Time Step During the Simulation

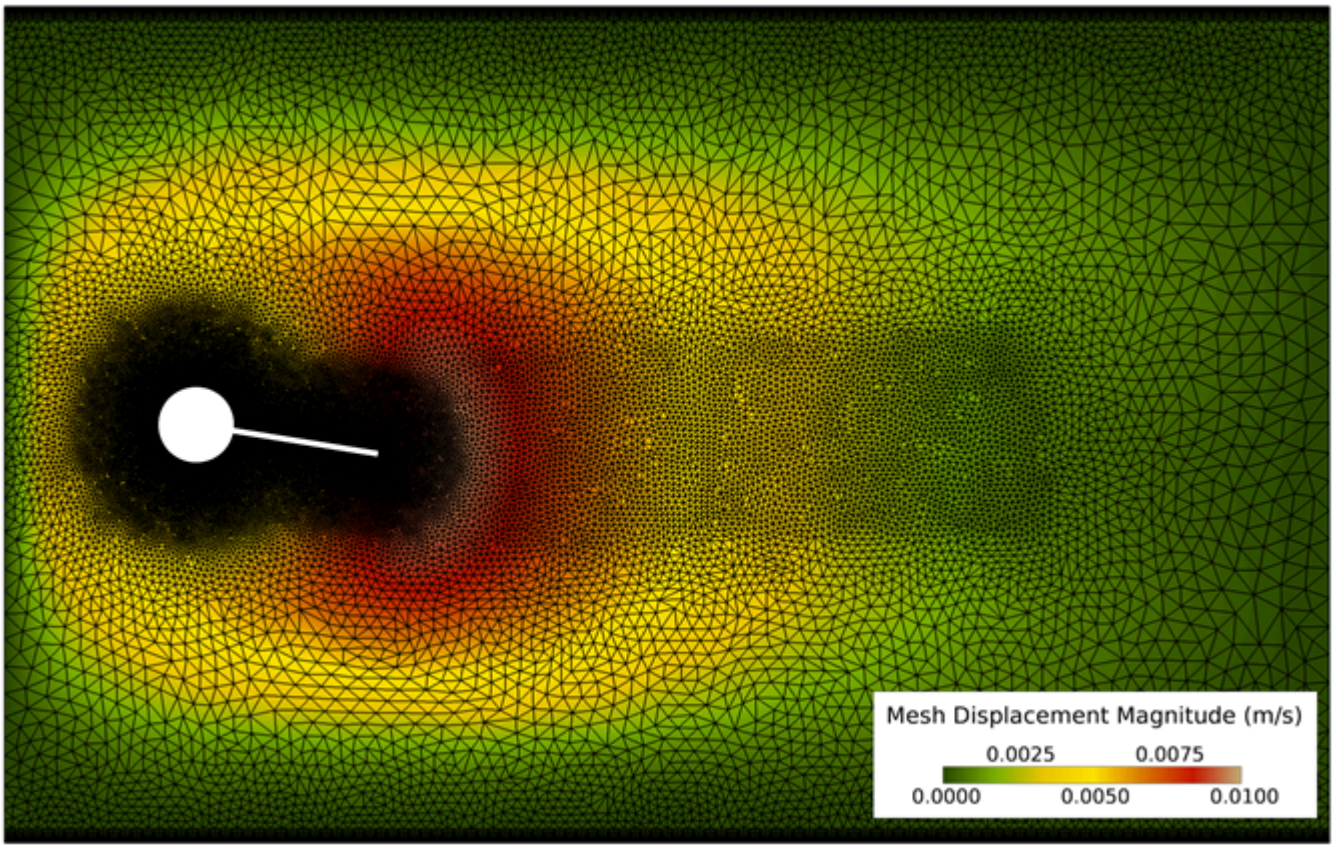


Figure 76: Mesh Displacement Contours Near the Assembly for a Single Time Step During the Simulation

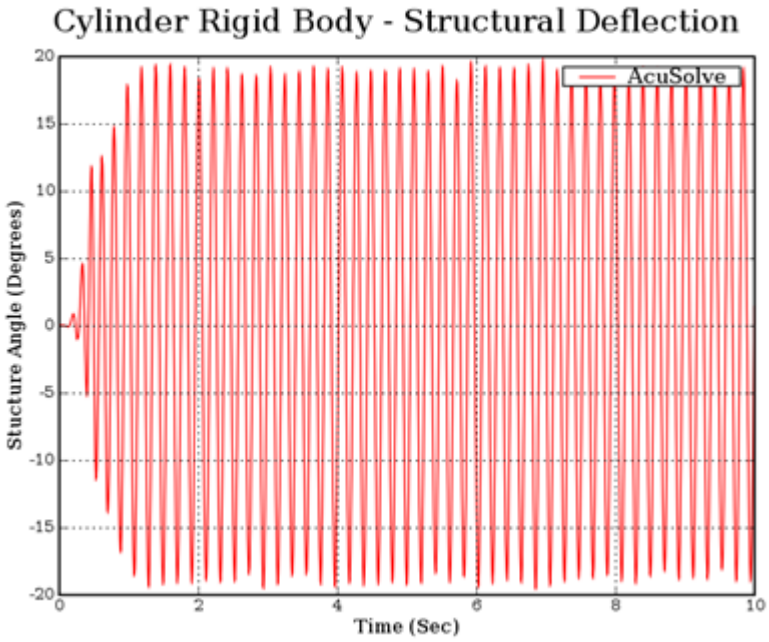


Figure 77: Rigid Body Displacement of the Assembly as a Function of Time, Showing the Oscillation Develop into the Pseudo-Steady Motion

The dominant frequency of the oscillation is easily identified in the Fast Fourier Transform (FFT) of the deflection angle, shown in the plot below.

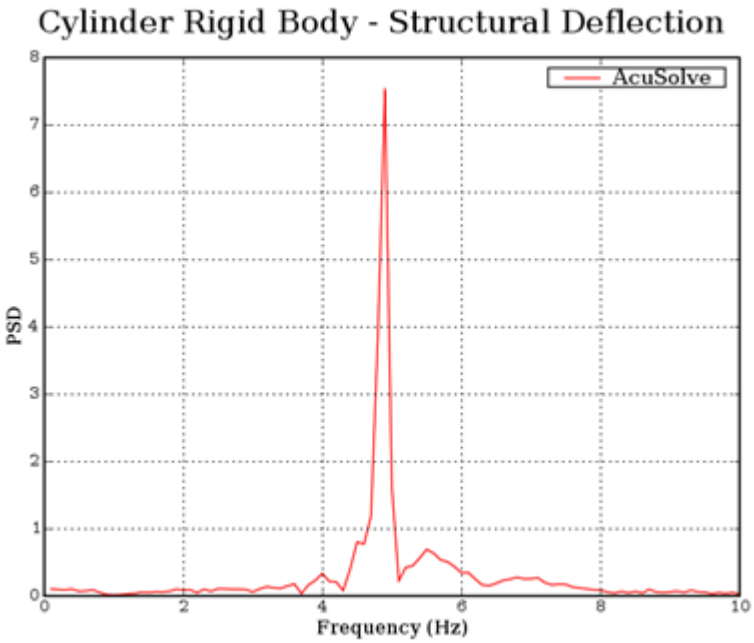


Figure 78: FFT of the Rigid Body Displacement Angle, Showing Power Spectral Density as a Function of Frequency

Summary

The AcuSolve solution compares well with experimental data for flow past an oscillating cylinder/plate assembly. In this application, water moves over the cylinder/plate assembly, giving rise to unsteady loading that causes the body to rotate as a rigid body. The good agreement with the natural frequency of oscillation compared to the experimental data demonstrates that AcuSolve is capable of predicting fluid forced motion with an internal rigid body dynamic solver.

Simulation Settings for Turbulent Flow Over an Oscillating Rigid Body Assembly

AcuConsole database file: `<your working directory>\cylinder_rigidbody_turbulent\cylinder_rigidbody_turbulent.acs`

Global

- Problem Description
  - Analysis type - Transient
  - Turbulence equation - SST
  - Mesh Type- Fully Specified
- Auto Solution Strategy
  - Final Time - `10.0`
  - Initial Time Increment- `0.005`
  - Convergence tolerance- `0.001`
  - Max stagger iterations- `3`
- Material Model
  - Water
    - Type- Constant
    - Density- `998.0` kg/m3
    - Viscosity- `0.00096806` kg/m*sec
- Mesh Motion
  - Interpolated
    - Type- Interpolated Motion
    - Interpolated motion surfaces
      1. Bottom
      2. Top
  - RigidBody
    - Type- Rigid Body Dynamic
      1. Z rotation- Active
      2. Mass- `0.2089` kg
      3. Dyadic
         1. X-X - `3.7 e-5` kg-m2
         2. Y-Y- `3.7 e-5` kg-m2
         3. Z-Z - `3.7 e-5` kg-m2

Model

- Volumes
  - Volume
    - Element Set
      1. Material model- Water
      2. Mesh motion- Interpolated
- Surfaces
  - Body
    - Simple Boundary Condition
      1. Type- Wall
      2. Mesh displacement BC type- Fixed
      3. Mesh motion- RigidBody
    - Interpolated Motion Surface
  - Bottom
    - Simple Boundary Condition
      1. Type- Wall
      2. Mesh displacement BC type- Fixed
    - Interpolated Motion Surface
  - Inflow
    - Simple Boundary Condition
      1. Type- Inflow
      2. Inflow type- Velocity
      3. X Velocity- `1.07` m/sec
      4. Turbulence input type- Auto
      5. Turbulence intensity type- High
    - Advanced Options
      1. Nodal Boundary Conditions
      2. X-velocity
         1. Type- Linear
         2. Precedence- `2`
         3. Curve fit variable- Y coordinate
         4. Curve fit values- Provided
      3. Y-velocity
         1. Type- Zero
      4. Z-velocity
         1. Type- Zero
  - Bottom
    - Simple Boundary Condition

1. Type- Wall
2. Mesh displacement BC type- Fixed
3. Mesh motion- RigidBody

- Interpolated Motion Surface

- Outflow
  - Simple Boundary Condition
    1. Type- Outflow
- Top
  - Simple Boundary Condition
    1. Type- Wall
    2. Mesh displacement BC type- Fixed
  - Interpolated Motion Surface
- maxZ
  - Simple Boundary Condition
    1. Type- Slip
- minZ
  - Simple Boundary Condition
    1. Type- Slip

References

Gomes, J. P. and Lienhart, H. (2009) Experimental Benchmark: Self-excited Fluid-structure Interaction Test Cases, in Fluid-Structure Interaction II: Modeling, Simulation, Optimization, Bungartz, H. J., Mehl, M., Schafer, M. (eds.), 383-412, Springer-Verlag.Ryhming.

Turbulent Flow Through a 180 Degree Curved Channel

In this application, AcuSolve is used to simulate turbulent flow through a strongly curved two dimensional 180 degree U-duct channel. AcuSolve results are compared with experimental results adapted from Rumsey et al. (2000). The close agreement of AcuSolve results with experimental results validates the ability of AcuSolve to model turbulent cases with strong curvature effects.

Problem Description

The problem consists of a fluid with properties similar to air flowing through a curved channel, as shown in the following image, which is not drawn to scale. The inlet channel height and remaining duct height is 0.0381 m. The bulk velocity (v) normal to the inlet is 31.1 m/s and an integrated outflow pressure is specified to allow the flow to pass through the channel. The flow develops into fully turbulent flow at a Reynolds's number (Re) of approximately 1,000,000. The density of the flow medium is 1.0 kg/m3 and the dynamic viscosity is 1.1818 X 10-6 kg/m-s. The simulation is conducted with the Reynolds Averaged Navier-Stokes equations using the Spalart Allmaras, Shear Stress Transport (SST), K-ω and Realizable K-ε turbulence models. The velocity field from the simulations is compared against experimental data at select measurement locations.

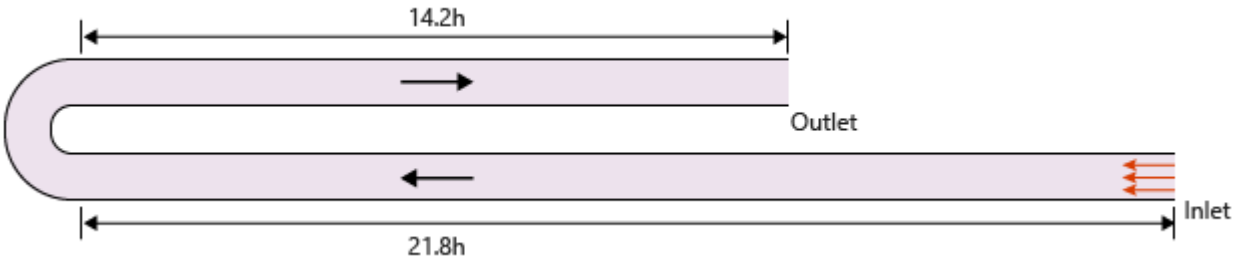
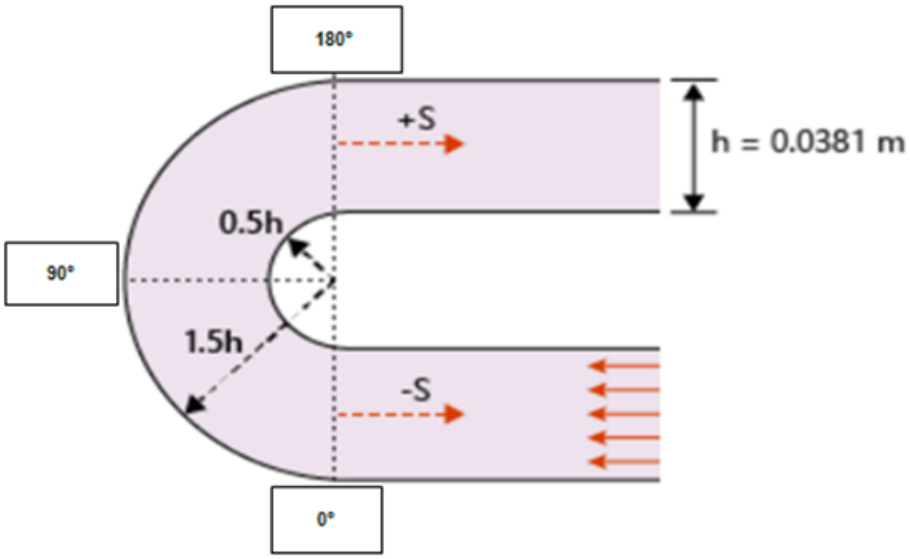


Figure 79: Critical Dimensions and Parameters for Simulating Turbulent Flow in the 180 degree U-Duct



The simulation was performed as a two dimensional problem by restricting flow in the out-of-plane direction through the use of a mesh that is one element thick. The upper and lower walls are specified as no-slip, the inlet velocity and eddy viscosity are specified normal to the inlet face to match the experimental Reynolds Number.

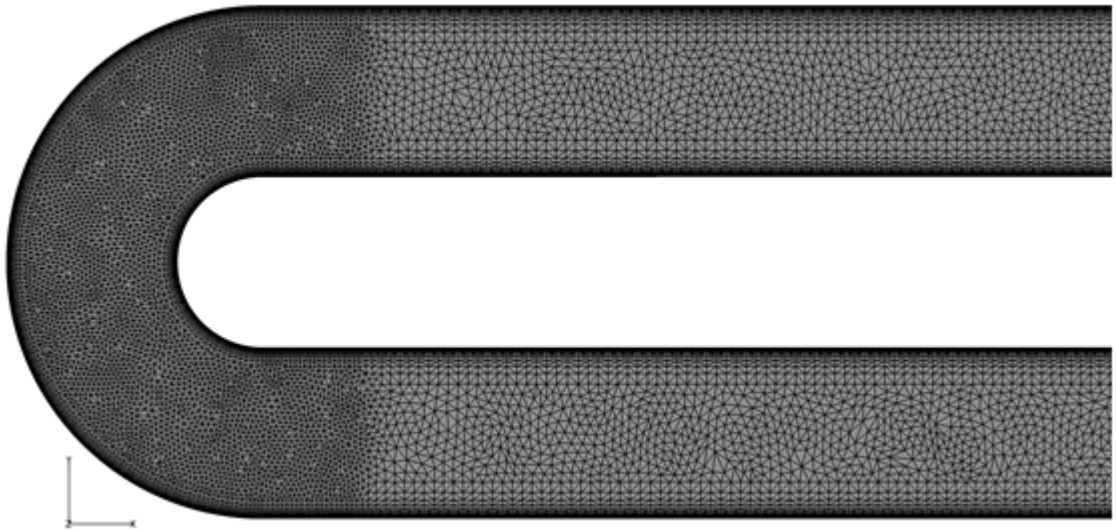


Figure 80: Mesh Used for Simulating Turbulent Flow in the 180 Degree U-Duct

AcuSolve Results

The AcuSolve solution converged to a steady state and the results reflect the mean flow conditions. As the flow passes the inner convex wall it begins to accelerate before decelerating directly past the curved section due to the adverse pressure gradient that eventually leads to a local recirculation zone. On the outer concave wall, the flow remains attached, but is influenced by the adverse pressure gradient above the recirculation region.

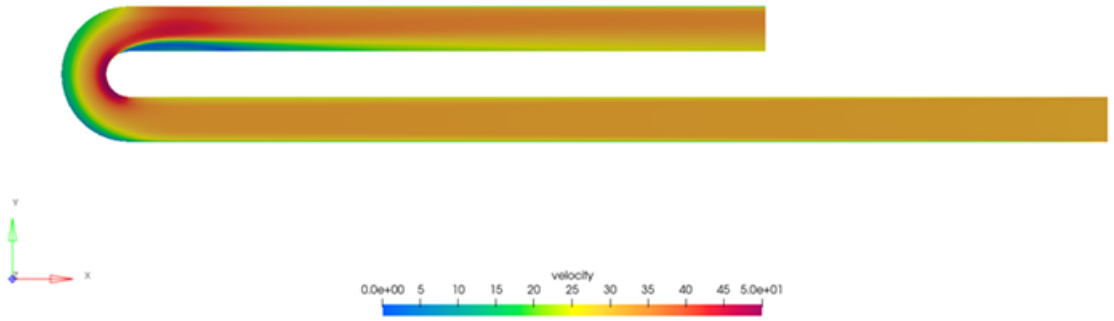


Figure 81: Velocity Contours in Stream Wise Plane

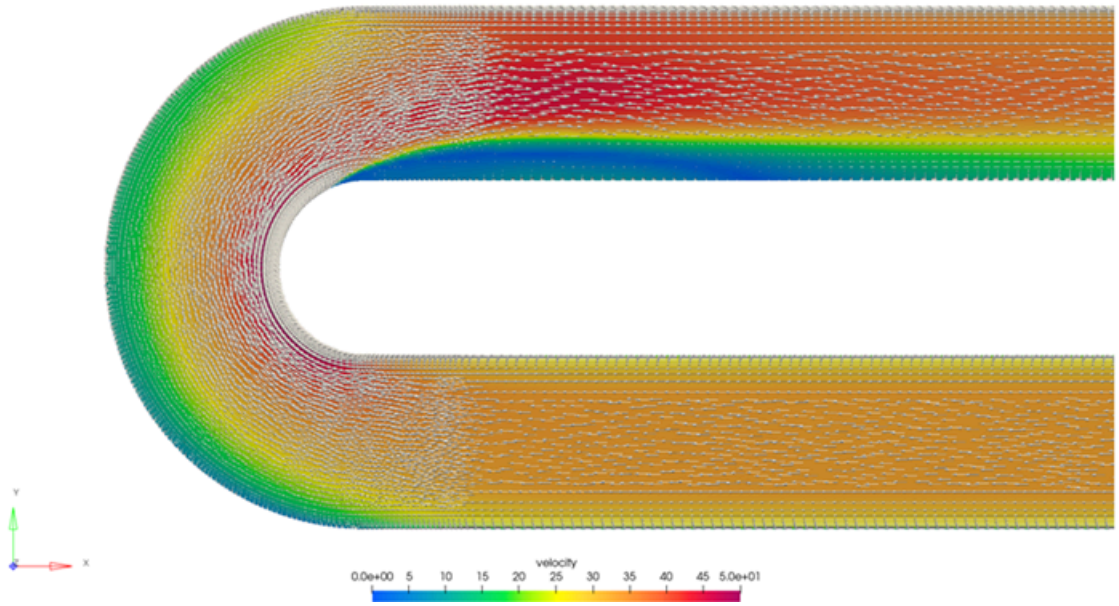


Figure 82: Close up View of Velocity Vectors and Velocity Contours at 180 Degree Bend

The experimental value for the ratio of Velocity magnitude (Vm) to inlet bulk velocity (Vb=31.1 m/s) at different sections of the U-duct is presented with the corresponding AcuSolve result for each of the turbulence models tested in the following images. The images show black circles representing the experimental measurements (Rumsey 2000), solid red lines for the SA model, solid blue lines for the SST model, solid green lines for the K-ω model and solid cyan lines for the K-ε model.

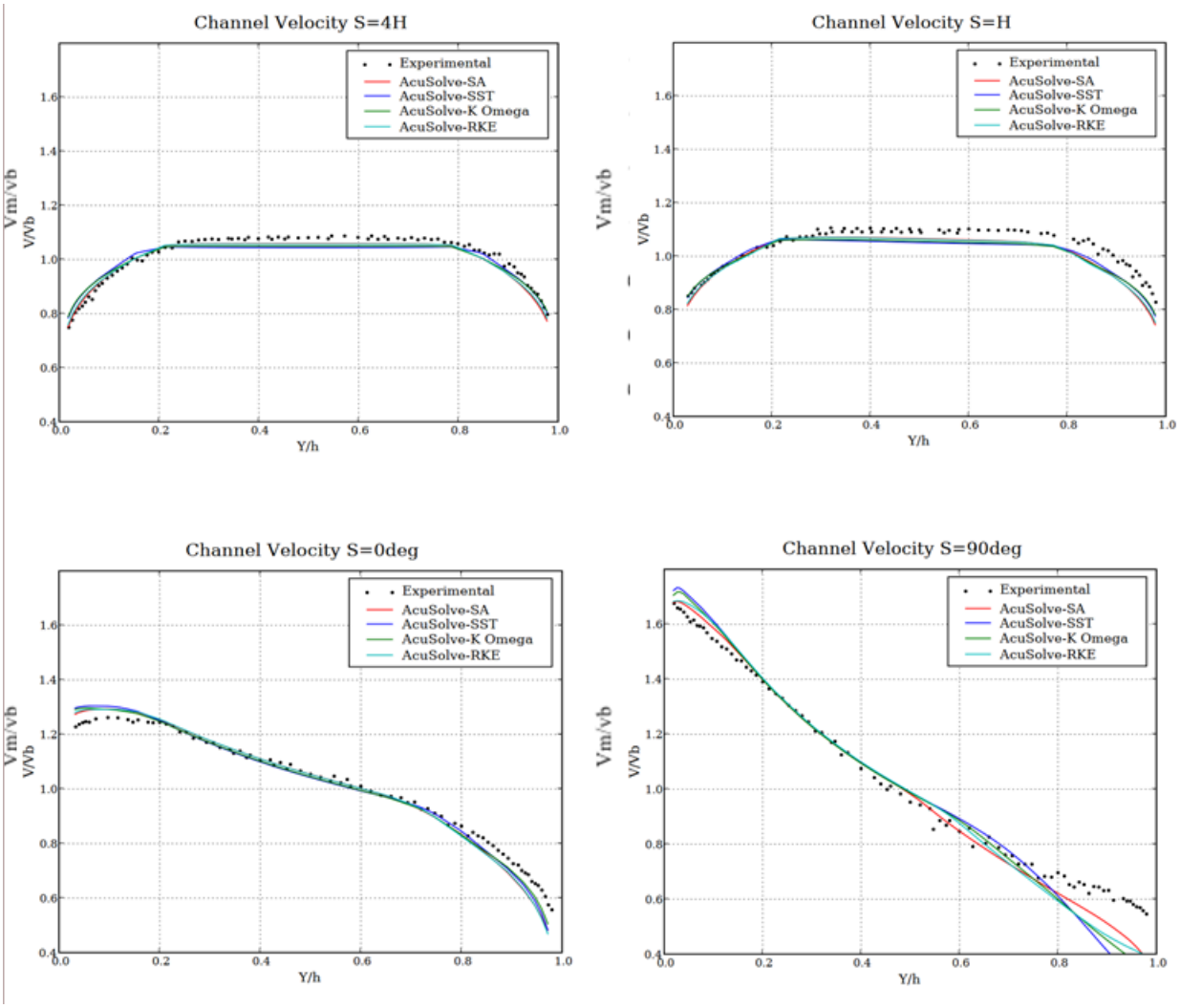


Figure 83:

Summary

The AcuSolve solution compares well with experimental results for flow past the 180 degree U-duct. The experimental value for the ratio of Velocity magnitude to inlet bulk velocity at different sections of the U-duct is presented with the corresponding AcuSolve result for various turbulence models. The performance of the Spalart Allmaras turbulence model was found to improve when the rotation curvature correction is included in the numerical formulation (enabled by default). In this application, AcuSolve demonstrates the ability to predict the complex boundary layer separation and reattachment resulting from the curvature of the channel.

Simulation Settings for Turbulent Flow Through a 180 Degree Curved Channel

HyperWorks CFD database file: `<your working directory>\curved_channel_simple_turbulent \curved_channel_simple_turbulent.hm`

Global

- Problem Description

    - Analysis type - Steady State
    - Turbulence equation - Realizable K-Epsilon
- Auto Solution Strategy
    - Relaxation factor - `0.4`
- Material Model
    - Air
        - Type- Constant
        - Density- `1.0` kg/m3
        - Viscosity- `1.1818e-006` kg/m-sec

  Model
- Volumes
    - Fluid
        - Element Set
            1. Material model- Air
- Surfaces
    - Inlet
        - Simple Boundary Condition
            1. Type- Wall
            2. Inflow type- Velocity
            3. Inflow velocity type- Normal
            4. Normal velocity- `31.1` m/sec
            5. Turbulence input type- Direct
            6. Eddy viscosity- `3.5547e-06` m2/sec
    - ext1
        - Simple Boundary Condition- Symmetry
    - ext2
        - Simple Boundary Condition- Symmetry
    - Outlet
        - Simple Boundary Condition
            1. Type- Outflow
    - wall-bottom
        - Simple Boundary Condition
            1. Type- Wall
            2. Turbulence wall type- Low Reynolds Number
    - wall-top
        - Simple Boundary Condition
            1. Type- Wall

2 Turbulence wall type- Low Reynolds Number

References

Christopher L. Rumsey, Thomas B. Gatski, and Joseph H. Morrison. "Turbulence Model Predictions of Strongly Curved Flow in a U-Duct", AIAA Journal, Vol. 38, No. 8 (2000), pp. 1394-1402.

Turbulent Mixing Layers in an Open Channel

In this application, AcuSolve is used to simulate the mixing of two streams of fluid with different velocities moving past a splitter plate. AcuSolve results are compared with experimental results as described in J. Delville, et al. (1989). The close agreement of AcuSolve results with the experimental results validates the ability of AcuSolve to model mixing layers in the turbulent flow regime.

Problem Description

The problem consists of two streams of fluid having material properties of standard air with density of 1.2 kg /m^3 and molecular viscosity of 1.7189 kg/m-sec. The two fluid streams enter an open channel separated by a splitter plate at two streamwise locations with differing velocities. The length of the channel is 1.8 m for the top portion and 1.5 m for the bottom portion. The inlet velocity of the top section is 41.54 m/s, producing a Reynolds's number of 2900, based on l=1.0 mm, while the inlet velocity of the lower section is 22.4 m/s, giving a Reynolds's number of 1200, as shown in the following image, which is not drawn to scale. The model is simulated as steady state with constant inflow conditions, using the Spalart Allmaras (SA) turbulence model. The velocity profile is computed for several locations downstream of the splitter plate and compared against the experimental data, as described in Delville, 1989.

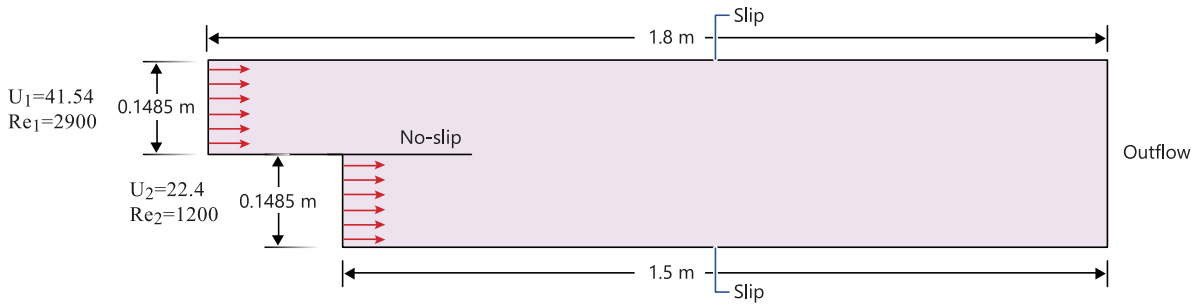


Figure 84: Critical Dimensions and Parameters Used for Simulating the Turbulent Mixing Layer

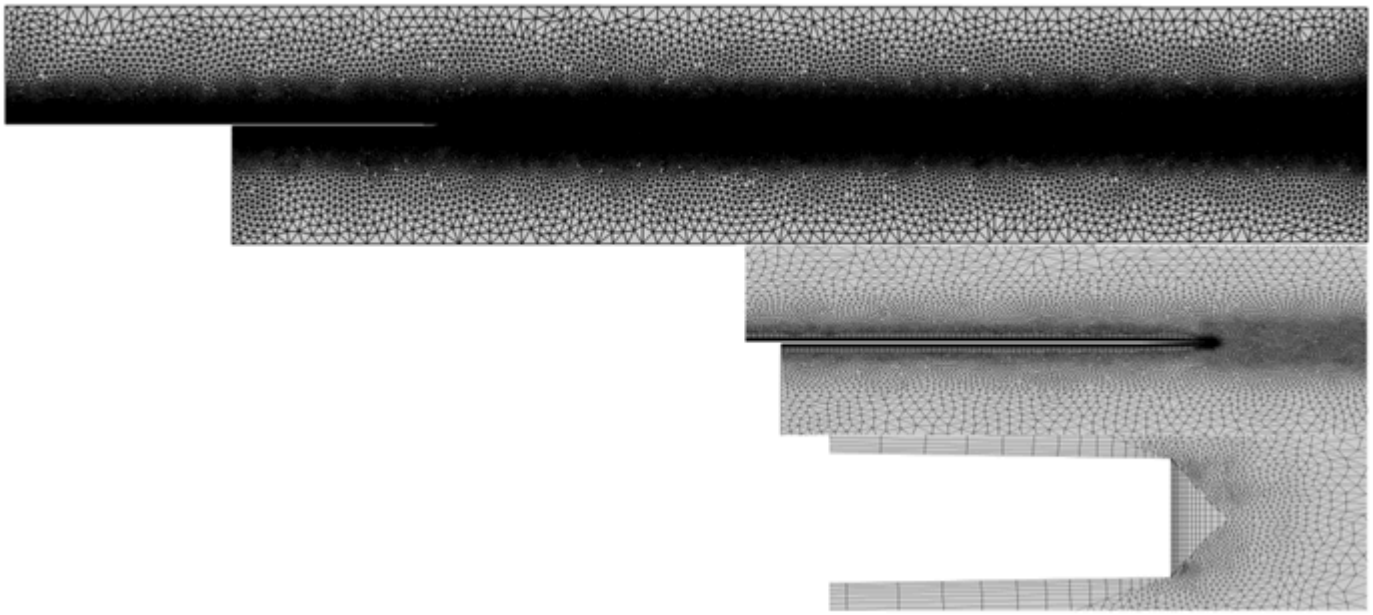


Figure 85: Mesh used for Simulating the Turbulent Mixing Layer Showing Close up Images Near the Trailing Edge of the Plate

The simulation was performed as a two dimensional problem by constructing a volume mesh that contains a single layer of elements extruded in the cross stream direction, normal to the flow plane and by imposing symmetry boundary conditions on the extruded planes. The upper and lower walls are specified as slip, the splitter plate is specified as no-slip and the inlet velocity and eddy viscosity are prescribed as constant values.

AcuSolve Results

The AcuSolve solution converged to a steady state and the results reflect the mean flow conditions within the open channel. The simulation result shows a developing flow field with the fluids fully separated as they pass the edge of the splitter plate. As the fluid travels downstream of the splitter plate, the dissimilar velocity fields produce a shear layer that results in momentum exchange between the two streams. The shear layer diffuses as the fluid travels further downstream. The relative velocity as a function of the normalized boundary layer height is computed from AcuSolve and compared with experimental data at three measurement stations, 0.2 m, 0.65 m and 0.95 m away from the trailing edge of the plate, as described in Delville, 1989. The image below shows black circles representing the experimental data and a solid red line for the AcuSolve results.

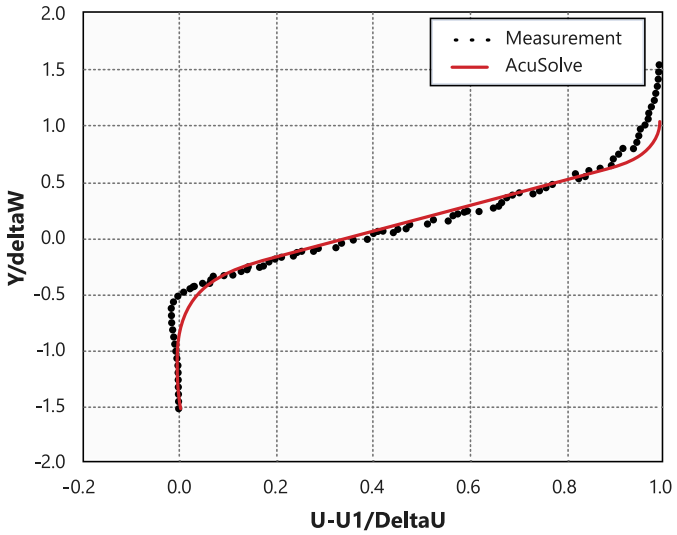


Figure 86: Relative Velocity within the Channel Compared Against Experimental Data Showing Experimental and Simulated Results for the SA Turbulence Model

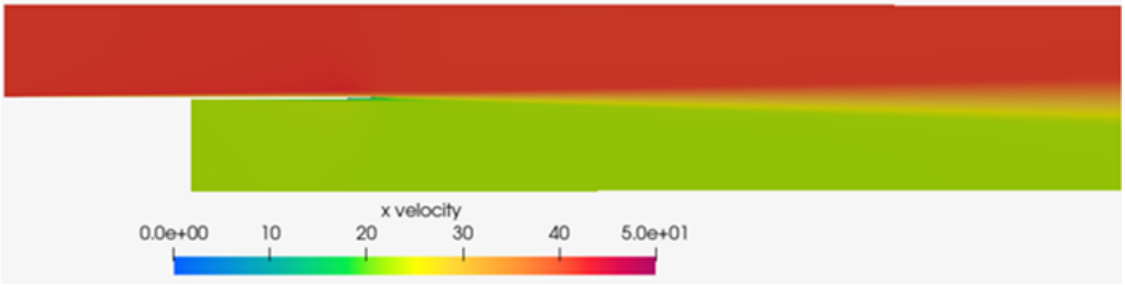


Figure 87: Velocity Magnitude Within the Channel

Summary

The AcuSolve solution compares well with experimental data for turbulent mixing within an open channel. In this application, the shear layer resulting from the dissimilar velocities of the incoming fluid streams results in an exchange of momentum within the channel. The amount of numerical dissipation from the grid is kept to a minimum to produce a good agreement with the experimental data. The good agreement with experimental results for the simulated turbulence model compares well with the measurement and previously published results, demonstrating that AcuSolve is capable of predicting turbulent mixing layers with relatively modest grid levels and the one equation turbulence model.

Simulation Settings for Turbulent Mixing Layers in an Open Channel

HyperWorks CFD database file: `<your working directory>\mixing_layer_turbulent\mixing_layer_turbulent.hm`

Global

- Problem Description
  - Analysis type - Steady State
  - Turbulence equation - Spalart Allmaras

- Auto Solution Strategy
  - Max time steps - `100`
  - Convergence tolerance - `0.001`
  - Relaxation Factor- `0.4`
- Material Model
  - Air
    - Type - Constant
    - Density - `1.2` kg/m3
    - Viscosity - `1.7189e-5` kg/m*sec

  Model
- Volumes
  - Volume
    - Element Set
      1. Material model - Air
- Surfaces
  - Back
    - Simple Boundary Condition
      1. Type- Symmetry
  - Front
    - Simple Boundary Condition
      1. Type- Symmetry
  - InletLower
    - Simple Boundary Condition
      1. Type- Inflow
      2. Inflow type- Velocity
      3. X Velocity- `22.4` m/sec
      4. Turbulence input type- Direct
      5. Eddy Viscosity- `0.0001432`
  - InletUpper
    - Simple Boundary Condition
      1. Type- Inflow
      2. Inflow type- Velocity
      3. X Velocity- `41.54` m/sec
      4. Turbulence input type- Direct
      5. Eddy Viscosity- `0.0001432`
  - Outlet
    - Simple Boundary Condition
      1. Type - Outflow

- Slip
  - Simple Boundary Condition
    1. Type- Slip
- SplitterPlate
  - Simple Boundary Condition
    1. Type - Wall
- TE
  - Simple Boundary Condition
    1. Type- Wall

References

Delville, J., Bellin, S., Garem, J. H., and Bonnet J. P., "Analysis of Structures in a Turbulent, Plane Mixing Layer by Use of a Pseudo Flow Visualization Method Based on Hot-Wire Anemometry," in: Advances in Turbulence 2, eds: H.-H. Fernholz and H. E. Fiedler, Proceedings of the Second European Turbulence Conference, Berlin, Aug. 30-Sept. 2, 1988, Springer Verlag, Berlin, 1989, pp. 251-256.

Turbulent Flow Through a Heated Periodic Channel

In this application, AcuSolve is used to solve for the flow and temperature field within a channel containing a heated wall. The wall is maintained at a constant temperature, inducing heat flux into the fluid, to predict the thermal law of the wall. The non dimensional temperature versus the non dimensional height above the wall is compared to the analytical correlation provided by Kader.

Problem Description

The problem consists of a fluid having material properties close to air with a density of 1.0 kg/m^3, molecular viscosity of 0.0001 kg/m-s, specific heat of 1005.0 J/kg-K and thermal conductivity of 0.139 W/m-K. The properties are specified to obtain a Prandtl number of 0.72. The velocity is defined as periodic and is driven by a constant acceleration body force equal to 2.0 m/s^2. The temperature is specified as periodic+unknown ratio allowing it to develop until it reaches a steady solution. The simulation description is shown in the following image, which is not drawn to scale. The model is simulated using the one equation Spalart Allmaras turbulence model along with the advective-diffusive temperature equation. The thermal wall distribution is validated against correlation data published by Kader 1981.

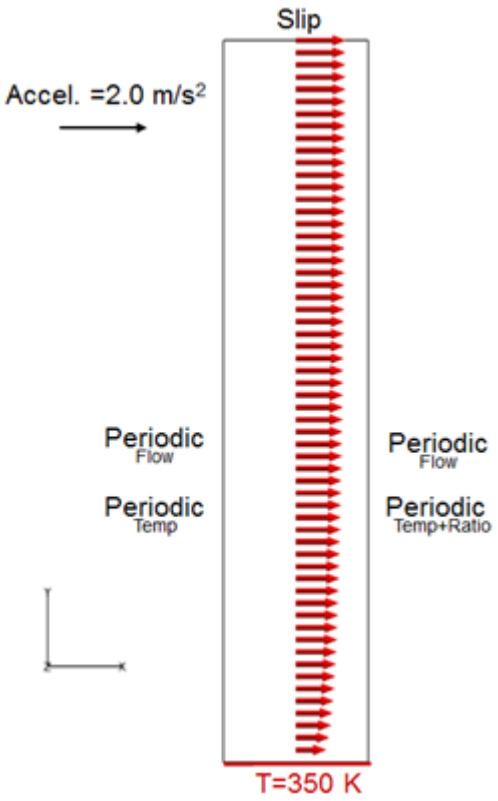


Figure 88: Critical Parameters used For Simulating Periodic Flow Within a Heated Channel

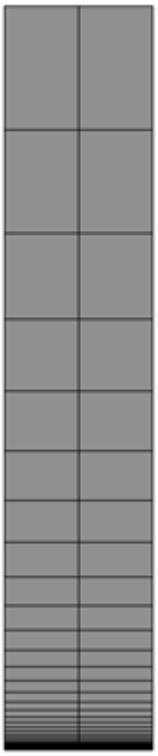


Figure 89: Mesh used For Simulating Periodic Flow Within a Heated Channel

The simulation was performed as a two dimensional problem by constructing a volume mesh that contains a single layer of elements extruded in the cross stream direction, normal to the flow plane and by imposing periodic boundary conditions on the extruded planes. The streamwise direction contains two elements allowing the flow and temperature solution to develop. Only the lower half of the channel is modeled, assuming the solution is mirror across the top slip plane.

AcuSolve Results

The AcuSolve solution converged to a steady state and the results reflect the mean flow conditions within the channel. The simulation results demonstrate that the channel wall induces a thermal flux into the flow field, producing a temperature distribution dependent on the distance from the wall. The thermal law of the wall computed from the AcuSolve results is compared with correlation data for the corresponding Prandtl number, as demonstrated in Kader 1981. The plot shown below gives the non dimensional value of T+ as a function of Y+, where T+ and Y+ are computed per the following relationships:

$$T+ = \frac{(Tw - T)\rho C p u\tau}{\dot{Q}} T \tag{2}$$

$$Y+ = \frac{yu\tau}{v} \tag{3}$$

$$u\tau = \sqrt{\tau w / \rho} \tag{4}$$

Where $T+$, Tw is the fixed wall temperature, T is the temperature away from the wall, ρ is the fluid density, Cp is the fluid specific heat, uT is computed from the magnitude of the shear stress and $\dot{Q}_i$ is the local surface heat flux.

The image below shows black circles representing the correlation data and a solid red line for the AcuSolve results. The results demonstrate that the temperature distribution away from the wall is resolved properly and compares well with the correlation. Since an empirical relationship for T+ is used for comparison, there will be minor discrepancies compared with the simulation results. Additional comparisons have been made against DNS results for T+ from Kawamura et al. 1998.

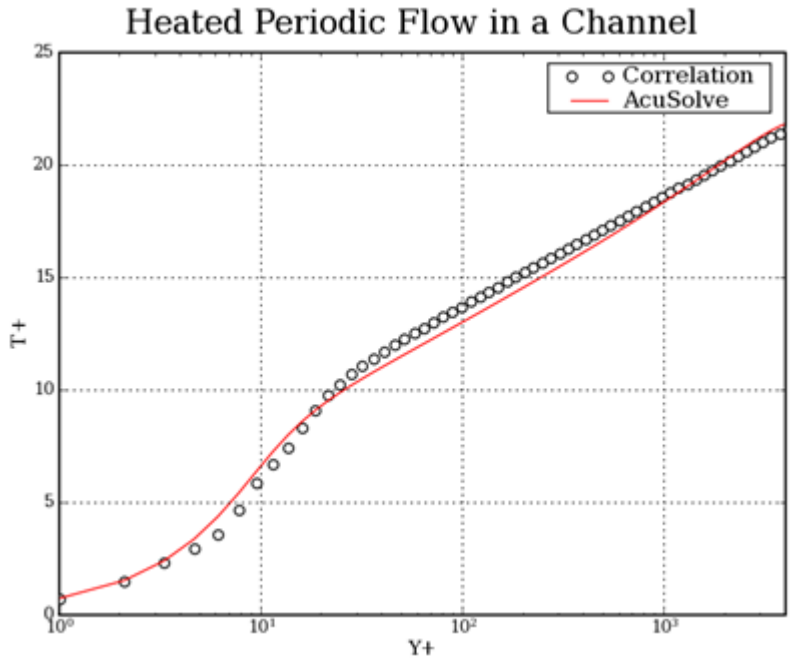


Figure 90: Thermal Boundary Layer Within the Heated Channel Compared Against the Correlation Data

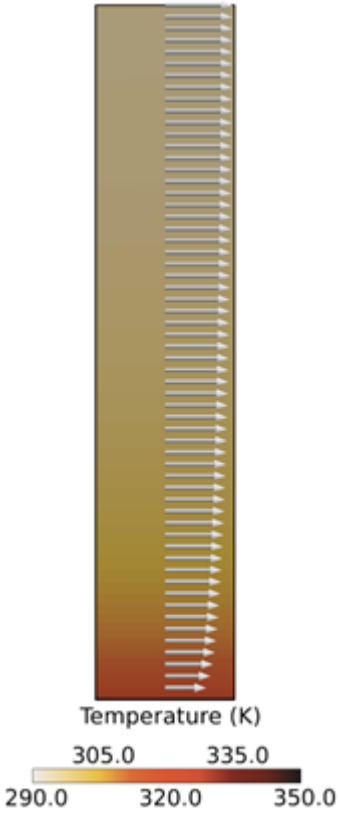


Figure 91: Contours of Temperature and Vectors Representing the Fluid Velocity Within the Channel

Summary

The AcuSolve solution compares well with the correlation data for turbulent flow within a heated channel. In this application, the constant temperature wall induces a surface heat flux, giving rise to a temperature gradient within the channel. AcuSolve can capture the correct temperature gradient at any location above the wall if an appropriate first layer height is selected to resolve a Y+ value of 1.0. The good agreement with correlation data for T+ demonstrates that AcuSolve can predict the locally varying temperature distribution within a turbulent channel.

Simulation Settings for Turbulent Flow Through a Heated Periodic Channel

AcuConsole database file: `<your working directory>\channel_periodic_heat\channel_periodic_heat.acs`

Global

- Problem Description
  - Analysis type - Steady State
  - Temperature equation - Advective Diffusive
  - Turbulence equation - Spalart Allmaras
- Auto Solution Strategy
  - Max time steps - `50`

- Convergence tolerance - `0.0001`
- Relaxation Factor - `0.4`
- Temperature - On

- Material Model
  - Fluid
    - Type - Constant
    - Density - `1.0` kg/m3
    - Viscosity - `1.0e-4` kg/m*sec
    - Specific Heat - `1005.0` J/kg*K
    - Conductivity - `0.139` W/m*K
- Body Force
  - BodyForce
    - Gravity
      1. X-component - `2.0` m/sec2

Model

- Volumes
  - Fluid
    - Element Set
      1. Material model - Fluid
      2. Body force - BodyForce
- Surfaces
  - Symmetry_1
    - Simple Boundary Condition - (disabled to allow for periodic conditions to be set)
  - Symmetry_2
    - Simple Boundary Condition - (disabled to allow for periodic conditions to be set)
  - Inflow
    - Simple Boundary Condition - (combination of integrated BC and periodic BC set)
    - Advanced Options
      1. Integrated Boundary Conditions - Temperature - `300.0` K
  - Outflow
    - Simple Boundary Condition - (disabled to allow for periodic conditions to be set)
  - Slip_surface
    - Simple Boundary Condition
      1. Type- Slip
  - Wall_surface
    - Simple Boundary Condition
      1. Type- Wall

        2. Temperature BC type - Value
        3. Temperature - `350.0` K

- Periodics
  - 2D
    - Periodic Boundary Conditions
      1. Type - Periodic
  - Flow
    - Periodic Boundary Conditions
      1. Type - Periodic
  - Temperature
    - Individual Periodic BCs
      1. Temperature: Type - Single Unknown Ratio
- Nodes
  - Fixed_pressure
    - Pressure: Type - Zero
  - Zero_z-velocity
    - Z-Velocity: Type - Zero

References

B.A. Kader, "Temperature and concentration profiles in fully turbulent boundary layers", International Journal of Heat and Mass Transfer, Volume 24, Issue 9, 1981, Pages 1541-1544.

H. Kawamura, K. Ohsaka, H. Abe and K. Yamamoto, "DNS of turbulent heat transfer in channel flow with low to medium-high Prandtl number fluid", International Journal of Heat and Mass Transfer, 19:482-491, 1998.

Two-Phase Nucleate Boiling in a Cylindrical Pipe

In this application, AcuSolve is used to simulate the changes in wall temperature due to two-phase nucleate boiling at the heated walls of a pipe with water flowing through it. AcuSolve results are compared with experimental results adapted from Koncar and others (2015). The close agreement of AcuSolve results with experimental results validates the ability of AcuSolve to model two-phase nucleate boiling problems.

Problem Description

The problem consists of a pipe with heated surrounding walls, as shown in the following image, which is not drawn to scale. The length of the pipe is 2 m and the radius is 0.0017 m. Mass flux at the inlet is 900 kg/m^2 and the temperature of the fluid entering the pipe is 473 K. A heat flux of 570,000 W/m^2 is applied on the walls. The preheated water enters the inlet and heat is transferred to the fluid from the walls. The heat causes sub-cooled boiling to occur in the region close to the wall and leads to the formation of bubbles at nucleation sites.

During sub-cooled boiling flow, heat and mass exchange between the phases takes place on the heated wall and in sub-cooled liquid flow. On the heated surface the vapor bubbles are generated and as they move through the sub-cooled liquid they condense and release the latent heat.

The AcuSolve simulation is set up to model transient state heat transfer to determine the temperature along the centerline of the pipe and along the heated pipe walls of the model. AcuSolve computes the two-phase nucleate boiling by simulating the three-dimensional flow in a heated pipe for two-phase boiling flow, as described in Koncar (2005). The temperatures along the centerline of the pipe and along the pipe walls are compared against the experimental measurements, as described in Koncar, et al. (2005).

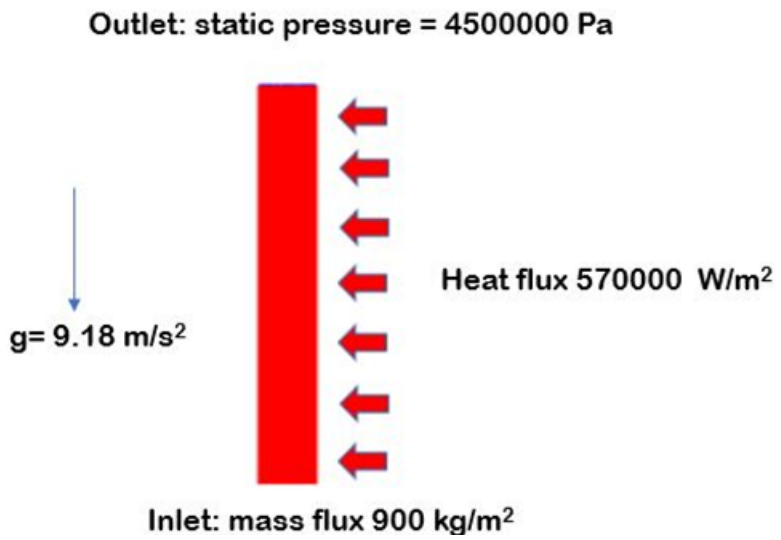


Figure 92: Parameters for Simulating a Two-Phase Nucleate Boiling Problem of a Pipe

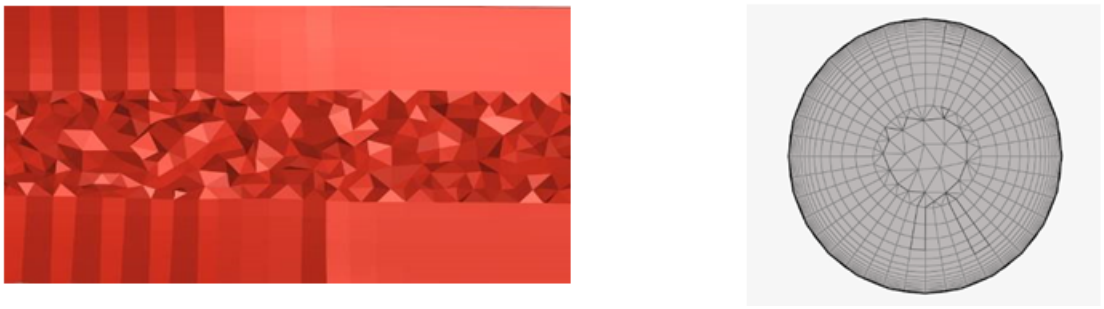


Figure 93: Mesh used for Simulating Two-Phase Flow in a Pipe

AcuSolve Results

The AcuSolve solution is run for a heat flux of 570,000 W/m^2 and the results are presented in the following image. The experimental values of wall temperature are presented with the corresponding AcuSolve results along the centerline of the pipe and along the pipe wall. The AcuSolve results show good agreement with the experimental results for the temperature, indicating that the two-phase nucleate boiling is properly captured.

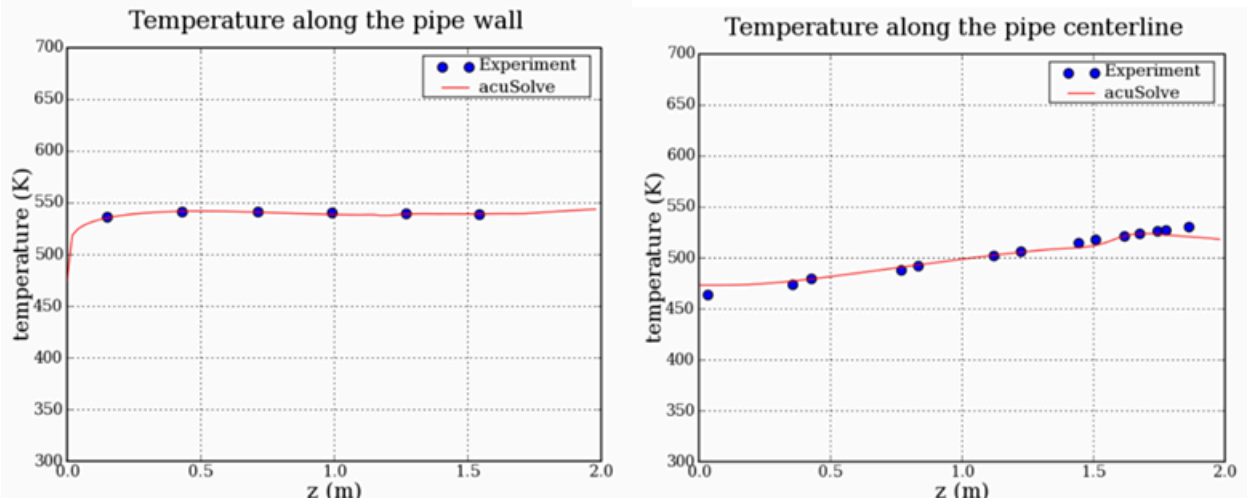


Figure 94: Temperature Values for Varying Streamwise Distance Compared to Experimental Data

Summary

The AcuSolve solution compares well with experimental results for two-phase nucleate boiling simulations. In this application, the temperature of the wall as the onset of boiling approaches are simulated with AcuSolve using the nucleate boiling feature and the SA turbulence model. The experimental values of temperature are presented with the corresponding AcuSolve results. A good agreement of simulation results with the experiment validates the ability to solve two-phase nucleate boiling using the nucleate boiling capabilities of AcuSolve.

Simulation Settings for Two-Phase Nucleate Boiling in a Cylindrical Pipe

HyperWorks database file: `<your working directory>\pipe_two_phase_boiling\pipe_two_phase_boiling.hm`.

Global

- Problem Description
  - Analysis type – Transient
  - Turbulence equation – SA
  - Temperature equation – Advective Diffusive
- Auto Solution Strategy
  - Maximum time steps – `500`
  - Initial time increment – `0.003`
  - Convergence Tolerance – `0.001` sec
  - Relaxation factor – `0.3`
- Surface Tension Model (“Water_NB-Vapor_NB”)
  - Type – Constant
  - Surface Tension – `0.02382`
- Material Model
  - Vapor_NB
    - Type – Constant
    - Density – `23.75` kg/m^3
    - Viscosity – `1.79e-05` kg/m-sec
    - Specific Heat – `4225` J/kg-K
    - Latent Heat – `1675570`
    - Latent Heat Temperature – `530.55` K
    - Conductivity – `0.02528` W/m-K
  - Water_NB
    - Type – Constant
    - Density – `800` kg/m3
    - Viscosity – `0.0001339` kg/m-sec
    - Specific Heat – `4500` J/kg-K
    - Conductivity – `0.65` W/m-K
- Multifield parameter (Field interaction model)
  - Type – Algebraic Eulerian
  - Phase change type – Wall Boiling
  - Carrier field - Water
  - Disperse field – Vapor
  - Disperse field diameter type – Boiling kurul exponential
  - Drag model – Ishii zuber
  - Lift Model – Legendre Magnaudet

Model

- Volumes
  - Fluid
    - Material – Vapor_Water
- Surfaces
  - Inflow
    - Simple Boundary Condition – Inflow
    - Inflow type – Mass Flux Rate
    - Mass Flux Rate – `0.167634` kg/sec
    - Temperature – `473` K
  - Outflow
    - Simple Boundary Condition – Outflow
    - Pressure – `4500000` N/m2
  - Wall
    - Simple Boundary Condition – Wall
    - Temperature type – Flux
    - Heat Flux – `570000` W/m2

References

B. Koncar, E. Krapper, Y. Egorov, 2005, "CFD MODELING OF SUBCOOLED FLOW BOILING FOR NUCLEAR ENGINEERING APPLICATIONS", International Conference Nuclear Energy for New Europe 2005, Bled, Slovenia, September 5-8,2005.

Supersonic Flow Through a Converging-Diverging Nozzle

In this application, AcuSolve is used to simulate the high-speed turbulent flow in a converging and then diverging nozzle. The flow within the nozzle enters as subsonic, reaches sonic at the throat and shortly after develops a normal shock. AcuSolve results are compared with experimental results adapted from Bogar and Sajben (1983). The close agreement of AcuSolve results to experimental measurements validates the ability of AcuSolve to simulate internal supersonic flows where normal shocks are present.

Problem Description

The problem consists of a converging and then diverging nozzle represented as an extruded planar surface, as shown in the image below, which is not drawn to scale. The length of the domain is 0.213 m with a throat height of 0.044 m. The stagnation pressure and static temperature are constrained at the inlet to 135,000 Pa and 265.98 K, respectively. The static pressure is defined using the outflow boundary condition, where P_{static}=97216.08 Pa. The flow in the diffuser has an inlet Reynolds number of $6.5x10^5$. The upper and lower walls are set to no-slip and the side walls are set to slip, while the exterior walls are specified to be adiabatic. Images of the numerical mesh are shown below.

The AcuSolve simulation is prepared to model the pseudo-transient state to determine the shock location and corresponding scalar quantities within the diffuser. AcuSolve computes the flow and thermal solution by simulating a planar, two-dimensional flow problem with physical dimensions and input quantities as described in the Sajben Diffuser case presented by Bogar and Sajben (1983). The gas in the simulation domain enters at subsonic conditions and is forced to accelerate beyond Mach=1.0 as it passes through the throat. After reaching supersonic speed a normal shock wave develops causing the flow speed to reduce back below sonic. The pressure along the bottom wall of the diffuser is compared against experimental measurements to demonstrate the solver's capability to solve supersonic cases.

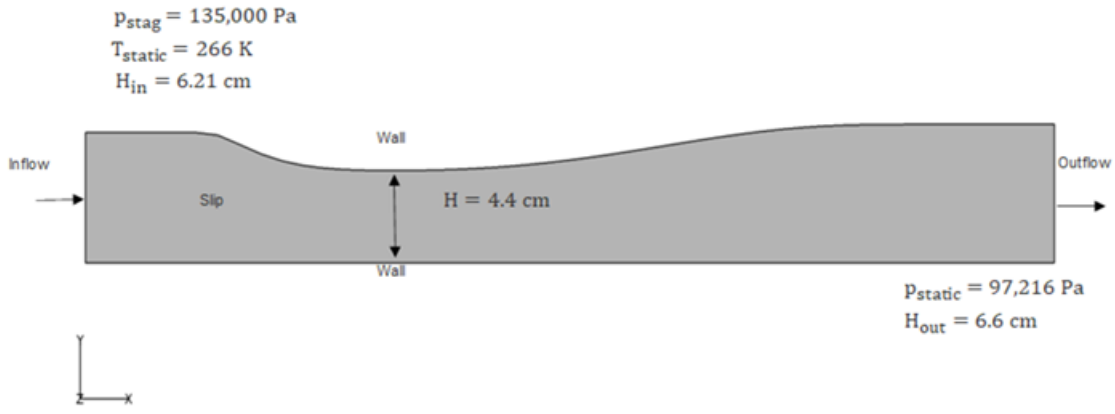


Figure 95: Parameters for Simulating Compressible Flow within a Converging-Diverging Nozzle

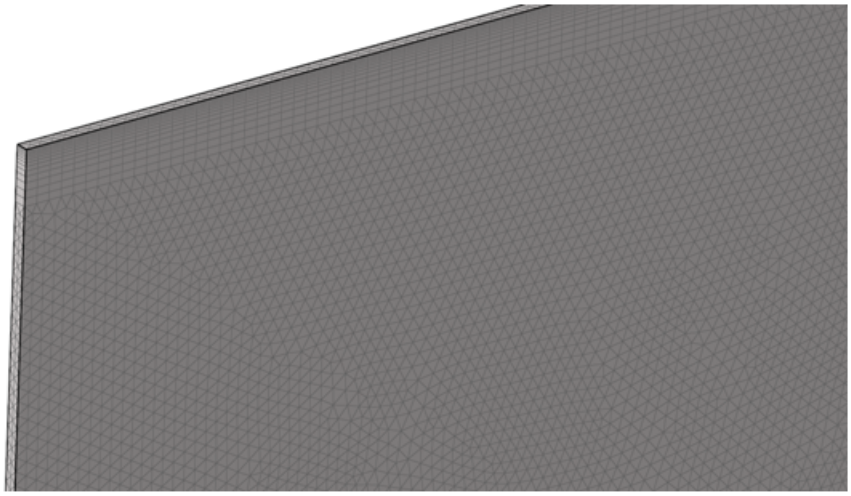


Figure 96: Mesh used for Simulating Compressible Flow in a Converging-Diverging Nozzle

AcuSolve Results

The AcuSolve solution is run for 0.025 seconds (6,250 timesteps with dt=4.0x10^{-6}sec) and converges to a pseudo-steady solution. The change in pressure from the inlet to outlet causes the flow to accelerate within the throat of the diffuser until it reaches approximately Mach=1.35. A normal shock is present just downstream of where the cross-sectional area of the nozzle increases, as shown in the image below. The numerical solution can be compared with the reference after normalizing the pressure along the wall by the inlet stagnation pressure (135 kPa) and the distance along the bottom wall by the nozzle throat height (0.044 m). The image below shows the normalized pressure versus normalized distance in comparison to NASA reference and experimental results. The image shows black circles representing the experimental measurements (Bogar and Sajben 1983), a dashed blue line representing the SA solution as obtained through NASA publication (Mohler 2005) and a solid red line representing the AcuSolve results with the Spalart-Allmaras turbulence model. The non-dimensional pressure within the diffuser agrees well with the reference data, demonstrating the correct physical location of the normal shock and expected moderate flow speed reduction within the constant cross-section diffuser portion of the nozzle.

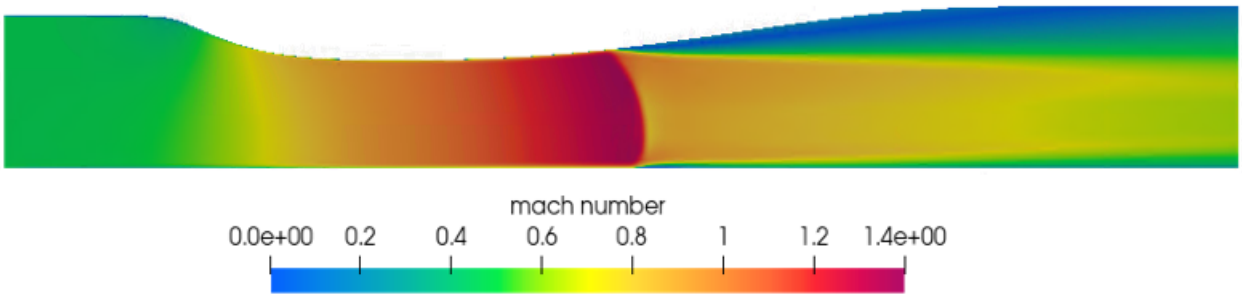


Figure 97: Contours of Mach Number within a Converging-Diverging Nozzle

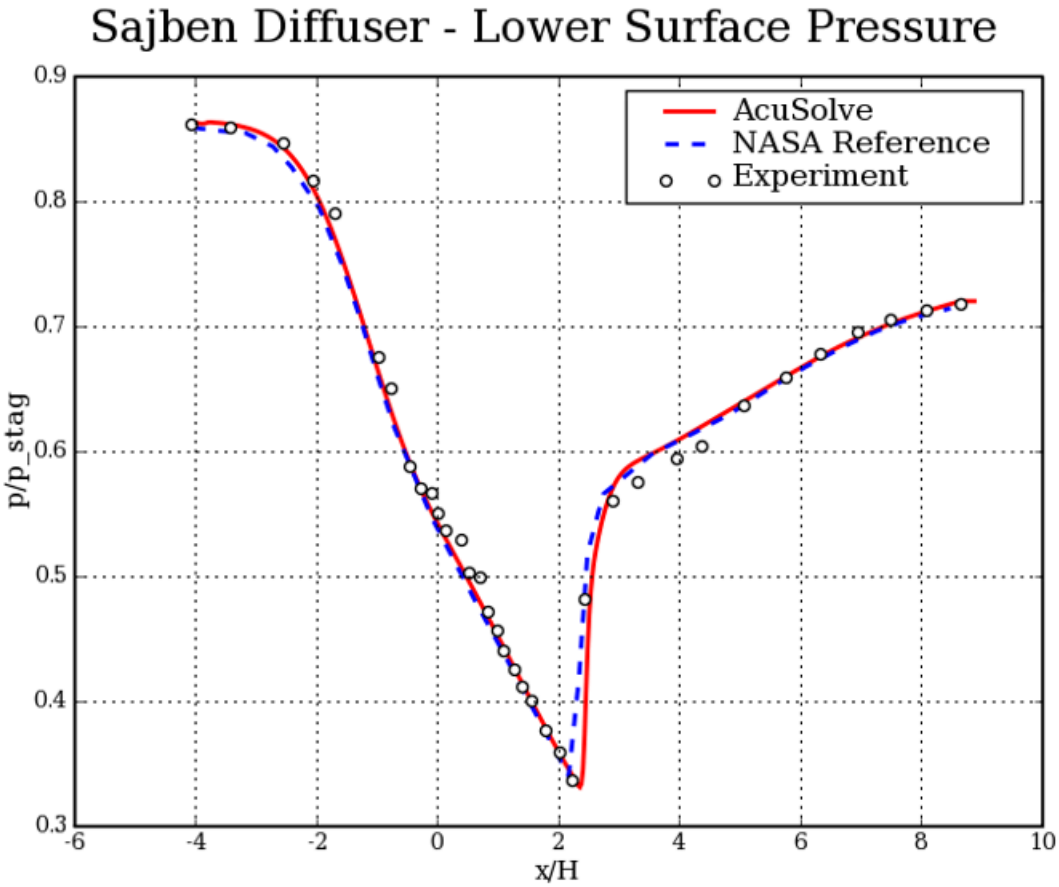


Figure 98: Normalized Pressure Versus Normalized Distance in Comparison to NASA Reference and Experimental Results

Summary

The AcuSolve solution compares well with experimental and numerical results for the described simulation. In this application, compressibility effects are accounted for using the coupled compressible flow solver with the ideal gas material definition. The thermal and momentum exchange within the nozzle is computed with AcuSolve using the compressible Navier-Stokes solver with the Spalart-Allmaras turbulence model. The experimental values of pressure are presented with the corresponding AcuSolve results and show good agreement, validating the ability to solve compressible cases with the presence of normal shocks. The results indicate that AcuSolve is able to properly predict the peak pressure magnitude and location within the diffuser while maintaining the normal shock when the time-step is selected to result in a maximum CFL of approximately 30.

Simulation Settings for Supersonic Flow Through a Converging-Diverging Nozzle

HyperWorks CFD database file: `<your working directory>\diffuser_compressible\diffuser_compressible.hm`

Global

- Problem Description

    - Flow – Compressible Navier Stokes
    - Analysis type – Transient
    - Turbulence equation – SA
    - Temperature equation – Advective Diffusive
- Auto Solution Strategy
    - Initial time increment – `4.0E-6`
    - Final time – `0.025` sec
    - Convergence Tolerance – `0.001` sec
    - Relaxation factor – `0.5`
- Material Model
    - Air-Ideal Gas
        - Type – Ideal_Gas
        - Viscosity – `1.781e-05` kg/m-sec
        - Specific Heat – `1005` J/kg-K
        - Conductivity – `0.02521` W/m-K
        - Gas Constant – `287.058` J/kg-K

Model

- Volumes
    - Fluid
        - Material – Air-Ideal Gas
- Surfaces
    - Inflow
        - Simple Boundary Condition – Inflow
        - Inflow type – Stagnation Pressure
        - Stagnation Pressure – `135000.0` N/m2
        - Turbulence_input_type – Direct
        - Eddy Viscosity – `1e-6` m^2/s
        - Temperature – `265.98` K
    - Outflow
        - Simple Boundary Condition – Outflow
        - Pressure – `97216.08` N/m2
    - Wall_1
        - Simple Boundary Condition – Wall
        - Type – auto_wall
    - Wall_2
        - Simple Boundary Condition – Wall
        - Type – auto_wall
    - Slip_1

        - Simple Boundary Condition – Slip
    - Slip_2
        - Simple Boundary Condition – Slip

References

Bogar, T. J., Sajben, M., and Kroutil, J. C. (1983) "Characteristic Frequencies of Transonic Diffuser Flow Oscillations," AIAA Journal, Vol. 21, No. 9, pp. 1232-1240.

Mohler, S.R., "Wind-US Unstructured Flow Solutions for a Transonic Diffuser," NASA CR-2005-213417, January 2005.

Steady Flow

3

This section includes validation cases that consider steady state flow simulations.

This chapter covers the following:

- Flow Between Concentric Cylinders (p. 137)
- Laminar Flow Through a Pipe With Imposed Heat Flux (p. 143)
- Turbulent Flow Through a Pipe (p. 148)
- Laminar Couette Flow with Imposed Pressure Gradient (p. 152)
- Laminar Couette Flow with Imposed Pressure Gradient and Heated Walls (p. 158)
- Laminar Poiseuille Flow Through a Pipe (p. 164)
- Laminar Flow Through a Pipe with Species Transport (p. 168)
- Flow Inside a Rotating Cavity (p. 174)
- Natural Convection in a Concentric Annulus (p. 182)
- Laminar Flow Past a 90° T-Junction (p. 188)
- Turbulent Flow Through a Wavy Channel (p. 193)
- Laminar Flow Through a Channel with Heated Walls (p. 201)
- Turbulent Flow Behind an Open-Slit V (p. 206)
- Turbulent Flow Over a NACA 0012 Airfoil (p. 213)
- Turbulent Natural Convection Inside a Tall Cavity (p. 221)
- Viscous Heating Inside a Rotating Annulus (p. 229)
- Separated Laminar Flow Over a Blunt Plate (p. 236)
- Laminar Flow Through a Pipe with Constant Wall Temperature (p. 243)
- Turbulent Flow with Separation in an Asymmetric Diffuser (p. 248)
- Turbulent Flow with Separation in an Axisymmetric Diffuser (p. 256)
- Turbulent Flow Over a Backward-Facing Step (p. 264)
- Turbulent Flow Past a Convex Curve in a Channel (p. 271)
- Turbulent Flow Past a Wall-Mounted Hump (p. 278)
- Heat Transfer Between Radiating Concentric Cylinders (p. 286)
- Turbulent Mixing Layers in an Open Channel (p. 292)
- Laminar to Turbulent Transition Over an Airfoil (p. 297)
- Turbulent Flow Through a 180 Degree Curved Channel (p. 302)
- Turbulent Flow Through a Heated Periodic Channel (p. 308)
- Heat Transfer Between Radiating Concentric Spheres (p. 314)
- Radiation Heat Transfer Through a Cube with a Specular Interface (p. 319)
- Single-Phase Nucleate Boiling in a Rectangular Channel (p. 326)

Flow Between Concentric Cylinders

In this application, AcuSolve is used to simulate the flow of water between concentric cylinders. The outer cylinder is held stationary while the inner cylinder rotates with a constant speed. AcuSolve results are compared with analytical results as described in White (1991). The close agreement of AcuSolve results with analytical results validates the ability of AcuSolve to model cases containing thin annular gaps with flow induced by rotating walls.

Problem Description

The problem consists of two concentric pipes with water filling the void between them, as shown in the following image, which is not drawn to scale. The radius of the outer pipe is 0.0468 m and the radius of the inner pipe is 0.0178 m. The inner cylinder rotates at 1 rad/sec and the outer cylinder is fixed. The induced flow is laminar and exhibits a steady state behavior. The rotation of the inner cylinder causes the fluid to rotate due to viscous shearing near the wall. As the outer cylinder is fixed, a velocity gradient is generated as a function of radius within the flow domain.

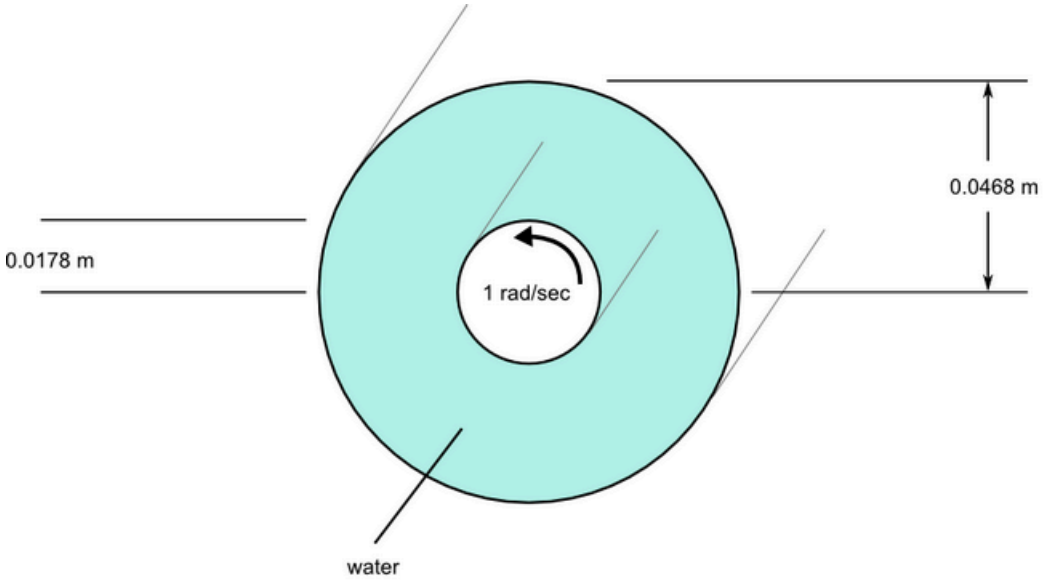


Figure 99: Critical Dimensions and Parameters for Simulating Flow Between Concentric Cylinders

The simulation was performed as a two dimensional problem by restricting flow in the out-of-plane direction through the use of a mesh that is one element thick.

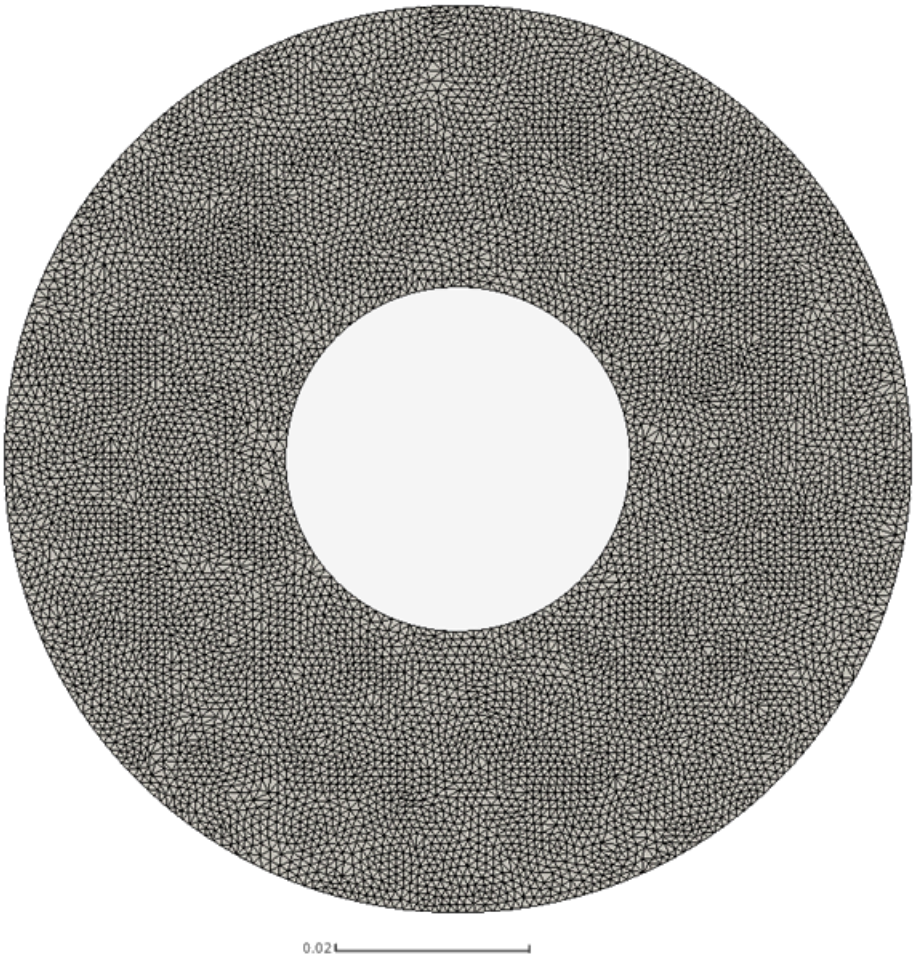


Figure 100: Mesh Used for Simulating Flow Between Concentric Cylinders

AcuSolve Results

The AcuSolve solution converged to a steady state and the results reflect the mean flow conditions. The velocity of the fluid within the cavity is greatest near the rotating inner cylinder. There is a nonlinear decrease in velocity as a function of distance away from the inner cylinder.

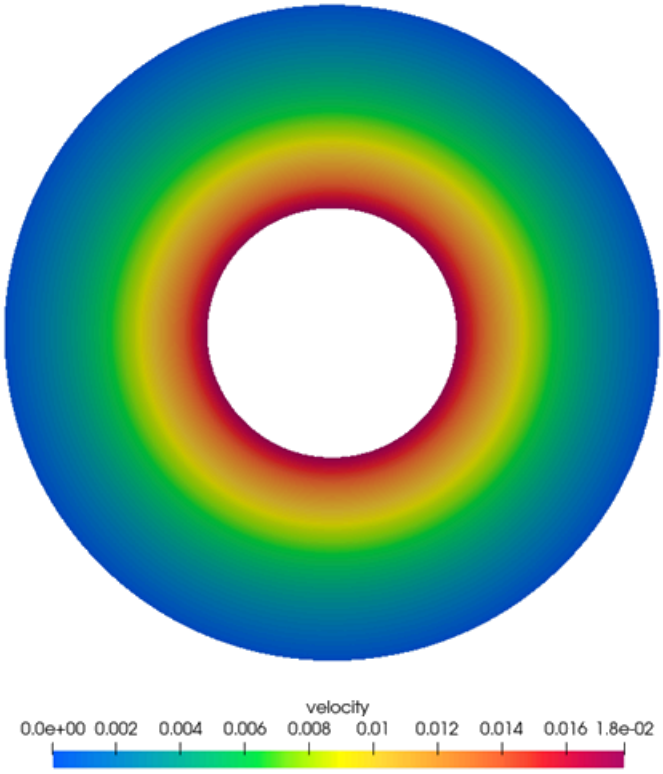


Figure 101: Contours of Tangential Velocity Between the Concentric Cylinders

Analytical tangential velocity at four distances away from the center of the rotating inner cylinder are presented with the corresponding AcuSolve results in the following table.

Table 4:

Distance from the center of rotating cylinder (m)	Analytical tangential velocity (m/s)	AcuSolve tangential velocity (m/s)	Percent deviation from analytical
0.020	0.01514	0.01514	0.04
0.025	0.01059	0.01058	0.10
0.030	0.00727	0.00727	0.06
0.035	0.00466	0.00466	0.10

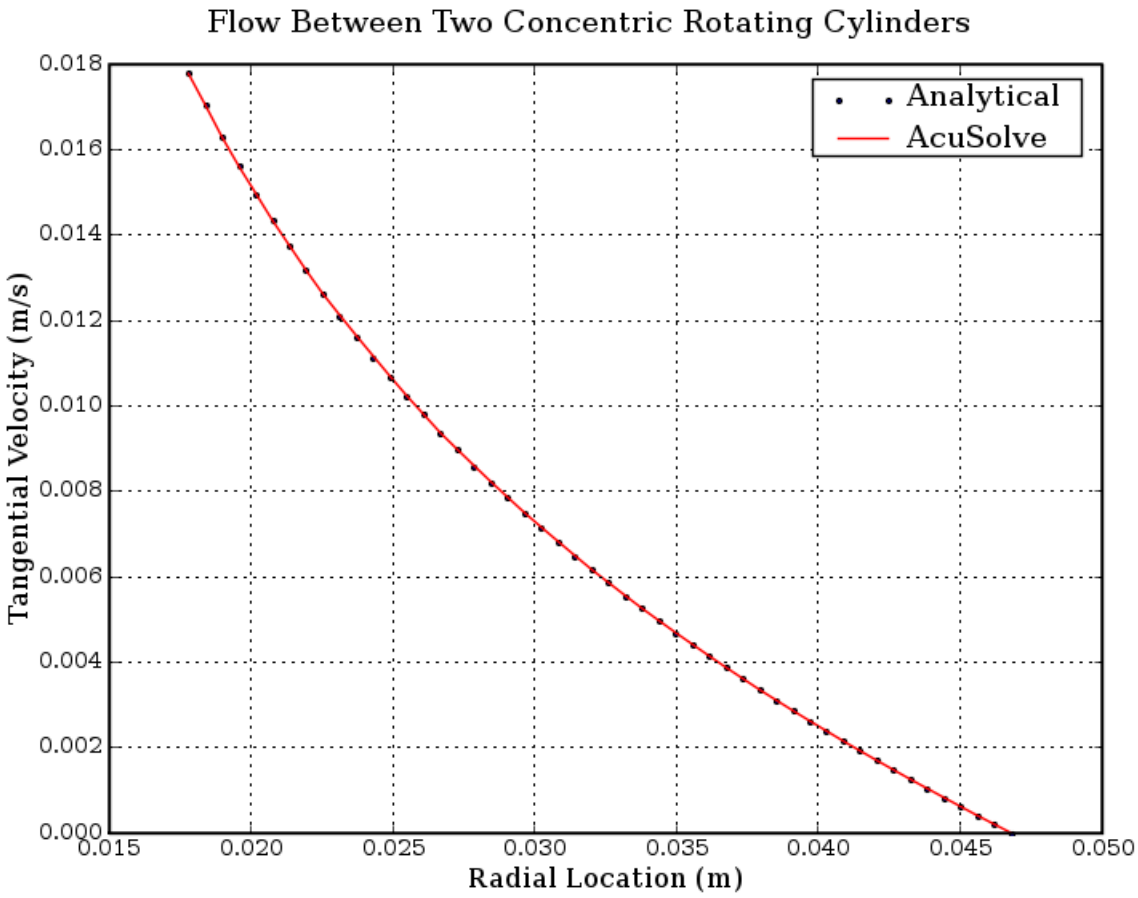


Figure 102: Tangential Velocity Plotted Against Distance from the Center of the Rotating Cylinder

Summary

The AcuSolve solution compares well with analytical results for the flow between concentric cylinders. In this application, the velocity in the annular fluid region is driven by the viscous stresses on the rotating wall. The AcuSolve tangential velocity is within 0.1 percent of the analytical solution at all radial locations.

Simulation Settings for Flow Between Concentric Cylinders

HyperWorks CFD database file: `<your working directory>\annulus_rotating\annulus_rotating.hm`

Global

- Problem Description
  - Analysis type - Steady State
  - Turbulence equation - Laminar
- Auto Solution Strategy
  - Relaxation Factor - `0.2`
- Material Model

- Water
  - Density - `1000.0` kg/m3
  - Viscosity - `0.001` kg/m-sec
- Reference Frame
  - Rotating_Cylinder
    - Rotation center
      1. X-coordinate - `0.0` m
      2. Y-coordinate - `0.0` m
      3. Z-coordinate - `0.0` m
    - Angular velocity
      1. X-component - `0.0` rad/sec
      2. Y-component - `0.0` rad/sec
      3. Z-component - `-1.0` rad/sec

Model

- Volumes
  - Volume
    - Element set
      1. Material model - Water
- Surfaces
  - Boundary1
    - Simple Boundary Condition
      1. Type - Symmetry
  - Boundary2
    - Simple Boundary Condition
      1. Type - Symmetry
  - Inner
    - Simple Boundary Condition
      1. Type - Wall
      2. Reference Frame - Rotating_Cylinder
  - Outer
    - Simple Boundary Condition
      1. Type - Wall
- Nodes
  - Fixed
    - Pressure
      1. Type - Zero

References

F. M. White. "Viscous Fluid Flow". Section 3-2.3. McGraw-Hill Book Co., Inc. New York. 1991.

Laminar Flow Through a Pipe With Imposed Heat Flux

In this application, AcuSolve is used to simulate the flow of mercury through a heated pipe. The AcuSolve results are compared with analytical results for pressure drop as described in White (1991), and with temperature changes as described in Incropera and DeWitt (1981). The close agreement of AcuSolve results with analytical results validates the ability of AcuSolve to model cases with flow and imposed heat flux.

Problem Description

The problem consists of mercury flowing through a heated, circular pipe that is 0.005 m in diameter and 0.1 m long, as shown in the following image, which is not drawn to scale. Mercury enters the pipe with a constant temperature of 300 K. The pipe has an imposed heat flux of 2000 W/m^2. The laminar velocity field is modeled as periodic to achieve a fully developed velocity profile. As the fluid moves through the pipe it is slowly heated by the heat flux on the wall, resulting in an increased centerline temperature. Pressure decreases along the pipe length due to the friction imposed by the viscous stresses near the pipe wall.

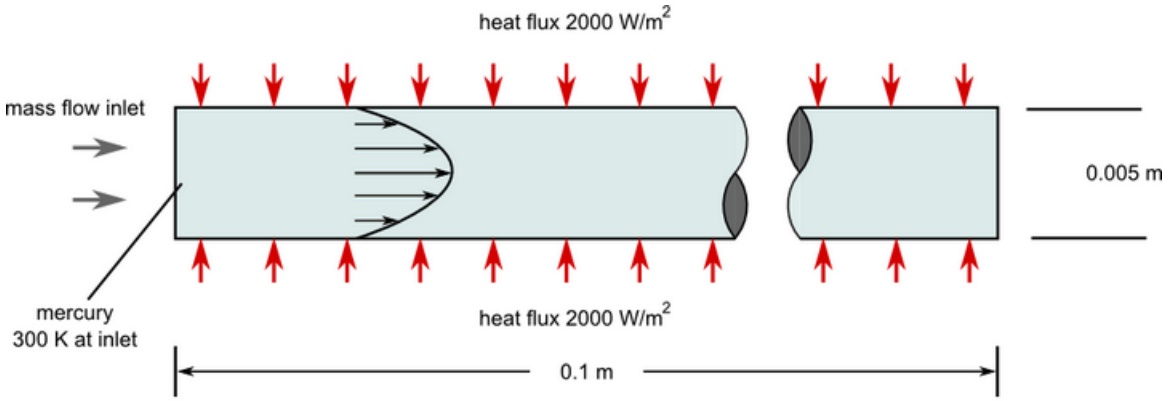


Figure 103: Critical Dimensions and Parameters for Simulating Laminar Flow through a Pipe with Imposed Heat Flux

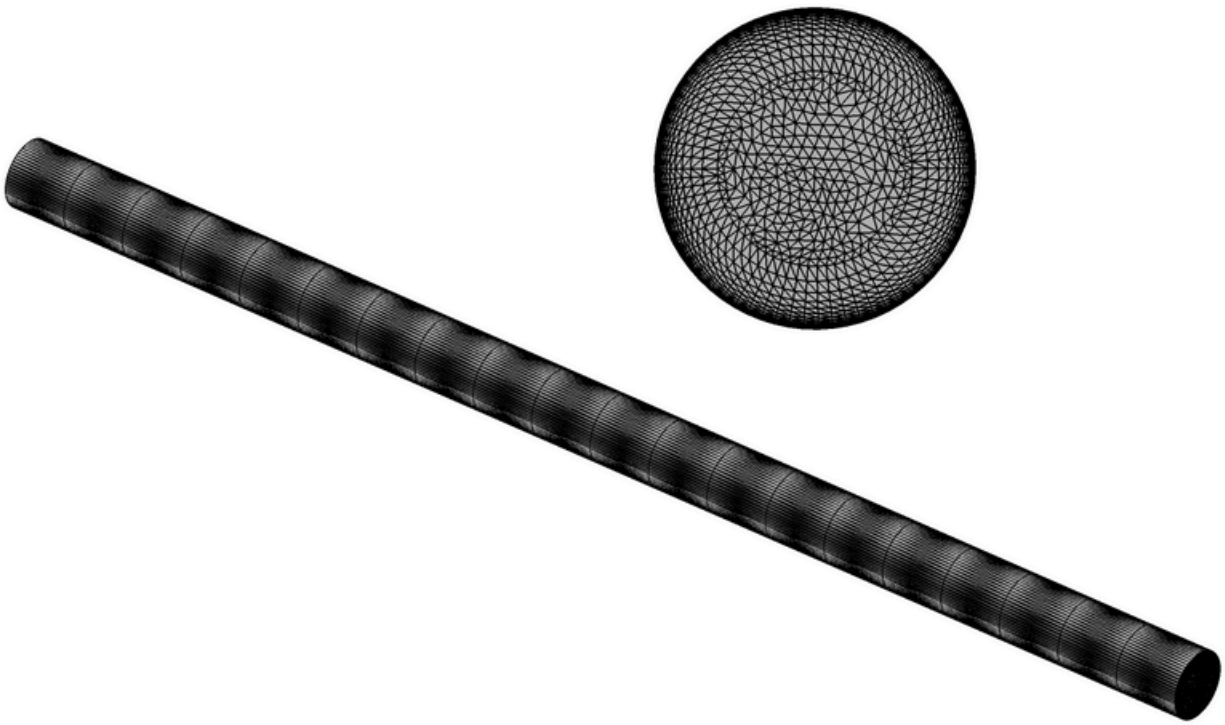


Figure 104: Mesh used for Simulating Laminar Flow Through a Pipe with Imposed Heat Flux

AcuSolve Results

The AcuSolve solution converged to a steady state and the results reflect the mean flow conditions. The greatest pressure is at the inlet, with pressure decreasing as a function of distance away from the inlet. The temperature of the mercury in the pipe increases as a function of distance from the inlet due to the impact of the heat flux on the pipe walls.

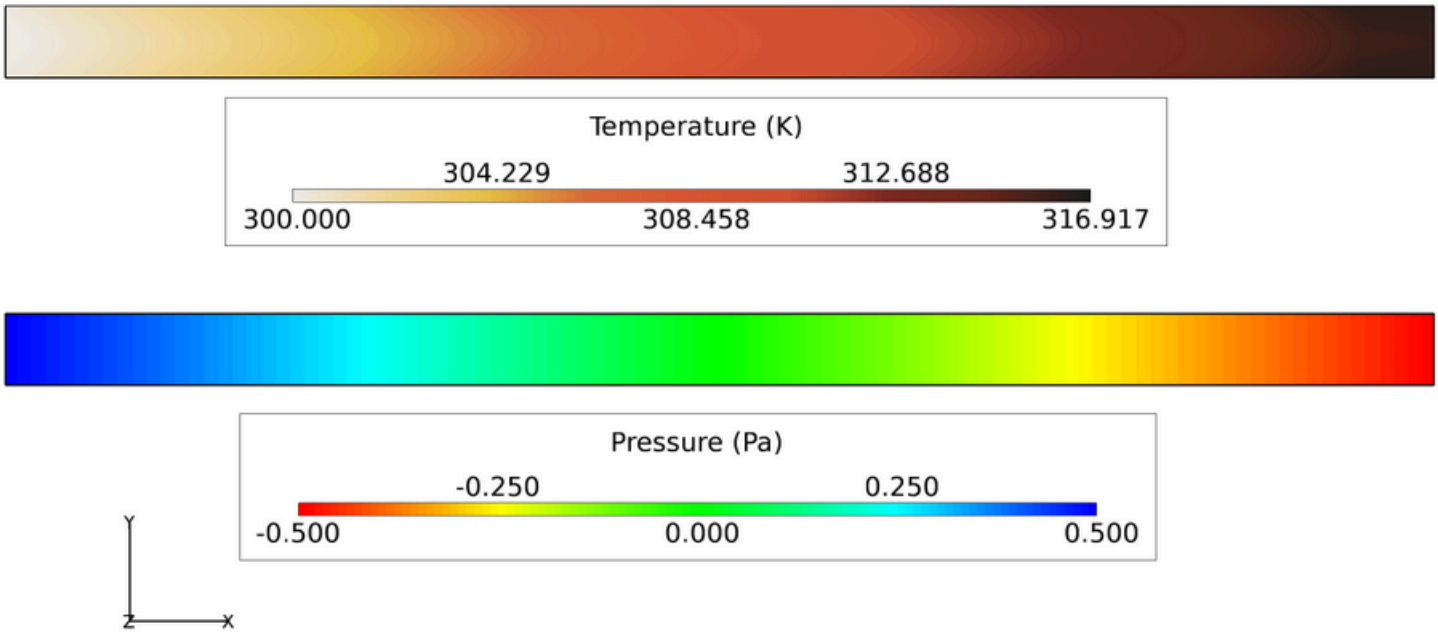


Figure 105: Temperature and Pressure Contours of Mercury Flow Through a Heated Pipe

The analytical solution for the pressure drop, between the inlet and outlet, as well as the analytical solution for the temperature of the mercury at the center of the outlet are presented with the corresponding AcuSolve results in the following table.

Table 5:

	Analytical solution	AcuSolve solution	Percent deviation from analytical
Pressure drop (Pa)	0.991	0.994	0.303
Centerline temperature of flow at outlet (K)	316.917	316.269	0.204

Summary

The AcuSolve solution compares well with analytical results for flow through a pipe with an imposed heat flux. In this application, the pressure drop in the fluid region is driven by the viscous stresses near the pipe wall. The temperature in the fluid region is influenced by the imposed heat flux on the walls. The values of pressure and temperature that are predicted by AcuSolve are within 0.3 percent of the analytical solution.

Simulation Settings for Laminar Flow Through a Pipe With Imposed Heat Flux

AcuConsole database file: `<your working directory>\pipe_laminar_heat\pipe_laminar_heat.acs`

Global

- Problem Description
  - Analysis type - Steady State
  - Temperature equation - Advective Diffusive
  - Turbulence equation - Laminar
- Auto Solution Strategy
  - Relaxation Factor - `0.2`
- Material Model
  - Mercury
    - Density - `13579.0` kg/m3
    - Viscosity - `0.001548` kg/m-sec

  Model
- Volume
  - Fluid
    - Element Set
      1. Material model - Mercury
- Surfaces
  - Inflow
    - Simple Boundary Condition - (disabled to allow for periodic conditions to be set)
    - Advanced Options
      1. Integrated Boundary Conditions
         1. Mass Flux
            1. Type - Constant
            2. Constant value - `-1.33e-3` kg/sec
         2. Temperature
            1. Type - Constant
            2. Constant value - `300.0` K
  - Outflow
    - Simple Boundary Condition - (disabled to allow for periodic conditions to be set)
  - Wall

        - Simple Boundary Condition
            1. Type - Wall
            2. Temperature BC type - Flux
            3. Heat flux - `2000.0` W/m2
- Periodics
    - Periodic 1
        - Individual Periodic BCs
            1. Velocity
                1. Type - Periodic
            2. Pressure
                1. Type - Single Unknown Offset
            3. Temperature
                1. Type - Single Unknown Offset

References

F. M. White. "Viscous Fluid Flow". Section 3-2.1. McGraw-Hill Book Co., Inc.. New York. 1991.

F. P. Incropera and D. P. DeWitt. "Fundamentals of Heat Transfer". John Wiley & Sons. New York. 1981.

Turbulent Flow Through a Pipe

In this application, turbulent flow of air through a pipe is simulated. AcuSolve results are compared with experimental results as described in White (1991) and extracted from the Moody chart. The close agreement of AcuSolve results with experimental results validates the ability of AcuSolve to model turbulent flow within pipes.

Problem Description

The problem consists of air flowing through a pipe 0.004 m in diameter and 0.02 m long, as shown in the following image, which is not drawn to scale. The AcuSolve simulation utilizes periodic boundary conditions to obtain the fully developed profile within the pipe. The defined pressure drop, applied as a body force on the fluid volume, offsets the change in pressure due to the friction created by the no-slip walls of the pipe. The Reynolds number for this problem is approximately 8,250.

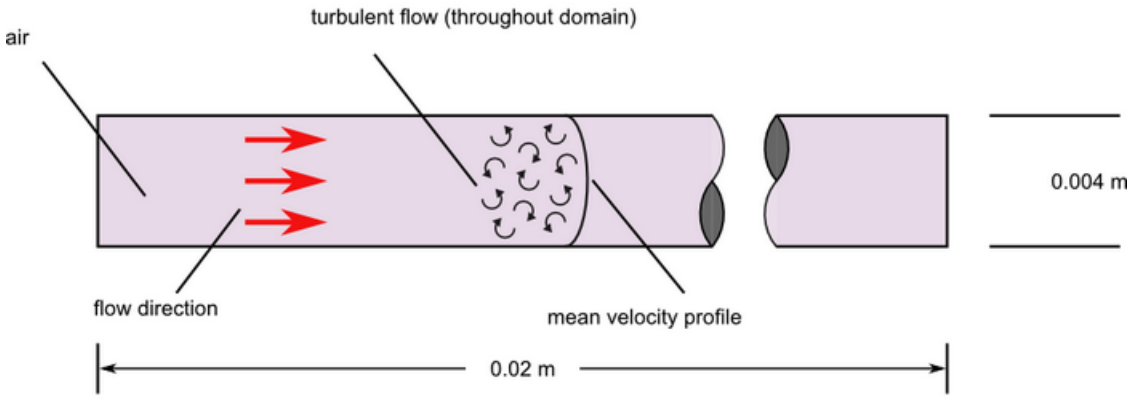


Figure 106: Critical Dimensions and Parameters for Simulating Turbulent Flow Through a Pipe

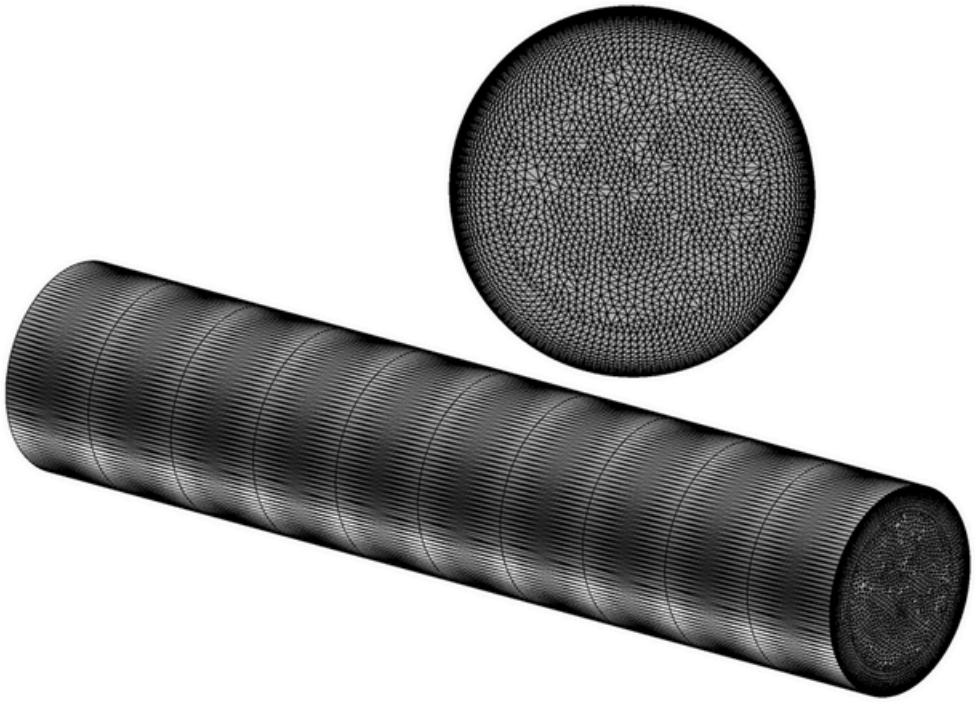


Figure 107: Mesh of a Periodic Segment Used for Simulating Turbulent Flow Through a Pipe

AcuSolve Results

The AcuSolve solution converged to a steady state and the results reflect the mean flow conditions with a turbulent velocity profile that is fully developed. The simulation was performed using the Spalart-Allmaras single-equation turbulence model. The velocity and eddy viscosity profiles are constant along the length of the pipe.

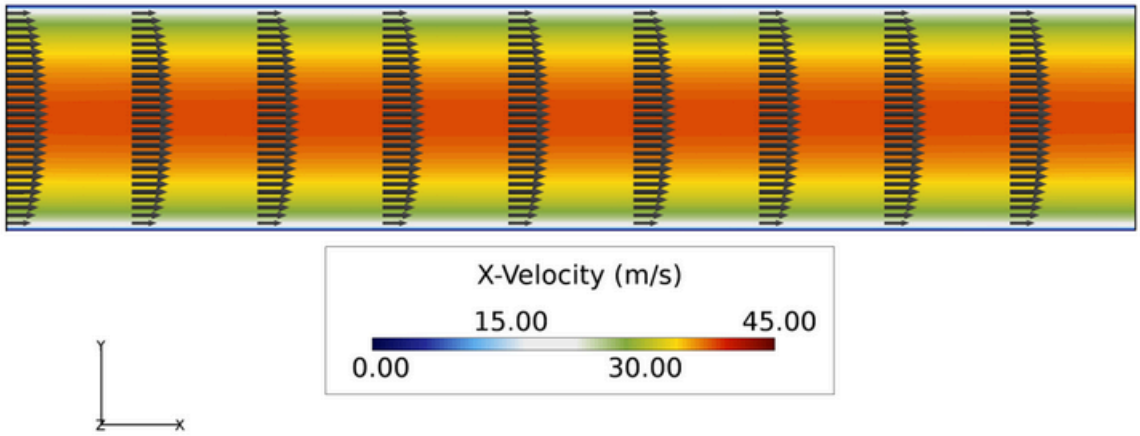


Figure 108: Velocity Contours and Periodic Velocity Vectors for the Averaged Turbulent Flow

The experimental result for average velocity at the inlet is presented with the corresponding AcuSolve prediction in the following table.

Table 6:

	Experimental result	AcuSolve prediction	Percent deviation from experimental
Average inlet velocity	30.0	29.71	0.971

Summary

The AcuSolve solution compares well with the experimental result for average inlet velocity for turbulent flow through a pipe. In this application, the applied body force counteracts the change in pressure due to the viscous stresses near the pipe wall. The resulting friction factor for a smooth wall pipe and the specified Reynolds number is approximately 0.0326. With the imposed pressure drop defining the flow, the AcuSolve prediction of average inlet velocity is within 1.0 percent of the Darcy-Weisbach approximation.

Simulation Settings for Turbulent Flow Through a Pipe

AcuConsole database file: `<your working directory >\pipe_turbulent\pipe_turbulent.acs`.

Global

- Problem Description
  - Analysis type - Steady State
  - Turbulence equation - Spalart Allmaras
- Auto Solution Strategy

    - Relaxation factor - `0.4`
- Material Model
    - Air
        - Density - `1.225` kg/m3
        - Viscosity - `1.781e-05` kg/m-sec
- Body Force
    - dpdx
        - Gravity
            1. X-component - `3739.98` m/s2

  Model
- Volumes
    - Fluid
        - Element Set
            1. Material model - Air
            2. Body force - dpdx
- Surfaces
    - Inlet
        - Simple Boundary Condition - (disabled to allow for periodic conditions to be set)
    - Outlet
        - Simple Boundary Condition - (disabled to allow for periodic conditions to be set)
    - Wall
        - Simple Boundary Condition
            1. Type - Wall
            2. Roughness height - `0.0` mm
- Periodics
    - Periodic 1
        - Periodic Boundary Condition
            1. Type - Periodic

References

F. M. White. "Viscous Fluid Flow". Section 3-2.1. McGraw-Hill Book Co., Inc.. New York. 1991.

Experimental solution adapted from Darcy-Weisbach equation based on friction factor taken from the Moody chart with a Reynolds number of approximately 8,250.

Laminar Couette Flow with Imposed Pressure Gradient

In this application, AcuSolve is used to simulate the viscous flow of water between a moving and a stationary plate with an imposed pressure gradient. AcuSolve results are compared with analytical results described in White (1991). The close agreement of AcuSolve results with analytical results validates the ability of AcuSolve to model cases with imposed pressure gradients.

Problem Description

The problem consists of air between two plates in a two dimensional domain, as shown in the following image, which is not drawn to scale. The domain is 1.0 m high and 1.5 m long. The top plate moves with a constant velocity of 3.0 m/sec and the bottom plate is fixed. There is a mean-pressure gradient of -12 Pa/m applied to the bulk fluid in the streamwise direction. The problem is simulated with periodic boundaries in the streamwise direction. The induced flow field is laminar and exhibits a steady state behavior. The flow field develops from the pressure gradient, the motion of the top plate, and the viscous shear stresses near the plates.

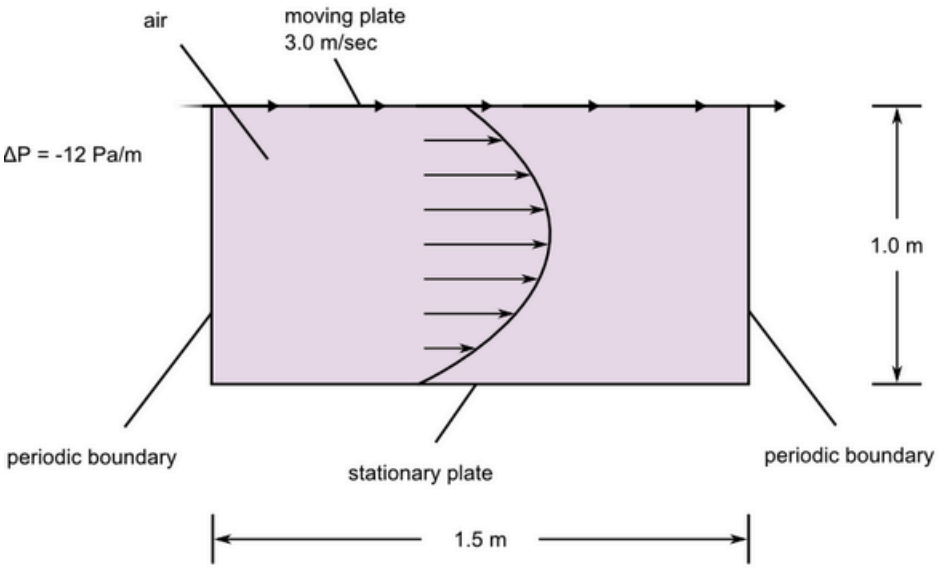


Figure 109: Critical Dimensions and Parameters for Simulating Laminar Couette Flow with an Imposed Pressure Gradient

The simulation was performed as a two dimensional problem by restricting flow in the out-of-plane direction through the use of a mesh that is one element thick.

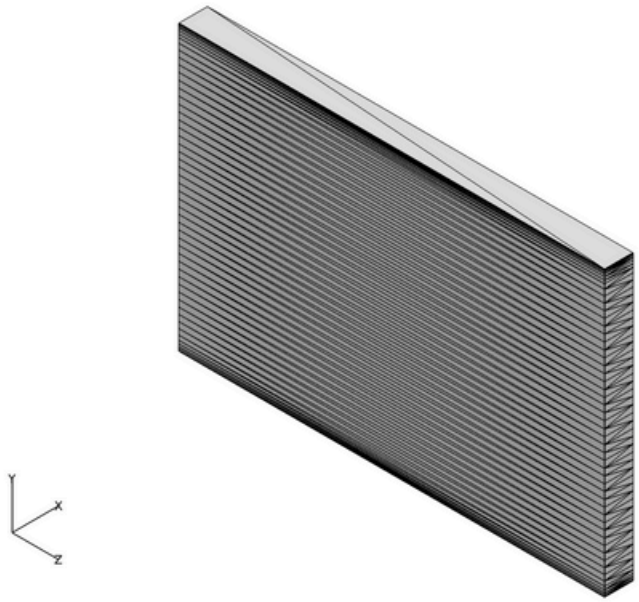


Figure 110: Mesh used for Simulating Laminar Couette Flow with an Imposed Pressure Gradient

AcuSolve Results

The AcuSolve solution converged to a steady state and the results reflect the mean flow conditions. The greatest velocity is located at approximately 40 percent of the channel height, closer to the moving plate. The flow develops as a result of the pressure gradient and the shear stress acting on the fluid near both the moving plate and the stationary plate.

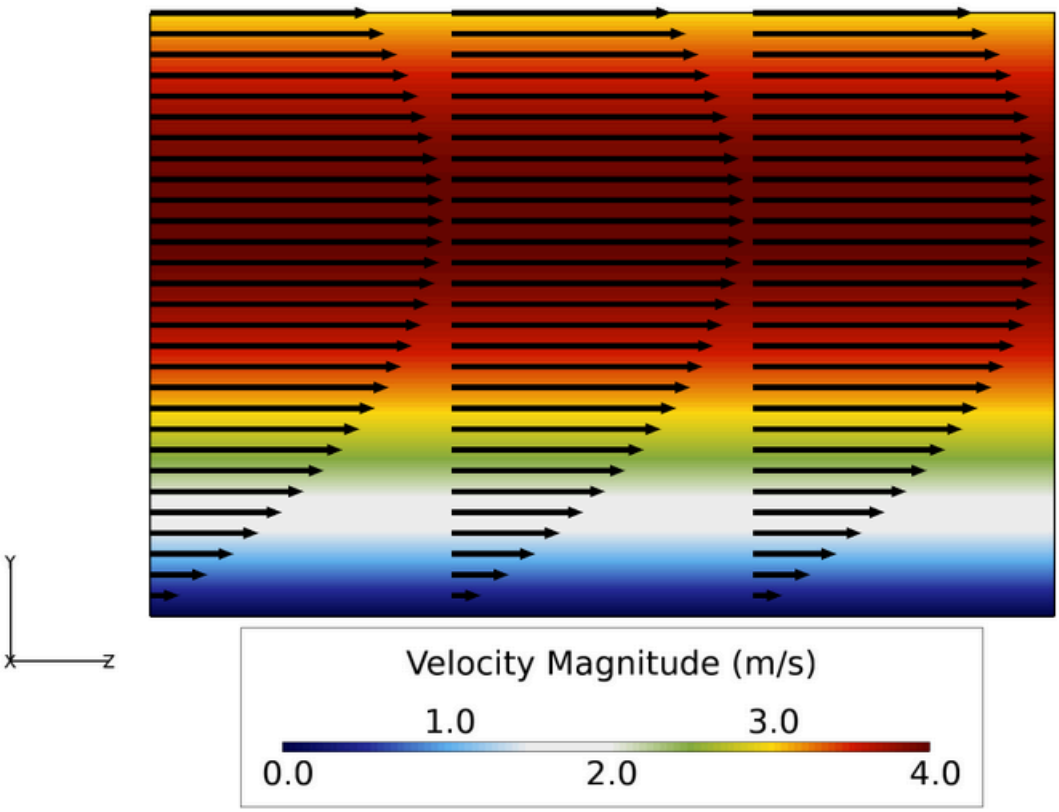


Figure 111: Z-Velocity Contours and Velocity Vectors

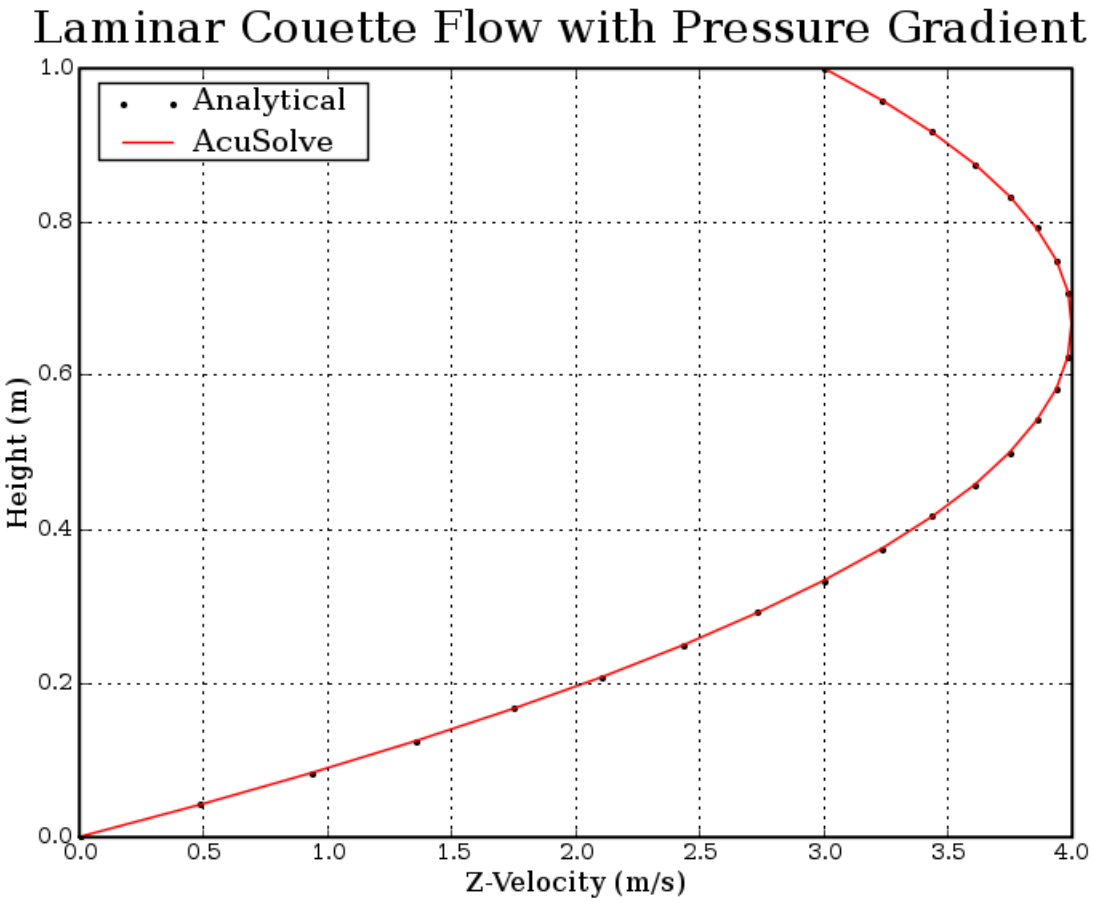


Figure 112: Z Velocity Plotted Against Height Above the Bottom of the Flow Field (Z Velocity is Presented on the X Axis to Better Represent the Velocity Profile in the Direction of Flow)

Summary

The velocity profile computed by AcuSolve agrees well with the analytical solution for this application. The velocity profile arises due to the combination of the imposed pressure gradient and the constant upper-wall velocity. Note that the combination of these effects results in the asymmetric velocity profile that is reflected in the results.

Simulation Settings for Laminar Couette Flow with Imposed Pressure Gradient

AcuConsole database file: `<your working directory>\couette_flow\couette_flow.acs`

Global

- Problem Description
  - Analysis Type - Steady State
  - Turbulence equation - Laminar
- Auto Solution Strategy
  - Relaxation factor - `0.2`

- Material Model
  - Air
    - Density - `1.0` kg/m3
    - Viscosity - `1.0` kg/m-sec
- Body Force
  - DP/DL
    - Gravity
      1. Z-component - `18.0` m/sec2

  Model
- Volumes
  - Fluid
    - Element set
      1. Material model - Air
      2. Body force - DP/DL
- Surfaces
  - Max_X
    - Simple Boundary Condition
      1. Type - Symmetry
  - Max_Y
    - Simple Boundary Condition
      1. Type - Wall
      2. Wall velocity type - Cartesian
      3. Z-velocity - `3.0` m/s
  - Max_Z
    - Simple Boundary Condition - (disabled to allow for periodic conditions to be set)
  - Min_X
    - Simple Boundary Condition
      1. Type - Symmetry
  - Min_Y
    - Simple Boundary Condition
      1. Type - Wall
  - Min_Z
    - Simple Boundary Condition - (disabled to allow for periodic conditions to be set)
- Periodics
  - Periodic 1
    - Periodic Boundary Conditions
      1. Type - Periodic

References

F. M. White. "Viscous Fluid Flow". Section 3-2.3. McGraw-Hill Book Co., Inc.. New York. 1991.

Laminar Couette Flow with Imposed Pressure Gradient and Heated Walls

In this application, AcuSolve is used to simulate the flow of a highly viscous fluid between a moving and a stationary plate with an imposed pressure gradient and fixed temperature on the walls. AcuSolve results are compared with analytical results described in White (1991). The close agreement of AcuSolve results with analytical results validates the ability of AcuSolve to model cases with imposed pressure gradients and viscous heating.

Problem Description

The problem consists of a viscous fluid between two plates in a two dimensional domain, as shown in the following image, which is not drawn to scale. The domain is 1.0 m high and 1.5 m long. The top plate moves with a constant velocity of 3.0 m/sec and the bottom plate is fixed. To simulate a fully developed flow with a relatively short length domain there is a mean-pressure gradient of -12 Pa/m applied to the fluid in the streamwise direction, defined as a body force acting on the entire fluid. The lower wall is held at a fixed temperature of 273.0 K, while the upper wall is held at a fixed temperature of 274.0 K. The problem is simulated with periodic boundaries in the streamwise direction. The Reynolds number of the flow, based on the distance between the plates is 0.3, indicating laminar flow. The flow field develops from the pressure gradient, the motion of the top plate, and the viscous shear stresses near the plates. The shear stress within the domain causes the temperature to increase within the channel.

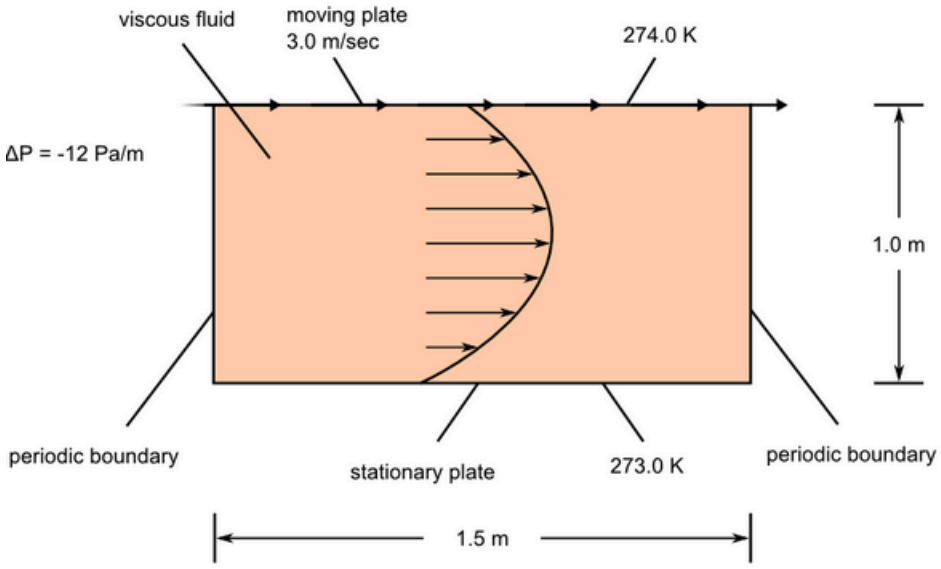


Figure 113: Critical Dimensions and Parameters for Simulating Laminar Couette Flow with an Imposed Pressure Gradient and Heated Walls

The simulation was performed as a two dimensional problem by constructing a volume mesh that contains a single layer of elements extruded in the cross stream direction, normal to the flow plane and by imposing symmetry boundary conditions on the extruded planes. Due to the periodic natural of the flow, a single element extrusion in the streamwise direction is used to reduce the model size.

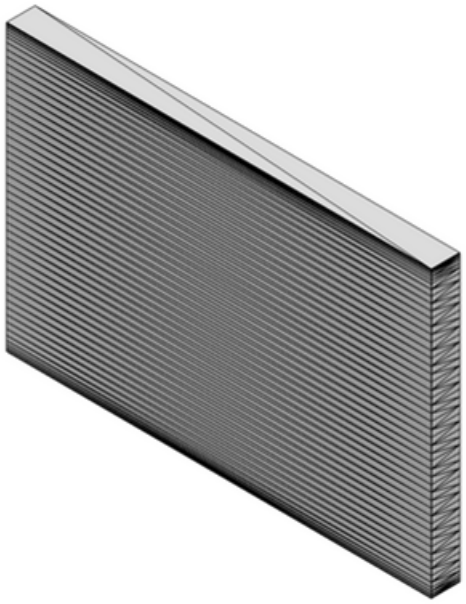


Figure 114: Mesh used for Simulating Laminar Couette Flow with an Imposed Pressure Gradient and Heated Walls

AcuSolve Results

The AcuSolve solution converged to a steady state and the results reflect the mean flow conditions. The simulation results show a flow field with a nearly linear distribution of velocity, with the peak at the top wall. The flow develops primarily as a result of the shear stress acting on the fluid near both the moving plate and the stationary plate. The temperature variation between the two plates develops due to the viscous heating effects that increase the temperature within the channel, with the maximum near the central height of the domain. The following figure shows the temperature distribution between the two plates and velocity vectors indicating the velocity profile.

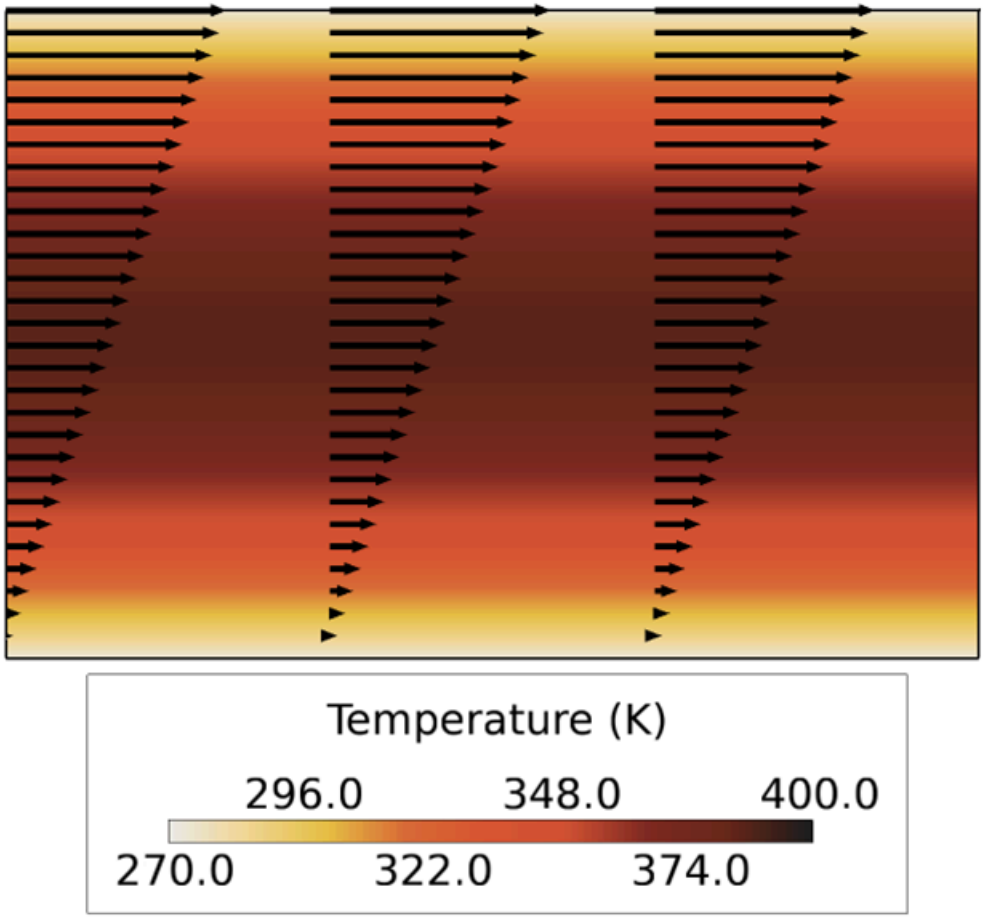


Figure 115: Contours of Temperature Between the Plates, with Velocity Vectors

The following image demonstrates the accuracy of the solution compared to the analytical results as computed by the solution for viscous heating within a channel with a moving upper boundary.

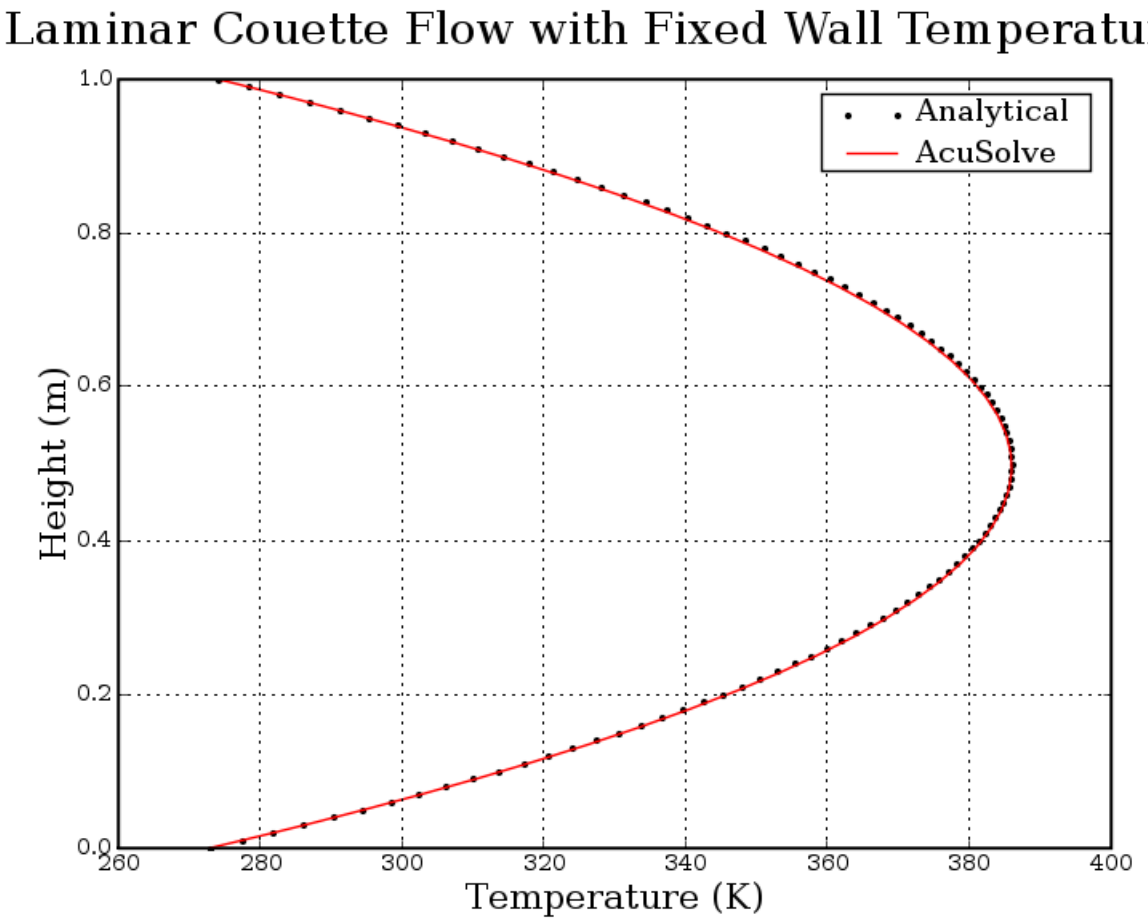


Figure 116: Temperature Plotted Against Height above the Bottom of the Flow Field (Temperature is Presented on the X Axis to Better Represent the Distribution Between the Plates in the Streamwise Direction)

Summary

In this application, a fully developed laminar flow between two plates with fixed temperature is studied and compared against analytical data. The AcuSolve results compare well with the analytical data for the temperature distribution between the two plates. The simulation indicates that the velocity profile arises due to the combination of the viscous shearing and the velocity of the upper plate. The velocity and temperature profiles computed by AcuSolve demonstrate how highly viscous fluids tend to direct the flow regime. AcuSolve demonstrates the ability to predict the analytical solution for viscous heating between two flat plates with moving and stationary boundaries and an imposed pressure gradient.

Simulation Settings for Laminar Couette Flow with Imposed Pressure Gradient and Heated Walls

AcuConsole database file: `<your working directory>\couette_laminar_heat\couette_laminar_heat.acs`

Global

- Problem Description

    - Analysis Type - Steady State
    - Temperature equation - Advective Diffusive
    - Turbulence equation - Laminar
- Auto Solution Strategy
    - Relaxation factor - `0.2`
- Material Model
    - Fluid
        - Density - `1.0` kg/m3
        - Specific Heat - `1.0` J/kg-K
        - Viscosity - `100.0` kg/m-sec
- Body Force
    - DP/DL
        - Gravity
            1. Z-component - `18.0` m/sec2

Model

- Volumes
    - Fluid
        - Element set
            1. Material model - Fluid
            2. Body force - DP/DL
            3. Viscous heating - on
- Surfaces
    - Max_X
        - Simple Boundary Condition
            1. Type - Symmetry
    - Max_Y
        - Simple Boundary Condition
            1. Type - Wall
            2. Wall velocity type - Cartesian
            3. Z-velocity - `3.0` m/s
            4. Temperature - `274.0` K
    - Max_Z
        - Simple Boundary Condition - (disabled to allow for periodic conditions to be set)
    - Min_X
        - Simple Boundary Condition
            1. Type - Symmetry
    - Min_Y

        - Simple Boundary Condition
            1. Type - Wall
            2. Temperature - `273.0` K
    - Min_Z
        - Simple Boundary Condition - (disabled to allow for periodic conditions to be set)
- Periodics
    - Periodic 1 all
        - Periodic Boundary Conditions
            1. Type - Periodic

References

F. M. White. "Viscous Fluid Flow". Section 3-3.2. McGraw-Hill Book Co., Inc. New York. 1991.

Laminar Poiseuille Flow Through a Pipe

In this application, AcuSolve is used to simulate the flow of carbon dioxide (CO_2) entering a pipe with a fixed velocity. AcuSolve results are compared with analytical results using the Hagen-Poiseuille approach as described in White (1991). The close agreement of AcuSolve results with analytical results validates the ability of AcuSolve to model cases with constant flow velocity.

Problem Description

The problem consists of CO_2 flowing through a circular pipe 0.0025 m in diameter and 0.01 m long, as shown in the following image, which is not drawn to scale. The CO_2 enters the pipe with an average inlet velocity of 3.0 m/s. The flow field develops as a result of the viscous shearing on the fluid at the pipe wall.

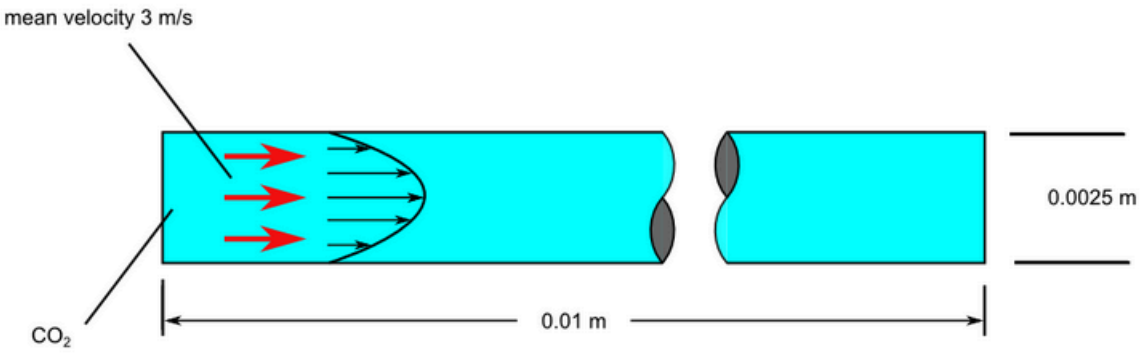


Figure 117: Critical Dimensions and Parameters for Simulating Laminar Poiseuille Flow Through a Pipe



Figure 118: Mesh Used for Simulating Laminar Poiseuille Flow Through a Pipe

AcuSolve Results

The AcuSolve solution converged to a steady state and the results reflect the mean flow conditions. The pressure decreases along the length of the pipe.

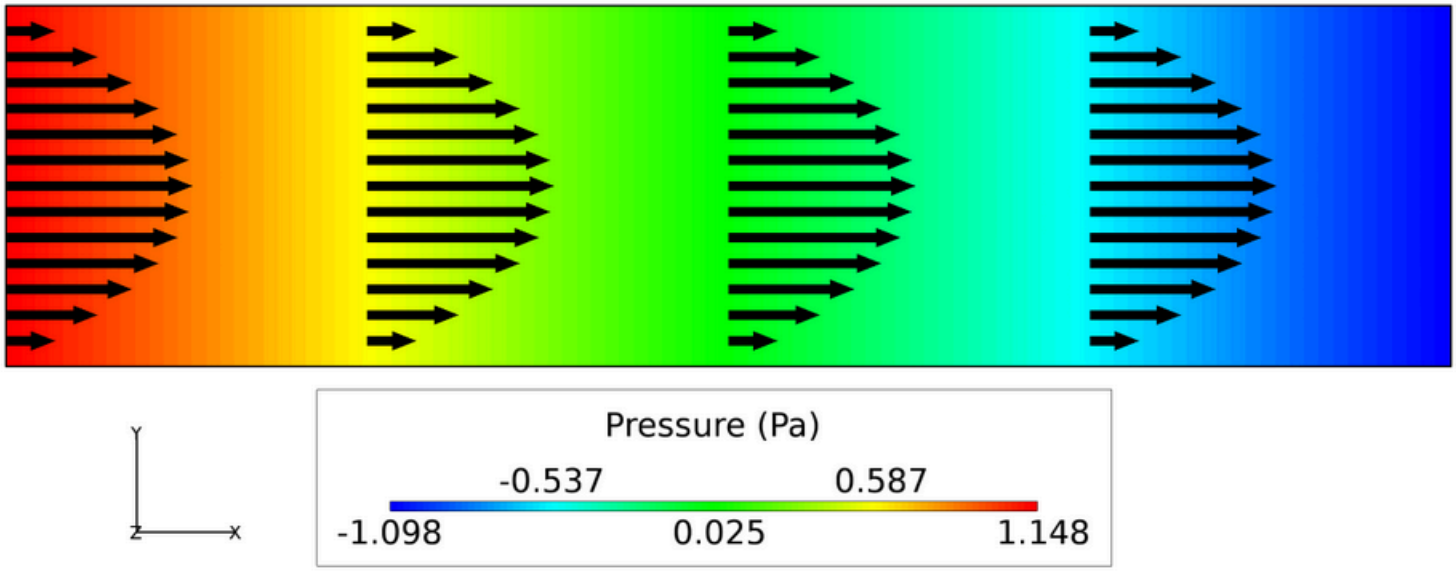


Figure 119: Pressure Contours and Velocity Vectors

The analytical pressure drop between the inlet and the outlet is presented with the corresponding AcuSolve result in the following table.

Table 7:

	Analytical pressure drop (Pa)	**AcuSolve pressure drop (Pa)**	**Percent deviation from analytical**
Inlet to outlet pressure drop	2.242	2.245	0.099

Summary

The AcuSolve solution compares well with analytical results for laminar flow through a pipe. In this application, the pressure drop along the length of the pipe is caused by the viscous shearing near the pipe wall. The AcuSolve steady state solution compares well with the analytical solution, with less than 0.1 percent error.

Simulation Settings for Laminar Poiseuille Flow Through a Pipe

AcuConsole database file: `<your working directory>\pipe_laminar\pipe_laminar.acs`

Global

- Problem Description
  - Analysis type - Steady State
  - Turbulence equation - Laminar
- Auto Solution Strategy
  - Relaxation factor - `0.2`
- Material Model
  - CO2
    - Density `1.808` kg/m3
    - Viscosity `1.46e-5` kg/m-sec

  Model
- Volumes
  - Fluid
    - Element Set
      1. Material Model - CO2
- Surfaces
  - Inflow
    - Simple Boundary Condition - (disabled to allow for periodic conditions to be set)
    - Advanced Options
      1. Integrated Boundary Conditions
         1. Mass Flux
            1. Type - Constant
            2. Constant value - `-2.6625e-05` kg/sec
  - Outflow
    - Simple Boundary Condition - (disabled to allow for periodic conditions to be set)
  - Wall
    - Simple Boundary Condition
      1. Type - Wall
- Periodics
  - Periodic 1
    - Individual Periodic BCs
      1. Velocity
         1. Type - Periodic
      2. Pressure
         1. Type - Single Unknown Offset

References

F. M. White. "Viscous Fluid Flow". Section 3-2.1. McGraw-Hill Book Co., Inc.. New York. 1991.

Laminar Flow Through a Pipe with Species Transport

In this application, AcuSolve is used to simulate the transport of a passive scalar species in a fully developed laminar flow. AcuSolve results are compared with analytical results as described in Kays and Crawford (1993). The close agreement of AcuSolve results with analytical results validates the ability of AcuSolve to model cases with species transport.

Problem Description

The problem consists of species transport in a pipe 0.005 m in diameter and 0.1 m long, as shown in the following image, which is not drawn to scale. The species transport equation is bounded at the inlet with a value of 1.0, while the boundary condition at the wall is 0.0. These constraints impose a concentration gradient within the fluid. The concentration gradient causes the fraction of species 1 to decrease near the pipe wall due to diffusion. The reduced concentration of the species is transported downstream in the pipe via advection, and leads to a continued decrease in the concentration as flow propagates through the pipe.

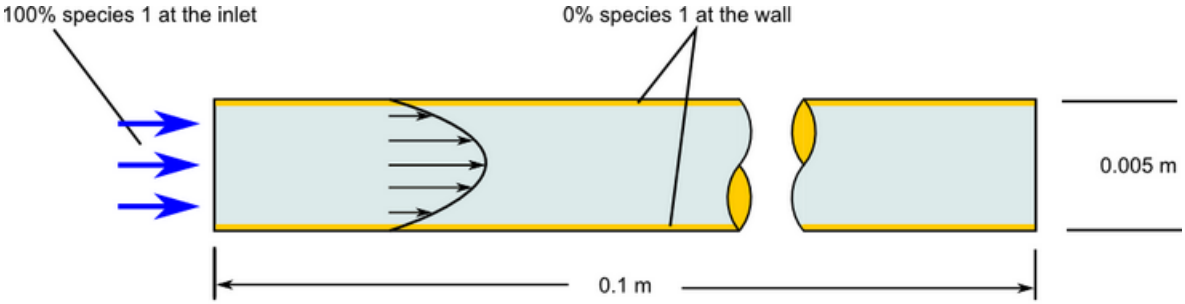


Figure 120: Critical Dimensions and Parameters for Simulating Laminar Flow Through a Pipe with Species Transport

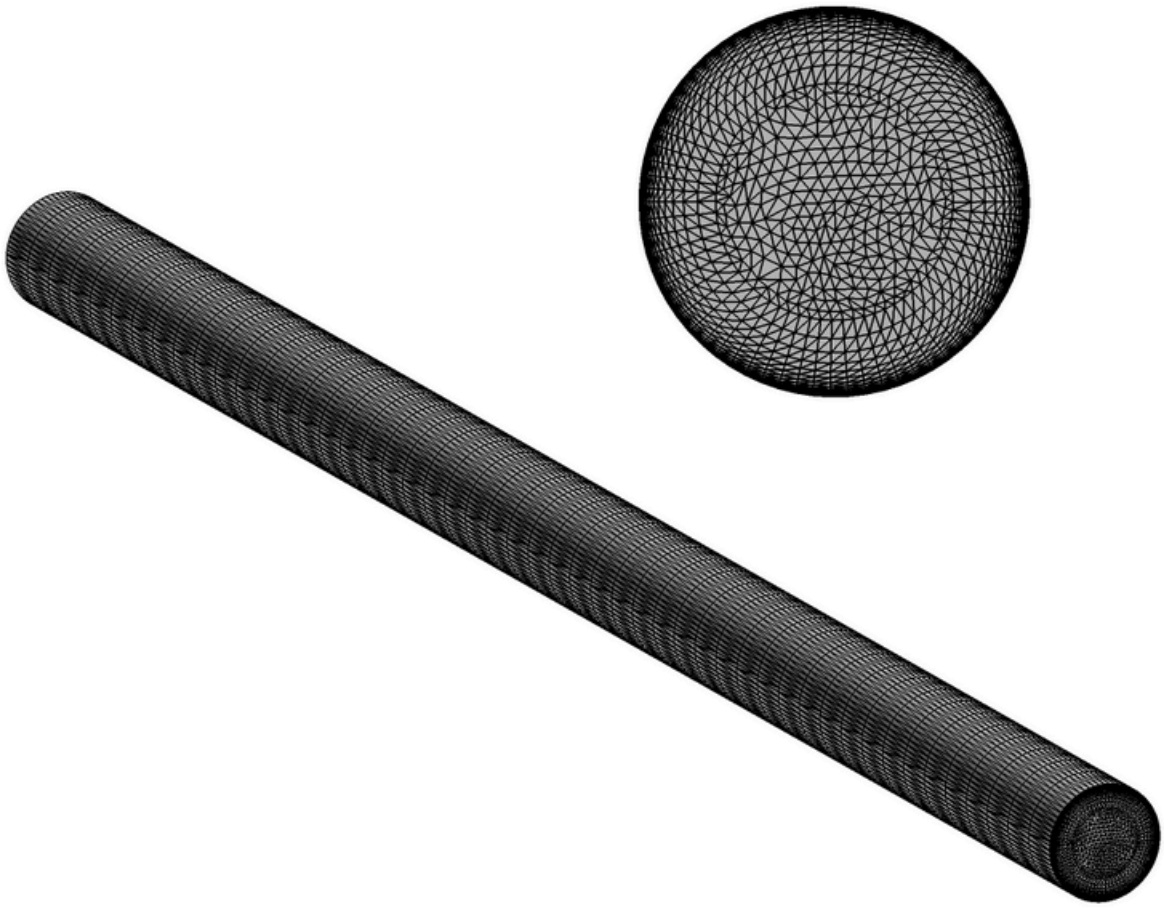


Figure 121: Mesh used for Simulating Laminar Flow Through a Pipe with Species Transport

AcuSolve Results

The AcuSolve solution converged to a steady state and the results reflect the mean flow conditions with the species fraction changing along the length of the pipe. At the inlet, the concentration of species 1 is 100 percent. The fraction of species 1 decreases along the length of the pipe, developing a parabolic concentration profile due to the no-slip walls and the specified concentration at the wall.

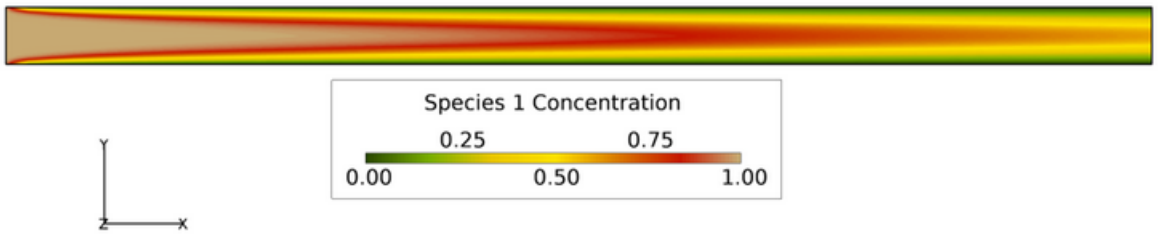


Figure 122: Contours of Concentration for Species 1

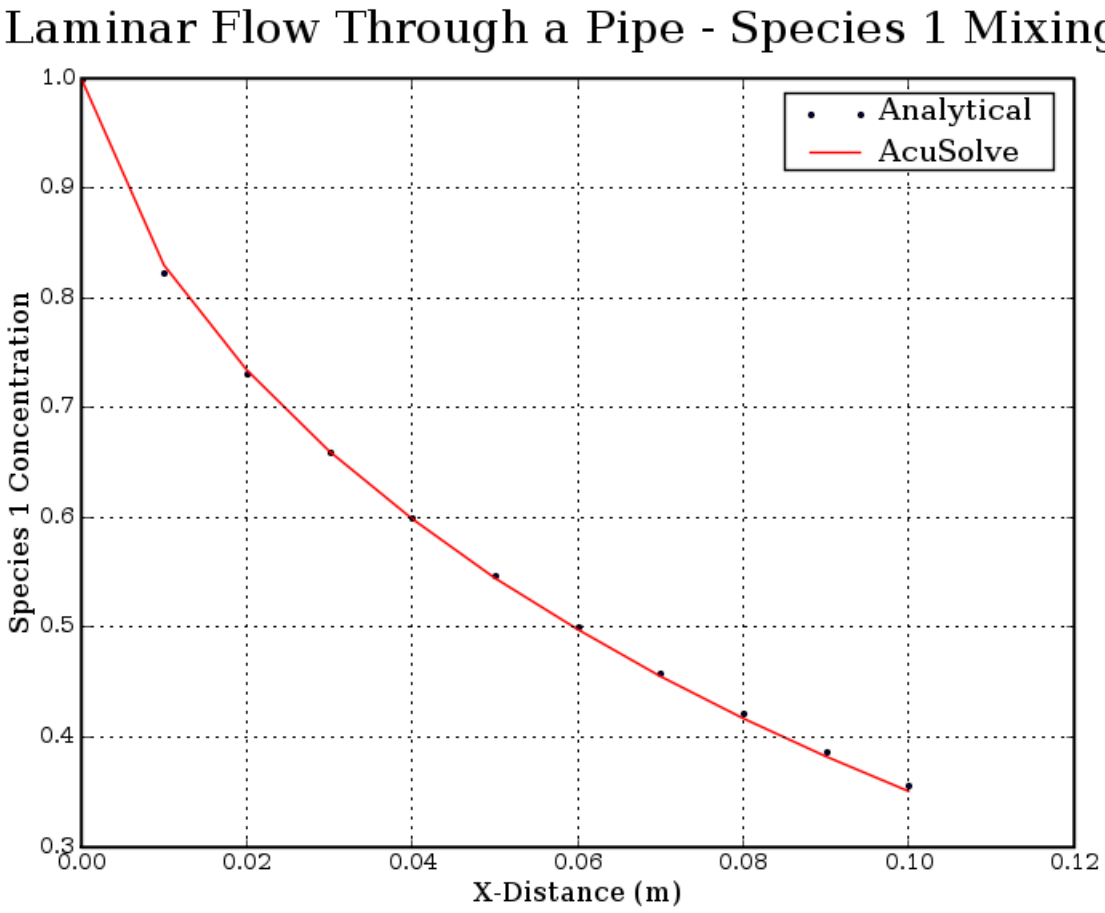


Figure 123: Species 1 Concentration Plotted Against Distance from the Pipe Inlet

Analytical values of the species fraction at different distances along the pipe are presented with the corresponding AcuSolve results in the following table. The analytical solution contains a series of five terms that are summed to yield the values shown in the table.

Table 8:

Distance along pipe (m)	Analytical species 1 fraction	AcuSolve species 1 fraction	Percent deviation from analytical
0	1.0000*	1.0000	0.00
0.01	0.8225	0.8298	0.90
0.02	0.7308	0.7344	0.49
0.03	0.6593	0.6603	0.15
0.04	0.5992	0.5988	0.06
0.05	0.5469	0.5448	0.38
0.06	0.5006	0.4981	0.49
0.07	0.4589	0.4554	0.78
0.08	0.4212	0.4171	0.98
0.09	0.3869	0.3824	1.15
0.1	0.3555	0.3507	1.35

* The theoretical species fraction at the inlet is shown rather than the analytical. In order for the analytical solution to correspond exactly with the theoretical results, additional terms in the series summation would need to be evaluated.

Summary

The AcuSolve solution compares well with analytical results for flow through a pipe with species transport. In this application, a fully developed laminar profile is achieved by enforcing periodic constraints on the pressure and velocity fields. The spatially developing species field is achieved by not enforcing periodicity and allowing the concentration to evolve along the full length of the model. The change in concentration along the pipe length is due to advection in the streamwise direction and diffusion of the species to the outer walls where the concentration is zero. The AcuSolve solution for fraction of species 1 is within 1.35 percent of analytical results.

Simulation Settings for Laminar Flow Through a Pipe with Species Mixing

AcuConsole database file: `<your working directory>\pipe_laminar_species \pipe_laminar_species.acs`.

Global

- Problem Description
  - Analysis type - Steady State

- Species equation - Advective Diffusive
- Num. species - `1`
- Turbulence equation - Laminar

- Auto Solution Strategy
  - Relaxation factor - `0.2`
- Material Model
  - Species1
    - Density - `1.0` kg/m3
    - Viscosity - `1.0e-5` kg/m-sec
    - Diffusivity
      1. 1
         1. Diffusivity - `1.43e-5` kg/m-sec

  Model
- Volumes
  - Fluid
    - Element Set
      1. Material model - Species1
- Surfaces
  - Inflow
    - Simple Boundary Condition - (disabled to allow for periodic conditions to be set)
    - Advanced Options
      1. Nodal Boundary Conditions
         1. Species 1
            1. Type - Constant
            2. Constant value - `1.0`
      2. Integrated Boundary Conditions
         1. Mass Flux
            1. Type - Constant
            2. Constant value - `1.96e-05` kg/sec
  - Outflow
    - Simple Boundary Condition - (disabled to allow for periodic conditions to be set)
  - Wall
    - Simple Boundary Condition
      1. Type - Wall
      2. Species 1 BC type - Value
      3. Species 1 - `0.0`
- Periodics

- Periodic 1
  - Individual Periodic BCs
    1. Velocity
       1. Type - Periodic
    2. Pressure
    3. Type - Single Unknown Offset

References

W. M. Kays and M. E. Crawford. "Convective Heat and Mass Transfer", 3rd Edition. pp. 126-134. McGraw-Hill Book Co., Inc. New York. 1993.

Flow Inside a Rotating Cavity

In this application, AcuSolve is used to simulate the flow of air in an enclosed cylindrical cavity with a rotating top and a fixed bottom. AcuSolve results are compared with experimental data adapted from Michelsen (1986). The close agreement of AcuSolve results with experimental data validates the ability of AcuSolve to model cases containing enclosed cavities with flow induced by rotating walls.

Problem Description

The problem consists of air in an enclosed cylinder 1.0 m tall with a radius of 1.0 m, as shown in the following image, which is not drawn to scale. The top of the cylinder rotates about its center at 1 rad/s, while the bottom of the cylinder is fixed. As the container top spins, the viscous stresses on the fluid induce a circumferential (swirl) velocity throughout the height of the cylinder. In order to conserve mass and momentum, the fluid generates a radial velocity that changes direction based on distance away from the rotation center of the cylinder.

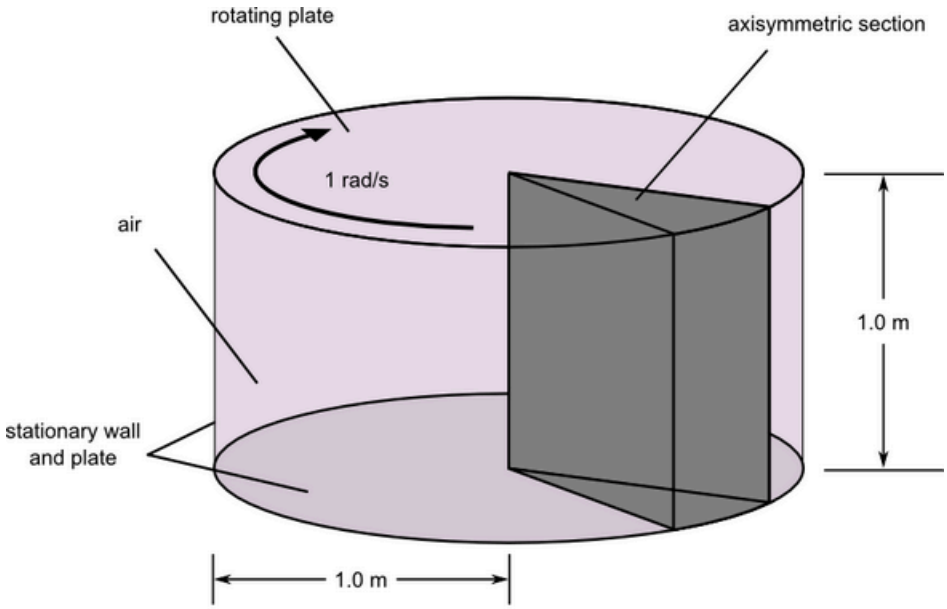


Figure 124: Critical Dimensions and Parameters for Simulating Flow Inside a Rotating Cavity

The flow domain is modeled with axisymmetric periodicity in the circumferential direction, which allows for accurate simulation of the flow while minimizing computational time.

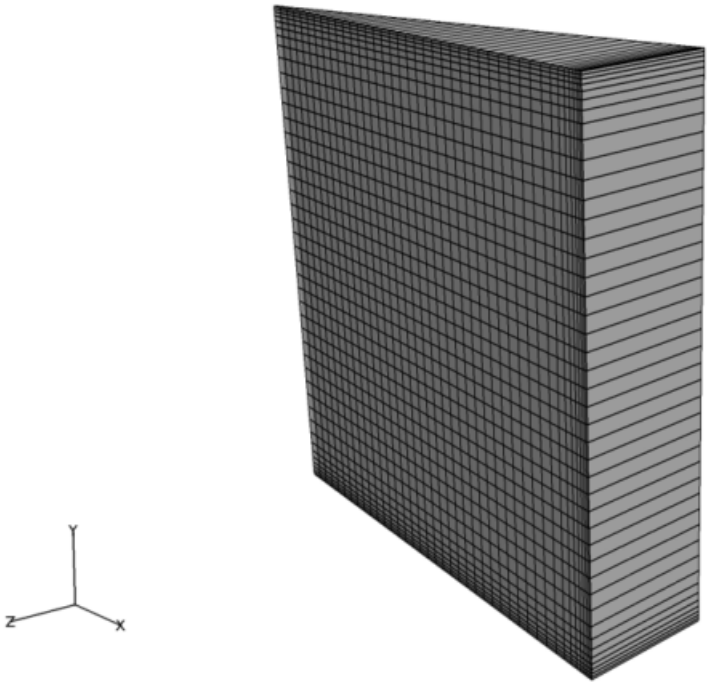


Figure 125: Mesh of Periodic Section Used for Simulating Flow Inside a Rotating Cylinder

AcuSolve Results

The AcuSolve solution converged to a steady state and the results reflect the mean flow conditions. The velocity varies with both vertical location and with distance from the rotation center. The complex flow field develops from a combination of the viscous stresses acting at the rotating cylinder top and at the stationary bottom.

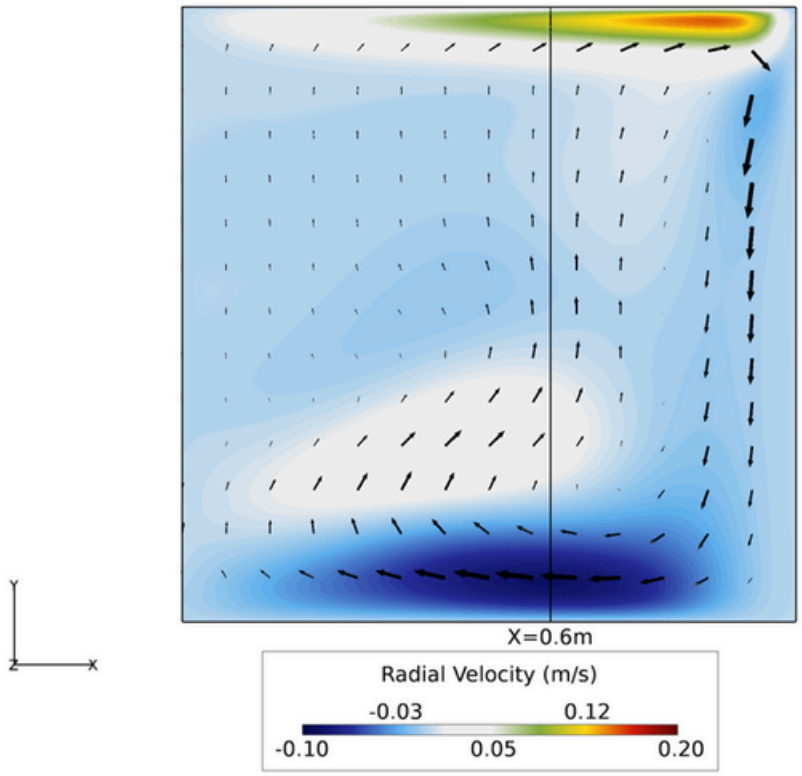


Figure 126: Contours of Radial Velocity with Velocity Vectors. This Image Shows the Front Face of the Modeled Cylinder Wedge, with the Center of Rotation on the Left Edge. The Vertical Line Represents a Radial Location 0.6 m From the Center of Rotation.

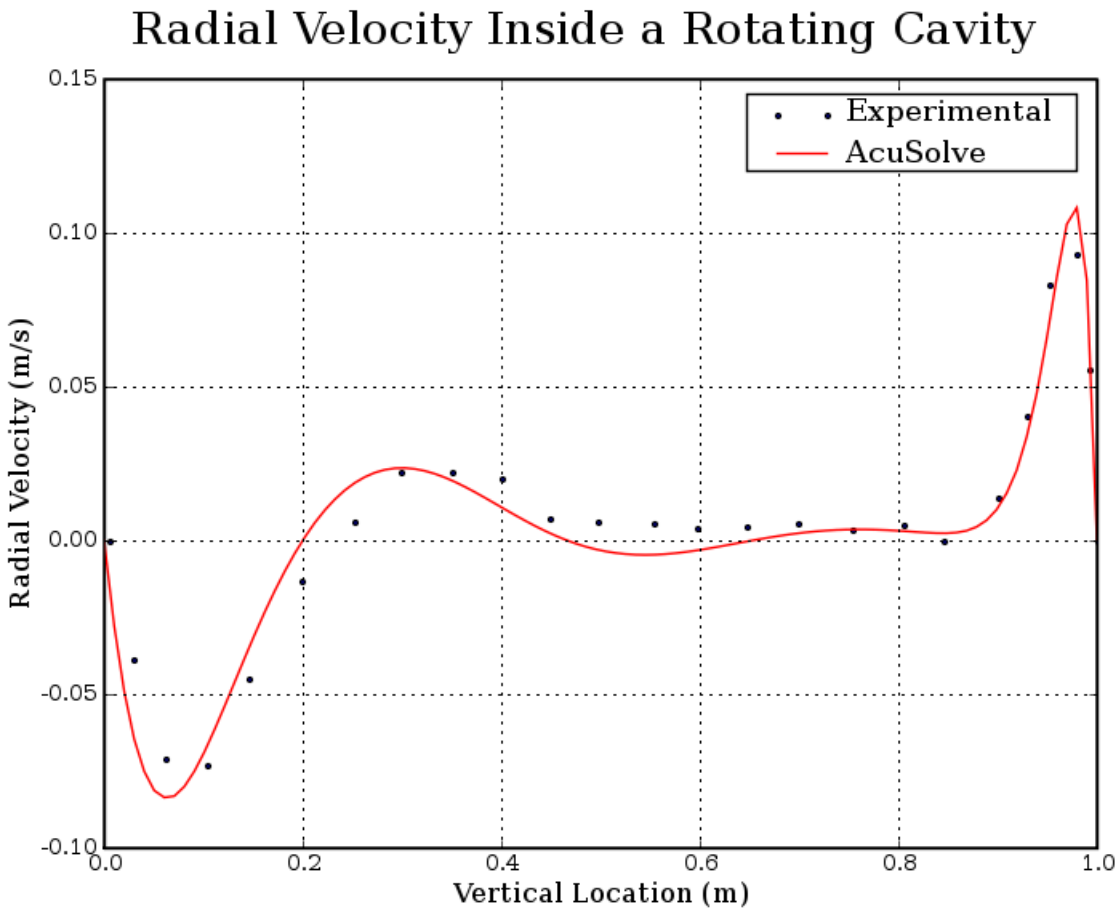


Figure 127: Radial Velocity (at 0.6 m From the Center of Rotation) as a Function of Vertical Location From Cylinder Bottom

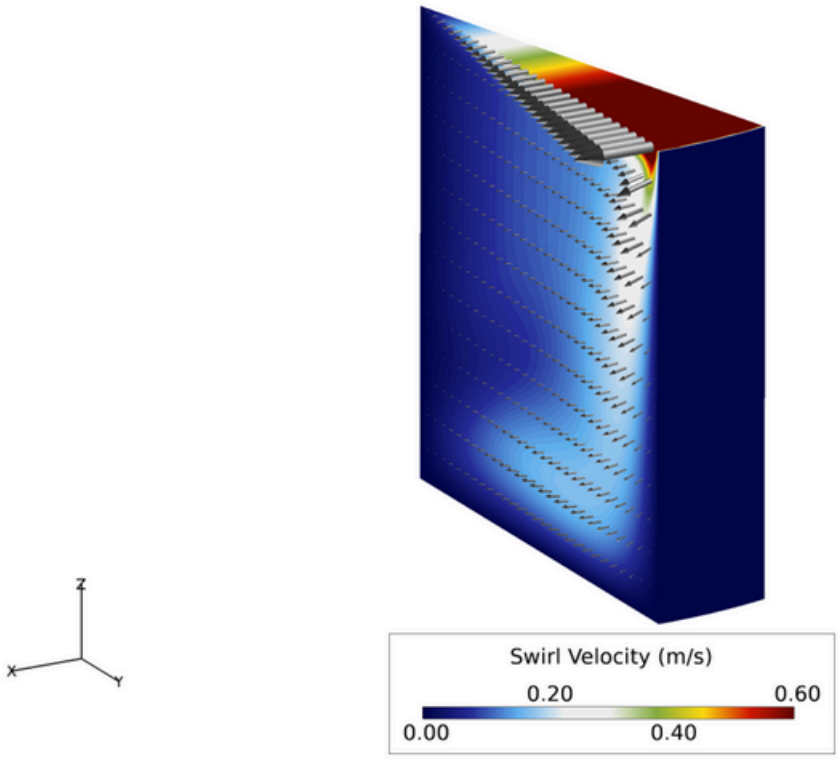


Figure 128: Contours of Swirl Velocity with Velocity Vectors

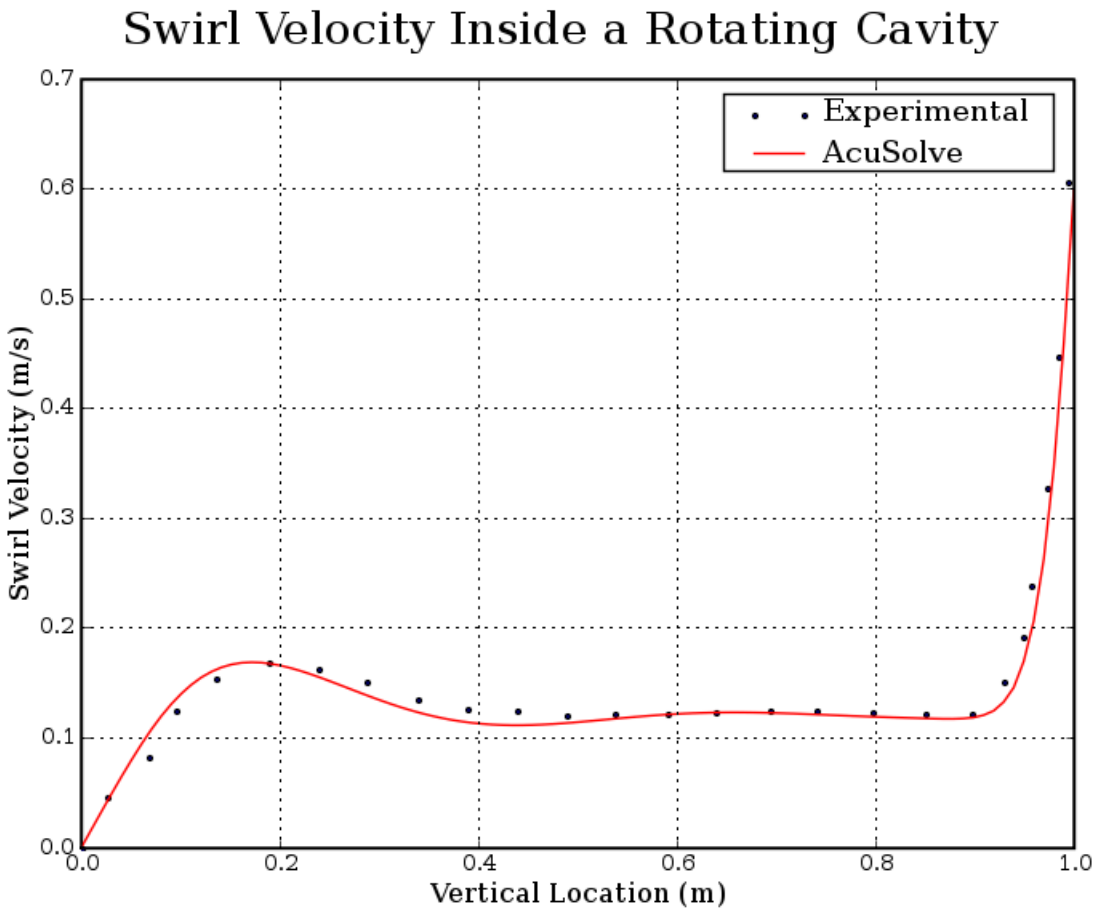


Figure 129: Swirl Velocity (at 0.6 m From Center of Rotation) as a Function of Vertical Location From the Cylinder Bottom

Summary

The AcuSolve solution compares well with the experimental data for flow induced by a rotating top of an enclosed cylinder. In this application, the flow in the fluid region is driven by the viscous stresses near the rotating top. Viscous stresses drag the fluid in a circular direction near the spinning wall. The angular velocity of the fluid decreases as distance from the top wall increases. Radial velocity develops as a result of the migration of the fluid toward the outer wall in regions of high angular velocity. The AcuSolve radial and swirl velocities compare very closely with the experimental data.

Simulation Settings for Flow Inside a Rotating Cavity

AcuConsole database file: `<your working directory>\cavity_rotating\cavity_rotating.acs`

Global

- Problem Description
  - Analysis type - Steady State
  - Turbulence Equation - Laminar
- Auto Solution Strategy

    - Relaxation Factor - `0.4`
- Material Model
    - Air
        - Density - `1.0` kg/m3
        - Viscosity - `0.000556` kg/m-sec
- Reference Frame
    - Cavity Rotation
        - Rotation center
            1. X-coordinate - `0.0`
            2. Y-coordinate - `0.0`
            3. Z-coordinate - `0.0`
        - Angular velocity
            1. X-component - `0.0`
            2. Y-component - `-1.0` rad/sec
            3. Z-component - `0.0`

    Model
- Volumes
    - Fluid
        - Element Set
            1. Material model - Air
- Surfaces
    - Bottom
        - Simple Boundary Condition
            1. Type - Wall
    - Max_X
        - Simple Boundary Condition
            1. Type - Wall
    - Max_Z
        - Simple Boundary Condition - (disabled to allow for periodic conditions to be set)
    - Min_Z
        - Simple Boundary Condition - (disabled to allow for periodic conditions to be set)
    - Top
        - Simple Boundary Condition
            1. Type - Wall
            2. Reference frame - Cavity Rotation
- Periodics
    - Periodic 1

- Periodic Boundary Condition
  1. Type - Axisymmetric
  2. Rotation axis
     1. point 1
        1. X-coordinate - `0.0` m
        2. Y-coordinate - `0.0` m
        3. Z-coordinate - `0.0` m
     2. point 2
        1. X-coordinate - `0.0` m
        2. Y-coordinate - `1.0` m
        3. Z-coordinate - `0.0` m

References

J. A. Michelsen. "Modeling of Laminar Incompressible Rotating Fluid Flow". AFM 86-05. Ph.D. thesis, Department of Fluid Mechanics, Technical University of Denmark. 1986.

Natural Convection in a Concentric Annulus

In this application, AcuSolve is used to simulate natural convection in the annular space between a heated inner pipe and an outer concentric pipe. AcuSolve results are compared with experimental results adapted from Kuehn and Goldstein (1978). The close agreement of AcuSolve results with experimental results validates the ability of AcuSolve to model cases with flow induced by natural convection.

Problem Description

The problem consists of two concentric cylinders with air filling the void between them, as shown in the following image, which is not drawn to scale. The radius of the inner cylinder is 0.0178 m and the radius of the outer cylinder is 0.0463 m. The inner cylinder is held at a fixed temperature of 373 K while the outer cylinder is held at 327 K. The temperature gradient drives the flow due to buoyancy effects.

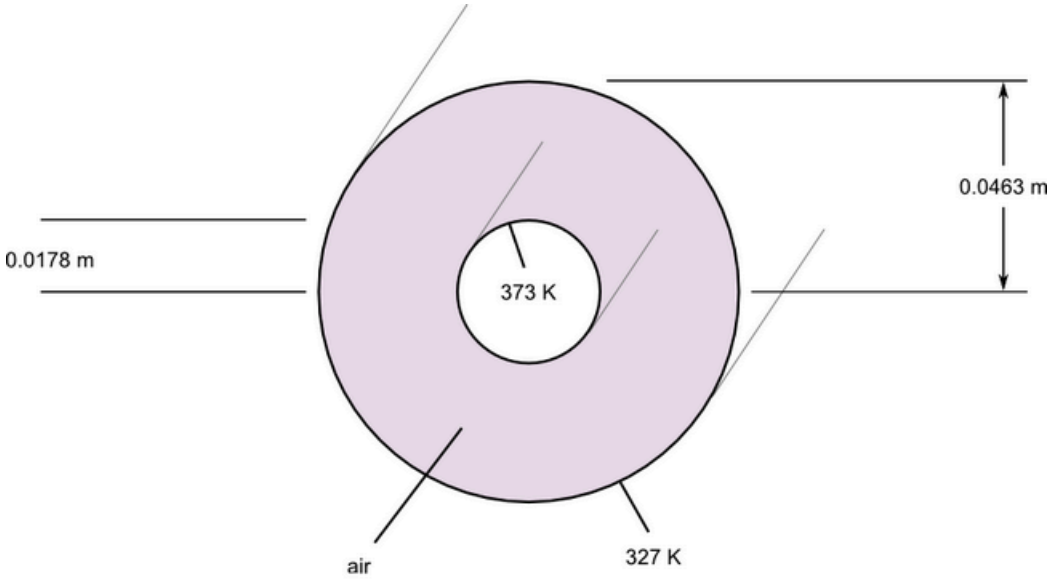


Figure 130: Critical Dimensions and Parameters for Simulating Natural Convection in a Concentric Annulus

The simulation was performed as a two dimensional problem by restricting flow in the out-of-plane direction through the use of a mesh that is one element thick. In addition, the half symmetry of the geometry is exploited to allow for modeling only half of the geometry. These characteristics allow for accurate simulation of the flow while minimizing computational time.

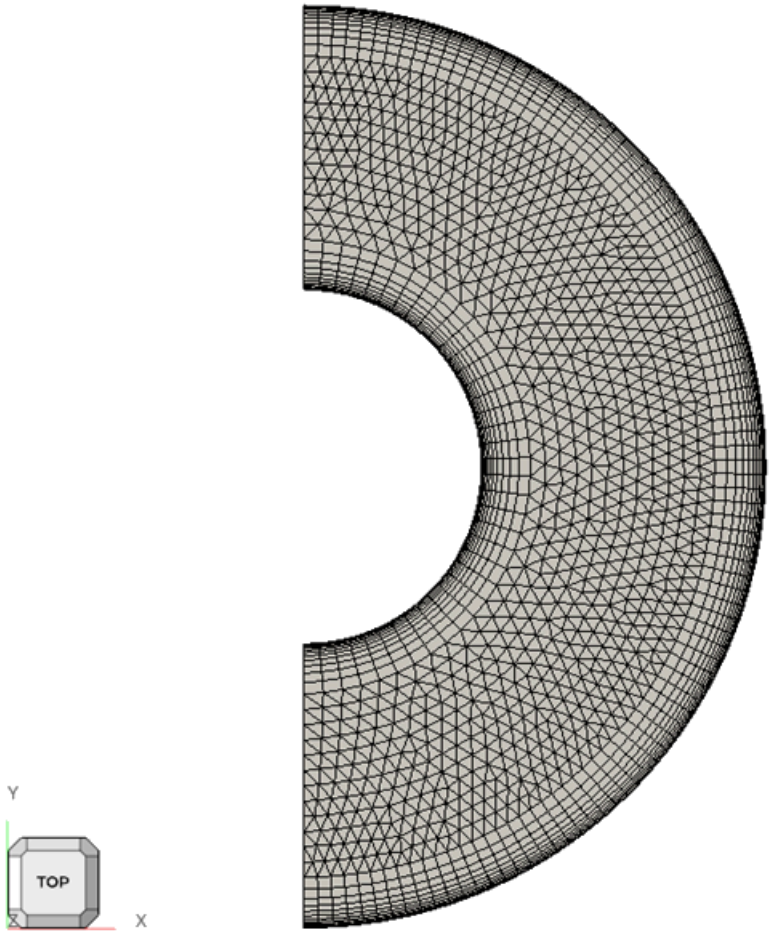


Figure 131: Mesh (Half of a Concentric Annulus) used for Simulating Natural Convection in a Concentric Annulus

AcuSolve Results

The AcuSolve solution converged to a steady state and the results reflect the mean flow conditions. Air density decreases due to heating by the inner cylinder, leading to convective currents within the annulus. As air approaches the outer cylinder, it is cooled by the outer wall, causing the density to increase. This results in heavier air sinking toward the bottom of the assembly.

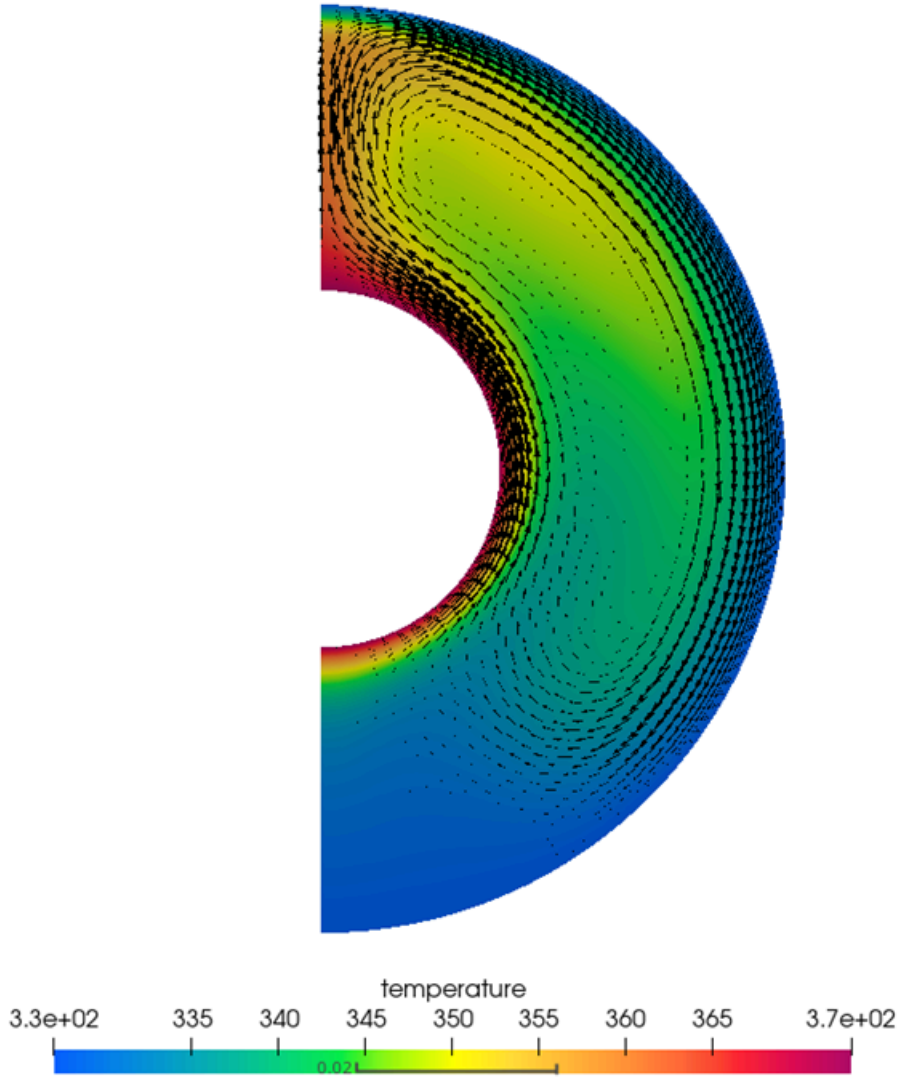


Figure 132: Temperature Contours and Velocity Vectors

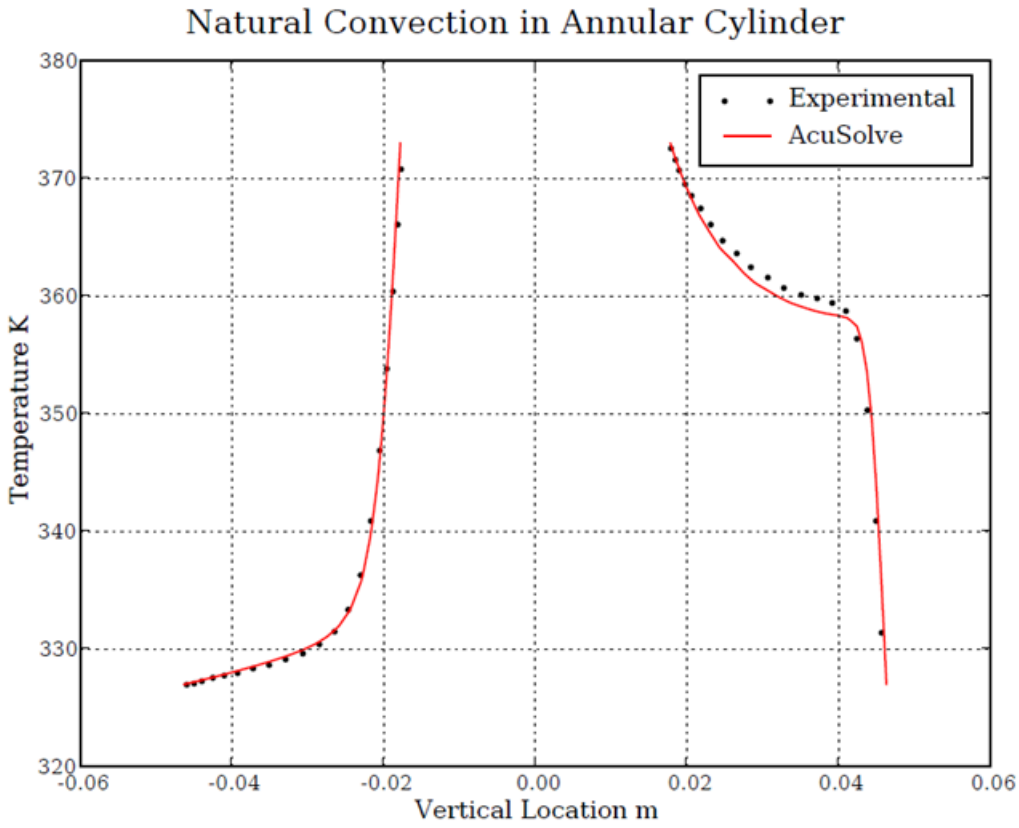


Figure 133: Temperature as a Function of Distance From the Center of the Inner Cylinder

Summary

The AcuSolve solution compares well with analytical results for natural convection in a concentric annulus. In this application, flow is driven by a decrease in density as air is heated. The local variations in density result in the higher density fluid sinking to the bottom of the annulus while the lower density fluid rises to the top. This transfer of momentum is a continuous process which results in the convective currents that are visible in the solution. The AcuSolve temperature results compare very closely with the experimental results.

Simulation Settings for Natural Convection in a Concentric Annulus

HyperWorks CFD database file: `<your working directory>\annulus_heat\annulus_heat.hm`

Global

- Problem Description
  - Analysis type - Steady State
  - Abs. pressure offset - `101325.0` N/m2
  - Temperature equation - Advective Diffusive
  - Turbulence equation - Laminar
  - Gravitational acceleration - { 0, -9.80665, 0 }
- Auto Solution Strategy

- Relaxation factor - `0.2`
- Flow - On
- Temperature - On

- Material Model
  - Air
    - Type - Boussinesq
    - Density - `1.225` kg/m3
    - Expansivity - `0.0034722` 1/K
    - Reference temperature - `288` K
    - Isothermal compressibility - `0.0` m2/N
    - Viscosity - `2.081e-5` kg/m-sec

  Model
- Volumes
  - Fluid
    - Element Set
      1. Material model - Air
  - Surfaces
    - ID
      1. Simple Boundary Condition
         1. Type - Wall
         2. Temperature BC type - Value
         3. Temperature - `373.0` K
    - Max_Z
      1. Simple Boundary Condition
      2. Type - Symmetry
    - Min_Z
      1. Simple Boundary Condition
      2. Type - Symmetry
    - OD
      1. Simple Boundary Condition
         1. Type - Wall
         2. Temperature BC type - Value
         3. Temperature - `327.0` K
    - Symmetry
      1. Simple Boundary Condition
      2. Type - Symmetry
  - Nodes
    - Node 1

1 Pressure

1 Type - Zero

References

T.H. Kuehn and R. J. Goldstein. "An Experimental Study of Natural Convection Heat Transfer in Concentric and Eccentric Horizontal Cylindrical Annuli". Journal of Heat Transfer 100:635-640. 1978.

Laminar Flow Past a 90° T-Junction

In this application, AcuSolve is used to simulate laminar flow through a channel with two outlets forming a T-junction. AcuSolve results are compared with experimental results adapted from Hayes and others (1989). The close agreement of AcuSolve results with experimental results validates the ability of AcuSolve to model cases with multiple outlet paths.

Problem Description

The problem consists of air flowing past a T-junction in a channel, as shown in the following image, which is not drawn to scale. Air enters the channel with an average velocity of 0.667 m/s and travels past the T-junction 2.0 m from the inlet. A portion of the flow will travel out of the branch of the channel due to the pressure difference between the bulk flow and the outlet of the branch.

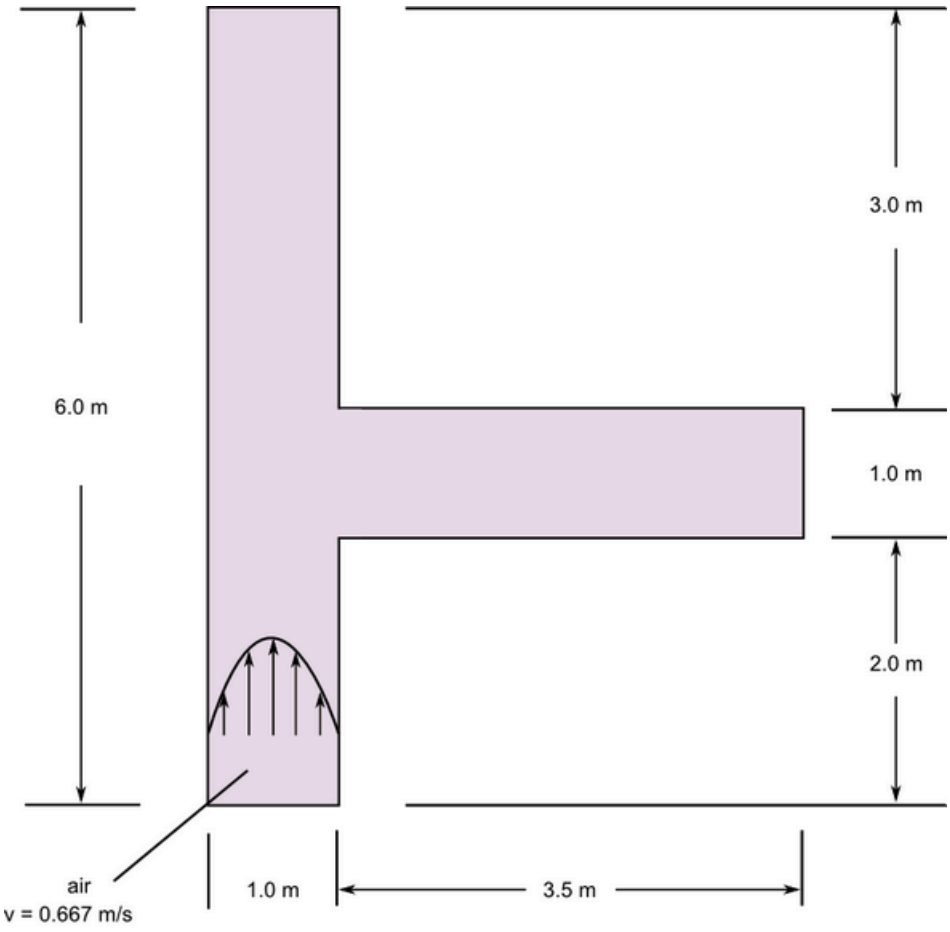


Figure 134: Critical Dimensions and Parameters for Simulating Laminar Flow Past a 90° T-Junction

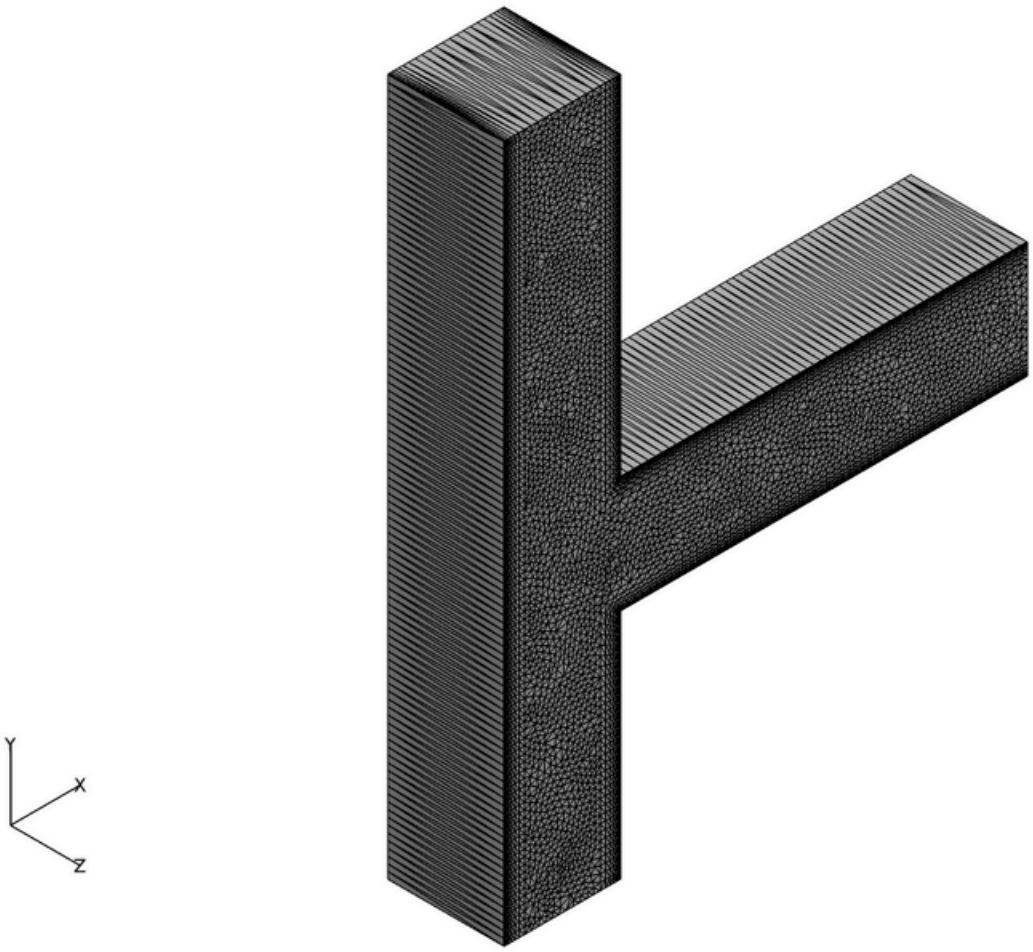


Figure 135: Mesh Used for Simulating Laminar Flow past a 90° T-Junction

AcuSolve Results

The AcuSolve solution converged to a steady state and the results reflect the mean flow conditions. As the air flows past the junction, a portion of it is diverted into the branch. A small recirculation region develops at the top of the junction and collapses before the flow exits the domain through the right branch.

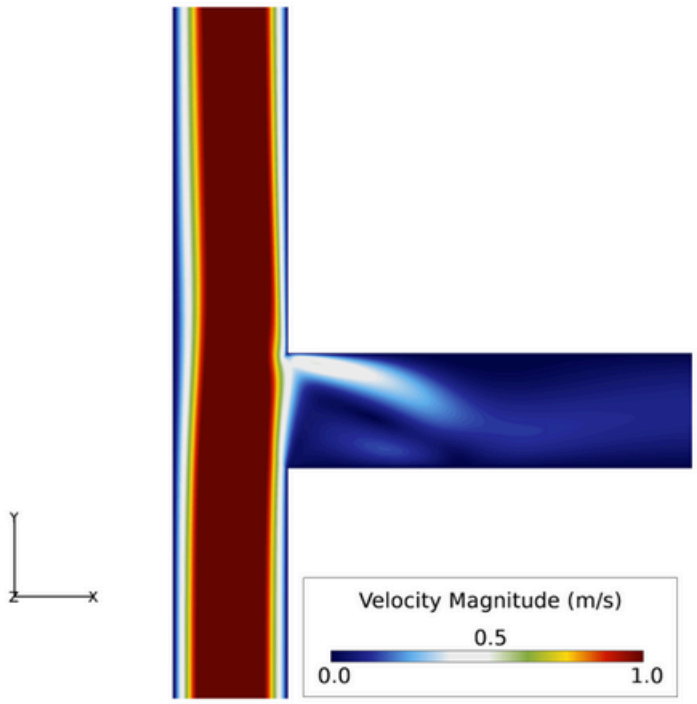


Figure 136: Velocity Contours in a T-Junction

The experimental value for the fraction of flow exiting the top branch of the channel is presented with the corresponding AcuSolve result in the following table.

Table 9:

	Experimental fractional flow	**AcuSolve fractional flow**	**Percent deviation from experimental**
Fractional flow exiting the upper branch	0.887	0.883	0.451

Summary

The AcuSolve solution compares well with experimental results for flow past a T-junction. In this application, flow is driven by a fixed flow rate at the inlet to the main branch. A portion of the flow from the main branch is diverted into the right branch of the T-junction, giving rise to recirculation just downstream of the junction. This recirculation collapses before the flow exits the side branch. The AcuSolve result for fractional flow exiting the top branch is within 0.451 percent of the experimental results.

Simulation Settings for Laminar Flow Past a 90° T-Junction

AcuConsole database file: `<your working directory>\T_junction_laminar\T_junction_laminar.acs`

Global

- Problem Description
  - Analysis type - Steady State
  - Turbulence equation - Laminar
- Auto Solution Strategy
  - Relaxation factor - `0.2`
- Material Model
  - Air
    - Type - Constant
    - Density - `1.0` kg/m3
    - Viscosity - `0.003333` kg/m-sec

  Model
- Volumes
  - Fluid
    - Element Set
      1. Material model - Air
- Surfaces
  - Inflow
    - Simple Boundary Condition
      1. Type - Inflow
      2. Inflow type - Average Velocity
      3. Average velocity - `0.6667` m/sec
  - Max_Z
    - Simple Boundary Condition - (disabled to allow for periodic conditions to be set)
  - Min_Z
    - Simple Boundary Condition - (disabled to allow for periodic conditions to be set)
  - Outflow
    - Simple Boundary Condition
      1. Type - Outflow
  - T_Out
    - Simple Boundary Condition
      1. Type - Outflow
  - Walls
    - Simple Boundary Condition

1 Type - Wall

- Periodics
  - Periodic 1
    - Periodic Boundary Condition
      1 Type - Periodic

References

R. E. Hayes, K. Nandkumar, and H. Nasr-El-Din. "Steady Laminar Flow in a 90 Degree Planar Branch". Computers and Fluids 17(4): 537-553. 1989.

Turbulent Flow Through a Wavy Channel

In this application, AcuSolve is used to simulate turbulent flow through a channel with a lower wall shaped as a sinusoidal wave. AcuSolve results are compared with experimental results adapted from Kuzan (1986). The close agreement of AcuSolve results with experimental results validates the ability of AcuSolve to model cases with internal flow through a channel with wavy walls.

Problem Description

The problem consists of air flowing through a channel with a wavy bottom wall. The channel is 1.1 m high, 1.0 m wide, and is modeled as a section 1.0 m in length, as shown in the following image, which is not drawn to scale. The bottom wall wave shape has an amplitude of 0.1 m and a wavelength of 1 m. The mass flow rate through the channel is set to a constant value of 0.816 kg/s. The flow field develops as a result of the non-planar bottom wall and viscous stresses acting near the top and bottom walls. Collision of air with the peak of the wave on the channel floor causes an acceleration of the flow, followed by recirculation as the flow area expands into the valley.

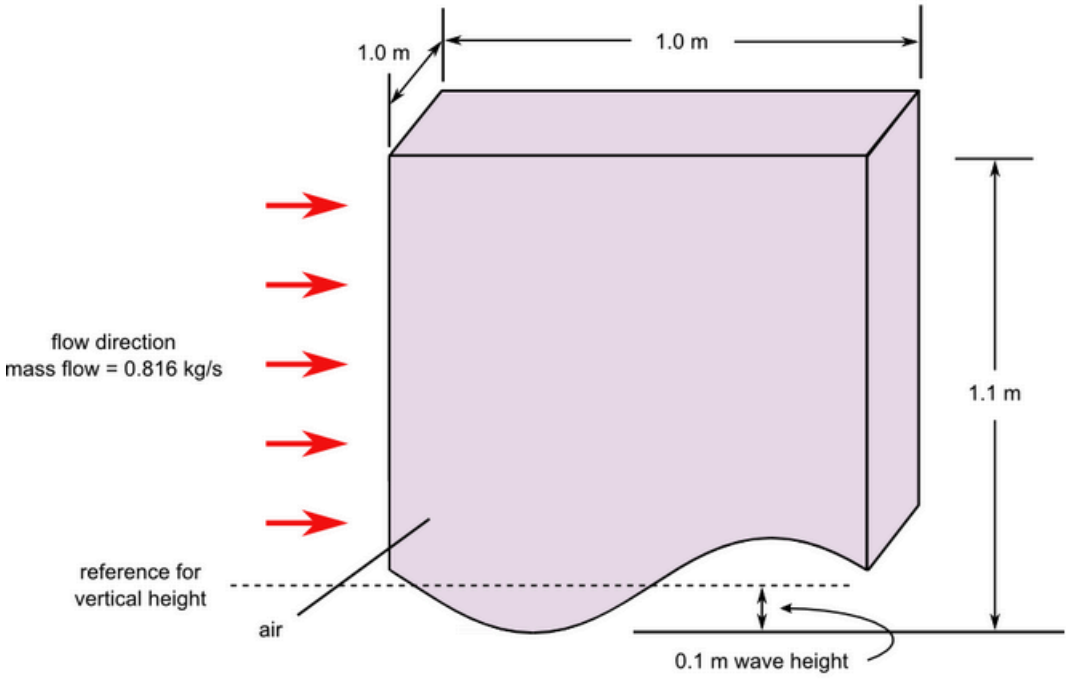


Figure 137: Critical Dimensions and Parameters for Simulating Turbulent Flow Through a Wavy Channel

The simulation was performed as a two dimensional problem by restricting flow in the out-of-plane direction through the use of a mesh that is one element thick. The elements were extruded to the width of the channel.

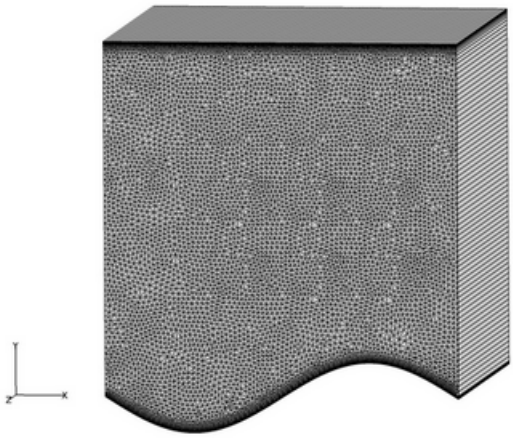


Figure 138: Mesh Used for Simulating Turbulent Flow Through a Wavy Channel

AcuSolve Results

The AcuSolve solution converged to a steady state and the results reflect the mean flow conditions. The expansion of the cross section as the air passes the trough in the wave causes an adverse pressure gradient to form. This results in separation of the flow along the downward-slanting walls of the wavy surfaces. The recirculation zone establishes itself within the troughs of the wave. The remaining flow above the troughs maintains its velocity in the streamwise direction and distributes throughout the channel. The flow accelerates as it travels over the wave peak and the velocity continues to increase as a function of distance from the wall until it reaches a maximum velocity approximately 0.3 m away from the upper wall.

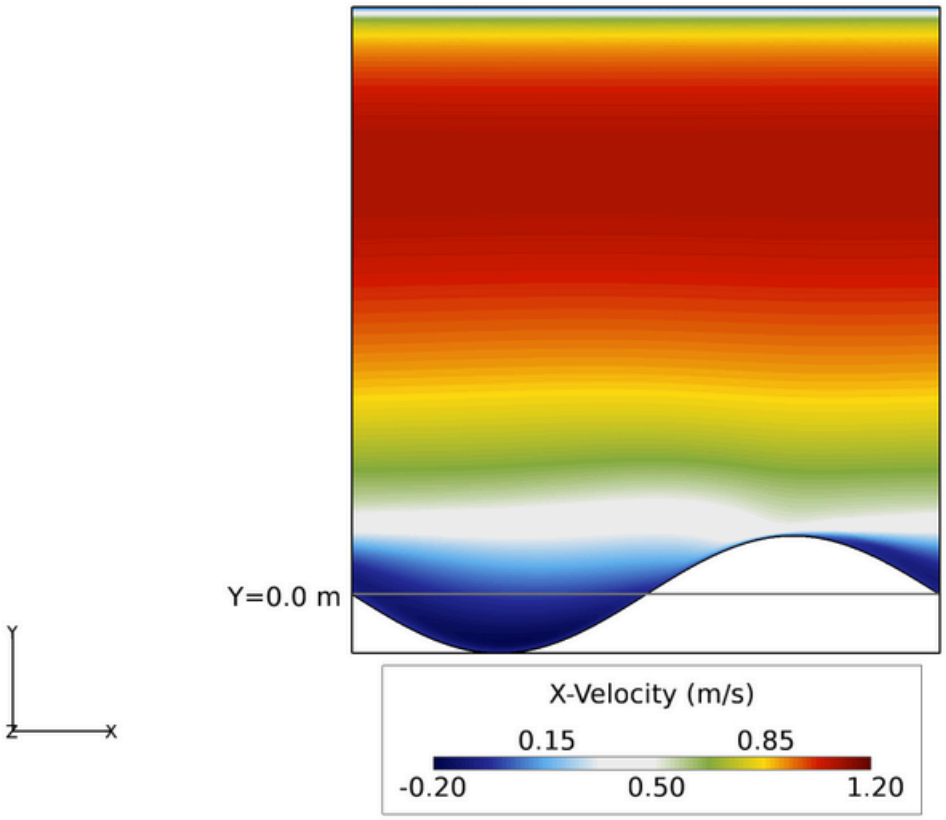


Figure 139: Velocity Contours in the X-Y Plane in a Wavy Channel (the Horizontal Line Represents the Reference for Wave Height - the Wave Crest is 0.1 m Above The Reference Height, and the Wave Valley is 0.1 m Below the Reference Height)

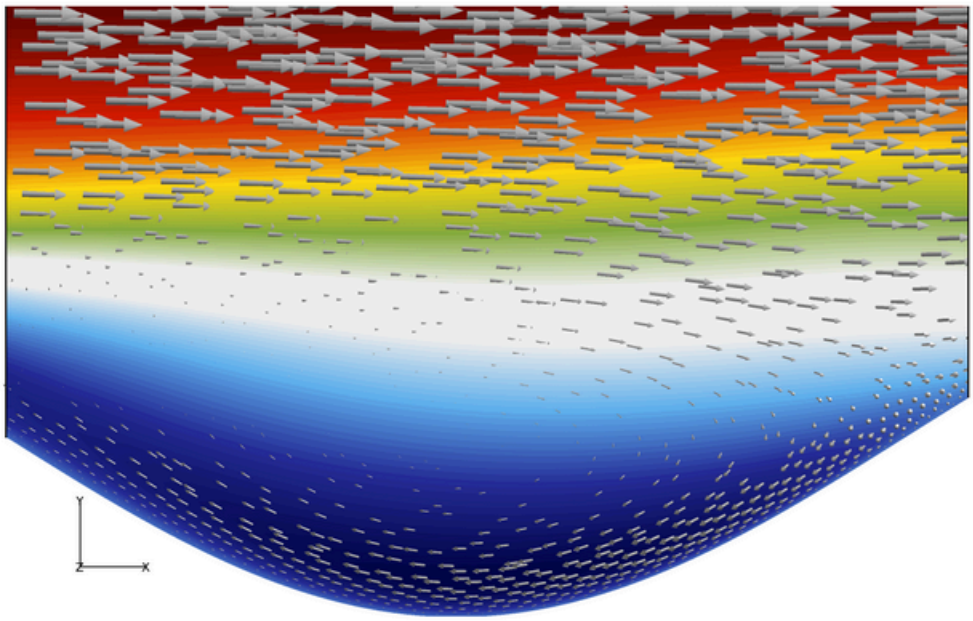


Figure 140: Close-Up View of Velocity Contours and Velocity Vectors in the X-Y Plane Near the Valley of a Wave

The X-velocity directly over the center of the wave valley initially decreases (backflow) as distance away from the bottom wall increases, with a maximum velocity in the -X direction at approximately 0.03 m above the valley floor. The X-velocity then increases to zero m/sec at 0.1 m above the valley, reflecting an end of the recirculation.

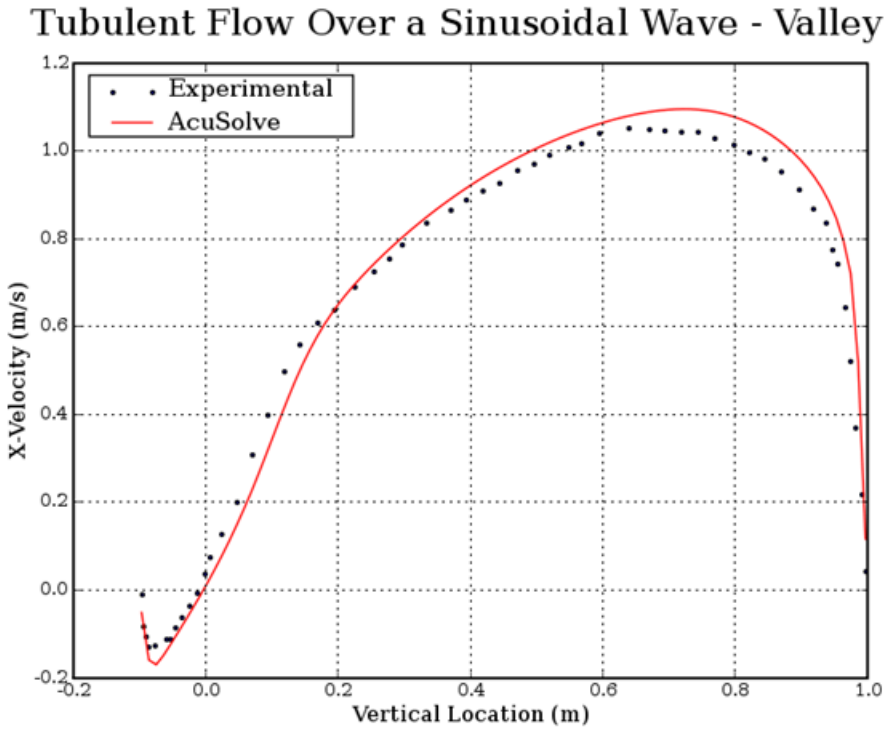


Figure 141: X-Velocity Plotted Against Vertical Location in the Channel Above the Valley Center (the Valley Floor is 0.1 m Below the Reference Height)

The X-velocity directly over the wave peak has different behavior due to the lack of recirculation. The velocity above the peak increases as distance away from the bottom wall increases, with a maximum velocity in the X direction at approximately 0.75 m. The velocity then decreases to zero at the top wall.

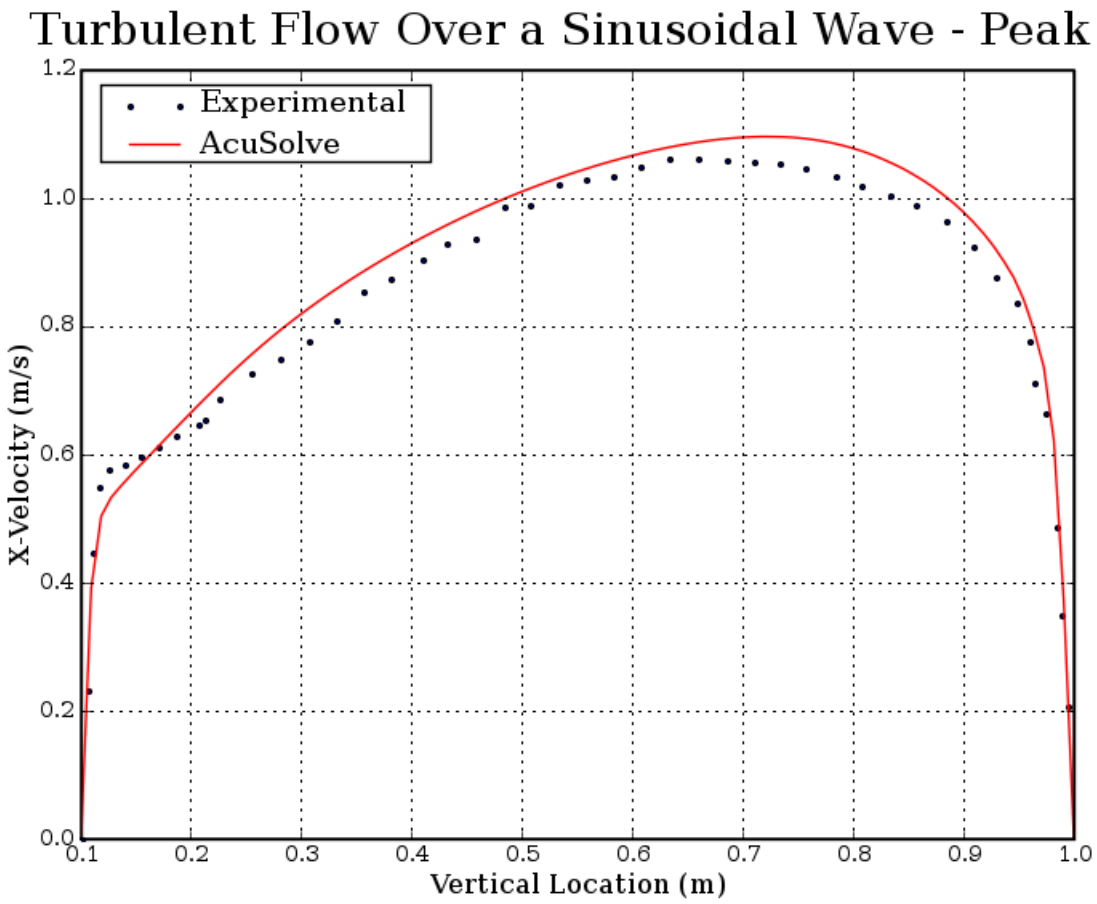


Figure 142: X-Velocity Plotted Against Vertical Location in the Channel Above the Wave Peak (the Wave Peak is 0.1 m Above the Reference Height)

Summary

The AcuSolve results compare well with the experimental data for X-velocity in a channel with a wavy floor. In this application, the flow is driven with a constant mass flow rate and periodic constraints are used to model a repeating array of channel segments with a wavy bottom wall. Separation of the flow occurs as a result of the adverse pressure gradient created by the changes in area. This leads to recirculation within the wave valleys. The flow separation occurs along the smoothly tapered wave wall, illustrating the ability of AcuSolve to accurately predict the separation point in this type of application. The X-velocity predicted by AcuSolve matches the experimental results with an overall coefficient of determination (R2) of 0.99 for each location shown in the plots.

Simulation Settings for Turbulent Flow Through a Wavy Channel

AcuConsole database file: `<your working directory>\wavy_channel_turbulent\wavy_channel_turbulent.acs`

Global

- Problem Description

- Analysis type - Steady State
- Turbulence equation - Spalart Allmaras

- Auto Solution Strategy
  - Relaxation factor - `0.4`
- Material Model
  - Air
    - Density - `1.0` kg/m3
    - Viscosity - `0.0001` kg/m-sec

  Model
- Volumes
  - Fluid
    - Element Set
      1. Material model - Air
- Surfaces
  - Max_X
    - Simple Boundary Condition - (disabled to allow for periodic conditions to be set)
  - Max_Y
    - Simple Boundary Condition
      1. Type - Wall
  - Max_Z
    - Simple Boundary Condition - (disabled to allow for periodic conditions to be set)
  - Min_X
    - Simple Boundary Condition - (disabled to allow for periodic conditions to be set)
    - Advanced Options
      1. Integrated Boundary Conditions
         1. Mass Flux
            1. Type - Constant
            2. Constant value - `-0.816` kg/sec
  - Min_Y
    - Simple Boundary Condition
      1. Type - Wall
  - Min_Z
    - Simple Boundary Condition - (disabled to allow for periodic conditions to be set)
- Periodics
  - Periodic-Crossflow
    - Periodic Boundary Condition
      1. Type - Periodic

- Periodic-Streamwise
  - Periodic Boundary Condition
    1. Type - Periodic
  - Individual Periodic BCs
    1. Velocity
       1. Type - Periodic
    2. Pressure
       1. Type - Single Unknown Offset
    3. Eddy Viscosity
       1. Type - Periodic

References

J. D. Kuzan."Velocity Measurements for Turbulent Separated and Near-Separated Flows Over Solid Waves". Ph.D. thesis. Deptartment of Chemical Engineering. University of Illinois. University of Illinois. Urbana, IL. 1986

Laminar Flow Through a Channel with Heated Walls

In this application, AcuSolve is used to simulate high Peclet number laminar flow through a channel with heated walls. AcuSolve results are compared with analytical results adapted from Hua and Pillai (2010). The close agreement of AcuSolve results with analytical results validates the ability of AcuSolve to model cases involving heat transfer to a moving fluid with a high Peclet number.

Problem Description

The problem consists of water at 20 °C flowing through a channel of infinite width with top and bottom walls heated to 75 °C. The channel is 0.2 m high and 0.8 m long, as shown in the following image, which is not drawn to scale. A centrally located slice 0.02 m wide is modeled with slip boundary conditions so that side-wall influences can be ignored. Water enters the channel with an average velocity of 0.003 m/s. As the fluid flows through the channel, it is heated by the top and bottom plates.

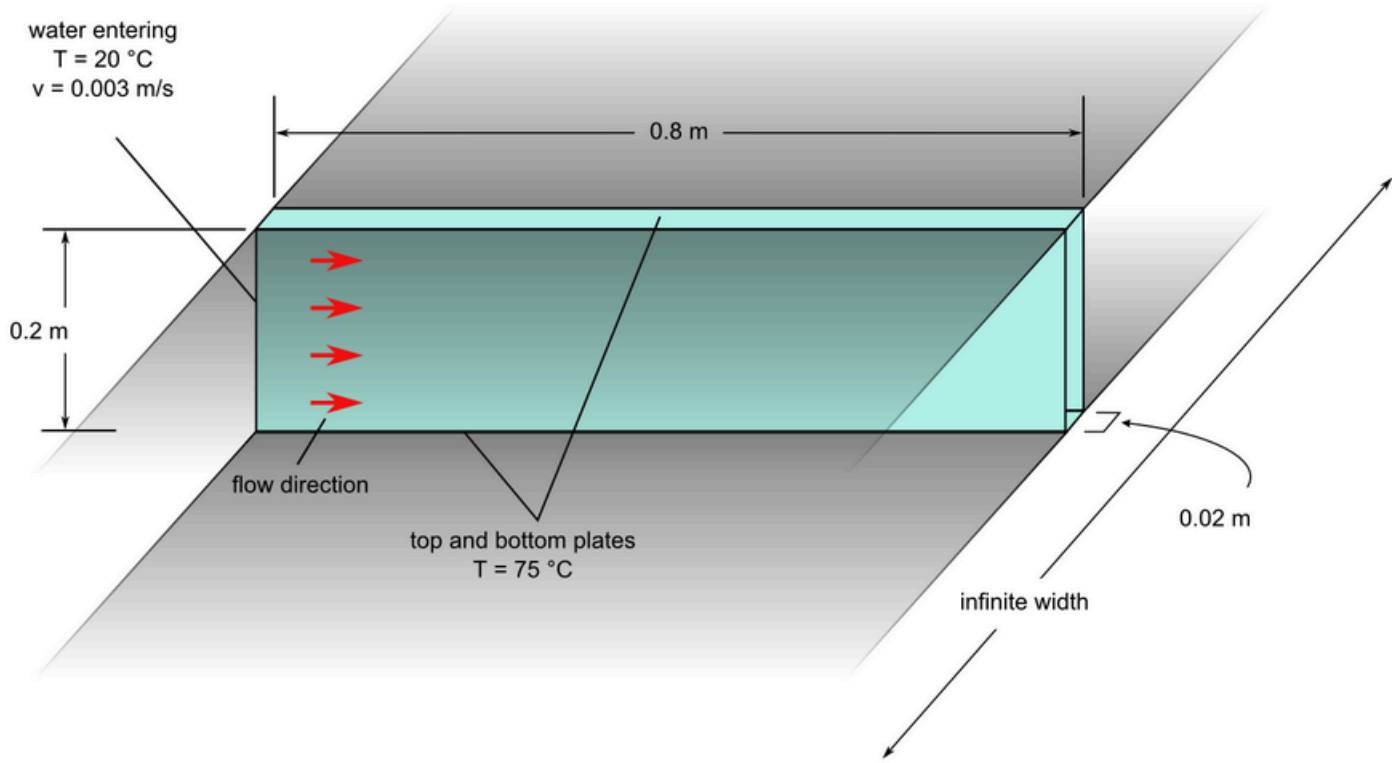


Figure 143: Critical Dimensions and Parameters for Simulating Laminar Flow Through a Channel with Heated Walls

The simulation was performed as a two dimensional problem by restricting flow in the out-of-plane direction through the use of a mesh that is one element thick. In addition, the symmetry of the geometry in the height direction is exploited to allow for modeling only half of the geometry. These characteristics allow for accurate simulation of flow while minimizing computational time.

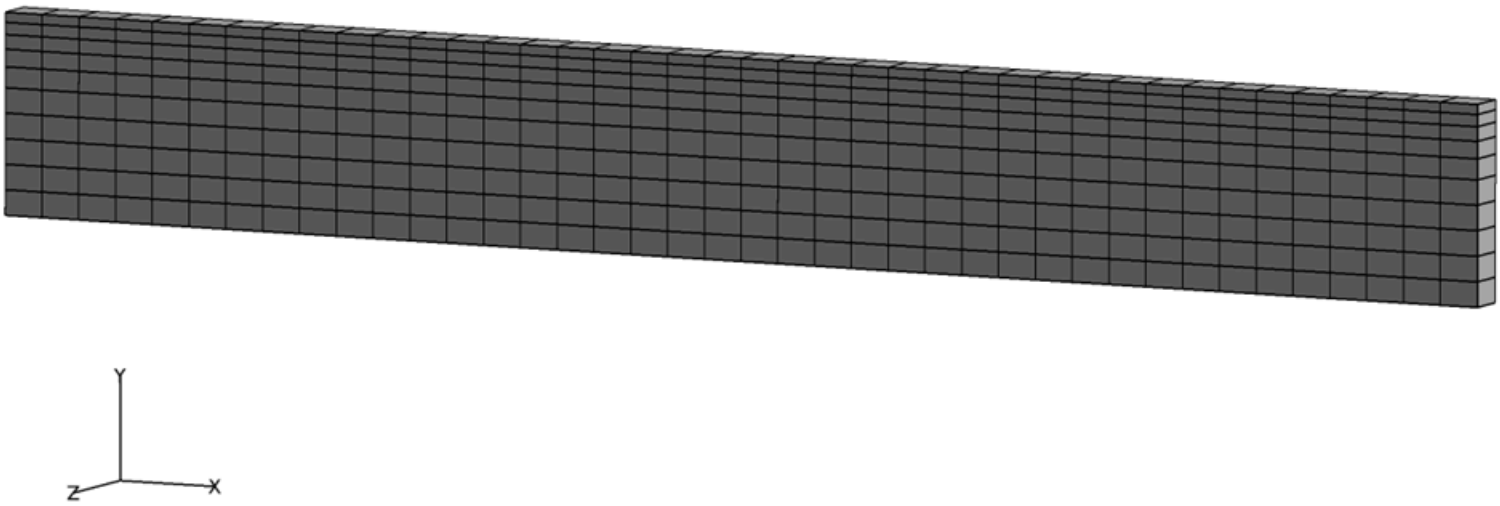


Figure 144: Mesh (Top Half of the Channel) used for Simulating Laminar Flow Through a Channel with Heated Walls

AcuSolve Results

The AcuSolve solution converged to a steady state and the results reflect the mean flow conditions. As the cool water enters the channel at temperature less than that of the walls, heat is transferred to the water by conduction. As the fluid travels along the channel, the temperature differential between the wall and the adjacent water decreases. The thermal boundary layer within the water develops as the flow propagates downstream.

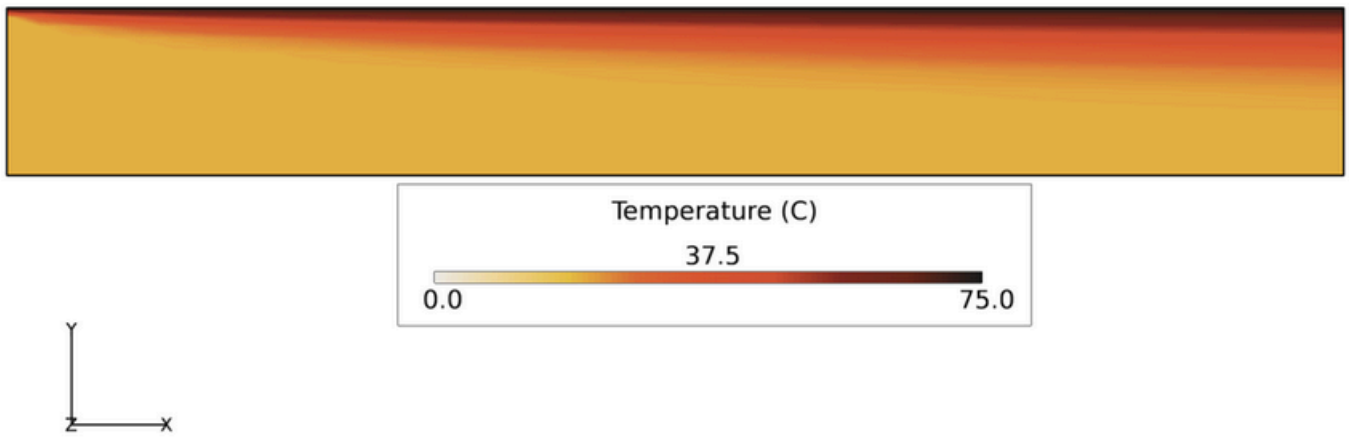


Figure 145: Temperature Contours Along the Top Half of a Heated Channel

Temperature at a specified vertical position in the channel increases along the length of the channel. The nature of that temperature change is dependent on proximity to the heated wall. Water in the center of the flow will have the least temperature change. Since this problem was solved for symmetrical flow, only the top half of the flow region was modeled. The vertical position for results

shown in the following figure are based on the center of flow having a Y-position of 0. For a vertical position near the center of flow (Y=0.0595) there is minimal change in temperature.

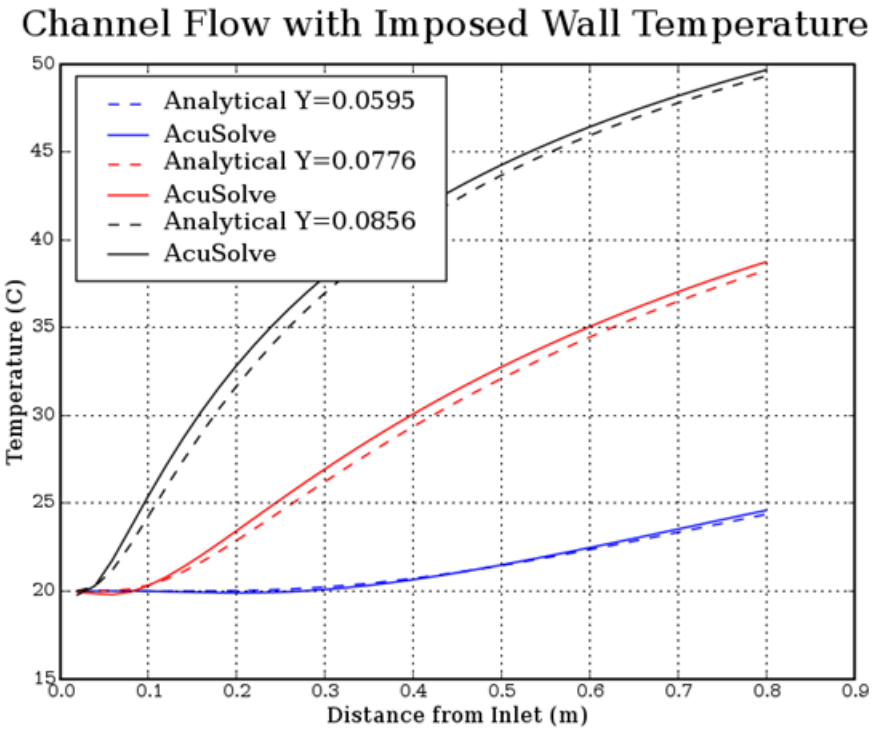


Figure 146: Temperature Plotted Against Distance from Inlet for 3 Different Heights from the Channel Center Line

Summary

The AcuSolve results compare well with the analytical results for the development of a thermal boundary layer in a heated channel. In this application, the model is set up to yield large gradients as the flow convects away from the inlet. The boundary conditions and mesh size were chosen specifically to yield a high Peclet number. The element Peclet number in the flow direction in this case is Pe=30.0, as calculated from the following equation.

$$Pe = \frac{\rho C p |v| he}{k} \tag{5}$$

where ρ is the density, CP the heat capacity, v the velocity, he the length, and k the thermal conductivity.

This example shows the robustness of the stabilized technique in AcuSolve when element Peclet number is high. Note that standard Galerkin finite element formulations become unstable when the element Peclet number is greater than 1.0.

Simulation Settings for Laminar Flow Through a Channel with Heated Walls

AcuConsole database file: `<your working directory>\channel_laminar_heat\channel_laminar_heat.acs`

Global

- Problem Description
  - Analysis type - Steady State
  - Temperature equation - Advective Diffusive
  - Turbulence equation - Laminar
- Auto Solution Strategy
  - Relaxation factor - `0.4`
- Material Model
  - Fluid_Material
    - Density - `1000.0` kg/m3
    - Specific Heat - `1000` J/kg-K
    - Viscosity - `1.0e-12` kg/m-sec
    - Conductivitiy - 1.0 W/m-K

  Model
- Volumes
  - Fluid
    - Element Set
      1. Material model - Fluid_Material
- Surfaces
  - Inlet
    - Simple Boundary Condition
      1. Type - Inflow
      2. Inflow type - Velocity
      3. X velocity - `0.003` m/sec
      4. Temperature - `20` °C
  - Outlet
    - Simple Boundary Condition
      1. Type - Outflow
  - Symm_MaxZ
    - Simple Boundary Condition
      1. Type - Slip
  - Symm_MinY
    - Simple Boundary Condition
      1. Type - Slip
  - Symm_MinZ
    - Simple Boundary Condition
      1. Type - Slip
  - Wall

- Simple Boundary Condition
  1. Type - Wall
  2. Temperature BC type - Value
  3. Temperature - 75 °C

References

Hua Tan and K. M. Pillai. "Numerical Simulation of Reactive Flow in Liquid Composite Molding Using Flux-Corrected Transport (FCT) Based Finite Element/Control Volume (FE/CV) Method". International Journal of Heat and Mass Transfer. 53:2256-2271, 2010.

Turbulent Flow Behind an Open-Slit V

In this application, AcuSolve is used to simulate turbulent flow of air through and behind a two dimensional open-slit V. AcuSolve results are compared with experimental results adapted from Yang and Tsai (1993). The close agreement of AcuSolve results with experimental results validates the ability of AcuSolve to model the Coandă effect.

Problem Description

The problem consists of air flowing through and past an open-slit V positioned within a flow domain, as shown in the following image, which is not drawn to scale. The flow domain is 0.3 m long and 0.1 m high. The narrow end of the V is positioned 0.05 m from the domain inlet. The slit in the V is 0.002 m high. The V widens to 0.022 m at 0.075 m from the domain inlet. Air enters the domain with a constant velocity of 20 m/s. The upper and lower limits of the domain are defined as no-slip boundary conditions.

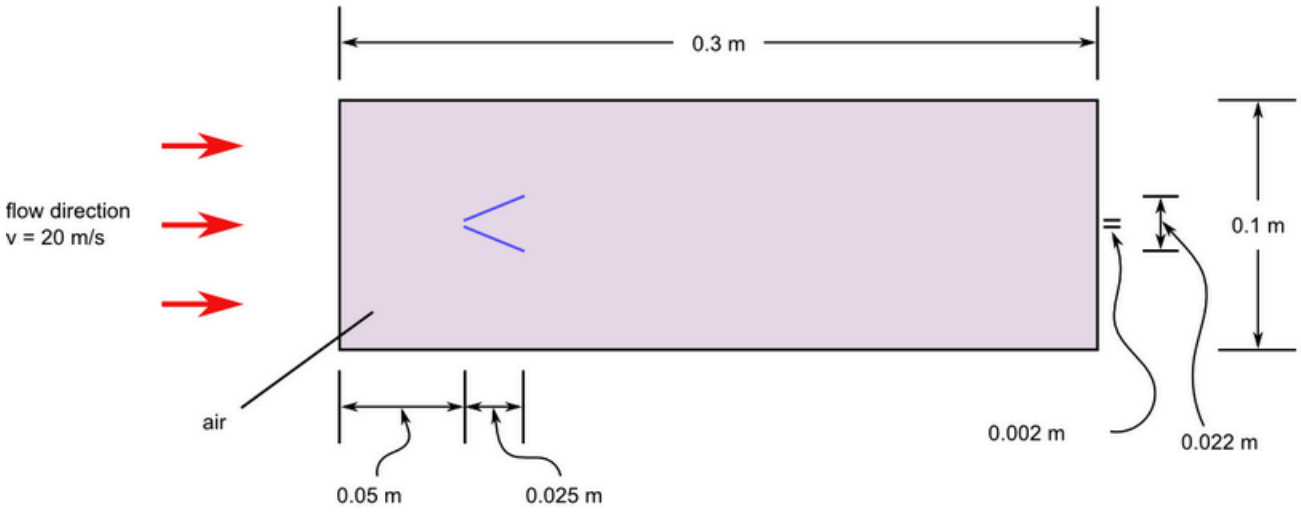


Figure 147: Critical Dimensions and Parameters for Simulating Turbulent Flow Behind an Open-Slit V

The simulation was performed as a two dimensional problem by restricting flow in the out-of-plane direction through the use of a mesh that is one element thick. A coarse mesh is used throughout much of the domain, with mesh refinement closer to the V.

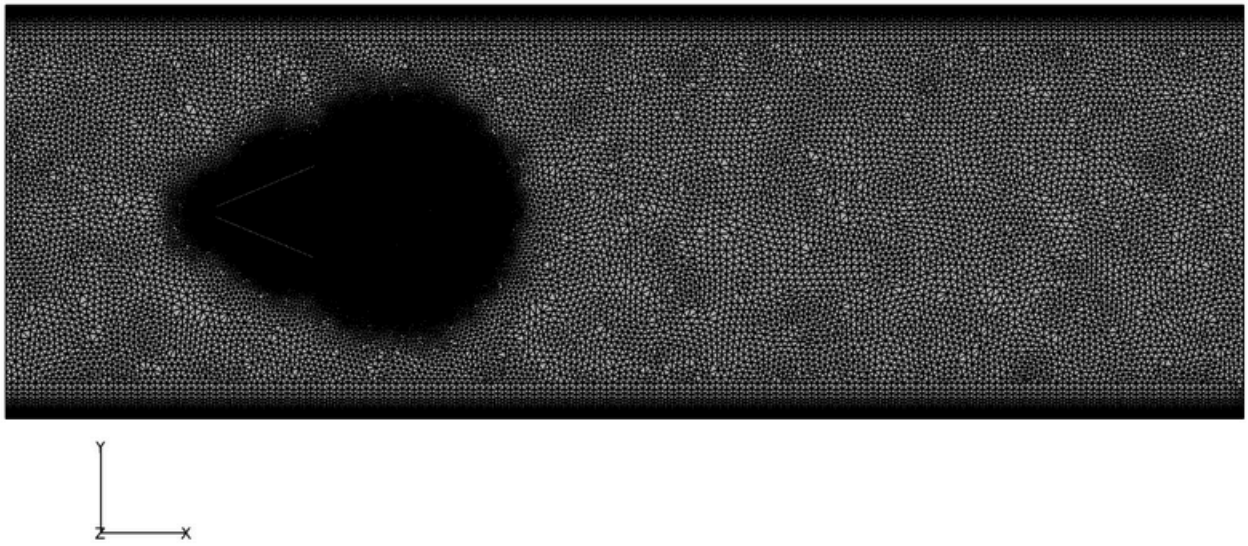


Figure 148: Mesh used for Simulating Turbulent Flow Behind an Open-Slit V (the V Lies Within the Dense Area of the Mesh)

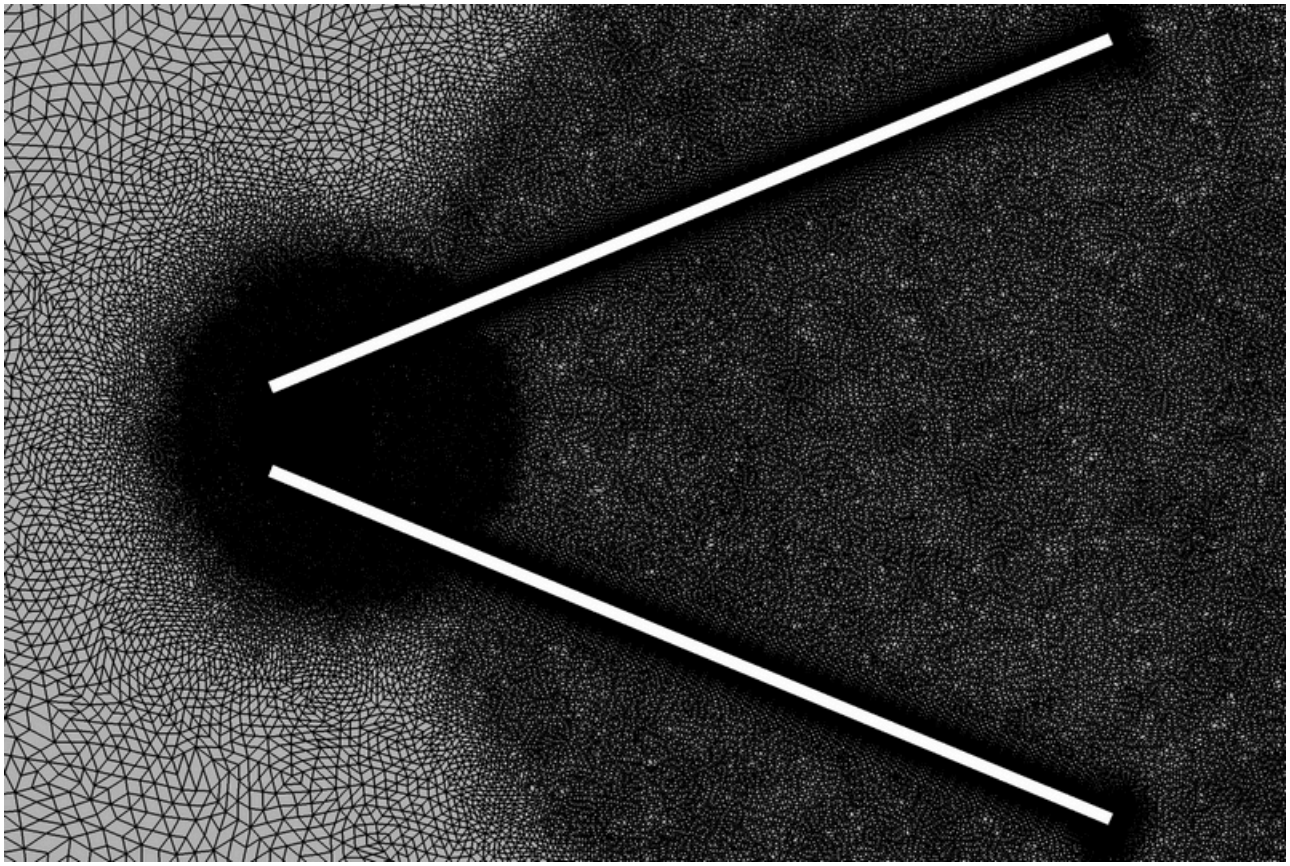


Figure 149: Mesh Surrounding the Open-Slit V

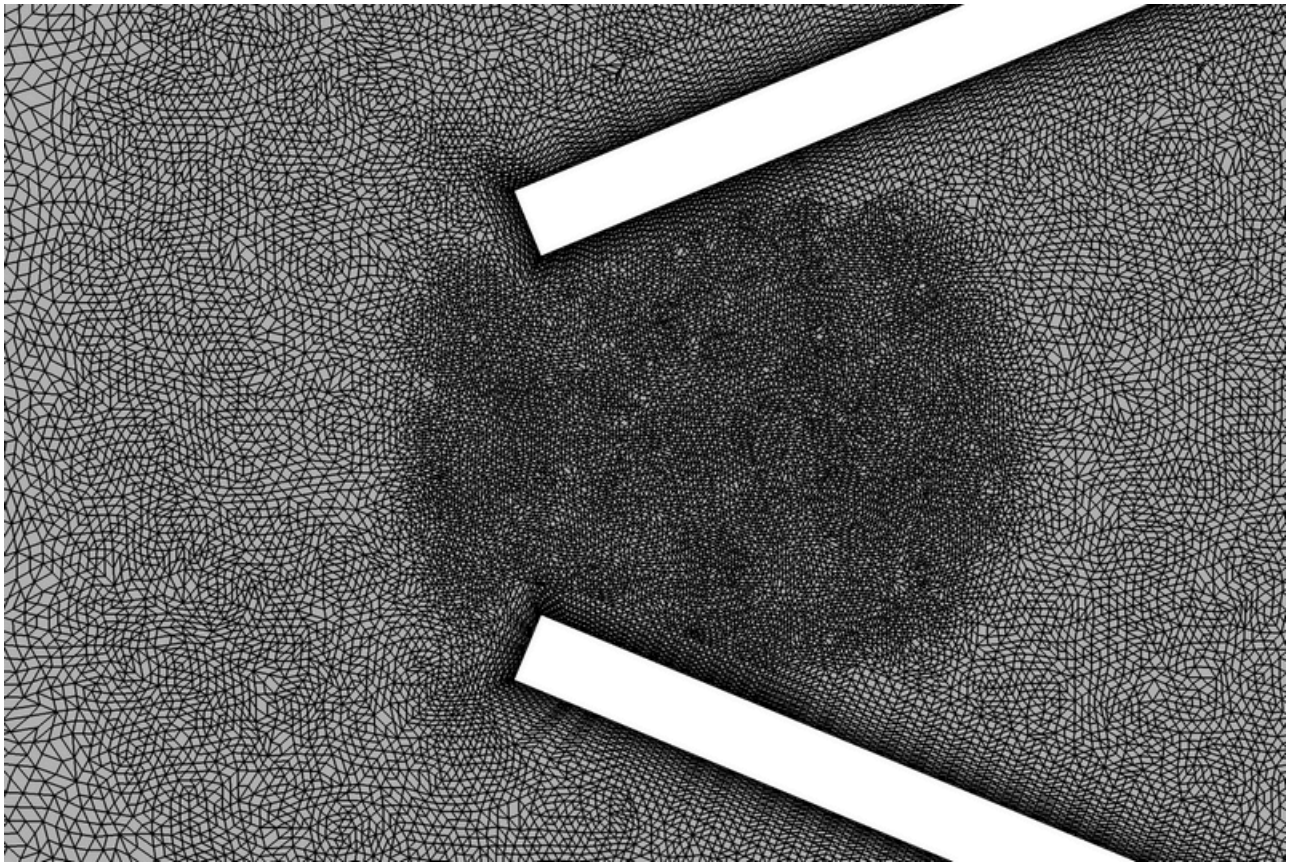


Figure 150: Mesh Near the Open Slit

AcuSolve Results

The AcuSolve solution converged to a steady state and the results reflect the mean flow conditions. Air flows through the open slit in the V and accelerates while being forced to one side due to the Coandă effect. As air encounters the exterior of the widening gutter, velocity increases and the wake induces recirculation near the exit of the V. The recirculation zone extends downstream of the V gutter.

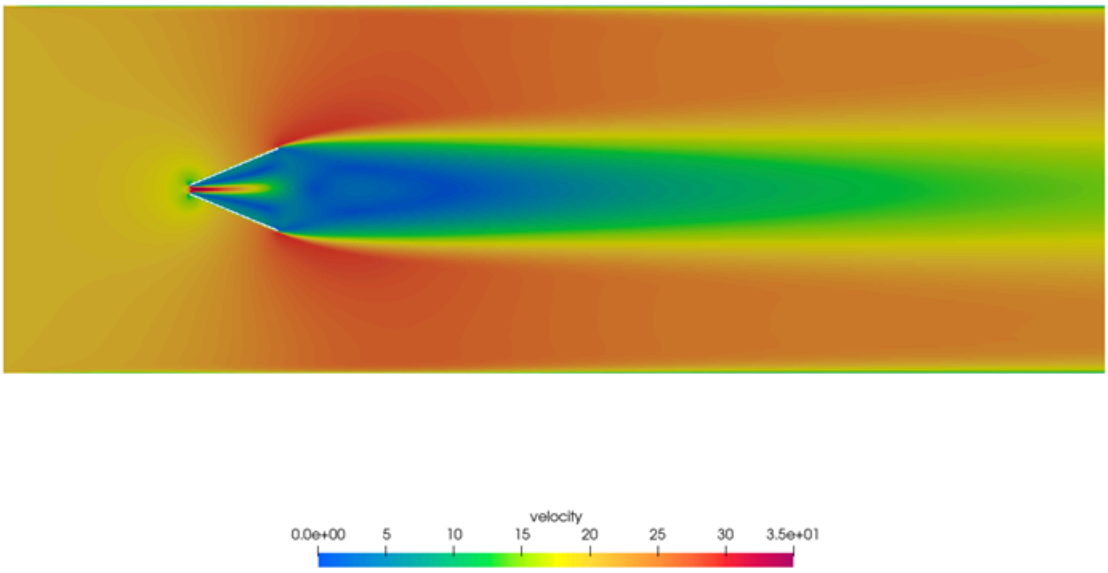


Figure 151: Contours of X-Velocity of Flow Through and Around an Open-Slit V (the Vertical Line Represents the Location, 0.022 m Downstream from the V exit, at Which Experimental Data is Compared to AcuSolve Results)

AcuSolve results were compared to experimental results at different heights 0.022 m behind the V exit. X-velocity is near zero at the bottom of the domain (height = -0.05 m), rising steeply with distance from the wall. The velocity gradient decreases until approximately 0.018 m below the center line of the domain, which is slightly below the bottom of the V exit. The velocity behind the V drops sharply with an increase in height, due to the blockage caused by the presence of the slanted walls. The lowest velocity is just above the center line of the domain.

The slight asymmetry in the velocity profile in the wake of the V is expected due to the Coandă effect.

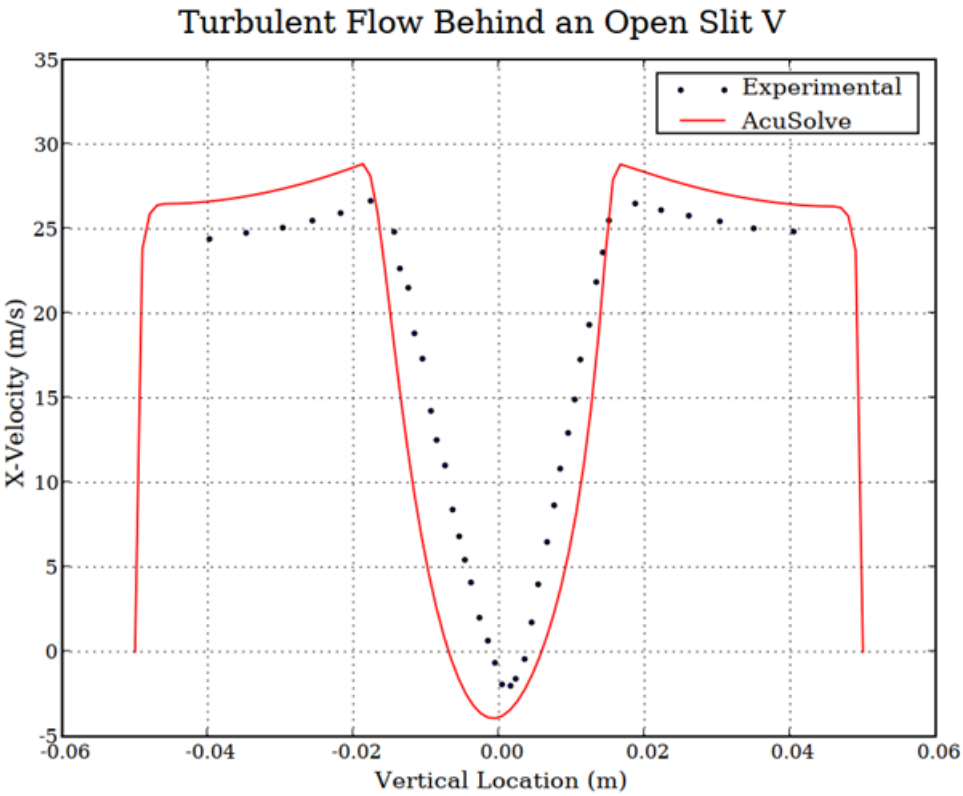


Figure 152: X-Velocity Plotted Against Vertical Location 0.0022 m Downstream of the V Exit

Summary

The AcuSolve results compare well with the experimental results for flow through and around an open-slit V. In this application, the V-shaped geometry diverts flow towards the side walls of the channel and also creates a high-velocity jet through the slit. The low pressure associated with the jet causes a deflection towards the walls of the V, resulting in an asymmetric flow field within the V shape. This application illustrates the ability of AcuSolve to accurately predict the Coandă effect. The acceleration of the flow due to the deflection along the V-shaped walls and the momentum deficit in the wake of the V is captured accurately.

Simulation Settings for Turbulent Flow Behind an Open-Slit V

HyperWorks CFD database file: `<your working directory>\v_gutter_turbulent\v_gutter_turbulent.hm`

Global

- Problem Description
  - Analysis type - Steady State
  - Turbulence equation - Spalart Allmaras
- Auto Solution Strategy
  - Relaxation factor - `0.5`
- Material Model

    - Air
        - Density - `1.0` kg/m3
        - Viscosity - `1.8333e-05` kg/m-sec

  Model
- Volumes
    - Fluid
        - Element Set
            1. Material model - Air
- Surfaces
    - Inlet
        - Simple Boundary Condition
            1. Type - Inflow
            2. Inflow type - Velocity
            3. X velocity - `20.0` m/sec
            4. Eddy viscosity - `0.000800426` m2/sec
    - LE_TE
        - Simple Boundary Condition
            1. Type - Wall
    - Outlet
        - Simple Boundary Condition
            1. Type - Outflow
    - Symm_MaxZ
        - Simple Boundary Condition
            1. Type - Slip
    - Symm_MinZ
        - Simple Boundary Condition
            1. Type - Slip
    - V_Walls
        - Simple Boundary Condition
            1. Type - Wall
    - Walls
        - Simple Boundary Condition
            1. Type - Wall

References

J.-T. Yang and G.-L. Tsai. "Near-wake flow of a v-gutter with slit bleed". Journal of Fluid Engineering. 115:13-20. March, 1993.

Turbulent Flow Over a NACA 0012 Airfoil

In this application, AcuSolve is used to simulate turbulent flow of a fluid over a NACA 0012 airfoil at 3 angles of attack, 0 degrees, 10 degrees, and 15 degrees. AcuSolve results are compared with experimental results for coefficients of pressure, lift, and drag reported by NASA. The close agreement of AcuSolve results with experimental results validates the ability of AcuSolve to model external aerodynamics.

Problem Description

The problem consists of a NACA 0012 airfoil located in the center of a cylindrical domain, as shown in the following image, which is not drawn to scale. Fluid enters the domain with a velocity of 1.0 m/s. The domain edges are distant, 500 chord lengths, from the airfoil to minimize any far field effects. The problem is set up to simulate high Reynolds number flow, with Re = 6,000,000.

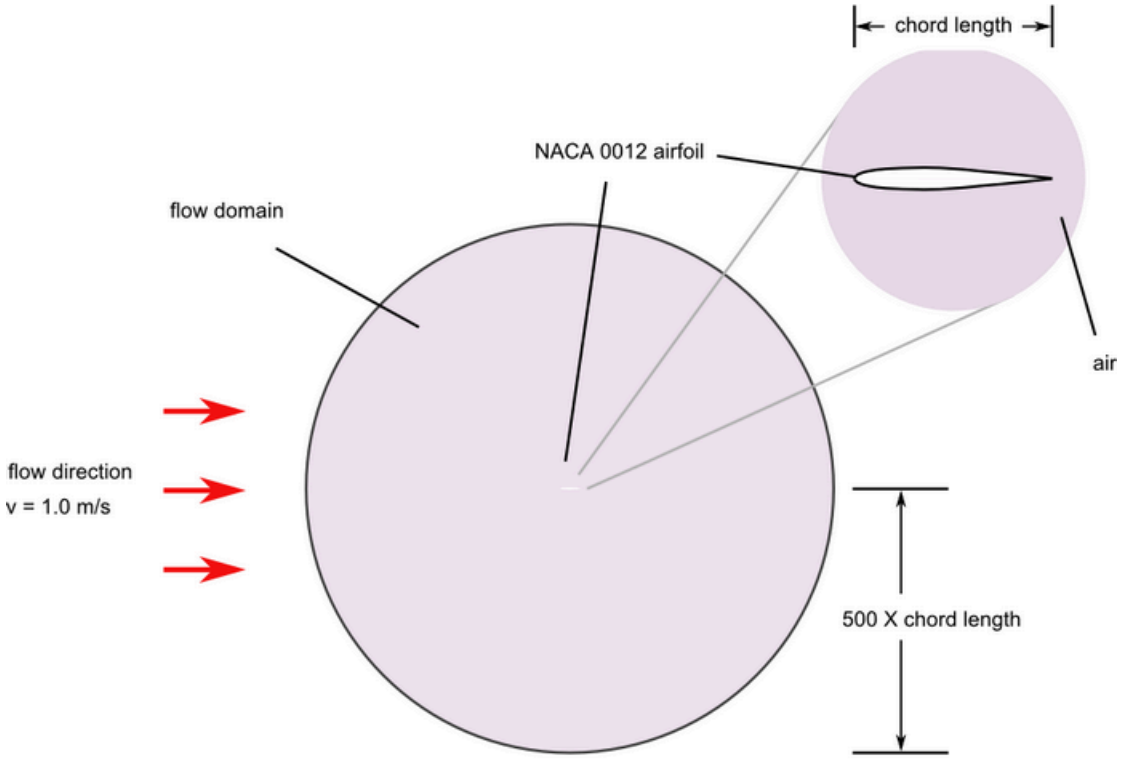


Figure 153: Critical Dimensions and Parameters for Simulating Turbulent Flow over a NACA 0012 Airfoil

The simulation was performed as a two dimensional problem by restricting flow in the out-of-plane direction through the use of a mesh that is one element thick.

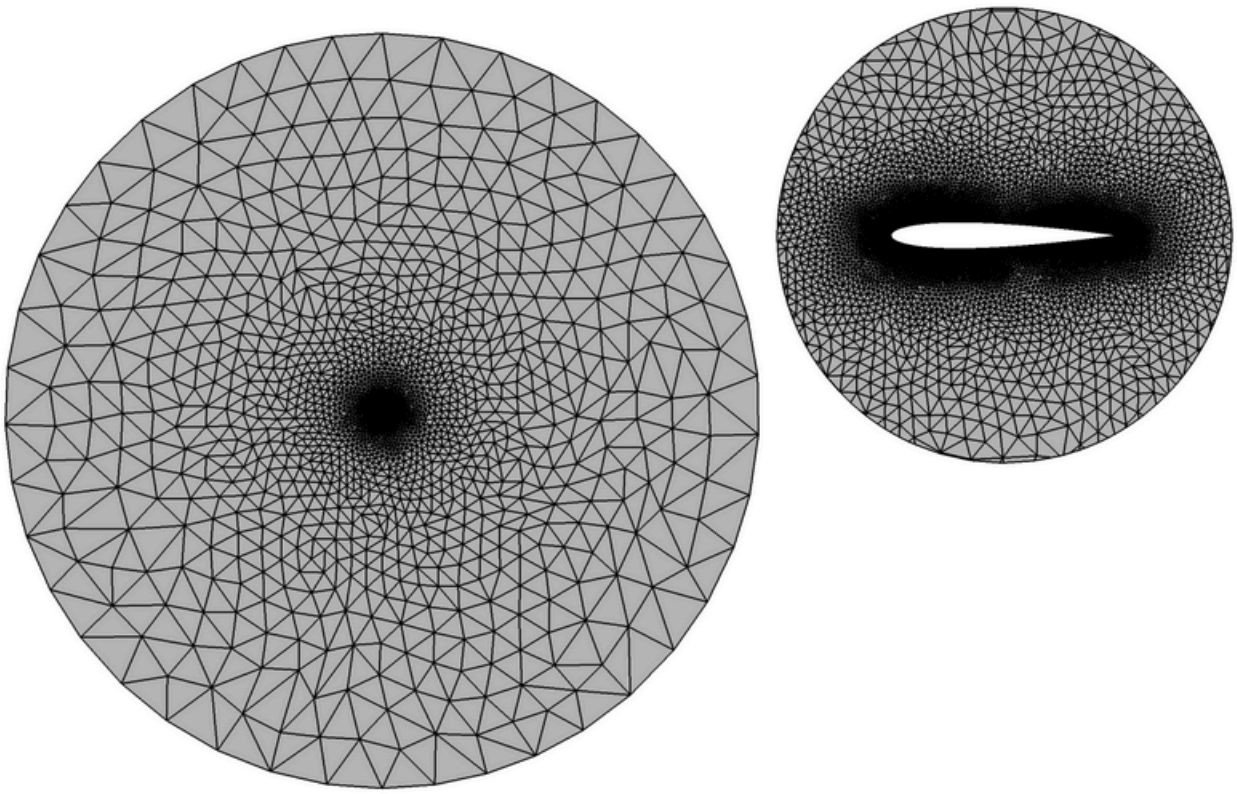


Figure 154: Mesh Used for Simulating Turbulent Flow over a NACA 0012 Airfoil (the Image on the Left Represents the Full Mesh, the Image on the Right Represents Mesh Details near the Airfoil)

AcuSolve Results

The AcuSolve solution converged to a steady state and the results reflect the mean flow conditions for each of the three angles of attack, 0 degrees, 10 degrees, and 15 degrees. For each case, the angle of attack was varied by changing the angle of the incident flow. Note that this enables the use of a single mesh for all of the simulations.

With a 0 degree angle of attack, the flow field is symmetric as the fluid flows over and under the airfoil. The airfoil impedes the flow, causing stagnation at the leading edge. As the fluid passes over and under the airfoil, velocity increases. As the fluid passes over the blunt trailing edge, a minor amount of flow separation occurs. The flow reattaches shortly after it passes the trailing edge and recovers the mean velocity in the distant far field.

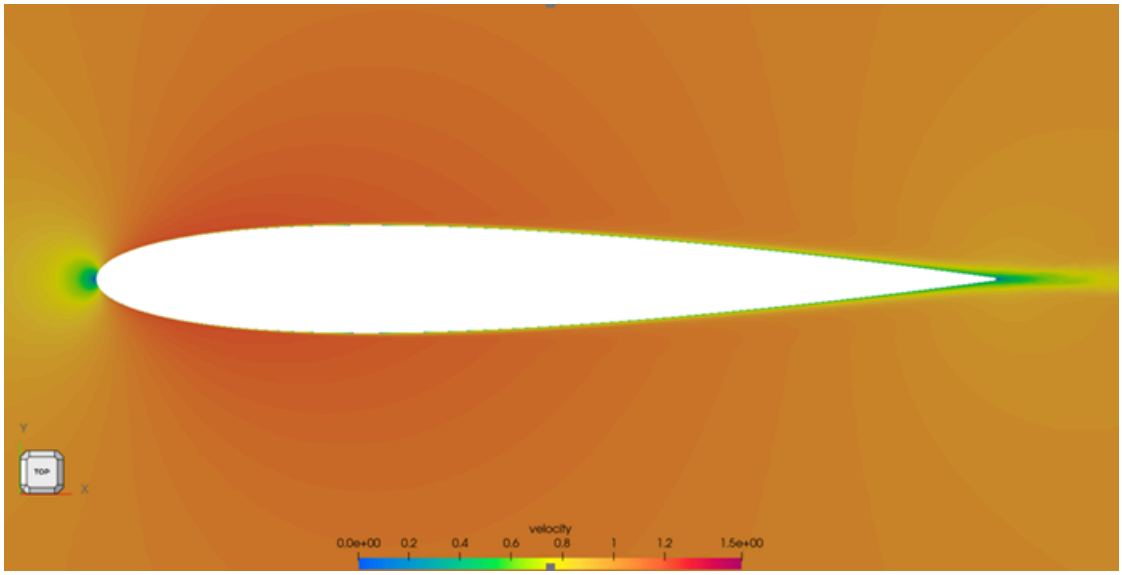


Figure 155: Contours of Velocity Magnitude Where Angle of Attack = 0 Degrees

With a 10 degree angle of attack, the stagnation point is shifted downward (relative to the airfoil), reflective of the shifted angle of attack. Fluid velocity above the airfoil is markedly different than that below the airfoil. A small low-velocity region is evident on the suction side of the airfoil, indicating some separation toward the trailing edge.

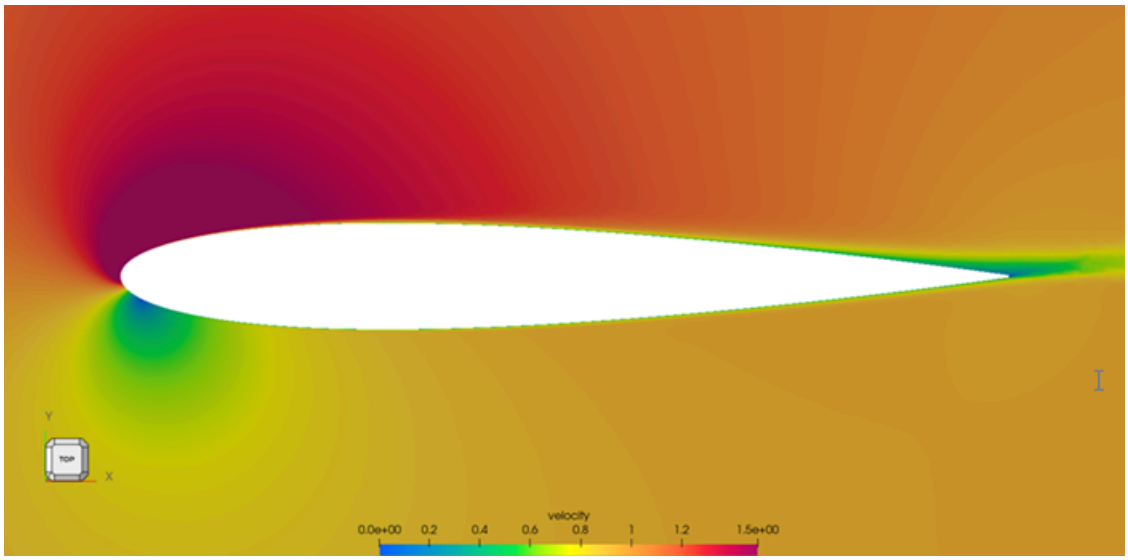


Figure 156: Contours of Velocity Magnitude Where Angle of Attack = 10 degrees

With a 15 degree angle of attack, the stagnation at the front of the airfoil is shifted even farther downward (relative to the airfoil), reflective of the shifted angle of attack. Additionally, the low-velocity wake increases in size, reflecting separation along the suction surface of the airfoil.

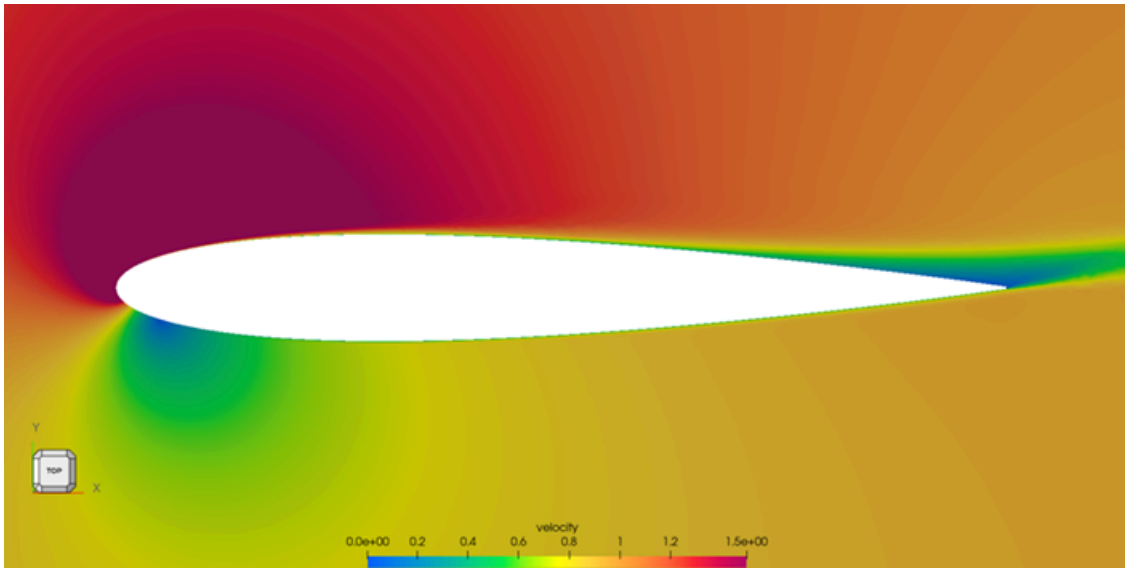


Figure 157: Contours of Velocity Magnitude Where Angle of Attack = 15 Degrees

Experimental values of coefficient of lift (CL) at angles of attack (α) of 10 degrees and 15 degrees and values of drag coefficient (cd) at angles of attack (α) of 0 degrees,10 degrees, and 15 degrees are presented with the corresponding AcuSolve results in the following table.

Table 10:

	CL (α=10)	**CL (α=15)**	**cd (α=0)**	**cd (α=10)**	**cd (α=15)**
Experimental	1.0941	1.5576	0.0082	0.0123	0.0207
AcuSolve	1.0905	1.5428	0.0081	0.0124	0.0208
Percent deviation from experimental	0.33	0.95	1.22	0.81	0.48

AcuSolve values for coefficient of pressure are plotted against experimental results for angles of attack (α) of 0 degrees, 10 degrees, and 15 degrees in the following plots. The results are presented for normalized distance along the airfoil, given by x/c, where x is the distance from the leading edge and c is the chord length.

For each case, AcuSolve is able to predict the flow characteristics at each point along the airfoil surface.

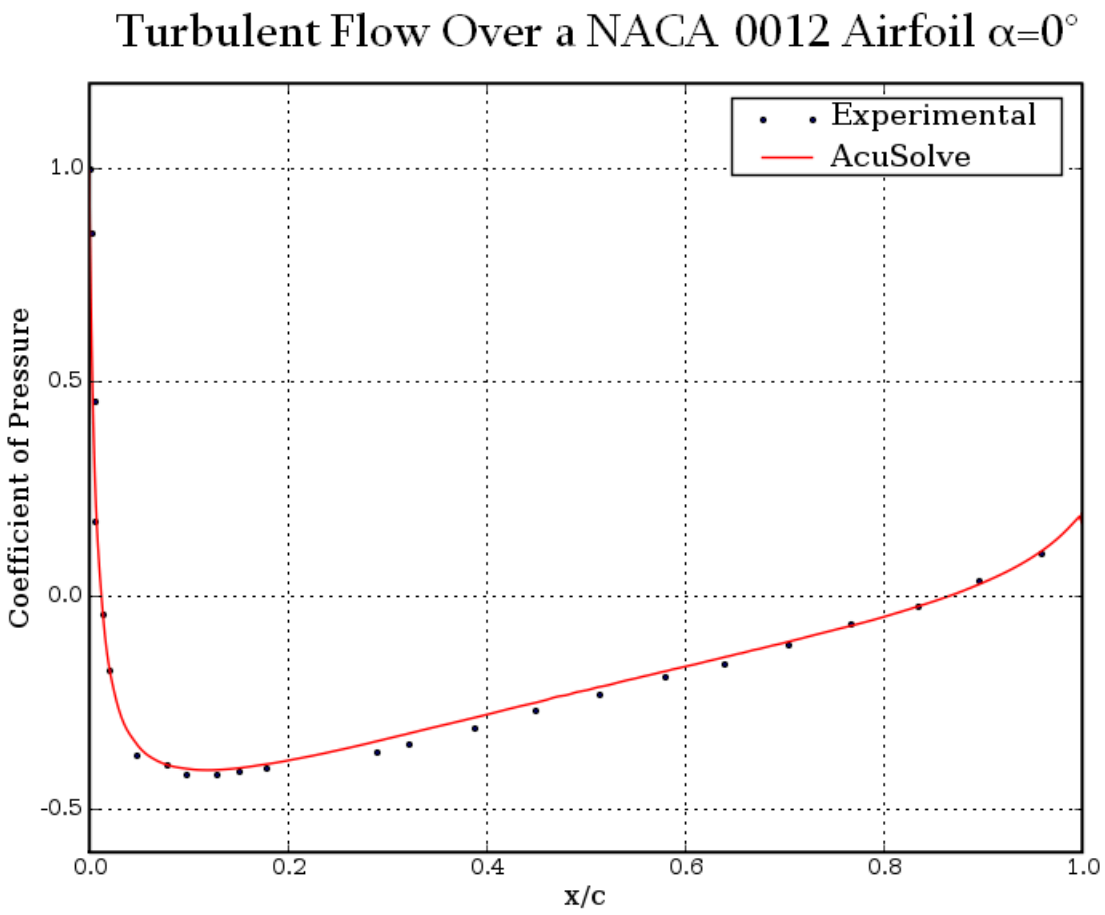


Figure 158: Coefficient of Pressure Plotted Against Normalized Distance Along the Airfoil for Angle of Attack (a) = 0 Degrees

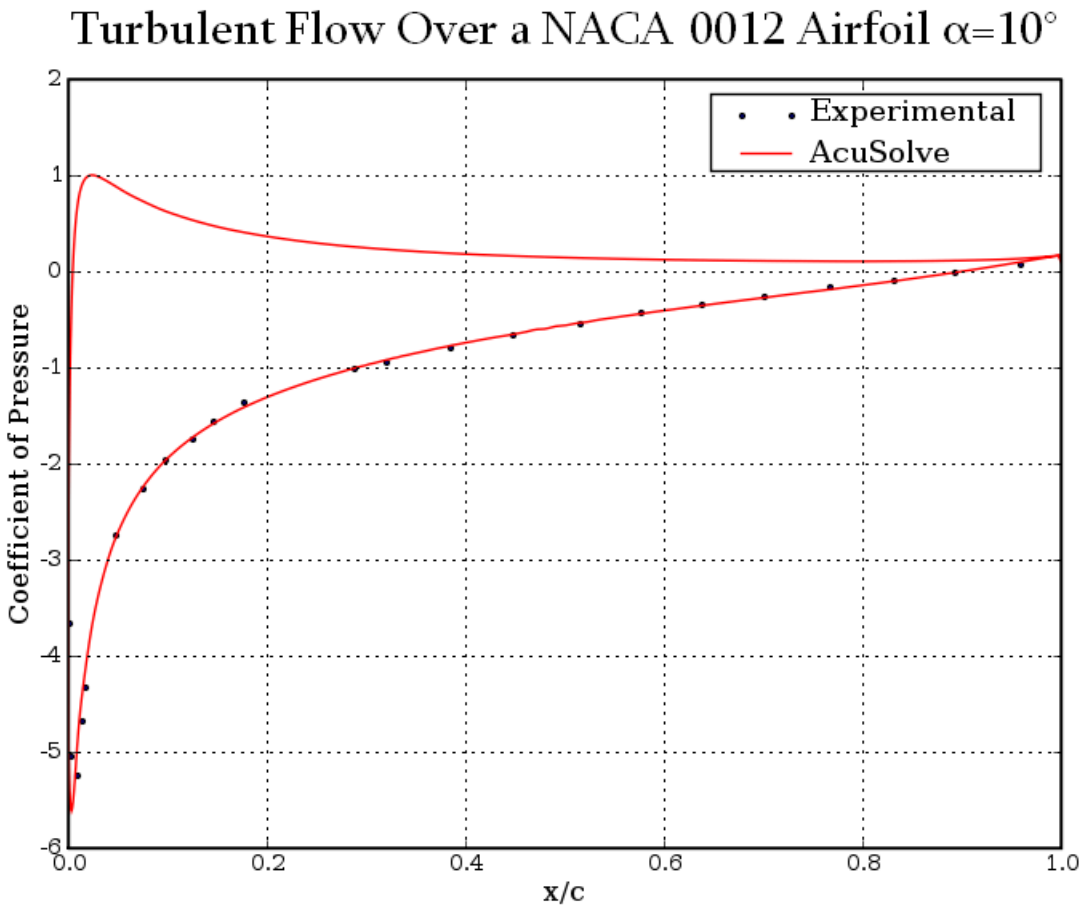


Figure 159: Coefficient of Pressure Plotted Against Normalized Distance Along the Airfoil For Angle of Attack (a) = 10 Degrees

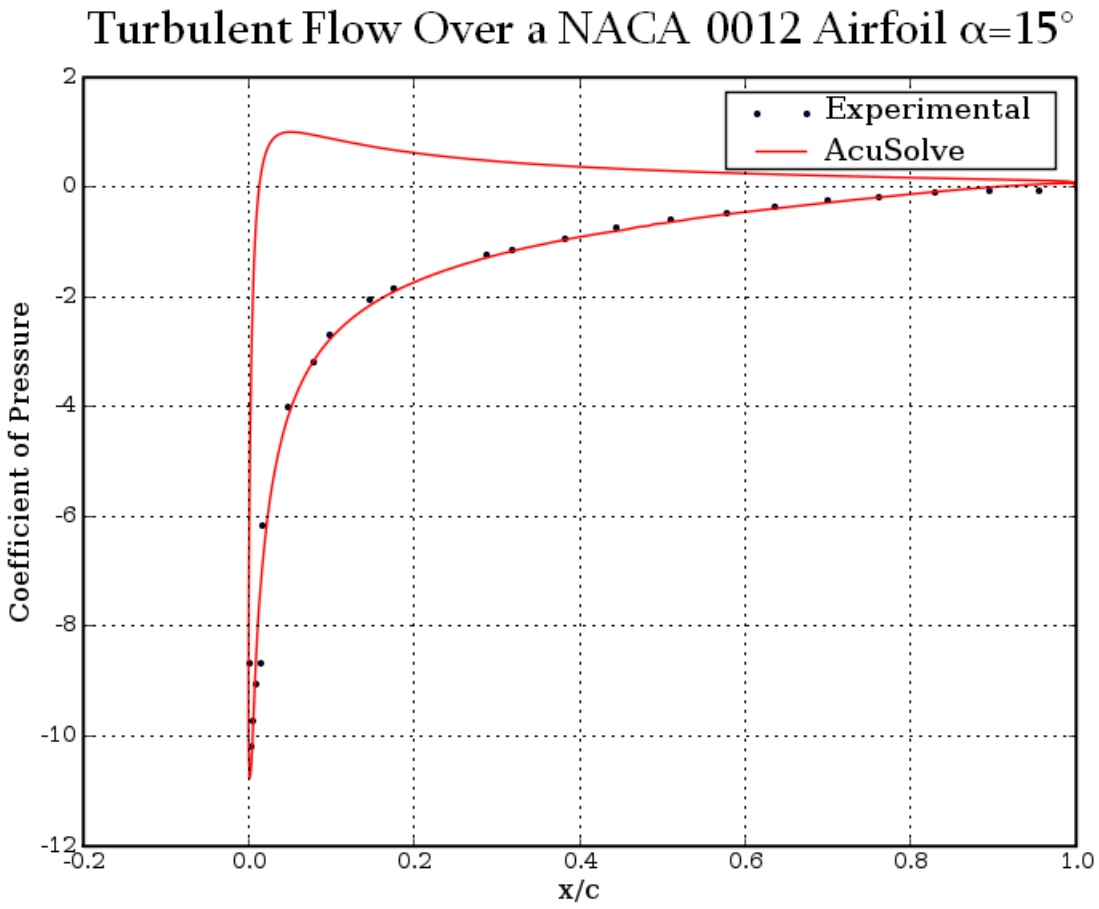


Figure 160: Coefficient of Pressure Plotted Against Normalized Distance Along the Airfoil for Angle of Attack (a) = 15 Degrees

Summary

The AcuSolve results compare well with the experimental results for flow over a NACA 0012 airfoil. In this application, a constant-velocity flow field impinges on the airfoil surface. As the flow convects in the streamwise direction along the airfoil surface, a boundary layer develops. The rate at which the boundary layer develops has significant impact on the viscous stresses present on the airfoil surface. At low angles of attack these stresses dominate the drag on the airfoil. As the angle of attack increases, the flow over the airfoil is no longer symmetric, which leads to the generation of lift. For non-zero angles of attack, the asymmetric pressure distribution on the airfoil creates another source of drag that is combined with the viscous stresses to determine the total drag on the airfoil. The AcuSolve results for coefficients of lift and drag at the 15 percent angle of attack are within 0.91 percent and 0.5 percent of experimental values, respectively. AcuSolve results for coefficient of pressure closely agree with experimental results along the length of the airfoil for all three angles of attack that were investigated.

Simulation Settings for Turbulent Flow Over a NACA0012 Airfoil

HyperWorks CFD database file: `<your working directory>\airfoil_turbulent\airfoil_turbulent.hm`

Global

- Problem Description
  - Analysis type - Steady State
  - Turbulence equation - Spalart Allmaras
- Auto Solution Strategy
  - Convergence tolerance - `0.0001`
  - Relaxation factor - `0.4`
- Material Model
  - Fluid
    - Density - `1.0` kg/m3
    - Viscosity - `1.667e-7` kg/m-sec

  Model
- Volumes
  - Fluid
    - Element Set
      1. Material model - Fluid
- Surfaces
  - +z slip
    - Simple Boundary Condition
      1. Type - Slip
  - -z slip
    - Simple Boundary Condition
      1. Type - Slip
  - airfoil surface
    - Simple Boundary Condition
      1. Type - Wall
  - farfield
    - Simple Boundary Condition
      1. Type - Far Field
      2. X velocity - cos(α) m/sec
      3. Y velocity - sin(α) m/sec
- Eddy viscosity - `1.0e-9` m2/sec

References

NASA - Langley Research Center. http://turbmodels.larc.nasa.gov/naca0012_val_sa.html

Turbulent Natural Convection Inside a Tall Cavity

In this application, AcuSolve is used to simulate the natural convection of a turbulent flow field within a tall rectangular cavity. AcuSolve results are compared with experimental results as described in Betts and Bokhari (2000). The close agreement of AcuSolve results with experimental results validates the ability of AcuSolve to model cases with natural convection of turbulent flow within a tall cavity.

Problem Description

The problem consists of air within a tall cavity with a hot wall and a cold wall, as shown in the following image, which is not drawn to scale. The cavity is 2.18 m tall, 0.0762 m wide, and 0.52 m deep. The cavity's vertical walls differ in temperature, causing the fluid to transfer the heat, leading to natural convection. The temperature of the hot wall is 307.85 K, while the temperature of the cold wall is 288.25 K. The horizontal walls of the cavity are adiabatic. The length-to-width ratio of 28.6 and temperature difference of 19.6 K produce a turbulent flow field within the cavity with a Rayleigh number of $8.6X10^{5}$ (Betts and Bokhari 2000). The flow medium is air, with a Boussinesq approximation for density, a specific heat of 1005 J/kg-K, and a viscosity of $1.781 X 10^{-5}$ kg/m-s. Gravity is applied globally to the volume of air.

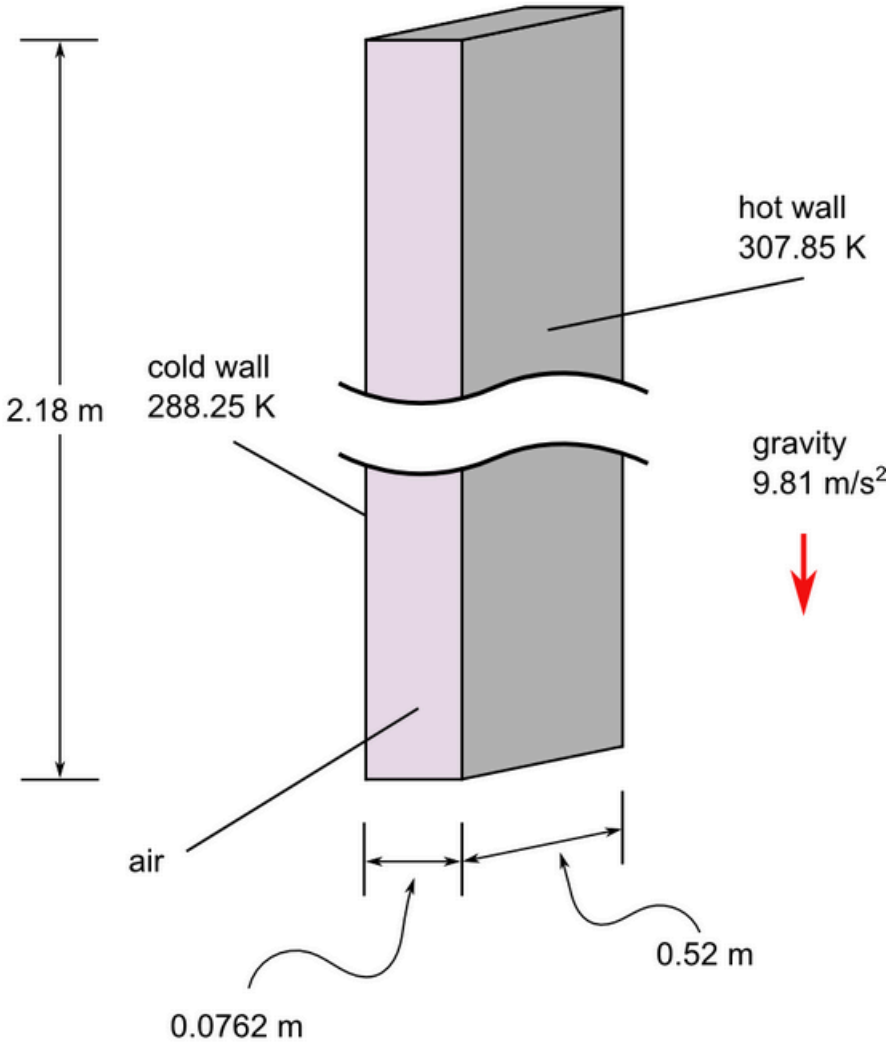


Figure 161: Critical Dimensions and Parameters for Simulating Turbulent Natural Convection in a Tall Cavity

The simulation was performed as a two dimensional problem by constructing a volume mesh that contains a single layer of elements in the extruded direction, normal to the flow plane and by imposing symmetry boundary conditions on the extruded planes.

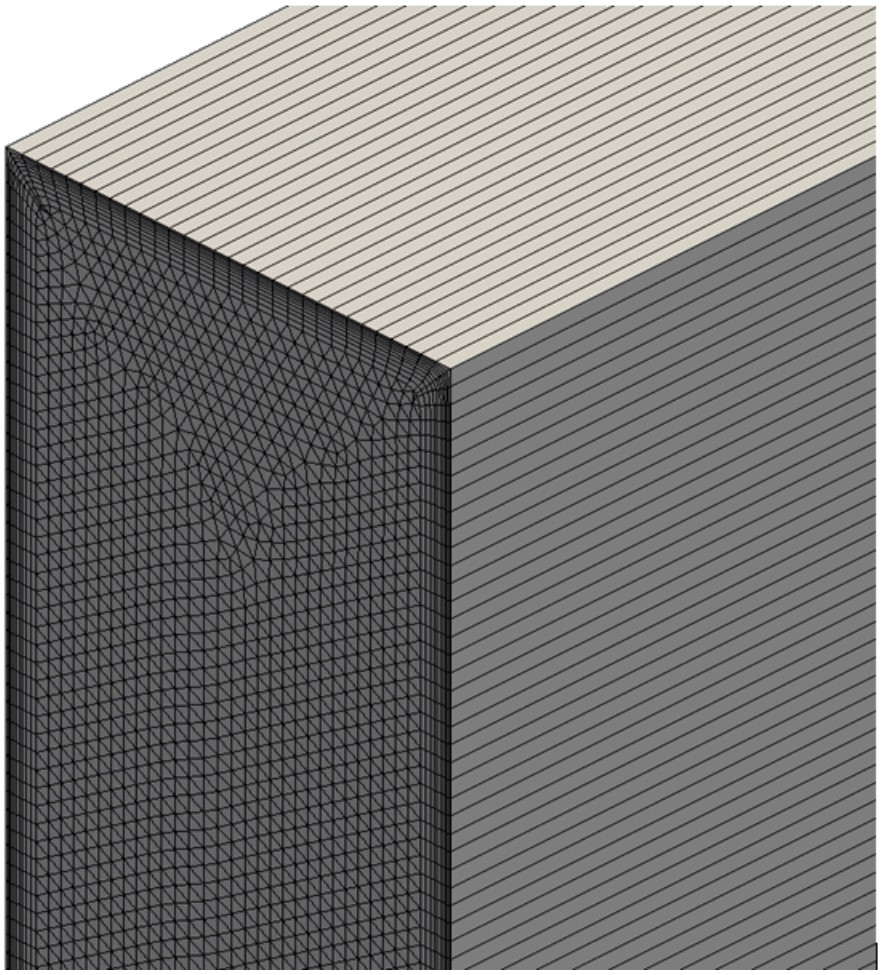


Figure 162: Mesh used for Simulating the Natural Convection of Turbulent Flow in a Tall Cavity

AcuSolve Results

The AcuSolve solution converged to a steady state and the results reflect the mean flow conditions. The natural convection of the flow is generated by heat transfer from the vertical walls to the fluid in the cavity. The temperature gradients created by this heat transfer cause differing densities within the flow region. The warmer air rises to the top of the cavity due to its lower density while the colder air sinks to the bottom of the cavity due to its higher density. This produces flow near the hot vertical wall in the positive vertical direction and flow near the cold wall in the negative vertical direction.

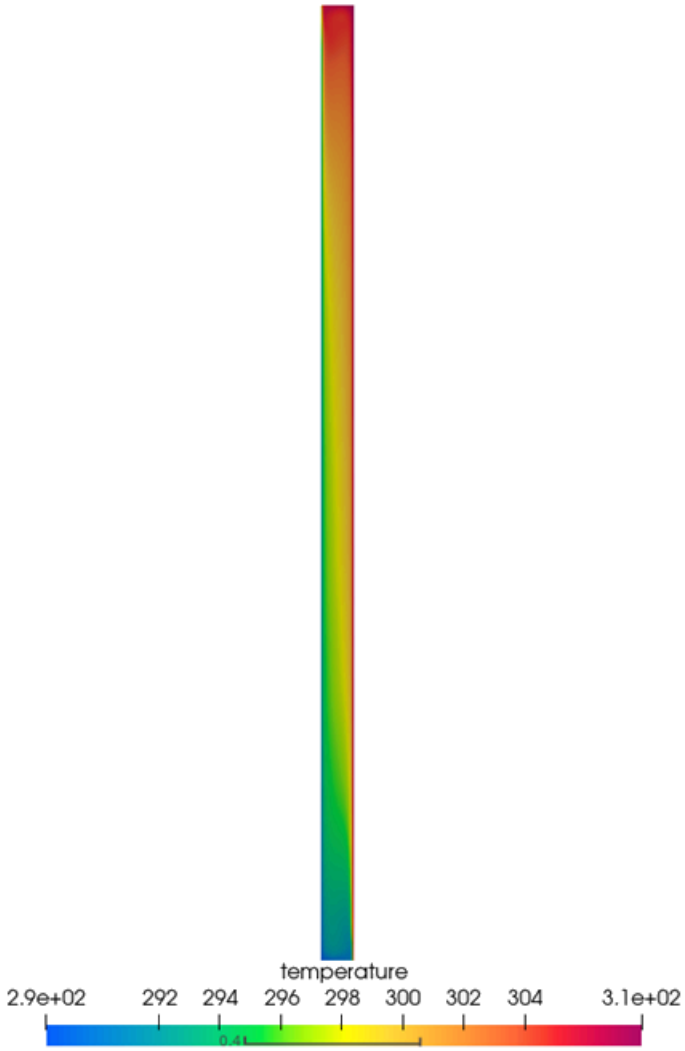


Figure 163: Temperature Contours Throughout Tall Cavity in the X-Y Plane

The AcuSolve results of the temperature and vertical velocity within the cavity are compared to the corresponding experimental values in the plots shown below. The temperature of the air is lowest near the cold vertical wall, remains relatively steady in the middle of the cavity, and then peaks near the hot vertical wall. Following a similar trend, the AcuSolve results show that the velocity is lowest near the cold vertical wall, due to the air sinking, and then steadily increases as the air begins to rise near the hot vertical wall. The velocity at the walls is zero due to the no-slip boundary condition. Additional comparisons are made to evaluate the performance of four turbulence models, Spalart-Allmaras (SA), shear stress transport (SST), K-Omega and K-ε.

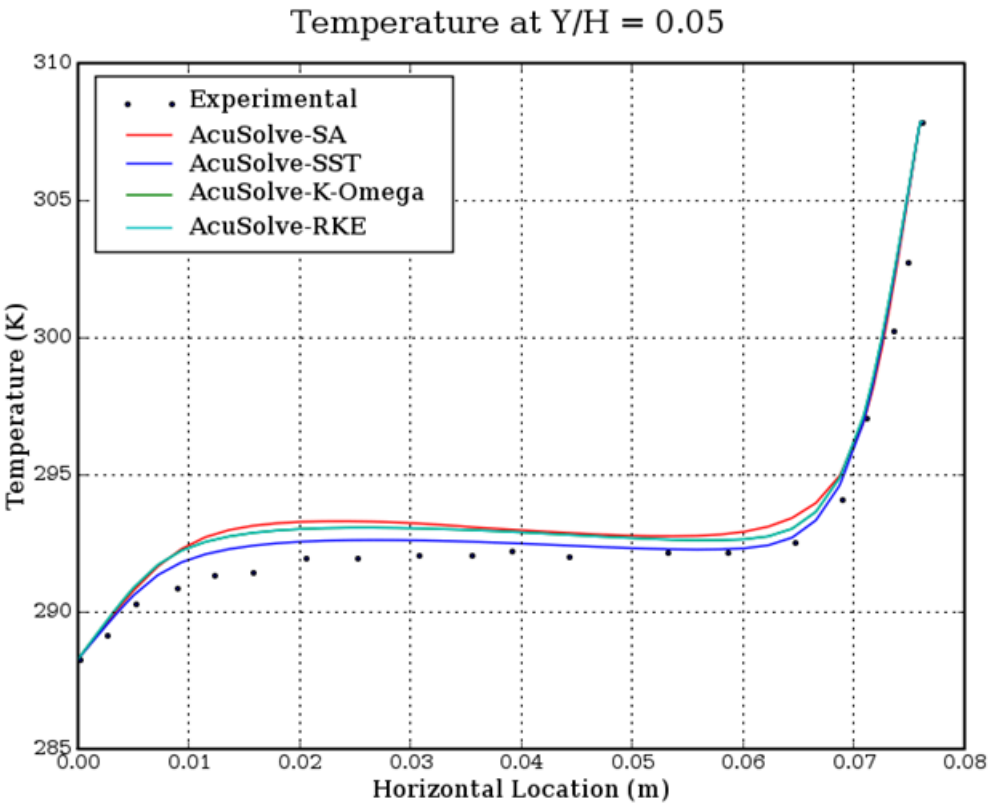


Figure 164: Temperature Plotted against Location along Horizontal at a Position of y/H=0.05 in the Cavity, where H is the Cavity Height and y is the Distance from the Bottom Wall

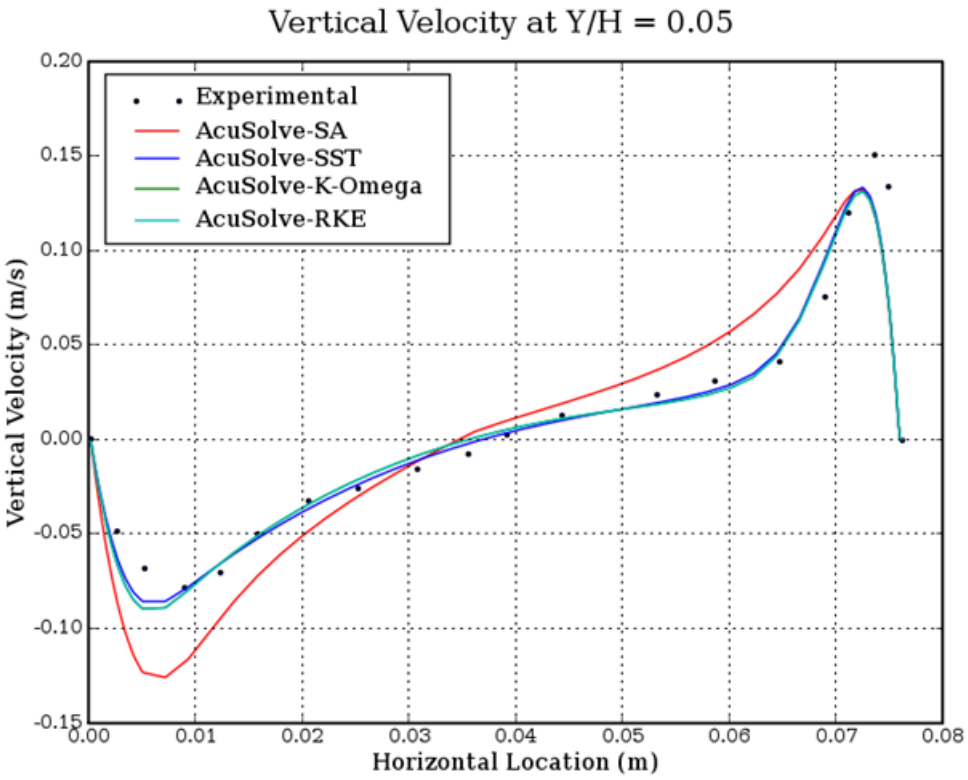


Figure 165: Vertical Velocity Plotted against Location along Horizontal at a Position of y/H=0.05 in the Cavity, where H is the Cavity Height and y is the Distance from the Bottom Wall

Summary

In this application, turbulent flow developed by natural convection, at a Rayleigh number of 8.6X105, is studied within a tall cavity. The AcuSolve results compare well with the experimental data for temperature and vertical velocity along a horizontal line at a location of y/H=0.05 in the tall cavity, with the two-equation models capturing the velocity gradient with greater accuracy. A temperature difference occurs within the flow region due to the heat transfer from the vertical walls of the cavity. The hotter, less-dense air rises to the top of the cavity while the colder, denser air sinks to the bottom, giving rise to recirculation. AcuSolve demonstrates the ability to accurately predict the natural convection of turbulent flow within a tall cavity.

Simulation Settings for Turbulent Natural Convection Inside a Tall Cavity

HyperWorks CFD database file: `<your working directory\cavity_turbulent_heat \cavity_turbulent_heat.hm`

Global

- Problem Description
  - Analysis type - Steady State
  - Turbulence equation - SST
- Auto Solution Strategy
  - Relaxation factor - `0.5`

    - Convergence tolerance - `0.005`
- Material Model
    - Air
        - Type - Boussinesq
        - Density - `1.225` kg/m3
        - Specific Heat - `1005` J/kg-K
        - Viscosity - `1.781e-5` kg/m-sec

  Model
- Volumes
    - Volume
        - Element Set
            1. Material model - Air
- Surfaces
    - Back
        - Simple Boundary Condition
            1. Type - Symmetry
    - Bottom
        - **Simple Boundary Condition**
            1. Type - Wall
            2. Temperature BC type - Flux
            3. Heat Flux - `0.0` W/m2
    - Cold
        - **Simple Boundary Condition**
            1. Type - Wall
            2. Temperature BC type - Value
            3. Temperature - `288.25` K
    - Front
        - Simple Boundary Condition
            1. Type - Symmetry
    - Hot
        - Simple Boundary Condition
            1. Type - Wall
            2. Temperature BC type - Value
            3. Temperature - `307.85` K
    - Top
        - Simple Boundary Condition
            1. Type - Wall

2 Temperature BC type - Flux

3 Heat Flux - `0.0` W/m2

References

P.L. Betts and I.H. Bokhari. "Experiments on Turbulent Natural Convection in an Enclosed Tall Cavity". International Journal of Heat and Fluid Flow 21:675-683. 2000.

Viscous Heating Inside a Rotating Annulus

In this application, AcuSolve is used to simulate fluid flow and viscous heating in an annulus formed by concentric cylinders. AcuSolve results are compared with analytical results adapted from Bird and others (1960). The close agreement of AcuSolve results with analytical results validates the ability of AcuSolve to model cases with viscous heating.

Problem Description

The problem consists of a viscous fluid filling the annulus between two concentric cylinders, as shown in the following image, which is not drawn to scale. The inner cylinder has a radius of 1.0 m and is fixed in place. The outer cylinder has a radius of 2.0 m and rotates with a constant angular velocity of 0.5 rad/s. The inner cylinder is held at a constant temperature of 273 K and the outer cylinder is held at 274 K.

The rotation of the outer cylinder causes the fluid to rotate due to the viscous shearing near the wall. As the inner cylinder is fixed, a velocity gradient is generated as a function of distance from the inner cylinder center. Viscous stresses within the domain generate significant amounts of heat, leading to a substantial increase in the fluid temperature in regions of high shear.

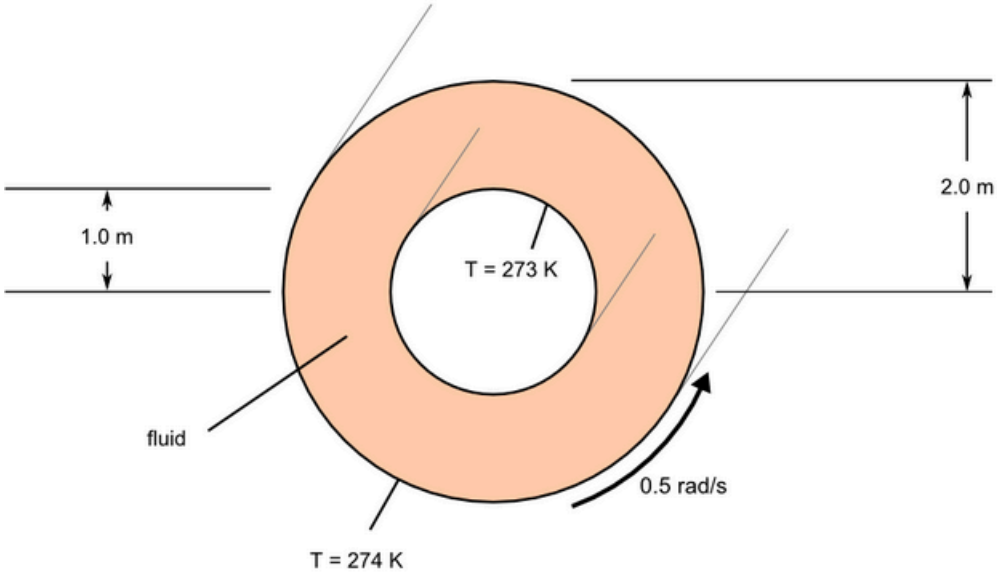


Figure 166: Critical Dimensions and Parameters for Simulating Viscous Heating Inside a Rotating Annulus

The simulation was performed as a two dimensional problem by constructing a volume mesh that contains a single layer of elements in the extruded direction, normal to the flow plane, and by imposing symmetry boundary conditions on the extruded planes.

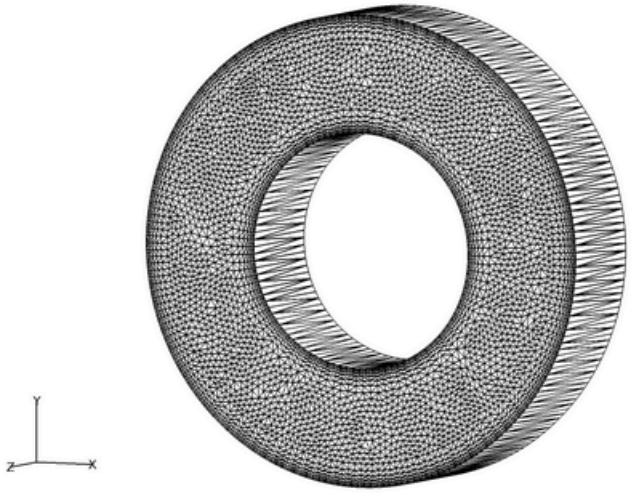


Figure 167: Mesh used for Simulating Viscous Heating Inside a Rotating Annulus

AcuSolve Results

The AcuSolve solution converged to a steady state and the results reflect the mean flow conditions. Flow is induced by the viscous shearing near the outer wall, creating a velocity gradient with the highest velocity near the moving wall.

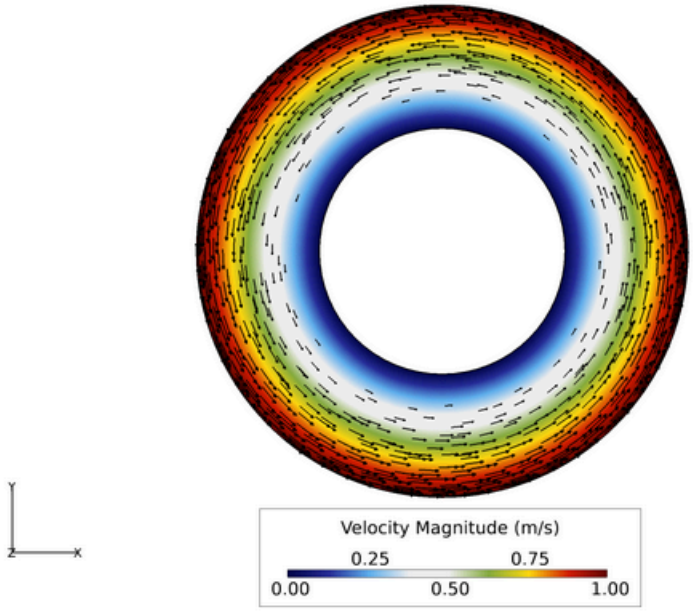


Figure 168: Contours of Velocity Magnitude and Velocity Vectors

The velocity gradient causes viscous heating, causing the fluid temperature to increase. The resulting temperature profile is nonlinear with the highest temperatures occurring in the space between the cylinders.

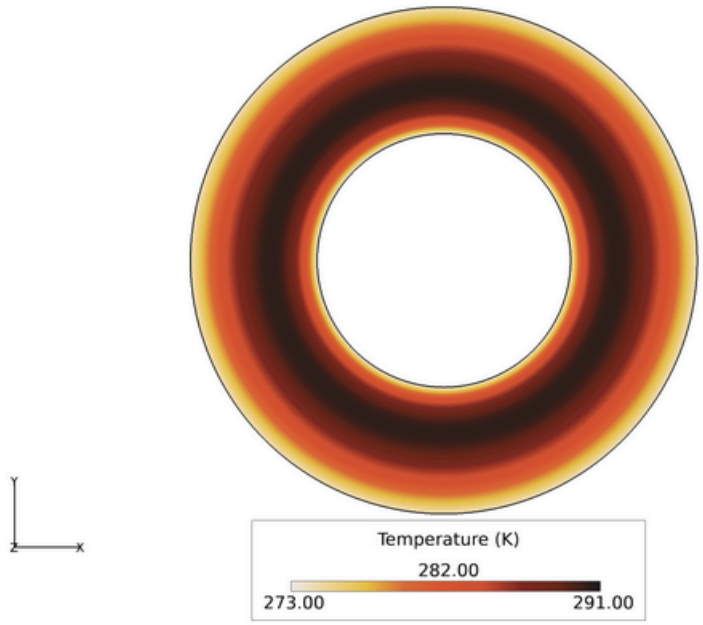


Figure 169: Contours of Temperature

AcuSolve results were compared to analytical results for velocity and for temperature across a range of radial locations.

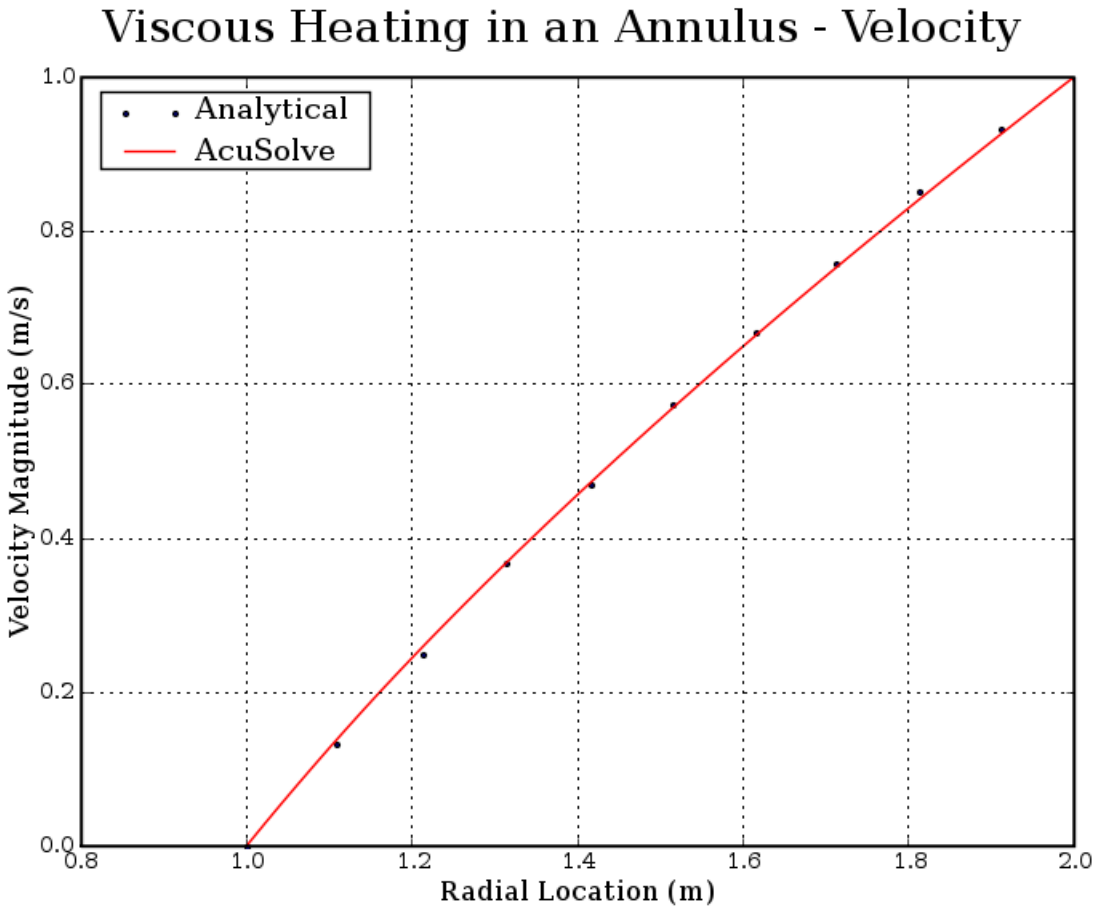


Figure 170: Velocity Magnitude Plotted Against Radial Location from the Center of the Inner Cylinder

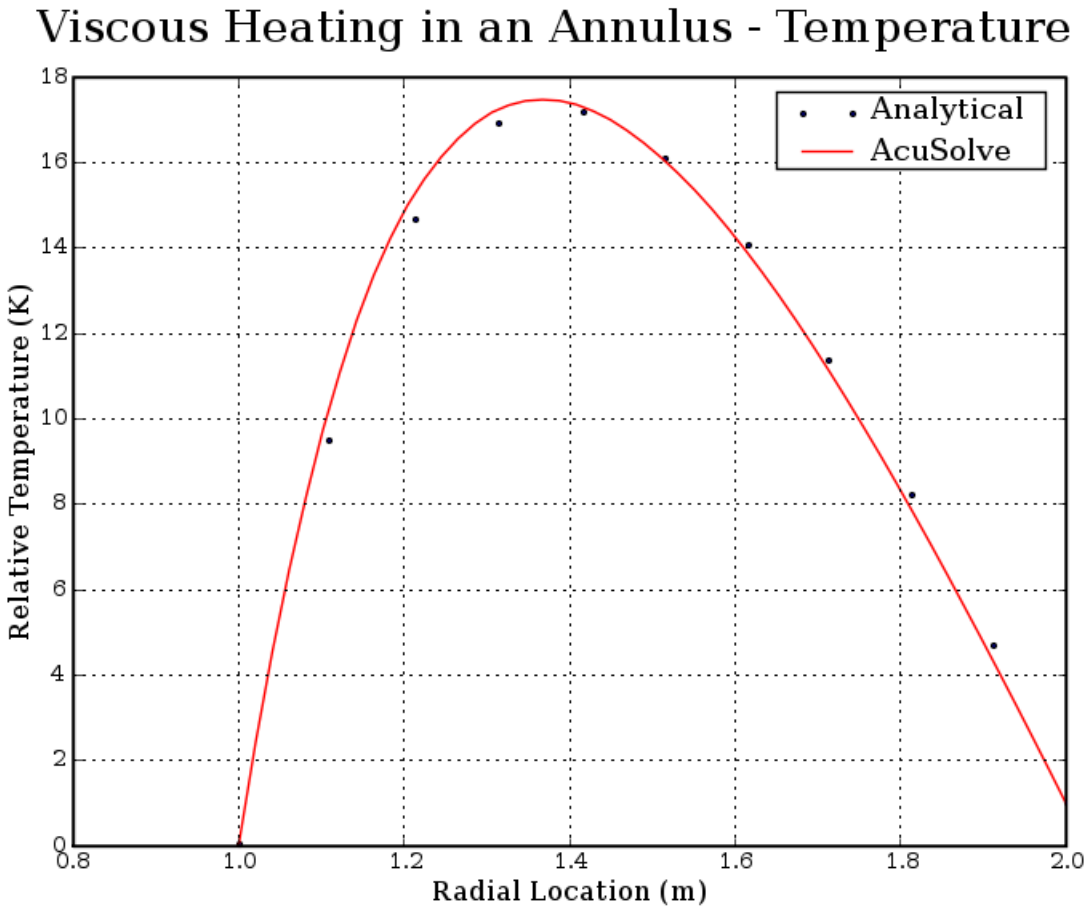


Figure 171: Temperature (Relative to the Inner Cylinder Wall Temperature) Plotted Against Radial Location from the Center of the Inner Pipe

Summary

The AcuSolve results compare well with the analytical results for both the flow field and the temperature across the annulus. In this application, flow is induced due to the viscous stresses generated by the rotation of the exterior cylinder. Velocity gradients between the cylinders give rise to shear stresses that induce frictional heating of the fluid. Due to the high viscosity of the fluid, the viscous heating is significant and leads to large increases in the temperature between the cylinders. This application validates the ability of AcuSolve to simulate flows where the viscous heating contribution is significant.

Simulation Settings for Viscous Heating Inside a Rotating Annulus

AcuConsole database file: `<your working directory>\annulus_rotating_heat\annulus_rotating_heat.acs`

Global

- Problem Description
  - Analysis type - Steady State
  - Temperature equation - Advective Diffusive

    - Turbulence equation - Laminar
- Auto Solution Strategy
    - Relaxation factor - `0.2`
- Material Model
    - Fluid
        - Density - `1.0` kg/m3
        - Viscosity - `300` kg/m-sec
        - Conductivity - `1.0` W/m-K
- Reference Frame
    - Outer_Rotation
        - Angular Velocity
            1. X-component - `0.0` rad/sec
            2. Y-component - `0.0` rad/sec
            3. Z-component - `0.5` rad/sec

Model

- Volumes
    - Fluid
        - Element Set
            1. Material model - Fluid
            2. Viscous heating - On
- Surfaces
    - Inner_Cylinder
        - Simple Boundary Condition
            1. Type - Wall
            2. Temperature BC type - Value
            3. Temperature - `273.0` K
    - Outer_Cylinder
        - Simple Boundary Condition
            1. Type - Wall
            2. Reference frame - Outer_Rotation
            3. Temperature BC type - Value
            4. Temperature - `274.0` K
    - Symm_MaxZ
        - Simple Boundary Condition
            1. Type - Symmetry
    - Symm_MinZ
        - Simple Boundary Condition

1 Type - Symmetry

- Nodes
  - Node 1
    - Pressure
      1 Type - Zero

References

R. B. Bird, W. E. Stewart, and E. N. Lightfoot. "Transport phenomena". New York, John Wiley and Sons, 1960

Separated Laminar Flow Over a Blunt Plate

In this application, AcuSolve is used to simulate the separation of laminar flow over a blunt plate. AcuSolve results are compared with experimental results as described in J.C. Lane and R.I. Loehrke (1980). The close agreement of AcuSolve results with the experimental results validates the ability of AcuSolve to model cases with external laminar flow including separation.

Problem Description

The problem consists of external, laminar flow over a blunt plate 1.5 m long and 0.09 m thick, as shown in the following image, which is not drawn to scale. The fluid flows with a uniform horizontal velocity (v) of 0.045133 m/s. The fluid material used for the simulation has a density of 1.0 kg/m^3 and a dynamic viscosity of 1.7894 X 10^{-5} kg/m-s. The resulting Reynolds number for the flow, based on the plate thickness, is approximately 227. This indicates that the flow over the plate is laminar. As the fluid flows past the leading edge of the plate, the pressure decreases, resulting in a separation region downstream of the leading edge. At some distance downstream from the leading edge, the pressure gradient decreases, and viscous forces cause the recirculation zone to dissipate, allowing the flow to reattach to the plate.

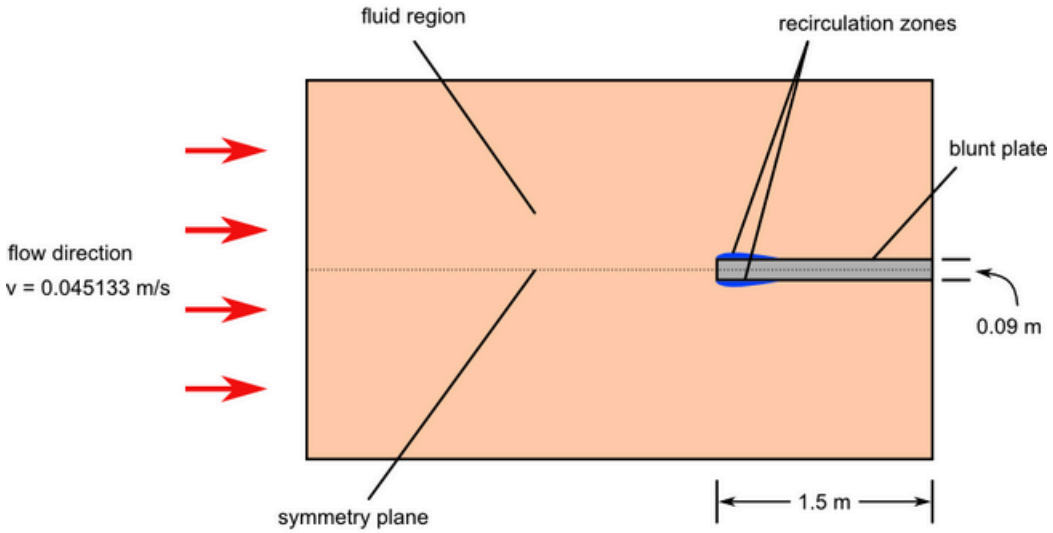


Figure 172:

The simulation was performed as a two dimensional problem by constructing a volume mesh that contains a single layer of elements in the extruded direction, normal to the flow plane, and by imposing symmetry boundary conditions on the extruded planes. In addition, the half symmetry of the geometry was exploited to allow for modeling only the top half of the geometry. These characteristics allow for accurate simulation of the flow while minimizing computational time. The following images show the mesh distribution and a refined mesh zone around the blunt plate.

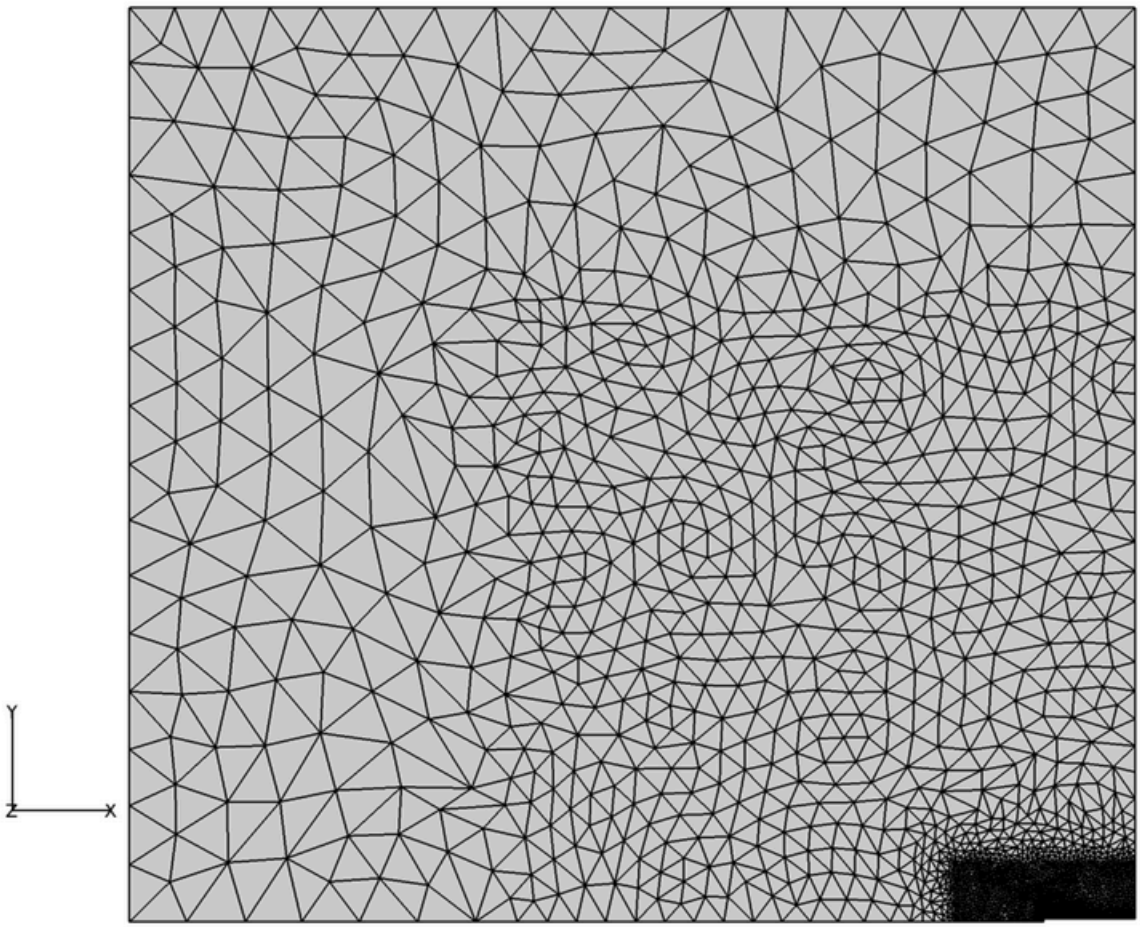


Figure 173: Mesh used for Simulating Separated Laminar Flow over a Blunt Plate

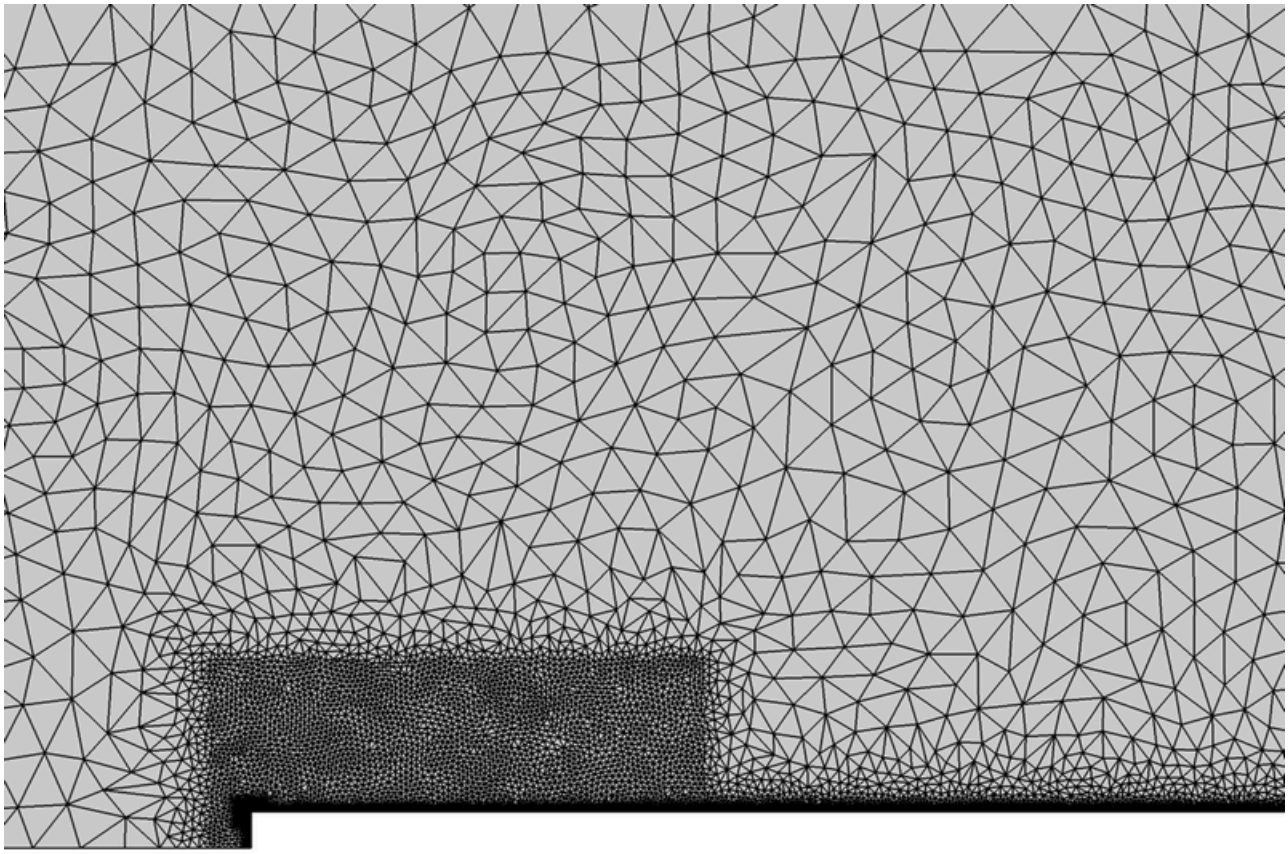


Figure 174: Mesh Detail Showing Refinement Zones at the Leading Edge of the Blunt Plate

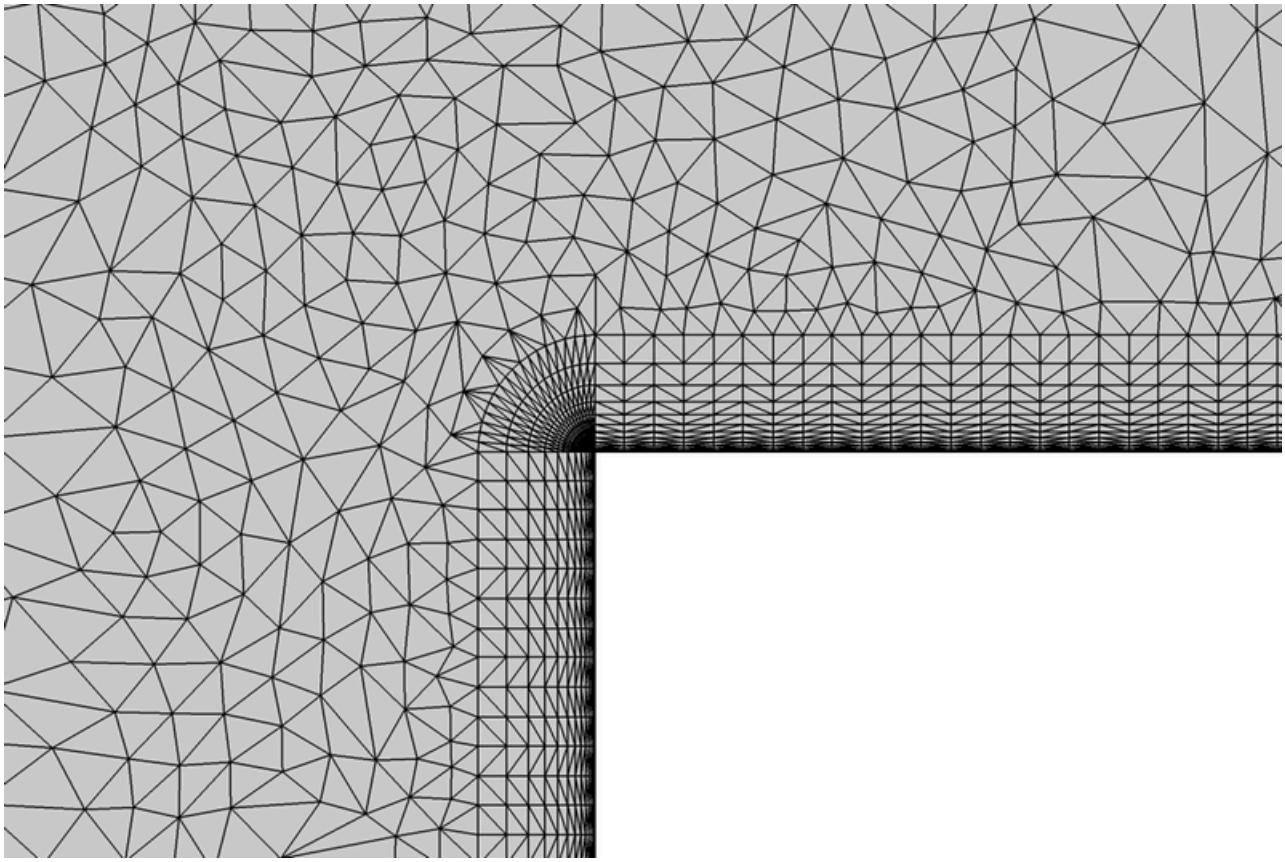


Figure 175: Mesh Detail Showing Mesh Elements Near the Leading Edge of the Blunt Plate

AcuSolve Results

The AcuSolve solution converged to a steady state and the results reflect the mean flow conditions over the blunt plate. The flow velocity is reduced to zero at the leading face, forming a stagnation point at the center. The flow reaches a maximum velocity as it flows around the leading edges and separates from the plate. Flow separation (shear stress parallel to the wall becomes negative) occurs downstream of the leading edge, leading to a recirculation zone. The flow reattaches 0.37 m downstream of the leading edge. The velocity in the laminar boundary layer increases from zero at the wall to free-stream velocity at the boundary layer edge. Along the plate length, the boundary layer slowly grows in thickness. The following image shows the contours of the flow velocity parallel to the streamwise direction and the recirculation region in the wake of the plate edge.

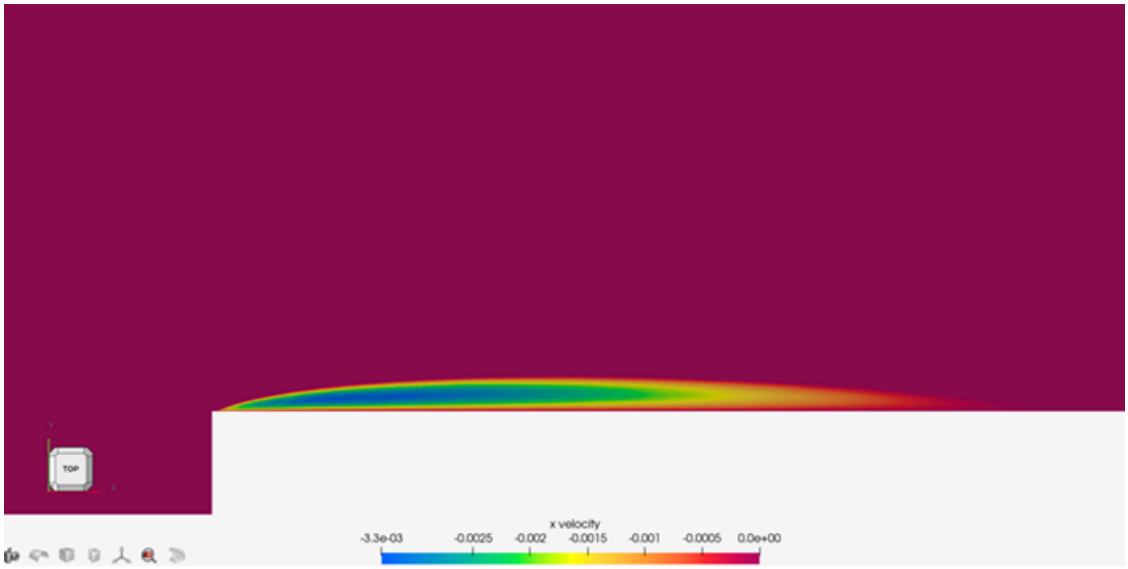


Figure 176: X-Velocity Contours Near the Leading Edge of the Blunt Plate

Downstream of the leading edge, the flow eventually reattaches to the plate at the point where the shear stress parallel to the wall passes from negative through zero to positive. The reattachment point is 0.37 m from the leading edge of the plate and corresponds to the trailing edge of the contours.

The results for the predicted and experimental reattachment length (xreattach) are presented in the table below. T represents the plate thickness.

Table 11:

AcuSolve xreattach	AcuSolve xreattach/T	Experimental xreattach/T	Percent error (%)
0.37	4.11	4.0	2.8

Summary

In this application, a constant flow inlet velocity and symmetric boundary conditions were used to model 2D flow over a blunt plate. The AcuSolve solution compares well with experimental results for the separation of laminar flow over a blunt plate. The non-dimensional reattachment length obtained from the AcuSolve steady state solution compares well with the experimental solution, with an error of less than 3.0 percent. The results of this simulation validate the ability of AcuSolve to accurately predict the reattachment point in cases with external, laminar flow with separation.

Simulation Settings for Separated Laminar Flow over a Blunt Plate

HyperWorks CFD database file: `<your working directory>\blunt_plate_laminar\blunt_plate_laminar.hm`

Global

- Problem Description

- Analysis type - Steady State
- Turbulence equation - Laminar

- Auto Solution Strategy
  - Relaxation Factor - `0.2`
- Material Model
  - Fluid
    - Density - `1.0` kg/m3
    - Viscosity - `1.7894e-005` kg/m-sec

  Model
- Volumes
  - Fluid
    - Element Set
      1. Material model - Fluid
- Surfaces
  - Back
    - Simple Boundary Condition
      1. Type - Symmetry
  - Freestream
    - Simple Boundary Condition
      1. Type - Slip
  - Front
    - Simple Boundary Condition
      1. Type - Symmetry
  - Inlet
    - Simple Boundary Condition
      1. Type - Inflow
      2. Inflow type - Velocity
      3. Inflow velocity type - Cartesian
      4. X Velocity - `0.045133` m/s
  - Outflow
    - Simple Boundary Condition
      1. Type - Outflow
  - Plate
    - Simple Boundary Condition
      1. Type - Wall
  - Symmetry
    - Simple Boundary Condition

1 Type - Symmetry

References

J.C. Lane and R.I. Loehrke. "Leading Edge Separation from a Blunt Plate at Low Reynolds Number". Journal of Fluids Engineering. 102(4):494-496. 1980.

Laminar Flow Through a Pipe with Constant Wall Temperature

In this application, AcuSolve is used to simulate the flow of mercury through a heated pipe. The AcuSolve results are compared with analytical results for pressure drop as described in White (1991), and with temperature changes as described in Incropera and DeWitt (1981). The close agreement of AcuSolve results with analytical results validates the ability of AcuSolve to model cases with flow and imposed temperature constraints.

Problem Description

The problem consists of mercury flowing through a circular pipe that is 0.005 m in diameter and 0.1 m long, as shown in the following image, which is not drawn to scale. Mercury enters the pipe with a constant temperature of 300 K and with a fully developed velocity profile with an average velocity of 0.005 m/s. The pipe wall has a constant temperature of 500 K. These constraints impose a temperature gradient within the fluid. As the fluid moves through the pipe it is slowly heated by the wall, resulting in an increased centerline temperature. Pressure decreases along the pipe length due to the friction imposed by the viscous stresses near the pipe wall. A periodic boundary condition is imposed on the inlet and outlet to allow the pressure to change with a constant offset, while the velocity is fully periodic.

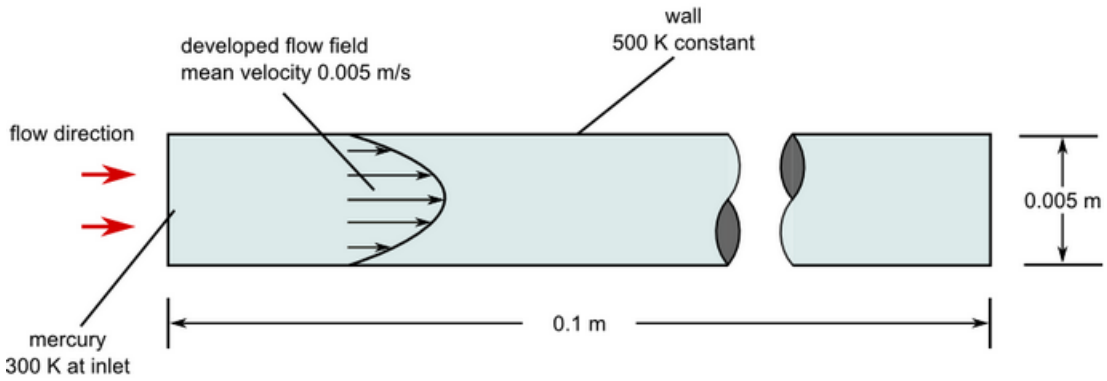


Figure 177: Critical Dimensions and Parameters for Simulating Laminar Flow through a Pipe with Constant Wall Temperature

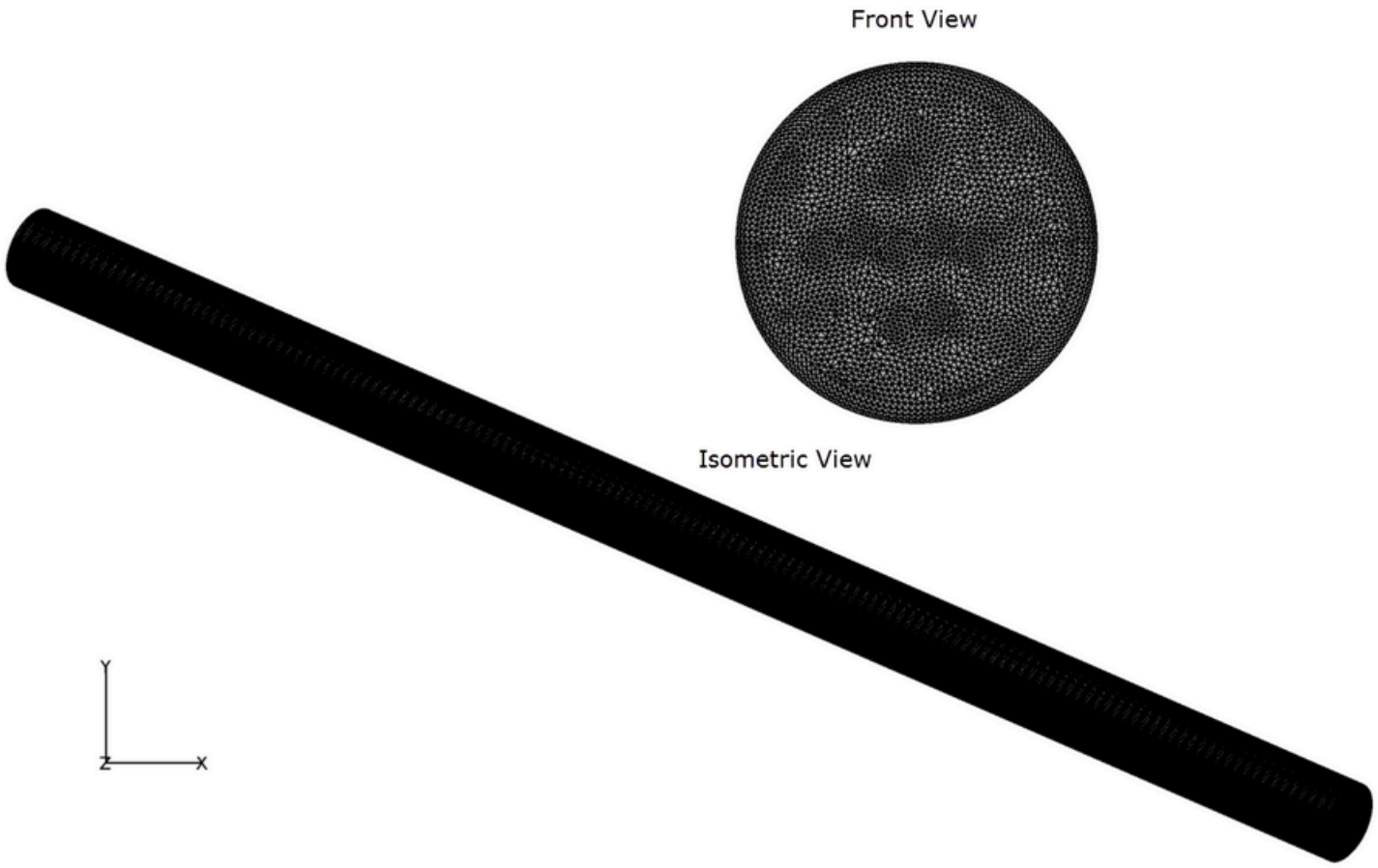


Figure 178: Mesh used for Simulating Laminar Flow Through a Pipe with Constant Wall Temperature

AcuSolve Results

The AcuSolve solution converged to a steady state and the results reflect the mean flow conditions. In this application, a fully developed laminar profile is achieved by enforcing periodic constraints on the pressure and velocity fields. The spatially developing temperature field is achieved by allowing the fluid's temperature to evolve along the full length of the model. The change in temperature along the pipe length is due to advection in the streamwise direction and heat conduction from the outer walls where the temperature is greater than the initial flow temperature. The temperature rises along the length of the pipe and the pressure drops along the length of the pipe. At the inlet, the temperature of the mercury is 300 K and the pressure is 0.496 Pa. At the outlet centerline, the temperature of the mercury has risen to 500.0 K and the pressure has dropped to -0.4965 Pa.

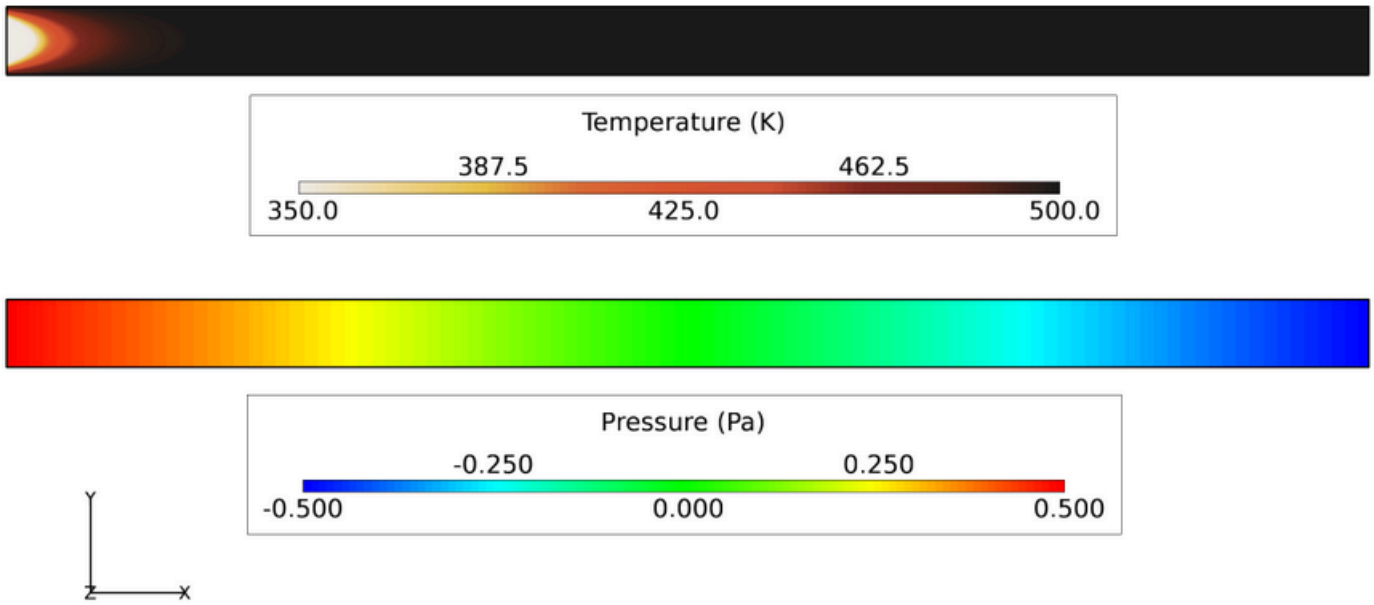


Figure 179: Temperature and Pressure Contours of Mercury Flow Through a Pipe with Prescribed Temperature Boundary

The following table shows the comparison of AcuSolve results with the analytical solutions from White (1994). Comparisons were made for the pressure drop between the inlet and outlet and the temperature at the center of the outlet.

Table 12:

	Analytical solution	**AcuSolve solution**	**Percent deviation from analytical**
Pressure drop (Pa)	0.991	0.9925	0.15
Centerline temperature of flow at outlet (K)	500.0	500.0	< 0.0001

Summary

The AcuSolve solution compares well with analytical results for flow through a pipe with constant temperature boundary conditions. The AcuSolve solution for the centerline temperature is nearly identical with the analytical results and the pressure reduces as expected for the prescribed flow conditions. The results of this simulation validate the ability of AcuSolve to accurately predict the heating of fluid flowing through a pipe with constant wall temperature.

Simulation Settings for Laminar Flow Through a Pipe With Constant Wall Temperature

AcuConsole database file: `<your working directory>\pipe_laminar_heatDirichlet\pipe_laminar_heatDirichlet.acs`

Global

- Problem Description
  - Analysis type - Steady State
  - Temperature equation - Advective Diffusive
  - Turbulence equation - Laminar
- Auto Solution Strategy
  - Relaxation Factor - `0.2`
- Material Model
  - Mercury
    - Density - `13579.0` kg/m3
    - Specific Heat - `139.3` J/kg-K
    - Viscosity - `0.001548` kg/m-sec
    - Conductivity - `8.69` W/m-K

  Model
- Volume
  - Fluid
    - Element Set
      1. Material model - Mercury
- Surfaces
  - Inflow
    - Simple Boundary Condition - (disabled to allow for periodic conditions to be set)
    - Advanced Options
      1. Integrated Boundary Conditions
         1. Mass Flux
            1. Type - Constant
            2. Constant value - `1.33e-3` kg/sec
      2. Temperature
         1. Type - Constant
         2. Constant value - `300.0` K
  - Outflow
    - Simple Boundary Condition - (disabled to allow for periodic conditions to be set)
  - Wall
    - Simple Boundary Condition
      1. Type - Wall

2 Temperature BC type - Value
3 Temperature - `500.0` K

- Periodics
  - Periodic 1
    - Individual Periodic BCs
      1 Velocity
        1 Type - Periodic
      2 Pressure
        1 Type - Single Unknown Offset

References

F. M. White. "Fluid Mechanics". 3rd Edition. McGraw-Hill Book Co., Inc. New York. 1994.

F. P. Incropera and D. P. DeWitt. "Fundamentals of Heat Transfer". John Wiley & Sons. New York. 1981.

Turbulent Flow with Separation in an Asymmetric Diffuser

In this application, AcuSolve is used to simulate fully developed turbulent flow through an asymmetric diffuser with a divergent lower wall and a straight upper wall. AcuSolve results are compared with experimental results as described in Buice and Eaton (2000). The close agreement of AcuSolve results with experimental results validates the ability of AcuSolve to model cases with internal turbulent flow with flow separation and reattachment in an asymmetric diffuser.

Problem Description

The problem consists of air flowing through an asymmetric diffuser with a divergent lower wall and a straight upper wall, as shown in the following image, which is not drawn to scale. The diffuser inlet has a height of 1.5 cm (H) and extends 9 cm (6H) to the divergent section. The lower wall of the diffuser diverges at an angle of 10° and expands to 7.05 cm (4.7H). The divergent section has a horizontal length of 31.5 cm (21H). The expanded section of the diffuser extends 84 cm (56H) to the outlet. Air, with a density of 1.225 kg/m^3 and a viscosity of 1.8325 X 10^{-5} kg/m-s enters the diffuser through the inlet of the diffuser with a fully developed turbulent profile at a Reynolds's number of 20,000. The simulation was conducted with the Reynolds Averaged Navier-Stokes equations using four turbulence models, Spalart Allmaras, Shear Stress Transport (SST), K-ω and Realizable K-ε.

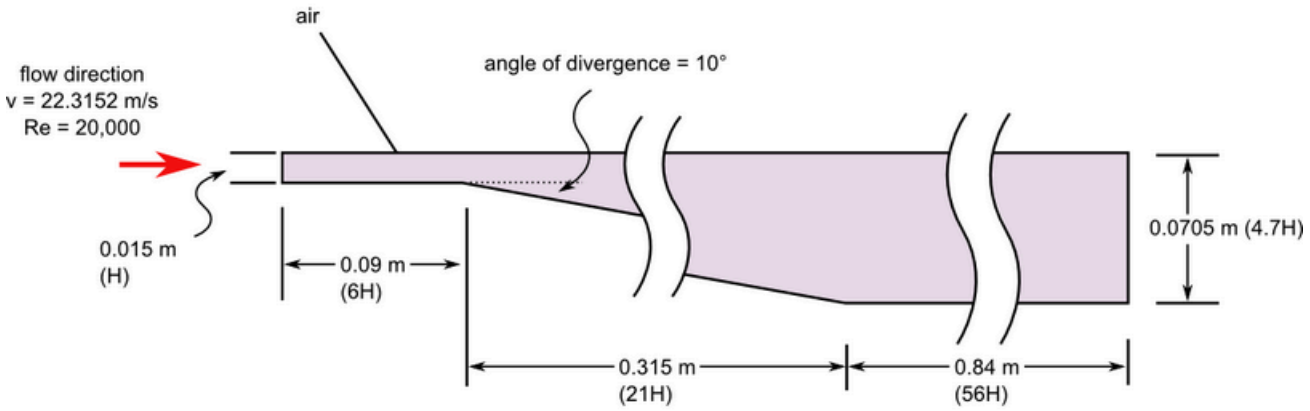


Figure 180: Critical Dimensions and Parameters for Simulating Turbulent Flow with Separation in an Asymmetric Diffuser

The simulation was performed as a two dimensional problem by constructing a volume mesh that contains a single layer of elements extruded in the cross stream direction (perpendicular to the flow plane) and by imposing symmetry boundary conditions on the extruded planes.



Figure 181: Mesh Details Near the Inlet and Divergent Section of Diffuser

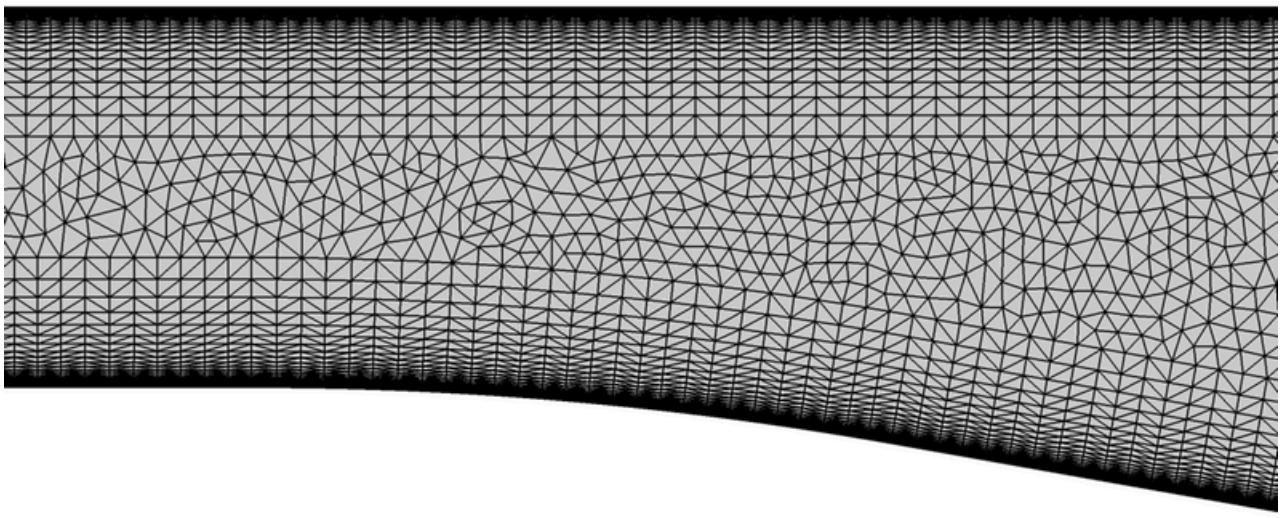


Figure 182: Mesh Details at the Beginning of the Divergence of the Lower Wall in the Diffuser

AcuSolve Results

The AcuSolve solution converged to a steady state and the results reflect the mean flow conditions. As the fully developed turbulent flow enters the divergent section, the peak velocity is maintained until the expansion of the cross-sectional height, forms an adverse pressure gradient. After the flow enters the divergent section, the velocity decreases significantly, due to the expansion of the cross-section height. This causes separation of the flow along the divergent wall and results in an area of recirculation.
The bulk of the flow above the divergent wall maintains its streamwise direction, while a portion of it reverses direction before reattaching further downstream of the divergent section. The following images show the steady state flow solution for flow within the diffuser.

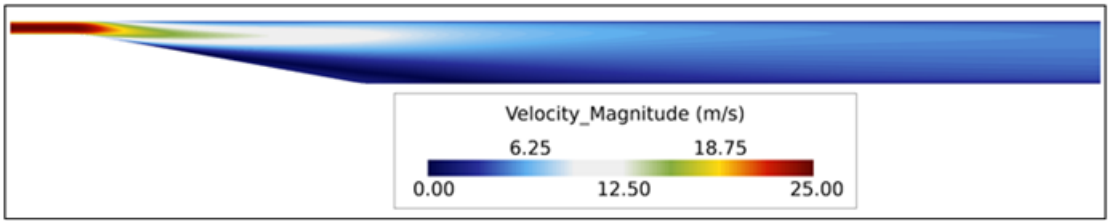


Figure 183: Velocity Contours Within the Diffuser

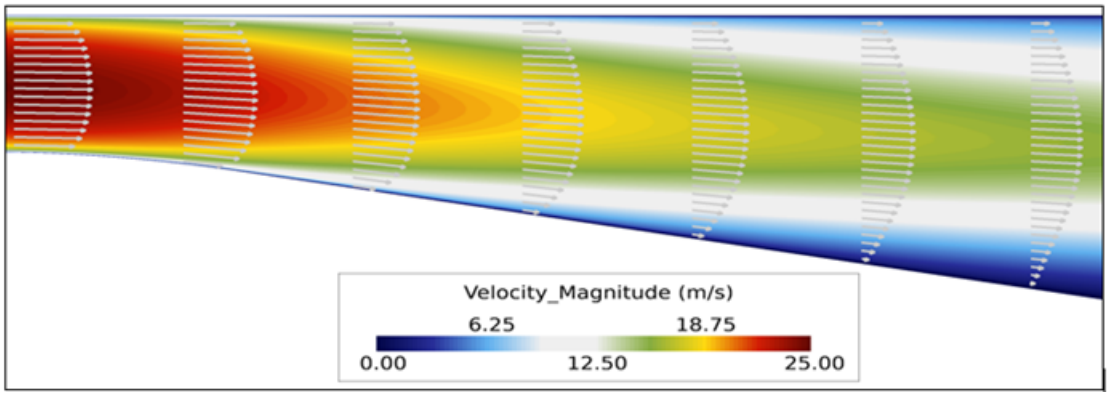


Figure 184: Close up View of Velocity Vectors and Contours of Velocity Magnitude in the Diffuser

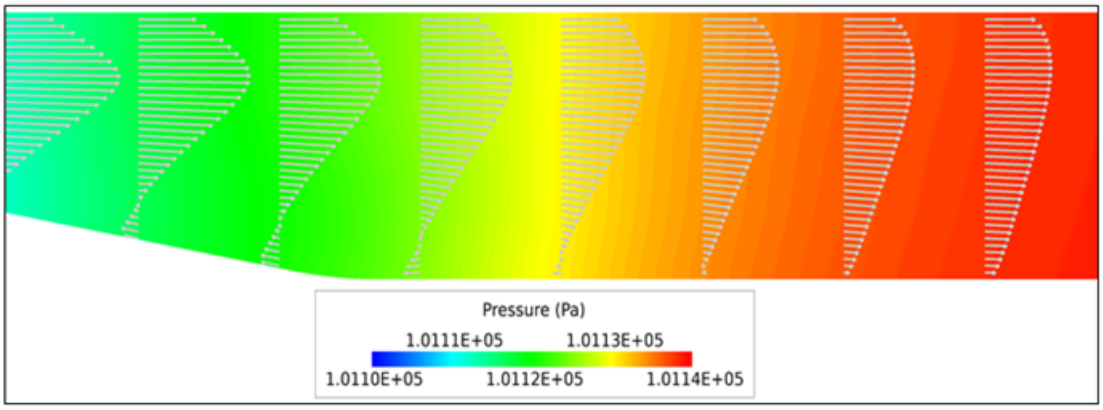


Figure 185: Close up View of Velocity Vectors and Contours of Pressure to Show Recirculation as it Approaches the Reattachment Point

Upstream of the diffuser section, the streamline velocity increases as the distance from the lower wall increases until it reaches the maximum velocity at the center of the channel. As the flow enters the divergent section of the channel, the streamwise velocity decreases near the bottom wall. The images below show the velocity profiles at three locations as measured from the midpoint of the curve where the bottom wall begins to diverge (X=0.0) for each of the tested turbulence models. The first location, where X/H = -5.944, is close to the inlet. The second location, where X/H = 13.468, is approximately 0.2 m downstream of the divergent section (~ 0.1 m from the fully expanded section). The third location, where X/H = 24.066, is approximately 0.16 m downstream of the point where the diffuser has reached the maximum height. In these plots the black circles represent the experimental measurements (Buice and Eaton 2000), the solid red lines for the prediction for the Spalart Allmaras model, solid blue lines for the prediction for the SST model, solid green lines for the prediction for the K-ω model and solid cyan lines for the K-ε model, representing the AcuSolve results. The non-dimensional height is represented by the fraction of the vertical height (Y) divided by the inlet height (H) and the velocity is normalized by the inlet velocity (Uref).

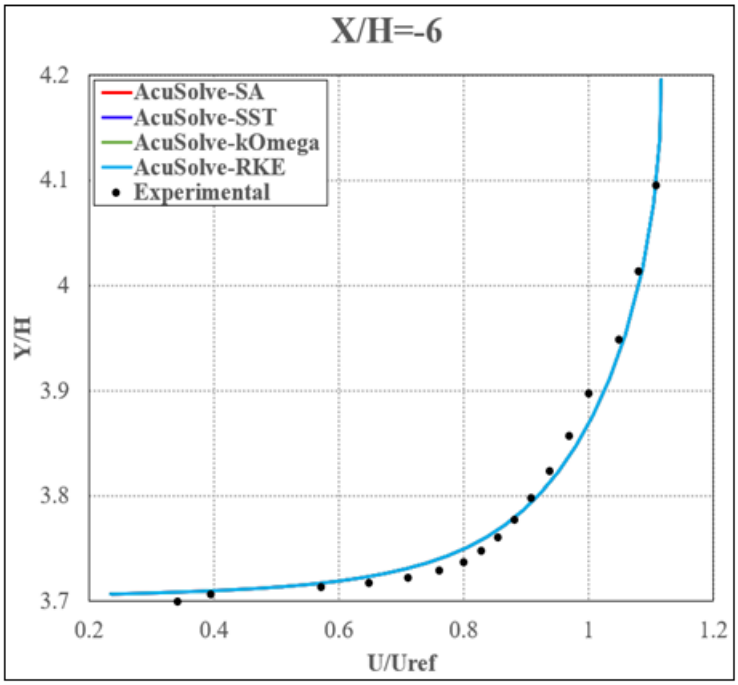


Figure 186: Non-Dimensional Streamwise Velocity Plotted Against Vertical Location Near the Inlet (X/H=-5.9442, Where the Reference Point is 6H Downstream of the Inlet)

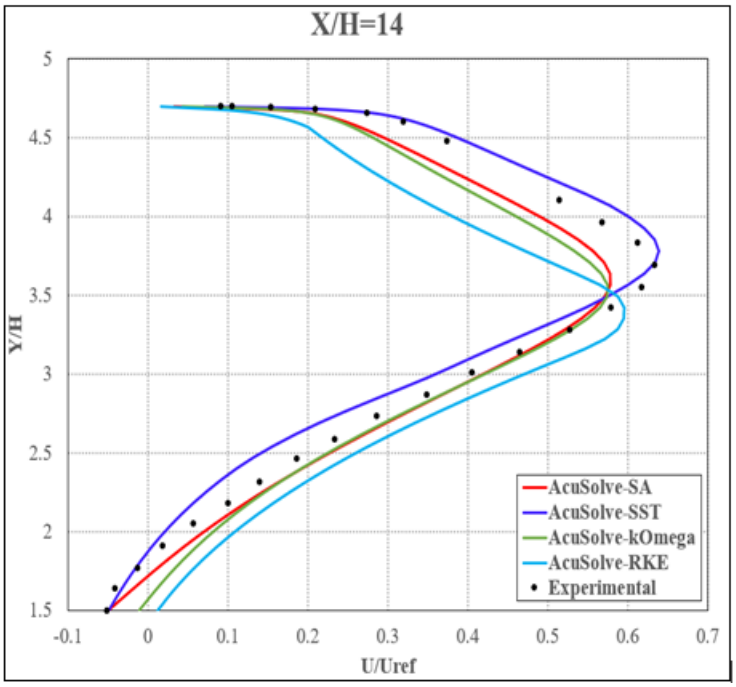


Figure 187: Non-Dimensional Streamwise Velocity Plotted Against Vertical Location Approximately 0.2 m Downstream of the Divergence (X/H = 13.468, Where the Reference Point is 6H Downstream of the Inlet)

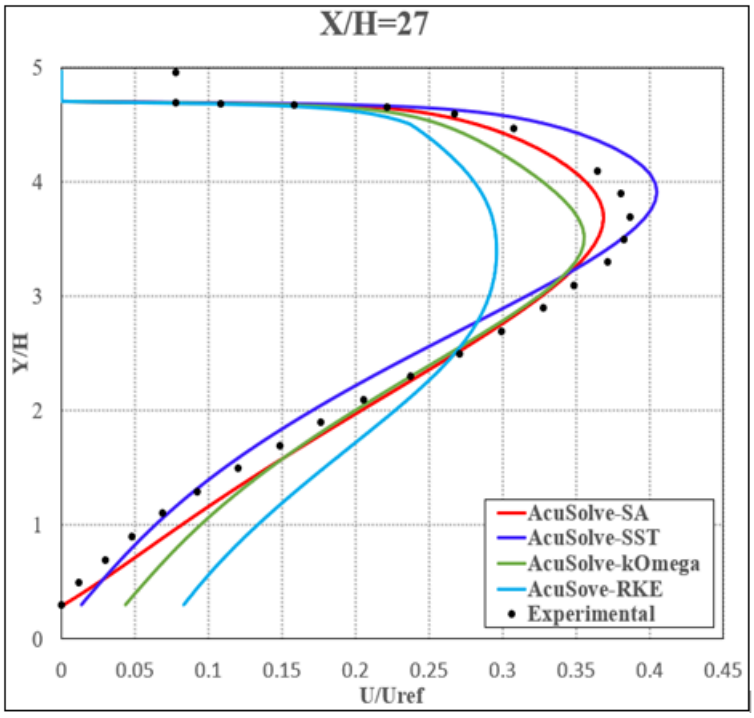


Figure 188: Non-Dimensional Streamwise Velocity Plotted Against Vertical Location Approximately 0.2 m Downstream of the Transition to the Fully Divergent Section (X/H = 27.066, Where the Reference Point is 6H Downstream of the Inlet)

The non-dimensional pressure coefficient (Cp), defined by the integrated inlet pressure and Uref predicted by AcuSolve along the bottom of the diffuser is compared to experimental results. The figure below shows Cp, along a constant vertical height, as a function of the streamwise distance from the inlet of the channel. The results demonstrate that AcuSolve is capable of accurately predicting the pressure within the diffuser within the expected range based on the type of turbulence model used. The performance of the three turbulence models were found to be consistent with previously published results for flow through the diffuser as published by Buice and Eaton (2000), with the SST model predicting the pressure distribution most accurately. Note that the inlet of the experimental duct was 6H longer than that modeled - AcuSolve values where X/H < -6 are reported as the inlet value.

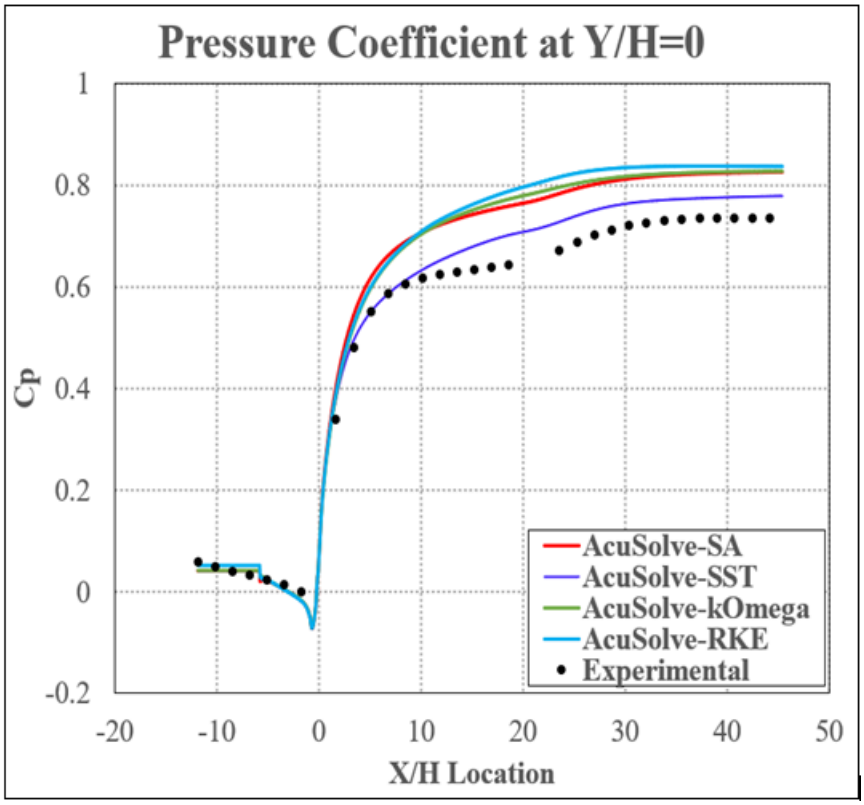


Figure 189: Non-Dimensional Pressure Coefficient (Cp) Plotted Against Relative Distance Along the Diffuser at a Constant Height Equal to the Bottom of the Inlet

Summary

In this application, a fully developed turbulent flow at a Reynolds number of 20,000 is studied. Due to the adverse pressure gradient, separation of flow occurs and causes recirculation in the divergent section of the diffuser. The results were found to be consistent with previously published computational studies and experimental data. The results of this validation demonstrate the ability of AcuSolve to accurately predict the separation point, the recirculation that occurs along the divergent wall, and the reattachment point in the straight section of the diffuser.

Simulation Settings for Turbulent Flow with Separation in an Asymmetric Diffuser

HyperWorks CFD database file: `<your working directory>\asymmetric_diffuser_turbulent\asymmetric_diffuser_turbulent.hm`

Global

- Problem Description
  - Analysis type - Steady State
  - Turbulence equation - Spalart Allmaras
- Auto Solution Strategy
  - Max time steps - `150`
  - Relaxation Factor - `0.2`
- Material Model
  - Air
    - Density - `1.225.0` kg/m3
    - Viscosity - `1.8325e-5` kg/m-sec

  Model
- Volume
  - Volume
    - Element Set
      1. Material model - Air
- Surfaces
  - Bottom
    - Simple Boundary Condition
      1. Type - Wall
  - Inlet
    - Simple Boundary Condition (disabled to allow for nodal boundary conditions to be set)
    - Advanced Options
      1. Nodal Boundary Conditions
         1. X-Velocity
            1. Type - Linear
            2. Precedence - `2`
            3. Curve fit variable - Y coordinate
            4. Curve fit values (included in database)
         2. Y-Velocity
            1. Type - Linear
            2. Precedence - `2`
            3. Curve fit variable - Y coordinate
            4. Curve fit values (included in database)
         3. Eddy Viscosity
            1. Type - Linear
            2. Precedence - `2`

3 Curve fit variable - Y coordinate
4 Curve fit values (included in database)

- Outlet
  - Simple Boundary Condition
    1 Type - Outflow - 101139.0 Pa
- Side 1
  - Simple Boundary Condition
    1 Type - Symmetry
- Side 2
  - Simple Boundary Condition
    1 Type - Symmetry
- Top
  - Simple Boundary Condition
    1 Type - Wall

References

C.U. Buice, and J.K., Eaton. "Experimental Investigation of Flow Through an Asymmetric Plane Diffuser". Journal of Fluids Engineering 122:433-435. June 2000.

S. Obi, K. Aoki and S. Masuda. "Experimental and Computational Study of Turbulent Separating Flow in an Asymmetric Plane Diffuser". Ninth Symposium on Turbulent Shear Flows. p. 305. Kyoto, Japan. August 16-19, 1993.

Turbulent Flow with Separation in an Axisymmetric Diffuser

In this application, AcuSolve is used to simulate fully developed turbulent flow through an axisymmetric diffuser with a divergent upper wall and a straight lower wall. AcuSolve results are compared with experimental results as described in Driver (1991) and on the NASA Langley Research Center Turbulence Modeling Resource webpage. The close agreement of AcuSolve results with experimental data and reference turbulence model performance validates the ability of AcuSolve to model cases with turbulent flow with separation due to an adverse pressure gradient within an axisymmetric geometry.

Problem Description

The problem consists of a fluid with material properties close to air flowing around a cylinder through an axisymmetric diffuser, as shown in the following image, which is not drawn to scale. The diffuser has a divergent section designed to generate an adverse pressure gradient. The inlet height between the cylinder and the upper section of the diffuser is 0.0355 m. The diffuser is constructed such that the section is axisymmetric around a cylinder with a diameter of 0.14 m. The inflow of the diffuser is set to produce a fully developed turbulent flow profile at a Reynolds number (Re) of 2,000,000. The upper section is modeled with a slip boundary condition, in order to match experimental conditions. The density of the fluid is 1.0 kg/m^3 and with a dynamic viscosity of 1.5 X 10-5 kg/m-s. The simulation was conducted with the Reynolds Averaged Navier-Stokes equations using four turbulence models, Spalart Allmaras, Shear Stress Transport (SST), K-ω and Realizable K-ε.

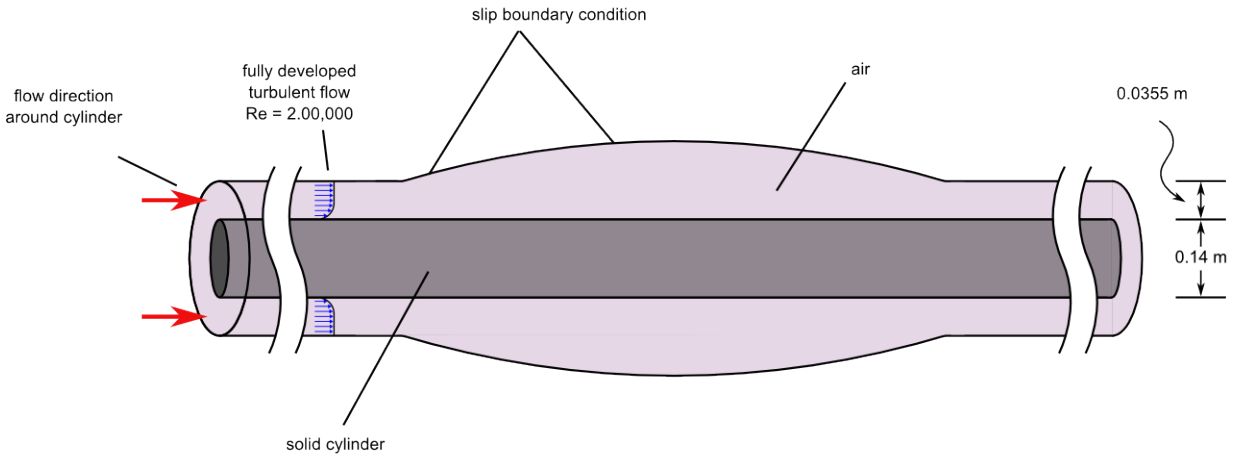


Figure 190: Critical Dimensions and Parameters for Simulating Turbulent Flow Through an Axisymmetric Diffuser

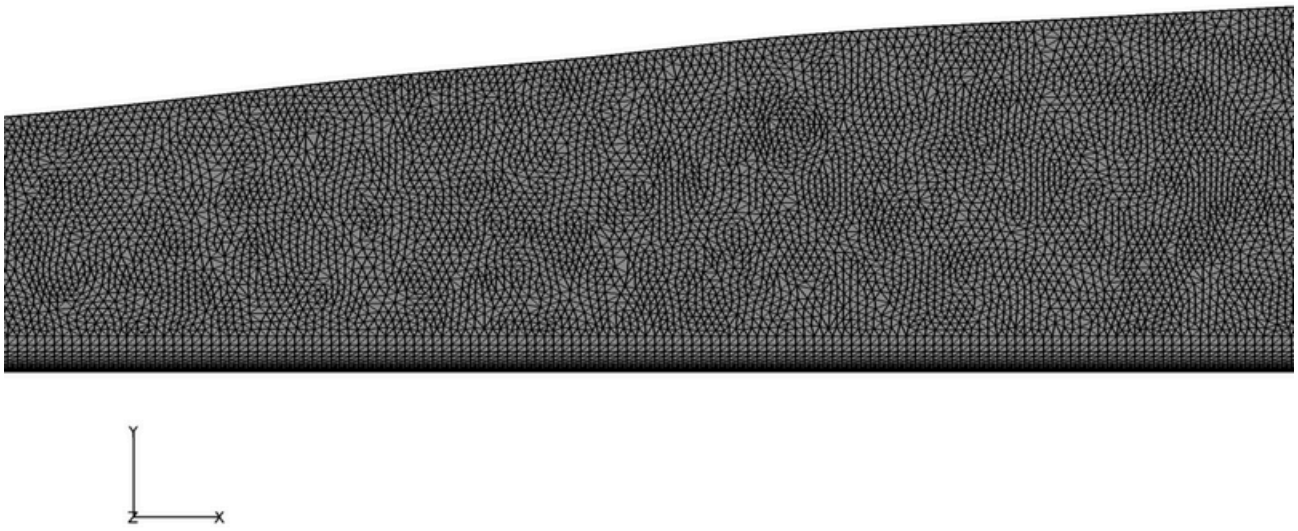


Figure 191: Mesh Detail Near the Divergence of the Walls in the Mesh used for Simulating Turbulent Flow Through an Axisymmetric Diffuser

The problem is simulated as axisymmetric by considering a 1 degree portion of the diffuser with the axisymmetric boundary condition applied on the cross-stream surfaces. The mesh elements were extruded in the axisymmetric direction to create a mesh with two elements spanning the simulated section.



Figure 192: Cross Section (Perpendicular to Flow) of Mesh used for Simulating Turbulent Flow Through an Axisymmetric Diffuser

AcuSolve Results

The AcuSolve solution converged to a steady state and the results reflect the mean flow conditions. As the fully developed turbulent flow enters the divergent section, the expansion of the cross-sectional height causes the streamwise velocity to decrease. This causes separation of the flow along the cylinder wall and results in an area of recirculation that eventually recovers downstream. After the flow enters the diffuser, the velocity decreases significantly from the inlet velocity, due to the rapid expansion of the cross section height in the divergent section. A separation bubble forms within the diffuser, with decreased flow velocity and increased pressure near the lower wall.

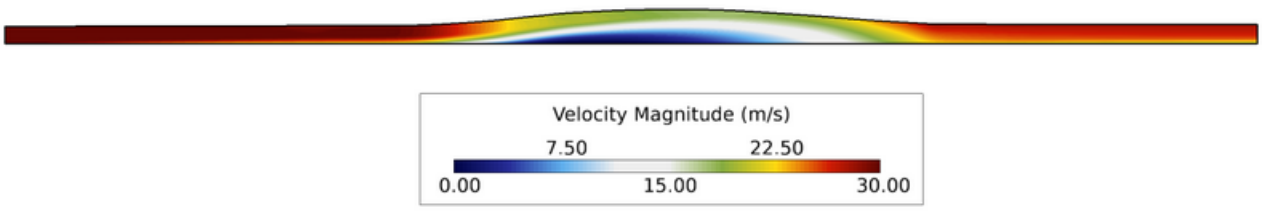


Figure 193: Velocity Contours Within the Diffuser

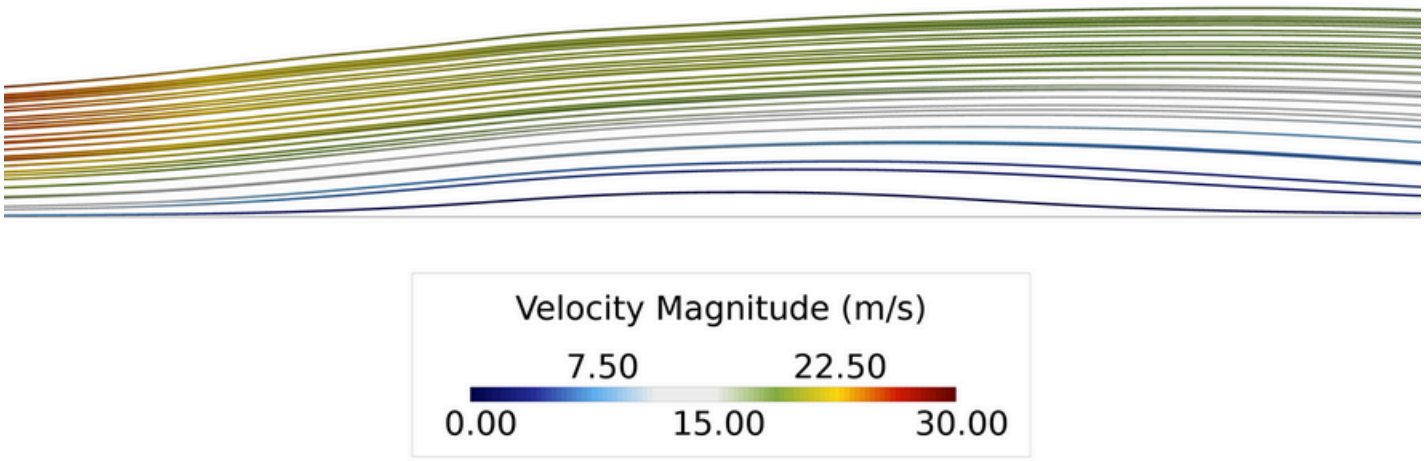


Figure 194:

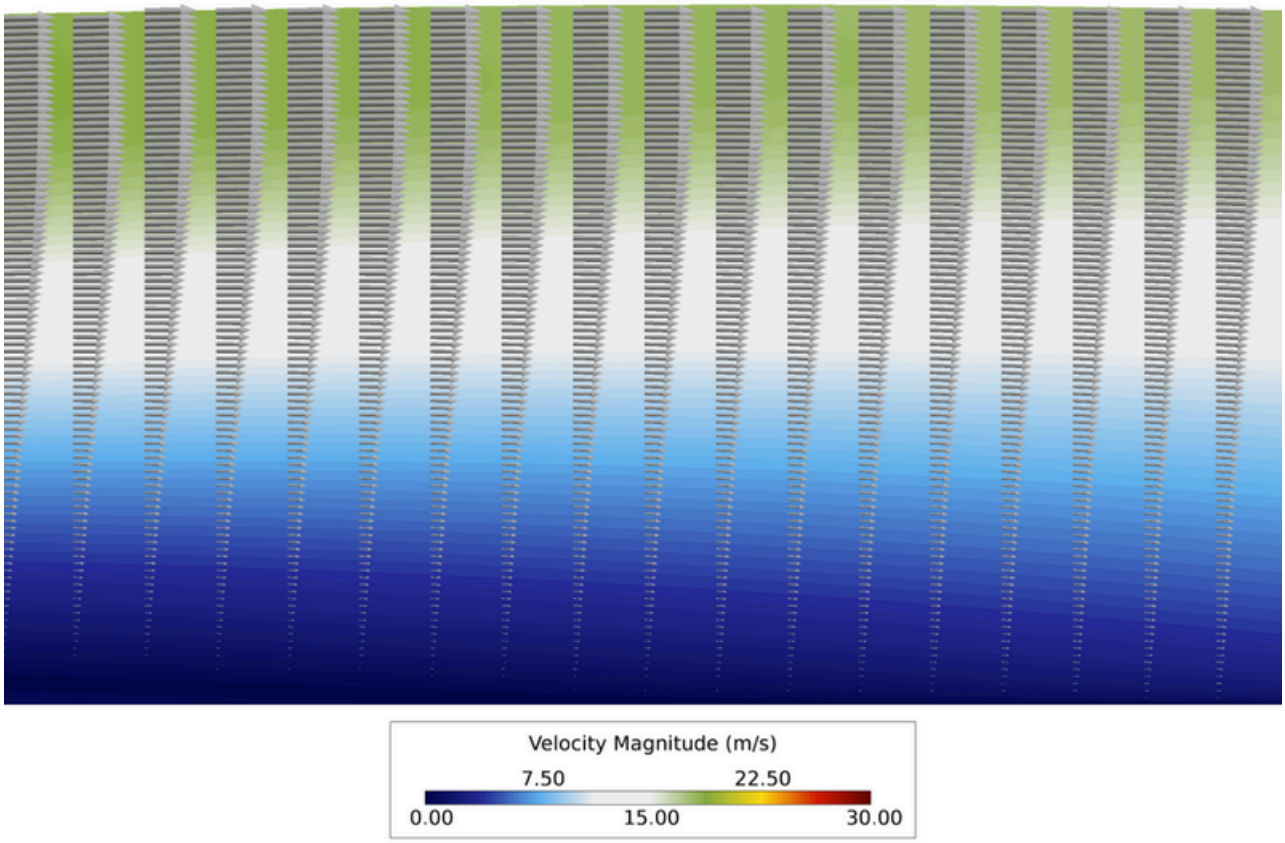


Figure 195: Close up View of Velocity Vectors and Contours in the Streamwise Plane Near the Reattachment Point

Upstream of the diffuser section, the streamwise velocity increases as the distance from the cylinder wall increases, with no influence from the top wall of the diffuser. As the flow enters into the divergent section, the streamwise velocity decreases near the cylinder wall and changes direction in the

recirculation region. Within the recirculation region, the reduced speed of the streamwise flow causes the wall shear stress to decrease and eventually change direction for a short distance along the cylinder surface. The images below show the coefficient of pressure (Cp) and coefficient of skin friction (Cf) along the cylinder wall in the diffuser compared against experimental results. The non-dimensional values are defined by the integrated inlet pressure and the magnitude of the inlet velocity. In the images black circles represent the experimental measurements (Driver 1991), solid red lines represent the prediction for the SA model, solid blue lines represent the prediction for the SST model, solid green lines represent the prediction for the K-ω model and solid cyan lines for the K-ε model, representing the AcuSolve results. There are minor differences in the prediction of the pressure coefficient within the diffuser between the three turbulence models. The SA model predicts a slightly higher value of pressure as the flow separates from the cylinder wall compared to both SST and K- ω. The shearing on the cylinder wall shows similar behavior, with the SA model predicting a slightly longer recirculation region and with the K- ω model predicting the separation further upstream. It was found that all three turbulence models predict the separation point further upstream than what is shown in the experiment. This is shown to be consistent with previous studies for each of the turbulence models used (NASA 2014).

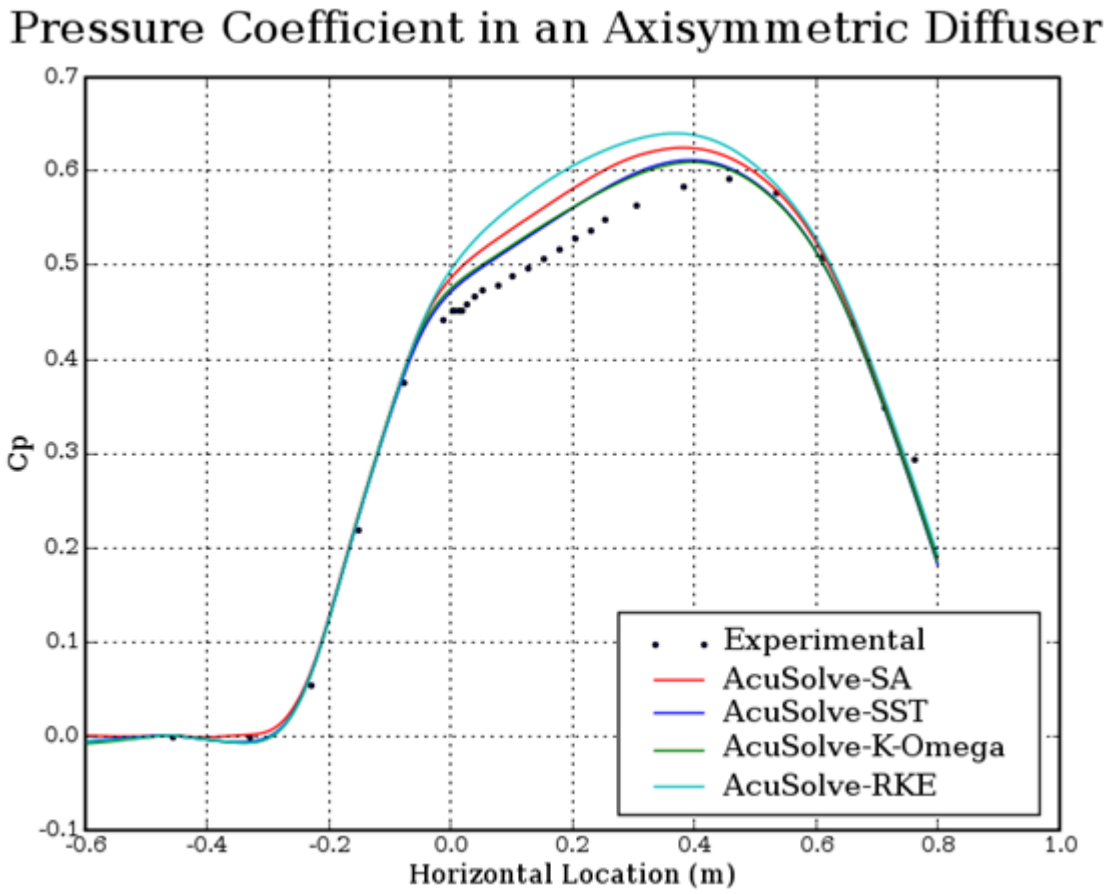


Figure 196: Coefficient of Pressure Along the Cylinder Wall Within the Diffuser Section (Horizontal Location = ~ 2.7m at the Midpoint of the Expanded Region of the Diffuser)

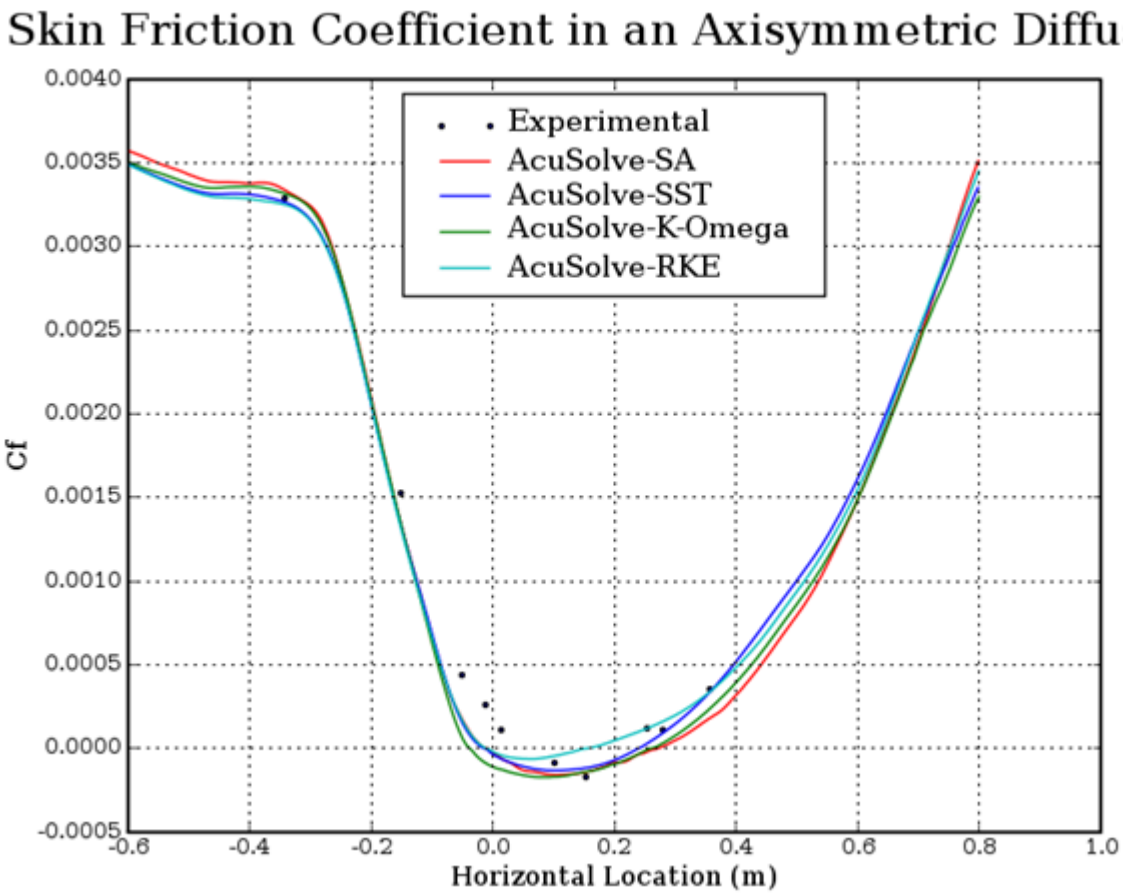


Figure 197: Skin Friction Coefficient Along the Cylinder Wall Within the Diffuser Section (Horizontal Location = 0 at the Point Where Flow Separation is Expected to Begin)

Summary

In this application, a fully developed turbulent flow at a Reynolds number of 2,000,000 is studied and compared against experimental data. The AcuSolve results compare well with the experimental data for pressure coefficient and skin friction coefficient. The recirculation region is slightly over predicted by the turbulence models studied, but the results still show a reasonable trend compared to experimental results. The performance of the three turbulence models was found to be consistent with previously published results for flow within an axisymmetric diffuser (NASA 2014). The results of this validation demonstrate the ability of AcuSolve to accurately predict flow recirculation with axisymmetric boundary conditions.

Simulation Settings for Turbulent Flow with Separation in an Axisymmetric Diffuser

AcuConsole database file: `<your working directory>\axisymmetric_diffuser_turbulent \axisymmetric_diffuser_turbulent.acs`

Global

- Problem Description
  - Analysis type - Steady State

    - Turbulence equation - Spalart Allmaras
- Auto Solution Strategy
    - Max time steps - `150`
    - Relaxation Factor - `0.4`
- Material Model
    - Fluid
        - Density - `1.0` kg/m3
        - Viscosity - `1.5e-5` kg/m-sec

  Model
- Volume
    - Fluid
        - Element Set
            1. Material model - Fluid
- Surfaces
    - Axisymmetric_maxZ
        - Simple Boundary Condition - (disabled to allow for periodic conditions to be set)
    - Axisymmetric_minZ
        - Simple Boundary Condition - (disabled to allow for periodic conditions to be set)
    - Inlet
        - Simple Boundary Condition
            1. Type - Inflow
            2. Inflow type - Velocity
            3. X velocity - `30.0` m/sec
            4. Turbulence input type - Direct
            5. Eddy viscosity - `1.5e-5` m2/sec
    - Outlet
        - Simple Boundary Condition
            1. Type - Outflow
    - Slip_maxY
        - Simple Boundary Condition
            1. Type - Slip
    - Wall_minY
        - Simple Boundary Condition
            1. Type - Wall
- Periodics
    - Axisymmetric
        - Periodic Boundary Condition

1 Type - Axisymmetric
2 Rotation Axis
    1 Point 1
        1 x-coordinate - `1.4` m
        2 y-coordinate - `0.0` m
        3 z-coordinate - `0.0` m
    2 Point 2
        1 x-coordinate - `-1.5` m
        2 y-coordinate - `0.0` m
        3 z-coordinate - `0.0` m

References

D. M. Driver. "Reynolds Shear Stress Measurements in a Separated Boundary Layer Flow". AIAA Paper 91-1787 from the AIAA 22nd Fluid Dynamics, Plasma Dynamics, and Lasers Conference. Honolulu, HI. June 1991.

NASA Langley Research Center Turbulence Modeling Resource webpage, http://turbmodels.larc.nasa.gov/driver_val.html. Accessed December 2014.

Turbulent Flow Over a Backward-Facing Step

In this application, AcuSolve is used to simulate fully developed turbulent flow over a backward-facing step. AcuSolve results are compared with experimental results as described in Driver (1985) and on the NASA Langley Research Center Turbulence Modeling Resource web page. The close agreement of AcuSolve results with experimental data and reference turbulence model performance validates the ability of AcuSolve to model cases with turbulent flow that forms a shear layer, recirculates and then reattaches downstream of the divergent step.

Problem Description

The problem consists of a fluid with material properties close to air flowing through a channel containing a sharp expansion, as shown in the following image, which is not drawn to scale. The step causes the flow to recirculate before reattaching downstream of the step. The inlet height of the channel is 8.0 m and expands as a step function to 9.0 m at a distance 20.0 m downstream of the inlet. This expanded section of the channel extends 50 m downstream of the step. The inflow of the channel is defined as fully developed at a Reynolds number (Re) of 36,000, based on the step height to match the experimental conditions. The density of the flow medium is 1.1837 kg/m^3 and the dynamic viscosity is 1.457 X 10^{-3} kg/m-s. The simulation was conducted with the Reynolds Averaged Navier-Stokes equations using four turbulence models, Spalart Allmaras, Shear Stress Transport (SST), K-ω and K-ε.

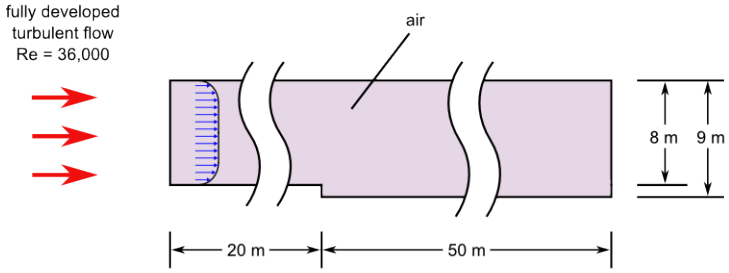


Figure 198: Critical Dimensions and Parameters for Simulating Turbulent Flow Through a Channel with a Backward-Facing Step

The simulation was performed as a two-dimensional problem by constructing a volume mesh that contains a single layer of elements extruded in the cross-stream direction, normal to the flow plane and by imposing symmetry boundary conditions on the extruded planes. The upper and lower walls are specified as no-slip, the inlet velocity and eddy viscosity are specified to match the conditions in the experiment (Driver 1985) at a distance of 20 m upstream of the step.

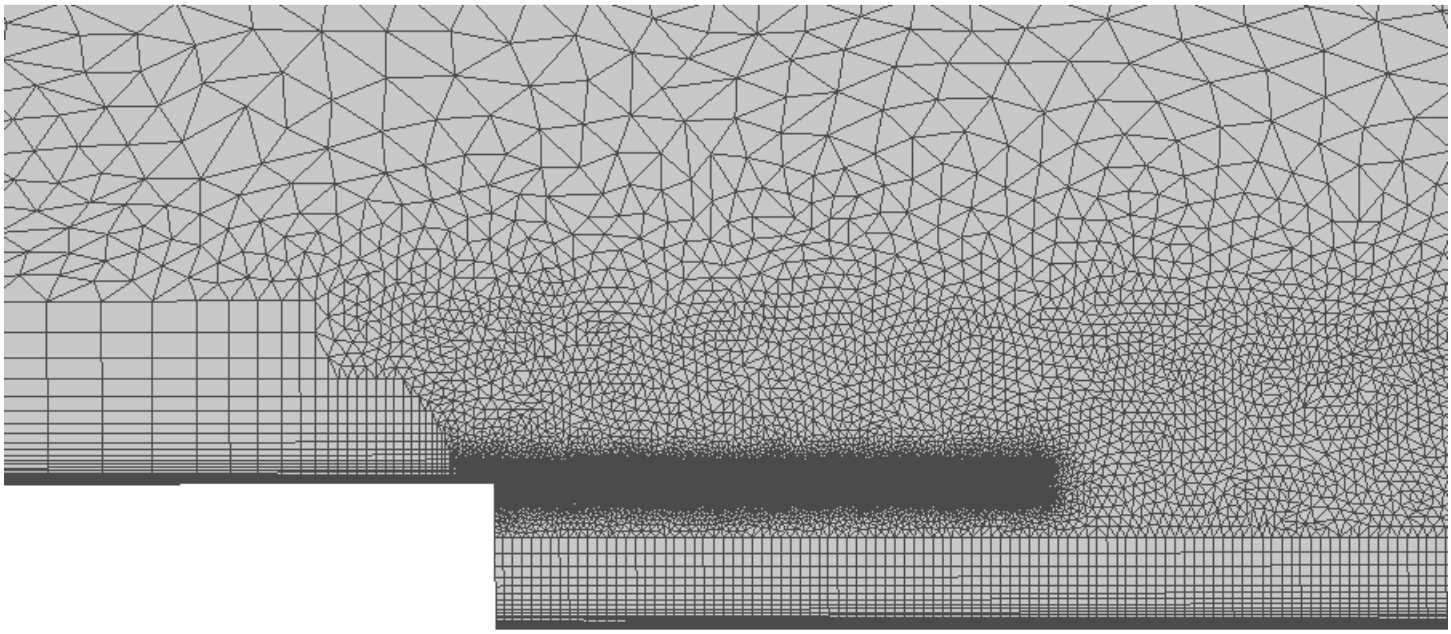


Figure 199: Detail of Mesh Near the Backward-Facing Step

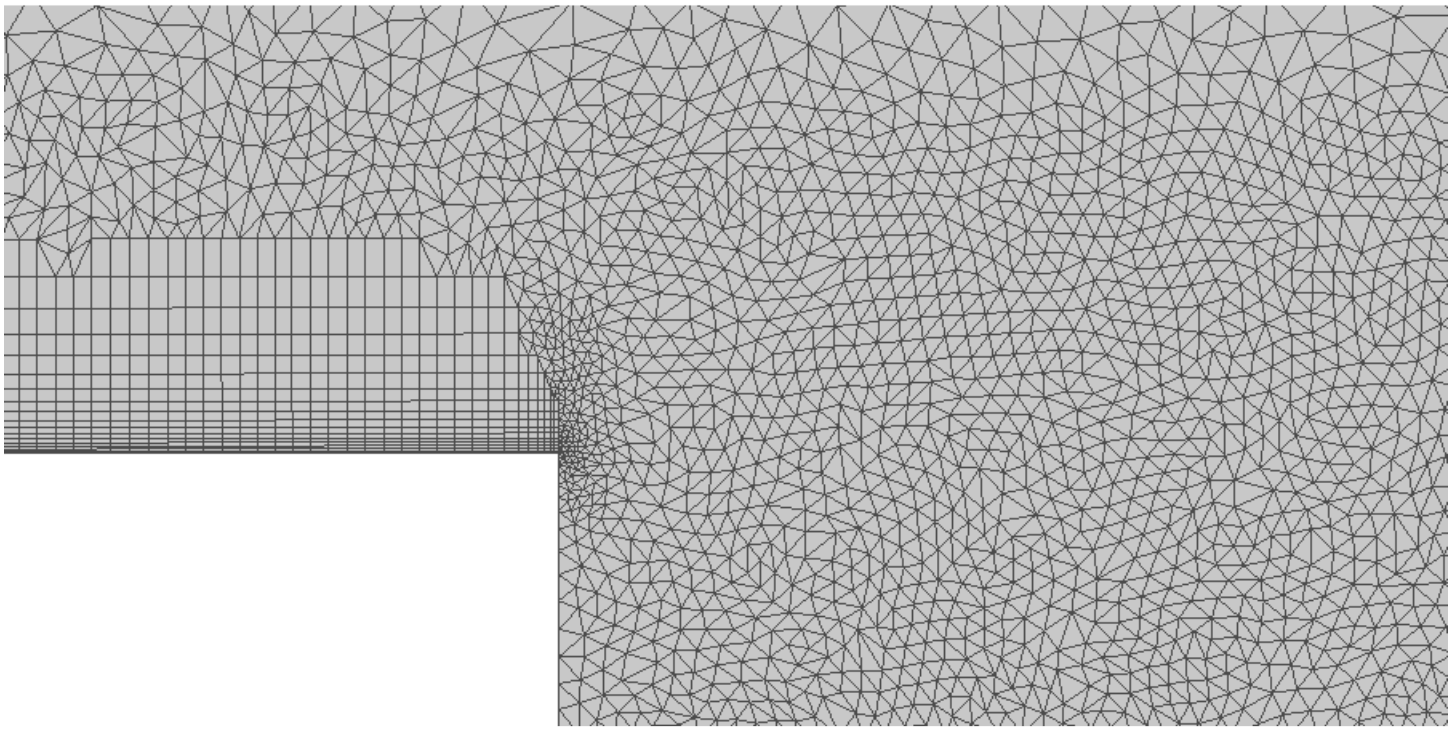


Figure 200: Finer Detail of Mesh Near the Backward-Facing Step

AcuSolve Results

The AcuSolve solution converged to a steady state and the results reflect the mean flow conditions. As the fully developed turbulent flow enters the divergent section, the expansion of the cross-sectional height causes a shear layer to develop above the lower wall. The expansion causes two recirculation zones; one immediately near the step wall and one that extends further downstream near the lower wall. The recirculation region eventually recovers downstream and the flow reattaches. The following images show the flow solution within the channel, demonstrating the recirculation region and reattachment point.

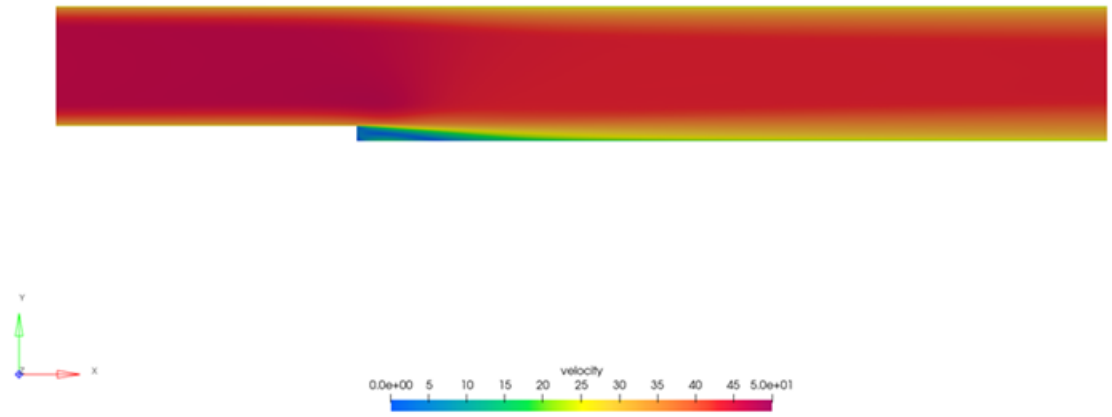


Figure 201: Velocity Contours Showing Low Velocity Near the Step Wall

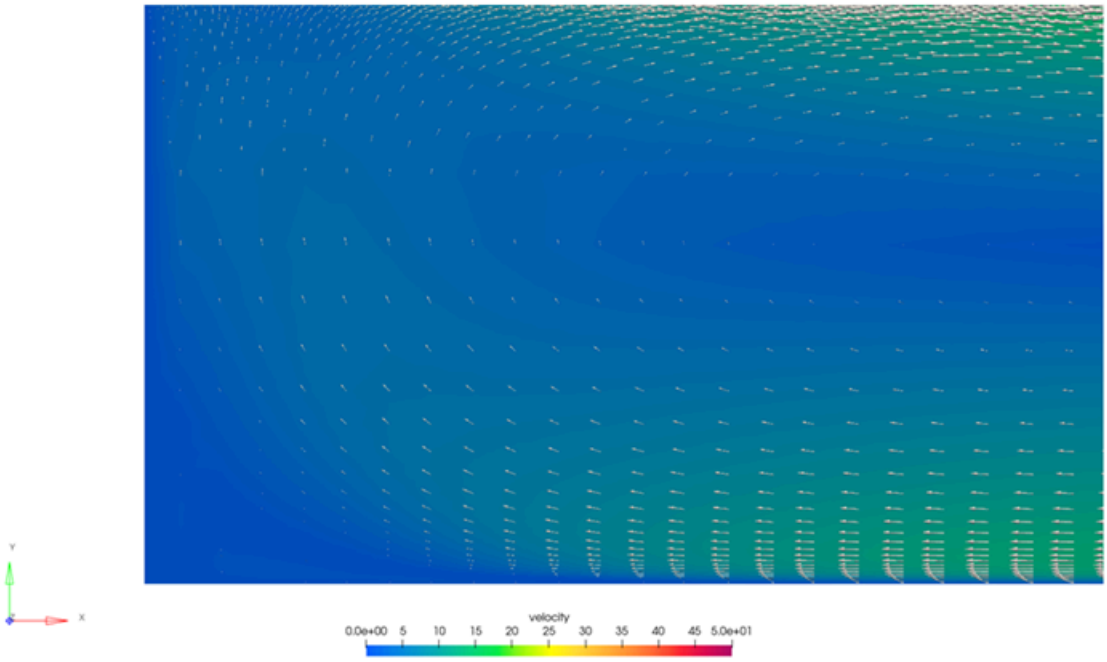


Figure 202: Close-Up View of Velocity Vectors and Contours in the Cross-Stream Plane Directly After the Step

Upstream of the expansion section, the streamwise velocity increases as the distance from the lower wall increases until it reaches the centerline of the channel and then begins decreasing until it reaches zero at the top wall. As the flow passes the step, it expands into the region directly downstream of the step wall, separating from the wall and recirculating until it recovers further downstream. The image below shows the coefficient of pressure along the lower wall of the step compared against experimental results. The non-dimensional values are defined by the integrated inlet pressure and the magnitude of the inlet velocity. The image shows black circles representing the experimental measurements (Driver 1985), a solid red line for the SA model, a solid blue line for the SST model, a solid green line for the K-ω model and a solid cyan line for the K-ε model, representing the AcuSolve results. The resulting pressure coefficient within the channel demonstrates minor differences between the three turbulence models. The SA model predicts a slightly larger recirculation region and does not reach the peak pressure in the wake of the step, compared to the SST model.

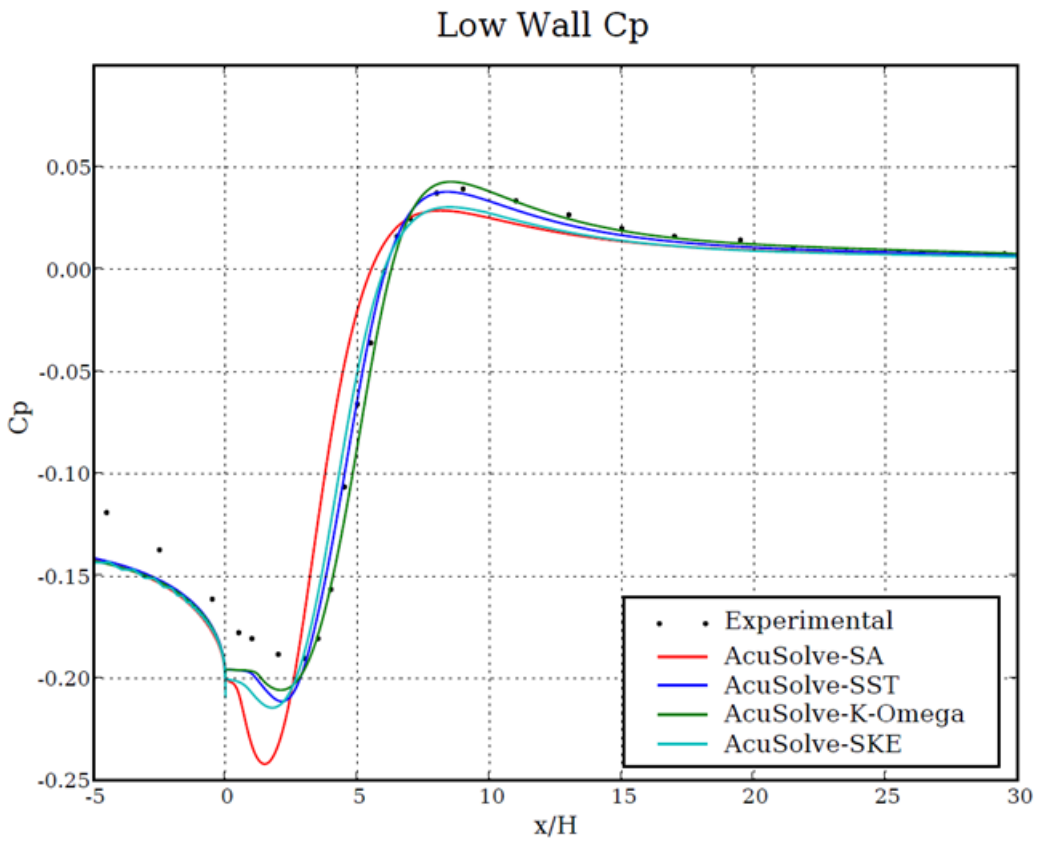


Figure 203: Coefficient of Pressure Plotted Against Location Along the Lower Wall Before and After the Step

Summary

In this application, a fully developed turbulent flow at a Reynolds number of 36,000 is studied and compared against experimental data. The AcuSolve results compare well with the experimental data for pressure coefficient. The performance of the Spalart Allmaras turbulence model was found to be consistent with previously published results for flow over a backward facing step (NASA 2015). The K-ω model appears to perform the best out of the three, predicting the reattachment and pressure distribution most accurately. AcuSolve demonstrates the ability to predict the shear layer in this type of application, the recirculation that occurs downstream of the step, as well as the reattachment point within the channel.

Simulation Settings for Turbulent Flow over a Backward-Facing Step

HyperWorks CFD database file: `<your working directory>\backstep_turbulent\backstep_turbulent.hm`

Global

- Problem Description
  - Analysis type - Steady State
  - Turbulence equation - Shear Stress Transport
- Auto Solution Strategy

    - Max time steps - `100`
    - Relaxation Factor - `0.5`
- Material Model
    - Air
        - Density - `1.183` kg/m3
        - Viscosity - `1.4575e-3` kg/m-sec

  Model
- Volume
    - Fluid
        - Element Set
            1. Material model - Air
- Surfaces
    - +Z
        - Simple Boundary Condition
            1. Type - Slip
    - -Z
        - Simple Boundary Condition
            1. Type - Slip
    - Inlet
        - Simple Boundary Condition - (disabled to allow for nodal boundary conditions to be set)
        - Advanced Options
            1. Nodal Boundary Conditions
                1. X-Velocity
                    1. Type - Linear
                    2. Precedence - Always
                    3. Curve fit variable - Y reference coordinate
                    4. Curve fit values - (included in database)
                2. Y-Velocity
                    1. Type - Linear
                    2. Precedence - Always
                    3. Curve fit variable - Y reference coordinate
                    4. Curve fit values - (included in database)
                3. Z-Velocity
                    1. Type - Zero
                4. Kinetic Energy
                    1. Type - Linear
                    2. Precedence - Always

3 Curve fit variable - Y reference coordinate
4 Curve fit values - (included in database)
5 Eddy Frequency
1 Type - Linear
2 Precedence - Always
3 Curve fit variable - Y reference coordinate
4 Curve fit values - (included in database)

- Outlet
  - Simple Boundary Condition
    1 Type - Outflow
- Wall - Lower - Downstream
  - Simple Boundary Condition
    1 Type - Wall
    2 Turbulence wall type - Low Reynolds Number
- Wall - Lower - Upstream
  - Simple Boundary Condition
    1 Type - Wall
    2 Turbulence wall type - Low Reynolds Number
- Wall - Step
  - Simple Boundary Condition
    1 Type - Wall
    2 Turbulence wall type - Wall Function
- Wall - Upper
  - Simple Boundary Condition
    1 Type - Wall
    2 Turbulence wall type - Low Reynolds Number

References

D. M. Driver and H. L. Seegmiller. "Features of Reattaching Turbulent Shear Layer in Divergent Channel Flow". AIAA Journal, 23(2): 163-171. Feb 1985.

NASA Langley Research Center Turbulence Modeling Resource webpage. http://turbmodels.larc.nasa.gov/backstep_val.html. Accessed June 2021.

Turbulent Flow Past a Convex Curve in a Channel

In this application, AcuSolve is used to simulate fully developed turbulent flow through a channel containing a convex curve in the lower wall. AcuSolve results are compared with experimental results as described in Smits (1979) and on the NASA Langley Research Center Turbulence Modeling Resource webpage. The close agreement of AcuSolve results with experimental data and reference turbulence model performance validates the ability of AcuSolve to model cases with turbulent flow moving past a convex curved wall.

Problem Description

The problem consists of a fluid with material properties close to air flowing through a channel containing a 30° swept wall, with a lower convex wall. The inlet channel height and remaining duct height is 0.127 m. The bulk velocity (v) normal to the inlet is 31.9 m/s and an integrated outflow pressure is specified to allow the flow to pass through the channel. The flow develops into fully turbulent flow at a Reynolds's number (Re) of 2,100,000. The density of the flow medium is 1.225 kg/m3 and the dynamic viscosity is 1.8608 X 10-5 kg/m-s. The simulation is conducted with the Reynolds Averaged Navier-Stokes equations using the Spalart Allmaras, Shear Stress Transport (SST), K-ω and Realizable K-ε turbulence models. The flow conditions are compared against experimental data and the current state-of-the-art performance for coefficient of pressure and coefficient of friction.

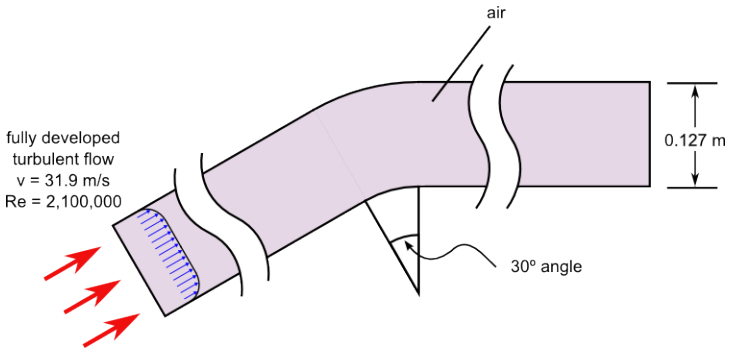


Figure 204: Critical Dimensions and Parameters for Simulating Turbulent Flow Through a Convex Channel

The simulation was performed as a two dimensional problem by restricting flow in the out-of-plane direction through the use of a mesh that is one element thick. The upper and lower walls are specified as no-slip, the inlet velocity and eddy viscosity are specified normal to the inlet face to match the experimental Reynolds Number.

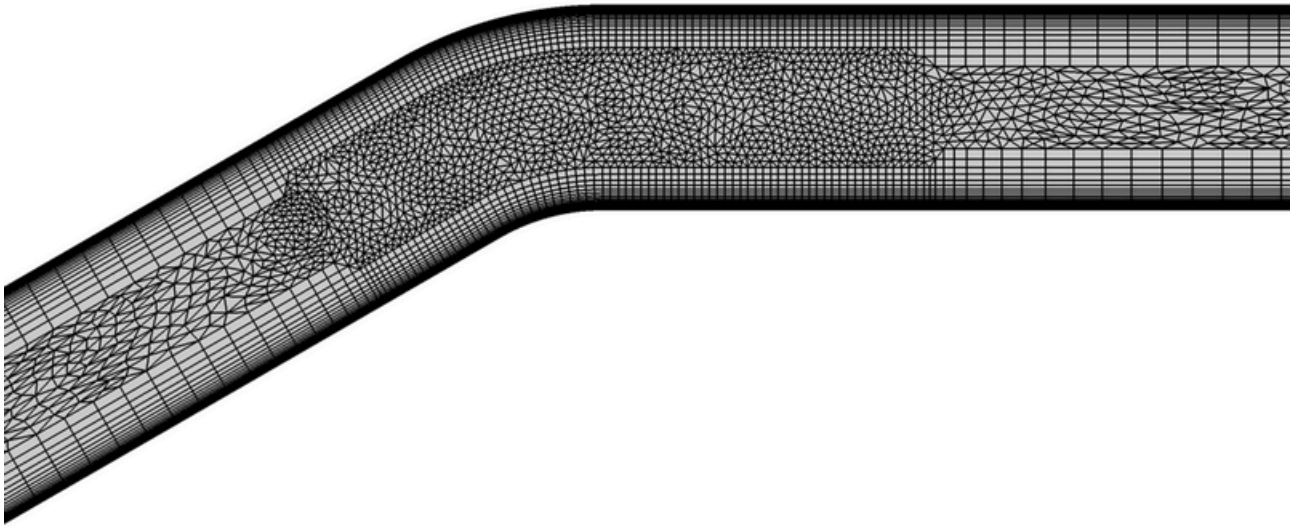


Figure 205: Detail of the Mesh used for Simulating Turbulent Flow Through a Convex Channel

AcuSolve Results

The AcuSolve solution converged to a steady state and the results reflect the mean flow conditions within the channel. As the fluid enters the channel it develops into fully turbulent flow exhibiting a steep parabolic velocity profile across the width of the channel. The flow begins to accelerate near the lower wall and decelerate near the top wall as it approaches the 30° bend. The results show that the upper (concave) wall destabilizes the boundary layer, increasing the eddy viscosity and forcing the flow velocity to decrease. The following figures show the flow conditions within the channel.

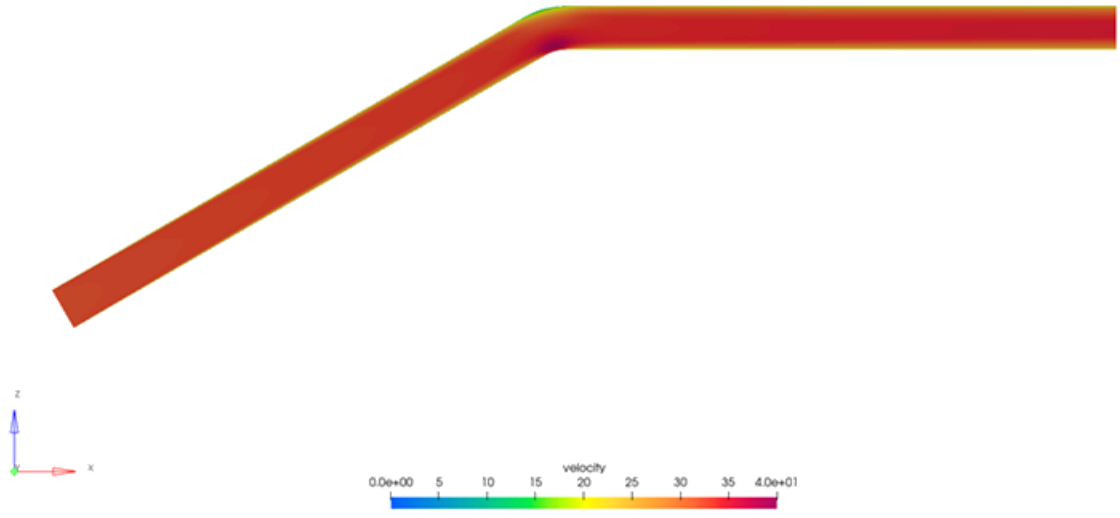


Figure 206: Velocity Contours in the Streamwise Plane

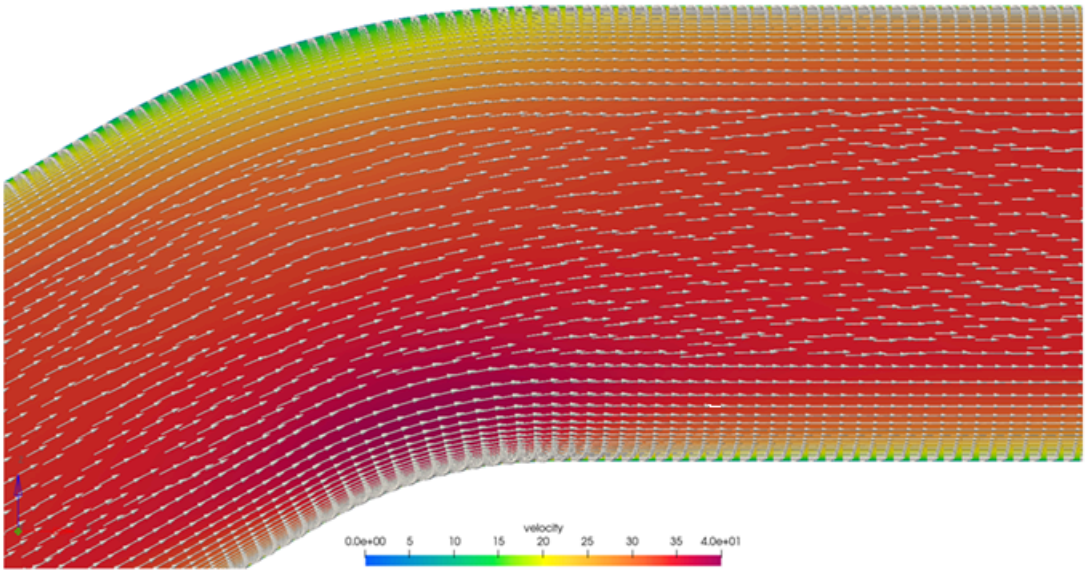


Figure 207: Close up View of Velocity Vectors and Velocity Contours at the 30° Bend

Upstream of the curved section of the channel, the flow normal to the channel opening increases as the distance from the lower wall increases until it reaches the centerline of the channel and then begins decreasing until it reaches zero at the top wall. As the flow approaches the curved section, it begins to accelerate, requiring that the flow velocity near the upper wall decrease to conserve momentum. The relatively low angle of curvature in the channel does not cause the accelerated fluid to recirculate. The images below show the coefficient of pressure (Cp) and coefficient of skin friction (Cf) along the lower wall of the channel. The images show black circles representing the experimental measurements (Smiths 1979), solid red lines for the SA model, solid blue lines for the SST model, solid green lines for the K-ω model and a solid cyan line for the K-ε model, representing the AcuSolve results. The coefficient of pressure within the channel is predicted nearly identically compared to the experiment for each of the turbulence models. It appears that the SST and K-ε models capture the low velocity region with the best accuracy, demonstrating that the flow velocity decreases significantly, but does not recirculate within the channel. This is shown in the friction coefficient plot, where the coefficient of friction, and subsequently the wall shear stress, does not decrease below zero.

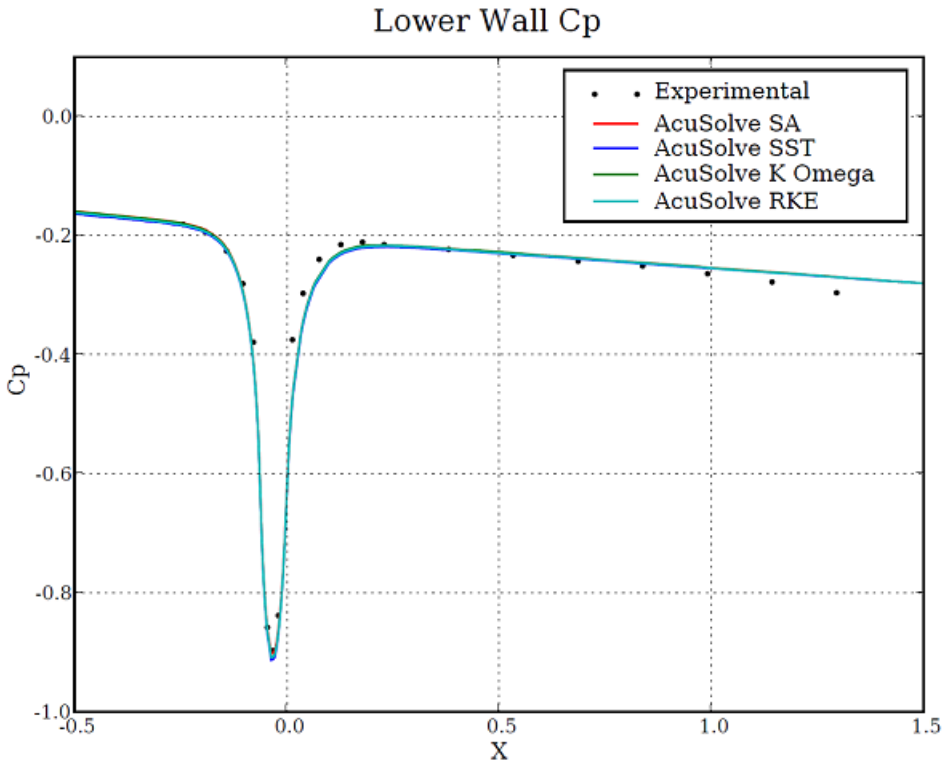


Figure 208: Coefficient of Pressure Plotted Against Relative Distance Along the Lower Wall from the Curve

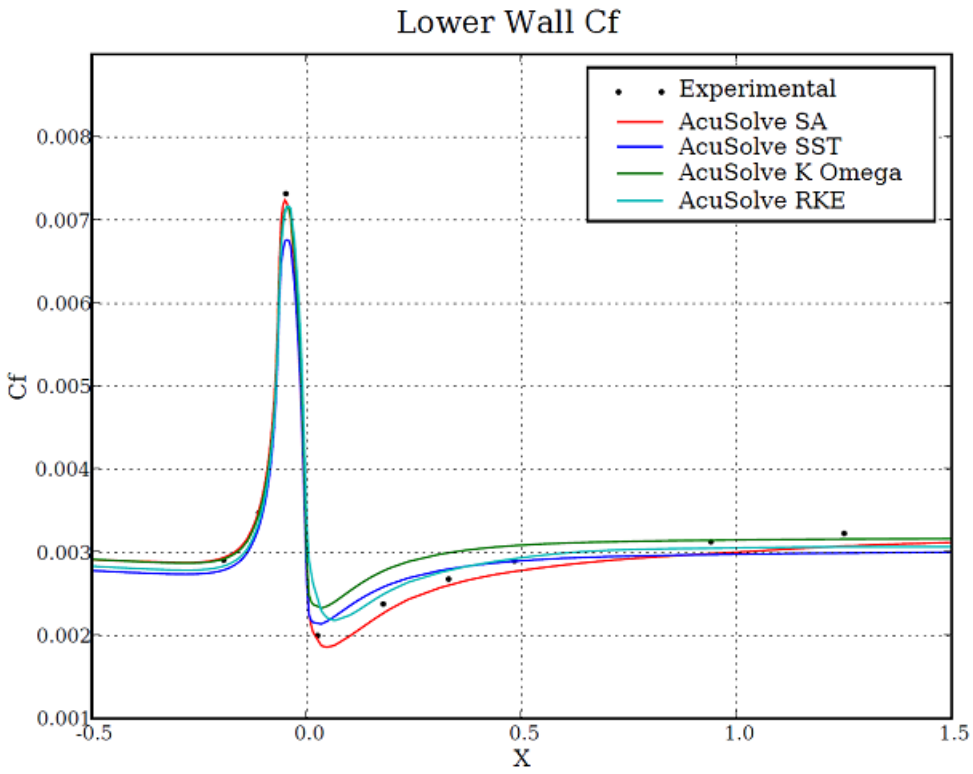


Figure 209: Skin Friction Coefficient Plotted Against Relative Distance Along the Lower Wall from the Curve

Summary

In this application, a turbulent flow through a curved channel at a Reynolds number of 2,100,000 is simulated and compared against experimental data. The AcuSolve results compare well with the experimental data for pressure coefficient and skin friction coefficient within the channel. The performance of the Spalart Allmaras turbulence model was found to be consistent with previously published results for flow through a convex-curved channel (NASA 2015) and the SST turbulence model appears to predict the shear stress on the lower wall most accurately. AcuSolve demonstrates the ability to predict the complex boundary layers resulting from the curvature of the channel and accurately predicts the propagation of the flow further downstream.

Simulation Settings for Turbulent Flow past a Convex Curve in a Channel

HyperWorks CFD database file: `<your working directory>\convex_curvature_turbulent \convex_curvature_turbulent.hm`

Global

- Problem Description
  - Analysis type - Steady State
  - Turbulence equation - Spalart Allmaras
- Auto Solution Strategy
  - Max time steps - `100`
  - Convergence tolerance - `0.0001`

    - Relaxation factor - `0.4`
- Material Model
    - Fluid
        - Density - `1.225` kg/m3
        - Viscosity - `1.8603e-5` kg/m-sec

  Model
- Volumes
    - Fluid - elbow
        - Element Set
            1. Material model - Fluid
    - Fluid - inlet
        - Element Set
            1. Material model - Fluid
    - Fluid - outlet
        - Element Set
            1. Material model - Fluid
- Surfaces
    - -Y
        - Simple Boundary Condition
            1. Type - Slip
    - +Y
        - 1. Type - Slip
    - Inlet
        - Simple Boundary Condition
            1. Type - Inflow
            2. Inflow type - Velocity
            3. Inflow velocity type - Normal
            4. Normal velocity - `31.9` m/sec
            5. Turbulence input type - Direct
            6. Eddy viscosity - `1.3671e-7` m2/sec
- Internal
    - Simple Boundary Condition - (disabled)
- Lower Wall
    - Simple Boundary Condition
        - Type - Wall
        - Turbulence wall type - Low Reynolds Number
- Outlet

    - Simple Boundary Condition
        - Type - Outflow
- Upper Wall
    - Simple Boundary Condition
        - Type - Wall
        - Turbulence wall type - Low Reynolds Number

References

A. J. Smits, S. T. B. Young, and P. Bradshaw. "The Effect of Short Regions of High Surface Curvature on Turbulent Boundary Layers". Journal of Fluid Mechanics. 94(2):209-242. 1979

NASA Langley Research Center Turbulence Modeling Resource webpage. http://turbmodels.larc.nasa.gov/smitscurve_val.html. Accessed May 2021.

Turbulent Flow Past a Wall-Mounted Hump

In this application, AcuSolve is used to simulate fully developed turbulent flow past a smooth hump on the lower wall of a flow domain. AcuSolve results are compared with experimental results as described in Seifert and Pack (2002) and on the NASA Langley Research Center Turbulence Modeling Resource web page. The close agreement of AcuSolve results with experimental data and reference turbulence model performance validates the ability of AcuSolve to model cases with turbulent flow moving past a wall protrusion resulting in flow separation and recovery.

Problem Description

The problem consists of a fluid with material properties close to air flowing through a flow domain containing a well-defined smooth hump with a slit opening at approximately 65 percent of the hump chord. The inlet of the domain is defined with an inflow velocity in the streamwise direction that develops into fully turbulent flow at a Reynolds number (Re) of 936,000, based on the hump chord length of 1.0 m. The density of the flow medium is 1.0 kg/m^3 and the dynamic viscosity is 1.0684 X 10^{-6} kg/m-s. The simulation is conducted with the Reynolds Averaged Navier-Stokes equations using the Spalart Allmaras turbulence model, shear stress transport (SST) model, the K-ω model and Realizable K-ε model to evaluate the performance of the turbulence models. The flow predictions from AcuSolve are compared against experimental data and previously published turbulence model performance for pressure and friction coefficients within the domain.

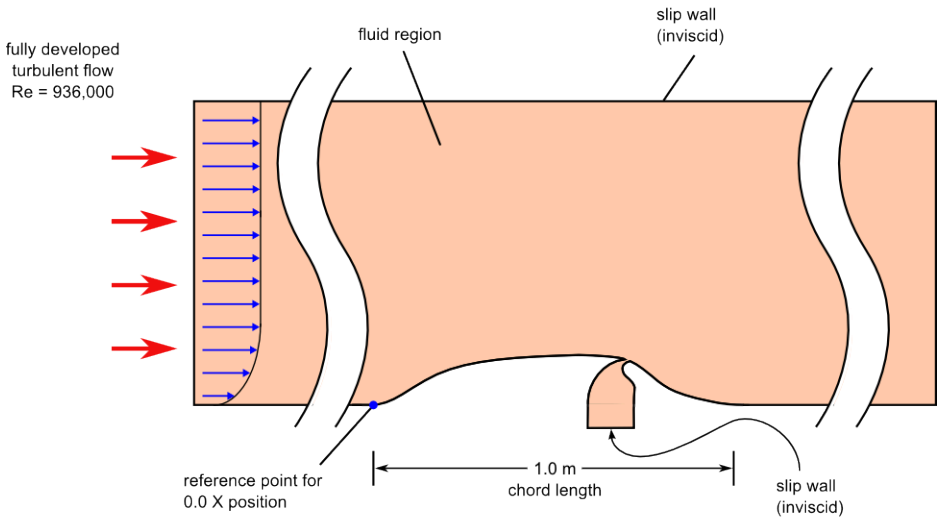


Figure 210: Critical Dimensions and Parameters for Simulating Turbulent Flow Through a Domain with a Wall-Mounted Hump

The upper walls of the domain are specified as slip (inviscid) and the lower walls are specified as no-slip. The inlet velocity and appropriate turbulence parameters are specified in the streamwise direction to match the desired Reynolds Number of 936,000. The outflow pressure is set to zero, and the lower wall on cavity below the hump is set to slip. The problem is simulated as two dimensional with a single layer of elements extruded in the cross stream direction and by defining the side walls as slip.

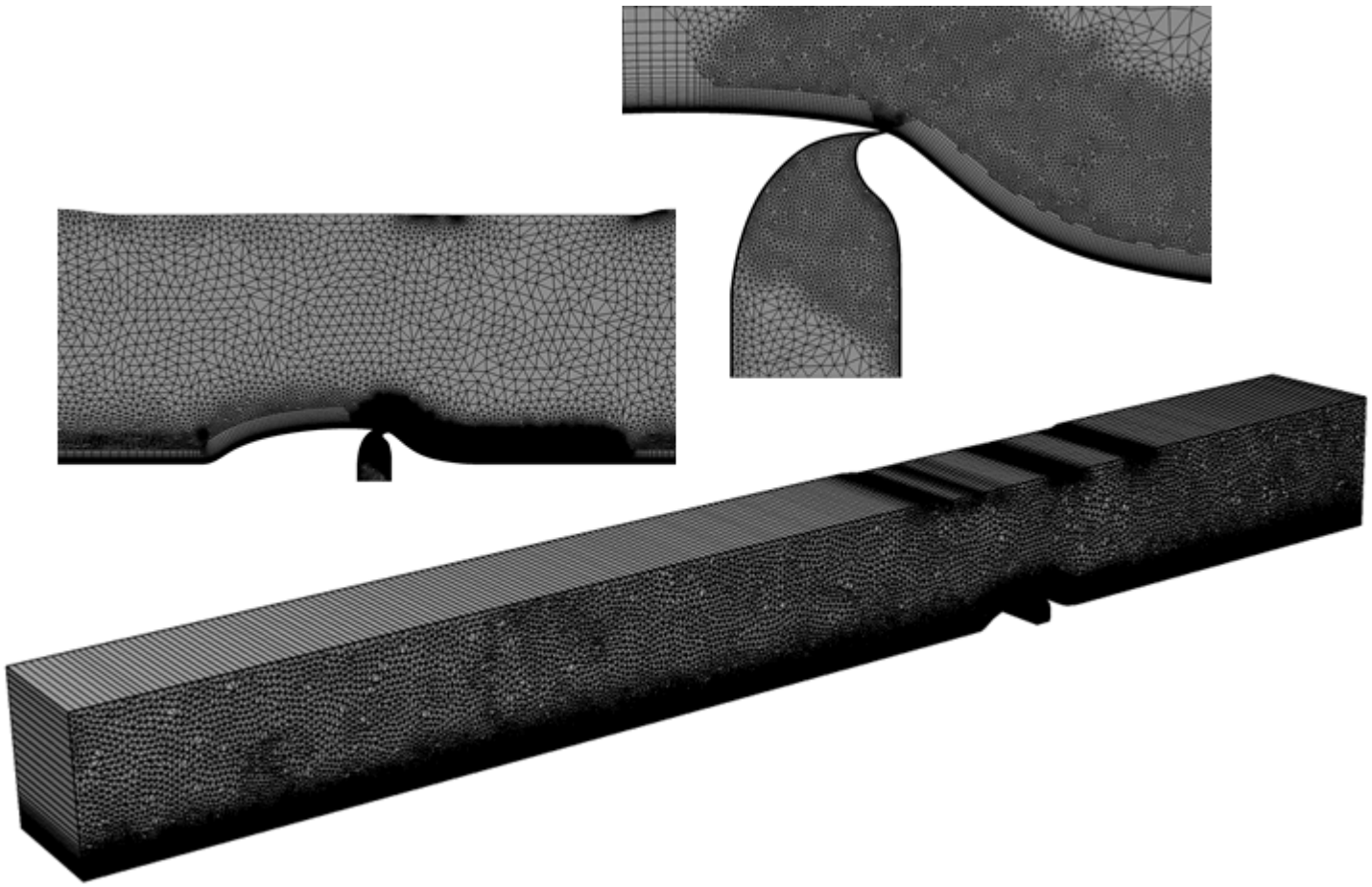


Figure 211: Three Views of the Mesh Used for Simulating Turbulent Flow over a Wall-Mounted Hump (Full Mesh is Shown on the Bottom, with Increased Resolution in Clockwise Views)

AcuSolve Results

The AcuSolve solution converged to a steady state and the results reflect the mean flow conditions within the domain. The images below show contours of velocity within the domain as well as the recirculation region directly downstream of the hump. As the flow enters the domain with a bulk velocity, it begins to develop a turbulent boundary layer near the lower wall prior to reaching the hump. As the flow approaches the hump section, the velocity near the lower wall decreases, but does not recirculate in front of the hump. It then accelerates over the top of the hump and separates immediately after reaching the cavity opening. The recirculation region propagates downstream, before the flow recovers and reattaches to the lower wall.

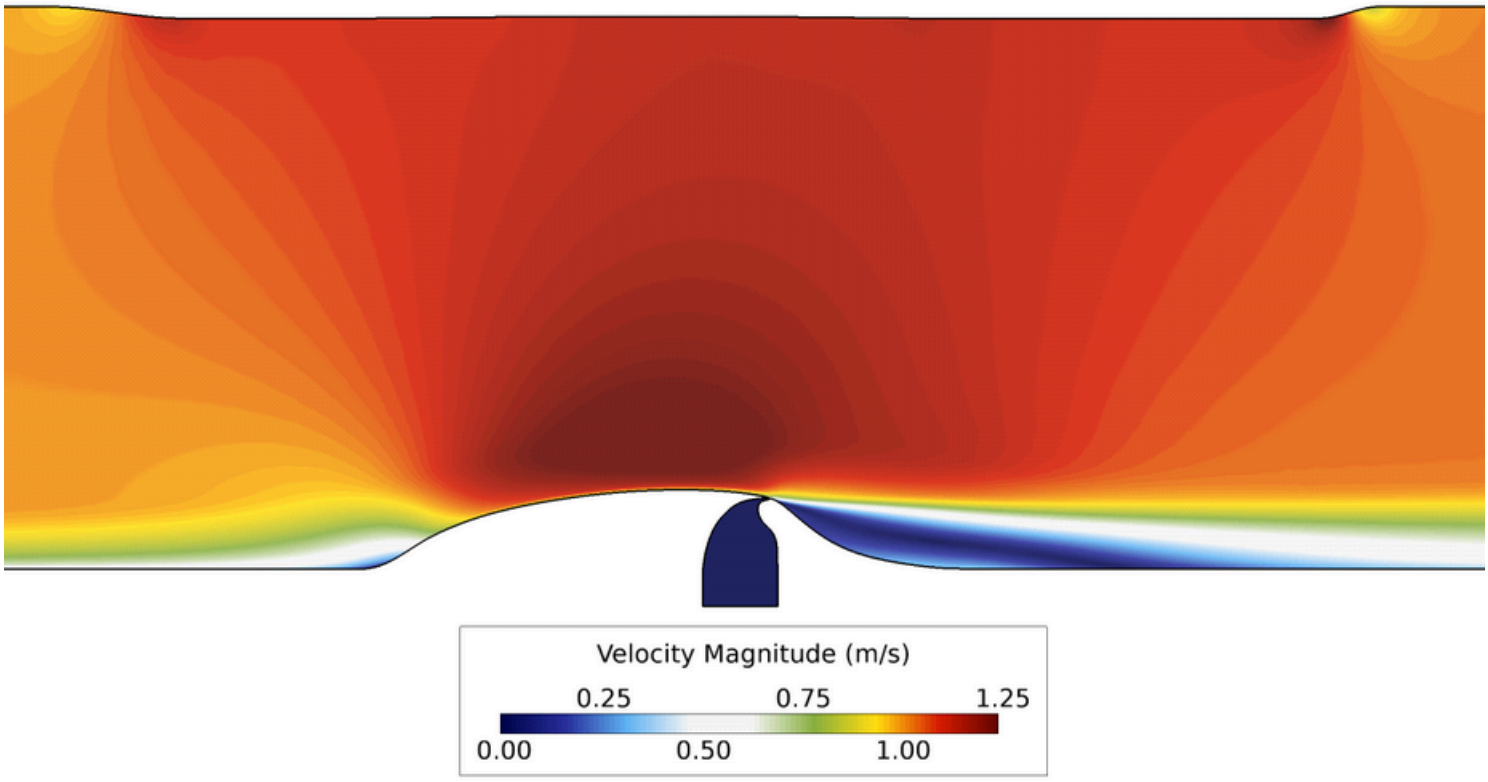


Figure 212: Velocity Contours on the Boundaries of the Domain, Showing Velocity Magnitude

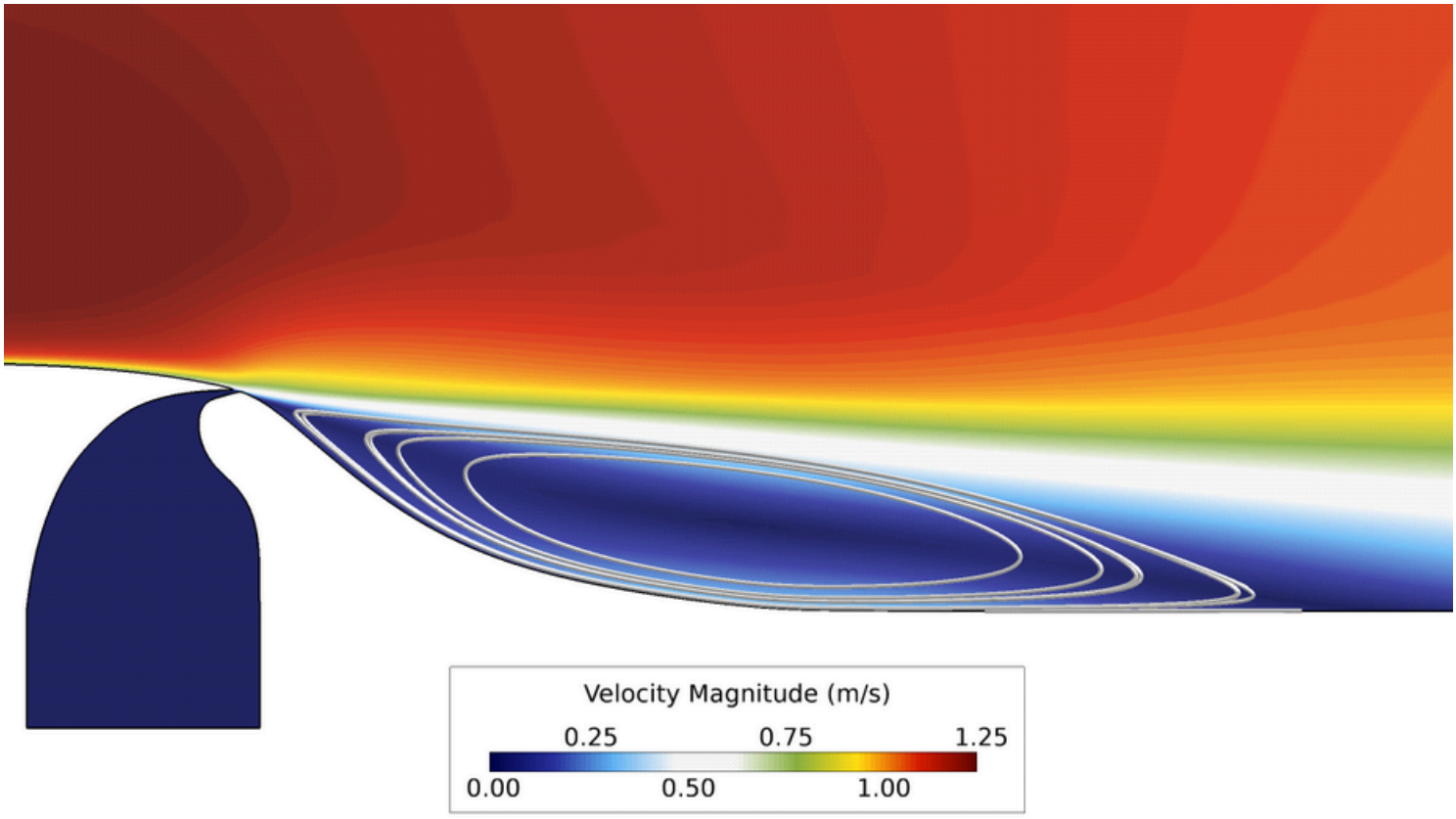


Figure 213: Close up View of Velocity Contours Showing the Recirculation Region with Streamlines (White Lines) Representing the Region of Backflow

The images below show the coefficient of pressure and coefficient of skin friction along the lower wall of the flow domain plotted with experimental results. The non-dimensional values are defined by the integrated inlet pressure and the magnitude of the inlet velocity. The images show black circles representing the experimental measurements (Seifert and Pack 2002), solid red lines for the SA model, solid blue lines for the SST model, solid green lines for the K-ω model and solid cyan lines for the K-ε model, representing the AcuSolve results. The resulting pressure coefficient within the domain demonstrates that there are minor differences between the three turbulence models. All three models are shown to perform accurately in predicting the increase in surface pressure on the front of the hump, but tend to over predict the skin friction in the wake of the hump, leading to an over prediction of the reattachment location. The SA model predicts a slightly larger recirculation region, and does not meet the expected recovery pressure compared to SST, K- ω and K-ε. This performance was found to be consistent with comparisons to other one equation models (NASA 2015).

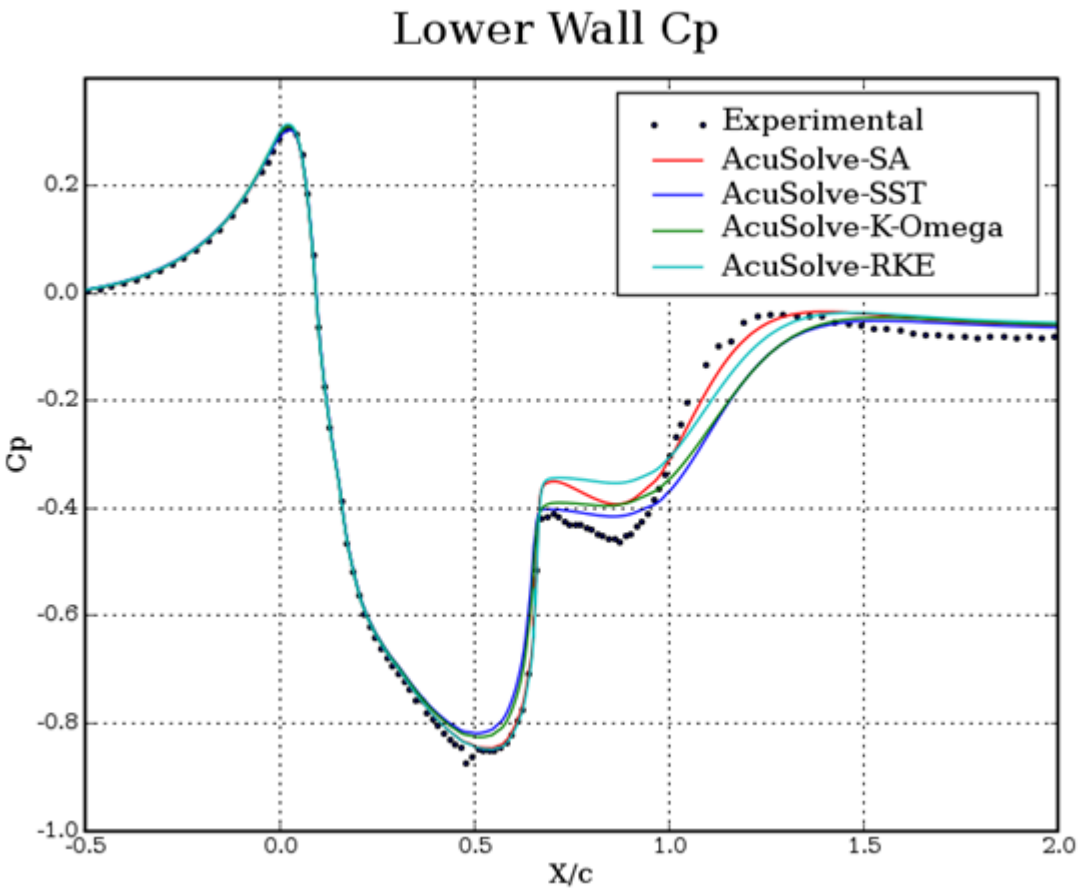


Figure 214: Coefficient of Pressure Along the Lower Wall as the Flow Moves Past the Hump, Where c is the Hump Chord Length and 0.0 is the Reference Location at the Front of the Hump in the X-Direction (Streamwise)

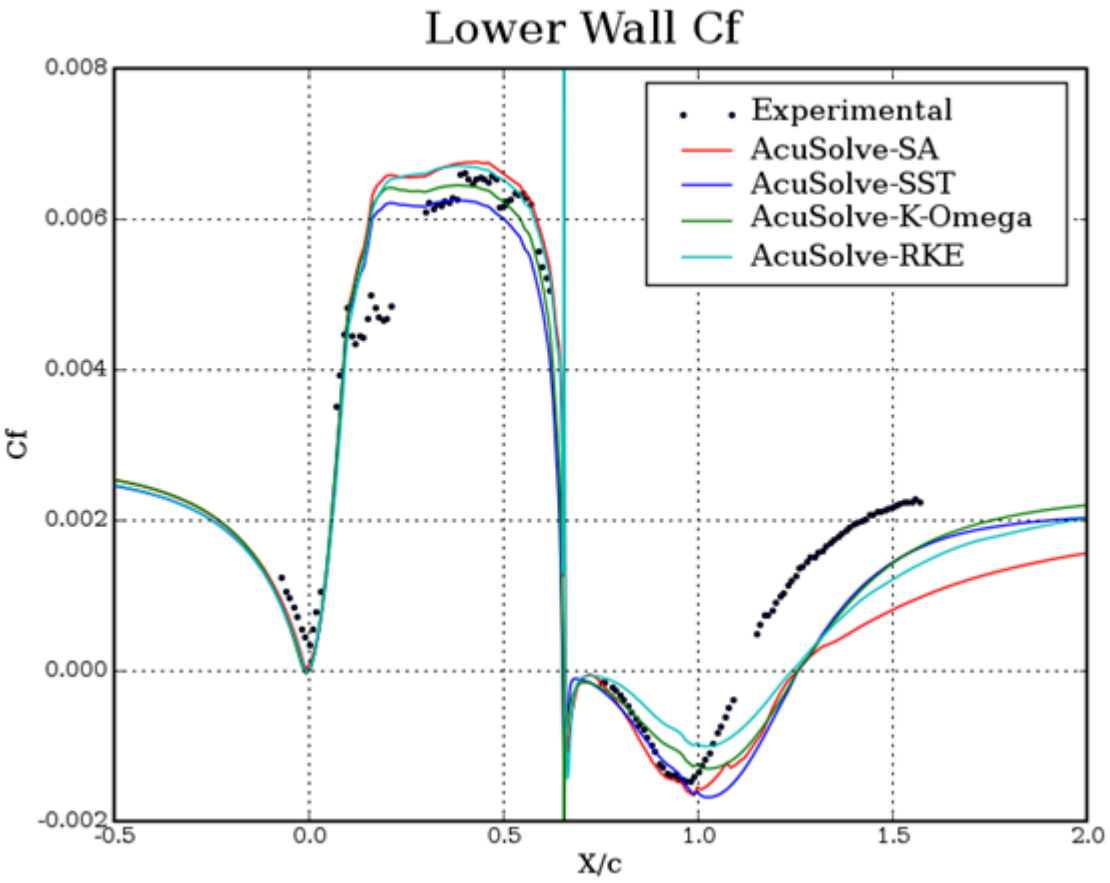


Figure 215: Skin Friction Coefficient Along the Lower Wall as the Flow Moves Past the Hump, Where c is the Hump Chord Length and 0.0 is the Reference Location at the Front of the Hump in the X-Direction (Streamwise)

Summary

In this application, a bulk turbulent flow at a Reynolds number of 936,000 within a flow domain containing a wall-mounted hump is studied and compared against experimental data. The AcuSolve results compare well with the experimental data for pressure coefficient and skin friction coefficient near the hump and downstream. The performance of the three turbulence models were found to be consistent with previously published results for flow over a wall-mounted hump (NASA 2015). For this application, the two equation models appear to outperform the one equation turbulence model, with better agreement for the downstream pressure on the wall. This application demonstrates AcuSolve's ability to predict the distribution of pressure and shear stress on protruding bodies within a turbulent flow field and serves to validate current turbulence modeling capabilities.

Simulation Settings for Turbulent Flow past a Wall-Mounted Hump

AcuConsole database file: `<your working directory>\wall_mounted_hump_turbulent\wall_mounted_hump_turbulent.acs`

Global

- Problem Description

    - Analysis type - Steady State
    - Turbulence equation - Spalart Allmaras
- Auto Solution Strategy
    - Max time steps - `100`
    - Convergence tolerance - `0.001`
    - Relaxation factor - `0.4`
- Material Model
    - Fluid
        - Density - `1.0` kg/m3
        - Viscosity - `1.0684e-6` kg/m-sec

  Model
- Volumes
    - Fluid
        - Element Set
            1. Material model - Fluid
- Surfaces
    - +Y
        - Simple Boundary Condition
            1. Type - Slip
    - -Y
        - Simple Boundary Condition
            1. Type - Slip
    - Cavity walls
        - Simple Boundary Condition
            1. Type - Wall
            2. Turbulence wall type - Wall Function
    - Hump walls
        - Simple Boundary Condition
            1. Type - Wall
            2. Turbulence wall type - Wall Function
    - Hump walls - downstream
        - Simple Boundary Condition
            1. Type - Wall
            2. Turbulence wall type - Wall Function
    - Inlet
        - Simple Boundary Condition
            1. Type - Inflow

2. Inflow type - Velocity
3. Inflow velocity type - Cartesian
4. X Velocity - `1.0` m/sec
5. Turbulence input type - Direct
6. Eddy viscosity - `3.205128e-6` m2/sec

- Lower slip
  - Simple Boundary Condition
    1. Type - Slip
- Lower wall
  - Simple Boundary Condition
    1. Type - Wall
    2. Turbulence wall type - Wall Function
- Nozzle walls
  - Simple Boundary Condition
    1. Type - Wall
    2. Turbulence wall type - Wall Function

- Outlet
  - Simple Boundary Condition
    - Type - Outflow
- Slip
  - Simple Boundary Condition
    - Type - Slip

References

A Seifert and L.G. Pack. "Active Flow Separation Control on Wall-Mounted Hump at High Reynolds Numbers". AIAA Journal. 40(7). 2002.

NASA Langley Research Center Turbulence Modeling Resource web page. http://turbmodels.larc.nasa.gov/nasahump_val.html. Accessed June 2015.

Heat Transfer Between Radiating Concentric Cylinders

In this application, AcuSolve is used to simulate the heat transfer due to radiation between concentric cylinders. The inner and outer cylinders are held at constant temperature and are defined to be radiation surfaces. AcuSolve results are compared with analytical results for temperature as described in Incropera (2006). The close agreement of AcuSolve results with analytical results validates the ability of AcuSolve to model cases with radiation heat transfer requiring view factor computation.

Problem Description

The problem consists of a fluid with arbitrary material properties between two infinitely long concentric cylinders, as shown in the following image, which is not drawn to scale. The radius of the outer cylinder is 0.046 m and the radius of the inner cylinder is 0.018 m. The inner cylinder is defined to have a constant wall temperature at 773.0 K (500 °C). The outer cylinder is defined to have a constant wall temperature at 300.0 K (27 °C). Both cylinders are specified to radiate as grey bodies, with emissivity set to 0.03778.

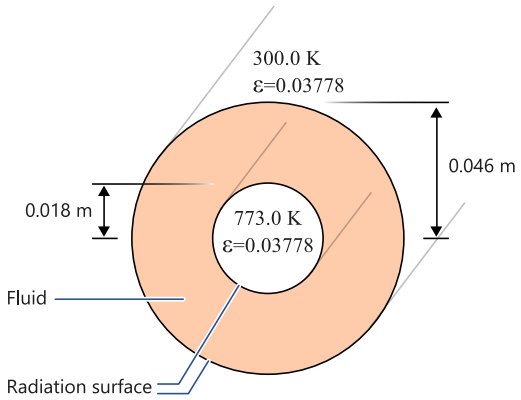


Figure 216: Critical Dimensions and Parameters Used for Simulating Radiation Between Two Concentric Cylinders

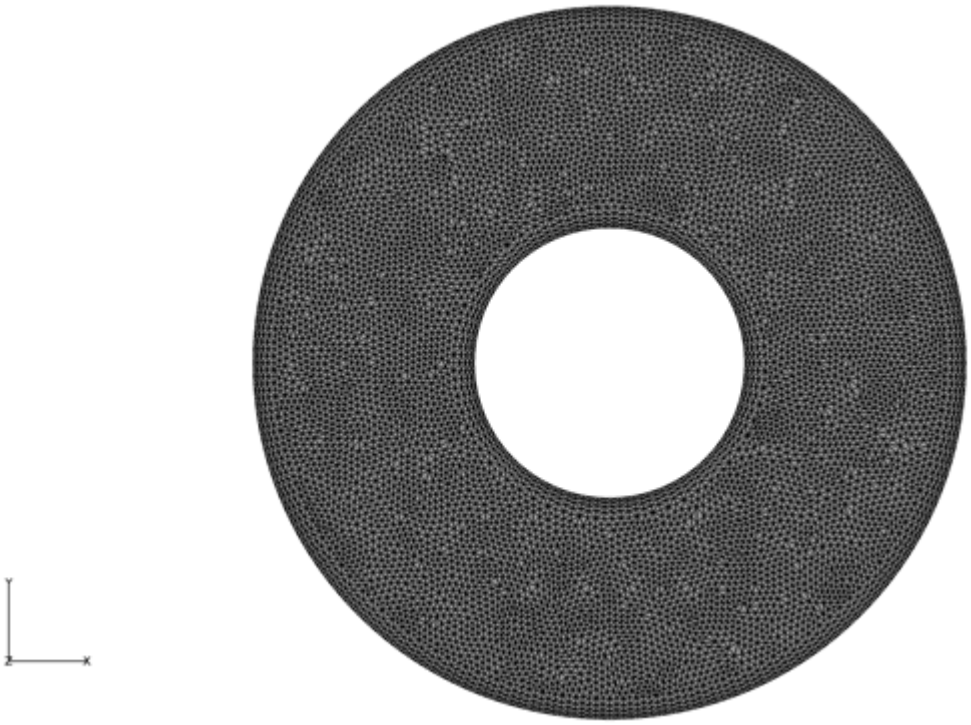


Figure 217: Mesh used for Simulating Radiation Between Two Concentric Cylinders

The simulation was performed as a two dimensional problem by constructing a volume mesh that contains a single layer of elements normal to the radial and circumferential directions.

AcuSolve Results

The AcuSolve solution converges to a steady state and the results reflect the mean temperature distribution. As the inner diameter is considerably hotter than the outer, a heat flux, due to radiation, is present between the cylinders. The temperature within the medium reduces logarithmically as a function of the radius. The following images show the temperature with the medium as a function of radius from the center. The temperature is compared with the analytical solution as described in Incropera (2006). The image below shows black circles representing the analytical solution and a solid red line for the AcuSolve results.

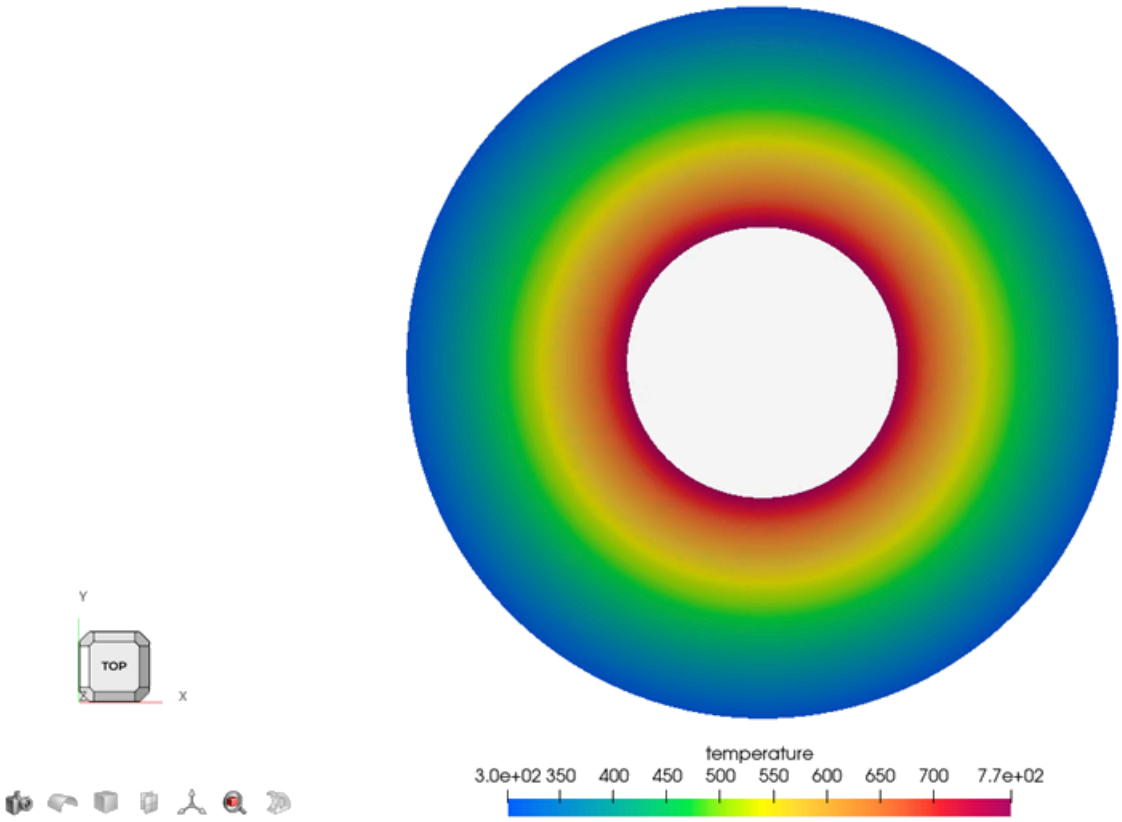


Figure 218: Contours of Temperature Between the Concentric Cylinders

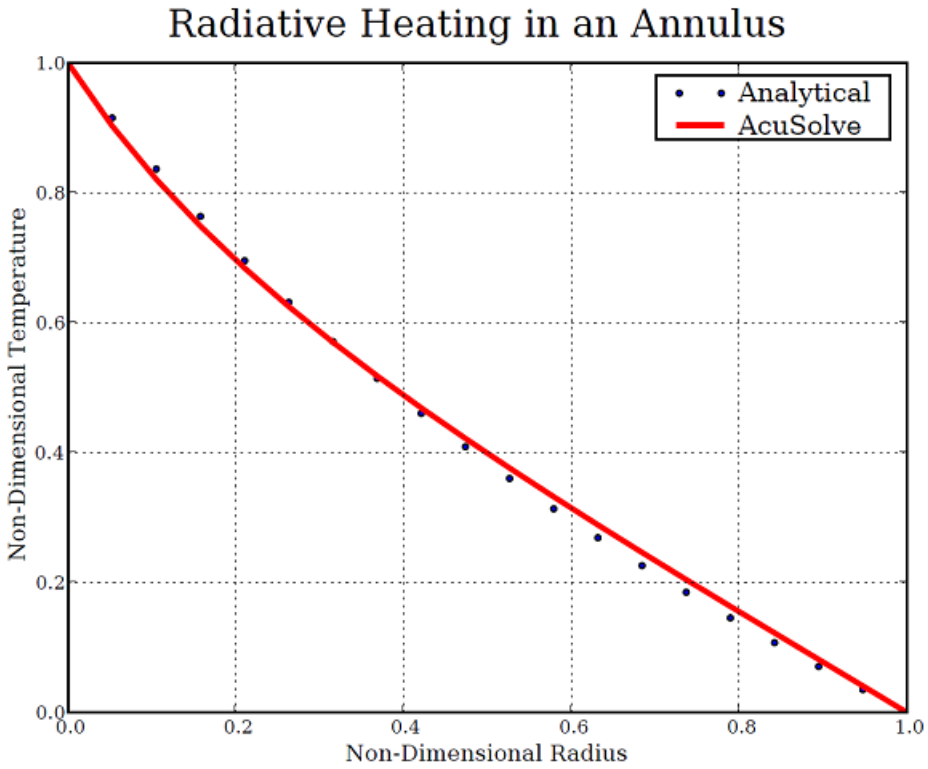


Figure 219: Non Dimensional Temperature Distribution Within the Annulus as a Function of Non Dimensional Radius

Summary

The AcuSolve solution compares well with analytical results for heat transfer due to radiation between two concentric cylinders. In this application, an arbitrary material is subjected to a heat flux that is calculated based on the view factors within the model. As a result of radiative heat flux a temperature distribution between the two cylinders develops. The AcuSolve solution for the temperature as a function of radius matches well compared to the analytical solution.

Heat Transfer Between Radiating Concentric Cylinders

HyperWorks CFD database file: `<your working directory>\annulus_radiation\annulus_radiation.hm`

Global

- Problem Description
  - Analysis type - Steady State
  - Temperature equation - Advective Diffusive
  - Radiation equation- Enclosure
- Auto Solution Strategy
  - Convergence tolerance - `0.0001`
  - Relaxation Factor- `0.4`
  - Flow- off

    - Enclosure radiation- on
- Material Model
    - Material
        - Conductivity
            1. Type - Constant
            2. Conductivity- `1.0`
- Emissivity Model
    - Grey Body
        - Emissivity- `0.03778`
    - Black Body
        - Emissivity- `1.0`

  Model
- Volumes
    - Medium
        - Element Set
            1. Medium - Fluid
            2. Material model- Material
- Surfaces
    - ID
        - Simple Boundary Condition
            1. Type- Wall
            2. Temperature BC type- Value
            3. Temperature- `773.0` K
        - Radiation Surface
            1. Type- Wall
            2. Emissivity model- Grey Body
    - Max_Z
        - Simple Boundary Condition
            1. Type- Symmetry
        - Radiation Surface
            1. Type- Wall
            2. Emissivity model- Black Body
    - Min_Z
        - Simple Boundary Condition
            1. Type- Symmetry
        - Radiation Surface
            1. Type- Wall

2. Emissivity model- Black Body

- OD
  - Simple Boundary Condition
    1. Type- Wall
    2. Temperature BC type- Value
    3. Temperature- `300.0` K
  - Radiation Surface
    1. Type- Wall
    2. Emissivity model- Grey Body

References

F. P. Incropera and D. P. DeWitt. "Fundamentals of Heat Transfer - Sixth Edition". John Wiley & Sons. New York. 2006.

Turbulent Mixing Layers in an Open Channel

In this application, AcuSolve is used to simulate the mixing of two streams of fluid with different velocities moving past a splitter plate. AcuSolve results are compared with experimental results as described in J. Delville, et al. (1989). The close agreement of AcuSolve results with the experimental results validates the ability of AcuSolve to model mixing layers in the turbulent flow regime.

Problem Description

The problem consists of two streams of fluid having material properties of standard air with density of 1.2 kg /m^3 and molecular viscosity of 1.7189 kg/m-sec. The two fluid streams enter an open channel separated by a splitter plate at two streamwise locations with differing velocities. The length of the channel is 1.8 m for the top portion and 1.5 m for the bottom portion. The inlet velocity of the top section is 41.54 m/s, producing a Reynolds's number of 2900, based on l=1.0 mm, while the inlet velocity of the lower section is 22.4 m/s, giving a Reynolds's number of 1200, as shown in the following image, which is not drawn to scale. The model is simulated as steady state with constant inflow conditions, using the Spalart Allmaras (SA) turbulence model. The velocity profile is computed for several locations downstream of the splitter plate and compared against the experimental data, as described in Delville, 1989.

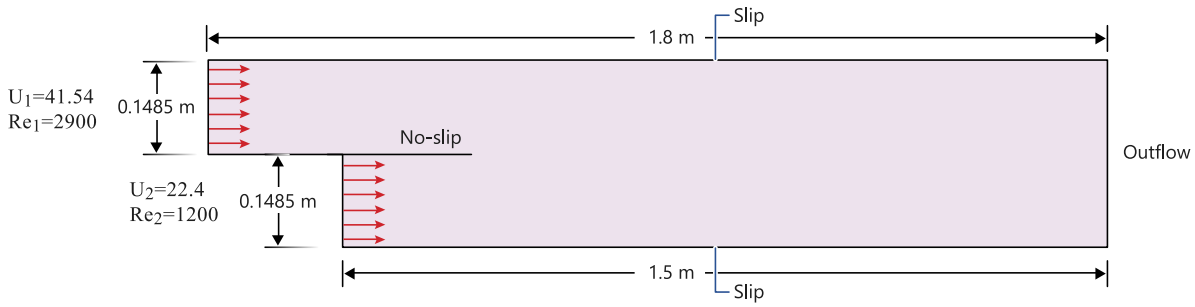


Figure 220: Critical Dimensions and Parameters Used for Simulating the Turbulent Mixing Layer

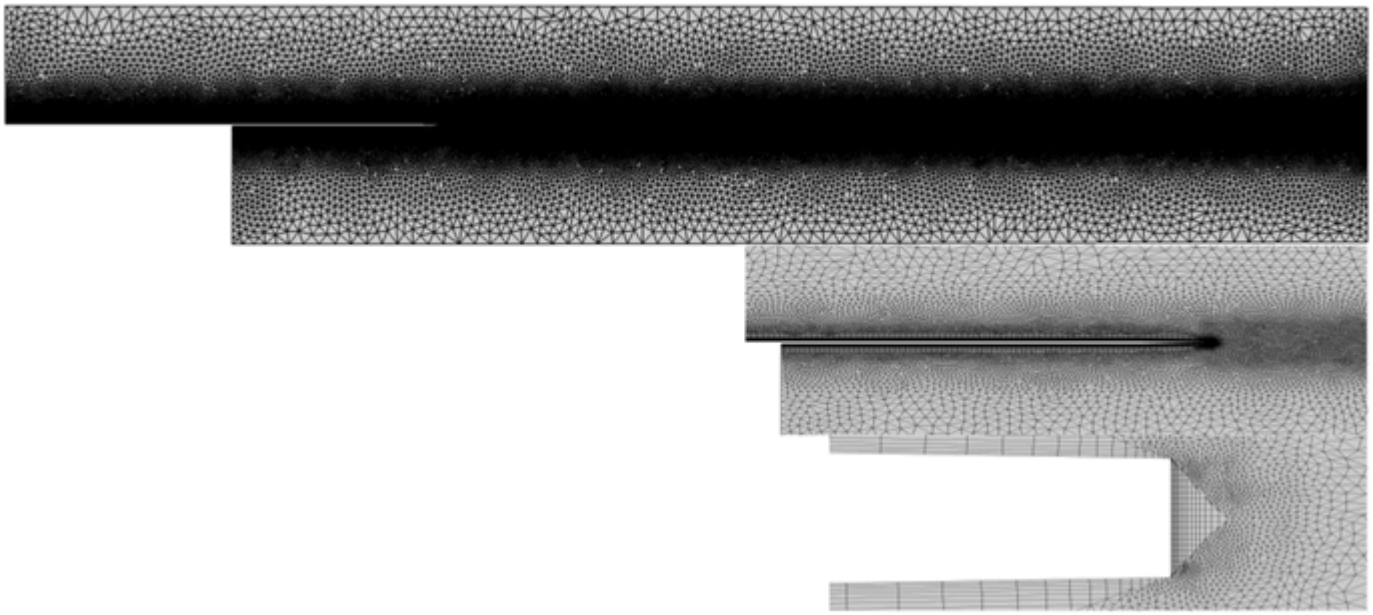


Figure 221: Mesh used for Simulating the Turbulent Mixing Layer Showing Close up Images Near the Trailing Edge of the Plate

The simulation was performed as a two dimensional problem by constructing a volume mesh that contains a single layer of elements extruded in the cross stream direction, normal to the flow plane and by imposing symmetry boundary conditions on the extruded planes. The upper and lower walls are specified as slip, the splitter plate is specified as no-slip and the inlet velocity and eddy viscosity are prescribed as constant values.

AcuSolve Results

The AcuSolve solution converged to a steady state and the results reflect the mean flow conditions within the open channel. The simulation result shows a developing flow field with the fluids fully separated as they pass the edge of the splitter plate. As the fluid travels downstream of the splitter plate, the dissimilar velocity fields produce a shear layer that results in momentum exchange between the two streams. The shear layer diffuses as the fluid travels further downstream. The relative velocity as a function of the normalized boundary layer height is computed from AcuSolve and compared with experimental data at three measurement stations, 0.2 m, 0.65 m and 0.95 m away from the trailing edge of the plate, as described in Delville, 1989. The image below shows black circles representing the experimental data and a solid red line for the AcuSolve results.

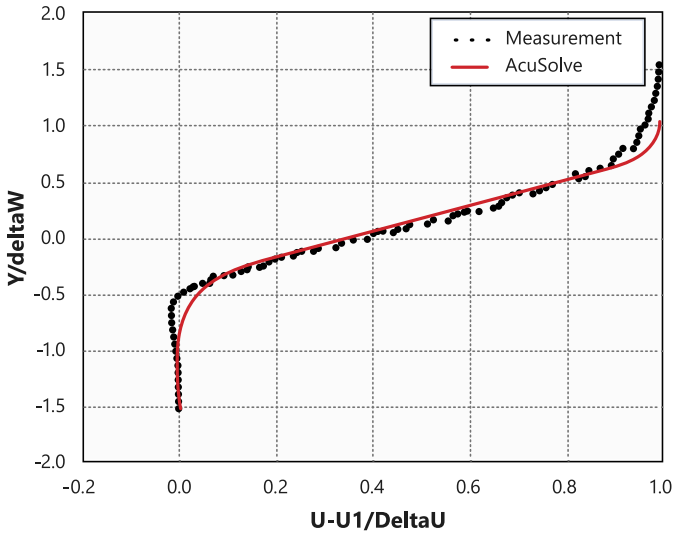


Figure 222: Relative Velocity within the Channel Compared Against Experimental Data Showing Experimental and Simulated Results for the SA Turbulence Model

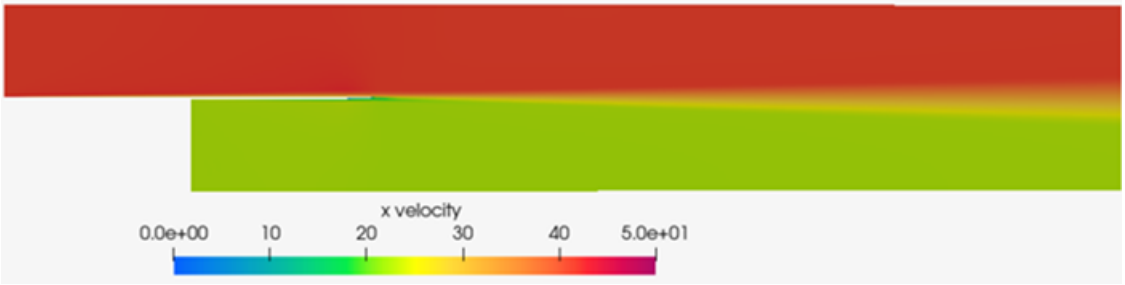


Figure 223: Velocity Magnitude Within the Channel

Summary

The AcuSolve solution compares well with experimental data for turbulent mixing within an open channel. In this application, the shear layer resulting from the dissimilar velocities of the incoming fluid streams results in an exchange of momentum within the channel. The amount of numerical dissipation from the grid is kept to a minimum to produce a good agreement with the experimental data. The good agreement with experimental results for the simulated turbulence model compares well with the measurement and previously published results, demonstrating that AcuSolve is capable of predicting turbulent mixing layers with relatively modest grid levels and the one equation turbulence model.

Simulation Settings for Turbulent Mixing Layers in an Open Channel

HyperWorks CFD database file: `<your working directory>\mixing_layer_turbulent \mixing_layer_turbulent.hm`

Global

- Problem Description
  - Analysis type - Steady State
  - Turbulence equation - Spalart Allmaras

- Auto Solution Strategy
  - Max time steps - `100`
  - Convergence tolerance - `0.001`
  - Relaxation Factor- `0.4`
- Material Model
  - Air
    - Type - Constant
    - Density - `1.2` kg/m3
    - Viscosity - `1.7189e-5` kg/m*sec

  Model
- Volumes
  - Volume
    - Element Set
      1. Material model - Air
- Surfaces
  - Back
    - Simple Boundary Condition
      1. Type- Symmetry
  - Front
    - Simple Boundary Condition
      1. Type- Symmetry
  - InletLower
    - Simple Boundary Condition
      1. Type- Inflow
      2. Inflow type- Velocity
      3. X Velocity- `22.4` m/sec
      4. Turbulence input type- Direct
      5. Eddy Viscosity- `0.0001432`
  - InletUpper
    - Simple Boundary Condition
      1. Type- Inflow
      2. Inflow type- Velocity
      3. X Velocity- `41.54` m/sec
      4. Turbulence input type- Direct
      5. Eddy Viscosity- `0.0001432`
  - Outlet
    - Simple Boundary Condition
      1. Type - Outflow

- Slip
  - Simple Boundary Condition
    1. Type- Slip
- SplitterPlate
  - Simple Boundary Condition
    1. Type - Wall
- TE
  - Simple Boundary Condition
    1. Type- Wall

References

Delville, J., Bellin, S., Garem, J. H., and Bonnet J. P., "Analysis of Structures in a Turbulent, Plane Mixing Layer by Use of a Pseudo Flow Visualization Method Based on Hot-Wire Anemometry," in: Advances in Turbulence 2, eds: H.-H. Fernholz and H. E. Fiedler, Proceedings of the Second European Turbulence Conference, Berlin, Aug. 30-Sept. 2, 1988, Springer Verlag, Berlin, 1989, pp. 251-256.

Laminar to Turbulent Transition Over an Airfoil

In this application, AcuSolve is used to solve for the flow field around a high lift airfoil with inflow conditions that lead to transitional flow on the pressure and suction side of the airfoil's surface. The moderate level of turbulence intensity at the inlet, low angle of attack and shape of the airfoil induce a transition to turbulent flow after a separation bubble develops on the surface. The coefficient of pressure is compared against experimental data from laboratory experiments.

Problem Description

The problem consists of a fluid having material properties close to air with density of 1.0 kg /m3 and molecular viscosity specified to produce a Reynolds number of 2.0e6, assuming a chord length of 1.0 m and an inlet velocity of 1.0 m/s, as is shown in the following image, which is not drawn to scale. The inflow velocity is oriented to simulate a 1 degree angle of attack. The model is simulated as steady state with constant inflow conditions using the farfield boundary condition. The two-equation gamma-ReTheta (γ- Reθ) transition model, used with the one equation Spalart Allmaras turbulence model, is validated against experimental data obtained from the experimental studies conducted by Somers, 1997.

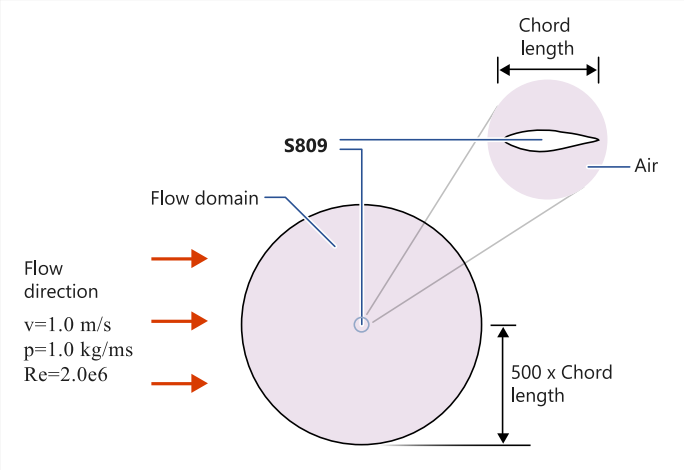


Figure 224: Critical Dimensions and Parameters used for Simulating Transitional Flow over the S809 Airfoil

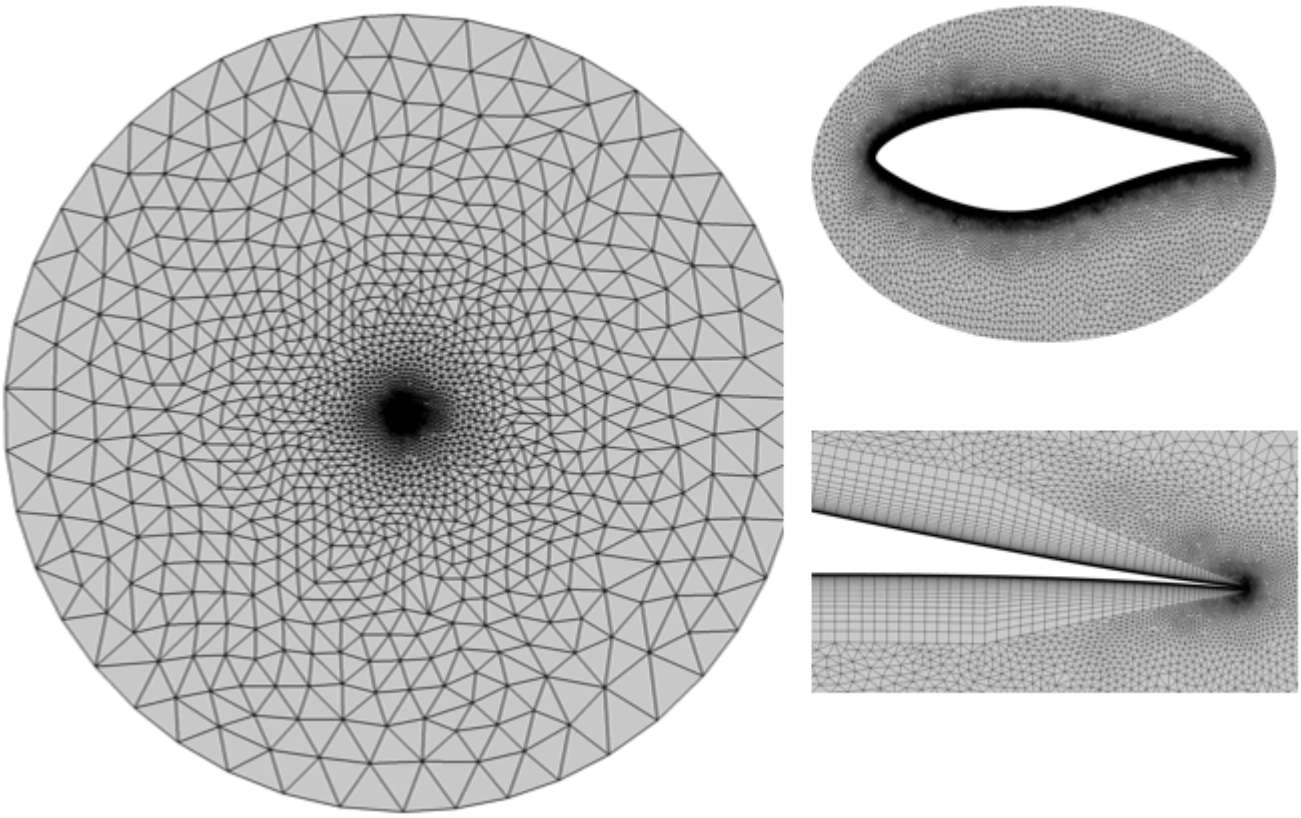


Figure 225: Mesh Used for Simulating Transitional over the S809 Airfoil

The simulation was performed as a two-dimensional problem by constructing a volume mesh that contains a single layer of elements extruded in the cross-stream direction, normal to the flow plane and by imposing symmetry boundary conditions on the extruded planes. The airfoil walls are specified as no-slip and the inlet velocity and eddy viscosity are specified at the farfield boundary.

AcuSolve Results

The AcuSolve solution converged to a steady state and the results reflect the mean flow conditions over the airfoil. The simulation results show that the flow field is laminar at the leading edge until approximately 50 percent chord on the pressure side and until approximately 55 percent on the suction side, then transitions to turbulent as it moves further downstream. The onset is caused by small separation bubbles at these locations. The following images show the negative pressure coefficient (-Cp) on the surface of the airfoil. The mean pressure at a reference point upstream of the airfoil is subtracted from the surface pressure and divided by the inlet velocity and air density to arrive at Cp. The Cp computed from AcuSolve is compared with experimental data, as described in Somers, 1997. The image shows black circles representing the experimental data and a solid red line for the AcuSolve results. Additional plots show contours of intermittency that illustrate the transition from laminar to turbulent flow.

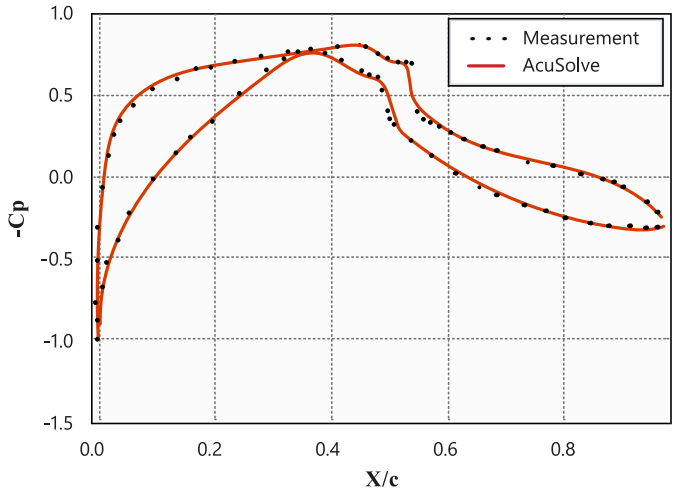


Figure 226: Negative pressure coefficient on the airfoil surface showing experimental and simulated results for the SA two equation (γ- Reθ) transition model

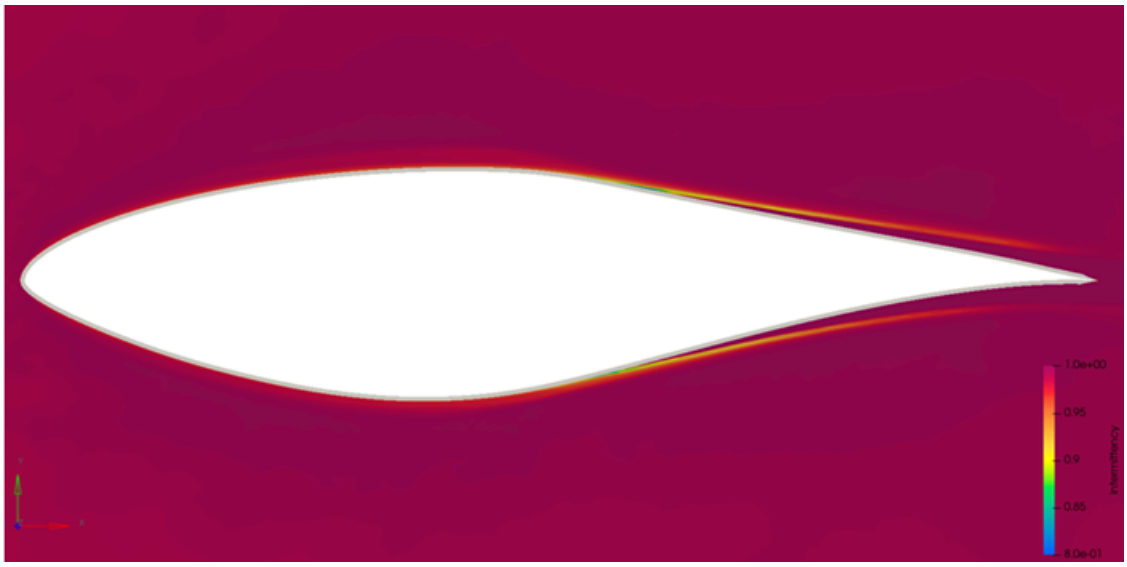


Figure 227: Contours of Intermittency Demonstrate the Onset Location from Laminar to Turbulent over the Airfoil

Summary

The AcuSolve solution compares well with experimental data for transitional flow over the S809 airfoil at a low angle of attack. Additional simulations and measurements for the full drag polar have been tested and compare well with considerably better accuracy when transition closure is included into the RANS solution. The good agreement with experimental results for the transition location and magnitude of expected pressure demonstrate that AcuSolve can predict the transition onset location for flow over surfaces with mild to moderate pressure gradients.

Simulation Settings for Laminar to Turbulent Transition Over an Airfoil

HyperWorks CFD database file: `<your working directory>\airfoil_transition\airfoil_transition.hm`

Global

- Problem Description
  - Analysis type - Steady State
  - Turbulence equation - Spalart Allmaras
  - Turbulence transition model- Gamma-ReTheta
- Auto Solution Strategy
  - Max time steps - `100`
  - Convergence tolerance - `0.0001`
  - Relaxation Factor- `0.5`
  - Turbulence transition- on
- Material Model
  - Air
    - Type - Constant
    - Density - `1.0` kg/m3
    - Viscosity - `5.0e-7` kg/m*sec

  Model
- Volumes
  - Fluid
    - Element Set
      1. Material model - Air
- Surfaces
  - +z slip
    - Simple Boundary Condition
      1. Type- Slip
  - -z slip
    - Simple Boundary Condition
      1. Type- Slip
  - farfield
    - Simple Boundary Condition
      1. Type- Far Field
      2. X velocity = `1.0` *cos(α), where α is the angle of attack in radians
      3. Y velocity = `1.0` *sin(α), where α is the angle of attack in radians
      4. Turbulence input type- Auto
      5. Turbulence intensity type- Value
      6. Turbulence intensity percent- `0.025`
  - airfoil surface
    - Simple Boundary Condition

1 Type- Wall

References

Somers, D., Design and Experimental Results for the S809 Airfoil. NREL/SR-440-6918. 1997

Turbulent Flow Through a 180 Degree Curved Channel

In this application, AcuSolve is used to simulate turbulent flow through a strongly curved two dimensional 180 degree U-duct channel. AcuSolve results are compared with experimental results adapted from Rumsey et al. (2000). The close agreement of AcuSolve results with experimental results validates the ability of AcuSolve to model turbulent cases with strong curvature effects.

Problem Description

The problem consists of a fluid with properties similar to air flowing through a curved channel, as shown in the following image, which is not drawn to scale. The inlet channel height and remaining duct height is 0.0381 m. The bulk velocity (v) normal to the inlet is 31.1 m/s and an integrated outflow pressure is specified to allow the flow to pass through the channel. The flow develops into fully turbulent flow at a Reynolds's number (Re) of approximately 1,000,000. The density of the flow medium is 1.0 kg/m3 and the dynamic viscosity is 1.1818 X 10-6 kg/m-s. The simulation is conducted with the Reynolds Averaged Navier-Stokes equations using the Spalart Allmaras, Shear Stress Transport (SST), K-ω and Realizable K-ε turbulence models. The velocity field from the simulations is compared against experimental data at select measurement locations.

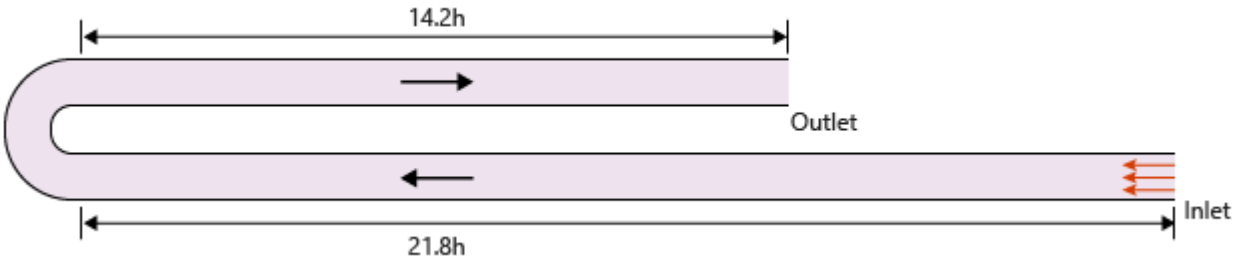
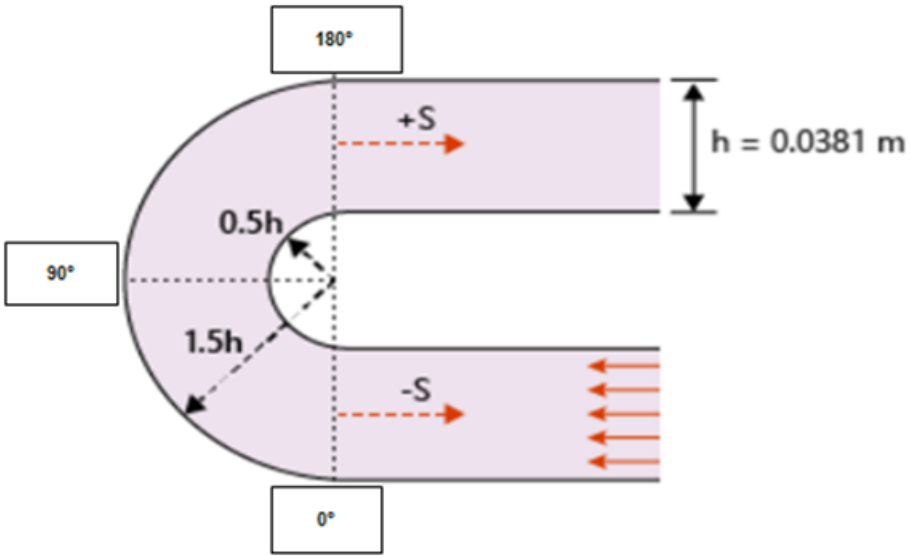


Figure 228: Critical Dimensions and Parameters for Simulating Turbulent Flow in the 180 degree U-Duct



The simulation was performed as a two dimensional problem by restricting flow in the out-of-plane direction through the use of a mesh that is one element thick. The upper and lower walls are specified as no-slip, the inlet velocity and eddy viscosity are specified normal to the inlet face to match the experimental Reynolds Number.

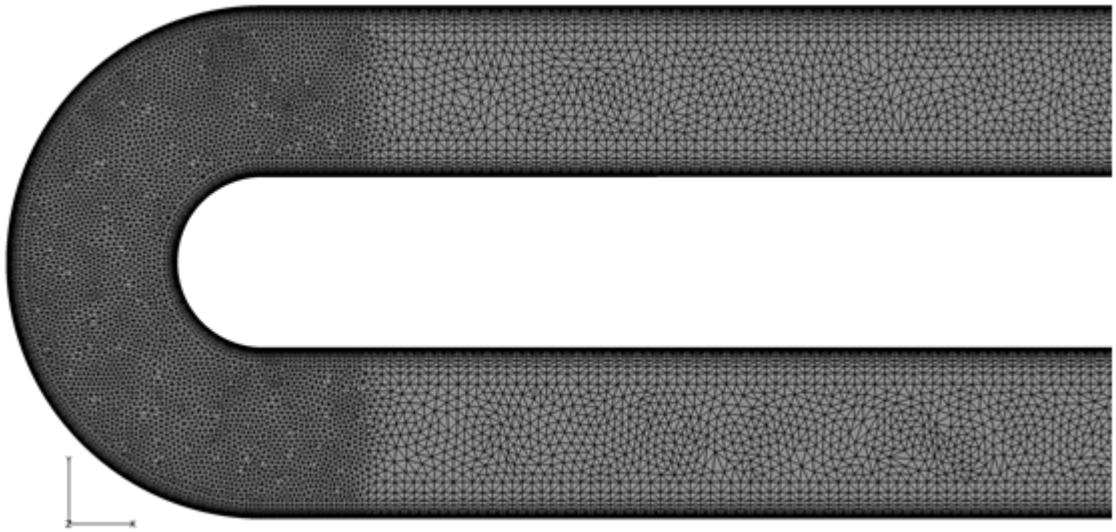


Figure 229: Mesh Used for Simulating Turbulent Flow in the 180 Degree U-Duct

AcuSolve Results

The AcuSolve solution converged to a steady state and the results reflect the mean flow conditions. As the flow passes the inner convex wall it begins to accelerate before decelerating directly past the curved section due to the adverse pressure gradient that eventually leads to a local recirculation zone. On the outer concave wall, the flow remains attached, but is influenced by the adverse pressure gradient above the recirculation region.

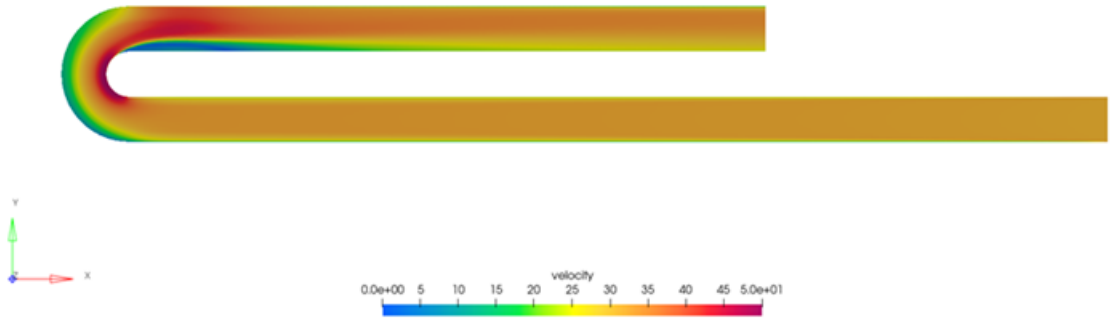


Figure 230: Velocity Contours in Stream Wise Plane

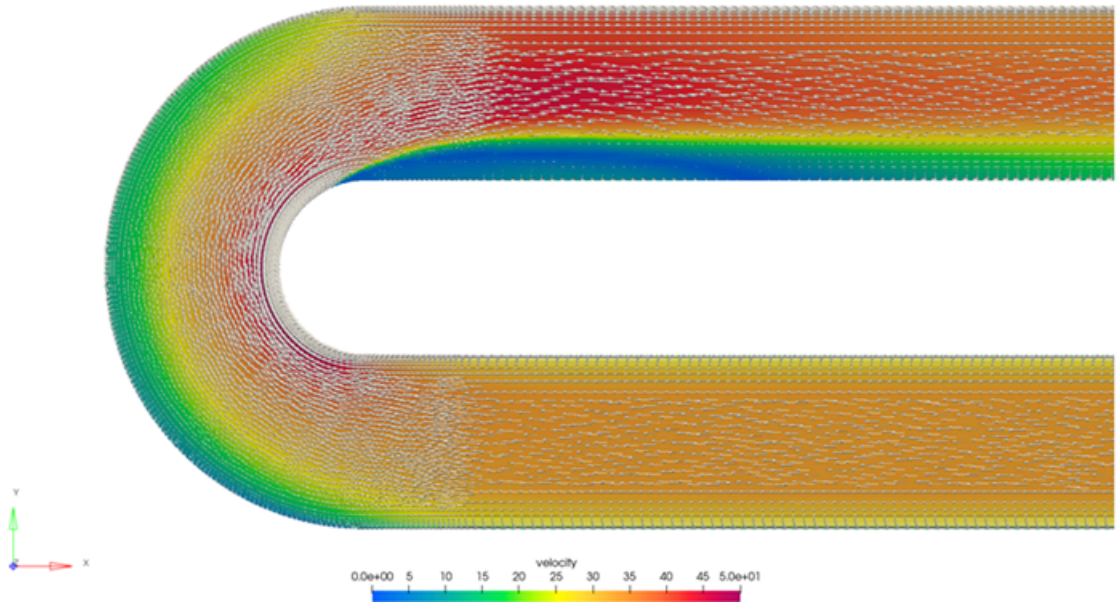


Figure 231: Close up View of Velocity Vectors and Velocity Contours at 180 Degree Bend

The experimental value for the ratio of Velocity magnitude (Vm) to inlet bulk velocity (Vb=31.1 m/s) at different sections of the U-duct is presented with the corresponding AcuSolve result for each of the turbulence models tested in the following images. The images show black circles representing the experimental measurements (Rumsey 2000), solid red lines for the SA model, solid blue lines for the SST model, solid green lines for the K-ω model and solid cyan lines for the K-ε model.

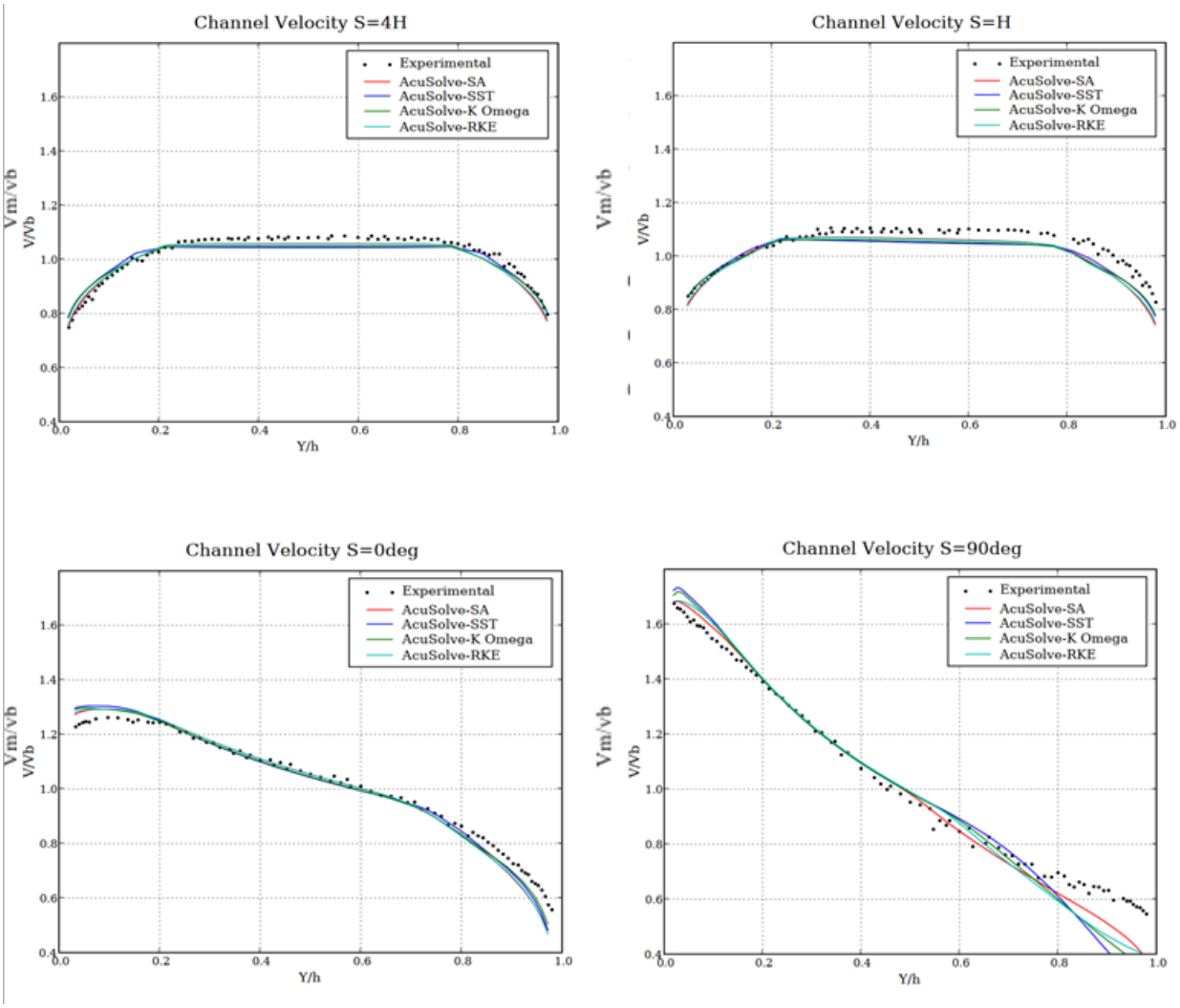


Figure 232:

Summary

The AcuSolve solution compares well with experimental results for flow past the 180 degree U-duct. The experimental value for the ratio of Velocity magnitude to inlet bulk velocity at different sections of the U-duct is presented with the corresponding AcuSolve result for various turbulence models. The performance of the Spalart Allmaras turbulence model was found to improve when the rotation curvature correction is included in the numerical formulation (enabled by default). In this application, AcuSolve demonstrates the ability to predict the complex boundary layer separation and reattachment resulting from the curvature of the channel.

Simulation Settings for Turbulent Flow Through a 180 Degree Curved Channel

HyperWorks CFD database file: `<your working directory>\curved_channel_simple_turbulent \curved_channel_simple_turbulent.hm`

Global

- Problem Description

    - Analysis type - Steady State
    - Turbulence equation - Realizable K-Epsilon
- Auto Solution Strategy
    - Relaxation factor - `0.4`
- Material Model
    - Air
        - Type- Constant
        - Density- `1.0` kg/m3
        - Viscosity- `1.1818e-006` kg/m-sec

  Model
- Volumes
    - Fluid
        - Element Set
            1. Material model- Air
- Surfaces
    - Inlet
        - Simple Boundary Condition
            1. Type- Wall
            2. Inflow type- Velocity
            3. Inflow velocity type- Normal
            4. Normal velocity- `31.1` m/sec
            5. Turbulence input type- Direct
            6. Eddy viscosity- `3.5547e-06` m2/sec
    - ext1
        - Simple Boundary Condition- Symmetry
    - ext2
        - Simple Boundary Condition- Symmetry
    - Outlet
        - Simple Boundary Condition
            1. Type- Outflow
    - wall-bottom
        - Simple Boundary Condition
            1. Type- Wall
            2. Turbulence wall type- Low Reynolds Number
    - wall-top
        - Simple Boundary Condition
            1. Type- Wall

2 Turbulence wall type- Low Reynolds Number

References

Christopher L. Rumsey, Thomas B. Gatski, and Joseph H. Morrison. "Turbulence Model Predictions of Strongly Curved Flow in a U-Duct", AIAA Journal, Vol. 38, No. 8 (2000), pp. 1394-1402.

Turbulent Flow Through a Heated Periodic Channel

In this application, AcuSolve is used to solve for the flow and temperature field within a channel containing a heated wall. The wall is maintained at a constant temperature, inducing heat flux into the fluid, to predict the thermal law of the wall. The non dimensional temperature versus the non dimensional height above the wall is compared to the analytical correlation provided by Kader.

Problem Description

The problem consists of a fluid having material properties close to air with a density of 1.0 kg/m^3, molecular viscosity of 0.0001 kg/m-s, specific heat of 1005.0 J/kg-K and thermal conductivity of 0.139 W/m-K. The properties are specified to obtain a Prandtl number of 0.72. The velocity is defined as periodic and is driven by a constant acceleration body force equal to 2.0 m/s^2. The temperature is specified as periodic+unknown ratio allowing it to develop until it reaches a steady solution. The simulation description is shown in the following image, which is not drawn to scale. The model is simulated using the one equation Spalart Allmaras turbulence model along with the advective-diffusive temperature equation. The thermal wall distribution is validated against correlation data published by Kader 1981.

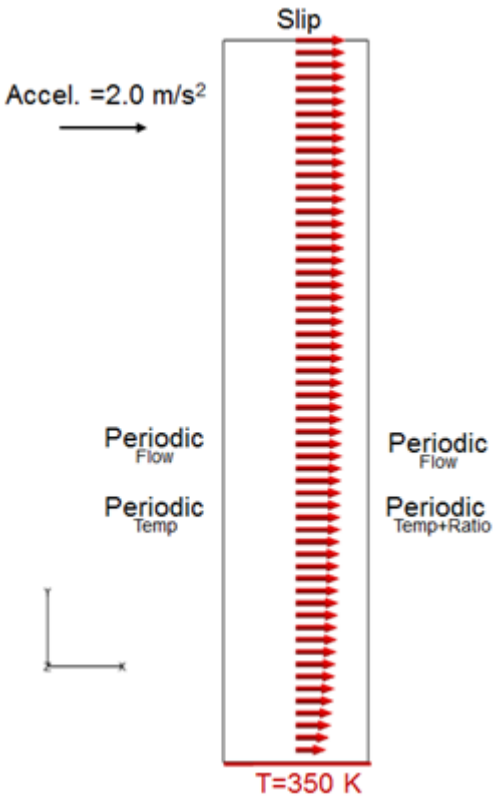


Figure 233: Critical Parameters used For Simulating Periodic Flow Within a Heated Channel

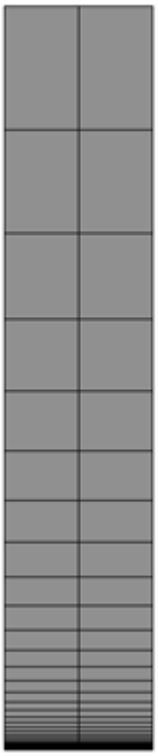


Figure 234: Mesh used For Simulating Periodic Flow Within a Heated Channel

The simulation was performed as a two dimensional problem by constructing a volume mesh that contains a single layer of elements extruded in the cross stream direction, normal to the flow plane and by imposing periodic boundary conditions on the extruded planes. The streamwise direction contains two elements allowing the flow and temperature solution to develop. Only the lower half of the channel is modeled, assuming the solution is mirror across the top slip plane.

AcuSolve Results

The AcuSolve solution converged to a steady state and the results reflect the mean flow conditions within the channel. The simulation results demonstrate that the channel wall induces a thermal flux into the flow field, producing a temperature distribution dependent on the distance from the wall. The thermal law of the wall computed from the AcuSolve results is compared with correlation data for the corresponding Prandtl number, as demonstrated in Kader 1981. The plot shown below gives the non dimensional value of T+ as a function of Y+, where T+ and Y+ are computed per the following relationships:

$$T+ = \frac{(Tw - T)\rho C p u\tau}{\dot{Q}} T \tag{6}$$

$$Y+ = \frac{yu\tau}{v} \tag{7}$$

$$u\tau = \sqrt{\tau w / \rho} \tag{8}$$

Where $T+$, Tw is the fixed wall temperature, T is the temperature away from the wall, ρ is the fluid density, Cp is the fluid specific heat, uT is computed from the magnitude of the shear stress and $\dot{Q}_i$ is the local surface heat flux.

The image below shows black circles representing the correlation data and a solid red line for the AcuSolve results. The results demonstrate that the temperature distribution away from the wall is resolved properly and compares well with the correlation. Since an empirical relationship for T+ is used for comparison, there will be minor discrepancies compared with the simulation results. Additional comparisons have been made against DNS results for T+ from Kawamura et al. 1998.

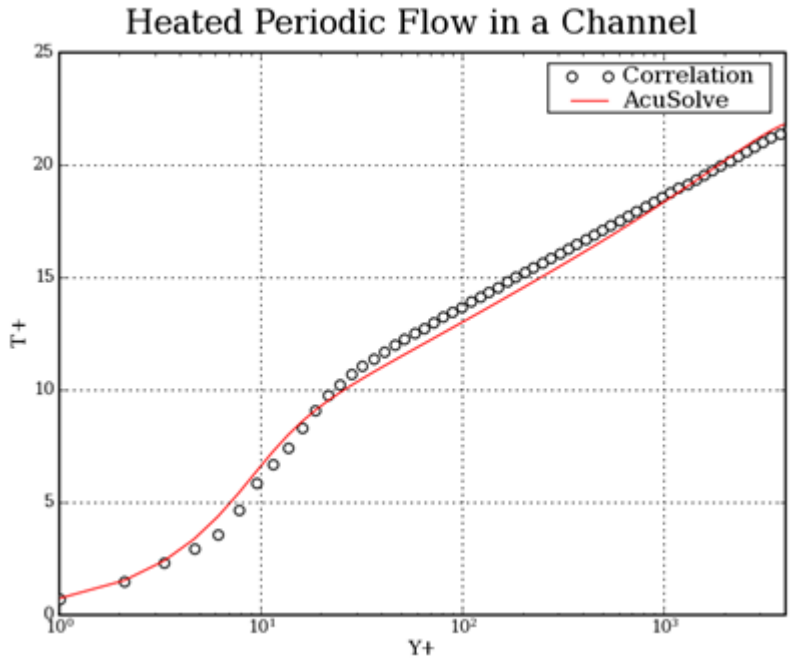


Figure 235: Thermal Boundary Layer Within the Heated Channel Compared Against the Correlation Data

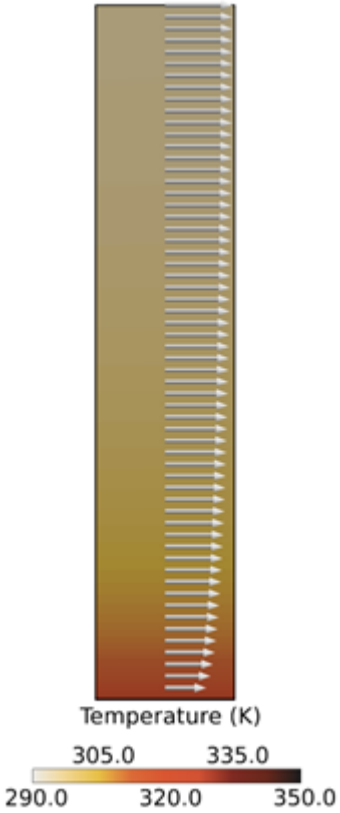


Figure 236: Contours of Temperature and Vectors Representing the Fluid Velocity Within the Channel

Summary

The AcuSolve solution compares well with the correlation data for turbulent flow within a heated channel. In this application, the constant temperature wall induces a surface heat flux, giving rise to a temperature gradient within the channel. AcuSolve can capture the correct temperature gradient at any location above the wall if an appropriate first layer height is selected to resolve a Y+ value of 1.0. The good agreement with correlation data for T+ demonstrates that AcuSolve can predict the locally varying temperature distribution within a turbulent channel.

Simulation Settings for Turbulent Flow Through a Heated Periodic Channel

AcuConsole database file: `<your working directory>\channel_periodic_heat\channel_periodic_heat.acs`

Global

- Problem Description
  - Analysis type - Steady State
  - Temperature equation - Advective Diffusive
  - Turbulence equation - Spalart Allmaras
- Auto Solution Strategy
  - Max time steps - `50`

    - Convergence tolerance - `0.0001`
    - Relaxation Factor - `0.4`
    - Temperature - On
- Material Model
    - Fluid
        - Type - Constant
        - Density - `1.0` kg/m3
        - Viscosity - `1.0e-4` kg/m*sec
        - Specific Heat - `1005.0` J/kg*K
        - Conductivity - `0.139` W/m*K
- Body Force
    - BodyForce
        - Gravity
            1. X-component - `2.0` m/sec2

Model

- Volumes
    - Fluid
        - Element Set
            1. Material model - Fluid
            2. Body force - BodyForce
- Surfaces
    - Symmetry_1
        - Simple Boundary Condition - (disabled to allow for periodic conditions to be set)
    - Symmetry_2
        - Simple Boundary Condition - (disabled to allow for periodic conditions to be set)
    - Inflow
        - Simple Boundary Condition - (combination of integrated BC and periodic BC set)
        - Advanced Options
            1. Integrated Boundary Conditions - Temperature - `300.0` K
    - Outflow
        - Simple Boundary Condition - (disabled to allow for periodic conditions to be set)
    - Slip_surface
        - Simple Boundary Condition
            1. Type- Slip
    - Wall_surface
        - Simple Boundary Condition
            1. Type- Wall

2 Temperature BC type - Value
3 Temperature - `350.0` K

- Periodics
  - 2D
    - Periodic Boundary Conditions
      1 Type - Periodic
  - Flow
    - Periodic Boundary Conditions
      1 Type - Periodic
  - Temperature
    - Individual Periodic BCs
      1 Temperature: Type - Single Unknown Ratio
- Nodes
  - Fixed_pressure
    - Pressure: Type - Zero
  - Zero_z-velocity
    - Z-Velocity: Type - Zero

References

B.A. Kader, "Temperature and concentration profiles in fully turbulent boundary layers", International Journal of Heat and Mass Transfer, Volume 24, Issue 9, 1981, Pages 1541-1544.

H. Kawamura, K. Ohsaka, H. Abe and K. Yamamoto, "DNS of turbulent heat transfer in channel flow with low to medium-high Prandtl number fluid", International Journal of Heat and Mass Transfer, 19:482-491, 1998.

Heat Transfer Between Radiating Concentric Spheres

In this application, AcuSolve is used to simulate the heat transfer due to conduction and radiation between concentric spheres. The inside surface of the inner and the outside surface of the outer sphere are both held at constant temperature, while the gap between them radiates the heat from one sphere to the other.

AcuSolve results are compared with analytical results for temperature and heat flux as described in Incropera (2006) and Salazar, et al. (2016). The close agreement of AcuSolve results with analytical results validates the ability of AcuSolve to model cases with radiation heat transfer and conjugate heat transfer with enclosure radiation modeling and the discrete ordinate (DO) radiation model.

Problem Description

The problem consists of a fluid region with arbitrary material properties between two concentric spheres with surfaces held at fixed temperature, as shown in the following image, which is not drawn to scale. The radius of the outer sphere is 0.04 m and the radius of the inner sphere is 0.01 m. The inner surface of the inner sphere is defined to have a constant wall temperature at 300.0 K (27 ºC). The outer surface of the outer sphere is defined to have a constant wall temperature at 1300.0 K (1027 ºC). The fluid within the spheres is defined as a non-conducting material, allowing heat to transfer via radiation only. The solid and fluid regions equilibrate to a steady temperature and can be compared with a semi-analytical solution for the temperature and heat flux at the fluid boundaries.

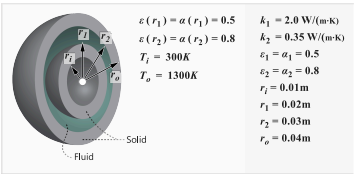


Figure 237: Critical Dimensions and Parameters used for Simulating Conduction and Radiation Between two Concentric Spheres



Figure 238: Mesh used for Simulating Radiation Between two Concentric Spheres

The simulation was performed as a three dimensional problem by constructing a volume mesh that contains a layer of boundary elements normal to the radial direction.

AcuSolve Results

The AcuSolve solution converges to a steady state and the results reflect the mean temperature distribution within the spheres. As the outer diameter is considerably hotter than the inner, a heat flux is present between the spheres. The temperature within the mediums increases as a function of the radius, with a slope corresponding to the temperature difference and the specified emissivity of the shells. The following image shows the temperature contour within the spheres along with the two-dimensional plot of the temperature versus radius in the solid mediums. The temperature and heat flux at the radiation surfaces are compared with the analytical solution as described in Salazar, et al. (2016).

Table 13: The Analytical Solution for the Temperature and Heat Flux at r1 and r2 are Presented with the Corresponding AcuSolve Results for the Enclosure (Surface to Surface) Model and the DO

	T(r1) (K)	T(r2) (K)	Q(r1) (W)	Q(r2) (W)
Analytical	578.2	1035.0	-27822.5	12365.6
AcuSolve (Enclosure)	578.4	1035.1	-27827	12364.2
AcuSolve (DO)	561.8	1023.6	-26175	12897.0
Percent Difference (Enclosure)	0.034%	0.010%	-0.015%	-0.011%
Percent Difference (DO)	2.8%	-1.11%	5.92%	4.3%

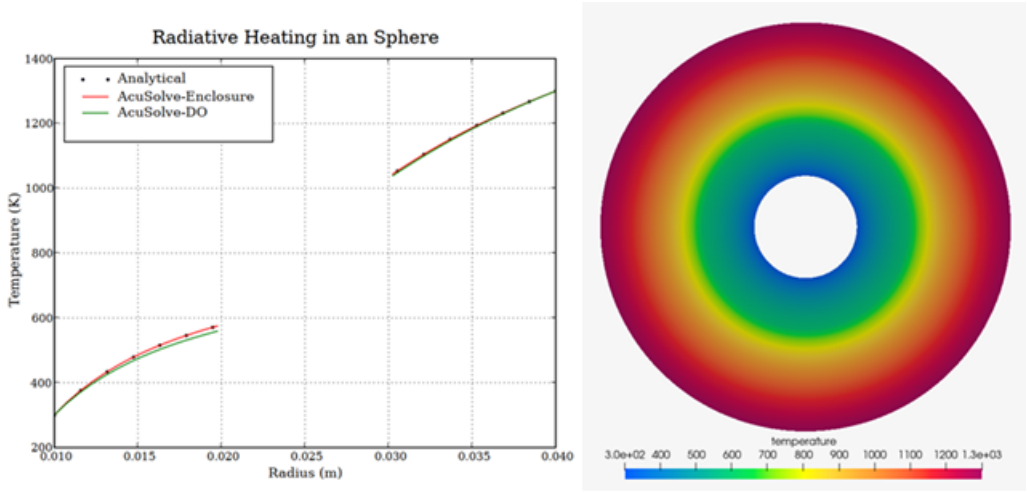


Figure 239: Two-Dimensional Plot and Contours of Temperature Between the Concentric Spheres

Summary

The AcuSolve solution compares well with analytical results for heat transfer due to conduction and radiation between two concentric spheres. In this application, an arbitrary material is subjected to a heat flux that is calculated based on the view factors or the DO model within the simulation. As a result of the conjugate heat transfer and the radiative heat flux a temperature distribution between the two spheres develops. The AcuSolve solution for the temperature and heat flux at the radiation surfaces matches well compared to the analytical solution with only a minor difference for the enclosure radiation model. The enclosure radiation model was found to have a higher accuracy for this application compared to the DO model, as expected due to the relatively low optical thickness in this simulation.

Heat Transfer Between Radiating Concentric Spheres

HyperWorks CFD database file: `<your working directory>\sphere_radiation\sphere_radiation.hm`.

Global

- Problem Description
  - Analysis type - Steady State
  - Turbulence equation - Advective Diffusive
  - Radiation equation - Enclosure
- Auto Solution Strategy
  - Convergence tolerance - `1.0e-5`
  - Relaxation Factor - `0.4`
  - Flow - off
  - Enclosure radiation - on
- Material Model
  - Inner
  - Conductivity

        - Type - Constant
        - Conductivity - `2.0`
    - Outer
    - Conductivity
        - Type - Constant
        - Conductivity - `0.35`
    - Radiating
    - Conductivity
        - Type - Constant
        - Conductivity - `1.0e-6`
- Emissivity Model
- Inner
    - Emissivity - `0.5`
- Outer
    - Emissivity - `0.8`

  Model
- Volumes
    - Inner
        - Element Set
            1. Medium- Solid
            2. Material model - Inner
        - Outer
            1. Element Set
                1. Medium - Solid
                2. Material model - Outer
        - Radiating
            1. Element Set
                1. Medium - Fluid
                2. Material model - Radiating
- Surfaces
    - Inner_Inner_r1
        - Simple Boundary Condition - (disabled to allow for heat flux)
    - Inner_Inner_ri
        - Simple Boundary Condition
            1. Type - Wall
            2. Temperature BC type - Value
            3. Temperature - `300.0` K

- Inner_Radiating_r1
  - Simple Boundary Condition (disabled to allow for heat flux)
  - Radiation Surface
    1. Type - Wall
    2. Emissivity model - Inner
- Outer_Outer_r2
  - Simple Boundary Condition (disabled to allow for heat flux)
- Inner_Outer_ro
  - Simple Boundary Condition
    1. Type - Wall
    2. Temperature BC type - Value
    3. Temperature - `1300.0` K
- Outer_Radiating_r2
  - Simple Boundary Condition (disabled to allow for heat flux)
  - Radiation Surface
    1. Type - Wall
    2. Emissivity model - Outer

References

F. P. Incropera and D. P. DeWitt. "Fundamentals of Heat Transfer – Sixth Edition". John Wiley & Sons. New York. 2006.

Salazar, G., Droba, J., Oliver, B., & Amar, A. J. (2016). Development and Verification of Enclosure Radiation Capabilities in the CHarring Ablator Response (CHAR) code. 46th AIAA Thermophysics Conference.

Radiation Heat Transfer Through a Cube with a Specular Interface

In this application, AcuSolve is used to simulate the heat transfer due to radiation through a specular interface within an absorbing, emitting, but not scattering solid cube. One of the cube's walls is modeled with an isotropic external radiation source while the remainder of the cube is held at fixed temperature conditions and modeled with pure radiation, neglecting the effects of conduction.

The internal surface between the two equal solid portions of the cube is specified to be a completely specular boundary condition. AcuSolve results are compared with accepted numerically derived results of incident radiation, as described in Muresan (2004) and Łapka (2012). The close agreement of the AcuSolve results and the published data validates the solver's ability to model cases with semi-transparent media with differing material properties using the discrete ordinates radiation model.

Problem Description

The problem consists of a solid region with fixed material properties similar to glass separated into two equal size cuboids to form a symmetrical cube with a side length of 1.0 m. The left most wall (minimum z) receives an external radiation source at a fixed temperature of 450.0 K (177 ºC) while the right most wall (maximum z) is prescribed a fixed temperature of 375.0 K (102 ºC), as shown in the following image, not drawn to scale. The solid, semi-transparent material is specified for each glass cuboid with n1=1.5, κ1=0.2 for glass1 and n2=1.25, κ2=2.0 for glass2. Only the solution to the radiative transfer equation on a discrete number of ordinate directions is considered, thus neglecting conduction. The solid regions equilibrate to a steady radiative state and are compared with a semi-analytical solution for the incident radiation across the centerline of the cube.

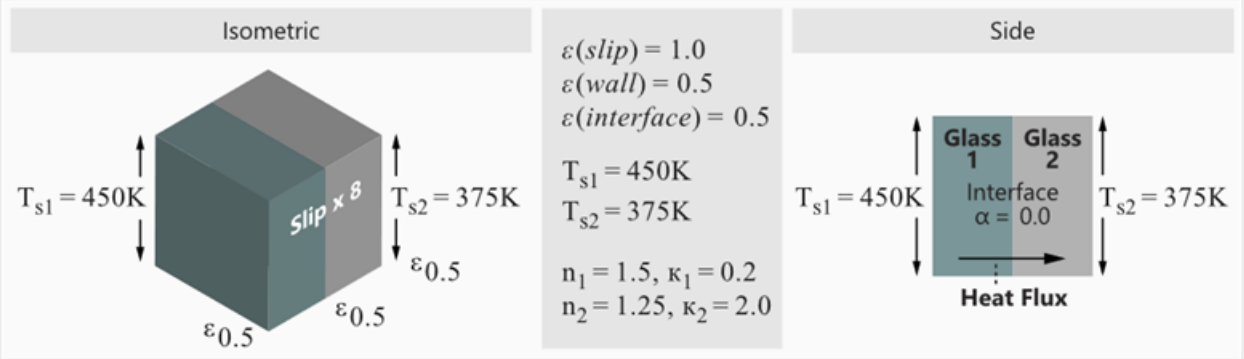


Figure 240: Critical Dimensions and Parameters Used for Simulating Radiation Heat Transfer Through a Cube with a Specular Interface

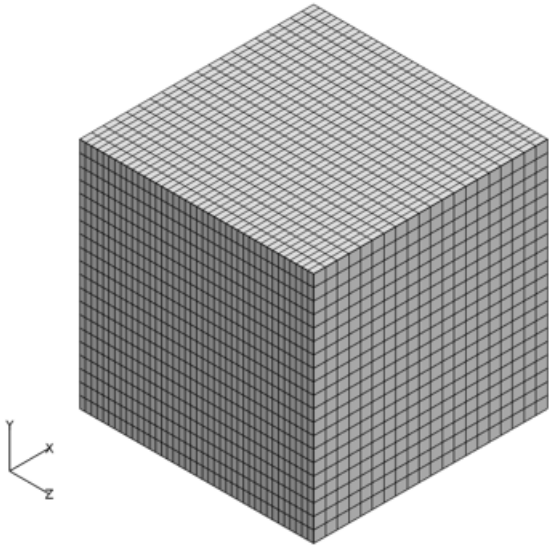


Figure 241: Mesh Used for Simulating Radiation Heat Transfer Through a Cube with a Specular Interface

The simulation was performed as a three-dimensional problem by constructing a volume mesh that contains all hexahedral elements with 20, 20, 40 cells in the x, y, z directions.

AcuSolve Results

The AcuSolve solution converges to a steady state and the results reflect the mean radiative state within the cube. Since the left side of the cube receives the external radiation source, the incident radiation is highest at that location. The transmission of the radiation decreases linearly within the first cuboid until it reaches the interface between the two materials. The discontinuity in the radiation field is demonstrated at the interface location, resulting from the specular reflection of radiation as it tries to travel from one material to the other. As the incident radiation passes through the second glass material, the simulation demonstrates how the material's higher absorption properties will produce a non-linear irradiance distribution. The following image shows the incident radiation contour within the two media along with the two-dimensional plot of the normalized incident radiation as a function of the non-dimensional cube length, where the incident radiation is normalized by $G^* = \sigma T^4$. The incident radiation is compared with the numerical solution as described in Muresan, et al. (2004).

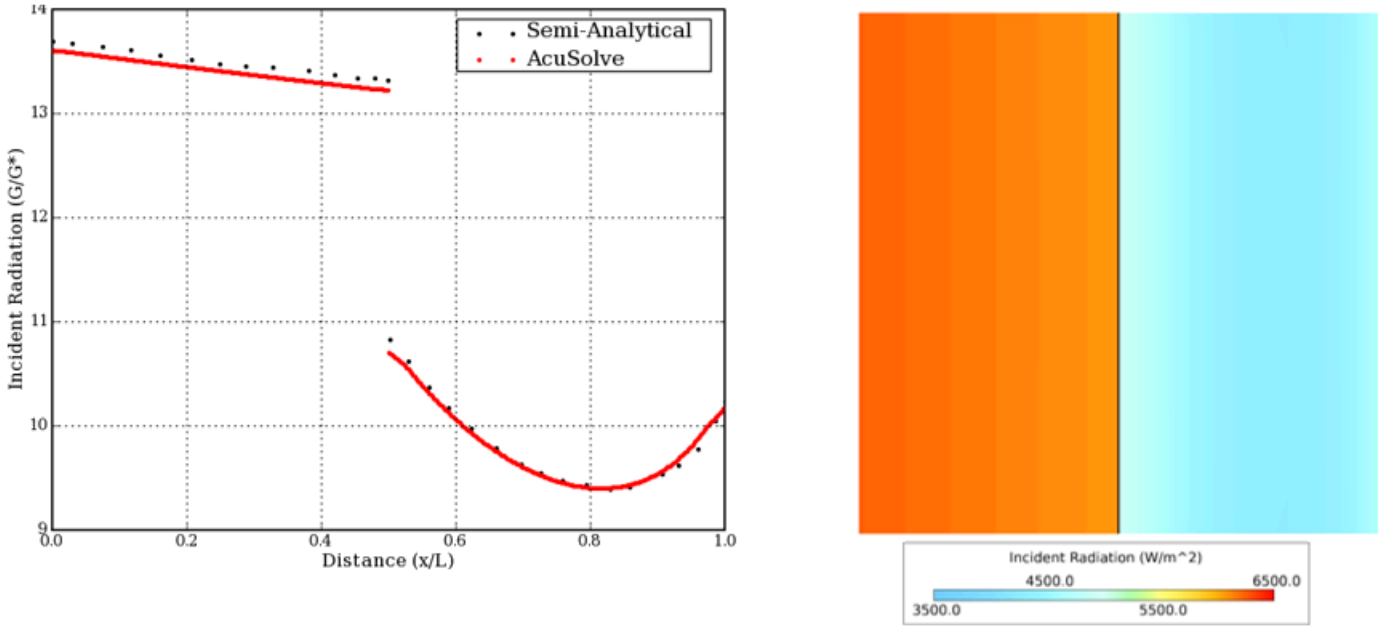


Figure 242: Two-Dimensional Plot and Contours of Incident Through a Cube with a Specular Interface

Summary

The AcuSolve solution compares well with numerical results for heat transfer due to radiation within a cube containing a specular interface. In this application, two arbitrary materials are subjected to a constant external radiative heat source and the media are defined to absorb, emit, but not scatter the irradiation. As a result of the prescribed radiative heat flux on the left most wall and the fixed temperature constraint across the entire domain, each media receives a non-trivial, varying amount of incident radiation. The AcuSolve solution for the incident radiation across the interface matches well compared to the numerical solution with only a minor difference at the far-right hand side of the domain. The discrete ordinate model requires a fairly large number of ordinate directions in order to obtain the highest accuracy solution. The published results are produced using the S14 quadrature, which is equivalent to 224 discrete ordinate directions.

Radiation Heat Transfer Through a Cube with a Specular Interface

HyperMesh database file: `<your working directory>\cube_specular_radiation\cube_specular_radiation.hm`.

Global

- Problem Description
  - Analysis type - Steady State
  - Turbulence equation - Advective Diffusive
  - Radiation equation - Discrete Ordinate
  - Radiation Ordinate - S14
- Solver Settings
  - Convergence tolerance - `1.0e-3`
  - Relaxation Factor - `0.3`

    - Flow - off
    - Temperature - off
- Nodal_Initial_Condition
    - Temperature
        - Type - Constant
        - Default Value - `300.0` K

Materials

- Glass_HM
    - Density
        - Type - Constant
        - Density - `2500.0`
    - Specific Heat
        - Type - Constant
        - Conductivity - `830`
    - Conductivity
        - Type - Constant
        - Conductivity - `1.3`
    - Radiation Properties
        - Allow Participating Media Radiation - On
        - Absorption Coefficient - `0.2`
        - Scattering Coefficient - `0.0`
        - Phase Coefficient - `0.0`
        - Refractive Index - `1.5`
- Glass2_HM
    - Density
        - Type - Constant
        - Density - `2500.0`
    - Specific Heat
        - Type - Constant
        - Conductivity - `830`
    - Conductivity
        - Type - Constant
        - Conductivity - `1.3`
    - Radiation Properties
        - Allow Participating Media Radiation - On
        - Absorption Coefficient - `2.0`
        - Scattering Coefficient - `0.0`

- Phase Coefficient - `0.0`
- Refractive Index - `1.25`

Emissivity Model

- BB05
  - Emissivity - `0.5`
- BB
  - Emissivity - `1.0`

Volumes

- S1
  - Type - Solid
  - Material model - Glass_HM
- S2
  - Type - Solid
  - Material model - Glass2_HM

Surfaces

- Wall_S1
  - Simple Boundary Condition
    1. Type - Wall
    2. Temperature BC type - Value
    3. Temperature - `450.0 K`
  - Radiation Surface
    1. Type - radiation interface
    2. Radiation interface type - external
    3. External emissivity model - BB
    4. Diffused fraction - `0.0`
- Wall_S2
  - Simple Boundary Condition
    1. Type - Outflow
  - Radiation Surface
    1. Type - Opening
    2. Opening temperature - 375.0 K
    3. Emissivity model - BB05
    4. Diffused fraction - `0.0`
- Interface_S1
  - Simple Boundary Condition
    1. Type - Auto Wall
  - Radiation Surface

1. Type - Radiation interface
2. Radiation interface type - internal
3. Diffused fraction - `0.0`

- Interface_S2
  - Simple Boundary Condition
    1. Type - Auto Wall
  - Radiation Surface
    1. Type - Radiation interface
    2. Radiation interface type - internal
    3. Diffused fraction - `0.0`
- Slip_1_S1
  - Simple Boundary Condition
    1. Type - Slip
- Slip_2_S1
  - Simple Boundary Condition
    1. Type – Slip
- Slip_3_S1
  - Simple Boundary Condition
    1. Type - Slip
- Slip_4_S1
  - Simple Boundary Condition
    1. Type - Slip
- Slip_1_S2
  - Simple Boundary Condition
    1. Type - Slip
- Slip_2_S2
  - Simple Boundary Condition
    1. Type - Slip
- Slip_3_S2
  - Simple Boundary Condition
    1. Type - Slip
- Slip_4_S2
  - Simple Boundary Condition
    1. Type - Slip

References

Muresan, Cristian & Vaillon, Rodolphe & Ménézo, Christophe & Morlot, Rodolphe. (2004). Discrete ordinates solution of coupled conductive radiative heat transfer in a two-layer slab with Fresnel

interfaces subject to diffuse and obliquely collimated irradiation. Journal of Quantitative Spectroscopy and Radiative Transfer. 84. 551-562. 10.1016/S0022-4073(03)00271-1.

Łapka, Piotr & Furmański, Piotr. (2012). Fixed Cartesian grid based numerical model for solidification process of semi-transparent materials II: Reflection and refraction or transmission of the thermal radiation at the solid–liquid interface. International Journal of Heat and Mass Transfer. 55. 4953–4964. 10.1016/j.ijheatmasstransfer.2012.03.077.

Single-Phase Nucleate Boiling in a Rectangular Channel

In this application, AcuSolve is used to simulate the wall heat flux due to nucleate boiling at a heated wall inside a rectangular channel with water flow. Results are compared with experimental heat flux measurements as reported by Steiner, et al. (2005). The close agreement of AcuSolve results with experimental results validates the ability of AcuSolve to model single phase nucleate boiling problems.

Problem Description

The problem consists of a channel with a heated wall at the bottom. The temperature of the wall is selected to onset the nucleate boiling at the heated wall. The dimensions of the inlet are 0.03 x 0.04 m; the inlet velocity (v) is 0.39 m/s and the temperature (T) of the fluid entering the inlets is varied from 373.15 K (100 C) to 406.15 (133 C)), while the atmospheric pressure is specified to be 2 bar. The pre-heated water enters the inlets and heat is transferred into the fluid from the heated walls. The heat causes sub-cooled boiling to occur in the region close to the wall and leads to the formation of bubbles at nucleation sites. The surface tension and vapor phase models are specified to emulate the physical process of water changing state to water vapor.

The heat transfer in this regime is dominated by two effects, the macro convection due to the motion of the bulk liquid and the latent heat transport associated with the evaporation of the liquid micro-layer between the bubble and the heated wall. Each of these effects are modeled with AcuSolve and the prediction of their processes is demonstrated in the following results.

The AcuSolve simulation is prepared as a steady state heat transfer simulation to determine the temperature and heat flux on the heated walls of the model. AcuSolve computes the single-phase nucleate boiling by employing Chen’s model for two-phase boiling flow described in Chen (1966). The heat flux values for different wall temperatures are compared against the experimental measurements, as described in Steiner, et al. (2005).

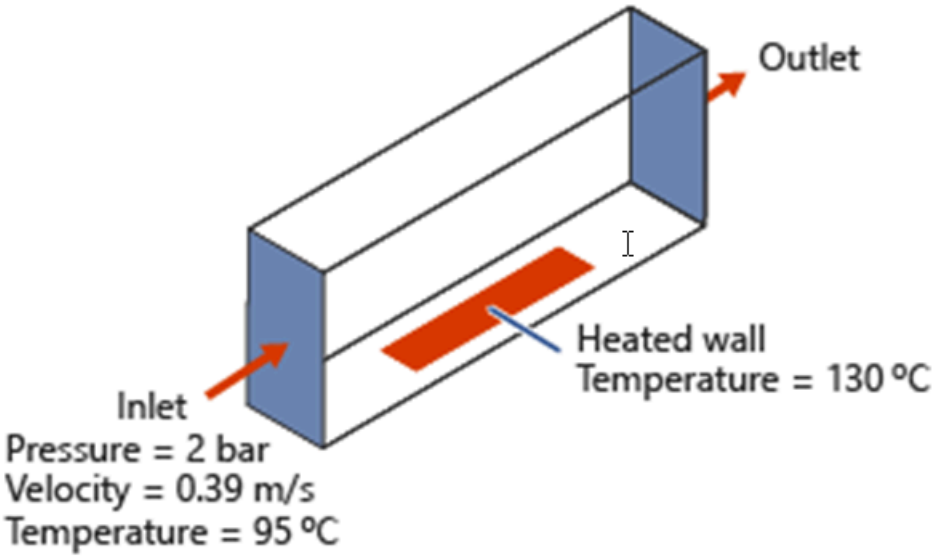


Figure 243: Critical Dimensions and Parameters for Simulating a Single-Phase Nucleate Boiling in a Rectangular Channel

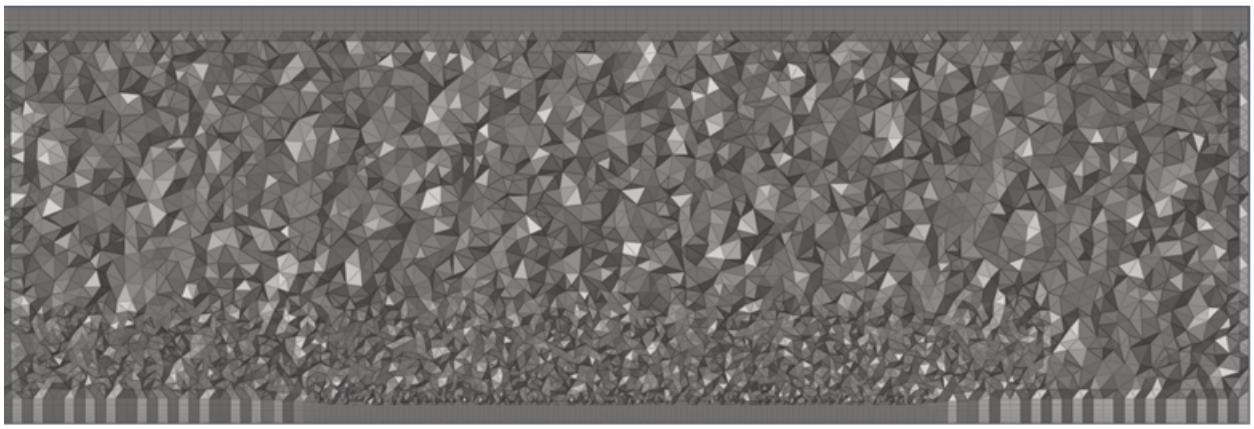


Figure 244: Mesh Used for Simulating a Single-Phase Nucleate Boiling in a Rectangular Channel

AcuSolve Results

The AcuSolve solution is run for heated wall temperature values of 100 C, 105 C, 110 C, 115 C, 120 C, 125 C, 130 C, 133 C and the results presented reflect the heat flux from the wall as the temperature nears the saturation temperature. The experimental values of heat flux (MW/m2) and wall temperature are presented with the corresponding AcuSolve results at seven temperature values. The AcuSolve results show good agreement with the experimental results for the heat flux, indicating that the single-phase nucleate boiling is properly captured.

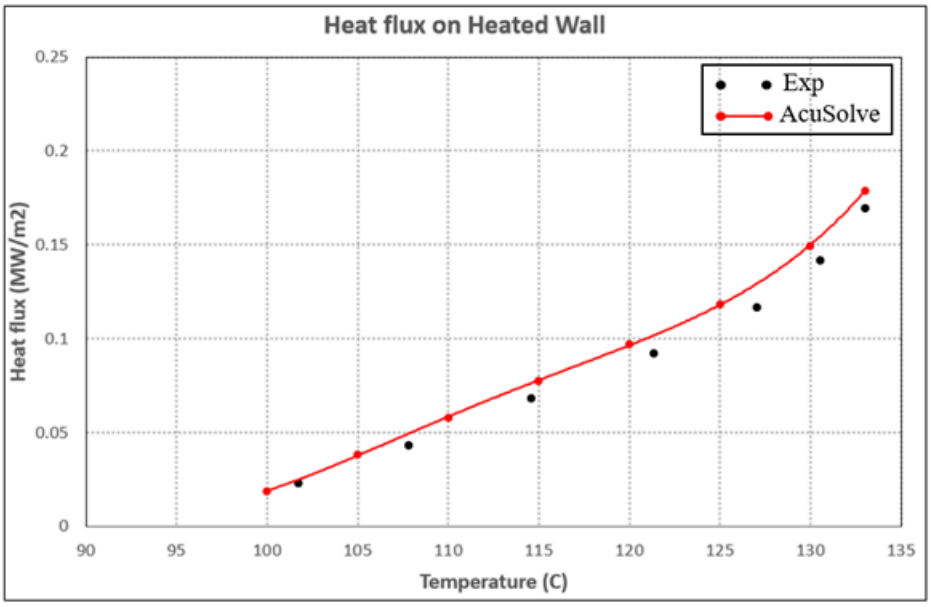


Figure 245: Heat Flux Values for Varying Wall Temperatures Compared to Experimental Data

Summary

The AcuSolve solution compares well with experimental results for single-phase nucleate boiling simulations. In this application, heat flux generated by the wall as the onset of boiling approaches are simulated with AcuSolve using the nucleate boiling feature and the RKE turbulence model. The experimental values of heat flux for the wall temperature range are presented with the corresponding AcuSolve results. A good agreement of simulation results with the experiment validates the ability to solve single-phase nucleate boiling using the nucleate boiling capabilities of AcuSolve.

Simulation Settings for Single-Phase Nucleate Boiling in a Rectangular Channel

HyperWorks CFD database file: `<your working directory>\channel_single_phase_boiling \channel_single_phase_boiling.hm`.

Global

- Problem Description
  - Analysis type – Steady
  - Turbulence equation – RKE
  - Temperature equation – Advective Diffusive
  - Nucleate Boiling Single Phase – On
- Auto Solution Strategy
  - Convergence Tolerance – `0.001` sec
  - Relaxation factor – `0.4`
- Surface Tension Model (“Water-srfTns”)
  - Type – Constant
  - Surface Tension – `0.07`

- Material Model
  - Vapor
    - Type – Constant
    - Density – `1.128` kg/m^3
    - Viscosity – `1.29e-5` kg/m-sec
    - Specific Heat – `2174.59` J/kg-K
    - Latent Heat – `2256000`
    - Latent Heat Temperature – `393.45` K
    - Conductivity – `0.02749` W/m-K
    - Turbulent Prandtl number – `1.0`
  - Water
    - Type – Constant
    - Density – `965.36` kg/m^3
    - Viscosity – `0.000314` kg/m-sec
    - Specific Heat – `4204.8` J/kg-K
    - Conductivity – `0.675` W/m-K
    - Turbulent Prandtl number – `0.91`
    - Vapor phase model – Vapor
    - Surface Tension model – Water-srfTns

Model

- Volumes
  - Fluid
    - Material– Water
- Surfaces
  - Inflow
    - Simple Boundary Condition – Inflow
    - Inflow type – Average Velocity
    - Average Velocity – `0.39` m/sec
    - Temperature – `368.15` K
  - Outflow
    - Simple Boundary Condition – Outflow
    - Back flow condition – On
    - Temperature back flow type – Mass flux average
    - Kinetic energy back flow type – Mass flux average
    - Dissipation rate back flow type – Mass flux average
  - Bottom
    - Simple Boundary Condition – Wall
  - Top

        - Simple Boundary Condition – Wall
    - Side_MinY
        - Simple Boundary Condition – Wall
    - Side_MaxY
        - Simple Boundary Condition – Wall
    - Heated Wall
        - Simple Boundary Condition – Wall
        - Temperature type – Value
        - Temperature – [373.15, 378.15, 383.15, 388.15, 393.15, 398.15, 403.15, 406.15] K

References

Helfried Steiner, Alexander Kobor, Ludwig Gebhard, 2005, "A wall heat transfer model for subcooled boiling flow", International Journal of Heat and Mass Transfer, Vol 48, pp. 4161- 4173.

Chen, J.C., 1966, "Correlation for Boiling Heat Transfer to Saturated Fluids in Convective Flow", United States: N. p., 1962. Web. doi:10.2172/4636495.

Laminar Flow

4

This section includes validation cases that do not require a turbulence model to be used.

This chapter covers the following:

- Circumferential Flow in a Cylinder Induced by a Rotating Solid (p. 332)
- Laminar Flow Through a Pipe With Imposed Heat Flux (p. 338)
- Laminar Couette Flow with Imposed Pressure Gradient (p. 343)
- Laminar Couette Flow with Imposed Pressure Gradient and Heated Walls (p. 349)
- Laminar Flow Through a Pipe with Species Transport (p. 355)
- Flow Inside a Rotating Cavity (p. 361)
- Laminar Flow Past a 90° T-Junction (p. 369)
- Laminar Flow Through a Channel with Heated Walls (p. 374)
- Viscous Heating Inside a Rotating Annulus (p. 379)
- Oscillating Laminar Flow Around a Circular Cylinder (p. 386)
- Ideal Gas Compression in an Actuating Piston (p. 391)
- Separated Laminar Flow Over a Blunt Plate (p. 398)
- Laminar Flow Through a Pipe with Constant Wall Temperature (p. 405)
- Laminar Free Surface Flow Inside a Rotating Cavity (p. 410)
- Natural Convection in a Concentric Annulus (p. 416)
- Flow Between Concentric Cylinders (p. 422)
- Laminar Poiseuille Flow Through a Pipe (p. 428)
- Heat Transfer Between Radiating Concentric Cylinders (p. 432)

Circumferential Flow in a Cylinder Induced by a Rotating Solid

In this application, AcuSolve is used to simulate the flow of air between concentric cylinders that is initiated by the rotation of the solid inner cylinder. The outer cylinder is held stationary while the inner cylinder rotates with a constant speed. AcuSolve results are compared with analytical results as described in White (1991). The close agreement of AcuSolve results with analytical results validates the ability of AcuSolve to maintain a continuous velocity across a non-conformal guide surface interface.

Problem Description

The problem consists of a fluid with material properties of a viscous fluid with the density of air rotating between two infinitely long concentric cylinders, as shown in the following image, which is not drawn to scale. The radius of the outer cylinder is 3.0 m and the radius of the inner cylinder is 1.5 m. The inner cylinder is defined as a solid medium and rotates at 1 rad/sec. The inner cylinder's surface velocity is mapped to the adjacent surface within the fluid medium, while the outer cylinder is fixed. The induced flow is laminar and exhibits a steady state behavior after running for a short period of physical time. The rotation of the inner cylinder causes the fluid to rotate due to viscous shearing near the wall. As the outer cylinder is fixed, a velocity gradient is generated as a function of radius within the flow domain.

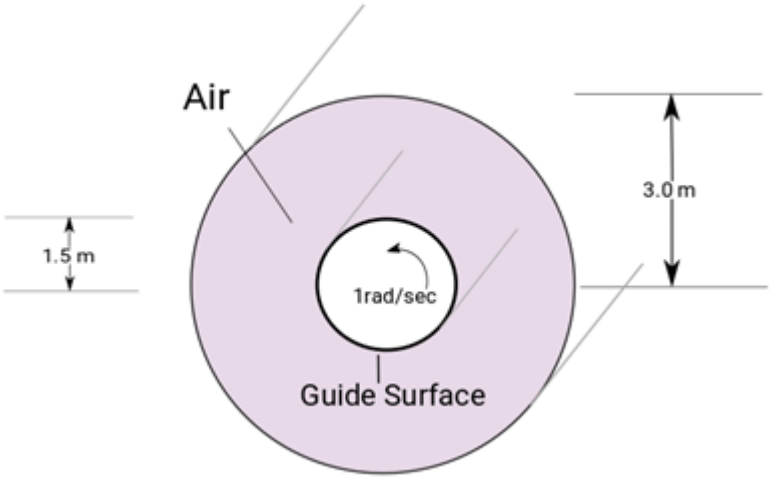


Figure 246: Critical Dimensions and Parameters Used for Simulating Flow Between Two Concentric Cylinders Split with a Guide Surface

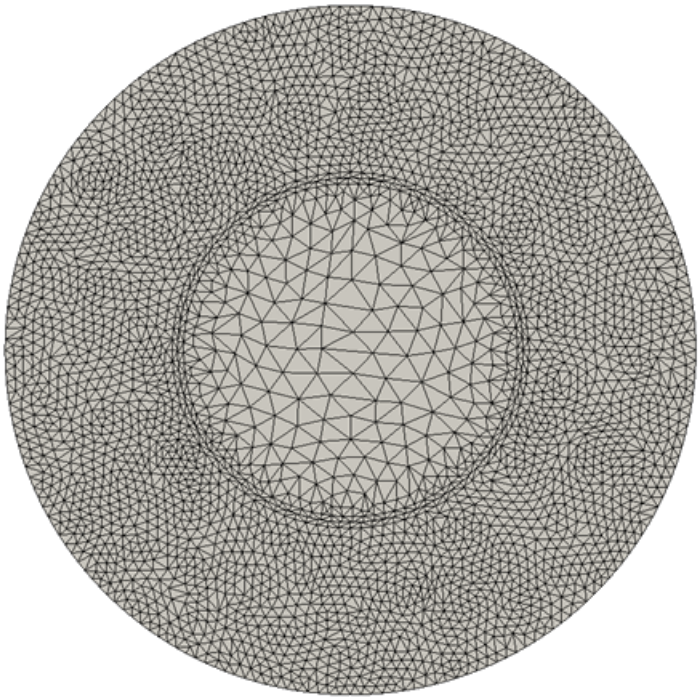


Figure 247: Mesh Used for Simulating Flow Between Two Concentric Cylinders

The simulation was performed as a two dimensional problem by constructing a volume mesh that contains a single layer of elements in the extruded direction, normal to the flow plane and by imposing slip flow and mesh boundary conditions on the extruded planes.

AcuSolve Results

The AcuSolve solution reaches a quasi-static result with the velocity between the two cylinders reaching a steady state at the simulation end time. As the solid inner cylinder rotates, it acts as a guide surface for the fluid elements to track and inherit the two velocity components. The velocity at the edge of the inner cylinder is equal to exactly the rotational speed multiplied by the radius. As the radius increases, the flow velocity reduces until it reaches zero at the outer diameter. The following images show the tangential velocity within the fluid as a function of radius from the center. The tangential velocity is compared with the analytical solution. The image below shows black circles representing the analytical solution and a solid red line for the AcuSolve results.

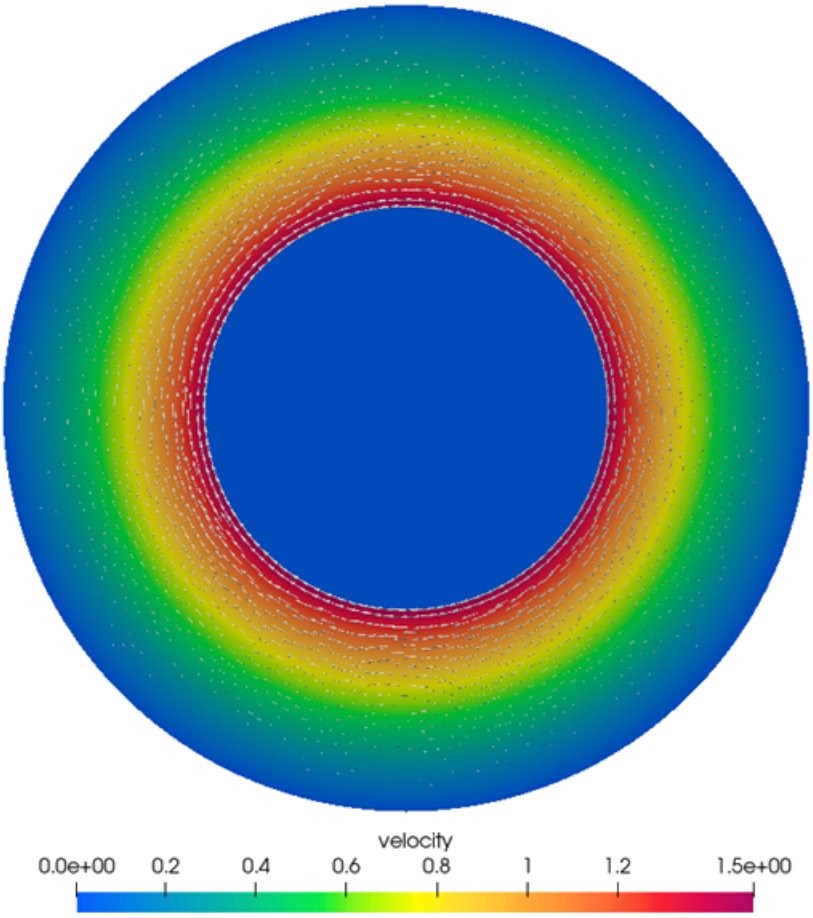


Figure 248: Contours and Vectors of Velocity Between the Concentric Cylinders

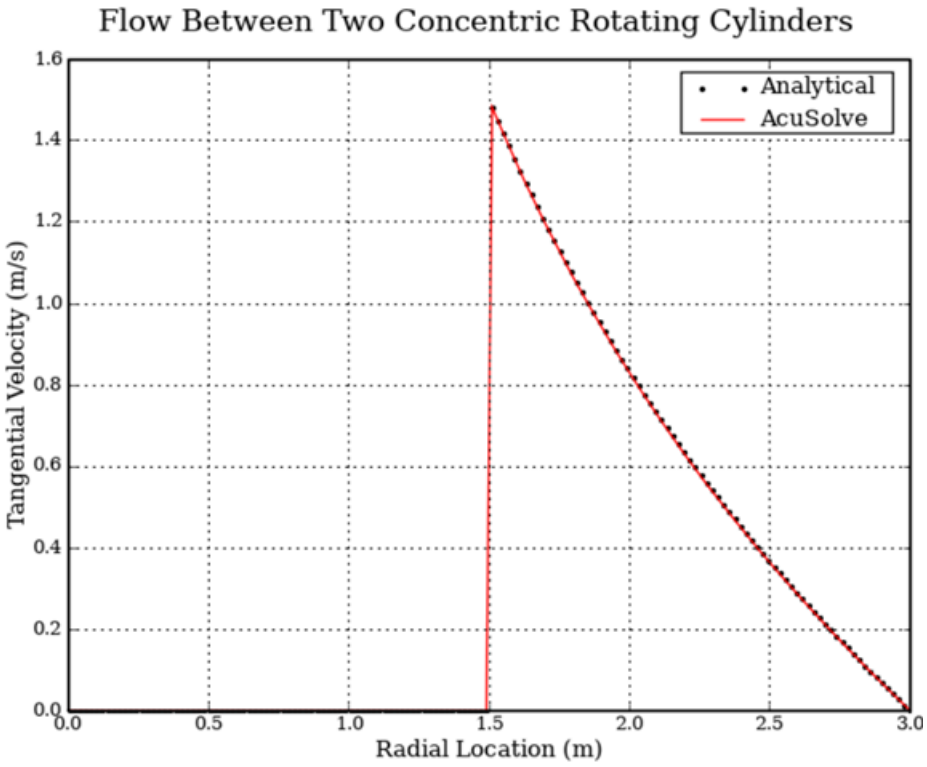


Figure 249: Tangential Velocity Within the Solid and Fluid as a Function of Radial Distance from the Center at the Final Timestep

Summary

The AcuSolve solution compares well with analytical results for laminar flow between concentric cylinders, where the inner cylinder guides the adjacent fluid elements. In this application, a fluid initially at rest inherits the angular velocity from the inner cylinder while the outer cylinder does not rotate. As a result of the inherited velocity and viscosity of the fluid, flow develops between the two cylinders. The AcuSolve solution for the tangential velocity as a function of radius matches exactly with the analytical results.

Simulation Settings for Flow Between Concentric Split Cylinders

HyperWorks CFD database file: `<your working directory>\annulus_split_rotating \annulus_split_rotating.hm`

- Problem Description
  - Analysis type - Transient
  - Flow equation - Navier Stokes
  - Turbulence equation - Laminar
  - Mesh type - Arbitrary Mesh Movement (ALE)
- Auto Solution Strategy
  - Max time steps - `40`
  - Initial time increment- `0.02` sec

    - Convergence tolerance - `0.001`
    - Min stagger iterations - `2`
    - Max stagger iterations - `4`
- Material Model
    - Air
        - Density
            1. Type - Constant
            2. Density - `1.225` kg/m3
        - Viscosity
            1. Type - Constant
            2. Viscosity - `1.781` kg/m-sec
- Mesh Motion
    - Rotation
        - Rotation Center
            1. X-coordinate - `2.0` m
            2. Y-coordinate - `0.0` m
            3. Z-coordinate - `0.0` m
        - Angular velocity
            1. X-component - `1.0` rad/sec
            2. Y-component- `0.0` rad/sec
            3. Z-component - `0.0` rad/sec

    Model
- Volumes
    - CylinderInner
        - Element Set
            1. Medium - Solid
            2. Material model - Aluminum
    - CylinderOuter
        - Element Set
            1. Medium - Fluid
            2. Material model - Air
- Surfaces
    - InBottom
        - Simple Boundary Condition
            1. Type- Slip
            2. Mesh displacement type- Slip
    - InInterf

        - Simple Boundary Condition
            1. Type- Wall
            2. Mesh displacement type- Fixed
            3. Mesh motion- Rotation
        - Guide Surface
            1. Type- Faceted
    - InTop
        - Simple Boundary Condition
            1. Type- Slip
            2. Mesh displacement type- Slip
    - OutBottom
        - Simple Boundary Condition
            1. Type- Slip
            2. Mesh displacement type- Slip
    - OutInterf
        - Simple Boundary Condition
            1. Type- Wall
            2. Wall velocity type- Match Mesh Velocity
            3. Mesh displacement type- Guide surface
            4. Guide surface- InInterf
    - OutTop
        - Simple Boundary Condition
            1. Type- Slip
            2. Mesh displacement type- Slip
    - OutWall
        - Simple Boundary Condition
            1. Type- Wall
            2. Mesh displacement type- Fixed
- Nodes
    - PressurePoint
        - Pressure
            1. Type- Zero

References

F. M. White. "Viscous Fluid Flow". Section 3-2.3. McGraw-Hill Book Co., Inc. New York. 1991.

Laminar Flow Through a Pipe With Imposed Heat Flux

In this application, AcuSolve is used to simulate the flow of mercury through a heated pipe. The AcuSolve results are compared with analytical results for pressure drop as described in White (1991), and with temperature changes as described in Incropera and DeWitt (1981). The close agreement of AcuSolve results with analytical results validates the ability of AcuSolve to model cases with flow and imposed heat flux.

Problem Description

The problem consists of mercury flowing through a heated, circular pipe that is 0.005 m in diameter and 0.1 m long, as shown in the following image, which is not drawn to scale. Mercury enters the pipe with a constant temperature of 300 K. The pipe has an imposed heat flux of 2000 W/m^2. The laminar velocity field is modeled as periodic to achieve a fully developed velocity profile. As the fluid moves through the pipe it is slowly heated by the heat flux on the wall, resulting in an increased centerline temperature. Pressure decreases along the pipe length due to the friction imposed by the viscous stresses near the pipe wall.

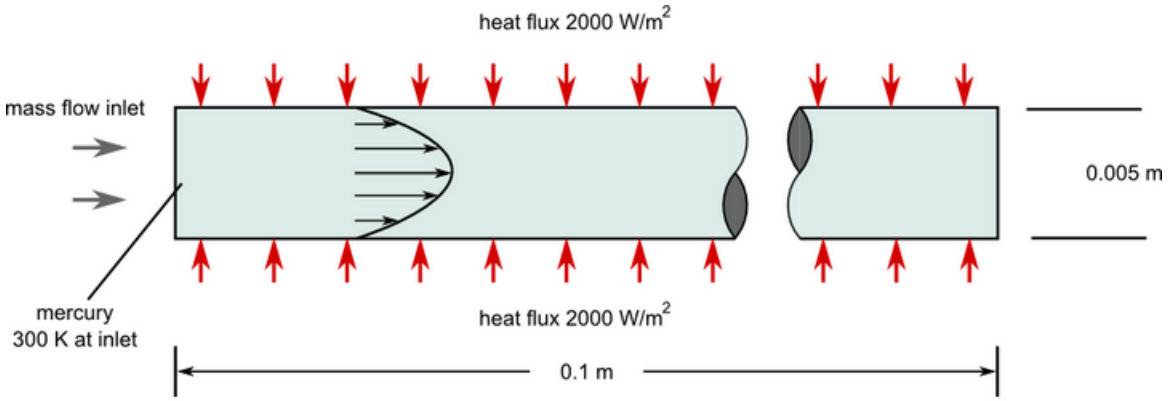


Figure 250: Critical Dimensions and Parameters for Simulating Laminar Flow through a Pipe with Imposed Heat Flux

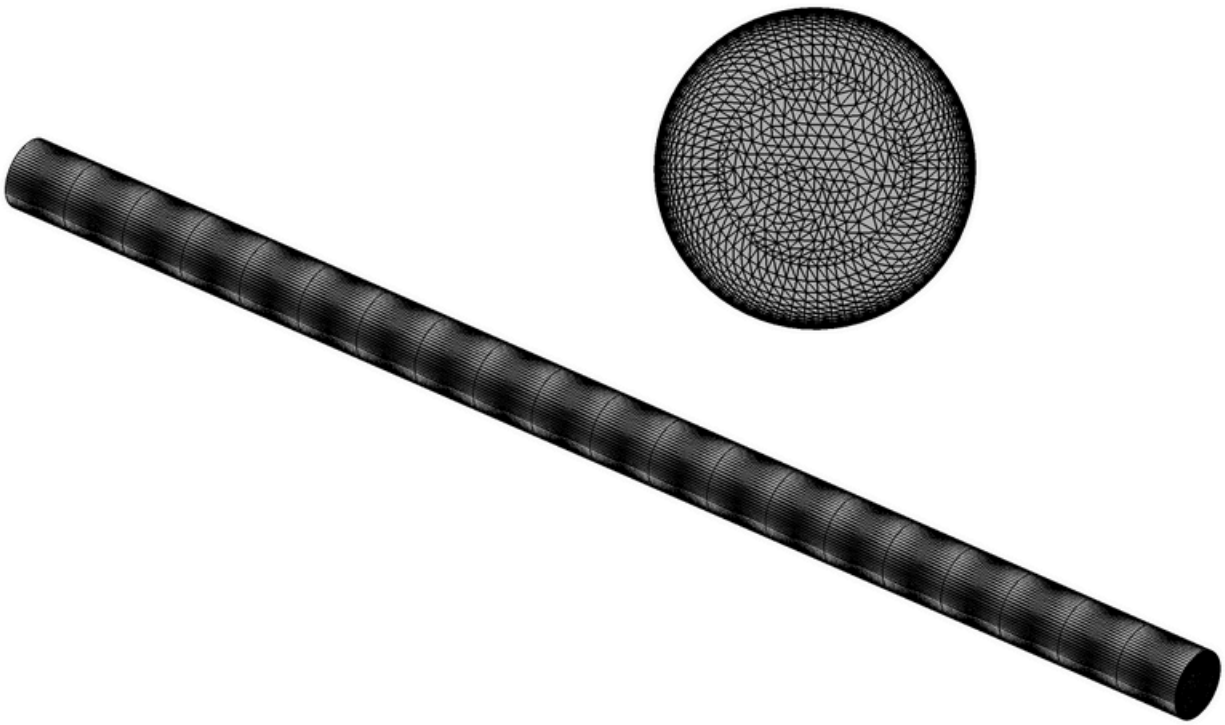


Figure 251: Mesh used for Simulating Laminar Flow Through a Pipe with Imposed Heat Flux

AcuSolve Results

The AcuSolve solution converged to a steady state and the results reflect the mean flow conditions. The greatest pressure is at the inlet, with pressure decreasing as a function of distance away from the inlet. The temperature of the mercury in the pipe increases as a function of distance from the inlet due to the impact of the heat flux on the pipe walls.

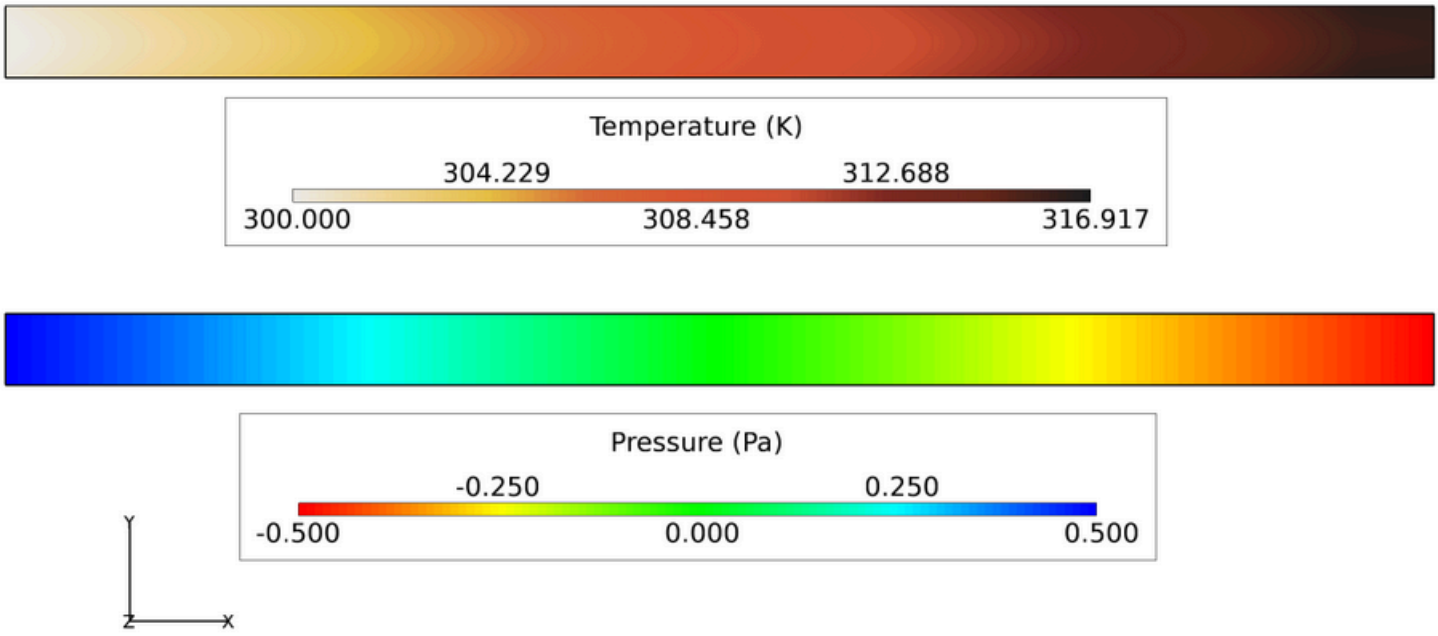


Figure 252: Temperature and Pressure Contours of Mercury Flow Through a Heated Pipe

The analytical solution for the pressure drop, between the inlet and outlet, as well as the analytical solution for the temperature of the mercury at the center of the outlet are presented with the corresponding AcuSolve results in the following table.

Table 14:

	Analytical solution	AcuSolve solution	Percent deviation from analytical
Pressure drop (Pa)	0.991	0.994	0.303
Centerline temperature of flow at outlet (K)	316.917	316.269	0.204

Summary

The AcuSolve solution compares well with analytical results for flow through a pipe with an imposed heat flux. In this application, the pressure drop in the fluid region is driven by the viscous stresses near the pipe wall. The temperature in the fluid region is influenced by the imposed heat flux on the walls. The values of pressure and temperature that are predicted by AcuSolve are within 0.3 percent of the analytical solution.

Simulation Settings for Laminar Flow Through a Pipe With Imposed Heat Flux

AcuConsole database file: `<your working directory>\pipe_laminar_heat\pipe_laminar_heat.acs`

Global

- Problem Description
  - Analysis type - Steady State
  - Temperature equation - Advective Diffusive
  - Turbulence equation - Laminar
- Auto Solution Strategy
  - Relaxation Factor - `0.2`
- Material Model
  - Mercury
    - Density - `13579.0` kg/m3
    - Viscosity - `0.001548` kg/m-sec

  Model
- Volume
  - Fluid
    - Element Set
      1. Material model - Mercury
- Surfaces
  - Inflow
    - Simple Boundary Condition - (disabled to allow for periodic conditions to be set)
    - Advanced Options
      1. Integrated Boundary Conditions
         1. Mass Flux
            1. Type - Constant
            2. Constant value - `-1.33e-3` kg/sec
         2. Temperature
            1. Type - Constant
            2. Constant value - `300.0` K
  - Outflow
    - Simple Boundary Condition - (disabled to allow for periodic conditions to be set)
  - Wall

        - Simple Boundary Condition
            1. Type - Wall
            2. Temperature BC type - Flux
            3. Heat flux - `2000.0` W/m2

- Periodics
    - Periodic 1
        - Individual Periodic BCs
            1. Velocity
                1. Type - Periodic
            2. Pressure
                1. Type - Single Unknown Offset
            3. Temperature
                1. Type - Single Unknown Offset

References

F. M. White. "Viscous Fluid Flow". Section 3-2.1. McGraw-Hill Book Co., Inc.. New York. 1991.

F. P. Incropera and D. P. DeWitt. "Fundamentals of Heat Transfer". John Wiley & Sons. New York. 1981.

Laminar Couette Flow with Imposed Pressure Gradient

In this application, AcuSolve is used to simulate the viscous flow of water between a moving and a stationary plate with an imposed pressure gradient. AcuSolve results are compared with analytical results described in White (1991). The close agreement of AcuSolve results with analytical results validates the ability of AcuSolve to model cases with imposed pressure gradients.

Problem Description

The problem consists of air between two plates in a two dimensional domain, as shown in the following image, which is not drawn to scale. The domain is 1.0 m high and 1.5 m long. The top plate moves with a constant velocity of 3.0 m/sec and the bottom plate is fixed. There is a mean-pressure gradient of -12 Pa/m applied to the bulk fluid in the streamwise direction. The problem is simulated with periodic boundaries in the streamwise direction. The induced flow field is laminar and exhibits a steady state behavior. The flow field develops from the pressure gradient, the motion of the top plate, and the viscous shear stresses near the plates.

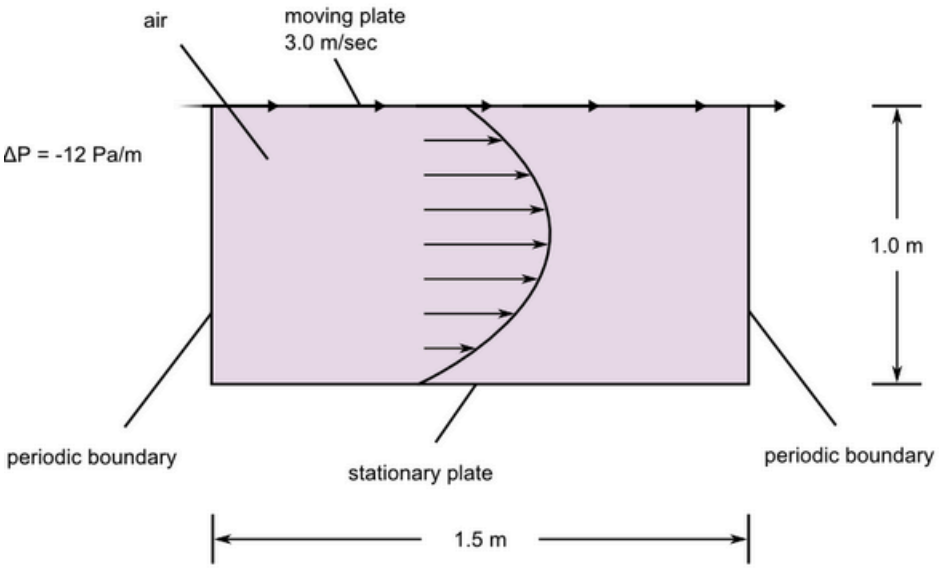


Figure 253: Critical Dimensions and Parameters for Simulating Laminar Couette Flow with an Imposed Pressure Gradient

The simulation was performed as a two dimensional problem by restricting flow in the out-of-plane direction through the use of a mesh that is one element thick.

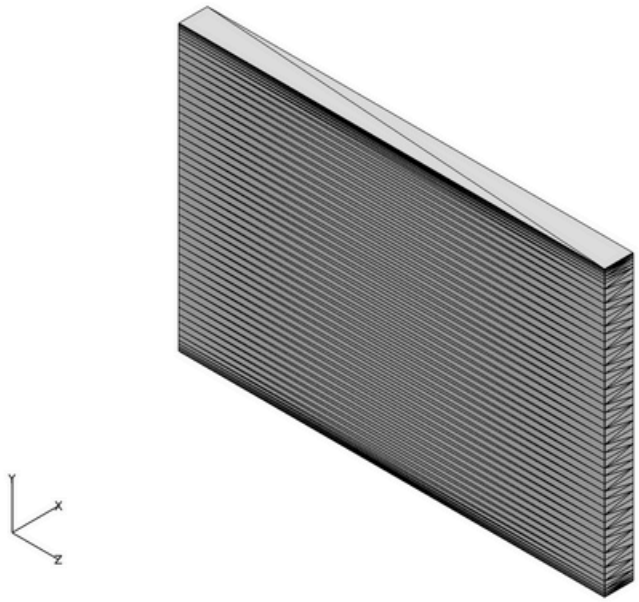


Figure 254: Mesh used for Simulating Laminar Couette Flow with an Imposed Pressure Gradient

AcuSolve Results

The AcuSolve solution converged to a steady state and the results reflect the mean flow conditions. The greatest velocity is located at approximately 40 percent of the channel height, closer to the moving plate. The flow develops as a result of the pressure gradient and the shear stress acting on the fluid near both the moving plate and the stationary plate.

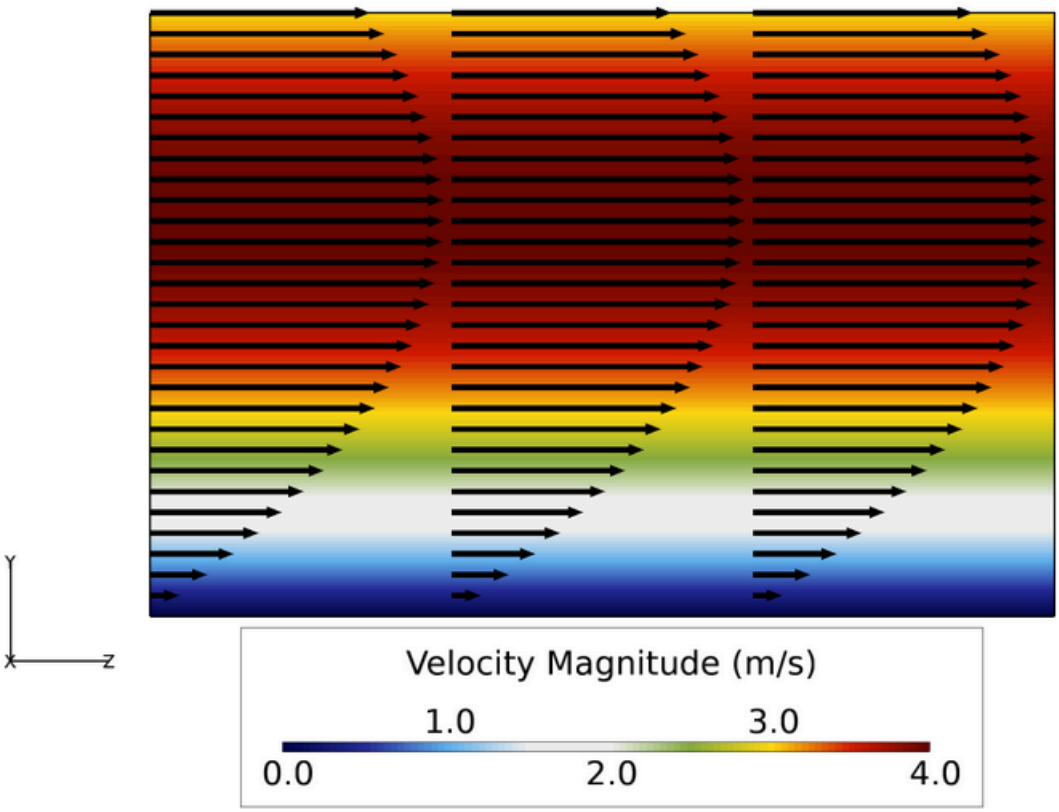


Figure 255: Z-Velocity Contours and Velocity Vectors

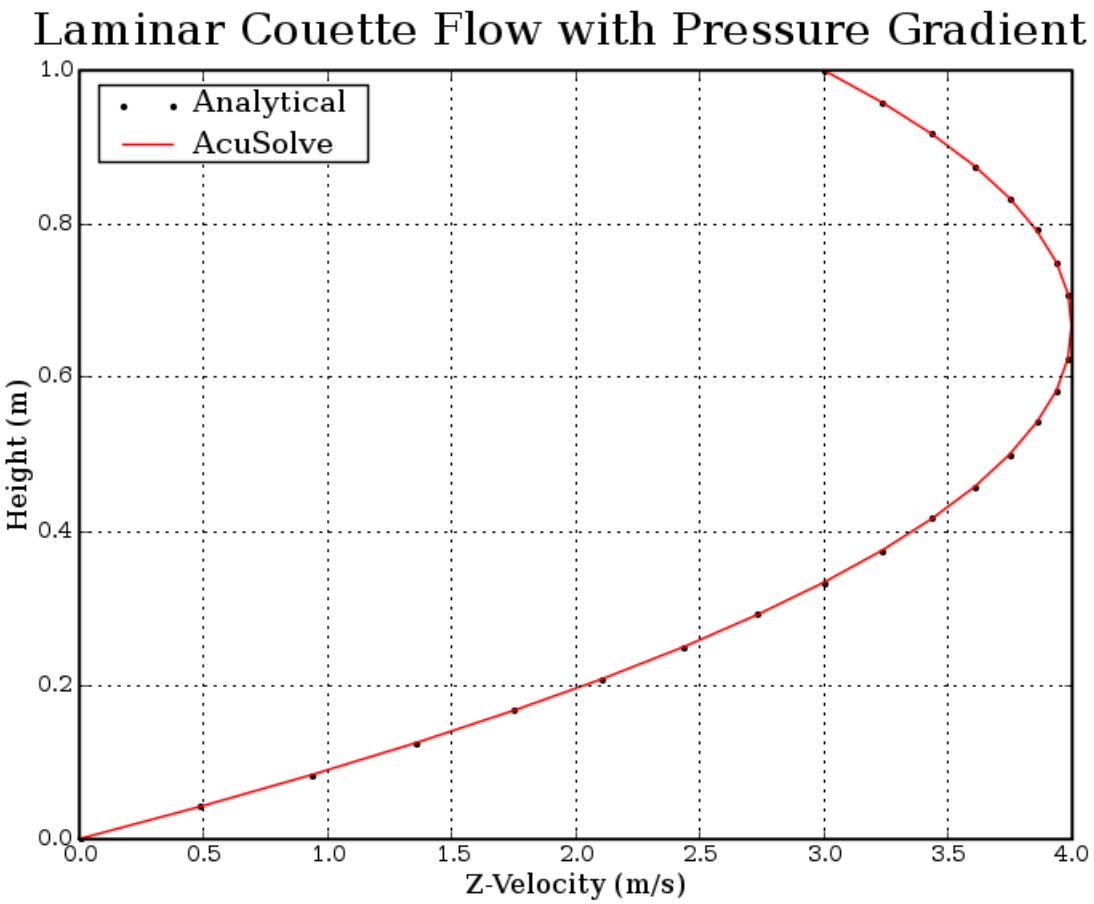


Figure 256: Z Velocity Plotted Against Height Above the Bottom of the Flow Field (Z Velocity is Presented on the X Axis to Better Represent the Velocity Profile in the Direction of Flow)

Summary

The velocity profile computed by AcuSolve agrees well with the analytical solution for this application. The velocity profile arises due to the combination of the imposed pressure gradient and the constant upper-wall velocity. Note that the combination of these effects results in the asymmetric velocity profile that is reflected in the results.

Simulation Settings for Laminar Couette Flow with Imposed Pressure Gradient

AcuConsole database file: `<your working directory>\couette_flow\couette_flow.acs`

Global

- Problem Description
  - Analysis Type - Steady State
  - Turbulence equation - Laminar
- Auto Solution Strategy
  - Relaxation factor - `0.2`

- Material Model
  - Air
    - Density - `1.0` kg/m3
    - Viscosity - `1.0` kg/m-sec
- Body Force
  - DP/DL
    - Gravity
      1. Z-component - `18.0` m/sec2

Model

- Volumes
  - Fluid
    - Element set
      1. Material model - Air
      2. Body force - DP/DL
- Surfaces
  - Max_X
    - Simple Boundary Condition
      1. Type - Symmetry
  - Max_Y
    - Simple Boundary Condition
      1. Type - Wall
      2. Wall velocity type - Cartesian
      3. Z-velocity - `3.0` m/s
  - Max_Z
    - Simple Boundary Condition - (disabled to allow for periodic conditions to be set)
  - Min_X
    - Simple Boundary Condition
      1. Type - Symmetry
  - Min_Y
    - Simple Boundary Condition
      1. Type - Wall
  - Min_Z
    - Simple Boundary Condition - (disabled to allow for periodic conditions to be set)
- Periodics
  - Periodic 1
    - Periodic Boundary Conditions
      1. Type - Periodic

References

F. M. White. "Viscous Fluid Flow". Section 3-2.3. McGraw-Hill Book Co., Inc.. New York. 1991.

Laminar Couette Flow with Imposed Pressure Gradient and Heated Walls

In this application, AcuSolve is used to simulate the flow of a highly viscous fluid between a moving and a stationary plate with an imposed pressure gradient and fixed temperature on the walls. AcuSolve results are compared with analytical results described in White (1991). The close agreement of AcuSolve results with analytical results validates the ability of AcuSolve to model cases with imposed pressure gradients and viscous heating.

Problem Description

The problem consists of a viscous fluid between two plates in a two dimensional domain, as shown in the following image, which is not drawn to scale. The domain is 1.0 m high and 1.5 m long. The top plate moves with a constant velocity of 3.0 m/sec and the bottom plate is fixed. To simulate a fully developed flow with a relatively short length domain there is a mean-pressure gradient of -12 Pa/m applied to the fluid in the streamwise direction, defined as a body force acting on the entire fluid. The lower wall is held at a fixed temperature of 273.0 K, while the upper wall is held at a fixed temperature of 274.0 K. The problem is simulated with periodic boundaries in the streamwise direction. The Reynolds number of the flow, based on the distance between the plates is 0.3, indicating laminar flow. The flow field develops from the pressure gradient, the motion of the top plate, and the viscous shear stresses near the plates. The shear stress within the domain causes the temperature to increase within the channel.

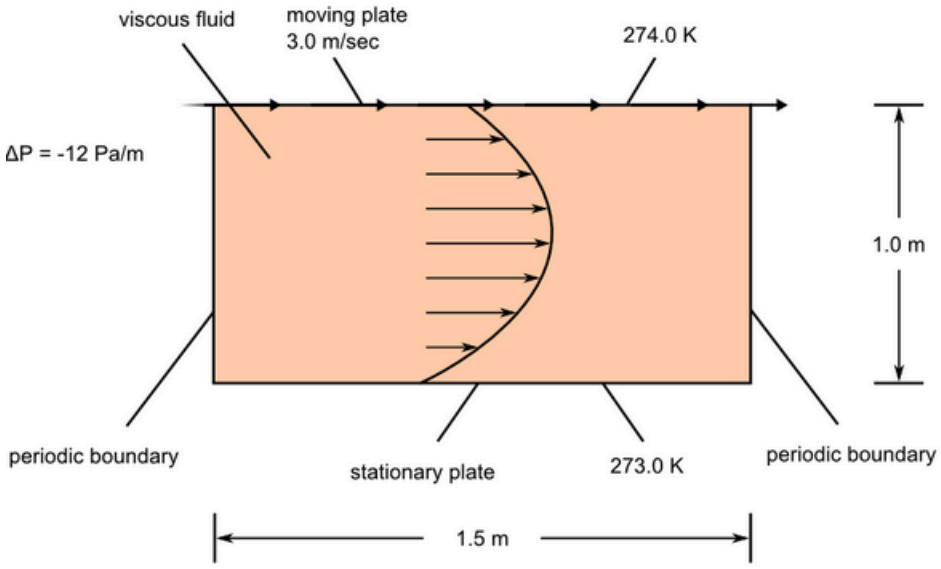


Figure 257: Critical Dimensions and Parameters for Simulating Laminar Couette Flow with an Imposed Pressure Gradient and Heated Walls

The simulation was performed as a two dimensional problem by constructing a volume mesh that contains a single layer of elements extruded in the cross stream direction, normal to the flow plane and by imposing symmetry boundary conditions on the extruded planes. Due to the periodic natural of the flow, a single element extrusion in the streamwise direction is used to reduce the model size.

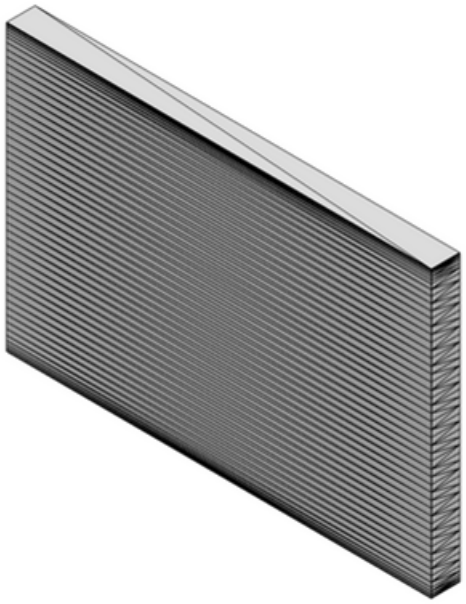


Figure 258: Mesh used for Simulating Laminar Couette Flow with an Imposed Pressure Gradient and Heated Walls

AcuSolve Results

The AcuSolve solution converged to a steady state and the results reflect the mean flow conditions. The simulation results show a flow field with a nearly linear distribution of velocity, with the peak at the top wall. The flow develops primarily as a result of the shear stress acting on the fluid near both the moving plate and the stationary plate. The temperature variation between the two plates develops due to the viscous heating effects that increase the temperature within the channel, with the maximum near the central height of the domain. The following figure shows the temperature distribution between the two plates and velocity vectors indicating the velocity profile.

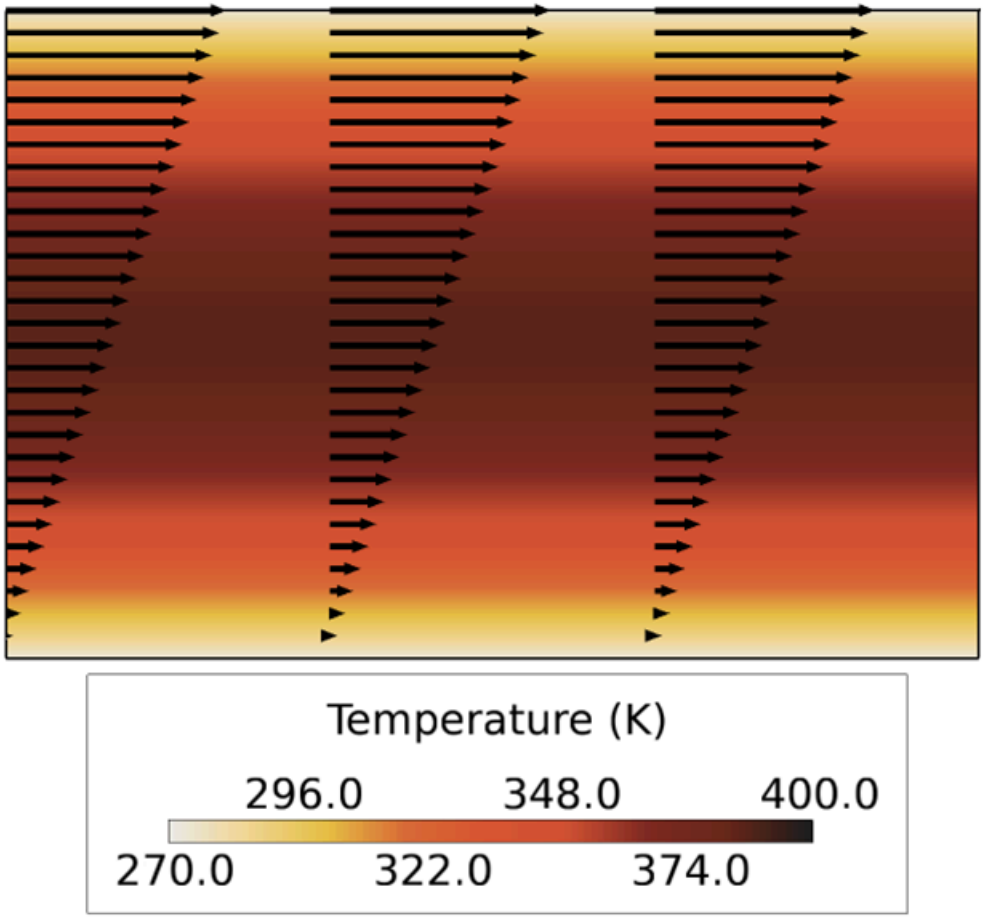


Figure 259: Contours of Temperature Between the Plates, with Velocity Vectors

The following image demonstrates the accuracy of the solution compared to the analytical results as computed by the solution for viscous heating within a channel with a moving upper boundary.

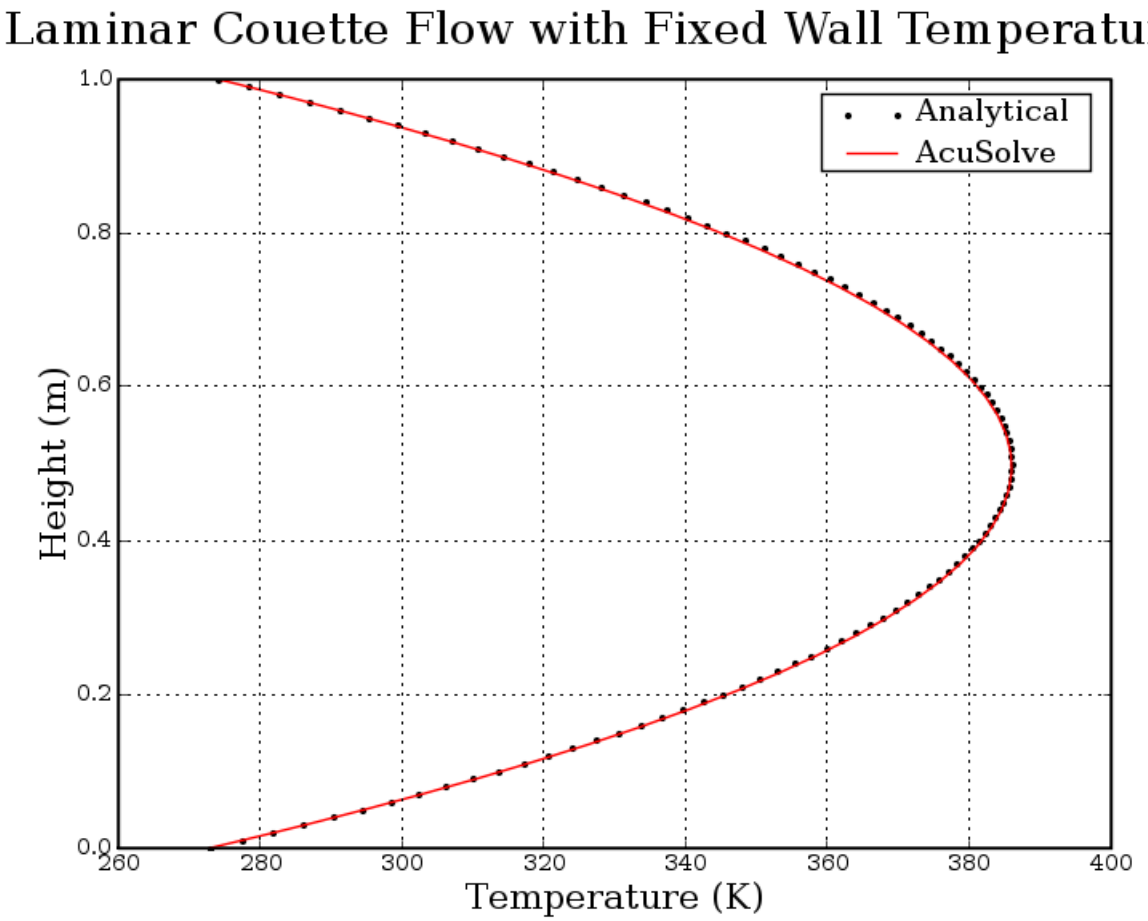


Figure 260: Temperature Plotted Against Height above the Bottom of the Flow Field (Temperature is Presented on the X Axis to Better Represent the Distribution Between the Plates in the Streamwise Direction)

Summary

In this application, a fully developed laminar flow between two plates with fixed temperature is studied and compared against analytical data. The AcuSolve results compare well with the analytical data for the temperature distribution between the two plates. The simulation indicates that the velocity profile arises due to the combination of the viscous shearing and the velocity of the upper plate. The velocity and temperature profiles computed by AcuSolve demonstrate how highly viscous fluids tend to direct the flow regime. AcuSolve demonstrates the ability to predict the analytical solution for viscous heating between two flat plates with moving and stationary boundaries and an imposed pressure gradient.

Simulation Settings for Laminar Couette Flow with Imposed Pressure Gradient and Heated Walls

AcuConsole database file: `<your working directory>\couette_laminar_heat\couette_laminar_heat.acs`

Global

- Problem Description

    - Analysis Type - Steady State
    - Temperature equation - Advective Diffusive
    - Turbulence equation - Laminar
- Auto Solution Strategy
    - Relaxation factor - `0.2`
- Material Model
    - Fluid
        - Density - `1.0` kg/m3
        - Specific Heat - `1.0` J/kg-K
        - Viscosity - `100.0` kg/m-sec
- Body Force
    - DP/DL
        - Gravity
            1. Z-component - `18.0` m/sec2

Model

- Volumes
    - Fluid
        - Element set
            1. Material model - Fluid
            2. Body force - DP/DL
            3. Viscous heating - on
- Surfaces
    - Max_X
        - Simple Boundary Condition
            1. Type - Symmetry
    - Max_Y
        - Simple Boundary Condition
            1. Type - Wall
            2. Wall velocity type - Cartesian
            3. Z-velocity - `3.0` m/s
            4. Temperature - `274.0` K
    - Max_Z
        - Simple Boundary Condition - (disabled to allow for periodic conditions to be set)
    - Min_X
        - Simple Boundary Condition
            1. Type - Symmetry
    - Min_Y

        - Simple Boundary Condition
            1. Type - Wall
            2. Temperature - `273.0` K
    - Min_Z
        - Simple Boundary Condition - (disabled to allow for periodic conditions to be set)
- Periodics
    - Periodic 1 all
        - Periodic Boundary Conditions
            1. Type - Periodic

References

F. M. White. "Viscous Fluid Flow". Section 3-3.2. McGraw-Hill Book Co., Inc. New York. 1991.

Laminar Flow Through a Pipe with Species Transport

In this application, AcuSolve is used to simulate the transport of a passive scalar species in a fully developed laminar flow. AcuSolve results are compared with analytical results as described in Kays and Crawford (1993). The close agreement of AcuSolve results with analytical results validates the ability of AcuSolve to model cases with species transport.

Problem Description

The problem consists of species transport in a pipe 0.005 m in diameter and 0.1 m long, as shown in the following image, which is not drawn to scale. The species transport equation is bounded at the inlet with a value of 1.0, while the boundary condition at the wall is 0.0. These constraints impose a concentration gradient within the fluid. The concentration gradient causes the fraction of species 1 to decrease near the pipe wall due to diffusion. The reduced concentration of the species is transported downstream in the pipe via advection, and leads to a continued decrease in the concentration as flow propagates through the pipe.

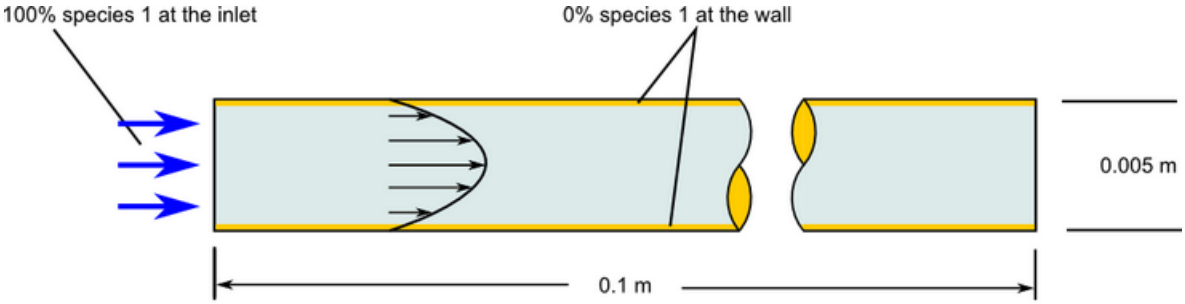


Figure 261: Critical Dimensions and Parameters for Simulating Laminar Flow Through a Pipe with Species Transport

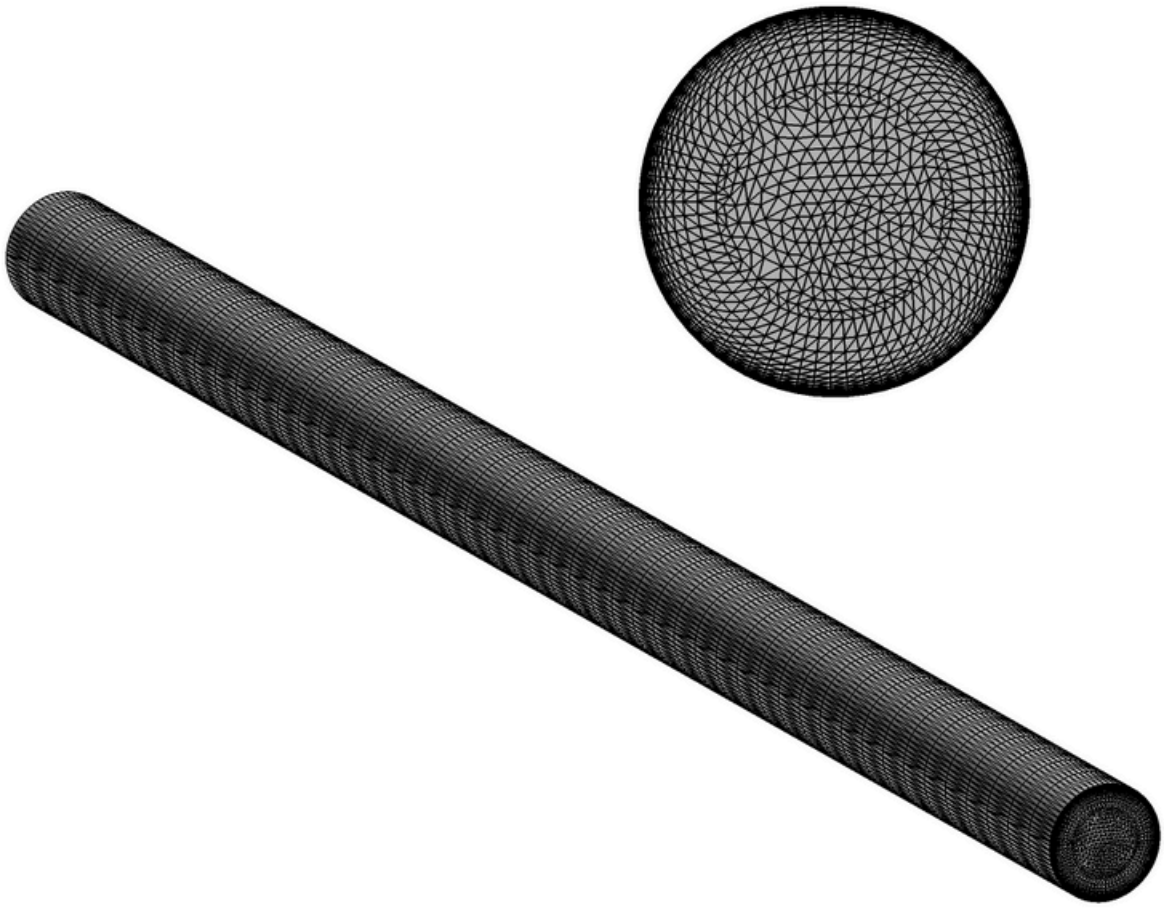


Figure 262: Mesh used for Simulating Laminar Flow Through a Pipe with Species Transport

AcuSolve Results

The AcuSolve solution converged to a steady state and the results reflect the mean flow conditions with the species fraction changing along the length of the pipe. At the inlet, the concentration of species 1 is 100 percent. The fraction of species 1 decreases along the length of the pipe, developing a parabolic concentration profile due to the no-slip walls and the specified concentration at the wall.

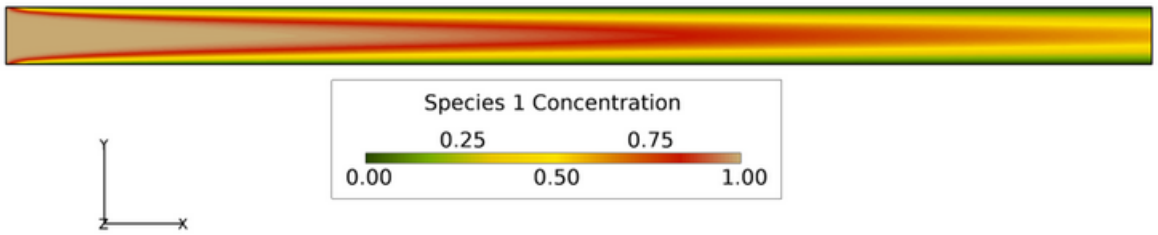


Figure 263: Contours of Concentration for Species 1

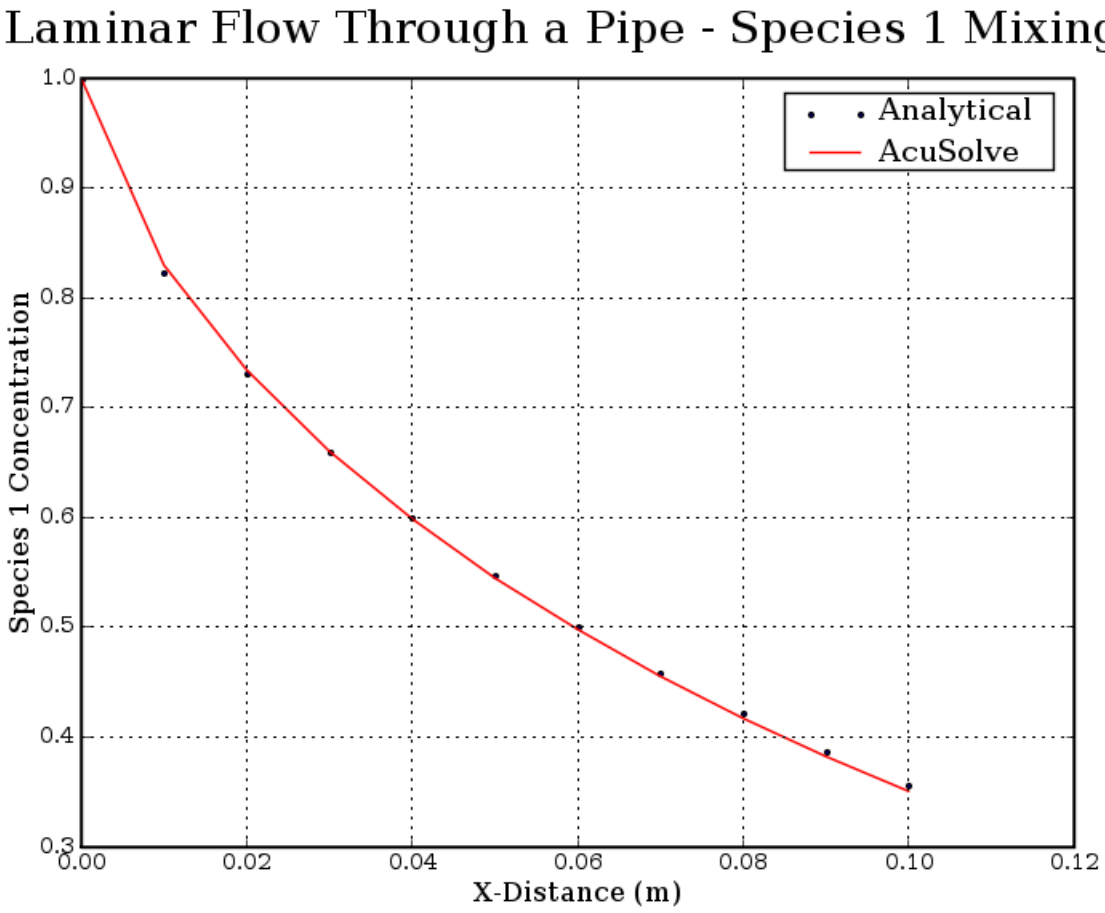


Figure 264: Species 1 Concentration Plotted Against Distance from the Pipe Inlet

Analytical values of the species fraction at different distances along the pipe are presented with the corresponding AcuSolve results in the following table. The analytical solution contains a series of five terms that are summed to yield the values shown in the table.

Table 15:

Distance along pipe (m)	Analytical species 1 fraction	AcuSolve species 1 fraction	Percent deviation from analytical
0	1.0000*	1.0000	0.00
0.01	0.8225	0.8298	0.90
0.02	0.7308	0.7344	0.49
0.03	0.6593	0.6603	0.15
0.04	0.5992	0.5988	0.06
0.05	0.5469	0.5448	0.38
0.06	0.5006	0.4981	0.49
0.07	0.4589	0.4554	0.78
0.08	0.4212	0.4171	0.98
0.09	0.3869	0.3824	1.15
0.1	0.3555	0.3507	1.35

* The theoretical species fraction at the inlet is shown rather than the analytical. In order for the analytical solution to correspond exactly with the theoretical results, additional terms in the series summation would need to be evaluated.

Summary

The AcuSolve solution compares well with analytical results for flow through a pipe with species transport. In this application, a fully developed laminar profile is achieved by enforcing periodic constraints on the pressure and velocity fields. The spatially developing species field is achieved by not enforcing periodicity and allowing the concentration to evolve along the full length of the model. The change in concentration along the pipe length is due to advection in the streamwise direction and diffusion of the species to the outer walls where the concentration is zero. The AcuSolve solution for fraction of species 1 is within 1.35 percent of analytical results.

Simulation Settings for Laminar Flow Through a Pipe with Species Mixing

AcuConsole database file: `<your working directory>\pipe_laminar_species \pipe_laminar_species.acs`.

Global

- Problem Description
  - Analysis type - Steady State

- Species equation - Advective Diffusive
- Num. species - `1`
- Turbulence equation - Laminar

- Auto Solution Strategy
  - Relaxation factor - `0.2`
- Material Model
  - Species1
    - Density - `1.0` kg/m3
    - Viscosity - `1.0e-5` kg/m-sec
    - Diffusivity
      1. 1
         1. Diffusivity - `1.43e-5` kg/m-sec

  Model
- Volumes
  - Fluid
    - Element Set
      1. Material model - Species1
- Surfaces
  - Inflow
    - Simple Boundary Condition - (disabled to allow for periodic conditions to be set)
    - Advanced Options
      1. Nodal Boundary Conditions
         1. Species 1
            1. Type - Constant
            2. Constant value - `1.0`
      2. Integrated Boundary Conditions
         1. Mass Flux
            1. Type - Constant
            2. Constant value - `1.96e-05` kg/sec
  - Outflow
    - Simple Boundary Condition - (disabled to allow for periodic conditions to be set)
  - Wall
    - Simple Boundary Condition
      1. Type - Wall
      2. Species 1 BC type - Value
      3. Species 1 - `0.0`
- Periodics

- Periodic 1
  - Individual Periodic BCs
    1. Velocity
       1. Type - Periodic
    2. Pressure
    3. Type - Single Unknown Offset

References

W. M. Kays and M. E. Crawford. "Convective Heat and Mass Transfer", 3rd Edition. pp. 126-134. McGraw-Hill Book Co., Inc. New York. 1993.

Flow Inside a Rotating Cavity

In this application, AcuSolve is used to simulate the flow of air in an enclosed cylindrical cavity with a rotating top and a fixed bottom. AcuSolve results are compared with experimental data adapted from Michelsen (1986). The close agreement of AcuSolve results with experimental data validates the ability of AcuSolve to model cases containing enclosed cavities with flow induced by rotating walls.

Problem Description

The problem consists of air in an enclosed cylinder 1.0 m tall with a radius of 1.0 m, as shown in the following image, which is not drawn to scale. The top of the cylinder rotates about its center at 1 rad/s, while the bottom of the cylinder is fixed. As the container top spins, the viscous stresses on the fluid induce a circumferential (swirl) velocity throughout the height of the cylinder. In order to conserve mass and momentum, the fluid generates a radial velocity that changes direction based on distance away from the rotation center of the cylinder.

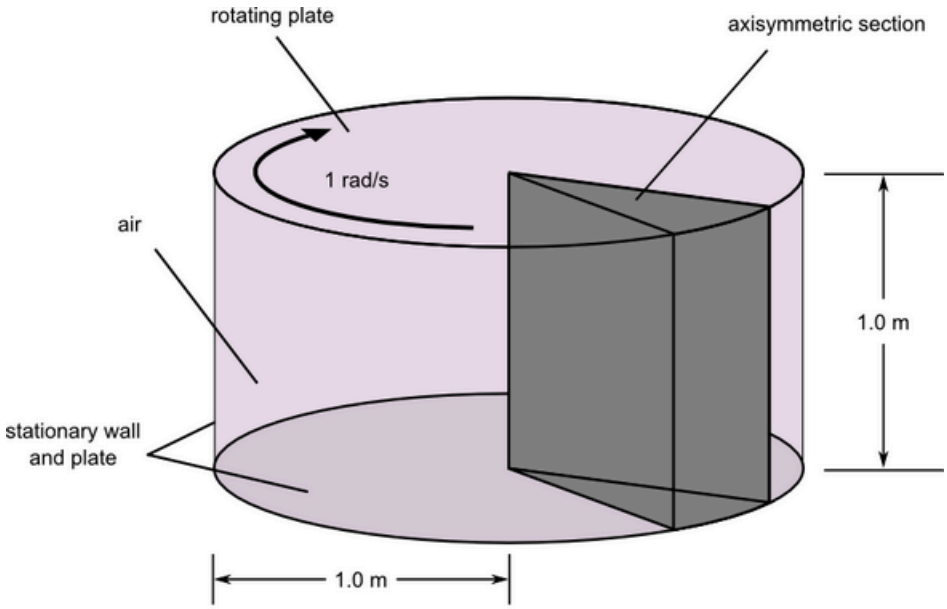


Figure 265: Critical Dimensions and Parameters for Simulating Flow Inside a Rotating Cavity

The flow domain is modeled with axisymmetric periodicity in the circumferential direction, which allows for accurate simulation of the flow while minimizing computational time.

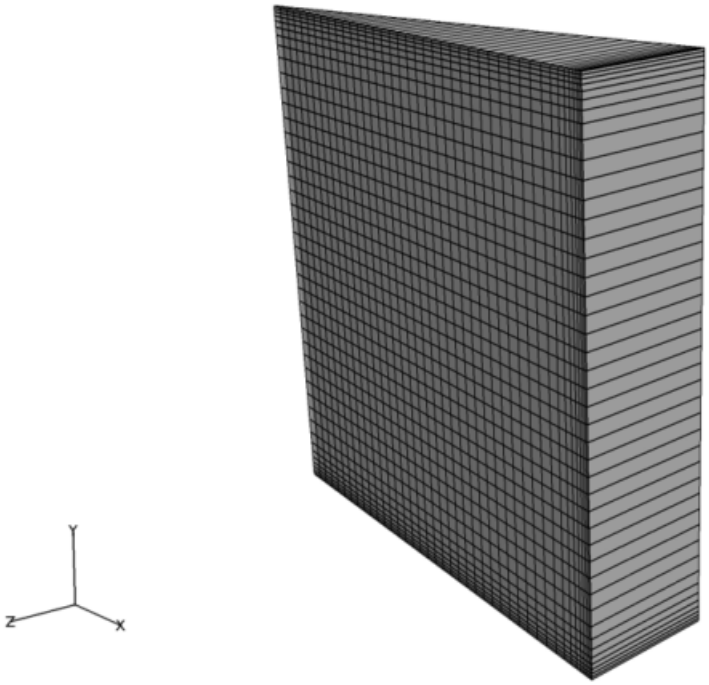


Figure 266: Mesh of Periodic Section Used for Simulating Flow Inside a Rotating Cylinder

AcuSolve Results

The AcuSolve solution converged to a steady state and the results reflect the mean flow conditions. The velocity varies with both vertical location and with distance from the rotation center. The complex flow field develops from a combination of the viscous stresses acting at the rotating cylinder top and at the stationary bottom.

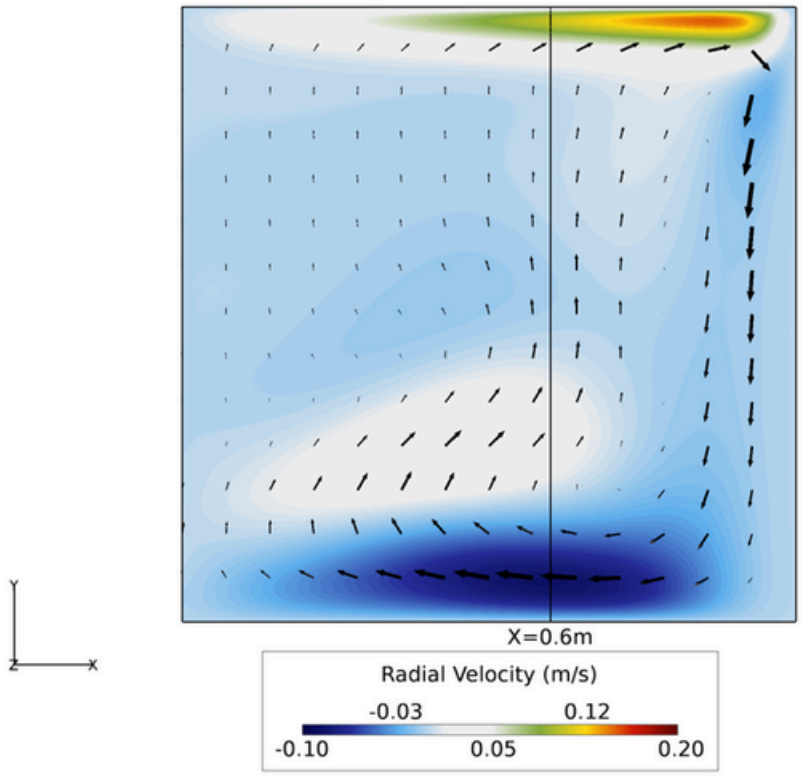


Figure 267: Contours of Radial Velocity with Velocity Vectors. This Image Shows the Front Face of the Modeled Cylinder Wedge, with the Center of Rotation on the Left Edge. The Vertical Line Represents a Radial Location 0.6 m From the Center of Rotation.

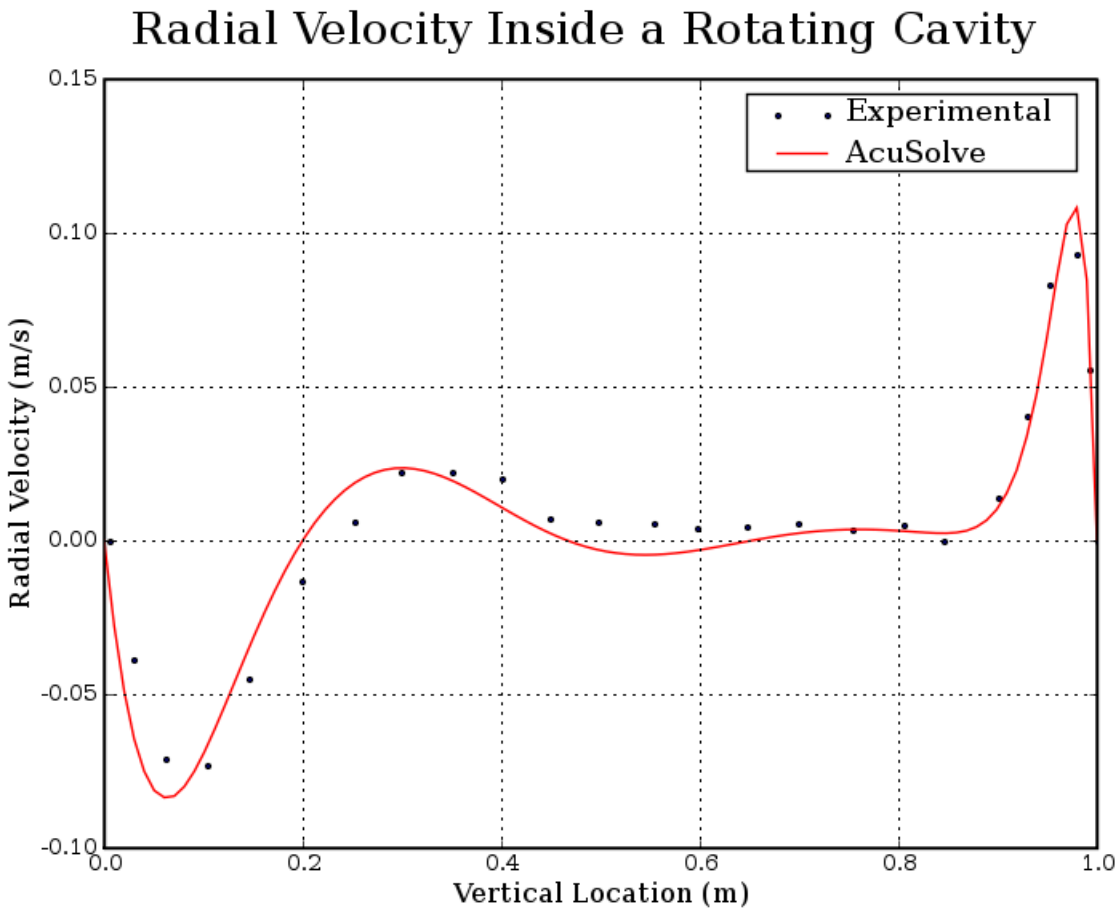


Figure 268: Radial Velocity (at 0.6 m From the Center of Rotation) as a Function of Vertical Location From Cylinder Bottom

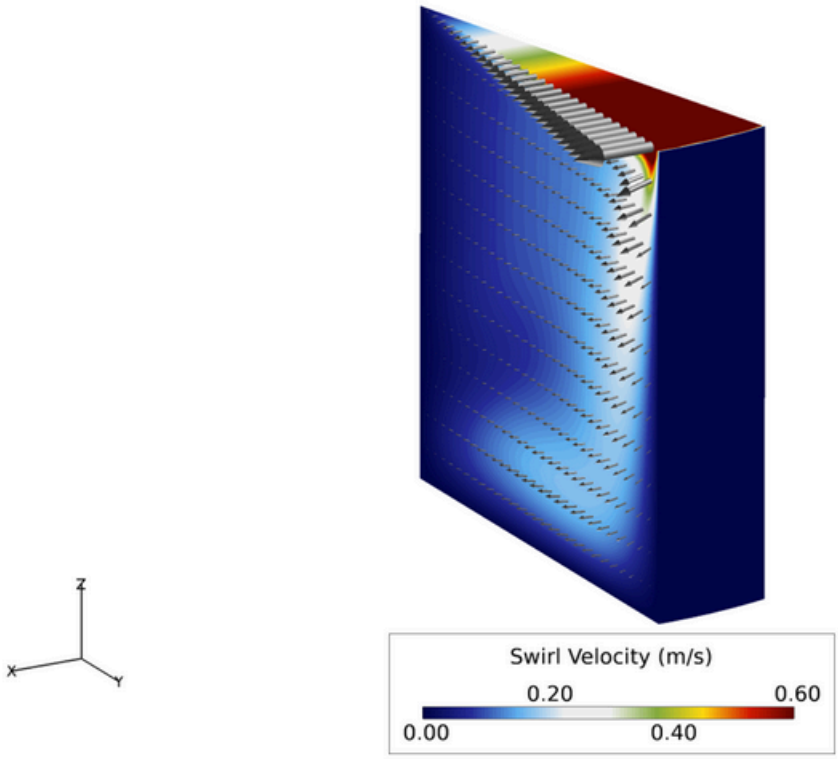


Figure 269: Contours of Swirl Velocity with Velocity Vectors

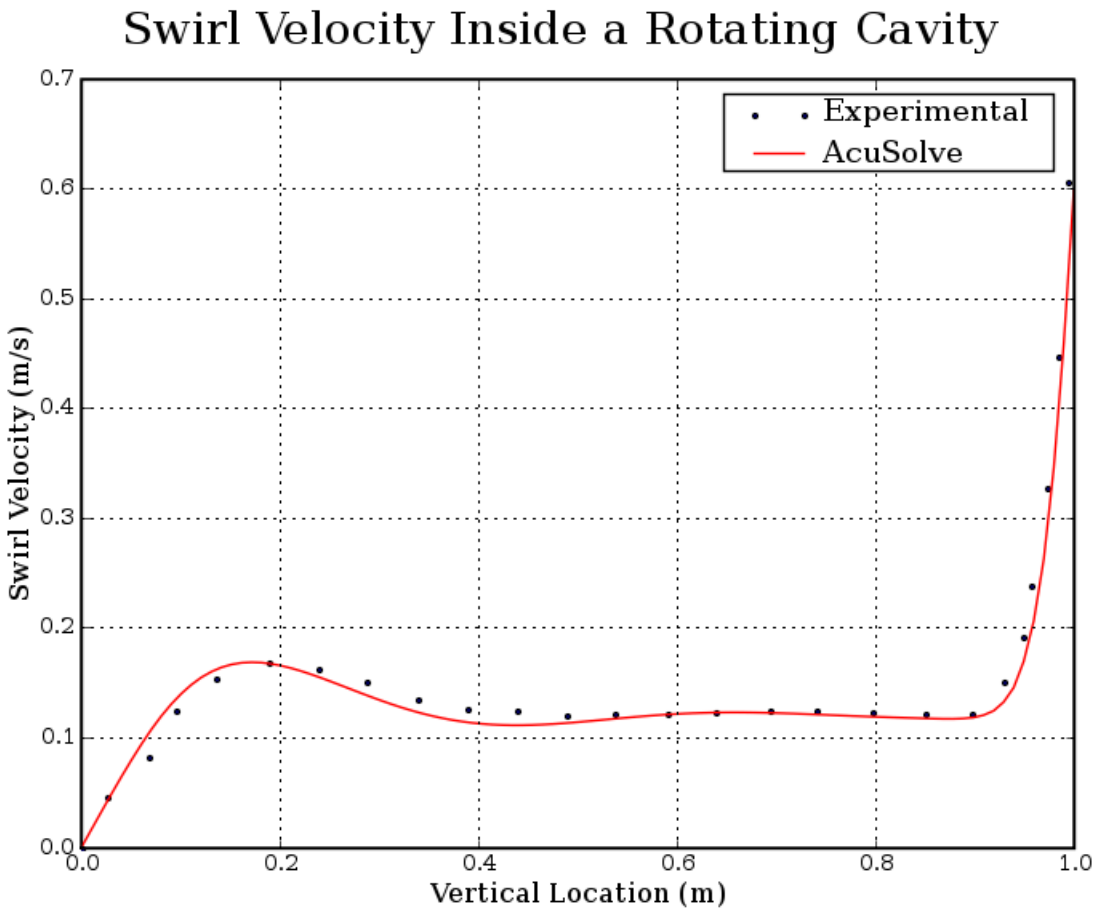


Figure 270: Swirl Velocity (at 0.6 m From Center of Rotation) as a Function of Vertical Location From the Cylinder Bottom

Summary

The AcuSolve solution compares well with the experimental data for flow induced by a rotating top of an enclosed cylinder. In this application, the flow in the fluid region is driven by the viscous stresses near the rotating top. Viscous stresses drag the fluid in a circular direction near the spinning wall. The angular velocity of the fluid decreases as distance from the top wall increases. Radial velocity develops as a result of the migration of the fluid toward the outer wall in regions of high angular velocity. The AcuSolve radial and swirl velocities compare very closely with the experimental data.

Simulation Settings for Flow Inside a Rotating Cavity

AcuConsole database file: `<your working directory>\cavity_rotating\cavity_rotating.acs`

Global

- Problem Description
  - Analysis type - Steady State
  - Turbulence Equation - Laminar
- Auto Solution Strategy

    - Relaxation Factor - `0.4`
- Material Model
    - Air
        - Density - `1.0` kg/m3
        - Viscosity - `0.000556` kg/m-sec
- Reference Frame
    - Cavity Rotation
        - Rotation center
            1. X-coordinate - `0.0`
            2. Y-coordinate - `0.0`
            3. Z-coordinate - `0.0`
        - Angular velocity
            1. X-component - `0.0`
            2. Y-component - `-1.0` rad/sec
            3. Z-component - `0.0`

    Model
- Volumes
    - Fluid
        - Element Set
            1. Material model - Air
- Surfaces
    - Bottom
        - Simple Boundary Condition
            1. Type - Wall
    - Max_X
        - Simple Boundary Condition
            1. Type - Wall
    - Max_Z
        - Simple Boundary Condition - (disabled to allow for periodic conditions to be set)
    - Min_Z
        - Simple Boundary Condition - (disabled to allow for periodic conditions to be set)
    - Top
        - Simple Boundary Condition
            1. Type - Wall
            2. Reference frame - Cavity Rotation
- Periodics
    - Periodic 1

- Periodic Boundary Condition
  1. Type - Axisymmetric
  2. Rotation axis
     1. point 1
        1. X-coordinate - `0.0` m
        2. Y-coordinate - `0.0` m
        3. Z-coordinate - `0.0` m
     2. point 2
        1. X-coordinate - `0.0` m
        2. Y-coordinate - `1.0` m
        3. Z-coordinate - `0.0` m

References

J. A. Michelsen. "Modeling of Laminar Incompressible Rotating Fluid Flow". AFM 86-05. Ph.D. thesis, Department of Fluid Mechanics, Technical University of Denmark. 1986.

Laminar Flow Past a 90° T-Junction

In this application, AcuSolve is used to simulate laminar flow through a channel with two outlets forming a T-junction. AcuSolve results are compared with experimental results adapted from Hayes and others (1989). The close agreement of AcuSolve results with experimental results validates the ability of AcuSolve to model cases with multiple outlet paths.

Problem Description

The problem consists of air flowing past a T-junction in a channel, as shown in the following image, which is not drawn to scale. Air enters the channel with an average velocity of 0.667 m/s and travels past the T-junction 2.0 m from the inlet. A portion of the flow will travel out of the branch of the channel due to the pressure difference between the bulk flow and the outlet of the branch.

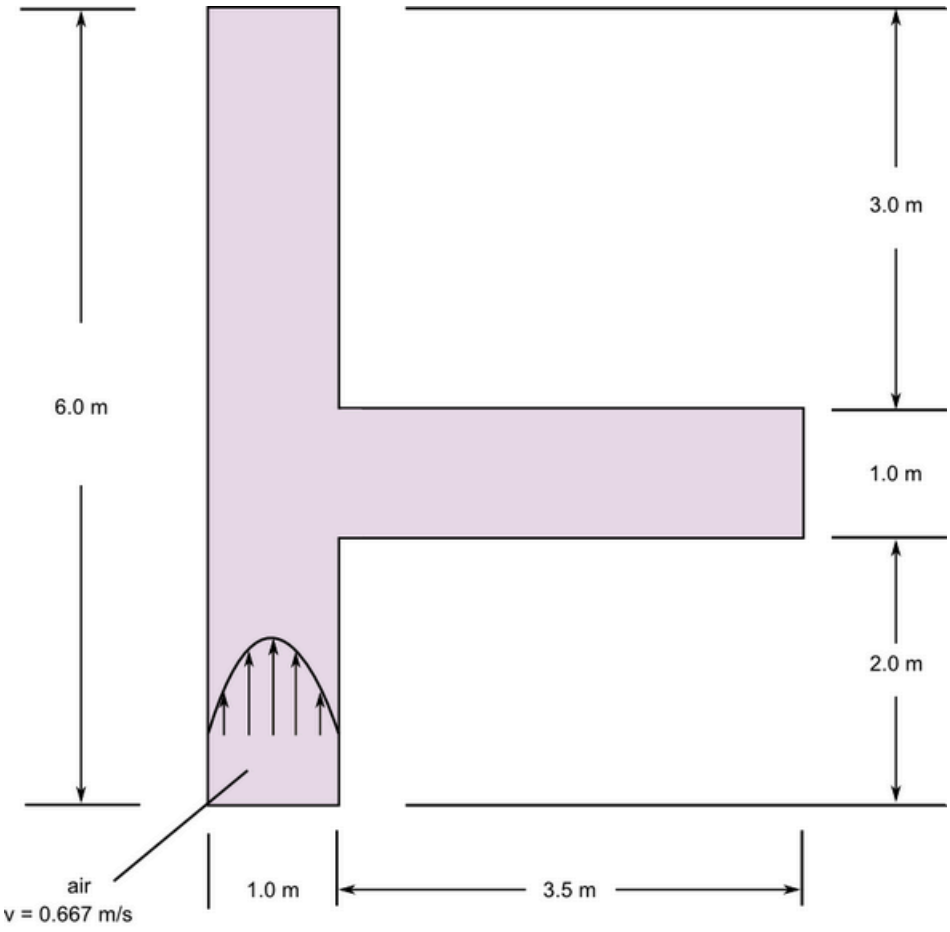


Figure 271: Critical Dimensions and Parameters for Simulating Laminar Flow Past a 90° T-Junction

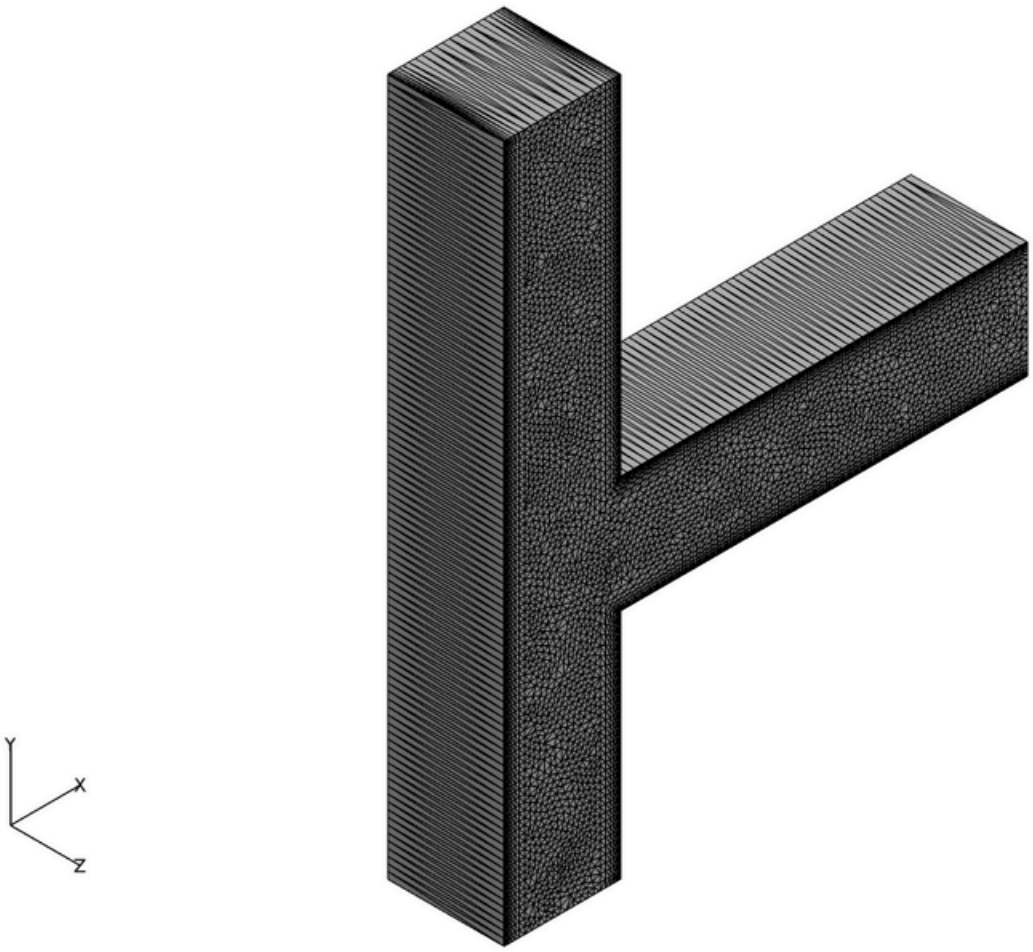


Figure 272: Mesh Used for Simulating Laminar Flow past a 90° T-Junction

AcuSolve Results

The AcuSolve solution converged to a steady state and the results reflect the mean flow conditions. As the air flows past the junction, a portion of it is diverted into the branch. A small recirculation region develops at the top of the junction and collapses before the flow exits the domain through the right branch.

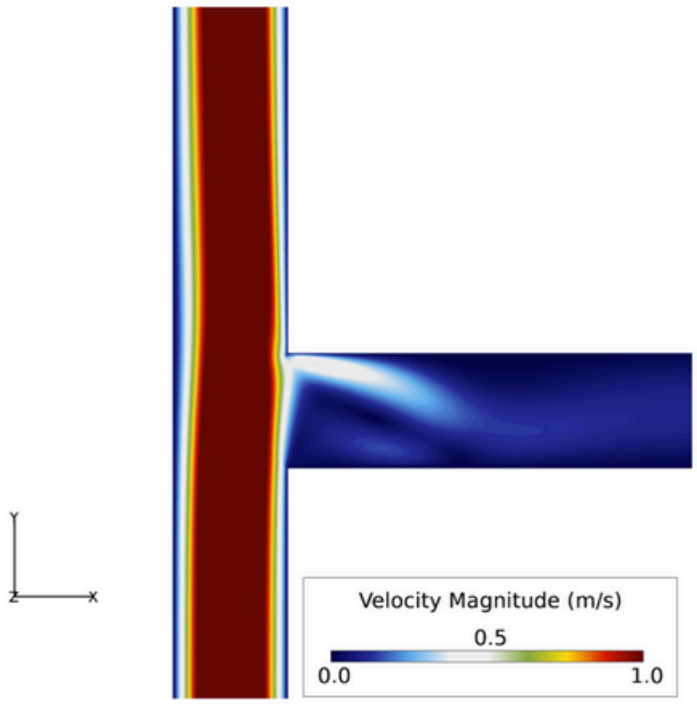


Figure 273: Velocity Contours in a T-Junction

The experimental value for the fraction of flow exiting the top branch of the channel is presented with the corresponding AcuSolve result in the following table.

Table 16:

	Experimental fractional flow	**AcuSolve fractional flow**	**Percent deviation from experimental**
Fractional flow exiting the upper branch	0.887	0.883	0.451

Summary

The AcuSolve solution compares well with experimental results for flow past a T-junction. In this application, flow is driven by a fixed flow rate at the inlet to the main branch. A portion of the flow from the main branch is diverted into the right branch of the T-junction, giving rise to recirculation just downstream of the junction. This recirculation collapses before the flow exits the side branch. The AcuSolve result for fractional flow exiting the top branch is within 0.451 percent of the experimental results.

Simulation Settings for Laminar Flow Past a 90° T-Junction

AcuConsole database file: `<your working directory>\T_junction_laminar\T_junction_laminar.acs`

Global

- Problem Description
  - Analysis type - Steady State
  - Turbulence equation - Laminar
- Auto Solution Strategy
  - Relaxation factor - `0.2`
- Material Model
  - Air
    - Type - Constant
    - Density - `1.0` kg/m3
    - Viscosity - `0.003333` kg/m-sec

  Model
- Volumes
  - Fluid
    - Element Set
      1. Material model - Air
- Surfaces
  - Inflow
    - Simple Boundary Condition
      1. Type - Inflow
      2. Inflow type - Average Velocity
      3. Average velocity - `0.6667` m/sec
  - Max_Z
    - Simple Boundary Condition - (disabled to allow for periodic conditions to be set)
  - Min_Z
    - Simple Boundary Condition - (disabled to allow for periodic conditions to be set)
  - Outflow
    - Simple Boundary Condition
      1. Type - Outflow
  - T_Out
    - Simple Boundary Condition
      1. Type - Outflow
  - Walls
    - Simple Boundary Condition

1 Type - Wall

- Periodics
  - Periodic 1
    - Periodic Boundary Condition
      1 Type - Periodic

References

R. E. Hayes, K. Nandkumar, and H. Nasr-El-Din. "Steady Laminar Flow in a 90 Degree Planar Branch". Computers and Fluids 17(4): 537-553. 1989.

Laminar Flow Through a Channel with Heated Walls

In this application, AcuSolve is used to simulate high Peclet number laminar flow through a channel with heated walls. AcuSolve results are compared with analytical results adapted from Hua and Pillai (2010). The close agreement of AcuSolve results with analytical results validates the ability of AcuSolve to model cases involving heat transfer to a moving fluid with a high Peclet number.

Problem Description

The problem consists of water at 20 °C flowing through a channel of infinite width with top and bottom walls heated to 75 °C. The channel is 0.2 m high and 0.8 m long, as shown in the following image, which is not drawn to scale. A centrally located slice 0.02 m wide is modeled with slip boundary conditions so that side-wall influences can be ignored. Water enters the channel with an average velocity of 0.003 m/s. As the fluid flows through the channel, it is heated by the top and bottom plates.

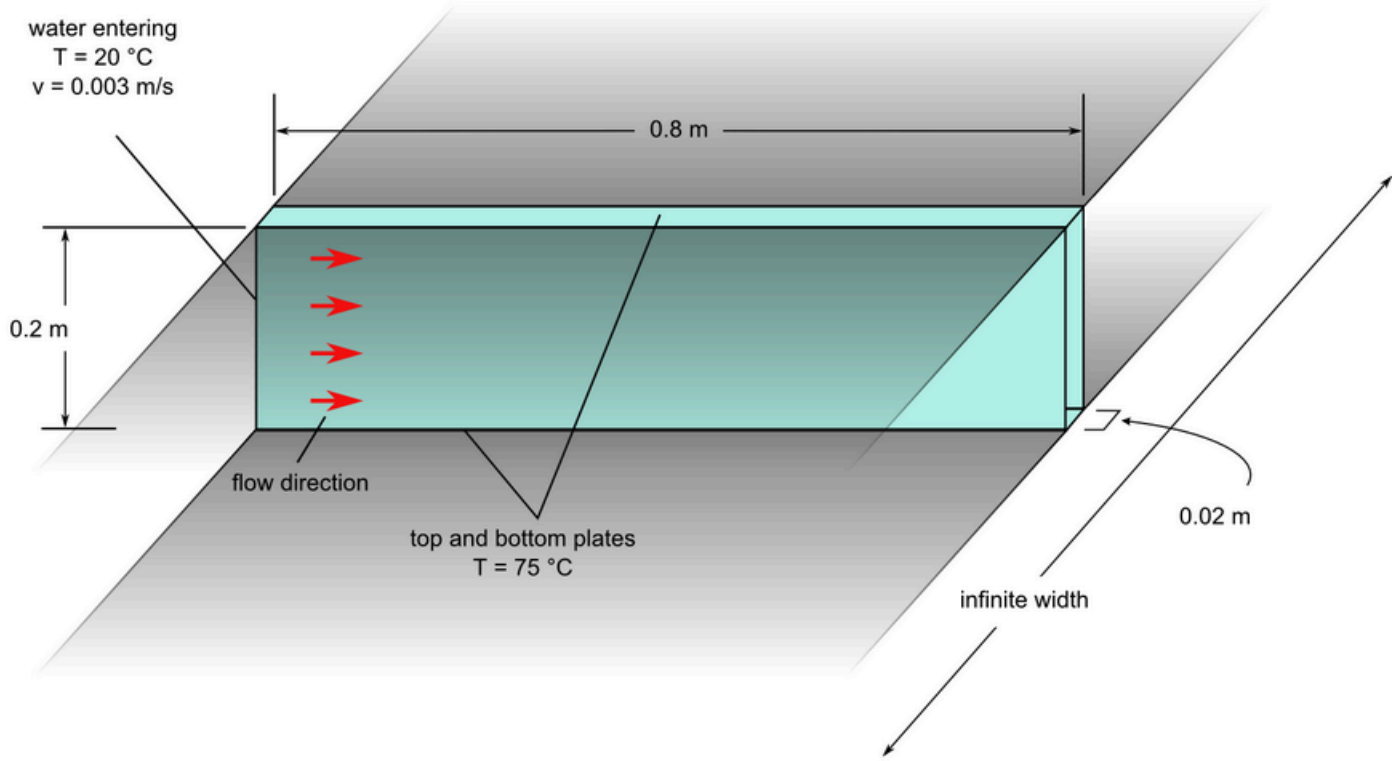


Figure 274: Critical Dimensions and Parameters for Simulating Laminar Flow Through a Channel with Heated Walls

The simulation was performed as a two dimensional problem by restricting flow in the out-of-plane direction through the use of a mesh that is one element thick. In addition, the symmetry of the geometry in the height direction is exploited to allow for modeling only half of the geometry. These characteristics allow for accurate simulation of flow while minimizing computational time.

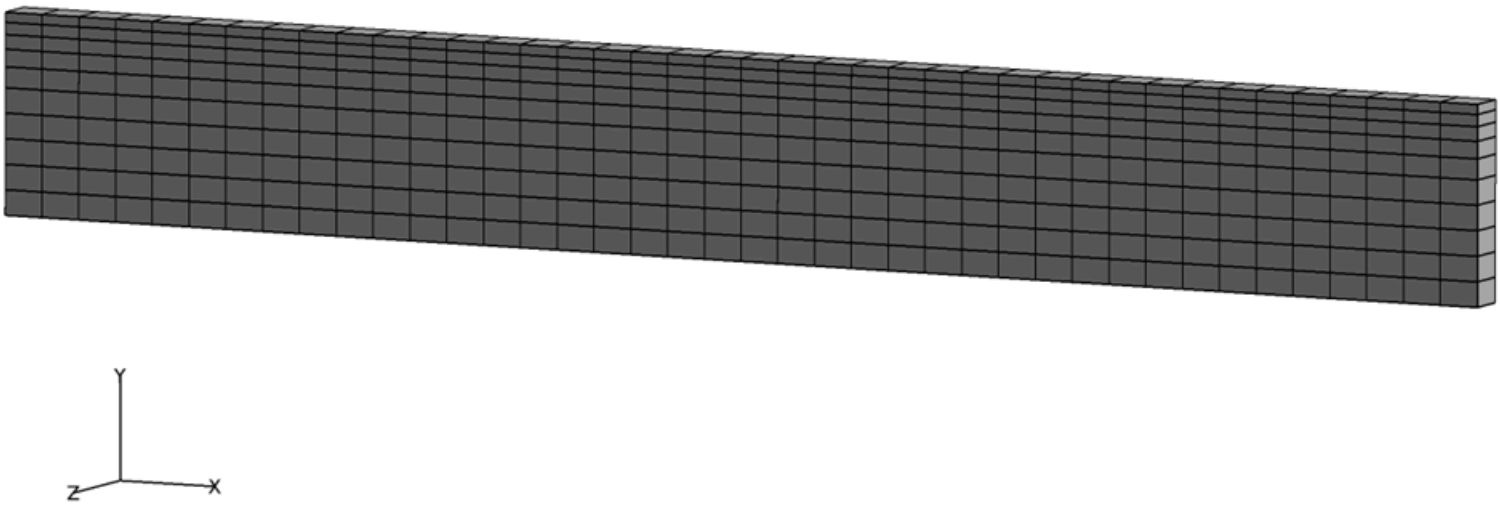


Figure 275: Mesh (Top Half of the Channel) used for Simulating Laminar Flow Through a Channel with Heated Walls

AcuSolve Results

The AcuSolve solution converged to a steady state and the results reflect the mean flow conditions. As the cool water enters the channel at temperature less than that of the walls, heat is transferred to the water by conduction. As the fluid travels along the channel, the temperature differential between the wall and the adjacent water decreases. The thermal boundary layer within the water develops as the flow propagates downstream.

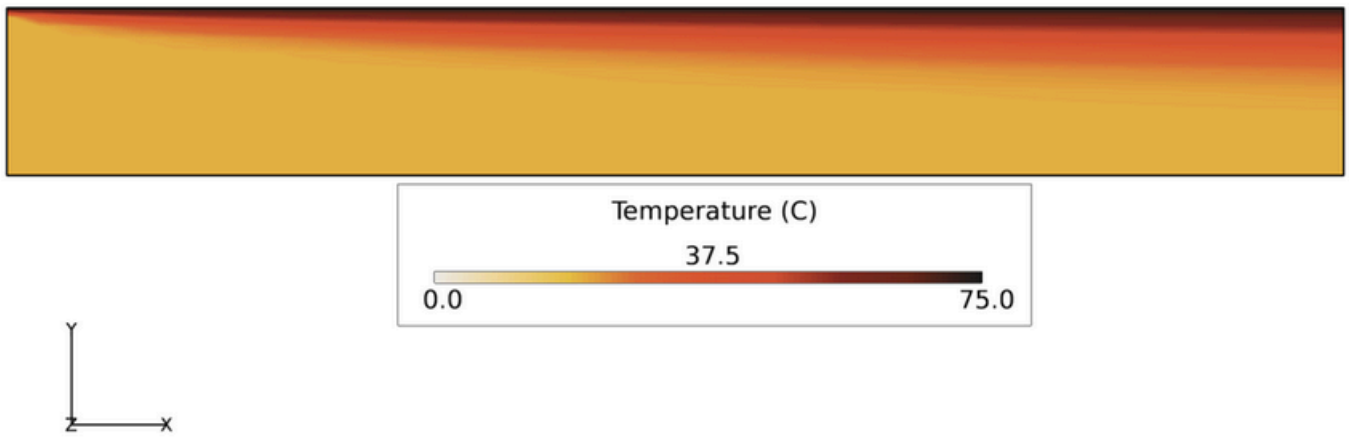


Figure 276: Temperature Contours Along the Top Half of a Heated Channel

Temperature at a specified vertical position in the channel increases along the length of the channel. The nature of that temperature change is dependent on proximity to the heated wall. Water in the center of the flow will have the least temperature change. Since this problem was solved for symmetrical flow, only the top half of the flow region was modeled. The vertical position for results

shown in the following figure are based on the center of flow having a Y-position of 0. For a vertical position near the center of flow (Y=0.0595) there is minimal change in temperature.

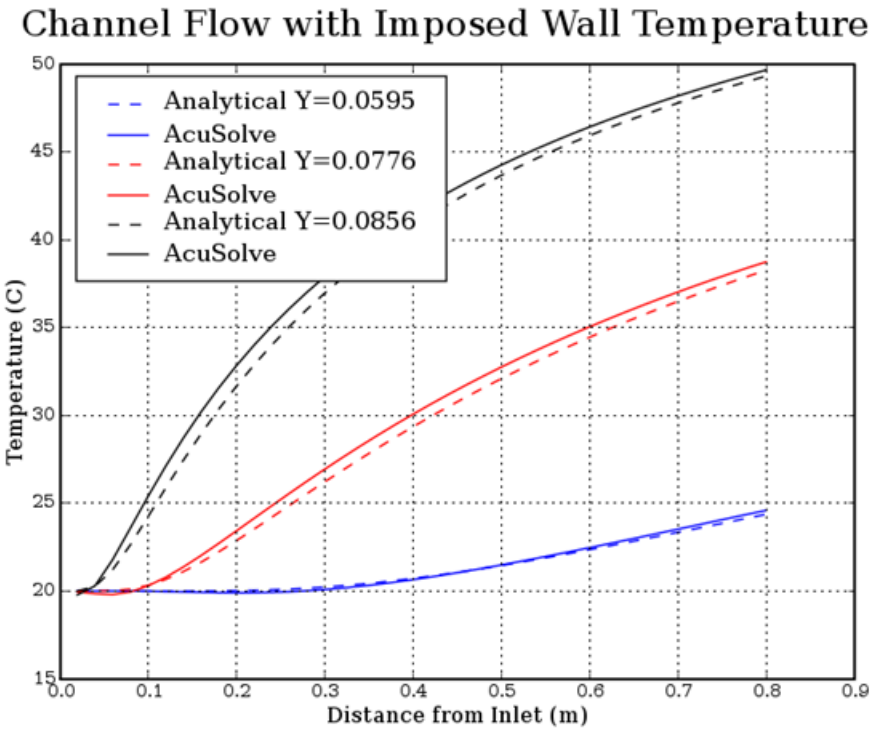


Figure 277: Temperature Plotted Against Distance from Inlet for 3 Different Heights from the Channel Center Line

Summary

The AcuSolve results compare well with the analytical results for the development of a thermal boundary layer in a heated channel. In this application, the model is set up to yield large gradients as the flow convects away from the inlet. The boundary conditions and mesh size were chosen specifically to yield a high Peclet number. The element Peclet number in the flow direction in this case is Pe=30.0, as calculated from the following equation.

$$Pe = \frac{\rho C p |v| he}{k} \tag{9}$$

where ρ is the density, CP the heat capacity, v the velocity, he the length, and k the thermal conductivity.

This example shows the robustness of the stabilized technique in AcuSolve when element Peclet number is high. Note that standard Galerkin finite element formulations become unstable when the element Peclet number is greater than 1.0.

Simulation Settings for Laminar Flow Through a Channel with Heated Walls

AcuConsole database file: `<your working directory>\channel_laminar_heat\channel_laminar_heat.acs`

Global

- Problem Description
  - Analysis type - Steady State
  - Temperature equation - Advective Diffusive
  - Turbulence equation - Laminar
- Auto Solution Strategy
  - Relaxation factor - `0.4`
- Material Model
  - Fluid_Material
    - Density - `1000.0` kg/m3
    - Specific Heat - `1000` J/kg-K
    - Viscosity - `1.0e-12` kg/m-sec
    - Conductivitiy - 1.0 W/m-K

  Model
- Volumes
  - Fluid
    - Element Set
      1. Material model - Fluid_Material
- Surfaces
  - Inlet
    - Simple Boundary Condition
      1. Type - Inflow
      2. Inflow type - Velocity
      3. X velocity - `0.003` m/sec
      4. Temperature - `20` °C
  - Outlet
    - Simple Boundary Condition
      1. Type - Outflow
  - Symm_MaxZ
    - Simple Boundary Condition
      1. Type - Slip
  - Symm_MinY
    - Simple Boundary Condition
      1. Type - Slip
  - Symm_MinZ
    - Simple Boundary Condition
      1. Type - Slip
  - Wall

- Simple Boundary Condition
  1. Type - Wall
  2. Temperature BC type - Value
  3. Temperature - 75 °C

References

Hua Tan and K. M. Pillai. "Numerical Simulation of Reactive Flow in Liquid Composite Molding Using Flux-Corrected Transport (FCT) Based Finite Element/Control Volume (FE/CV) Method". International Journal of Heat and Mass Transfer. 53:2256-2271, 2010.

Viscous Heating Inside a Rotating Annulus

In this application, AcuSolve is used to simulate fluid flow and viscous heating in an annulus formed by concentric cylinders. AcuSolve results are compared with analytical results adapted from Bird and others (1960). The close agreement of AcuSolve results with analytical results validates the ability of AcuSolve to model cases with viscous heating.

Problem Description

The problem consists of a viscous fluid filling the annulus between two concentric cylinders, as shown in the following image, which is not drawn to scale. The inner cylinder has a radius of 1.0 m and is fixed in place. The outer cylinder has a radius of 2.0 m and rotates with a constant angular velocity of 0.5 rad/s. The inner cylinder is held at a constant temperature of 273 K and the outer cylinder is held at 274 K.

The rotation of the outer cylinder causes the fluid to rotate due to the viscous shearing near the wall. As the inner cylinder is fixed, a velocity gradient is generated as a function of distance from the inner cylinder center. Viscous stresses within the domain generate significant amounts of heat, leading to a substantial increase in the fluid temperature in regions of high shear.

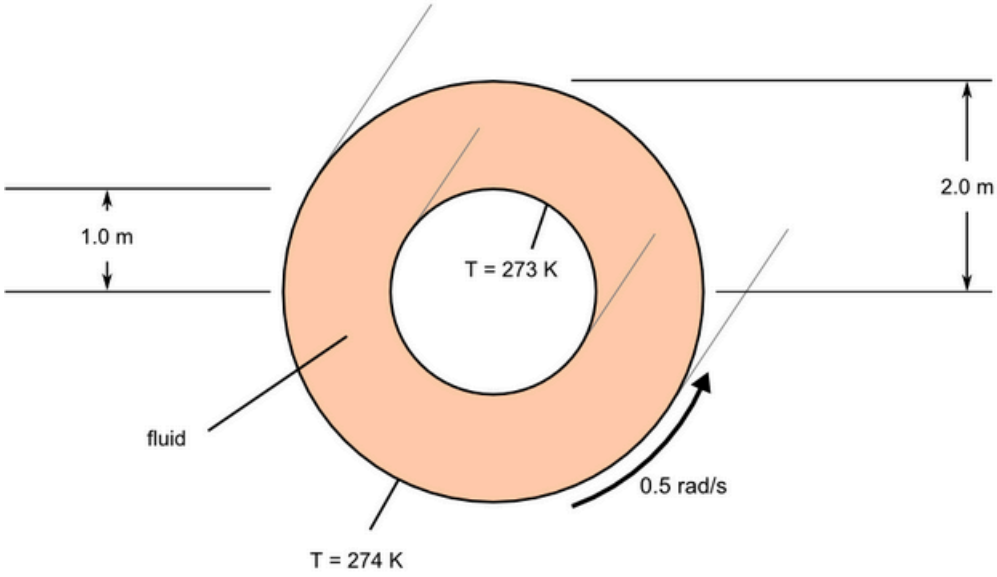


Figure 278: Critical Dimensions and Parameters for Simulating Viscous Heating Inside a Rotating Annulus

The simulation was performed as a two dimensional problem by constructing a volume mesh that contains a single layer of elements in the extruded direction, normal to the flow plane, and by imposing symmetry boundary conditions on the extruded planes.

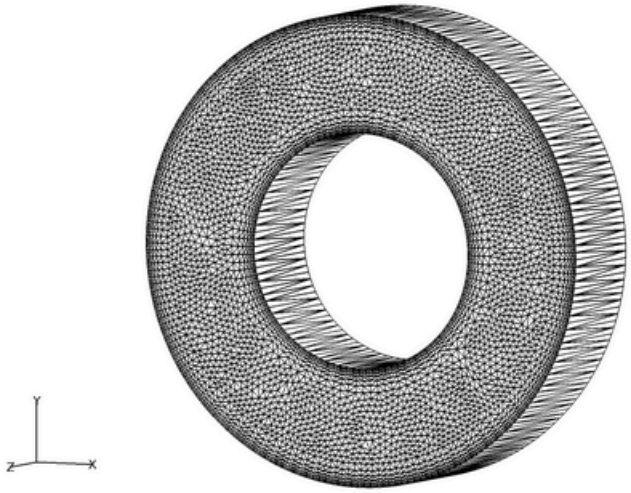


Figure 279: Mesh used for Simulating Viscous Heating Inside a Rotating Annulus

AcuSolve Results

The AcuSolve solution converged to a steady state and the results reflect the mean flow conditions. Flow is induced by the viscous shearing near the outer wall, creating a velocity gradient with the highest velocity near the moving wall.

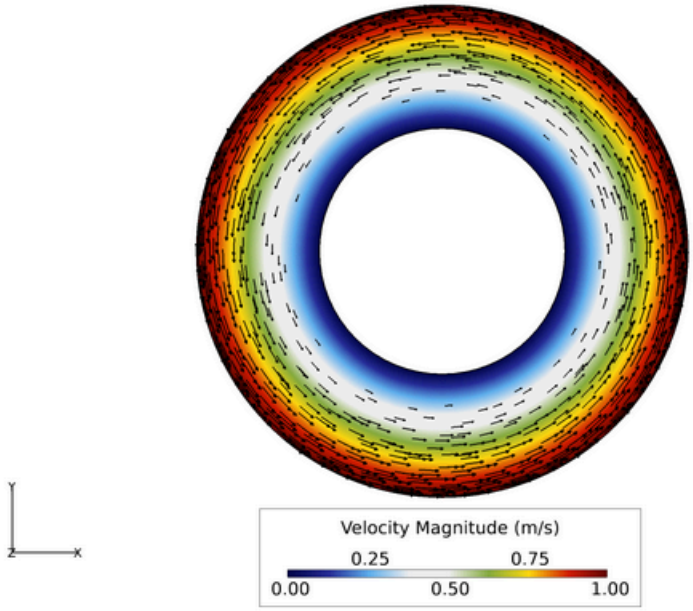


Figure 280: Contours of Velocity Magnitude and Velocity Vectors

The velocity gradient causes viscous heating, causing the fluid temperature to increase. The resulting temperature profile is nonlinear with the highest temperatures occurring in the space between the cylinders.

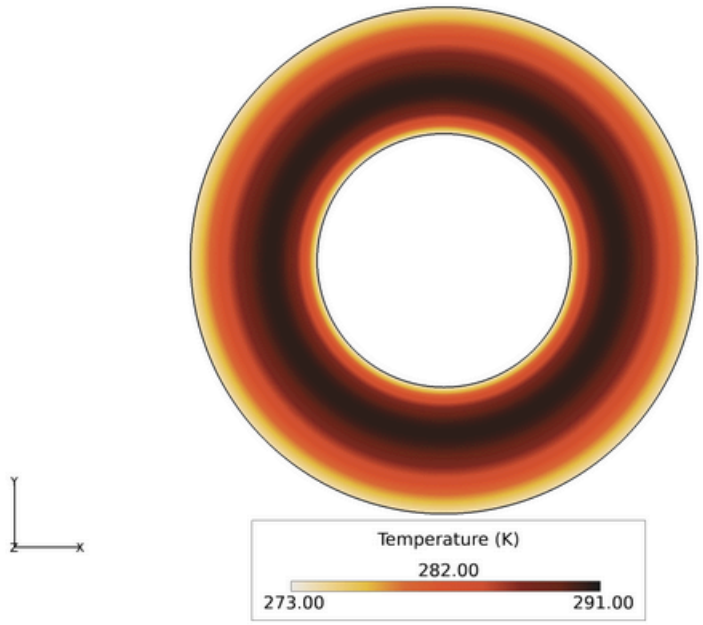


Figure 281: Contours of Temperature

AcuSolve results were compared to analytical results for velocity and for temperature across a range of radial locations.

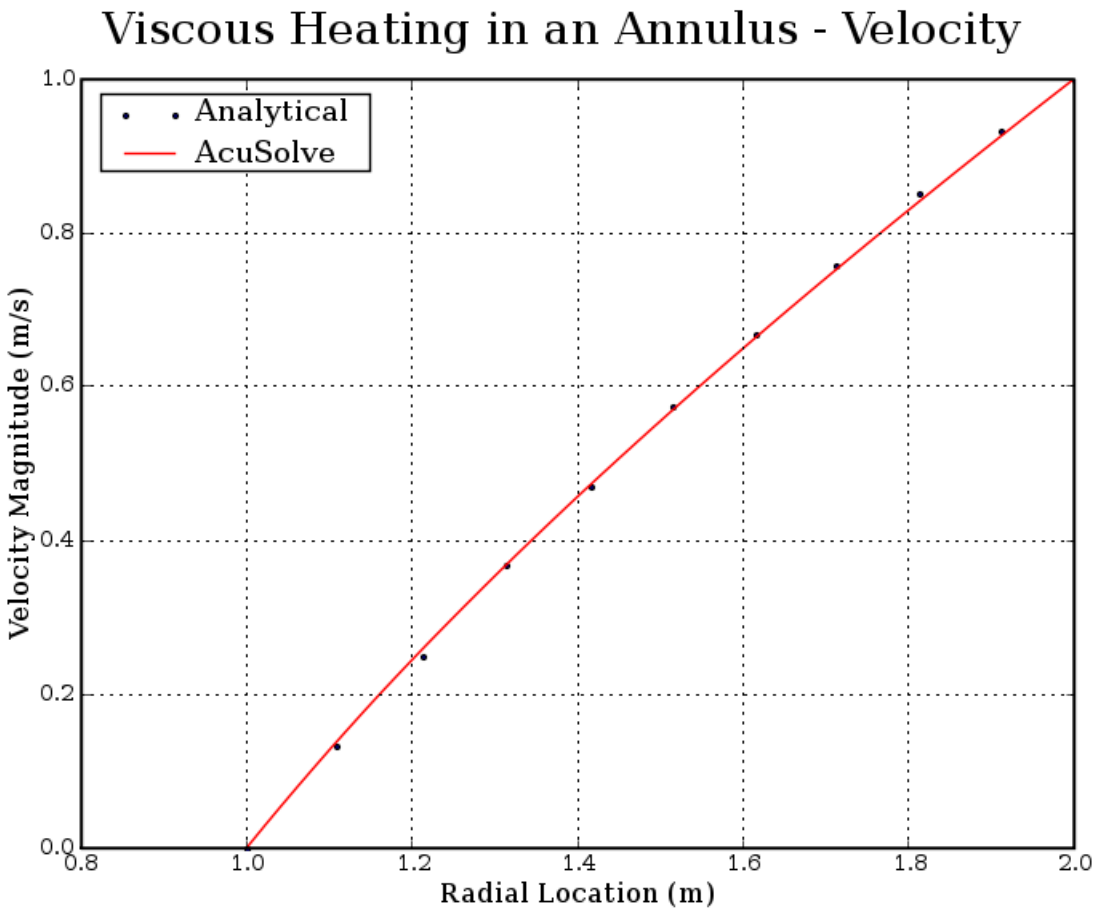


Figure 282: Velocity Magnitude Plotted Against Radial Location from the Center of the Inner Cylinder

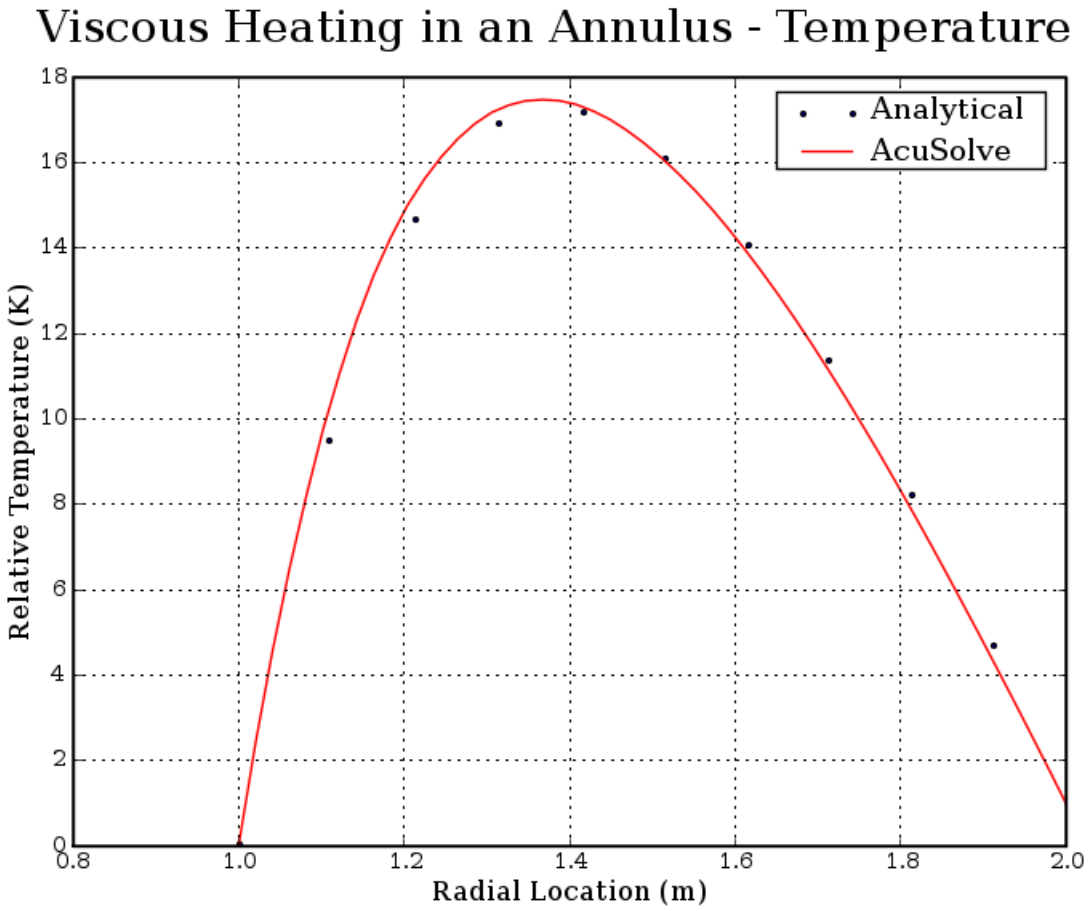


Figure 283: Temperature (Relative to the Inner Cylinder Wall Temperature) Plotted Against Radial Location from the Center of the Inner Pipe

Summary

The AcuSolve results compare well with the analytical results for both the flow field and the temperature across the annulus. In this application, flow is induced due to the viscous stresses generated by the rotation of the exterior cylinder. Velocity gradients between the cylinders give rise to shear stresses that induce frictional heating of the fluid. Due to the high viscosity of the fluid, the viscous heating is significant and leads to large increases in the temperature between the cylinders. This application validates the ability of AcuSolve to simulate flows where the viscous heating contribution is significant.

Simulation Settings for Viscous Heating Inside a Rotating Annulus

AcuConsole database file: `<your working directory>\annulus_rotating_heat\annulus_rotating_heat.acs`

Global

- Problem Description
  - Analysis type - Steady State
  - Temperature equation - Advective Diffusive

    - Turbulence equation - Laminar
- Auto Solution Strategy
    - Relaxation factor - `0.2`
- Material Model
    - Fluid
        - Density - `1.0` kg/m3
        - Viscosity - `300` kg/m-sec
        - Conductivity - `1.0` W/m-K
- Reference Frame
    - Outer_Rotation
        - Angular Velocity
            1. X-component - `0.0` rad/sec
            2. Y-component - `0.0` rad/sec
            3. Z-component - `0.5` rad/sec

Model

- Volumes
    - Fluid
        - Element Set
            1. Material model - Fluid
            2. Viscous heating - On
- Surfaces
    - Inner_Cylinder
        - Simple Boundary Condition
            1. Type - Wall
            2. Temperature BC type - Value
            3. Temperature - `273.0` K
    - Outer_Cylinder
        - Simple Boundary Condition
            1. Type - Wall
            2. Reference frame - Outer_Rotation
            3. Temperature BC type - Value
            4. Temperature - `274.0` K
    - Symm_MaxZ
        - Simple Boundary Condition
            1. Type - Symmetry
    - Symm_MinZ
        - Simple Boundary Condition

1 Type - Symmetry

- Nodes
  - Node 1
    - Pressure
      1 Type - Zero

References

R. B. Bird, W. E. Stewart, and E. N. Lightfoot. "Transport phenomena". New York, John Wiley and Sons, 1960

Oscillating Laminar Flow Around a Circular Cylinder

In this application, AcuSolve is used to simulate two dimensional, laminar flow over a cylinder to predict separation of flow from the cylinder surface and the flow in the wake area. AcuSolve results are compared with experimental results as described in Tritton (1959). The close agreement of AcuSolve results with experimental results validates the ability of AcuSolve to model cases with unsteady oscillating vortex streets.

Problem Description

The problem consists of a cylinder located in a rectangular domain, as shown in the following image, which is not drawn to scale. A fluid enters the domain with a low velocity (v) of 0.5 m/s. The diameter (D) of the cylinder is 20 cm. The domain extends 10 X D upstream of the cylinder center, 5D above and below the cylinder center, and 40D downstream of the cylinder center. The density of the working fluid is 1 kg/m^3 and the viscosity is 0.001 kg/m-s. The Reynolds number for this problem is 100.

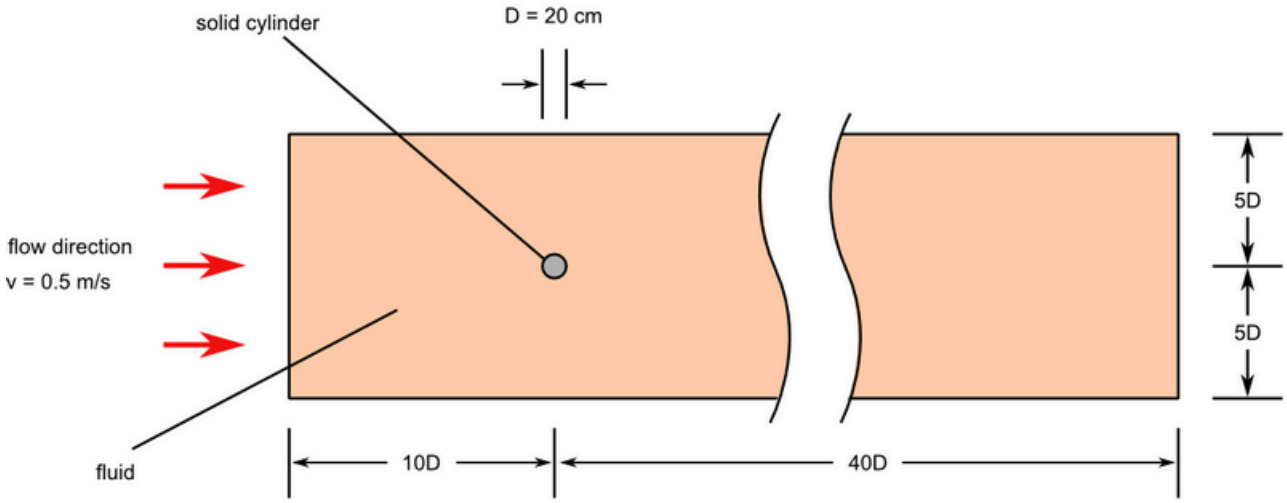


Figure 284: Critical Dimensions and Parameters for Simulating Oscillating Laminar Flow Around a Circular Cylinder

The simulation was performed as a two dimensional problem by constructing a volume mesh that contains a single layer of elements in the extruded direction, normal to the flow plane, and by imposing symmetry boundary conditions on the extruded planes.

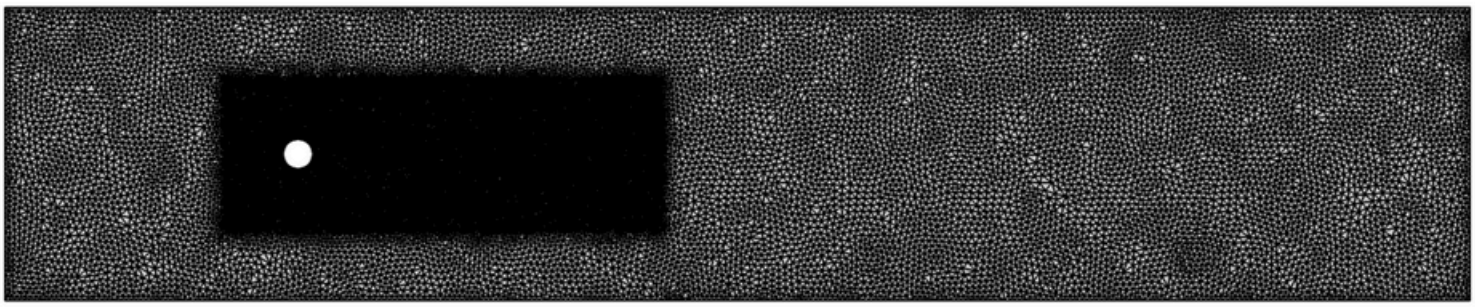


Figure 285: Mesh used for Simulating Oscillating Laminar Flow Around a Circular Cylinder

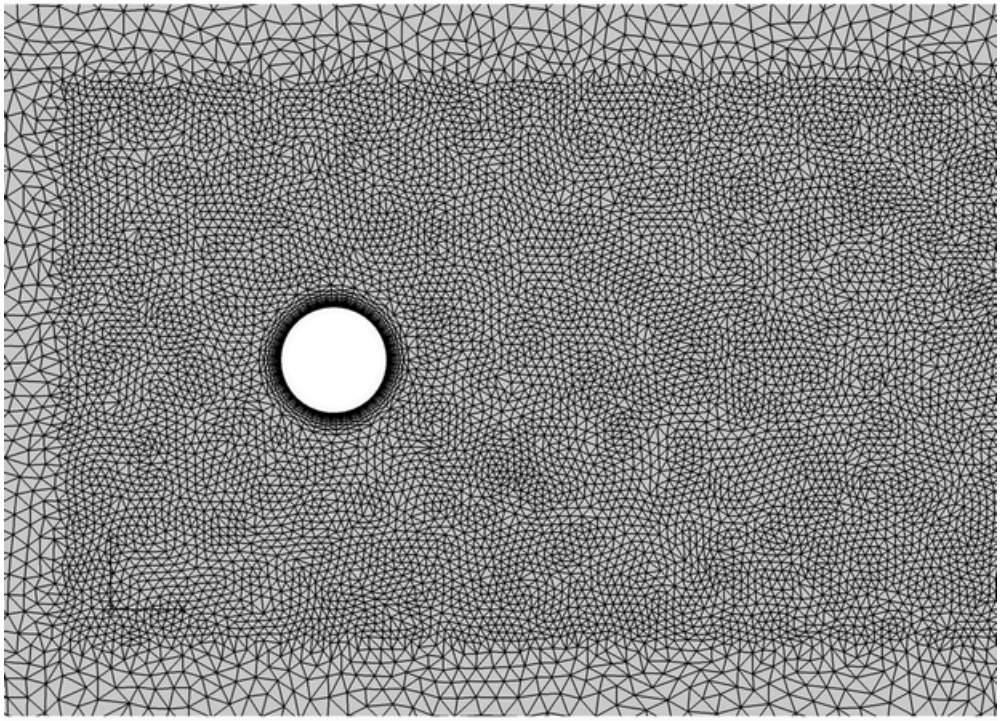


Figure 286: Details of the Mesh Showing Refinement Zone Around the Cylinder

AcuSolve Results

The simulation was run as transient for a time record sufficient to ensure that the vortex shedding in the wake reached a stabilized oscillation frequency. The AcuSolve solution shows an unsteady, oscillating flow field with flow around the cylinder separating from the cylinder surface. A wake area is developed downstream of the cylinder with alternating vortices shedding at a regular frequency from the top and bottom of the cylinder surface. This results in oscillating lift forces that act on the cylinder as shown in the following images.

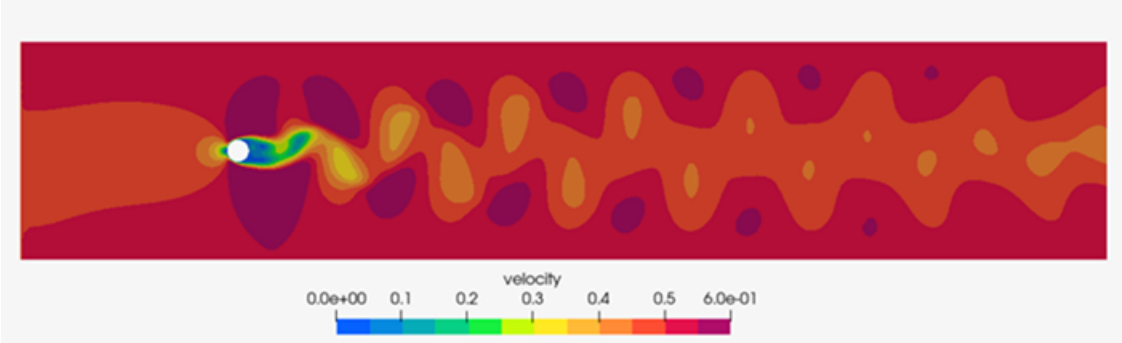


Figure 287: Contours of Velocity Magnitude

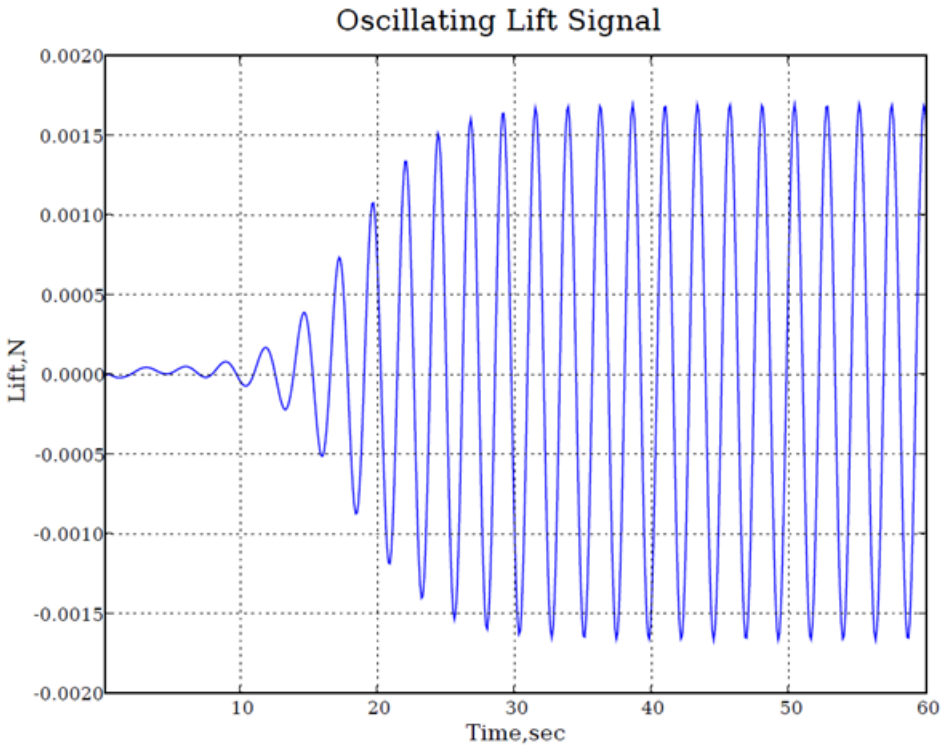


Figure 288: Lift Coefficient (lift force perpendicular to flow) plotted against time. Simulation was run for 600 time steps for a duration of 60 s

The Strouhal number for this simulation, a dimensionless number describing oscillating flows, is used to validate AcuSolve results. The experimental Strouhal number for this problem is given by

$$St = \frac{\omega^* L}{v} = 0.165 \qquad (10)$$

where ω is the dominant frequency of oscillations, L is the diameter of the cylinder, and v is the flow velocity.

The peak frequency of the oscillating lift force was computed by transforming the time dependent data into frequency space with a Fourier transform. From the Fourier transform, the AcuSolve-based Strouhal

number was calculated. The table below shows the comparison of the Strouhal number provided by the AcuSolve prediction and the measurement given by Tritton (1959).

Table 17:

	Experimental	**AcuSolve**
Strouhal number	0.165	0.173

Summary

In this application, two dimensional flow over a cylinder is achieved by enforcing symmetry conditions on the front and back surfaces of the flow domain. The laminar, unsteady simulation shows the flow separation that leads to alternating vortex shedding. Frequency of the lift force acting on the cylinder is calculated to evaluate the Strouhal number. The AcuSolve solution compares well with results reported by Tritton (1959), differing slightly from the experimental results. In this application, AcuSolve demonstrates the ability to accurately predict oscillating laminar flow around a circular cylinder.

Simulation Settings for Oscillating Laminar Flow Around a Circular Cylinder

HyperWorks CFD database file: `<your working directory>\cylinder_laminar\cylinder_laminar.hm`

Global

- Problem Description
  - Analysis type - Transient
  - Turbulence equation - Laminar
- Auto Solution Strategy
  - Analysis type - Transient
  - Max time - `600` sec
  - Initial time increment - `0.1` sec
- Material Model
  - Fluid
    - Density - `1.0` kg/m3
    - Viscosity - `1.0e-3` kg/m-sec

  Model
- Volumes
  - Volume
    - Element Set
      1. Material model - Fluid
- Surfaces
  - Back
    - Simple Boundary Condition
      1. Type - Symmetry

- Base
  - Simple Boundary Condition
    1. Type - Slip
- Front
  - Simple Boundary Condition
    1. Type - Symmetry
- Inflow
  - Simple Boundary Condition
    1. Type - Inflow
    2. Inflow Type - Average velocity
    3. Average Velocity - `0.5` m/sec
- Outflow
  - Simple Boundary Condition
    1. Type - Outflow
- Top
  - Simple Boundary Condition
    1. Type - Slip

References

D.J. Tritton. "Experiments on the Flow around a Circular Cylinder at Low Reynolds Number". Journal of Fluid Mech. 6(04):547-567. 1959

Ideal Gas Compression in an Actuating Piston

In this application, AcuSolve is used to simulate pressure and temperature inside an actuating piston using the ideal gas relationship and fully defined mesh motion. AcuSolve results are compared with analytical results as described in Moran and Shapiro (2000). The close agreement of AcuSolve results with analytical results validates the ability of AcuSolve to model cases with material properties defined by the ideal gas law subjected to significant mesh distortion.

Problem Description

The problem consists of air compressed by a piston within a cylinder 10 m long with a diameter of π (3.14159) m, as shown in the following image, which is not drawn to scale. The piston is driven by a crankshaft 4 m long attached to a connecting rod 6 m long. The crankshaft rotates at 60o/s around a center point. At time (t) = 0.0 s the crank and piston are at top dead center (TDC) with an initial cylinder volume of 80 m^3. At t = 3.0 s the piston is at bottom dead center (BDC), at which point the volume in the cylinder is reduced to 16 m^3. The piston then moves back to TDC at t = 6.0 s. Air at atmospheric conditions, with material properties of an ideal gas and a dynamic viscosity of 1.781 X 10^5 kg/m-sec is the fluid modeled in the domain.

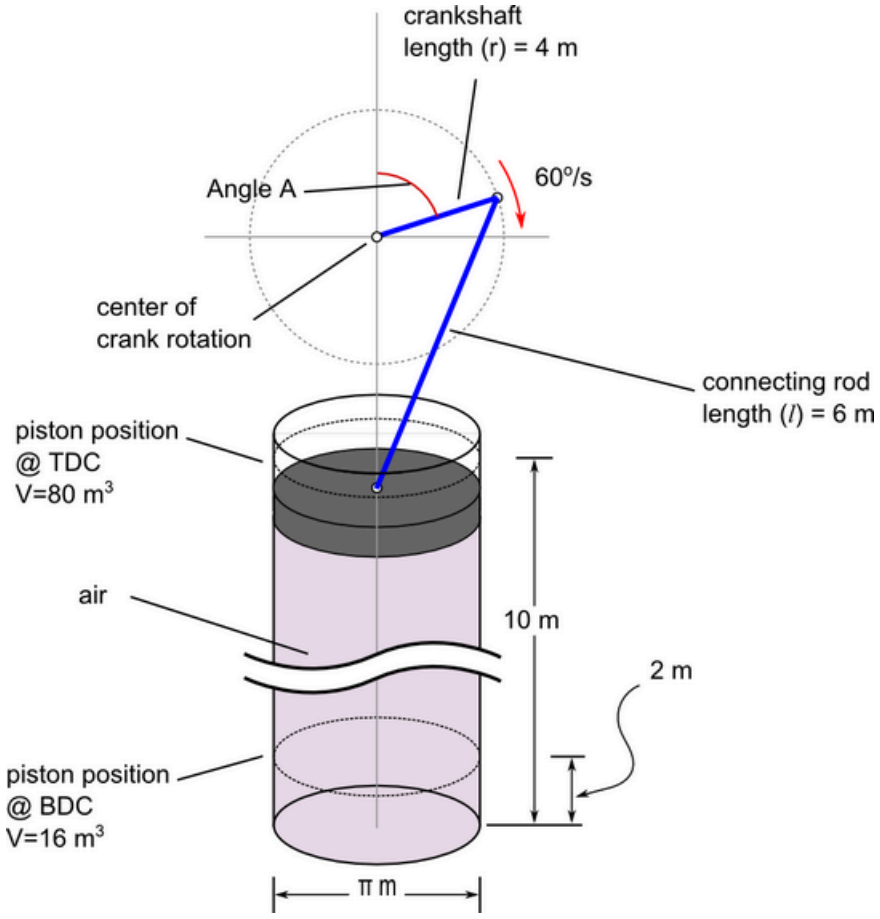


Figure 289: Critical Dimensions and Parameters for Simulating Ideal Gas Compression in an Actuating Piston

The motion of the piston is described by the following equation.

$$x = r*\cos A + \sqrt{l^2 - r^2 \sin^2 A} \quad (11)$$

Where

- x is the distance of the piston from TDC
- r is the length of the connecting rod, 4 m
- A is the crank angle as a function of time (t)
- l is the connecting rod length, 6 m

During the simulation, the top surface of the cylinder, representing the piston, moves with an applied mesh motion that mimics the motion of the reciprocating crank, rod, and piston assembly. The ideal gas is compressed by contracting the mesh according to the motion of that assembly and by allowing the fluid properties to change as a function of time.

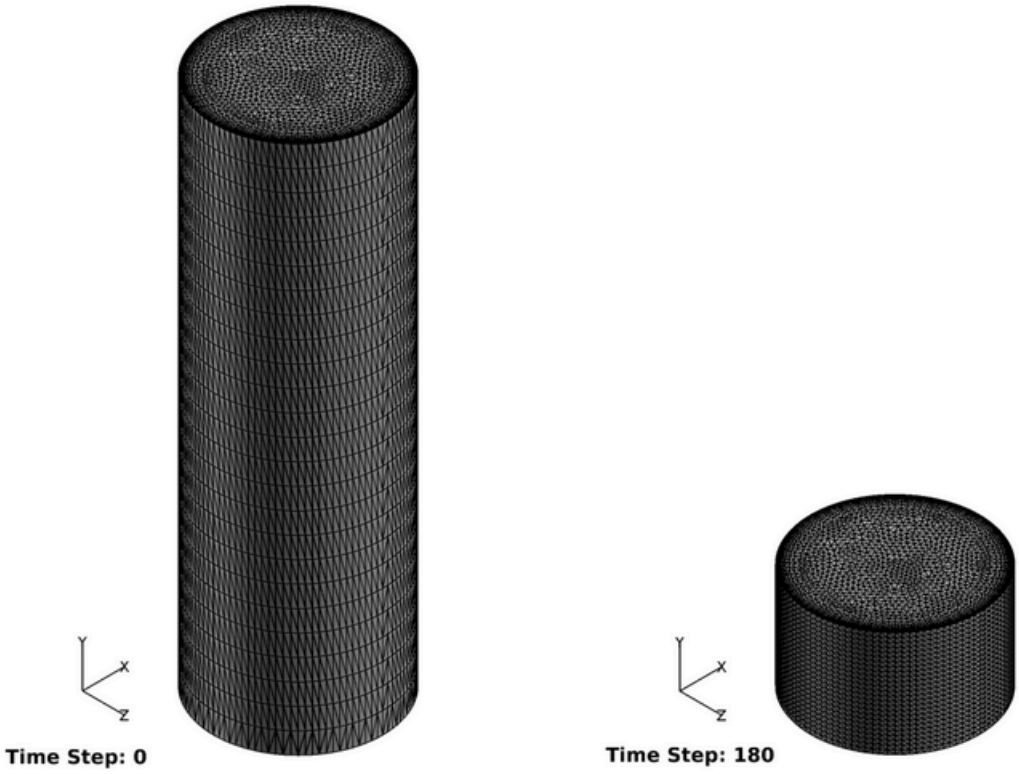


Figure 290: Mesh Used for Simulating Ideal Gas Compression in an Actuating Pistion at Time Step 0 and Time Step 180 (3 s)

AcuSolve Results

The simulation was run as transient for a total of 360 time steps with a duration of 6.0 seconds. The AcuSolve solution shows time dependent pressure and temperature in a cylinder volume that compresses and expands in a 6.0 second cycle. Pressure and temperature increase as the cylinder volume decreases, and returns toward initial conditions as the cylinder volume expands. The contours of pressure and temperature within the cylinder at the initial stage (t = 0.0 s) and the half cycle (t = 3.0 s) are shown in the following images.

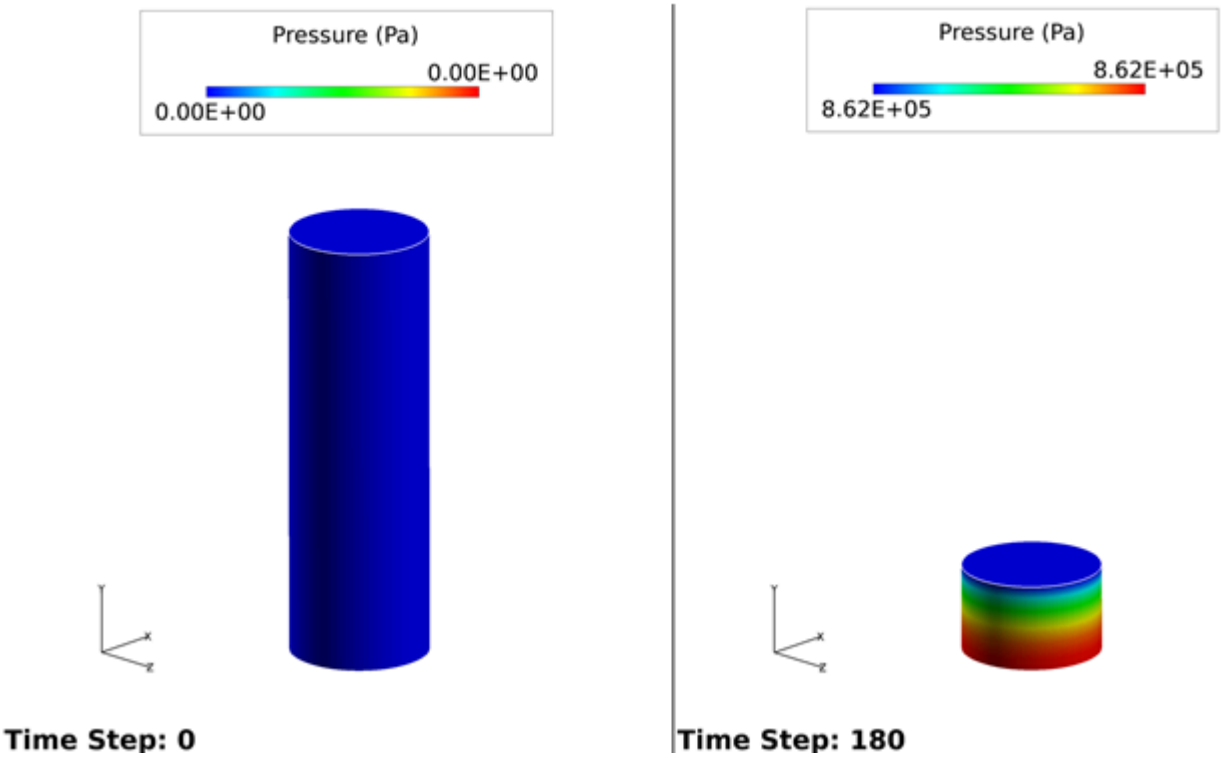


Figure 291: Pressure Distribution Within the Domain with the Piston at TDC and BDC

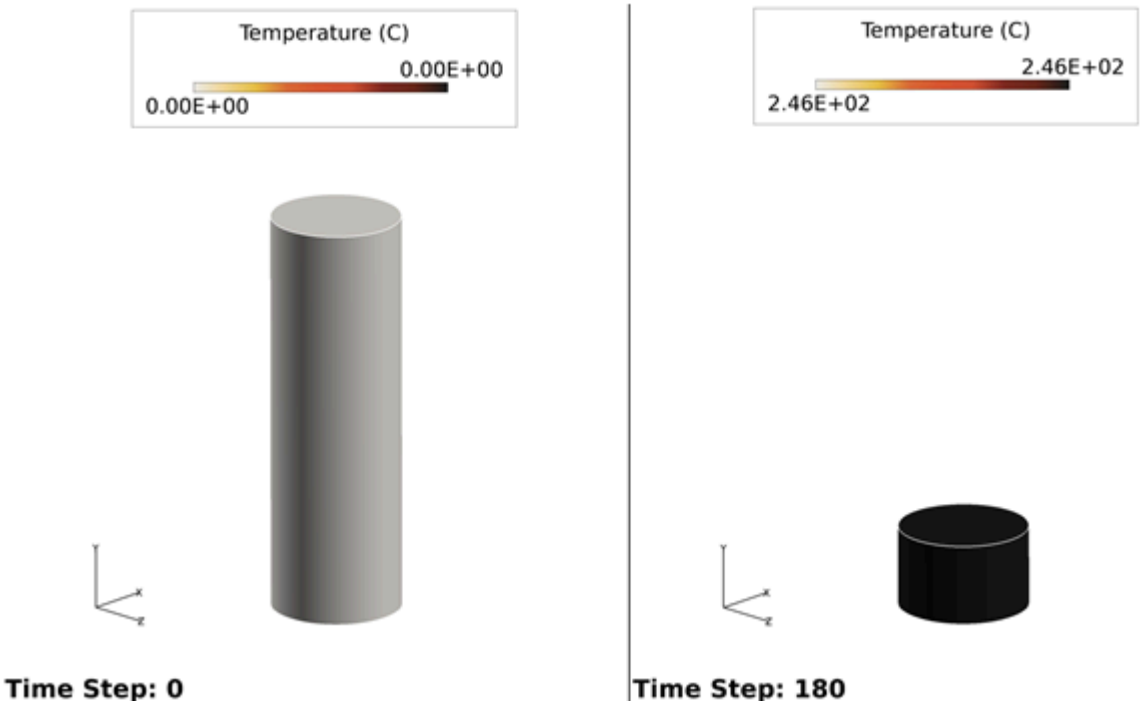


Figure 292: Temperature Distribution Within the Domain with the Piston at TDC and BDC

Comparison of time history plots of the AcuSolve and analytical solutions shows that the AcuSolve solution is nearly identical to the analytical solution. The AcuSolve computed internal pressure reaches a maximum of 8.62 X 105 Pa and the temperature reaches a maximum of 246.45 degrees C.

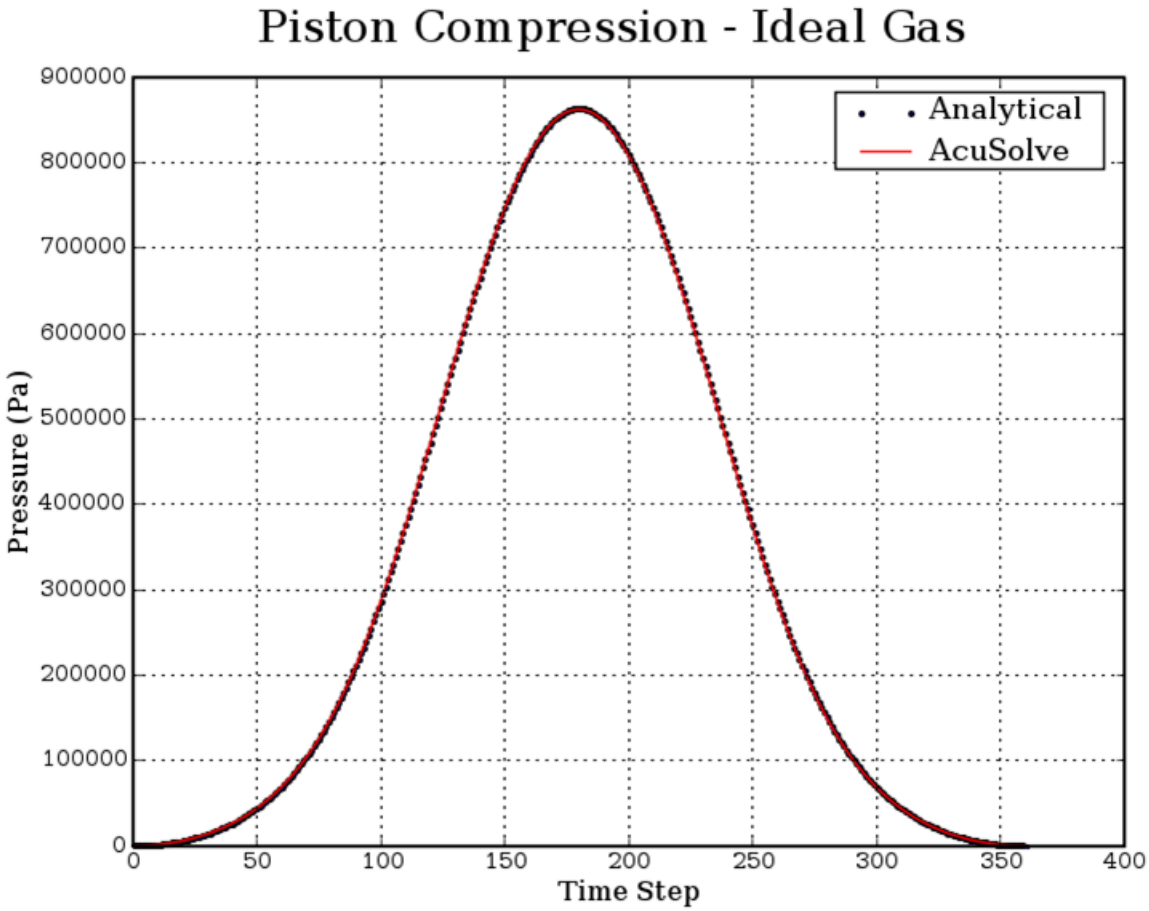


Figure 293: History Plots of Pressure for AcuSolve and Analytical Solutions

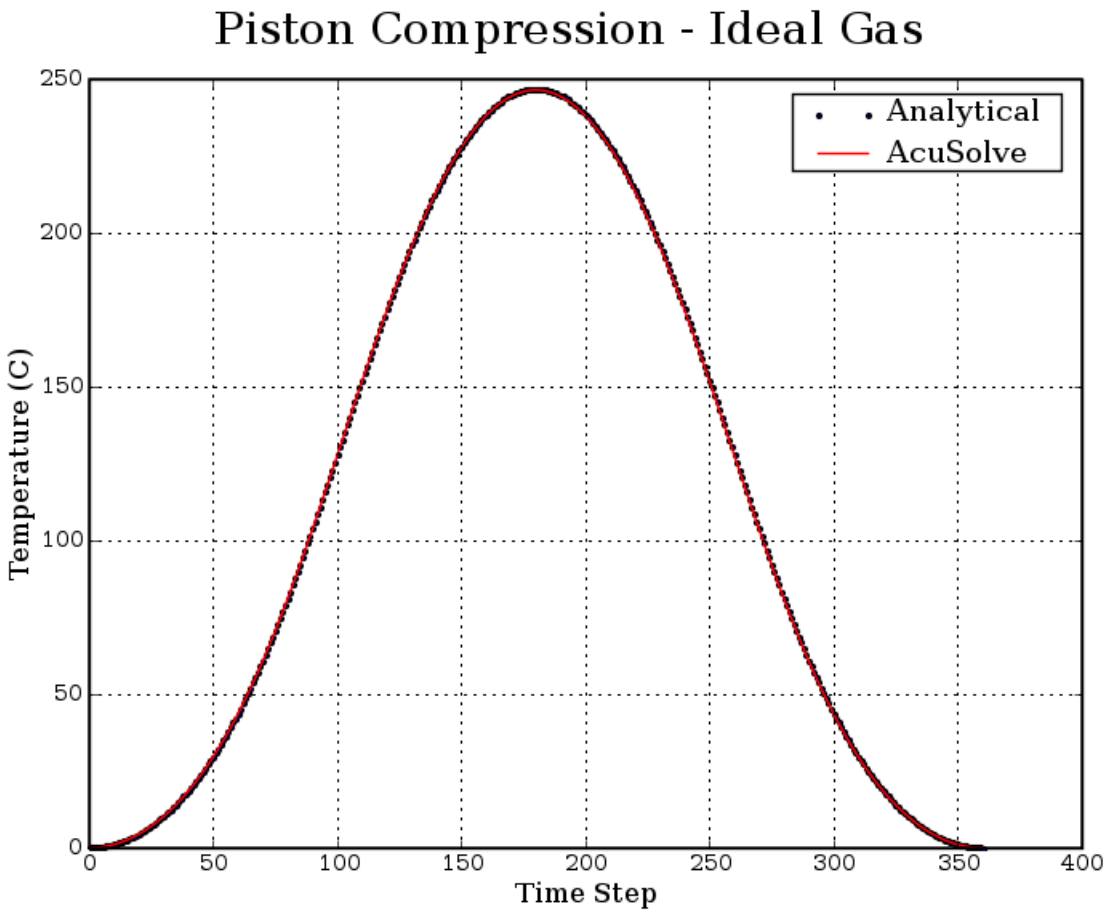


Figure 294: History Plots of Temperature for AcuSolve and Analytical Solutions

Summary

The AcuSolve solution compares well with analytical results for ideal gas compression in an actuating piston. The AcuSolve transient solution compares nearly identically with the analytical solution, with 0.1 percent and 0.16 percent error for the maximum pressure and temperature, respectively. As a result, AcuSolve demonstrates the ability to predict ideal gas compression in an actuating piston.

Simulation Settings for Ideal Gas Compression in an Actuating Piston

AcuConsole database file: `<your working directory>\cylinder_piston_compression\cylinder_piston_compression.acs`

Global

- Problem Description
  - Analysis type - Transient
  - Temperature equation - Advective Diffusive
  - Turbulence equation - Laminar
  - Mesh type - Fully Specified

- Auto Solution Strategy
  - Max time steps - `360`
  - Initial time increment - `0.01667` sec
  - Convergence tolerance - `1.0e-5` sec
  - Max stagger iterations - `10`
- Multiplier Function
  - Piston
    - Type - Piecewise Linear
    - Curve fit variable - Time
    - Curve fit values - (included in `.acs` based on equation discussed in problem description)
- Material Model
  - Air
    - Density
      1. Type - Ideal Gas
      2. Gas constant - `286.9` J/kg-K
      3. Abs. pressure offset - `101325.0` N/m2
      4. Abs. temperature offset - `273.15` K
    - Viscosity - `1.781e-5` kg/m-sec
- Mesh Motion
  - Piston
    - Type - Translation
    - Translation velocity - `0.0`, `-1.0`, `0.0`
    - Velocity variable - Multiplier Function
    - Translation multiplier function - Piston

  Model
- Volumes
  - Fluid
    - Element Set
      1. Material model - Air
      2. Compression heating - On
    - Element Output - on
- Surfaces
  - BDC
    - Simple Boundary Condition
      1. Type - Wall
      2. Wall velocity type - Match Mesh Velocity
      3. Mesh displacement BC type - Fixed
  - SideWall

        - Simple Boundary Condition
            1. Type - Wall
            2. Wall velocity type - Match Mesh Velocity
            3. Mesh displacement BC type - Fixed
    - TDC
        - Simple Boundary Condition
            1. Type - Wall
            2. Mesh displacement BC type - Fixed
            3. Mesh motion - Piston
- Nodes
    - VolumeNodes
        - Mesh X-Displacement
            1. Type - Zero
        - Mesh Y-Displacement
            1. Type - Linear
            2. Mesh motion - Piston
            3. Curve fit variable - Y reference coordinate
                1. X1 - `10.0` m
                2. Y1 - `1.0` m
                3. Y2 - `0.0` m
        - Mesh Z-Displacement
            1. Type - Zero

References

M.J. Moran and H.N Shapiro. "Fundamentals of Engineering Thermodynamics". Wiley. 4th Ed. 2000.

Separated Laminar Flow Over a Blunt Plate

In this application, AcuSolve is used to simulate the separation of laminar flow over a blunt plate. AcuSolve results are compared with experimental results as described in J.C. Lane and R.I. Loehrke (1980). The close agreement of AcuSolve results with the experimental results validates the ability of AcuSolve to model cases with external laminar flow including separation.

Problem Description

The problem consists of external, laminar flow over a blunt plate 1.5 m long and 0.09 m thick, as shown in the following image, which is not drawn to scale. The fluid flows with a uniform horizontal velocity (v) of 0.045133 m/s. The fluid material used for the simulation has a density of 1.0 kg/m^3 and a dynamic viscosity of 1.7894 X 10^{-5} kg/m-s. The resulting Reynolds number for the flow, based on the plate thickness, is approximately 227. This indicates that the flow over the plate is laminar. As the fluid flows past the leading edge of the plate, the pressure decreases, resulting in a separation region downstream of the leading edge. At some distance downstream from the leading edge, the pressure gradient decreases, and viscous forces cause the recirculation zone to dissipate, allowing the flow to reattach to the plate.

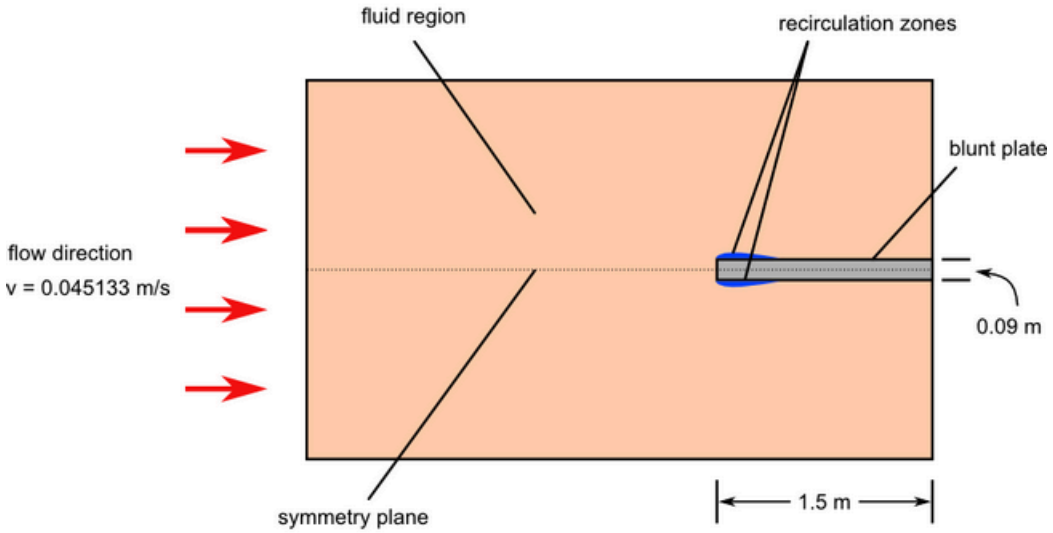


Figure 295:

The simulation was performed as a two dimensional problem by constructing a volume mesh that contains a single layer of elements in the extruded direction, normal to the flow plane, and by imposing symmetry boundary conditions on the extruded planes. In addition, the half symmetry of the geometry was exploited to allow for modeling only the top half of the geometry. These characteristics allow for accurate simulation of the flow while minimizing computational time. The following images show the mesh distribution and a refined mesh zone around the blunt plate.

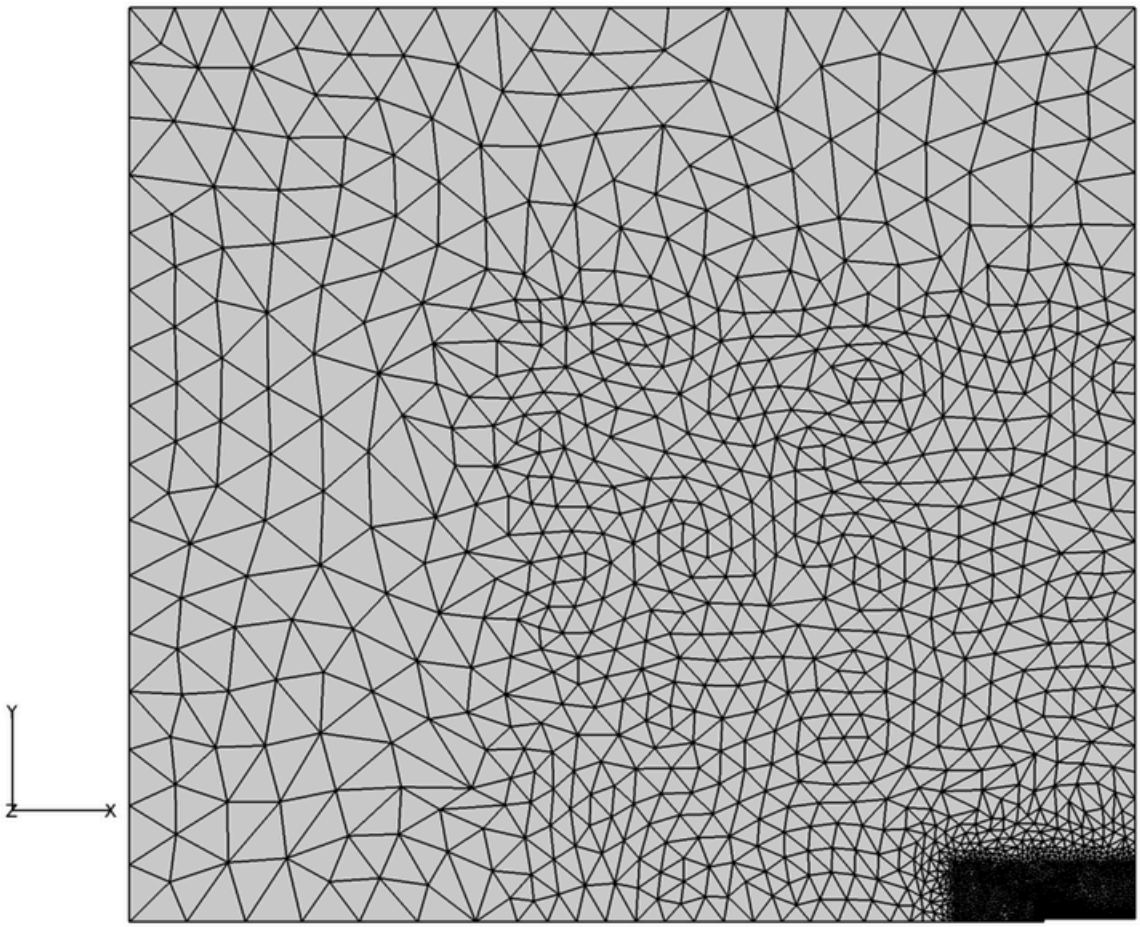


Figure 296: Mesh used for Simulating Separated Laminar Flow over a Blunt Plate

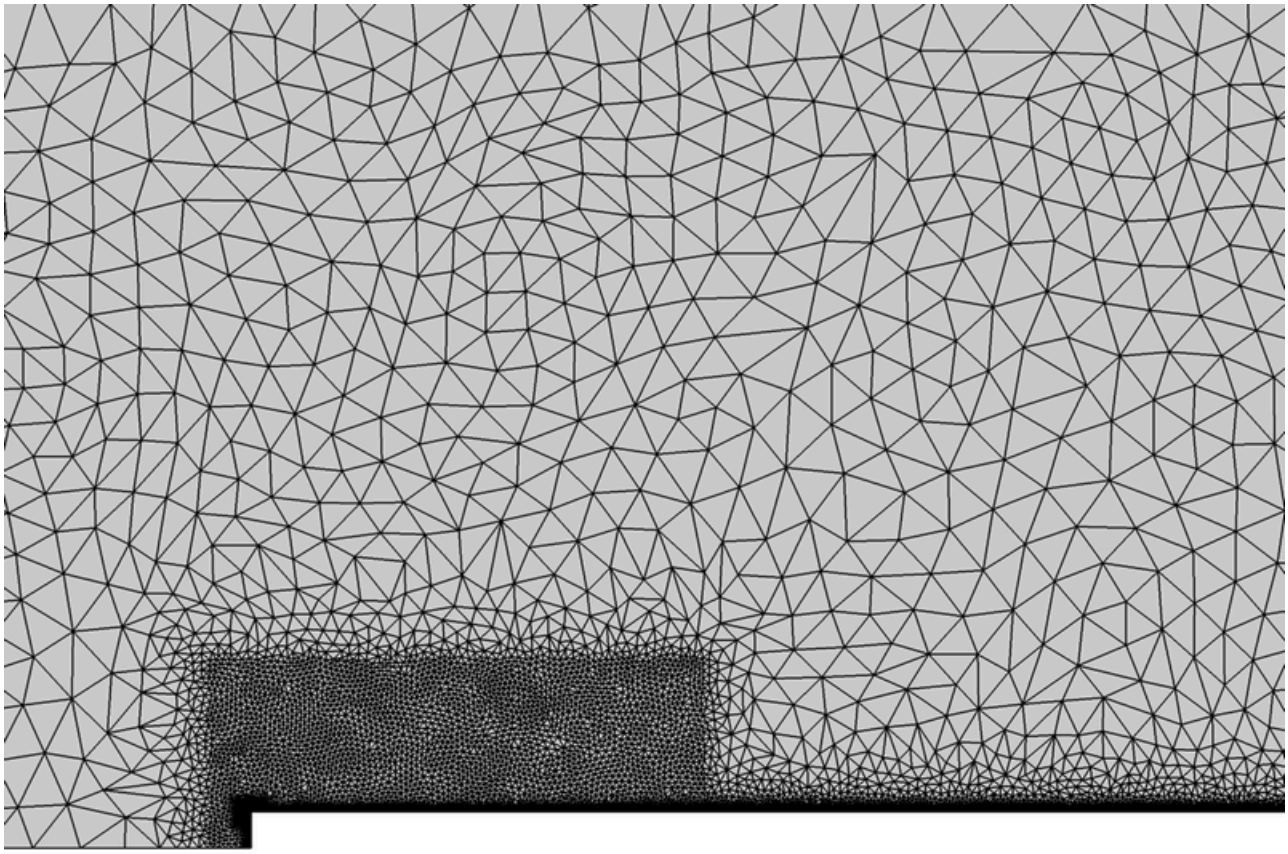


Figure 297: Mesh Detail Showing Refinement Zones at the Leading Edge of the Blunt Plate

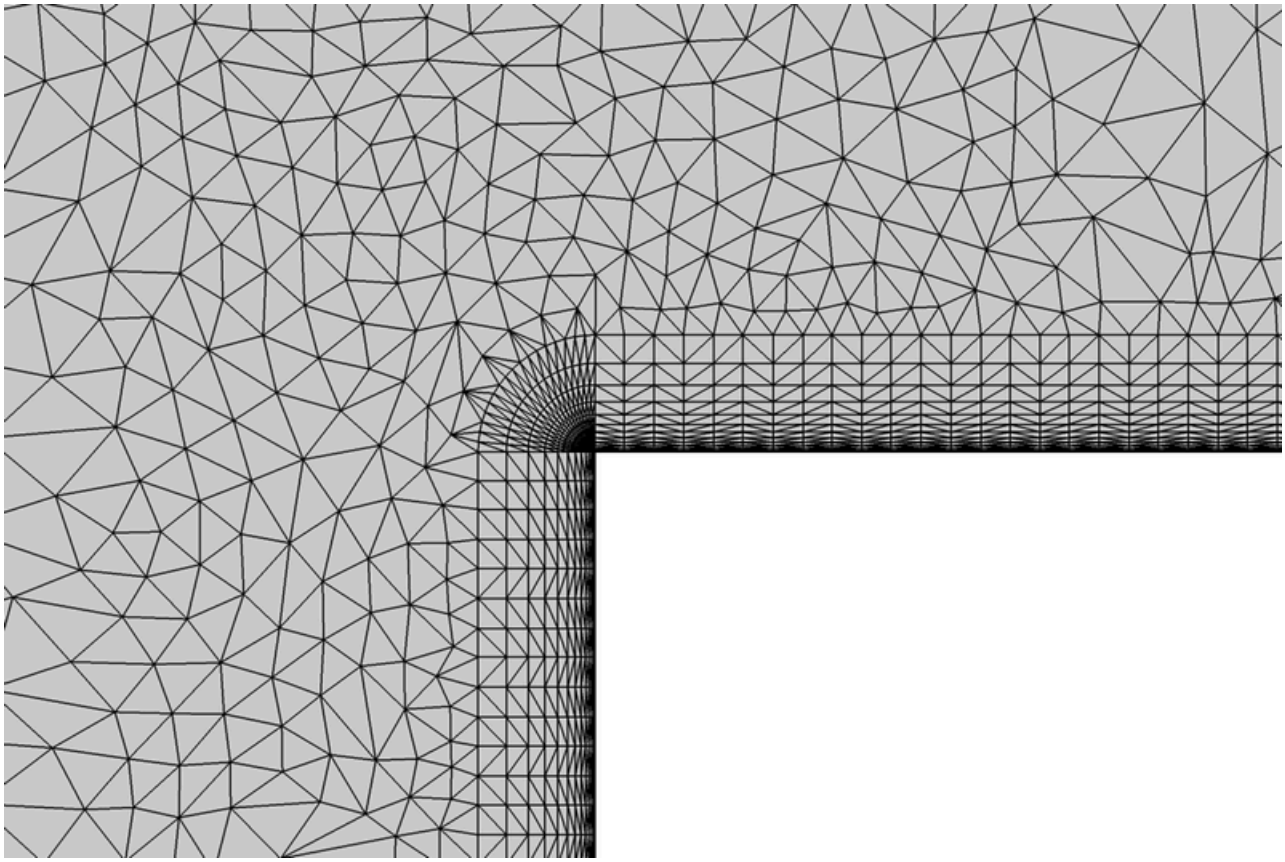


Figure 298: Mesh Detail Showing Mesh Elements Near the Leading Edge of the Blunt Plate

AcuSolve Results

The AcuSolve solution converged to a steady state and the results reflect the mean flow conditions over the blunt plate. The flow velocity is reduced to zero at the leading face, forming a stagnation point at the center. The flow reaches a maximum velocity as it flows around the leading edges and separates from the plate. Flow separation (shear stress parallel to the wall becomes negative) occurs downstream of the leading edge, leading to a recirculation zone. The flow reattaches 0.37 m downstream of the leading edge. The velocity in the laminar boundary layer increases from zero at the wall to free-stream velocity at the boundary layer edge. Along the plate length, the boundary layer slowly grows in thickness. The following image shows the contours of the flow velocity parallel to the streamwise direction and the recirculation region in the wake of the plate edge.

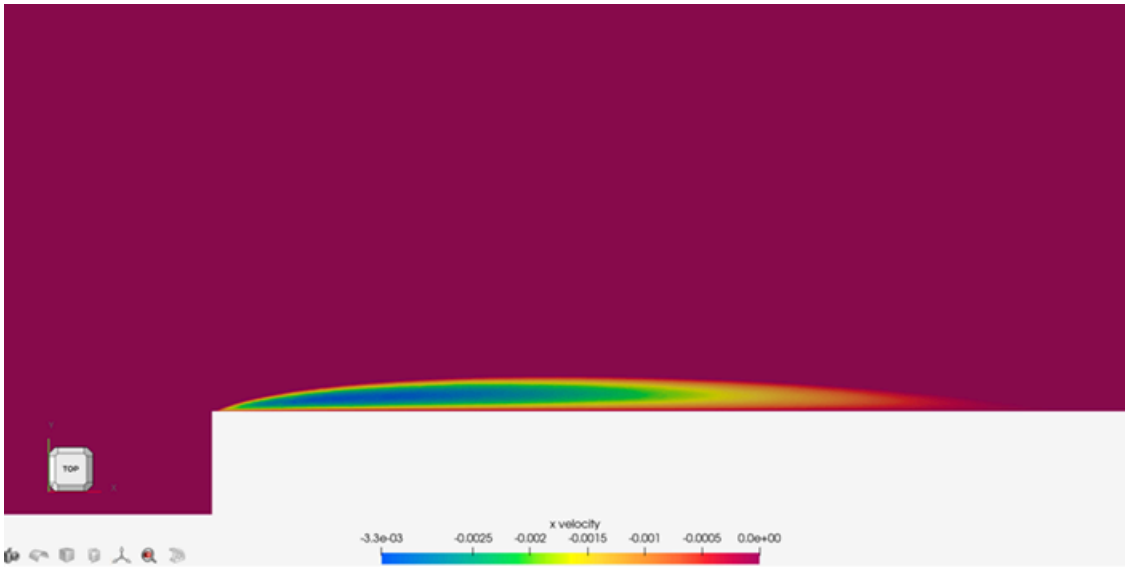


Figure 299: X-Velocity Contours Near the Leading Edge of the Blunt Plate

Downstream of the leading edge, the flow eventually reattaches to the plate at the point where the shear stress parallel to the wall passes from negative through zero to positive. The reattachment point is 0.37 m from the leading edge of the plate and corresponds to the trailing edge of the contours.

The results for the predicted and experimental reattachment length (xreattach) are presented in the table below. T represents the plate thickness.

Table 18:

AcuSolve xreattach	AcuSolve xreattach/T	Experimental xreattach/T	Percent error (%)
0.37	4.11	4.0	2.8

Summary

In this application, a constant flow inlet velocity and symmetric boundary conditions were used to model 2D flow over a blunt plate. The AcuSolve solution compares well with experimental results for the separation of laminar flow over a blunt plate. The non-dimensional reattachment length obtained from the AcuSolve steady state solution compares well with the experimental solution, with an error of less than 3.0 percent. The results of this simulation validate the ability of AcuSolve to accurately predict the reattachment point in cases with external, laminar flow with separation.

Simulation Settings for Separated Laminar Flow over a Blunt Plate

HyperWorks CFD database file: `<your working directory>\blunt_plate_laminar\blunt_plate_laminar.hm`

Global

- Problem Description

    - Analysis type - Steady State
    - Turbulence equation - Laminar
- Auto Solution Strategy
    - Relaxation Factor - `0.2`
- Material Model
    - Fluid
        - Density - `1.0` kg/m3
        - Viscosity - `1.7894e-005` kg/m-sec

  Model
- Volumes
    - Fluid
        - Element Set
            1. Material model - Fluid
- Surfaces
    - Back
        - Simple Boundary Condition
            1. Type - Symmetry
    - Freestream
        - Simple Boundary Condition
            1. Type - Slip
    - Front
        - Simple Boundary Condition
            1. Type - Symmetry
    - Inlet
        - Simple Boundary Condition
            1. Type - Inflow
            2. Inflow type - Velocity
            3. Inflow velocity type - Cartesian
            4. X Velocity - `0.045133` m/s
    - Outflow
        - Simple Boundary Condition
            1. Type - Outflow
    - Plate
        - Simple Boundary Condition
            1. Type - Wall
    - Symmetry
        - Simple Boundary Condition

1 Type - Symmetry

References

J.C. Lane and R.I. Loehrke. "Leading Edge Separation from a Blunt Plate at Low Reynolds Number". Journal of Fluids Engineering. 102(4):494-496. 1980.

Laminar Flow Through a Pipe with Constant Wall Temperature

In this application, AcuSolve is used to simulate the flow of mercury through a heated pipe. The AcuSolve results are compared with analytical results for pressure drop as described in White (1991), and with temperature changes as described in Incropera and DeWitt (1981). The close agreement of AcuSolve results with analytical results validates the ability of AcuSolve to model cases with flow and imposed temperature constraints.

Problem Description

The problem consists of mercury flowing through a circular pipe that is 0.005 m in diameter and 0.1 m long, as shown in the following image, which is not drawn to scale. Mercury enters the pipe with a constant temperature of 300 K and with a fully developed velocity profile with an average velocity of 0.005 m/s. The pipe wall has a constant temperature of 500 K. These constraints impose a temperature gradient within the fluid. As the fluid moves through the pipe it is slowly heated by the wall, resulting in an increased centerline temperature. Pressure decreases along the pipe length due to the friction imposed by the viscous stresses near the pipe wall. A periodic boundary condition is imposed on the inlet and outlet to allow the pressure to change with a constant offset, while the velocity is fully periodic.

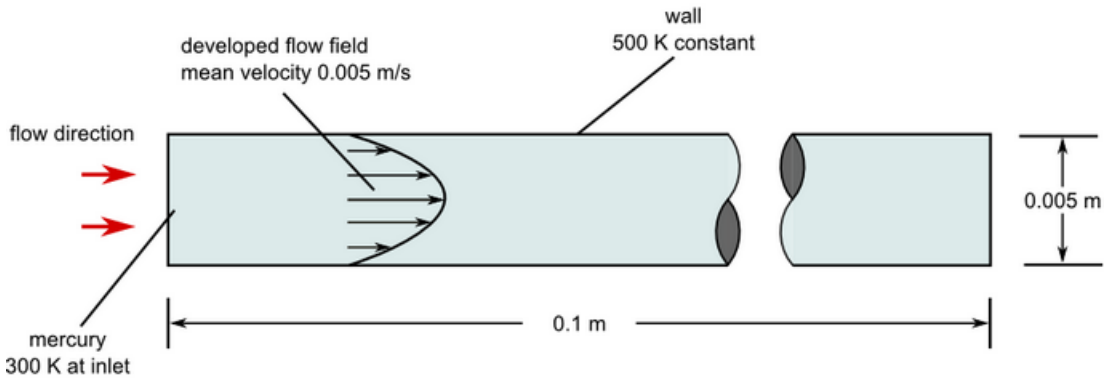


Figure 300: Critical Dimensions and Parameters for Simulating Laminar Flow through a Pipe with Constant Wall Temperature

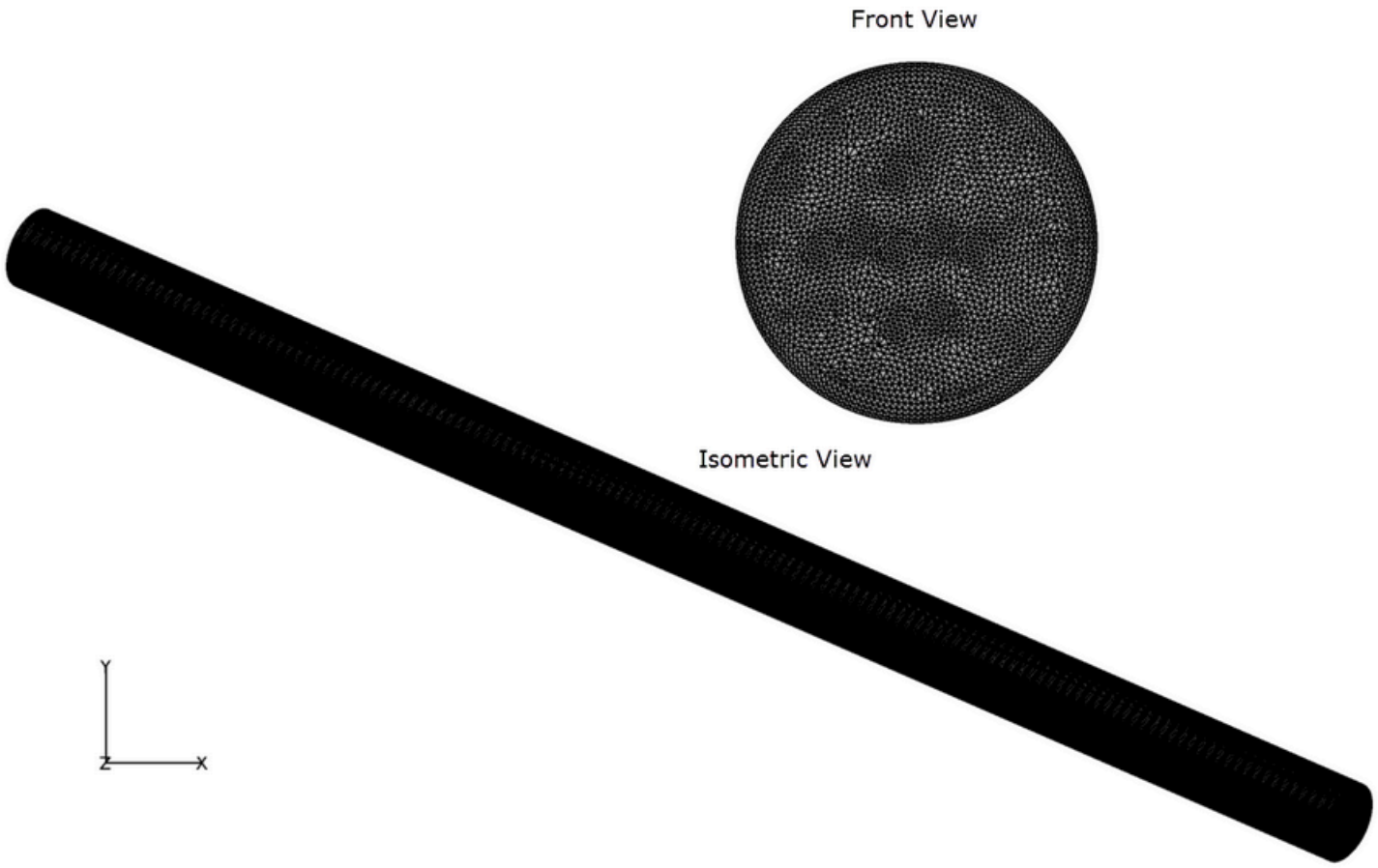


Figure 301: Mesh used for Simulating Laminar Flow Through a Pipe with Constant Wall Temperature

AcuSolve Results

The AcuSolve solution converged to a steady state and the results reflect the mean flow conditions. In this application, a fully developed laminar profile is achieved by enforcing periodic constraints on the pressure and velocity fields. The spatially developing temperature field is achieved by allowing the fluid's temperature to evolve along the full length of the model. The change in temperature along the pipe length is due to advection in the streamwise direction and heat conduction from the outer walls where the temperature is greater than the initial flow temperature. The temperature rises along the length of the pipe and the pressure drops along the length of the pipe. At the inlet, the temperature of the mercury is 300 K and the pressure is 0.496 Pa. At the outlet centerline, the temperature of the mercury has risen to 500.0 K and the pressure has dropped to -0.4965 Pa.

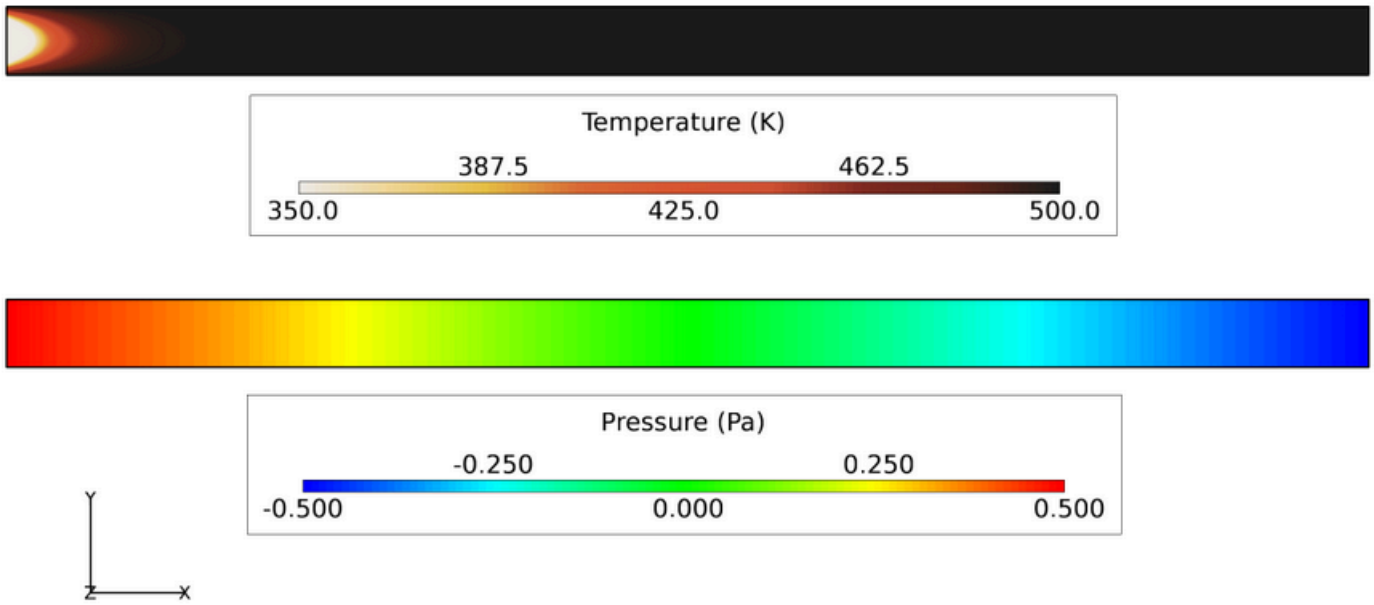


Figure 302: Temperature and Pressure Contours of Mercury Flow Through a Pipe with Prescribed Temperature Boundary

The following table shows the comparison of AcuSolve results with the analytical solutions from White (1994). Comparisons were made for the pressure drop between the inlet and outlet and the temperature at the center of the outlet.

Table 19:

	Analytical solution	**AcuSolve solution**	**Percent deviation from analytical**
Pressure drop (Pa)	0.991	0.9925	0.15
Centerline temperature of flow at outlet (K)	500.0	500.0	< 0.0001

Summary

The AcuSolve solution compares well with analytical results for flow through a pipe with constant temperature boundary conditions. The AcuSolve solution for the centerline temperature is nearly identical with the analytical results and the pressure reduces as expected for the prescribed flow conditions. The results of this simulation validate the ability of AcuSolve to accurately predict the heating of fluid flowing through a pipe with constant wall temperature.

Simulation Settings for Laminar Flow Through a Pipe With Constant Wall Temperature

AcuConsole database file: `<your working directory>\pipe_laminar_heatDirichlet\pipe_laminar_heatDirichlet.acs`

Global

- Problem Description
  - Analysis type - Steady State
  - Temperature equation - Advective Diffusive
  - Turbulence equation - Laminar
- Auto Solution Strategy
  - Relaxation Factor - `0.2`
- Material Model
  - Mercury
    - Density - `13579.0` kg/m3
    - Specific Heat - `139.3` J/kg-K
    - Viscosity - `0.001548` kg/m-sec
    - Conductivity - `8.69` W/m-K

  Model
- Volume
  - Fluid
    - Element Set
      1. Material model - Mercury
- Surfaces
  - Inflow
    - Simple Boundary Condition - (disabled to allow for periodic conditions to be set)
    - Advanced Options
      1. Integrated Boundary Conditions
         1. Mass Flux
            1. Type - Constant
            2. Constant value - `1.33e-3` kg/sec
      2. Temperature
         1. Type - Constant
         2. Constant value - `300.0` K
  - Outflow
    - Simple Boundary Condition - (disabled to allow for periodic conditions to be set)
  - Wall
    - Simple Boundary Condition
      1. Type - Wall

2 Temperature BC type - Value
3 Temperature - `500.0` K

- Periodics
  - Periodic 1
    - Individual Periodic BCs
      1 Velocity
        1 Type - Periodic
      2 Pressure
        1 Type - Single Unknown Offset

References

F. M. White. "Fluid Mechanics". 3rd Edition. McGraw-Hill Book Co., Inc. New York. 1994.

F. P. Incropera and D. P. DeWitt. "Fundamentals of Heat Transfer". John Wiley & Sons. New York. 1981.

Laminar Free Surface Flow Inside a Rotating Cavity

In this application, AcuSolve is used to solve for the flow field within a rotating cavity with the top of the cavity free to move as if it was exposed to air. The height of the free surface is determined and compared against the analytical solution for the same rotational velocity under the standard gravitational force.

Problem Description

The problem consists of a fluid with arbitrary material properties rotating within an axisymmetric cavity. The cavity is 1.0 m in height with a radius of 0.5 m and is rotating at a constant speed of 3.0 rad/sec, as shown in the following image, which is not drawn to scale. The model is simulated as transient with the fluid initially at rest within the cavity. The radial velocity applied to the cavity walls causes the fluid's free surface to creep up the side wall forming a parabolic shape. The height of this surface is compared against the analytical solution as described in White, 2003.

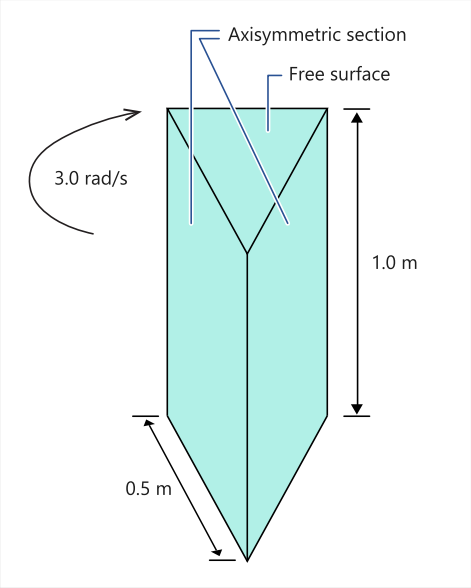


Figure 303: Critical Dimensions and Parameters used for Simulating a Laminar Free Surface Inside a Rotating Cavity

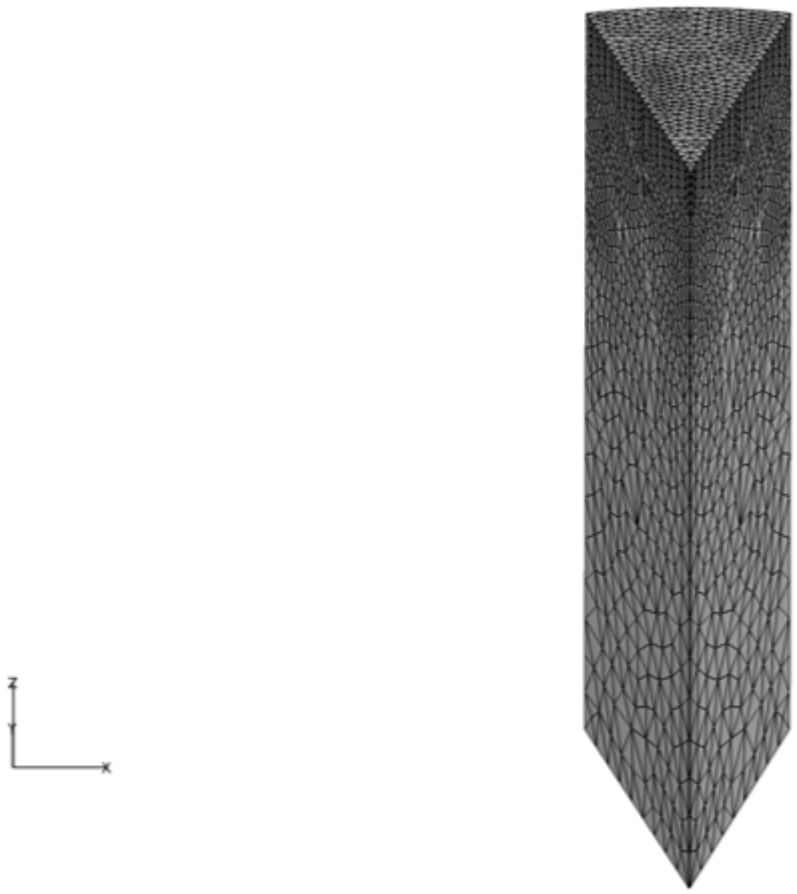


Figure 304: Mesh used for Simulating Laminar Free Surface Flow Inside a Rotating Cavity

The problem is simulated as axisymmetric by considering a 30 degree portion of the cavity with rotationally periodic boundary conditions applied on the planar surfaces representing the cut faces of the cavity.

AcuSolve Results

The AcuSolve solution reaches a quasi-static result with the free surface height stabilizing, demonstrating the final flow conditions of the simulation. As the fluid within the cavity is subjected to the multiple reference frame simulating the rotating boundaries the free surface begins to deform. At the center of the cavity the fluid height decreases and in order to conserve mass the height steadily increases as a function of the radial distance from the center. The surface height takes the form of a parabola as described in White, 2003. The following image demonstrates the shape that the fluid forms within the cavity, showing the vertical displacement of the rotating fluid. The free surface height is compared with the analytical solution where the image shows black circles representing the analytical solution and a solid red line for the AcuSolve results.

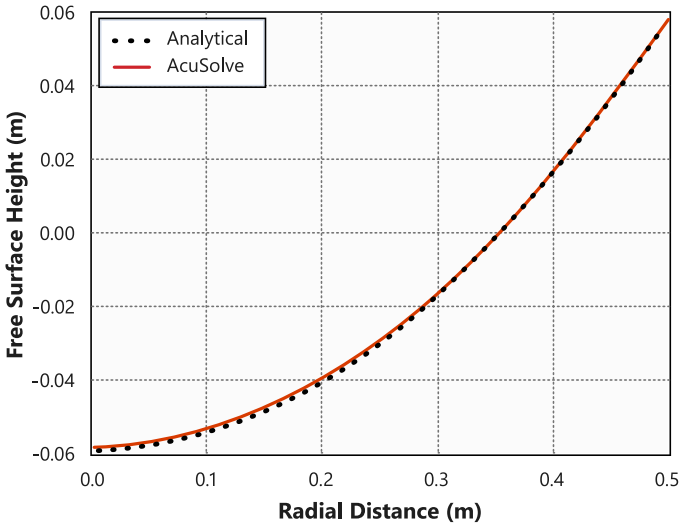


Figure 305: Free Surface Height of the Fluid Within the Cavity as a Function of Distance from the Center of the Domain at the Final Timestep

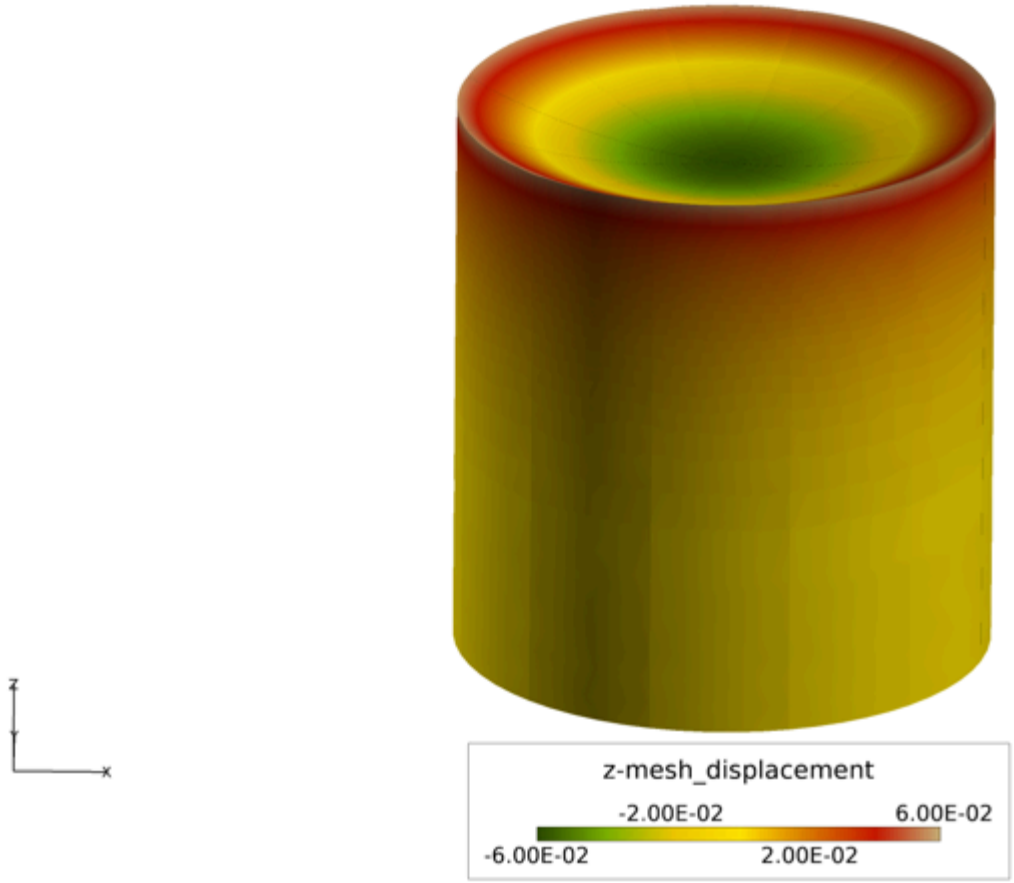


Figure 306: Vertical Mesh Displacement Within the Rotating Cavity at the Final Time Step (Shown as the Complete Cavity, using the Results from the Axisymmetric Section)

Summary

The AcuSolve solution compares well with analytical results for laminar free surface flow inside a rotating cavity. In this application, a fluid initially at rest is subjected to an angular velocity about the center of the cavity. As a result of the prescribed velocity, the fluid is forced to the outer wall of the cavity and develops a free surface profile in the shape of a parabola. The AcuSolve solution for the free surface height matches nearly exactly with the analytical results, with only minor differences based on the convergence criteria that you specified.

Simulation Settings for Laminar Free Surface Flow Inside a Rotating Cavity Fluid

Global

- Problem Description
  - Analysis type - Transient
  - Flow equation - Navier Stokes
  - Turbulence equation - Laminar
  - Mesh type - Arbitrary Mesh Movement (ALE)
- Auto Solution Strategy
  - Final time - `15.0` sec
  - Initial time increment- `0.05` sec
  - Convergence tolerance - `0.001`
  - Min stagger iterations - `0`
  - Max stagger iterations - `4`
- Material Model
  - Fluid
    - Density
      1. Type - Constant
      2. Density - `10` kg/m3
    - Viscosity
      1. Type - Constant
      2. Viscosity - `3.0` kg/m-sec
- Reference Frame
  - Omega
    - Rotation Center
      1. X-coordinate - `0.0` m
      2. Y-coordinate - `0.0` m
      3. Z-coordinate - `0.0` m
    - Angular velocity
      1. X-component - `0.0` rad/sec
      2. Y-component- `0.0` rad/sec
      3. Z-component - `3.0` rad/sec

Model

- Volumes
  - Fluid
    - Element Set
      1. Material model - Fluid
      2. Body force - Gravity
      3. Reference frame - Omega
- Surfaces
  - + Y
    - Simple Boundary Condition - (disabled to allow for nodal boundary conditions)
    - Advanced Options
      1. Nodal Boundary Conditions
         1. X-velocity
            1. Type - Constant
            2. Reference frame - Omega
            3. Constant value - `0.0`
         2. Y-velocity
            1. Type - Constant
            2. Reference frame - Omega
            3. Constant value - `0.0`
         3. Mesh X-Displacement
            1. Type- Zero
         4. Mesh Y-Displacement
            1. Type- Zero
  - -Z
    - Simple Boundary Condition
      1. Type - Wall
      2. Reference frame - Omega
      3. Mesh displacement BC type - Fixed
  - Axisymmetric +X
    - Simple Boundary Condition (disabled to allow for nodal boundary conditions)
  - Axisymmetric -X
    - Simple Boundary Condition (disabled to allow for nodal boundary conditions)
  - Free_Surface
    - Simple Boundary Condition
      1. # Type - Free Surface
- Periodics

- Axisymmetric Condition
- Periodic Boundary Condition
  - Type - Axisymmetric
  - Rotation Axis
    1. Point 1
       1. x-coordinate - 0.0 m
       2. y-coordinate - 0.0m
       3. z-coordinate - 0.0m
    2. Point 2
       1. x-coordinate - 0.0 m
       2. y-coordinate - 0.0m
       3. z-coordinate - 1.0m
- Nodes
  - All
    1. Mesh X-Displacement
       1. Type - Zero
    2. Mesh Y-Displacement
       1. Type - Zero
  - Centerline
    1. X-Velocity
       1. Type - Zero
    2. Y-velocity
       1. Type - Zero
    3. Mesh X-Displacement
       1. Type - Zero
    4. Mesh Y-Displacement
       1. Type - Zero

References

White, F. Fluid Mechanics. New York: McGrawHill. 2003

Natural Convection in a Concentric Annulus

In this application, AcuSolve is used to simulate natural convection in the annular space between a heated inner pipe and an outer concentric pipe. AcuSolve results are compared with experimental results adapted from Kuehn and Goldstein (1978). The close agreement of AcuSolve results with experimental results validates the ability of AcuSolve to model cases with flow induced by natural convection.

Problem Description

The problem consists of two concentric cylinders with air filling the void between them, as shown in the following image, which is not drawn to scale. The radius of the inner cylinder is 0.0178 m and the radius of the outer cylinder is 0.0463 m. The inner cylinder is held at a fixed temperature of 373 K while the outer cylinder is held at 327 K. The temperature gradient drives the flow due to buoyancy effects.

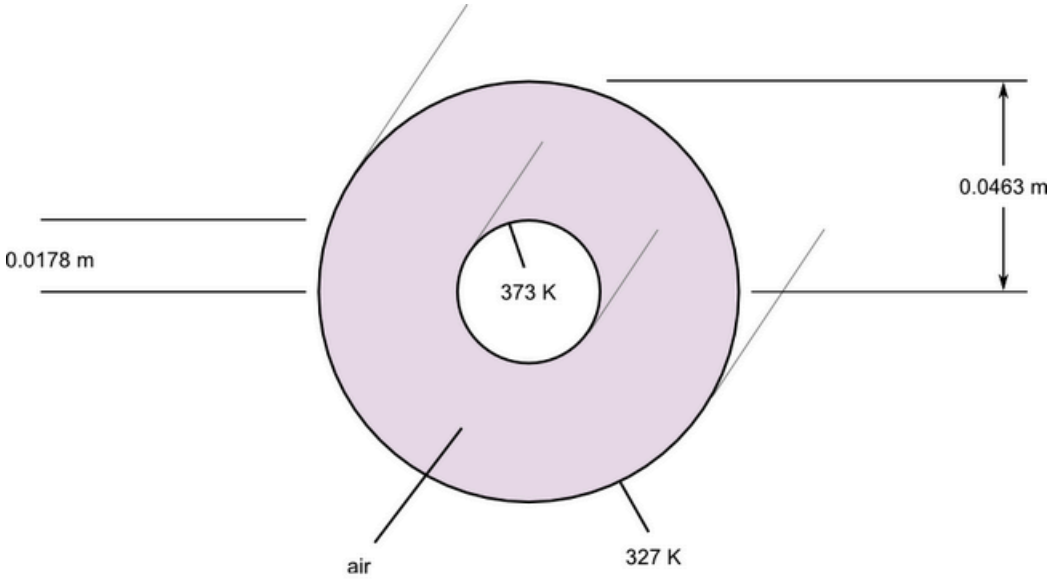


Figure 307: Critical Dimensions and Parameters for Simulating Natural Convection in a Concentric Annulus

The simulation was performed as a two dimensional problem by restricting flow in the out-of-plane direction through the use of a mesh that is one element thick. In addition, the half symmetry of the geometry is exploited to allow for modeling only half of the geometry. These characteristics allow for accurate simulation of the flow while minimizing computational time.

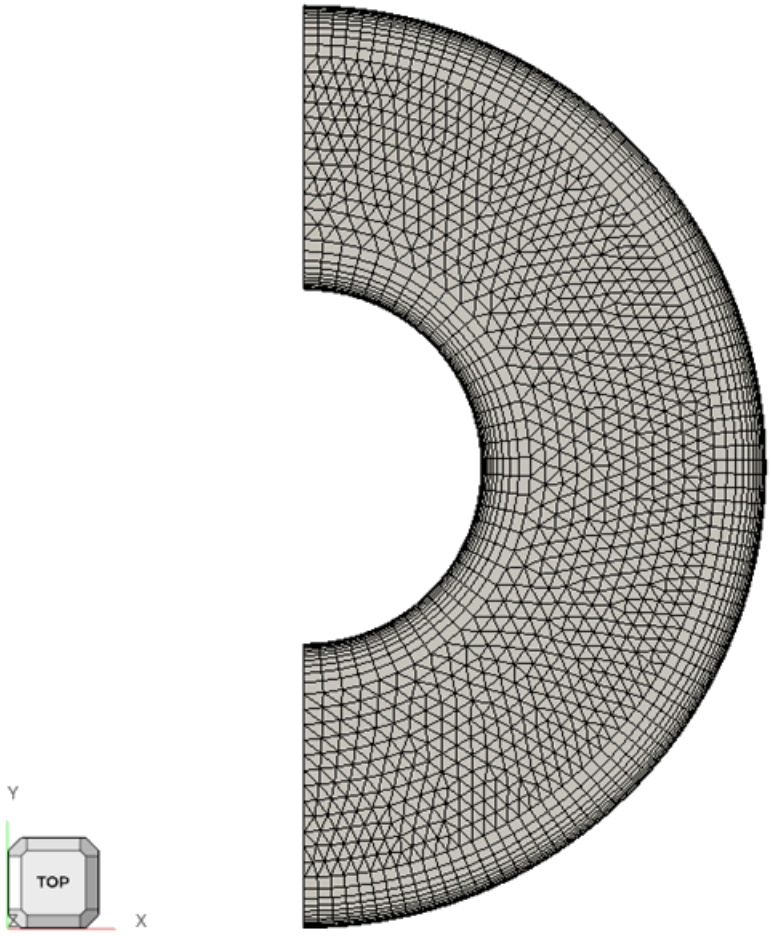


Figure 308: Mesh (Half of a Concentric Annulus) used for Simulating Natural Convection in a Concentric Annulus

AcuSolve Results

The AcuSolve solution converged to a steady state and the results reflect the mean flow conditions. Air density decreases due to heating by the inner cylinder, leading to convective currents within the annulus. As air approaches the outer cylinder, it is cooled by the outer wall, causing the density to increase. This results in heavier air sinking toward the bottom of the assembly.

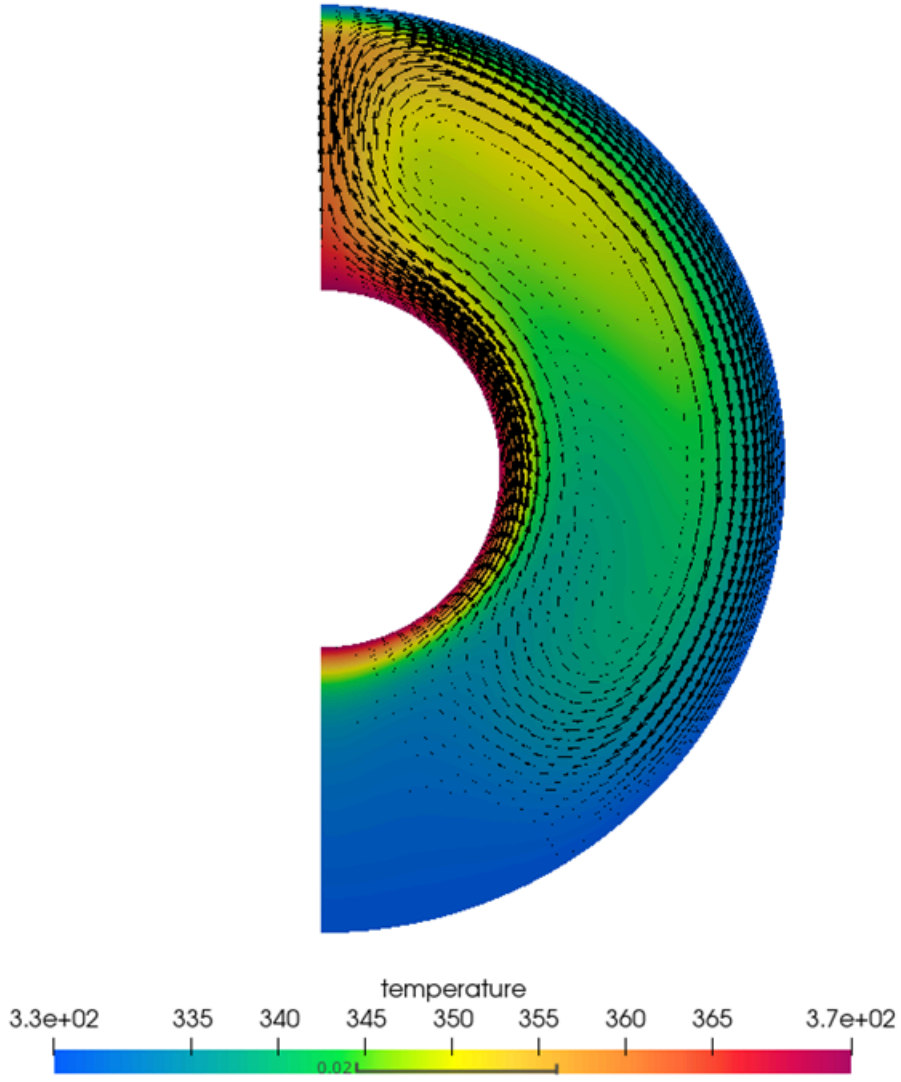


Figure 309: Temperature Contours and Velocity Vectors

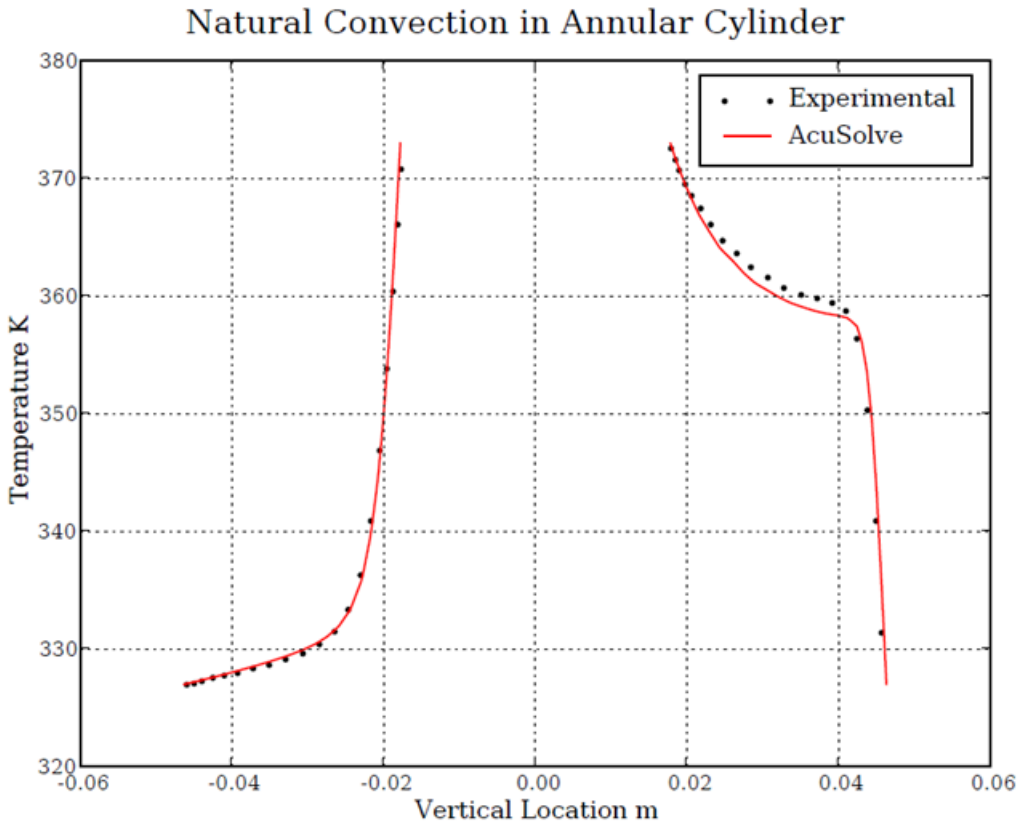


Figure 310: Temperature as a Function of Distance From the Center of the Inner Cylinder

Summary

The AcuSolve solution compares well with analytical results for natural convection in a concentric annulus. In this application, flow is driven by a decrease in density as air is heated. The local variations in density result in the higher density fluid sinking to the bottom of the annulus while the lower density fluid rises to the top. This transfer of momentum is a continuous process which results in the convective currents that are visible in the solution. The AcuSolve temperature results compare very closely with the experimental results.

Simulation Settings for Natural Convection in a Concentric Annulus

HyperWorks CFD database file: `<your working directory>\annulus_heat\annulus_heat.hm`

Global

- Problem Description
  - Analysis type - Steady State
  - Abs. pressure offset - `101325.0` N/m2
  - Temperature equation - Advective Diffusive
  - Turbulence equation - Laminar
  - Gravitational acceleration - { 0, -9.80665, 0 }
- Auto Solution Strategy

    - Relaxation factor - `0.2`
    - Flow - On
    - Temperature - On
- Material Model
    - Air
        - Type - Boussinesq
        - Density - `1.225` kg/m3
        - Expansivity - `0.0034722` 1/K
        - Reference temperature - `288` K
        - Isothermal compressibility - `0.0` m2/N
        - Viscosity - `2.081e-5` kg/m-sec

    Model
- Volumes
    - Fluid
        - Element Set
            1. Material model - Air
    - Surfaces
        - ID
            1. Simple Boundary Condition
                1. Type - Wall
                2. Temperature BC type - Value
                3. Temperature - `373.0` K
        - Max_Z
            1. Simple Boundary Condition
            2. Type - Symmetry
        - Min_Z
            1. Simple Boundary Condition
            2. Type - Symmetry
        - OD
            1. Simple Boundary Condition
                1. Type - Wall
                2. Temperature BC type - Value
                3. Temperature - `327.0` K
        - Symmetry
            1. Simple Boundary Condition
            2. Type - Symmetry
    - Nodes
        - Node 1

1 Pressure

1 Type - Zero

References

T.H. Kuehn and R. J. Goldstein. "An Experimental Study of Natural Convection Heat Transfer in Concentric and Eccentric Horizontal Cylindrical Annuli". Journal of Heat Transfer 100:635-640. 1978.

Flow Between Concentric Cylinders

In this application, AcuSolve is used to simulate the flow of water between concentric cylinders. The outer cylinder is held stationary while the inner cylinder rotates with a constant speed. AcuSolve results are compared with analytical results as described in White (1991). The close agreement of AcuSolve results with analytical results validates the ability of AcuSolve to model cases containing thin annular gaps with flow induced by rotating walls.

Problem Description

The problem consists of two concentric pipes with water filling the void between them, as shown in the following image, which is not drawn to scale. The radius of the outer pipe is 0.0468 m and the radius of the inner pipe is 0.0178 m. The inner cylinder rotates at 1 rad/sec and the outer cylinder is fixed. The induced flow is laminar and exhibits a steady state behavior. The rotation of the inner cylinder causes the fluid to rotate due to viscous shearing near the wall. As the outer cylinder is fixed, a velocity gradient is generated as a function of radius within the flow domain.

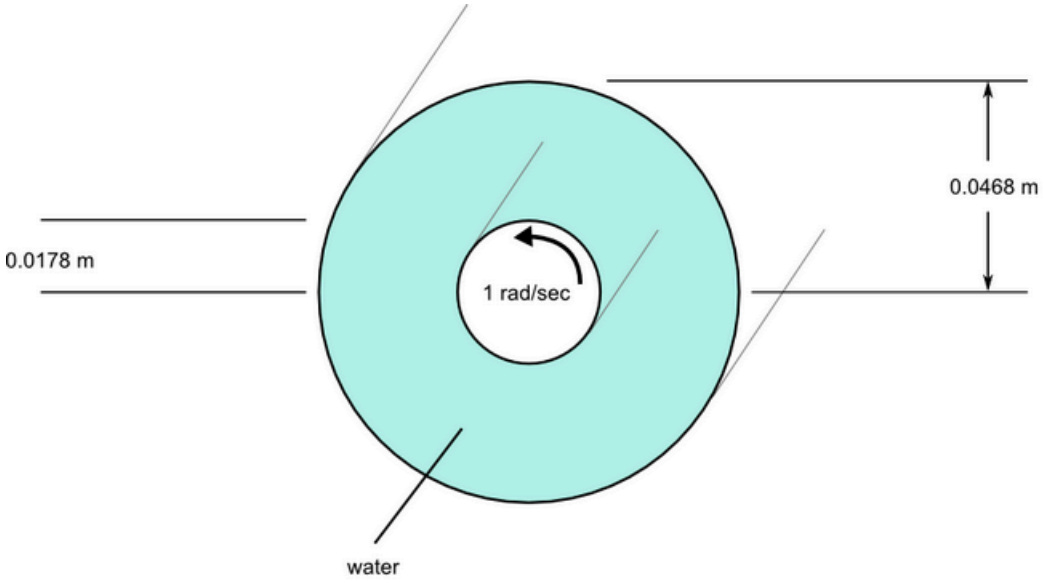


Figure 311: Critical Dimensions and Parameters for Simulating Flow Between Concentric Cylinders

The simulation was performed as a two dimensional problem by restricting flow in the out-of-plane direction through the use of a mesh that is one element thick.

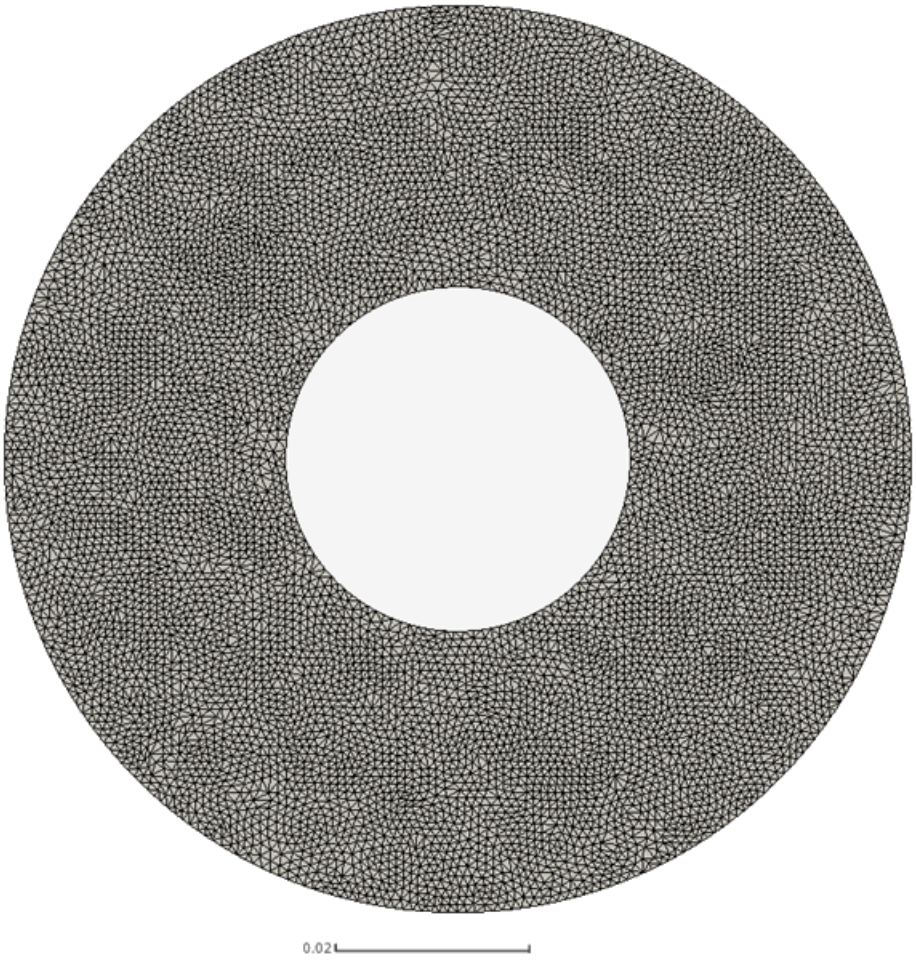


Figure 312: Mesh Used for Simulating Flow Between Concentric Cylinders

AcuSolve Results

The AcuSolve solution converged to a steady state and the results reflect the mean flow conditions. The velocity of the fluid within the cavity is greatest near the rotating inner cylinder. There is a nonlinear decrease in velocity as a function of distance away from the inner cylinder.

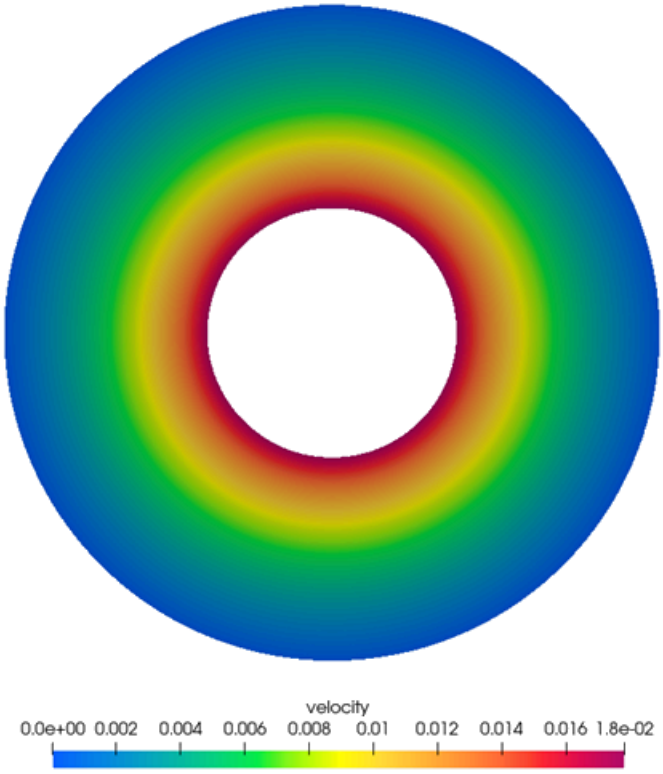


Figure 313: Contours of Tangential Velocity Between the Concentric Cylinders

Analytical tangential velocity at four distances away from the center of the rotating inner cylinder are presented with the corresponding AcuSolve results in the following table.

Table 20:

Distance from the center of rotating cylinder (m)	Analytical tangential velocity (m/s)	AcuSolve tangential velocity (m/s)	Percent deviation from analytical
0.020	0.01514	0.01514	0.04
0.025	0.01059	0.01058	0.10
0.030	0.00727	0.00727	0.06
0.035	0.00466	0.00466	0.10

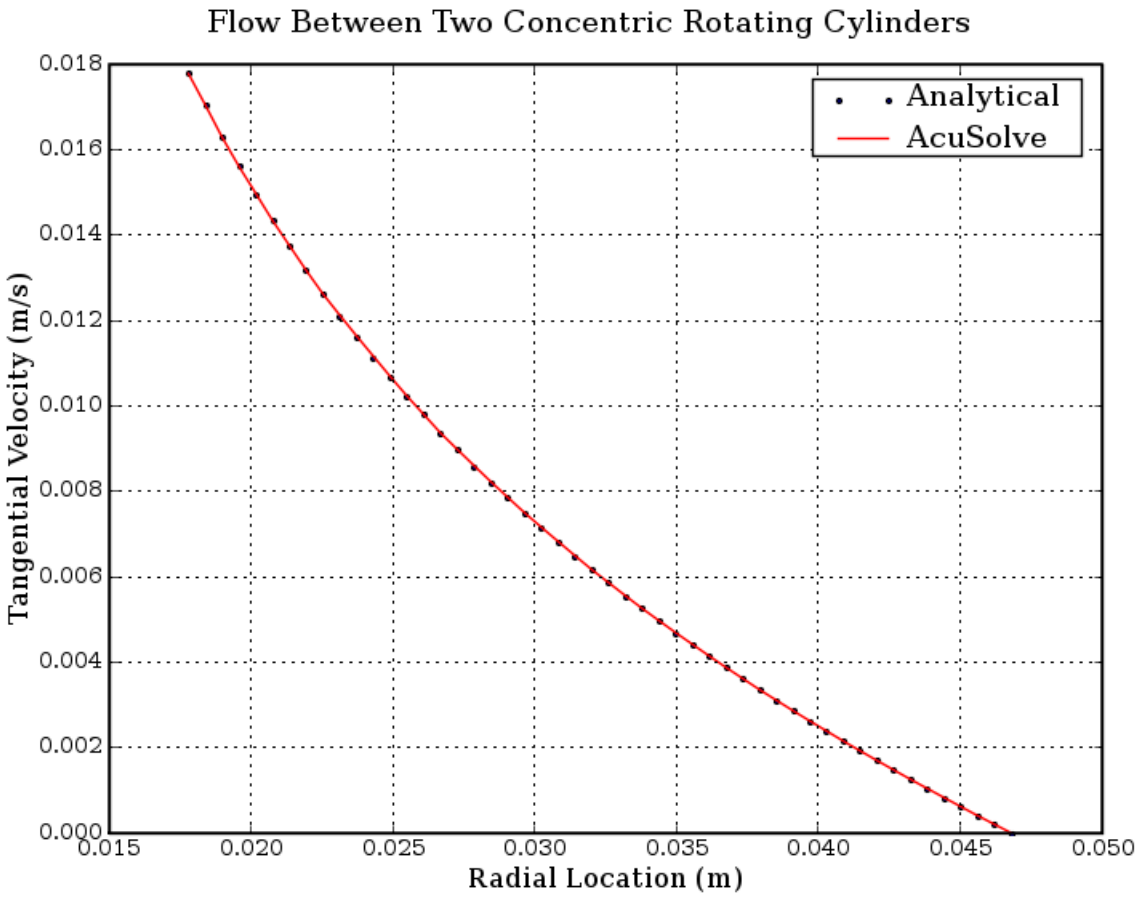


Figure 314: Tangential Velocity Plotted Against Distance from the Center of the Rotating Cylinder

Summary

The AcuSolve solution compares well with analytical results for the flow between concentric cylinders. In this application, the velocity in the annular fluid region is driven by the viscous stresses on the rotating wall. The AcuSolve tangential velocity is within 0.1 percent of the analytical solution at all radial locations.

Simulation Settings for Flow Between Concentric Cylinders

HyperWorks CFD database file: `<your working directory>\annulus_rotating\annulus_rotating.hm`

Global

- Problem Description
  - Analysis type - Steady State
  - Turbulence equation - Laminar
- Auto Solution Strategy
  - Relaxation Factor - `0.2`
- Material Model

    - Water
        - Density - `1000.0` kg/m3
        - Viscosity - `0.001` kg/m-sec
- Reference Frame
    - Rotating_Cylinder
        - Rotation center
            1. X-coordinate - `0.0` m
            2. Y-coordinate - `0.0` m
            3. Z-coordinate - `0.0` m
        - Angular velocity
            1. X-component - `0.0` rad/sec
            2. Y-component - `0.0` rad/sec
            3. Z-component - `-1.0` rad/sec

Model

- Volumes
    - Volume
        - Element set
            1. Material model - Water
- Surfaces
    - Boundary1
        - Simple Boundary Condition
            1. Type - Symmetry
    - Boundary2
        - Simple Boundary Condition
            1. Type - Symmetry
    - Inner
        - Simple Boundary Condition
            1. Type - Wall
            2. Reference Frame - Rotating_Cylinder
    - Outer
        - Simple Boundary Condition
            1. Type - Wall
- Nodes
    - Fixed
        - Pressure
            1. Type - Zero

References

F. M. White. "Viscous Fluid Flow". Section 3-2.3. McGraw-Hill Book Co., Inc. New York. 1991.

Laminar Poiseuille Flow Through a Pipe

In this application, AcuSolve is used to simulate the flow of carbon dioxide (CO_2) entering a pipe with a fixed velocity. AcuSolve results are compared with analytical results using the Hagen-Poiseuille approach as described in White (1991). The close agreement of AcuSolve results with analytical results validates the ability of AcuSolve to model cases with constant flow velocity.

Problem Description

The problem consists of CO_2 flowing through a circular pipe 0.0025 m in diameter and 0.01 m long, as shown in the following image, which is not drawn to scale. The CO_2 enters the pipe with an average inlet velocity of 3.0 m/s. The flow field develops as a result of the viscous shearing on the fluid at the pipe wall.

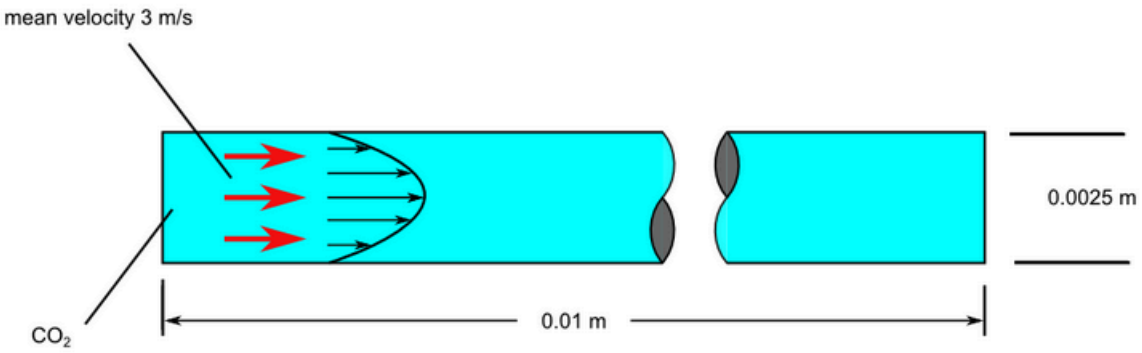


Figure 315: Critical Dimensions and Parameters for Simulating Laminar Poiseuille Flow Through a Pipe



Figure 316: Mesh Used for Simulating Laminar Poiseuille Flow Through a Pipe

AcuSolve Results

The AcuSolve solution converged to a steady state and the results reflect the mean flow conditions. The pressure decreases along the length of the pipe.

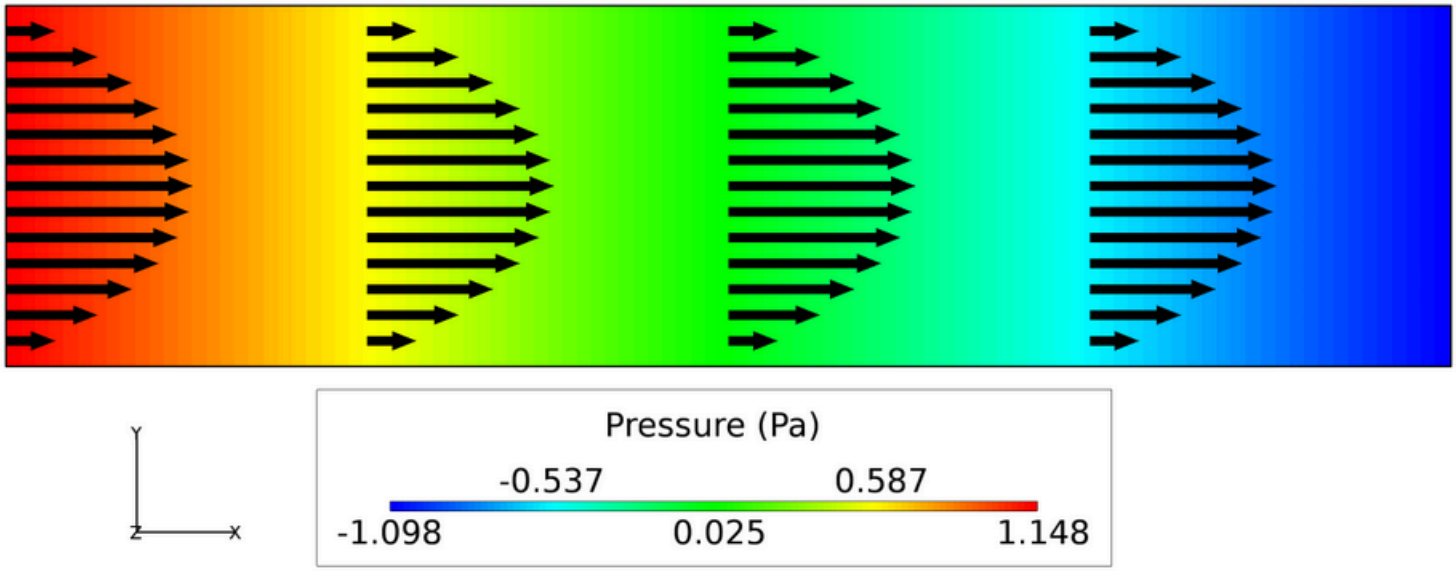


Figure 317: Pressure Contours and Velocity Vectors

The analytical pressure drop between the inlet and the outlet is presented with the corresponding AcuSolve result in the following table.

Table 21:

	Analytical pressure drop (Pa)	**AcuSolve pressure drop (Pa)**	**Percent deviation from analytical**
Inlet to outlet pressure drop	2.242	2.245	0.099

Summary

The AcuSolve solution compares well with analytical results for laminar flow through a pipe. In this application, the pressure drop along the length of the pipe is caused by the viscous shearing near the pipe wall. The AcuSolve steady state solution compares well with the analytical solution, with less than 0.1 percent error.

Simulation Settings for Laminar Poiseuille Flow Through a Pipe

AcuConsole database file: `<your working directory>\pipe_laminar\pipe_laminar.acs`

Global

- Problem Description
  - Analysis type - Steady State
  - Turbulence equation - Laminar
- Auto Solution Strategy
  - Relaxation factor - `0.2`
- Material Model
  - CO2
    - Density `1.808` kg/m3
    - Viscosity `1.46e-5` kg/m-sec

  Model
- Volumes
  - Fluid
    - Element Set
      1. Material Model - CO2
- Surfaces
  - Inflow
    - Simple Boundary Condition - (disabled to allow for periodic conditions to be set)
    - Advanced Options
      1. Integrated Boundary Conditions
         1. Mass Flux
            1. Type - Constant
            2. Constant value - `-2.6625e-05` kg/sec
  - Outflow
    - Simple Boundary Condition - (disabled to allow for periodic conditions to be set)
  - Wall
    - Simple Boundary Condition
      1. Type - Wall
- Periodics
  - Periodic 1
    - Individual Periodic BCs
      1. Velocity
         1. Type - Periodic
      2. Pressure
         1. Type - Single Unknown Offset

References

F. M. White. "Viscous Fluid Flow". Section 3-2.1. McGraw-Hill Book Co., Inc.. New York. 1991.

Heat Transfer Between Radiating Concentric Cylinders

In this application, AcuSolve is used to simulate the heat transfer due to radiation between concentric cylinders. The inner and outer cylinders are held at constant temperature and are defined to be radiation surfaces. AcuSolve results are compared with analytical results for temperature as described in Incropera (2006). The close agreement of AcuSolve results with analytical results validates the ability of AcuSolve to model cases with radiation heat transfer requiring view factor computation.

Problem Description

The problem consists of a fluid with arbitrary material properties between two infinitely long concentric cylinders, as shown in the following image, which is not drawn to scale. The radius of the outer cylinder is 0.046 m and the radius of the inner cylinder is 0.018 m. The inner cylinder is defined to have a constant wall temperature at 773.0 K (500 °C). The outer cylinder is defined to have a constant wall temperature at 300.0 K (27 °C). Both cylinders are specified to radiate as grey bodies, with emissivity set to 0.03778.

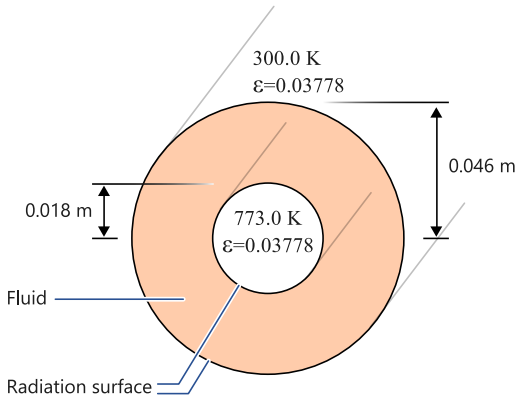


Figure 318: Critical Dimensions and Parameters Used for Simulating Radiation Between Two Concentric Cylinders

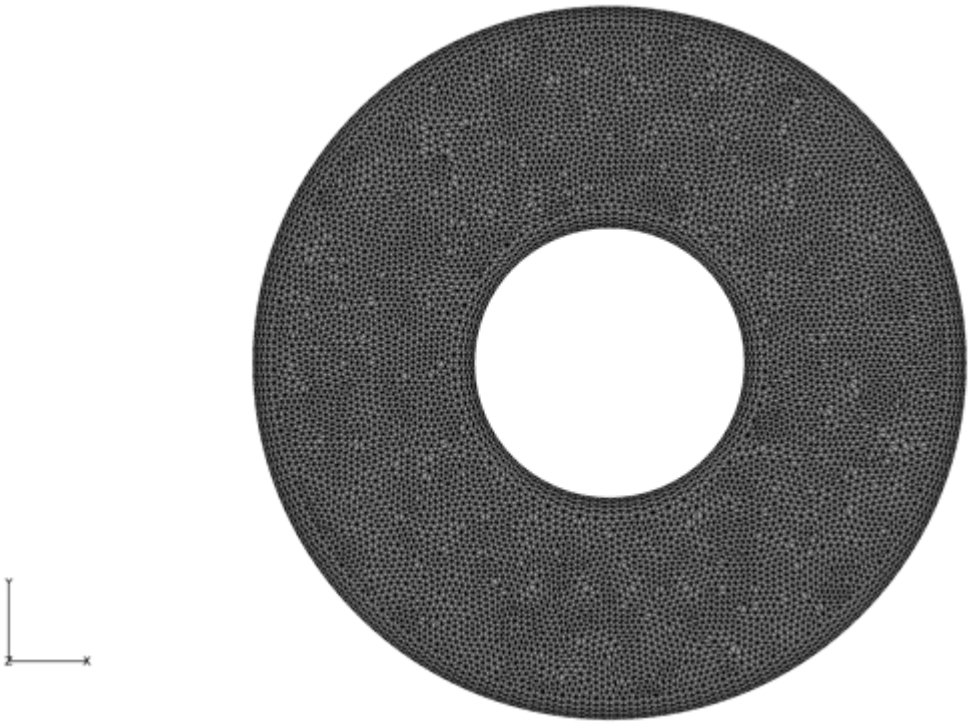


Figure 319: Mesh used for Simulating Radiation Between Two Concentric Cylinders

The simulation was performed as a two dimensional problem by constructing a volume mesh that contains a single layer of elements normal to the radial and circumferential directions.

AcuSolve Results

The AcuSolve solution converges to a steady state and the results reflect the mean temperature distribution. As the inner diameter is considerably hotter than the outer, a heat flux, due to radiation, is present between the cylinders. The temperature within the medium reduces logarithmically as a function of the radius. The following images show the temperature with the medium as a function of radius from the center. The temperature is compared with the analytical solution as described in Incropera (2006). The image below shows black circles representing the analytical solution and a solid red line for the AcuSolve results.

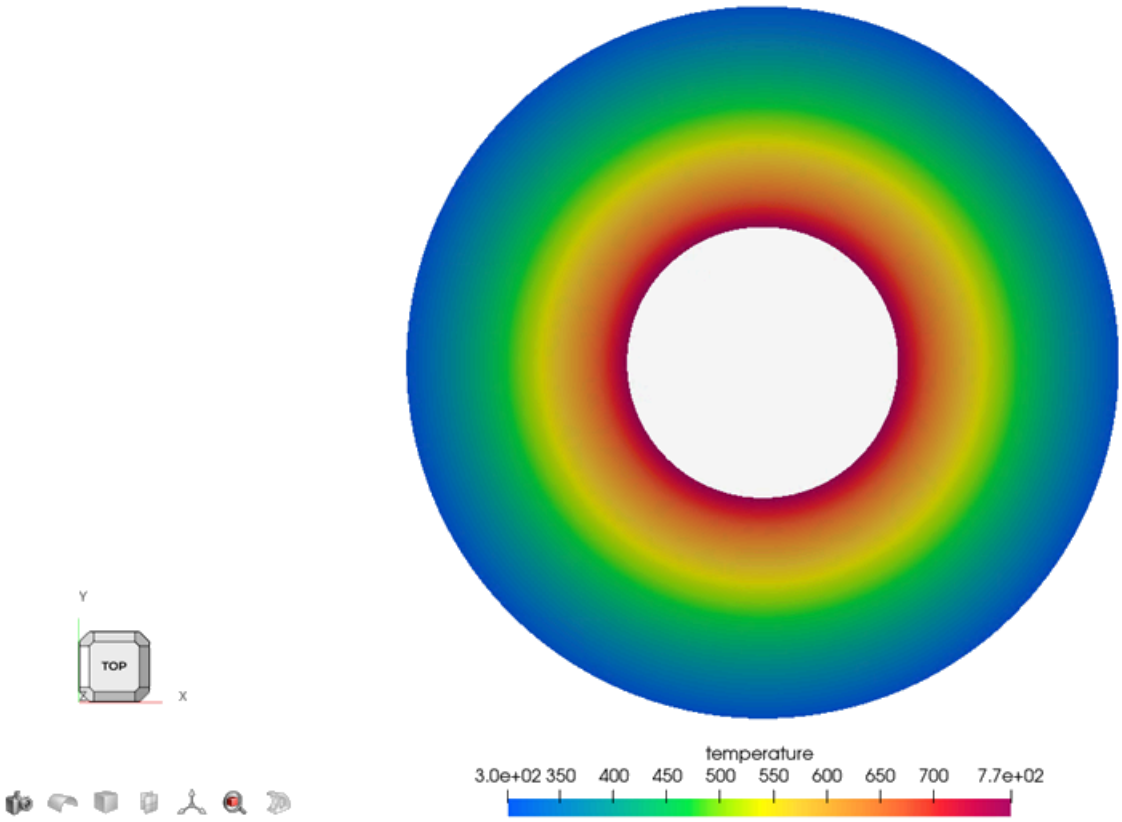


Figure 320: Contours of Temperature Between the Concentric Cylinders

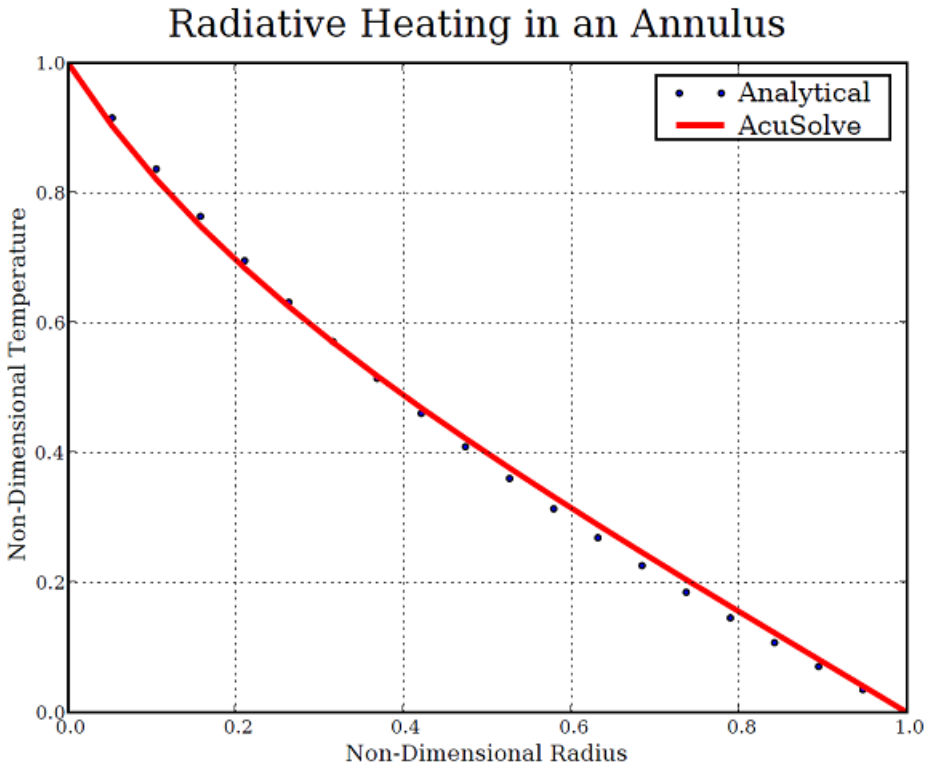


Figure 321: Non Dimensional Temperature Distribution Within the Annulus as a Function of Non Dimensional Radius

Summary

The AcuSolve solution compares well with analytical results for heat transfer due to radiation between two concentric cylinders. In this application, an arbitrary material is subjected to a heat flux that is calculated based on the view factors within the model. As a result of radiative heat flux a temperature distribution between the two cylinders develops. The AcuSolve solution for the temperature as a function of radius matches well compared to the analytical solution.

Heat Transfer Between Radiating Concentric Cylinders

HyperWorks CFD database file: `<your working directory>\annulus_radiation\annulus_radiation.hm`

Global

- Problem Description
  - Analysis type - Steady State
  - Temperature equation - Advective Diffusive
  - Radiation equation- Enclosure
- Auto Solution Strategy
  - Convergence tolerance - `0.0001`
  - Relaxation Factor- `0.4`
  - Flow- off

    - Enclosure radiation- on
- Material Model
    - Material
        - Conductivity
            1. Type - Constant
            2. Conductivity- `1.0`
- Emissivity Model
    - Grey Body
        - Emissivity- `0.03778`
    - Black Body
        - Emissivity- `1.0`

  Model
- Volumes
    - Medium
        - Element Set
            1. Medium - Fluid
            2. Material model- Material
- Surfaces
    - ID
        - Simple Boundary Condition
            1. Type- Wall
            2. Temperature BC type- Value
            3. Temperature- `773.0` K
        - Radiation Surface
            1. Type- Wall
            2. Emissivity model- Grey Body
    - Max_Z
        - Simple Boundary Condition
            1. Type- Symmetry
        - Radiation Surface
            1. Type- Wall
            2. Emissivity model- Black Body
    - Min_Z
        - Simple Boundary Condition
            1. Type- Symmetry
        - Radiation Surface
            1. Type- Wall

2. Emissivity model- Black Body

- OD
  - Simple Boundary Condition
    1. Type- Wall
    2. Temperature BC type- Value
    3. Temperature- `300.0` K
  - Radiation Surface
    1. Type- Wall
    2. Emissivity model- Grey Body

References

F. P. Incropera and D. P. DeWitt. "Fundamentals of Heat Transfer - Sixth Edition". John Wiley & Sons. New York. 2006.

Internal Flow

5

This section includes validation cases that consider wall bounded simulation domains with internally constrained fluid medium.

This chapter covers the following:

- Flow Between Concentric Cylinders (p. 440)
- Laminar Flow Through a Pipe With Imposed Heat Flux (p. 446)
- Turbulent Flow Through a Pipe (p. 451)
- Laminar Couette Flow with Imposed Pressure Gradient (p. 455)
- Laminar Couette Flow with Imposed Pressure Gradient and Heated Walls (p. 461)
- Laminar Poiseuille Flow Through a Pipe (p. 467)
- Laminar Flow Through a Pipe with Species Transport (p. 471)
- Flow Inside a Rotating Cavity (p. 477)
- Natural Convection in a Concentric Annulus (p. 485)
- Laminar Flow Past a 90° T-Junction (p. 491)
- Turbulent Flow Through a Wavy Channel (p. 496)
- Laminar Flow Through a Channel with Heated Walls (p. 504)
- Turbulent Natural Convection Inside a Tall Cavity (p. 509)
- Viscous Heating Inside a Rotating Annulus (p. 517)
- Ideal Gas Compression in an Actuating Piston (p. 524)
- Laminar Flow Through a Pipe with Constant Wall Temperature (p. 531)
- Turbulent Flow with Separation in an Asymmetric Diffuser (p. 536)
- Turbulent Flow with Separation in an Axisymmetric Diffuser (p. 544)
- Turbulent Flow Over a Backward-Facing Step (p. 552)
- Turbulent Flow Past a Convex Curve in a Channel (p. 559)
- Turbulent Flow Past a Wall-Mounted Hump (p. 566)
- Laminar Free Surface Flow Inside a Rotating Cavity (p. 574)
- Heat Transfer Between Radiating Concentric Cylinders (p. 580)
- Turbulent Flow Through a 180 Degree Curved Channel (p. 586)
- Circumferential Flow in a Cylinder Induced by a Rotating Solid (p. 592)
- Turbulent Flow Through a Heated Periodic Channel (p. 598)
- Multiphase Flow Within a Sloshing Tank (p. 604)
- Heat Transfer Between Radiating Concentric Spheres (p. 611)
- Radiation Heat Transfer Through a Cube with a Specular Interface (p. 616)
- Two-Phase Nucleate Boiling in a Cylindrical Pipe (p. 623)
- Single-Phase Nucleate Boiling in a Rectangular Channel (p. 627)

- Supersonic Flow Through a Converging-Diverging Nozzle (p. 632)

Flow Between Concentric Cylinders

In this application, AcuSolve is used to simulate the flow of water between concentric cylinders. The outer cylinder is held stationary while the inner cylinder rotates with a constant speed. AcuSolve results are compared with analytical results as described in White (1991). The close agreement of AcuSolve results with analytical results validates the ability of AcuSolve to model cases containing thin annular gaps with flow induced by rotating walls.

Problem Description

The problem consists of two concentric pipes with water filling the void between them, as shown in the following image, which is not drawn to scale. The radius of the outer pipe is 0.0468 m and the radius of the inner pipe is 0.0178 m. The inner cylinder rotates at 1 rad/sec and the outer cylinder is fixed. The induced flow is laminar and exhibits a steady state behavior. The rotation of the inner cylinder causes the fluid to rotate due to viscous shearing near the wall. As the outer cylinder is fixed, a velocity gradient is generated as a function of radius within the flow domain.

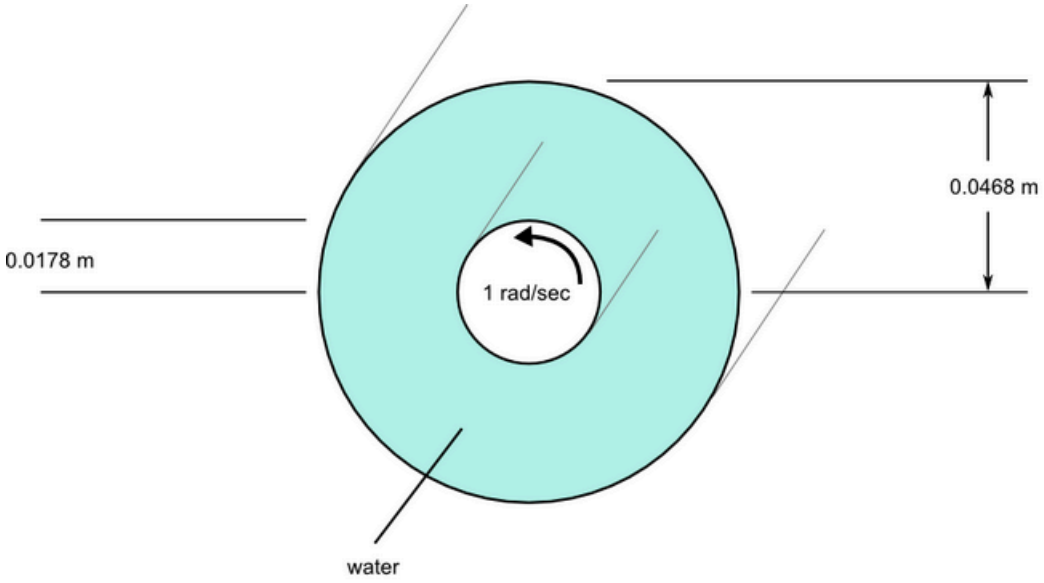


Figure 322: Critical Dimensions and Parameters for Simulating Flow Between Concentric Cylinders

The simulation was performed as a two dimensional problem by restricting flow in the out-of-plane direction through the use of a mesh that is one element thick.

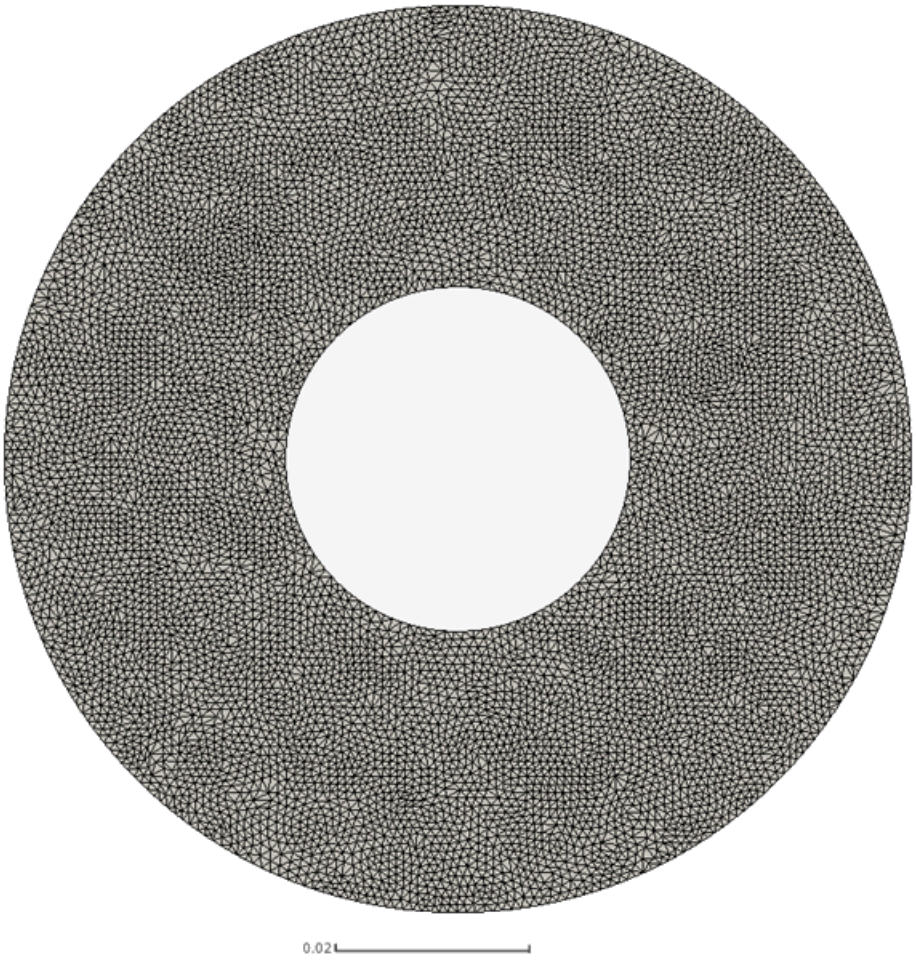


Figure 323: Mesh Used for Simulating Flow Between Concentric Cylinders

AcuSolve Results

The AcuSolve solution converged to a steady state and the results reflect the mean flow conditions. The velocity of the fluid within the cavity is greatest near the rotating inner cylinder. There is a nonlinear decrease in velocity as a function of distance away from the inner cylinder.

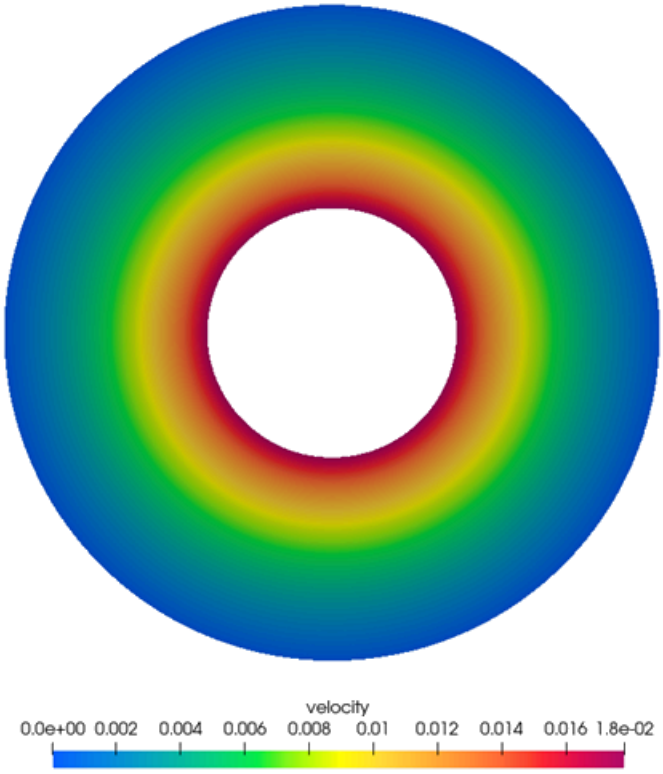


Figure 324: Contours of Tangential Velocity Between the Concentric Cylinders

Analytical tangential velocity at four distances away from the center of the rotating inner cylinder are presented with the corresponding AcuSolve results in the following table.

Table 22:

Distance from the center of rotating cylinder (m)	**Analytical tangential velocity (m/s)**	**AcuSolve tangential velocity (m/s)**	**Percent deviation from analytical**
0.020	0.01514	0.01514	0.04
0.025	0.01059	0.01058	0.10
0.030	0.00727	0.00727	0.06
0.035	0.00466	0.00466	0.10

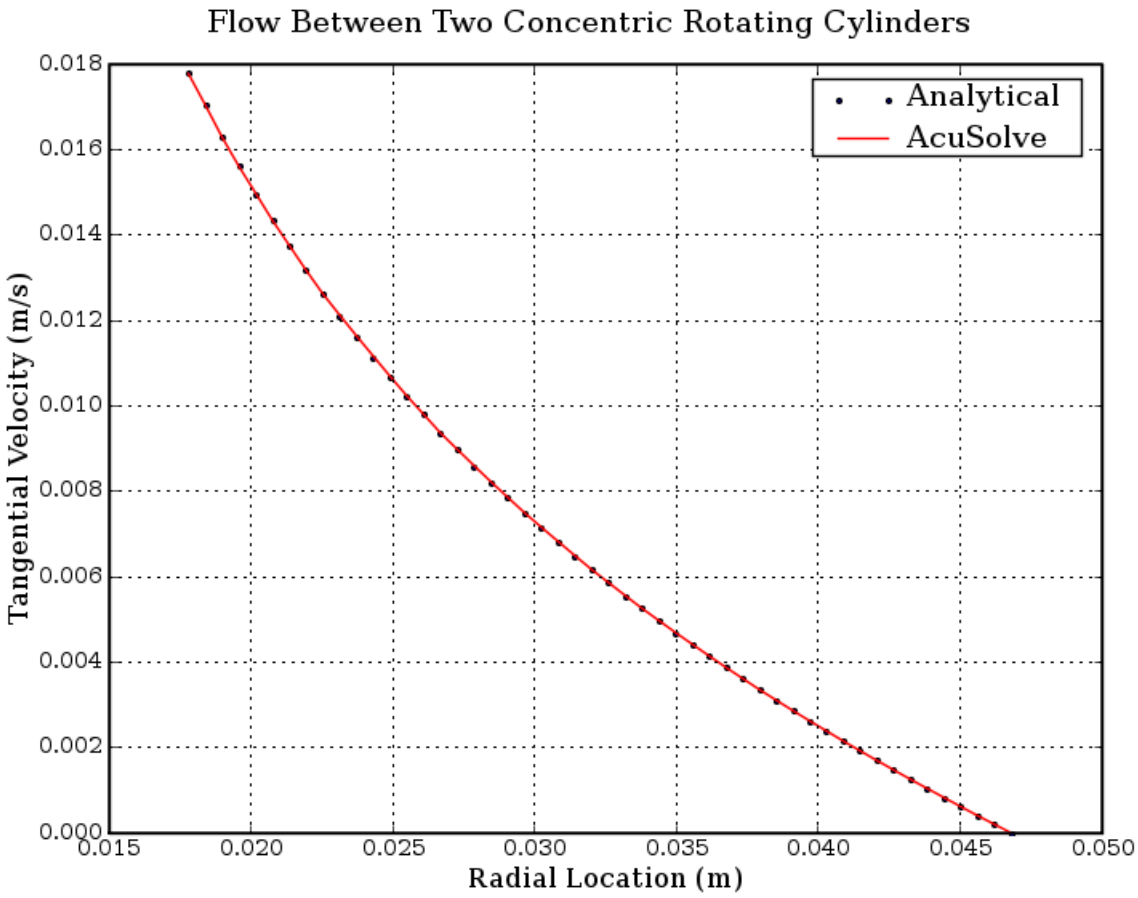


Figure 325: Tangential Velocity Plotted Against Distance from the Center of the Rotating Cylinder

Summary

The AcuSolve solution compares well with analytical results for the flow between concentric cylinders. In this application, the velocity in the annular fluid region is driven by the viscous stresses on the rotating wall. The AcuSolve tangential velocity is within 0.1 percent of the analytical solution at all radial locations.

Simulation Settings for Flow Between Concentric Cylinders

HyperWorks CFD database file: `<your working directory>\annulus_rotating\annulus_rotating.hm`

Global

- Problem Description
  - Analysis type - Steady State
  - Turbulence equation - Laminar
- Auto Solution Strategy
  - Relaxation Factor - `0.2`
- Material Model

    - Water
        - Density - `1000.0` kg/m3
        - Viscosity - `0.001` kg/m-sec
- Reference Frame
    - Rotating_Cylinder
        - Rotation center
            1. X-coordinate - `0.0` m
            2. Y-coordinate - `0.0` m
            3. Z-coordinate - `0.0` m
        - Angular velocity
            1. X-component - `0.0` rad/sec
            2. Y-component - `0.0` rad/sec
            3. Z-component - `-1.0` rad/sec

Model

- Volumes
    - Volume
        - Element set
            1. Material model - Water
- Surfaces
    - Boundary1
        - Simple Boundary Condition
            1. Type - Symmetry
    - Boundary2
        - Simple Boundary Condition
            1. Type - Symmetry
    - Inner
        - Simple Boundary Condition
            1. Type - Wall
            2. Reference Frame - Rotating_Cylinder
    - Outer
        - Simple Boundary Condition
            1. Type - Wall
- Nodes
    - Fixed
        - Pressure
            1. Type - Zero

References

F. M. White. "Viscous Fluid Flow". Section 3-2.3. McGraw-Hill Book Co., Inc. New York. 1991.

Laminar Flow Through a Pipe With Imposed Heat Flux

In this application, AcuSolve is used to simulate the flow of mercury through a heated pipe. The AcuSolve results are compared with analytical results for pressure drop as described in White (1991), and with temperature changes as described in Incropera and DeWitt (1981). The close agreement of AcuSolve results with analytical results validates the ability of AcuSolve to model cases with flow and imposed heat flux.

Problem Description

The problem consists of mercury flowing through a heated, circular pipe that is 0.005 m in diameter and 0.1 m long, as shown in the following image, which is not drawn to scale. Mercury enters the pipe with a constant temperature of 300 K. The pipe has an imposed heat flux of 2000 W/m^2. The laminar velocity field is modeled as periodic to achieve a fully developed velocity profile. As the fluid moves through the pipe it is slowly heated by the heat flux on the wall, resulting in an increased centerline temperature. Pressure decreases along the pipe length due to the friction imposed by the viscous stresses near the pipe wall.

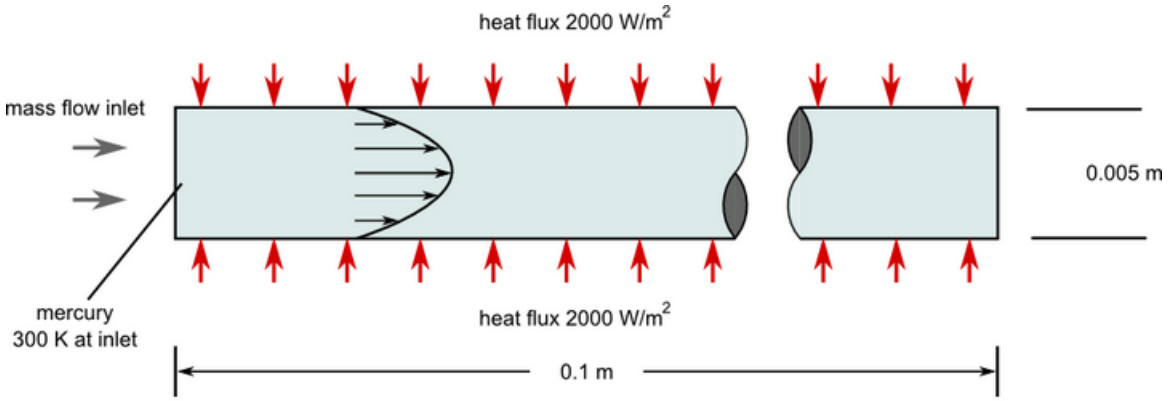


Figure 326: Critical Dimensions and Parameters for Simulating Laminar Flow through a Pipe with Imposed Heat Flux

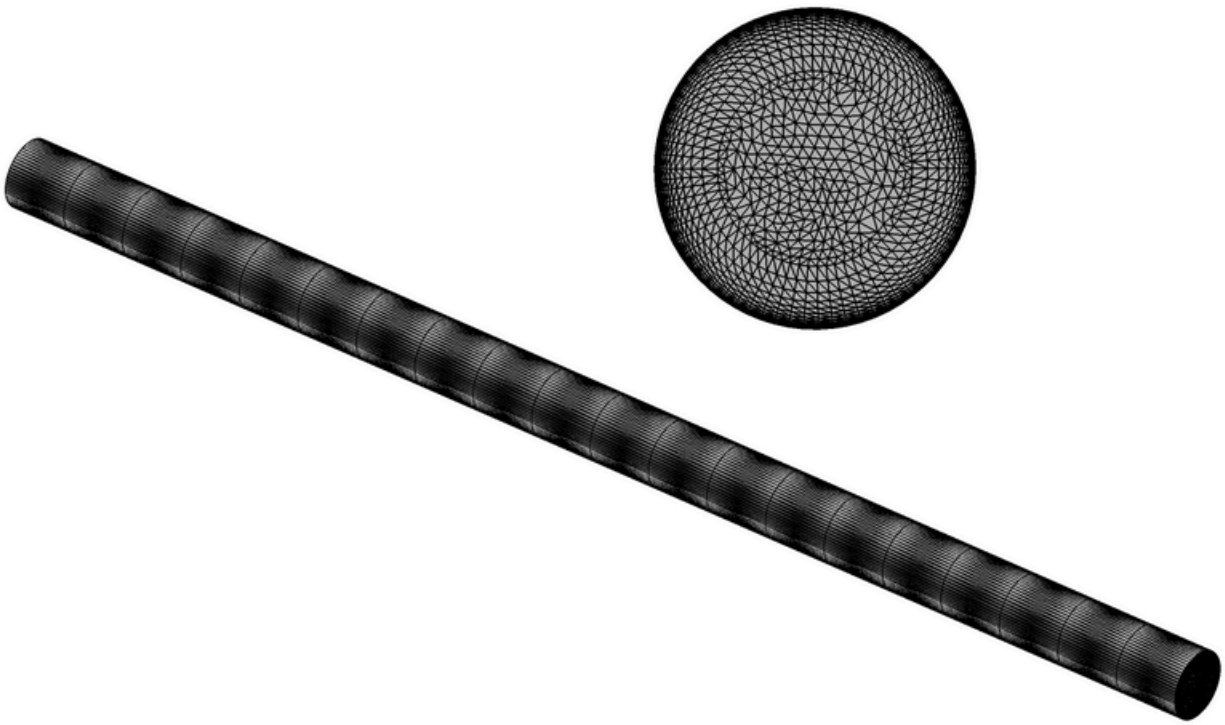


Figure 327: Mesh used for Simulating Laminar Flow Through a Pipe with Imposed Heat Flux

AcuSolve Results

The AcuSolve solution converged to a steady state and the results reflect the mean flow conditions. The greatest pressure is at the inlet, with pressure decreasing as a function of distance away from the inlet. The temperature of the mercury in the pipe increases as a function of distance from the inlet due to the impact of the heat flux on the pipe walls.

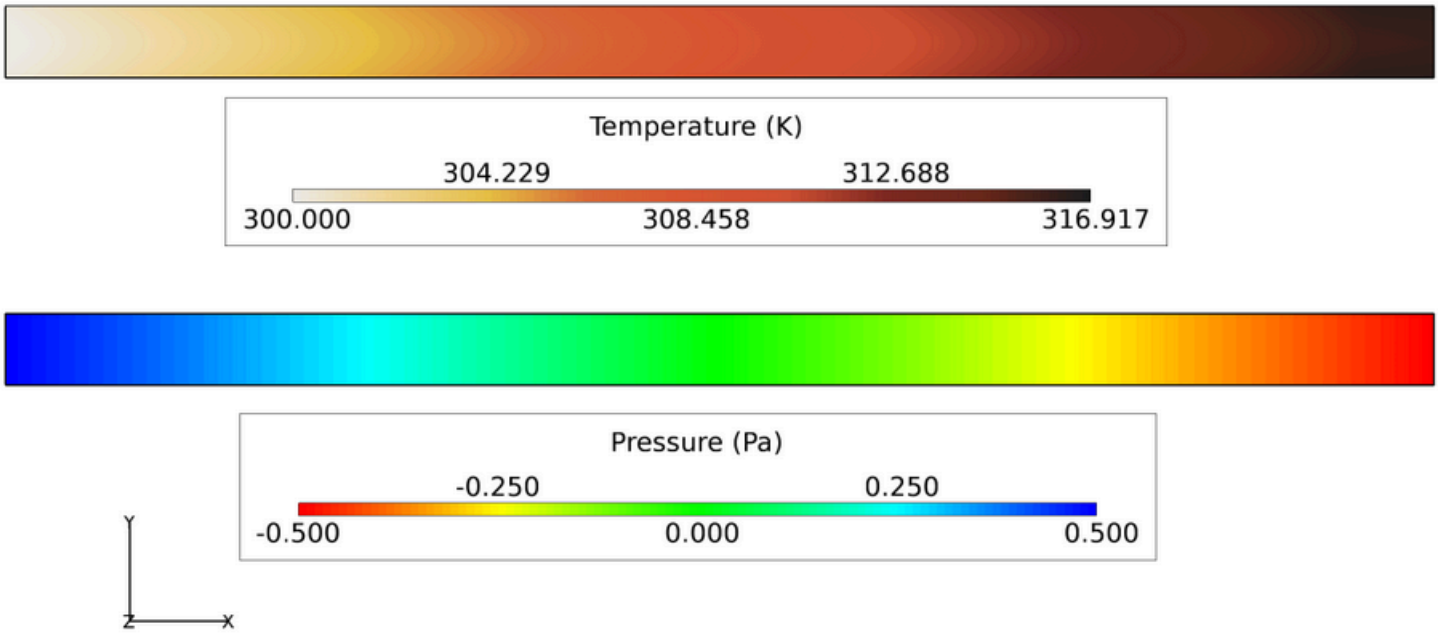


Figure 328: Temperature and Pressure Contours of Mercury Flow Through a Heated Pipe

The analytical solution for the pressure drop, between the inlet and outlet, as well as the analytical solution for the temperature of the mercury at the center of the outlet are presented with the corresponding AcuSolve results in the following table.

Table 23:

	Analytical solution	AcuSolve solution	Percent deviation from analytical
Pressure drop (Pa)	0.991	0.994	0.303
Centerline temperature of flow at outlet (K)	316.917	316.269	0.204

Summary

The AcuSolve solution compares well with analytical results for flow through a pipe with an imposed heat flux. In this application, the pressure drop in the fluid region is driven by the viscous stresses near the pipe wall. The temperature in the fluid region is influenced by the imposed heat flux on the walls. The values of pressure and temperature that are predicted by AcuSolve are within 0.3 percent of the analytical solution.

Simulation Settings for Laminar Flow Through a Pipe With Imposed Heat Flux

AcuConsole database file: `<your working directory>\pipe_laminar_heat\pipe_laminar_heat.acs`

Global

- Problem Description
  - Analysis type - Steady State
  - Temperature equation - Advective Diffusive
  - Turbulence equation - Laminar
- Auto Solution Strategy
  - Relaxation Factor - `0.2`
- Material Model
  - Mercury
    - Density - `13579.0` kg/m3
    - Viscosity - `0.001548` kg/m-sec

  Model
- Volume
  - Fluid
    - Element Set
      1. Material model - Mercury
- Surfaces
  - Inflow
    - Simple Boundary Condition - (disabled to allow for periodic conditions to be set)
    - Advanced Options
      1. Integrated Boundary Conditions
         1. Mass Flux
            1. Type - Constant
            2. Constant value - `-1.33e-3` kg/sec
         2. Temperature
            1. Type - Constant
            2. Constant value - `300.0` K
  - Outflow
    - Simple Boundary Condition - (disabled to allow for periodic conditions to be set)
  - Wall

        - Simple Boundary Condition
            1. Type - Wall
            2. Temperature BC type - Flux
            3. Heat flux - `2000.0` W/m2
- Periodics
    - Periodic 1
        - Individual Periodic BCs
            1. Velocity
                1. Type - Periodic
            2. Pressure
                1. Type - Single Unknown Offset
            3. Temperature
                1. Type - Single Unknown Offset

References

F. M. White. "Viscous Fluid Flow". Section 3-2.1. McGraw-Hill Book Co., Inc.. New York. 1991.

F. P. Incropera and D. P. DeWitt. "Fundamentals of Heat Transfer". John Wiley & Sons. New York. 1981.

Turbulent Flow Through a Pipe

In this application, turbulent flow of air through a pipe is simulated. AcuSolve results are compared with experimental results as described in White (1991) and extracted from the Moody chart. The close agreement of AcuSolve results with experimental results validates the ability of AcuSolve to model turbulent flow within pipes.

Problem Description

The problem consists of air flowing through a pipe 0.004 m in diameter and 0.02 m long, as shown in the following image, which is not drawn to scale. The AcuSolve simulation utilizes periodic boundary conditions to obtain the fully developed profile within the pipe. The defined pressure drop, applied as a body force on the fluid volume, offsets the change in pressure due to the friction created by the no-slip walls of the pipe. The Reynolds number for this problem is approximately 8,250.

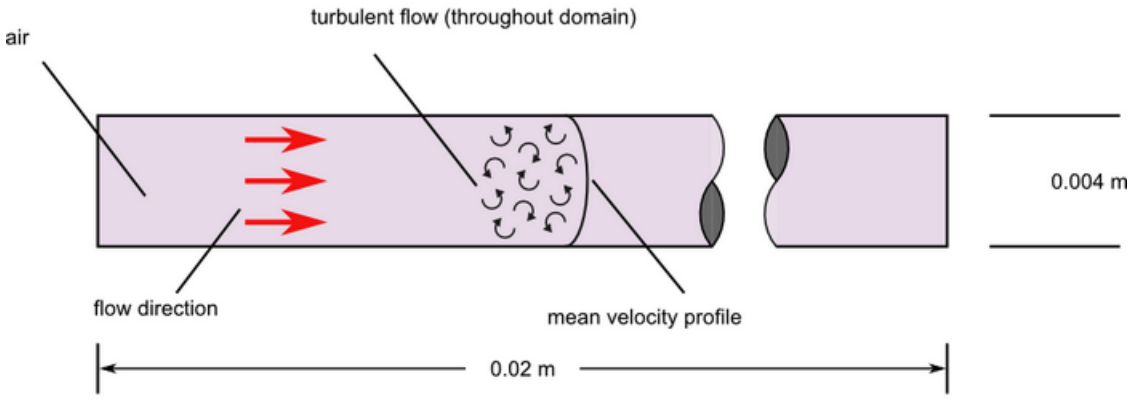


Figure 329: Critical Dimensions and Parameters for Simulating Turbulent Flow Through a Pipe

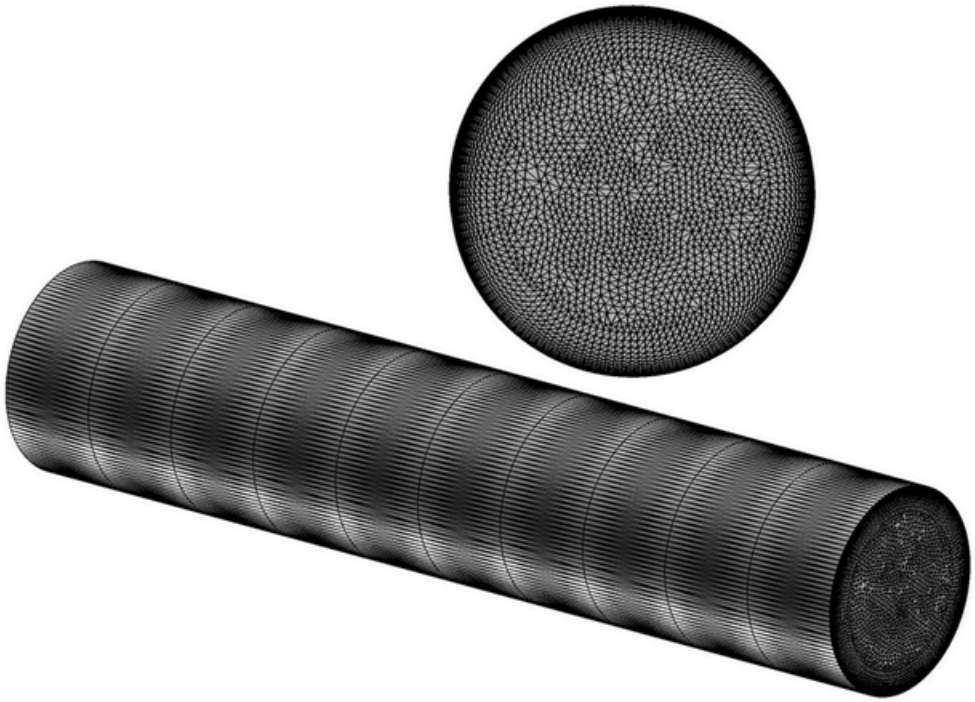


Figure 330: Mesh of a Periodic Segment Used for Simulating Turbulent Flow Through a Pipe

AcuSolve Results

The AcuSolve solution converged to a steady state and the results reflect the mean flow conditions with a turbulent velocity profile that is fully developed. The simulation was performed using the Spalart-Allmaras single-equation turbulence model. The velocity and eddy viscosity profiles are constant along the length of the pipe.

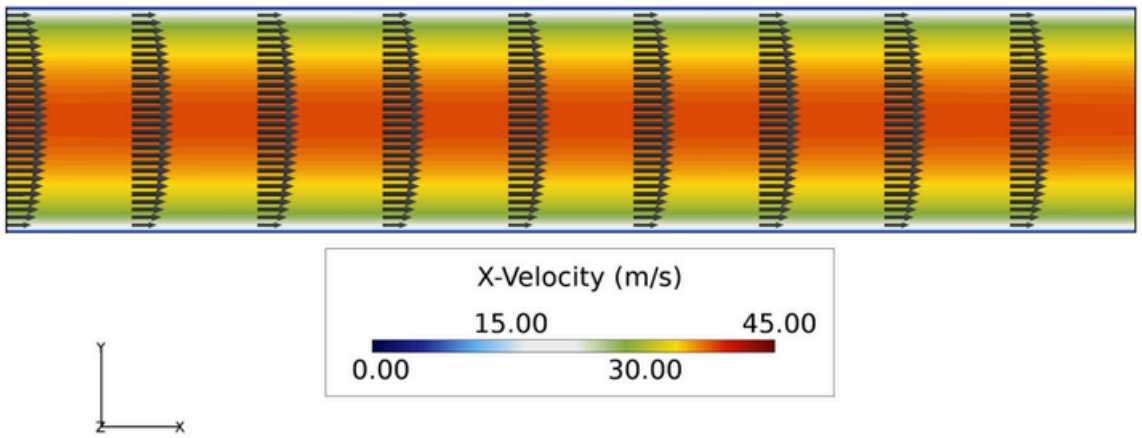


Figure 331: Velocity Contours and Periodic Velocity Vectors for the Averaged Turbulent Flow

The experimental result for average velocity at the inlet is presented with the corresponding AcuSolve prediction in the following table.

Table 24:

	Experimental result	AcuSolve prediction	Percent deviation from experimental
Average inlet velocity	30.0	29.71	0.971

Summary

The AcuSolve solution compares well with the experimental result for average inlet velocity for turbulent flow through a pipe. In this application, the applied body force counteracts the change in pressure due to the viscous stresses near the pipe wall. The resulting friction factor for a smooth wall pipe and the specified Reynolds number is approximately 0.0326. With the imposed pressure drop defining the flow, the AcuSolve prediction of average inlet velocity is within 1.0 percent of the Darcy-Weisbach approximation.

Simulation Settings for Turbulent Flow Through a Pipe

AcuConsole database file: `<your working directory >\pipe_turbulent\pipe_turbulent.acs`.

Global

- Problem Description
  - Analysis type - Steady State
  - Turbulence equation - Spalart Allmaras
- Auto Solution Strategy

    - Relaxation factor - `0.4`
- Material Model
    - Air
        - Density - `1.225` kg/m3
        - Viscosity - `1.781e-05` kg/m-sec
- Body Force
    - dpdx
        - Gravity
            1. X-component - `3739.98` m/s2

    Model
- Volumes
    - Fluid
        - Element Set
            1. Material model - Air
            2. Body force - dpdx
- Surfaces
    - Inlet
        - Simple Boundary Condition - (disabled to allow for periodic conditions to be set)
    - Outlet
        - Simple Boundary Condition - (disabled to allow for periodic conditions to be set)
    - Wall
        - Simple Boundary Condition
            1. Type - Wall
            2. Roughness height - `0.0` mm
- Periodics
    - Periodic 1
        - Periodic Boundary Condition
            1. Type - Periodic

References

F. M. White. "Viscous Fluid Flow". Section 3-2.1. McGraw-Hill Book Co., Inc.. New York. 1991.

Experimental solution adapted from Darcy-Weisbach equation based on friction factor taken from the Moody chart with a Reynolds number of approximately 8,250.

Laminar Couette Flow with Imposed Pressure Gradient

In this application, AcuSolve is used to simulate the viscous flow of water between a moving and a stationary plate with an imposed pressure gradient. AcuSolve results are compared with analytical results described in White (1991). The close agreement of AcuSolve results with analytical results validates the ability of AcuSolve to model cases with imposed pressure gradients.

Problem Description

The problem consists of air between two plates in a two dimensional domain, as shown in the following image, which is not drawn to scale. The domain is 1.0 m high and 1.5 m long. The top plate moves with a constant velocity of 3.0 m/sec and the bottom plate is fixed. There is a mean-pressure gradient of -12 Pa/m applied to the bulk fluid in the streamwise direction. The problem is simulated with periodic boundaries in the streamwise direction. The induced flow field is laminar and exhibits a steady state behavior. The flow field develops from the pressure gradient, the motion of the top plate, and the viscous shear stresses near the plates.

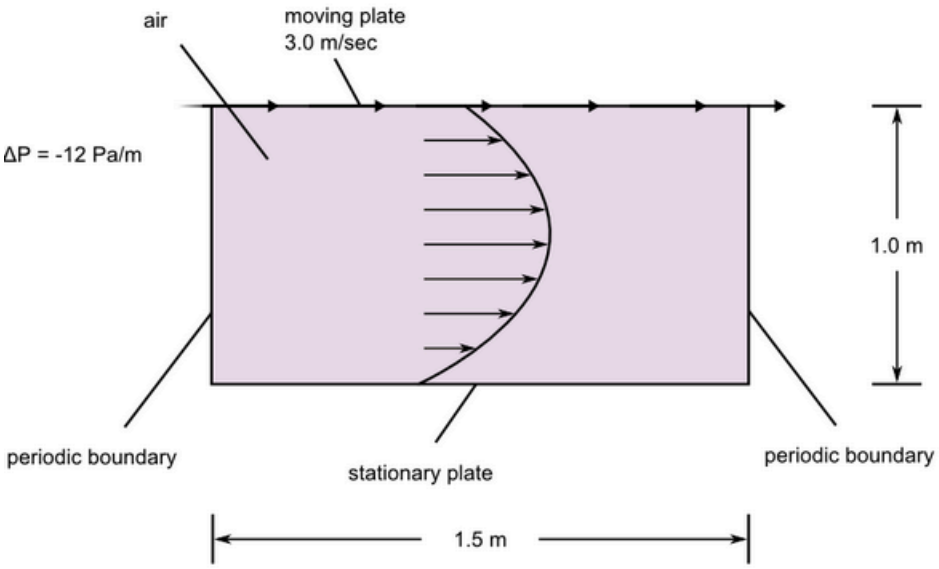


Figure 332: Critical Dimensions and Parameters for Simulating Laminar Couette Flow with an Imposed Pressure Gradient

The simulation was performed as a two dimensional problem by restricting flow in the out-of-plane direction through the use of a mesh that is one element thick.

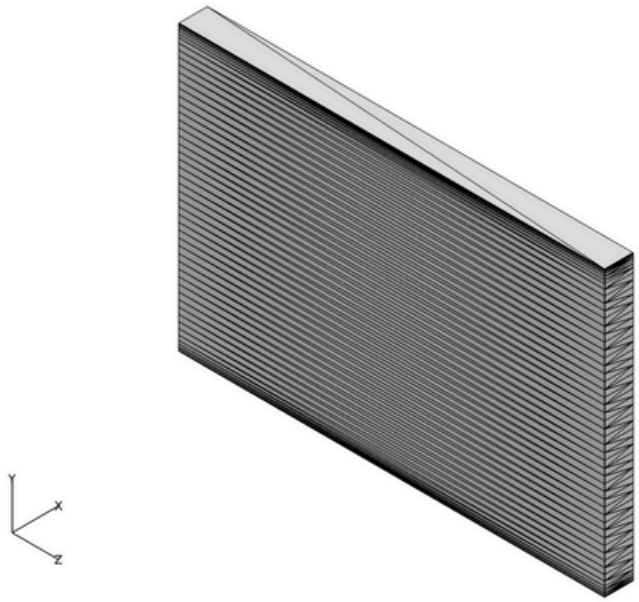


Figure 333: Mesh used for Simulating Laminar Couette Flow with an Imposed Pressure Gradient

AcuSolve Results

The AcuSolve solution converged to a steady state and the results reflect the mean flow conditions. The greatest velocity is located at approximately 40 percent of the channel height, closer to the moving plate. The flow develops as a result of the pressure gradient and the shear stress acting on the fluid near both the moving plate and the stationary plate.

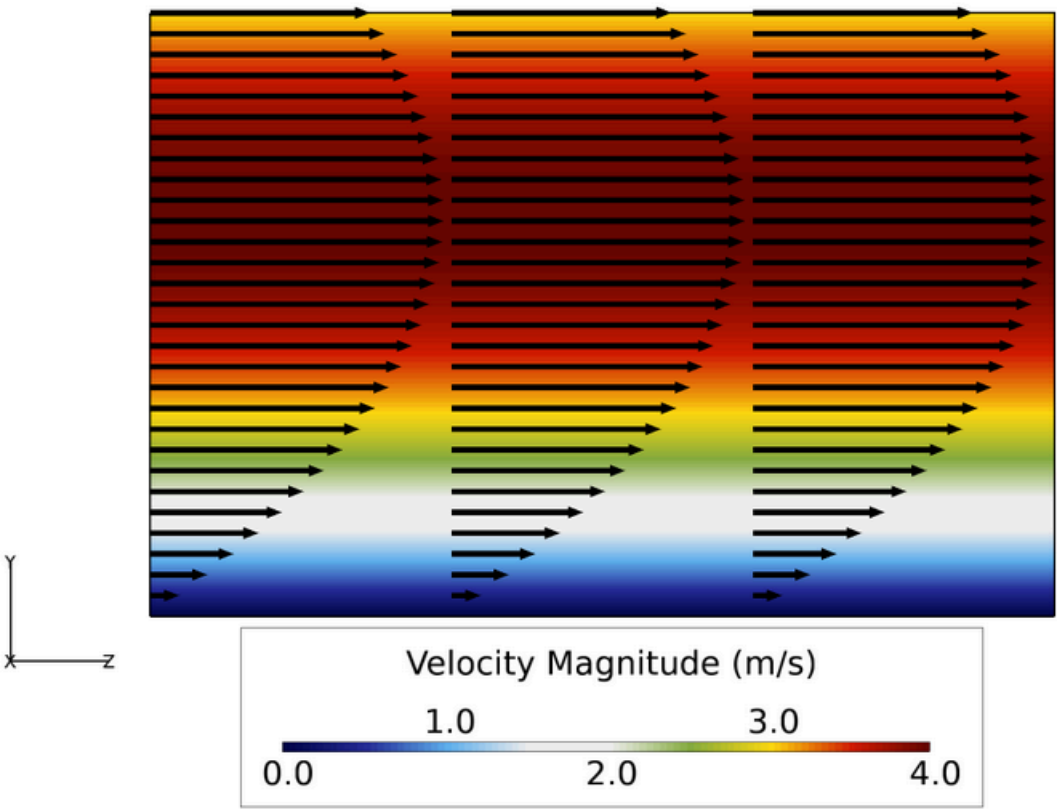


Figure 334: Z-Velocity Contours and Velocity Vectors

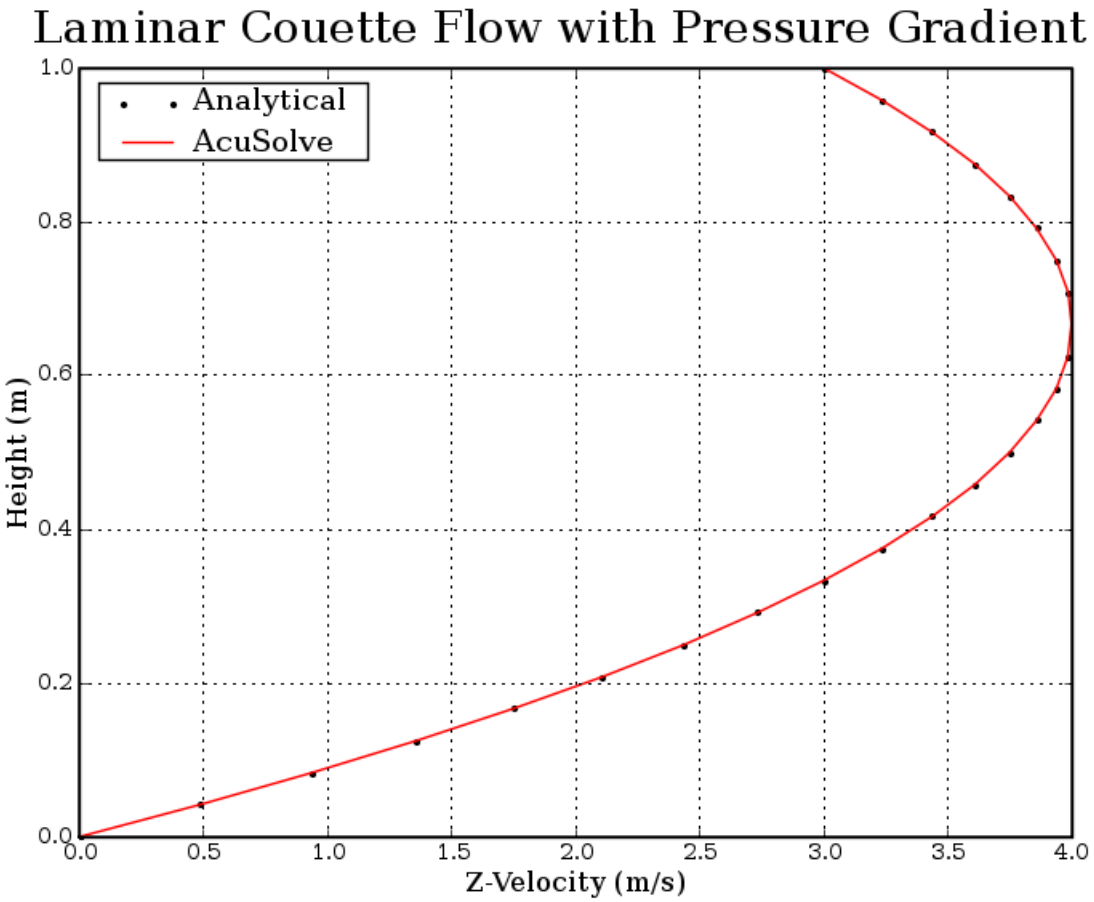


Figure 335: Z Velocity Plotted Against Height Above the Bottom of the Flow Field (Z Velocity is Presented on the X Axis to Better Represent the Velocity Profile in the Direction of Flow)

Summary

The velocity profile computed by AcuSolve agrees well with the analytical solution for this application. The velocity profile arises due to the combination of the imposed pressure gradient and the constant upper-wall velocity. Note that the combination of these effects results in the asymmetric velocity profile that is reflected in the results.

Simulation Settings for Laminar Couette Flow with Imposed Pressure Gradient

AcuConsole database file: `<your working directory>\couette_flow\couette_flow.acs`

Global

- Problem Description
  - Analysis Type - Steady State
  - Turbulence equation - Laminar
- Auto Solution Strategy
  - Relaxation factor - `0.2`

- Material Model
  - Air
    - Density - `1.0` kg/m3
    - Viscosity - `1.0` kg/m-sec
- Body Force
  - DP/DL
    - Gravity
      1. Z-component - `18.0` m/sec2

  Model
- Volumes
  - Fluid
    - Element set
      1. Material model - Air
      2. Body force - DP/DL
- Surfaces
  - Max_X
    - Simple Boundary Condition
      1. Type - Symmetry
  - Max_Y
    - Simple Boundary Condition
      1. Type - Wall
      2. Wall velocity type - Cartesian
      3. Z-velocity - `3.0` m/s
  - Max_Z
    - Simple Boundary Condition - (disabled to allow for periodic conditions to be set)
  - Min_X
    - Simple Boundary Condition
      1. Type - Symmetry
  - Min_Y
    - Simple Boundary Condition
      1. Type - Wall
  - Min_Z
    - Simple Boundary Condition - (disabled to allow for periodic conditions to be set)
- Periodics
  - Periodic 1
    - Periodic Boundary Conditions
      1. Type - Periodic

References

F. M. White. "Viscous Fluid Flow". Section 3-2.3. McGraw-Hill Book Co., Inc.. New York. 1991.

Laminar Couette Flow with Imposed Pressure Gradient and Heated Walls

In this application, AcuSolve is used to simulate the flow of a highly viscous fluid between a moving and a stationary plate with an imposed pressure gradient and fixed temperature on the walls. AcuSolve results are compared with analytical results described in White (1991). The close agreement of AcuSolve results with analytical results validates the ability of AcuSolve to model cases with imposed pressure gradients and viscous heating.

Problem Description

The problem consists of a viscous fluid between two plates in a two dimensional domain, as shown in the following image, which is not drawn to scale. The domain is 1.0 m high and 1.5 m long. The top plate moves with a constant velocity of 3.0 m/sec and the bottom plate is fixed. To simulate a fully developed flow with a relatively short length domain there is a mean-pressure gradient of -12 Pa/m applied to the fluid in the streamwise direction, defined as a body force acting on the entire fluid. The lower wall is held at a fixed temperature of 273.0 K, while the upper wall is held at a fixed temperature of 274.0 K. The problem is simulated with periodic boundaries in the streamwise direction. The Reynolds number of the flow, based on the distance between the plates is 0.3, indicating laminar flow. The flow field develops from the pressure gradient, the motion of the top plate, and the viscous shear stresses near the plates. The shear stress within the domain causes the temperature to increase within the channel.

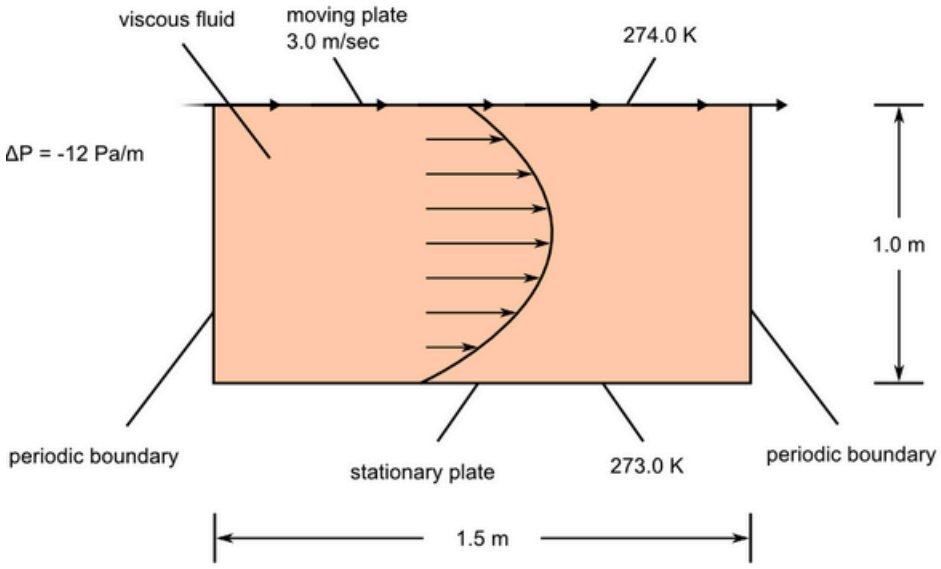


Figure 336: Critical Dimensions and Parameters for Simulating Laminar Couette Flow with an Imposed Pressure Gradient and Heated Walls

The simulation was performed as a two dimensional problem by constructing a volume mesh that contains a single layer of elements extruded in the cross stream direction, normal to the flow plane and by imposing symmetry boundary conditions on the extruded planes. Due to the periodic natural of the flow, a single element extrusion in the streamwise direction is used to reduce the model size.

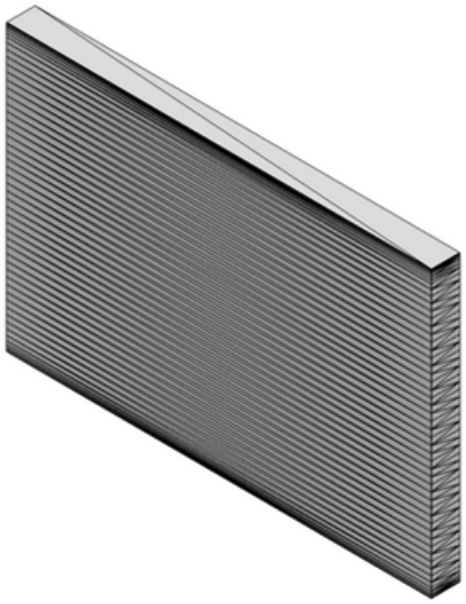


Figure 337: Mesh used for Simulating Laminar Couette Flow with an Imposed Pressure Gradient and Heated Walls

AcuSolve Results

The AcuSolve solution converged to a steady state and the results reflect the mean flow conditions. The simulation results show a flow field with a nearly linear distribution of velocity, with the peak at the top wall. The flow develops primarily as a result of the shear stress acting on the fluid near both the moving plate and the stationary plate. The temperature variation between the two plates develops due to the viscous heating effects that increase the temperature within the channel, with the maximum near the central height of the domain. The following figure shows the temperature distribution between the two plates and velocity vectors indicating the velocity profile.

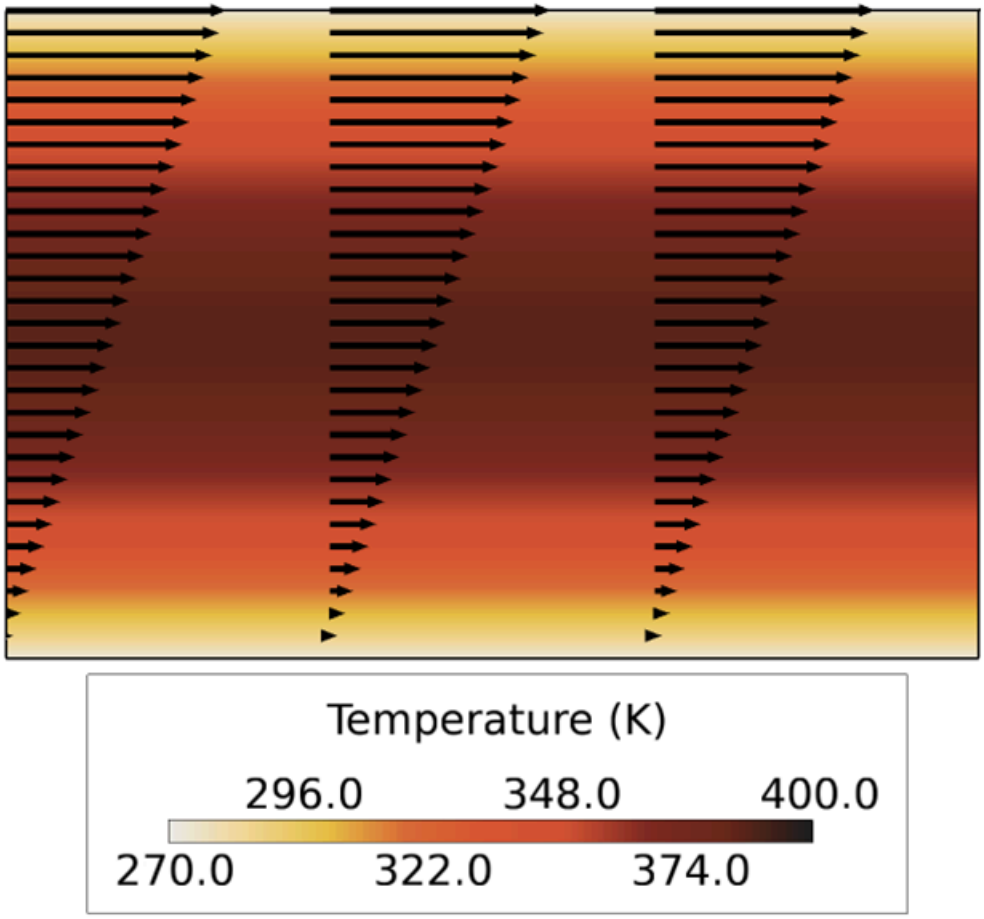


Figure 338: Contours of Temperature Between the Plates, with Velocity Vectors

The following image demonstrates the accuracy of the solution compared to the analytical results as computed by the solution for viscous heating within a channel with a moving upper boundary.

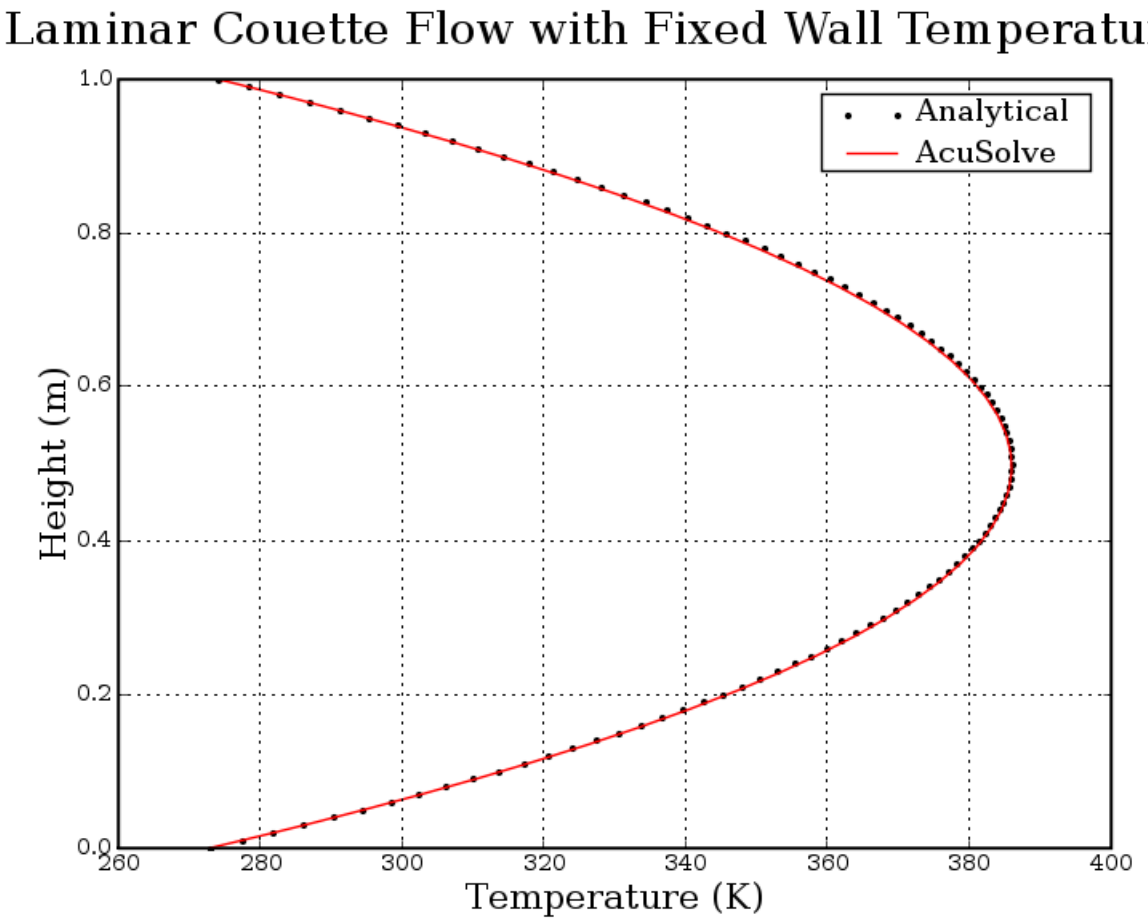


Figure 339: Temperature Plotted Against Height above the Bottom of the Flow Field (Temperature is Presented on the X Axis to Better Represent the Distribution Between the Plates in the Streamwise Direction)

Summary

In this application, a fully developed laminar flow between two plates with fixed temperature is studied and compared against analytical data. The AcuSolve results compare well with the analytical data for the temperature distribution between the two plates. The simulation indicates that the velocity profile arises due to the combination of the viscous shearing and the velocity of the upper plate. The velocity and temperature profiles computed by AcuSolve demonstrate how highly viscous fluids tend to direct the flow regime. AcuSolve demonstrates the ability to predict the analytical solution for viscous heating between two flat plates with moving and stationary boundaries and an imposed pressure gradient.

Simulation Settings for Laminar Couette Flow with Imposed Pressure Gradient and Heated Walls

AcuConsole database file: `<your working directory>\couette_laminar_heat\couette_laminar_heat.acs`

Global

- Problem Description

    - Analysis Type - Steady State
    - Temperature equation - Advective Diffusive
    - Turbulence equation - Laminar
- Auto Solution Strategy
    - Relaxation factor - `0.2`
- Material Model
    - Fluid
        - Density - `1.0` kg/m3
        - Specific Heat - `1.0` J/kg-K
        - Viscosity - `100.0` kg/m-sec
- Body Force
    - DP/DL
        - Gravity
            1. Z-component - `18.0` m/sec2

    Model
- Volumes
    - Fluid
        - Element set
            1. Material model - Fluid
            2. Body force - DP/DL
            3. Viscous heating - on
- Surfaces
    - Max_X
        - Simple Boundary Condition
            1. Type - Symmetry
    - Max_Y
        - Simple Boundary Condition
            1. Type - Wall
            2. Wall velocity type - Cartesian
            3. Z-velocity - `3.0` m/s
            4. Temperature - `274.0` K
    - Max_Z
        - Simple Boundary Condition - (disabled to allow for periodic conditions to be set)
    - Min_X
        - Simple Boundary Condition
            1. Type - Symmetry
    - Min_Y

        - Simple Boundary Condition
            1. Type - Wall
            2. Temperature - `273.0` K
    - Min_Z
        - Simple Boundary Condition - (disabled to allow for periodic conditions to be set)
- Periodics
    - Periodic 1 all
        - Periodic Boundary Conditions
            1. Type - Periodic

References

F. M. White. "Viscous Fluid Flow". Section 3-3.2. McGraw-Hill Book Co., Inc. New York. 1991.

Laminar Poiseuille Flow Through a Pipe

In this application, AcuSolve is used to simulate the flow of carbon dioxide (CO_2) entering a pipe with a fixed velocity. AcuSolve results are compared with analytical results using the Hagen-Poiseuille approach as described in White (1991). The close agreement of AcuSolve results with analytical results validates the ability of AcuSolve to model cases with constant flow velocity.

Problem Description

The problem consists of CO_2 flowing through a circular pipe 0.0025 m in diameter and 0.01 m long, as shown in the following image, which is not drawn to scale. The CO_2 enters the pipe with an average inlet velocity of 3.0 m/s. The flow field develops as a result of the viscous shearing on the fluid at the pipe wall.

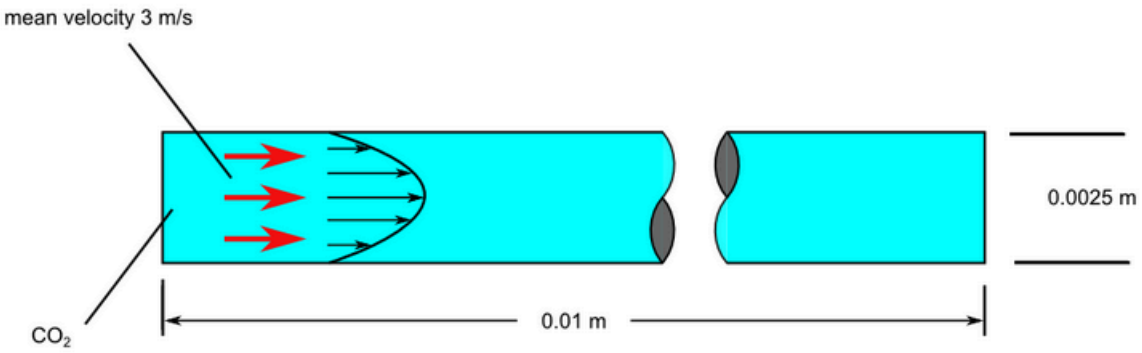


Figure 340: Critical Dimensions and Parameters for Simulating Laminar Poiseuille Flow Through a Pipe



Figure 341: Mesh Used for Simulating Laminar Poiseuille Flow Through a Pipe

AcuSolve Results

The AcuSolve solution converged to a steady state and the results reflect the mean flow conditions. The pressure decreases along the length of the pipe.

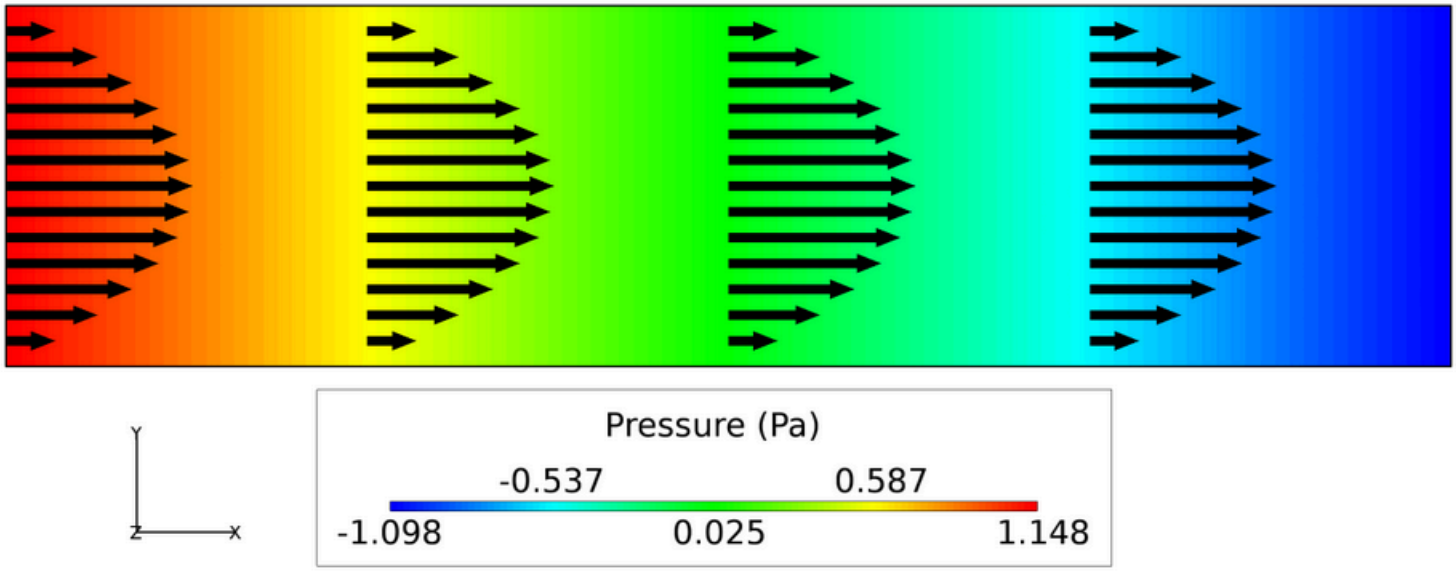


Figure 342: Pressure Contours and Velocity Vectors

The analytical pressure drop between the inlet and the outlet is presented with the corresponding AcuSolve result in the following table.

Table 25:

	Analytical pressure drop (Pa)	**AcuSolve pressure drop (Pa)**	**Percent deviation from analytical**
Inlet to outlet pressure drop	2.242	2.245	0.099

Summary

The AcuSolve solution compares well with analytical results for laminar flow through a pipe. In this application, the pressure drop along the length of the pipe is caused by the viscous shearing near the pipe wall. The AcuSolve steady state solution compares well with the analytical solution, with less than 0.1 percent error.

Simulation Settings for Laminar Poiseuille Flow Through a Pipe

AcuConsole database file: `<your working directory>\pipe_laminar\pipe_laminar.acs`

Global

- Problem Description
  - Analysis type - Steady State
  - Turbulence equation - Laminar
- Auto Solution Strategy
  - Relaxation factor - `0.2`
- Material Model
  - CO2
    - Density `1.808` kg/m3
    - Viscosity `1.46e-5` kg/m-sec

  Model
- Volumes
  - Fluid
    - Element Set
      1. Material Model - CO2
- Surfaces
  - Inflow
    - Simple Boundary Condition - (disabled to allow for periodic conditions to be set)
    - Advanced Options
      1. Integrated Boundary Conditions
         1. Mass Flux
            1. Type - Constant
            2. Constant value - `-2.6625e-05` kg/sec
  - Outflow
    - Simple Boundary Condition - (disabled to allow for periodic conditions to be set)
  - Wall
    - Simple Boundary Condition
      1. Type - Wall
- Periodics
  - Periodic 1
    - Individual Periodic BCs
      1. Velocity
         1. Type - Periodic
      2. Pressure
         1. Type - Single Unknown Offset

References

F. M. White. "Viscous Fluid Flow". Section 3-2.1. McGraw-Hill Book Co., Inc.. New York. 1991.

Laminar Flow Through a Pipe with Species Transport

In this application, AcuSolve is used to simulate the transport of a passive scalar species in a fully developed laminar flow. AcuSolve results are compared with analytical results as described in Kays and Crawford (1993). The close agreement of AcuSolve results with analytical results validates the ability of AcuSolve to model cases with species transport.

Problem Description

The problem consists of species transport in a pipe 0.005 m in diameter and 0.1 m long, as shown in the following image, which is not drawn to scale. The species transport equation is bounded at the inlet with a value of 1.0, while the boundary condition at the wall is 0.0. These constraints impose a concentration gradient within the fluid. The concentration gradient causes the fraction of species 1 to decrease near the pipe wall due to diffusion. The reduced concentration of the species is transported downstream in the pipe via advection, and leads to a continued decrease in the concentration as flow propagates through the pipe.

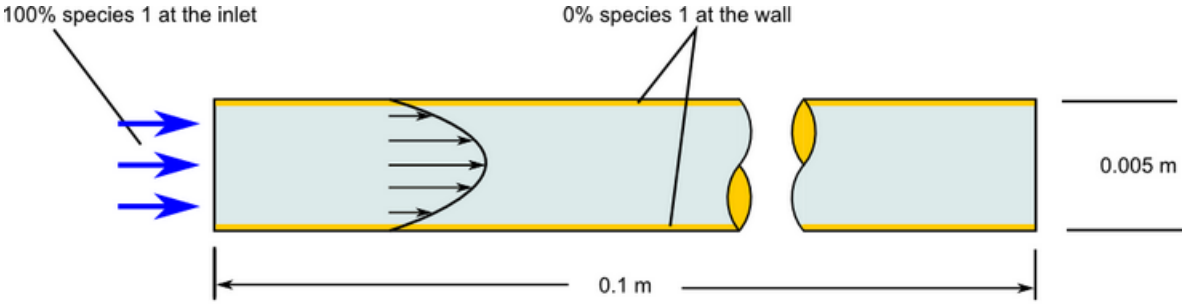


Figure 343: Critical Dimensions and Parameters for Simulating Laminar Flow Through a Pipe with Species Transport

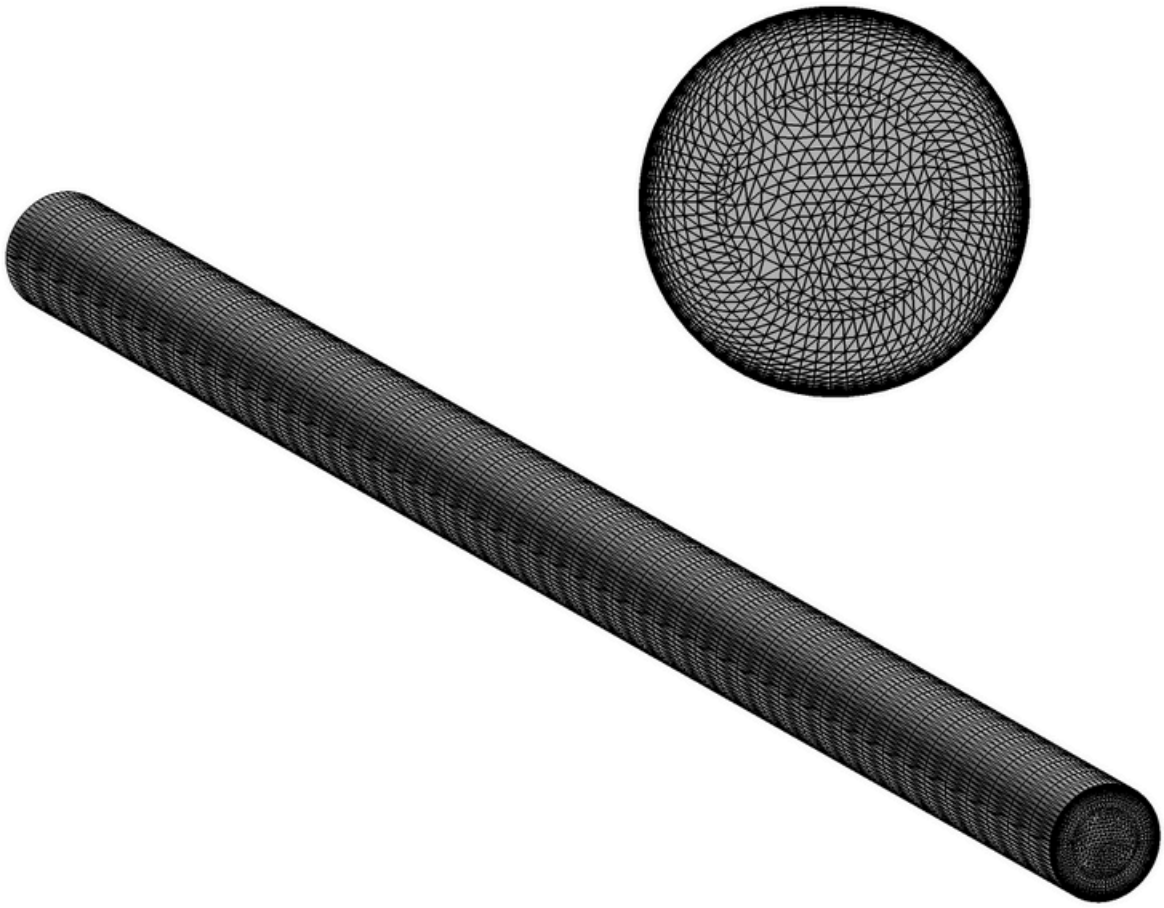


Figure 344: Mesh used for Simulating Laminar Flow Through a Pipe with Species Transport

AcuSolve Results

The AcuSolve solution converged to a steady state and the results reflect the mean flow conditions with the species fraction changing along the length of the pipe. At the inlet, the concentration of species 1 is 100 percent. The fraction of species 1 decreases along the length of the pipe, developing a parabolic concentration profile due to the no-slip walls and the specified concentration at the wall.

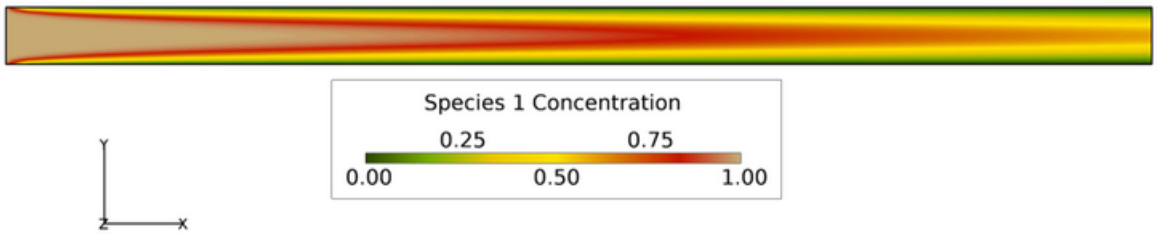


Figure 345: Contours of Concentration for Species 1

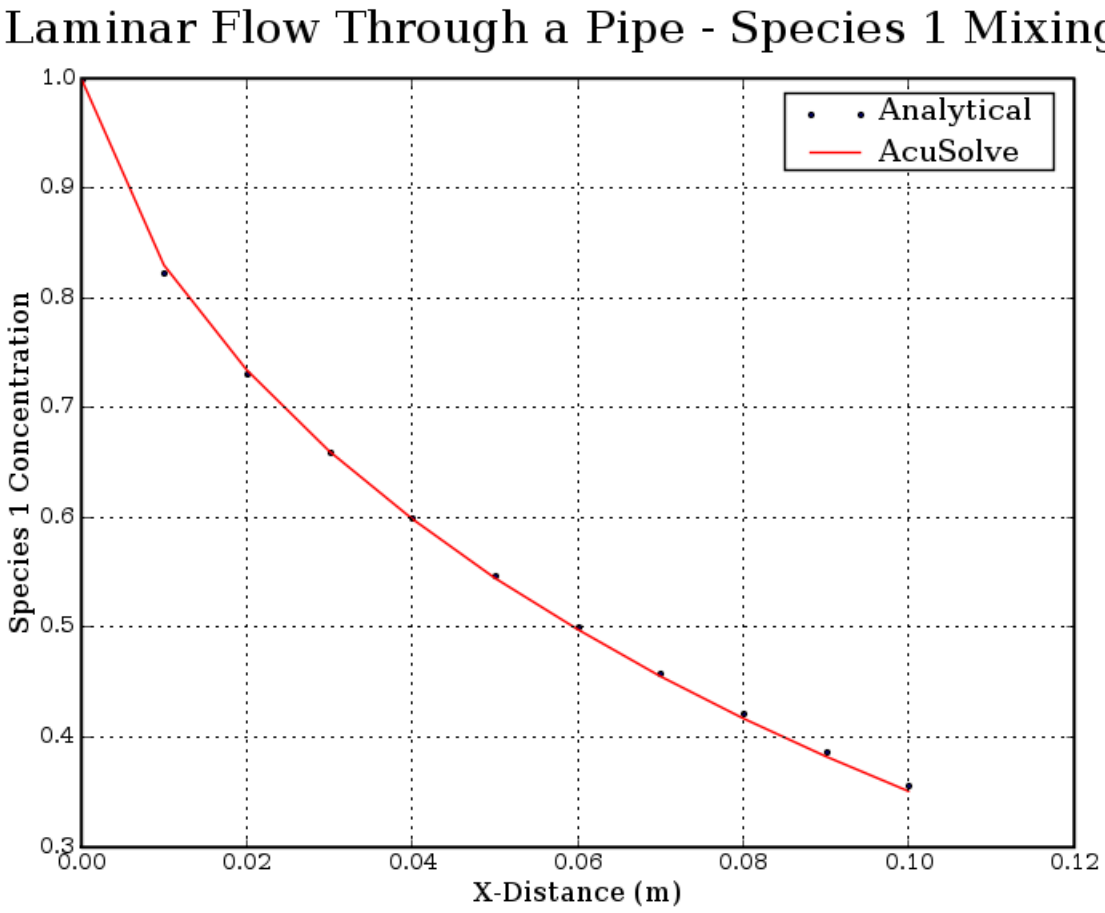


Figure 346: Species 1 Concentration Plotted Against Distance from the Pipe Inlet

Analytical values of the species fraction at different distances along the pipe are presented with the corresponding AcuSolve results in the following table. The analytical solution contains a series of five terms that are summed to yield the values shown in the table.

Table 26:

Distance along pipe (m)	Analytical species 1 fraction	AcuSolve species 1 fraction	Percent deviation from analytical
0	1.0000*	1.0000	0.00
0.01	0.8225	0.8298	0.90
0.02	0.7308	0.7344	0.49
0.03	0.6593	0.6603	0.15
0.04	0.5992	0.5988	0.06
0.05	0.5469	0.5448	0.38
0.06	0.5006	0.4981	0.49
0.07	0.4589	0.4554	0.78
0.08	0.4212	0.4171	0.98
0.09	0.3869	0.3824	1.15
0.1	0.3555	0.3507	1.35

* The theoretical species fraction at the inlet is shown rather than the analytical. In order for the analytical solution to correspond exactly with the theoretical results, additional terms in the series summation would need to be evaluated.

Summary

The AcuSolve solution compares well with analytical results for flow through a pipe with species transport. In this application, a fully developed laminar profile is achieved by enforcing periodic constraints on the pressure and velocity fields. The spatially developing species field is achieved by not enforcing periodicity and allowing the concentration to evolve along the full length of the model. The change in concentration along the pipe length is due to advection in the streamwise direction and diffusion of the species to the outer walls where the concentration is zero. The AcuSolve solution for fraction of species 1 is within 1.35 percent of analytical results.

Simulation Settings for Laminar Flow Through a Pipe with Species Mixing

AcuConsole database file: `<your working directory>\pipe_laminar_species\pipe_laminar_species.acs`.

Global

- Problem Description
  - Analysis type - Steady State

- Species equation - Advective Diffusive
- Num. species - `1`
- Turbulence equation - Laminar

- Auto Solution Strategy
  - Relaxation factor - `0.2`
- Material Model
  - Species1
    - Density - `1.0` kg/m3
    - Viscosity - `1.0e-5` kg/m-sec
    - Diffusivity
      1. 1
         1. Diffusivity - `1.43e-5` kg/m-sec

  Model
- Volumes
  - Fluid
    - Element Set
      1. Material model - Species1
- Surfaces
  - Inflow
    - Simple Boundary Condition - (disabled to allow for periodic conditions to be set)
    - Advanced Options
      1. Nodal Boundary Conditions
         1. Species 1
            1. Type - Constant
            2. Constant value - `1.0`
      2. Integrated Boundary Conditions
         1. Mass Flux
            1. Type - Constant
            2. Constant value - `1.96e-05` kg/sec
  - Outflow
    - Simple Boundary Condition - (disabled to allow for periodic conditions to be set)
  - Wall
    - Simple Boundary Condition
      1. Type - Wall
      2. Species 1 BC type - Value
      3. Species 1 - `0.0`
- Periodics

- Periodic 1
  - Individual Periodic BCs
    1. Velocity
       1. Type - Periodic
    2. Pressure
    3. Type - Single Unknown Offset

References

W. M. Kays and M. E. Crawford. "Convective Heat and Mass Transfer", 3rd Edition. pp. 126-134. McGraw-Hill Book Co., Inc. New York. 1993.

Flow Inside a Rotating Cavity

In this application, AcuSolve is used to simulate the flow of air in an enclosed cylindrical cavity with a rotating top and a fixed bottom. AcuSolve results are compared with experimental data adapted from Michelsen (1986). The close agreement of AcuSolve results with experimental data validates the ability of AcuSolve to model cases containing enclosed cavities with flow induced by rotating walls.

Problem Description

The problem consists of air in an enclosed cylinder 1.0 m tall with a radius of 1.0 m, as shown in the following image, which is not drawn to scale. The top of the cylinder rotates about its center at 1 rad/s, while the bottom of the cylinder is fixed. As the container top spins, the viscous stresses on the fluid induce a circumferential (swirl) velocity throughout the height of the cylinder. In order to conserve mass and momentum, the fluid generates a radial velocity that changes direction based on distance away from the rotation center of the cylinder.

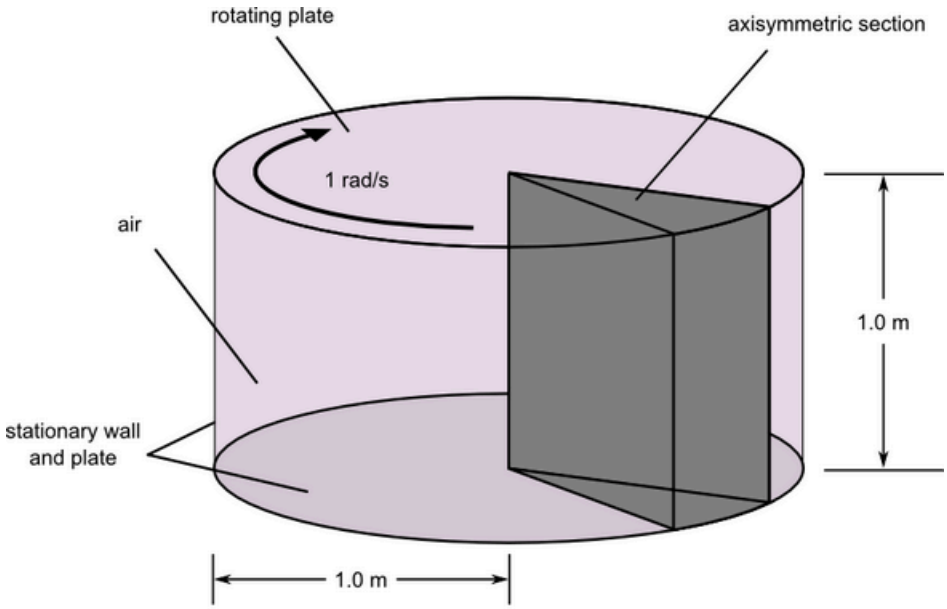


Figure 347: Critical Dimensions and Parameters for Simulating Flow Inside a Rotating Cavity

The flow domain is modeled with axisymmetric periodicity in the circumferential direction, which allows for accurate simulation of the flow while minimizing computational time.

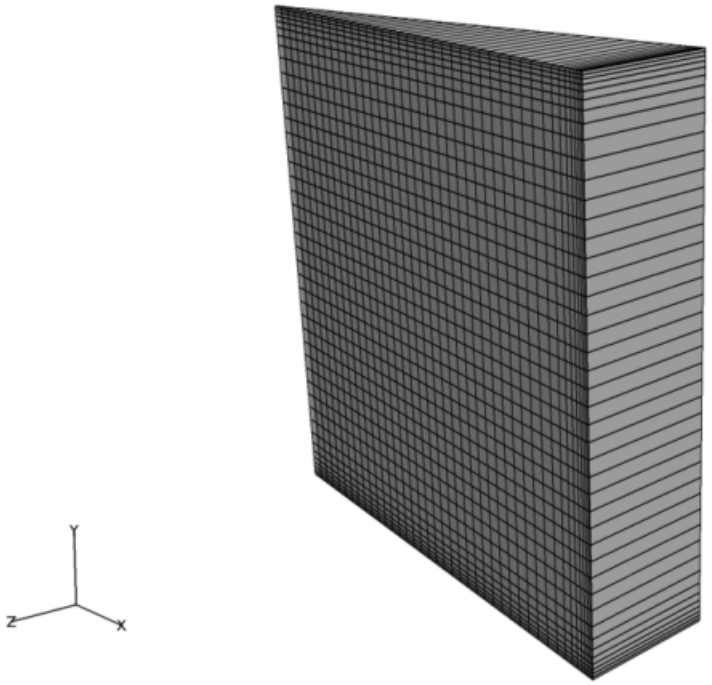


Figure 348: Mesh of Periodic Section Used for Simulating Flow Inside a Rotating Cylinder

AcuSolve Results

The AcuSolve solution converged to a steady state and the results reflect the mean flow conditions. The velocity varies with both vertical location and with distance from the rotation center. The complex flow field develops from a combination of the viscous stresses acting at the rotating cylinder top and at the stationary bottom.

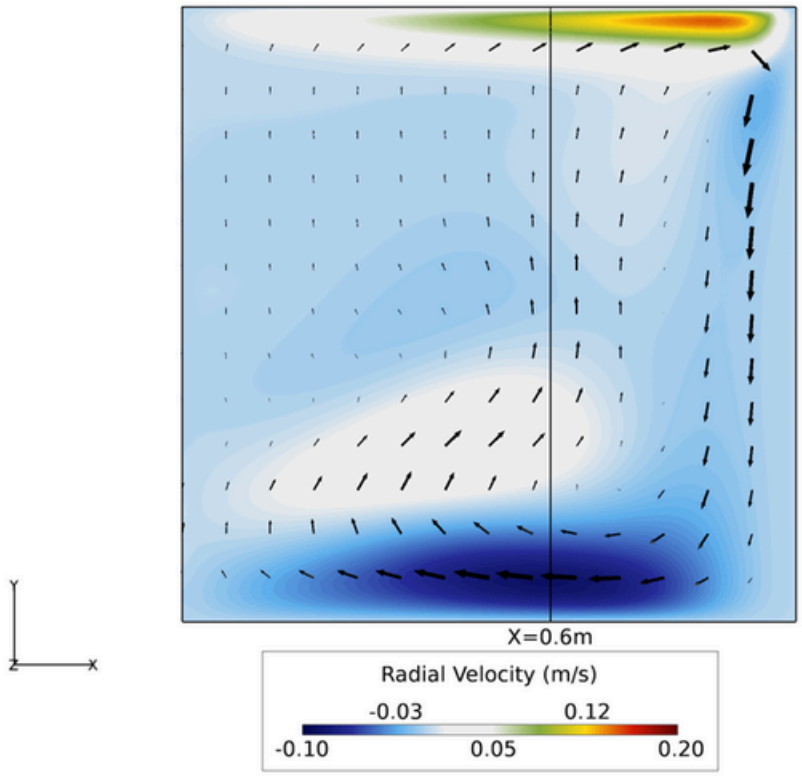


Figure 349: Contours of Radial Velocity with Velocity Vectors. This Image Shows the Front Face of the Modeled Cylinder Wedge, with the Center of Rotation on the Left Edge. The Vertical Line Represents a Radial Location 0.6 m From the Center of Rotation.

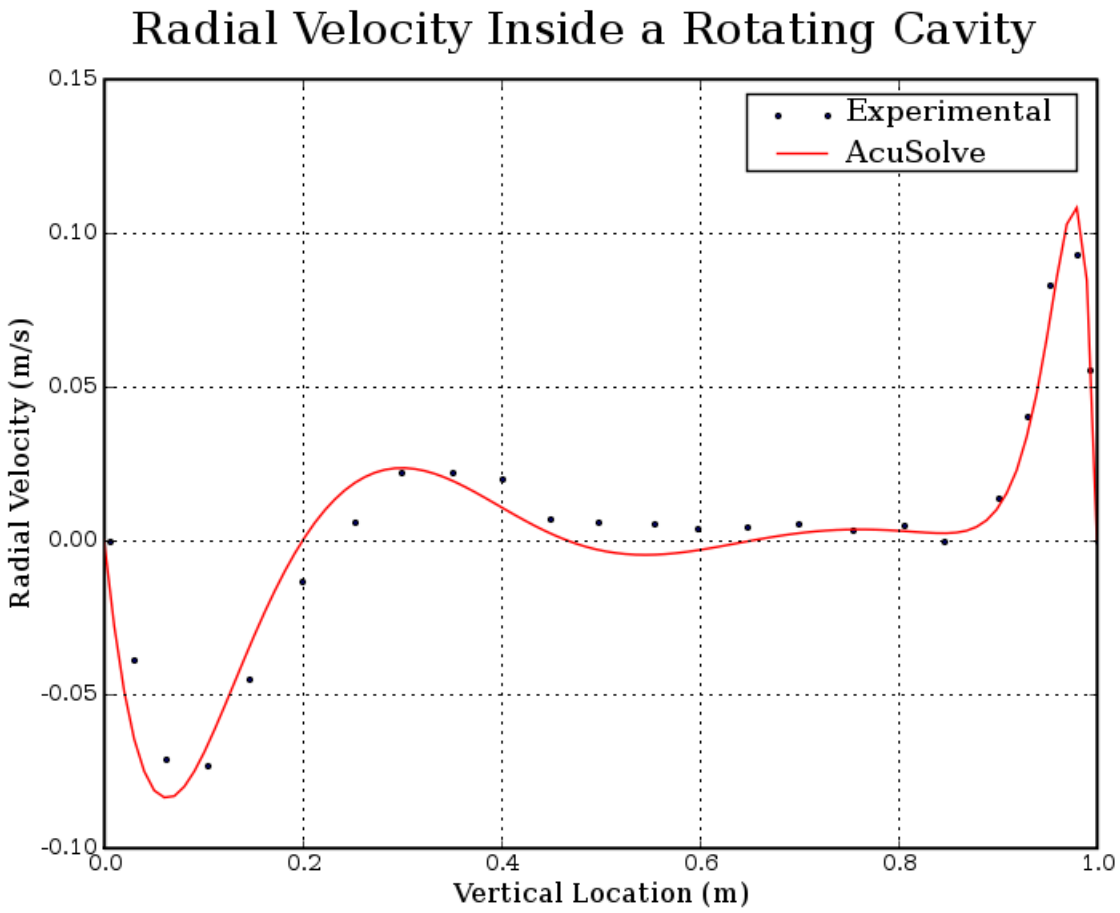


Figure 350: Radial Velocity (at 0.6 m From the Center of Rotation) as a Function of Vertical Location From Cylinder Bottom

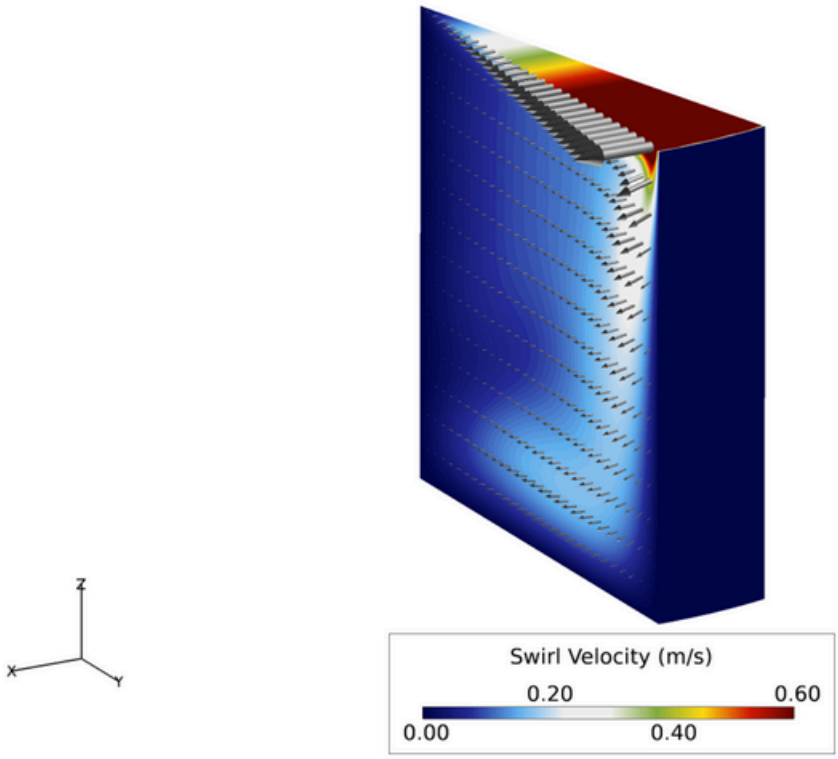


Figure 351: Contours of Swirl Velocity with Velocity Vectors

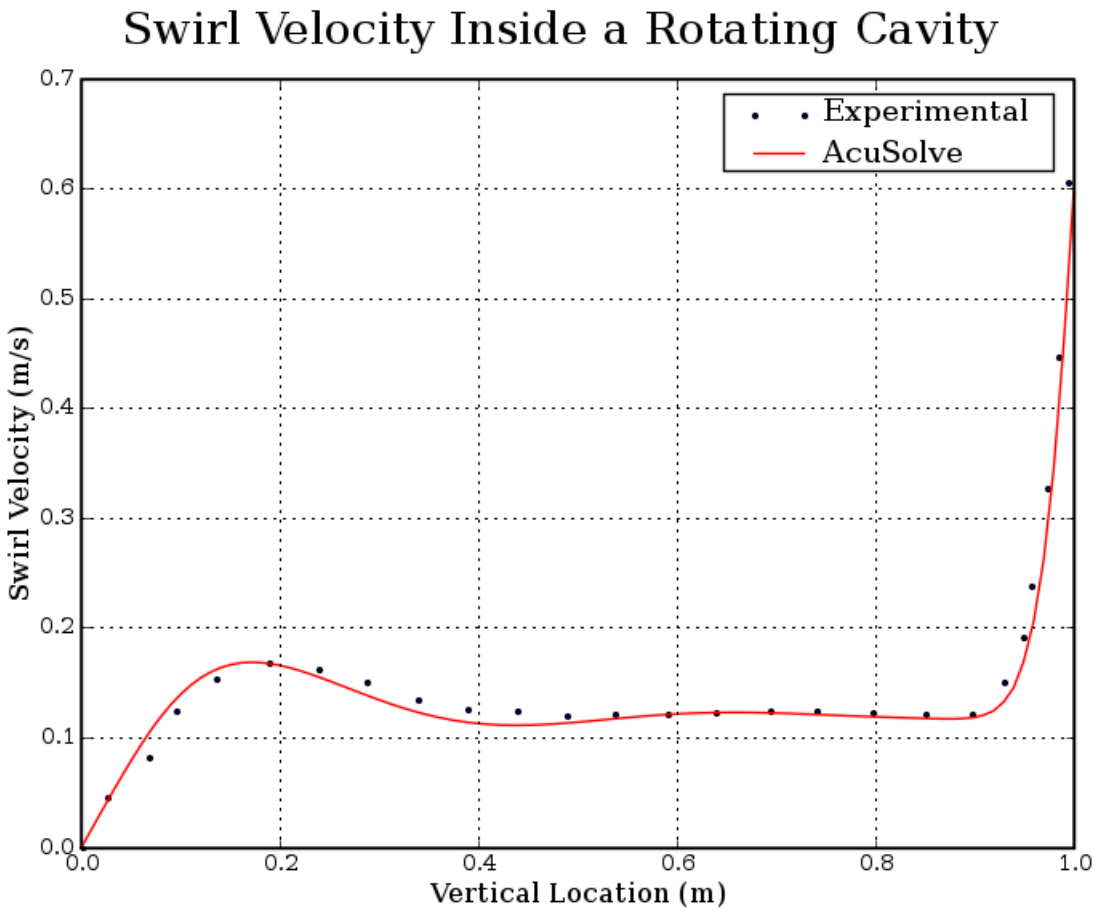


Figure 352: Swirl Velocity (at 0.6 m From Center of Rotation) as a Function of Vertical Location From the Cylinder Bottom

Summary

The AcuSolve solution compares well with the experimental data for flow induced by a rotating top of an enclosed cylinder. In this application, the flow in the fluid region is driven by the viscous stresses near the rotating top. Viscous stresses drag the fluid in a circular direction near the spinning wall. The angular velocity of the fluid decreases as distance from the top wall increases. Radial velocity develops as a result of the migration of the fluid toward the outer wall in regions of high angular velocity. The AcuSolve radial and swirl velocities compare very closely with the experimental data.

Simulation Settings for Flow Inside a Rotating Cavity

AcuConsole database file: `<your working directory>\cavity_rotating\cavity_rotating.acs`

Global

- Problem Description
  - Analysis type - Steady State
  - Turbulence Equation - Laminar
- Auto Solution Strategy

    - Relaxation Factor - 0.4
- Material Model
    - Air
        - Density - 1.0 kg/m3
        - Viscosity - 0.000556 kg/m-sec
- Reference Frame
    - Cavity Rotation
        - Rotation center
            1. X-coordinate - 0.0
            2. Y-coordinate - 0.0
            3. Z-coordinate - 0.0
        - Angular velocity
            1. X-component - 0.0
            2. Y-component - -1.0 rad/sec
            3. Z-component - 0.0

    Model
- Volumes
    - Fluid
        - Element Set
            1. Material model - Air
- Surfaces
    - Bottom
        - Simple Boundary Condition
            1. Type - Wall
    - Max_X
        - Simple Boundary Condition
            1. Type - Wall
    - Max_Z
        - Simple Boundary Condition - (disabled to allow for periodic conditions to be set)
    - Min_Z
        - Simple Boundary Condition - (disabled to allow for periodic conditions to be set)
    - Top
        - Simple Boundary Condition
            1. Type - Wall
            2. Reference frame - Cavity Rotation
- Periodics
    - Periodic 1

- Periodic Boundary Condition
  1. Type - Axisymmetric
  2. Rotation axis
     1. point 1
        1. X-coordinate - `0.0` m
        2. Y-coordinate - `0.0` m
        3. Z-coordinate - `0.0` m
     2. point 2
        1. X-coordinate - `0.0` m
        2. Y-coordinate - `1.0` m
        3. Z-coordinate - `0.0` m

References

J. A. Michelsen. "Modeling of Laminar Incompressible Rotating Fluid Flow". AFM 86-05. Ph.D. thesis, Department of Fluid Mechanics, Technical University of Denmark. 1986.

Natural Convection in a Concentric Annulus

In this application, AcuSolve is used to simulate natural convection in the annular space between a heated inner pipe and an outer concentric pipe. AcuSolve results are compared with experimental results adapted from Kuehn and Goldstein (1978). The close agreement of AcuSolve results with experimental results validates the ability of AcuSolve to model cases with flow induced by natural convection.

Problem Description

The problem consists of two concentric cylinders with air filling the void between them, as shown in the following image, which is not drawn to scale. The radius of the inner cylinder is 0.0178 m and the radius of the outer cylinder is 0.0463 m. The inner cylinder is held at a fixed temperature of 373 K while the outer cylinder is held at 327 K. The temperature gradient drives the flow due to buoyancy effects.

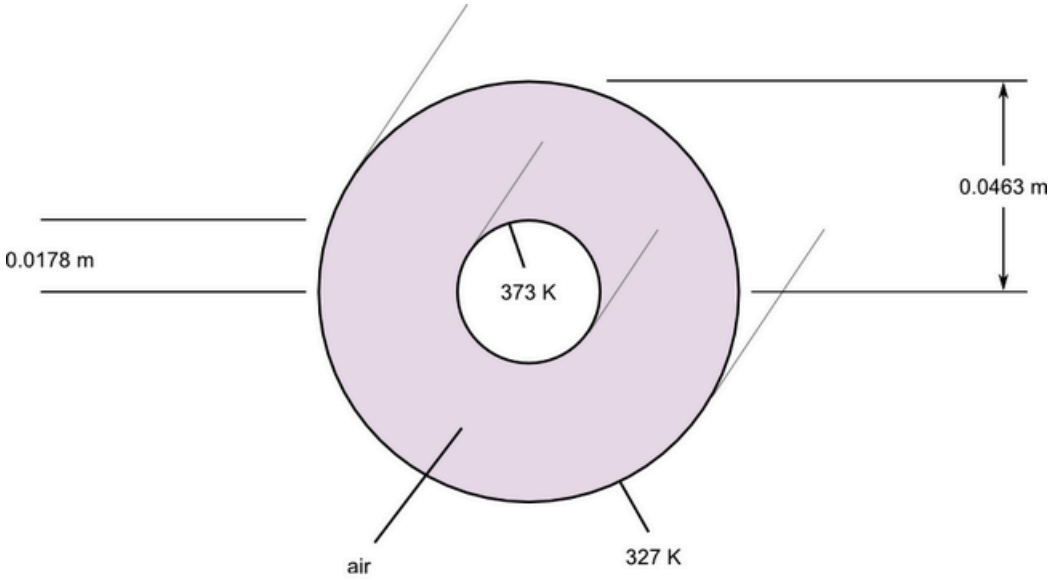


Figure 353: Critical Dimensions and Parameters for Simulating Natural Convection in a Concentric Annulus

The simulation was performed as a two dimensional problem by restricting flow in the out-of-plane direction through the use of a mesh that is one element thick. In addition, the half symmetry of the geometry is exploited to allow for modeling only half of the geometry. These characteristics allow for accurate simulation of the flow while minimizing computational time.

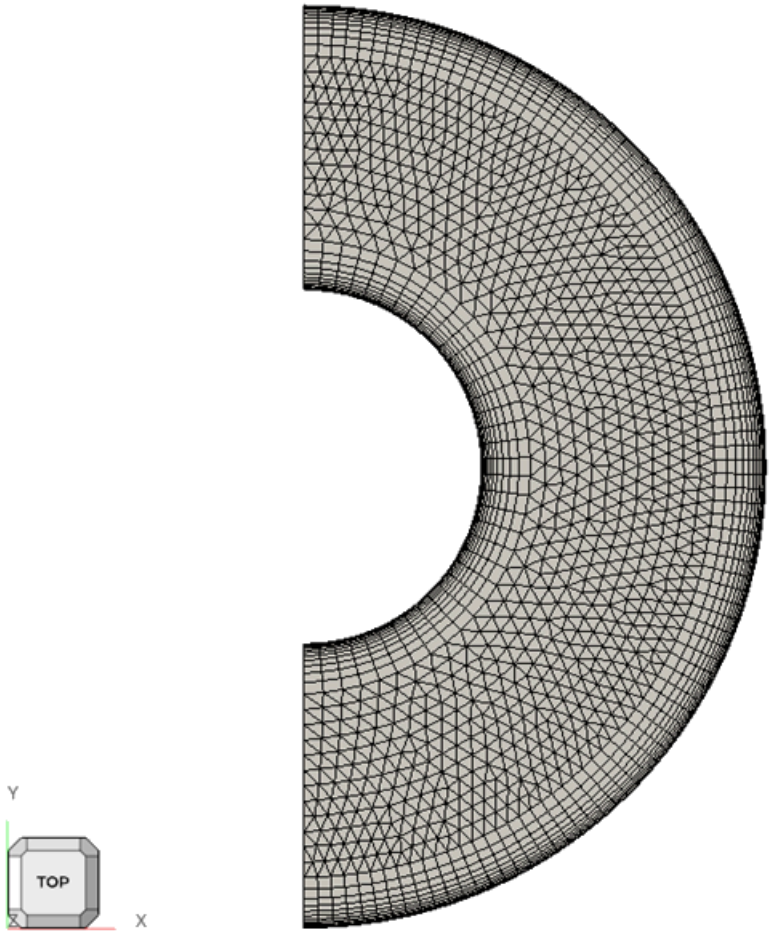


Figure 354: Mesh (Half of a Concentric Annulus) used for Simulating Natural Convection in a Concentric Annulus

AcuSolve Results

The AcuSolve solution converged to a steady state and the results reflect the mean flow conditions. Air density decreases due to heating by the inner cylinder, leading to convective currents within the annulus. As air approaches the outer cylinder, it is cooled by the outer wall, causing the density to increase. This results in heavier air sinking toward the bottom of the assembly.

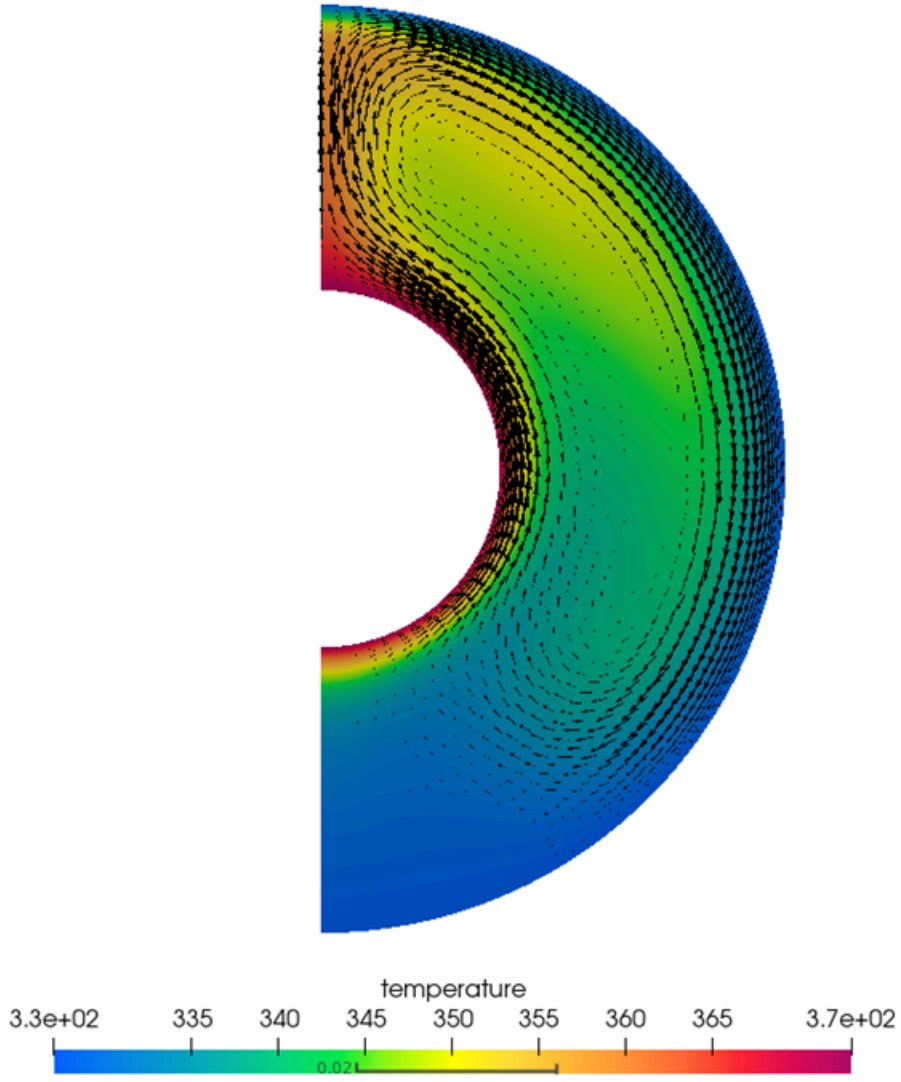


Figure 355: Temperature Contours and Velocity Vectors

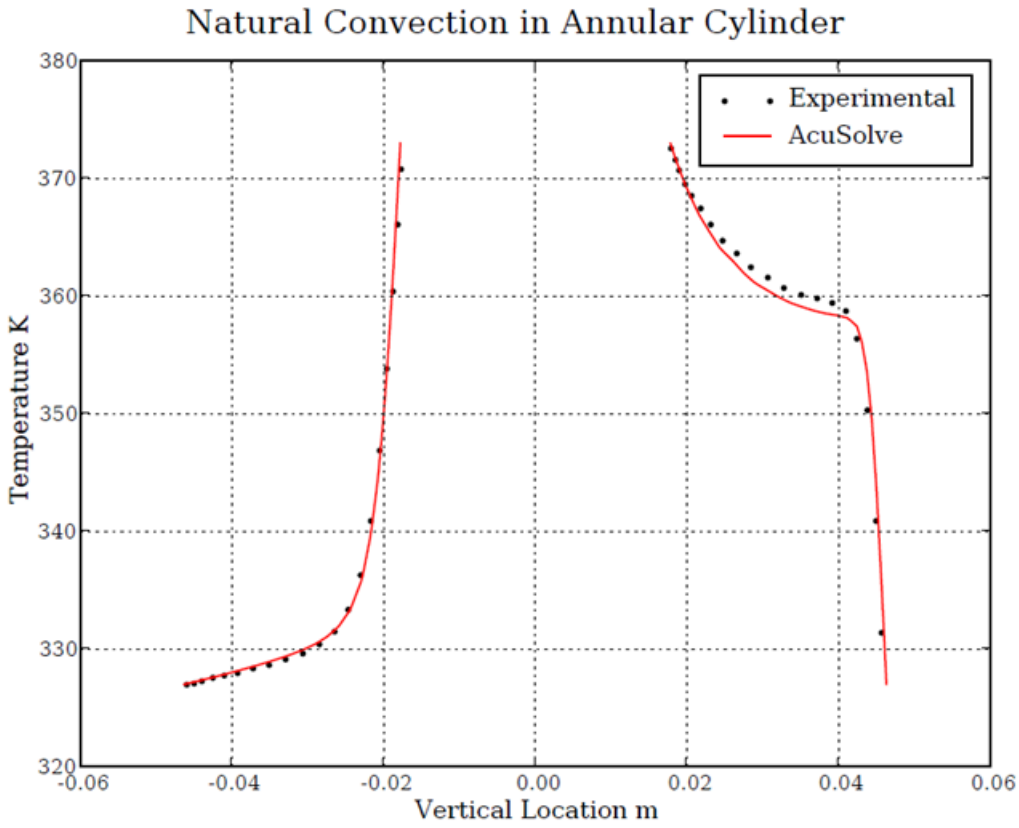


Figure 356: Temperature as a Function of Distance From the Center of the Inner Cylinder

Summary

The AcuSolve solution compares well with analytical results for natural convection in a concentric annulus. In this application, flow is driven by a decrease in density as air is heated. The local variations in density result in the higher density fluid sinking to the bottom of the annulus while the lower density fluid rises to the top. This transfer of momentum is a continuous process which results in the convective currents that are visible in the solution. The AcuSolve temperature results compare very closely with the experimental results.

Simulation Settings for Natural Convection in a Concentric Annulus

HyperWorks CFD database file: `<your working directory>\annulus_heat\annulus_heat.hm`

Global

- Problem Description
  - Analysis type - Steady State
  - Abs. pressure offset - `101325.0` N/m2
  - Temperature equation - Advective Diffusive
  - Turbulence equation - Laminar
  - Gravitational acceleration - { 0, -9.80665, 0 }
- Auto Solution Strategy

- Relaxation factor - `0.2`
- Flow - On
- Temperature - On

- Material Model
  - Air
    - Type - Boussinesq
    - Density - `1.225` kg/m3
    - Expansivity - `0.0034722` 1/K
    - Reference temperature - `288` K
    - Isothermal compressibility - `0.0` m2/N
    - Viscosity - `2.081e-5` kg/m-sec

  Model
- Volumes
  - Fluid
    - Element Set
      1. Material model - Air
  - Surfaces
    - ID
      1. Simple Boundary Condition
         1. Type - Wall
         2. Temperature BC type - Value
         3. Temperature - `373.0` K
    - Max_Z
      1. Simple Boundary Condition
      2. Type - Symmetry
    - Min_Z
      1. Simple Boundary Condition
      2. Type - Symmetry
    - OD
      1. Simple Boundary Condition
         1. Type - Wall
         2. Temperature BC type - Value
         3. Temperature - `327.0` K
    - Symmetry
      1. Simple Boundary Condition
      2. Type - Symmetry
  - Nodes
    - Node 1

1 Pressure

1 Type - Zero

References

T.H. Kuehn and R. J. Goldstein. "An Experimental Study of Natural Convection Heat Transfer in Concentric and Eccentric Horizontal Cylindrical Annuli". Journal of Heat Transfer 100:635-640. 1978.

Laminar Flow Past a 90° T-Junction

In this application, AcuSolve is used to simulate laminar flow through a channel with two outlets forming a T-junction. AcuSolve results are compared with experimental results adapted from Hayes and others (1989). The close agreement of AcuSolve results with experimental results validates the ability of AcuSolve to model cases with multiple outlet paths.

Problem Description

The problem consists of air flowing past a T-junction in a channel, as shown in the following image, which is not drawn to scale. Air enters the channel with an average velocity of 0.667 m/s and travels past the T-junction 2.0 m from the inlet. A portion of the flow will travel out of the branch of the channel due to the pressure difference between the bulk flow and the outlet of the branch.

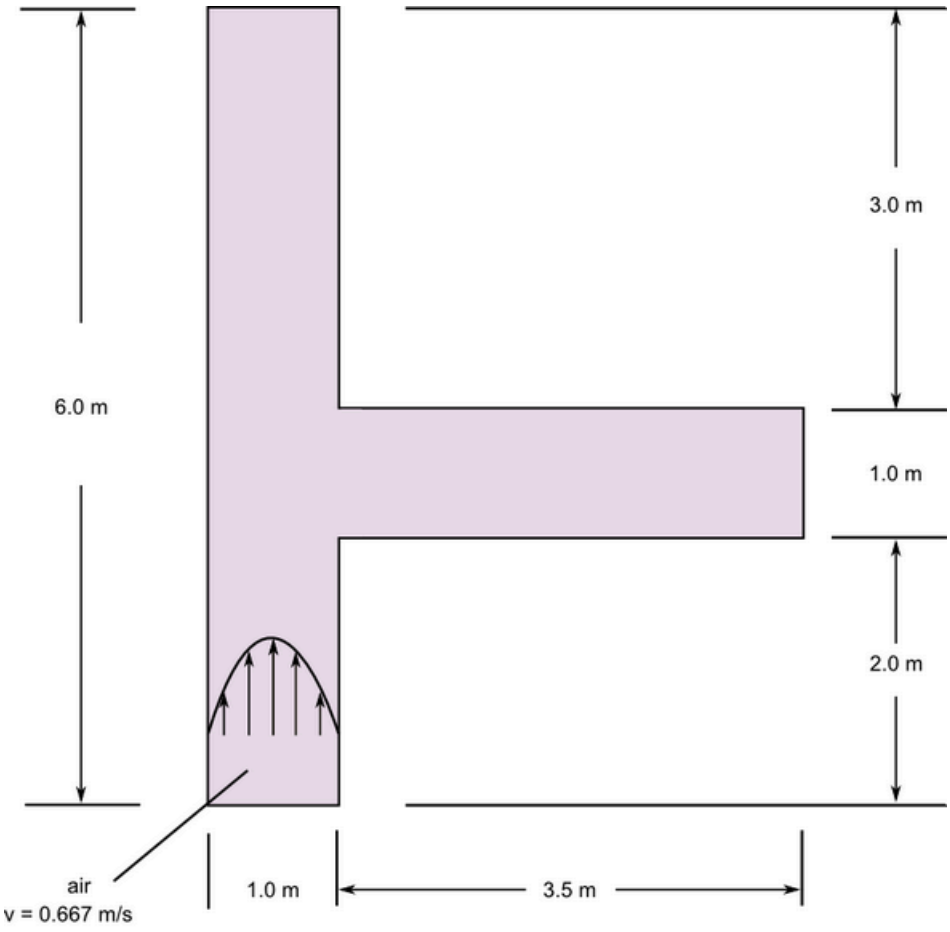


Figure 357: Critical Dimensions and Parameters for Simulating Laminar Flow Past a 90° T-Junction

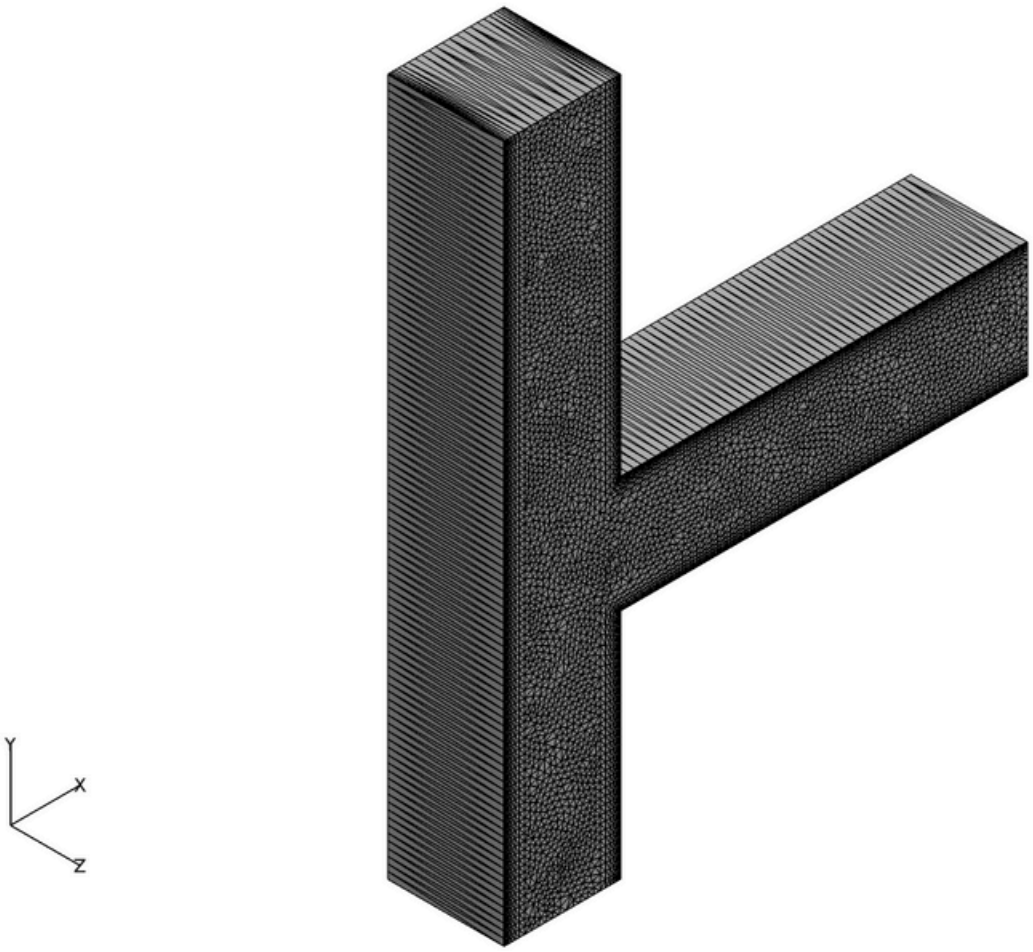


Figure 358: Mesh Used for Simulating Laminar Flow past a 90° T-Junction

AcuSolve Results

The AcuSolve solution converged to a steady state and the results reflect the mean flow conditions. As the air flows past the junction, a portion of it is diverted into the branch. A small recirculation region develops at the top of the junction and collapses before the flow exits the domain through the right branch.

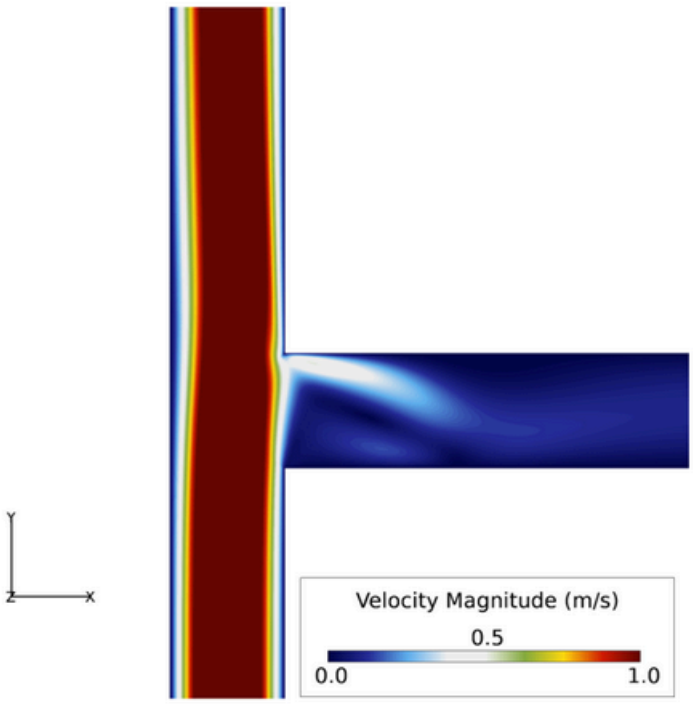


Figure 359: Velocity Contours in a T-Junction

The experimental value for the fraction of flow exiting the top branch of the channel is presented with the corresponding AcuSolve result in the following table.

Table 27:

	Experimental fractional flow	**AcuSolve fractional flow**	**Percent deviation from experimental**
Fractional flow exiting the upper branch	0.887	0.883	0.451

Summary

The AcuSolve solution compares well with experimental results for flow past a T-junction. In this application, flow is driven by a fixed flow rate at the inlet to the main branch. A portion of the flow from the main branch is diverted into the right branch of the T-junction, giving rise to recirculation just downstream of the junction. This recirculation collapses before the flow exits the side branch. The AcuSolve result for fractional flow exiting the top branch is within 0.451 percent of the experimental results.

Simulation Settings for Laminar Flow Past a 90° T-Junction

AcuConsole database file: `<your working directory>\T_junction_laminar\T_junction_laminar.acs`

Global

- Problem Description
  - Analysis type - Steady State
  - Turbulence equation - Laminar
- Auto Solution Strategy
  - Relaxation factor - `0.2`
- Material Model
  - Air
    - Type - Constant
    - Density - `1.0` kg/m3
    - Viscosity - `0.003333` kg/m-sec

  Model
- Volumes
  - Fluid
    - Element Set
      1. Material model - Air
- Surfaces
  - Inflow
    - Simple Boundary Condition
      1. Type - Inflow
      2. Inflow type - Average Velocity
      3. Average velocity - `0.6667` m/sec
  - Max_Z
    - Simple Boundary Condition - (disabled to allow for periodic conditions to be set)
  - Min_Z
    - Simple Boundary Condition - (disabled to allow for periodic conditions to be set)
  - Outflow
    - Simple Boundary Condition
      1. Type - Outflow
  - T_Out
    - Simple Boundary Condition
      1. Type - Outflow
  - Walls
    - Simple Boundary Condition

1 Type - Wall

- Periodics
  - Periodic 1
    - Periodic Boundary Condition
      1 Type - Periodic

References

R. E. Hayes, K. Nandkumar, and H. Nasr-El-Din. "Steady Laminar Flow in a 90 Degree Planar Branch". Computers and Fluids 17(4): 537-553. 1989.

Turbulent Flow Through a Wavy Channel

In this application, AcuSolve is used to simulate turbulent flow through a channel with a lower wall shaped as a sinusoidal wave. AcuSolve results are compared with experimental results adapted from Kuzan (1986). The close agreement of AcuSolve results with experimental results validates the ability of AcuSolve to model cases with internal flow through a channel with wavy walls.

Problem Description

The problem consists of air flowing through a channel with a wavy bottom wall. The channel is 1.1 m high, 1.0 m wide, and is modeled as a section 1.0 m in length, as shown in the following image, which is not drawn to scale. The bottom wall wave shape has an amplitude of 0.1 m and a wavelength of 1 m. The mass flow rate through the channel is set to a constant value of 0.816 kg/s. The flow field develops as a result of the non-planar bottom wall and viscous stresses acting near the top and bottom walls. Collision of air with the peak of the wave on the channel floor causes an acceleration of the flow, followed by recirculation as the flow area expands into the valley.

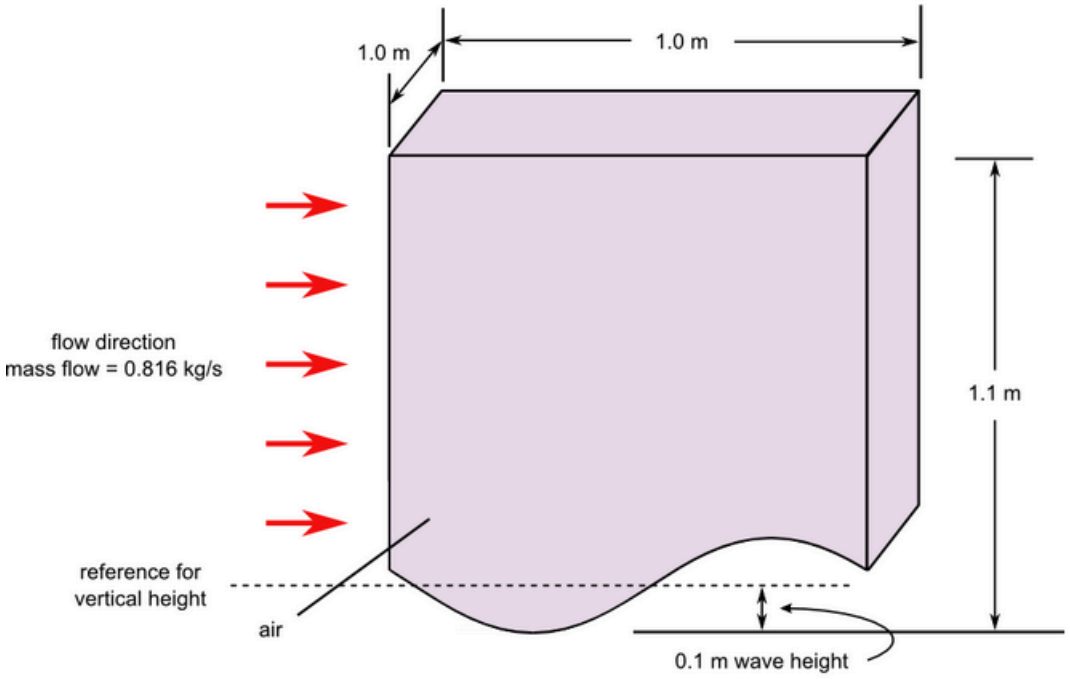


Figure 360: Critical Dimensions and Parameters for Simulating Turbulent Flow Through a Wavy Channel

The simulation was performed as a two dimensional problem by restricting flow in the out-of-plane direction through the use of a mesh that is one element thick. The elements were extruded to the width of the channel.

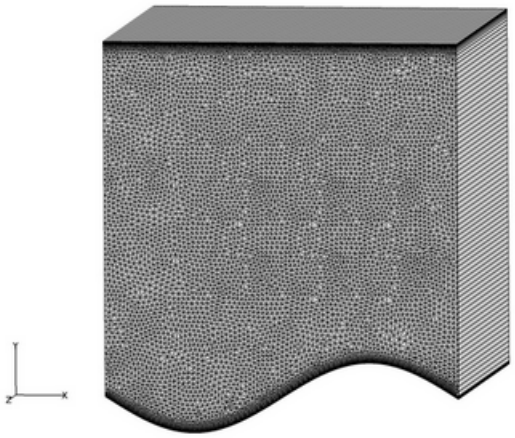


Figure 361: Mesh Used for Simulating Turbulent Flow Through a Wavy Channel

AcuSolve Results

The AcuSolve solution converged to a steady state and the results reflect the mean flow conditions. The expansion of the cross section as the air passes the trough in the wave causes an adverse pressure gradient to form. This results in separation of the flow along the downward-slanting walls of the wavy surfaces. The recirculation zone establishes itself within the troughs of the wave. The remaining flow above the troughs maintains its velocity in the streamwise direction and distributes throughout the channel. The flow accelerates as it travels over the wave peak and the velocity continues to increase as a function of distance from the wall until it reaches a maximum velocity approximately 0.3 m away from the upper wall.

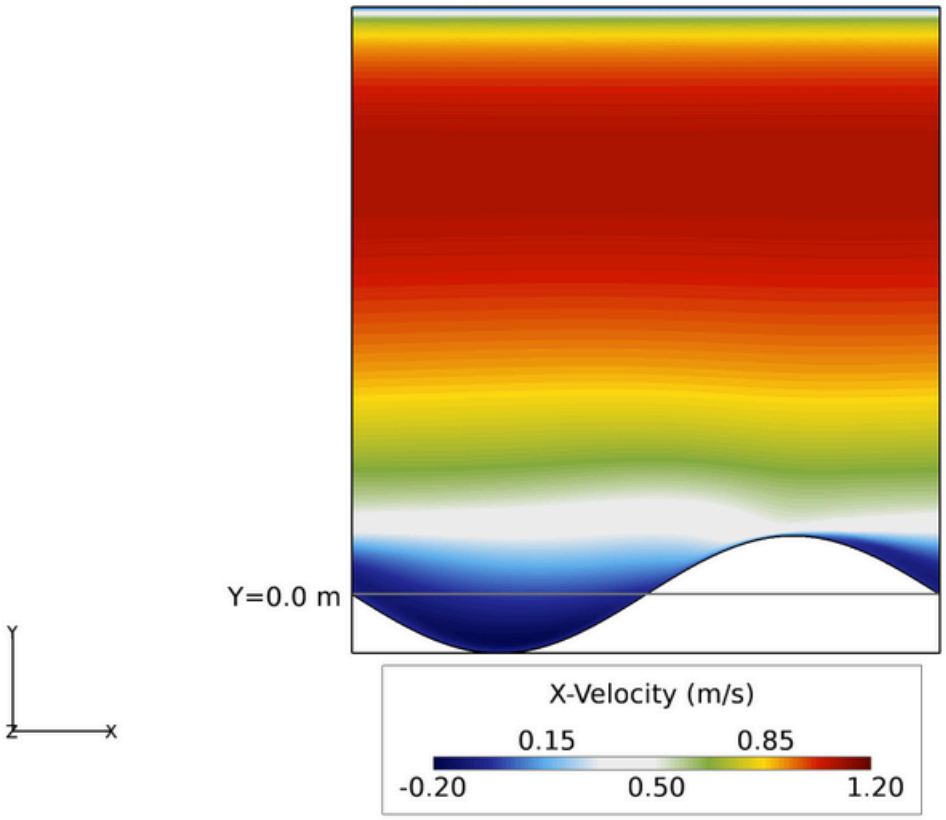


Figure 362: Velocity Contours in the X-Y Plane in a Wavy Channel (the Horizontal Line Represents the Reference for Wave Height - the Wave Crest is 0.1 m Above The Reference Height, and the Wave Valley is 0.1 m Below the Reference Height)

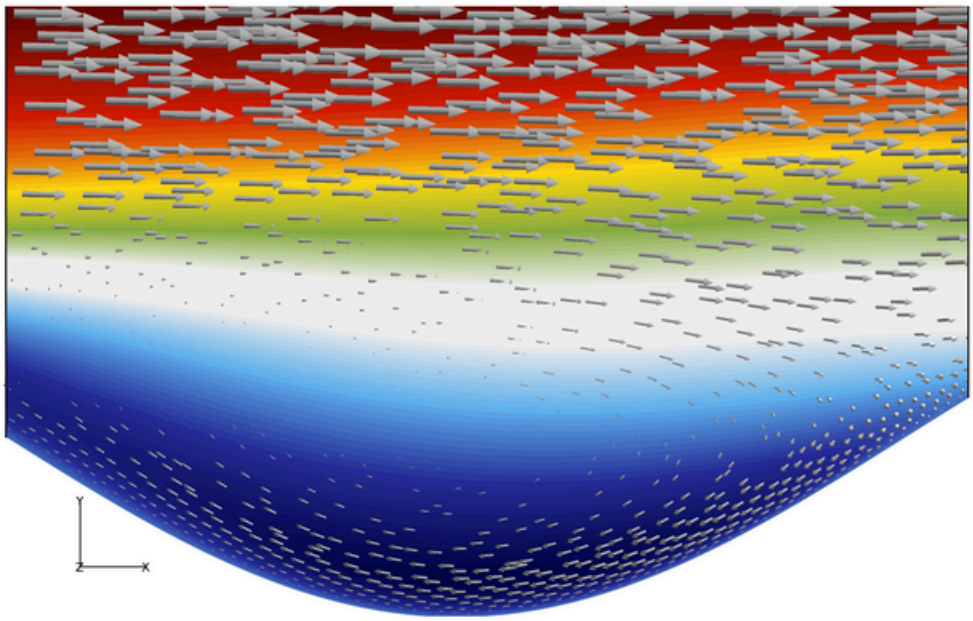


Figure 363: Close-Up View of Velocity Contours and Velocity Vectors in the X-Y Plane Near the Valley of a Wave

The X-velocity directly over the center of the wave valley initially decreases (backflow) as distance away from the bottom wall increases, with a maximum velocity in the -X direction at approximately 0.03 m above the valley floor. The X-velocity then increases to zero m/sec at 0.1 m above the valley, reflecting an end of the recirculation.

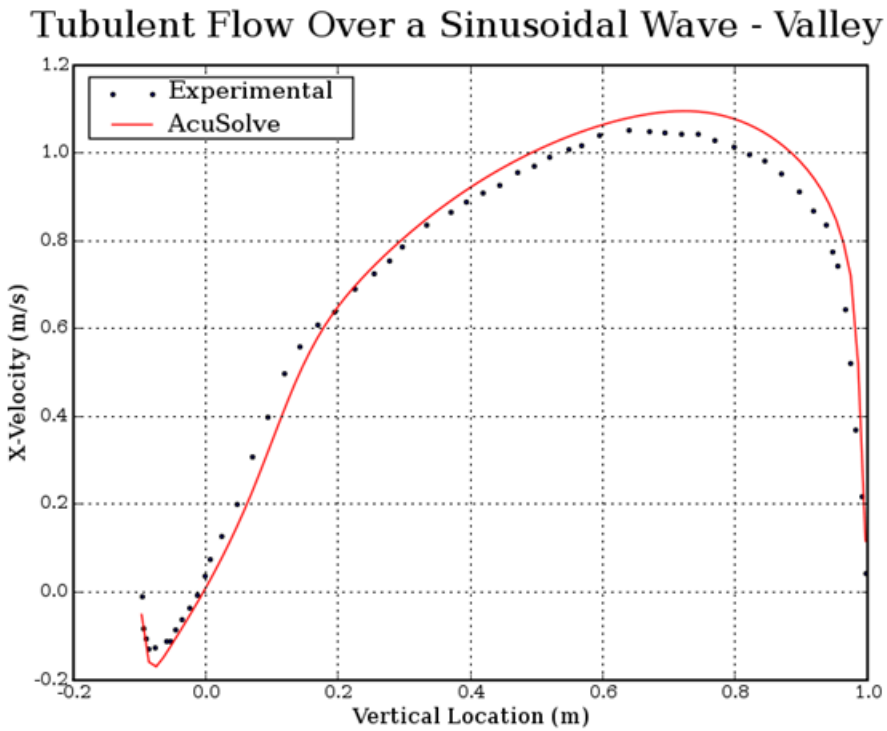


Figure 364: X-Velocity Plotted Against Vertical Location in the Channel Above the Valley Center (the Valley Floor is 0.1 m Below the Reference Height)

The X-velocity directly over the wave peak has different behavior due to the lack of recirculation. The velocity above the peak increases as distance away from the bottom wall increases, with a maximum velocity in the X direction at approximately 0.75 m. The velocity then decreases to zero at the top wall.

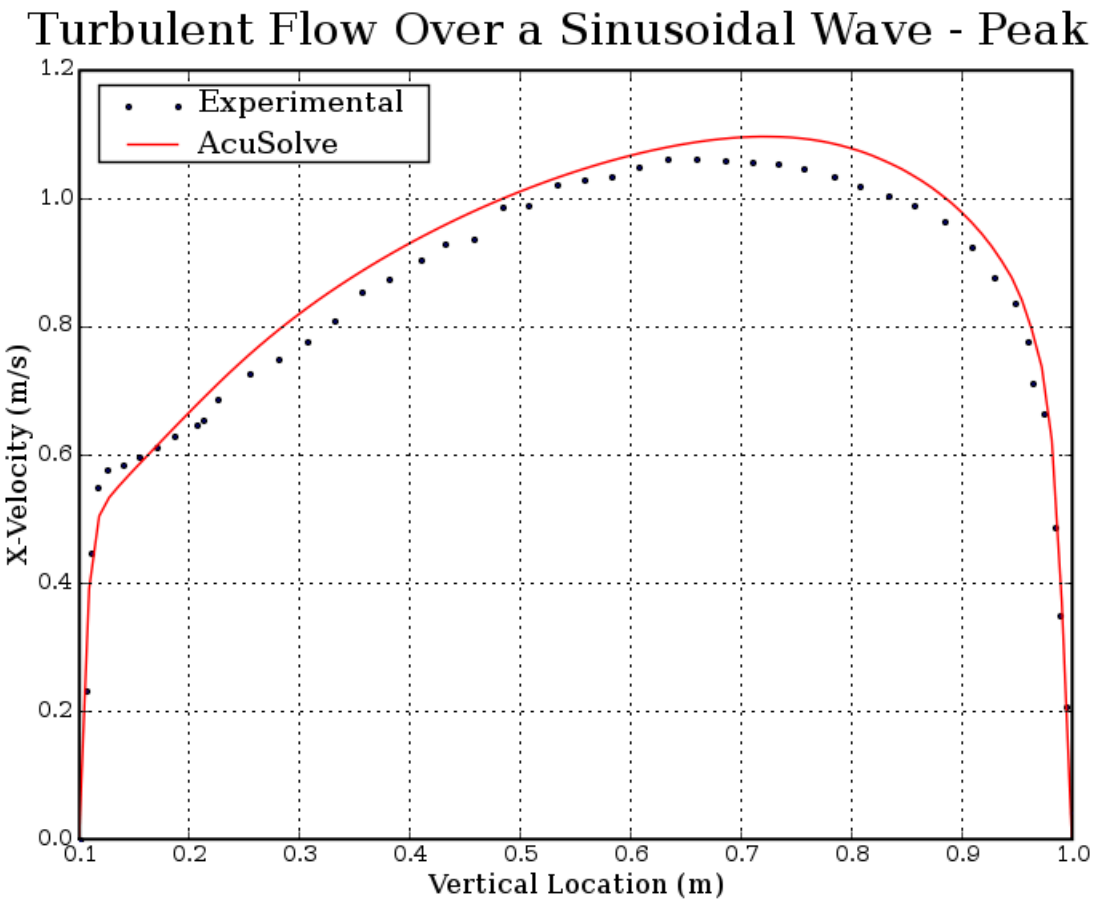


Figure 365: X-Velocity Plotted Against Vertical Location in the Channel Above the Wave Peak (the Wave Peak is 0.1 m Above the Reference Height)

Summary

The AcuSolve results compare well with the experimental data for X-velocity in a channel with a wavy floor. In this application, the flow is driven with a constant mass flow rate and periodic constraints are used to model a repeating array of channel segments with a wavy bottom wall. Separation of the flow occurs as a result of the adverse pressure gradient created by the changes in area. This leads to recirculation within the wave valleys. The flow separation occurs along the smoothly tapered wave wall, illustrating the ability of AcuSolve to accurately predict the separation point in this type of application. The X-velocity predicted by AcuSolve matches the experimental results with an overall coefficient of determination (R2) of 0.99 for each location shown in the plots.

Simulation Settings for Turbulent Flow Through a Wavy Channel

AcuConsole database file: `<your working directory>\wavy_channel_turbulent\wavy_channel_turbulent.acs`

Global

- Problem Description

- Analysis type - Steady State
- Turbulence equation - Spalart Allmaras

- Auto Solution Strategy
  - Relaxation factor - `0.4`
- Material Model
  - Air
    - Density - `1.0` kg/m3
    - Viscosity - `0.0001` kg/m-sec

  Model
- Volumes
  - Fluid
    - Element Set
      1. Material model - Air
- Surfaces
  - Max_X
    - Simple Boundary Condition - (disabled to allow for periodic conditions to be set)
  - Max_Y
    - Simple Boundary Condition
      1. Type - Wall
  - Max_Z
    - Simple Boundary Condition - (disabled to allow for periodic conditions to be set)
  - Min_X
    - Simple Boundary Condition - (disabled to allow for periodic conditions to be set)
    - Advanced Options
      1. Integrated Boundary Conditions
         1. Mass Flux
            1. Type - Constant
            2. Constant value - `-0.816` kg/sec
  - Min_Y
    - Simple Boundary Condition
      1. Type - Wall
  - Min_Z
    - Simple Boundary Condition - (disabled to allow for periodic conditions to be set)
- Periodics
  - Periodic-Crossflow
    - Periodic Boundary Condition
      1. Type - Periodic

- Periodic-Streamwise
  - Periodic Boundary Condition
    1. Type - Periodic
  - Individual Periodic BCs
    1. Velocity
       1. Type - Periodic
    2. Pressure
       1. Type - Single Unknown Offset
    3. Eddy Viscosity
       1. Type - Periodic

References

J. D. Kuzan."Velocity Measurements for Turbulent Separated and Near-Separated Flows Over Solid Waves". Ph.D. thesis. Deptartment of Chemical Engineering. University of Illinois. University of Illinois. Urbana, IL. 1986

Laminar Flow Through a Channel with Heated Walls

In this application, AcuSolve is used to simulate high Peclet number laminar flow through a channel with heated walls. AcuSolve results are compared with analytical results adapted from Hua and Pillai (2010). The close agreement of AcuSolve results with analytical results validates the ability of AcuSolve to model cases involving heat transfer to a moving fluid with a high Peclet number.

Problem Description

The problem consists of water at 20 °C flowing through a channel of infinite width with top and bottom walls heated to 75 °C. The channel is 0.2 m high and 0.8 m long, as shown in the following image, which is not drawn to scale. A centrally located slice 0.02 m wide is modeled with slip boundary conditions so that side-wall influences can be ignored. Water enters the channel with an average velocity of 0.003 m/s. As the fluid flows through the channel, it is heated by the top and bottom plates.

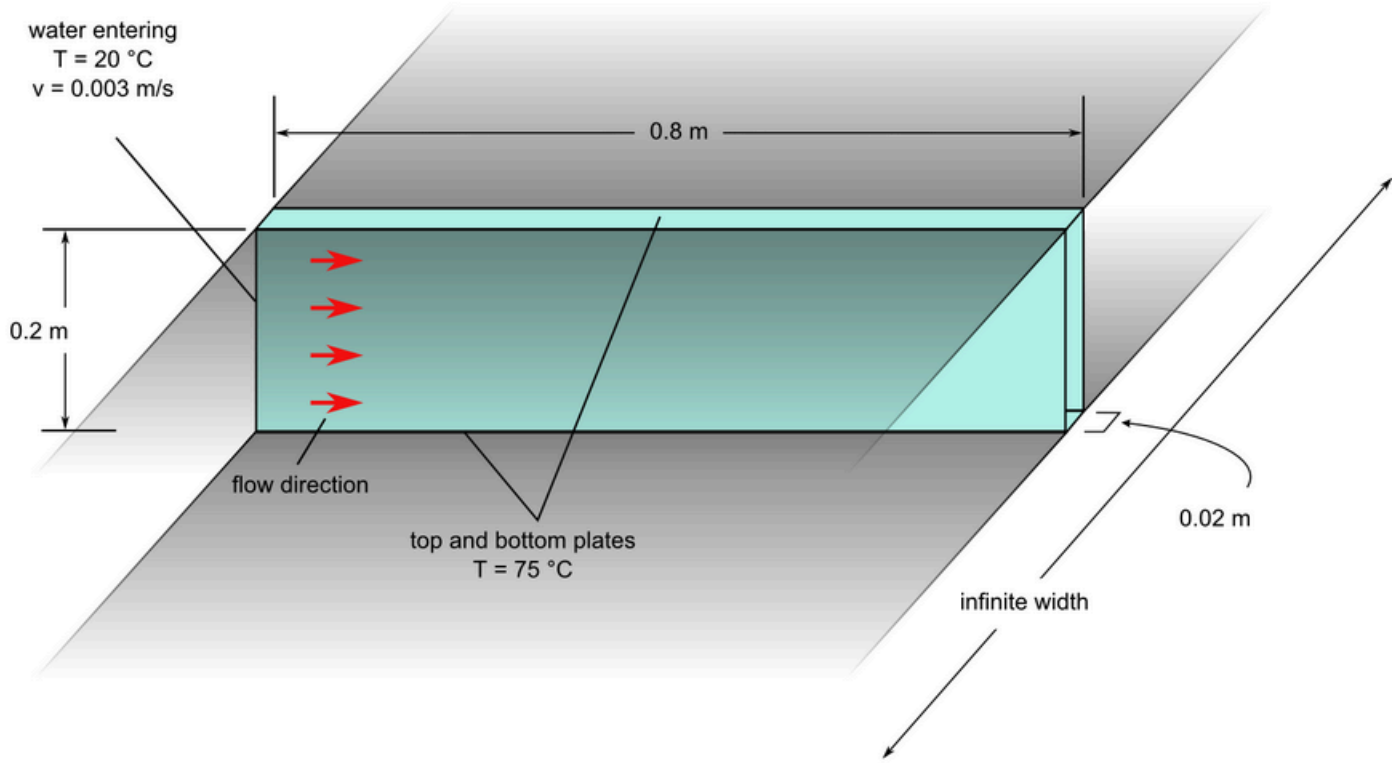


Figure 366: Critical Dimensions and Parameters for Simulating Laminar Flow Through a Channel with Heated Walls

The simulation was performed as a two dimensional problem by restricting flow in the out-of-plane direction through the use of a mesh that is one element thick. In addition, the symmetry of the geometry in the height direction is exploited to allow for modeling only half of the geometry. These characteristics allow for accurate simulation of flow while minimizing computational time.

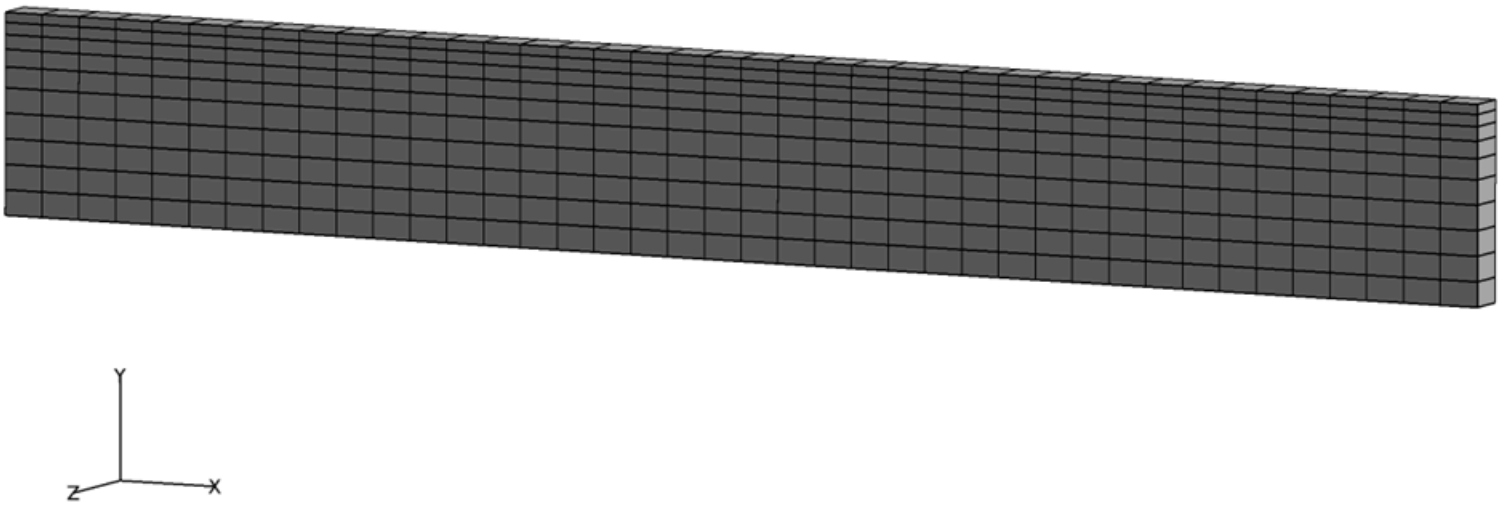


Figure 367: Mesh (Top Half of the Channel) used for Simulating Laminar Flow Through a Channel with Heated Walls

AcuSolve Results

The AcuSolve solution converged to a steady state and the results reflect the mean flow conditions. As the cool water enters the channel at temperature less than that of the walls, heat is transferred to the water by conduction. As the fluid travels along the channel, the temperature differential between the wall and the adjacent water decreases. The thermal boundary layer within the water develops as the flow propagates downstream.

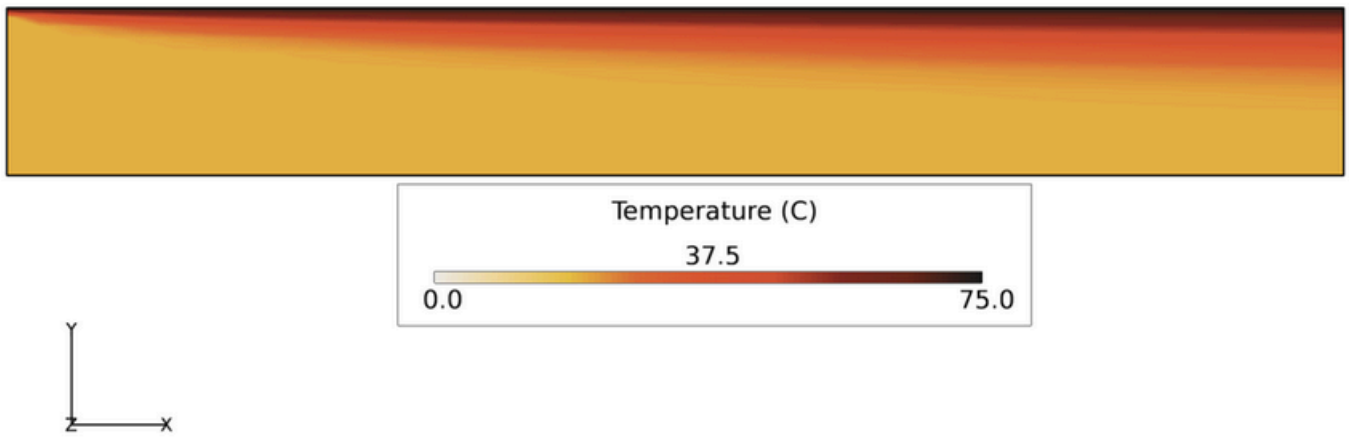


Figure 368: Temperature Contours Along the Top Half of a Heated Channel

Temperature at a specified vertical position in the channel increases along the length of the channel. The nature of that temperature change is dependent on proximity to the heated wall. Water in the center of the flow will have the least temperature change. Since this problem was solved for symmetrical flow, only the top half of the flow region was modeled. The vertical position for results

shown in the following figure are based on the center of flow having a Y-position of 0. For a vertical position near the center of flow (Y=0.0595) there is minimal change in temperature.

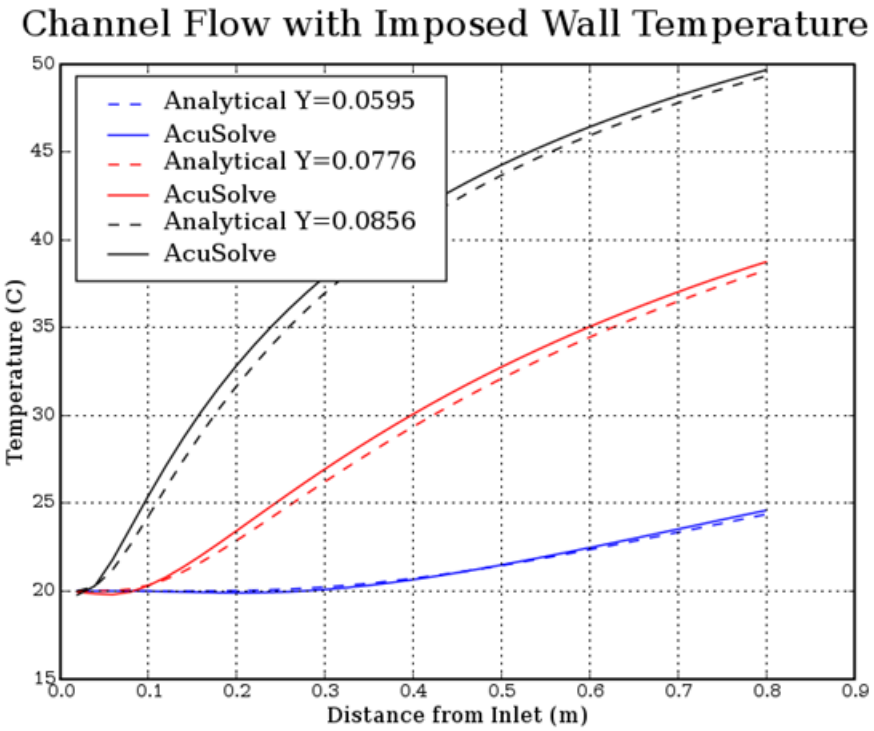


Figure 369: Temperature Plotted Against Distance from Inlet for 3 Different Heights from the Channel Center Line

Summary

The AcuSolve results compare well with the analytical results for the development of a thermal boundary layer in a heated channel. In this application, the model is set up to yield large gradients as the flow convects away from the inlet. The boundary conditions and mesh size were chosen specifically to yield a high Peclet number. The element Peclet number in the flow direction in this case is Pe=30.0, as calculated from the following equation.

$$Pe = \frac{\rho C p |v| he}{k} \tag{12}$$

where ρ is the density, CP the heat capacity, v the velocity, he the length, and k the thermal conductivity.

This example shows the robustness of the stabilized technique in AcuSolve when element Peclet number is high. Note that standard Galerkin finite element formulations become unstable when the element Peclet number is greater than 1.0.

Simulation Settings for Laminar Flow Through a Channel with Heated Walls

AcuConsole database file: `<your working directory>\channel_laminar_heat\channel_laminar_heat.acs`

Global

- Problem Description
  - Analysis type - Steady State
  - Temperature equation - Advective Diffusive
  - Turbulence equation - Laminar
- Auto Solution Strategy
  - Relaxation factor - `0.4`
- Material Model
  - Fluid_Material
    - Density - `1000.0` kg/m3
    - Specific Heat - `1000` J/kg-K
    - Viscosity - `1.0e-12` kg/m-sec
    - Conductivitiy - 1.0 W/m-K

  Model
- Volumes
  - Fluid
    - Element Set
      1. Material model - Fluid_Material
- Surfaces
  - Inlet
    - Simple Boundary Condition
      1. Type - Inflow
      2. Inflow type - Velocity
      3. X velocity - `0.003` m/sec
      4. Temperature - `20` °C
  - Outlet
    - Simple Boundary Condition
      1. Type - Outflow
  - Symm_MaxZ
    - Simple Boundary Condition
      1. Type - Slip
  - Symm_MinY
    - Simple Boundary Condition
      1. Type - Slip
  - Symm_MinZ
    - Simple Boundary Condition
      1. Type - Slip
  - Wall

- Simple Boundary Condition
  1. Type - Wall
  2. Temperature BC type - Value
  3. Temperature - 75 °C

References

Hua Tan and K. M. Pillai. "Numerical Simulation of Reactive Flow in Liquid Composite Molding Using Flux-Corrected Transport (FCT) Based Finite Element/Control Volume (FE/CV) Method". International Journal of Heat and Mass Transfer. 53:2256-2271, 2010.

Turbulent Natural Convection Inside a Tall Cavity

In this application, AcuSolve is used to simulate the natural convection of a turbulent flow field within a tall rectangular cavity. AcuSolve results are compared with experimental results as described in Betts and Bokhari (2000). The close agreement of AcuSolve results with experimental results validates the ability of AcuSolve to model cases with natural convection of turbulent flow within a tall cavity.

Problem Description

The problem consists of air within a tall cavity with a hot wall and a cold wall, as shown in the following image, which is not drawn to scale. The cavity is 2.18 m tall, 0.0762 m wide, and 0.52 m deep. The cavity's vertical walls differ in temperature, causing the fluid to transfer the heat, leading to natural convection. The temperature of the hot wall is 307.85 K, while the temperature of the cold wall is 288.25 K. The horizontal walls of the cavity are adiabatic. The length-to-width ratio of 28.6 and temperature difference of 19.6 K produce a turbulent flow field within the cavity with a Rayleigh number of $8.6X10^{5}$ (Betts and Bokhari 2000). The flow medium is air, with a Boussinesq approximation for density, a specific heat of 1005 J/kg-K, and a viscosity of $1.781 X 10^{-5}$ kg/m-s. Gravity is applied globally to the volume of air.

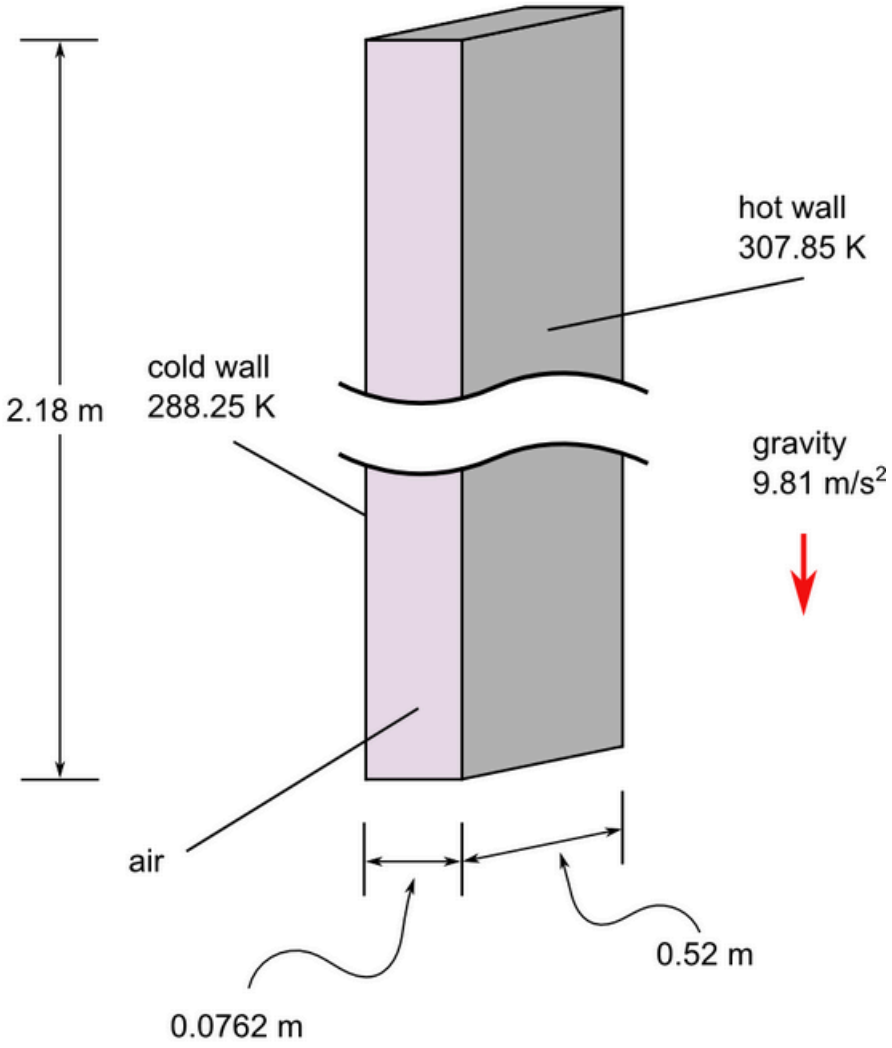


Figure 370: Critical Dimensions and Parameters for Simulating Turbulent Natural Convection in a Tall Cavity

The simulation was performed as a two dimensional problem by constructing a volume mesh that contains a single layer of elements in the extruded direction, normal to the flow plane and by imposing symmetry boundary conditions on the extruded planes.

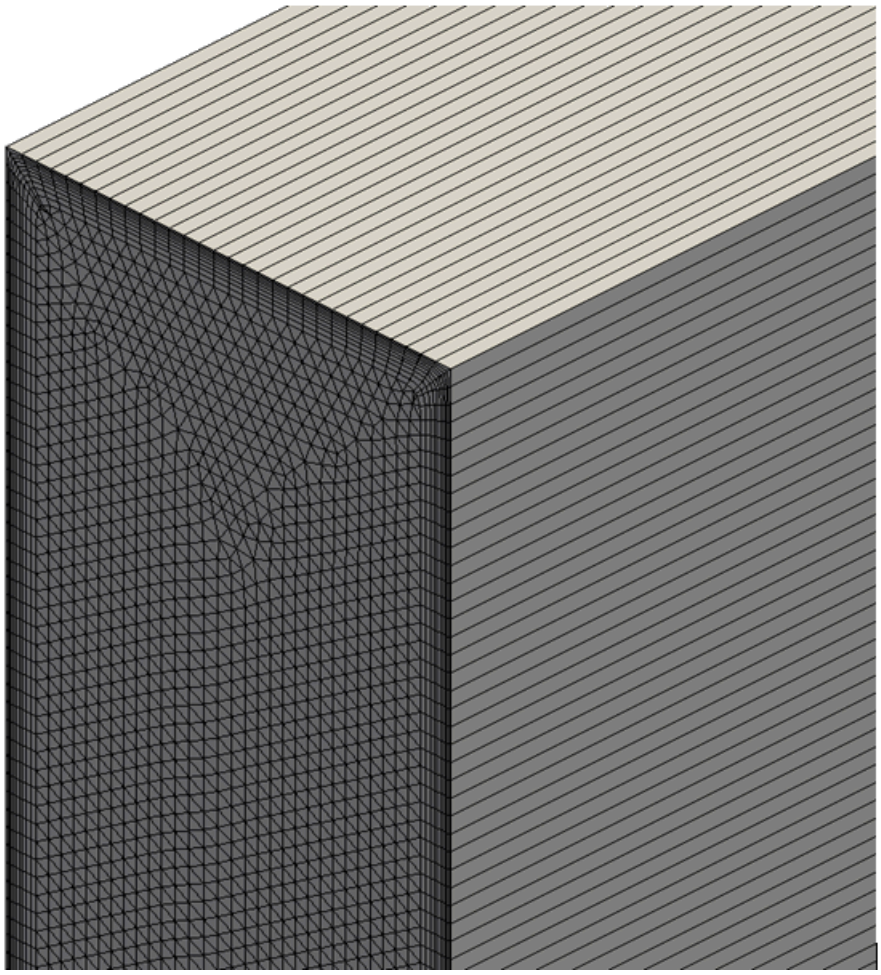


Figure 371: Mesh used for Simulating the Natural Convection of Turbulent Flow in a Tall Cavity

AcuSolve Results

The AcuSolve solution converged to a steady state and the results reflect the mean flow conditions. The natural convection of the flow is generated by heat transfer from the vertical walls to the fluid in the cavity. The temperature gradients created by this heat transfer cause differing densities within the flow region. The warmer air rises to the top of the cavity due to its lower density while the colder air sinks to the bottom of the cavity due to its higher density. This produces flow near the hot vertical wall in the positive vertical direction and flow near the cold wall in the negative vertical direction.

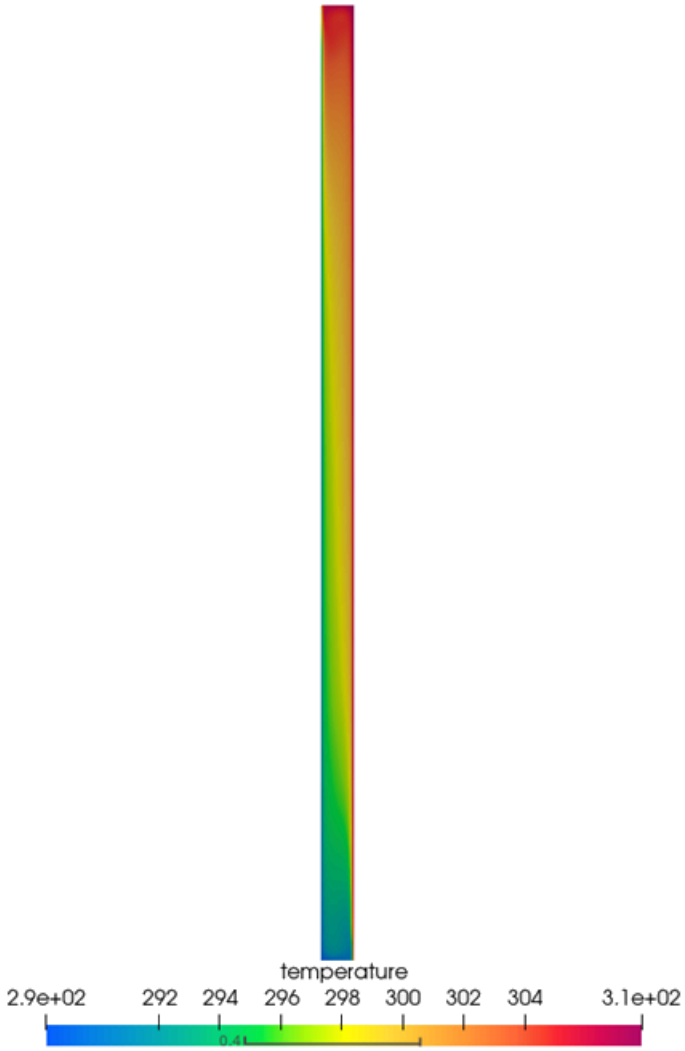


Figure 372: Temperature Contours Throughout Tall Cavity in the X-Y Plane

The AcuSolve results of the temperature and vertical velocity within the cavity are compared to the corresponding experimental values in the plots shown below. The temperature of the air is lowest near the cold vertical wall, remains relatively steady in the middle of the cavity, and then peaks near the hot vertical wall. Following a similar trend, the AcuSolve results show that the velocity is lowest near the cold vertical wall, due to the air sinking, and then steadily increases as the air begins to rise near the hot vertical wall. The velocity at the walls is zero due to the no-slip boundary condition. Additional comparisons are made to evaluate the performance of four turbulence models, Spalart-Allmaras (SA), shear stress transport (SST), K-Omega and K-ε.

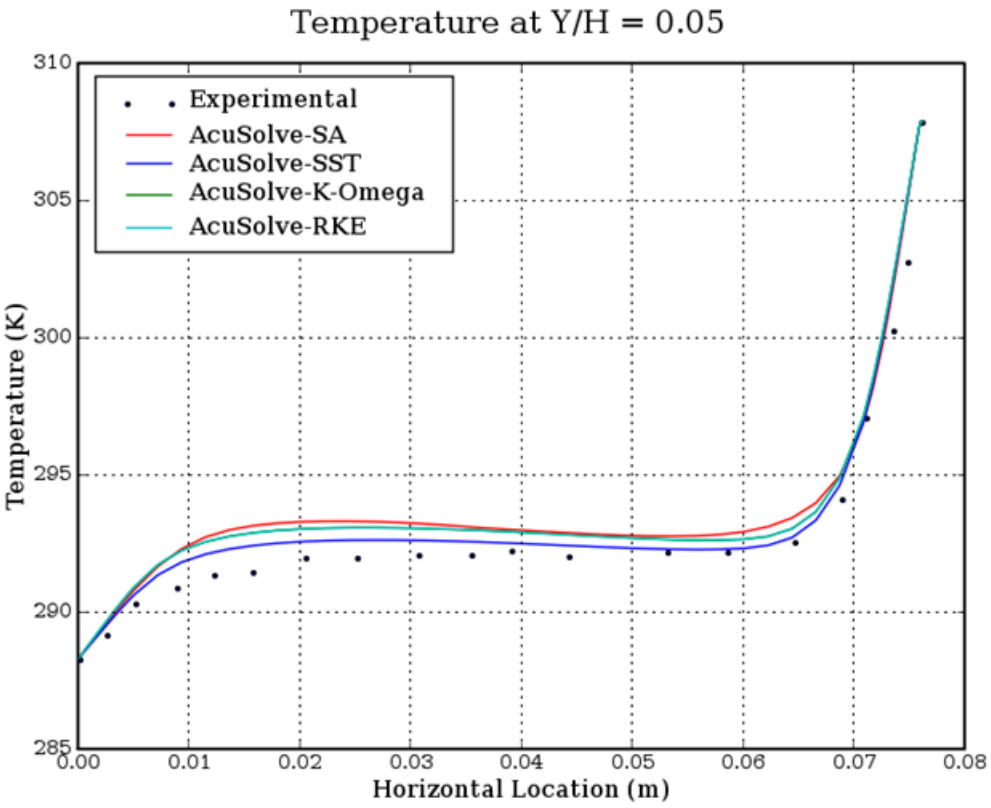


Figure 373: Temperature Plotted against Location along Horizontal at a Position of y/H=0.05 in the Cavity, where H is the Cavity Height and y is the Distance from the Bottom Wall

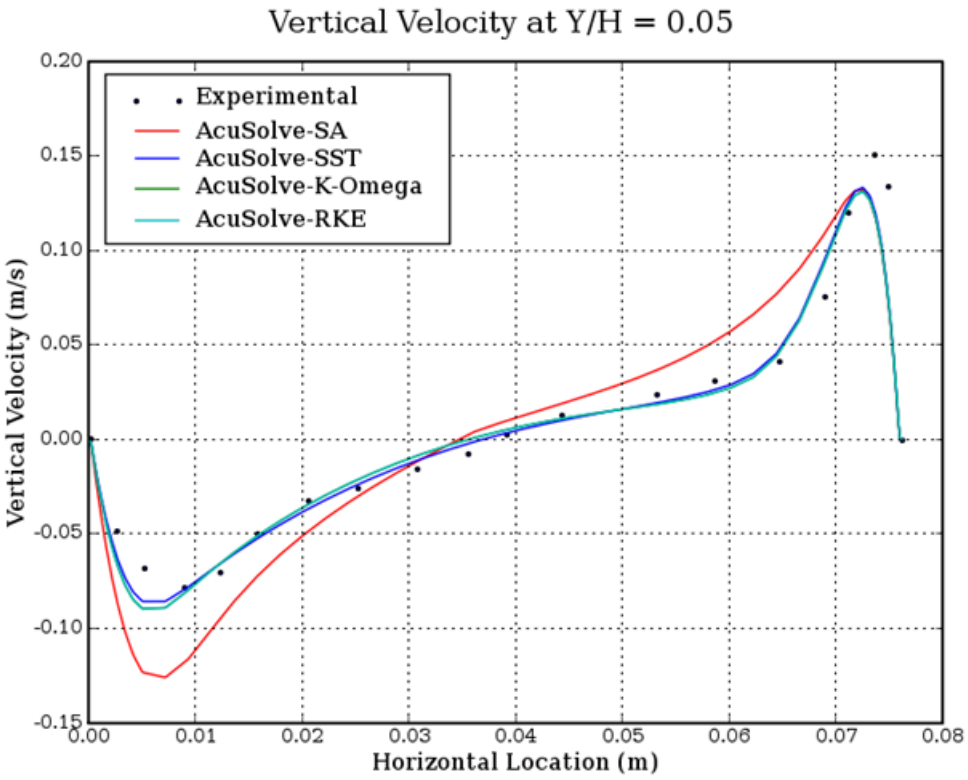


Figure 374: Vertical Velocity Plotted against Location along Horizontal at a Position of y/H=0.05 in the Cavity, where H is the Cavity Height and y is the Distance from the Bottom Wall

Summary

In this application, turbulent flow developed by natural convection, at a Rayleigh number of 8.6X105, is studied within a tall cavity. The AcuSolve results compare well with the experimental data for temperature and vertical velocity along a horizontal line at a location of y/H=0.05 in the tall cavity, with the two-equation models capturing the velocity gradient with greater accuracy. A temperature difference occurs within the flow region due to the heat transfer from the vertical walls of the cavity. The hotter, less-dense air rises to the top of the cavity while the colder, denser air sinks to the bottom, giving rise to recirculation. AcuSolve demonstrates the ability to accurately predict the natural convection of turbulent flow within a tall cavity.

Simulation Settings for Turbulent Natural Convection Inside a Tall Cavity

HyperWorks CFD database file: `<your working directory\cavity_turbulent_heat\cavity_turbulent_heat.hm`

Global

- Problem Description
  - Analysis type - Steady State
  - Turbulence equation - SST
- Auto Solution Strategy
  - Relaxation factor - `0.5`

    - Convergence tolerance - `0.005`
- Material Model
    - Air
        - Type - Boussinesq
        - Density - `1.225` kg/m3
        - Specific Heat - `1005` J/kg-K
        - Viscosity - `1.781e-5` kg/m-sec

  Model
- Volumes
    - Volume
        - Element Set
            1. Material model - Air
- Surfaces
    - Back
        - Simple Boundary Condition
            1. Type - Symmetry
    - Bottom
        - **Simple Boundary Condition**
            1. Type - Wall
            2. Temperature BC type - Flux
            3. Heat Flux - `0.0` W/m2
    - Cold
        - **Simple Boundary Condition**
            1. Type - Wall
            2. Temperature BC type - Value
            3. Temperature - `288.25` K
    - Front
        - Simple Boundary Condition
            1. Type - Symmetry
    - Hot
        - Simple Boundary Condition
            1. Type - Wall
            2. Temperature BC type - Value
            3. Temperature - `307.85` K
    - Top
        - Simple Boundary Condition
            1. Type - Wall

2 Temperature BC type - Flux

3 Heat Flux - `0.0` W/m2

References

P.L. Betts and I.H. Bokhari. "Experiments on Turbulent Natural Convection in an Enclosed Tall Cavity". International Journal of Heat and Fluid Flow 21:675-683. 2000.

Viscous Heating Inside a Rotating Annulus

In this application, AcuSolve is used to simulate fluid flow and viscous heating in an annulus formed by concentric cylinders. AcuSolve results are compared with analytical results adapted from Bird and others (1960). The close agreement of AcuSolve results with analytical results validates the ability of AcuSolve to model cases with viscous heating.

Problem Description

The problem consists of a viscous fluid filling the annulus between two concentric cylinders, as shown in the following image, which is not drawn to scale. The inner cylinder has a radius of 1.0 m and is fixed in place. The outer cylinder has a radius of 2.0 m and rotates with a constant angular velocity of 0.5 rad/s. The inner cylinder is held at a constant temperature of 273 K and the outer cylinder is held at 274 K.

The rotation of the outer cylinder causes the fluid to rotate due to the viscous shearing near the wall. As the inner cylinder is fixed, a velocity gradient is generated as a function of distance from the inner cylinder center. Viscous stresses within the domain generate significant amounts of heat, leading to a substantial increase in the fluid temperature in regions of high shear.

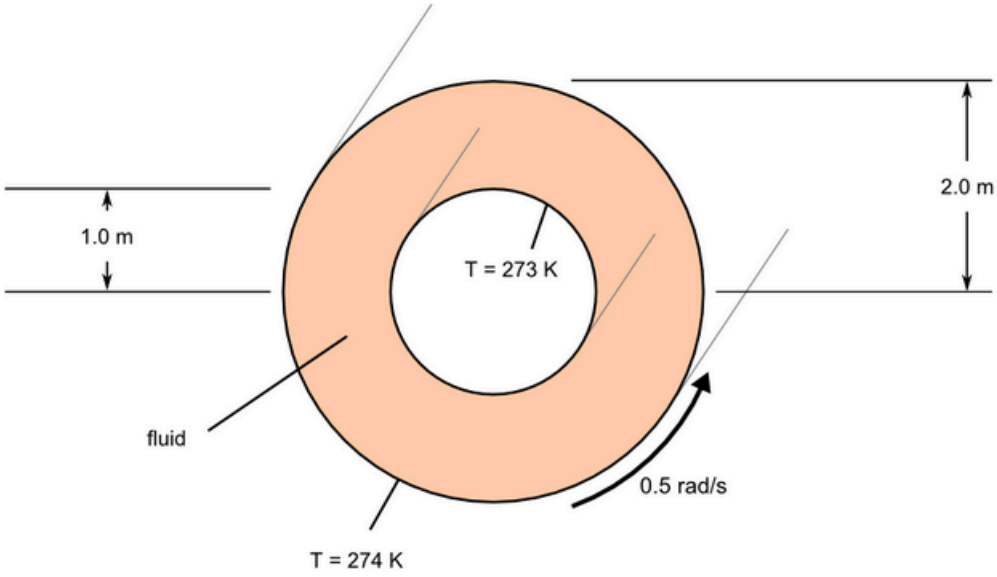


Figure 375: Critical Dimensions and Parameters for Simulating Viscous Heating Inside a Rotating Annulus

The simulation was performed as a two dimensional problem by constructing a volume mesh that contains a single layer of elements in the extruded direction, normal to the flow plane, and by imposing symmetry boundary conditions on the extruded planes.

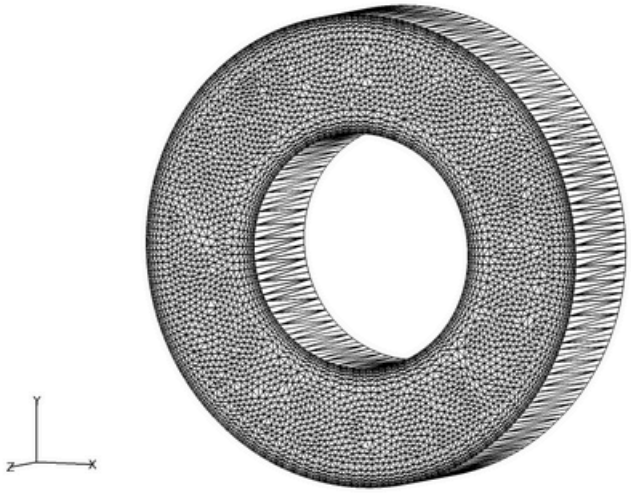


Figure 376: Mesh used for Simulating Viscous Heating Inside a Rotating Annulus

AcuSolve Results

The AcuSolve solution converged to a steady state and the results reflect the mean flow conditions. Flow is induced by the viscous shearing near the outer wall, creating a velocity gradient with the highest velocity near the moving wall.

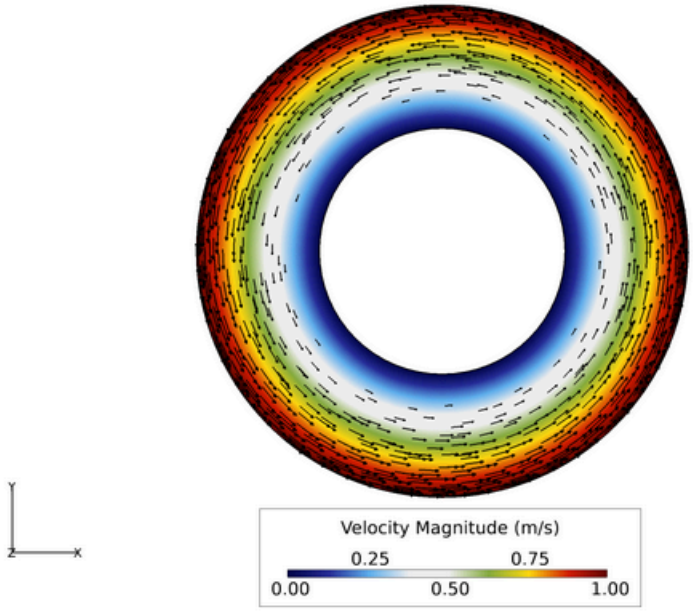


Figure 377: Contours of Velocity Magnitude and Velocity Vectors

The velocity gradient causes viscous heating, causing the fluid temperature to increase. The resulting temperature profile is nonlinear with the highest temperatures occurring in the space between the cylinders.

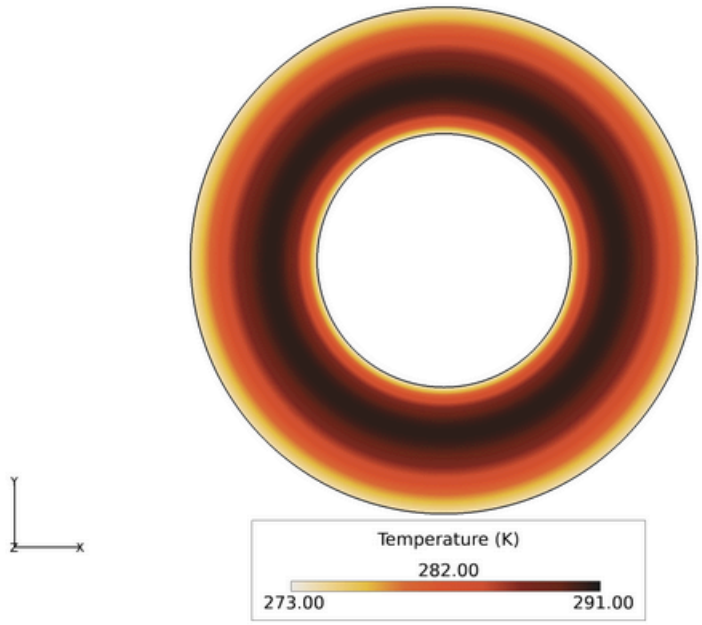


Figure 378: Contours of Temperature

AcuSolve results were compared to analytical results for velocity and for temperature across a range of radial locations.

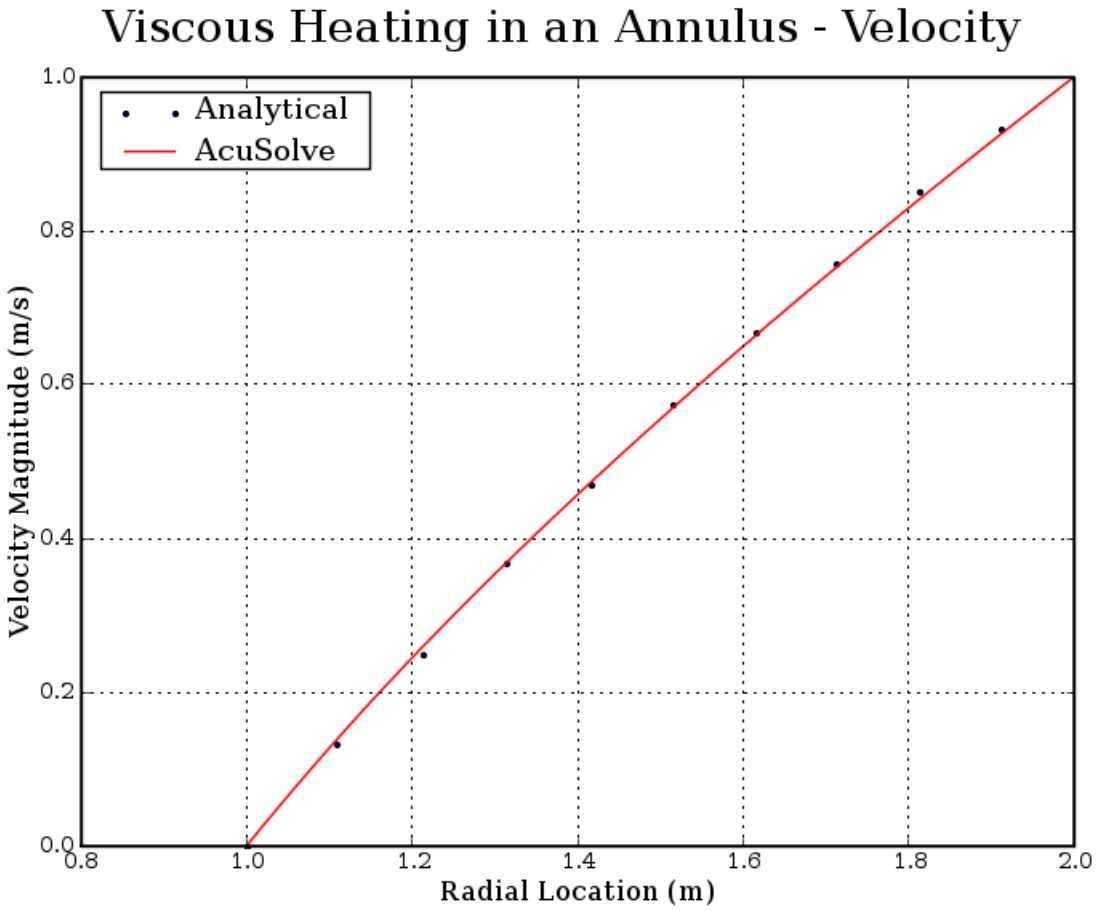


Figure 379: Velocity Magnitude Plotted Against Radial Location from the Center of the Inner Cylinder

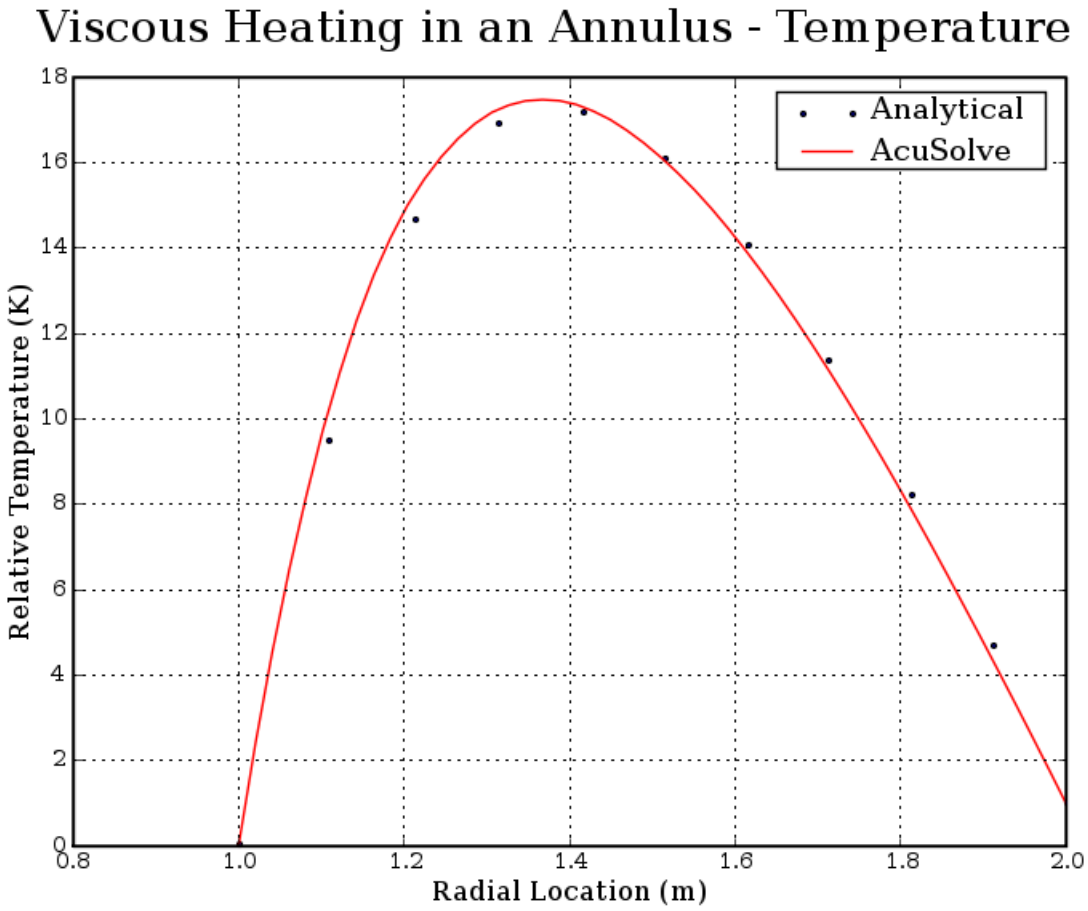


Figure 380: Temperature (Relative to the Inner Cylinder Wall Temperature) Plotted Against Radial Location from the Center of the Inner Pipe

Summary

The AcuSolve results compare well with the analytical results for both the flow field and the temperature across the annulus. In this application, flow is induced due to the viscous stresses generated by the rotation of the exterior cylinder. Velocity gradients between the cylinders give rise to shear stresses that induce frictional heating of the fluid. Due to the high viscosity of the fluid, the viscous heating is significant and leads to large increases in the temperature between the cylinders. This application validates the ability of AcuSolve to simulate flows where the viscous heating contribution is significant.

Simulation Settings for Viscous Heating Inside a Rotating Annulus

AcuConsole database file: `<your working directory>\annulus_rotating_heat\annulus_rotating_heat.acs`

Global

- Problem Description
  - Analysis type - Steady State
  - Temperature equation - Advective Diffusive

    - Turbulence equation - Laminar
- Auto Solution Strategy
    - Relaxation factor - `0.2`
- Material Model
    - Fluid
        - Density - `1.0` kg/m3
        - Viscosity - `300` kg/m-sec
        - Conductivity - `1.0` W/m-K
- Reference Frame
    - Outer_Rotation
        - Angular Velocity
            1. X-component - `0.0` rad/sec
            2. Y-component - `0.0` rad/sec
            3. Z-component - `0.5` rad/sec

Model

- Volumes
    - Fluid
        - Element Set
            1. Material model - Fluid
            2. Viscous heating - On
- Surfaces
    - Inner_Cylinder
        - Simple Boundary Condition
            1. Type - Wall
            2. Temperature BC type - Value
            3. Temperature - `273.0` K
    - Outer_Cylinder
        - Simple Boundary Condition
            1. Type - Wall
            2. Reference frame - Outer_Rotation
            3. Temperature BC type - Value
            4. Temperature - `274.0` K
    - Symm_MaxZ
        - Simple Boundary Condition
            1. Type - Symmetry
    - Symm_MinZ
        - Simple Boundary Condition

1 Type - Symmetry

- Nodes
  - Node 1
    - Pressure
      1 Type - Zero

References

R. B. Bird, W. E. Stewart, and E. N. Lightfoot. "Transport phenomena". New York, John Wiley and Sons, 1960

Ideal Gas Compression in an Actuating Piston

In this application, AcuSolve is used to simulate pressure and temperature inside an actuating piston using the ideal gas relationship and fully defined mesh motion. AcuSolve results are compared with analytical results as described in Moran and Shapiro (2000). The close agreement of AcuSolve results with analytical results validates the ability of AcuSolve to model cases with material properties defined by the ideal gas law subjected to significant mesh distortion.

Problem Description

The problem consists of air compressed by a piston within a cylinder 10 m long with a diameter of π (3.14159) m, as shown in the following image, which is not drawn to scale. The piston is driven by a crankshaft 4 m long attached to a connecting rod 6 m long. The crankshaft rotates at 60o/s around a center point. At time (t) = 0.0 s the crank and piston are at top dead center (TDC) with an initial cylinder volume of 80 m^3. At t = 3.0 s the piston is at bottom dead center (BDC), at which point the volume in the cylinder is reduced to 16 m^3. The piston then moves back to TDC at t = 6.0 s. Air at atmospheric conditions, with material properties of an ideal gas and a dynamic viscosity of 1.781 X 10^5 kg/m-sec is the fluid modeled in the domain.

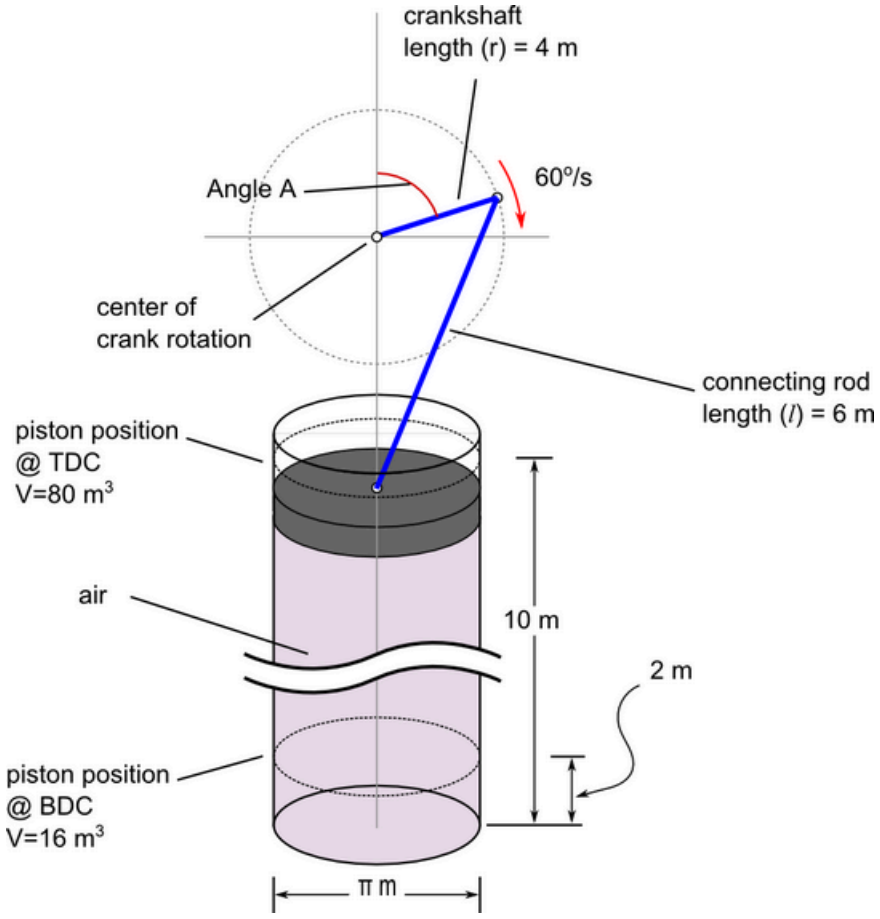


Figure 381: Critical Dimensions and Parameters for Simulating Ideal Gas Compression in an Actuating Piston

The motion of the piston is described by the following equation.

$$x = r*\cos A + \sqrt{l^2 - r^2 \sin^2 A} \quad (13)$$

Where

- x is the distance of the piston from TDC
- r is the length of the connecting rod, 4 m
- A is the crank angle as a function of time (t)
- l is the connecting rod length, 6 m

During the simulation, the top surface of the cylinder, representing the piston, moves with an applied mesh motion that mimics the motion of the reciprocating crank, rod, and piston assembly. The ideal gas is compressed by contracting the mesh according to the motion of that assembly and by allowing the fluid properties to change as a function of time.

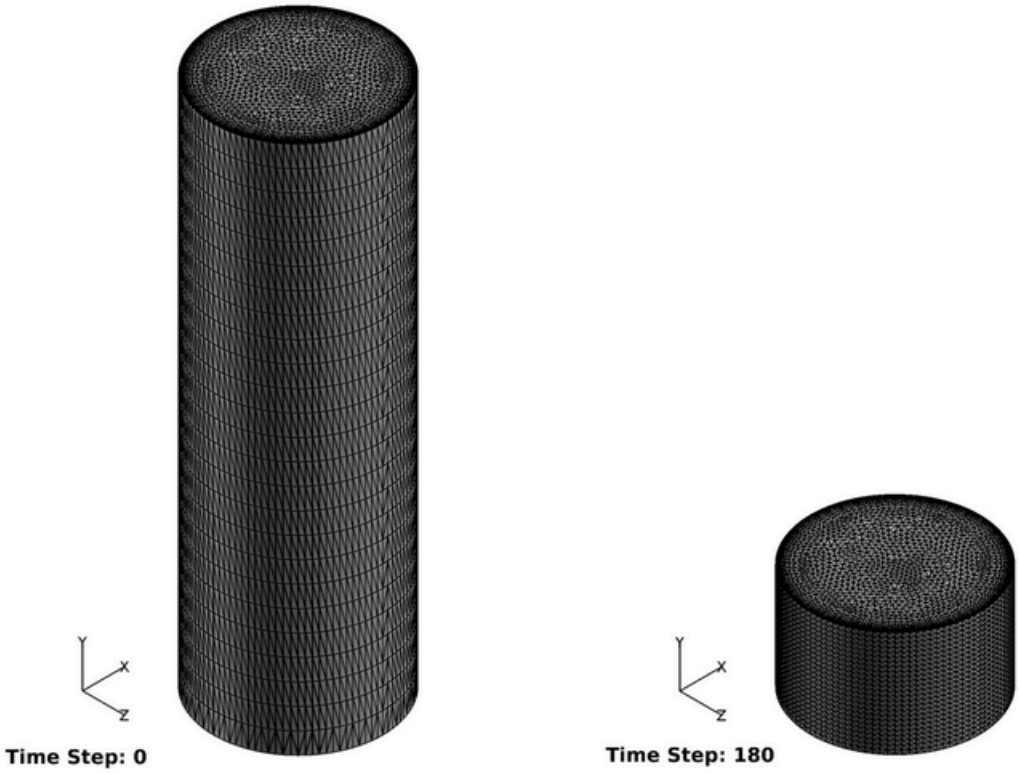


Figure 382: Mesh Used for Simulating Ideal Gas Compression in an Actuating Pistion at Time Step 0 and Time Step 180 (3 s)

AcuSolve Results

The simulation was run as transient for a total of 360 time steps with a duration of 6.0 seconds. The AcuSolve solution shows time dependent pressure and temperature in a cylinder volume that compresses and expands in a 6.0 second cycle. Pressure and temperature increase as the cylinder volume decreases, and returns toward initial conditions as the cylinder volume expands. The contours of pressure and temperature within the cylinder at the initial stage (t = 0.0 s) and the half cycle (t = 3.0 s) are shown in the following images.

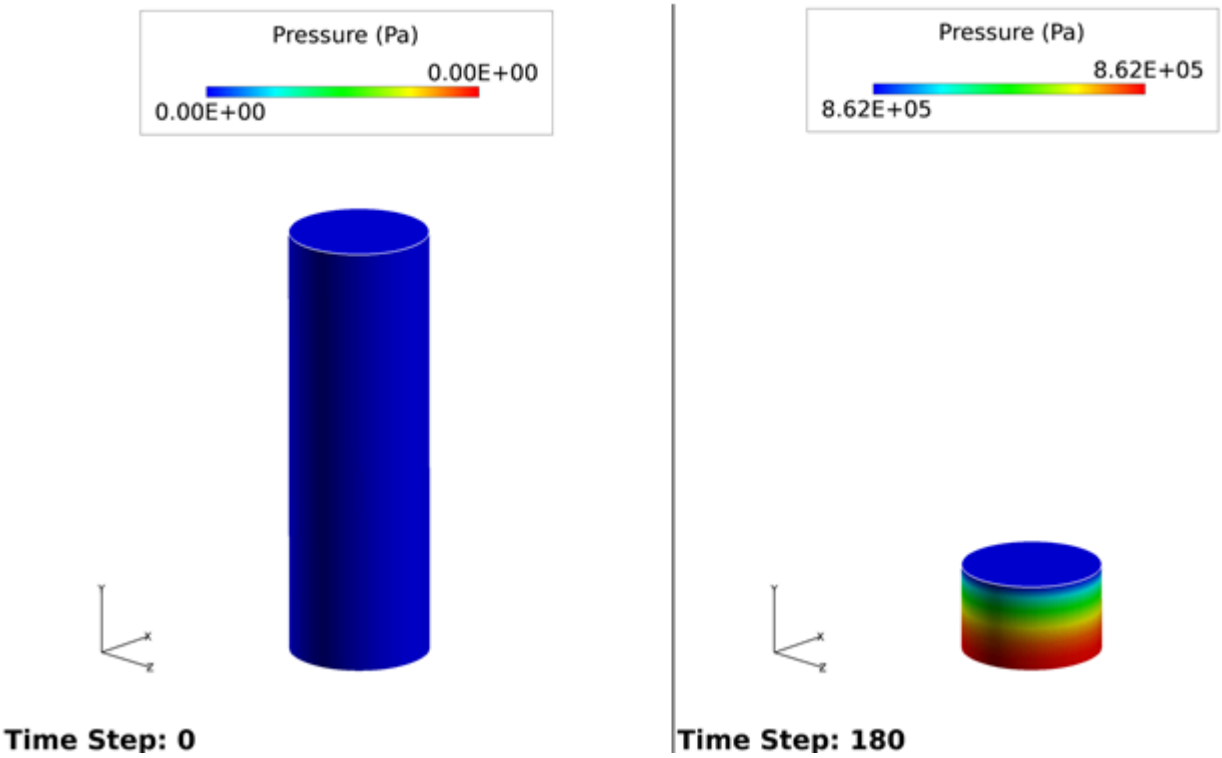


Figure 383: Pressure Distribution Within the Domain with the Piston at TDC and BDC

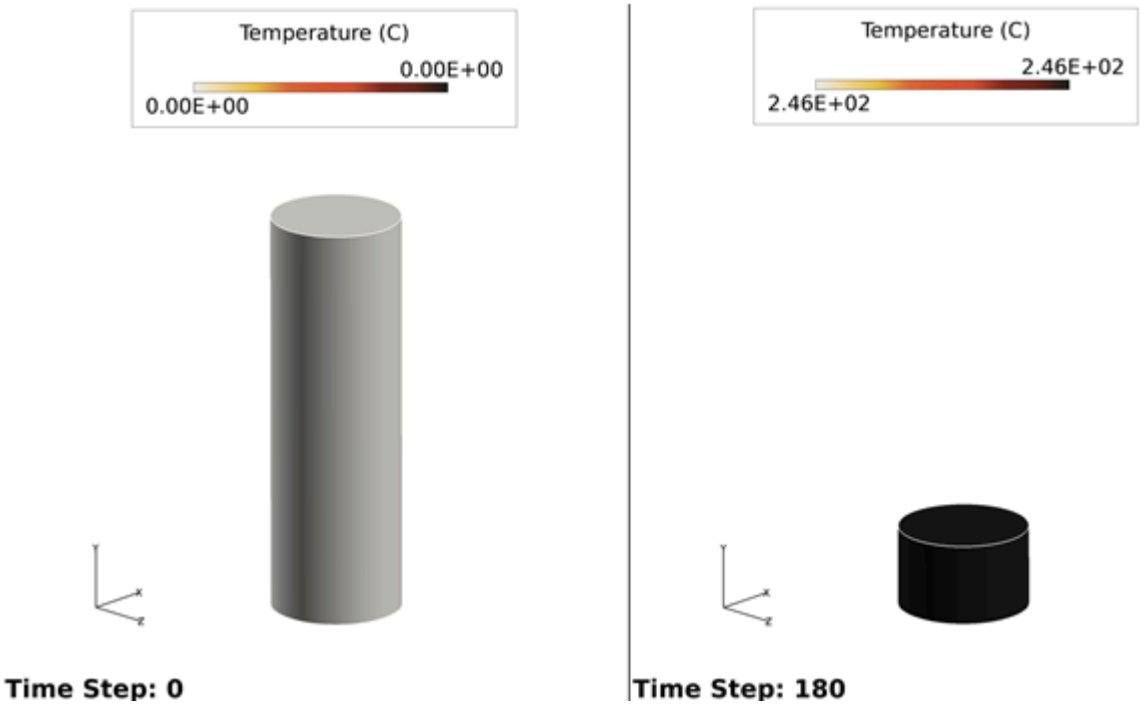


Figure 384: Temperature Distribution Within the Domain with the Piston at TDC and BDC

Comparison of time history plots of the AcuSolve and analytical solutions shows that the AcuSolve solution is nearly identical to the analytical solution. The AcuSolve computed internal pressure reaches a maximum of 8.62 X 105 Pa and the temperature reaches a maximum of 246.45 degrees C.

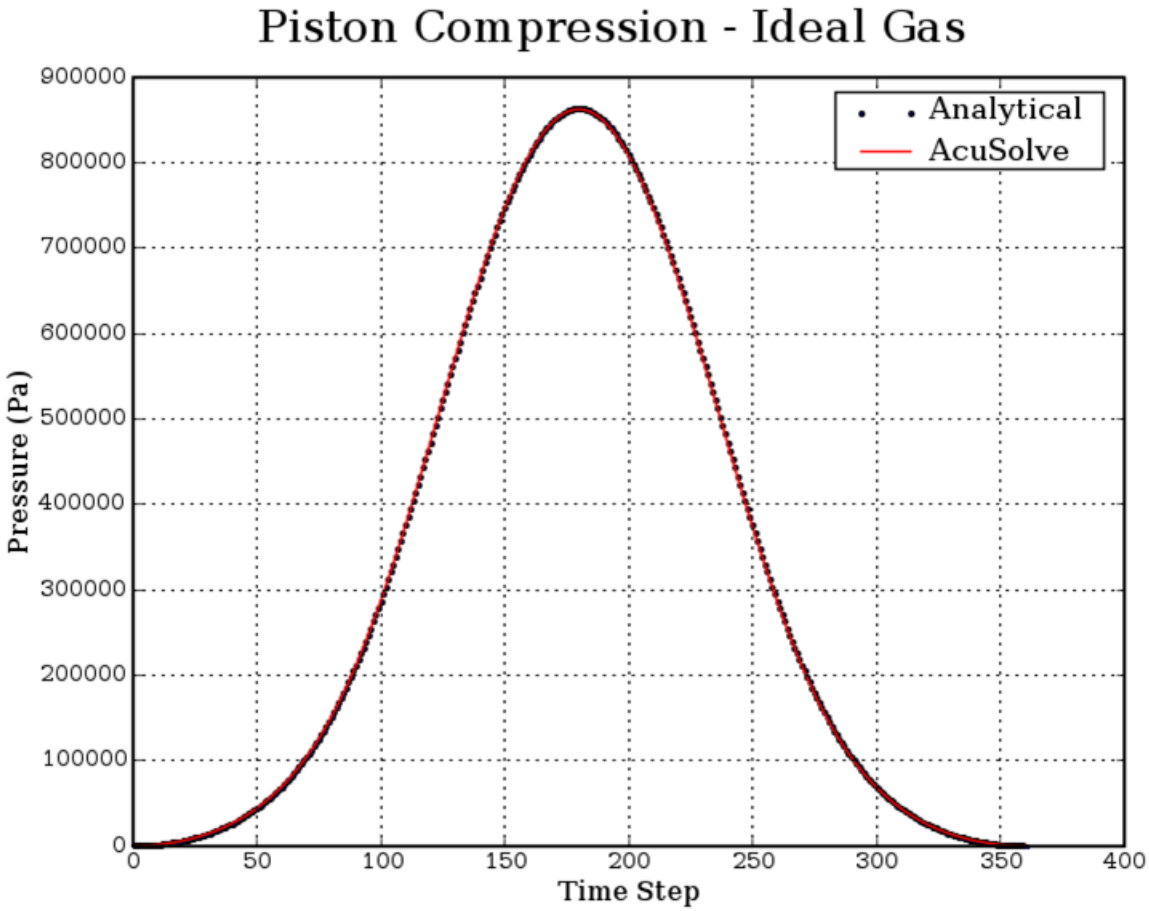


Figure 385: History Plots of Pressure for AcuSolve and Analytical Solutions

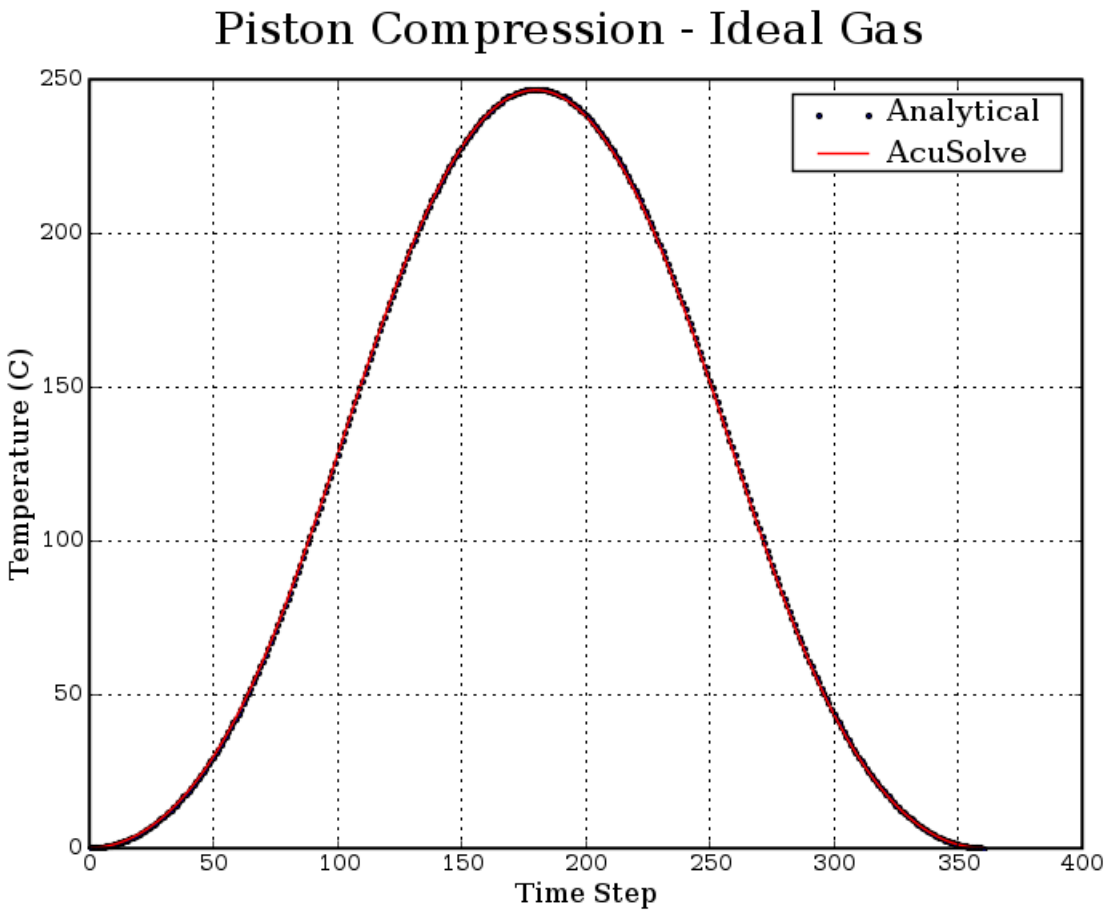


Figure 386: History Plots of Temperature for AcuSolve and Analytical Solutions

Summary

The AcuSolve solution compares well with analytical results for ideal gas compression in an actuating piston. The AcuSolve transient solution compares nearly identically with the analytical solution, with 0.1 percent and 0.16 percent error for the maximum pressure and temperature, respectively. As a result, AcuSolve demonstrates the ability to predict ideal gas compression in an actuating piston.

Simulation Settings for Ideal Gas Compression in an Actuating Piston

AcuConsole database file: `<your working directory>\cylinder_piston_compression\cylinder_piston_compression.acs`

Global

- Problem Description
  - Analysis type - Transient
  - Temperature equation - Advective Diffusive
  - Turbulence equation - Laminar
  - Mesh type - Fully Specified

- Auto Solution Strategy
  - Max time steps - `360`
  - Initial time increment - `0.01667` sec
  - Convergence tolerance - `1.0e-5` sec
  - Max stagger iterations - `10`
- Multiplier Function
  - Piston
    - Type - Piecewise Linear
    - Curve fit variable - Time
    - Curve fit values - (included in `.acs` based on equation discussed in problem description)
- Material Model
  - Air
    - Density
      1. Type - Ideal Gas
      2. Gas constant - `286.9` J/kg-K
      3. Abs. pressure offset - `101325.0` N/m2
      4. Abs. temperature offset - `273.15` K
    - Viscosity - `1.781e-5` kg/m-sec
- Mesh Motion
  - Piston
    - Type - Translation
    - Translation velocity - `0.0`, `-1.0`, `0.0`
    - Velocity variable - Multiplier Function
    - Translation multiplier function - Piston

  Model
- Volumes
  - Fluid
    - Element Set
      1. Material model - Air
      2. Compression heating - On
    - Element Output - on
- Surfaces
  - BDC
    - Simple Boundary Condition
      1. Type - Wall
      2. Wall velocity type - Match Mesh Velocity
      3. Mesh displacement BC type - Fixed
  - SideWall

        - Simple Boundary Condition
            1. Type - Wall
            2. Wall velocity type - Match Mesh Velocity
            3. Mesh displacement BC type - Fixed
    - TDC
        - Simple Boundary Condition
            1. Type - Wall
            2. Mesh displacement BC type - Fixed
            3. Mesh motion - Piston
- Nodes
    - VolumeNodes
        - Mesh X-Displacement
            1. Type - Zero
        - Mesh Y-Displacement
            1. Type - Linear
            2. Mesh motion - Piston
            3. Curve fit variable - Y reference coordinate
                1. X1 - `10.0` m
                2. Y1 - `1.0` m
                3. Y2 - `0.0` m
        - Mesh Z-Displacement
            1. Type - Zero

References

M.J. Moran and H.N Shapiro. "Fundamentals of Engineering Thermodynamics". Wiley. 4th Ed. 2000.

Laminar Flow Through a Pipe with Constant Wall Temperature

In this application, AcuSolve is used to simulate the flow of mercury through a heated pipe. The AcuSolve results are compared with analytical results for pressure drop as described in White (1991), and with temperature changes as described in Incropera and DeWitt (1981). The close agreement of AcuSolve results with analytical results validates the ability of AcuSolve to model cases with flow and imposed temperature constraints.

Problem Description

The problem consists of mercury flowing through a circular pipe that is 0.005 m in diameter and 0.1 m long, as shown in the following image, which is not drawn to scale. Mercury enters the pipe with a constant temperature of 300 K and with a fully developed velocity profile with an average velocity of 0.005 m/s. The pipe wall has a constant temperature of 500 K. These constraints impose a temperature gradient within the fluid. As the fluid moves through the pipe it is slowly heated by the wall, resulting in an increased centerline temperature. Pressure decreases along the pipe length due to the friction imposed by the viscous stresses near the pipe wall. A periodic boundary condition is imposed on the inlet and outlet to allow the pressure to change with a constant offset, while the velocity is fully periodic.

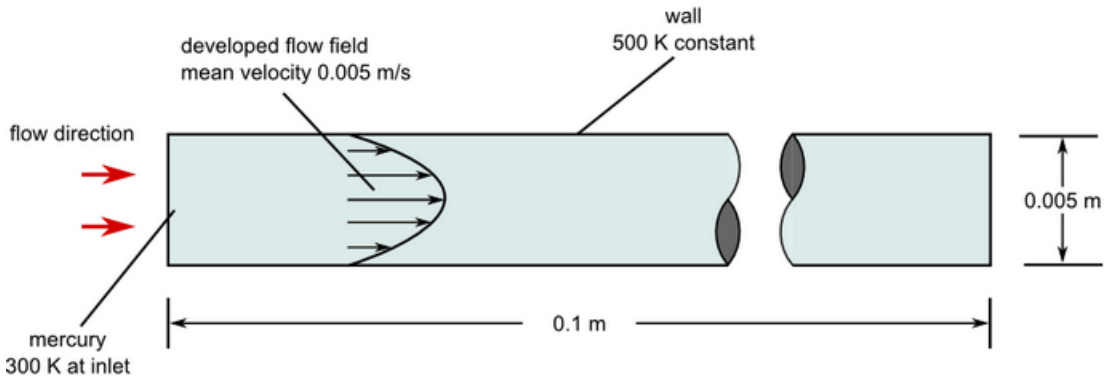


Figure 387: Critical Dimensions and Parameters for Simulating Laminar Flow through a Pipe with Constant Wall Temperature

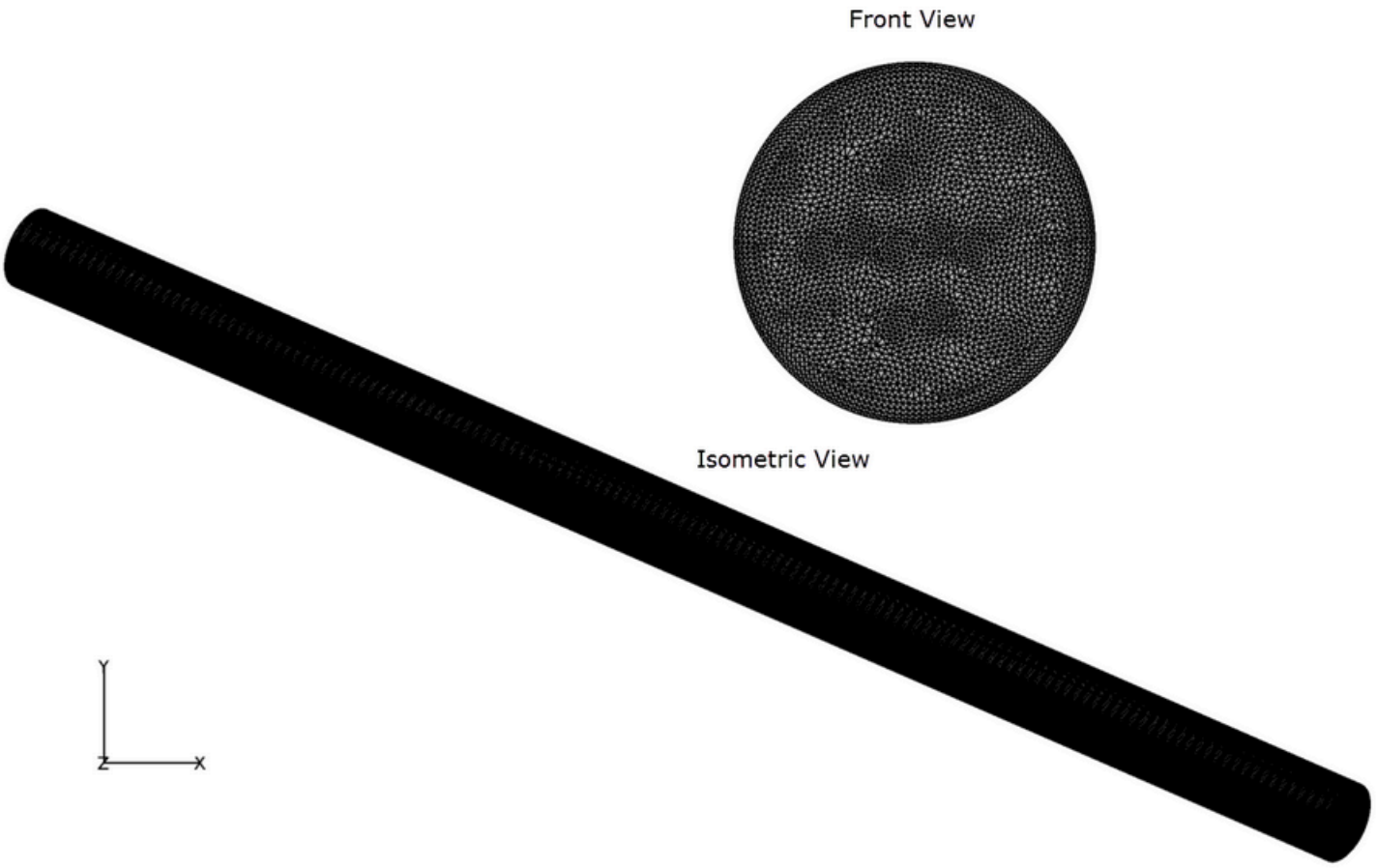


Figure 388: Mesh used for Simulating Laminar Flow Through a Pipe with Constant Wall Temperature

AcuSolve Results

The AcuSolve solution converged to a steady state and the results reflect the mean flow conditions. In this application, a fully developed laminar profile is achieved by enforcing periodic constraints on the pressure and velocity fields. The spatially developing temperature field is achieved by allowing the fluid's temperature to evolve along the full length of the model. The change in temperature along the pipe length is due to advection in the streamwise direction and heat conduction from the outer walls where the temperature is greater than the initial flow temperature. The temperature rises along the length of the pipe and the pressure drops along the length of the pipe. At the inlet, the temperature of the mercury is 300 K and the pressure is 0.496 Pa. At the outlet centerline, the temperature of the mercury has risen to 500.0 K and the pressure has dropped to -0.4965 Pa.

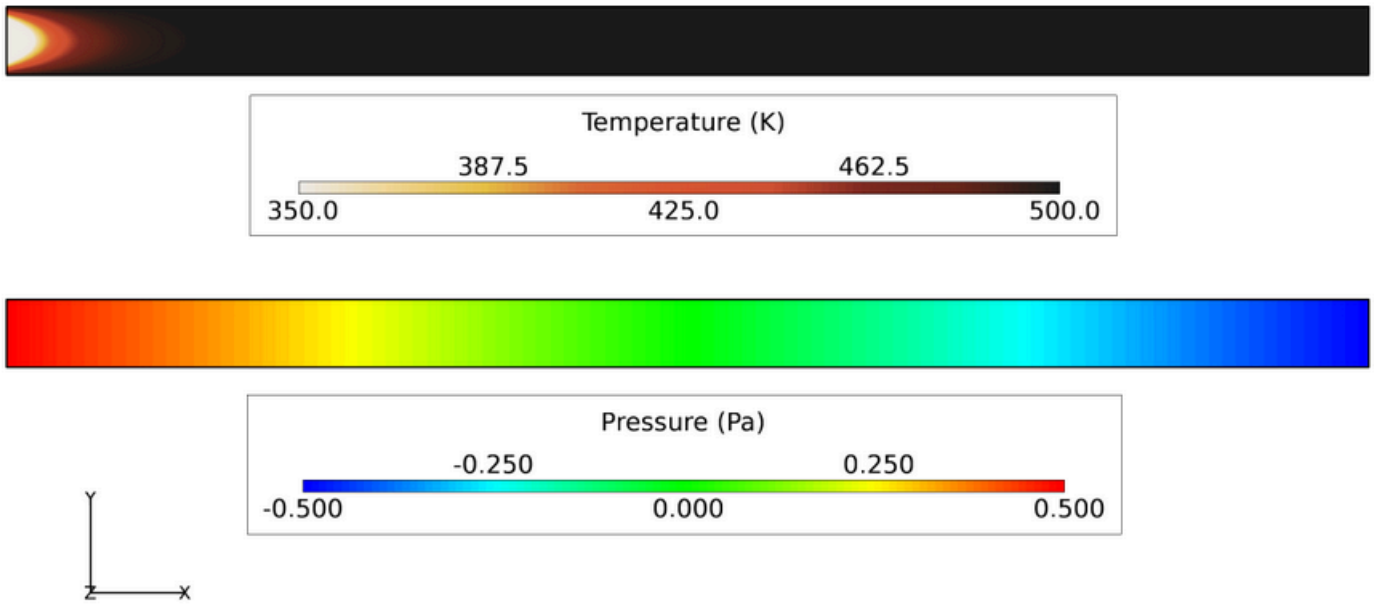


Figure 389: Temperature and Pressure Contours of Mercury Flow Through a Pipe with Prescribed Temperature Boundary

The following table shows the comparison of AcuSolve results with the analytical solutions from White (1994). Comparisons were made for the pressure drop between the inlet and outlet and the temperature at the center of the outlet.

Table 28:

	Analytical solution	**AcuSolve solution**	**Percent deviation from analytical**
Pressure drop (Pa)	0.991	0.9925	0.15
Centerline temperature of flow at outlet (K)	500.0	500.0	< 0.0001

Summary

The AcuSolve solution compares well with analytical results for flow through a pipe with constant temperature boundary conditions. The AcuSolve solution for the centerline temperature is nearly identical with the analytical results and the pressure reduces as expected for the prescribed flow conditions. The results of this simulation validate the ability of AcuSolve to accurately predict the heating of fluid flowing through a pipe with constant wall temperature.

Simulation Settings for Laminar Flow Through a Pipe With Constant Wall Temperature

AcuConsole database file: `<your working directory>\pipe_laminar_heatDirichlet\pipe_laminar_heatDirichlet.acs`

Global

- Problem Description
  - Analysis type - Steady State
  - Temperature equation - Advective Diffusive
  - Turbulence equation - Laminar
- Auto Solution Strategy
  - Relaxation Factor - `0.2`
- Material Model
  - Mercury
    - Density - `13579.0` kg/m3
    - Specific Heat - `139.3` J/kg-K
    - Viscosity - `0.001548` kg/m-sec
    - Conductivity - `8.69` W/m-K

  Model
- Volume
  - Fluid
    - Element Set
      1. Material model - Mercury
- Surfaces
  - Inflow
    - Simple Boundary Condition - (disabled to allow for periodic conditions to be set)
    - Advanced Options
      1. Integrated Boundary Conditions
         1. Mass Flux
            1. Type - Constant
            2. Constant value - `1.33e-3` kg/sec
      2. Temperature
         1. Type - Constant
         2. Constant value - `300.0` K
  - Outflow
    - Simple Boundary Condition - (disabled to allow for periodic conditions to be set)
  - Wall
    - Simple Boundary Condition
      1. Type - Wall

2 Temperature BC type - Value
3 Temperature - `500.0` K

- Periodics
  - Periodic 1
    - Individual Periodic BCs
      1 Velocity
        1 Type - Periodic
      2 Pressure
        1 Type - Single Unknown Offset

References

F. M. White. "Fluid Mechanics". 3rd Edition. McGraw-Hill Book Co., Inc. New York. 1994.

F. P. Incropera and D. P. DeWitt. "Fundamentals of Heat Transfer". John Wiley & Sons. New York. 1981.

Turbulent Flow with Separation in an Asymmetric Diffuser

In this application, AcuSolve is used to simulate fully developed turbulent flow through an asymmetric diffuser with a divergent lower wall and a straight upper wall. AcuSolve results are compared with experimental results as described in Buice and Eaton (2000). The close agreement of AcuSolve results with experimental results validates the ability of AcuSolve to model cases with internal turbulent flow with flow separation and reattachment in an asymmetric diffuser.

Problem Description

The problem consists of air flowing through an asymmetric diffuser with a divergent lower wall and a straight upper wall, as shown in the following image, which is not drawn to scale. The diffuser inlet has a height of 1.5 cm (H) and extends 9 cm (6H) to the divergent section. The lower wall of the diffuser diverges at an angle of 10° and expands to 7.05 cm (4.7H). The divergent section has a horizontal length of 31.5 cm (21H). The expanded section of the diffuser extends 84 cm (56H) to the outlet. Air, with a density of 1.225 kg/m^3 and a viscosity of 1.8325 X 10^{-5} kg/m-s enters the diffuser through the inlet of the diffuser with a fully developed turbulent profile at a Reynolds's number of 20,000. The simulation was conducted with the Reynolds Averaged Navier-Stokes equations using four turbulence models, Spalart Allmaras, Shear Stress Transport (SST), K-ω and Realizable K-ε.

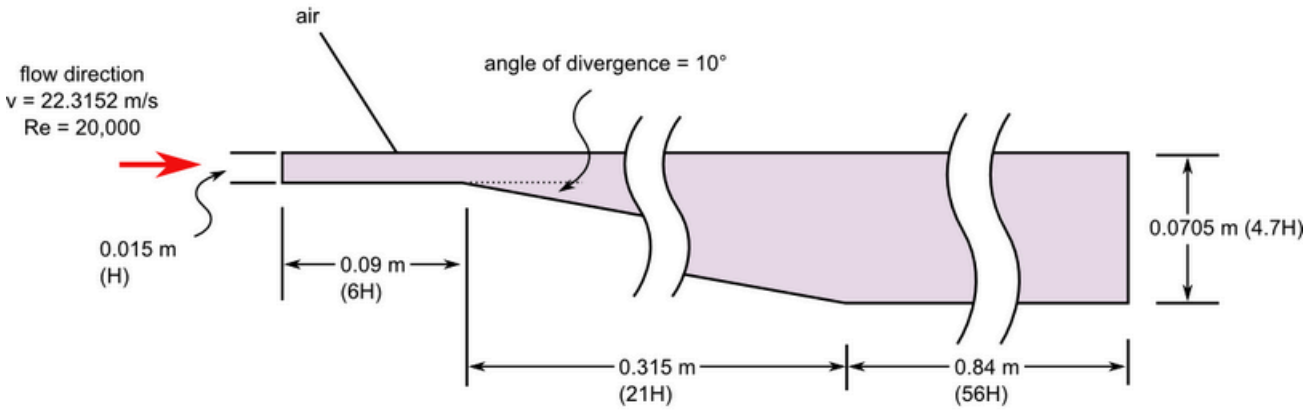


Figure 390: Critical Dimensions and Parameters for Simulating Turbulent Flow with Separation in an Asymmetric Diffuser

The simulation was performed as a two dimensional problem by constructing a volume mesh that contains a single layer of elements extruded in the cross stream direction (perpendicular to the flow plane) and by imposing symmetry boundary conditions on the extruded planes.



Figure 391: Mesh Details Near the Inlet and Divergent Section of Diffuser

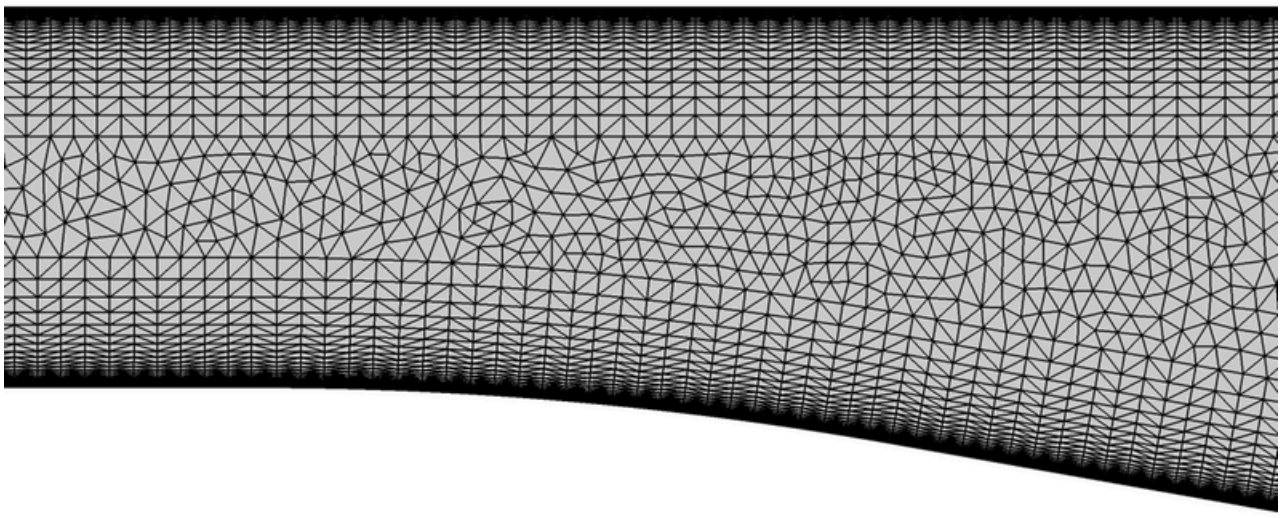


Figure 392: Mesh Details at the Beginning of the Divergence of the Lower Wall in the Diffuser

AcuSolve Results

The AcuSolve solution converged to a steady state and the results reflect the mean flow conditions. As the fully developed turbulent flow enters the divergent section, the peak velocity is maintained until the expansion of the cross-sectional height, forms an adverse pressure gradient. After the flow enters the divergent section, the velocity decreases significantly, due to the expansion of the cross-section height. This causes separation of the flow along the divergent wall and results in an area of recirculation.
The bulk of the flow above the divergent wall maintains its streamwise direction, while a portion of it reverses direction before reattaching further downstream of the divergent section. The following images show the steady state flow solution for flow within the diffuser.

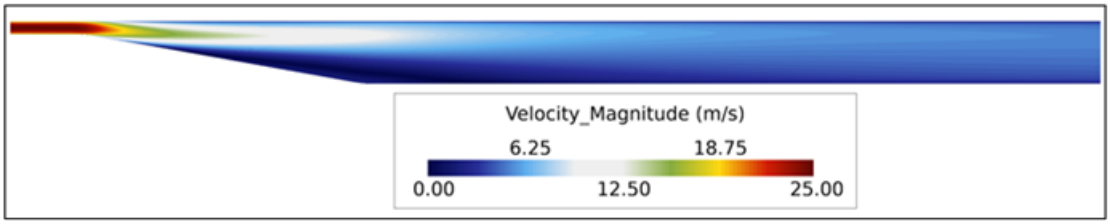


Figure 393: Velocity Contours Within the Diffuser

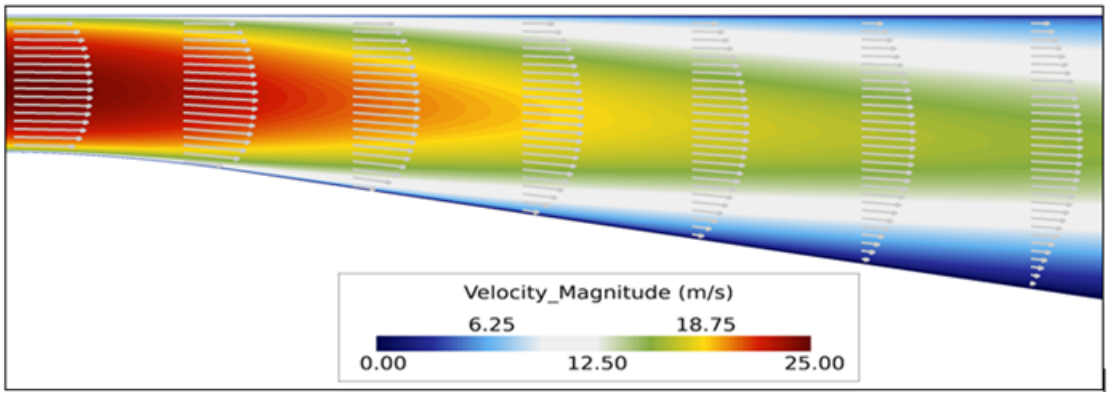


Figure 394: Close up View of Velocity Vectors and Contours of Velocity Magnitude in the Diffuser

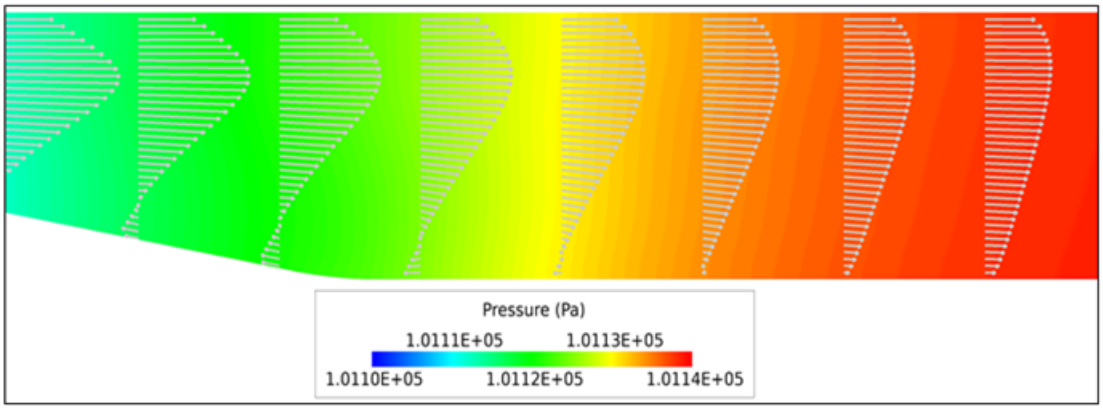


Figure 395: Close up View of Velocity Vectors and Contours of Pressure to Show Recirculation as it Approaches the Reattachment Point

Upstream of the diffuser section, the streamline velocity increases as the distance from the lower wall increases until it reaches the maximum velocity at the center of the channel. As the flow enters the divergent section of the channel, the streamwise velocity decreases near the bottom wall. The images below show the velocity profiles at three locations as measured from the midpoint of the curve where the bottom wall begins to diverge (X=0.0) for each of the tested turbulence models. The first location, where X/H = -5.944, is close to the inlet. The second location, where X/H = 13.468, is approximately 0.2 m downstream of the divergent section (~ 0.1 m from the fully expanded section). The third location, where X/H = 24.066, is approximately 0.16 m downstream of the point where the diffuser has reached the maximum height. In these plots the black circles represent the experimental measurements (Buice and Eaton 2000), the solid red lines for the prediction for the Spalart Allmaras model, solid blue lines for the prediction for the SST model, solid green lines for the prediction for the K-ω model and solid cyan lines for the K-ε model, representing the AcuSolve results. The non-dimensional height is represented by the fraction of the vertical height (Y) divided by the inlet height (H) and the velocity is normalized by the inlet velocity (Uref).

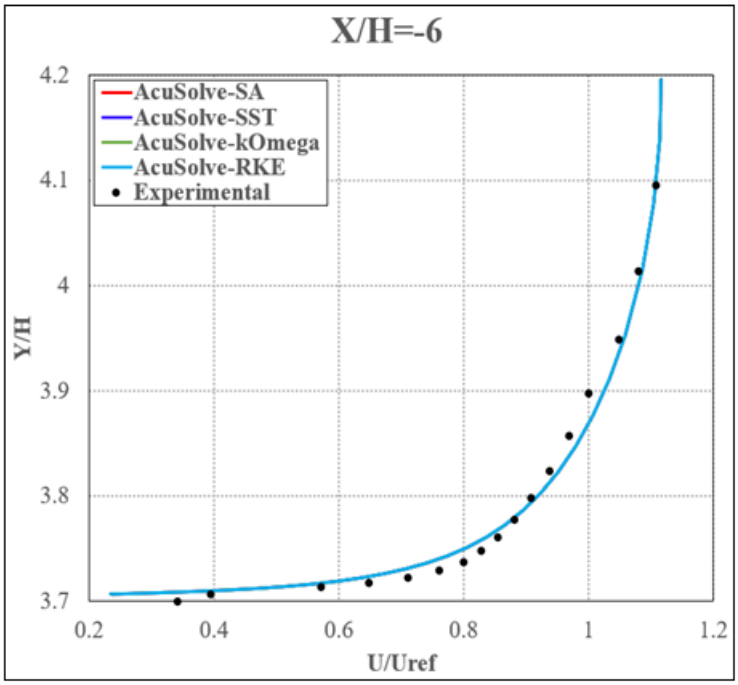


Figure 396: Non-Dimensional Streamwise Velocity Plotted Against Vertical Location Near the Inlet (X/H=-5.9442, Where the Reference Point is 6H Downstream of the Inlet)

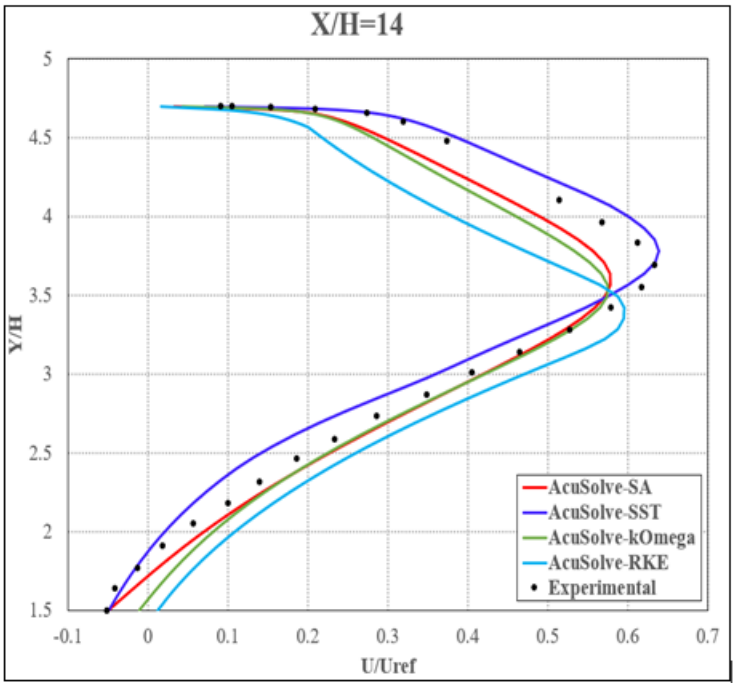


Figure 397: Non-Dimensional Streamwise Velocity Plotted Against Vertical Location Approximately 0.2 m Downstream of the Divergence (X/H = 13.468, Where the Reference Point is 6H Downstream of the Inlet)

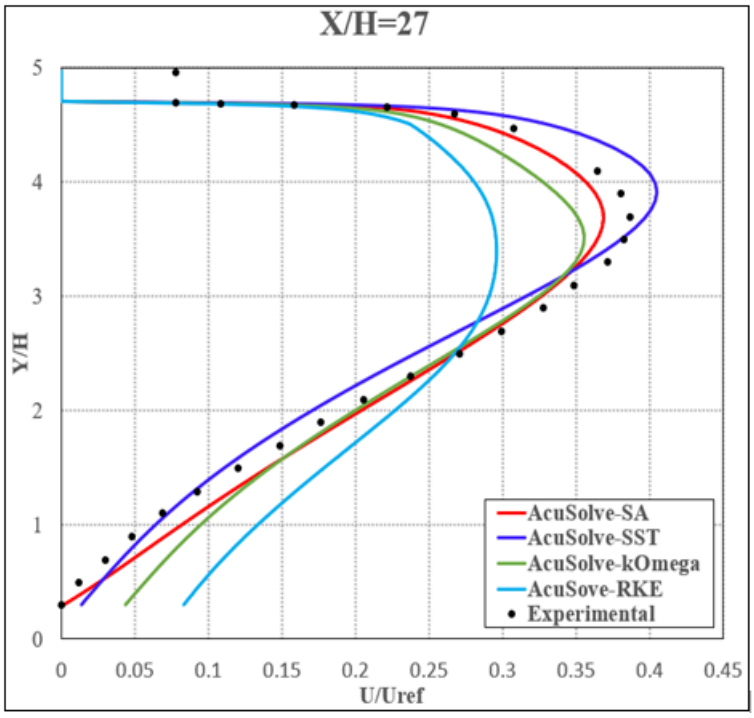


Figure 398: Non-Dimensional Streamwise Velocity Plotted Against Vertical Location Approximately 0.2 m Downstream of the Transition to the Fully Divergent Section (X/H = 27.066, Where the Reference Point is 6H Downstream of the Inlet)

The non-dimensional pressure coefficient (Cp), defined by the integrated inlet pressure and Uref predicted by AcuSolve along the bottom of the diffuser is compared to experimental results. The figure below shows Cp, along a constant vertical height, as a function of the streamwise distance from the inlet of the channel. The results demonstrate that AcuSolve is capable of accurately predicting the pressure within the diffuser within the expected range based on the type of turbulence model used. The performance of the three turbulence models were found to be consistent with previously published results for flow through the diffuser as published by Buice and Eaton (2000), with the SST model predicting the pressure distribution most accurately. Note that the inlet of the experimental duct was 6H longer than that modeled - AcuSolve values where X/H < -6 are reported as the inlet value.

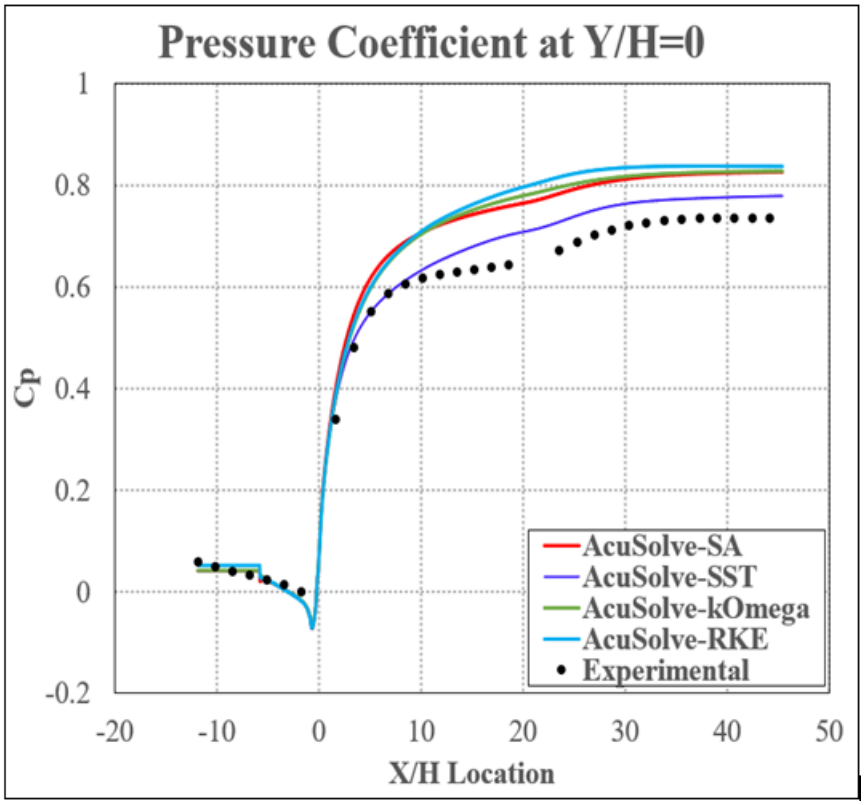


Figure 399: Non-Dimensional Pressure Coefficient (Cp) Plotted Against Relative Distance Along the Diffuser at a Constant Height Equal to the Bottom of the Inlet

Summary

In this application, a fully developed turbulent flow at a Reynolds number of 20,000 is studied. Due to the adverse pressure gradient, separation of flow occurs and causes recirculation in the divergent section of the diffuser. The results were found to be consistent with previously published computational studies and experimental data. The results of this validation demonstrate the ability of AcuSolve to accurately predict the separation point, the recirculation that occurs along the divergent wall, and the reattachment point in the straight section of the diffuser.

Simulation Settings for Turbulent Flow with Separation in an Asymmetric Diffuser

HyperWorks CFD database file: `<your working directory>\asymmetric_diffuser_turbulent\asymmetric_diffuser_turbulent.hm`

Global

- Problem Description
  - Analysis type - Steady State
  - Turbulence equation - Spalart Allmaras
- Auto Solution Strategy
  - Max time steps - `150`
  - Relaxation Factor - `0.2`
- Material Model
  - Air
    - Density - `1.225.0` kg/m3
    - Viscosity - `1.8325e-5` kg/m-sec

  Model
- Volume
  - Volume
    - Element Set
      1. Material model - Air
- Surfaces
  - Bottom
    - Simple Boundary Condition
      1. Type - Wall
  - Inlet
    - Simple Boundary Condition (disabled to allow for nodal boundary conditions to be set)
    - Advanced Options
      1. Nodal Boundary Conditions
         1. X-Velocity
            1. Type - Linear
            2. Precedence - `2`
            3. Curve fit variable - Y coordinate
            4. Curve fit values (included in database)
         2. Y-Velocity
            1. Type - Linear
            2. Precedence - `2`
            3. Curve fit variable - Y coordinate
            4. Curve fit values (included in database)
         3. Eddy Viscosity
            1. Type - Linear
            2. Precedence - `2`

3 Curve fit variable - Y coordinate
4 Curve fit values (included in database)

- Outlet
  - Simple Boundary Condition
    1 Type - Outflow - 101139.0 Pa
- Side 1
  - Simple Boundary Condition
    1 Type - Symmetry
- Side 2
  - Simple Boundary Condition
    1 Type - Symmetry
- Top
  - Simple Boundary Condition
    1 Type - Wall

References

C.U. Buice, and J.K., Eaton. "Experimental Investigation of Flow Through an Asymmetric Plane Diffuser". Journal of Fluids Engineering 122:433-435. June 2000.

S. Obi, K. Aoki and S. Masuda. "Experimental and Computational Study of Turbulent Separating Flow in an Asymmetric Plane Diffuser". Ninth Symposium on Turbulent Shear Flows. p. 305. Kyoto, Japan. August 16-19, 1993.

Turbulent Flow with Separation in an Axisymmetric Diffuser

In this application, AcuSolve is used to simulate fully developed turbulent flow through an axisymmetric diffuser with a divergent upper wall and a straight lower wall. AcuSolve results are compared with experimental results as described in Driver (1991) and on the NASA Langley Research Center Turbulence Modeling Resource webpage. The close agreement of AcuSolve results with experimental data and reference turbulence model performance validates the ability of AcuSolve to model cases with turbulent flow with separation due to an adverse pressure gradient within an axisymmetric geometry.

Problem Description

The problem consists of a fluid with material properties close to air flowing around a cylinder through an axisymmetric diffuser, as shown in the following image, which is not drawn to scale. The diffuser has a divergent section designed to generate an adverse pressure gradient. The inlet height between the cylinder and the upper section of the diffuser is 0.0355 m. The diffuser is constructed such that the section is axisymmetric around a cylinder with a diameter of 0.14 m. The inflow of the diffuser is set to produce a fully developed turbulent flow profile at a Reynolds number (Re) of 2,000,000. The upper section is modeled with a slip boundary condition, in order to match experimental conditions. The density of the fluid is 1.0 kg/m^3 and with a dynamic viscosity of 1.5 X 10-5 kg/m-s. The simulation was conducted with the Reynolds Averaged Navier-Stokes equations using four turbulence models, Spalart Allmaras, Shear Stress Transport (SST), K-ω and Realizable K-ε.

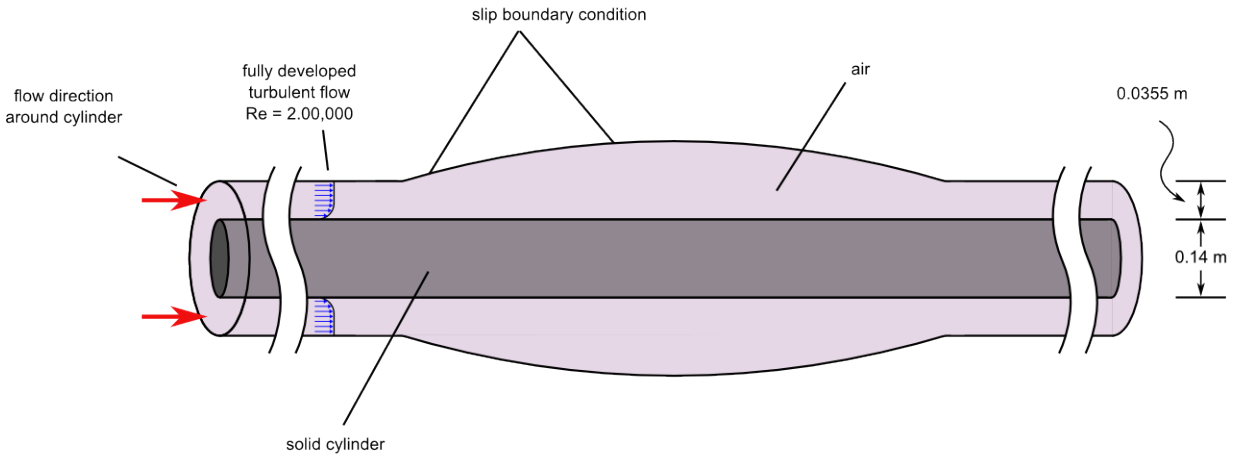


Figure 400: Critical Dimensions and Parameters for Simulating Turbulent Flow Through an Axisymmetric Diffuser

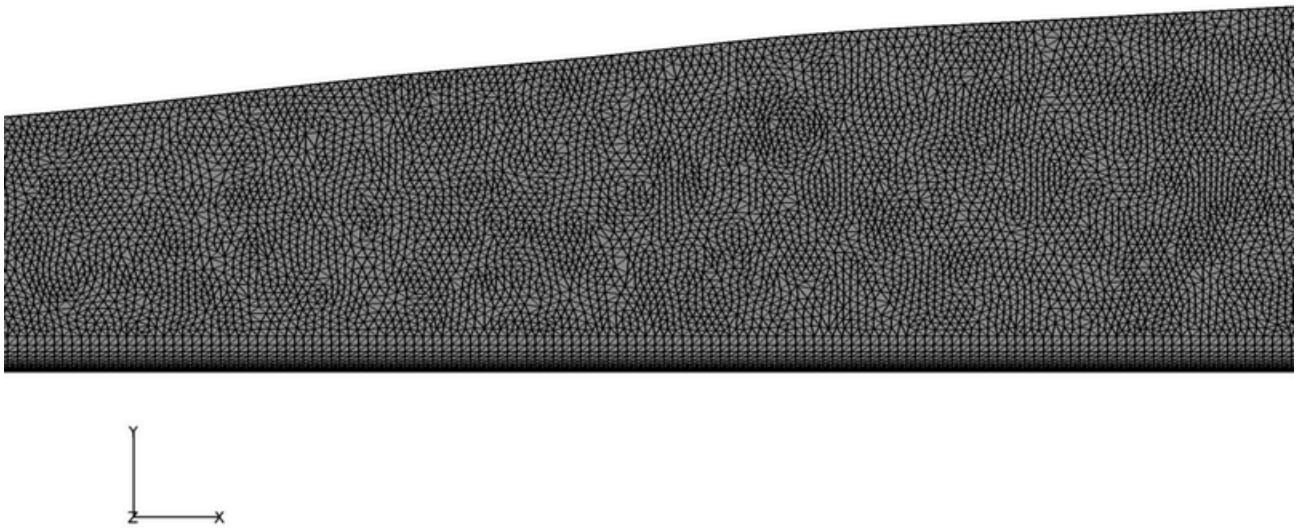


Figure 401: Mesh Detail Near the Divergence of the Walls in the Mesh used for Simulating Turbulent Flow Through an Axisymmetric Diffuser

The problem is simulated as axisymmetric by considering a 1 degree portion of the diffuser with the axisymmetric boundary condition applied on the cross-stream surfaces. The mesh elements were extruded in the axisymmetric direction to create a mesh with two elements spanning the simulated section.



Figure 402: Cross Section (Perpendicular to Flow) of Mesh used for Simulating Turbulent Flow Through an Axisymmetric Diffuser

AcuSolve Results

The AcuSolve solution converged to a steady state and the results reflect the mean flow conditions. As the fully developed turbulent flow enters the divergent section, the expansion of the cross-sectional height causes the streamwise velocity to decrease. This causes separation of the flow along the cylinder wall and results in an area of recirculation that eventually recovers downstream. After the flow enters the diffuser, the velocity decreases significantly from the inlet velocity, due to the rapid expansion of the cross section height in the divergent section. A separation bubble forms within the diffuser, with decreased flow velocity and increased pressure near the lower wall.

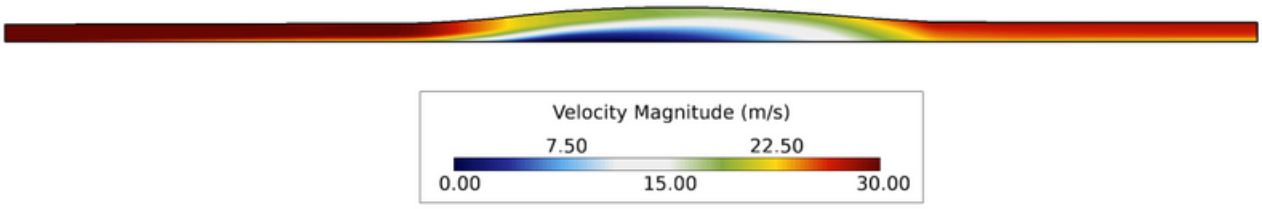


Figure 403: Velocity Contours Within the Diffuser

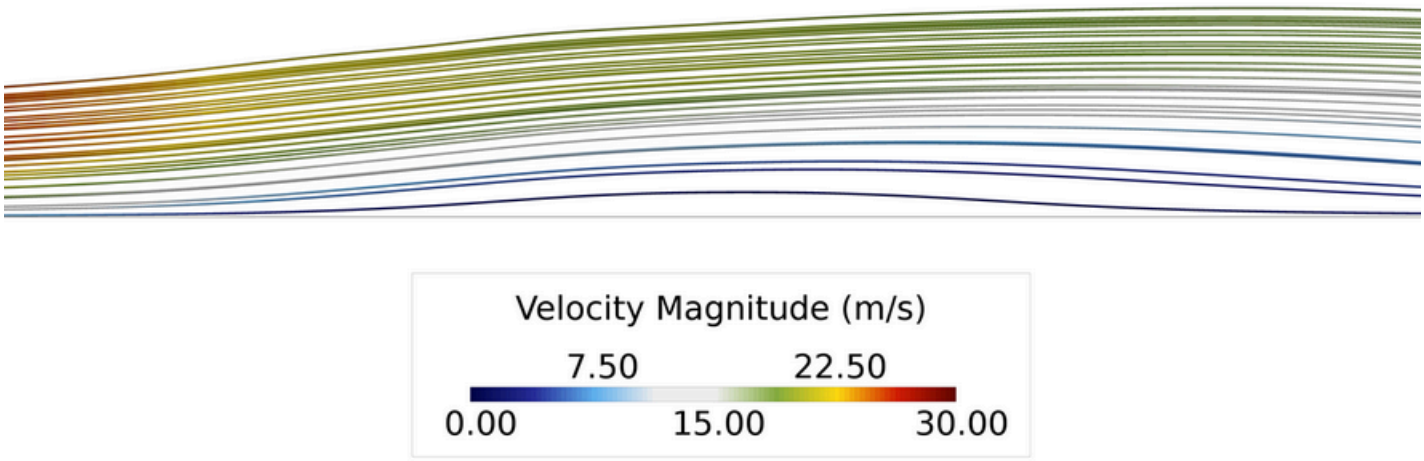


Figure 404:

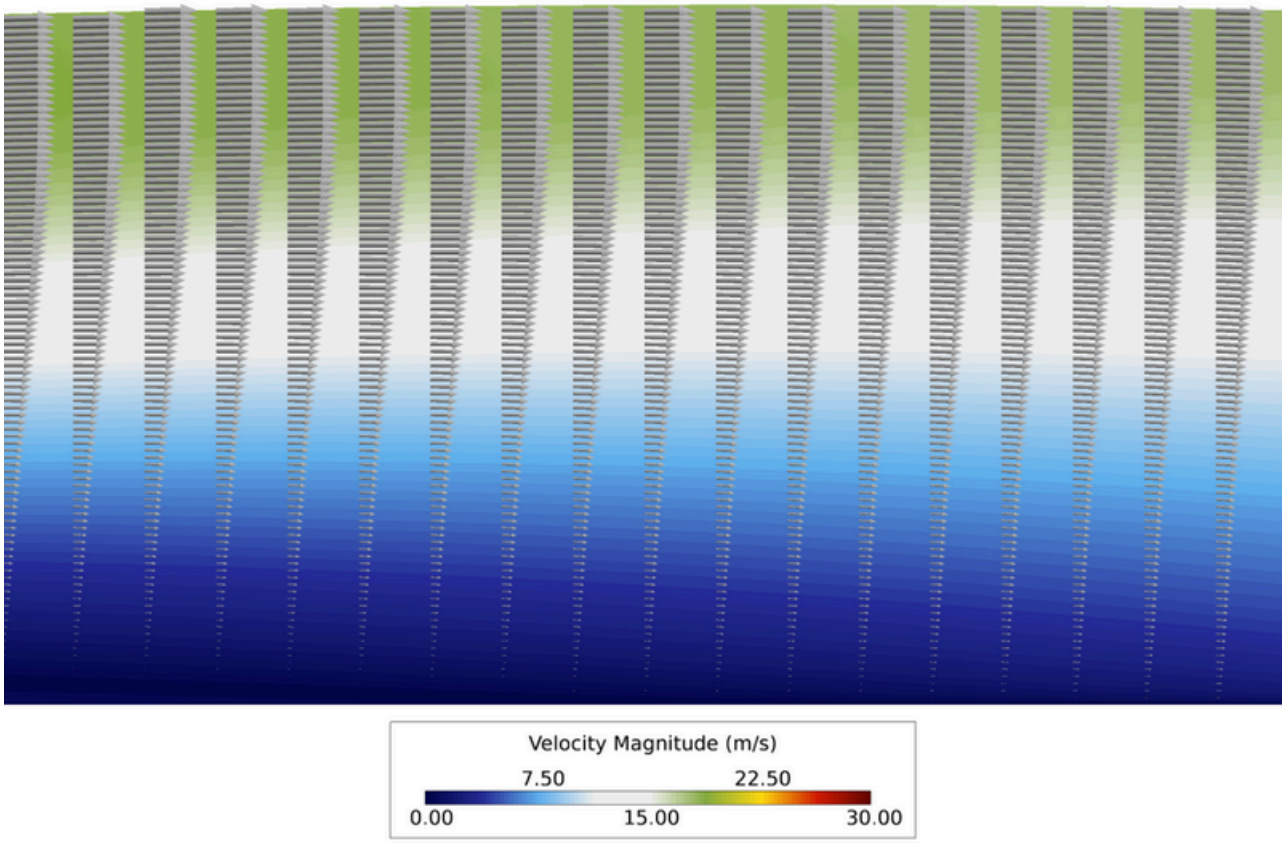


Figure 405: Close up View of Velocity Vectors and Contours in the Streamwise Plane Near the Reattachment Point

Upstream of the diffuser section, the streamwise velocity increases as the distance from the cylinder wall increases, with no influence from the top wall of the diffuser. As the flow enters into the divergent section, the streamwise velocity decreases near the cylinder wall and changes direction in the

recirculation region. Within the recirculation region, the reduced speed of the streamwise flow causes the wall shear stress to decrease and eventually change direction for a short distance along the cylinder surface. The images below show the coefficient of pressure (Cp) and coefficient of skin friction (Cf) along the cylinder wall in the diffuser compared against experimental results. The non-dimensional values are defined by the integrated inlet pressure and the magnitude of the inlet velocity. In the images black circles represent the experimental measurements (Driver 1991), solid red lines represent the prediction for the SA model, solid blue lines represent the prediction for the SST model, solid green lines represent the prediction for the K-ω model and solid cyan lines for the K-ε model, representing the AcuSolve results. There are minor differences in the prediction of the pressure coefficient within the diffuser between the three turbulence models. The SA model predicts a slightly higher value of pressure as the flow separates from the cylinder wall compared to both SST and K- ω. The shearing on the cylinder wall shows similar behavior, with the SA model predicting a slightly longer recirculation region and with the K- ω model predicting the separation further upstream. It was found that all three turbulence models predict the separation point further upstream than what is shown in the experiment. This is shown to be consistent with previous studies for each of the turbulence models used (NASA 2014).

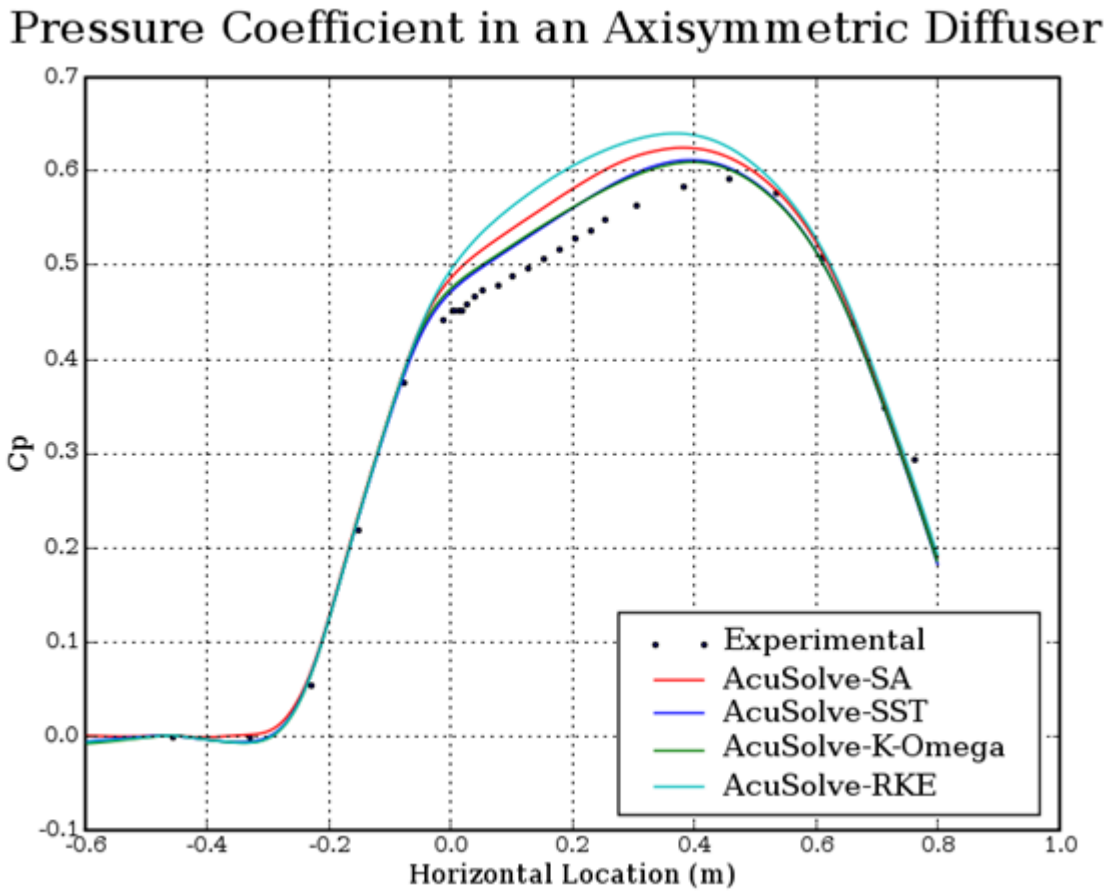


Figure 406: Coefficient of Pressure Along the Cylinder Wall Within the Diffuser Section (Horizontal Location = ~ 2.7m at the Midpoint of the Expanded Region of the Diffuser)

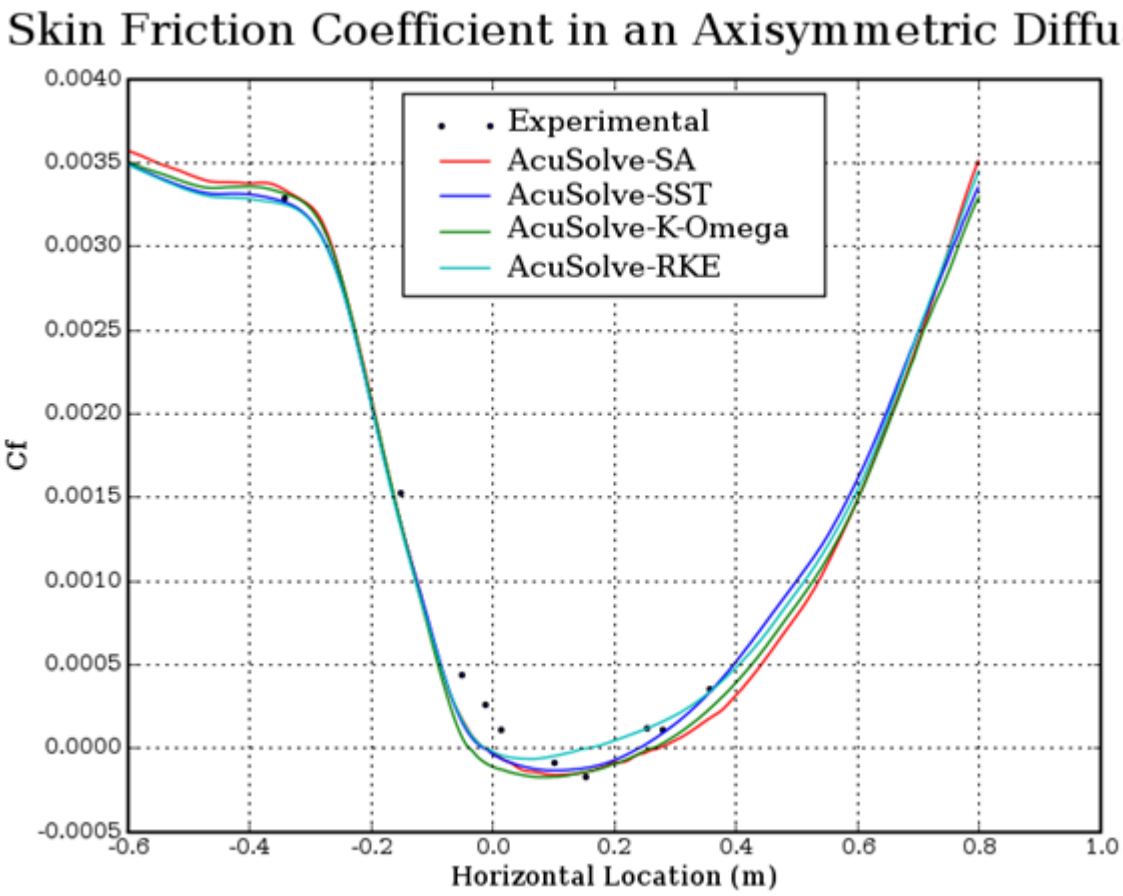


Figure 407: Skin Friction Coefficient Along the Cylinder Wall Within the Diffuser Section (Horizontal Location = 0 at the Point Where Flow Separation is Expected to Begin)

Summary

In this application, a fully developed turbulent flow at a Reynolds number of 2,000,000 is studied and compared against experimental data. The AcuSolve results compare well with the experimental data for pressure coefficient and skin friction coefficient. The recirculation region is slightly over predicted by the turbulence models studied, but the results still show a reasonable trend compared to experimental results. The performance of the three turbulence models was found to be consistent with previously published results for flow within an axisymmetric diffuser (NASA 2014). The results of this validation demonstrate the ability of AcuSolve to accurately predict flow recirculation with axisymmetric boundary conditions.

Simulation Settings for Turbulent Flow with Separation in an Axisymmetric Diffuser

AcuConsole database file: `<your working directory>\axisymmetric_diffuser_turbulent\axisymmetric_diffuser_turbulent.acs`

Global

- Problem Description
  - Analysis type - Steady State

    - Turbulence equation - Spalart Allmaras
- Auto Solution Strategy
    - Max time steps - `150`
    - Relaxation Factor - `0.4`
- Material Model
    - Fluid
        - Density - `1.0` kg/m3
        - Viscosity - `1.5e-5` kg/m-sec

  Model
- Volume
    - Fluid
        - Element Set
            1. Material model - Fluid
- Surfaces
    - Axisymmetric_maxZ
        - Simple Boundary Condition - (disabled to allow for periodic conditions to be set)
    - Axisymmetric_minZ
        - Simple Boundary Condition - (disabled to allow for periodic conditions to be set)
    - Inlet
        - Simple Boundary Condition
            1. Type - Inflow
            2. Inflow type - Velocity
            3. X velocity - `30.0` m/sec
            4. Turbulence input type - Direct
            5. Eddy viscosity - `1.5e-5` m2/sec
    - Outlet
        - Simple Boundary Condition
            1. Type - Outflow
    - Slip_maxY
        - Simple Boundary Condition
            1. Type - Slip
    - Wall_minY
        - Simple Boundary Condition
            1. Type - Wall
- Periodics
    - Axisymmetric
        - Periodic Boundary Condition

1 Type - Axisymmetric
2 Rotation Axis
    1 Point 1
        1 x-coordinate - `1.4` m
        2 y-coordinate - `0.0` m
        3 z-coordinate - `0.0` m
    2 Point 2
        1 x-coordinate - `-1.5` m
        2 y-coordinate - `0.0` m
        3 z-coordinate - `0.0` m

References

D. M. Driver. "Reynolds Shear Stress Measurements in a Separated Boundary Layer Flow". AIAA Paper 91-1787 from the AIAA 22nd Fluid Dynamics, Plasma Dynamics, and Lasers Conference. Honolulu, HI. June 1991.

NASA Langley Research Center Turbulence Modeling Resource webpage, http://turbmodels.larc.nasa.gov/driver_val.html. Accessed December 2014.

Turbulent Flow Over a Backward-Facing Step

In this application, AcuSolve is used to simulate fully developed turbulent flow over a backward-facing step. AcuSolve results are compared with experimental results as described in Driver (1985) and on the NASA Langley Research Center Turbulence Modeling Resource web page. The close agreement of AcuSolve results with experimental data and reference turbulence model performance validates the ability of AcuSolve to model cases with turbulent flow that forms a shear layer, recirculates and then reattaches downstream of the divergent step.

Problem Description

The problem consists of a fluid with material properties close to air flowing through a channel containing a sharp expansion, as shown in the following image, which is not drawn to scale. The step causes the flow to recirculate before reattaching downstream of the step. The inlet height of the channel is 8.0 m and expands as a step function to 9.0 m at a distance 20.0 m downstream of the inlet. This expanded section of the channel extends 50 m downstream of the step. The inflow of the channel is defined as fully developed at a Reynolds number (Re) of 36,000, based on the step height to match the experimental conditions. The density of the flow medium is 1.1837 kg/m^3 and the dynamic viscosity is 1.457 X 10^{-3} kg/m-s. The simulation was conducted with the Reynolds Averaged Navier-Stokes equations using four turbulence models, Spalart Allmaras, Shear Stress Transport (SST), K-ω and K-ε.

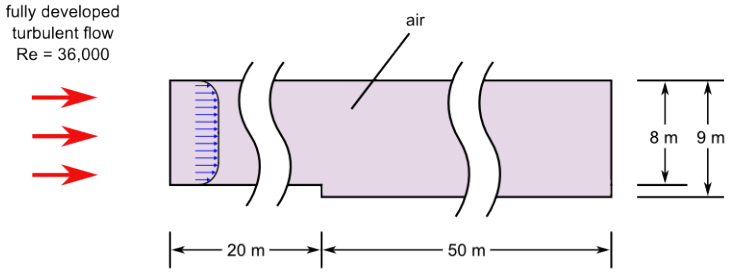


Figure 408: Critical Dimensions and Parameters for Simulating Turbulent Flow Through a Channel with a Backward-Facing Step

The simulation was performed as a two-dimensional problem by constructing a volume mesh that contains a single layer of elements extruded in the cross-stream direction, normal to the flow plane and by imposing symmetry boundary conditions on the extruded planes. The upper and lower walls are specified as no-slip, the inlet velocity and eddy viscosity are specified to match the conditions in the experiment (Driver 1985) at a distance of 20 m upstream of the step.

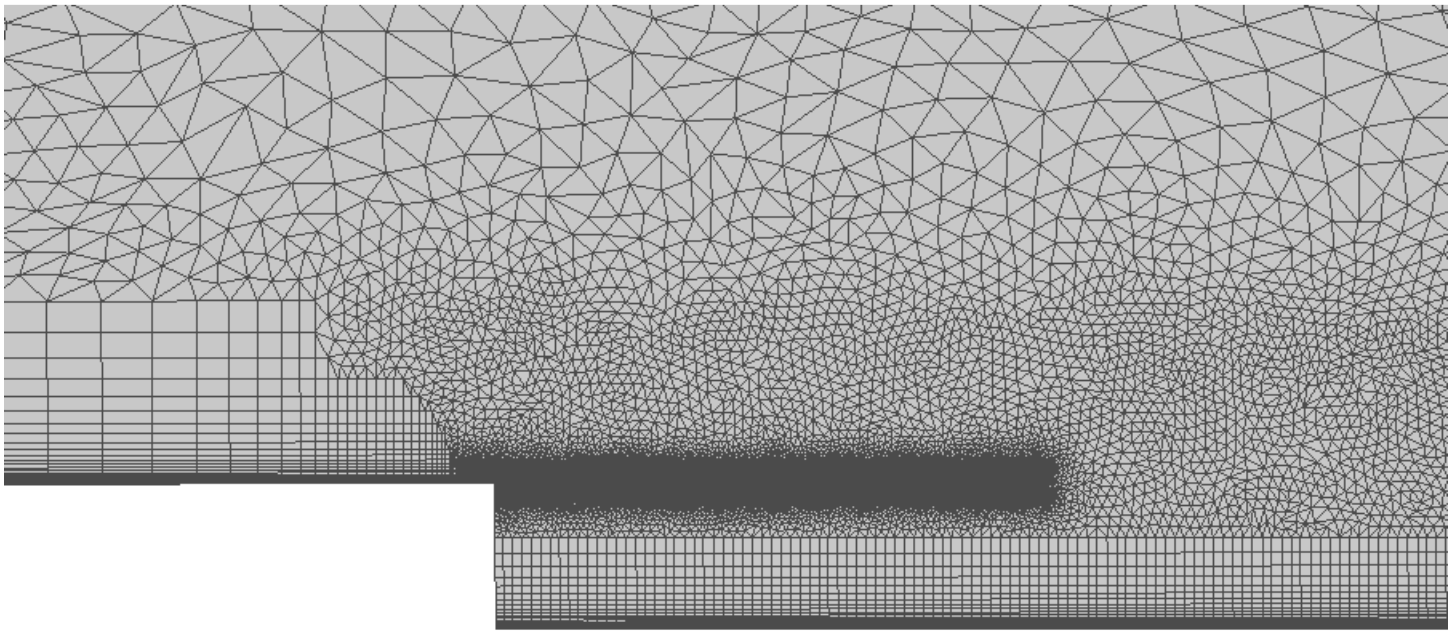


Figure 409: Detail of Mesh Near the Backward-Facing Step

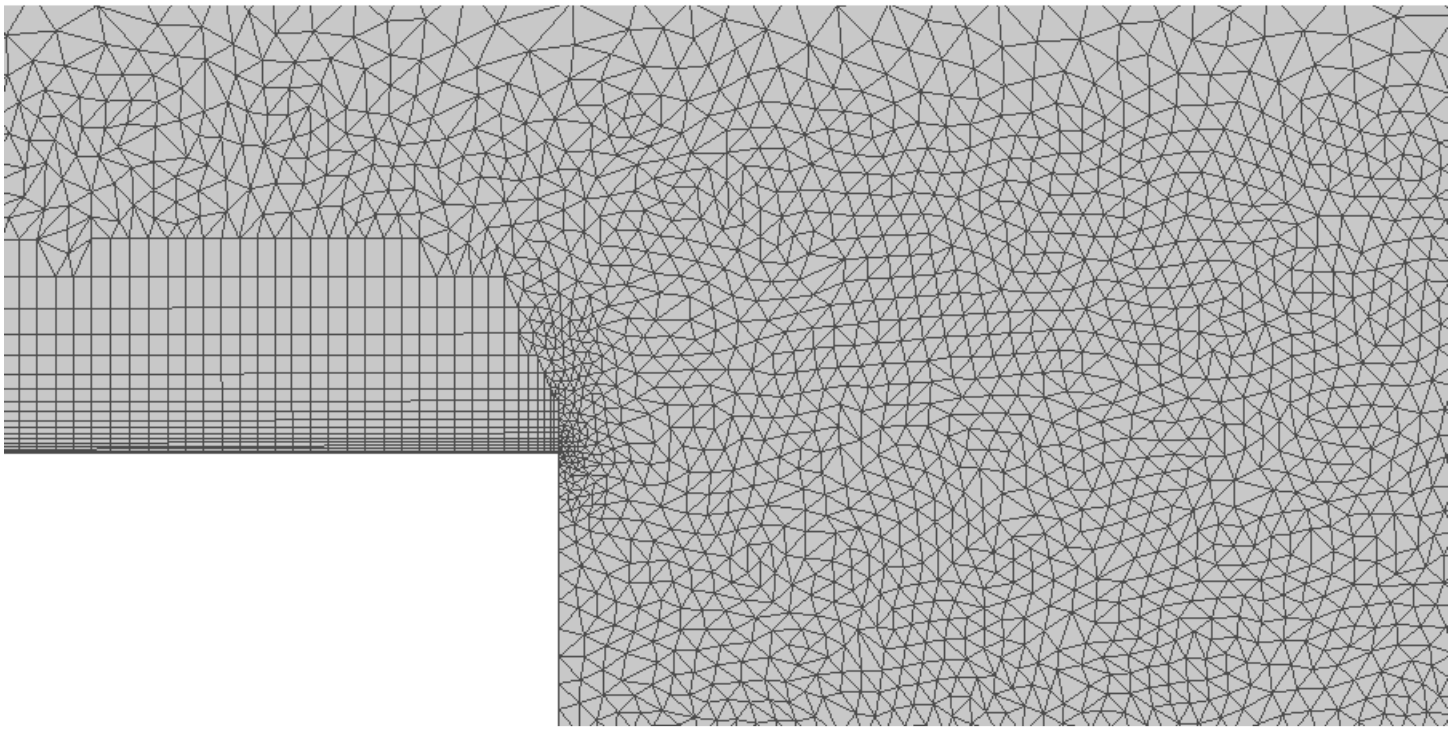


Figure 410: Finer Detail of Mesh Near the Backward-Facing Step

AcuSolve Results

The AcuSolve solution converged to a steady state and the results reflect the mean flow conditions. As the fully developed turbulent flow enters the divergent section, the expansion of the cross-sectional height causes a shear layer to develop above the lower wall. The expansion causes two recirculation zones; one immediately near the step wall and one that extends further downstream near the lower wall. The recirculation region eventually recovers downstream and the flow reattaches. The following images show the flow solution within the channel, demonstrating the recirculation region and reattachment point.

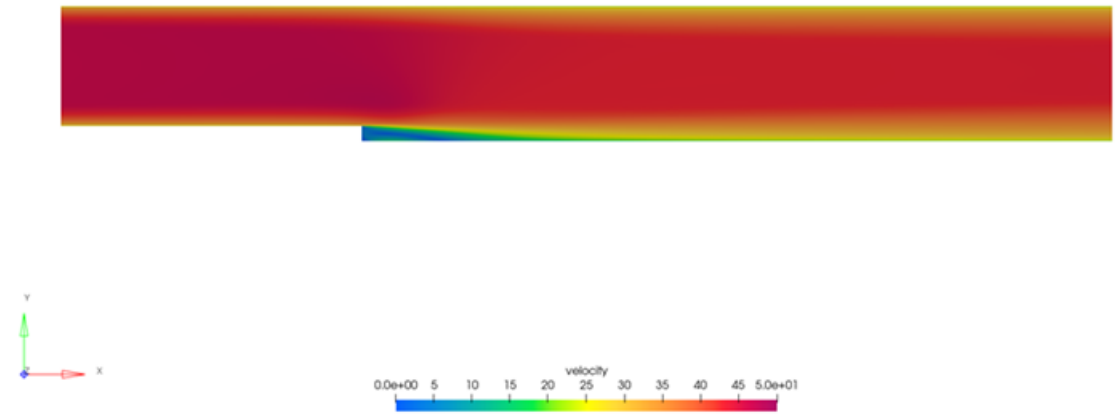


Figure 411: Velocity Contours Showing Low Velocity Near the Step Wall

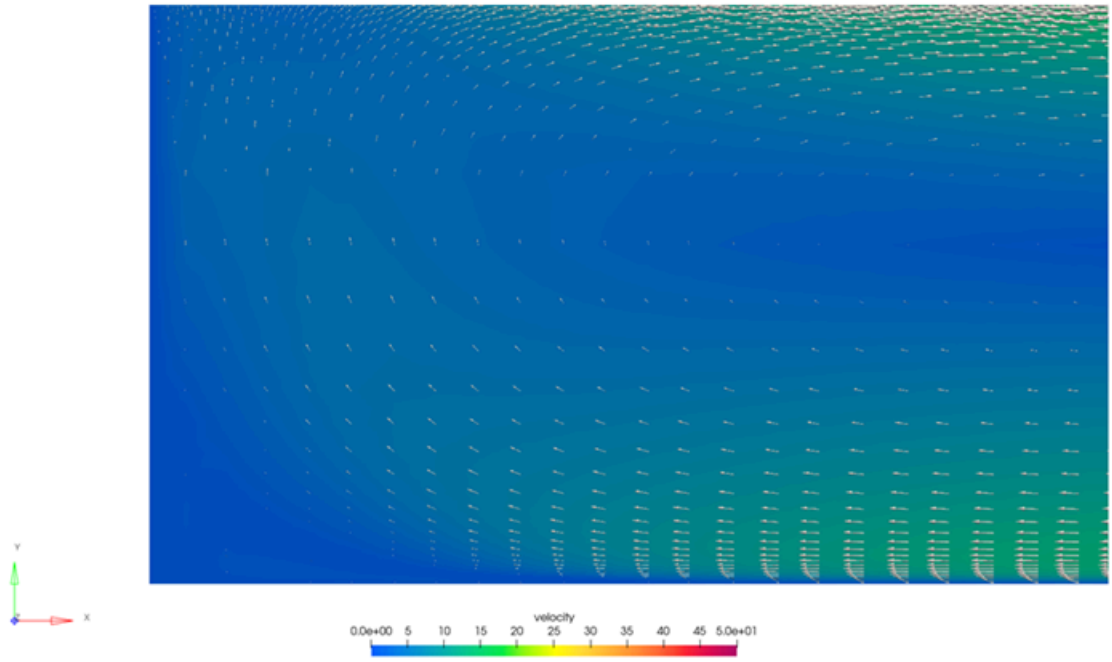


Figure 412: Close-Up View of Velocity Vectors and Contours in the Cross-Stream Plane Directly After the Step

Upstream of the expansion section, the streamwise velocity increases as the distance from the lower wall increases until it reaches the centerline of the channel and then begins decreasing until it reaches zero at the top wall. As the flow passes the step, it expands into the region directly downstream of the step wall, separating from the wall and recirculating until it recovers further downstream. The image below shows the coefficient of pressure along the lower wall of the step compared against experimental results. The non-dimensional values are defined by the integrated inlet pressure and the magnitude of the inlet velocity. The image shows black circles representing the experimental measurements (Driver 1985), a solid red line for the SA model, a solid blue line for the SST model, a solid green line for the K-ω model and a solid cyan line for the K-ε model, representing the AcuSolve results. The resulting pressure coefficient within the channel demonstrates minor differences between the three turbulence models. The SA model predicts a slightly larger recirculation region and does not reach the peak pressure in the wake of the step, compared to the SST model.

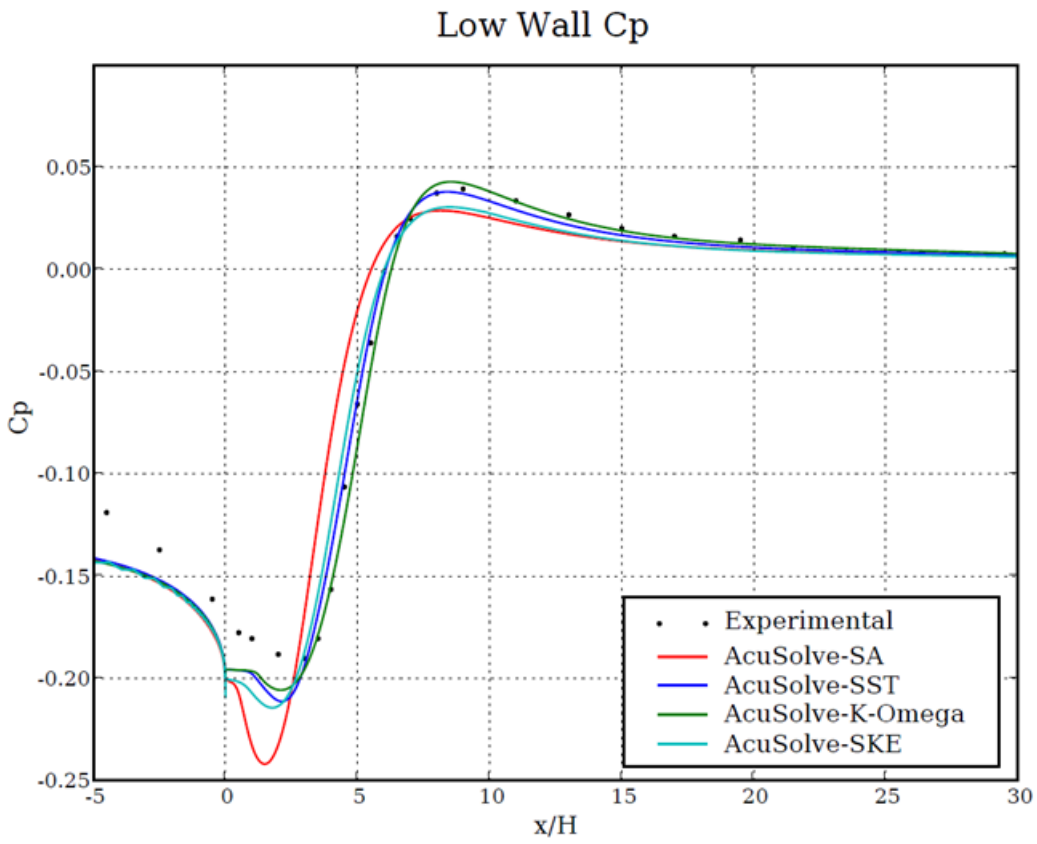


Figure 413: Coefficient of Pressure Plotted Against Location Along the Lower Wall Before and After the Step

Summary

In this application, a fully developed turbulent flow at a Reynolds number of 36,000 is studied and compared against experimental data. The AcuSolve results compare well with the experimental data for pressure coefficient. The performance of the Spalart Allmaras turbulence model was found to be consistent with previously published results for flow over a backward facing step (NASA 2015). The K-ω model appears to perform the best out of the three, predicting the reattachment and pressure distribution most accurately. AcuSolve demonstrates the ability to predict the shear layer in this type of application, the recirculation that occurs downstream of the step, as well as the reattachment point within the channel.

Simulation Settings for Turbulent Flow over a Backward-Facing Step

HyperWorks CFD database file: `<your working directory>\backstep_turbulent\backstep_turbulent.hm`

Global

- Problem Description
  - Analysis type - Steady State
  - Turbulence equation - Shear Stress Transport
- Auto Solution Strategy

    - Max time steps - `100`
    - Relaxation Factor - `0.5`
- Material Model
    - Air
        - Density - `1.183` kg/m3
        - Viscosity - `1.4575e-3` kg/m-sec

  Model
- Volume
    - Fluid
        - Element Set
            1. Material model - Air
- Surfaces
    - +Z
        - Simple Boundary Condition
            1. Type - Slip
    - -Z
        - Simple Boundary Condition
            1. Type - Slip
    - Inlet
        - Simple Boundary Condition - (disabled to allow for nodal boundary conditions to be set)
        - Advanced Options
            1. Nodal Boundary Conditions
                1. X-Velocity
                    1. Type - Linear
                    2. Precedence - Always
                    3. Curve fit variable - Y reference coordinate
                    4. Curve fit values - (included in database)
                2. Y-Velocity
                    1. Type - Linear
                    2. Precedence - Always
                    3. Curve fit variable - Y reference coordinate
                    4. Curve fit values - (included in database)
                3. Z-Velocity
                    1. Type - Zero
                4. Kinetic Energy
                    1. Type - Linear
                    2. Precedence - Always

3 Curve fit variable - Y reference coordinate
4 Curve fit values - (included in database)
5 Eddy Frequency
1 Type - Linear
2 Precedence - Always
3 Curve fit variable - Y reference coordinate
4 Curve fit values - (included in database)

- Outlet
  - Simple Boundary Condition
    1 Type - Outflow
- Wall - Lower - Downstream
  - Simple Boundary Condition
    1 Type - Wall
    2 Turbulence wall type - Low Reynolds Number
- Wall - Lower - Upstream
  - Simple Boundary Condition
    1 Type - Wall
    2 Turbulence wall type - Low Reynolds Number
- Wall - Step
  - Simple Boundary Condition
    1 Type - Wall
    2 Turbulence wall type - Wall Function
- Wall - Upper
  - Simple Boundary Condition
    1 Type - Wall
    2 Turbulence wall type - Low Reynolds Number

References

D. M. Driver and H. L. Seegmiller. "Features of Reattaching Turbulent Shear Layer in Divergent Channel Flow". AIAA Journal, 23(2): 163-171. Feb 1985.

NASA Langley Research Center Turbulence Modeling Resource webpage. http://turbmodels.larc.nasa.gov/backstep_val.html. Accessed June 2021.

Turbulent Flow Past a Convex Curve in a Channel

In this application, AcuSolve is used to simulate fully developed turbulent flow through a channel containing a convex curve in the lower wall. AcuSolve results are compared with experimental results as described in Smits (1979) and on the NASA Langley Research Center Turbulence Modeling Resource webpage. The close agreement of AcuSolve results with experimental data and reference turbulence model performance validates the ability of AcuSolve to model cases with turbulent flow moving past a convex curved wall.

Problem Description

The problem consists of a fluid with material properties close to air flowing through a channel containing a 30° swept wall, with a lower convex wall. The inlet channel height and remaining duct height is 0.127 m. The bulk velocity (v) normal to the inlet is 31.9 m/s and an integrated outflow pressure is specified to allow the flow to pass through the channel. The flow develops into fully turbulent flow at a Reynolds's number (Re) of 2,100,000. The density of the flow medium is 1.225 kg/m3 and the dynamic viscosity is 1.8608 X 10-5 kg/m-s. The simulation is conducted with the Reynolds Averaged Navier-Stokes equations using the Spalart Allmaras, Shear Stress Transport (SST), K-ω and Realizable K-ε turbulence models. The flow conditions are compared against experimental data and the current state-of-the-art performance for coefficient of pressure and coefficient of friction.

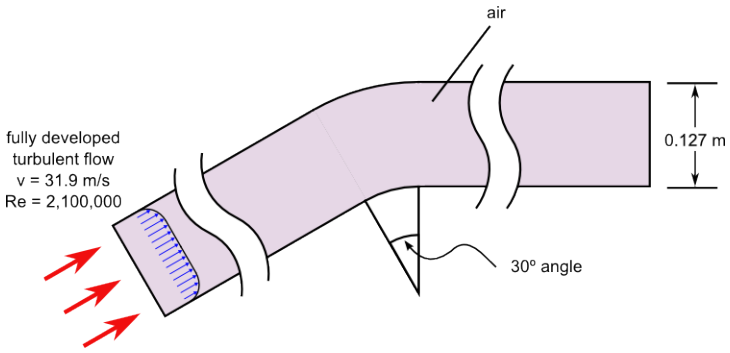


Figure 414: Critical Dimensions and Parameters for Simulating Turbulent Flow Through a Convex Channel

The simulation was performed as a two dimensional problem by restricting flow in the out-of-plane direction through the use of a mesh that is one element thick. The upper and lower walls are specified as no-slip, the inlet velocity and eddy viscosity are specified normal to the inlet face to match the experimental Reynolds Number.

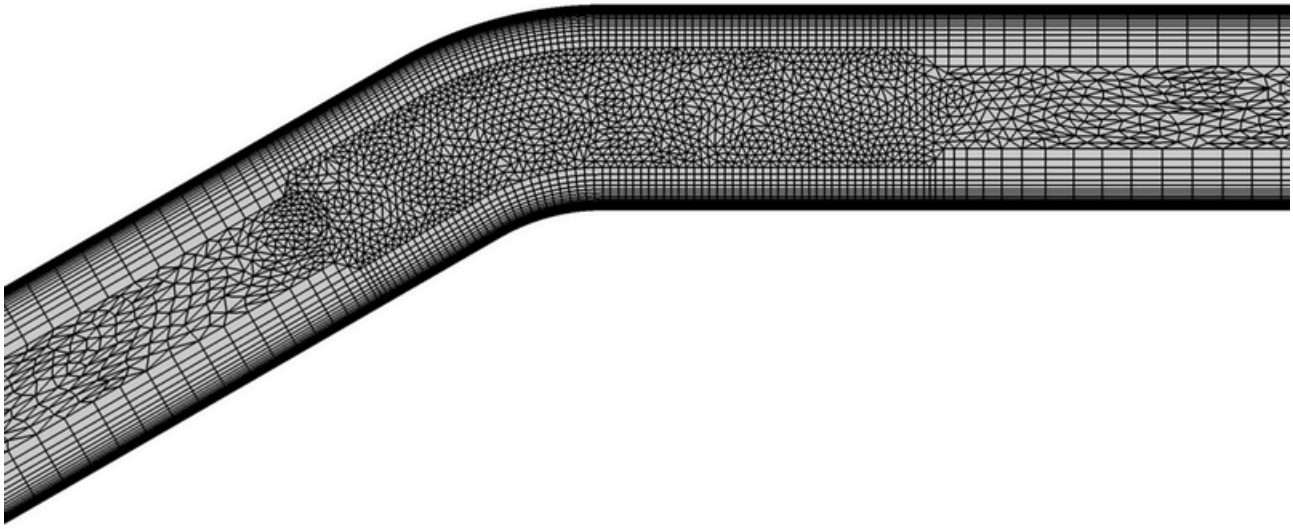


Figure 415: Detail of the Mesh used for Simulating Turbulent Flow Through a Convex Channel

AcuSolve Results

The AcuSolve solution converged to a steady state and the results reflect the mean flow conditions within the channel. As the fluid enters the channel it develops into fully turbulent flow exhibiting a steep parabolic velocity profile across the width of the channel. The flow begins to accelerate near the lower wall and decelerate near the top wall as it approaches the 30° bend. The results show that the upper (concave) wall destabilizes the boundary layer, increasing the eddy viscosity and forcing the flow velocity to decrease. The following figures show the flow conditions within the channel.

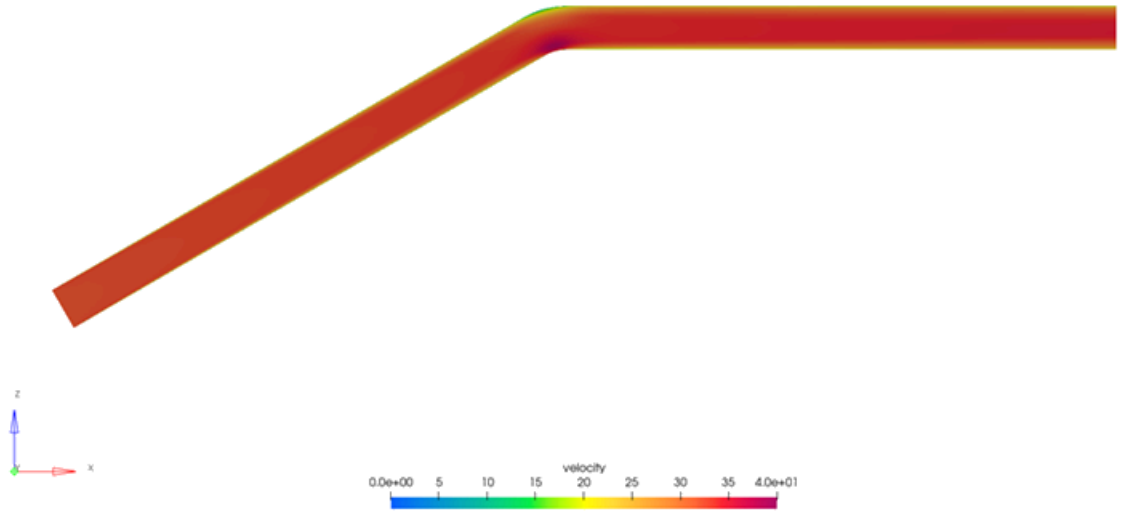


Figure 416: Velocity Contours in the Streamwise Plane

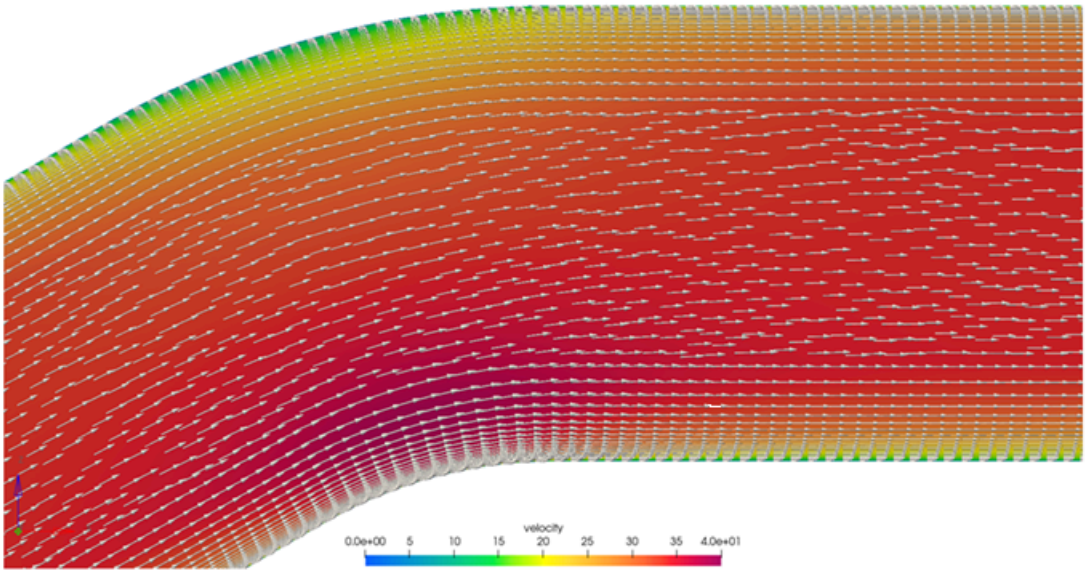


Figure 417: Close up View of Velocity Vectors and Velocity Contours at the 30° Bend

Upstream of the curved section of the channel, the flow normal to the channel opening increases as the distance from the lower wall increases until it reaches the centerline of the channel and then begins decreasing until it reaches zero at the top wall. As the flow approaches the curved section, it begins to accelerate, requiring that the flow velocity near the upper wall decrease to conserve momentum. The relatively low angle of curvature in the channel does not cause the accelerated fluid to recirculate. The images below show the coefficient of pressure (Cp) and coefficient of skin friction (Cf) along the lower wall of the channel. The images show black circles representing the experimental measurements (Smiths 1979), solid red lines for the SA model, solid blue lines for the SST model, solid green lines for the K-ω model and a solid cyan line for the K-ε model, representing the AcuSolve results. The coefficient of pressure within the channel is predicted nearly identically compared to the experiment for each of the turbulence models. It appears that the SST and K-ε models capture the low velocity region with the best accuracy, demonstrating that the flow velocity decreases significantly, but does not recirculate within the channel. This is shown in the friction coefficient plot, where the coefficient of friction, and subsequently the wall shear stress, does not decrease below zero.

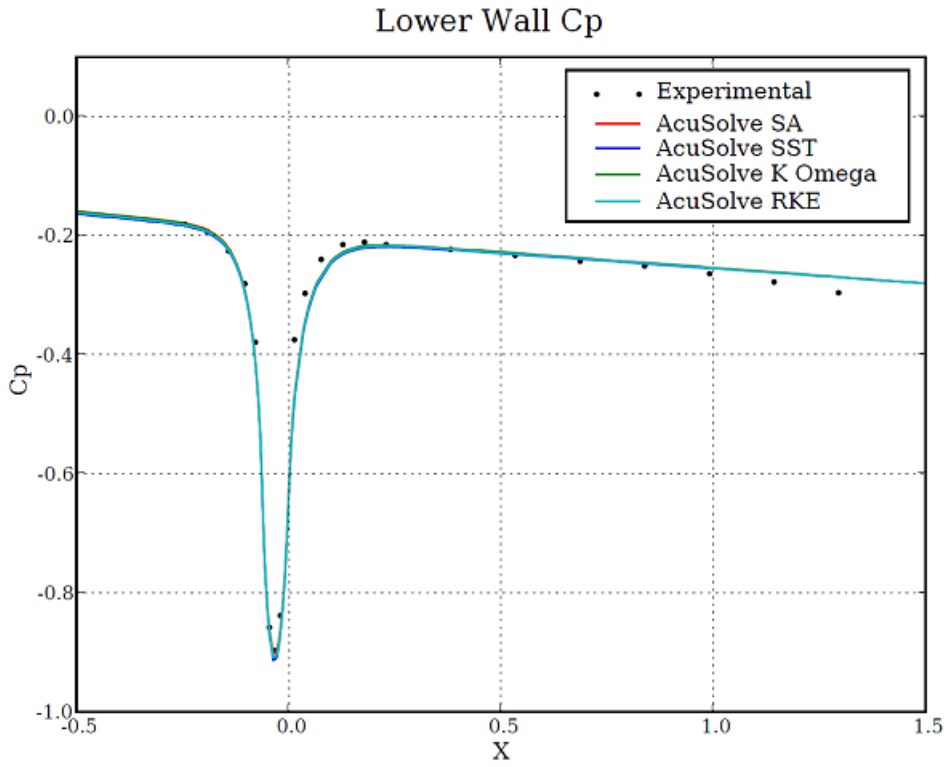


Figure 418: Coefficient of Pressure Plotted Against Relative Distance Along the Lower Wall from the Curve

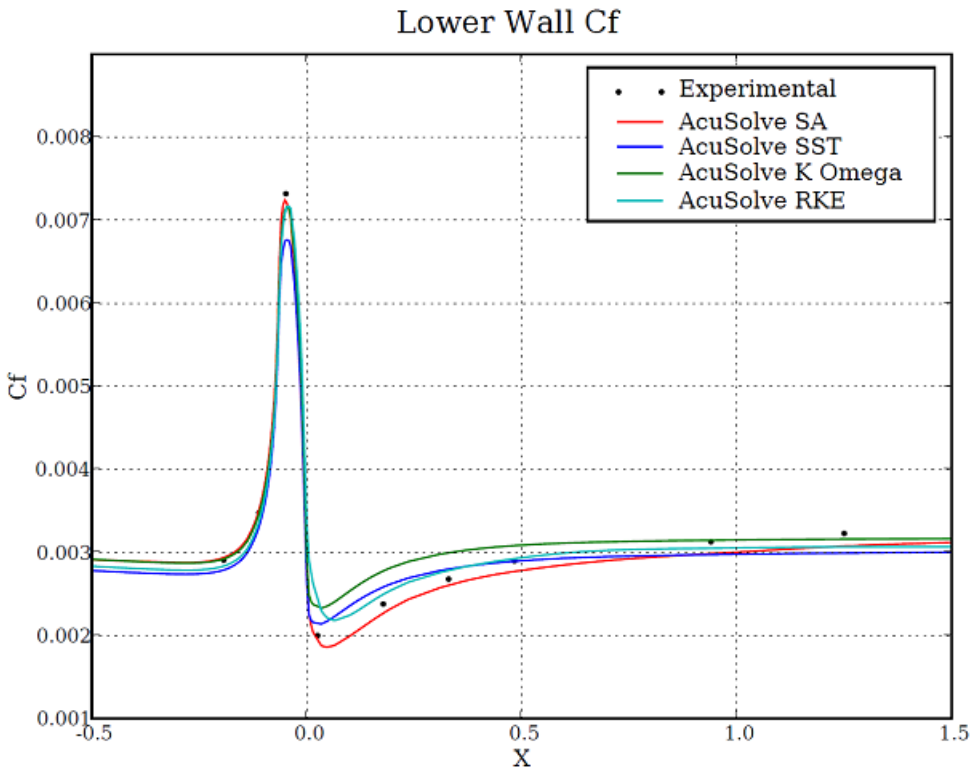


Figure 419: Skin Friction Coefficient Plotted Against Relative Distance Along the Lower Wall from the Curve

Summary

In this application, a turbulent flow through a curved channel at a Reynolds number of 2,100,000 is simulated and compared against experimental data. The AcuSolve results compare well with the experimental data for pressure coefficient and skin friction coefficient within the channel. The performance of the Spalart Allmaras turbulence model was found to be consistent with previously published results for flow through a convex-curved channel (NASA 2015) and the SST turbulence model appears to predict the shear stress on the lower wall most accurately. AcuSolve demonstrates the ability to predict the complex boundary layers resulting from the curvature of the channel and accurately predicts the propagation of the flow further downstream.

Simulation Settings for Turbulent Flow past a Convex Curve in a Channel

HyperWorks CFD database file: `<your working directory>\convex_curvature_turbulent \convex_curvature_turbulent.hm`

Global

- Problem Description
  - Analysis type - Steady State
  - Turbulence equation - Spalart Allmaras
- Auto Solution Strategy
  - Max time steps - `100`
  - Convergence tolerance - `0.0001`

    - Relaxation factor - `0.4`
- Material Model
    - Fluid
        - Density - `1.225` kg/m3
        - Viscosity - `1.8603e-5` kg/m-sec

  Model
- Volumes
    - Fluid - elbow
        - Element Set
            1. Material model - Fluid
    - Fluid - inlet
        - Element Set
            1. Material model - Fluid
    - Fluid - outlet
        - Element Set
            1. Material model - Fluid
- Surfaces
    - -Y
        - Simple Boundary Condition
            1. Type - Slip
    - +Y
        - 1. Type - Slip
    - Inlet
        - Simple Boundary Condition
            1. Type - Inflow
            2. Inflow type - Velocity
            3. Inflow velocity type - Normal
            4. Normal velocity - `31.9` m/sec
            5. Turbulence input type - Direct
            6. Eddy viscosity - `1.3671e-7` m2/sec
- Internal
    - Simple Boundary Condition - (disabled)
- Lower Wall
    - Simple Boundary Condition
        - Type - Wall
        - Turbulence wall type - Low Reynolds Number
- Outlet

    - Simple Boundary Condition
        - Type - Outflow
- Upper Wall
    - Simple Boundary Condition
        - Type - Wall
        - Turbulence wall type - Low Reynolds Number

References

A. J. Smits, S. T. B. Young, and P. Bradshaw. "The Effect of Short Regions of High Surface Curvature on Turbulent Boundary Layers". Journal of Fluid Mechanics. 94(2):209-242. 1979

NASA Langley Research Center Turbulence Modeling Resource webpage. http://turbmodels.larc.nasa.gov/smitscurve_val.html. Accessed May 2021.

Turbulent Flow Past a Wall-Mounted Hump

In this application, AcuSolve is used to simulate fully developed turbulent flow past a smooth hump on the lower wall of a flow domain. AcuSolve results are compared with experimental results as described in Seifert and Pack (2002) and on the NASA Langley Research Center Turbulence Modeling Resource web page. The close agreement of AcuSolve results with experimental data and reference turbulence model performance validates the ability of AcuSolve to model cases with turbulent flow moving past a wall protrusion resulting in flow separation and recovery.

Problem Description

The problem consists of a fluid with material properties close to air flowing through a flow domain containing a well-defined smooth hump with a slit opening at approximately 65 percent of the hump chord. The inlet of the domain is defined with an inflow velocity in the streamwise direction that develops into fully turbulent flow at a Reynolds number (Re) of 936,000, based on the hump chord length of 1.0 m. The density of the flow medium is 1.0 kg/m^3 and the dynamic viscosity is 1.0684 X 10^{-6} kg/m-s. The simulation is conducted with the Reynolds Averaged Navier-Stokes equations using the Spalart Allmaras turbulence model, shear stress transport (SST) model, the K-ω model and Realizable K-ε model to evaluate the performance of the turbulence models. The flow predictions from AcuSolve are compared against experimental data and previously published turbulence model performance for pressure and friction coefficients within the domain.

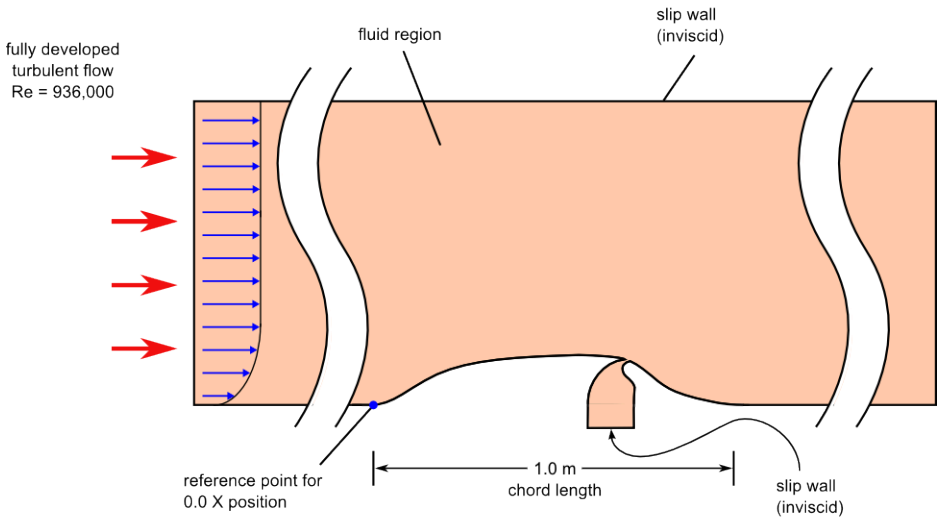


Figure 420: Critical Dimensions and Parameters for Simulating Turbulent Flow Through a Domain with a Wall-Mounted Hump

The upper walls of the domain are specified as slip (inviscid) and the lower walls are specified as no-slip. The inlet velocity and appropriate turbulence parameters are specified in the streamwise direction to match the desired Reynolds Number of 936,000. The outflow pressure is set to zero, and the lower wall on cavity below the hump is set to slip. The problem is simulated as two dimensional with a single layer of elements extruded in the cross stream direction and by defining the side walls as slip.

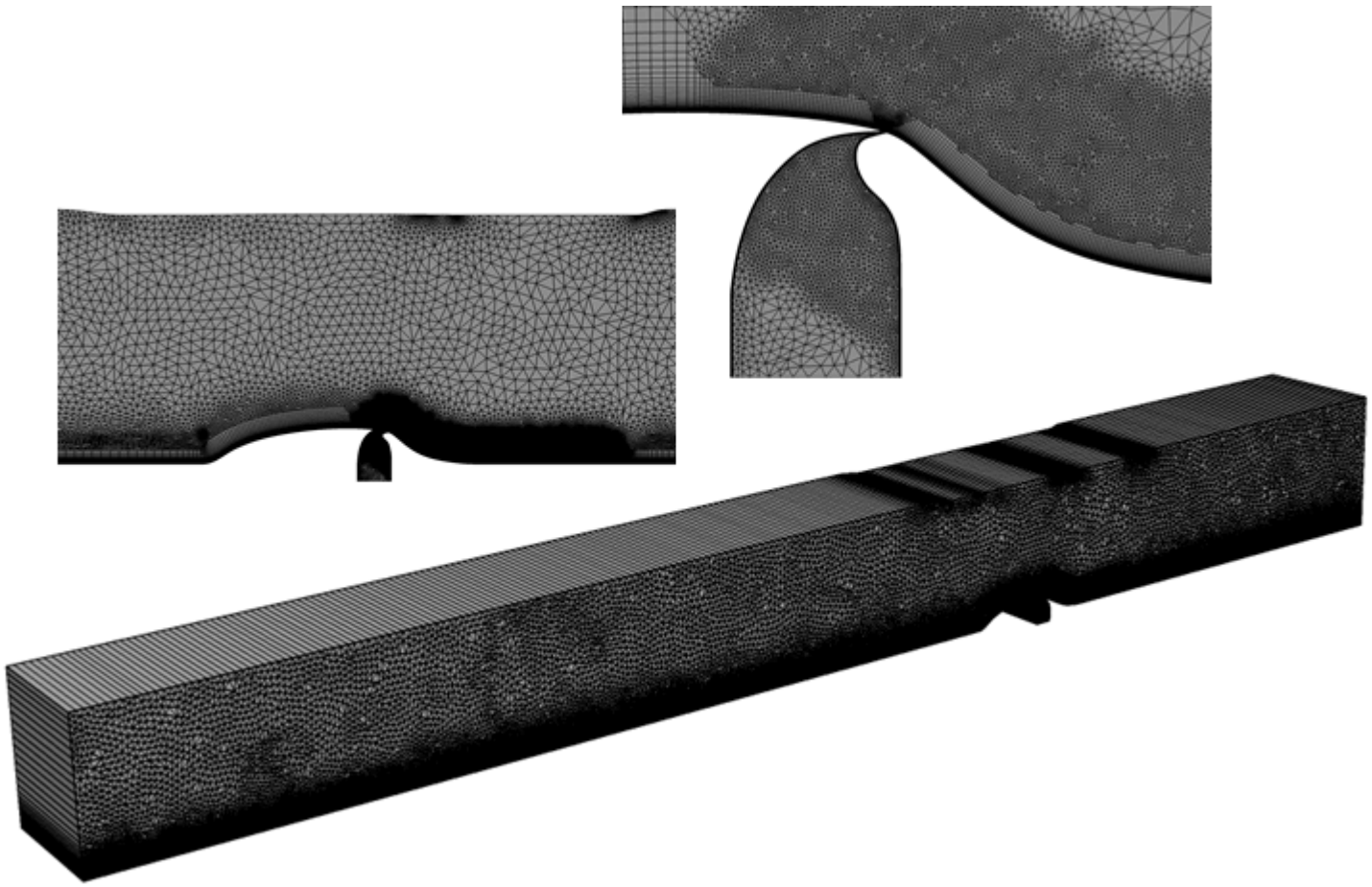


Figure 421: Three Views of the Mesh Used for Simulating Turbulent Flow over a Wall-Mounted Hump (Full Mesh is Shown on the Bottom, with Increased Resolution in Clockwise Views)

AcuSolve Results

The AcuSolve solution converged to a steady state and the results reflect the mean flow conditions within the domain. The images below show contours of velocity within the domain as well as the recirculation region directly downstream of the hump. As the flow enters the domain with a bulk velocity, it begins to develop a turbulent boundary layer near the lower wall prior to reaching the hump. As the flow approaches the hump section, the velocity near the lower wall decreases, but does not recirculate in front of the hump. It then accelerates over the top of the hump and separates immediately after reaching the cavity opening. The recirculation region propagates downstream, before the flow recovers and reattaches to the lower wall.

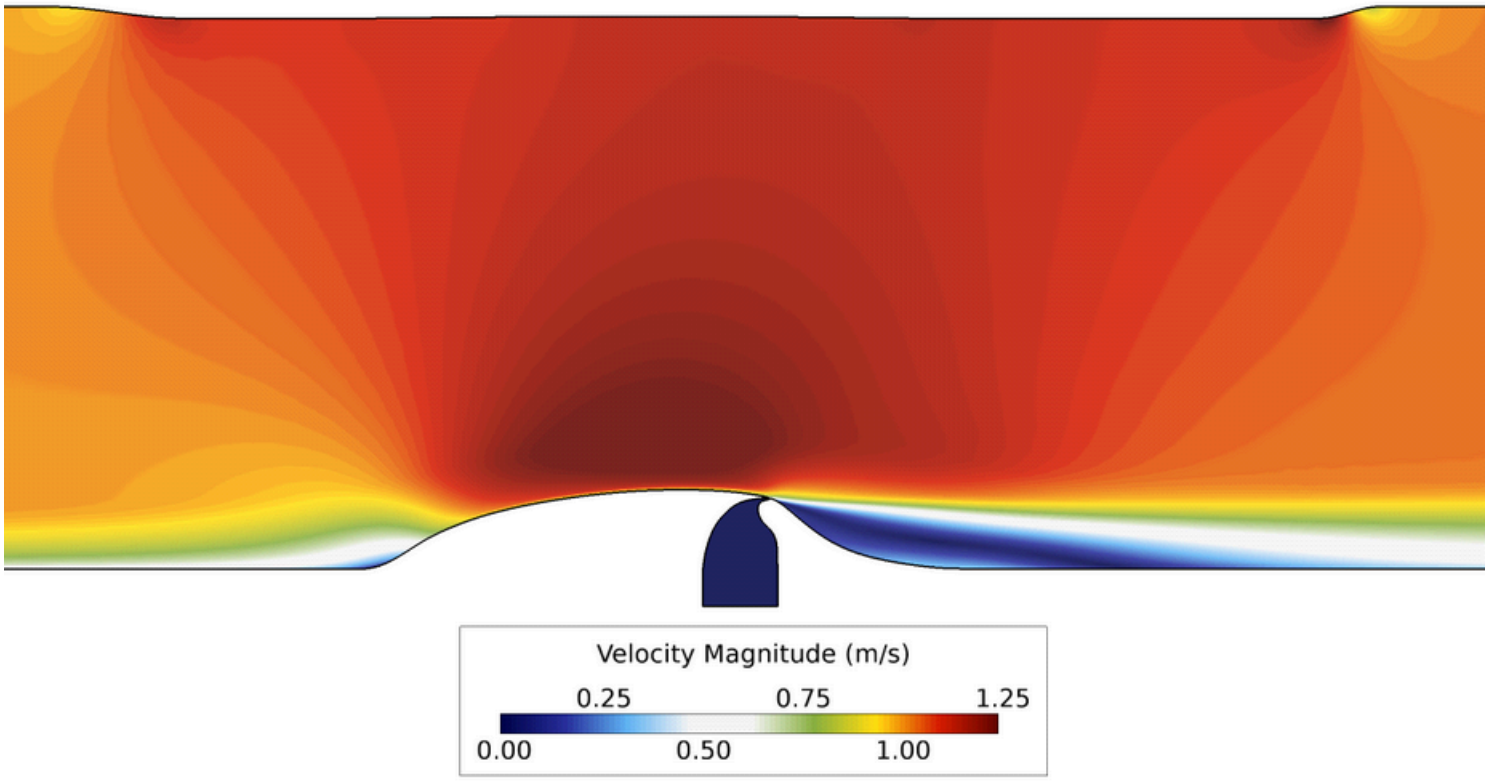


Figure 422: Velocity Contours on the Boundaries of the Domain, Showing Velocity Magnitude

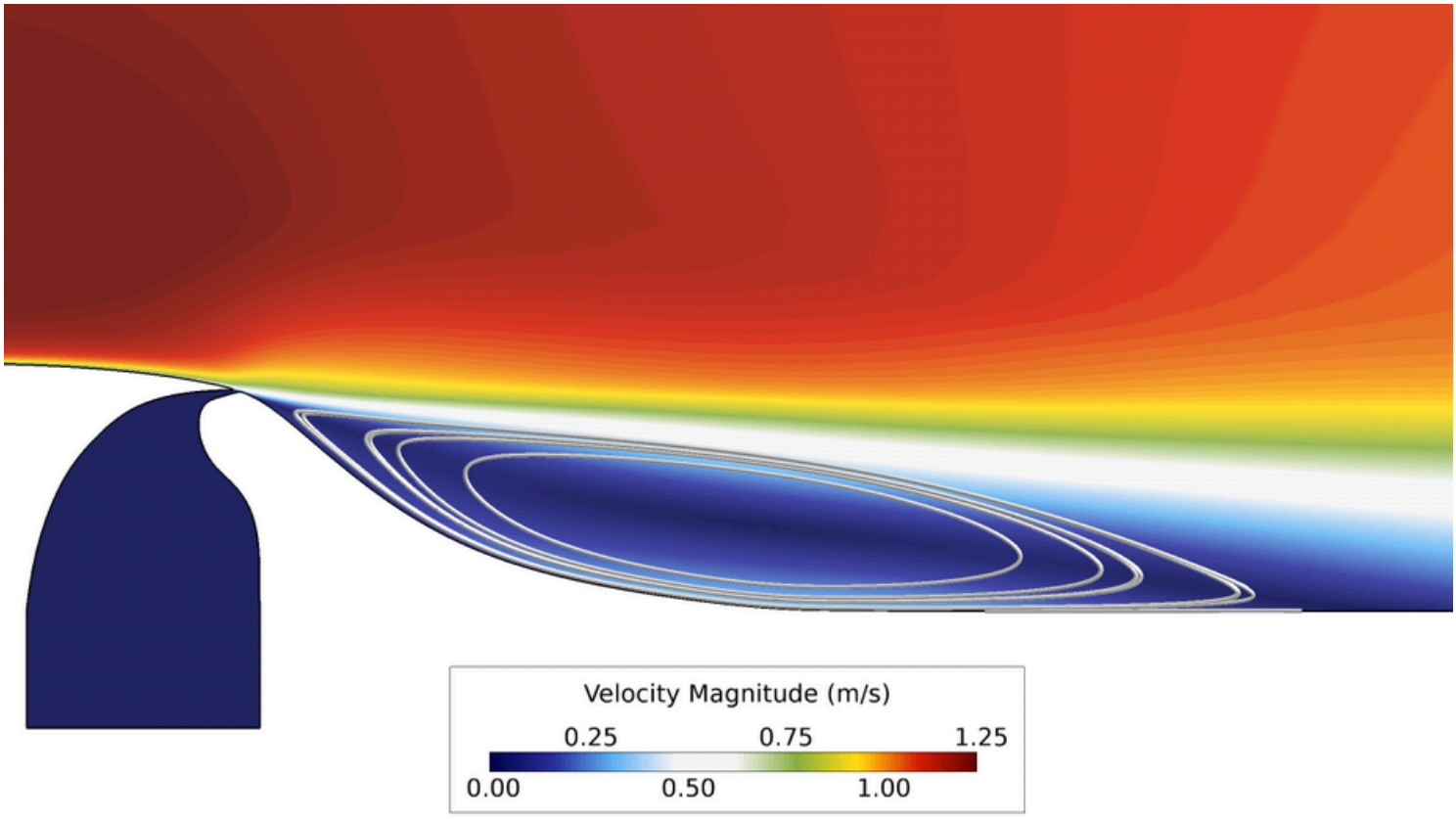


Figure 423: Close up View of Velocity Contours Showing the Recirculation Region with Streamlines (White Lines) Representing the Region of Backflow

The images below show the coefficient of pressure and coefficient of skin friction along the lower wall of the flow domain plotted with experimental results. The non-dimensional values are defined by the integrated inlet pressure and the magnitude of the inlet velocity. The images show black circles representing the experimental measurements (Seifert and Pack 2002), solid red lines for the SA model, solid blue lines for the SST model, solid green lines for the K-ω model and solid cyan lines for the K-ε model, representing the AcuSolve results. The resulting pressure coefficient within the domain demonstrates that there are minor differences between the three turbulence models. All three models are shown to perform accurately in predicting the increase in surface pressure on the front of the hump, but tend to over predict the skin friction in the wake of the hump, leading to an over prediction of the reattachment location. The SA model predicts a slightly larger recirculation region, and does not meet the expected recovery pressure compared to SST, K- ω and K-ε. This performance was found to be consistent with comparisons to other one equation models (NASA 2015).

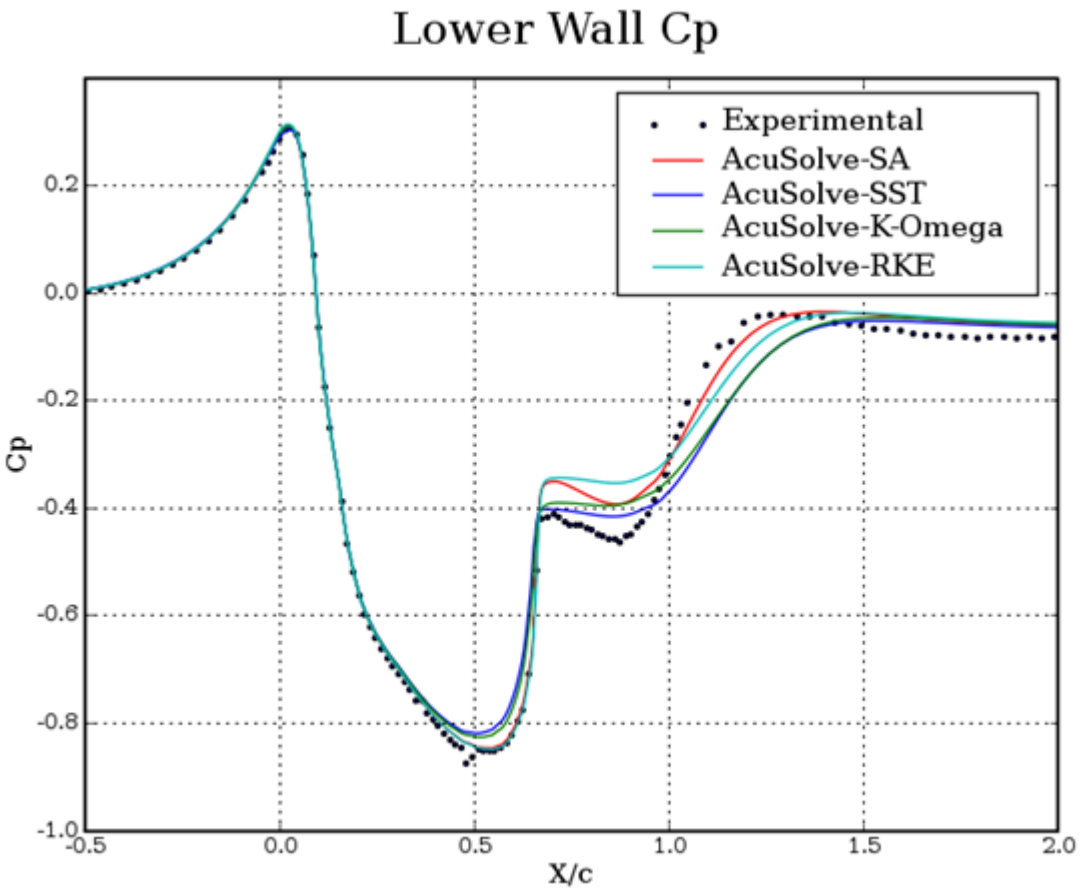


Figure 424: Coefficient of Pressure Along the Lower Wall as the Flow Moves Past the Hump, Where c is the Hump Chord Length and 0.0 is the Reference Location at the Front of the Hump in the X-Direction (Streamwise)

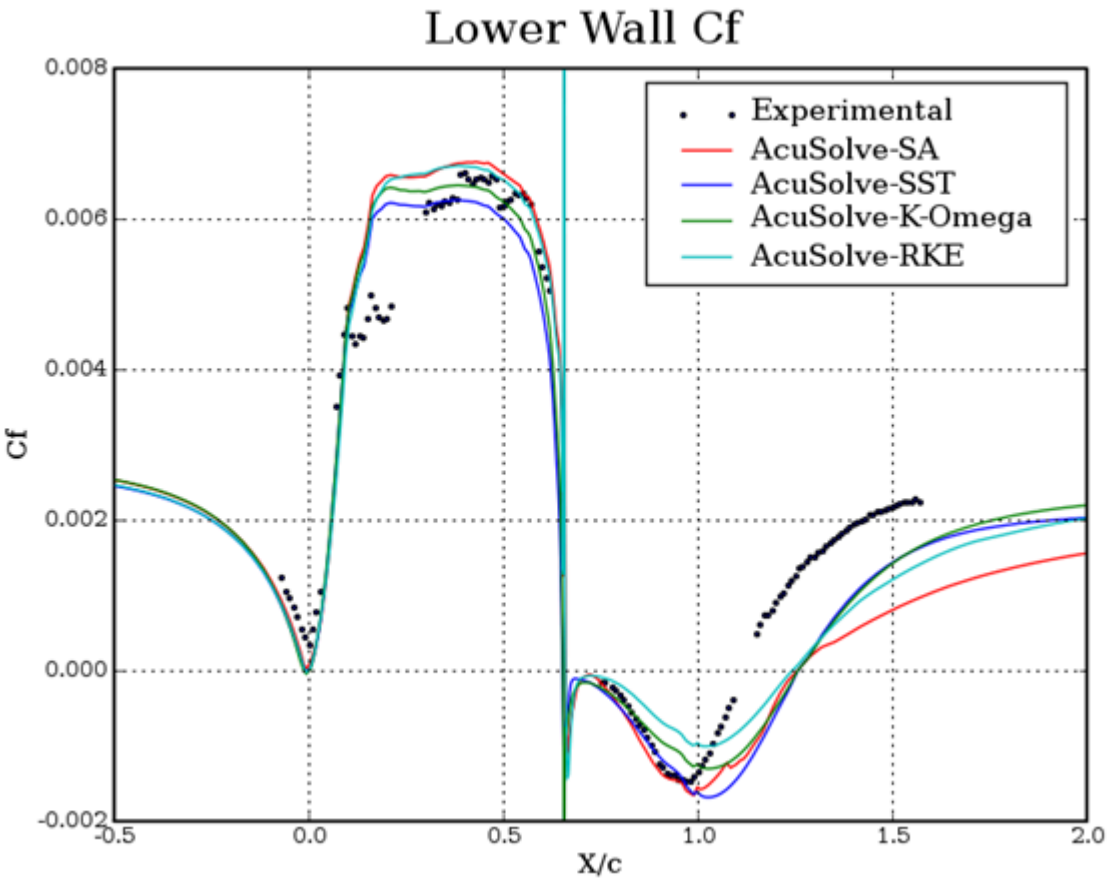


Figure 425: Skin Friction Coefficient Along the Lower Wall as the Flow Moves Past the Hump, Where c is the Hump Chord Length and 0.0 is the Reference Location at the Front of the Hump in the X-Direction (Streamwise)

Summary

In this application, a bulk turbulent flow at a Reynolds number of 936,000 within a flow domain containing a wall-mounted hump is studied and compared against experimental data. The AcuSolve results compare well with the experimental data for pressure coefficient and skin friction coefficient near the hump and downstream. The performance of the three turbulence models were found to be consistent with previously published results for flow over a wall-mounted hump (NASA 2015). For this application, the two equation models appear to outperform the one equation turbulence model, with better agreement for the downstream pressure on the wall. This application demonstrates AcuSolve's ability to predict the distribution of pressure and shear stress on protruding bodies within a turbulent flow field and serves to validate current turbulence modeling capabilities.

Simulation Settings for Turbulent Flow past a Wall-Mounted Hump

AcuConsole database file: `<your working directory>\wall_mounted_hump_turbulent\wall_mounted_hump_turbulent.acs`

Global

- Problem Description

- Analysis type - Steady State
- Turbulence equation - Spalart Allmaras

- Auto Solution Strategy
  - Max time steps - `100`
  - Convergence tolerance - `0.001`
  - Relaxation factor - `0.4`
- Material Model
  - Fluid
    - Density - `1.0` kg/m3
    - Viscosity - `1.0684e-6` kg/m-sec

  Model
- Volumes
  - Fluid
    - Element Set
      1. Material model - Fluid
- Surfaces
  - +Y
    - Simple Boundary Condition
      1. Type - Slip
  - -Y
    - Simple Boundary Condition
      1. Type - Slip
  - Cavity walls
    - Simple Boundary Condition
      1. Type - Wall
      2. Turbulence wall type - Wall Function
  - Hump walls
    - Simple Boundary Condition
      1. Type - Wall
      2. Turbulence wall type - Wall Function
  - Hump walls - downstream
    - Simple Boundary Condition
      1. Type - Wall
      2. Turbulence wall type - Wall Function
  - Inlet
    - Simple Boundary Condition
      1. Type - Inflow

2. Inflow type - Velocity
3. Inflow velocity type - Cartesian
4. X Velocity - `1.0` m/sec
5. Turbulence input type - Direct
6. Eddy viscosity - `3.205128e-6` m2/sec

- Lower slip
  - Simple Boundary Condition
    1. Type - Slip
- Lower wall
  - Simple Boundary Condition
    1. Type - Wall
    2. Turbulence wall type - Wall Function
- Nozzle walls
  - Simple Boundary Condition
    1. Type - Wall
    2. Turbulence wall type - Wall Function

- Outlet
  - Simple Boundary Condition
    - Type - Outflow
- Slip
  - Simple Boundary Condition
    - Type - Slip

References

A Seifert and L.G. Pack. "Active Flow Separation Control on Wall-Mounted Hump at High Reynolds Numbers". AIAA Journal. 40(7). 2002.

NASA Langley Research Center Turbulence Modeling Resource web page. http://turbmodels.larc.nasa.gov/nasahump_val.html. Accessed June 2015.

Laminar Free Surface Flow Inside a Rotating Cavity

In this application, AcuSolve is used to solve for the flow field within a rotating cavity with the top of the cavity free to move as if it was exposed to air. The height of the free surface is determined and compared against the analytical solution for the same rotational velocity under the standard gravitational force.

Problem Description

The problem consists of a fluid with arbitrary material properties rotating within an axisymmetric cavity. The cavity is 1.0 m in height with a radius of 0.5 m and is rotating at a constant speed of 3.0 rad/sec, as shown in the following image, which is not drawn to scale. The model is simulated as transient with the fluid initially at rest within the cavity. The radial velocity applied to the cavity walls causes the fluid's free surface to creep up the side wall forming a parabolic shape. The height of this surface is compared against the analytical solution as described in White, 2003.

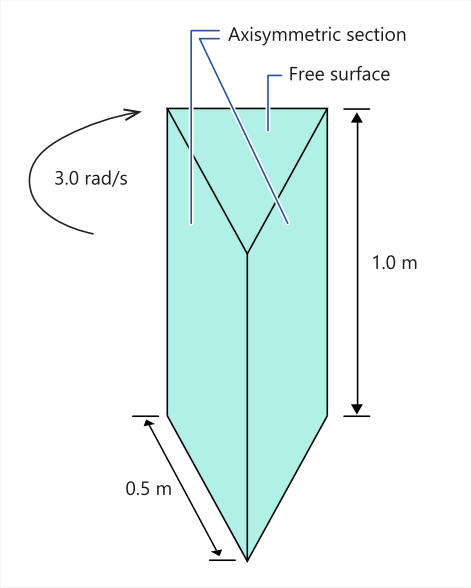


Figure 426: Critical Dimensions and Parameters used for Simulating a Laminar Free Surface Inside a Rotating Cavity

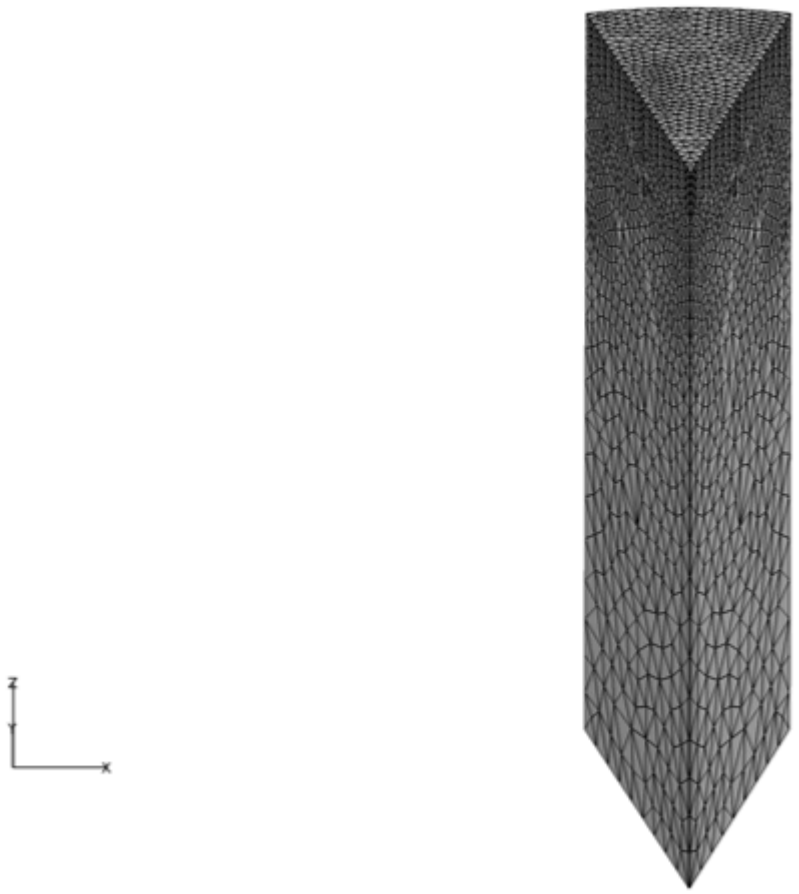


Figure 427: Mesh used for Simulating Laminar Free Surface Flow Inside a Rotating Cavity

The problem is simulated as axisymmetric by considering a 30 degree portion of the cavity with rotationally periodic boundary conditions applied on the planar surfaces representing the cut faces of the cavity.

AcuSolve Results

The AcuSolve solution reaches a quasi-static result with the free surface height stabilizing, demonstrating the final flow conditions of the simulation. As the fluid within the cavity is subjected to the multiple reference frame simulating the rotating boundaries the free surface begins to deform. At the center of the cavity the fluid height decreases and in order to conserve mass the height steadily increases as a function of the radial distance from the center. The surface height takes the form of a parabola as described in White, 2003. The following image demonstrates the shape that the fluid forms within the cavity, showing the vertical displacement of the rotating fluid. The free surface height is compared with the analytical solution where the image shows black circles representing the analytical solution and a solid red line for the AcuSolve results.

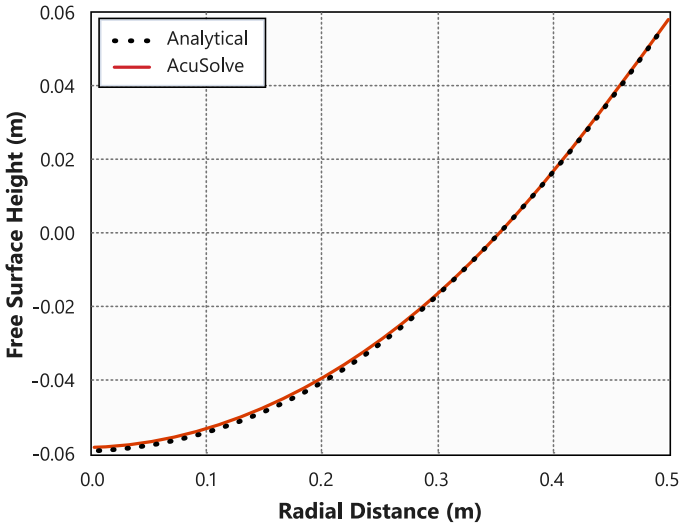


Figure 428: Free Surface Height of the Fluid Within the Cavity as a Function of Distance from the Center of the Domain at the Final Timestep

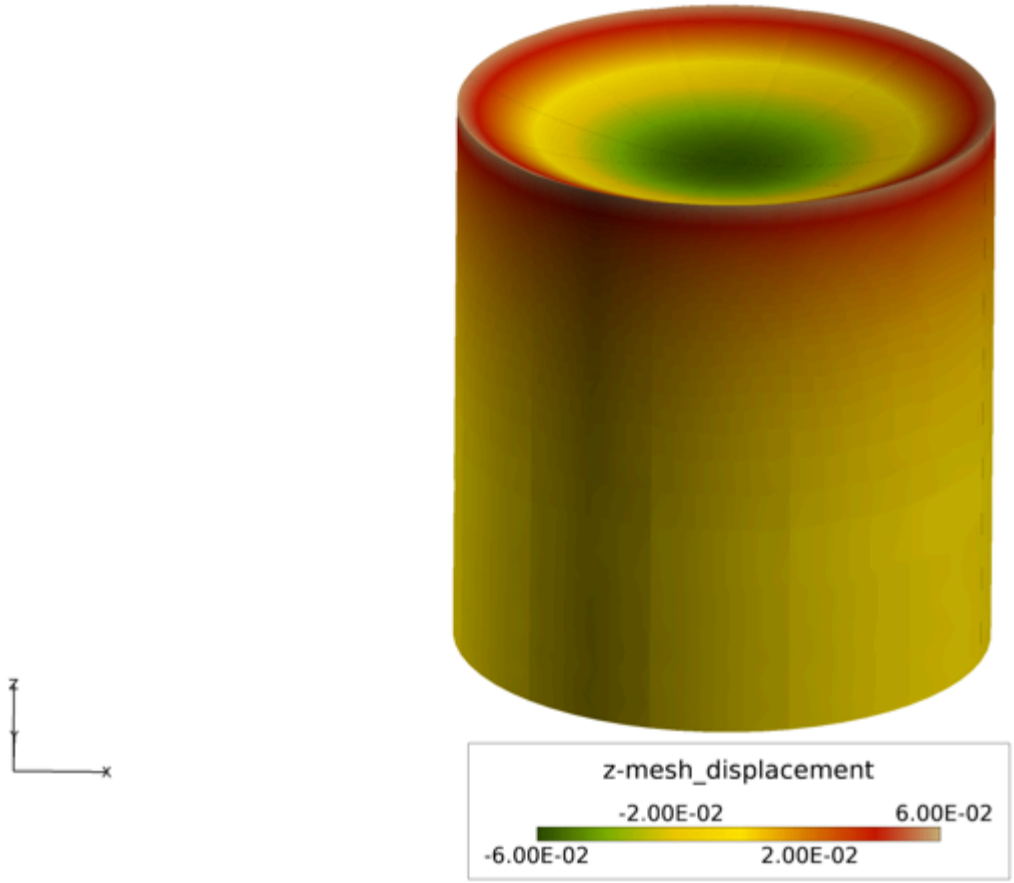


Figure 429: Vertical Mesh Displacement Within the Rotating Cavity at the Final Time Step (Shown as the Complete Cavity, using the Results from the Axisymmetric Section)

Summary

The AcuSolve solution compares well with analytical results for laminar free surface flow inside a rotating cavity. In this application, a fluid initially at rest is subjected to an angular velocity about the center of the cavity. As a result of the prescribed velocity, the fluid is forced to the outer wall of the cavity and develops a free surface profile in the shape of a parabola. The AcuSolve solution for the free surface height matches nearly exactly with the analytical results, with only minor differences based on the convergence criteria that you specified.

Simulation Settings for Laminar Free Surface Flow Inside a Rotating Cavity Fluid

Global

- Problem Description
  - Analysis type - Transient
  - Flow equation - Navier Stokes
  - Turbulence equation - Laminar
  - Mesh type - Arbitrary Mesh Movement (ALE)
- Auto Solution Strategy
  - Final time - `15.0` sec
  - Initial time increment- `0.05` sec
  - Convergence tolerance - `0.001`
  - Min stagger iterations - `0`
  - Max stagger iterations - `4`
- Material Model
  - Fluid
    - Density
      1. Type - Constant
      2. Density - `10` kg/m3
    - Viscosity
      1. Type - Constant
      2. Viscosity - `3.0` kg/m-sec
- Reference Frame
  - Omega
    - Rotation Center
      1. X-coordinate - `0.0` m
      2. Y-coordinate - `0.0` m
      3. Z-coordinate - `0.0` m
    - Angular velocity
      1. X-component - `0.0` rad/sec
      2. Y-component- `0.0` rad/sec
      3. Z-component - `3.0` rad/sec

Model

- Volumes
  - Fluid
    - Element Set
      1. Material model - Fluid
      2. Body force - Gravity
      3. Reference frame - Omega
- Surfaces
  - + Y
    - Simple Boundary Condition - (disabled to allow for nodal boundary conditions)
    - Advanced Options
      1. Nodal Boundary Conditions
         1. X-velocity
            1. Type - Constant
            2. Reference frame - Omega
            3. Constant value - `0.0`
         2. Y-velocity
            1. Type - Constant
            2. Reference frame - Omega
            3. Constant value - `0.0`
         3. Mesh X-Displacement
            1. Type- Zero
         4. Mesh Y-Displacement
            1. Type- Zero
  - -Z
    - Simple Boundary Condition
      1. Type - Wall
      2. Reference frame - Omega
      3. Mesh displacement BC type - Fixed
  - Axisymmetric +X
    - Simple Boundary Condition (disabled to allow for nodal boundary conditions)
  - Axisymmetric -X
    - Simple Boundary Condition (disabled to allow for nodal boundary conditions)
  - Free_Surface
    - Simple Boundary Condition
      1. # Type - Free Surface
- Periodics

- Axisymmetric Condition
- Periodic Boundary Condition
  - Type - Axisymmetric
  - Rotation Axis
    1. Point 1
       1. x-coordinate - 0.0 m
       2. y-coordinate - 0.0m
       3. z-coordinate - 0.0m
    2. Point 2
       1. x-coordinate - 0.0 m
       2. y-coordinate - 0.0m
       3. z-coordinate - 1.0m
- Nodes
  - All
    1. Mesh X-Displacement
       1. Type - Zero
    2. Mesh Y-Displacement
       1. Type - Zero
  - Centerline
    1. X-Velocity
       1. Type - Zero
    2. Y-velocity
       1. Type - Zero
    3. Mesh X-Displacement
       1. Type - Zero
    4. Mesh Y-Displacement
       1. Type - Zero

References

White, F. Fluid Mechanics. New York: McGrawHill. 2003

Heat Transfer Between Radiating Concentric Cylinders

In this application, AcuSolve is used to simulate the heat transfer due to radiation between concentric cylinders. The inner and outer cylinders are held at constant temperature and are defined to be radiation surfaces. AcuSolve results are compared with analytical results for temperature as described in Incropera (2006). The close agreement of AcuSolve results with analytical results validates the ability of AcuSolve to model cases with radiation heat transfer requiring view factor computation.

Problem Description

The problem consists of a fluid with arbitrary material properties between two infinitely long concentric cylinders, as shown in the following image, which is not drawn to scale. The radius of the outer cylinder is 0.046 m and the radius of the inner cylinder is 0.018 m. The inner cylinder is defined to have a constant wall temperature at 773.0 K (500 °C). The outer cylinder is defined to have a constant wall temperature at 300.0 K (27 °C). Both cylinders are specified to radiate as grey bodies, with emissivity set to 0.03778.

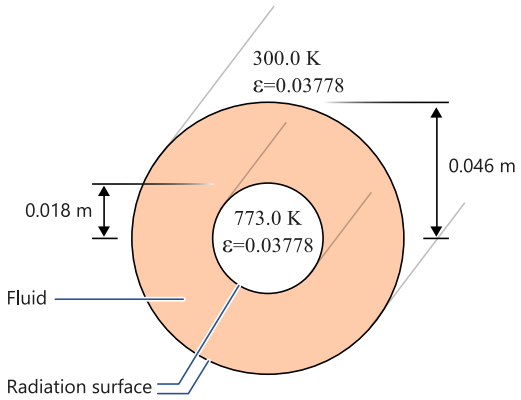


Figure 430: Critical Dimensions and Parameters Used for Simulating Radiation Between Two Concentric Cylinders

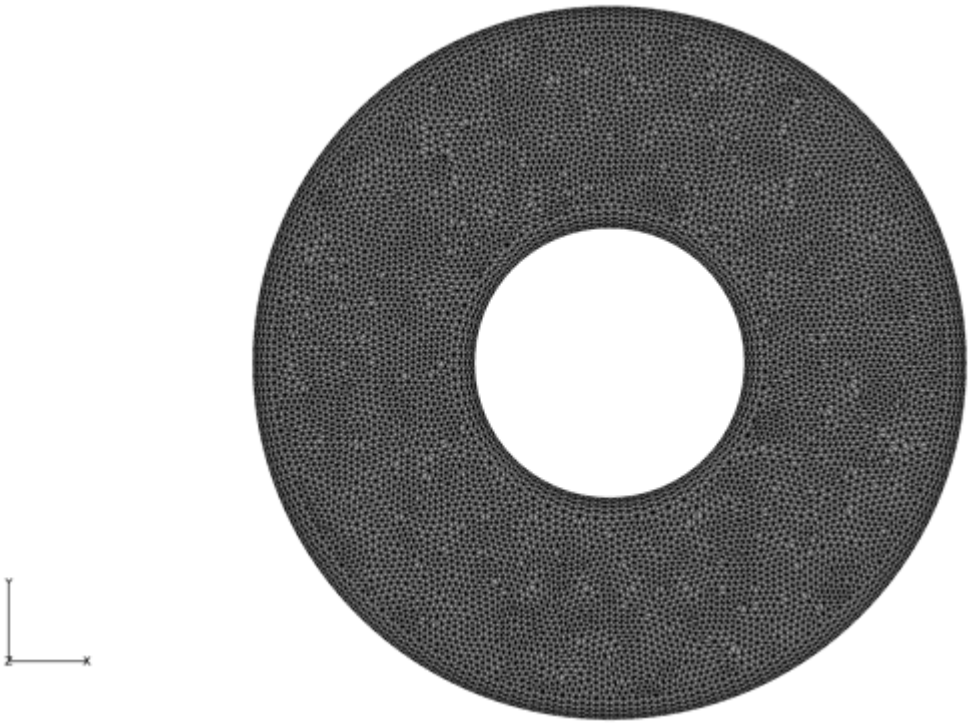


Figure 431: Mesh used for Simulating Radiation Between Two Concentric Cylinders

The simulation was performed as a two dimensional problem by constructing a volume mesh that contains a single layer of elements normal to the radial and circumferential directions.

AcuSolve Results

The AcuSolve solution converges to a steady state and the results reflect the mean temperature distribution. As the inner diameter is considerably hotter than the outer, a heat flux, due to radiation, is present between the cylinders. The temperature within the medium reduces logarithmically as a function of the radius. The following images show the temperature with the medium as a function of radius from the center. The temperature is compared with the analytical solution as described in Incropera (2006). The image below shows black circles representing the analytical solution and a solid red line for the AcuSolve results.

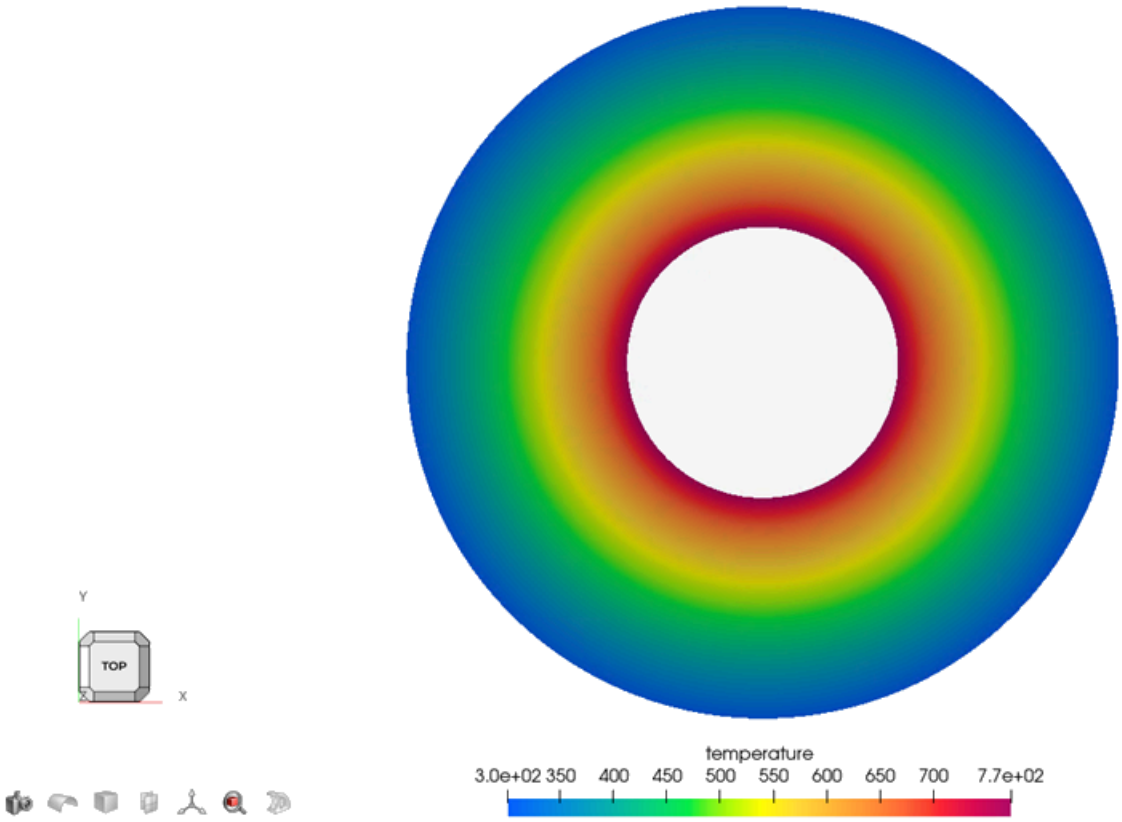


Figure 432: Contours of Temperature Between the Concentric Cylinders

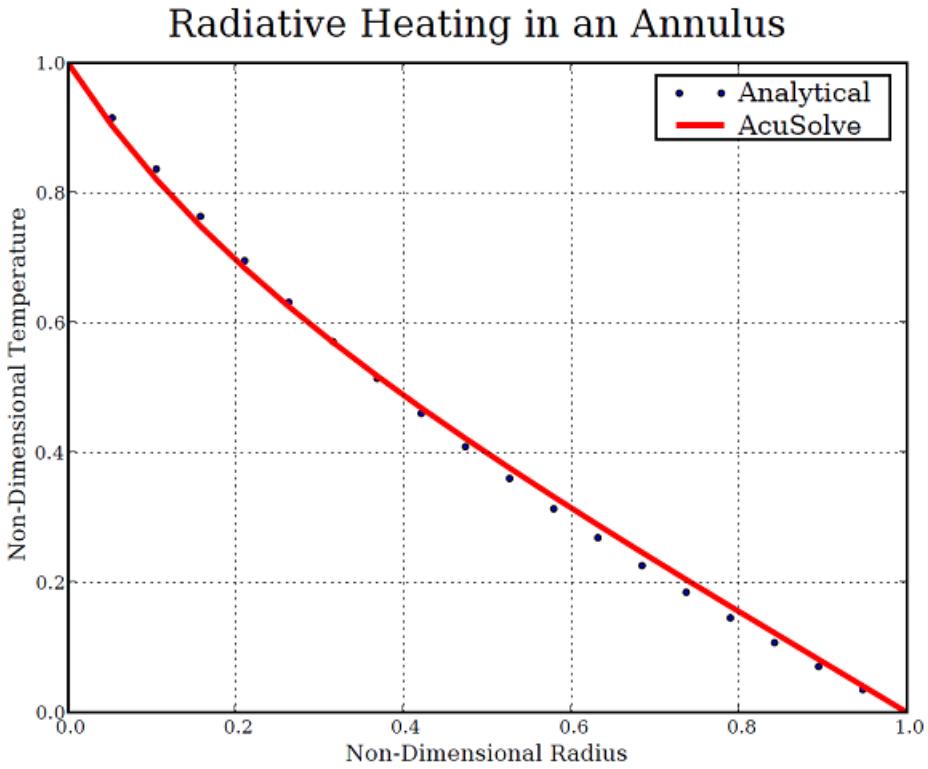


Figure 433: Non Dimensional Temperature Distribution Within the Annulus as a Function of Non Dimensional Radius

Summary

The AcuSolve solution compares well with analytical results for heat transfer due to radiation between two concentric cylinders. In this application, an arbitrary material is subjected to a heat flux that is calculated based on the view factors within the model. As a result of radiative heat flux a temperature distribution between the two cylinders develops. The AcuSolve solution for the temperature as a function of radius matches well compared to the analytical solution.

Heat Transfer Between Radiating Concentric Cylinders

HyperWorks CFD database file: `<your working directory>\annulus_radiation\annulus_radiation.hm`

Global

- Problem Description
  - Analysis type - Steady State
  - Temperature equation - Advective Diffusive
  - Radiation equation- Enclosure
- Auto Solution Strategy
  - Convergence tolerance - `0.0001`
  - Relaxation Factor- `0.4`
  - Flow- off

    - Enclosure radiation- on
- Material Model
    - Material
        - Conductivity
            1. Type - Constant
            2. Conductivity- `1.0`
- Emissivity Model
    - Grey Body
        - Emissivity- `0.03778`
    - Black Body
        - Emissivity- `1.0`

  Model
- Volumes
    - Medium
        - Element Set
            1. Medium - Fluid
            2. Material model- Material
- Surfaces
    - ID
        - Simple Boundary Condition
            1. Type- Wall
            2. Temperature BC type- Value
            3. Temperature- `773.0` K
        - Radiation Surface
            1. Type- Wall
            2. Emissivity model- Grey Body
    - Max_Z
        - Simple Boundary Condition
            1. Type- Symmetry
        - Radiation Surface
            1. Type- Wall
            2. Emissivity model- Black Body
    - Min_Z
        - Simple Boundary Condition
            1. Type- Symmetry
        - Radiation Surface
            1. Type- Wall

2. Emissivity model- Black Body

- OD
  - Simple Boundary Condition
    1. Type- Wall
    2. Temperature BC type- Value
    3. Temperature- `300.0` K
  - Radiation Surface
    1. Type- Wall
    2. Emissivity model- Grey Body

References

F. P. Incropera and D. P. DeWitt. "Fundamentals of Heat Transfer - Sixth Edition". John Wiley & Sons. New York. 2006.

Turbulent Flow Through a 180 Degree Curved Channel

In this application, AcuSolve is used to simulate turbulent flow through a strongly curved two dimensional 180 degree U-duct channel. AcuSolve results are compared with experimental results adapted from Rumsey et al. (2000). The close agreement of AcuSolve results with experimental results validates the ability of AcuSolve to model turbulent cases with strong curvature effects.

Problem Description

The problem consists of a fluid with properties similar to air flowing through a curved channel, as shown in the following image, which is not drawn to scale. The inlet channel height and remaining duct height is 0.0381 m. The bulk velocity (v) normal to the inlet is 31.1 m/s and an integrated outflow pressure is specified to allow the flow to pass through the channel. The flow develops into fully turbulent flow at a Reynolds's number (Re) of approximately 1,000,000. The density of the flow medium is 1.0 kg/m3 and the dynamic viscosity is 1.1818 X 10-6 kg/m-s. The simulation is conducted with the Reynolds Averaged Navier-Stokes equations using the Spalart Allmaras, Shear Stress Transport (SST), K-ω and Realizable K-ε turbulence models. The velocity field from the simulations is compared against experimental data at select measurement locations.

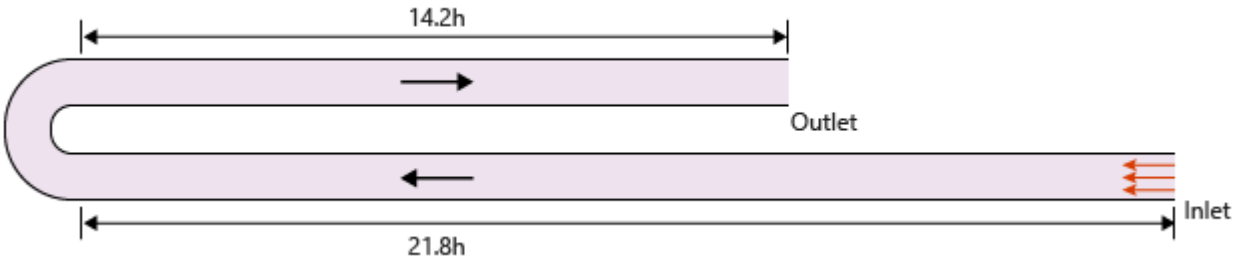
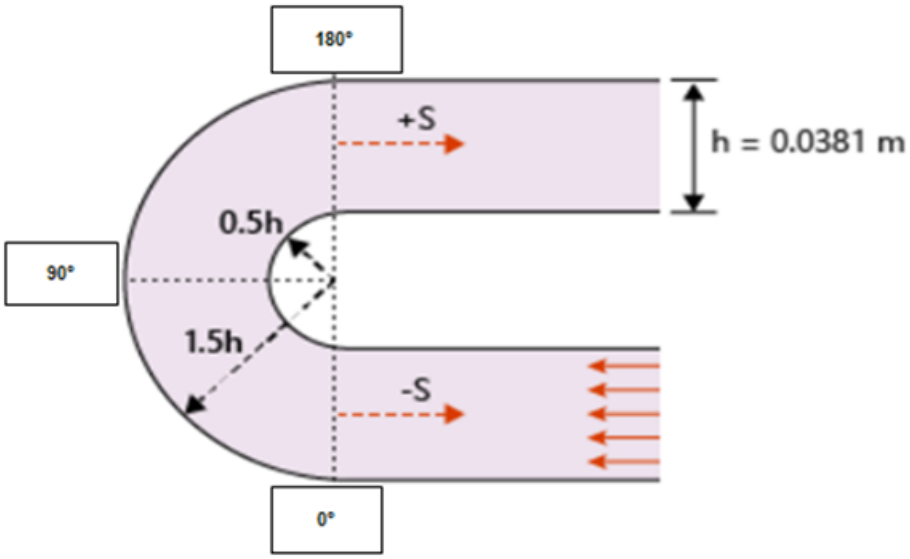


Figure 434: Critical Dimensions and Parameters for Simulating Turbulent Flow in the 180 degree U-Duct



The simulation was performed as a two dimensional problem by restricting flow in the out-of-plane direction through the use of a mesh that is one element thick. The upper and lower walls are specified as no-slip, the inlet velocity and eddy viscosity are specified normal to the inlet face to match the experimental Reynolds Number.

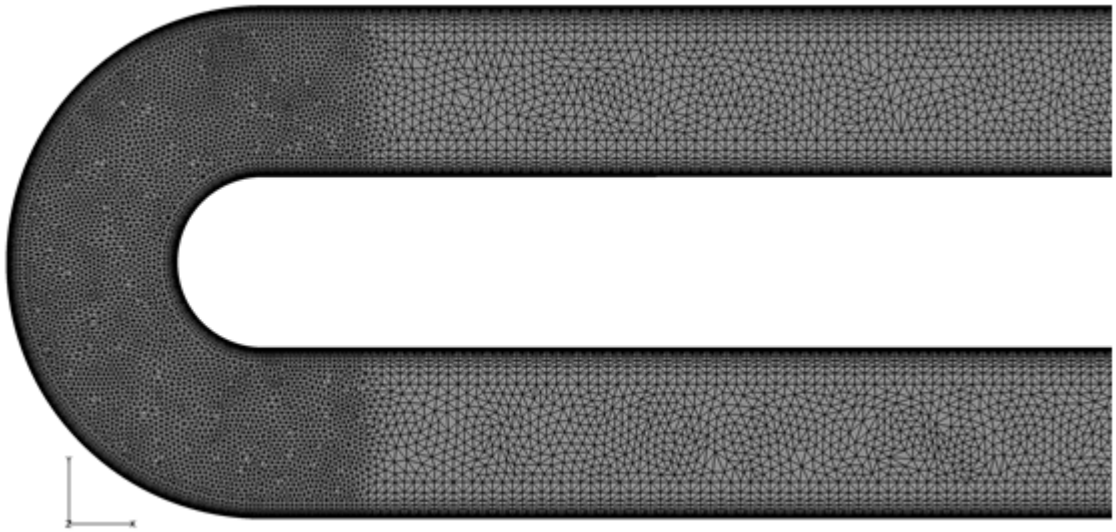


Figure 435: Mesh Used for Simulating Turbulent Flow in the 180 Degree U-Duct

AcuSolve Results

The AcuSolve solution converged to a steady state and the results reflect the mean flow conditions. As the flow passes the inner convex wall it begins to accelerate before decelerating directly past the curved section due to the adverse pressure gradient that eventually leads to a local recirculation zone. On the outer concave wall, the flow remains attached, but is influenced by the adverse pressure gradient above the recirculation region.

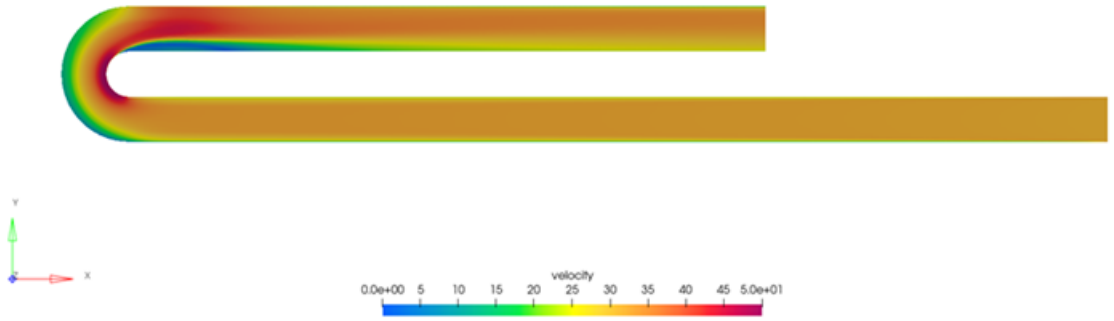


Figure 436: Velocity Contours in Stream Wise Plane

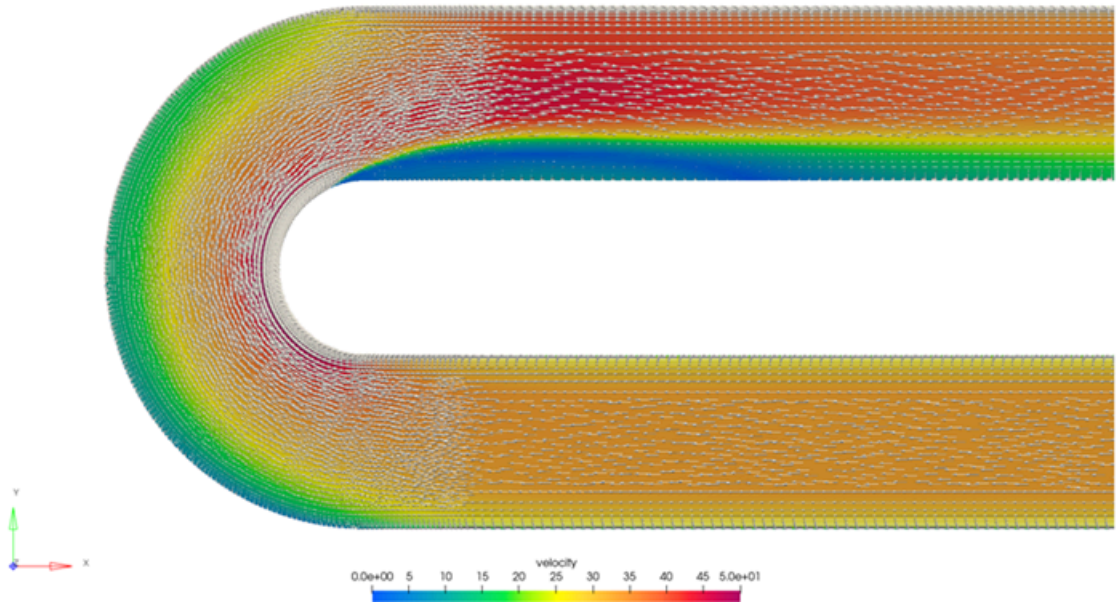


Figure 437: Close up View of Velocity Vectors and Velocity Contours at 180 Degree Bend

The experimental value for the ratio of Velocity magnitude (Vm) to inlet bulk velocity (Vb=31.1 m/s) at different sections of the U-duct is presented with the corresponding AcuSolve result for each of the turbulence models tested in the following images. The images show black circles representing the experimental measurements (Rumsey 2000), solid red lines for the SA model, solid blue lines for the SST model, solid green lines for the K-ω model and solid cyan lines for the K-ε model.

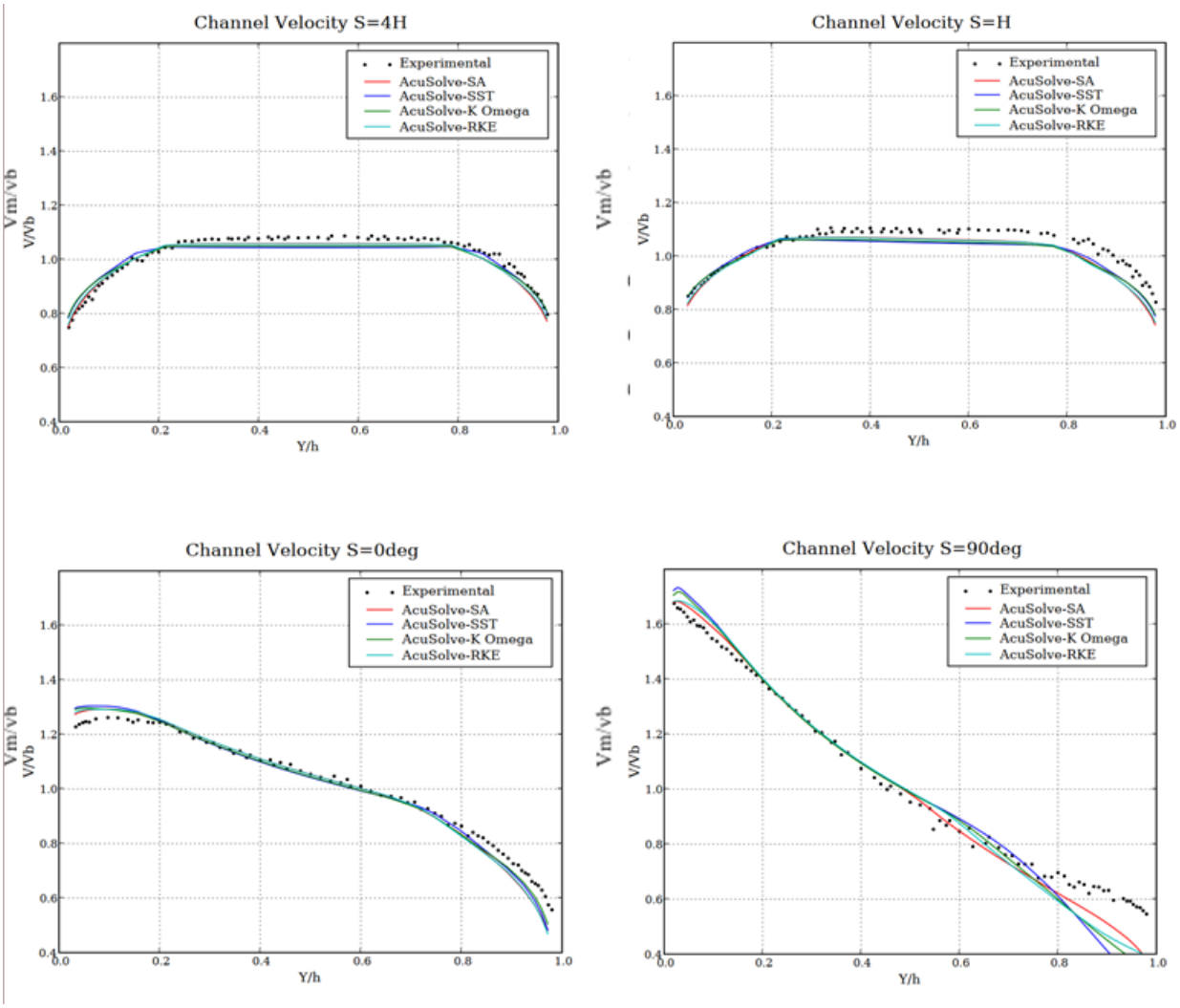


Figure 438:

Summary

The AcuSolve solution compares well with experimental results for flow past the 180 degree U-duct. The experimental value for the ratio of Velocity magnitude to inlet bulk velocity at different sections of the U-duct is presented with the corresponding AcuSolve result for various turbulence models. The performance of the Spalart Allmaras turbulence model was found to improve when the rotation curvature correction is included in the numerical formulation (enabled by default). In this application, AcuSolve demonstrates the ability to predict the complex boundary layer separation and reattachment resulting from the curvature of the channel.

Simulation Settings for Turbulent Flow Through a 180 Degree Curved Channel

HyperWorks CFD database file: `<your working directory>\curved_channel_simple_turbulent \curved_channel_simple_turbulent.hm`

Global

- Problem Description

    - Analysis type - Steady State
    - Turbulence equation - Realizable K-Epsilon
- Auto Solution Strategy
    - Relaxation factor - `0.4`
- Material Model
    - Air
        - Type- Constant
        - Density- `1.0` kg/m3
        - Viscosity- `1.1818e-006` kg/m-sec

  Model
- Volumes
    - Fluid
        - Element Set
            1. Material model- Air
- Surfaces
    - Inlet
        - Simple Boundary Condition
            1. Type- Wall
            2. Inflow type- Velocity
            3. Inflow velocity type- Normal
            4. Normal velocity- `31.1` m/sec
            5. Turbulence input type- Direct
            6. Eddy viscosity- `3.5547e-06` m2/sec
    - ext1
        - Simple Boundary Condition- Symmetry
    - ext2
        - Simple Boundary Condition- Symmetry
    - Outlet
        - Simple Boundary Condition
            1. Type- Outflow
    - wall-bottom
        - Simple Boundary Condition
            1. Type- Wall
            2. Turbulence wall type- Low Reynolds Number
    - wall-top
        - Simple Boundary Condition
            1. Type- Wall

2 Turbulence wall type- Low Reynolds Number

References

Christopher L. Rumsey, Thomas B. Gatski, and Joseph H. Morrison. "Turbulence Model Predictions of Strongly Curved Flow in a U-Duct", AIAA Journal, Vol. 38, No. 8 (2000), pp. 1394-1402.

Circumferential Flow in a Cylinder Induced by a Rotating Solid

In this application, AcuSolve is used to simulate the flow of air between concentric cylinders that is initiated by the rotation of the solid inner cylinder. The outer cylinder is held stationary while the inner cylinder rotates with a constant speed. AcuSolve results are compared with analytical results as described in White (1991). The close agreement of AcuSolve results with analytical results validates the ability of AcuSolve to maintain a continuous velocity across a non-conformal guide surface interface.

Problem Description

The problem consists of a fluid with material properties of a viscous fluid with the density of air rotating between two infinitely long concentric cylinders, as shown in the following image, which is not drawn to scale. The radius of the outer cylinder is 3.0 m and the radius of the inner cylinder is 1.5 m. The inner cylinder is defined as a solid medium and rotates at 1 rad/sec. The inner cylinder's surface velocity is mapped to the adjacent surface within the fluid medium, while the outer cylinder is fixed. The induced flow is laminar and exhibits a steady state behavior after running for a short period of physical time. The rotation of the inner cylinder causes the fluid to rotate due to viscous shearing near the wall. As the outer cylinder is fixed, a velocity gradient is generated as a function of radius within the flow domain.

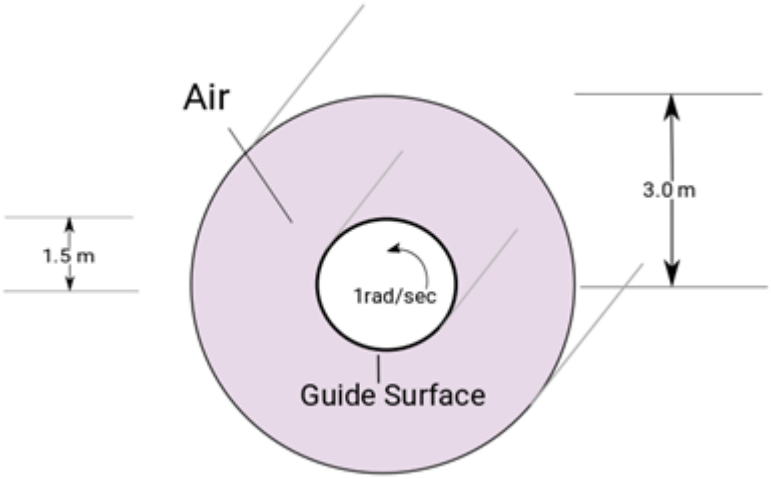


Figure 439: Critical Dimensions and Parameters Used for Simulating Flow Between Two Concentric Cylinders Split with a Guide Surface

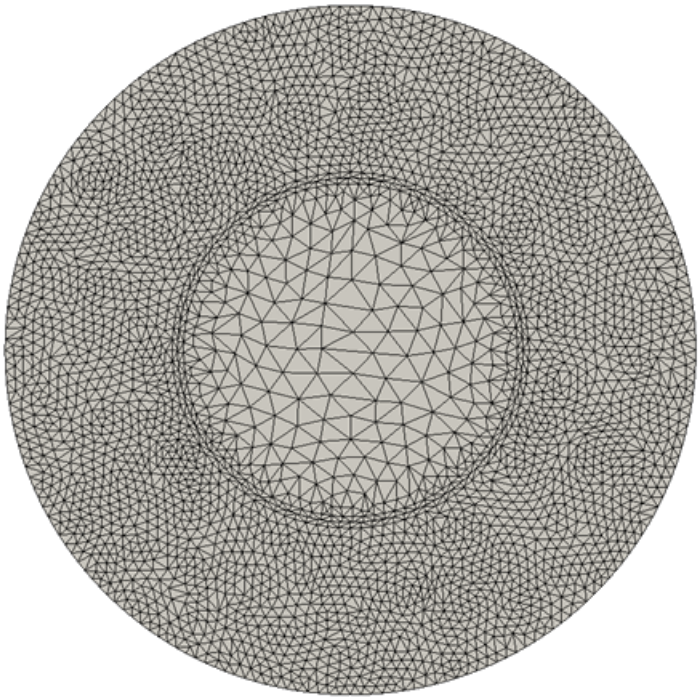


Figure 440: Mesh Used for Simulating Flow Between Two Concentric Cylinders

The simulation was performed as a two dimensional problem by constructing a volume mesh that contains a single layer of elements in the extruded direction, normal to the flow plane and by imposing slip flow and mesh boundary conditions on the extruded planes.

AcuSolve Results

The AcuSolve solution reaches a quasi-static result with the velocity between the two cylinders reaching a steady state at the simulation end time. As the solid inner cylinder rotates, it acts as a guide surface for the fluid elements to track and inherit the two velocity components. The velocity at the edge of the inner cylinder is equal to exactly the rotational speed multiplied by the radius. As the radius increases, the flow velocity reduces until it reaches zero at the outer diameter. The following images show the tangential velocity within the fluid as a function of radius from the center. The tangential velocity is compared with the analytical solution. The image below shows black circles representing the analytical solution and a solid red line for the AcuSolve results.

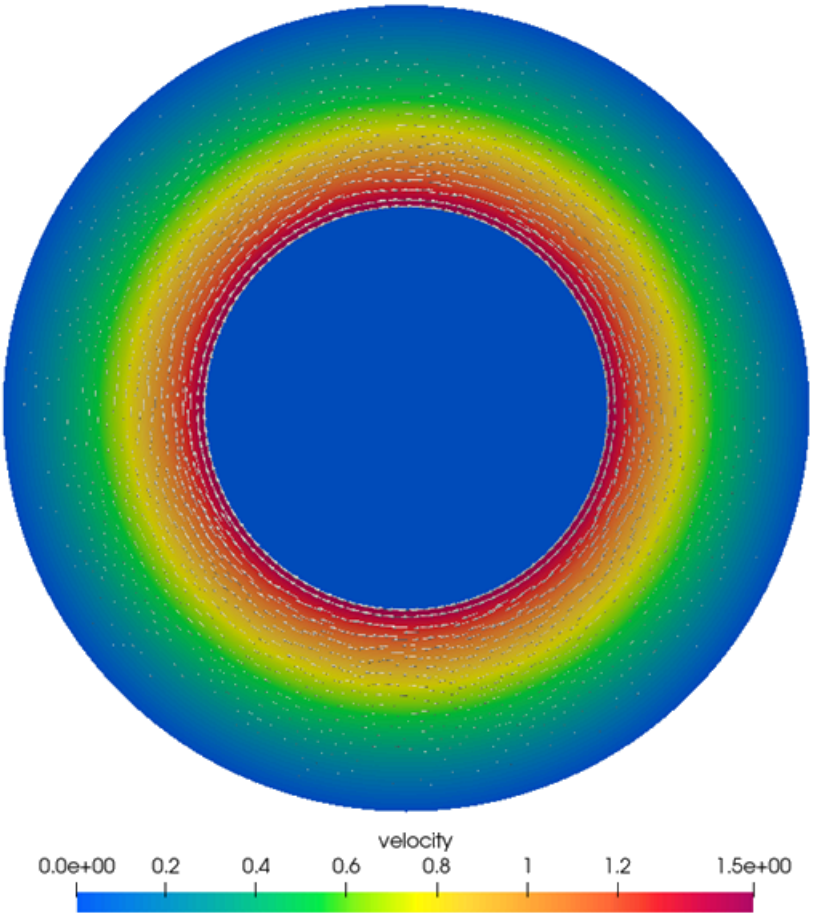


Figure 441: Contours and Vectors of Velocity Between the Concentric Cylinders

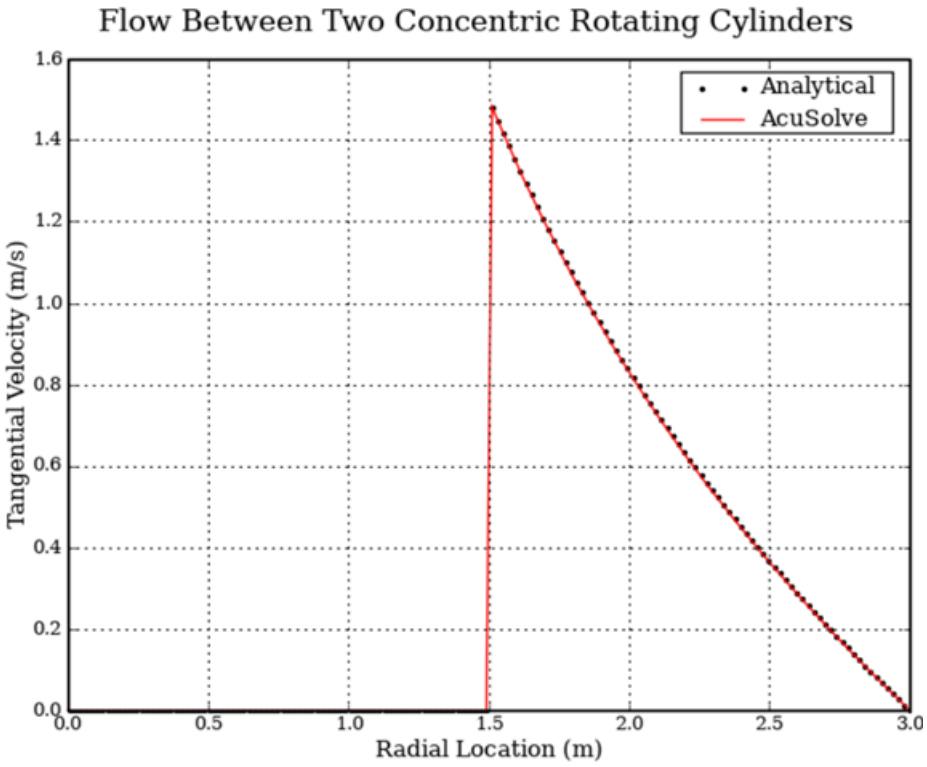


Figure 442: Tangential Velocity Within the Solid and Fluid as a Function of Radial Distance from the Center at the Final Timestep

Summary

The AcuSolve solution compares well with analytical results for laminar flow between concentric cylinders, where the inner cylinder guides the adjacent fluid elements. In this application, a fluid initially at rest inherits the angular velocity from the inner cylinder while the outer cylinder does not rotate. As a result of the inherited velocity and viscosity of the fluid, flow develops between the two cylinders. The AcuSolve solution for the tangential velocity as a function of radius matches exactly with the analytical results.

Simulation Settings for Flow Between Concentric Split Cylinders

HyperWorks CFD database file: `<your working directory>\annulus_split_rotating \annulus_split_rotating.hm`

- Problem Description
  - Analysis type - Transient
  - Flow equation - Navier Stokes
  - Turbulence equation - Laminar
  - Mesh type - Arbitrary Mesh Movement (ALE)
- Auto Solution Strategy
  - Max time steps - `40`
  - Initial time increment- `0.02` sec

- Convergence tolerance - `0.001`
- Min stagger iterations - `2`
- Max stagger iterations - `4`

- Material Model
  - Air
    - Density
      1. Type - Constant
      2. Density - `1.225` kg/m3
    - Viscosity
      1. Type - Constant
      2. Viscosity - `1.781` kg/m-sec
- Mesh Motion
  - Rotation
    - Rotation Center
      1. X-coordinate - `2.0` m
      2. Y-coordinate - `0.0` m
      3. Z-coordinate - `0.0` m
    - Angular velocity
      1. X-component - `1.0` rad/sec
      2. Y-component- `0.0` rad/sec
      3. Z-component - `0.0` rad/sec

  Model
- Volumes
  - CylinderInner
    - Element Set
      1. Medium - Solid
      2. Material model - Aluminum
  - CylinderOuter
    - Element Set
      1. Medium - Fluid
      2. Material model - Air
- Surfaces
  - InBottom
    - Simple Boundary Condition
      1. Type- Slip
      2. Mesh displacement type- Slip
  - InInterf

        - Simple Boundary Condition
            1. Type- Wall
            2. Mesh displacement type- Fixed
            3. Mesh motion- Rotation
        - Guide Surface
            1. Type- Faceted
    - InTop
        - Simple Boundary Condition
            1. Type- Slip
            2. Mesh displacement type- Slip
    - OutBottom
        - Simple Boundary Condition
            1. Type- Slip
            2. Mesh displacement type- Slip
    - OutInterf
        - Simple Boundary Condition
            1. Type- Wall
            2. Wall velocity type- Match Mesh Velocity
            3. Mesh displacement type- Guide surface
            4. Guide surface- InInterf
    - OutTop
        - Simple Boundary Condition
            1. Type- Slip
            2. Mesh displacement type- Slip
    - OutWall
        - Simple Boundary Condition
            1. Type- Wall
            2. Mesh displacement type- Fixed
- Nodes
    - PressurePoint
        - Pressure
            1. Type- Zero

References

F. M. White. "Viscous Fluid Flow". Section 3-2.3. McGraw-Hill Book Co., Inc. New York. 1991.

Turbulent Flow Through a Heated Periodic Channel

In this application, AcuSolve is used to solve for the flow and temperature field within a channel containing a heated wall. The wall is maintained at a constant temperature, inducing heat flux into the fluid, to predict the thermal law of the wall. The non dimensional temperature versus the non dimensional height above the wall is compared to the analytical correlation provided by Kader.

Problem Description

The problem consists of a fluid having material properties close to air with a density of 1.0 kg/m^3, molecular viscosity of 0.0001 kg/m-s, specific heat of 1005.0 J/kg-K and thermal conductivity of 0.139 W/m-K. The properties are specified to obtain a Prandtl number of 0.72. The velocity is defined as periodic and is driven by a constant acceleration body force equal to 2.0 m/s^2. The temperature is specified as periodic+unknown ratio allowing it to develop until it reaches a steady solution. The simulation description is shown in the following image, which is not drawn to scale. The model is simulated using the one equation Spalart Allmaras turbulence model along with the advective-diffusive temperature equation. The thermal wall distribution is validated against correlation data published by Kader 1981.

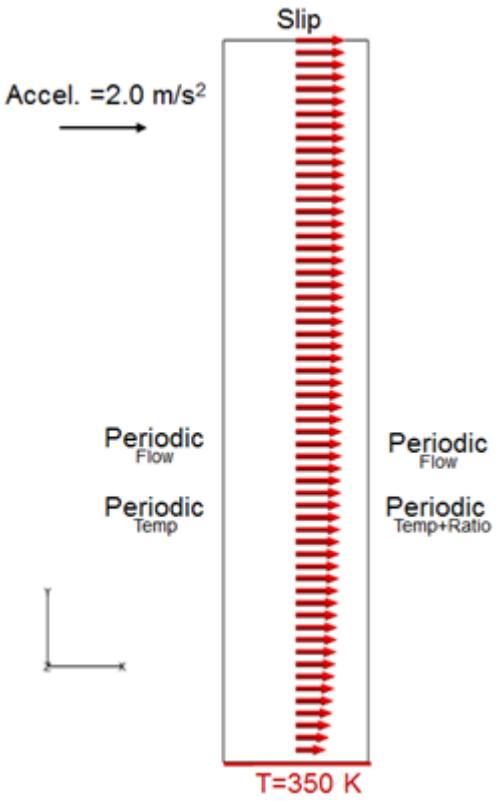


Figure 443: Critical Parameters used For Simulating Periodic Flow Within a Heated Channel

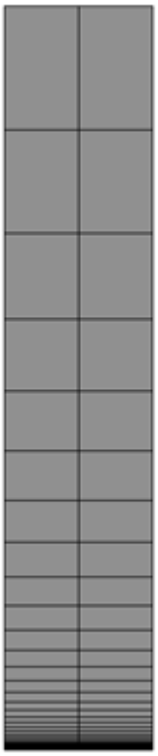


Figure 444: Mesh used For Simulating Periodic Flow Within a Heated Channel

The simulation was performed as a two dimensional problem by constructing a volume mesh that contains a single layer of elements extruded in the cross stream direction, normal to the flow plane and by imposing periodic boundary conditions on the extruded planes. The streamwise direction contains two elements allowing the flow and temperature solution to develop. Only the lower half of the channel is modeled, assuming the solution is mirror across the top slip plane.

AcuSolve Results

The AcuSolve solution converged to a steady state and the results reflect the mean flow conditions within the channel. The simulation results demonstrate that the channel wall induces a thermal flux into the flow field, producing a temperature distribution dependent on the distance from the wall. The thermal law of the wall computed from the AcuSolve results is compared with correlation data for the corresponding Prandtl number, as demonstrated in Kader 1981. The plot shown below gives the non dimensional value of T+ as a function of Y+, where T+ and Y+ are computed per the following relationships:

$$T+ = \frac{(Tw - T)\rho C p u\tau}{\dot{Q}} T \tag{14}$$

$$Y+ = \frac{yu\tau}{v} \tag{15}$$

$$u\tau = \sqrt{\tau w / \rho} \tag{16}$$

Where $T+$, Tw is the fixed wall temperature, T is the temperature away from the wall, ρ is the fluid density, Cp is the fluid specific heat, uT is computed from the magnitude of the shear stress and $\dot{Q}_i$ is the local surface heat flux.

The image below shows black circles representing the correlation data and a solid red line for the AcuSolve results. The results demonstrate that the temperature distribution away from the wall is resolved properly and compares well with the correlation. Since an empirical relationship for T+ is used for comparison, there will be minor discrepancies compared with the simulation results. Additional comparisons have been made against DNS results for T+ from Kawamura et al. 1998.

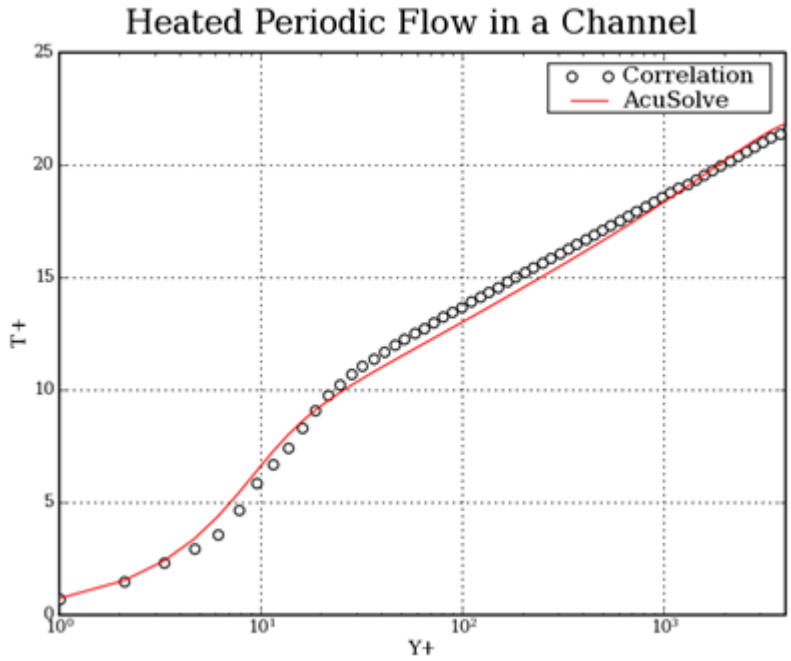


Figure 445: Thermal Boundary Layer Within the Heated Channel Compared Against the Correlation Data

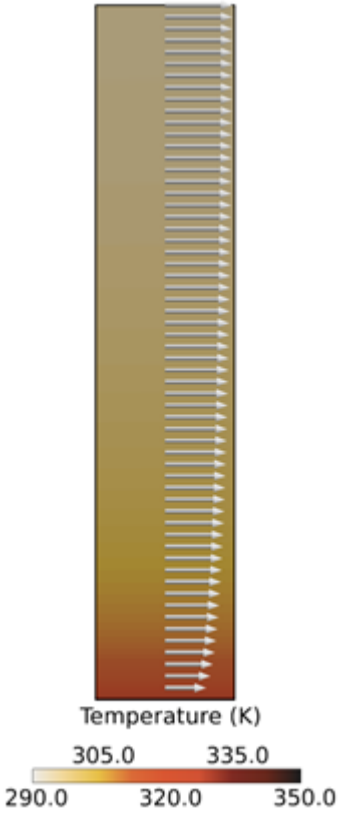


Figure 446: Contours of Temperature and Vectors Representing the Fluid Velocity Within the Channel

Summary

The AcuSolve solution compares well with the correlation data for turbulent flow within a heated channel. In this application, the constant temperature wall induces a surface heat flux, giving rise to a temperature gradient within the channel. AcuSolve can capture the correct temperature gradient at any location above the wall if an appropriate first layer height is selected to resolve a Y+ value of 1.0. The good agreement with correlation data for T+ demonstrates that AcuSolve can predict the locally varying temperature distribution within a turbulent channel.

Simulation Settings for Turbulent Flow Through a Heated Periodic Channel

AcuConsole database file: `<your working directory>\channel_periodic_heat\channel_periodic_heat.acs`

Global

- Problem Description
  - Analysis type - Steady State
  - Temperature equation - Advective Diffusive
  - Turbulence equation - Spalart Allmaras
- Auto Solution Strategy
  - Max time steps - `50`

- Convergence tolerance - `0.0001`
- Relaxation Factor - `0.4`
- Temperature - On

- Material Model
  - Fluid
    - Type - Constant
    - Density - `1.0` kg/m3
    - Viscosity - `1.0e-4` kg/m*sec
    - Specific Heat - `1005.0` J/kg*K
    - Conductivity - `0.139` W/m*K
- Body Force
  - BodyForce
    - Gravity
      1. X-component - `2.0` m/sec2

Model

- Volumes
  - Fluid
    - Element Set
      1. Material model - Fluid
      2. Body force - BodyForce
- Surfaces
  - Symmetry_1
    - Simple Boundary Condition - (disabled to allow for periodic conditions to be set)
  - Symmetry_2
    - Simple Boundary Condition - (disabled to allow for periodic conditions to be set)
  - Inflow
    - Simple Boundary Condition - (combination of integrated BC and periodic BC set)
    - Advanced Options
      1. Integrated Boundary Conditions - Temperature - `300.0` K
  - Outflow
    - Simple Boundary Condition - (disabled to allow for periodic conditions to be set)
  - Slip_surface
    - Simple Boundary Condition
      1. Type- Slip
  - Wall_surface
    - Simple Boundary Condition
      1. Type- Wall

2 Temperature BC type - Value
3 Temperature - `350.0` K

- Periodics
  - 2D
    - Periodic Boundary Conditions
      1 Type - Periodic
  - Flow
    - Periodic Boundary Conditions
      1 Type - Periodic
  - Temperature
    - Individual Periodic BCs
      1 Temperature: Type - Single Unknown Ratio
- Nodes
  - Fixed_pressure
    - Pressure: Type - Zero
  - Zero_z-velocity
    - Z-Velocity: Type - Zero

References

B.A. Kader, "Temperature and concentration profiles in fully turbulent boundary layers", International Journal of Heat and Mass Transfer, Volume 24, Issue 9, 1981, Pages 1541-1544.

H. Kawamura, K. Ohsaka, H. Abe and K. Yamamoto, "DNS of turbulent heat transfer in channel flow with low to medium-high Prandtl number fluid", International Journal of Heat and Mass Transfer, 19:482-491, 1998.

Multiphase Flow Within a Sloshing Tank

In this application, AcuSolve is used to simulate water and the time-dependent interface of air-water within a tank subject to a prescribed sloshing motion. AcuSolve results are compared with experimental pressure measurements as reported by Tankaka, et al. (2000) and Rhee (2005). The close agreement of AcuSolve results with experimental results validates the ability of AcuSolve to model multiphase flow problems with user-defined motion.

Problem Description

The problem consists of a tank filled to 20 percent capacity with water that is rotated or translated according to a user-defined function, as shown in the following image, which is not drawn to scale, where three monitoring locations, P1, P2 and P3, are denoted. The motion of the tank causes the fluid to begin sloshing rapidly, creating a time-dependent pressure field due to the height of the local water column. Non-slip boundary conditions for the top, bottom, left and right sides are applied with slip boundary conditions on the front and back faces. The SST turbulence model along with a global time-step of 0.001 seconds is used for the simulation. The pressure at each of the monitoring locations is compared against the experimental measurements as described in Tankaka, et al. (2000). It should be noted that the pressure computed and presented in the images represent the time-dependent dynamic pressure, static pressure is subtracted to be consistent with the measurements, at the specified point. Roll-Short is the case provided with the Validation Manual. The results for this case as well as Sway - Short are presented within this overview. In each case, the motion profile is defined with the following function and coefficients as defined in the table below.

$$x = A\sin(\omega t) \tag{17}$$

Where A = amplitude of oscillation, ω = frequency of oscillation = 2 π/T, t = time (sec) and T = Time period of oscillation (sec).

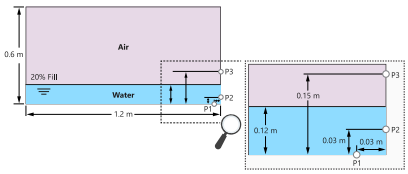


Figure 447: Critical Dimensions and Parameters for Simulating a 2D Tank Slosh with Mesh Motion

Table 29: Sine Function Scaling Parameters for Tank Motion Profile

Cases	Mesh Motion	Amplitude (A)	Time Periods (T)	Tank Filling Level
Sway – Base	Sway motion	0.06 m	1.94 sec	20% height

Cases	Mesh Motion	Amplitude (A)	Time Periods (T)	Tank Filling Level
Sway – Short	Sway motion	0.06 m	1.74 sec	20% height
Roll – Base	Rolling motion	10 degrees	2.25 sec	20% height
Roll – Short	Rolling motion	10 degrees	1.85 sec	20% height

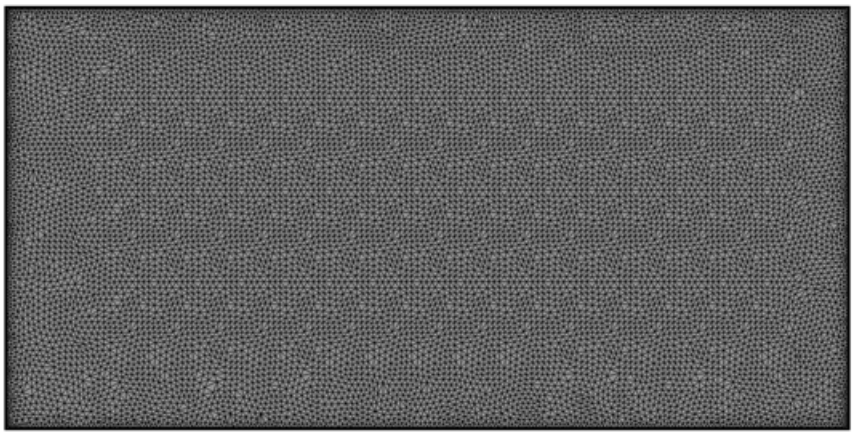


Figure 448: Mesh Used for Simulating Multiphase Sloshing Within a 2D Tank

AcuSolve Results

The AcuSolve solution is run for a time of t/T=5.0, 9.25 sec for Roll - Short, and the results presented reflect the transient motion of the water within the tank. The experimental values of pressure (kPa) and normalized simulation time are presented with the corresponding AcuSolve results at three measurement locations. The AcuSolve results show good agreement with the experimental results for pressure magnitude, the local water column height, as well as accurate timing of the peaks, indicating that the air-water interface is properly captured. Additional motion cases, as well as comparisons between two dimensional versus three dimensional simulations have been simulated with AcuSolve. The accuracy and solution requirements of these simulations are omitted for brevity but are available upon request. It was found that the differences between 2D and 3D simulations may be of interest for engineers, however the 2D results are shown to be adequate and less computationally expensive than 3D in the cases studied.

User-Defined Multiplier Function

This validation case relies on defining the motion of the elements within the tank, leading to the water sloshing in the presence of air. The motion is defined using an AcuSolve User-Defined Function (UDF) to specify the time-dependent multiplier function applied to the mesh motion command. The mesh motion is assigned to the Fluid element set, causing all of the elements to move according to the specified sine function. For the Roll - Short case, the mesh motion command is specified as rotation with the rotation multiplier function specified as rotation. If you are interested in simulating one of the other motion profiles, for example Sway - Base/Short, the type of mesh motion command would be changed to translation with the translation multiplier function assigned with the same UDF. The function name is designated at usrMotion and is contained within the source file `motion.c`. The source file, along with

pre-compiled binaries for Linux64 and Windows64 are provided with the validation case. Depending on your architecture it may be necessary to re-compile the source on the local system. Please refer to the *Programs Reference Manual* for details on using AcuMakeLib or AcuMakeDll for Linux and Windows, respectively.

Summary

The AcuSolve solution compares well with experimental results for tank sloshing simulations. In this application, the time dependent motion of the tank and the multiphase flow solution are simulated with AcuSolve using the level-set formulation and the SST turbulence model. The experimental values for instantaneous pressure at three locations and for two motion profiles are presented with the corresponding AcuSolve results. A good agreement of simulation results with the experiment validates the ability to solve time-dependent/accurate sloshing cases using the multiphase capabilities of AcuSolve.

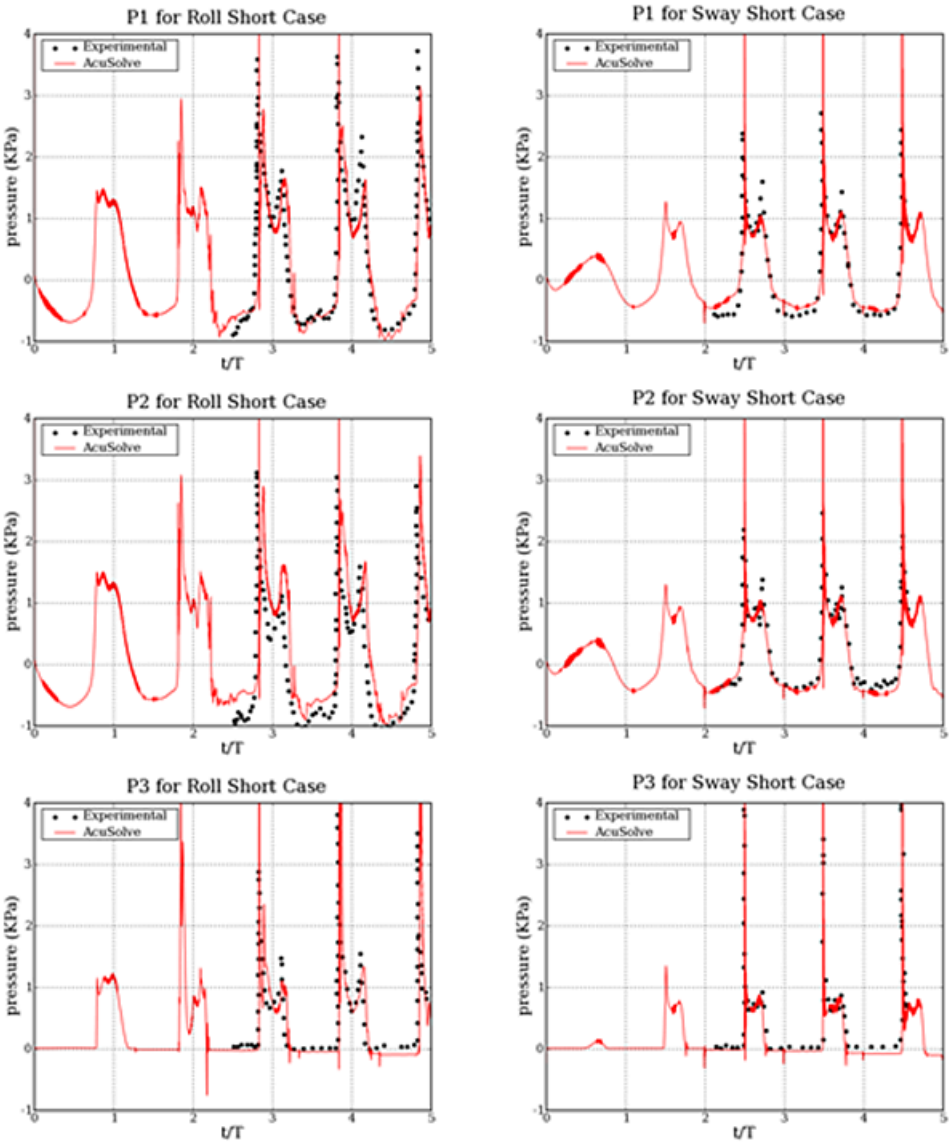


Figure 449: Time Dependent Pressure at Three Monitoring Locations Within the Sloshing Tank for Two Motion Profiles (Roll-Short, Left and Sway-Short, Right)

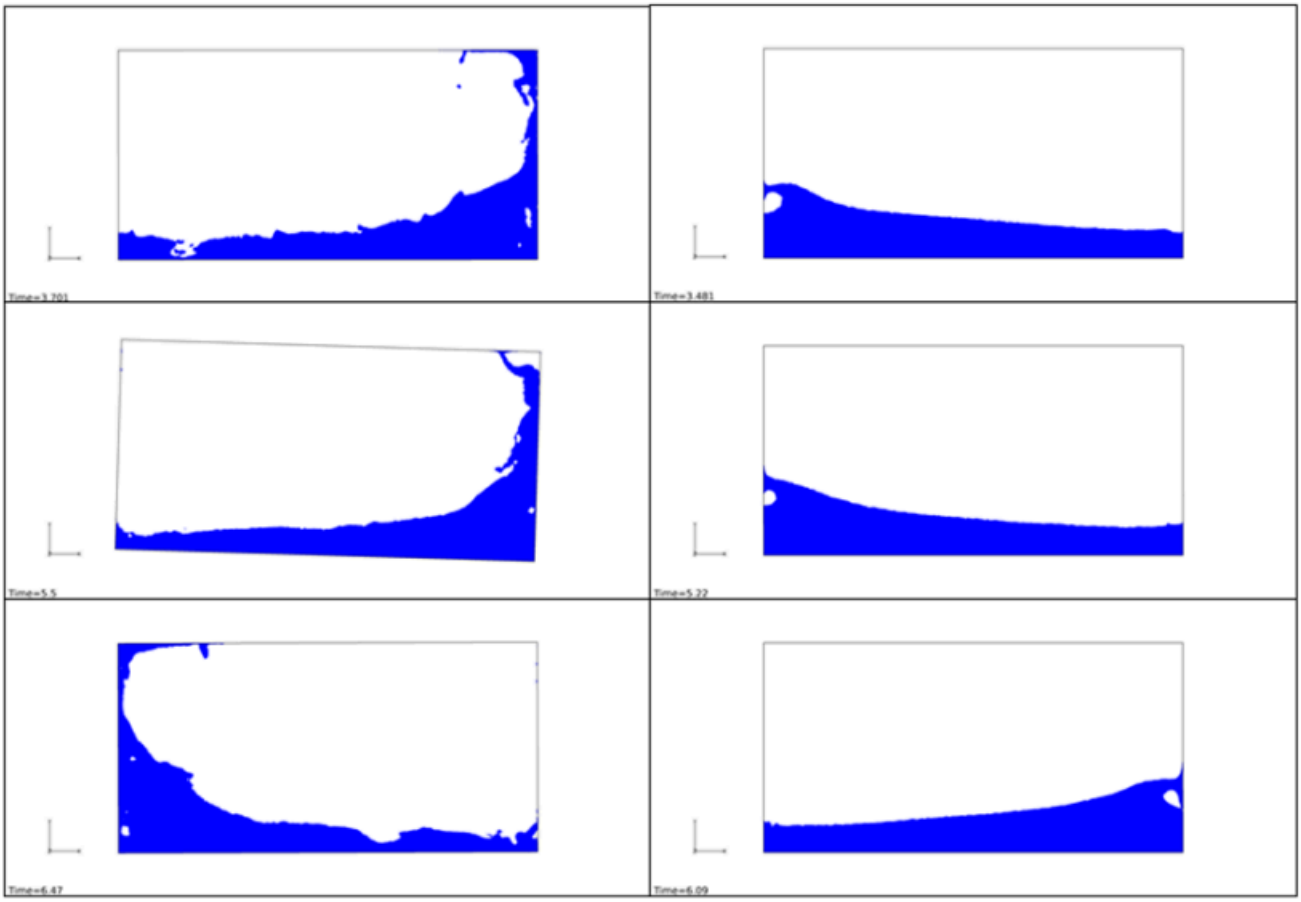


Figure 450: Instantaneous Volume Fraction Contour (Blue Showing Water) at Three Moments in Time (t/T=2.0, 3.0 and 3.5) for Two Motion Profiles (Roll-Short, Left and Sway-Short, Right)

Simulation Settings for Multiphase Flow Within a Sloshing Tank

AcuConsole database file: `<your working directory>\tank_sloshing_multiphase \tank_sloshing.acs`

Global

- Problem Description
  - Analysis type - Transient
  - Turbulence equation - SST
  - Multiphase equation – Level Set
- Auto Solution Strategy
  - Final time - `9.5` sec
  - Initial time increment - `0.001` sec
  - Min stagger iterations - `2`
  - Max stagger iterations - `10`
  - Fluid 1 - Water
  - Fluid 2 - Air

- Multiplier Function
  - rotation
    - Type - User Function
    - User function name - UsrMotion
    - User function values - `10.0`, `1.85`, `0.0`
- Material Model
  - Air
    - Type - Constant
    - Density - `1.225` kg/m^3
    - Velocity - `1.781e-5` kg/m-sec
  - Water
    - Type - Constant
    - Density - `1000` kg/m^3
    - Velocity - `0.001` kg/m-sec
- Mesh motion
  - rotation
    - Type - Rotation
    - Rotation center – `0.0`, `0.0`, `0.0`
    - Angular velocity – `0.0`, `0.0`, `0.0174533` (1.0 deg/sec)
    - Rotation variable – Multiplier Function
    - Rotation multiplier function – rotation

  Model
  - Volumes
    - Fluid
      1. Element Set
         1. Medium – Multiphase
         2. Multi field model – Water-Air
         3. Body force – Gravity
         4. Mesh motion – rotation
- Surfaces
  - x+
    - Simple Boundary Condition – Wall
  - x-
    - Simple Boundary Condition – Wall
  - y+
    - Simple Boundary Condition – Wall
  - y-
    - Simple Boundary Condition – Wall

- z+
  - Simple Boundary Condition – Slip
- z-
  - Simple Boundary Condition – Slip

References

Shin Hyung Rhee, 2005, "Unstructured Grid Based Reynolds-Averaged Navier-Stokes Method for Liquid Tank Sloshing", Journal of Fluids Engineering, Vol 127, pp. 572- 582.

Tanaka, Y., Ando, T., and Miyamoto, T., 2000, "Experimental Study on Sloshing Load Measured by Panel-Type Pressure Gauge," Proc. 74th. General Meeting of Ship Research Institute, Ship Research Institute, Tokyo, Japan, pp. 137-142.

Heat Transfer Between Radiating Concentric Spheres

In this application, AcuSolve is used to simulate the heat transfer due to conduction and radiation between concentric spheres. The inside surface of the inner and the outside surface of the outer sphere are both held at constant temperature, while the gap between them radiates the heat from one sphere to the other.

AcuSolve results are compared with analytical results for temperature and heat flux as described in Incropera (2006) and Salazar, et al. (2016). The close agreement of AcuSolve results with analytical results validates the ability of AcuSolve to model cases with radiation heat transfer and conjugate heat transfer with enclosure radiation modeling and the discrete ordinate (DO) radiation model.

Problem Description

The problem consists of a fluid region with arbitrary material properties between two concentric spheres with surfaces held at fixed temperature, as shown in the following image, which is not drawn to scale. The radius of the outer sphere is 0.04 m and the radius of the inner sphere is 0.01 m. The inner surface of the inner sphere is defined to have a constant wall temperature at 300.0 K (27 ºC). The outer surface of the outer sphere is defined to have a constant wall temperature at 1300.0 K (1027 ºC). The fluid within the spheres is defined as a non-conducting material, allowing heat to transfer via radiation only. The solid and fluid regions equilibrate to a steady temperature and can be compared with a semi-analytical solution for the temperature and heat flux at the fluid boundaries.

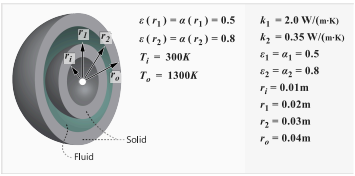


Figure 451: Critical Dimensions and Parameters used for Simulating Conduction and Radiation Between two Concentric Spheres



Figure 452: Mesh used for Simulating Radiation Between two Concentric Spheres

The simulation was performed as a three dimensional problem by constructing a volume mesh that contains a layer of boundary elements normal to the radial direction.

AcuSolve Results

The AcuSolve solution converges to a steady state and the results reflect the mean temperature distribution within the spheres. As the outer diameter is considerably hotter than the inner, a heat flux is present between the spheres. The temperature within the mediums increases as a function of the radius, with a slope corresponding to the temperature difference and the specified emissivity of the shells. The following image shows the temperature contour within the spheres along with the two-dimensional plot of the temperature versus radius in the solid mediums. The temperature and heat flux at the radiation surfaces are compared with the analytical solution as described in Salazar, et al. (2016).

Table 30: The Analytical Solution for the Temperature and Heat Flux at r1 and r2 are Presented with the Corresponding AcuSolve Results for the Enclosure (Surface to Surface) Model and the DO

	T(r1) (K)	T(r2) (K)	Q(r1) (W)	Q(r2) (W)
Analytical	578.2	1035.0	-27822.5	12365.6
AcuSolve (Enclosure)	578.4	1035.1	-27827	12364.2
AcuSolve (DO)	561.8	1023.6	-26175	12897.0
Percent Difference (Enclosure)	0.034%	0.010%	-0.015%	-0.011%
Percent Difference (DO)	2.8%	-1.11%	5.92%	4.3%

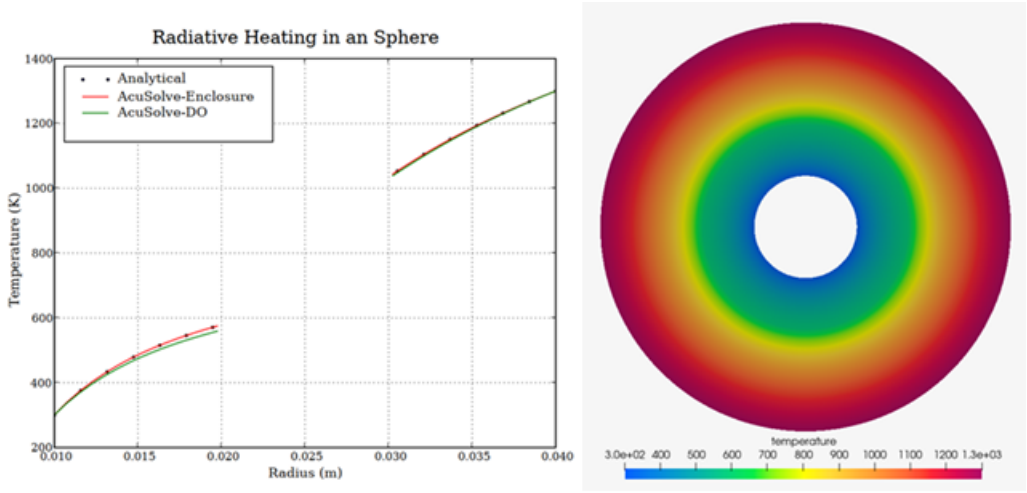


Figure 453: Two-Dimensional Plot and Contours of Temperature Between the Concentric Spheres

Summary

The AcuSolve solution compares well with analytical results for heat transfer due to conduction and radiation between two concentric spheres. In this application, an arbitrary material is subjected to a heat flux that is calculated based on the view factors or the DO model within the simulation. As a result of the conjugate heat transfer and the radiative heat flux a temperature distribution between the two spheres develops. The AcuSolve solution for the temperature and heat flux at the radiation surfaces matches well compared to the analytical solution with only a minor difference for the enclosure radiation model. The enclosure radiation model was found to have a higher accuracy for this application compared to the DO model, as expected due to the relatively low optical thickness in this simulation.

Heat Transfer Between Radiating Concentric Spheres

HyperWorks CFD database file: `<your working directory>\sphere_radiation\sphere_radiation.hm`.

Global

- Problem Description
  - Analysis type - Steady State
  - Turbulence equation - Advective Diffusive
  - Radiation equation - Enclosure
- Auto Solution Strategy
  - Convergence tolerance - `1.0e-5`
  - Relaxation Factor - `0.4`
  - Flow - off
  - Enclosure radiation - on
- Material Model
  - Inner
  - Conductivity

        - Type - Constant
        - Conductivity - `2.0`
    - Outer
    - Conductivity
        - Type - Constant
        - Conductivity - `0.35`
    - Radiating
    - Conductivity
        - Type - Constant
        - Conductivity - `1.0e-6`
- Emissivity Model
- Inner
    - Emissivity - `0.5`
- Outer
    - Emissivity - `0.8`

  Model
- Volumes
    - Inner
        - Element Set
            1. Medium- Solid
            2. Material model - Inner
        - Outer
            1. Element Set
                1. Medium - Solid
                2. Material model - Outer
        - Radiating
            1. Element Set
                1. Medium - Fluid
                2. Material model - Radiating
- Surfaces
    - Inner_Inner_r1
        - Simple Boundary Condition - (disabled to allow for heat flux)
    - Inner_Inner_ri
        - Simple Boundary Condition
            1. Type - Wall
            2. Temperature BC type - Value
            3. Temperature - `300.0` K

- Inner_Radiating_r1
  - Simple Boundary Condition (disabled to allow for heat flux)
  - Radiation Surface
    1. Type - Wall
    2. Emissivity model - Inner
- Outer_Outer_r2
  - Simple Boundary Condition (disabled to allow for heat flux)
- Inner_Outer_ro
  - Simple Boundary Condition
    1. Type - Wall
    2. Temperature BC type - Value
    3. Temperature - `1300.0` K
- Outer_Radiating_r2
  - Simple Boundary Condition (disabled to allow for heat flux)
  - Radiation Surface
    1. Type - Wall
    2. Emissivity model - Outer

References

F. P. Incropera and D. P. DeWitt. "Fundamentals of Heat Transfer – Sixth Edition". John Wiley & Sons. New York. 2006.

Salazar, G., Droba, J., Oliver, B., & Amar, A. J. (2016). Development and Verification of Enclosure Radiation Capabilities in the CHarring Ablator Response (CHAR) code. 46th AIAA Thermophysics Conference.

Radiation Heat Transfer Through a Cube with a Specular Interface

In this application, AcuSolve is used to simulate the heat transfer due to radiation through a specular interface within an absorbing, emitting, but not scattering solid cube. One of the cube's walls is modeled with an isotropic external radiation source while the remainder of the cube is held at fixed temperature conditions and modeled with pure radiation, neglecting the effects of conduction.

The internal surface between the two equal solid portions of the cube is specified to be a completely specular boundary condition. AcuSolve results are compared with accepted numerically derived results of incident radiation, as described in Muresan (2004) and Łapka (2012). The close agreement of the AcuSolve results and the published data validates the solver's ability to model cases with semi-transparent media with differing material properties using the discrete ordinates radiation model.

Problem Description

The problem consists of a solid region with fixed material properties similar to glass separated into two equal size cuboids to form a symmetrical cube with a side length of 1.0 m. The left most wall (minimum z) receives an external radiation source at a fixed temperature of 450.0 K (177 ºC) while the right most wall (maximum z) is prescribed a fixed temperature of 375.0 K (102 ºC), as shown in the following image, not drawn to scale. The solid, semi-transparent material is specified for each glass cuboid with n1=1.5, κ1=0.2 for glass1 and n2=1.25, κ2=2.0 for glass2. Only the solution to the radiative transfer equation on a discrete number of ordinate directions is considered, thus neglecting conduction. The solid regions equilibrate to a steady radiative state and are compared with a semi-analytical solution for the incident radiation across the centerline of the cube.

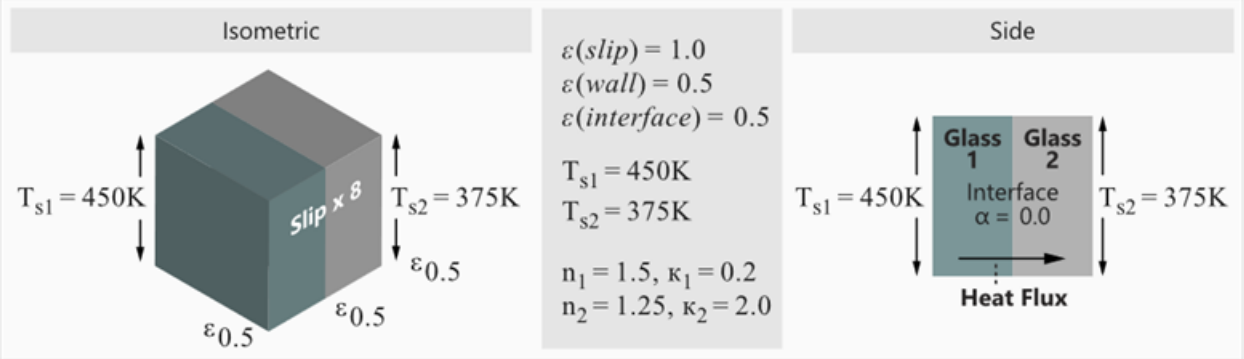


Figure 454: Critical Dimensions and Parameters Used for Simulating Radiation Heat Transfer Through a Cube with a Specular Interface

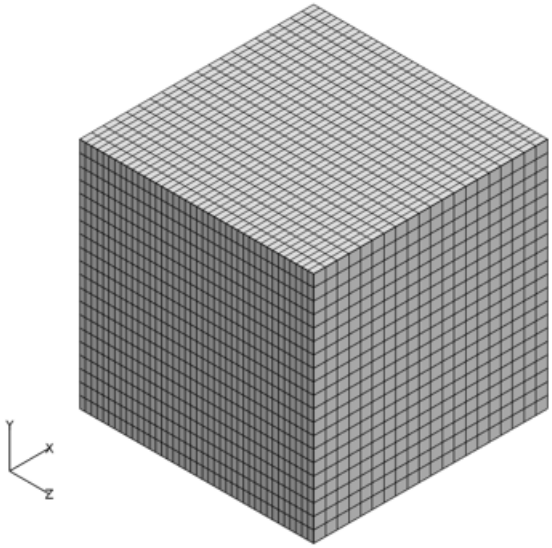


Figure 455: Mesh Used for Simulating Radiation Heat Transfer Through a Cube with a Specular Interface

The simulation was performed as a three-dimensional problem by constructing a volume mesh that contains all hexahedral elements with 20, 20, 40 cells in the x, y, z directions.

AcuSolve Results

The AcuSolve solution converges to a steady state and the results reflect the mean radiative state within the cube. Since the left side of the cube receives the external radiation source, the incident radiation is highest at that location. The transmission of the radiation decreases linearly within the first cuboid until it reaches the interface between the two materials. The discontinuity in the radiation field is demonstrated at the interface location, resulting from the specular reflection of radiation as it tries to travel from one material to the other. As the incident radiation passes through the second glass material, the simulation demonstrates how the material's higher absorption properties will produce a non-linear irradiance distribution. The following image shows the incident radiation contour within the two media along with the two-dimensional plot of the normalized incident radiation as a function of the non-dimensional cube length, where the incident radiation is normalized by $G^* = \sigma T^4$. The incident radiation is compared with the numerical solution as described in Muresan, et al. (2004).

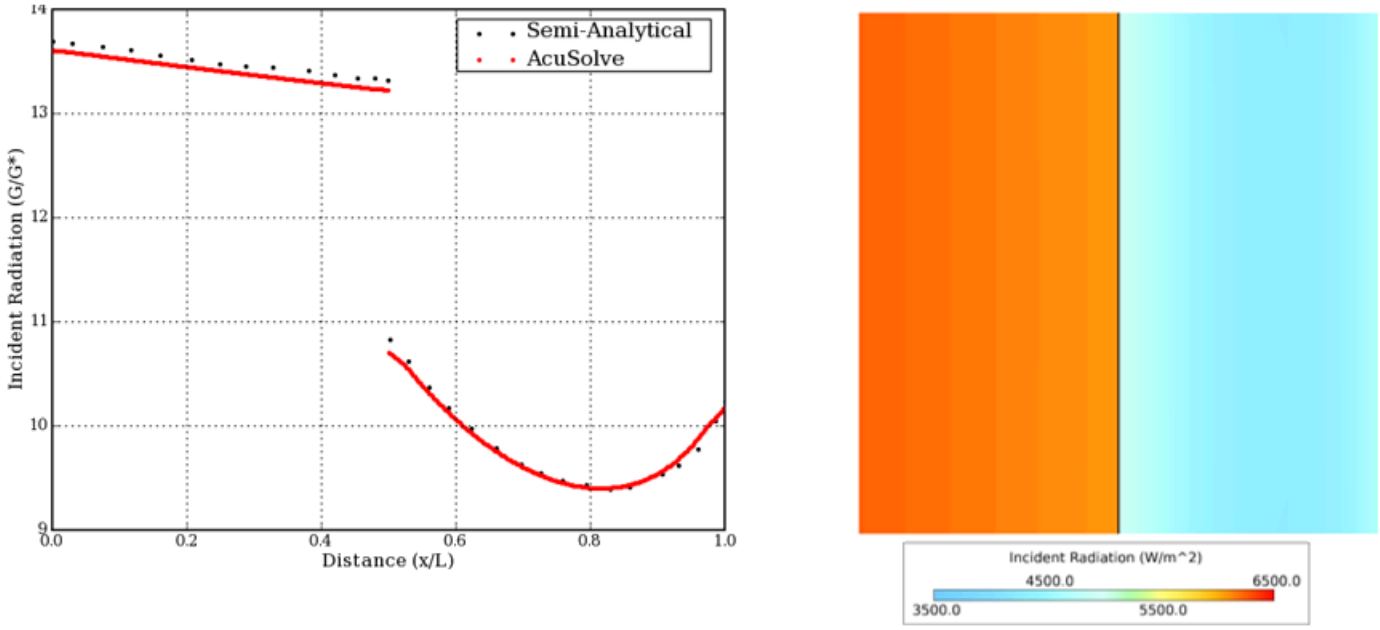


Figure 456: Two-Dimensional Plot and Contours of Incident Through a Cube with a Specular Interface

Summary

The AcuSolve solution compares well with numerical results for heat transfer due to radiation within a cube containing a specular interface. In this application, two arbitrary materials are subjected to a constant external radiative heat source and the media are defined to absorb, emit, but not scatter the irradiation. As a result of the prescribed radiative heat flux on the left most wall and the fixed temperature constraint across the entire domain, each media receives a non-trivial, varying amount of incident radiation. The AcuSolve solution for the incident radiation across the interface matches well compared to the numerical solution with only a minor difference at the far-right hand side of the domain. The discrete ordinate model requires a fairly large number of ordinate directions in order to obtain the highest accuracy solution. The published results are produced using the S14 quadrature, which is equivalent to 224 discrete ordinate directions.

Radiation Heat Transfer Through a Cube with a Specular Interface

HyperMesh database file: `<your working directory>\cube_specular_radiation\cube_specular_radiation.hm`.

Global

- Problem Description
  - Analysis type - Steady State
  - Turbulence equation - Advective Diffusive
  - Radiation equation - Discrete Ordinate
  - Radiation Ordinate - S14
- Solver Settings
  - Convergence tolerance - `1.0e-3`
  - Relaxation Factor - `0.3`

    - Flow - off
    - Temperature - off
- Nodal_Initial_Condition
    - Temperature
        - Type - Constant
        - Default Value - `300.0` K

Materials

- Glass_HM
    - Density
        - Type - Constant
        - Density - `2500.0`
    - Specific Heat
        - Type - Constant
        - Conductivity - `830`
    - Conductivity
        - Type - Constant
        - Conductivity - `1.3`
    - Radiation Properties
        - Allow Participating Media Radiation - On
        - Absorption Coefficient - `0.2`
        - Scattering Coefficient - `0.0`
        - Phase Coefficient - `0.0`
        - Refractive Index - `1.5`
- Glass2_HM
    - Density
        - Type - Constant
        - Density - `2500.0`
    - Specific Heat
        - Type - Constant
        - Conductivity - `830`
    - Conductivity
        - Type - Constant
        - Conductivity - `1.3`
    - Radiation Properties
        - Allow Participating Media Radiation - On
        - Absorption Coefficient - `2.0`
        - Scattering Coefficient - `0.0`

- Phase Coefficient - `0.0`
- Refractive Index - `1.25`

Emissivity Model

- BB05
  - Emissivity - `0.5`
- BB
  - Emissivity - `1.0`

Volumes

- S1
  - Type - Solid
  - Material model - Glass_HM
- S2
  - Type - Solid
  - Material model - Glass2_HM

Surfaces

- Wall_S1
  - Simple Boundary Condition
    1. Type - Wall
    2. Temperature BC type - Value
    3. Temperature - `450.0 K`
  - Radiation Surface
    1. Type - radiation interface
    2. Radiation interface type - external
    3. External emissivity model - BB
    4. Diffused fraction - `0.0`
- Wall_S2
  - Simple Boundary Condition
    1. Type - Outflow
  - Radiation Surface
    1. Type - Opening
    2. Opening temperature - 375.0 K
    3. Emissivity model - BB05
    4. Diffused fraction - `0.0`
- Interface_S1
  - Simple Boundary Condition
    1. Type - Auto Wall
  - Radiation Surface

1. Type - Radiation interface
2. Radiation interface type - internal
3. Diffused fraction - `0.0`

- Interface_S2
  - Simple Boundary Condition
    1. Type - Auto Wall
  - Radiation Surface
    1. Type - Radiation interface
    2. Radiation interface type - internal
    3. Diffused fraction - `0.0`
- Slip_1_S1
  - Simple Boundary Condition
    1. Type - Slip
- Slip_2_S1
  - Simple Boundary Condition
    1. Type – Slip
- Slip_3_S1
  - Simple Boundary Condition
    1. Type - Slip
- Slip_4_S1
  - Simple Boundary Condition
    1. Type - Slip
- Slip_1_S2
  - Simple Boundary Condition
    1. Type - Slip
- Slip_2_S2
  - Simple Boundary Condition
    1. Type - Slip
- Slip_3_S2
  - Simple Boundary Condition
    1. Type - Slip
- Slip_4_S2
  - Simple Boundary Condition
    1. Type - Slip

References

Muresan, Cristian & Vaillon, Rodolphe & Ménézo, Christophe & Morlot, Rodolphe. (2004). Discrete ordinates solution of coupled conductive radiative heat transfer in a two-layer slab with Fresnel

interfaces subject to diffuse and obliquely collimated irradiation. Journal of Quantitative Spectroscopy and Radiative Transfer. 84. 551-562. 10.1016/S0022-4073(03)00271-1.

Łapka, Piotr & Furmański, Piotr. (2012). Fixed Cartesian grid based numerical model for solidification process of semi-transparent materials II: Reflection and refraction or transmission of the thermal radiation at the solid–liquid interface. International Journal of Heat and Mass Transfer. 55. 4953–4964. 10.1016/j.ijheatmasstransfer.2012.03.077.

Two-Phase Nucleate Boiling in a Cylindrical Pipe

In this application, AcuSolve is used to simulate the changes in wall temperature due to two-phase nucleate boiling at the heated walls of a pipe with water flowing through it. AcuSolve results are compared with experimental results adapted from Koncar and others (2015). The close agreement of AcuSolve results with experimental results validates the ability of AcuSolve to model two-phase nucleate boiling problems.

Problem Description

The problem consists of a pipe with heated surrounding walls, as shown in the following image, which is not drawn to scale. The length of the pipe is 2 m and the radius is 0.0017 m. Mass flux at the inlet is 900 kg/m^2 and the temperature of the fluid entering the pipe is 473 K. A heat flux of 570,000 W/m^2 is applied on the walls. The preheated water enters the inlet and heat is transferred to the fluid from the walls. The heat causes sub-cooled boiling to occur in the region close to the wall and leads to the formation of bubbles at nucleation sites.

During sub-cooled boiling flow, heat and mass exchange between the phases takes place on the heated wall and in sub-cooled liquid flow. On the heated surface the vapor bubbles are generated and as they move through the sub-cooled liquid they condense and release the latent heat.

The AcuSolve simulation is set up to model transient state heat transfer to determine the temperature along the centerline of the pipe and along the heated pipe walls of the model. AcuSolve computes the two-phase nucleate boiling by simulating the three-dimensional flow in a heated pipe for two-phase boiling flow, as described in Koncar (2005). The temperatures along the centerline of the pipe and along the pipe walls are compared against the experimental measurements, as described in Koncar, et al. (2005).

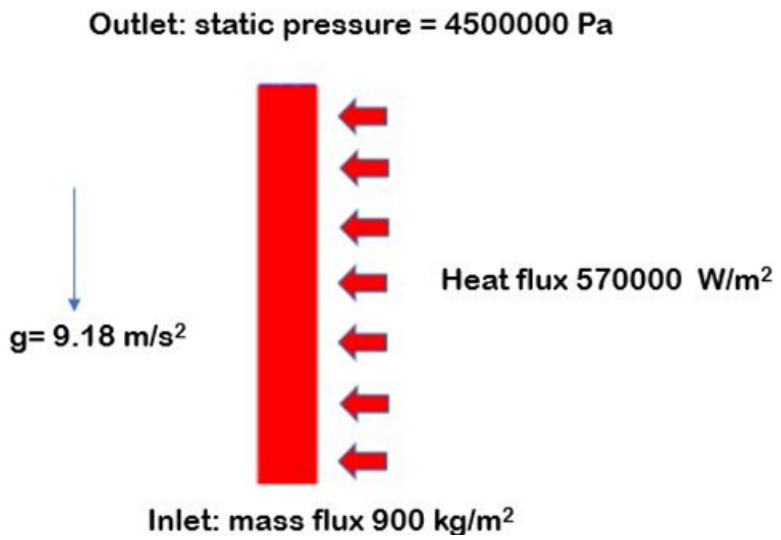


Figure 457: Parameters for Simulating a Two-Phase Nucleate Boiling Problem of a Pipe

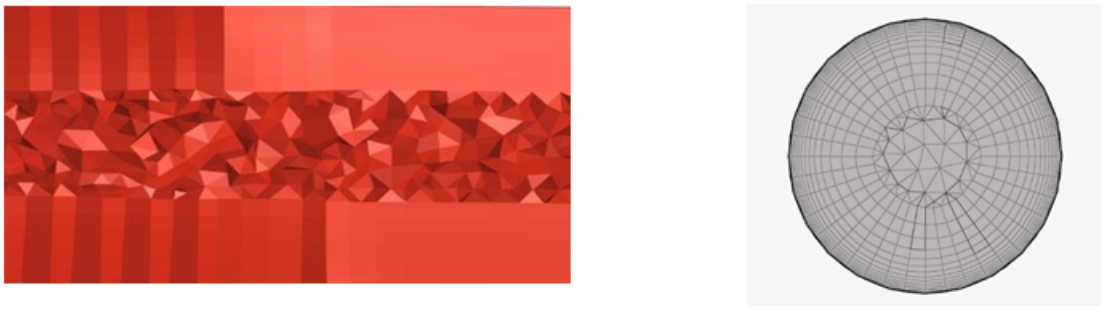


Figure 458: Mesh used for Simulating Two-Phase Flow in a Pipe

AcuSolve Results

The AcuSolve solution is run for a heat flux of 570,000 W/m^2 and the results are presented in the following image. The experimental values of wall temperature are presented with the corresponding AcuSolve results along the centerline of the pipe and along the pipe wall. The AcuSolve results show good agreement with the experimental results for the temperature, indicating that the two-phase nucleate boiling is properly captured.

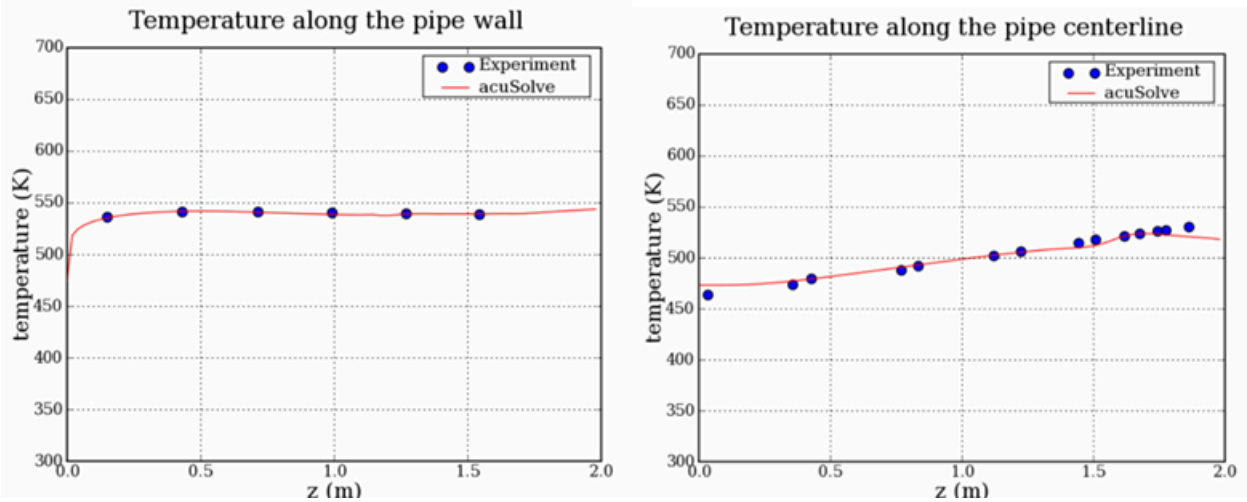


Figure 459: Temperature Values for Varying Streamwise Distance Compared to Experimental Data

Summary

The AcuSolve solution compares well with experimental results for two-phase nucleate boiling simulations. In this application, the temperature of the wall as the onset of boiling approaches are simulated with AcuSolve using the nucleate boiling feature and the SA turbulence model. The experimental values of temperature are presented with the corresponding AcuSolve results. A good agreement of simulation results with the experiment validates the ability to solve two-phase nucleate boiling using the nucleate boiling capabilities of AcuSolve.

Simulation Settings for Two-Phase Nucleate Boiling in a Cylindrical Pipe

HyperWorks database file: `<your working directory>\pipe_two_phase_boiling\pipe_two_phase_boiling.hm`.

Global

- Problem Description
  - Analysis type – Transient
  - Turbulence equation – SA
  - Temperature equation – Advective Diffusive
- Auto Solution Strategy
  - Maximum time steps – `500`
  - Initial time increment – `0.003`
  - Convergence Tolerance – `0.001` sec
  - Relaxation factor – `0.3`
- Surface Tension Model (“Water_NB-Vapor_NB”)
  - Type – Constant
  - Surface Tension – `0.02382`
- Material Model
  - Vapor_NB
    - Type – Constant
    - Density – `23.75` kg/m^3
    - Viscosity – `1.79e-05` kg/m-sec
    - Specific Heat – `4225` J/kg-K
    - Latent Heat – `1675570`
    - Latent Heat Temperature – `530.55` K
    - Conductivity – `0.02528` W/m-K
  - Water_NB
    - Type – Constant
    - Density – `800` kg/m3
    - Viscosity – `0.0001339` kg/m-sec
    - Specific Heat – `4500` J/kg-K
    - Conductivity – `0.65` W/m-K
- Multifield parameter (Field interaction model)
  - Type – Algebraic Eulerian
  - Phase change type – Wall Boiling
  - Carrier field - Water
  - Disperse field – Vapor
  - Disperse field diameter type – Boiling kurul exponential
  - Drag model – Ishii zuber
  - Lift Model – Legendre Magnaudet

Model

- Volumes
  - Fluid
    - Material – Vapor_Water
- Surfaces
  - Inflow
    - Simple Boundary Condition – Inflow
    - Inflow type – Mass Flux Rate
    - Mass Flux Rate – `0.167634` kg/sec
    - Temperature – `473` K
  - Outflow
    - Simple Boundary Condition – Outflow
    - Pressure – `4500000` N/m2
  - Wall
    - Simple Boundary Condition – Wall
    - Temperature type – Flux
    - Heat Flux – `570000` W/m2

References

B. Koncar, E. Krapper, Y. Egorov, 2005, "CFD MODELING OF SUBCOOLED FLOW BOILING FOR NUCLEAR ENGINEERING APPLICATIONS", International Conference Nuclear Energy for New Europe 2005, Bled, Slovenia, September 5-8,2005.

Single-Phase Nucleate Boiling in a Rectangular Channel

In this application, AcuSolve is used to simulate the wall heat flux due to nucleate boiling at a heated wall inside a rectangular channel with water flow. Results are compared with experimental heat flux measurements as reported by Steiner, et al. (2005). The close agreement of AcuSolve results with experimental results validates the ability of AcuSolve to model single phase nucleate boiling problems.

Problem Description

The problem consists of a channel with a heated wall at the bottom. The temperature of the wall is selected to onset the nucleate boiling at the heated wall. The dimensions of the inlet are 0.03 x 0.04 m; the inlet velocity (v) is 0.39 m/s and the temperature (T) of the fluid entering the inlets is varied from 373.15 K (100 C) to 406.15 (133 C)), while the atmospheric pressure is specified to be 2 bar. The pre-heated water enters the inlets and heat is transferred into the fluid from the heated walls. The heat causes sub-cooled boiling to occur in the region close to the wall and leads to the formation of bubbles at nucleation sites. The surface tension and vapor phase models are specified to emulate the physical process of water changing state to water vapor.

The heat transfer in this regime is dominated by two effects, the macro convection due to the motion of the bulk liquid and the latent heat transport associated with the evaporation of the liquid micro-layer between the bubble and the heated wall. Each of these effects are modeled with AcuSolve and the prediction of their processes is demonstrated in the following results.

The AcuSolve simulation is prepared as a steady state heat transfer simulation to determine the temperature and heat flux on the heated walls of the model. AcuSolve computes the single-phase nucleate boiling by employing Chen’s model for two-phase boiling flow described in Chen (1966). The heat flux values for different wall temperatures are compared against the experimental measurements, as described in Steiner, et al. (2005).

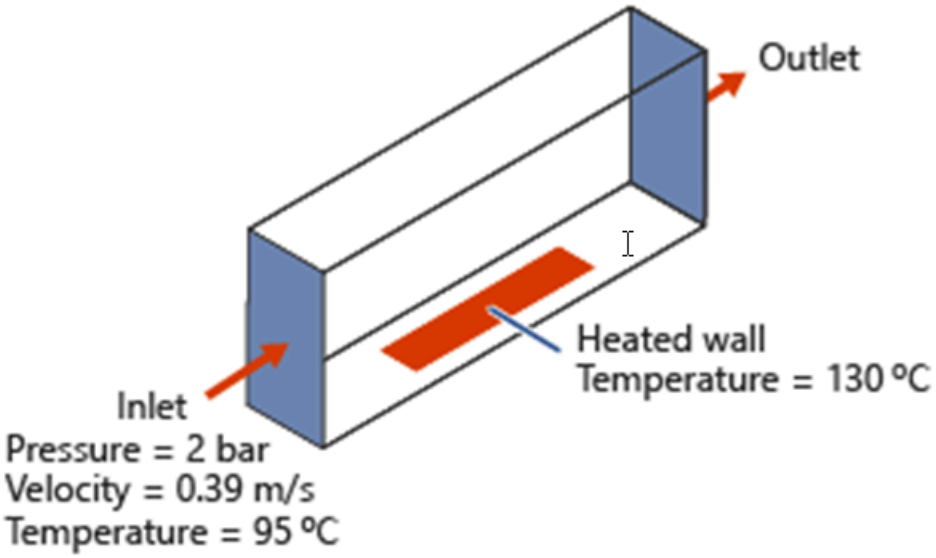


Figure 460: Critical Dimensions and Parameters for Simulating a Single-Phase Nucleate Boiling in a Rectangular Channel

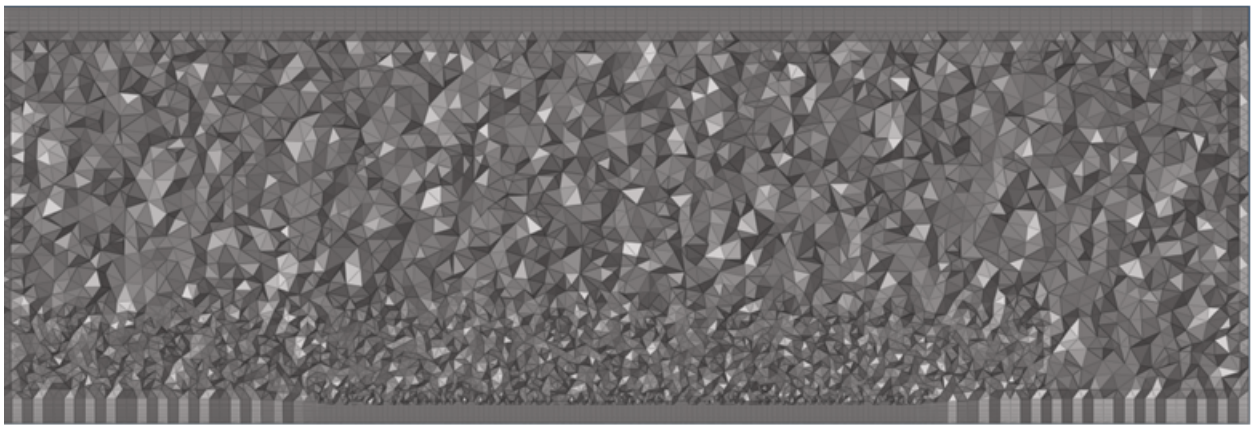


Figure 461: Mesh Used for Simulating a Single-Phase Nucleate Boiling in a Rectangular Channel

AcuSolve Results

The AcuSolve solution is run for heated wall temperature values of 100 C, 105 C, 110 C, 115 C, 120 C, 125 C, 130 C, 133 C and the results presented reflect the heat flux from the wall as the temperature nears the saturation temperature. The experimental values of heat flux (MW/m2) and wall temperature are presented with the corresponding AcuSolve results at seven temperature values. The AcuSolve results show good agreement with the experimental results for the heat flux, indicating that the single-phase nucleate boiling is properly captured.

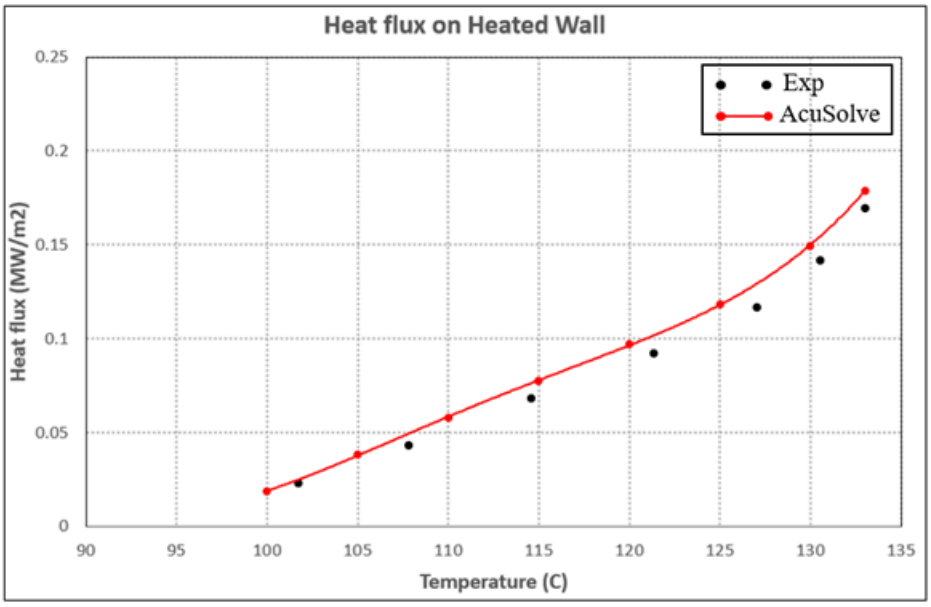


Figure 462: Heat Flux Values for Varying Wall Temperatures Compared to Experimental Data

Summary

The AcuSolve solution compares well with experimental results for single-phase nucleate boiling simulations. In this application, heat flux generated by the wall as the onset of boiling approaches are simulated with AcuSolve using the nucleate boiling feature and the RKE turbulence model. The experimental values of heat flux for the wall temperature range are presented with the corresponding AcuSolve results. A good agreement of simulation results with the experiment validates the ability to solve single-phase nucleate boiling using the nucleate boiling capabilities of AcuSolve.

Simulation Settings for Single-Phase Nucleate Boiling in a Rectangular Channel

HyperWorks CFD database file: `<your working directory>\channel_single_phase_boiling \channel_single_phase_boiling.hm`.

Global

- Problem Description
  - Analysis type – Steady
  - Turbulence equation – RKE
  - Temperature equation – Advective Diffusive
  - Nucleate Boiling Single Phase – On
- Auto Solution Strategy
  - Convergence Tolerance – `0.001` sec
  - Relaxation factor – `0.4`
- Surface Tension Model (“Water-srfTns”)
  - Type – Constant
  - Surface Tension – `0.07`

- Material Model
  - Vapor
    - Type – Constant
    - Density – `1.128` kg/m^3
    - Viscosity – `1.29e-5` kg/m-sec
    - Specific Heat – `2174.59` J/kg-K
    - Latent Heat – `2256000`
    - Latent Heat Temperature – `393.45` K
    - Conductivity – `0.02749` W/m-K
    - Turbulent Prandtl number – `1.0`
  - Water
    - Type – Constant
    - Density – `965.36` kg/m^3
    - Viscosity – `0.000314` kg/m-sec
    - Specific Heat – `4204.8` J/kg-K
    - Conductivity – `0.675` W/m-K
    - Turbulent Prandtl number – `0.91`
    - Vapor phase model – Vapor
    - Surface Tension model – Water-srfTns

Model

- Volumes
  - Fluid
    - Material– Water
- Surfaces
  - Inflow
    - Simple Boundary Condition – Inflow
    - Inflow type – Average Velocity
    - Average Velocity – `0.39` m/sec
    - Temperature – `368.15` K
  - Outflow
    - Simple Boundary Condition – Outflow
    - Back flow condition – On
    - Temperature back flow type – Mass flux average
    - Kinetic energy back flow type – Mass flux average
    - Dissipation rate back flow type – Mass flux average
  - Bottom
    - Simple Boundary Condition – Wall
  - Top

        - Simple Boundary Condition – Wall
    - Side_MinY
        - Simple Boundary Condition – Wall
    - Side_MaxY
        - Simple Boundary Condition – Wall
    - Heated Wall
        - Simple Boundary Condition – Wall
        - Temperature type – Value
        - Temperature – [373.15, 378.15, 383.15, 388.15, 393.15, 398.15, 403.15, 406.15] K

References

Helfried Steiner, Alexander Kobor, Ludwig Gebhard, 2005, "A wall heat transfer model for subcooled boiling flow", International Journal of Heat and Mass Transfer, Vol 48, pp. 4161- 4173.

Chen, J.C., 1966, "Correlation for Boiling Heat Transfer to Saturated Fluids in Convective Flow", United States: N. p., 1962. Web. doi:10.2172/4636495.

Supersonic Flow Through a Converging-Diverging Nozzle

In this application, AcuSolve is used to simulate the high-speed turbulent flow in a converging and then diverging nozzle. The flow within the nozzle enters as subsonic, reaches sonic at the throat and shortly after develops a normal shock. AcuSolve results are compared with experimental results adapted from Bogar and Sajben (1983). The close agreement of AcuSolve results to experimental measurements validates the ability of AcuSolve to simulate internal supersonic flows where normal shocks are present.

Problem Description

The problem consists of a converging and then diverging nozzle represented as an extruded planar surface, as shown in the image below, which is not drawn to scale. The length of the domain is 0.213 m with a throat height of 0.044 m. The stagnation pressure and static temperature are constrained at the inlet to 135,000 Pa and 265.98 K, respectively. The static pressure is defined using the outflow boundary condition, where P_{static}=97216.08 Pa. The flow in the diffuser has an inlet Reynolds number of $6.5x10^5$. The upper and lower walls are set to no-slip and the side walls are set to slip, while the exterior walls are specified to be adiabatic. Images of the numerical mesh are shown below.

The AcuSolve simulation is prepared to model the pseudo-transient state to determine the shock location and corresponding scalar quantities within the diffuser. AcuSolve computes the flow and thermal solution by simulating a planar, two-dimensional flow problem with physical dimensions and input quantities as described in the Sajben Diffuser case presented by Bogar and Sajben (1983). The gas in the simulation domain enters at subsonic conditions and is forced to accelerate beyond Mach=1.0 as it passes through the throat. After reaching supersonic speed a normal shock wave develops causing the flow speed to reduce back below sonic. The pressure along the bottom wall of the diffuser is compared against experimental measurements to demonstrate the solver's capability to solve supersonic cases.

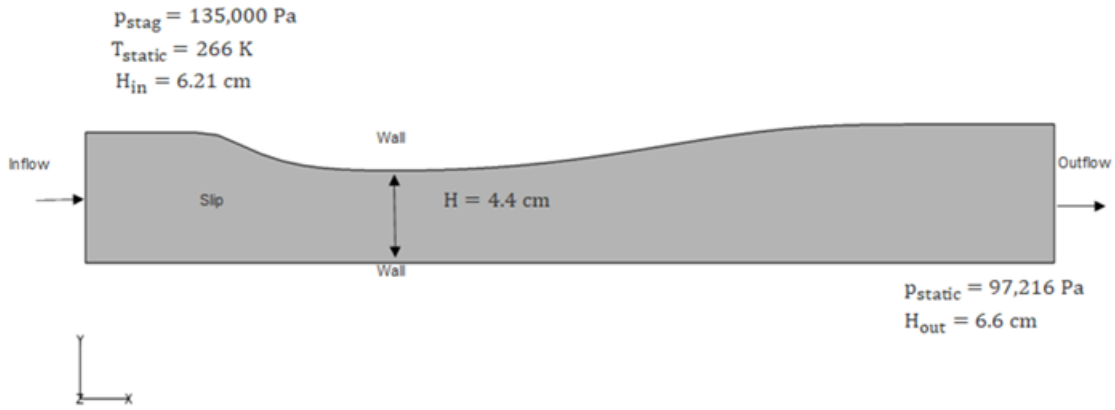


Figure 463: Parameters for Simulating Compressible Flow within a Converging-Diverging Nozzle

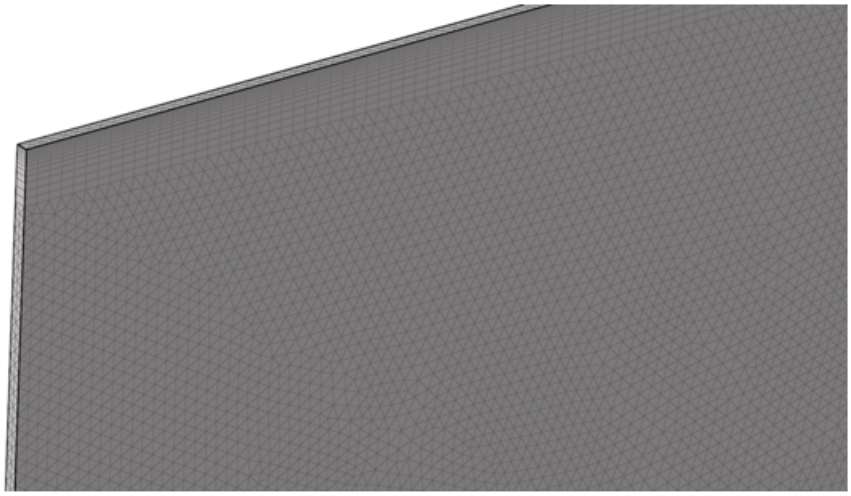


Figure 464: Mesh used for Simulating Compressible Flow in a Converging-Diverging Nozzle

AcuSolve Results

The AcuSolve solution is run for 0.025 seconds (6,250 timesteps with dt=4.0x10^{-6}sec) and converges to a pseudo-steady solution. The change in pressure from the inlet to outlet causes the flow to accelerate within the throat of the diffuser until it reaches approximately Mach=1.35. A normal shock is present just downstream of where the cross-sectional area of the nozzle increases, as shown in the image below. The numerical solution can be compared with the reference after normalizing the pressure along the wall by the inlet stagnation pressure (135 kPa) and the distance along the bottom wall by the nozzle throat height (0.044 m). The image below shows the normalized pressure versus normalized distance in comparison to NASA reference and experimental results. The image shows black circles representing the experimental measurements (Bogar and Sajben 1983), a dashed blue line representing the SA solution as obtained through NASA publication (Mohler 2005) and a solid red line representing the AcuSolve results with the Spalart-Allmaras turbulence model. The non-dimensional pressure within the diffuser agrees well with the reference data, demonstrating the correct physical location of the normal shock and expected moderate flow speed reduction within the constant cross-section diffuser portion of the nozzle.

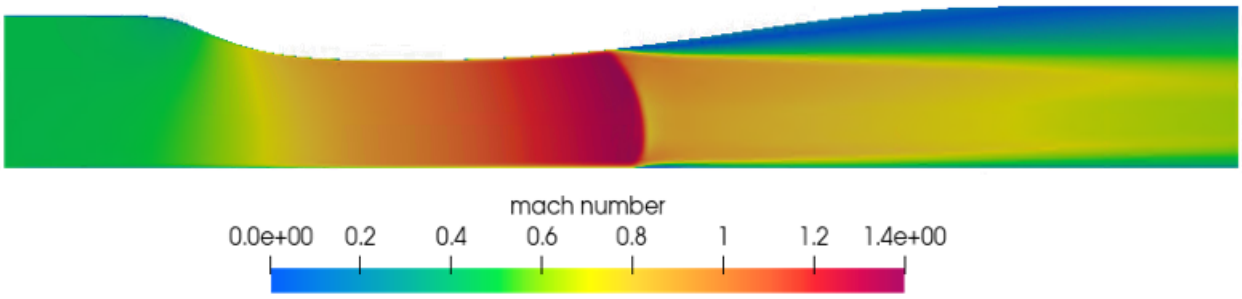


Figure 465: Contours of Mach Number within a Converging-Diverging Nozzle

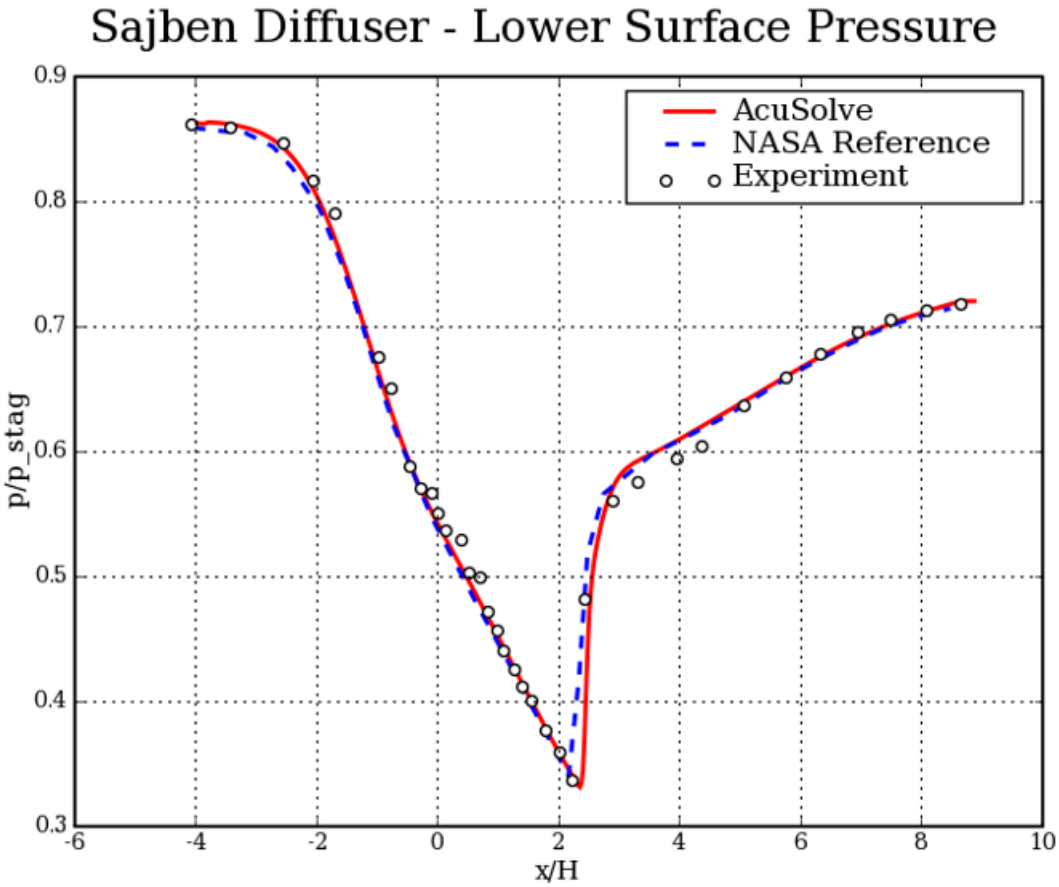


Figure 466: Normalized Pressure Versus Normalized Distance in Comparison to NASA Reference and Experimental Results

Summary

The AcuSolve solution compares well with experimental and numerical results for the described simulation. In this application, compressibility effects are accounted for using the coupled compressible flow solver with the ideal gas material definition. The thermal and momentum exchange within the nozzle is computed with AcuSolve using the compressible Navier-Stokes solver with the Spalart-Allmaras turbulence model. The experimental values of pressure are presented with the corresponding AcuSolve results and show good agreement, validating the ability to solve compressible cases with the presence of normal shocks. The results indicate that AcuSolve is able to properly predict the peak pressure magnitude and location within the diffuser while maintaining the normal shock when the time-step is selected to result in a maximum CFL of approximately 30.

Simulation Settings for Supersonic Flow Through a Converging-Diverging Nozzle

HyperWorks CFD database file: `<your working directory>\diffuser_compressible\diffuser_compressible.hm`

Global

- Problem Description

    - Flow – Compressible Navier Stokes
    - Analysis type – Transient
    - Turbulence equation – SA
    - Temperature equation – Advective Diffusive
- Auto Solution Strategy
    - Initial time increment – `4.0E-6`
    - Final time – `0.025` sec
    - Convergence Tolerance – `0.001` sec
    - Relaxation factor – `0.5`
- Material Model
    - Air-Ideal Gas
        - Type – Ideal_Gas
        - Viscosity – `1.781e-05` kg/m-sec
        - Specific Heat – `1005` J/kg-K
        - Conductivity – `0.02521` W/m-K
        - Gas Constant – `287.058` J/kg-K

Model

- Volumes
    - Fluid
        - Material – Air-Ideal Gas
- Surfaces
    - Inflow
        - Simple Boundary Condition – Inflow
        - Inflow type – Stagnation Pressure
        - Stagnation Pressure – `135000.0` N/m2
        - Turbulence_input_type – Direct
        - Eddy Viscosity – `1e-6` m^2/s
        - Temperature – `265.98` K
    - Outflow
        - Simple Boundary Condition – Outflow
        - Pressure – `97216.08` N/m2
    - Wall_1
        - Simple Boundary Condition – Wall
        - Type – auto_wall
    - Wall_2
        - Simple Boundary Condition – Wall
        - Type – auto_wall
    - Slip_1

        - Simple Boundary Condition – Slip
    - Slip_2
        - Simple Boundary Condition – Slip

References

Bogar, T. J., Sajben, M., and Kroutil, J. C. (1983) "Characteristic Frequencies of Transonic Diffuser Flow Oscillations," AIAA Journal, Vol. 21, No. 9, pp. 1232-1240.

Mohler, S.R., "Wind-US Unstructured Flow Solutions for a Transonic Diffuser," NASA CR-2005-213417, January 2005.

External Flow

6

This section includes validation cases that consider unbounded simulation domains where external flow is present over solid bodies, leading to free boundary layer development.

This chapter covers the following:

- Turbulent Flow Behind an Open-Slit V (p. 638)
- Turbulent Flow Over a NACA 0012 Airfoil (p. 645)
- Oscillating Laminar Flow Around a Circular Cylinder (p. 653)
- Separated Laminar Flow Over a Blunt Plate (p. 658)
- Turbulent Mixing Layers in an Open Channel (p. 665)
- Turbulent Flow Over an Oscillating Rigid Body Assembly (p. 670)
- Laminar to Turbulent Transition Over an Airfoil (p. 678)

Turbulent Flow Behind an Open-Slit V

In this application, AcuSolve is used to simulate turbulent flow of air through and behind a two dimensional open-slit V. AcuSolve results are compared with experimental results adapted from Yang and Tsai (1993). The close agreement of AcuSolve results with experimental results validates the ability of AcuSolve to model the Coandă effect.

Problem Description

The problem consists of air flowing through and past an open-slit V positioned within a flow domain, as shown in the following image, which is not drawn to scale. The flow domain is 0.3 m long and 0.1 m high. The narrow end of the V is positioned 0.05 m from the domain inlet. The slit in the V is 0.002 m high. The V widens to 0.022 m at 0.075 m from the domain inlet. Air enters the domain with a constant velocity of 20 m/s. The upper and lower limits of the domain are defined as no-slip boundary conditions.

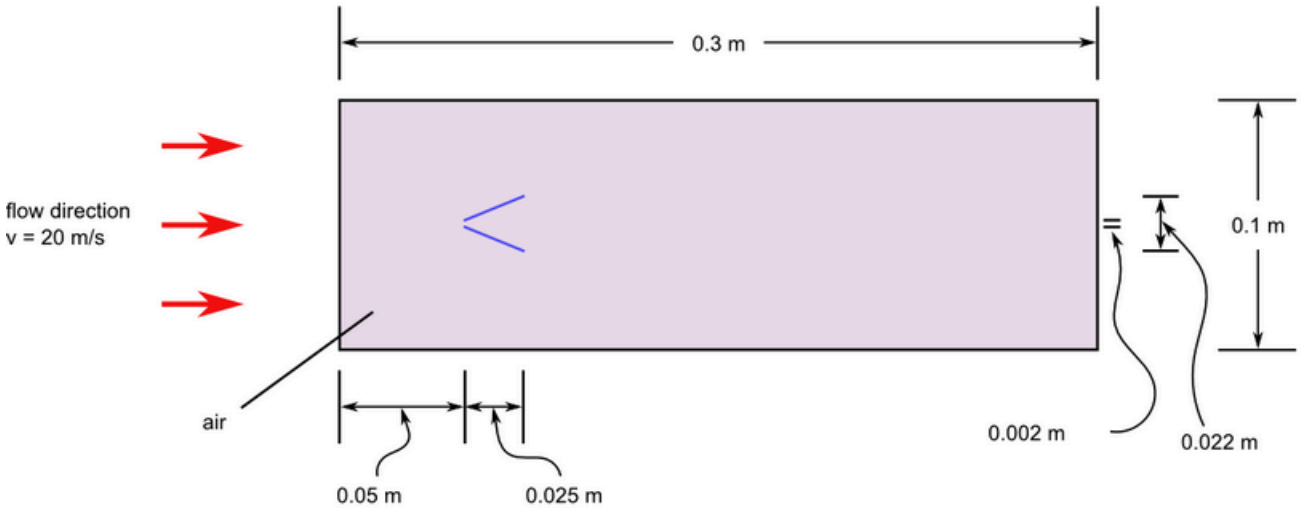


Figure 467: Critical Dimensions and Parameters for Simulating Turbulent Flow Behind an Open-Slit V

The simulation was performed as a two dimensional problem by restricting flow in the out-of-plane direction through the use of a mesh that is one element thick. A coarse mesh is used throughout much of the domain, with mesh refinement closer to the V.

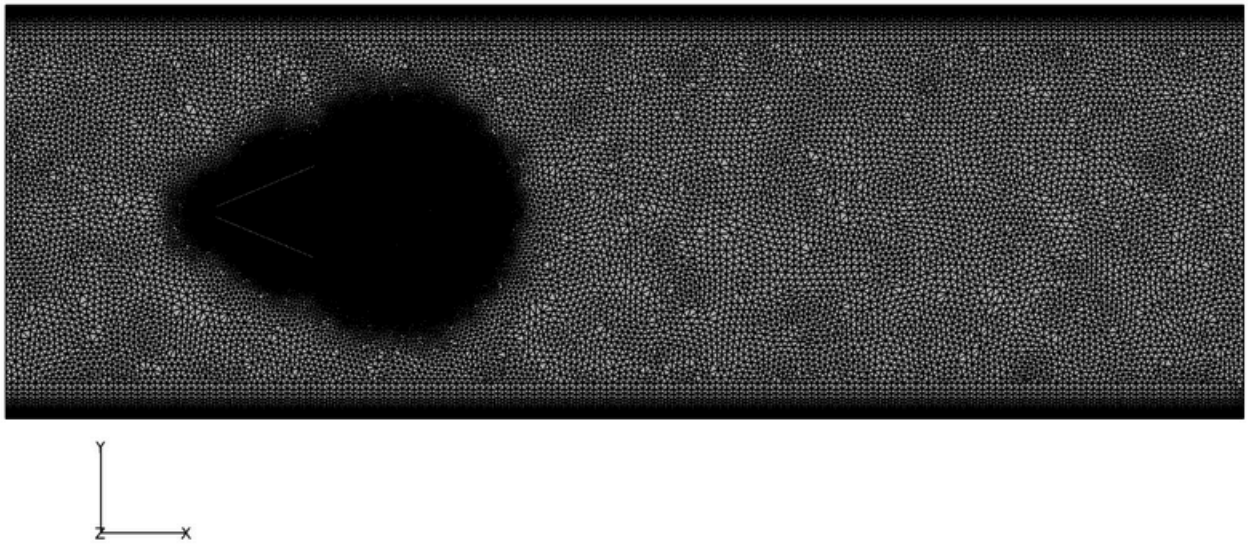


Figure 468: Mesh used for Simulating Turbulent Flow Behind an Open-Slit V (the V Lies Within the Dense Area of the Mesh)

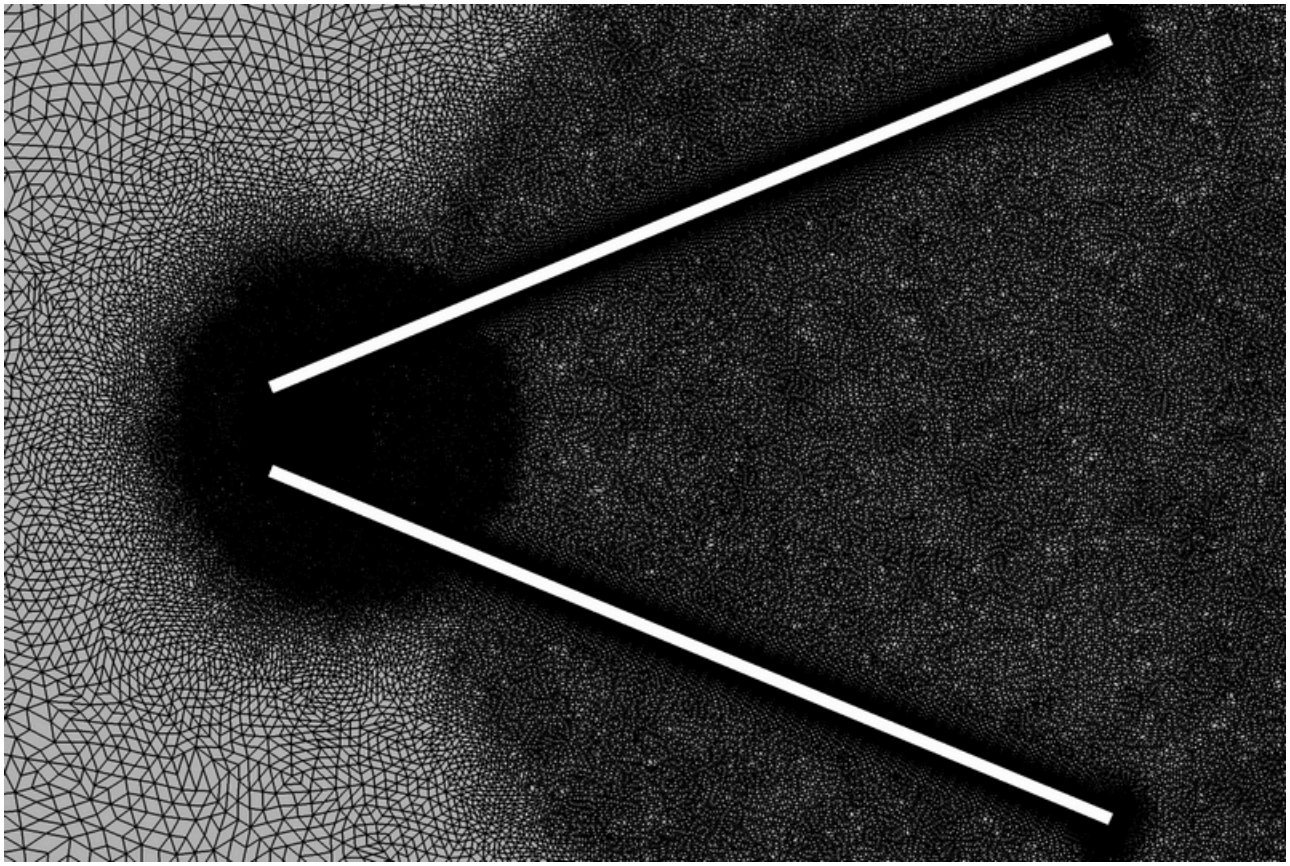


Figure 469: Mesh Surrounding the Open-Slit V

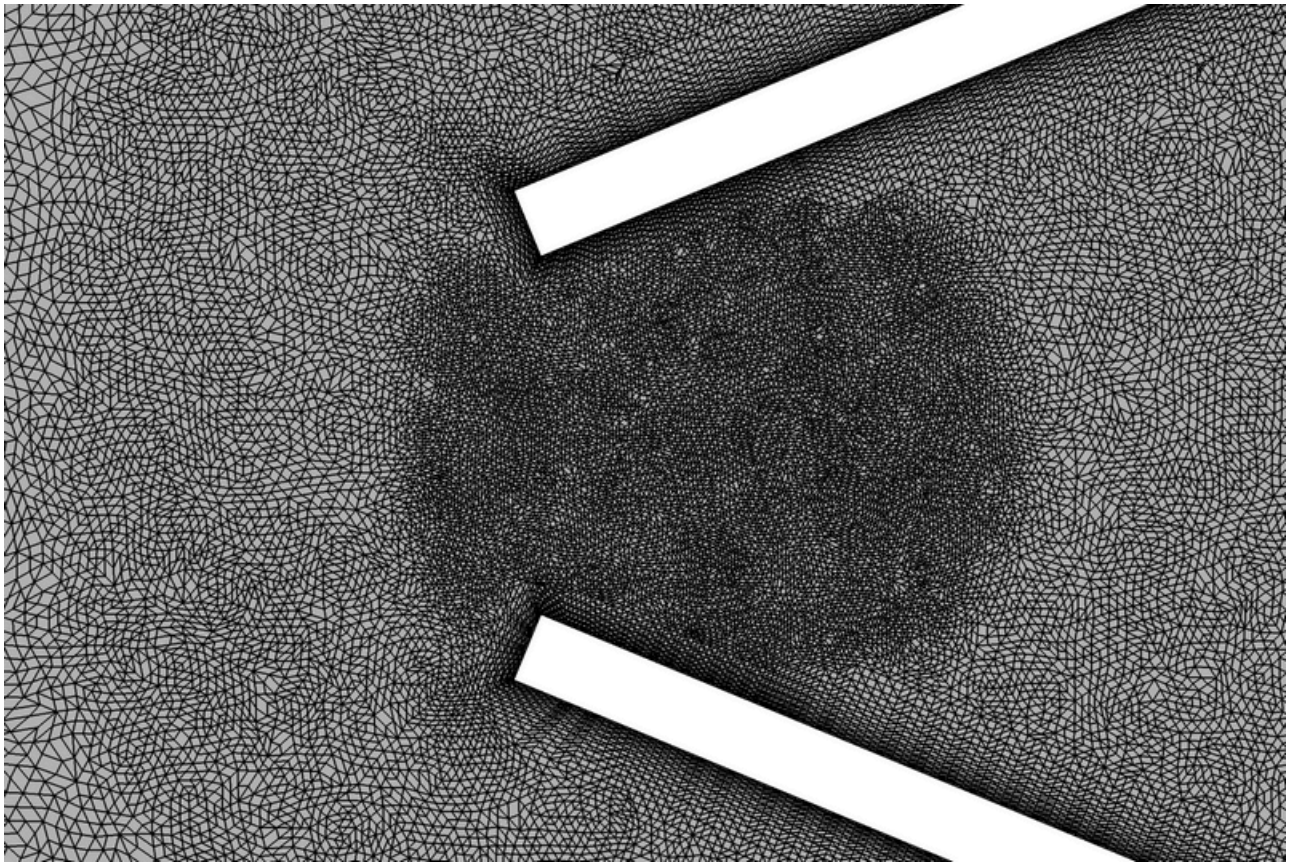


Figure 470: Mesh Near the Open Slit

AcuSolve Results

The AcuSolve solution converged to a steady state and the results reflect the mean flow conditions. Air flows through the open slit in the V and accelerates while being forced to one side due to the Coandă effect. As air encounters the exterior of the widening gutter, velocity increases and the wake induces recirculation near the exit of the V. The recirculation zone extends downstream of the V gutter.

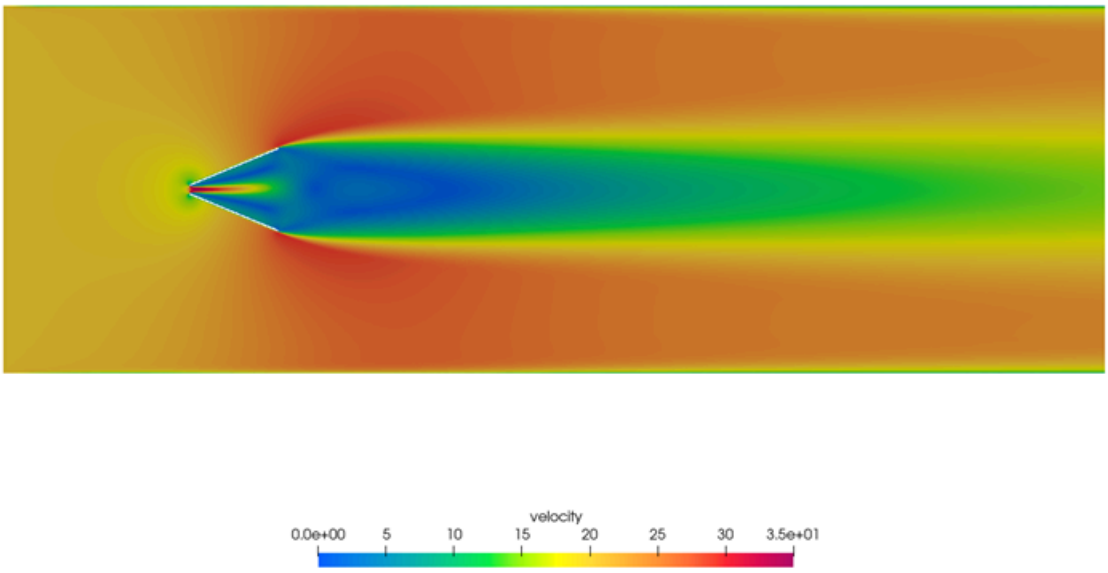


Figure 471: Contours of X-Velocity of Flow Through and Around an Open-Slit V (the Vertical Line Represents the Location, 0.022 m Downstream from the V exit, at Which Experimental Data is Compared to AcuSolve Results)

AcuSolve results were compared to experimental results at different heights 0.022 m behind the V exit. X-velocity is near zero at the bottom of the domain (height = -0.05 m), rising steeply with distance from the wall. The velocity gradient decreases until approximately 0.018 m below the center line of the domain, which is slightly below the bottom of the V exit. The velocity behind the V drops sharply with an increase in height, due to the blockage caused by the presence of the slanted walls. The lowest velocity is just above the center line of the domain.

The slight asymmetry in the velocity profile in the wake of the V is expected due to the Coandă effect.

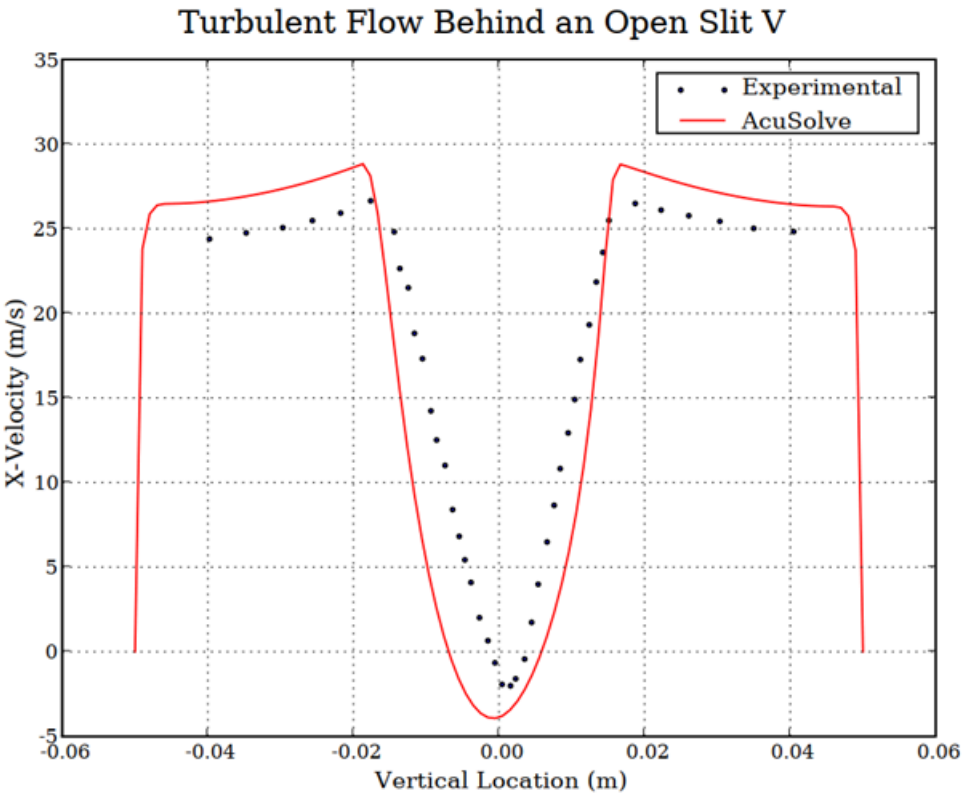


Figure 472: X-Velocity Plotted Against Vertical Location 0.0022 m Downstream of the V Exit

Summary

The AcuSolve results compare well with the experimental results for flow through and around an open-slit V. In this application, the V-shaped geometry diverts flow towards the side walls of the channel and also creates a high-velocity jet through the slit. The low pressure associated with the jet causes a deflection towards the walls of the V, resulting in an asymmetric flow field within the V shape. This application illustrates the ability of AcuSolve to accurately predict the Coandă effect. The acceleration of the flow due to the deflection along the V-shaped walls and the momentum deficit in the wake of the V is captured accurately.

Simulation Settings for Turbulent Flow Behind an Open-Slit V

HyperWorks CFD database file: `<your working directory>\v_gutter_turbulent\v_gutter_turbulent.hm`

Global

- Problem Description
  - Analysis type - Steady State
  - Turbulence equation - Spalart Allmaras
- Auto Solution Strategy
  - Relaxation factor - `0.5`
- Material Model

- Air
  - Density - `1.0` kg/m3
  - Viscosity - `1.8333e-05` kg/m-sec

Model

- Volumes
  - Fluid
    - Element Set
      1. Material model - Air
- Surfaces
  - Inlet
    - Simple Boundary Condition
      1. Type - Inflow
      2. Inflow type - Velocity
      3. X velocity - `20.0` m/sec
      4. Eddy viscosity - `0.000800426` m2/sec
  - LE_TE
    - Simple Boundary Condition
      1. Type - Wall
  - Outlet
    - Simple Boundary Condition
      1. Type - Outflow
  - Symm_MaxZ
    - Simple Boundary Condition
      1. Type - Slip
  - Symm_MinZ
    - Simple Boundary Condition
      1. Type - Slip
  - V_Walls
    - Simple Boundary Condition
      1. Type - Wall
  - Walls
    - Simple Boundary Condition
      1. Type - Wall

References

J.-T. Yang and G.-L. Tsai. "Near-wake flow of a v-gutter with slit bleed". Journal of Fluid Engineering. 115:13-20. March, 1993.

Turbulent Flow Over a NACA 0012 Airfoil

In this application, AcuSolve is used to simulate turbulent flow of a fluid over a NACA 0012 airfoil at 3 angles of attack, 0 degrees, 10 degrees, and 15 degrees. AcuSolve results are compared with experimental results for coefficients of pressure, lift, and drag reported by NASA. The close agreement of AcuSolve results with experimental results validates the ability of AcuSolve to model external aerodynamics.

Problem Description

The problem consists of a NACA 0012 airfoil located in the center of a cylindrical domain, as shown in the following image, which is not drawn to scale. Fluid enters the domain with a velocity of 1.0 m/s. The domain edges are distant, 500 chord lengths, from the airfoil to minimize any far field effects. The problem is set up to simulate high Reynolds number flow, with Re = 6,000,000.

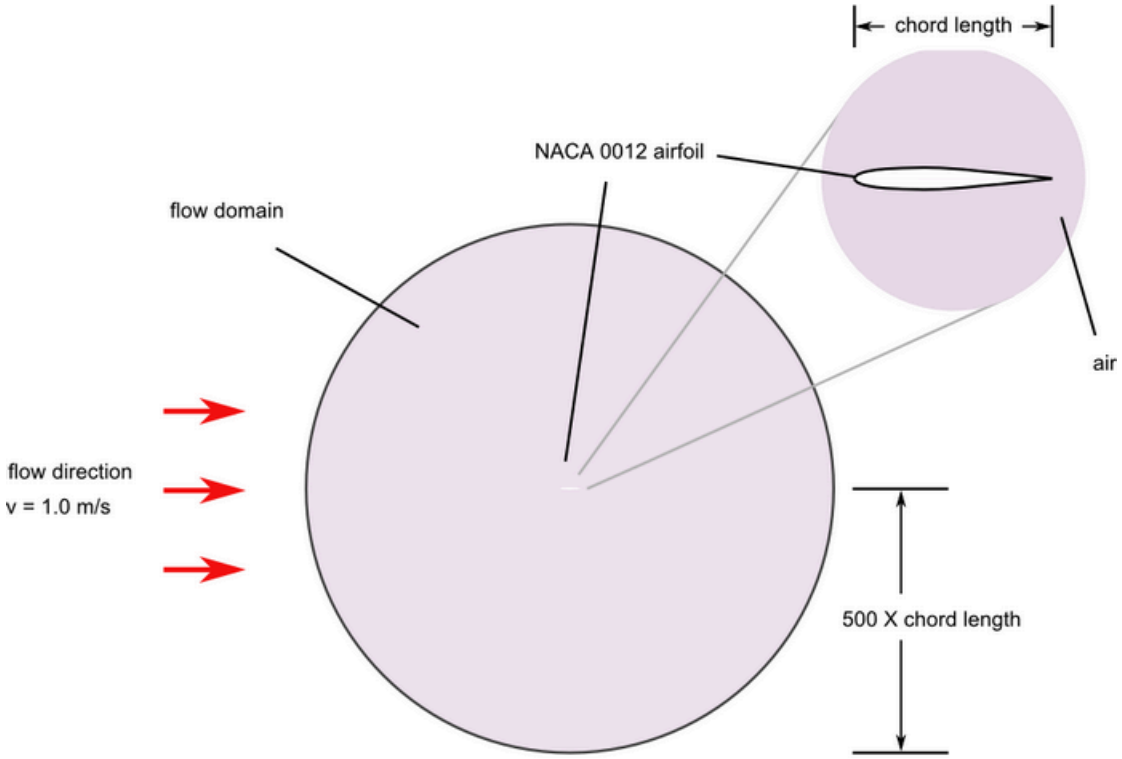


Figure 473: Critical Dimensions and Parameters for Simulating Turbulent Flow over a NACA 0012 Airfoil

The simulation was performed as a two dimensional problem by restricting flow in the out-of-plane direction through the use of a mesh that is one element thick.

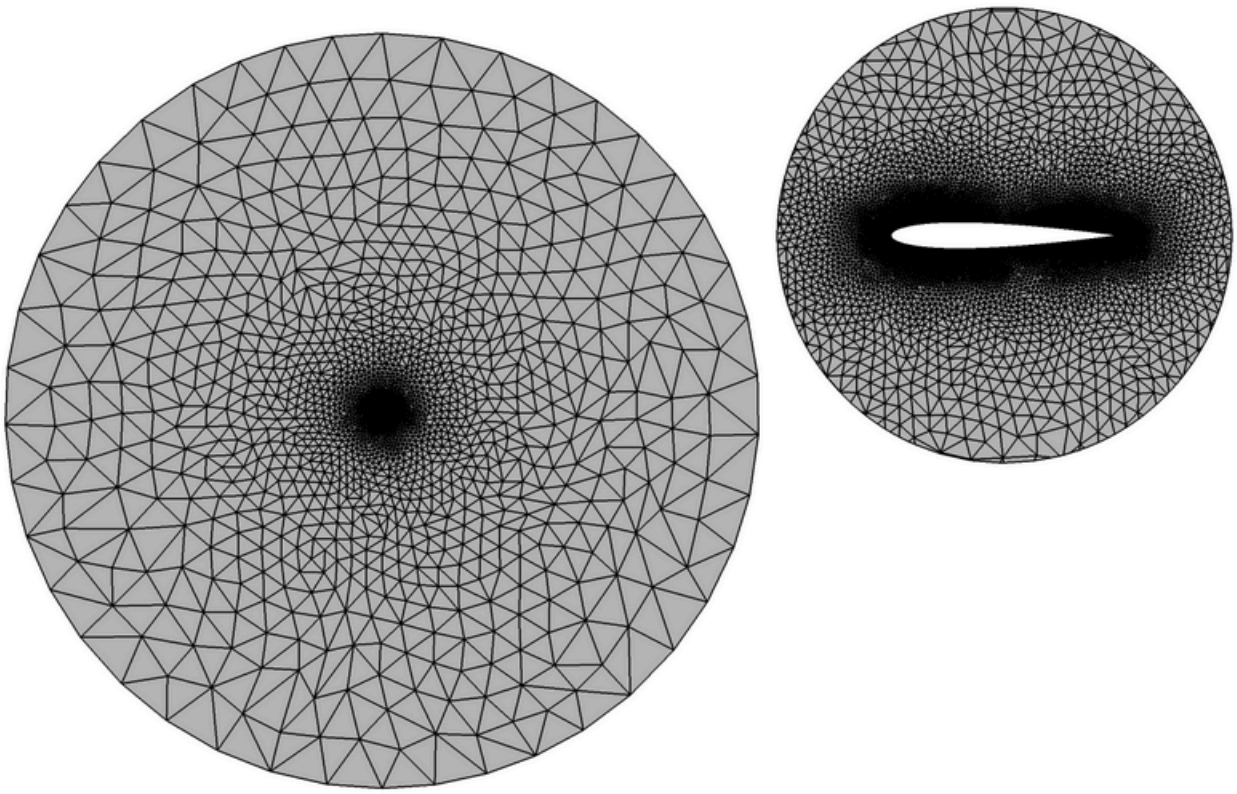


Figure 474: Mesh Used for Simulating Turbulent Flow over a NACA 0012 Airfoil (the Image on the Left Represents the Full Mesh, the Image on the Right Represents Mesh Details near the Airfoil)

AcuSolve Results

The AcuSolve solution converged to a steady state and the results reflect the mean flow conditions for each of the three angles of attack, 0 degrees, 10 degrees, and 15 degrees. For each case, the angle of attack was varied by changing the angle of the incident flow. Note that this enables the use of a single mesh for all of the simulations.

With a 0 degree angle of attack, the flow field is symmetric as the fluid flows over and under the airfoil. The airfoil impedes the flow, causing stagnation at the leading edge. As the fluid passes over and under the airfoil, velocity increases. As the fluid passes over the blunt trailing edge, a minor amount of flow separation occurs. The flow reattaches shortly after it passes the trailing edge and recovers the mean velocity in the distant far field.

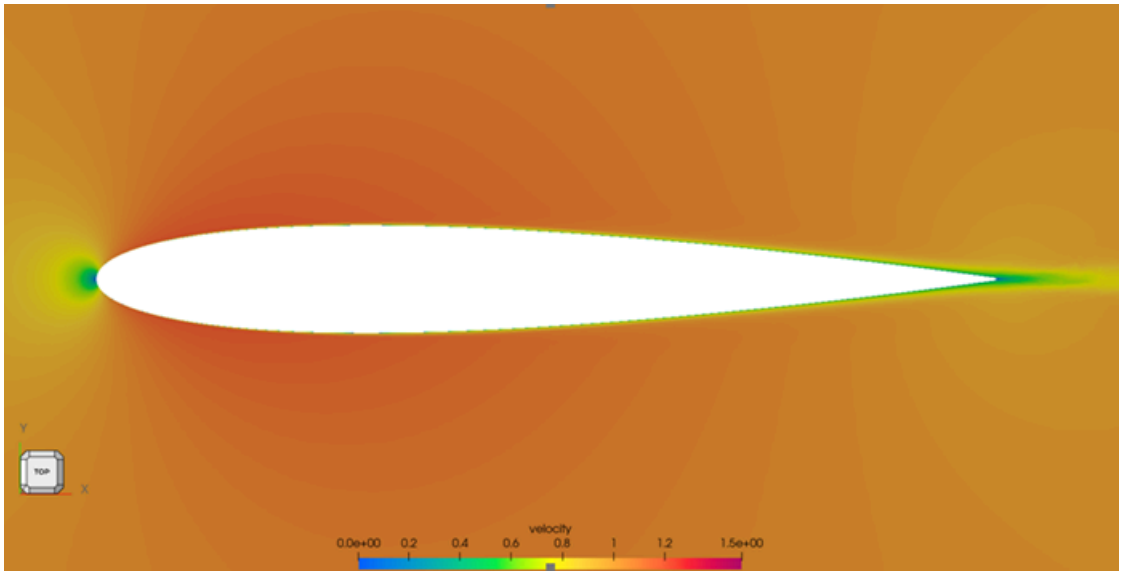


Figure 475: Contours of Velocity Magnitude Where Angle of Attack = 0 Degrees

With a 10 degree angle of attack, the stagnation point is shifted downward (relative to the airfoil), reflective of the shifted angle of attack. Fluid velocity above the airfoil is markedly different than that below the airfoil. A small low-velocity region is evident on the suction side of the airfoil, indicating some separation toward the trailing edge.

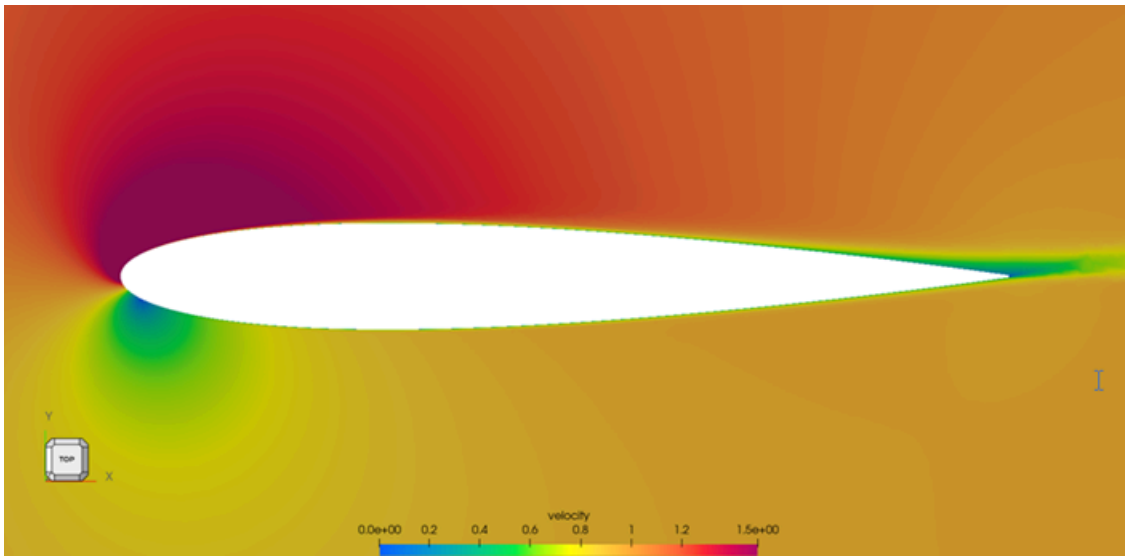


Figure 476: Contours of Velocity Magnitude Where Angle of Attack = 10 degrees

With a 15 degree angle of attack, the stagnation at the front of the airfoil is shifted even farther downward (relative to the airfoil), reflective of the shifted angle of attack. Additionally, the low-velocity wake increases in size, reflecting separation along the suction surface of the airfoil.

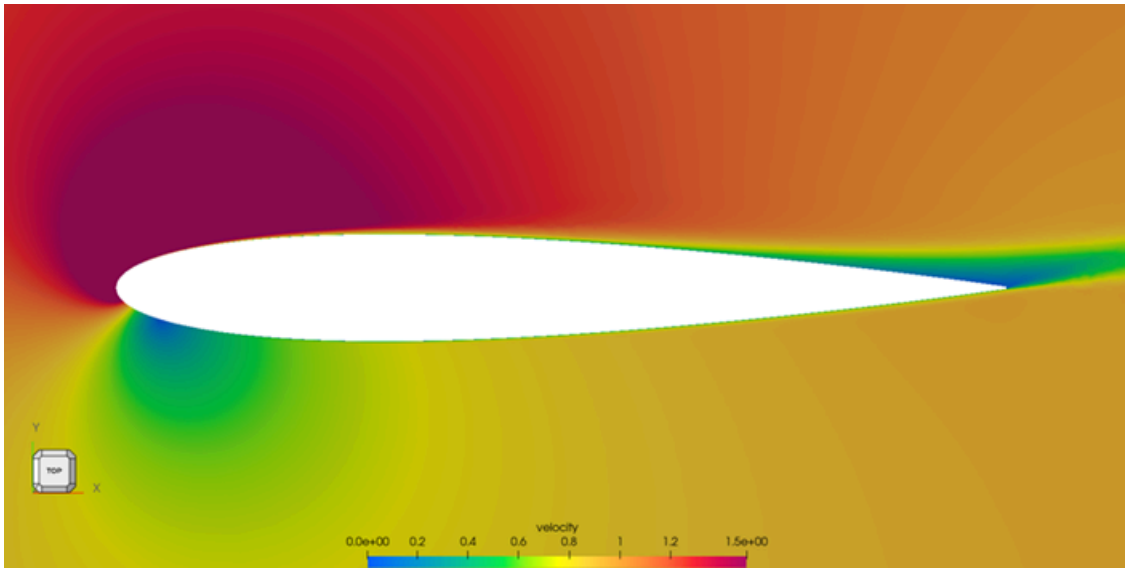


Figure 477: Contours of Velocity Magnitude Where Angle of Attack = 15 Degrees

Experimental values of coefficient of lift (CL) at angles of attack (α) of 10 degrees and 15 degrees and values of drag coefficient (cd) at angles of attack (α) of 0 degrees,10 degrees, and 15 degrees are presented with the corresponding AcuSolve results in the following table.

Table 31:

	CL (α=10)	**CL (α=15)**	**cd (α=0)**	**cd (α=10)**	**cd (α=15)**
Experimental	1.0941	1.5576	0.0082	0.0123	0.0207
AcuSolve	1.0905	1.5428	0.0081	0.0124	0.0208
Percent deviation from experimental	0.33	0.95	1.22	0.81	0.48

AcuSolve values for coefficient of pressure are plotted against experimental results for angles of attack (α) of 0 degrees, 10 degrees, and 15 degrees in the following plots. The results are presented for normalized distance along the airfoil, given by x/c, where x is the distance from the leading edge and c is the chord length.

For each case, AcuSolve is able to predict the flow characteristics at each point along the airfoil surface.

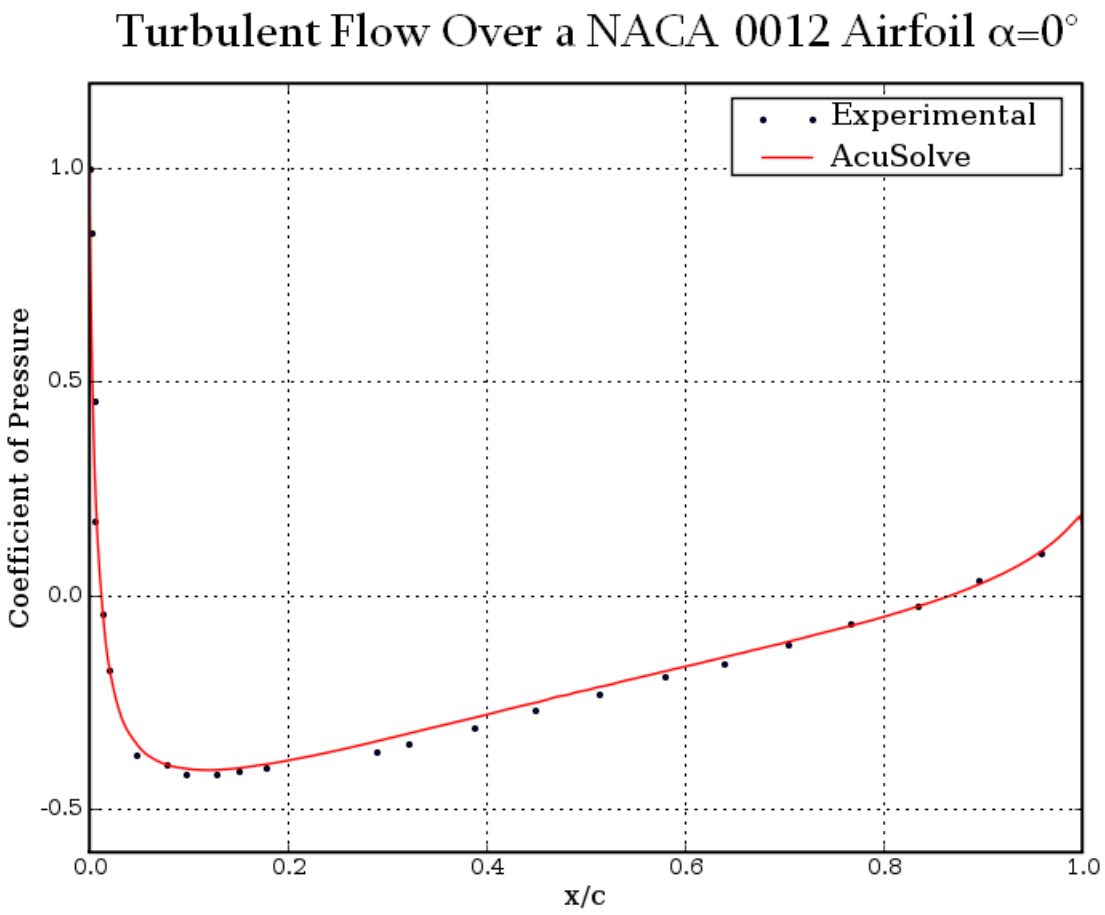


Figure 478: Coefficient of Pressure Plotted Against Normalized Distance Along the Airfoil for Angle of Attack (a) = 0 Degrees

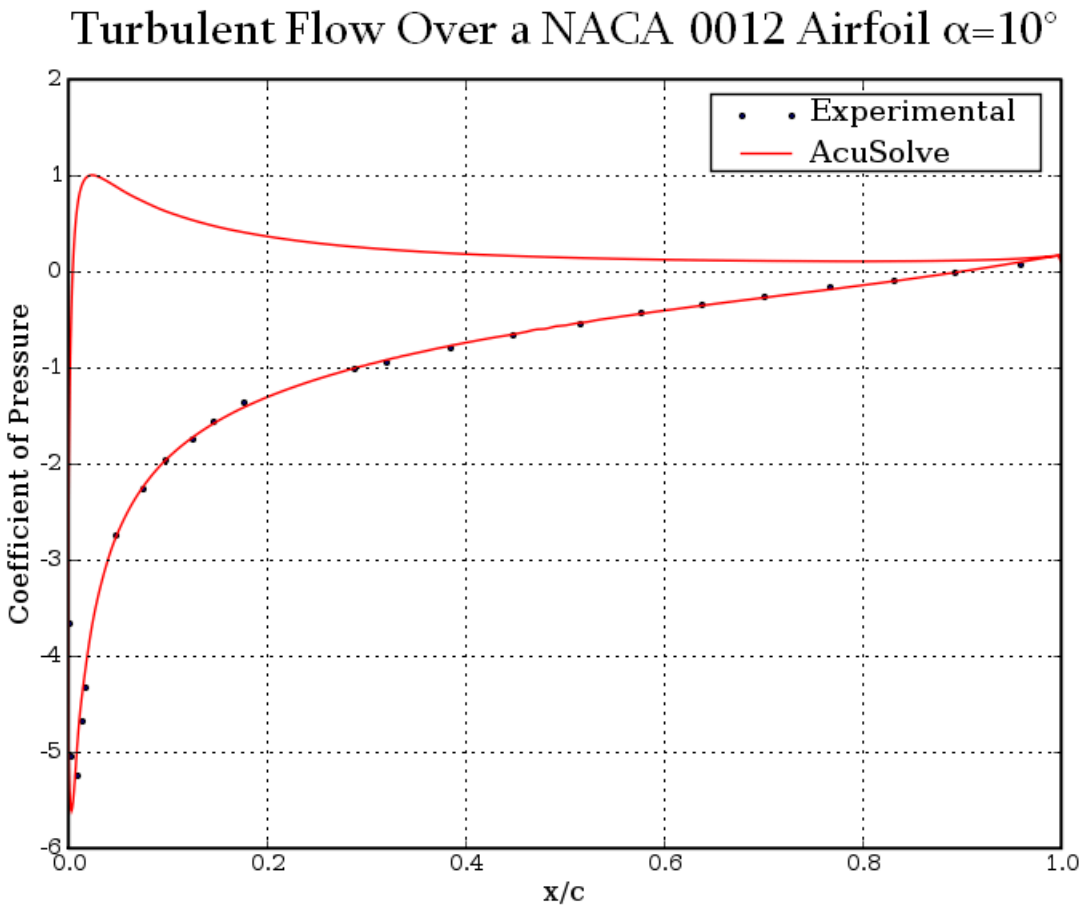


Figure 479: Coefficient of Pressure Plotted Against Normalized Distance Along the Airfoil For Angle of Attack (a) = 10 Degrees

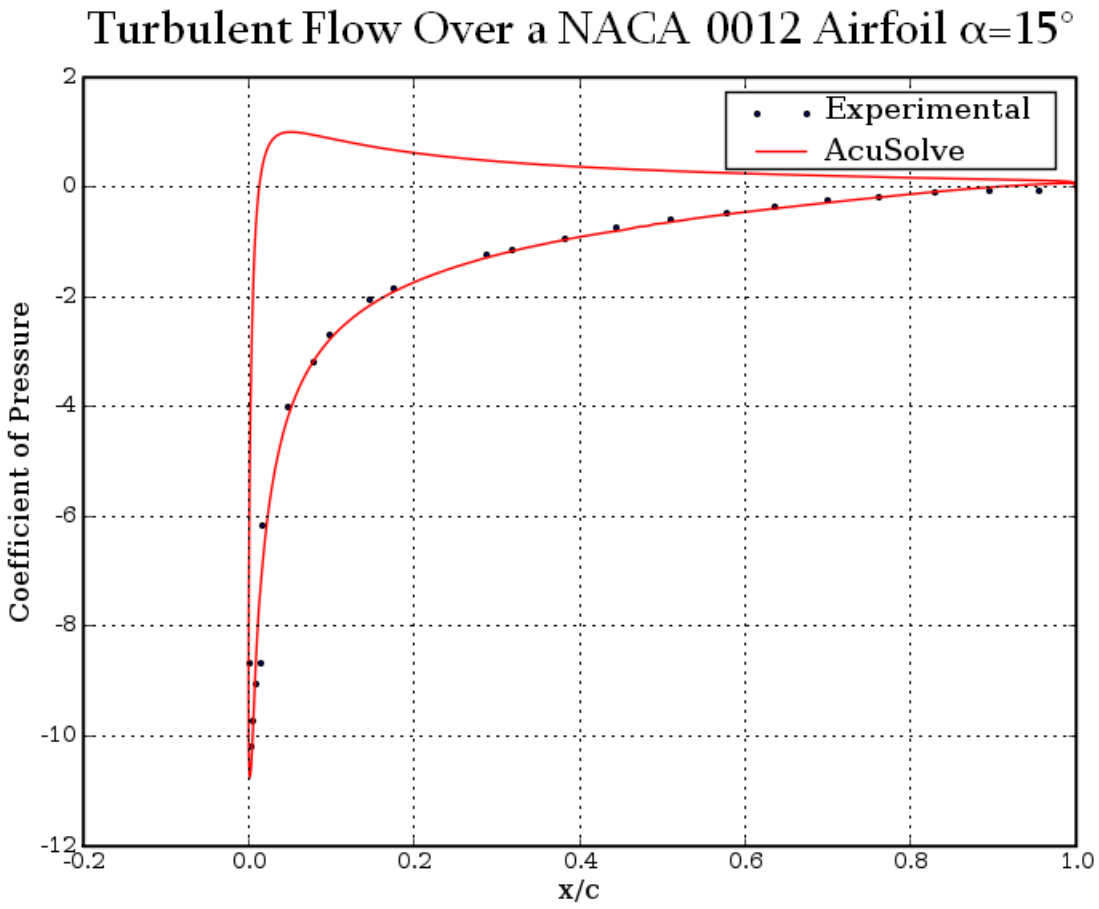


Figure 480: Coefficient of Pressure Plotted Against Normalized Distance Along the Airfoil for Angle of Attack (a) = 15 Degrees

Summary

The AcuSolve results compare well with the experimental results for flow over a NACA 0012 airfoil. In this application, a constant-velocity flow field impinges on the airfoil surface. As the flow convects in the streamwise direction along the airfoil surface, a boundary layer develops. The rate at which the boundary layer develops has significant impact on the viscous stresses present on the airfoil surface. At low angles of attack these stresses dominate the drag on the airfoil. As the angle of attack increases, the flow over the airfoil is no longer symmetric, which leads to the generation of lift. For non-zero angles of attack, the asymmetric pressure distribution on the airfoil creates another source of drag that is combined with the viscous stresses to determine the total drag on the airfoil. The AcuSolve results for coefficients of lift and drag at the 15 percent angle of attack are within 0.91 percent and 0.5 percent of experimental values, respectively. AcuSolve results for coefficient of pressure closely agree with experimental results along the length of the airfoil for all three angles of attack that were investigated.

Simulation Settings for Turbulent Flow Over a NACA0012 Airfoil

HyperWorks CFD database file: `<your working directory>\airfoil_turbulent\airfoil_turbulent.hm`

Global

- Problem Description
  - Analysis type - Steady State
  - Turbulence equation - Spalart Allmaras
- Auto Solution Strategy
  - Convergence tolerance - `0.0001`
  - Relaxation factor - `0.4`
- Material Model
  - Fluid
    - Density - `1.0` kg/m3
    - Viscosity - `1.667e-7` kg/m-sec

  Model
- Volumes
  - Fluid
    - Element Set
      1. Material model - Fluid
- Surfaces
  - +z slip
    - Simple Boundary Condition
      1. Type - Slip
  - -z slip
    - Simple Boundary Condition
      1. Type - Slip
  - airfoil surface
    - Simple Boundary Condition
      1. Type - Wall
  - farfield
    - Simple Boundary Condition
      1. Type - Far Field
      2. X velocity - cos(α) m/sec
      3. Y velocity - sin(α) m/sec
- Eddy viscosity - `1.0e-9` m2/sec

References

NASA - Langley Research Center. http://turbmodels.larc.nasa.gov/naca0012_val_sa.html

Oscillating Laminar Flow Around a Circular Cylinder

In this application, AcuSolve is used to simulate two dimensional, laminar flow over a cylinder to predict separation of flow from the cylinder surface and the flow in the wake area. AcuSolve results are compared with experimental results as described in Tritton (1959). The close agreement of AcuSolve results with experimental results validates the ability of AcuSolve to model cases with unsteady oscillating vortex streets.

Problem Description

The problem consists of a cylinder located in a rectangular domain, as shown in the following image, which is not drawn to scale. A fluid enters the domain with a low velocity (v) of 0.5 m/s. The diameter (D) of the cylinder is 20 cm. The domain extends 10 X D upstream of the cylinder center, 5D above and below the cylinder center, and 40D downstream of the cylinder center. The density of the working fluid is 1 kg/m^3 and the viscosity is 0.001 kg/m-s. The Reynolds number for this problem is 100.

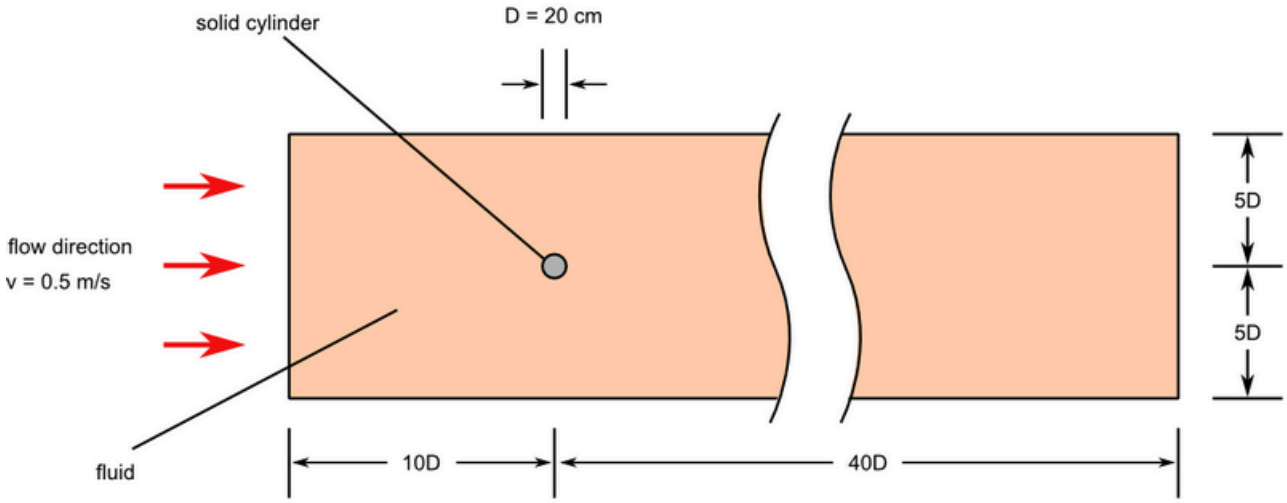


Figure 481: Critical Dimensions and Parameters for Simulating Oscillating Laminar Flow Around a Circular Cylinder

The simulation was performed as a two dimensional problem by constructing a volume mesh that contains a single layer of elements in the extruded direction, normal to the flow plane, and by imposing symmetry boundary conditions on the extruded planes.

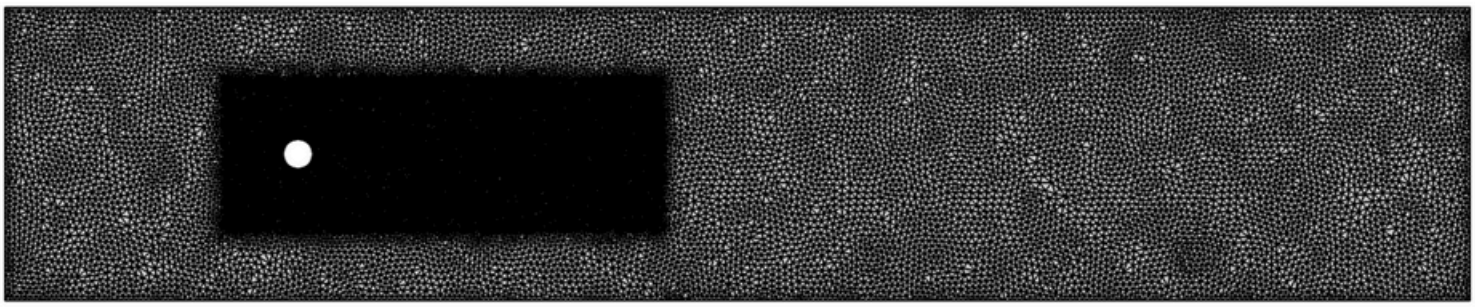


Figure 482: Mesh used for Simulating Oscillating Laminar Flow Around a Circular Cylinder

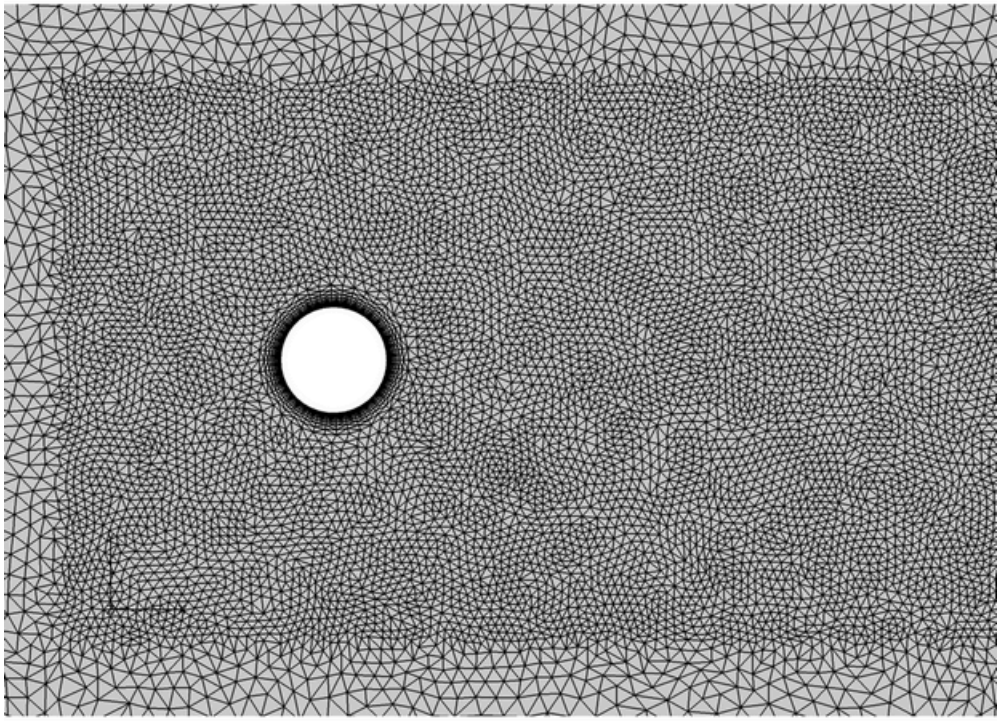


Figure 483: Details of the Mesh Showing Refinement Zone Around the Cylinder

AcuSolve Results

The simulation was run as transient for a time record sufficient to ensure that the vortex shedding in the wake reached a stabilized oscillation frequency. The AcuSolve solution shows an unsteady, oscillating flow field with flow around the cylinder separating from the cylinder surface. A wake area is developed downstream of the cylinder with alternating vortices shedding at a regular frequency from the top and bottom of the cylinder surface. This results in oscillating lift forces that act on the cylinder as shown in the following images.

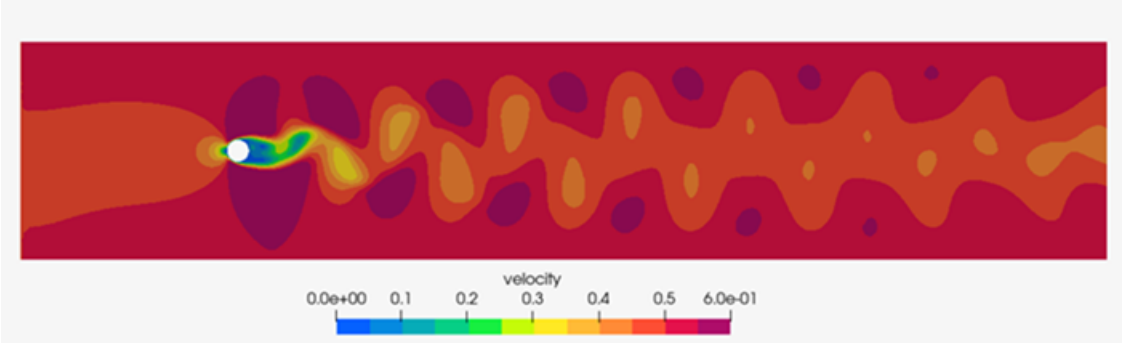


Figure 484: Contours of Velocity Magnitude

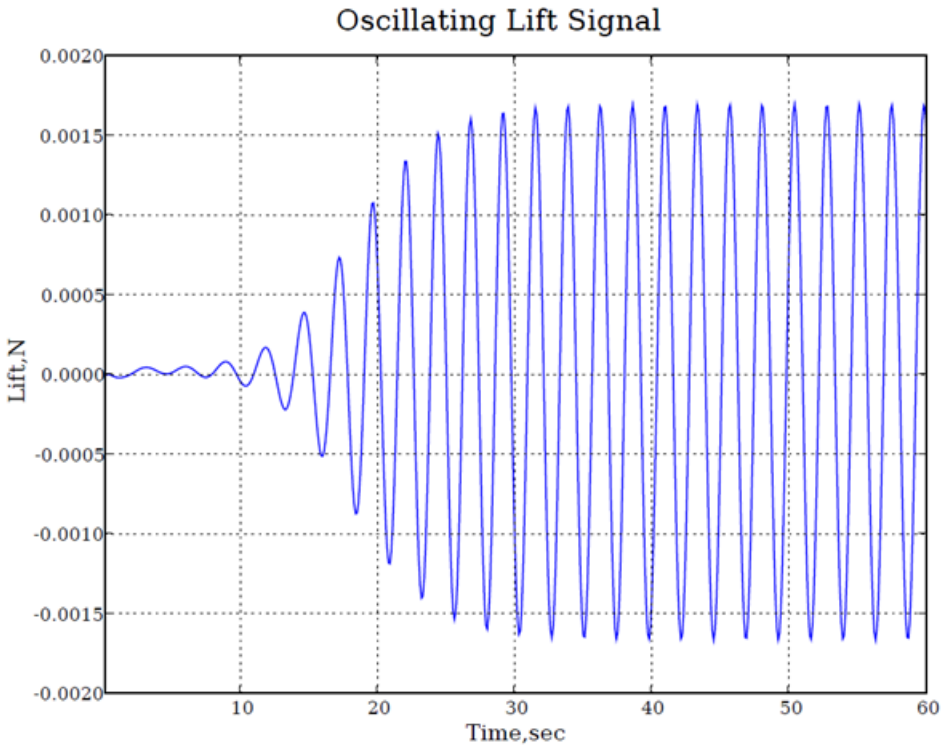


Figure 485: Lift Coefficient (lift force perpendicular to flow) plotted against time. Simulation was run for 600 time steps for a duration of 60 s

The Strouhal number for this simulation, a dimensionless number describing oscillating flows, is used to validate AcuSolve results. The experimental Strouhal number for this problem is given by

$$St = \frac{\omega^* L}{v} = 0.165 \qquad (18)$$

where ω is the dominant frequency of oscillations, L is the diameter of the cylinder, and v is the flow velocity.

The peak frequency of the oscillating lift force was computed by transforming the time dependent data into frequency space with a Fourier transform. From the Fourier transform, the AcuSolve-based Strouhal

number was calculated. The table below shows the comparison of the Strouhal number provided by the AcuSolve prediction and the measurement given by Tritton (1959).

Table 32:

	Experimental	**AcuSolve**
Strouhal number	0.165	0.173

Summary

In this application, two dimensional flow over a cylinder is achieved by enforcing symmetry conditions on the front and back surfaces of the flow domain. The laminar, unsteady simulation shows the flow separation that leads to alternating vortex shedding. Frequency of the lift force acting on the cylinder is calculated to evaluate the Strouhal number. The AcuSolve solution compares well with results reported by Tritton (1959), differing slightly from the experimental results. In this application, AcuSolve demonstrates the ability to accurately predict oscillating laminar flow around a circular cylinder.

Simulation Settings for Oscillating Laminar Flow Around a Circular Cylinder

HyperWorks CFD database file: `<your working directory>\cylinder_laminar\cylinder_laminar.hm`

Global

- Problem Description
  - Analysis type - Transient
  - Turbulence equation - Laminar
- Auto Solution Strategy
  - Analysis type - Transient
  - Max time - `600` sec
  - Initial time increment - `0.1` sec
- Material Model
  - Fluid
    - Density - `1.0` kg/m3
    - Viscosity - `1.0e-3` kg/m-sec

  Model
- Volumes
  - Volume
    - Element Set
      1. Material model - Fluid
- Surfaces
  - Back
    - Simple Boundary Condition
      1. Type - Symmetry

- Base
  - Simple Boundary Condition
    1. Type - Slip
- Front
  - Simple Boundary Condition
    1. Type - Symmetry
- Inflow
  - Simple Boundary Condition
    1. Type - Inflow
    2. Inflow Type - Average velocity
    3. Average Velocity - `0.5` m/sec
- Outflow
  - Simple Boundary Condition
    1. Type - Outflow
- Top
  - Simple Boundary Condition
    1. Type - Slip

References

D.J. Tritton. "Experiments on the Flow around a Circular Cylinder at Low Reynolds Number". Journal of Fluid Mech. 6(04):547-567. 1959

Separated Laminar Flow Over a Blunt Plate

In this application, AcuSolve is used to simulate the separation of laminar flow over a blunt plate. AcuSolve results are compared with experimental results as described in J.C. Lane and R.I. Loehrke (1980). The close agreement of AcuSolve results with the experimental results validates the ability of AcuSolve to model cases with external laminar flow including separation.

Problem Description

The problem consists of external, laminar flow over a blunt plate 1.5 m long and 0.09 m thick, as shown in the following image, which is not drawn to scale. The fluid flows with a uniform horizontal velocity (v) of 0.045133 m/s. The fluid material used for the simulation has a density of 1.0 kg/m^3 and a dynamic viscosity of 1.7894 X 10^{-5} kg/m-s. The resulting Reynolds number for the flow, based on the plate thickness, is approximately 227. This indicates that the flow over the plate is laminar. As the fluid flows past the leading edge of the plate, the pressure decreases, resulting in a separation region downstream of the leading edge. At some distance downstream from the leading edge, the pressure gradient decreases, and viscous forces cause the recirculation zone to dissipate, allowing the flow to reattach to the plate.

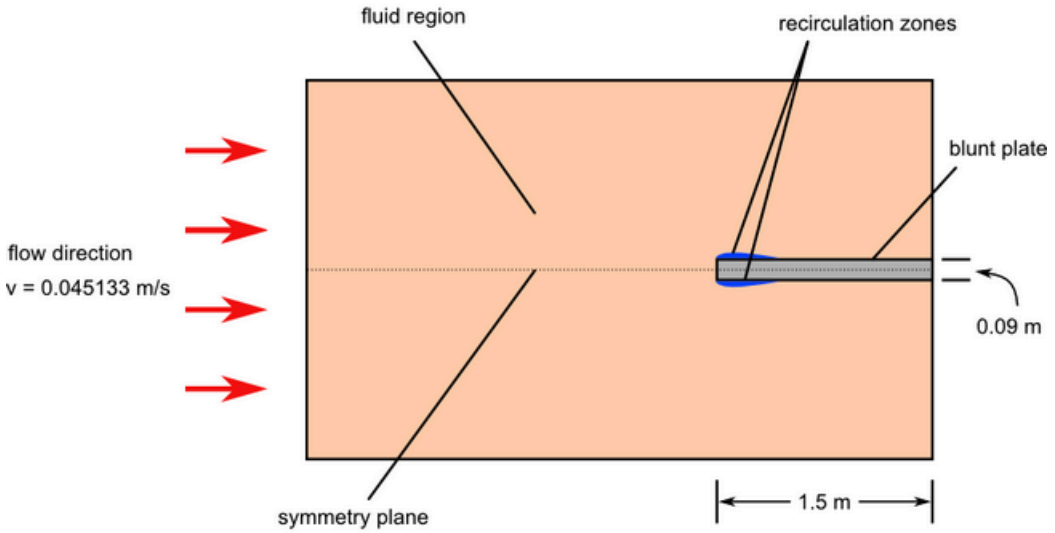


Figure 486:

The simulation was performed as a two dimensional problem by constructing a volume mesh that contains a single layer of elements in the extruded direction, normal to the flow plane, and by imposing symmetry boundary conditions on the extruded planes. In addition, the half symmetry of the geometry was exploited to allow for modeling only the top half of the geometry. These characteristics allow for accurate simulation of the flow while minimizing computational time. The following images show the mesh distribution and a refined mesh zone around the blunt plate.

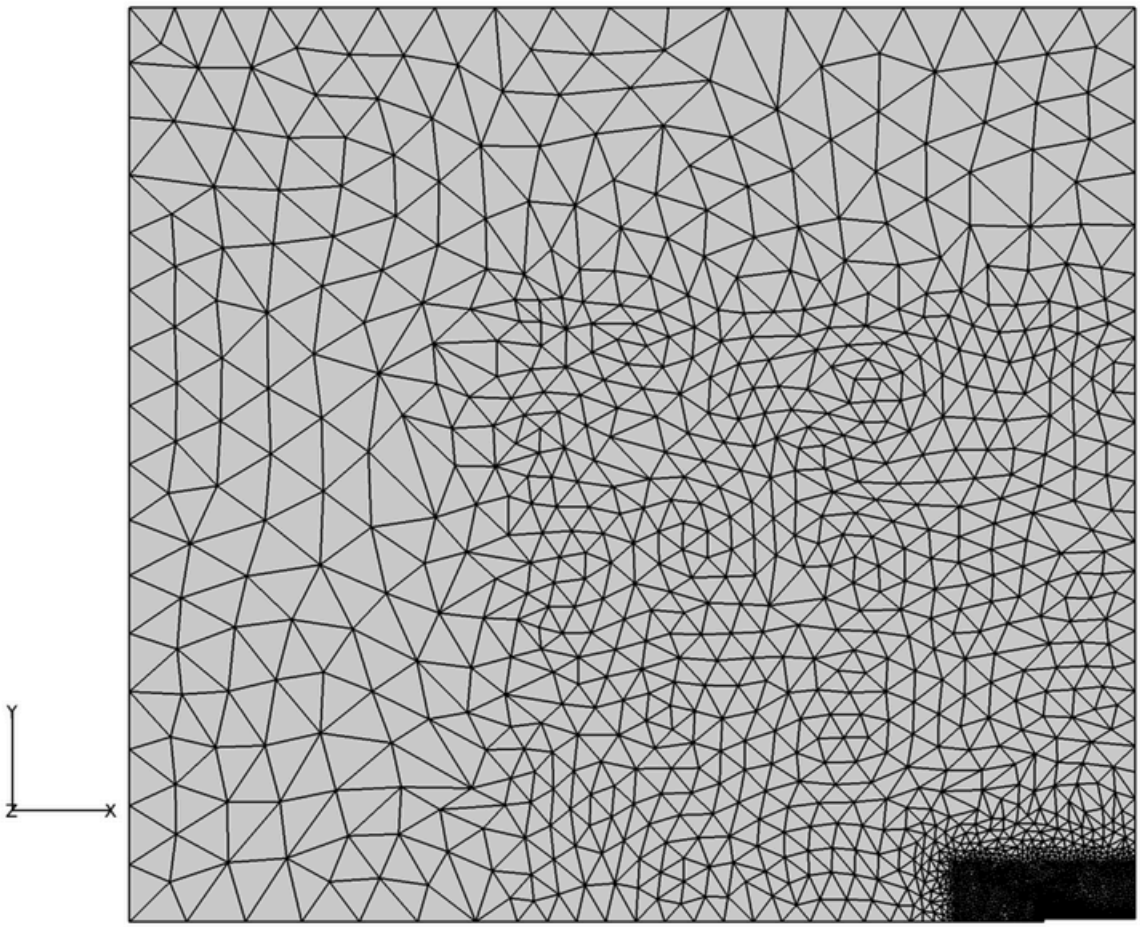


Figure 487: Mesh used for Simulating Separated Laminar Flow over a Blunt Plate

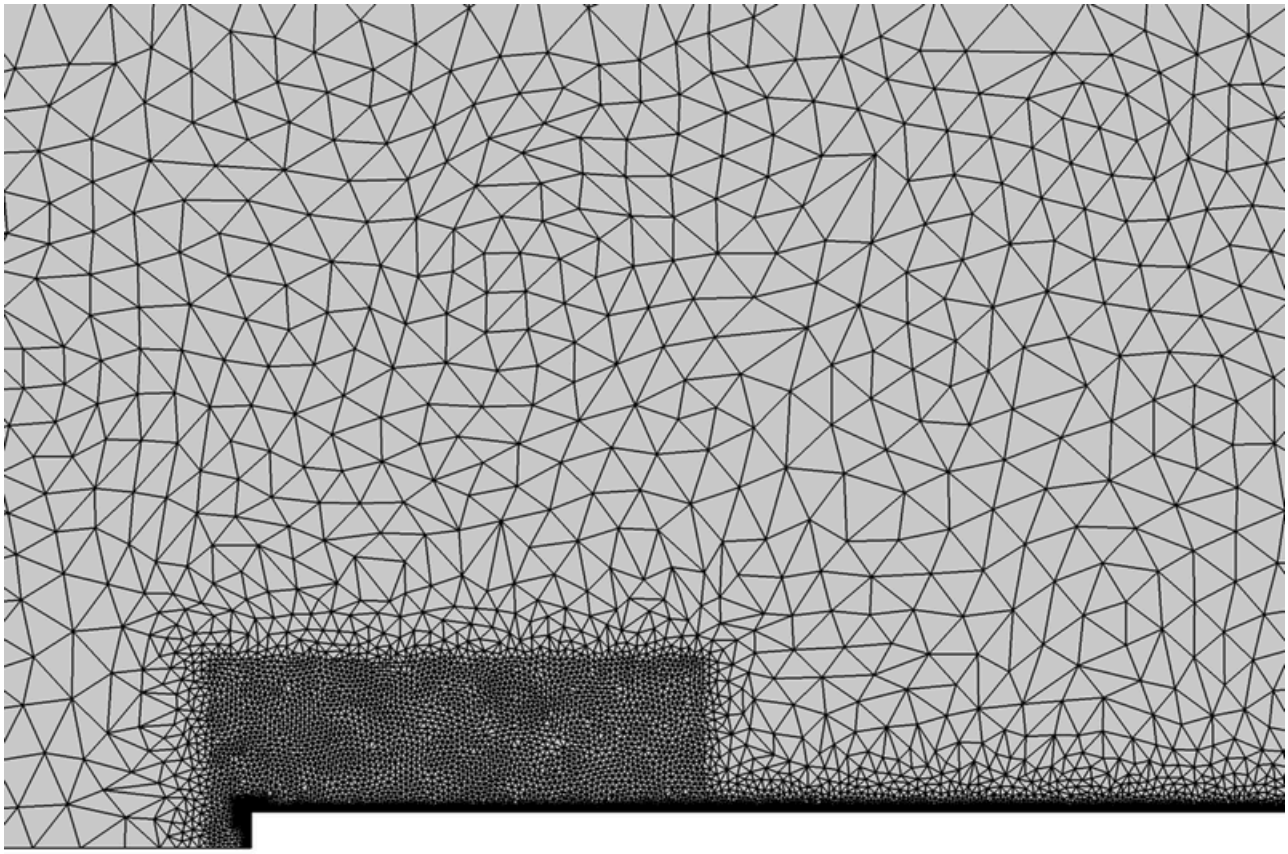


Figure 488: Mesh Detail Showing Refinement Zones at the Leading Edge of the Blunt Plate

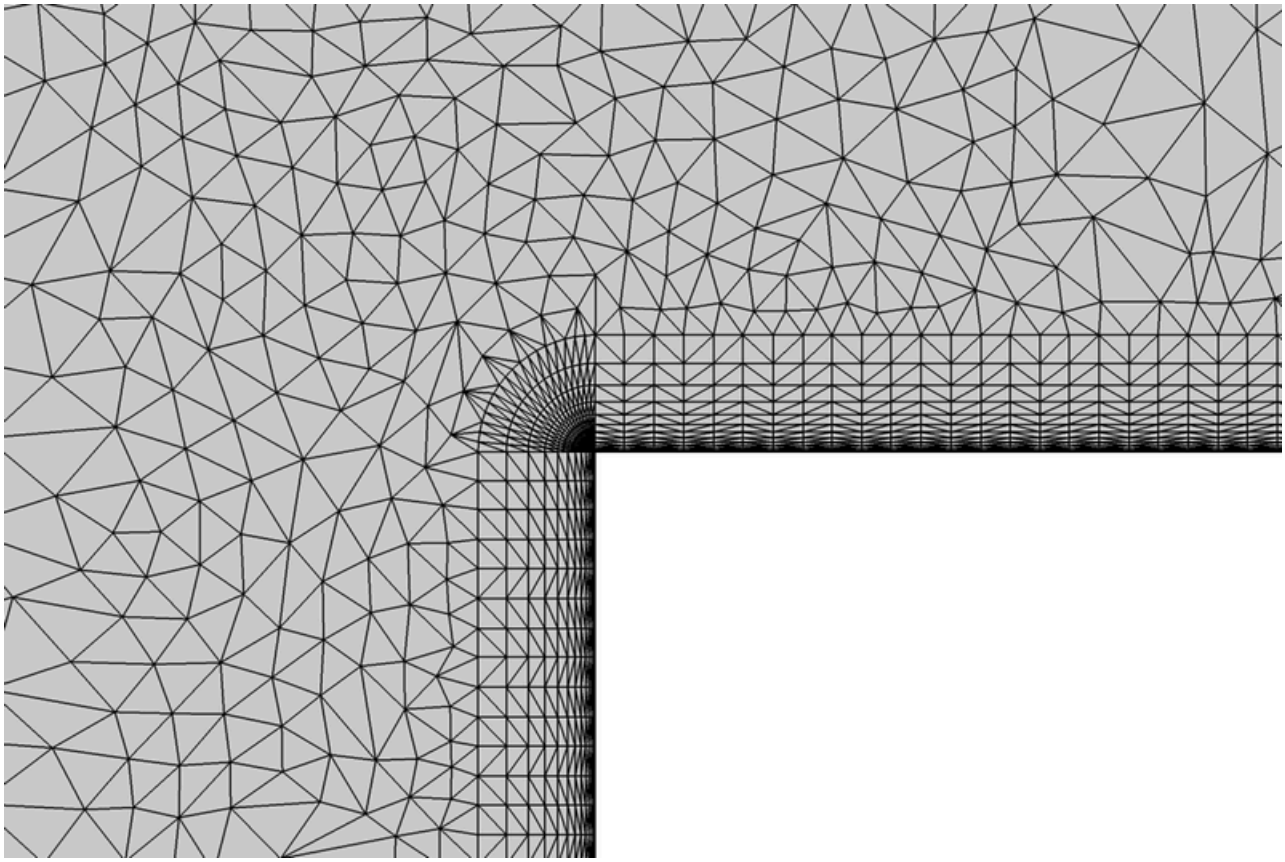


Figure 489: Mesh Detail Showing Mesh Elements Near the Leading Edge of the Blunt Plate

AcuSolve Results

The AcuSolve solution converged to a steady state and the results reflect the mean flow conditions over the blunt plate. The flow velocity is reduced to zero at the leading face, forming a stagnation point at the center. The flow reaches a maximum velocity as it flows around the leading edges and separates from the plate. Flow separation (shear stress parallel to the wall becomes negative) occurs downstream of the leading edge, leading to a recirculation zone. The flow reattaches 0.37 m downstream of the leading edge. The velocity in the laminar boundary layer increases from zero at the wall to free-stream velocity at the boundary layer edge. Along the plate length, the boundary layer slowly grows in thickness. The following image shows the contours of the flow velocity parallel to the streamwise direction and the recirculation region in the wake of the plate edge.

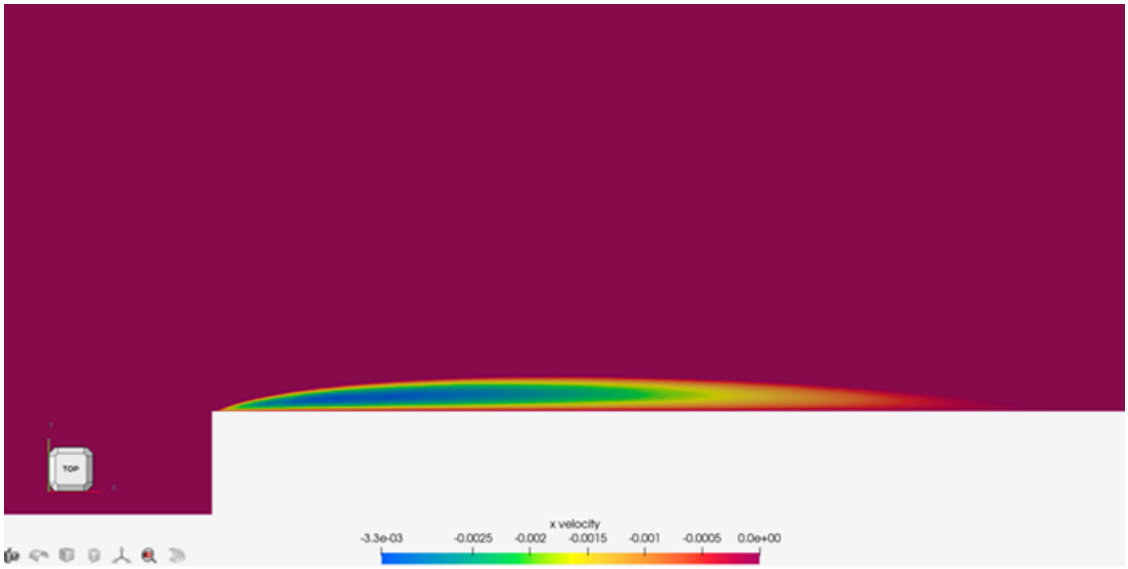


Figure 490: X-Velocity Contours Near the Leading Edge of the Blunt Plate

Downstream of the leading edge, the flow eventually reattaches to the plate at the point where the shear stress parallel to the wall passes from negative through zero to positive. The reattachment point is 0.37 m from the leading edge of the plate and corresponds to the trailing edge of the contours.

The results for the predicted and experimental reattachment length (xreattach) are presented in the table below. T represents the plate thickness.

Table 33:

AcuSolve xreattach	AcuSolve xreattach/T	Experimental xreattach/T	Percent error (%)
0.37	4.11	4.0	2.8

Summary

In this application, a constant flow inlet velocity and symmetric boundary conditions were used to model 2D flow over a blunt plate. The AcuSolve solution compares well with experimental results for the separation of laminar flow over a blunt plate. The non-dimensional reattachment length obtained from the AcuSolve steady state solution compares well with the experimental solution, with an error of less than 3.0 percent. The results of this simulation validate the ability of AcuSolve to accurately predict the reattachment point in cases with external, laminar flow with separation.

Simulation Settings for Separated Laminar Flow over a Blunt Plate

HyperWorks CFD database file: `<your working directory>\blunt_plate_laminar\blunt_plate_laminar.hm`

Global

- Problem Description

    - Analysis type - Steady State
    - Turbulence equation - Laminar
- Auto Solution Strategy
    - Relaxation Factor - `0.2`
- Material Model
    - Fluid
        - Density - `1.0` kg/m3
        - Viscosity - `1.7894e-005` kg/m-sec

  Model
- Volumes
    - Fluid
        - Element Set
            1. Material model - Fluid
- Surfaces
    - Back
        - Simple Boundary Condition
            1. Type - Symmetry
    - Freestream
        - Simple Boundary Condition
            1. Type - Slip
    - Front
        - Simple Boundary Condition
            1. Type - Symmetry
    - Inlet
        - Simple Boundary Condition
            1. Type - Inflow
            2. Inflow type - Velocity
            3. Inflow velocity type - Cartesian
            4. X Velocity - `0.045133` m/s
    - Outflow
        - Simple Boundary Condition
            1. Type - Outflow
    - Plate
        - Simple Boundary Condition
            1. Type - Wall
    - Symmetry
        - Simple Boundary Condition

1 Type - Symmetry

References

J.C. Lane and R.I. Loehrke. "Leading Edge Separation from a Blunt Plate at Low Reynolds Number". Journal of Fluids Engineering. 102(4):494-496. 1980.

Turbulent Mixing Layers in an Open Channel

In this application, AcuSolve is used to simulate the mixing of two streams of fluid with different velocities moving past a splitter plate. AcuSolve results are compared with experimental results as described in J. Delville, et al. (1989). The close agreement of AcuSolve results with the experimental results validates the ability of AcuSolve to model mixing layers in the turbulent flow regime.

Problem Description

The problem consists of two streams of fluid having material properties of standard air with density of 1.2 kg /m^3 and molecular viscosity of 1.7189 kg/m-sec. The two fluid streams enter an open channel separated by a splitter plate at two streamwise locations with differing velocities. The length of the channel is 1.8 m for the top portion and 1.5 m for the bottom portion. The inlet velocity of the top section is 41.54 m/s, producing a Reynolds's number of 2900, based on l=1.0 mm, while the inlet velocity of the lower section is 22.4 m/s, giving a Reynolds's number of 1200, as shown in the following image, which is not drawn to scale. The model is simulated as steady state with constant inflow conditions, using the Spalart Allmaras (SA) turbulence model. The velocity profile is computed for several locations downstream of the splitter plate and compared against the experimental data, as described in Delville, 1989.

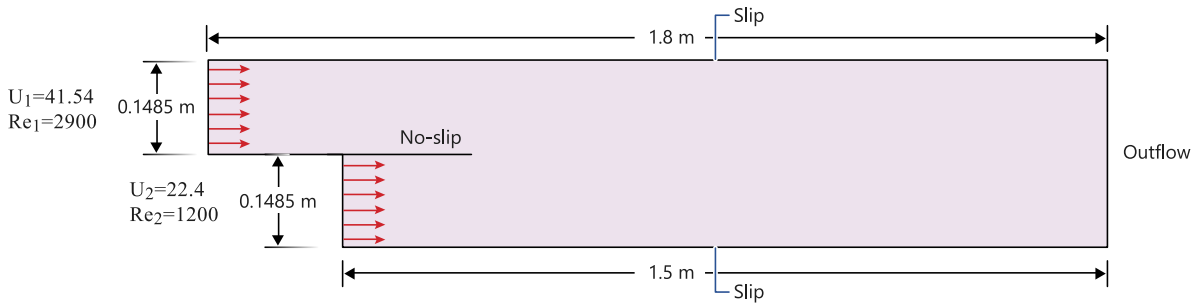


Figure 491: Critical Dimensions and Parameters Used for Simulating the Turbulent Mixing Layer

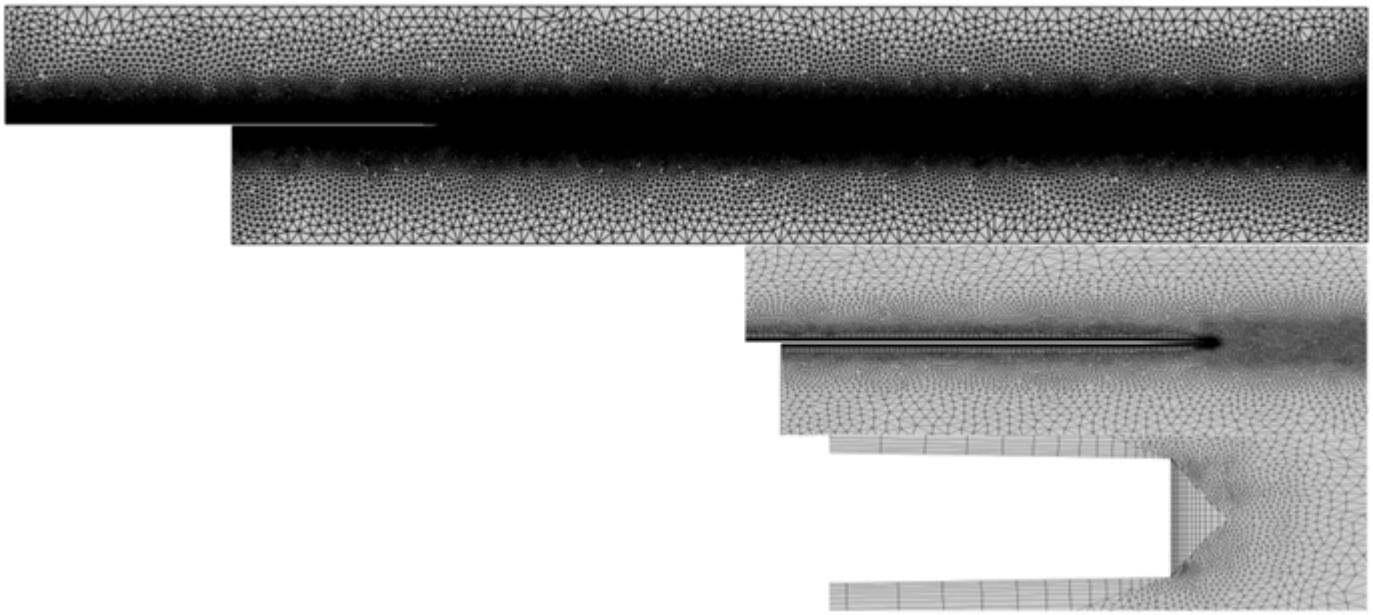


Figure 492: Mesh used for Simulating the Turbulent Mixing Layer Showing Close up Images Near the Trailing Edge of the Plate

The simulation was performed as a two dimensional problem by constructing a volume mesh that contains a single layer of elements extruded in the cross stream direction, normal to the flow plane and by imposing symmetry boundary conditions on the extruded planes. The upper and lower walls are specified as slip, the splitter plate is specified as no-slip and the inlet velocity and eddy viscosity are prescribed as constant values.

AcuSolve Results

The AcuSolve solution converged to a steady state and the results reflect the mean flow conditions within the open channel. The simulation result shows a developing flow field with the fluids fully separated as they pass the edge of the splitter plate. As the fluid travels downstream of the splitter plate, the dissimilar velocity fields produce a shear layer that results in momentum exchange between the two streams. The shear layer diffuses as the fluid travels further downstream. The relative velocity as a function of the normalized boundary layer height is computed from AcuSolve and compared with experimental data at three measurement stations, 0.2 m, 0.65 m and 0.95 m away from the trailing edge of the plate, as described in Delville, 1989. The image below shows black circles representing the experimental data and a solid red line for the AcuSolve results.

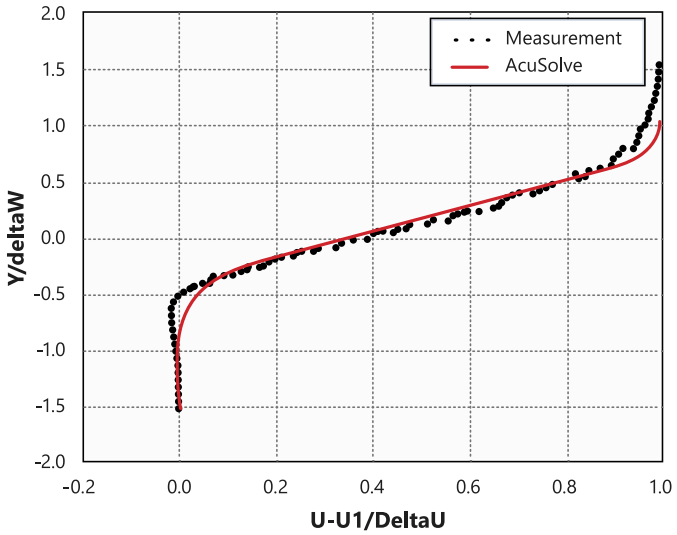


Figure 493: Relative Velocity within the Channel Compared Against Experimental Data Showing Experimental and Simulated Results for the SA Turbulence Model

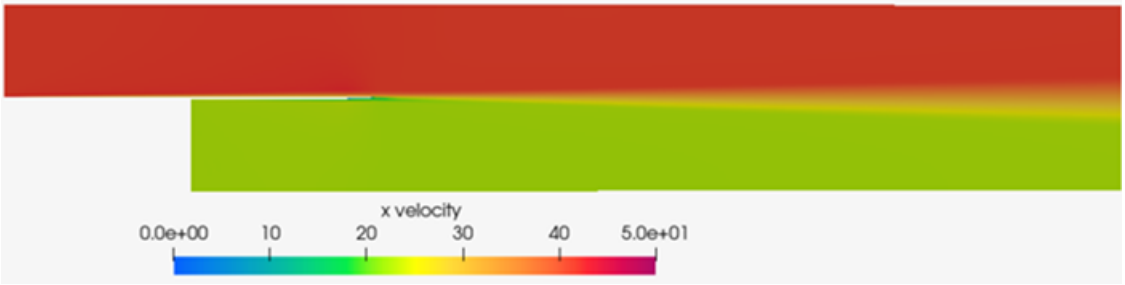


Figure 494: Velocity Magnitude Within the Channel

Summary

The AcuSolve solution compares well with experimental data for turbulent mixing within an open channel. In this application, the shear layer resulting from the dissimilar velocities of the incoming fluid streams results in an exchange of momentum within the channel. The amount of numerical dissipation from the grid is kept to a minimum to produce a good agreement with the experimental data. The good agreement with experimental results for the simulated turbulence model compares well with the measurement and previously published results, demonstrating that AcuSolve is capable of predicting turbulent mixing layers with relatively modest grid levels and the one equation turbulence model.

Simulation Settings for Turbulent Mixing Layers in an Open Channel

HyperWorks CFD database file: `<your working directory>\mixing_layer_turbulent \mixing_layer_turbulent.hm`

Global

- Problem Description
  - Analysis type - Steady State
  - Turbulence equation - Spalart Allmaras

- Auto Solution Strategy
  - Max time steps - `100`
  - Convergence tolerance - `0.001`
  - Relaxation Factor- `0.4`
- Material Model
  - Air
    - Type - Constant
    - Density - `1.2` kg/m3
    - Viscosity - `1.7189e-5` kg/m*sec

  Model
- Volumes
  - Volume
    - Element Set
      1. Material model - Air
- Surfaces
  - Back
    - Simple Boundary Condition
      1. Type- Symmetry
  - Front
    - Simple Boundary Condition
      1. Type- Symmetry
  - InletLower
    - Simple Boundary Condition
      1. Type- Inflow
      2. Inflow type- Velocity
      3. X Velocity- `22.4` m/sec
      4. Turbulence input type- Direct
      5. Eddy Viscosity- `0.0001432`
  - InletUpper
    - Simple Boundary Condition
      1. Type- Inflow
      2. Inflow type- Velocity
      3. X Velocity- `41.54` m/sec
      4. Turbulence input type- Direct
      5. Eddy Viscosity- `0.0001432`
  - Outlet
    - Simple Boundary Condition
      1. Type - Outflow

- Slip
  - Simple Boundary Condition
    1. Type- Slip
- SplitterPlate
  - Simple Boundary Condition
    1. Type - Wall
- TE
  - Simple Boundary Condition
    1. Type- Wall

References

Delville, J., Bellin, S., Garem, J. H., and Bonnet J. P., "Analysis of Structures in a Turbulent, Plane Mixing Layer by Use of a Pseudo Flow Visualization Method Based on Hot-Wire Anemometry," in: Advances in Turbulence 2, eds: H.-H. Fernholz and H. E. Fiedler, Proceedings of the Second European Turbulence Conference, Berlin, Aug. 30-Sept. 2, 1988, Springer Verlag, Berlin, 1989, pp. 251-256.

Turbulent Flow Over an Oscillating Rigid Body Assembly

In this application, AcuSolve is used to simulate the fluid-structure interaction of a fluid moving over a cylinder/plate assembly. AcuSolve results are compared with experimental results as described in Gomes and Lienhart (2009). The close agreement of AcuSolve results with the experimental results validates the ability of AcuSolve to model cases in which the fluid forces lead to structural motions.

Problem Description

The problem consists of a fluid having material properties of standard water with density of 998 kg / m^3 and kinematic viscosity of 0.97e-6 m^2/sec through a two dimensional channel over a cylinder and plate assembly. The diameter of the cylinder is 0.022 m and the plate length is 0.042 m, while the inlet velocity is specified to match experimental conditions with a max velocity of 1.07 m/sec, as is shown in the following image, which is not drawn to scale. The model is simulated as transient with constant inflow conditions, allowing an oscillatory motion of the assembly to develop. The Shear Stress Transport (SST) turbulence model is used to model the turbulent portion of the flow and AcuSolve's internal rigid body motion is used to capture the motion of the oscillating assembly.

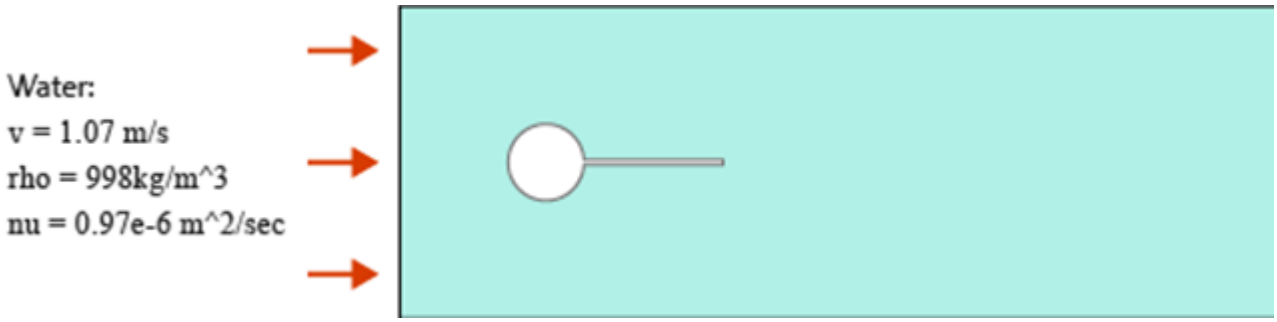


Figure 495: Critical Dimensions and Parameters used for Simulating Rigid Body Motion of Flow Past a Cylinder/Plate Assembly

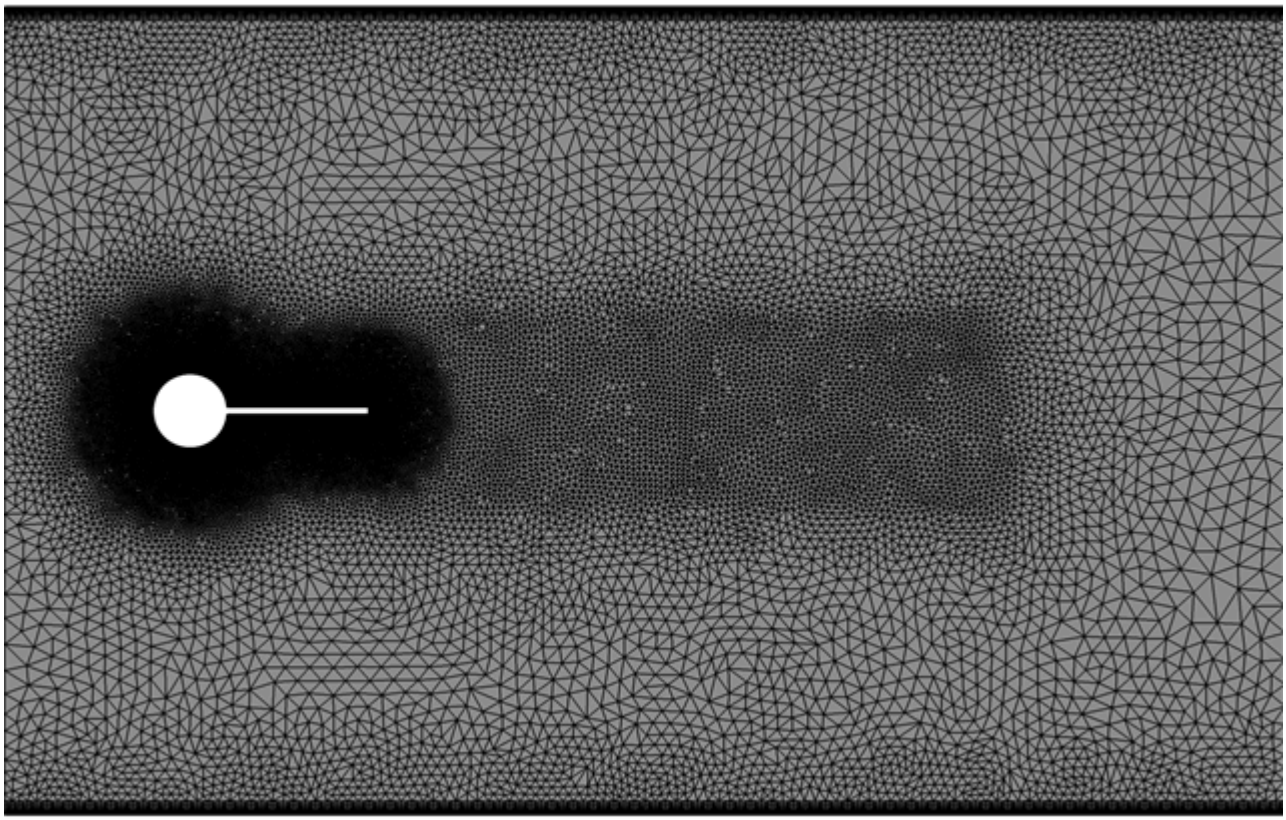


Figure 496: Mesh used for Simulating Rigid Body Motion of Flow Past a Cylinder/Plate Assembly

The simulation was performed as a two dimensional problem by constructing a volume mesh that contains a single layer of elements extruded in the cross stream direction, normal to the flow plane and by imposing symmetry boundary conditions on the extruded planes. The upper and lower walls are specified as no-slip and the inlet velocity is specified to match the conditions of the experiment (Gomes and Lienhart 2009).

AcuSolve Results

The AcuSolve solution reached a regularly repeating oscillatory state and the simulation was allowed to proceed for 10 seconds of physical time to obtain a sufficient number of cycles for statistical analysis. The motion of the cylinder/plate assembly is directly attributed to the vortices shedding in its wake. The fluctuating loads on the assembly that result from the vortex shedding lead to a repeating cycle of structural rotation. The dominant oscillation frequency from the simulation was found to match well with the experimental measurements, within approximately 3.5 percent. The images below show the rigid body displacement of the assembly as it oscillates within the flow. Contours of velocity magnitude demonstrate the forcing on the assembly, while the mesh motion around the structure is captured and plotted for a single time step. Two dimensional plots showing the angular displacement demonstrate the motion, showing a single red line for the AcuSolve results.

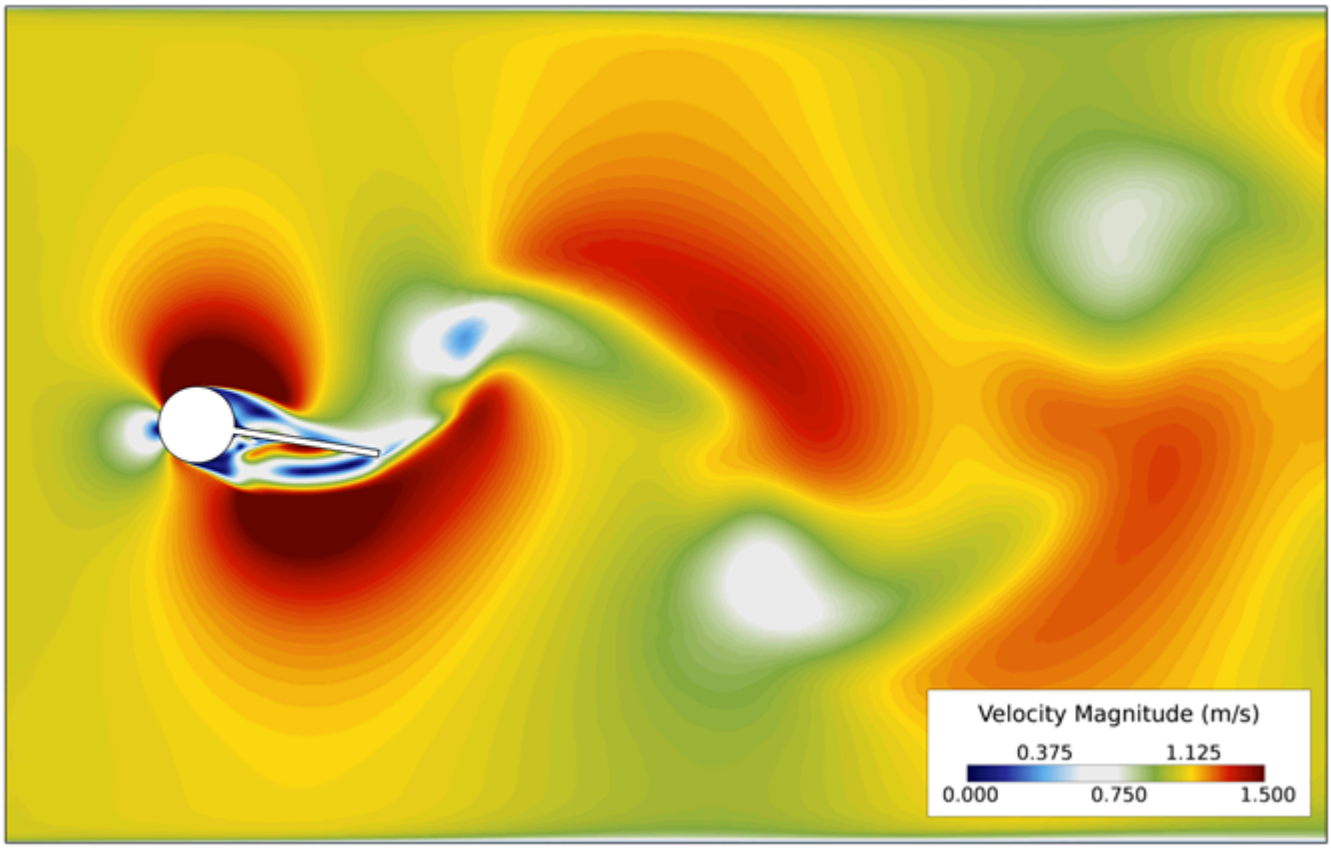


Figure 497: Velocity Contours Near the Assembly for a Single Time Step During the Simulation

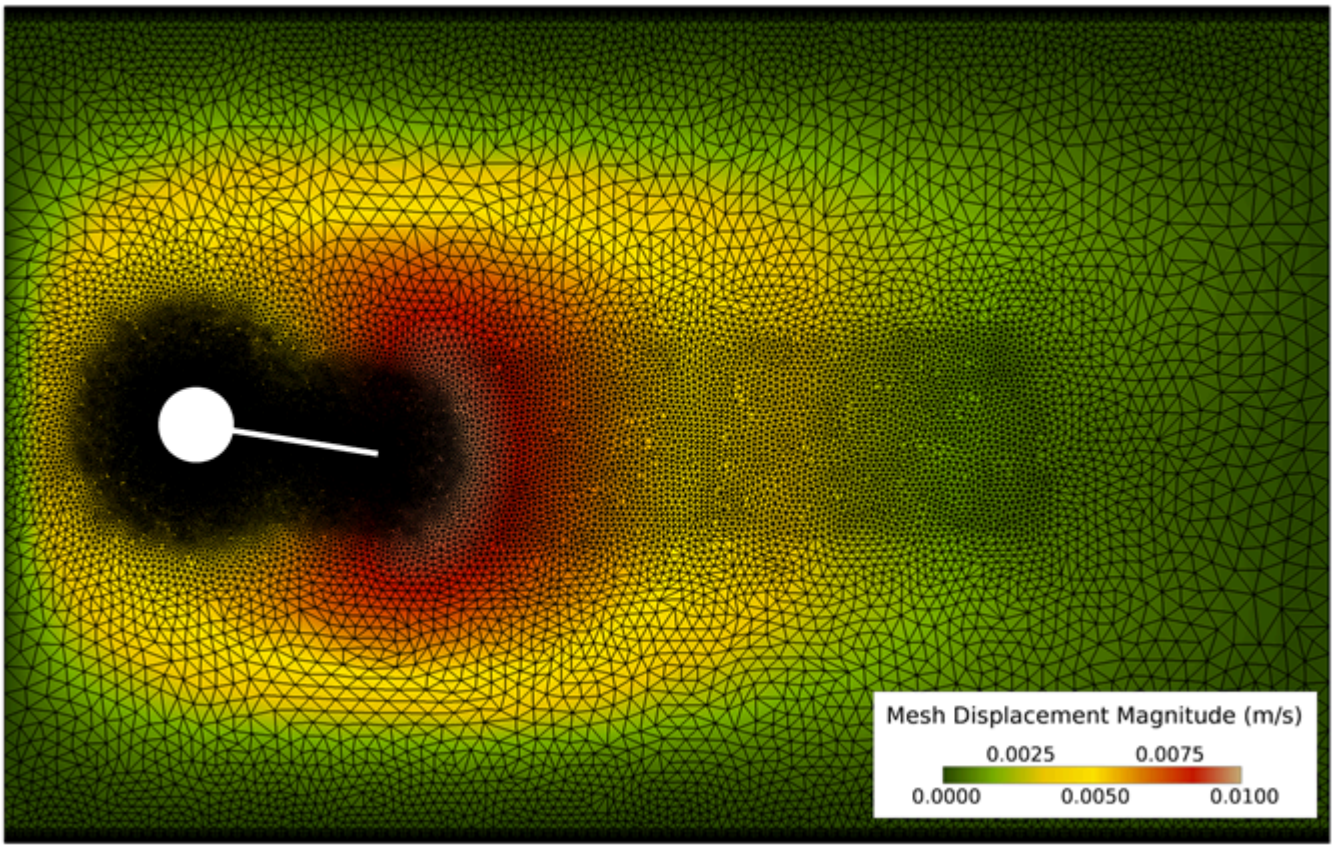


Figure 498: Mesh Displacement Contours Near the Assembly for a Single Time Step During the Simulation

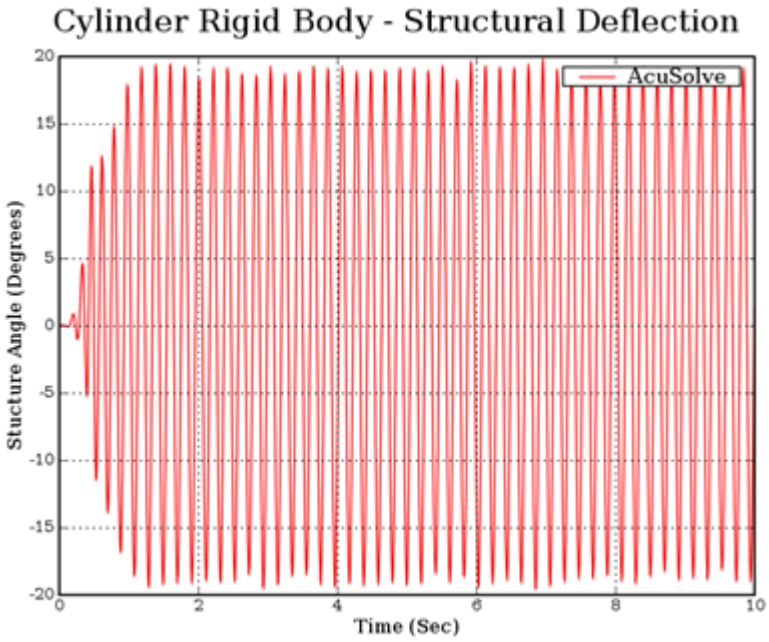


Figure 499: Rigid Body Displacement of the Assembly as a Function of Time, Showing the Oscillation Develop into the Pseudo-Steady Motion

The dominant frequency of the oscillation is easily identified in the Fast Fourier Transform (FFT) of the deflection angle, shown in the plot below.

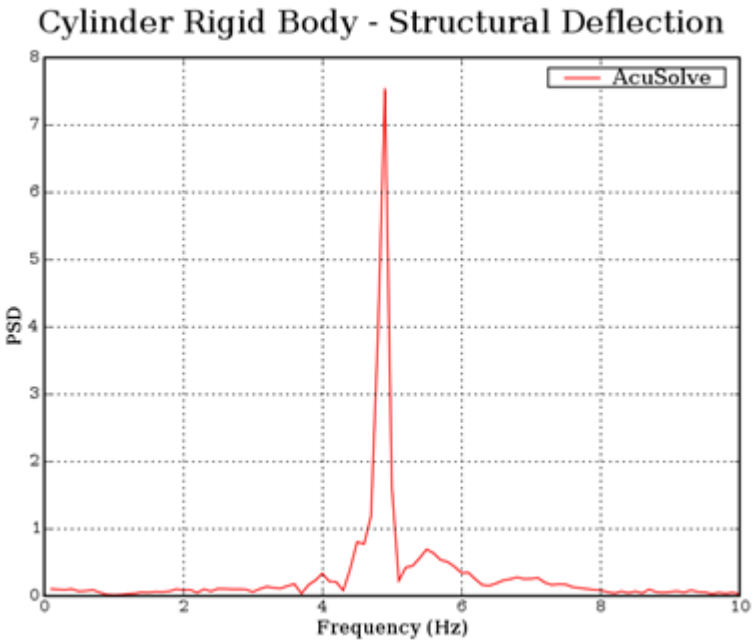


Figure 500: FFT of the Rigid Body Displacement Angle, Showing Power Spectral Density as a Function of Frequency

Summary

The AcuSolve solution compares well with experimental data for flow past an oscillating cylinder/plate assembly. In this application, water moves over the cylinder/plate assembly, giving rise to unsteady loading that causes the body to rotate as a rigid body. The good agreement with the natural frequency of oscillation compared to the experimental data demonstrates that AcuSolve is capable of predicting fluid forced motion with an internal rigid body dynamic solver.

Simulation Settings for Turbulent Flow Over an Oscillating Rigid Body Assembly

AcuConsole database file: `<your working directory>\cylinder_rigidbody_turbulent\cylinder_rigidbody_turbulent.acs`

Global

- Problem Description
  - Analysis type - Transient
  - Turbulence equation - SST
  - Mesh Type- Fully Specified
- Auto Solution Strategy
  - Final Time - `10.0`
  - Initial Time Increment- `0.005`
  - Convergence tolerance- `0.001`
  - Max stagger iterations- `3`
- Material Model
  - Water
    - Type- Constant
    - Density- `998.0` kg/m3
    - Viscosity- `0.00096806` kg/m*sec
- Mesh Motion
  - Interpolated
    - Type- Interpolated Motion
    - Interpolated motion surfaces
      1. Bottom
      2. Top
  - RigidBody
    - Type- Rigid Body Dynamic
      1. Z rotation- Active
      2. Mass- `0.2089` kg
      3. Dyadic
         1. X-X - `3.7 e-5` kg-m2
         2. Y-Y- `3.7 e-5` kg-m2
         3. Z-Z - `3.7 e-5` kg-m2

Model

- Volumes
  - Volume
    - Element Set
      1. Material model- Water
      2. Mesh motion- Interpolated
- Surfaces
  - Body
    - Simple Boundary Condition
      1. Type- Wall
      2. Mesh displacement BC type- Fixed
      3. Mesh motion- RigidBody
    - Interpolated Motion Surface
  - Bottom
    - Simple Boundary Condition
      1. Type- Wall
      2. Mesh displacement BC type- Fixed
    - Interpolated Motion Surface
  - Inflow
    - Simple Boundary Condition
      1. Type- Inflow
      2. Inflow type- Velocity
      3. X Velocity- `1.07` m/sec
      4. Turbulence input type- Auto
      5. Turbulence intensity type- High
    - Advanced Options
      1. Nodal Boundary Conditions
      2. X-velocity
         1. Type- Linear
         2. Precedence- `2`
         3. Curve fit variable- Y coordinate
         4. Curve fit values- Provided
      3. Y-velocity
         1. Type- Zero
      4. Z-velocity
         1. Type- Zero
  - Bottom
    - Simple Boundary Condition

1. Type- Wall
2. Mesh displacement BC type- Fixed
3. Mesh motion- RigidBody

- Interpolated Motion Surface

- Outflow
  - Simple Boundary Condition
    1. Type- Outflow
- Top
  - Simple Boundary Condition
    1. Type- Wall
    2. Mesh displacement BC type- Fixed
  - Interpolated Motion Surface
- maxZ
  - Simple Boundary Condition
    1. Type- Slip
- minZ
  - Simple Boundary Condition
    1. Type- Slip

References

Gomes, J. P. and Lienhart, H. (2009) Experimental Benchmark: Self-excited Fluid-structure Interaction Test Cases, in Fluid-Structure Interaction II: Modeling, Simulation, Optimization, Bungartz, H. J., Mehl, M., Schafer, M. (eds.), 383-412, Springer-Verlag.Ryhming.

Laminar to Turbulent Transition Over an Airfoil

In this application, AcuSolve is used to solve for the flow field around a high lift airfoil with inflow conditions that lead to transitional flow on the pressure and suction side of the airfoil's surface. The moderate level of turbulence intensity at the inlet, low angle of attack and shape of the airfoil induce a transition to turbulent flow after a separation bubble develops on the surface. The coefficient of pressure is compared against experimental data from laboratory experiments.

Problem Description

The problem consists of a fluid having material properties close to air with density of 1.0 kg /m3 and molecular viscosity specified to produce a Reynolds number of 2.0e6, assuming a chord length of 1.0 m and an inlet velocity of 1.0 m/s, as is shown in the following image, which is not drawn to scale. The inflow velocity is oriented to simulate a 1 degree angle of attack. The model is simulated as steady state with constant inflow conditions using the farfield boundary condition. The two-equation gamma-ReTheta (γ- Reθ) transition model, used with the one equation Spalart Allmaras turbulence model, is validated against experimental data obtained from the experimental studies conducted by Somers, 1997.

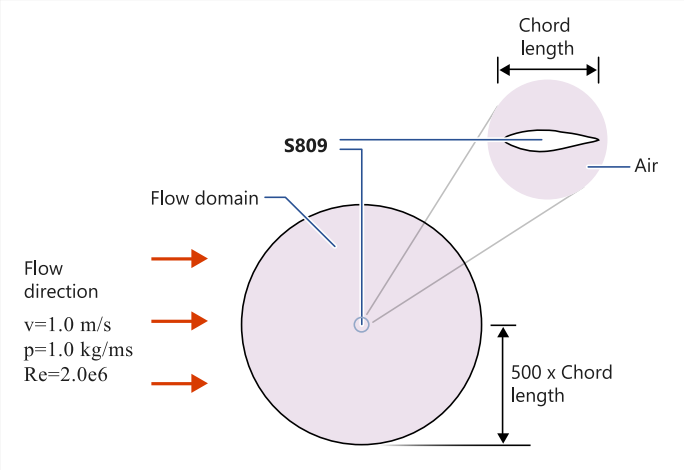


Figure 501: Critical Dimensions and Parameters used for Simulating Transitional Flow over the S809 Airfoil

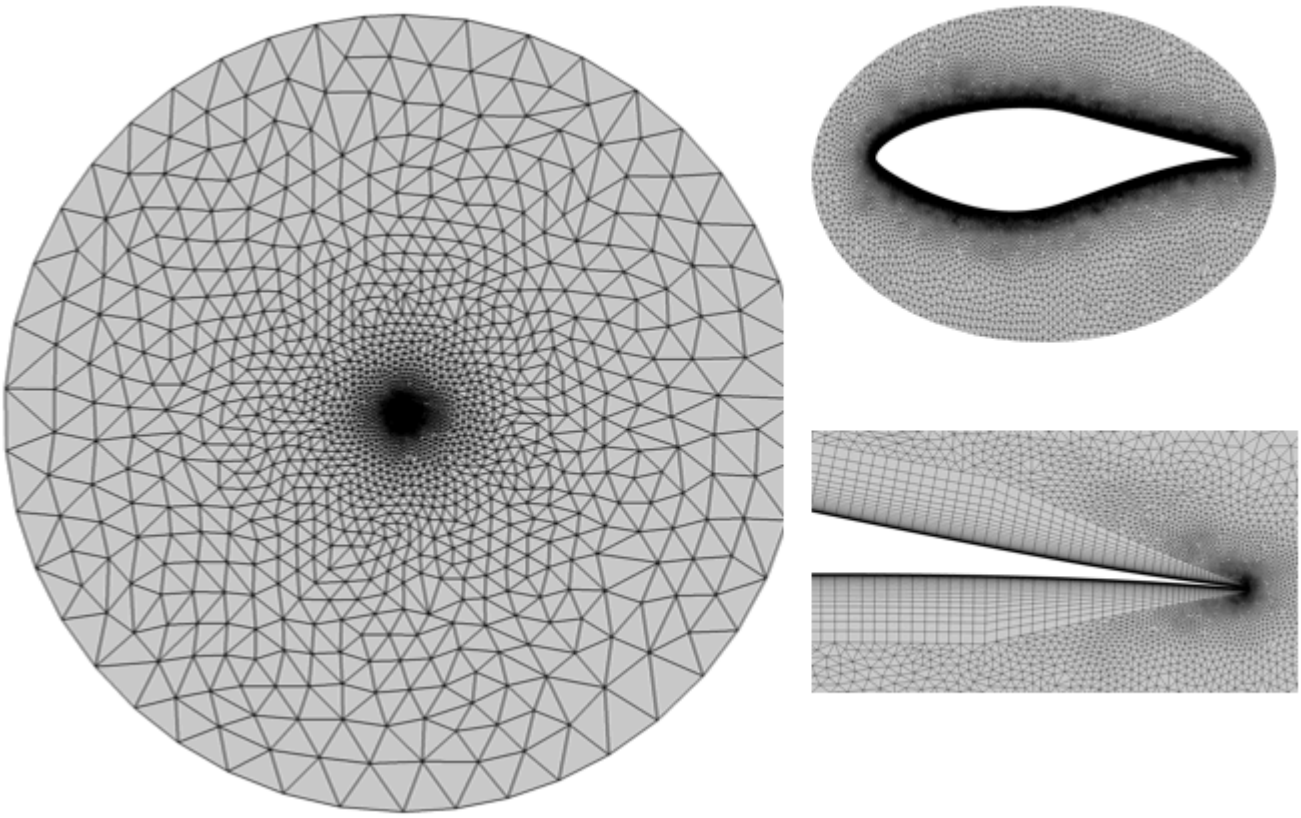


Figure 502: Mesh Used for Simulating Transitional over the S809 Airfoil

The simulation was performed as a two-dimensional problem by constructing a volume mesh that contains a single layer of elements extruded in the cross-stream direction, normal to the flow plane and by imposing symmetry boundary conditions on the extruded planes. The airfoil walls are specified as no-slip and the inlet velocity and eddy viscosity are specified at the farfield boundary.

AcuSolve Results

The AcuSolve solution converged to a steady state and the results reflect the mean flow conditions over the airfoil. The simulation results show that the flow field is laminar at the leading edge until approximately 50 percent chord on the pressure side and until approximately 55 percent on the suction side, then transitions to turbulent as it moves further downstream. The onset is caused by small separation bubbles at these locations. The following images show the negative pressure coefficient (-Cp) on the surface of the airfoil. The mean pressure at a reference point upstream of the airfoil is subtracted from the surface pressure and divided by the inlet velocity and air density to arrive at Cp. The Cp computed from AcuSolve is compared with experimental data, as described in Somers, 1997. The image shows black circles representing the experimental data and a solid red line for the AcuSolve results. Additional plots show contours of intermittency that illustrate the transition from laminar to turbulent flow.

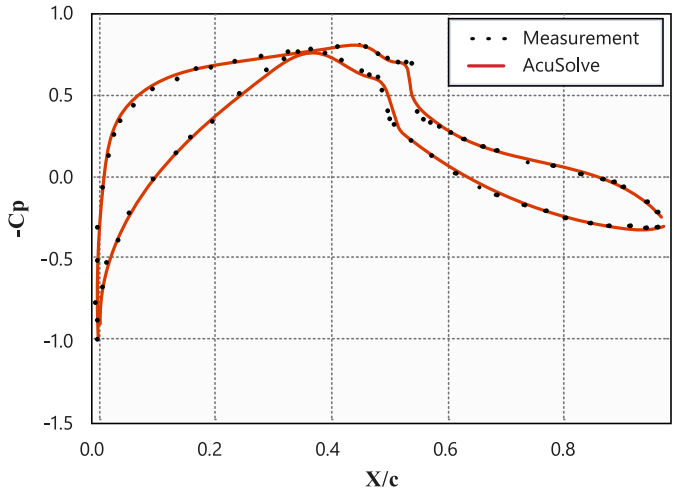


Figure 503: Negative pressure coefficient on the airfoil surface showing experimental and simulated results for the SA two equation (γ- Reθ) transition model

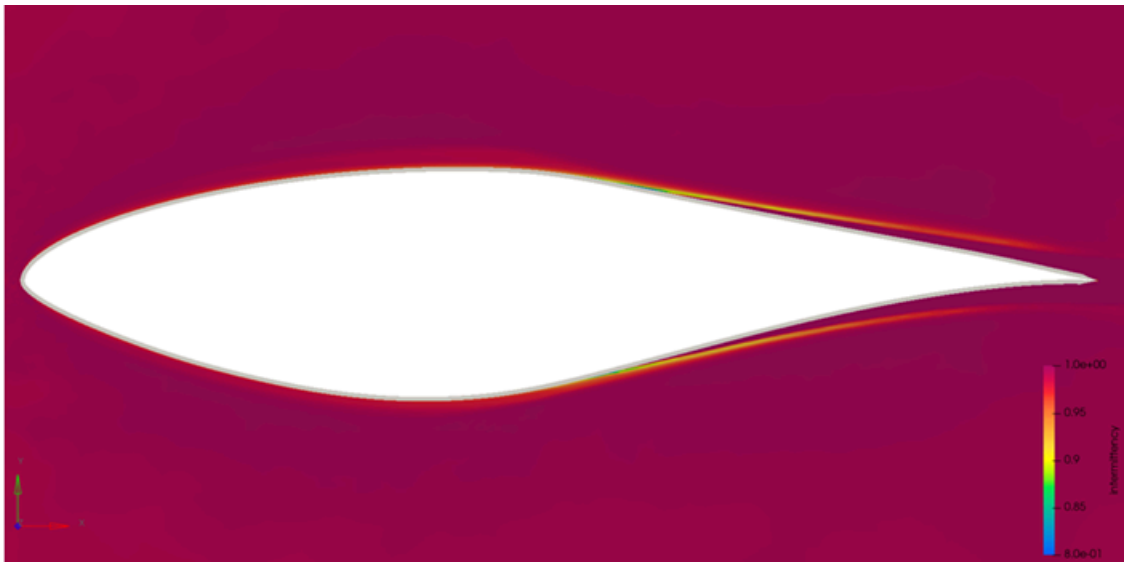


Figure 504: Contours of Intermittency Demonstrate the Onset Location from Laminar to Turbulent over the Airfoil

Summary

The AcuSolve solution compares well with experimental data for transitional flow over the S809 airfoil at a low angle of attack. Additional simulations and measurements for the full drag polar have been tested and compare well with considerably better accuracy when transition closure is included into the RANS solution. The good agreement with experimental results for the transition location and magnitude of expected pressure demonstrate that AcuSolve can predict the transition onset location for flow over surfaces with mild to moderate pressure gradients.

Simulation Settings for Laminar to Turbulent Transition Over an Airfoil

HyperWorks CFD database file: `<your working directory>\airfoil_transition\airfoil_transition.hm`

Global

- Problem Description
  - Analysis type - Steady State
  - Turbulence equation - Spalart Allmaras
  - Turbulence transition model- Gamma-ReTheta
- Auto Solution Strategy
  - Max time steps - `100`
  - Convergence tolerance - `0.0001`
  - Relaxation Factor- `0.5`
  - Turbulence transition- on
- Material Model
  - Air
    - Type - Constant
    - Density - `1.0` kg/m3
    - Viscosity - `5.0e-7` kg/m*sec

  Model
- Volumes
  - Fluid
    - Element Set
      1. Material model - Air
- Surfaces
  - +z slip
    - Simple Boundary Condition
      1. Type- Slip
  - -z slip
    - Simple Boundary Condition
      1. Type- Slip
  - farfield
    - Simple Boundary Condition
      1. Type- Far Field
      2. X velocity = `1.0` *cos(α), where α is the angle of attack in radians
      3. Y velocity = `1.0` *sin(α), where α is the angle of attack in radians
      4. Turbulence input type- Auto
      5. Turbulence intensity type- Value
      6. Turbulence intensity percent- `0.025`
  - airfoil surface
    - Simple Boundary Condition

1 Type- Wall

References

Somers, D., Design and Experimental Results for the S809 Airfoil. NREL/SR-440-6918. 1997

Transitional Flow

7

This section includes validation cases containing conditions producing laminar to turbulent flow that are simulated with a turbulence transition model.

This chapter covers the following:

- Laminar to Turbulent Transition Over an Airfoil (p. 684)

Laminar to Turbulent Transition Over an Airfoil

In this application, AcuSolve is used to solve for the flow field around a high lift airfoil with inflow conditions that lead to transitional flow on the pressure and suction side of the airfoil's surface. The moderate level of turbulence intensity at the inlet, low angle of attack and shape of the airfoil induce a transition to turbulent flow after a separation bubble develops on the surface. The coefficient of pressure is compared against experimental data from laboratory experiments.

Problem Description

The problem consists of a fluid having material properties close to air with density of 1.0 kg /m3 and molecular viscosity specified to produce a Reynolds number of 2.0e6, assuming a chord length of 1.0 m and an inlet velocity of 1.0 m/s, as is shown in the following image, which is not drawn to scale. The inflow velocity is oriented to simulate a 1 degree angle of attack. The model is simulated as steady state with constant inflow conditions using the farfield boundary condition. The two-equation gamma-ReTheta (γ- Reθ) transition model, used with the one equation Spalart Allmaras turbulence model, is validated against experimental data obtained from the experimental studies conducted by Somers, 1997.

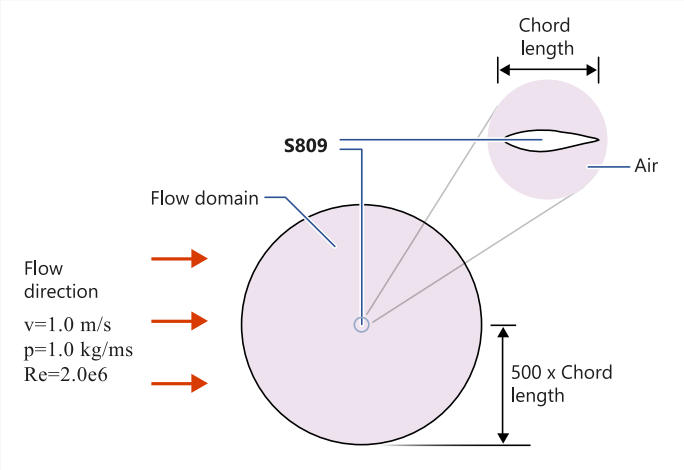


Figure 505: Critical Dimensions and Parameters used for Simulating Transitional Flow over the S809 Airfoil

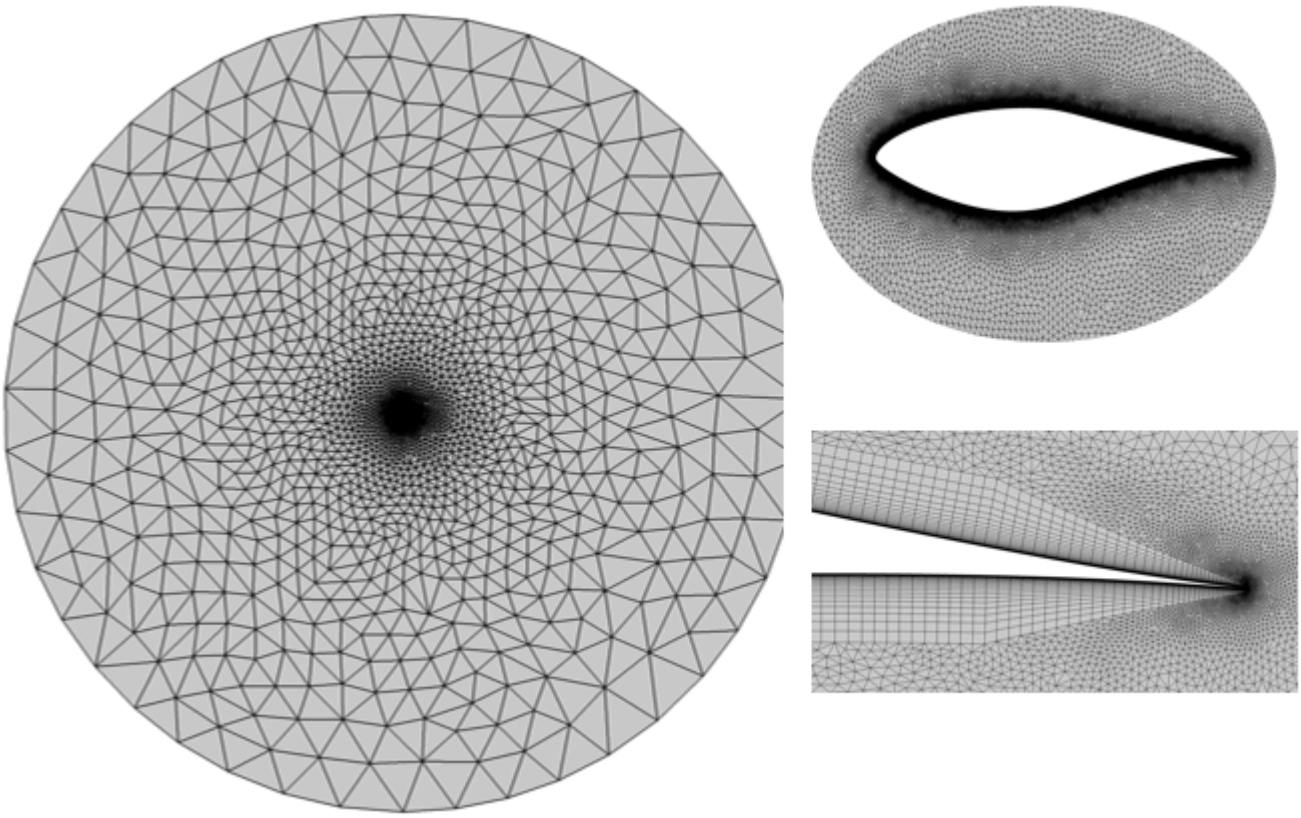


Figure 506: Mesh Used for Simulating Transitional over the S809 Airfoil

The simulation was performed as a two-dimensional problem by constructing a volume mesh that contains a single layer of elements extruded in the cross-stream direction, normal to the flow plane and by imposing symmetry boundary conditions on the extruded planes. The airfoil walls are specified as no-slip and the inlet velocity and eddy viscosity are specified at the farfield boundary.

AcuSolve Results

The AcuSolve solution converged to a steady state and the results reflect the mean flow conditions over the airfoil. The simulation results show that the flow field is laminar at the leading edge until approximately 50 percent chord on the pressure side and until approximately 55 percent on the suction side, then transitions to turbulent as it moves further downstream. The onset is caused by small separation bubbles at these locations. The following images show the negative pressure coefficient (-Cp) on the surface of the airfoil. The mean pressure at a reference point upstream of the airfoil is subtracted from the surface pressure and divided by the inlet velocity and air density to arrive at Cp. The Cp computed from AcuSolve is compared with experimental data, as described in Somers, 1997. The image shows black circles representing the experimental data and a solid red line for the AcuSolve results. Additional plots show contours of intermittency that illustrate the transition from laminar to turbulent flow.

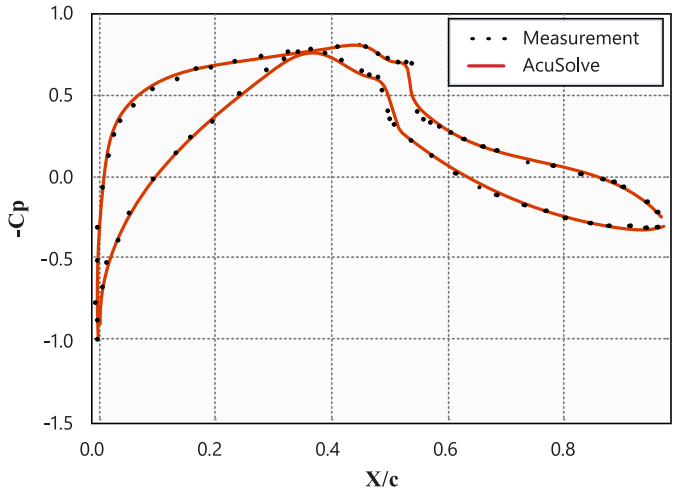


Figure 507: Negative pressure coefficient on the airfoil surface showing experimental and simulated results for the SA two equation (γ- Reθ) transition model

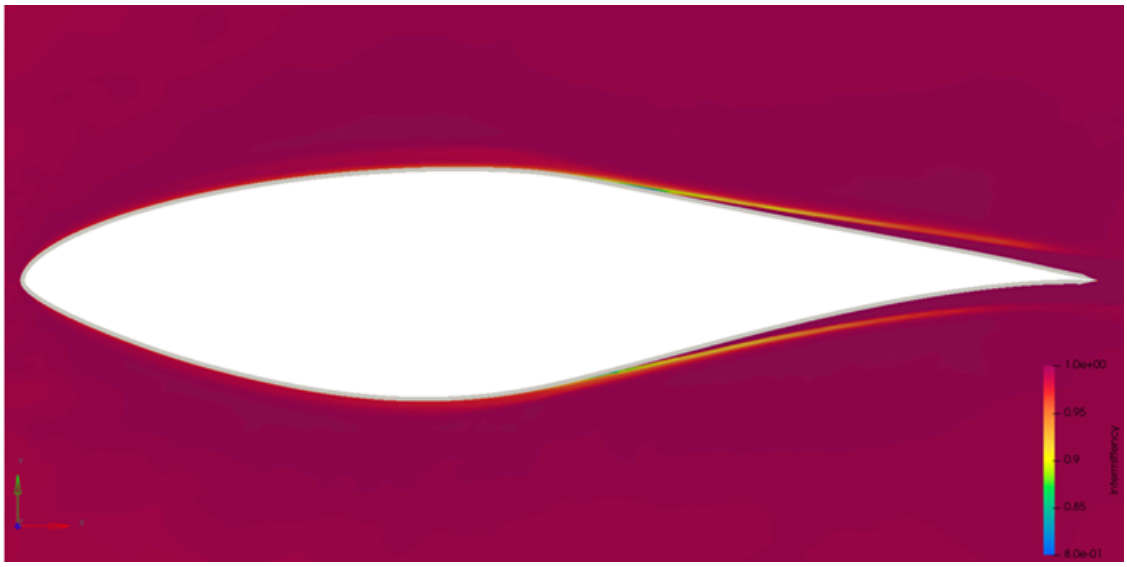


Figure 508: Contours of Intermittency Demonstrate the Onset Location from Laminar to Turbulent over the Airfoil

Summary

The AcuSolve solution compares well with experimental data for transitional flow over the S809 airfoil at a low angle of attack. Additional simulations and measurements for the full drag polar have been tested and compare well with considerably better accuracy when transition closure is included into the RANS solution. The good agreement with experimental results for the transition location and magnitude of expected pressure demonstrate that AcuSolve can predict the transition onset location for flow over surfaces with mild to moderate pressure gradients.

Simulation Settings for Laminar to Turbulent Transition Over an Airfoil

HyperWorks CFD database file: `<your working directory>\airfoil_transition\airfoil_transition.hm`

Global

- Problem Description
  - Analysis type - Steady State
  - Turbulence equation - Spalart Allmaras
  - Turbulence transition model- Gamma-ReTheta
- Auto Solution Strategy
  - Max time steps - `100`
  - Convergence tolerance - `0.0001`
  - Relaxation Factor- `0.5`
  - Turbulence transition- on
- Material Model
  - Air
    - Type - Constant
    - Density - `1.0` kg/m3
    - Viscosity - `5.0e-7` kg/m*sec

  Model
- Volumes
  - Fluid
    - Element Set
      1. Material model - Air
- Surfaces
  - +z slip
    - Simple Boundary Condition
      1. Type- Slip
  - -z slip
    - Simple Boundary Condition
      1. Type- Slip
  - farfield
    - Simple Boundary Condition
      1. Type- Far Field
      2. X velocity = `1.0` *cos(α), where α is the angle of attack in radians
      3. Y velocity = `1.0` *sin(α), where α is the angle of attack in radians
      4. Turbulence input type- Auto
      5. Turbulence intensity type- Value
      6. Turbulence intensity percent- `0.025`
  - airfoil surface
    - Simple Boundary Condition

1 Type- Wall

References

Somers, D., Design and Experimental Results for the S809 Airfoil. NREL/SR-440-6918. 1997

Transient Flow

8

This section includes validation cases that consider time dependent flow simulations.

This chapter covers the following:

- Oscillating Laminar Flow Around a Circular Cylinder (p. 690)
- Ideal Gas Compression in an Actuating Piston (p. 695)
- Laminar Free Surface Flow Inside a Rotating Cavity (p. 702)
- Turbulent Flow Over an Oscillating Rigid Body Assembly (p. 708)
- Circumferential Flow in a Cylinder Induced by a Rotating Solid (p. 716)
- Multiphase Flow Within a Sloshing Tank (p. 722)
- Two-Phase Nucleate Boiling in a Cylindrical Pipe (p. 729)
- Supersonic Flow Through a Converging-Diverging Nozzle (p. 733)

Oscillating Laminar Flow Around a Circular Cylinder

In this application, AcuSolve is used to simulate two dimensional, laminar flow over a cylinder to predict separation of flow from the cylinder surface and the flow in the wake area. AcuSolve results are compared with experimental results as described in Tritton (1959). The close agreement of AcuSolve results with experimental results validates the ability of AcuSolve to model cases with unsteady oscillating vortex streets.

Problem Description

The problem consists of a cylinder located in a rectangular domain, as shown in the following image, which is not drawn to scale. A fluid enters the domain with a low velocity (v) of 0.5 m/s. The diameter (D) of the cylinder is 20 cm. The domain extends 10 X D upstream of the cylinder center, 5D above and below the cylinder center, and 40D downstream of the cylinder center. The density of the working fluid is 1 kg/m^3 and the viscosity is 0.001 kg/m-s. The Reynolds number for this problem is 100.

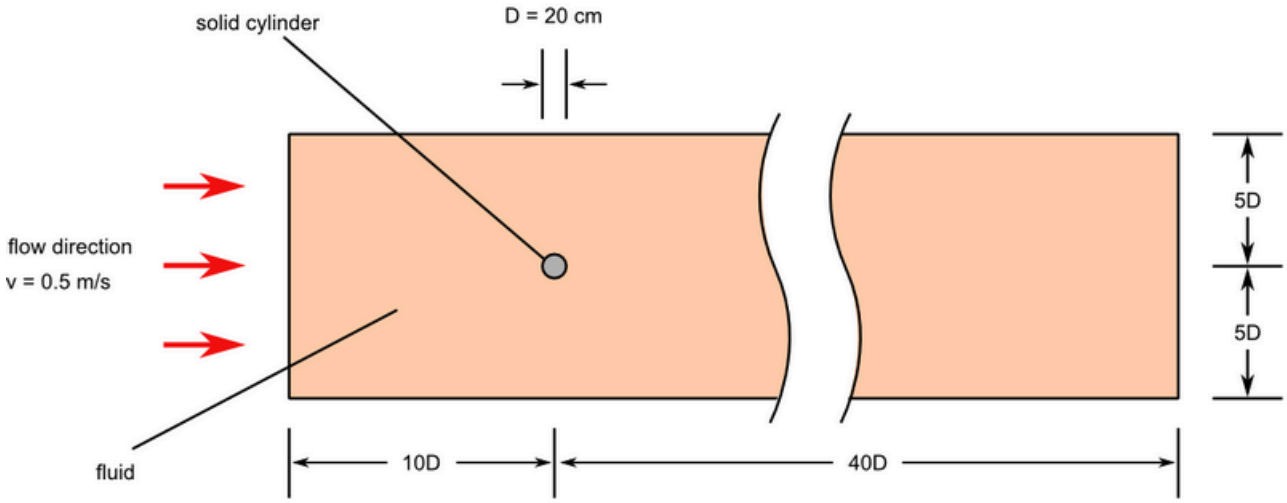


Figure 509: Critical Dimensions and Parameters for Simulating Oscillating Laminar Flow Around a Circular Cylinder

The simulation was performed as a two dimensional problem by constructing a volume mesh that contains a single layer of elements in the extruded direction, normal to the flow plane, and by imposing symmetry boundary conditions on the extruded planes.

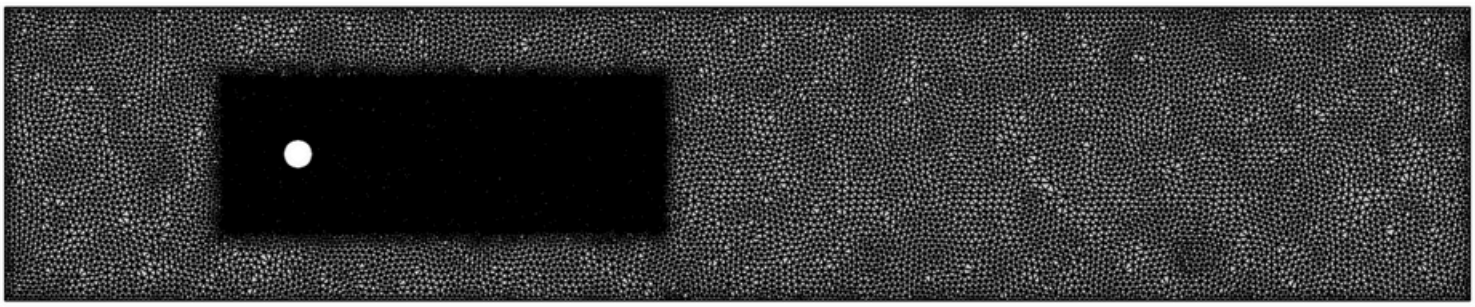


Figure 510: Mesh used for Simulating Oscillating Laminar Flow Around a Circular Cylinder

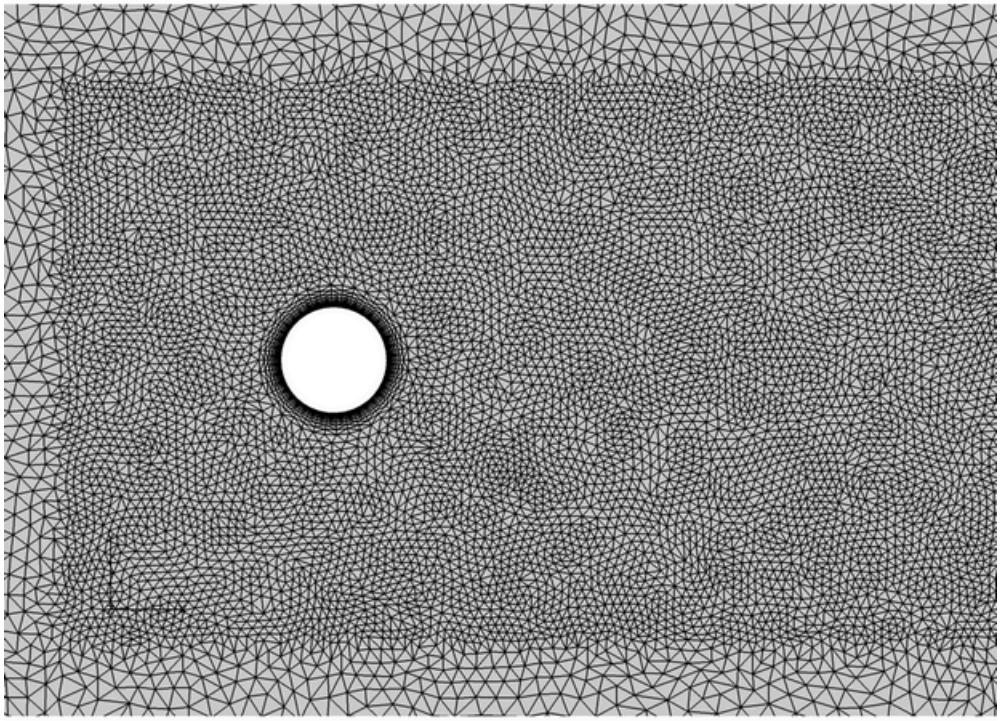


Figure 511: Details of the Mesh Showing Refinement Zone Around the Cylinder

AcuSolve Results

The simulation was run as transient for a time record sufficient to ensure that the vortex shedding in the wake reached a stabilized oscillation frequency. The AcuSolve solution shows an unsteady, oscillating flow field with flow around the cylinder separating from the cylinder surface. A wake area is developed downstream of the cylinder with alternating vortices shedding at a regular frequency from the top and bottom of the cylinder surface. This results in oscillating lift forces that act on the cylinder as shown in the following images.

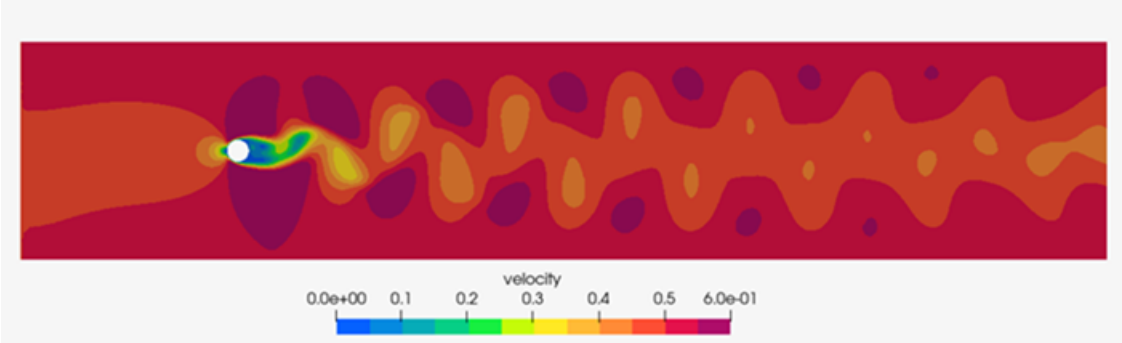


Figure 512: Contours of Velocity Magnitude

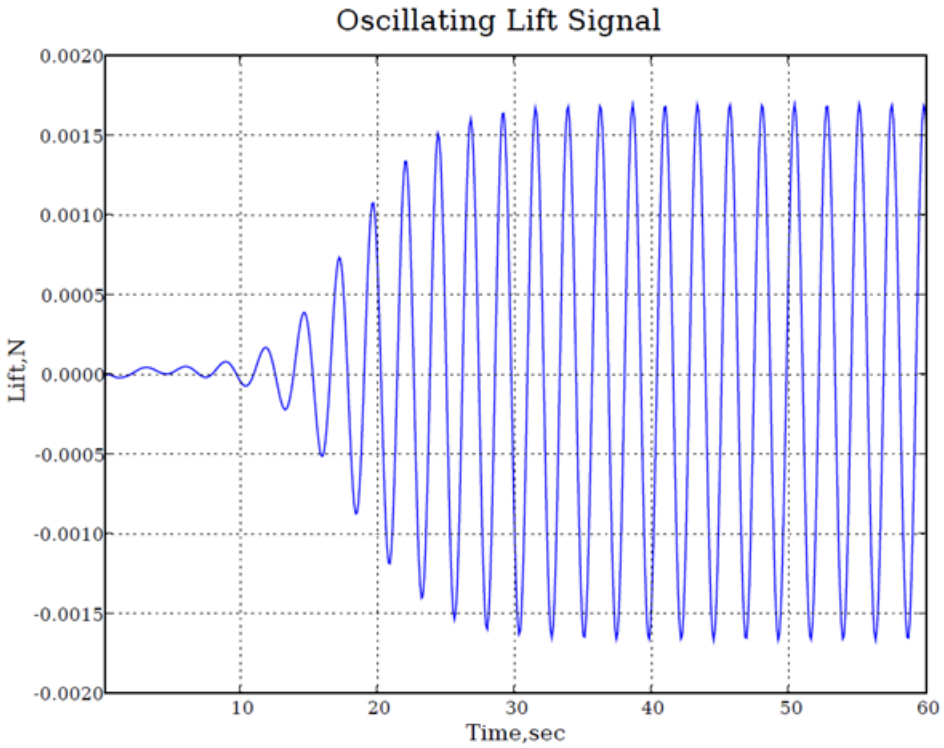


Figure 513: Lift Coefficient (lift force perpendicular to flow) plotted against time. Simulation was run for 600 time steps for a duration of 60 s

The Strouhal number for this simulation, a dimensionless number describing oscillating flows, is used to validate AcuSolve results. The experimental Strouhal number for this problem is given by

$$St = \frac{\omega^* L}{v} = 0.165 \tag{19}$$

where ω is the dominant frequency of oscillations, L is the diameter of the cylinder, and v is the flow velocity.

The peak frequency of the oscillating lift force was computed by transforming the time dependent data into frequency space with a Fourier transform. From the Fourier transform, the AcuSolve-based Strouhal

number was calculated. The table below shows the comparison of the Strouhal number provided by the AcuSolve prediction and the measurement given by Tritton (1959).

Table 34:

	Experimental	**AcuSolve**
Strouhal number	0.165	0.173

Summary

In this application, two dimensional flow over a cylinder is achieved by enforcing symmetry conditions on the front and back surfaces of the flow domain. The laminar, unsteady simulation shows the flow separation that leads to alternating vortex shedding. Frequency of the lift force acting on the cylinder is calculated to evaluate the Strouhal number. The AcuSolve solution compares well with results reported by Tritton (1959), differing slightly from the experimental results. In this application, AcuSolve demonstrates the ability to accurately predict oscillating laminar flow around a circular cylinder.

Simulation Settings for Oscillating Laminar Flow Around a Circular Cylinder

HyperWorks CFD database file: `<your working directory>\cylinder_laminar\cylinder_laminar.hm`

Global

- Problem Description
  - Analysis type - Transient
  - Turbulence equation - Laminar
- Auto Solution Strategy
  - Analysis type - Transient
  - Max time - `600` sec
  - Initial time increment - `0.1` sec
- Material Model
  - Fluid
    - Density - `1.0` kg/m3
    - Viscosity - `1.0e-3` kg/m-sec

  Model
- Volumes
  - Volume
    - Element Set
      1. Material model - Fluid
- Surfaces
  - Back
    - Simple Boundary Condition
      1. Type - Symmetry

- Base
  - Simple Boundary Condition
    1. Type - Slip
- Front
  - Simple Boundary Condition
    1. Type - Symmetry
- Inflow
  - Simple Boundary Condition
    1. Type - Inflow
    2. Inflow Type - Average velocity
    3. Average Velocity - `0.5` m/sec
- Outflow
  - Simple Boundary Condition
    1. Type - Outflow
- Top
  - Simple Boundary Condition
    1. Type - Slip

References

D.J. Tritton. "Experiments on the Flow around a Circular Cylinder at Low Reynolds Number". Journal of Fluid Mech. 6(04):547-567. 1959

Ideal Gas Compression in an Actuating Piston

In this application, AcuSolve is used to simulate pressure and temperature inside an actuating piston using the ideal gas relationship and fully defined mesh motion. AcuSolve results are compared with analytical results as described in Moran and Shapiro (2000). The close agreement of AcuSolve results with analytical results validates the ability of AcuSolve to model cases with material properties defined by the ideal gas law subjected to significant mesh distortion.

Problem Description

The problem consists of air compressed by a piston within a cylinder 10 m long with a diameter of π (3.14159) m, as shown in the following image, which is not drawn to scale. The piston is driven by a crankshaft 4 m long attached to a connecting rod 6 m long. The crankshaft rotates at 60o/s around a center point. At time (t) = 0.0 s the crank and piston are at top dead center (TDC) with an initial cylinder volume of 80 m^3. At t = 3.0 s the piston is at bottom dead center (BDC), at which point the volume in the cylinder is reduced to 16 m^3. The piston then moves back to TDC at t = 6.0 s. Air at atmospheric conditions, with material properties of an ideal gas and a dynamic viscosity of 1.781 X 10^5 kg/m-sec is the fluid modeled in the domain.

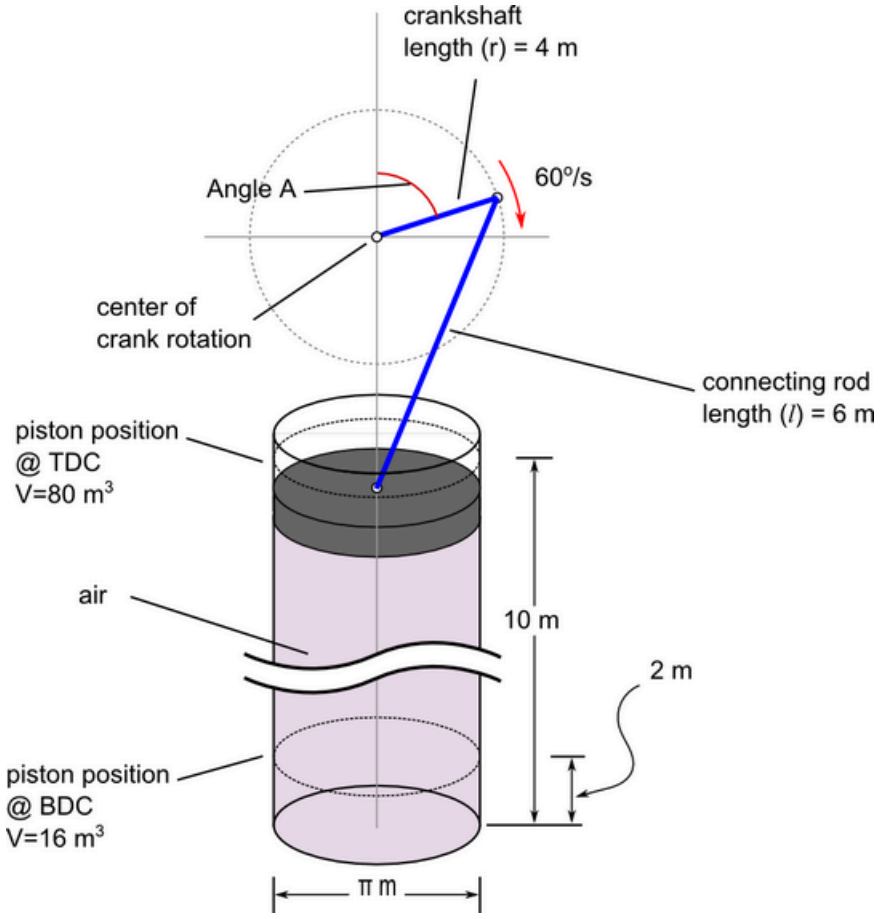


Figure 514: Critical Dimensions and Parameters for Simulating Ideal Gas Compression in an Actuating Piston

The motion of the piston is described by the following equation.

$$x = r*\cos A + \sqrt{l^2 - r^2 \sin^2 A} \quad (20)$$

Where

- x is the distance of the piston from TDC
- r is the length of the connecting rod, 4 m
- A is the crank angle as a function of time (t)
- l is the connecting rod length, 6 m

During the simulation, the top surface of the cylinder, representing the piston, moves with an applied mesh motion that mimics the motion of the reciprocating crank, rod, and piston assembly. The ideal gas is compressed by contracting the mesh according to the motion of that assembly and by allowing the fluid properties to change as a function of time.

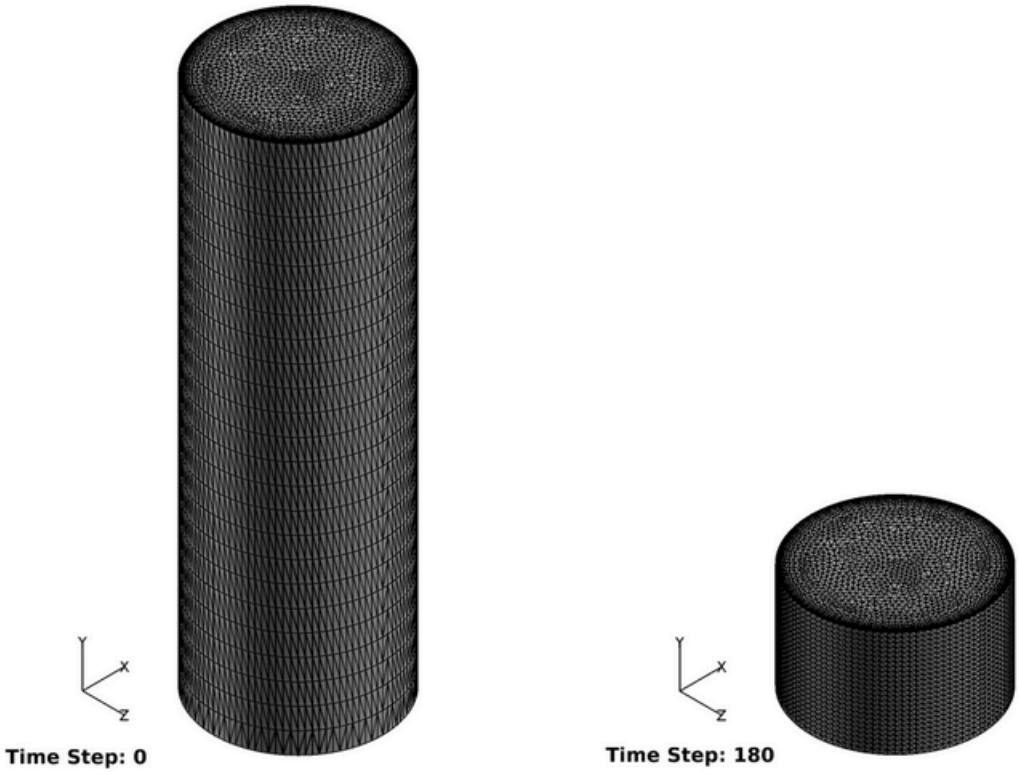


Figure 515: Mesh Used for Simulating Ideal Gas Compression in an Actuating Pistion at Time Step 0 and Time Step 180 (3 s)

AcuSolve Results

The simulation was run as transient for a total of 360 time steps with a duration of 6.0 seconds. The AcuSolve solution shows time dependent pressure and temperature in a cylinder volume that compresses and expands in a 6.0 second cycle. Pressure and temperature increase as the cylinder volume decreases, and returns toward initial conditions as the cylinder volume expands. The contours of pressure and temperature within the cylinder at the initial stage (t = 0.0 s) and the half cycle (t = 3.0 s) are shown in the following images.

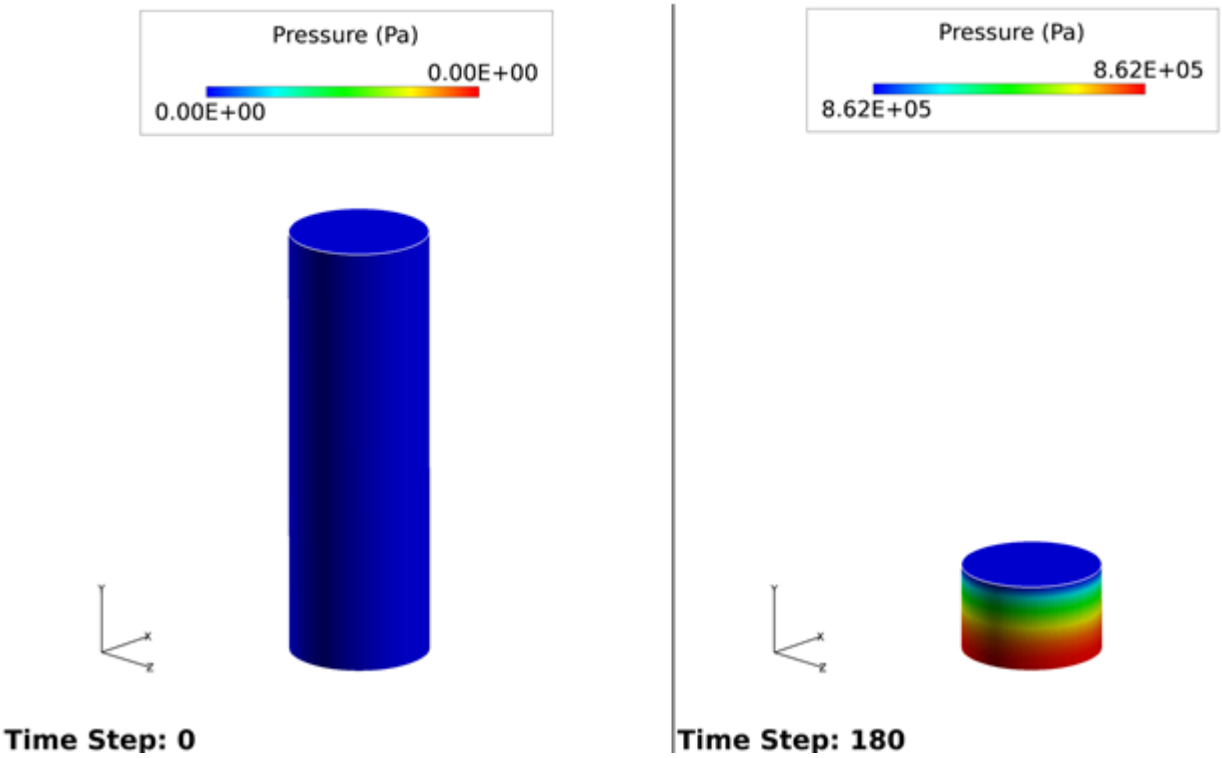


Figure 516: Pressure Distribution Within the Domain with the Piston at TDC and BDC

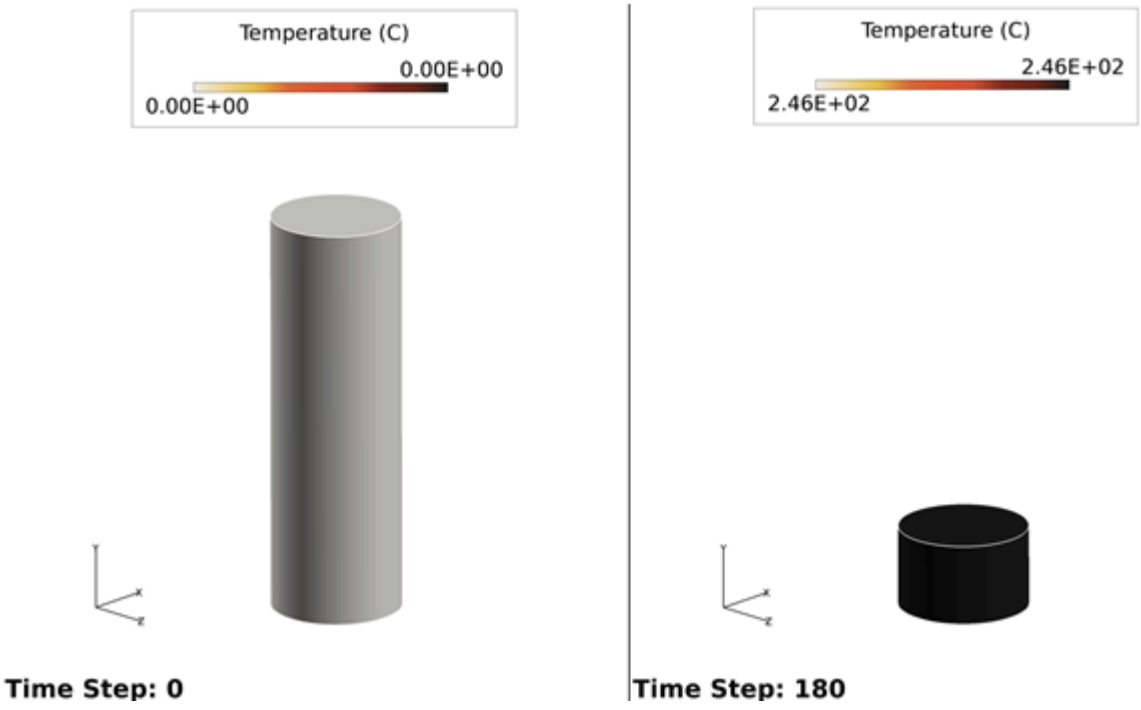


Figure 517: Temperature Distribution Within the Domain with the Piston at TDC and BDC

Comparison of time history plots of the AcuSolve and analytical solutions shows that the AcuSolve solution is nearly identical to the analytical solution. The AcuSolve computed internal pressure reaches a maximum of 8.62 X 105 Pa and the temperature reaches a maximum of 246.45 degrees C.

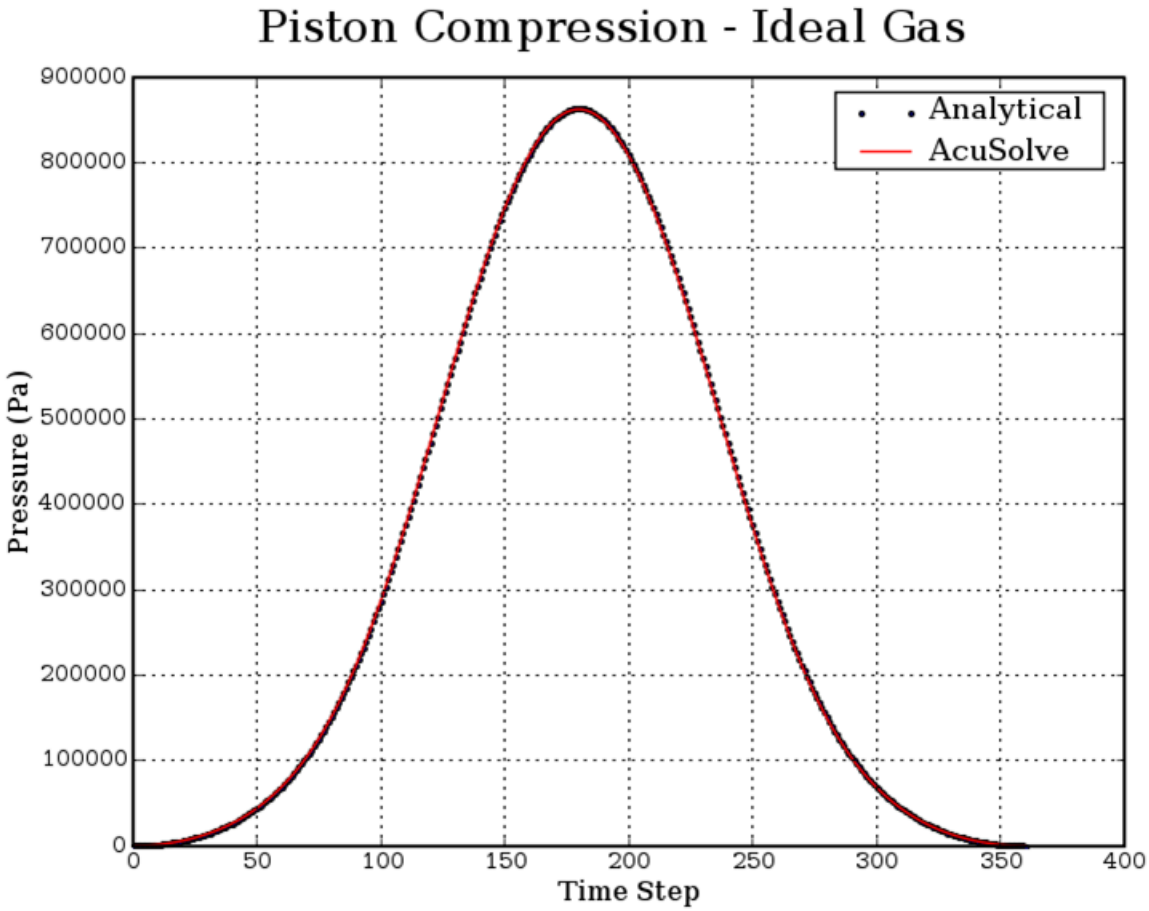


Figure 518: History Plots of Pressure for AcuSolve and Analytical Solutions

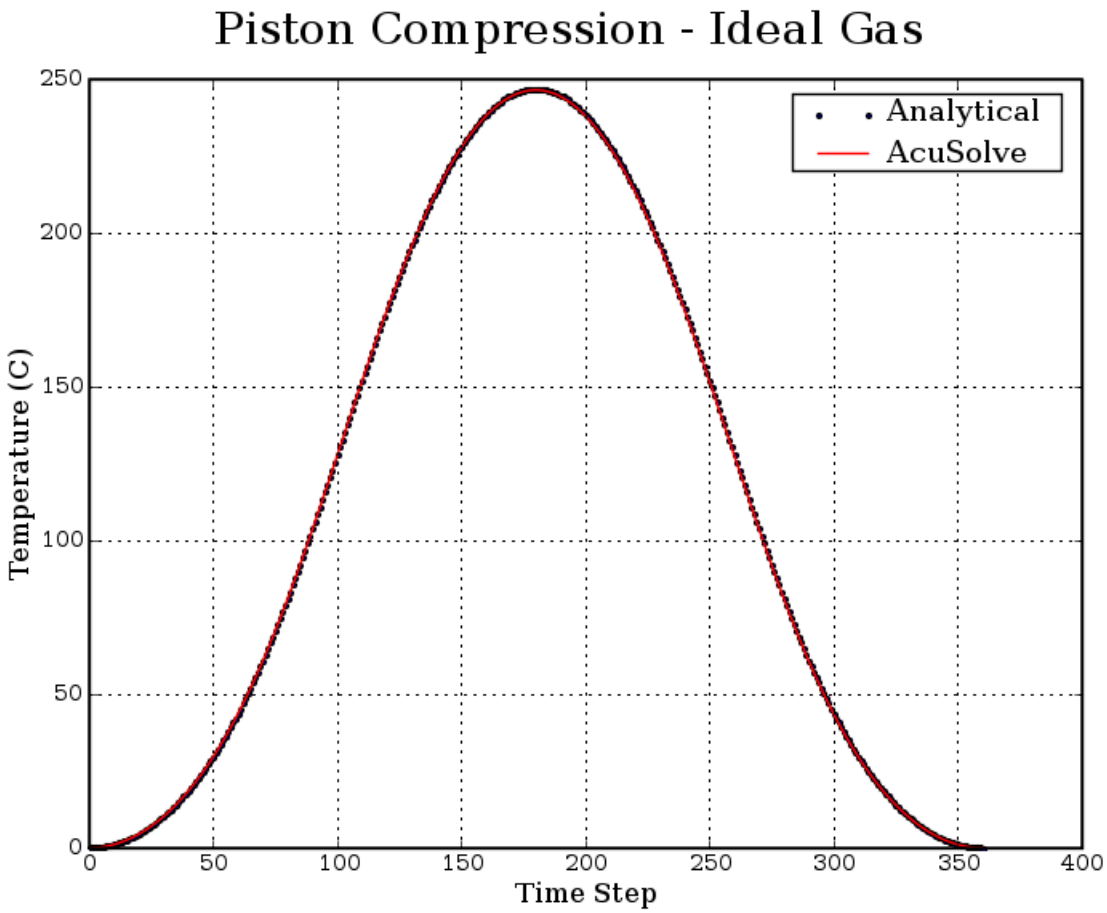


Figure 519: History Plots of Temperature for AcuSolve and Analytical Solutions

Summary

The AcuSolve solution compares well with analytical results for ideal gas compression in an actuating piston. The AcuSolve transient solution compares nearly identically with the analytical solution, with 0.1 percent and 0.16 percent error for the maximum pressure and temperature, respectively. As a result, AcuSolve demonstrates the ability to predict ideal gas compression in an actuating piston.

Simulation Settings for Ideal Gas Compression in an Actuating Piston

AcuConsole database file: `<your working directory>\cylinder_piston_compression\cylinder_piston_compression.acs`

Global

- Problem Description
  - Analysis type - Transient
  - Temperature equation - Advective Diffusive
  - Turbulence equation - Laminar
  - Mesh type - Fully Specified

- Auto Solution Strategy
  - Max time steps - `360`
  - Initial time increment - `0.01667` sec
  - Convergence tolerance - `1.0e-5` sec
  - Max stagger iterations - `10`
- Multiplier Function
  - Piston
    - Type - Piecewise Linear
    - Curve fit variable - Time
    - Curve fit values - (included in `.acs` based on equation discussed in problem description)
- Material Model
  - Air
    - Density
      1. Type - Ideal Gas
      2. Gas constant - `286.9` J/kg-K
      3. Abs. pressure offset - `101325.0` N/m2
      4. Abs. temperature offset - `273.15` K
    - Viscosity - `1.781e-5` kg/m-sec
- Mesh Motion
  - Piston
    - Type - Translation
    - Translation velocity - `0.0`, `-1.0`, `0.0`
    - Velocity variable - Multiplier Function
    - Translation multiplier function - Piston

  Model
- Volumes
  - Fluid
    - Element Set
      1. Material model - Air
      2. Compression heating - On
    - Element Output - on
- Surfaces
  - BDC
    - Simple Boundary Condition
      1. Type - Wall
      2. Wall velocity type - Match Mesh Velocity
      3. Mesh displacement BC type - Fixed
  - SideWall

        - Simple Boundary Condition
            1. Type - Wall
            2. Wall velocity type - Match Mesh Velocity
            3. Mesh displacement BC type - Fixed
    - TDC
        - Simple Boundary Condition
            1. Type - Wall
            2. Mesh displacement BC type - Fixed
            3. Mesh motion - Piston
- Nodes
    - VolumeNodes
        - Mesh X-Displacement
            1. Type - Zero
        - Mesh Y-Displacement
            1. Type - Linear
            2. Mesh motion - Piston
            3. Curve fit variable - Y reference coordinate
                1. X1 - `10.0` m
                2. Y1 - `1.0` m
                3. Y2 - `0.0` m
        - Mesh Z-Displacement
            1. Type - Zero

References

M.J. Moran and H.N Shapiro. "Fundamentals of Engineering Thermodynamics". Wiley. 4th Ed. 2000.

Laminar Free Surface Flow Inside a Rotating Cavity

In this application, AcuSolve is used to solve for the flow field within a rotating cavity with the top of the cavity free to move as if it was exposed to air. The height of the free surface is determined and compared against the analytical solution for the same rotational velocity under the standard gravitational force.

Problem Description

The problem consists of a fluid with arbitrary material properties rotating within an axisymmetric cavity. The cavity is 1.0 m in height with a radius of 0.5 m and is rotating at a constant speed of 3.0 rad/sec, as shown in the following image, which is not drawn to scale. The model is simulated as transient with the fluid initially at rest within the cavity. The radial velocity applied to the cavity walls causes the fluid's free surface to creep up the side wall forming a parabolic shape. The height of this surface is compared against the analytical solution as described in White, 2003.

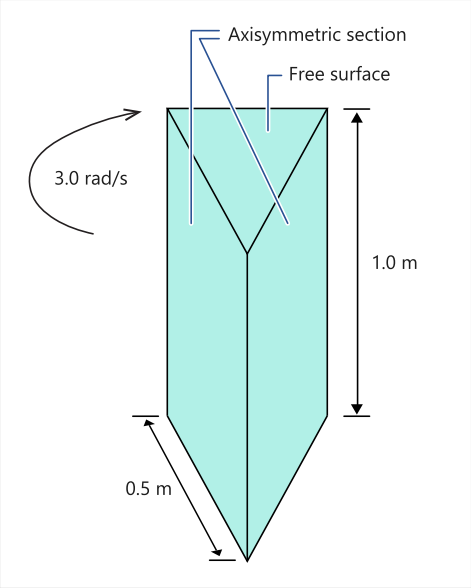


Figure 520: Critical Dimensions and Parameters used for Simulating a Laminar Free Surface Inside a Rotating Cavity

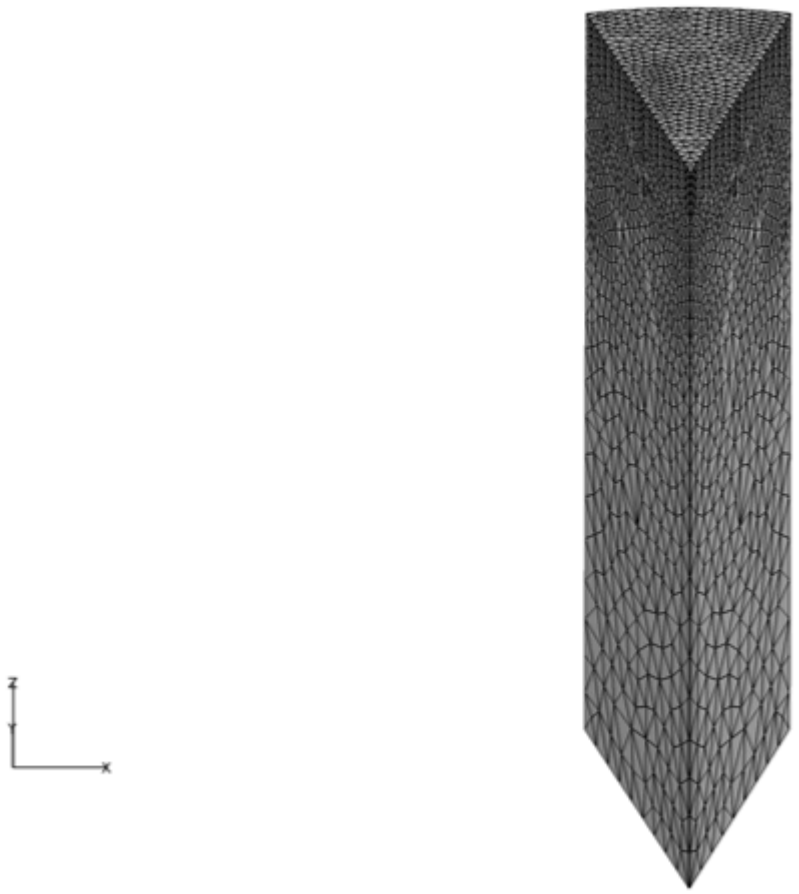


Figure 521: Mesh used for Simulating Laminar Free Surface Flow Inside a Rotating Cavity

The problem is simulated as axisymmetric by considering a 30 degree portion of the cavity with rotationally periodic boundary conditions applied on the planar surfaces representing the cut faces of the cavity.

AcuSolve Results

The AcuSolve solution reaches a quasi-static result with the free surface height stabilizing, demonstrating the final flow conditions of the simulation. As the fluid within the cavity is subjected to the multiple reference frame simulating the rotating boundaries the free surface begins to deform. At the center of the cavity the fluid height decreases and in order to conserve mass the height steadily increases as a function of the radial distance from the center. The surface height takes the form of a parabola as described in White, 2003. The following image demonstrates the shape that the fluid forms within the cavity, showing the vertical displacement of the rotating fluid. The free surface height is compared with the analytical solution where the image shows black circles representing the analytical solution and a solid red line for the AcuSolve results.

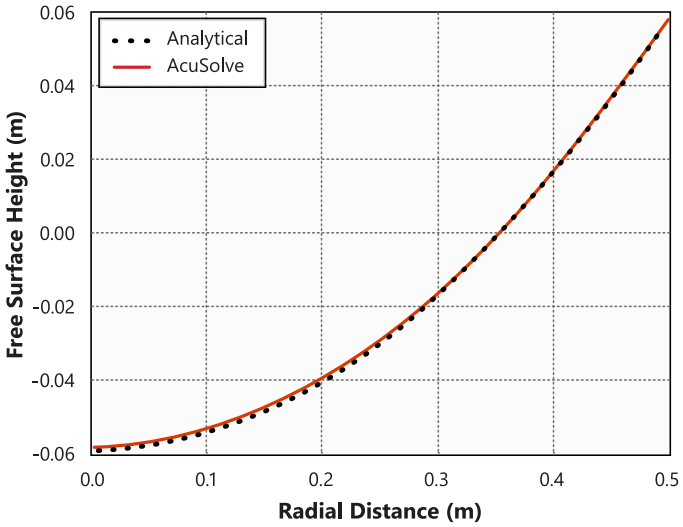


Figure 522: Free Surface Height of the Fluid Within the Cavity as a Function of Distance from the Center of the Domain at the Final Timestep

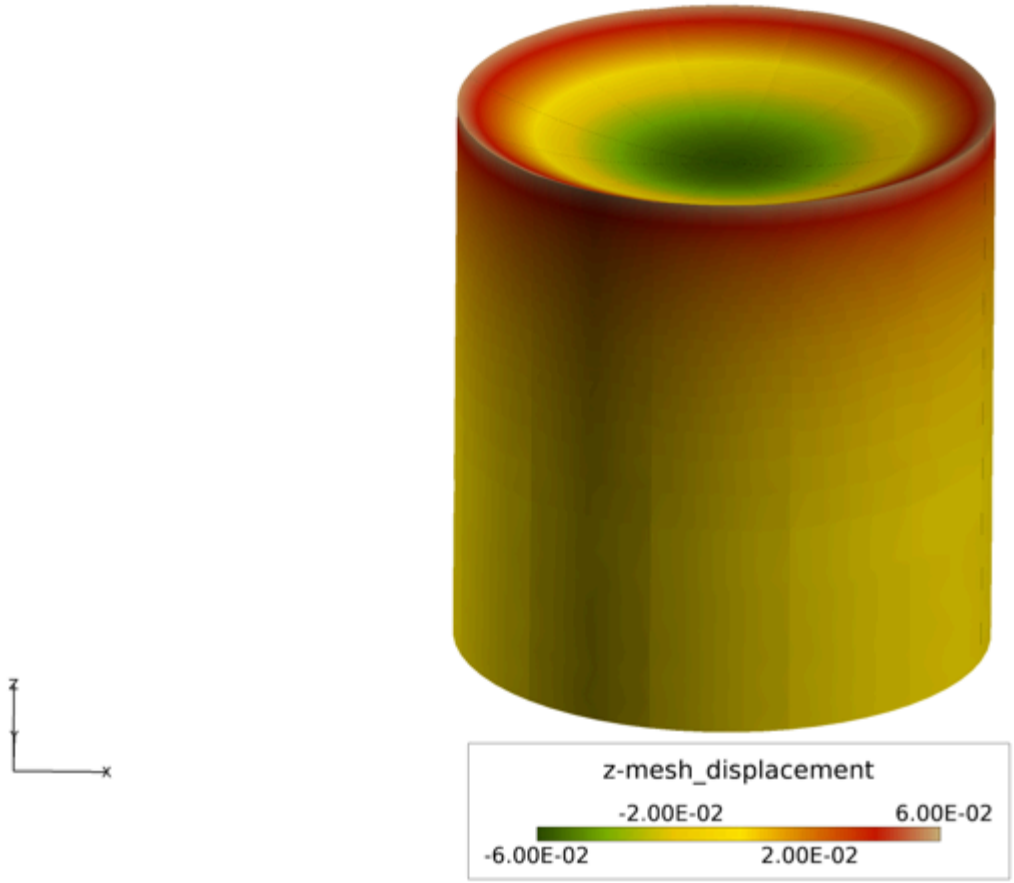


Figure 523: Vertical Mesh Displacement Within the Rotating Cavity at the Final Time Step (Shown as the Complete Cavity, using the Results from the Axisymmetric Section)

Summary

The AcuSolve solution compares well with analytical results for laminar free surface flow inside a rotating cavity. In this application, a fluid initially at rest is subjected to an angular velocity about the center of the cavity. As a result of the prescribed velocity, the fluid is forced to the outer wall of the cavity and develops a free surface profile in the shape of a parabola. The AcuSolve solution for the free surface height matches nearly exactly with the analytical results, with only minor differences based on the convergence criteria that you specified.

Simulation Settings for Laminar Free Surface Flow Inside a Rotating Cavity Fluid

Global

- Problem Description
  - Analysis type - Transient
  - Flow equation - Navier Stokes
  - Turbulence equation - Laminar
  - Mesh type - Arbitrary Mesh Movement (ALE)
- Auto Solution Strategy
  - Final time - `15.0` sec
  - Initial time increment- `0.05` sec
  - Convergence tolerance - `0.001`
  - Min stagger iterations - `0`
  - Max stagger iterations - `4`
- Material Model
  - Fluid
    - Density
      1. Type - Constant
      2. Density - `10` kg/m3
    - Viscosity
      1. Type - Constant
      2. Viscosity - `3.0` kg/m-sec
- Reference Frame
  - Omega
    - Rotation Center
      1. X-coordinate - `0.0` m
      2. Y-coordinate - `0.0` m
      3. Z-coordinate - `0.0` m
    - Angular velocity
      1. X-component - `0.0` rad/sec
      2. Y-component- `0.0` rad/sec
      3. Z-component - `3.0` rad/sec

Model

- Volumes
  - Fluid
    - Element Set
      1. Material model - Fluid
      2. Body force - Gravity
      3. Reference frame - Omega
- Surfaces
  - + Y
    - Simple Boundary Condition - (disabled to allow for nodal boundary conditions)
    - Advanced Options
      1. Nodal Boundary Conditions
         1. X-velocity
            1. Type - Constant
            2. Reference frame - Omega
            3. Constant value - `0.0`
         2. Y-velocity
            1. Type - Constant
            2. Reference frame - Omega
            3. Constant value - `0.0`
         3. Mesh X-Displacement
            1. Type- Zero
         4. Mesh Y-Displacement
            1. Type- Zero
  - -Z
    - Simple Boundary Condition
      1. Type - Wall
      2. Reference frame - Omega
      3. Mesh displacement BC type - Fixed
  - Axisymmetric +X
    - Simple Boundary Condition (disabled to allow for nodal boundary conditions)
  - Axisymmetric -X
    - Simple Boundary Condition (disabled to allow for nodal boundary conditions)
  - Free_Surface
    - Simple Boundary Condition
      1. # Type - Free Surface
- Periodics

- Axisymmetric Condition
- Periodic Boundary Condition
  - Type - Axisymmetric
  - Rotation Axis
    1. Point 1
       1. x-coordinate - 0.0 m
       2. y-coordinate - 0.0m
       3. z-coordinate - 0.0m
    2. Point 2
       1. x-coordinate - 0.0 m
       2. y-coordinate - 0.0m
       3. z-coordinate - 1.0m
- Nodes
  - All
    1. Mesh X-Displacement
       1. Type - Zero
    2. Mesh Y-Displacement
       1. Type - Zero
  - Centerline
    1. X-Velocity
       1. Type - Zero
    2. Y-velocity
       1. Type - Zero
    3. Mesh X-Displacement
       1. Type - Zero
    4. Mesh Y-Displacement
       1. Type - Zero

References

White, F. Fluid Mechanics. New York: McGrawHill. 2003

Turbulent Flow Over an Oscillating Rigid Body Assembly

In this application, AcuSolve is used to simulate the fluid-structure interaction of a fluid moving over a cylinder/plate assembly. AcuSolve results are compared with experimental results as described in Gomes and Lienhart (2009). The close agreement of AcuSolve results with the experimental results validates the ability of AcuSolve to model cases in which the fluid forces lead to structural motions.

Problem Description

The problem consists of a fluid having material properties of standard water with density of 998 kg / m^3 and kinematic viscosity of 0.97e-6 m^2/sec through a two dimensional channel over a cylinder and plate assembly. The diameter of the cylinder is 0.022 m and the plate length is 0.042 m, while the inlet velocity is specified to match experimental conditions with a max velocity of 1.07 m/sec, as is shown in the following image, which is not drawn to scale. The model is simulated as transient with constant inflow conditions, allowing an oscillatory motion of the assembly to develop. The Shear Stress Transport (SST) turbulence model is used to model the turbulent portion of the flow and AcuSolve's internal rigid body motion is used to capture the motion of the oscillating assembly.

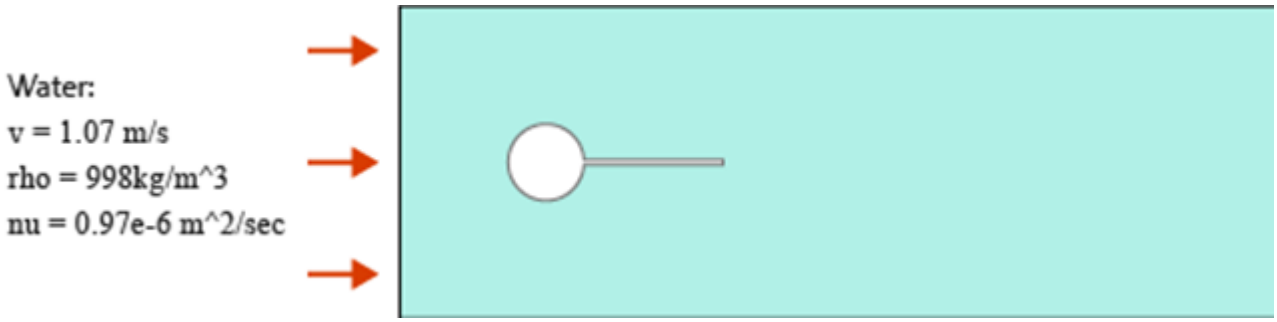


Figure 524: Critical Dimensions and Parameters used for Simulating Rigid Body Motion of Flow Past a Cylinder/Plate Assembly

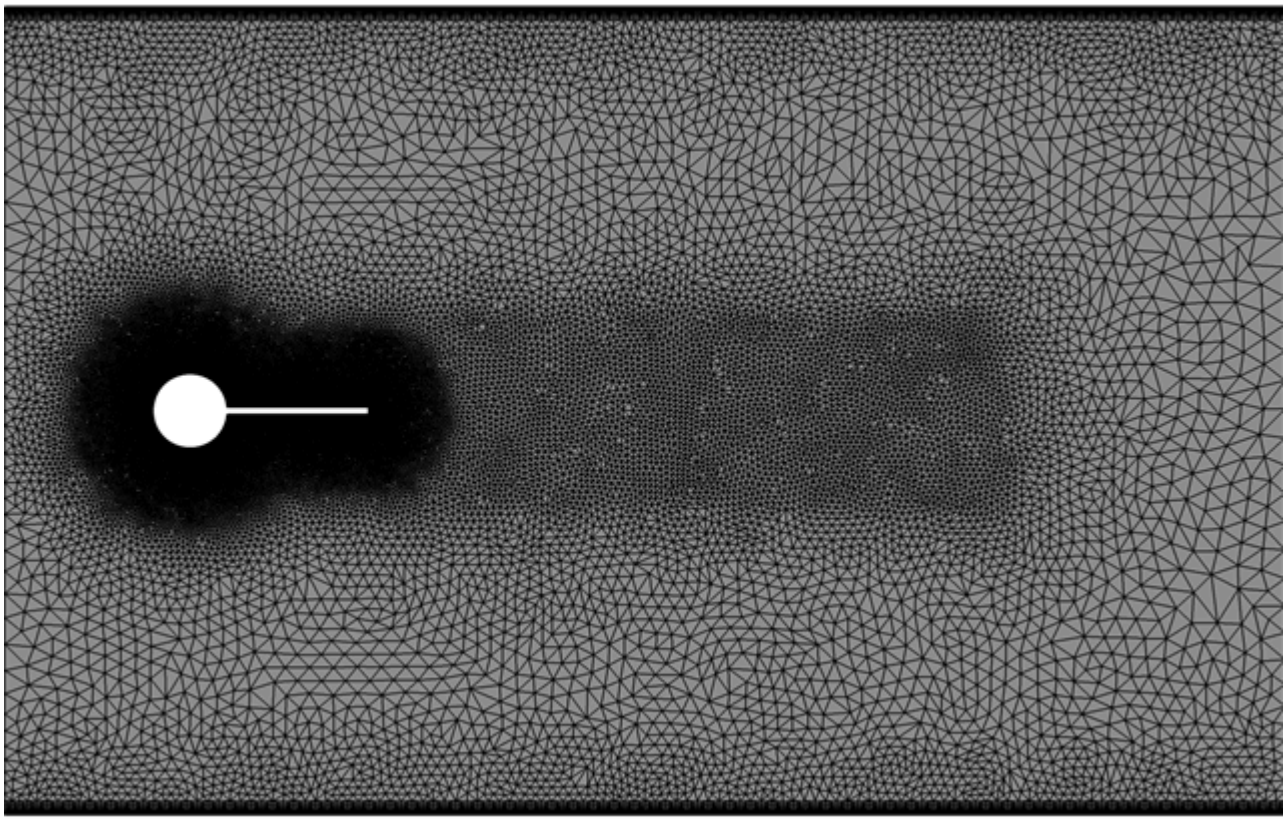


Figure 525: Mesh used for Simulating Rigid Body Motion of Flow Past a Cylinder/Plate Assembly

The simulation was performed as a two dimensional problem by constructing a volume mesh that contains a single layer of elements extruded in the cross stream direction, normal to the flow plane and by imposing symmetry boundary conditions on the extruded planes. The upper and lower walls are specified as no-slip and the inlet velocity is specified to match the conditions of the experiment (Gomes and Lienhart 2009).

AcuSolve Results

The AcuSolve solution reached a regularly repeating oscillatory state and the simulation was allowed to proceed for 10 seconds of physical time to obtain a sufficient number of cycles for statistical analysis. The motion of the cylinder/plate assembly is directly attributed to the vortices shedding in its wake. The fluctuating loads on the assembly that result from the vortex shedding lead to a repeating cycle of structural rotation. The dominant oscillation frequency from the simulation was found to match well with the experimental measurements, within approximately 3.5 percent. The images below show the rigid body displacement of the assembly as it oscillates within the flow. Contours of velocity magnitude demonstrate the forcing on the assembly, while the mesh motion around the structure is captured and plotted for a single time step. Two dimensional plots showing the angular displacement demonstrate the motion, showing a single red line for the AcuSolve results.

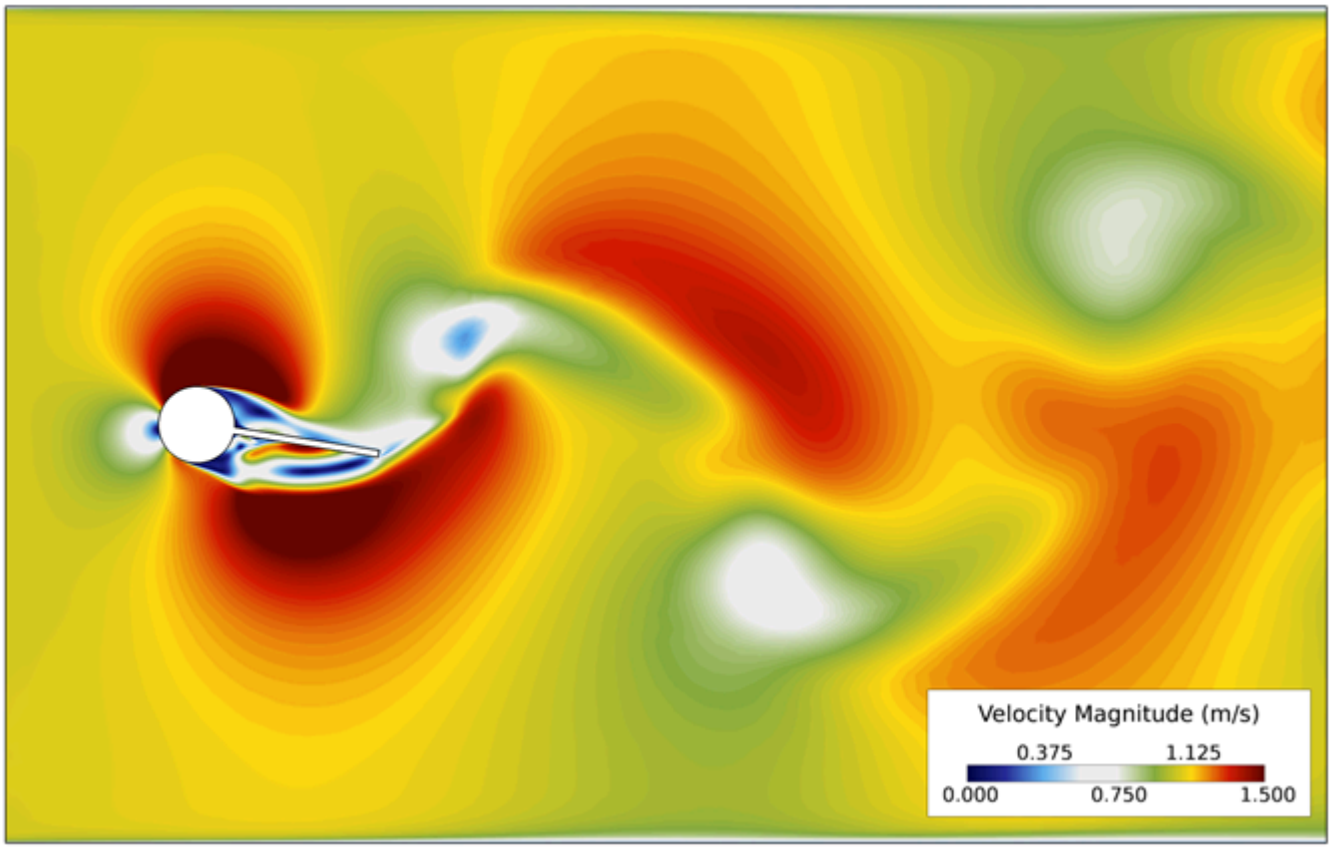


Figure 526: Velocity Contours Near the Assembly for a Single Time Step During the Simulation

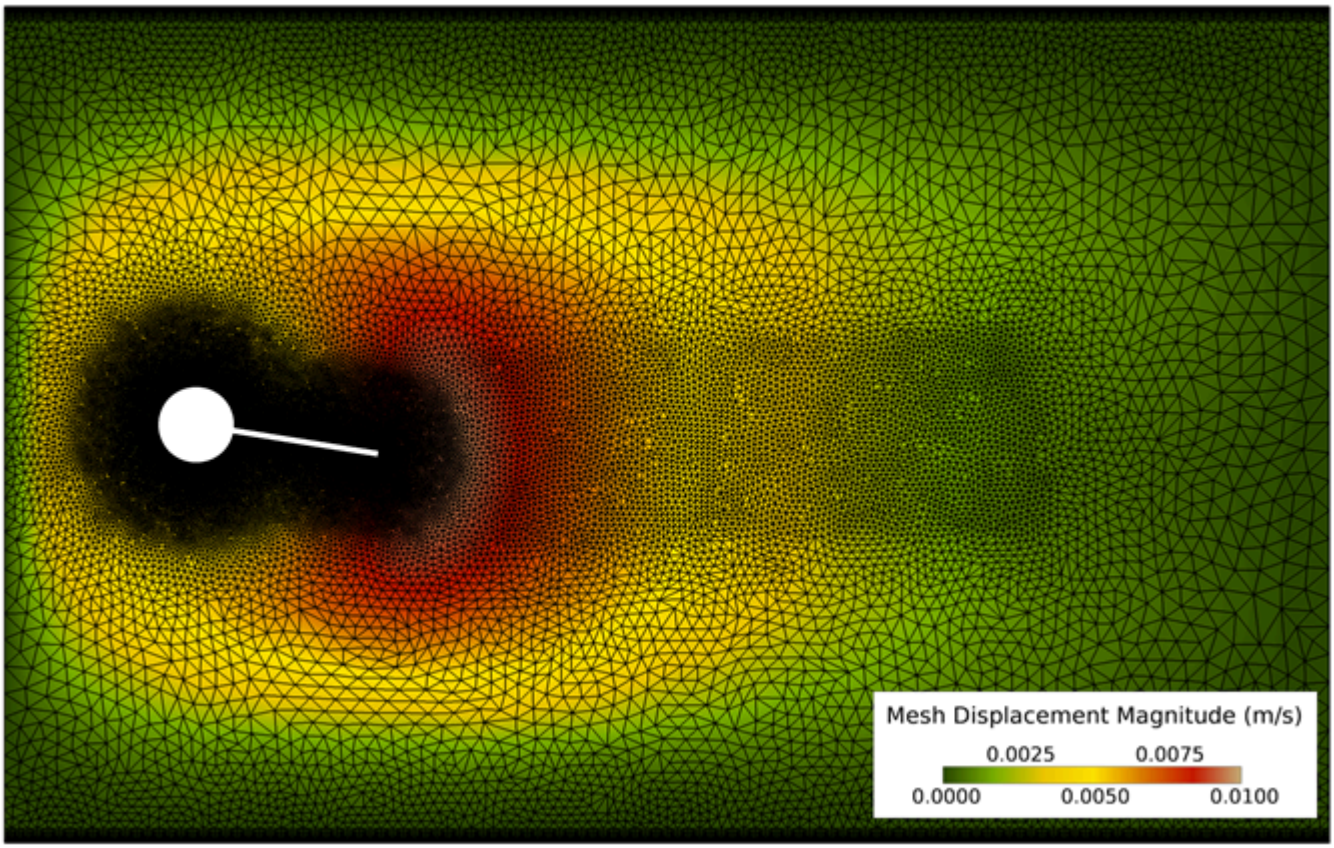


Figure 527: Mesh Displacement Contours Near the Assembly for a Single Time Step During the Simulation

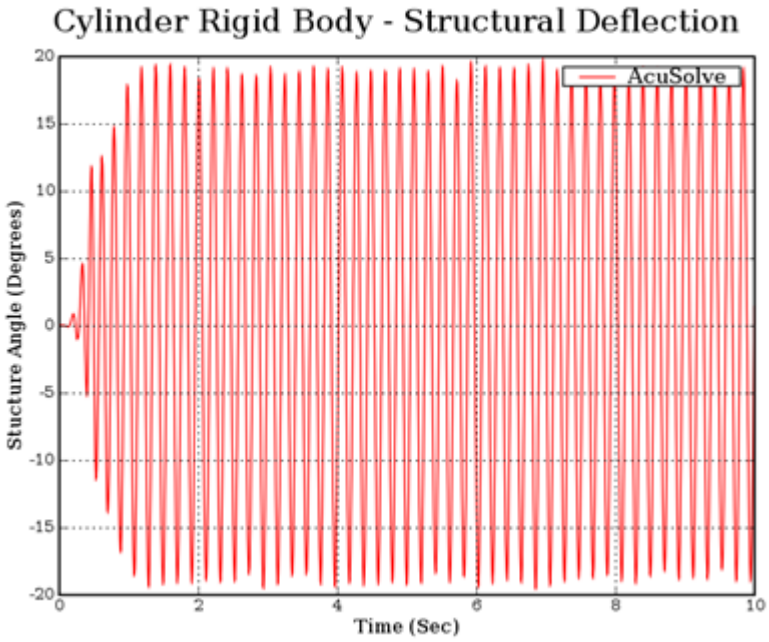


Figure 528: Rigid Body Displacement of the Assembly as a Function of Time, Showing the Oscillation Develop into the Pseudo-Steady Motion

The dominant frequency of the oscillation is easily identified in the Fast Fourier Transform (FFT) of the deflection angle, shown in the plot below.

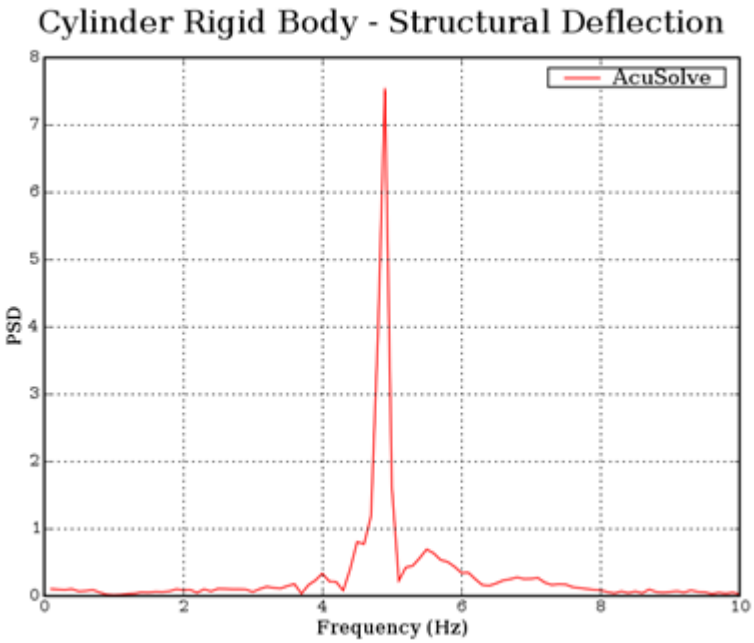


Figure 529: FFT of the Rigid Body Displacement Angle, Showing Power Spectral Density as a Function of Frequency

Summary

The AcuSolve solution compares well with experimental data for flow past an oscillating cylinder/plate assembly. In this application, water moves over the cylinder/plate assembly, giving rise to unsteady loading that causes the body to rotate as a rigid body. The good agreement with the natural frequency of oscillation compared to the experimental data demonstrates that AcuSolve is capable of predicting fluid forced motion with an internal rigid body dynamic solver.

Simulation Settings for Turbulent Flow Over an Oscillating Rigid Body Assembly

AcuConsole database file: `<your working directory>\cylinder_rigidbody_turbulent\cylinder_rigidbody_turbulent.acs`

Global

- Problem Description
  - Analysis type - Transient
  - Turbulence equation - SST
  - Mesh Type- Fully Specified
- Auto Solution Strategy
  - Final Time - `10.0`
  - Initial Time Increment- `0.005`
  - Convergence tolerance- `0.001`
  - Max stagger iterations- `3`
- Material Model
  - Water
    - Type- Constant
    - Density- `998.0` kg/m3
    - Viscosity- `0.00096806` kg/m*sec
- Mesh Motion
  - Interpolated
    - Type- Interpolated Motion
    - Interpolated motion surfaces
      1. Bottom
      2. Top
  - RigidBody
    - Type- Rigid Body Dynamic
      1. Z rotation- Active
      2. Mass- `0.2089` kg
      3. Dyadic
         1. X-X - `3.7 e-5` kg-m2
         2. Y-Y- `3.7 e-5` kg-m2
         3. Z-Z - `3.7 e-5` kg-m2

Model

- Volumes
  - Volume
    - Element Set
      1. Material model- Water
      2. Mesh motion- Interpolated
- Surfaces
  - Body
    - Simple Boundary Condition
      1. Type- Wall
      2. Mesh displacement BC type- Fixed
      3. Mesh motion- RigidBody
    - Interpolated Motion Surface
  - Bottom
    - Simple Boundary Condition
      1. Type- Wall
      2. Mesh displacement BC type- Fixed
    - Interpolated Motion Surface
  - Inflow
    - Simple Boundary Condition
      1. Type- Inflow
      2. Inflow type- Velocity
      3. X Velocity- `1.07` m/sec
      4. Turbulence input type- Auto
      5. Turbulence intensity type- High
    - Advanced Options
      1. Nodal Boundary Conditions
      2. X-velocity
         1. Type- Linear
         2. Precedence- `2`
         3. Curve fit variable- Y coordinate
         4. Curve fit values- Provided
      3. Y-velocity
         1. Type- Zero
      4. Z-velocity
         1. Type- Zero
  - Bottom
    - Simple Boundary Condition

1. Type- Wall
2. Mesh displacement BC type- Fixed
3. Mesh motion- RigidBody

- Interpolated Motion Surface

- Outflow
  - Simple Boundary Condition
    1. Type- Outflow
- Top
  - Simple Boundary Condition
    1. Type- Wall
    2. Mesh displacement BC type- Fixed
  - Interpolated Motion Surface
- maxZ
  - Simple Boundary Condition
    1. Type- Slip
- minZ
  - Simple Boundary Condition
    1. Type- Slip

References

Gomes, J. P. and Lienhart, H. (2009) Experimental Benchmark: Self-excited Fluid-structure Interaction Test Cases, in Fluid-Structure Interaction II: Modeling, Simulation, Optimization, Bungartz, H. J., Mehl, M., Schafer, M. (eds.), 383-412, Springer-Verlag.Ryhming.

Circumferential Flow in a Cylinder Induced by a Rotating Solid

In this application, AcuSolve is used to simulate the flow of air between concentric cylinders that is initiated by the rotation of the solid inner cylinder. The outer cylinder is held stationary while the inner cylinder rotates with a constant speed. AcuSolve results are compared with analytical results as described in White (1991). The close agreement of AcuSolve results with analytical results validates the ability of AcuSolve to maintain a continuous velocity across a non-conformal guide surface interface.

Problem Description

The problem consists of a fluid with material properties of a viscous fluid with the density of air rotating between two infinitely long concentric cylinders, as shown in the following image, which is not drawn to scale. The radius of the outer cylinder is 3.0 m and the radius of the inner cylinder is 1.5 m. The inner cylinder is defined as a solid medium and rotates at 1 rad/sec. The inner cylinder's surface velocity is mapped to the adjacent surface within the fluid medium, while the outer cylinder is fixed. The induced flow is laminar and exhibits a steady state behavior after running for a short period of physical time. The rotation of the inner cylinder causes the fluid to rotate due to viscous shearing near the wall. As the outer cylinder is fixed, a velocity gradient is generated as a function of radius within the flow domain.

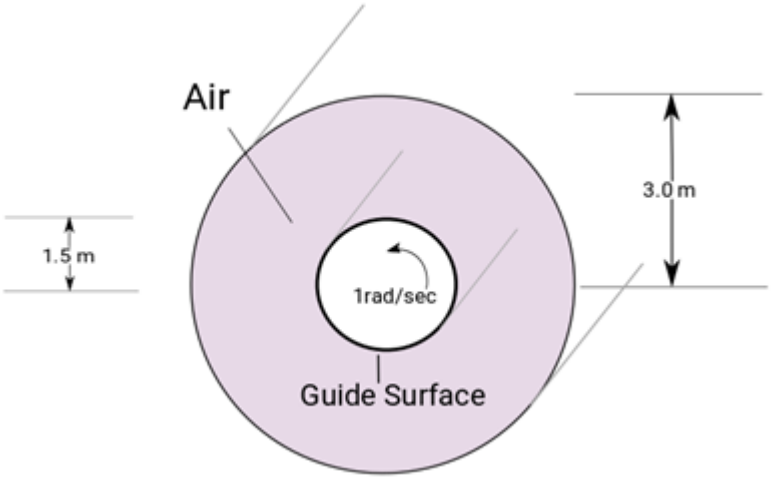


Figure 530: Critical Dimensions and Parameters Used for Simulating Flow Between Two Concentric Cylinders Split with a Guide Surface

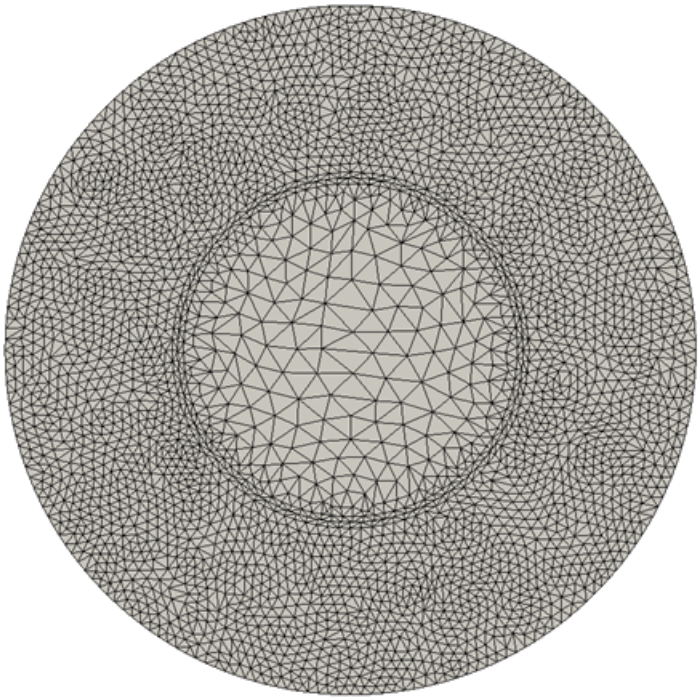


Figure 531: Mesh Used for Simulating Flow Between Two Concentric Cylinders

The simulation was performed as a two dimensional problem by constructing a volume mesh that contains a single layer of elements in the extruded direction, normal to the flow plane and by imposing slip flow and mesh boundary conditions on the extruded planes.

AcuSolve Results

The AcuSolve solution reaches a quasi-static result with the velocity between the two cylinders reaching a steady state at the simulation end time. As the solid inner cylinder rotates, it acts as a guide surface for the fluid elements to track and inherit the two velocity components. The velocity at the edge of the inner cylinder is equal to exactly the rotational speed multiplied by the radius. As the radius increases, the flow velocity reduces until it reaches zero at the outer diameter. The following images show the tangential velocity within the fluid as a function of radius from the center. The tangential velocity is compared with the analytical solution. The image below shows black circles representing the analytical solution and a solid red line for the AcuSolve results.

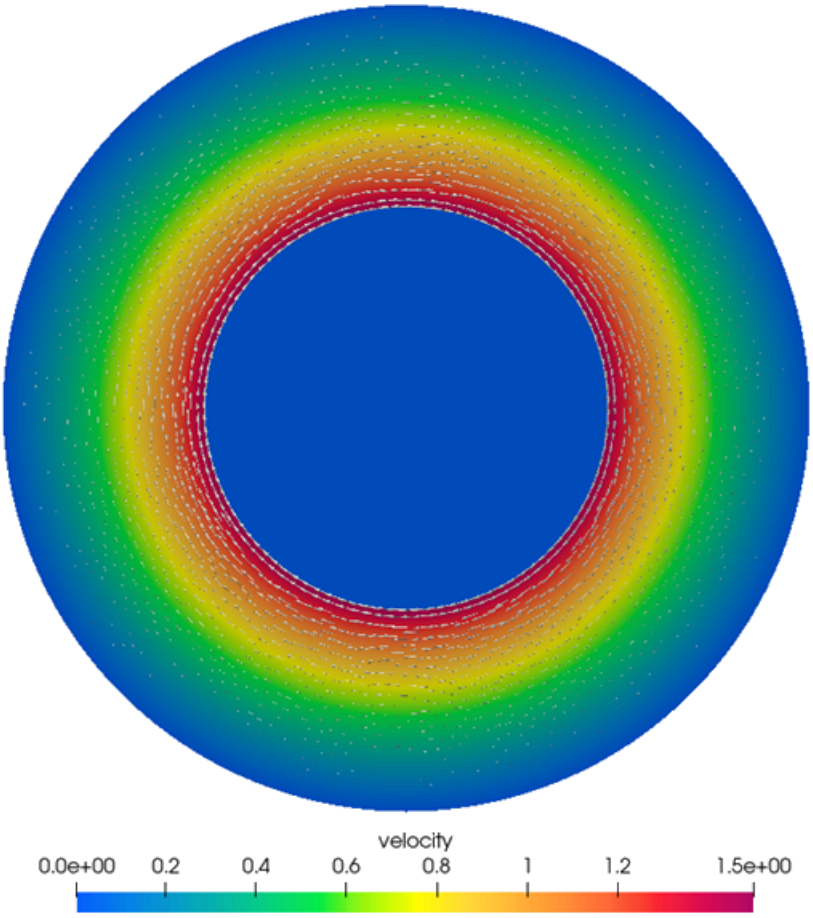


Figure 532: Contours and Vectors of Velocity Between the Concentric Cylinders

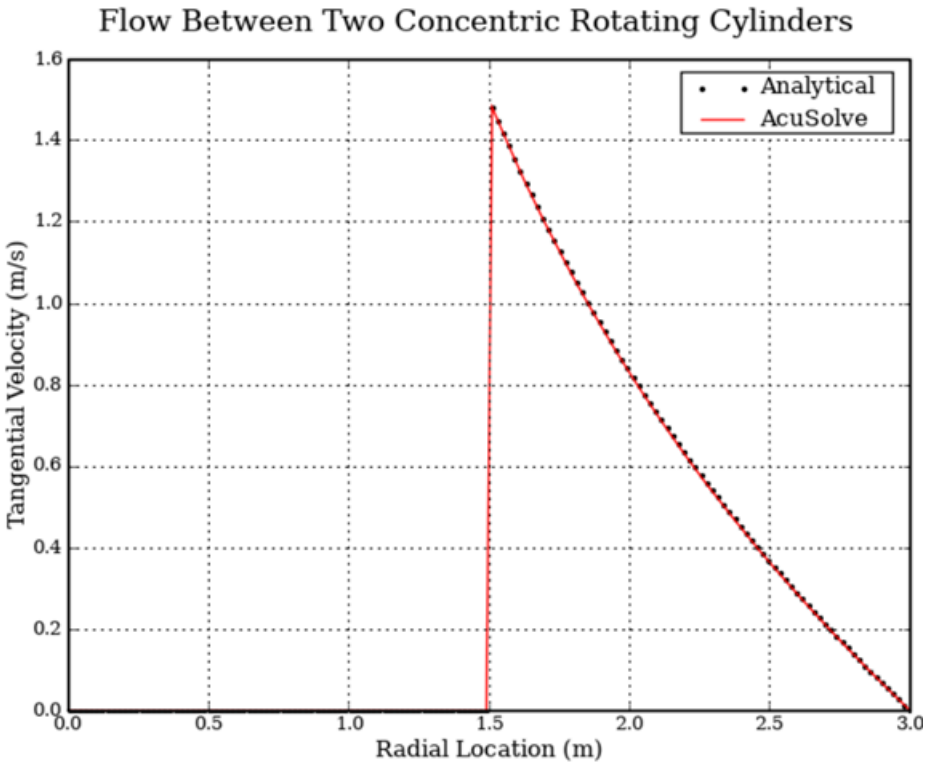


Figure 533: Tangential Velocity Within the Solid and Fluid as a Function of Radial Distance from the Center at the Final Timestep

Summary

The AcuSolve solution compares well with analytical results for laminar flow between concentric cylinders, where the inner cylinder guides the adjacent fluid elements. In this application, a fluid initially at rest inherits the angular velocity from the inner cylinder while the outer cylinder does not rotate. As a result of the inherited velocity and viscosity of the fluid, flow develops between the two cylinders. The AcuSolve solution for the tangential velocity as a function of radius matches exactly with the analytical results.

Simulation Settings for Flow Between Concentric Split Cylinders

HyperWorks CFD database file: `<your working directory>\annulus_split_rotating \annulus_split_rotating.hm`

- Problem Description
  - Analysis type - Transient
  - Flow equation - Navier Stokes
  - Turbulence equation - Laminar
  - Mesh type - Arbitrary Mesh Movement (ALE)
- Auto Solution Strategy
  - Max time steps - `40`
  - Initial time increment- `0.02` sec

- Convergence tolerance - `0.001`
- Min stagger iterations - `2`
- Max stagger iterations - `4`

- Material Model
  - Air
    - Density
      1. Type - Constant
      2. Density - `1.225` kg/m3
    - Viscosity
      1. Type - Constant
      2. Viscosity - `1.781` kg/m-sec
- Mesh Motion
  - Rotation
    - Rotation Center
      1. X-coordinate - `2.0` m
      2. Y-coordinate - `0.0` m
      3. Z-coordinate - `0.0` m
    - Angular velocity
      1. X-component - `1.0` rad/sec
      2. Y-component- `0.0` rad/sec
      3. Z-component - `0.0` rad/sec

  Model
- Volumes
  - CylinderInner
    - Element Set
      1. Medium - Solid
      2. Material model - Aluminum
  - CylinderOuter
    - Element Set
      1. Medium - Fluid
      2. Material model - Air
- Surfaces
  - InBottom
    - Simple Boundary Condition
      1. Type- Slip
      2. Mesh displacement type- Slip
  - InInterf

        - Simple Boundary Condition
            1. Type- Wall
            2. Mesh displacement type- Fixed
            3. Mesh motion- Rotation
        - Guide Surface
            1. Type- Faceted
    - InTop
        - Simple Boundary Condition
            1. Type- Slip
            2. Mesh displacement type- Slip
    - OutBottom
        - Simple Boundary Condition
            1. Type- Slip
            2. Mesh displacement type- Slip
    - OutInterf
        - Simple Boundary Condition
            1. Type- Wall
            2. Wall velocity type- Match Mesh Velocity
            3. Mesh displacement type- Guide surface
            4. Guide surface- InInterf
    - OutTop
        - Simple Boundary Condition
            1. Type- Slip
            2. Mesh displacement type- Slip
    - OutWall
        - Simple Boundary Condition
            1. Type- Wall
            2. Mesh displacement type- Fixed
- Nodes
    - PressurePoint
        - Pressure
            1. Type- Zero

References

F. M. White. "Viscous Fluid Flow". Section 3-2.3. McGraw-Hill Book Co., Inc. New York. 1991.

Multiphase Flow Within a Sloshing Tank

In this application, AcuSolve is used to simulate water and the time-dependent interface of air-water within a tank subject to a prescribed sloshing motion. AcuSolve results are compared with experimental pressure measurements as reported by Tankaka, et al. (2000) and Rhee (2005). The close agreement of AcuSolve results with experimental results validates the ability of AcuSolve to model multiphase flow problems with user-defined motion.

Problem Description

The problem consists of a tank filled to 20 percent capacity with water that is rotated or translated according to a user-defined function, as shown in the following image, which is not drawn to scale, where three monitoring locations, P1, P2 and P3, are denoted. The motion of the tank causes the fluid to begin sloshing rapidly, creating a time-dependent pressure field due to the height of the local water column. Non-slip boundary conditions for the top, bottom, left and right sides are applied with slip boundary conditions on the front and back faces. The SST turbulence model along with a global time-step of 0.001 seconds is used for the simulation. The pressure at each of the monitoring locations is compared against the experimental measurements as described in Tankaka, et al. (2000). It should be noted that the pressure computed and presented in the images represent the time-dependent dynamic pressure, static pressure is subtracted to be consistent with the measurements, at the specified point. Roll-Short is the case provided with the Validation Manual. The results for this case as well as Sway - Short are presented within this overview. In each case, the motion profile is defined with the following function and coefficients as defined in the table below.

$$x = A\sin(\omega t) \tag{21}$$

Where A = amplitude of oscillation, ω = frequency of oscillation = 2 π/T, t = time (sec) and T = Time period of oscillation (sec).

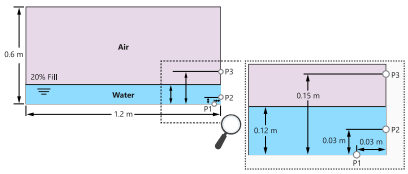


Figure 534: Critical Dimensions and Parameters for Simulating a 2D Tank Slosh with Mesh Motion

Table 35: Sine Function Scaling Parameters for Tank Motion Profile

Cases	Mesh Motion	Amplitude (A)	Time Periods (T)	Tank Filling Level
Sway – Base	Sway motion	0.06 m	1.94 sec	20% height

Cases	Mesh Motion	Amplitude (A)	Time Periods (T)	Tank Filling Level
Sway – Short	Sway motion	0.06 m	1.74 sec	20% height
Roll – Base	Rolling motion	10 degrees	2.25 sec	20% height
Roll – Short	Rolling motion	10 degrees	1.85 sec	20% height

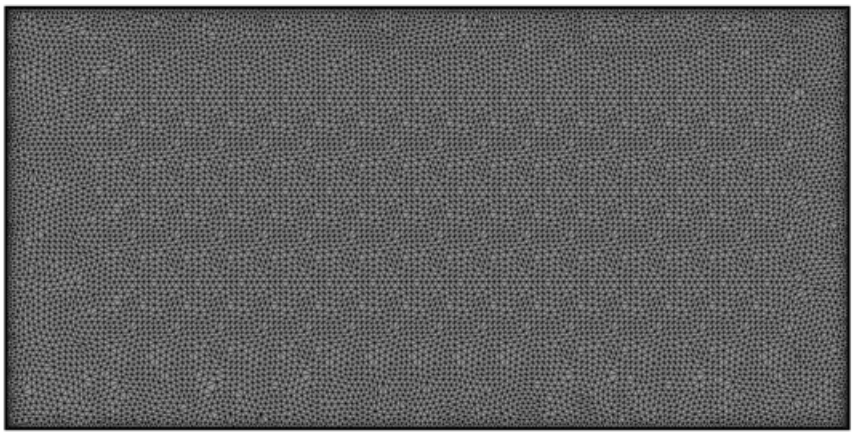


Figure 535: Mesh Used for Simulating Multiphase Sloshing Within a 2D Tank

AcuSolve Results

The AcuSolve solution is run for a time of t/T=5.0, 9.25 sec for Roll - Short, and the results presented reflect the transient motion of the water within the tank. The experimental values of pressure (kPa) and normalized simulation time are presented with the corresponding AcuSolve results at three measurement locations. The AcuSolve results show good agreement with the experimental results for pressure magnitude, the local water column height, as well as accurate timing of the peaks, indicating that the air-water interface is properly captured. Additional motion cases, as well as comparisons between two dimensional versus three dimensional simulations have been simulated with AcuSolve. The accuracy and solution requirements of these simulations are omitted for brevity but are available upon request. It was found that the differences between 2D and 3D simulations may be of interest for engineers, however the 2D results are shown to be adequate and less computationally expensive than 3D in the cases studied.

User-Defined Multiplier Function

This validation case relies on defining the motion of the elements within the tank, leading to the water sloshing in the presence of air. The motion is defined using an AcuSolve User-Defined Function (UDF) to specify the time-dependent multiplier function applied to the mesh motion command. The mesh motion is assigned to the Fluid element set, causing all of the elements to move according to the specified sine function. For the Roll - Short case, the mesh motion command is specified as rotation with the rotation multiplier function specified as rotation. If you are interested in simulating one of the other motion profiles, for example Sway - Base/Short, the type of mesh motion command would be changed to translation with the translation multiplier function assigned with the same UDF. The function name is designated at usrMotion and is contained within the source file `motion.c`. The source file, along with

pre-compiled binaries for Linux64 and Windows64 are provided with the validation case. Depending on your architecture it may be necessary to re-compile the source on the local system. Please refer to the *Programs Reference Manual* for details on using AcuMakeLib or AcuMakeDll for Linux and Windows, respectively.

Summary

The AcuSolve solution compares well with experimental results for tank sloshing simulations. In this application, the time dependent motion of the tank and the multiphase flow solution are simulated with AcuSolve using the level-set formulation and the SST turbulence model. The experimental values for instantaneous pressure at three locations and for two motion profiles are presented with the corresponding AcuSolve results. A good agreement of simulation results with the experiment validates the ability to solve time-dependent/accurate sloshing cases using the multiphase capabilities of AcuSolve.

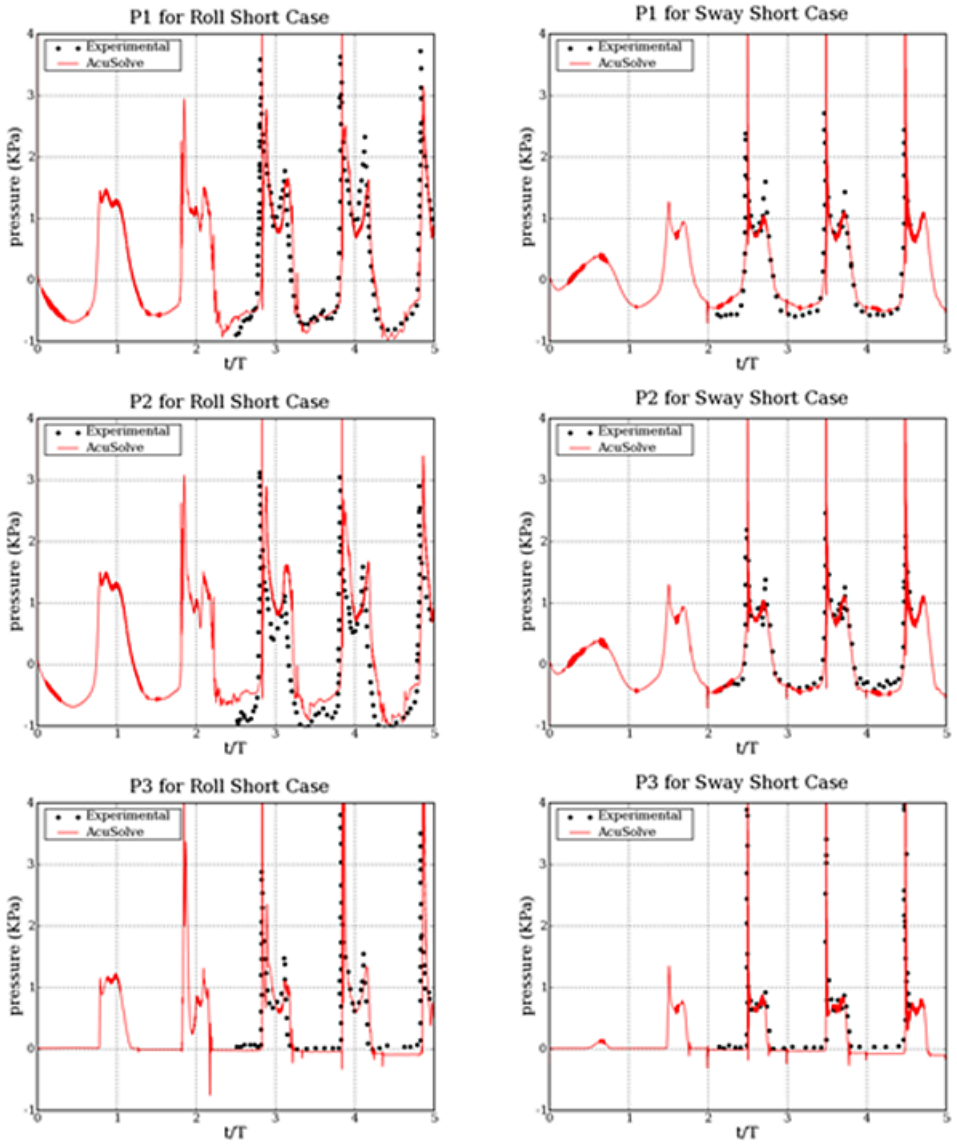


Figure 536: Time Dependent Pressure at Three Monitoring Locations Within the Sloshing Tank for Two Motion Profiles (Roll-Short, Left and Sway-Short, Right)

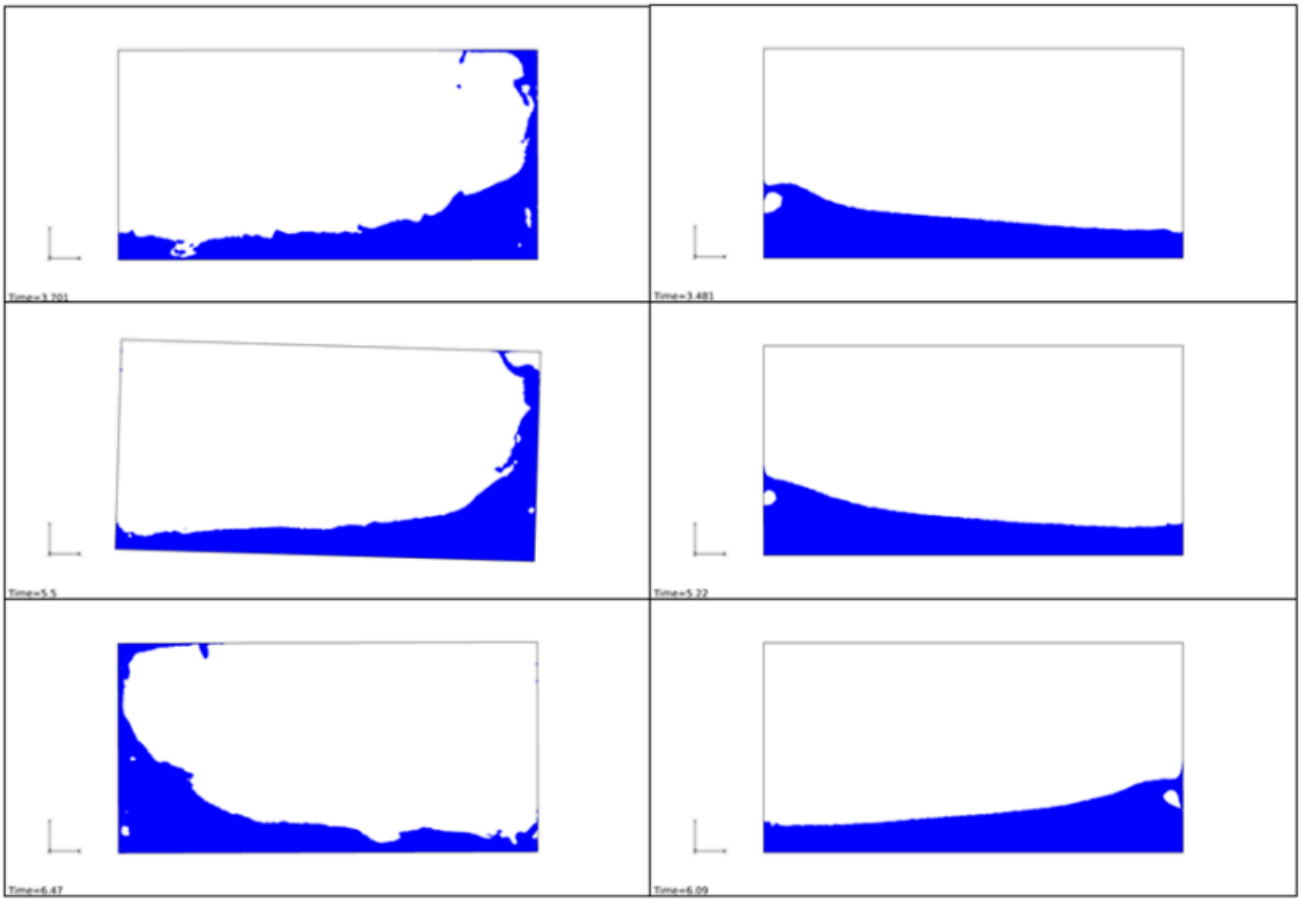


Figure 537: Instantaneous Volume Fraction Contour (Blue Showing Water) at Three Moments in Time (t/T=2.0, 3.0 and 3.5) for Two Motion Profiles (Roll-Short, Left and Sway-Short, Right)

Simulation Settings for Multiphase Flow Within a Sloshing Tank

AcuConsole database file: `<your working directory>\tank_sloshing_multiphase \tank_sloshing.acs`

Global

- Problem Description
  - Analysis type - Transient
  - Turbulence equation - SST
  - Multiphase equation – Level Set
- Auto Solution Strategy
  - Final time - `9.5` sec
  - Initial time increment - `0.001` sec
  - Min stagger iterations - `2`
  - Max stagger iterations - `10`
  - Fluid 1 - Water
  - Fluid 2 - Air

- Multiplier Function
  - rotation
    - Type - User Function
    - User function name - UsrMotion
    - User function values - `10.0`, `1.85`, `0.0`
- Material Model
  - Air
    - Type - Constant
    - Density - `1.225` kg/m^3
    - Velocity - `1.781e-5` kg/m-sec
  - Water
    - Type - Constant
    - Density - `1000` kg/m^3
    - Velocity - `0.001` kg/m-sec
- Mesh motion
  - rotation
    - Type - Rotation
    - Rotation center – `0.0`, `0.0`, `0.0`
    - Angular velocity – `0.0`, `0.0`, `0.0174533` (1.0 deg/sec)
    - Rotation variable – Multiplier Function
    - Rotation multiplier function – rotation

  Model
  - Volumes
    - Fluid
      1. Element Set
         1. Medium – Multiphase
         2. Multi field model – Water-Air
         3. Body force – Gravity
         4. Mesh motion – rotation
- Surfaces
  - x+
    - Simple Boundary Condition – Wall
  - x-
    - Simple Boundary Condition – Wall
  - y+
    - Simple Boundary Condition – Wall
  - y-
    - Simple Boundary Condition – Wall

- z+
  - Simple Boundary Condition – Slip
- z-
  - Simple Boundary Condition – Slip

References

Shin Hyung Rhee, 2005, "Unstructured Grid Based Reynolds-Averaged Navier-Stokes Method for Liquid Tank Sloshing", Journal of Fluids Engineering, Vol 127, pp. 572- 582.

Tanaka, Y., Ando, T., and Miyamoto, T., 2000, "Experimental Study on Sloshing Load Measured by Panel-Type Pressure Gauge," Proc. 74th. General Meeting of Ship Research Institute, Ship Research Institute, Tokyo, Japan, pp. 137-142.

Two-Phase Nucleate Boiling in a Cylindrical Pipe

In this application, AcuSolve is used to simulate the changes in wall temperature due to two-phase nucleate boiling at the heated walls of a pipe with water flowing through it. AcuSolve results are compared with experimental results adapted from Koncar and others (2015). The close agreement of AcuSolve results with experimental results validates the ability of AcuSolve to model two-phase nucleate boiling problems.

Problem Description

The problem consists of a pipe with heated surrounding walls, as shown in the following image, which is not drawn to scale. The length of the pipe is 2 m and the radius is 0.0017 m. Mass flux at the inlet is 900 kg/m^2 and the temperature of the fluid entering the pipe is 473 K. A heat flux of 570,000 W/m^2 is applied on the walls. The preheated water enters the inlet and heat is transferred to the fluid from the walls. The heat causes sub-cooled boiling to occur in the region close to the wall and leads to the formation of bubbles at nucleation sites.

During sub-cooled boiling flow, heat and mass exchange between the phases takes place on the heated wall and in sub-cooled liquid flow. On the heated surface the vapor bubbles are generated and as they move through the sub-cooled liquid they condense and release the latent heat.

The AcuSolve simulation is set up to model transient state heat transfer to determine the temperature along the centerline of the pipe and along the heated pipe walls of the model. AcuSolve computes the two-phase nucleate boiling by simulating the three-dimensional flow in a heated pipe for two-phase boiling flow, as described in Koncar (2005). The temperatures along the centerline of the pipe and along the pipe walls are compared against the experimental measurements, as described in Koncar, et al. (2005).

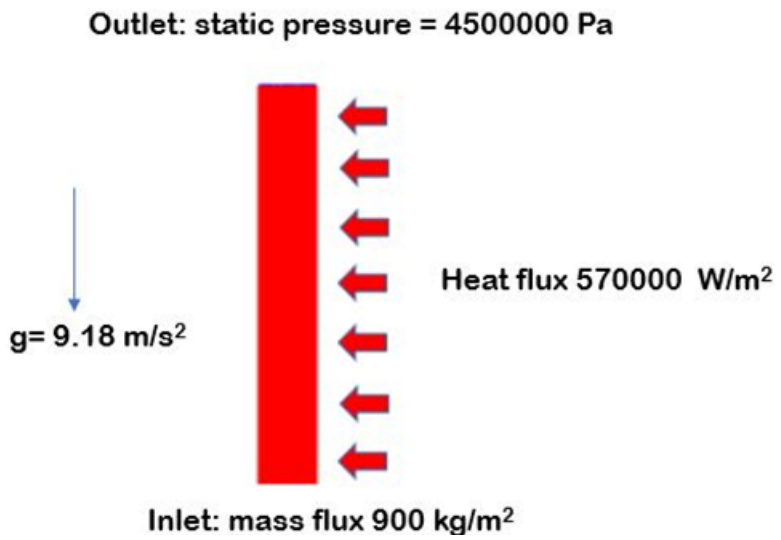


Figure 538: Parameters for Simulating a Two-Phase Nucleate Boiling Problem of a Pipe

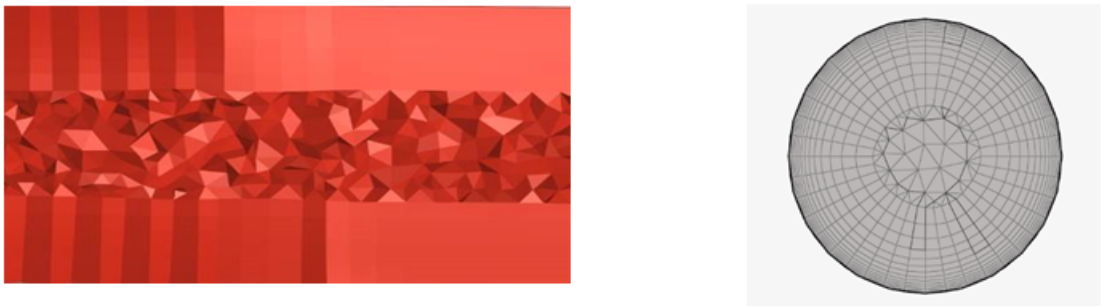


Figure 539: Mesh used for Simulating Two-Phase Flow in a Pipe

AcuSolve Results

The AcuSolve solution is run for a heat flux of 570,000 W/m^2 and the results are presented in the following image. The experimental values of wall temperature are presented with the corresponding AcuSolve results along the centerline of the pipe and along the pipe wall. The AcuSolve results show good agreement with the experimental results for the temperature, indicating that the two-phase nucleate boiling is properly captured.

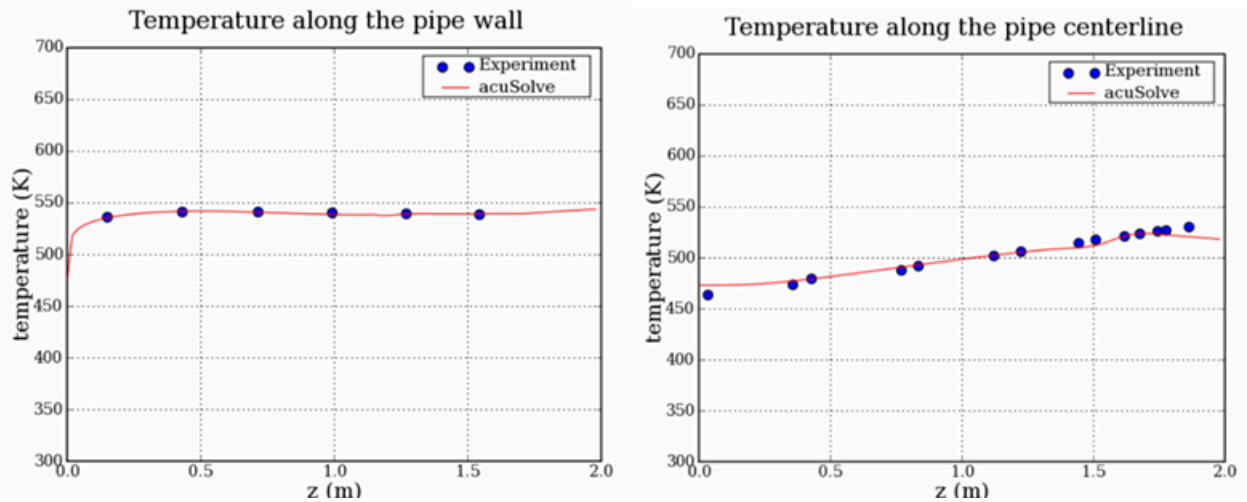


Figure 540: Temperature Values for Varying Streamwise Distance Compared to Experimental Data

Summary

The AcuSolve solution compares well with experimental results for two-phase nucleate boiling simulations. In this application, the temperature of the wall as the onset of boiling approaches are simulated with AcuSolve using the nucleate boiling feature and the SA turbulence model. The experimental values of temperature are presented with the corresponding AcuSolve results. A good agreement of simulation results with the experiment validates the ability to solve two-phase nucleate boiling using the nucleate boiling capabilities of AcuSolve.

Simulation Settings for Two-Phase Nucleate Boiling in a Cylindrical Pipe

HyperWorks database file: `<your working directory>\pipe_two_phase_boiling\pipe_two_phase_boiling.hm`.

Global

- Problem Description
  - Analysis type – Transient
  - Turbulence equation – SA
  - Temperature equation – Advective Diffusive
- Auto Solution Strategy
  - Maximum time steps – `500`
  - Initial time increment – `0.003`
  - Convergence Tolerance – `0.001` sec
  - Relaxation factor – `0.3`
- Surface Tension Model (“Water_NB-Vapor_NB”)
  - Type – Constant
  - Surface Tension – `0.02382`
- Material Model
  - Vapor_NB
    - Type – Constant
    - Density – `23.75` kg/m^3
    - Viscosity – `1.79e-05` kg/m-sec
    - Specific Heat – `4225` J/kg-K
    - Latent Heat – `1675570`
    - Latent Heat Temperature – `530.55` K
    - Conductivity – `0.02528` W/m-K
  - Water_NB
    - Type – Constant
    - Density – `800` kg/m3
    - Viscosity – `0.0001339` kg/m-sec
    - Specific Heat – `4500` J/kg-K
    - Conductivity – `0.65` W/m-K
- Multifield parameter (Field interaction model)
  - Type – Algebraic Eulerian
  - Phase change type – Wall Boiling
  - Carrier field - Water
  - Disperse field – Vapor
  - Disperse field diameter type – Boiling kurul exponential
  - Drag model – Ishii zuber
  - Lift Model – Legendre Magnaudet

Model

- Volumes
  - Fluid
    - Material – Vapor_Water
- Surfaces
  - Inflow
    - Simple Boundary Condition – Inflow
    - Inflow type – Mass Flux Rate
    - Mass Flux Rate – `0.167634` kg/sec
    - Temperature – `473` K
  - Outflow
    - Simple Boundary Condition – Outflow
    - Pressure – `4500000` N/m2
  - Wall
    - Simple Boundary Condition – Wall
    - Temperature type – Flux
    - Heat Flux – `570000` W/m2

References

B. Koncar, E. Krapper, Y. Egorov, 2005, "CFD MODELING OF SUBCOOLED FLOW BOILING FOR NUCLEAR ENGINEERING APPLICATIONS", International Conference Nuclear Energy for New Europe 2005, Bled, Slovenia, September 5-8,2005.

Supersonic Flow Through a Converging-Diverging Nozzle

In this application, AcuSolve is used to simulate the high-speed turbulent flow in a converging and then diverging nozzle. The flow within the nozzle enters as subsonic, reaches sonic at the throat and shortly after develops a normal shock. AcuSolve results are compared with experimental results adapted from Bogar and Sajben (1983). The close agreement of AcuSolve results to experimental measurements validates the ability of AcuSolve to simulate internal supersonic flows where normal shocks are present.

Problem Description

The problem consists of a converging and then diverging nozzle represented as an extruded planar surface, as shown in the image below, which is not drawn to scale. The length of the domain is 0.213 m with a throat height of 0.044 m. The stagnation pressure and static temperature are constrained at the inlet to 135,000 Pa and 265.98 K, respectively. The static pressure is defined using the outflow boundary condition, where P_{static}=97216.08 Pa. The flow in the diffuser has an inlet Reynolds number of $6.5x10^5$. The upper and lower walls are set to no-slip and the side walls are set to slip, while the exterior walls are specified to be adiabatic. Images of the numerical mesh are shown below.

The AcuSolve simulation is prepared to model the pseudo-transient state to determine the shock location and corresponding scalar quantities within the diffuser. AcuSolve computes the flow and thermal solution by simulating a planar, two-dimensional flow problem with physical dimensions and input quantities as described in the Sajben Diffuser case presented by Bogar and Sajben (1983). The gas in the simulation domain enters at subsonic conditions and is forced to accelerate beyond Mach=1.0 as it passes through the throat. After reaching supersonic speed a normal shock wave develops causing the flow speed to reduce back below sonic. The pressure along the bottom wall of the diffuser is compared against experimental measurements to demonstrate the solver's capability to solve supersonic cases.

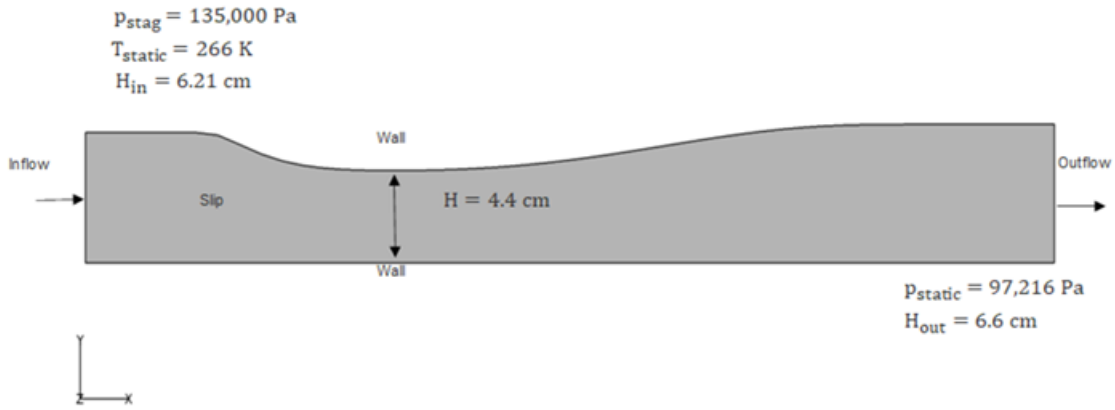


Figure 541: Parameters for Simulating Compressible Flow within a Converging-Diverging Nozzle

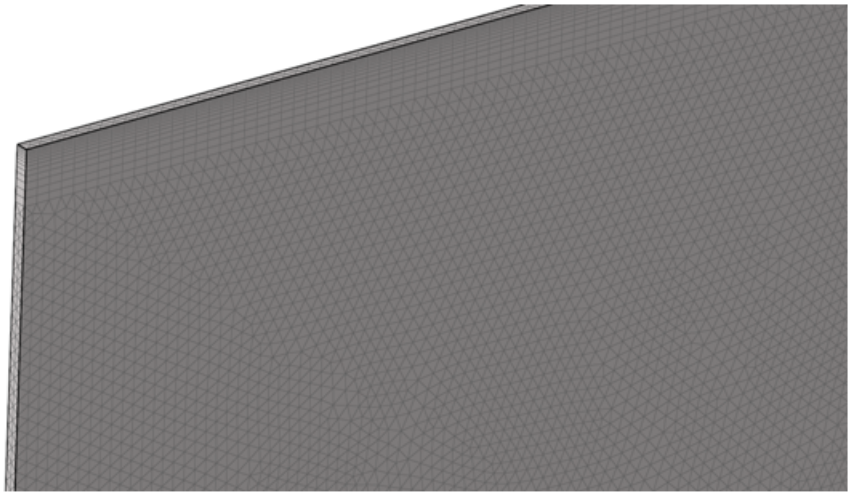


Figure 542: Mesh used for Simulating Compressible Flow in a Converging-Diverging Nozzle

AcuSolve Results

The AcuSolve solution is run for 0.025 seconds (6,250 timesteps with dt=4.0x10^{-6}sec) and converges to a pseudo-steady solution. The change in pressure from the inlet to outlet causes the flow to accelerate within the throat of the diffuser until it reaches approximately Mach=1.35. A normal shock is present just downstream of where the cross-sectional area of the nozzle increases, as shown in the image below. The numerical solution can be compared with the reference after normalizing the pressure along the wall by the inlet stagnation pressure (135 kPa) and the distance along the bottom wall by the nozzle throat height (0.044 m). The image below shows the normalized pressure versus normalized distance in comparison to NASA reference and experimental results. The image shows black circles representing the experimental measurements (Bogar and Sajben 1983), a dashed blue line representing the SA solution as obtained through NASA publication (Mohler 2005) and a solid red line representing the AcuSolve results with the Spalart-Allmaras turbulence model. The non-dimensional pressure within the diffuser agrees well with the reference data, demonstrating the correct physical location of the normal shock and expected moderate flow speed reduction within the constant cross-section diffuser portion of the nozzle.

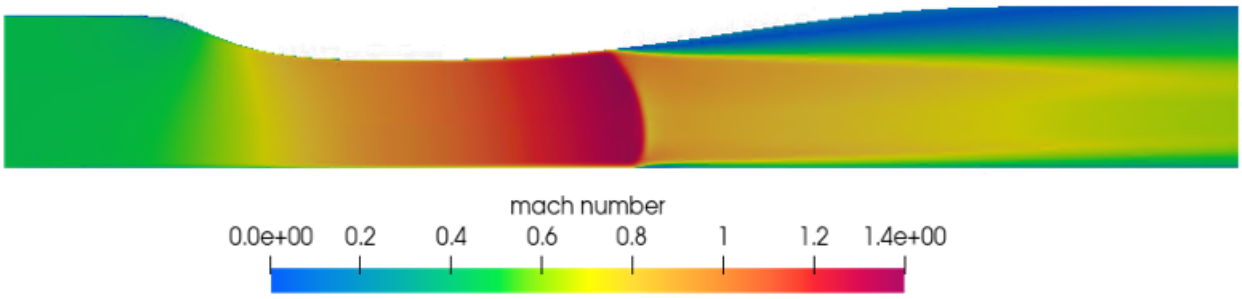


Figure 543: Contours of Mach Number within a Converging-Diverging Nozzle

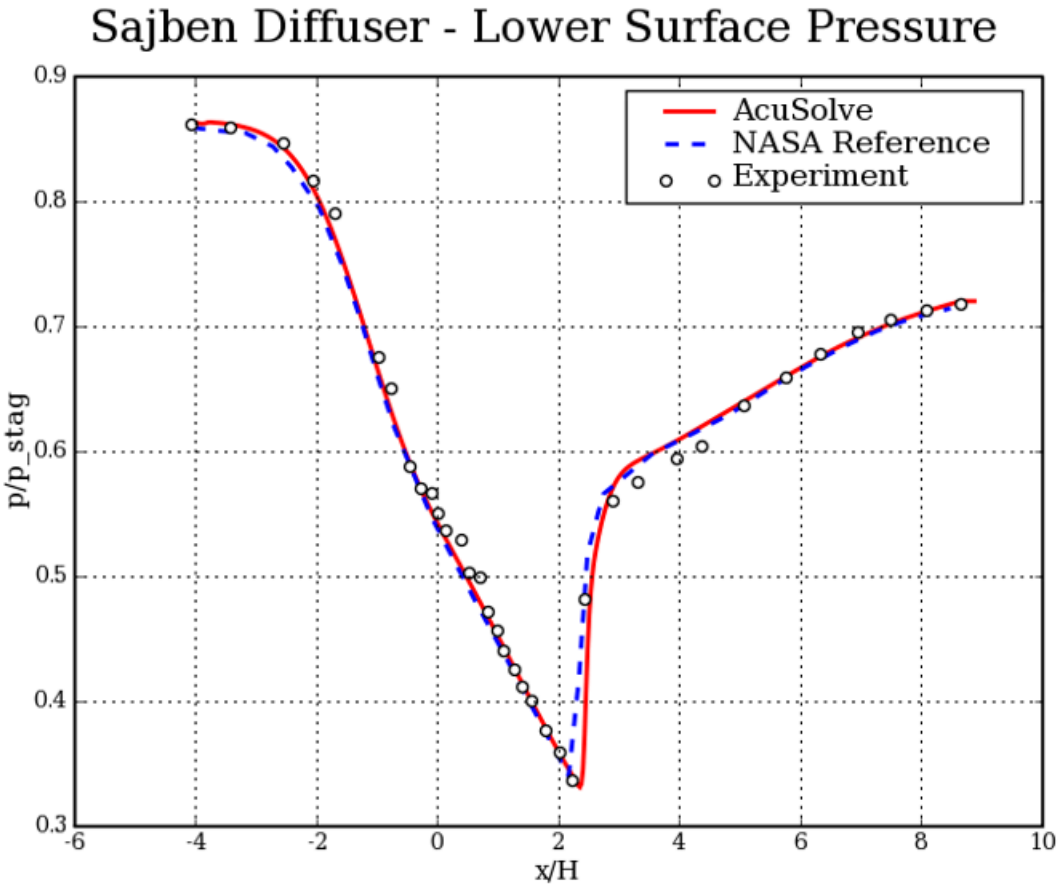


Figure 544: Normalized Pressure Versus Normalized Distance in Comparison to NASA Reference and Experimental Results

Summary

The AcuSolve solution compares well with experimental and numerical results for the described simulation. In this application, compressibility effects are accounted for using the coupled compressible flow solver with the ideal gas material definition. The thermal and momentum exchange within the nozzle is computed with AcuSolve using the compressible Navier-Stokes solver with the Spalart-Allmaras turbulence model. The experimental values of pressure are presented with the corresponding AcuSolve results and show good agreement, validating the ability to solve compressible cases with the presence of normal shocks. The results indicate that AcuSolve is able to properly predict the peak pressure magnitude and location within the diffuser while maintaining the normal shock when the time-step is selected to result in a maximum CFL of approximately 30.

Simulation Settings for Supersonic Flow Through a Converging-Diverging Nozzle

HyperWorks CFD database file: `<your working directory>\diffuser_compressible\diffuser_compressible.hm`

Global

- Problem Description

    - Flow – Compressible Navier Stokes
    - Analysis type – Transient
    - Turbulence equation – SA
    - Temperature equation – Advective Diffusive
- Auto Solution Strategy
    - Initial time increment – `4.0E-6`
    - Final time – `0.025` sec
    - Convergence Tolerance – `0.001` sec
    - Relaxation factor – `0.5`
- Material Model
    - Air-Ideal Gas
        - Type – Ideal_Gas
        - Viscosity – `1.781e-05` kg/m-sec
        - Specific Heat – `1005` J/kg-K
        - Conductivity – `0.02521` W/m-K
        - Gas Constant – `287.058` J/kg-K

Model

- Volumes
    - Fluid
        - Material – Air-Ideal Gas
- Surfaces
    - Inflow
        - Simple Boundary Condition – Inflow
        - Inflow type – Stagnation Pressure
        - Stagnation Pressure – `135000.0` N/m2
        - Turbulence_input_type – Direct
        - Eddy Viscosity – `1e-6` m^2/s
        - Temperature – `265.98` K
    - Outflow
        - Simple Boundary Condition – Outflow
        - Pressure – `97216.08` N/m2
    - Wall_1
        - Simple Boundary Condition – Wall
        - Type – auto_wall
    - Wall_2
        - Simple Boundary Condition – Wall
        - Type – auto_wall
    - Slip_1

        - Simple Boundary Condition – Slip
    - Slip_2
        - Simple Boundary Condition – Slip

References

Bogar, T. J., Sajben, M., and Kroutil, J. C. (1983) "Characteristic Frequencies of Transonic Diffuser Flow Oscillations," AIAA Journal, Vol. 21, No. 9, pp. 1232-1240.

Mohler, S.R., "Wind-US Unstructured Flow Solutions for a Transonic Diffuser," NASA CR-2005-213417, January 2005.

Heat Transfer/Radiation

9

This section includes validation cases that consider the temperature of the flow by simulating one or modes of heat transfer.

This chapter covers the following:

- Laminar Flow Through a Pipe With Imposed Heat Flux (p. 739)
- Laminar Couette Flow with Imposed Pressure Gradient and Heated Walls (p. 744)
- Natural Convection in a Concentric Annulus (p. 750)
- Laminar Flow Through a Channel with Heated Walls (p. 756)
- Turbulent Natural Convection Inside a Tall Cavity (p. 761)
- Viscous Heating Inside a Rotating Annulus (p. 769)
- Ideal Gas Compression in an Actuating Piston (p. 776)
- Laminar Flow Through a Pipe with Constant Wall Temperature (p. 783)
- Heat Transfer Between Radiating Concentric Cylinders (p. 788)
- Turbulent Flow Through a Heated Periodic Channel (p. 794)
- Heat Transfer Between Concentric Cylinders with Heat Source (p. 800)
- Heat Transfer Between Radiating Concentric Spheres (p. 805)
- Radiation Heat Transfer Through a Cube with a Specular Interface (p. 810)
- Two-Phase Nucleate Boiling in a Cylindrical Pipe (p. 817)
- Single-Phase Nucleate Boiling in a Rectangular Channel (p. 821)
- Supersonic Flow Through a Converging-Diverging Nozzle (p. 826)

Laminar Flow Through a Pipe With Imposed Heat Flux

In this application, AcuSolve is used to simulate the flow of mercury through a heated pipe. The AcuSolve results are compared with analytical results for pressure drop as described in White (1991), and with temperature changes as described in Incropera and DeWitt (1981). The close agreement of AcuSolve results with analytical results validates the ability of AcuSolve to model cases with flow and imposed heat flux.

Problem Description

The problem consists of mercury flowing through a heated, circular pipe that is 0.005 m in diameter and 0.1 m long, as shown in the following image, which is not drawn to scale. Mercury enters the pipe with a constant temperature of 300 K. The pipe has an imposed heat flux of 2000 W/m^2. The laminar velocity field is modeled as periodic to achieve a fully developed velocity profile. As the fluid moves through the pipe it is slowly heated by the heat flux on the wall, resulting in an increased centerline temperature. Pressure decreases along the pipe length due to the friction imposed by the viscous stresses near the pipe wall.

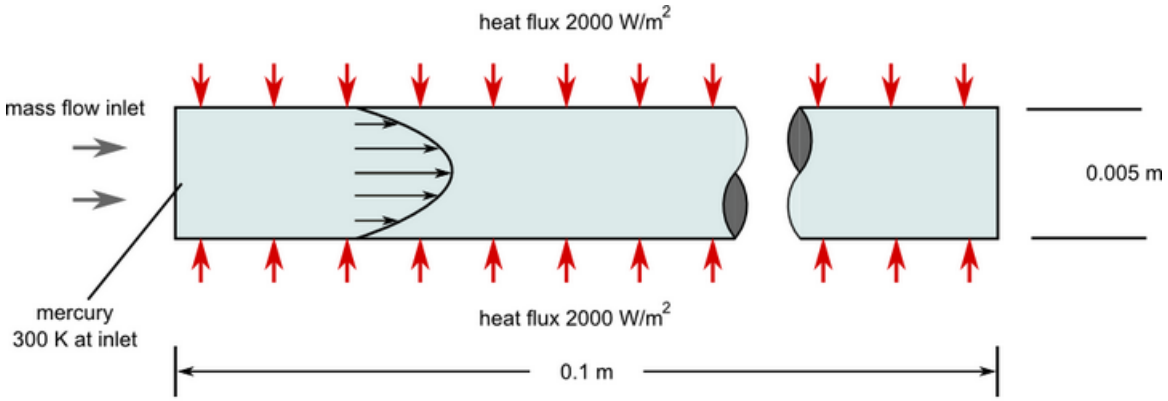


Figure 545: Critical Dimensions and Parameters for Simulating Laminar Flow through a Pipe with Imposed Heat Flux

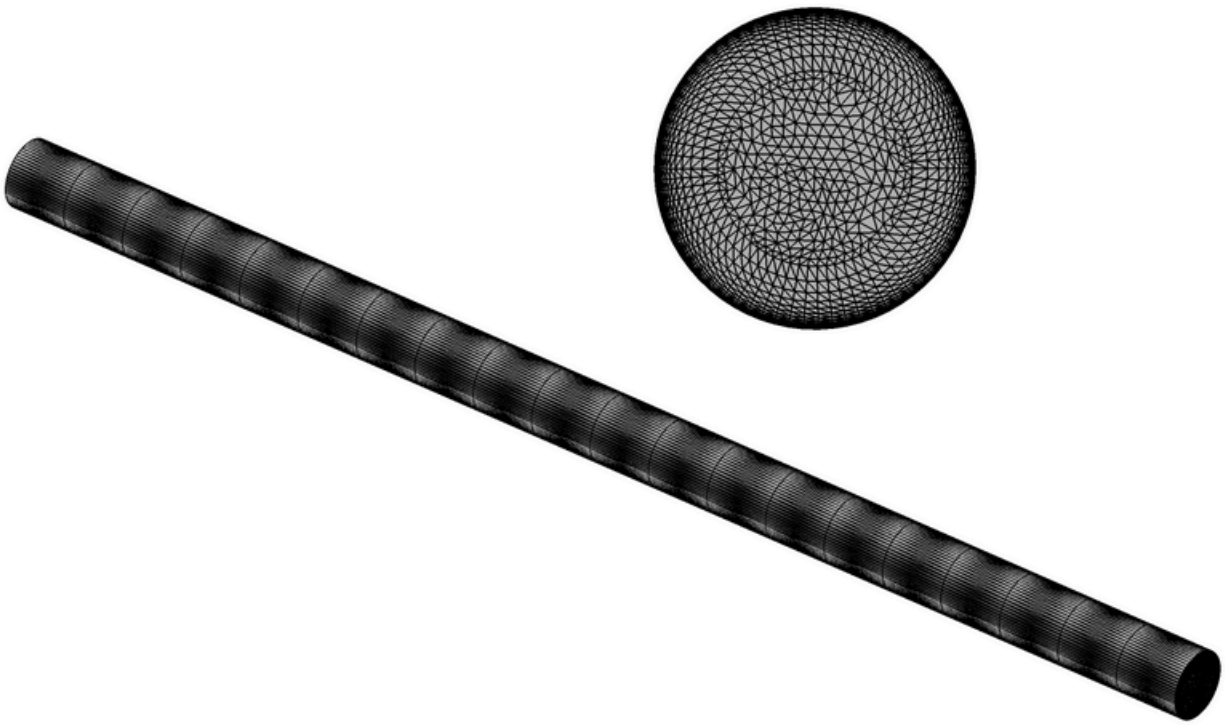


Figure 546: Mesh used for Simulating Laminar Flow Through a Pipe with Imposed Heat Flux

AcuSolve Results

The AcuSolve solution converged to a steady state and the results reflect the mean flow conditions. The greatest pressure is at the inlet, with pressure decreasing as a function of distance away from the inlet. The temperature of the mercury in the pipe increases as a function of distance from the inlet due to the impact of the heat flux on the pipe walls.

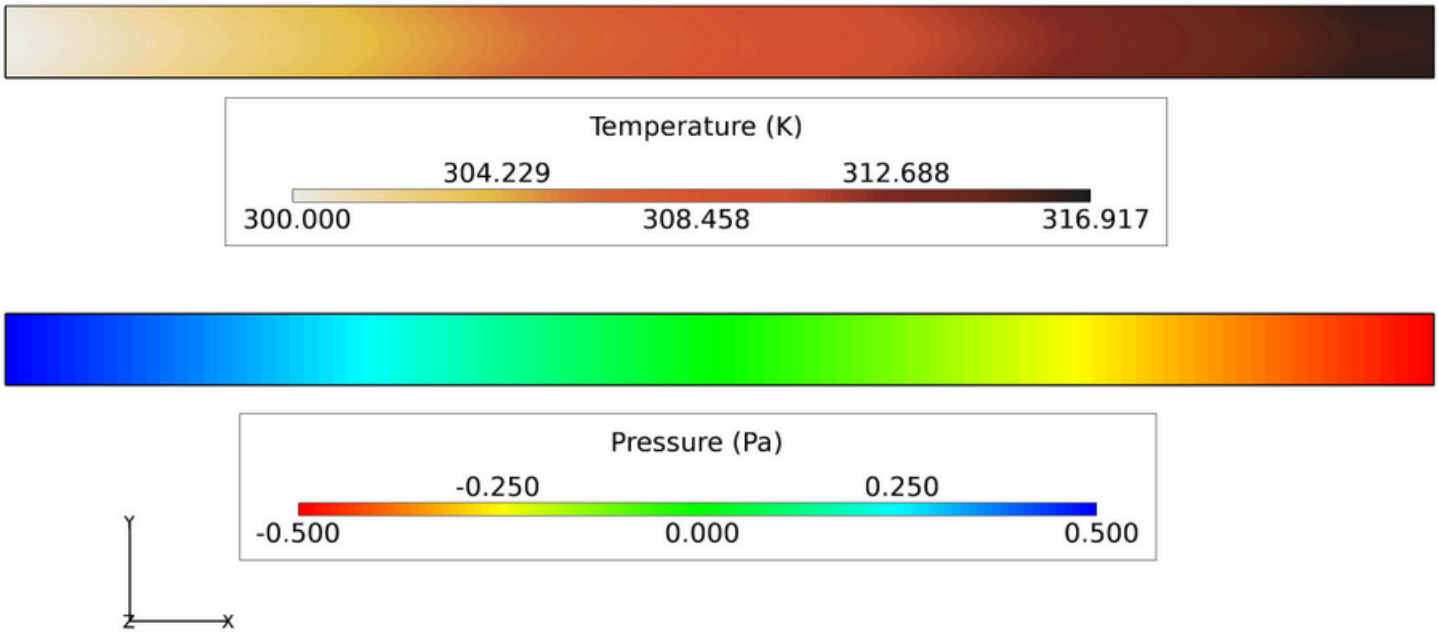


Figure 547: Temperature and Pressure Contours of Mercury Flow Through a Heated Pipe

The analytical solution for the pressure drop, between the inlet and outlet, as well as the analytical solution for the temperature of the mercury at the center of the outlet are presented with the corresponding AcuSolve results in the following table.

Table 36:

	Analytical solution	AcuSolve solution	Percent deviation from analytical
Pressure drop (Pa)	0.991	0.994	0.303
Centerline temperature of flow at outlet (K)	316.917	316.269	0.204

Summary

The AcuSolve solution compares well with analytical results for flow through a pipe with an imposed heat flux. In this application, the pressure drop in the fluid region is driven by the viscous stresses near the pipe wall. The temperature in the fluid region is influenced by the imposed heat flux on the walls. The values of pressure and temperature that are predicted by AcuSolve are within 0.3 percent of the analytical solution.

Simulation Settings for Laminar Flow Through a Pipe With Imposed Heat Flux

AcuConsole database file: `<your working directory>\pipe_laminar_heat\pipe_laminar_heat.acs`

Global

- Problem Description
  - Analysis type - Steady State
  - Temperature equation - Advective Diffusive
  - Turbulence equation - Laminar
- Auto Solution Strategy
  - Relaxation Factor - `0.2`
- Material Model
  - Mercury
    - Density - `13579.0` kg/m3
    - Viscosity - `0.001548` kg/m-sec

  Model
- Volume
  - Fluid
    - Element Set
      1. Material model - Mercury
- Surfaces
  - Inflow
    - Simple Boundary Condition - (disabled to allow for periodic conditions to be set)
    - Advanced Options
      1. Integrated Boundary Conditions
         1. Mass Flux
            1. Type - Constant
            2. Constant value - `-1.33e-3` kg/sec
         2. Temperature
            1. Type - Constant
            2. Constant value - `300.0` K
  - Outflow
    - Simple Boundary Condition - (disabled to allow for periodic conditions to be set)
  - Wall

        - Simple Boundary Condition
            1. Type - Wall
            2. Temperature BC type - Flux
            3. Heat flux - `2000.0` W/m2

- Periodics
    - Periodic 1
        - Individual Periodic BCs
            1. Velocity
                1. Type - Periodic
            2. Pressure
                1. Type - Single Unknown Offset
            3. Temperature
                1. Type - Single Unknown Offset

References

F. M. White. "Viscous Fluid Flow". Section 3-2.1. McGraw-Hill Book Co., Inc.. New York. 1991.

F. P. Incropera and D. P. DeWitt. "Fundamentals of Heat Transfer". John Wiley & Sons. New York. 1981.

Laminar Couette Flow with Imposed Pressure Gradient and Heated Walls

In this application, AcuSolve is used to simulate the flow of a highly viscous fluid between a moving and a stationary plate with an imposed pressure gradient and fixed temperature on the walls. AcuSolve results are compared with analytical results described in White (1991). The close agreement of AcuSolve results with analytical results validates the ability of AcuSolve to model cases with imposed pressure gradients and viscous heating.

Problem Description

The problem consists of a viscous fluid between two plates in a two dimensional domain, as shown in the following image, which is not drawn to scale. The domain is 1.0 m high and 1.5 m long. The top plate moves with a constant velocity of 3.0 m/sec and the bottom plate is fixed. To simulate a fully developed flow with a relatively short length domain there is a mean-pressure gradient of -12 Pa/m applied to the fluid in the streamwise direction, defined as a body force acting on the entire fluid. The lower wall is held at a fixed temperature of 273.0 K, while the upper wall is held at a fixed temperature of 274.0 K. The problem is simulated with periodic boundaries in the streamwise direction. The Reynolds number of the flow, based on the distance between the plates is 0.3, indicating laminar flow. The flow field develops from the pressure gradient, the motion of the top plate, and the viscous shear stresses near the plates. The shear stress within the domain causes the temperature to increase within the channel.

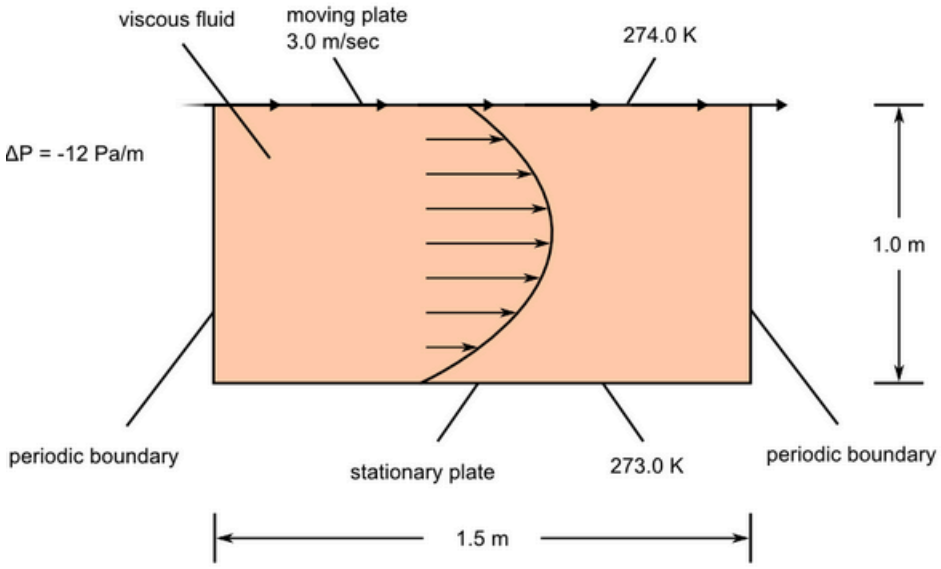


Figure 548: Critical Dimensions and Parameters for Simulating Laminar Couette Flow with an Imposed Pressure Gradient and Heated Walls

The simulation was performed as a two dimensional problem by constructing a volume mesh that contains a single layer of elements extruded in the cross stream direction, normal to the flow plane and by imposing symmetry boundary conditions on the extruded planes. Due to the periodic natural of the flow, a single element extrusion in the streamwise direction is used to reduce the model size.

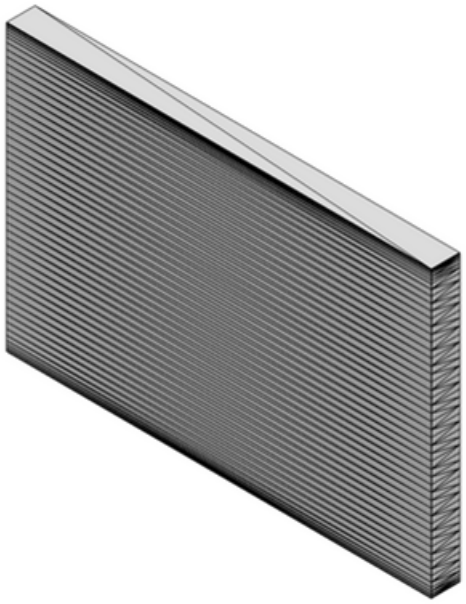


Figure 549: Mesh used for Simulating Laminar Couette Flow with an Imposed Pressure Gradient and Heated Walls

AcuSolve Results

The AcuSolve solution converged to a steady state and the results reflect the mean flow conditions. The simulation results show a flow field with a nearly linear distribution of velocity, with the peak at the top wall. The flow develops primarily as a result of the shear stress acting on the fluid near both the moving plate and the stationary plate. The temperature variation between the two plates develops due to the viscous heating effects that increase the temperature within the channel, with the maximum near the central height of the domain. The following figure shows the temperature distribution between the two plates and velocity vectors indicating the velocity profile.

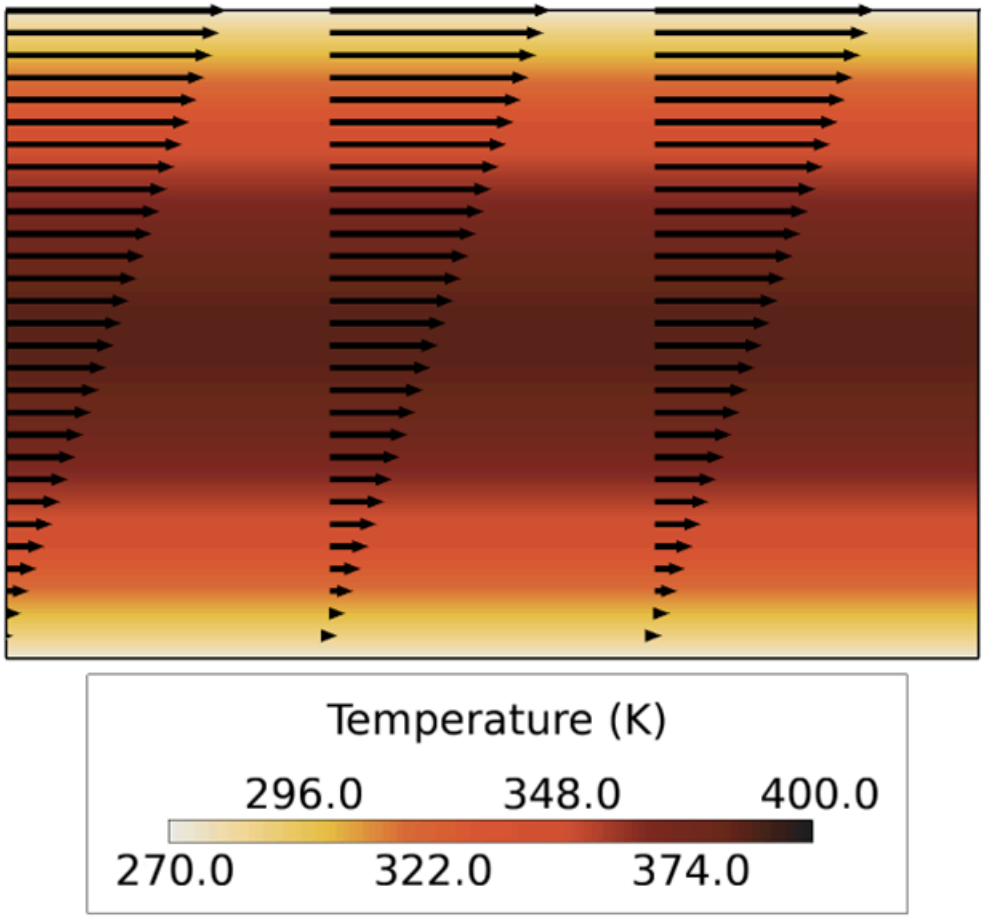


Figure 550: Contours of Temperature Between the Plates, with Velocity Vectors

The following image demonstrates the accuracy of the solution compared to the analytical results as computed by the solution for viscous heating within a channel with a moving upper boundary.

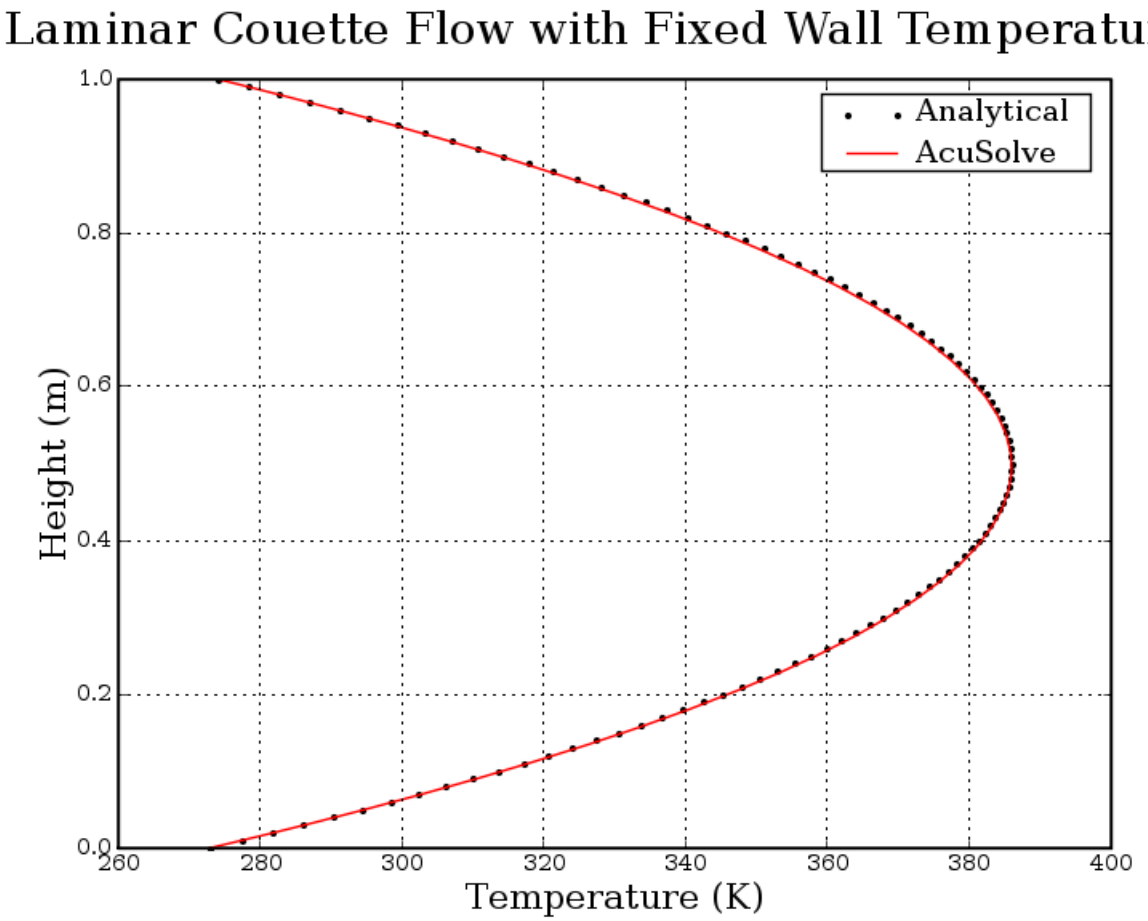


Figure 551: Temperature Plotted Against Height above the Bottom of the Flow Field (Temperature is Presented on the X Axis to Better Represent the Distribution Between the Plates in the Streamwise Direction)

Summary

In this application, a fully developed laminar flow between two plates with fixed temperature is studied and compared against analytical data. The AcuSolve results compare well with the analytical data for the temperature distribution between the two plates. The simulation indicates that the velocity profile arises due to the combination of the viscous shearing and the velocity of the upper plate. The velocity and temperature profiles computed by AcuSolve demonstrate how highly viscous fluids tend to direct the flow regime. AcuSolve demonstrates the ability to predict the analytical solution for viscous heating between two flat plates with moving and stationary boundaries and an imposed pressure gradient.

Simulation Settings for Laminar Couette Flow with Imposed Pressure Gradient and Heated Walls

AcuConsole database file: `<your working directory>\couette_laminar_heat\couette_laminar_heat.acs`

Global

- Problem Description

    - Analysis Type - Steady State
    - Temperature equation - Advective Diffusive
    - Turbulence equation - Laminar
- Auto Solution Strategy
    - Relaxation factor - `0.2`
- Material Model
    - Fluid
        - Density - `1.0` kg/m3
        - Specific Heat - `1.0` J/kg-K
        - Viscosity - `100.0` kg/m-sec
- Body Force
    - DP/DL
        - Gravity
            1. Z-component - `18.0` m/sec2

    Model
- Volumes
    - Fluid
        - Element set
            1. Material model - Fluid
            2. Body force - DP/DL
            3. Viscous heating - on
- Surfaces
    - Max_X
        - Simple Boundary Condition
            1. Type - Symmetry
    - Max_Y
        - Simple Boundary Condition
            1. Type - Wall
            2. Wall velocity type - Cartesian
            3. Z-velocity - `3.0` m/s
            4. Temperature - `274.0` K
    - Max_Z
        - Simple Boundary Condition - (disabled to allow for periodic conditions to be set)
    - Min_X
        - Simple Boundary Condition
            1. Type - Symmetry
    - Min_Y

        - Simple Boundary Condition
            1. Type - Wall
            2. Temperature - `273.0` K
    - Min_Z
        - Simple Boundary Condition - (disabled to allow for periodic conditions to be set)
- Periodics
    - Periodic 1 all
        - Periodic Boundary Conditions
            1. Type - Periodic

References

F. M. White. "Viscous Fluid Flow". Section 3-3.2. McGraw-Hill Book Co., Inc. New York. 1991.

Natural Convection in a Concentric Annulus

In this application, AcuSolve is used to simulate natural convection in the annular space between a heated inner pipe and an outer concentric pipe. AcuSolve results are compared with experimental results adapted from Kuehn and Goldstein (1978). The close agreement of AcuSolve results with experimental results validates the ability of AcuSolve to model cases with flow induced by natural convection.

Problem Description

The problem consists of two concentric cylinders with air filling the void between them, as shown in the following image, which is not drawn to scale. The radius of the inner cylinder is 0.0178 m and the radius of the outer cylinder is 0.0463 m. The inner cylinder is held at a fixed temperature of 373 K while the outer cylinder is held at 327 K. The temperature gradient drives the flow due to buoyancy effects.

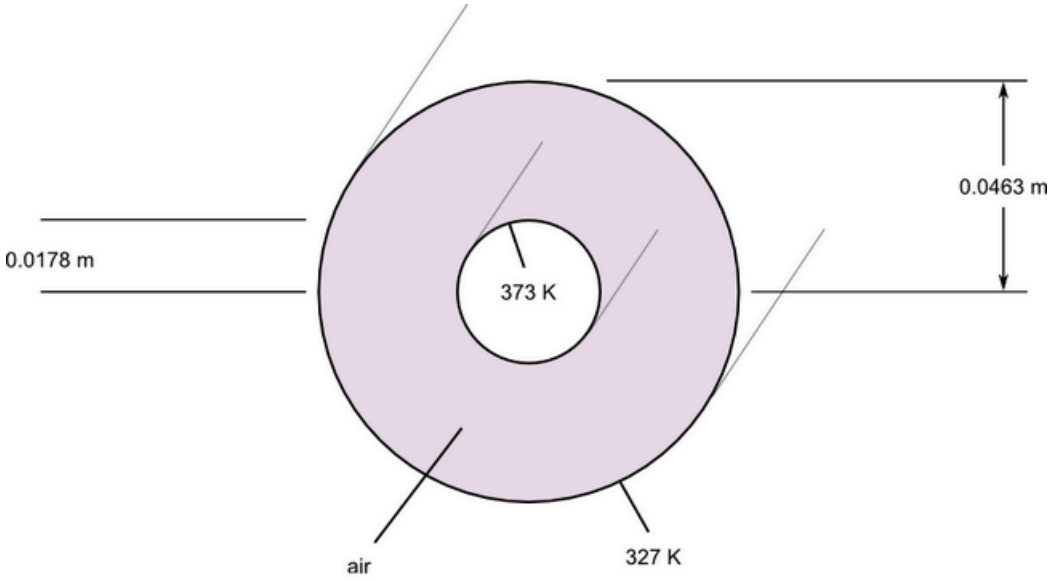


Figure 552: Critical Dimensions and Parameters for Simulating Natural Convection in a Concentric Annulus

The simulation was performed as a two dimensional problem by restricting flow in the out-of-plane direction through the use of a mesh that is one element thick. In addition, the half symmetry of the geometry is exploited to allow for modeling only half of the geometry. These characteristics allow for accurate simulation of the flow while minimizing computational time.

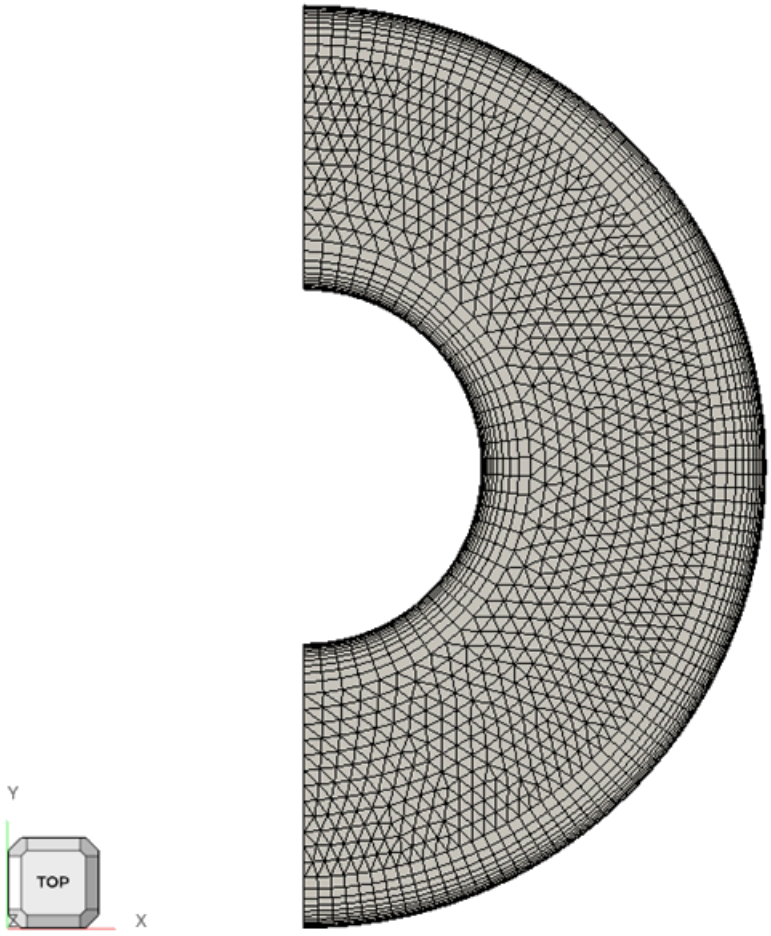


Figure 553: Mesh (Half of a Concentric Annulus) used for Simulating Natural Convection in a Concentric Annulus

AcuSolve Results

The AcuSolve solution converged to a steady state and the results reflect the mean flow conditions. Air density decreases due to heating by the inner cylinder, leading to convective currents within the annulus. As air approaches the outer cylinder, it is cooled by the outer wall, causing the density to increase. This results in heavier air sinking toward the bottom of the assembly.

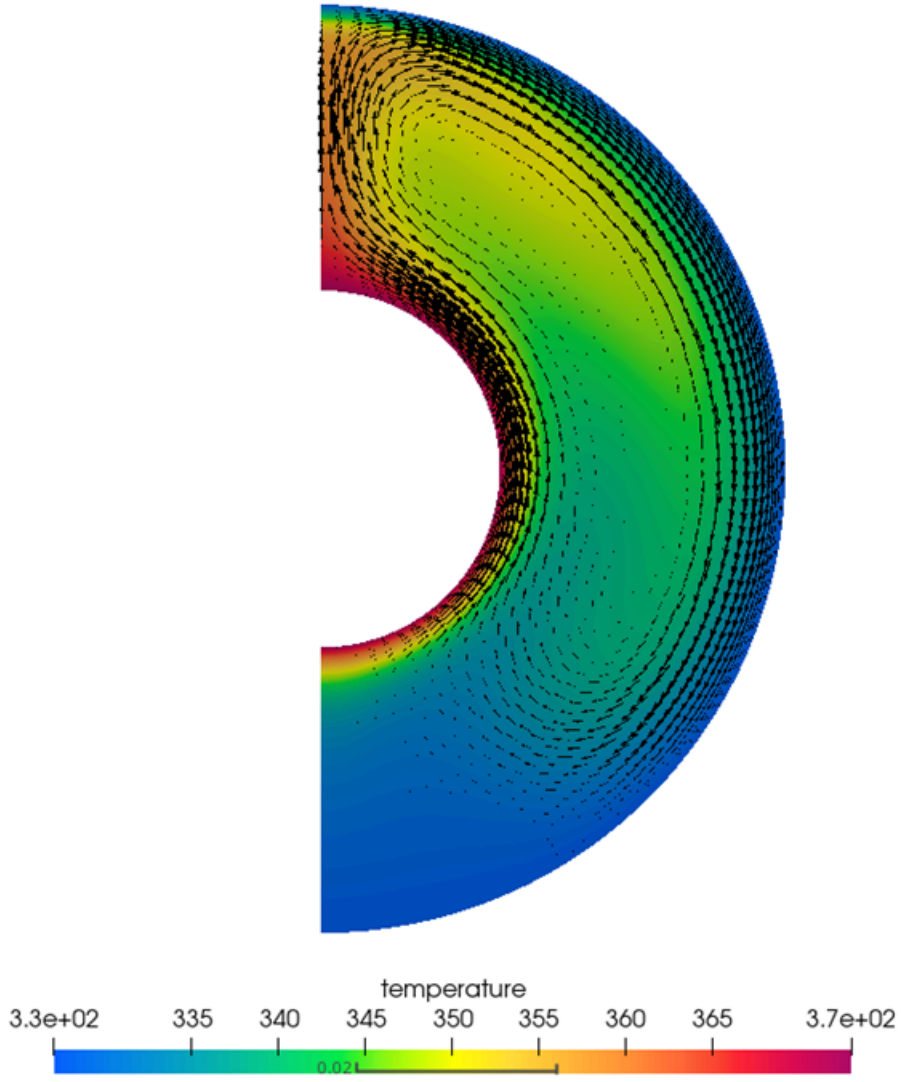


Figure 554: Temperature Contours and Velocity Vectors

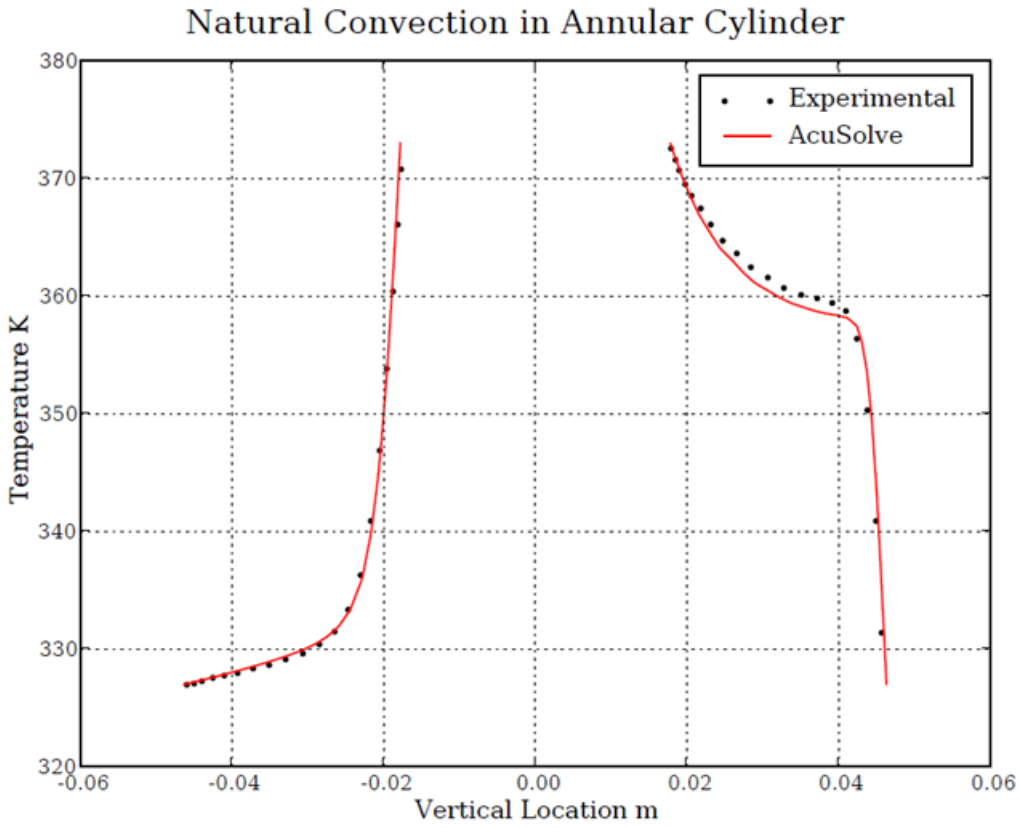


Figure 555: Temperature as a Function of Distance From the Center of the Inner Cylinder

Summary

The AcuSolve solution compares well with analytical results for natural convection in a concentric annulus. In this application, flow is driven by a decrease in density as air is heated. The local variations in density result in the higher density fluid sinking to the bottom of the annulus while the lower density fluid rises to the top. This transfer of momentum is a continuous process which results in the convective currents that are visible in the solution. The AcuSolve temperature results compare very closely with the experimental results.

Simulation Settings for Natural Convection in a Concentric Annulus

HyperWorks CFD database file: `<your working directory>\annulus_heat\annulus_heat.hm`

Global

- Problem Description
  - Analysis type - Steady State
  - Abs. pressure offset - `101325.0` N/m2
  - Temperature equation - Advective Diffusive
  - Turbulence equation - Laminar
  - Gravitational acceleration - { 0, -9.80665, 0 }
- Auto Solution Strategy

- Relaxation factor - `0.2`
- Flow - On
- Temperature - On

- Material Model
  - Air
    - Type - Boussinesq
    - Density - `1.225` kg/m3
    - Expansivity - `0.0034722` 1/K
    - Reference temperature - `288` K
    - Isothermal compressibility - `0.0` m2/N
    - Viscosity - `2.081e-5` kg/m-sec

  Model
- Volumes
  - Fluid
    - Element Set
      1. Material model - Air
  - Surfaces
    - ID
      1. Simple Boundary Condition
         1. Type - Wall
         2. Temperature BC type - Value
         3. Temperature - `373.0` K
    - Max_Z
      1. Simple Boundary Condition
      2. Type - Symmetry
    - Min_Z
      1. Simple Boundary Condition
      2. Type - Symmetry
    - OD
      1. Simple Boundary Condition
         1. Type - Wall
         2. Temperature BC type - Value
         3. Temperature - `327.0` K
    - Symmetry
      1. Simple Boundary Condition
      2. Type - Symmetry
  - Nodes
    - Node 1

1 Pressure

1 Type - Zero

References

T.H. Kuehn and R. J. Goldstein. "An Experimental Study of Natural Convection Heat Transfer in Concentric and Eccentric Horizontal Cylindrical Annuli". Journal of Heat Transfer 100:635-640. 1978.

Laminar Flow Through a Channel with Heated Walls

In this application, AcuSolve is used to simulate high Peclet number laminar flow through a channel with heated walls. AcuSolve results are compared with analytical results adapted from Hua and Pillai (2010). The close agreement of AcuSolve results with analytical results validates the ability of AcuSolve to model cases involving heat transfer to a moving fluid with a high Peclet number.

Problem Description

The problem consists of water at 20 °C flowing through a channel of infinite width with top and bottom walls heated to 75 °C. The channel is 0.2 m high and 0.8 m long, as shown in the following image, which is not drawn to scale. A centrally located slice 0.02 m wide is modeled with slip boundary conditions so that side-wall influences can be ignored. Water enters the channel with an average velocity of 0.003 m/s. As the fluid flows through the channel, it is heated by the top and bottom plates.

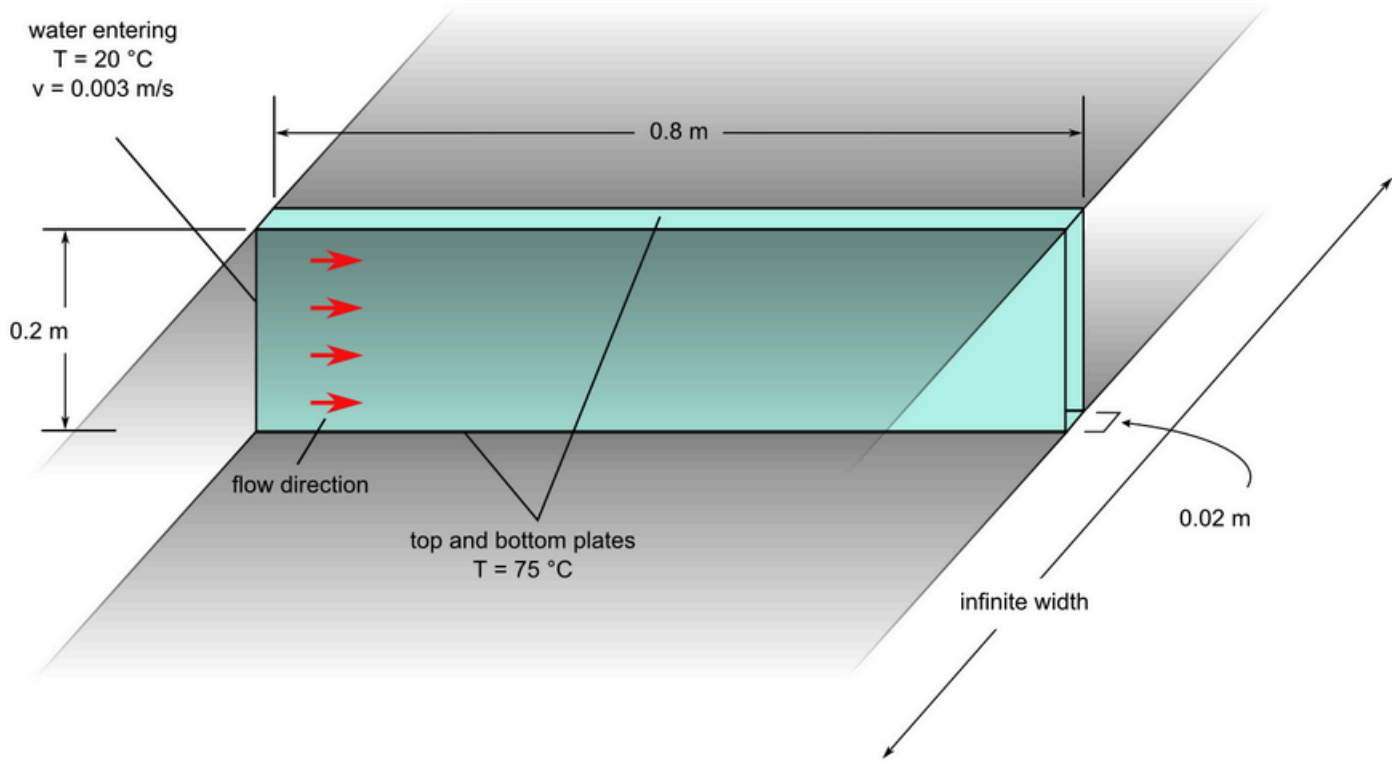


Figure 556: Critical Dimensions and Parameters for Simulating Laminar Flow Through a Channel with Heated Walls

The simulation was performed as a two dimensional problem by restricting flow in the out-of-plane direction through the use of a mesh that is one element thick. In addition, the symmetry of the geometry in the height direction is exploited to allow for modeling only half of the geometry. These characteristics allow for accurate simulation of flow while minimizing computational time.

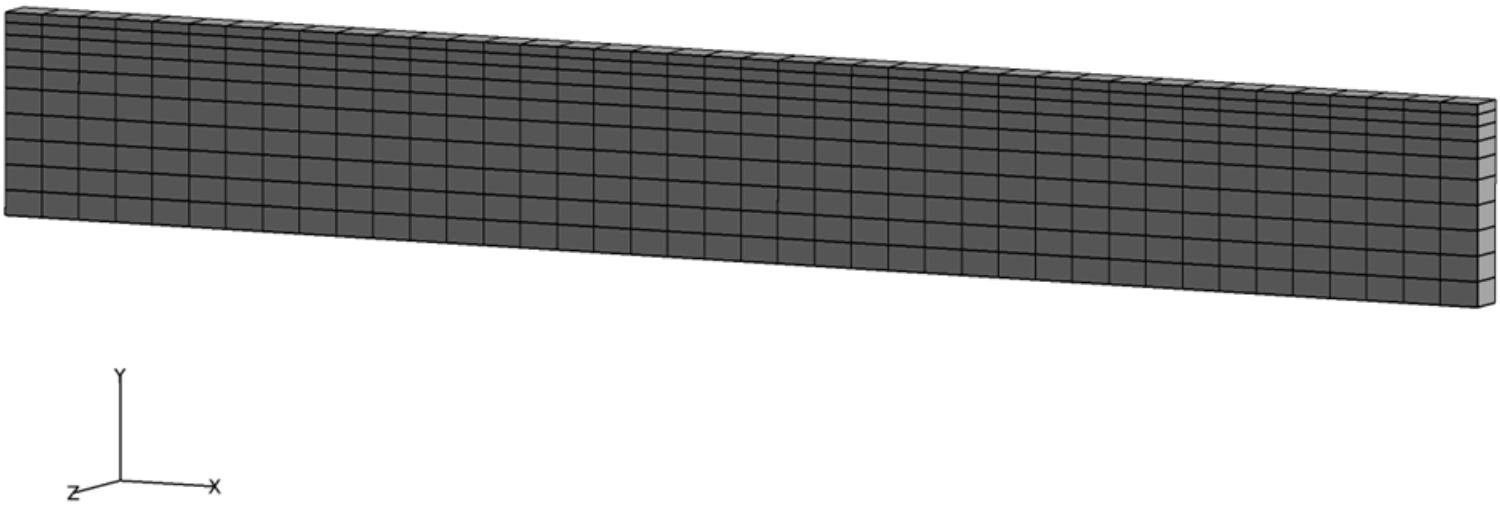


Figure 557: Mesh (Top Half of the Channel) used for Simulating Laminar Flow Through a Channel with Heated Walls

AcuSolve Results

The AcuSolve solution converged to a steady state and the results reflect the mean flow conditions. As the cool water enters the channel at temperature less than that of the walls, heat is transferred to the water by conduction. As the fluid travels along the channel, the temperature differential between the wall and the adjacent water decreases. The thermal boundary layer within the water develops as the flow propagates downstream.

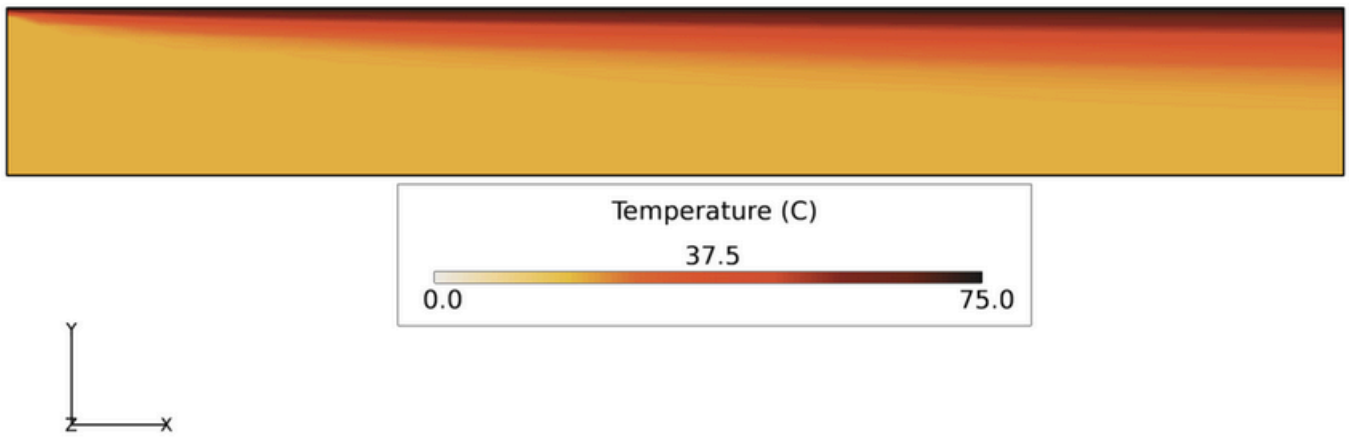


Figure 558: Temperature Contours Along the Top Half of a Heated Channel

Temperature at a specified vertical position in the channel increases along the length of the channel. The nature of that temperature change is dependent on proximity to the heated wall. Water in the center of the flow will have the least temperature change. Since this problem was solved for symmetrical flow, only the top half of the flow region was modeled. The vertical position for results

shown in the following figure are based on the center of flow having a Y-position of 0. For a vertical position near the center of flow (Y=0.0595) there is minimal change in temperature.

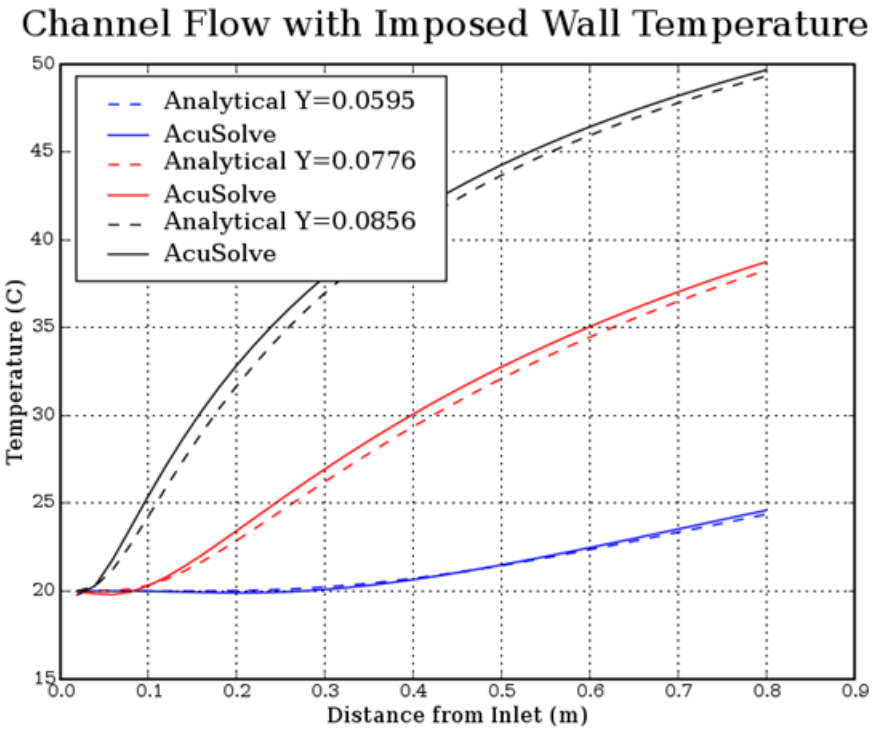


Figure 559: Temperature Plotted Against Distance from Inlet for 3 Different Heights from the Channel Center Line

Summary

The AcuSolve results compare well with the analytical results for the development of a thermal boundary layer in a heated channel. In this application, the model is set up to yield large gradients as the flow convects away from the inlet. The boundary conditions and mesh size were chosen specifically to yield a high Peclet number. The element Peclet number in the flow direction in this case is Pe=30.0, as calculated from the following equation.

$$Pe = \frac{\rho C p |v| he}{k} \tag{22}$$

where ρ is the density, CP the heat capacity, v the velocity, he the length, and k the thermal conductivity.

This example shows the robustness of the stabilized technique in AcuSolve when element Peclet number is high. Note that standard Galerkin finite element formulations become unstable when the element Peclet number is greater than 1.0.

Simulation Settings for Laminar Flow Through a Channel with Heated Walls

AcuConsole database file: `<your working directory>\channel_laminar_heat\channel_laminar_heat.acs`

Global

- Problem Description
  - Analysis type - Steady State
  - Temperature equation - Advective Diffusive
  - Turbulence equation - Laminar
- Auto Solution Strategy
  - Relaxation factor - `0.4`
- Material Model
  - Fluid_Material
    - Density - `1000.0` kg/m3
    - Specific Heat - `1000` J/kg-K
    - Viscosity - `1.0e-12` kg/m-sec
    - Conductivitiy - 1.0 W/m-K

  Model
- Volumes
  - Fluid
    - Element Set
      1. Material model - Fluid_Material
- Surfaces
  - Inlet
    - Simple Boundary Condition
      1. Type - Inflow
      2. Inflow type - Velocity
      3. X velocity - `0.003` m/sec
      4. Temperature - `20` °C
  - Outlet
    - Simple Boundary Condition
      1. Type - Outflow
  - Symm_MaxZ
    - Simple Boundary Condition
      1. Type - Slip
  - Symm_MinY
    - Simple Boundary Condition
      1. Type - Slip
  - Symm_MinZ
    - Simple Boundary Condition
      1. Type - Slip
  - Wall

- Simple Boundary Condition
  1. Type - Wall
  2. Temperature BC type - Value
  3. Temperature - 75 °C

References

Hua Tan and K. M. Pillai. "Numerical Simulation of Reactive Flow in Liquid Composite Molding Using Flux-Corrected Transport (FCT) Based Finite Element/Control Volume (FE/CV) Method". International Journal of Heat and Mass Transfer. 53:2256-2271, 2010.

Turbulent Natural Convection Inside a Tall Cavity

In this application, AcuSolve is used to simulate the natural convection of a turbulent flow field within a tall rectangular cavity. AcuSolve results are compared with experimental results as described in Betts and Bokhari (2000). The close agreement of AcuSolve results with experimental results validates the ability of AcuSolve to model cases with natural convection of turbulent flow within a tall cavity.

Problem Description

The problem consists of air within a tall cavity with a hot wall and a cold wall, as shown in the following image, which is not drawn to scale. The cavity is 2.18 m tall, 0.0762 m wide, and 0.52 m deep. The cavity's vertical walls differ in temperature, causing the fluid to transfer the heat, leading to natural convection. The temperature of the hot wall is 307.85 K, while the temperature of the cold wall is 288.25 K. The horizontal walls of the cavity are adiabatic. The length-to-width ratio of 28.6 and temperature difference of 19.6 K produce a turbulent flow field within the cavity with a Rayleigh number of $8.6X10^{5}$ (Betts and Bokhari 2000). The flow medium is air, with a Boussinesq approximation for density, a specific heat of 1005 J/kg-K, and a viscosity of $1.781 X 10^{-5}$ kg/m-s. Gravity is applied globally to the volume of air.

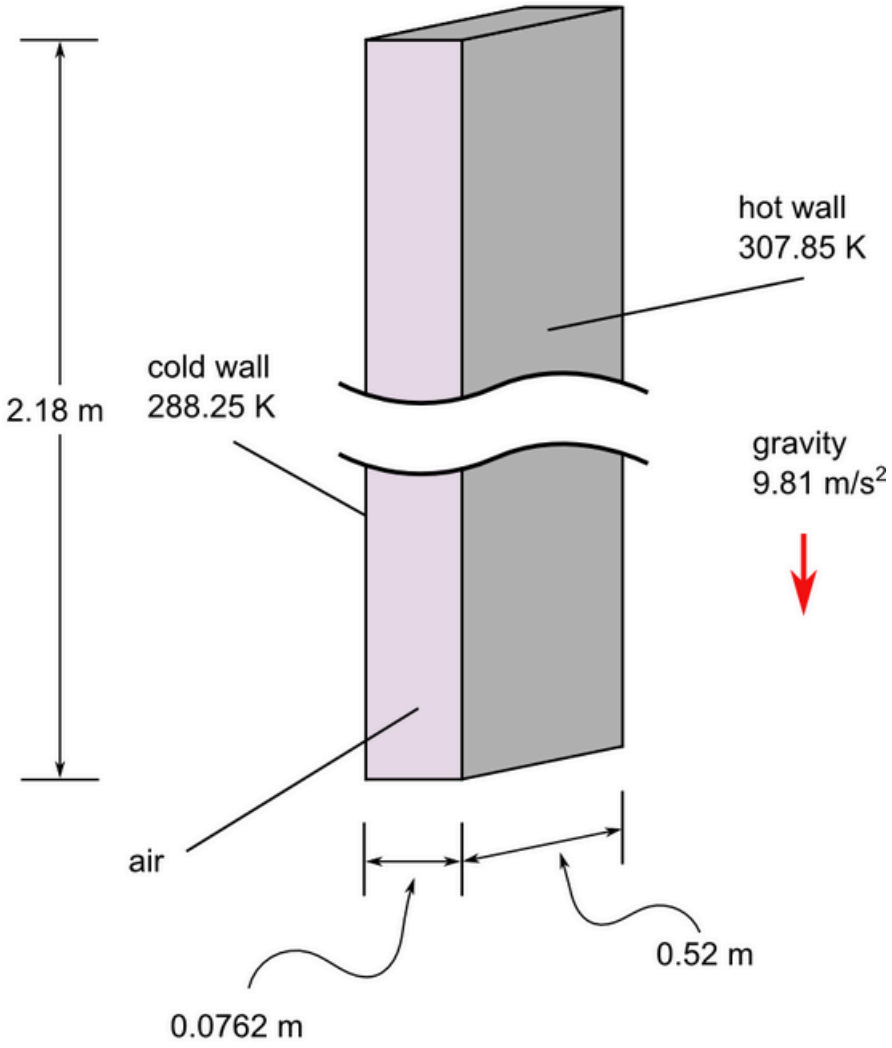


Figure 560: Critical Dimensions and Parameters for Simulating Turbulent Natural Convection in a Tall Cavity

The simulation was performed as a two dimensional problem by constructing a volume mesh that contains a single layer of elements in the extruded direction, normal to the flow plane and by imposing symmetry boundary conditions on the extruded planes.

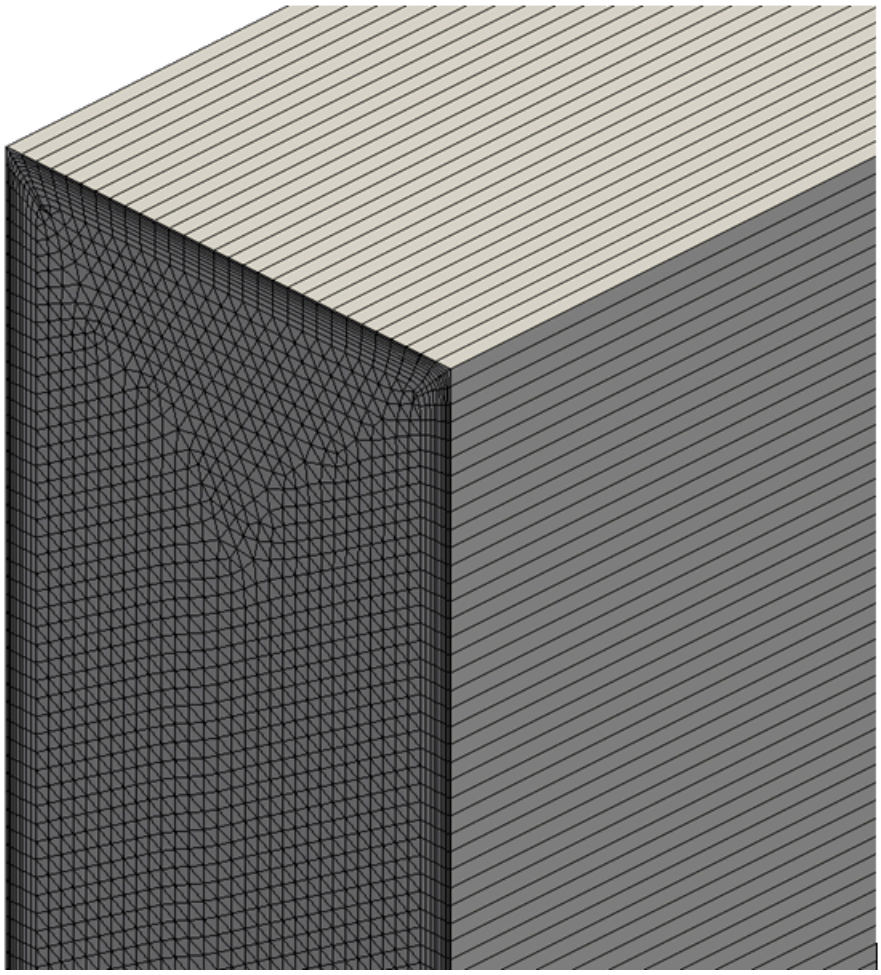


Figure 561: Mesh used for Simulating the Natural Convection of Turbulent Flow in a Tall Cavity

AcuSolve Results

The AcuSolve solution converged to a steady state and the results reflect the mean flow conditions. The natural convection of the flow is generated by heat transfer from the vertical walls to the fluid in the cavity. The temperature gradients created by this heat transfer cause differing densities within the flow region. The warmer air rises to the top of the cavity due to its lower density while the colder air sinks to the bottom of the cavity due to its higher density. This produces flow near the hot vertical wall in the positive vertical direction and flow near the cold wall in the negative vertical direction.

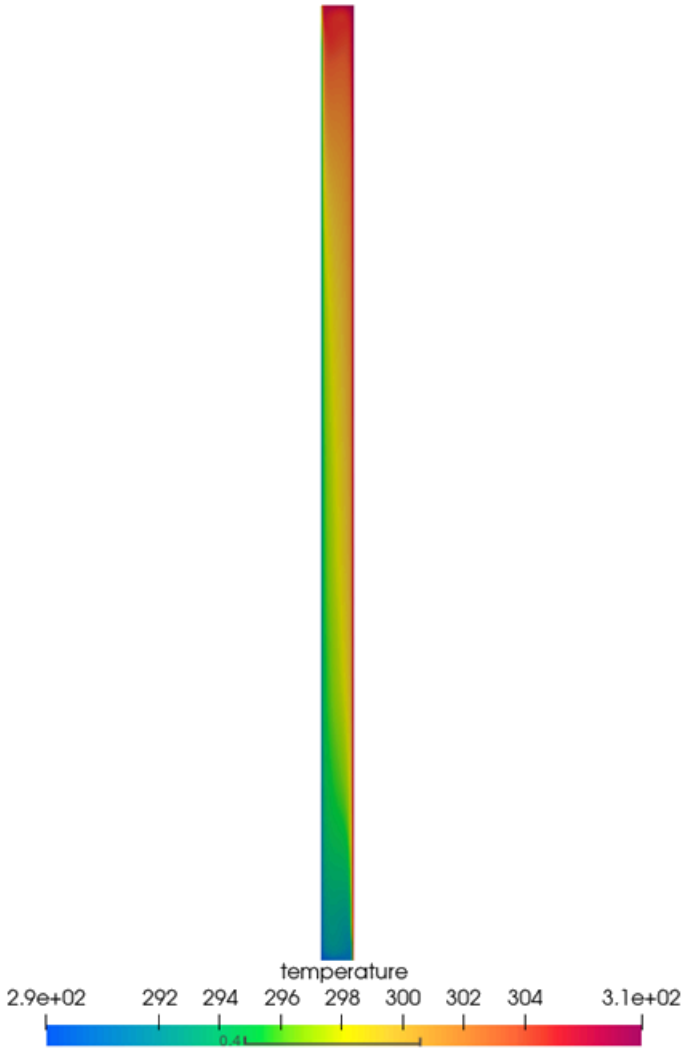


Figure 562: Temperature Contours Throughout Tall Cavity in the X-Y Plane

The AcuSolve results of the temperature and vertical velocity within the cavity are compared to the corresponding experimental values in the plots shown below. The temperature of the air is lowest near the cold vertical wall, remains relatively steady in the middle of the cavity, and then peaks near the hot vertical wall. Following a similar trend, the AcuSolve results show that the velocity is lowest near the cold vertical wall, due to the air sinking, and then steadily increases as the air begins to rise near the hot vertical wall. The velocity at the walls is zero due to the no-slip boundary condition. Additional comparisons are made to evaluate the performance of four turbulence models, Spalart-Allmaras (SA), shear stress transport (SST), K-Omega and K-ε.

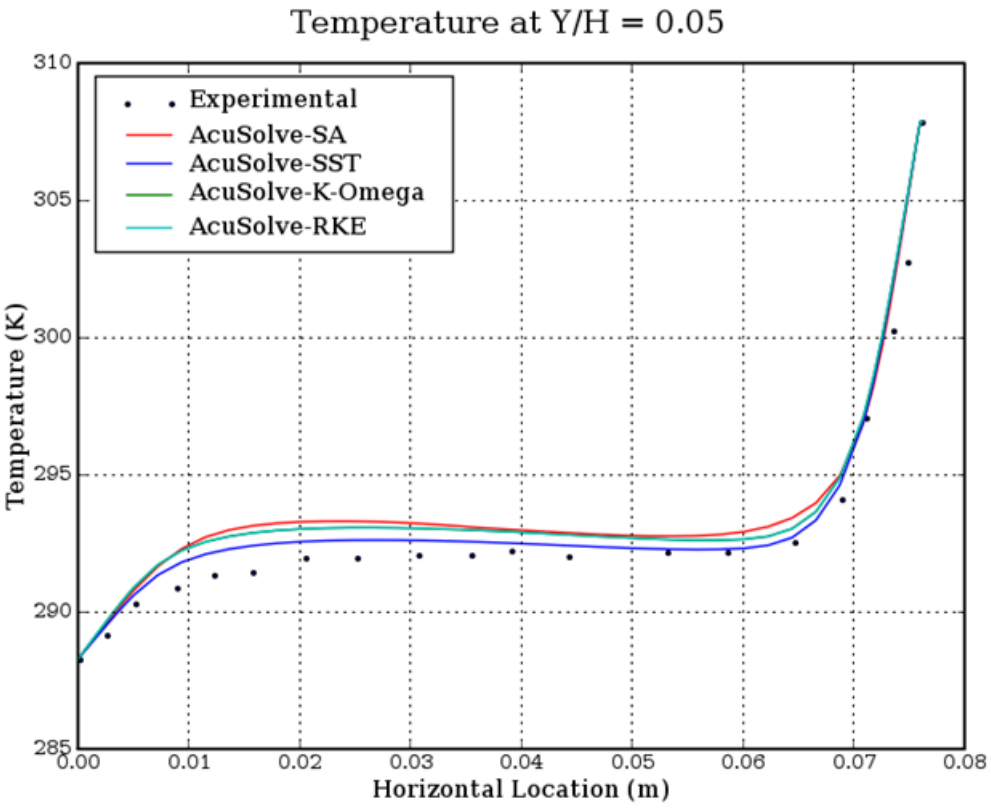


Figure 563: Temperature Plotted against Location along Horizontal at a Position of y/H=0.05 in the Cavity, where H is the Cavity Height and y is the Distance from the Bottom Wall

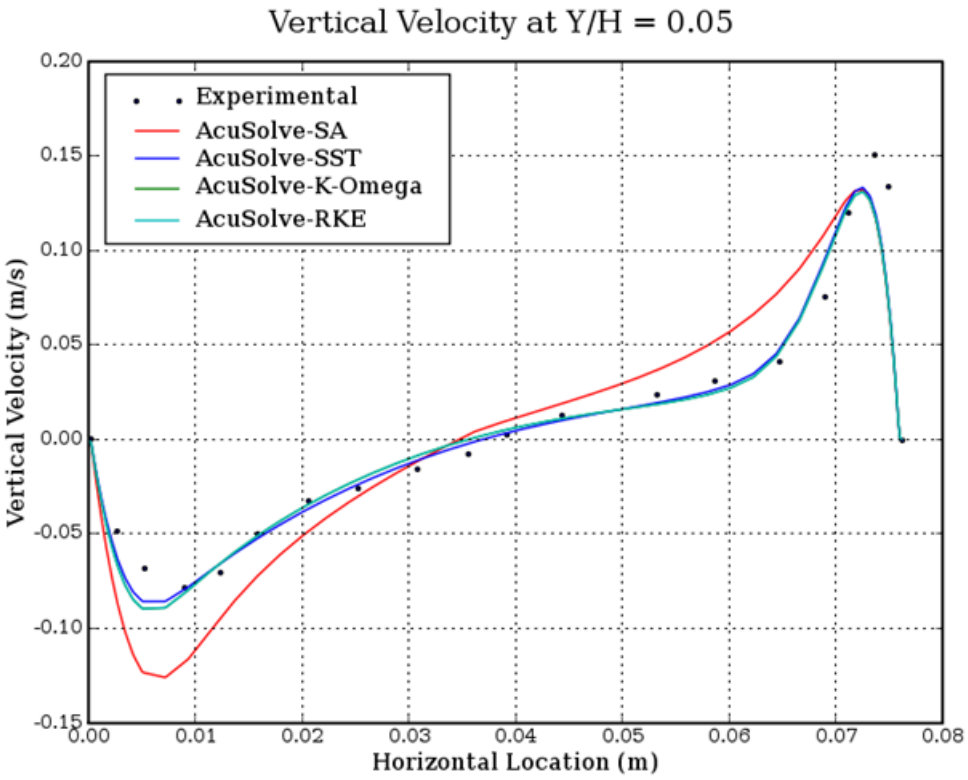


Figure 564: Vertical Velocity Plotted against Location along Horizontal at a Position of y/H=0.05 in the Cavity, where H is the Cavity Height and y is the Distance from the Bottom Wall

Summary

In this application, turbulent flow developed by natural convection, at a Rayleigh number of 8.6X105, is studied within a tall cavity. The AcuSolve results compare well with the experimental data for temperature and vertical velocity along a horizontal line at a location of y/H=0.05 in the tall cavity, with the two-equation models capturing the velocity gradient with greater accuracy. A temperature difference occurs within the flow region due to the heat transfer from the vertical walls of the cavity. The hotter, less-dense air rises to the top of the cavity while the colder, denser air sinks to the bottom, giving rise to recirculation. AcuSolve demonstrates the ability to accurately predict the natural convection of turbulent flow within a tall cavity.

Simulation Settings for Turbulent Natural Convection Inside a Tall Cavity

HyperWorks CFD database file: `<your working directory\cavity_turbulent_heat \cavity_turbulent_heat.hm`

Global

- Problem Description
  - Analysis type - Steady State
  - Turbulence equation - SST
- Auto Solution Strategy
  - Relaxation factor - `0.5`

    - Convergence tolerance - `0.005`
- Material Model
    - Air
        - Type - Boussinesq
        - Density - `1.225` kg/m3
        - Specific Heat - `1005` J/kg-K
        - Viscosity - `1.781e-5` kg/m-sec

  Model
- Volumes
    - Volume
        - Element Set
            1. Material model - Air
- Surfaces
    - Back
        - Simple Boundary Condition
            1. Type - Symmetry
    - Bottom
        - **Simple Boundary Condition**
            1. Type - Wall
            2. Temperature BC type - Flux
            3. Heat Flux - `0.0` W/m2
    - Cold
        - **Simple Boundary Condition**
            1. Type - Wall
            2. Temperature BC type - Value
            3. Temperature - `288.25` K
    - Front
        - Simple Boundary Condition
            1. Type - Symmetry
    - Hot
        - Simple Boundary Condition
            1. Type - Wall
            2. Temperature BC type - Value
            3. Temperature - `307.85` K
    - Top
        - Simple Boundary Condition
            1. Type - Wall

2 Temperature BC type - Flux

3 Heat Flux - `0.0` W/m2

References

P.L. Betts and I.H. Bokhari. "Experiments on Turbulent Natural Convection in an Enclosed Tall Cavity". International Journal of Heat and Fluid Flow 21:675-683. 2000.

Viscous Heating Inside a Rotating Annulus

In this application, AcuSolve is used to simulate fluid flow and viscous heating in an annulus formed by concentric cylinders. AcuSolve results are compared with analytical results adapted from Bird and others (1960). The close agreement of AcuSolve results with analytical results validates the ability of AcuSolve to model cases with viscous heating.

Problem Description

The problem consists of a viscous fluid filling the annulus between two concentric cylinders, as shown in the following image, which is not drawn to scale. The inner cylinder has a radius of 1.0 m and is fixed in place. The outer cylinder has a radius of 2.0 m and rotates with a constant angular velocity of 0.5 rad/s. The inner cylinder is held at a constant temperature of 273 K and the outer cylinder is held at 274 K.

The rotation of the outer cylinder causes the fluid to rotate due to the viscous shearing near the wall. As the inner cylinder is fixed, a velocity gradient is generated as a function of distance from the inner cylinder center. Viscous stresses within the domain generate significant amounts of heat, leading to a substantial increase in the fluid temperature in regions of high shear.

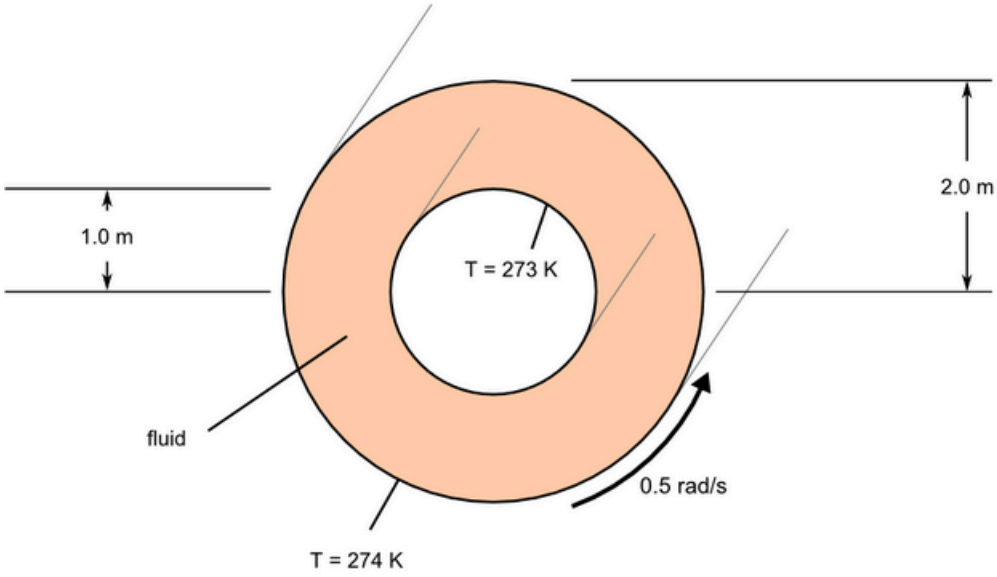


Figure 565: Critical Dimensions and Parameters for Simulating Viscous Heating Inside a Rotating Annulus

The simulation was performed as a two dimensional problem by constructing a volume mesh that contains a single layer of elements in the extruded direction, normal to the flow plane, and by imposing symmetry boundary conditions on the extruded planes.

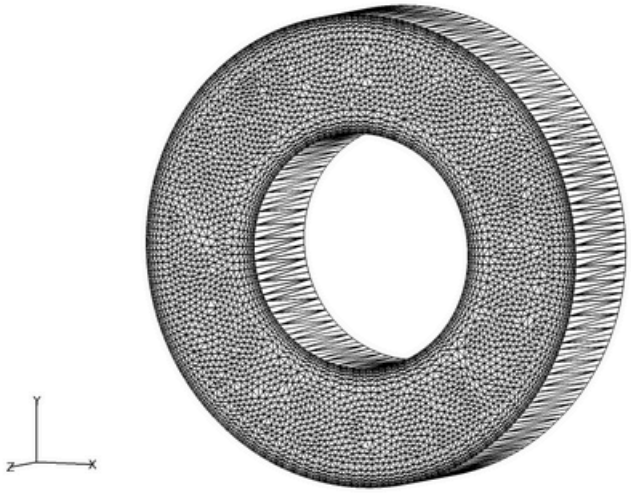


Figure 566: Mesh used for Simulating Viscous Heating Inside a Rotating Annulus

AcuSolve Results

The AcuSolve solution converged to a steady state and the results reflect the mean flow conditions. Flow is induced by the viscous shearing near the outer wall, creating a velocity gradient with the highest velocity near the moving wall.

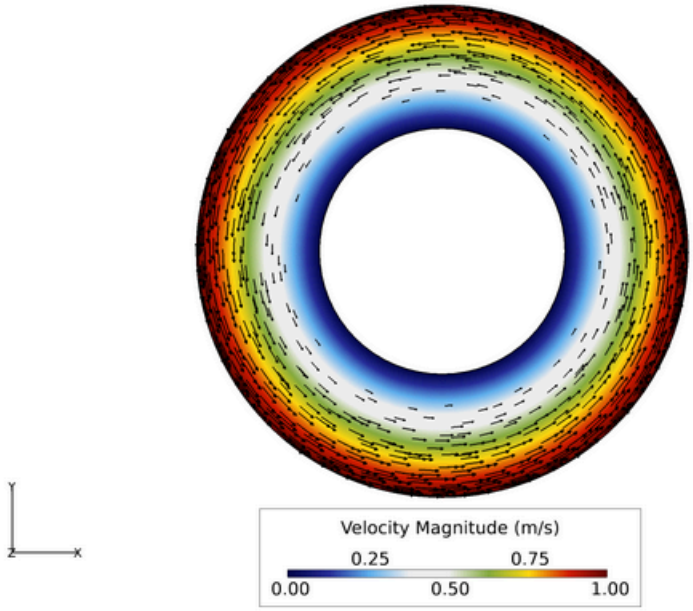


Figure 567: Contours of Velocity Magnitude and Velocity Vectors

The velocity gradient causes viscous heating, causing the fluid temperature to increase. The resulting temperature profile is nonlinear with the highest temperatures occurring in the space between the cylinders.

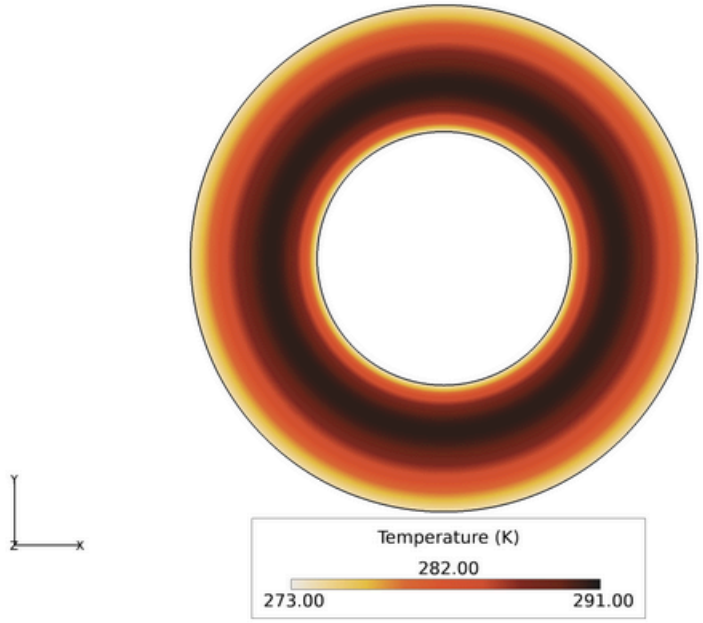


Figure 568: Contours of Temperature

AcuSolve results were compared to analytical results for velocity and for temperature across a range of radial locations.

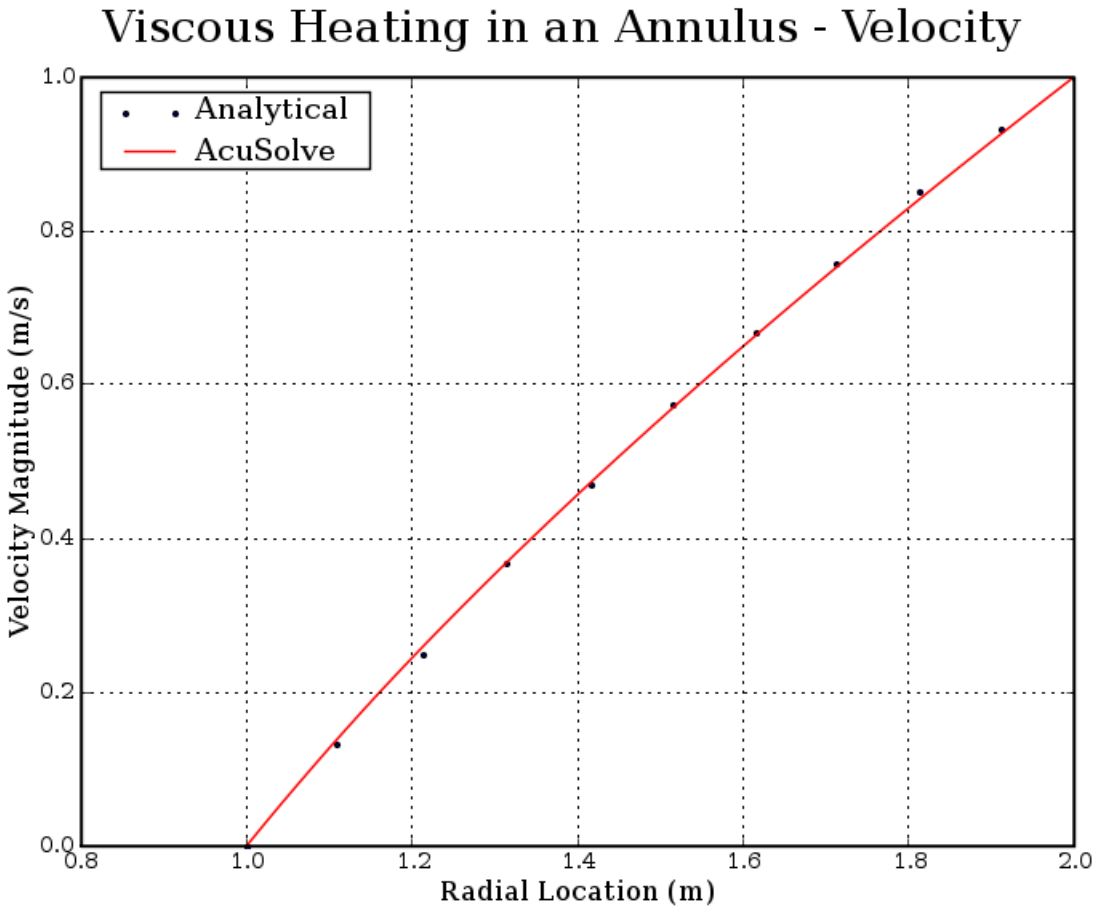


Figure 569: Velocity Magnitude Plotted Against Radial Location from the Center of the Inner Cylinder

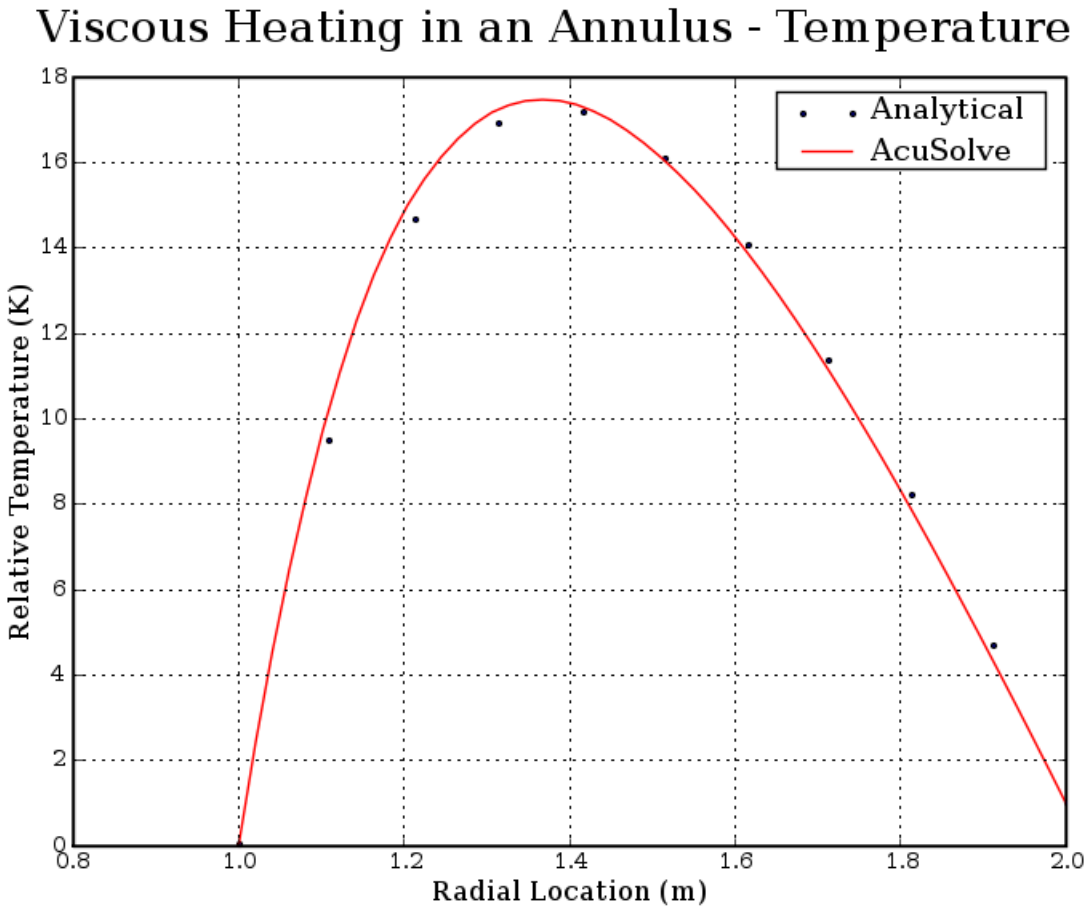


Figure 570: Temperature (Relative to the Inner Cylinder Wall Temperature) Plotted Against Radial Location from the Center of the Inner Pipe

Summary

The AcuSolve results compare well with the analytical results for both the flow field and the temperature across the annulus. In this application, flow is induced due to the viscous stresses generated by the rotation of the exterior cylinder. Velocity gradients between the cylinders give rise to shear stresses that induce frictional heating of the fluid. Due to the high viscosity of the fluid, the viscous heating is significant and leads to large increases in the temperature between the cylinders. This application validates the ability of AcuSolve to simulate flows where the viscous heating contribution is significant.

Simulation Settings for Viscous Heating Inside a Rotating Annulus

AcuConsole database file: `<your working directory>\annulus_rotating_heat\annulus_rotating_heat.acs`

Global

- Problem Description
  - Analysis type - Steady State
  - Temperature equation - Advective Diffusive

- Turbulence equation - Laminar
- Auto Solution Strategy
  - Relaxation factor - `0.2`
- Material Model
  - Fluid
    - Density - `1.0` kg/m3
    - Viscosity - `300` kg/m-sec
    - Conductivity - `1.0` W/m-K
- Reference Frame
  - Outer_Rotation
    - Angular Velocity
      1. X-component - `0.0` rad/sec
      2. Y-component - `0.0` rad/sec
      3. Z-component - `0.5` rad/sec

Model

- Volumes
  - Fluid
    - Element Set
      1. Material model - Fluid
      2. Viscous heating - On
- Surfaces
  - Inner_Cylinder
    - Simple Boundary Condition
      1. Type - Wall
      2. Temperature BC type - Value
      3. Temperature - `273.0` K
  - Outer_Cylinder
    - Simple Boundary Condition
      1. Type - Wall
      2. Reference frame - Outer_Rotation
      3. Temperature BC type - Value
      4. Temperature - `274.0` K
  - Symm_MaxZ
    - Simple Boundary Condition
      1. Type - Symmetry
  - Symm_MinZ
    - Simple Boundary Condition

1 Type - Symmetry

- Nodes
  - Node 1
    - Pressure
      1 Type - Zero

References

R. B. Bird, W. E. Stewart, and E. N. Lightfoot. "Transport phenomena". New York, John Wiley and Sons, 1960

Ideal Gas Compression in an Actuating Piston

In this application, AcuSolve is used to simulate pressure and temperature inside an actuating piston using the ideal gas relationship and fully defined mesh motion. AcuSolve results are compared with analytical results as described in Moran and Shapiro (2000). The close agreement of AcuSolve results with analytical results validates the ability of AcuSolve to model cases with material properties defined by the ideal gas law subjected to significant mesh distortion.

Problem Description

The problem consists of air compressed by a piston within a cylinder 10 m long with a diameter of π (3.14159) m, as shown in the following image, which is not drawn to scale. The piston is driven by a crankshaft 4 m long attached to a connecting rod 6 m long. The crankshaft rotates at 60o/s around a center point. At time (t) = 0.0 s the crank and piston are at top dead center (TDC) with an initial cylinder volume of 80 m^3. At t = 3.0 s the piston is at bottom dead center (BDC), at which point the volume in the cylinder is reduced to 16 m^3. The piston then moves back to TDC at t = 6.0 s. Air at atmospheric conditions, with material properties of an ideal gas and a dynamic viscosity of 1.781 X 10^5 kg/m-sec is the fluid modeled in the domain.

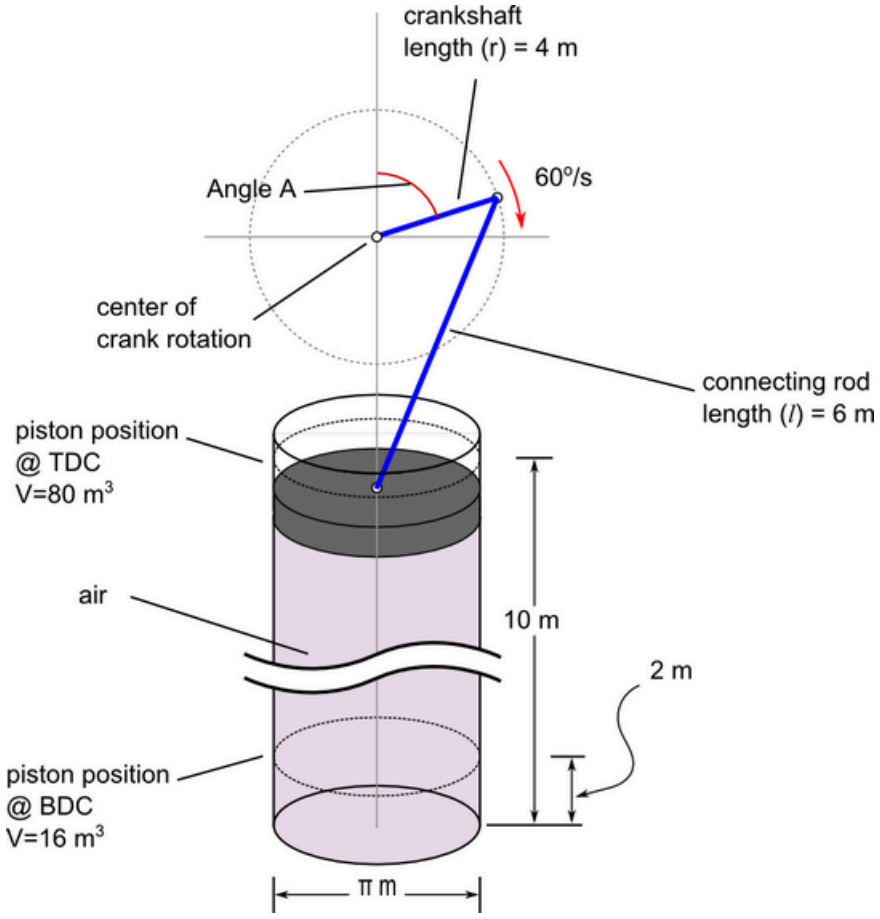


Figure 571: Critical Dimensions and Parameters for Simulating Ideal Gas Compression in an Actuating Piston

The motion of the piston is described by the following equation.

$$x = r*\cos A + \sqrt{l^2 - r^2 \sin^2 A} \quad (23)$$

Where

- x is the distance of the piston from TDC
- r is the length of the connecting rod, 4 m
- A is the crank angle as a function of time (t)
- l is the connecting rod length, 6 m

During the simulation, the top surface of the cylinder, representing the piston, moves with an applied mesh motion that mimics the motion of the reciprocating crank, rod, and piston assembly. The ideal gas is compressed by contracting the mesh according to the motion of that assembly and by allowing the fluid properties to change as a function of time.

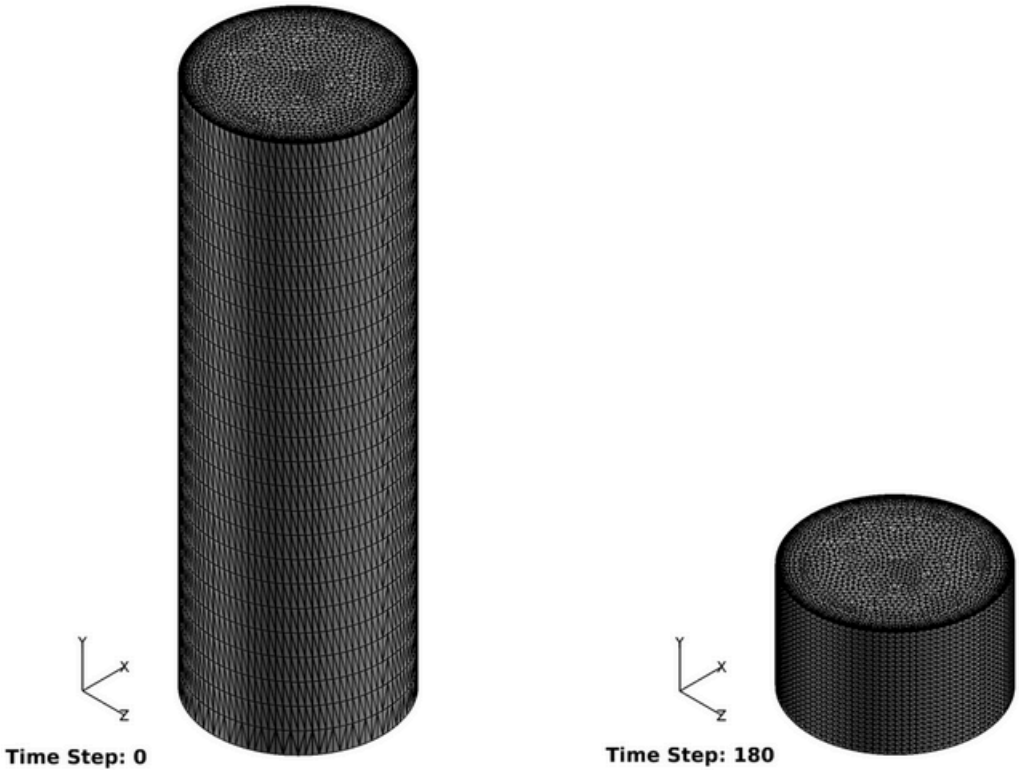


Figure 572: Mesh Used for Simulating Ideal Gas Compression in an Actuating Pistion at Time Step 0 and Time Step 180 (3 s)

AcuSolve Results

The simulation was run as transient for a total of 360 time steps with a duration of 6.0 seconds. The AcuSolve solution shows time dependent pressure and temperature in a cylinder volume that compresses and expands in a 6.0 second cycle. Pressure and temperature increase as the cylinder volume decreases, and returns toward initial conditions as the cylinder volume expands. The contours of pressure and temperature within the cylinder at the initial stage (t = 0.0 s) and the half cycle (t = 3.0 s) are shown in the following images.

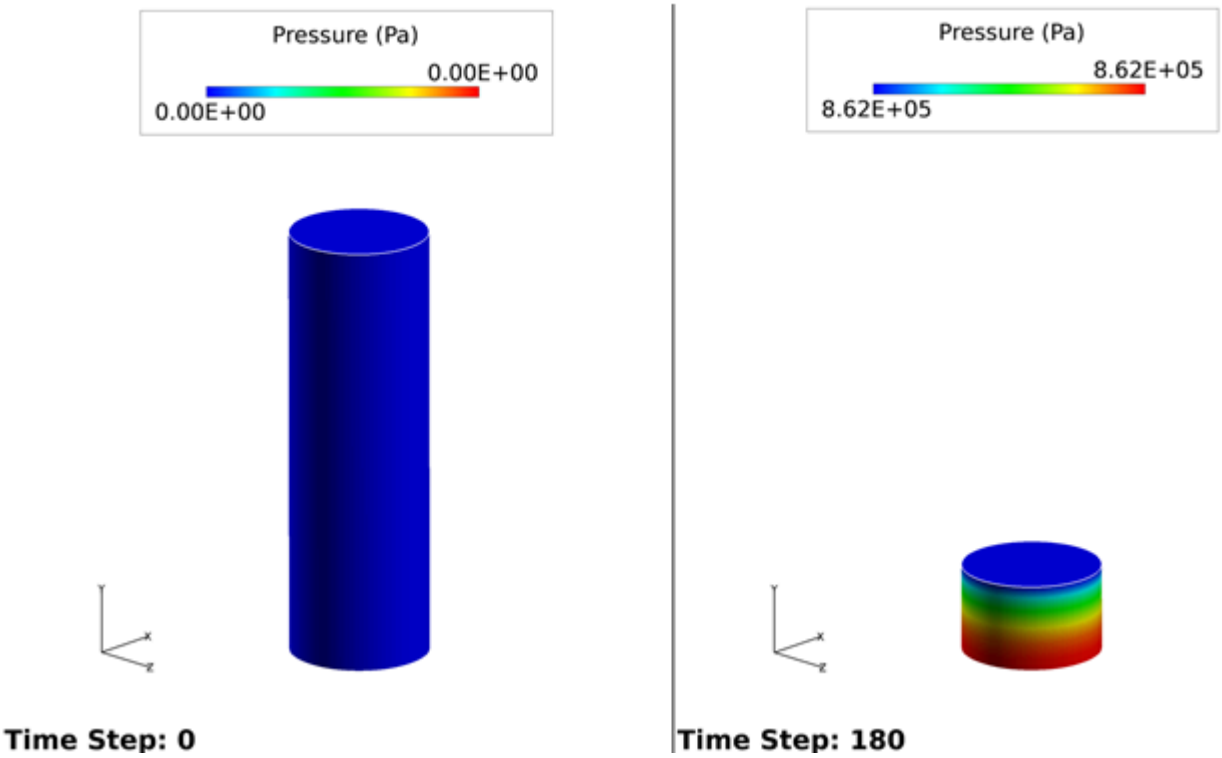


Figure 573: Pressure Distribution Within the Domain with the Piston at TDC and BDC

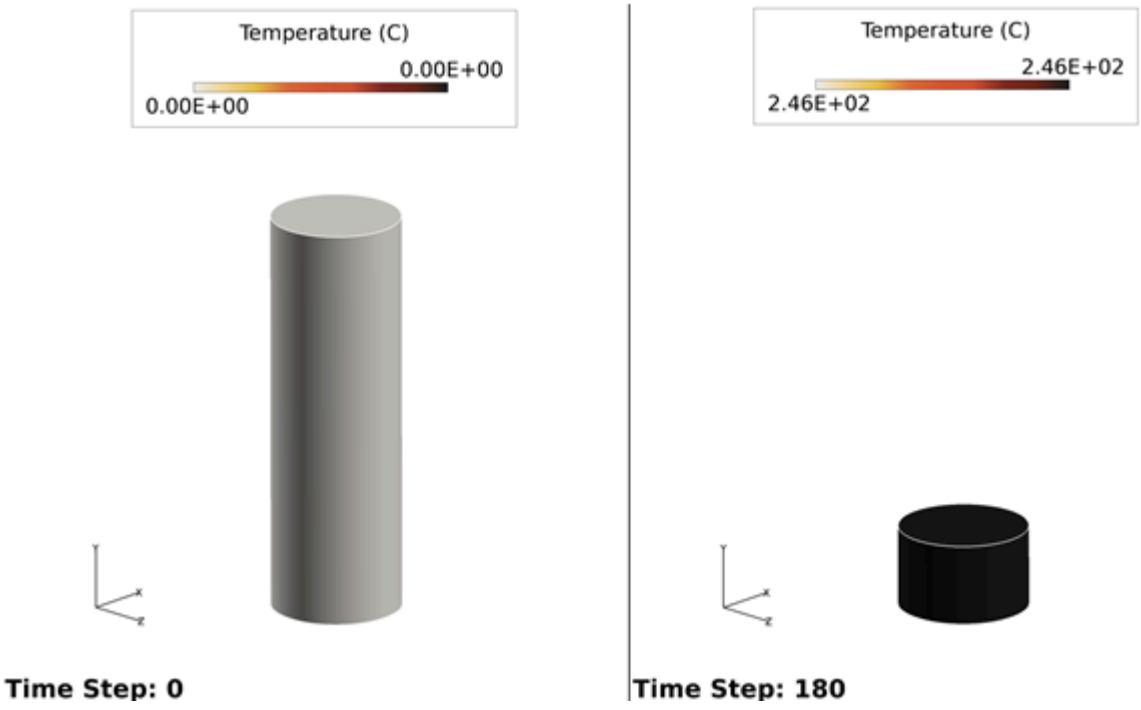


Figure 574: Temperature Distribution Within the Domain with the Piston at TDC and BDC

Comparison of time history plots of the AcuSolve and analytical solutions shows that the AcuSolve solution is nearly identical to the analytical solution. The AcuSolve computed internal pressure reaches a maximum of 8.62 X 105 Pa and the temperature reaches a maximum of 246.45 degrees C.

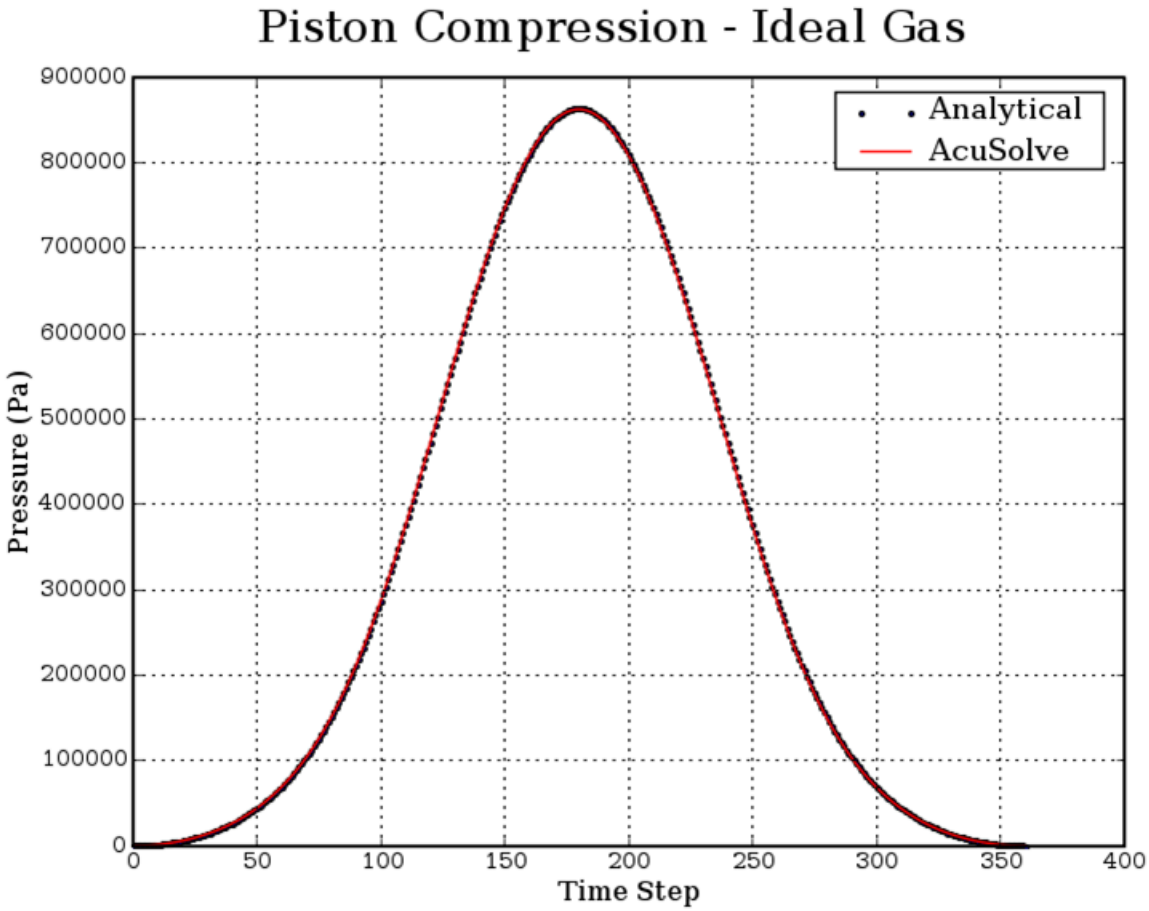


Figure 575: History Plots of Pressure for AcuSolve and Analytical Solutions

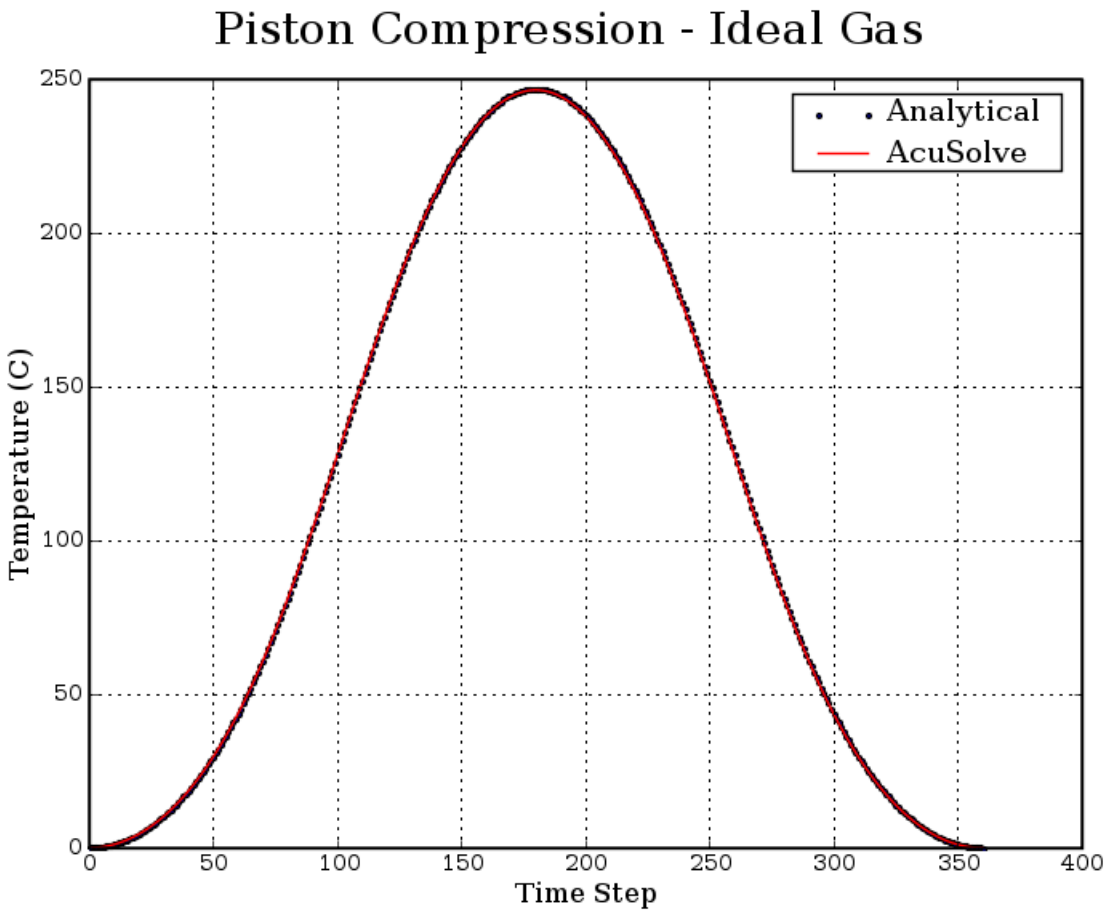


Figure 576: History Plots of Temperature for AcuSolve and Analytical Solutions

Summary

The AcuSolve solution compares well with analytical results for ideal gas compression in an actuating piston. The AcuSolve transient solution compares nearly identically with the analytical solution, with 0.1 percent and 0.16 percent error for the maximum pressure and temperature, respectively. As a result, AcuSolve demonstrates the ability to predict ideal gas compression in an actuating piston.

Simulation Settings for Ideal Gas Compression in an Actuating Piston

AcuConsole database file: `<your working directory>\cylinder_piston_compression\cylinder_piston_compression.acs`

Global

- Problem Description
  - Analysis type - Transient
  - Temperature equation - Advective Diffusive
  - Turbulence equation - Laminar
  - Mesh type - Fully Specified

- Auto Solution Strategy
  - Max time steps - `360`
  - Initial time increment - `0.01667` sec
  - Convergence tolerance - `1.0e-5` sec
  - Max stagger iterations - `10`
- Multiplier Function
  - Piston
    - Type - Piecewise Linear
    - Curve fit variable - Time
    - Curve fit values - (included in `.acs` based on equation discussed in problem description)
- Material Model
  - Air
    - Density
      1. Type - Ideal Gas
      2. Gas constant - `286.9` J/kg-K
      3. Abs. pressure offset - `101325.0` N/m2
      4. Abs. temperature offset - `273.15` K
    - Viscosity - `1.781e-5` kg/m-sec
- Mesh Motion
  - Piston
    - Type - Translation
    - Translation velocity - `0.0`, `-1.0`, `0.0`
    - Velocity variable - Multiplier Function
    - Translation multiplier function - Piston

  Model
- Volumes
  - Fluid
    - Element Set
      1. Material model - Air
      2. Compression heating - On
    - Element Output - on
- Surfaces
  - BDC
    - Simple Boundary Condition
      1. Type - Wall
      2. Wall velocity type - Match Mesh Velocity
      3. Mesh displacement BC type - Fixed
  - SideWall

        - Simple Boundary Condition
            1. Type - Wall
            2. Wall velocity type - Match Mesh Velocity
            3. Mesh displacement BC type - Fixed
    - TDC
        - Simple Boundary Condition
            1. Type - Wall
            2. Mesh displacement BC type - Fixed
            3. Mesh motion - Piston
- Nodes
    - VolumeNodes
        - Mesh X-Displacement
            1. Type - Zero
        - Mesh Y-Displacement
            1. Type - Linear
            2. Mesh motion - Piston
            3. Curve fit variable - Y reference coordinate
                1. X1 - `10.0` m
                2. Y1 - `1.0` m
                3. Y2 - `0.0` m
        - Mesh Z-Displacement
            1. Type - Zero

References

M.J. Moran and H.N Shapiro. "Fundamentals of Engineering Thermodynamics". Wiley. 4th Ed. 2000.

Laminar Flow Through a Pipe with Constant Wall Temperature

In this application, AcuSolve is used to simulate the flow of mercury through a heated pipe. The AcuSolve results are compared with analytical results for pressure drop as described in White (1991), and with temperature changes as described in Incropera and DeWitt (1981). The close agreement of AcuSolve results with analytical results validates the ability of AcuSolve to model cases with flow and imposed temperature constraints.

Problem Description

The problem consists of mercury flowing through a circular pipe that is 0.005 m in diameter and 0.1 m long, as shown in the following image, which is not drawn to scale. Mercury enters the pipe with a constant temperature of 300 K and with a fully developed velocity profile with an average velocity of 0.005 m/s. The pipe wall has a constant temperature of 500 K. These constraints impose a temperature gradient within the fluid. As the fluid moves through the pipe it is slowly heated by the wall, resulting in an increased centerline temperature. Pressure decreases along the pipe length due to the friction imposed by the viscous stresses near the pipe wall. A periodic boundary condition is imposed on the inlet and outlet to allow the pressure to change with a constant offset, while the velocity is fully periodic.

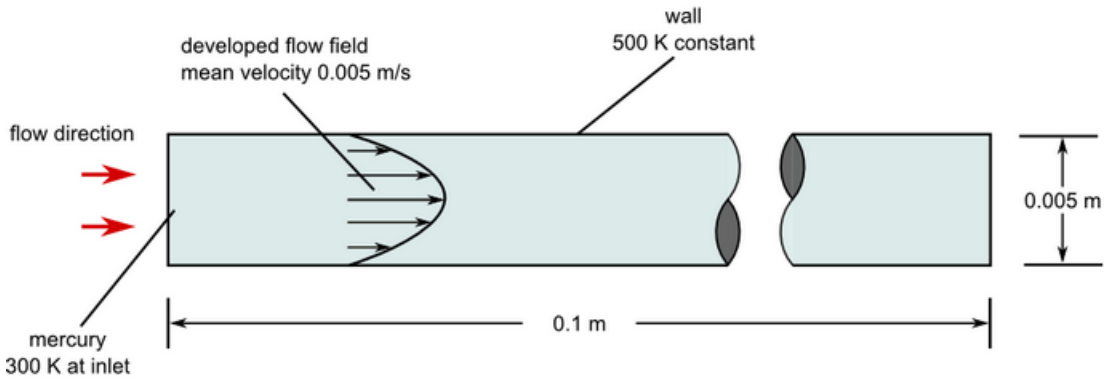


Figure 577: Critical Dimensions and Parameters for Simulating Laminar Flow through a Pipe with Constant Wall Temperature

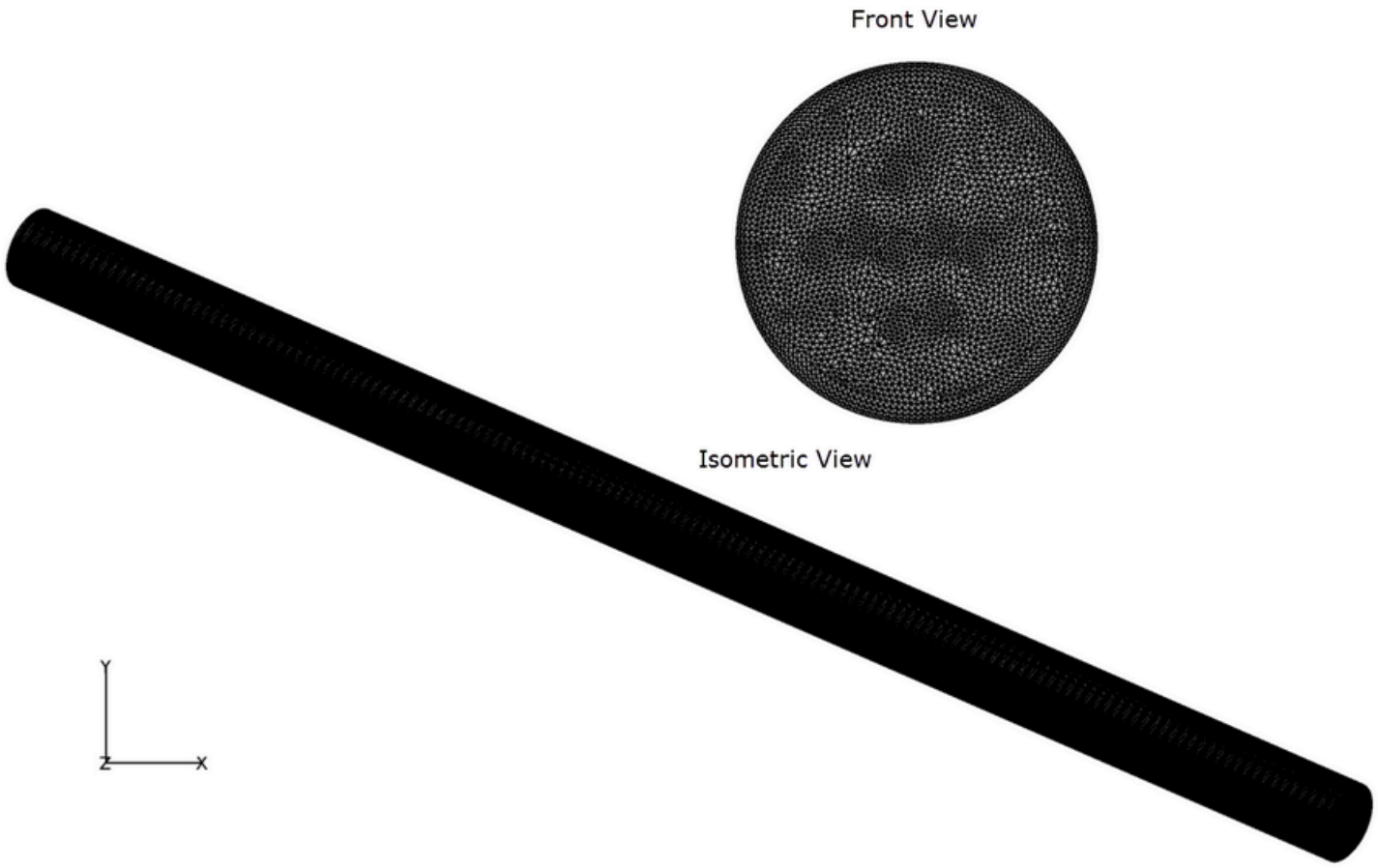


Figure 578: Mesh used for Simulating Laminar Flow Through a Pipe with Constant Wall Temperature

AcuSolve Results

The AcuSolve solution converged to a steady state and the results reflect the mean flow conditions. In this application, a fully developed laminar profile is achieved by enforcing periodic constraints on the pressure and velocity fields. The spatially developing temperature field is achieved by allowing the fluid's temperature to evolve along the full length of the model. The change in temperature along the pipe length is due to advection in the streamwise direction and heat conduction from the outer walls where the temperature is greater than the initial flow temperature. The temperature rises along the length of the pipe and the pressure drops along the length of the pipe. At the inlet, the temperature of the mercury is 300 K and the pressure is 0.496 Pa. At the outlet centerline, the temperature of the mercury has risen to 500.0 K and the pressure has dropped to -0.4965 Pa.

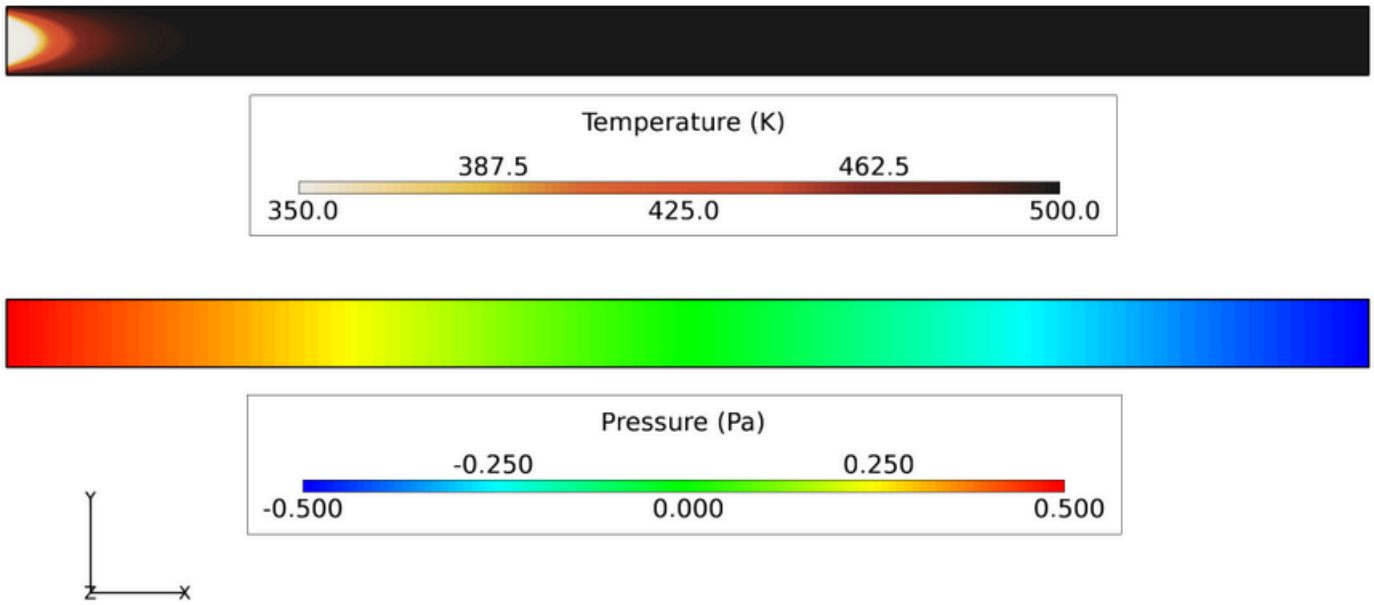


Figure 579: Temperature and Pressure Contours of Mercury Flow Through a Pipe with Prescribed Temperature Boundary

The following table shows the comparison of AcuSolve results with the analytical solutions from White (1994). Comparisons were made for the pressure drop between the inlet and outlet and the temperature at the center of the outlet.

Table 37:

	Analytical solution	**AcuSolve solution**	**Percent deviation from analytical**
Pressure drop (Pa)	0.991	0.9925	0.15
Centerline temperature of flow at outlet (K)	500.0	500.0	< 0.0001

Summary

The AcuSolve solution compares well with analytical results for flow through a pipe with constant temperature boundary conditions. The AcuSolve solution for the centerline temperature is nearly identical with the analytical results and the pressure reduces as expected for the prescribed flow conditions. The results of this simulation validate the ability of AcuSolve to accurately predict the heating of fluid flowing through a pipe with constant wall temperature.

Simulation Settings for Laminar Flow Through a Pipe With Constant Wall Temperature

AcuConsole database file: `<your working directory>\pipe_laminar_heatDirichlet\pipe_laminar_heatDirichlet.acs`

Global

- Problem Description
  - Analysis type - Steady State
  - Temperature equation - Advective Diffusive
  - Turbulence equation - Laminar
- Auto Solution Strategy
  - Relaxation Factor - `0.2`
- Material Model
  - Mercury
    - Density - `13579.0` kg/m3
    - Specific Heat - `139.3` J/kg-K
    - Viscosity - `0.001548` kg/m-sec
    - Conductivity - `8.69` W/m-K

  Model
- Volume
  - Fluid
    - Element Set
      1. Material model - Mercury
- Surfaces
  - Inflow
    - Simple Boundary Condition - (disabled to allow for periodic conditions to be set)
    - Advanced Options
      1. Integrated Boundary Conditions
         1. Mass Flux
            1. Type - Constant
            2. Constant value - `1.33e-3` kg/sec
      2. Temperature
         1. Type - Constant
         2. Constant value - `300.0` K
  - Outflow
    - Simple Boundary Condition - (disabled to allow for periodic conditions to be set)
  - Wall
    - Simple Boundary Condition
      1. Type - Wall

2. Temperature BC type - Value
3. Temperature - `500.0` K

- Periodics
  - Periodic 1
    - Individual Periodic BCs
      1. Velocity
         1. Type - Periodic
      2. Pressure
         1. Type - Single Unknown Offset

References

F. M. White. "Fluid Mechanics". 3rd Edition. McGraw-Hill Book Co., Inc. New York. 1994.

F. P. Incropera and D. P. DeWitt. "Fundamentals of Heat Transfer". John Wiley & Sons. New York. 1981.

Heat Transfer Between Radiating Concentric Cylinders

In this application, AcuSolve is used to simulate the heat transfer due to radiation between concentric cylinders. The inner and outer cylinders are held at constant temperature and are defined to be radiation surfaces. AcuSolve results are compared with analytical results for temperature as described in Incropera (2006). The close agreement of AcuSolve results with analytical results validates the ability of AcuSolve to model cases with radiation heat transfer requiring view factor computation.

Problem Description

The problem consists of a fluid with arbitrary material properties between two infinitely long concentric cylinders, as shown in the following image, which is not drawn to scale. The radius of the outer cylinder is 0.046 m and the radius of the inner cylinder is 0.018 m. The inner cylinder is defined to have a constant wall temperature at 773.0 K (500 °C). The outer cylinder is defined to have a constant wall temperature at 300.0 K (27 °C). Both cylinders are specified to radiate as grey bodies, with emissivity set to 0.03778.

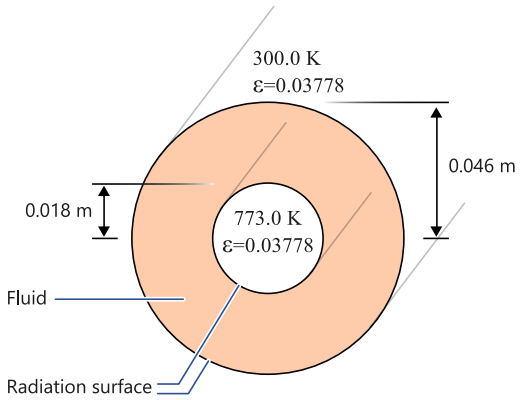


Figure 580: Critical Dimensions and Parameters Used for Simulating Radiation Between Two Concentric Cylinders

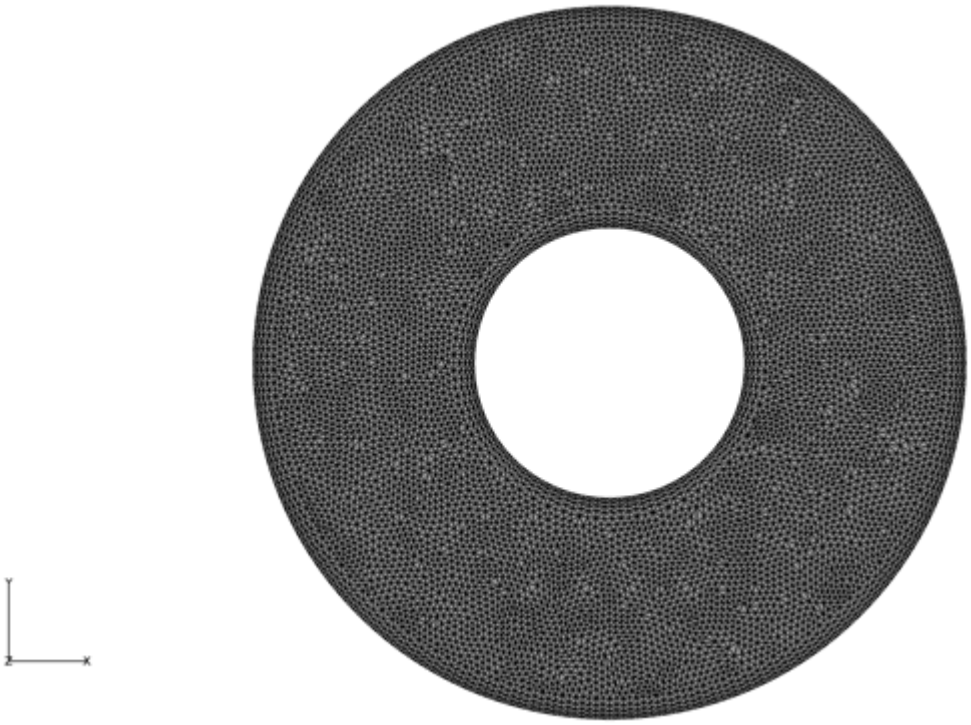


Figure 581: Mesh used for Simulating Radiation Between Two Concentric Cylinders

The simulation was performed as a two dimensional problem by constructing a volume mesh that contains a single layer of elements normal to the radial and circumferential directions.

AcuSolve Results

The AcuSolve solution converges to a steady state and the results reflect the mean temperature distribution. As the inner diameter is considerably hotter than the outer, a heat flux, due to radiation, is present between the cylinders. The temperature within the medium reduces logarithmically as a function of the radius. The following images show the temperature with the medium as a function of radius from the center. The temperature is compared with the analytical solution as described in Incropera (2006). The image below shows black circles representing the analytical solution and a solid red line for the AcuSolve results.

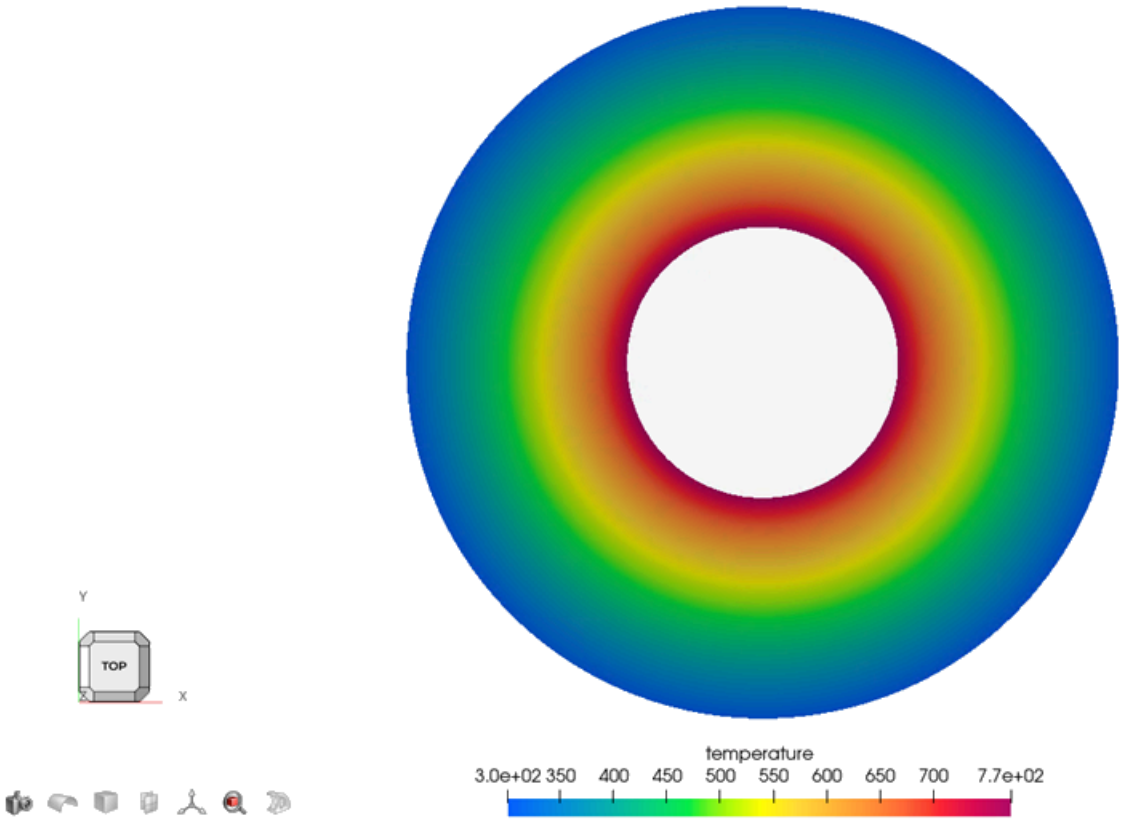


Figure 582: Contours of Temperature Between the Concentric Cylinders

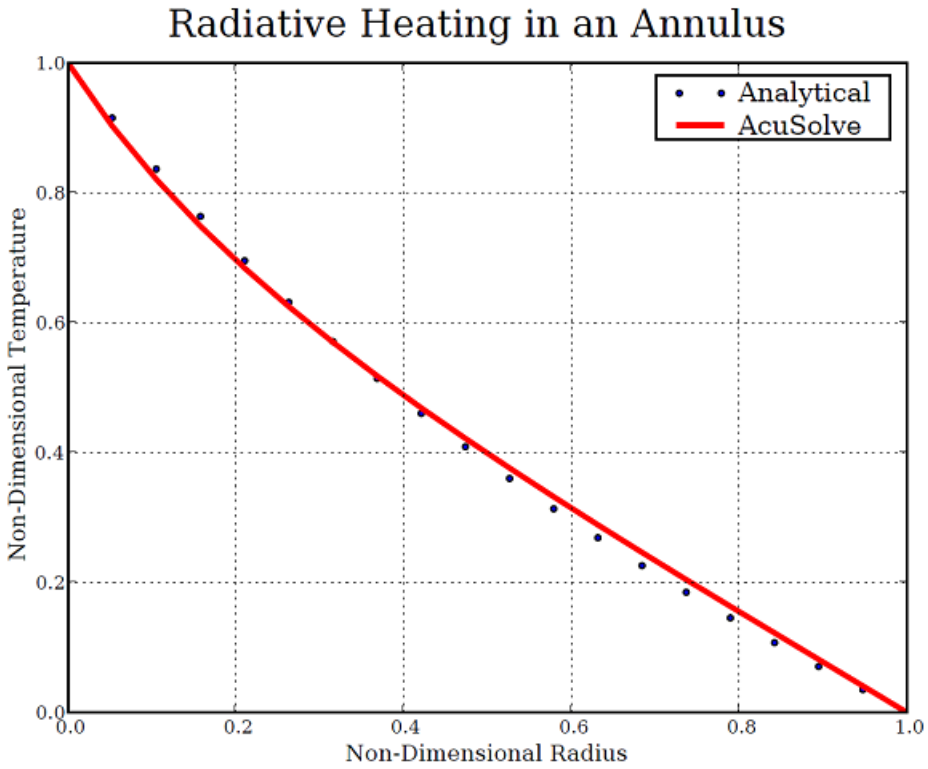


Figure 583: Non Dimensional Temperature Distribution Within the Annulus as a Function of Non Dimensional Radius

Summary

The AcuSolve solution compares well with analytical results for heat transfer due to radiation between two concentric cylinders. In this application, an arbitrary material is subjected to a heat flux that is calculated based on the view factors within the model. As a result of radiative heat flux a temperature distribution between the two cylinders develops. The AcuSolve solution for the temperature as a function of radius matches well compared to the analytical solution.

Heat Transfer Between Radiating Concentric Cylinders

HyperWorks CFD database file: `<your working directory>\annulus_radiation\annulus_radiation.hm`

Global

- Problem Description
  - Analysis type - Steady State
  - Temperature equation - Advective Diffusive
  - Radiation equation- Enclosure
- Auto Solution Strategy
  - Convergence tolerance - `0.0001`
  - Relaxation Factor- `0.4`
  - Flow- off

    - Enclosure radiation- on
- Material Model
    - Material
        - Conductivity
            1. Type - Constant
            2. Conductivity- `1.0`
- Emissivity Model
    - Grey Body
        - Emissivity- `0.03778`
    - Black Body
        - Emissivity- `1.0`

  Model
- Volumes
    - Medium
        - Element Set
            1. Medium - Fluid
            2. Material model- Material
- Surfaces
    - ID
        - Simple Boundary Condition
            1. Type- Wall
            2. Temperature BC type- Value
            3. Temperature- `773.0` K
        - Radiation Surface
            1. Type- Wall
            2. Emissivity model- Grey Body
    - Max_Z
        - Simple Boundary Condition
            1. Type- Symmetry
        - Radiation Surface
            1. Type- Wall
            2. Emissivity model- Black Body
    - Min_Z
        - Simple Boundary Condition
            1. Type- Symmetry
        - Radiation Surface
            1. Type- Wall

2. Emissivity model- Black Body

- OD
  - Simple Boundary Condition
    1. Type- Wall
    2. Temperature BC type- Value
    3. Temperature- `300.0` K
  - Radiation Surface
    1. Type- Wall
    2. Emissivity model- Grey Body

References

F. P. Incropera and D. P. DeWitt. "Fundamentals of Heat Transfer - Sixth Edition". John Wiley & Sons. New York. 2006.

Turbulent Flow Through a Heated Periodic Channel

In this application, AcuSolve is used to solve for the flow and temperature field within a channel containing a heated wall. The wall is maintained at a constant temperature, inducing heat flux into the fluid, to predict the thermal law of the wall. The non dimensional temperature versus the non dimensional height above the wall is compared to the analytical correlation provided by Kader.

Problem Description

The problem consists of a fluid having material properties close to air with a density of 1.0 kg/m^3, molecular viscosity of 0.0001 kg/m-s, specific heat of 1005.0 J/kg-K and thermal conductivity of 0.139 W/m-K. The properties are specified to obtain a Prandtl number of 0.72. The velocity is defined as periodic and is driven by a constant acceleration body force equal to 2.0 m/s^2. The temperature is specified as periodic+unknown ratio allowing it to develop until it reaches a steady solution. The simulation description is shown in the following image, which is not drawn to scale. The model is simulated using the one equation Spalart Allmaras turbulence model along with the advective-diffusive temperature equation. The thermal wall distribution is validated against correlation data published by Kader 1981.

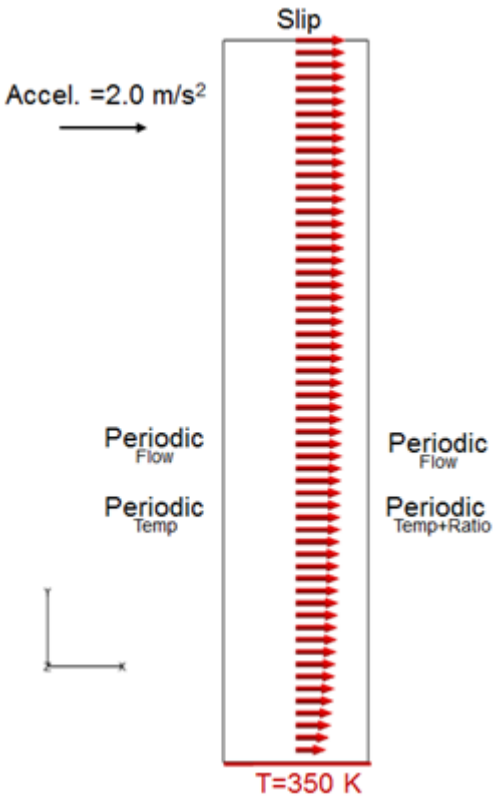


Figure 584: Critical Parameters used For Simulating Periodic Flow Within a Heated Channel

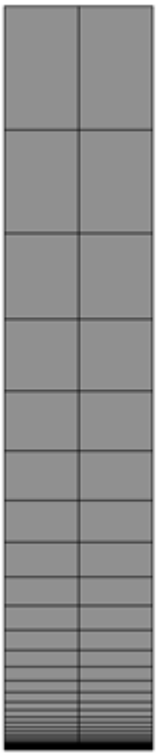


Figure 585: Mesh used For Simulating Periodic Flow Within a Heated Channel

The simulation was performed as a two dimensional problem by constructing a volume mesh that contains a single layer of elements extruded in the cross stream direction, normal to the flow plane and by imposing periodic boundary conditions on the extruded planes. The streamwise direction contains two elements allowing the flow and temperature solution to develop. Only the lower half of the channel is modeled, assuming the solution is mirror across the top slip plane.

AcuSolve Results

The AcuSolve solution converged to a steady state and the results reflect the mean flow conditions within the channel. The simulation results demonstrate that the channel wall induces a thermal flux into the flow field, producing a temperature distribution dependent on the distance from the wall. The thermal law of the wall computed from the AcuSolve results is compared with correlation data for the corresponding Prandtl number, as demonstrated in Kader 1981. The plot shown below gives the non dimensional value of T+ as a function of Y+, where T+ and Y+ are computed per the following relationships:

$$T+ = \frac{(Tw - T)\rho C p u\tau}{\dot{Q}} T \tag{24}$$

$$Y+ = \frac{yu\tau}{v} \tag{25}$$

$$u\tau = \sqrt{\tau w / \rho} \tag{26}$$

Where $T+$, Tw is the fixed wall temperature, T is the temperature away from the wall, ρ is the fluid density, Cp is the fluid specific heat, uT is computed from the magnitude of the shear stress and $\dot{Q}_i$ is the local surface heat flux.

The image below shows black circles representing the correlation data and a solid red line for the AcuSolve results. The results demonstrate that the temperature distribution away from the wall is resolved properly and compares well with the correlation. Since an empirical relationship for T+ is used for comparison, there will be minor discrepancies compared with the simulation results. Additional comparisons have been made against DNS results for T+ from Kawamura et al. 1998.

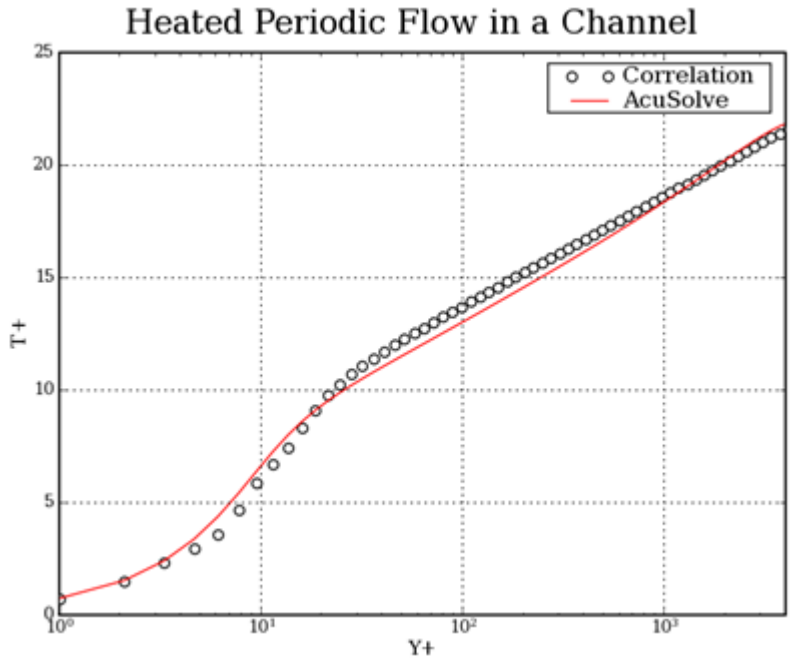


Figure 586: Thermal Boundary Layer Within the Heated Channel Compared Against the Correlation Data

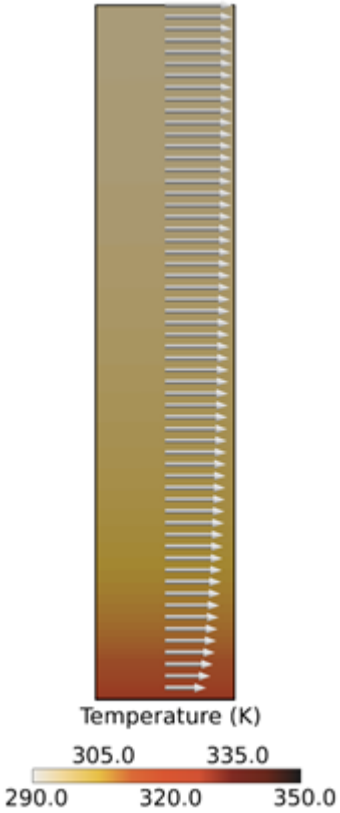


Figure 587: Contours of Temperature and Vectors Representing the Fluid Velocity Within the Channel

Summary

The AcuSolve solution compares well with the correlation data for turbulent flow within a heated channel. In this application, the constant temperature wall induces a surface heat flux, giving rise to a temperature gradient within the channel. AcuSolve can capture the correct temperature gradient at any location above the wall if an appropriate first layer height is selected to resolve a Y+ value of 1.0. The good agreement with correlation data for T+ demonstrates that AcuSolve can predict the locally varying temperature distribution within a turbulent channel.

Simulation Settings for Turbulent Flow Through a Heated Periodic Channel

AcuConsole database file: `<your working directory>\channel_periodic_heat\channel_periodic_heat.acs`

Global

- Problem Description
  - Analysis type - Steady State
  - Temperature equation - Advective Diffusive
  - Turbulence equation - Spalart Allmaras
- Auto Solution Strategy
  - Max time steps - `50`

    - Convergence tolerance - `0.0001`
    - Relaxation Factor - `0.4`
    - Temperature - On
- Material Model
    - Fluid
        - Type - Constant
        - Density - `1.0` kg/m3
        - Viscosity - `1.0e-4` kg/m*sec
        - Specific Heat - `1005.0` J/kg*K
        - Conductivity - `0.139` W/m*K
- Body Force
    - BodyForce
        - Gravity
            1. X-component - `2.0` m/sec2

Model

- Volumes
    - Fluid
        - Element Set
            1. Material model - Fluid
            2. Body force - BodyForce
- Surfaces
    - Symmetry_1
        - Simple Boundary Condition - (disabled to allow for periodic conditions to be set)
    - Symmetry_2
        - Simple Boundary Condition - (disabled to allow for periodic conditions to be set)
    - Inflow
        - Simple Boundary Condition - (combination of integrated BC and periodic BC set)
        - Advanced Options
            1. Integrated Boundary Conditions - Temperature - `300.0` K
    - Outflow
        - Simple Boundary Condition - (disabled to allow for periodic conditions to be set)
    - Slip_surface
        - Simple Boundary Condition
            1. Type- Slip
    - Wall_surface
        - Simple Boundary Condition
            1. Type- Wall

2 Temperature BC type - Value
3 Temperature - `350.0` K

- Periodics
  - 2D
    - Periodic Boundary Conditions
      1 Type - Periodic
  - Flow
    - Periodic Boundary Conditions
      1 Type - Periodic
  - Temperature
    - Individual Periodic BCs
      1 Temperature: Type - Single Unknown Ratio
- Nodes
  - Fixed_pressure
    - Pressure: Type - Zero
  - Zero_z-velocity
    - Z-Velocity: Type - Zero

References

B.A. Kader, "Temperature and concentration profiles in fully turbulent boundary layers", International Journal of Heat and Mass Transfer, Volume 24, Issue 9, 1981, Pages 1541-1544.

H. Kawamura, K. Ohsaka, H. Abe and K. Yamamoto, "DNS of turbulent heat transfer in channel flow with low to medium-high Prandtl number fluid", International Journal of Heat and Mass Transfer, 19:482-491, 1998.

Heat Transfer Between Concentric Cylinders with Heat Source

In this application, AcuSolve is used to simulate a 2D cable problem to demonstrate one way Flux-AcuSolve coupling. The 2D cable is used to demonstrate how the volumetric heat load conducts through a solid. AcuSolve results are compared with analytical results as described in Incropera (2006). The close agreement of AcuSolve results with analytical results validates the ability of AcuSolve to model cases with volumetric heat source applied on a solid volume.

Problem Description

The problem consists of two solid cylinders in contact with each other wherein the inner solid cylinder is provided with a volumetric heat source of 1.46686 W and is in contact with the outer solid cylinder, the outer surface of which is maintained at a temperature of 20 degrees C (293K). The radius of the inner cylinder is 0.002 m and the radius of the outer cylinder is 0.003 m. This problem forms the basis of a simple conduction analysis between two concentric cylinders. The only difference from the basic problem is that the heat source is calculated using another software called Flux and is provided using AcuConsole's EMag (Electromagnetics) Manager to account for volumetric losses from Flux to AcuSolve.

$$T_1 - T_2 = \frac{\Phi}{2.0\pi\lambda L} ln\left(\frac{R_2}{R_1}\right)$$

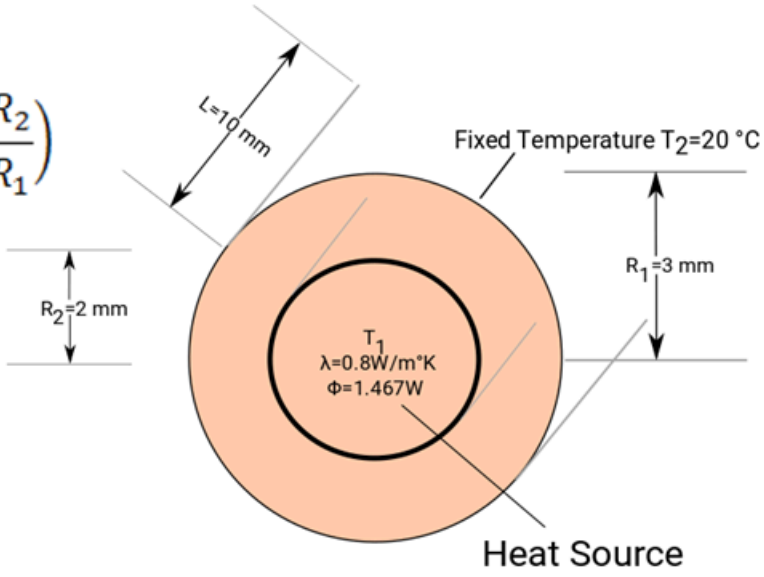


Figure 588: Critical Dimensions and Parameters used for Simulating Two Concentric Cylinders with an Internal Heat Source

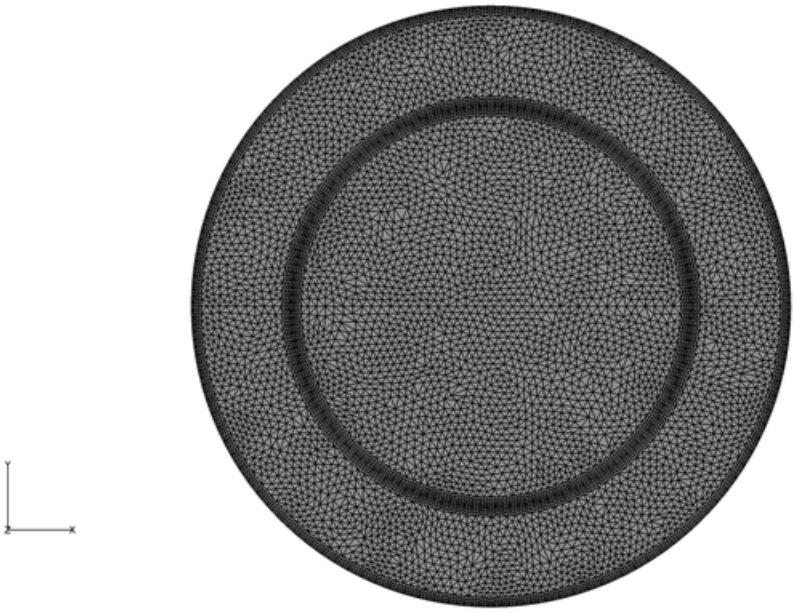


Figure 589: Mesh Used for Simulating Two Concentric Cylinders with an Internal Heat Source

The simulation was performed as a two dimensional problem by constructing a volume mesh that contains a single layer of elements normal to the radial and circumferential directions.

AcuSolve Results

The AcuSolve solution converges to a steady state and the results reflect the mean temperature distribution. The heated volume (inner cylinder) is at the highest temperature due to the heat source provided and conducts through the outer cylinder volume and forms a temperature gradient along the radial direction between both the inner and outer solid volume. The temperature within the medium increases logarithmically as a function of the radius. The following images show the temperature with the medium as a function of radius from the edge of the inner cylinder. The temperature is compared with the analytical solution as described in Incropera (2006). The image below shows black circles representing the analytical solution and a solid red line for the AcuSolve results.

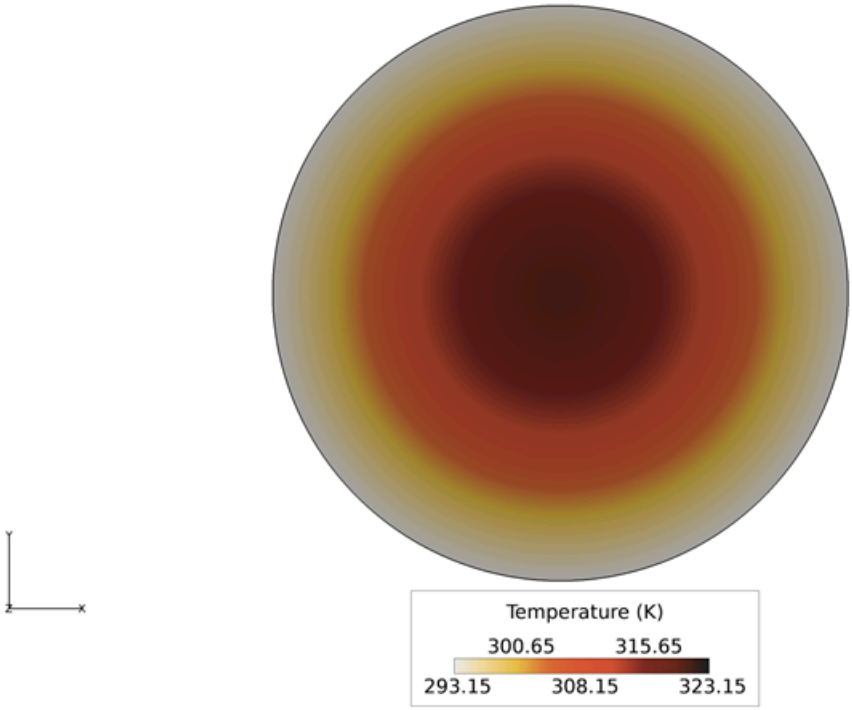


Figure 590: Contours of Temperature Between the Concentric Cylinders

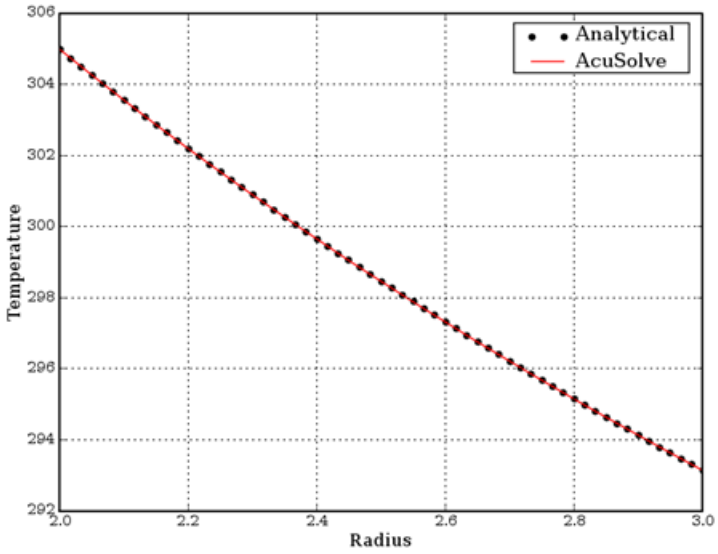


Figure 591: Temperature Distribution within the Outer Cylinder as a Function of Radius

Summary

The AcuSolve solution compares well with analytical results for the 2D solid conduction model case with volumetric heat source applied on a solid volume. In this application, the temperature within the cylinders is driven by a gradient along the outer and inner solid volumes, due to the volumetric

heat source and fixed temperature. The AcuSolve solution for the temperature as a function of radius matches well compared to the analytical solution.

Heat Transfer Between Concentric Cylinders with Heat Source

AcuConsole database file: `<your working directory>\annulus_heat_source\annulus_heat_source.acs`

Global

- Problem Description
  - Analysis type - Steady State
  - Turbulence equation - Advective Diffusive
  - Absolute temperature offset - `273.15`
- Auto Solution Strategy
  - Convergence tolerance - `0.0001`
  - Relaxation Factor - `0.4`
  - Flow - off
  - Temperature - on
- Material Model
  - Insulation
    - Density
    - Type - Constant
    - Conductivity - `2702.0`
  - Specific Heat
    - Type - Constant
    - Conductivity - `908.0`
  - Conductivity
    - Type - Constant
    - Conductivity - `0.8`

  Model
- Volumes
  - Solid
    - Element Set
      1. Medium - Solid
      2. Material model - Insulation
  - SolidHeated
    - Element Set
      1. Medium - Solid
      2. Material model - Insulation
      3. Total heat source - 1.46686 (applied through EMag Manager)

- Surfaces
  - +ZInner
    - Simple Boundary Condition - (disabled, no BC needed)
  - +ZOuter
    - Simple Boundary Condition - (disabled, no BC needed)
  - -ZInner
    - Simple Boundary Condition - (disabled, no BC needed)
  - -ZOuter
    - Simple Boundary Condition - (disabled, no BC needed)
  - InterfaceAll
    - Simple Boundary Condition - (disabled, no BC needed)
  - InterfaceInner
    - Simple Boundary Condition - (disabled, no BC needed)
  - InterfaceOuter
    - Simple Boundary Condition - (disabled, no BC needed)
  - OuterWall
    - Simple Boundary Condition
      1. Type - Wall
      2. Temperature BC type - Value
      3. Temperature - `20.0` K

References

F. P. Incropera and D. P. DeWitt. "Fundamentals of Heat Transfer – Sixth Edition". John Wiley & Sons. New York. 2006.

Heat Transfer Between Radiating Concentric Spheres

In this application, AcuSolve is used to simulate the heat transfer due to conduction and radiation between concentric spheres. The inside surface of the inner and the outside surface of the outer sphere are both held at constant temperature, while the gap between them radiates the heat from one sphere to the other.

AcuSolve results are compared with analytical results for temperature and heat flux as described in Incropera (2006) and Salazar, et al. (2016). The close agreement of AcuSolve results with analytical results validates the ability of AcuSolve to model cases with radiation heat transfer and conjugate heat transfer with enclosure radiation modeling and the discrete ordinate (DO) radiation model.

Problem Description

The problem consists of a fluid region with arbitrary material properties between two concentric spheres with surfaces held at fixed temperature, as shown in the following image, which is not drawn to scale. The radius of the outer sphere is 0.04 m and the radius of the inner sphere is 0.01 m. The inner surface of the inner sphere is defined to have a constant wall temperature at 300.0 K (27 ºC). The outer surface of the outer sphere is defined to have a constant wall temperature at 1300.0 K (1027 ºC). The fluid within the spheres is defined as a non-conducting material, allowing heat to transfer via radiation only. The solid and fluid regions equilibrate to a steady temperature and can be compared with a semi-analytical solution for the temperature and heat flux at the fluid boundaries.

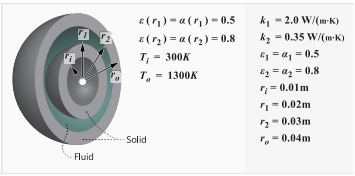


Figure 592: Critical Dimensions and Parameters used for Simulating Conduction and Radiation Between two Concentric Spheres



Figure 593: Mesh used for Simulating Radiation Between two Concentric Spheres

The simulation was performed as a three dimensional problem by constructing a volume mesh that contains a layer of boundary elements normal to the radial direction.

AcuSolve Results

The AcuSolve solution converges to a steady state and the results reflect the mean temperature distribution within the spheres. As the outer diameter is considerably hotter than the inner, a heat flux is present between the spheres. The temperature within the mediums increases as a function of the radius, with a slope corresponding to the temperature difference and the specified emissivity of the shells. The following image shows the temperature contour within the spheres along with the two-dimensional plot of the temperature versus radius in the solid mediums. The temperature and heat flux at the radiation surfaces are compared with the analytical solution as described in Salazar, et al. (2016).

Table 38: The Analytical Solution for the Temperature and Heat Flux at r1 and r2 are Presented with the Corresponding AcuSolve Results for the Enclosure (Surface to Surface) Model and the DO

	T(r1) (K)	T(r2) (K)	Q(r1) (W)	Q(r2) (W)
Analytical	578.2	1035.0	-27822.5	12365.6
AcuSolve (Enclosure)	578.4	1035.1	-27827	12364.2
AcuSolve (DO)	561.8	1023.6	-26175	12897.0
Percent Difference (Enclosure)	0.034%	0.010%	-0.015%	-0.011%
Percent Difference (DO)	2.8%	-1.11%	5.92%	4.3%

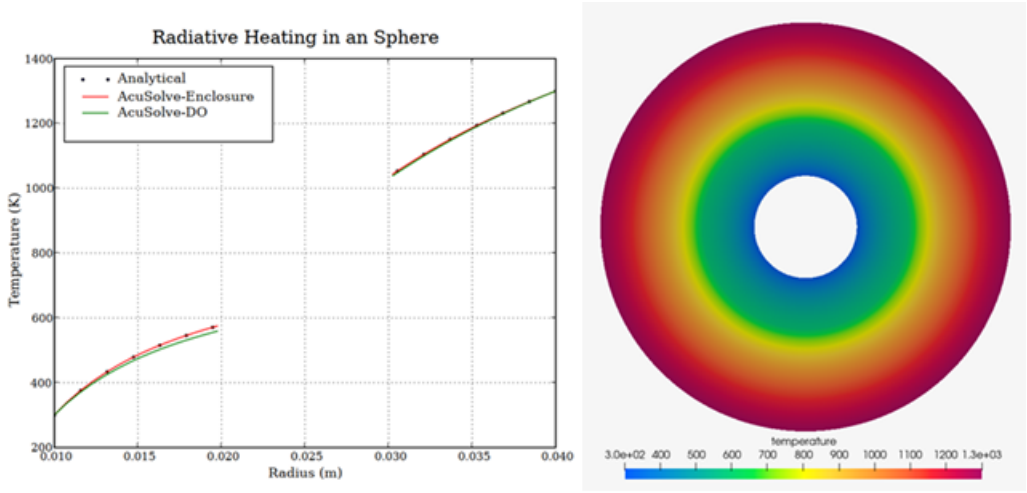


Figure 594: Two-Dimensional Plot and Contours of Temperature Between the Concentric Spheres

Summary

The AcuSolve solution compares well with analytical results for heat transfer due to conduction and radiation between two concentric spheres. In this application, an arbitrary material is subjected to a heat flux that is calculated based on the view factors or the DO model within the simulation. As a result of the conjugate heat transfer and the radiative heat flux a temperature distribution between the two spheres develops. The AcuSolve solution for the temperature and heat flux at the radiation surfaces matches well compared to the analytical solution with only a minor difference for the enclosure radiation model. The enclosure radiation model was found to have a higher accuracy for this application compared to the DO model, as expected due to the relatively low optical thickness in this simulation.

Heat Transfer Between Radiating Concentric Spheres

HyperWorks CFD database file: `<your working directory>\sphere_radiation\sphere_radiation.hm`.

Global

- Problem Description
  - Analysis type - Steady State
  - Turbulence equation - Advective Diffusive
  - Radiation equation - Enclosure
- Auto Solution Strategy
  - Convergence tolerance - `1.0e-5`
  - Relaxation Factor - `0.4`
  - Flow - off
  - Enclosure radiation - on
- Material Model
  - Inner
  - Conductivity

        - Type - Constant
        - Conductivity - `2.0`
    - Outer
    - Conductivity
        - Type - Constant
        - Conductivity - `0.35`
    - Radiating
    - Conductivity
        - Type - Constant
        - Conductivity - `1.0e-6`
- Emissivity Model
- Inner
    - Emissivity - `0.5`
- Outer
    - Emissivity - `0.8`

  Model
- Volumes
    - Inner
        - Element Set
            1. Medium- Solid
            2. Material model - Inner
        - Outer
            1. Element Set
                1. Medium - Solid
                2. Material model - Outer
        - Radiating
            1. Element Set
                1. Medium - Fluid
                2. Material model - Radiating
- Surfaces
    - Inner_Inner_r1
        - Simple Boundary Condition - (disabled to allow for heat flux)
    - Inner_Inner_ri
        - Simple Boundary Condition
            1. Type - Wall
            2. Temperature BC type - Value
            3. Temperature - `300.0` K

- Inner_Radiating_r1
  - Simple Boundary Condition (disabled to allow for heat flux)
  - Radiation Surface
    1. Type - Wall
    2. Emissivity model - Inner
- Outer_Outer_r2
  - Simple Boundary Condition (disabled to allow for heat flux)
- Inner_Outer_ro
  - Simple Boundary Condition
    1. Type - Wall
    2. Temperature BC type - Value
    3. Temperature - `1300.0` K
- Outer_Radiating_r2
  - Simple Boundary Condition (disabled to allow for heat flux)
  - Radiation Surface
    1. Type - Wall
    2. Emissivity model - Outer

References

F. P. Incropera and D. P. DeWitt. "Fundamentals of Heat Transfer – Sixth Edition". John Wiley & Sons. New York. 2006.

Salazar, G., Droba, J., Oliver, B., & Amar, A. J. (2016). Development and Verification of Enclosure Radiation Capabilities in the CHarring Ablator Response (CHAR) code. 46th AIAA Thermophysics Conference.

Radiation Heat Transfer Through a Cube with a Specular Interface

In this application, AcuSolve is used to simulate the heat transfer due to radiation through a specular interface within an absorbing, emitting, but not scattering solid cube. One of the cube's walls is modeled with an isotropic external radiation source while the remainder of the cube is held at fixed temperature conditions and modeled with pure radiation, neglecting the effects of conduction.

The internal surface between the two equal solid portions of the cube is specified to be a completely specular boundary condition. AcuSolve results are compared with accepted numerically derived results of incident radiation, as described in Muresan (2004) and Łapka (2012). The close agreement of the AcuSolve results and the published data validates the solver's ability to model cases with semi-transparent media with differing material properties using the discrete ordinates radiation model.

Problem Description

The problem consists of a solid region with fixed material properties similar to glass separated into two equal size cuboids to form a symmetrical cube with a side length of 1.0 m. The left most wall (minimum z) receives an external radiation source at a fixed temperature of 450.0 K (177 ºC) while the right most wall (maximum z) is prescribed a fixed temperature of 375.0 K (102 ºC), as shown in the following image, not drawn to scale. The solid, semi-transparent material is specified for each glass cuboid with n1=1.5, κ1=0.2 for glass1 and n2=1.25, κ2=2.0 for glass2. Only the solution to the radiative transfer equation on a discrete number of ordinate directions is considered, thus neglecting conduction. The solid regions equilibrate to a steady radiative state and are compared with a semi-analytical solution for the incident radiation across the centerline of the cube.

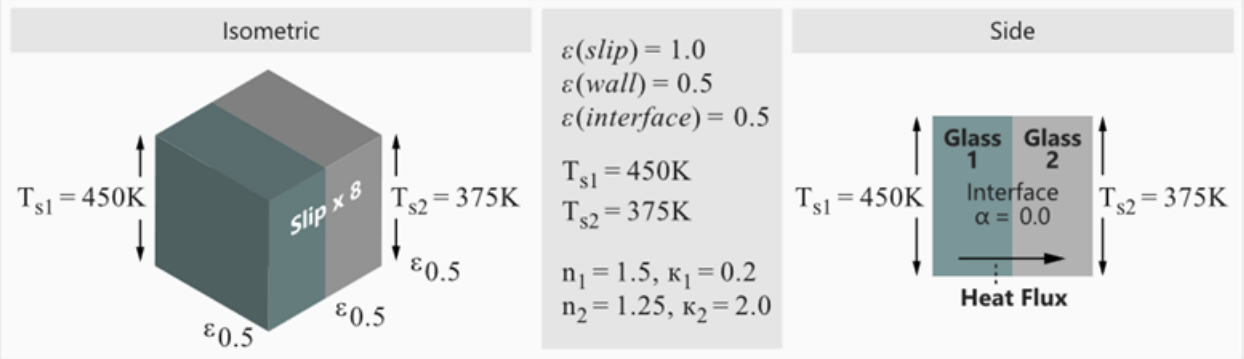


Figure 595: Critical Dimensions and Parameters Used for Simulating Radiation Heat Transfer Through a Cube with a Specular Interface

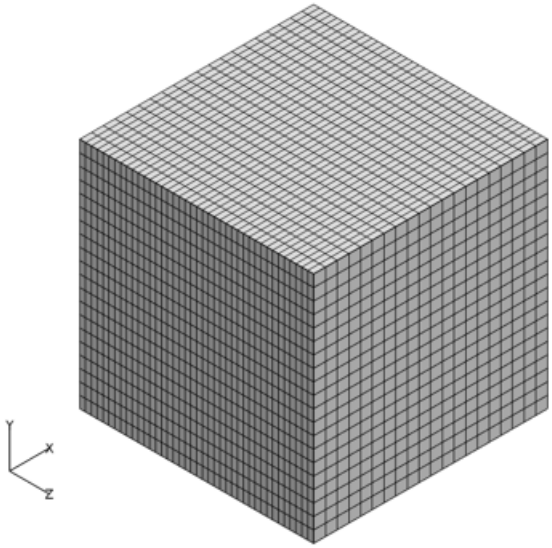


Figure 596: Mesh Used for Simulating Radiation Heat Transfer Through a Cube with a Specular Interface

The simulation was performed as a three-dimensional problem by constructing a volume mesh that contains all hexahedral elements with 20, 20, 40 cells in the x, y, z directions.

AcuSolve Results

The AcuSolve solution converges to a steady state and the results reflect the mean radiative state within the cube. Since the left side of the cube receives the external radiation source, the incident radiation is highest at that location. The transmission of the radiation decreases linearly within the first cuboid until it reaches the interface between the two materials. The discontinuity in the radiation field is demonstrated at the interface location, resulting from the specular reflection of radiation as it tries to travel from one material to the other. As the incident radiation passes through the second glass material, the simulation demonstrates how the material's higher absorption properties will produce a non-linear irradiance distribution. The following image shows the incident radiation contour within the two media along with the two-dimensional plot of the normalized incident radiation as a function of the non-dimensional cube length, where the incident radiation is normalized by $G^* = \sigma T^4$. The incident radiation is compared with the numerical solution as described in Muresan, et al. (2004).

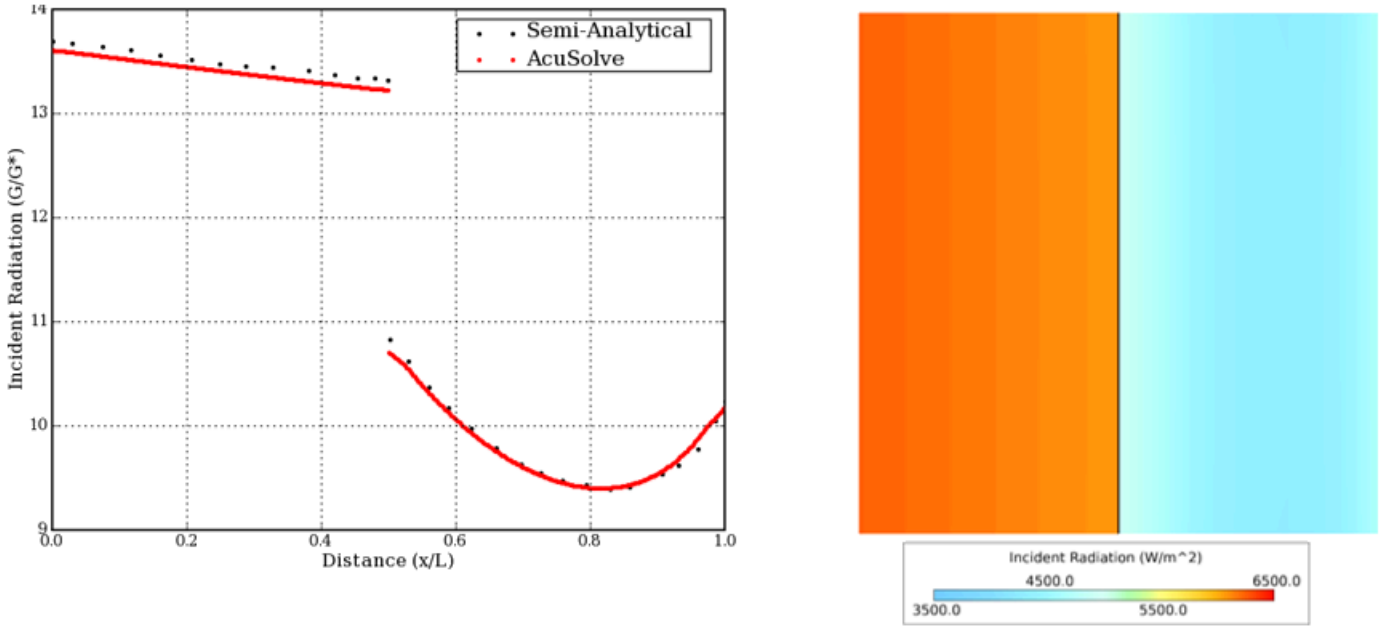


Figure 597: Two-Dimensional Plot and Contours of Incident Through a Cube with a Specular Interface

Summary

The AcuSolve solution compares well with numerical results for heat transfer due to radiation within a cube containing a specular interface. In this application, two arbitrary materials are subjected to a constant external radiative heat source and the media are defined to absorb, emit, but not scatter the irradiation. As a result of the prescribed radiative heat flux on the left most wall and the fixed temperature constraint across the entire domain, each media receives a non-trivial, varying amount of incident radiation. The AcuSolve solution for the incident radiation across the interface matches well compared to the numerical solution with only a minor difference at the far-right hand side of the domain. The discrete ordinate model requires a fairly large number of ordinate directions in order to obtain the highest accuracy solution. The published results are produced using the S14 quadrature, which is equivalent to 224 discrete ordinate directions.

Radiation Heat Transfer Through a Cube with a Specular Interface

HyperMesh database file: `<your working directory>\cube_specular_radiation\cube_specular_radiation.hm`.

Global

- Problem Description
  - Analysis type - Steady State
  - Turbulence equation - Advective Diffusive
  - Radiation equation - Discrete Ordinate
  - Radiation Ordinate - S14
- Solver Settings
  - Convergence tolerance - `1.0e-3`
  - Relaxation Factor - `0.3`

    - Flow - off
    - Temperature - off
- Nodal_Initial_Condition
    - Temperature
        - Type - Constant
        - Default Value - `300.0` K

Materials

- Glass_HM
    - Density
        - Type - Constant
        - Density - `2500.0`
    - Specific Heat
        - Type - Constant
        - Conductivity - `830`
    - Conductivity
        - Type - Constant
        - Conductivity - `1.3`
    - Radiation Properties
        - Allow Participating Media Radiation - On
        - Absorption Coefficient - `0.2`
        - Scattering Coefficient - `0.0`
        - Phase Coefficient - `0.0`
        - Refractive Index - `1.5`
- Glass2_HM
    - Density
        - Type - Constant
        - Density - `2500.0`
    - Specific Heat
        - Type - Constant
        - Conductivity - `830`
    - Conductivity
        - Type - Constant
        - Conductivity - `1.3`
    - Radiation Properties
        - Allow Participating Media Radiation - On
        - Absorption Coefficient - `2.0`
        - Scattering Coefficient - `0.0`

- Phase Coefficient - `0.0`
- Refractive Index - `1.25`

Emissivity Model

- BB05
  - Emissivity - `0.5`
- BB
  - Emissivity - `1.0`

Volumes

- S1
  - Type - Solid
  - Material model - Glass_HM
- S2
  - Type - Solid
  - Material model - Glass2_HM

Surfaces

- Wall_S1
  - Simple Boundary Condition
    1. Type - Wall
    2. Temperature BC type - Value
    3. Temperature - `450.0 K`
  - Radiation Surface
    1. Type - radiation interface
    2. Radiation interface type - external
    3. External emissivity model - BB
    4. Diffused fraction - `0.0`
- Wall_S2
  - Simple Boundary Condition
    1. Type - Outflow
  - Radiation Surface
    1. Type - Opening
    2. Opening temperature - 375.0 K
    3. Emissivity model - BB05
    4. Diffused fraction - `0.0`
- Interface_S1
  - Simple Boundary Condition
    1. Type - Auto Wall
  - Radiation Surface

1. Type - Radiation interface
2. Radiation interface type - internal
3. Diffused fraction - `0.0`

- Interface_S2
  - Simple Boundary Condition
    1. Type - Auto Wall
  - Radiation Surface
    1. Type - Radiation interface
    2. Radiation interface type - internal
    3. Diffused fraction - `0.0`
- Slip_1_S1
  - Simple Boundary Condition
    1. Type - Slip
- Slip_2_S1
  - Simple Boundary Condition
    1. Type – Slip
- Slip_3_S1
  - Simple Boundary Condition
    1. Type - Slip
- Slip_4_S1
  - Simple Boundary Condition
    1. Type - Slip
- Slip_1_S2
  - Simple Boundary Condition
    1. Type - Slip
- Slip_2_S2
  - Simple Boundary Condition
    1. Type - Slip
- Slip_3_S2
  - Simple Boundary Condition
    1. Type - Slip
- Slip_4_S2
  - Simple Boundary Condition
    1. Type - Slip

References

Muresan, Cristian & Vaillon, Rodolphe & Ménézo, Christophe & Morlot, Rodolphe. (2004). Discrete ordinates solution of coupled conductive radiative heat transfer in a two-layer slab with Fresnel

interfaces subject to diffuse and obliquely collimated irradiation. Journal of Quantitative Spectroscopy and Radiative Transfer. 84. 551-562. 10.1016/S0022-4073(03)00271-1.

Łapka, Piotr & Furmański, Piotr. (2012). Fixed Cartesian grid based numerical model for solidification process of semi-transparent materials II: Reflection and refraction or transmission of the thermal radiation at the solid–liquid interface. International Journal of Heat and Mass Transfer. 55. 4953–4964. 10.1016/j.ijheatmasstransfer.2012.03.077.

Two-Phase Nucleate Boiling in a Cylindrical Pipe

In this application, AcuSolve is used to simulate the changes in wall temperature due to two-phase nucleate boiling at the heated walls of a pipe with water flowing through it. AcuSolve results are compared with experimental results adapted from Koncar and others (2015). The close agreement of AcuSolve results with experimental results validates the ability of AcuSolve to model two-phase nucleate boiling problems.

Problem Description

The problem consists of a pipe with heated surrounding walls, as shown in the following image, which is not drawn to scale. The length of the pipe is 2 m and the radius is 0.0017 m. Mass flux at the inlet is 900 kg/m^2 and the temperature of the fluid entering the pipe is 473 K. A heat flux of 570,000 W/m^2 is applied on the walls. The preheated water enters the inlet and heat is transferred to the fluid from the walls. The heat causes sub-cooled boiling to occur in the region close to the wall and leads to the formation of bubbles at nucleation sites.

During sub-cooled boiling flow, heat and mass exchange between the phases takes place on the heated wall and in sub-cooled liquid flow. On the heated surface the vapor bubbles are generated and as they move through the sub-cooled liquid they condense and release the latent heat.

The AcuSolve simulation is set up to model transient state heat transfer to determine the temperature along the centerline of the pipe and along the heated pipe walls of the model. AcuSolve computes the two-phase nucleate boiling by simulating the three-dimensional flow in a heated pipe for two-phase boiling flow, as described in Koncar (2005). The temperatures along the centerline of the pipe and along the pipe walls are compared against the experimental measurements, as described in Koncar, et al. (2005).

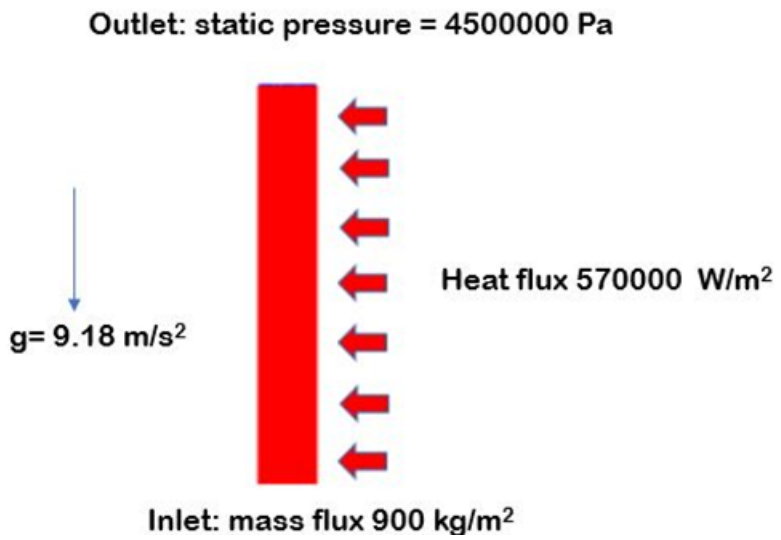


Figure 598: Parameters for Simulating a Two-Phase Nucleate Boiling Problem of a Pipe

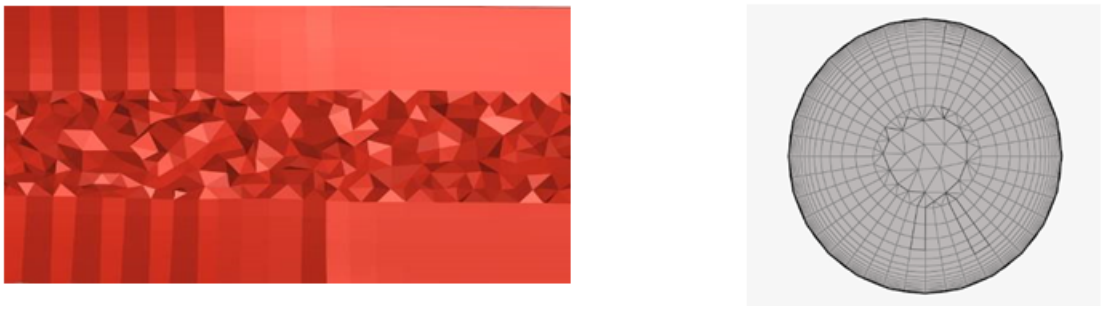


Figure 599: Mesh used for Simulating Two-Phase Flow in a Pipe

AcuSolve Results

The AcuSolve solution is run for a heat flux of 570,000 W/m^2 and the results are presented in the following image. The experimental values of wall temperature are presented with the corresponding AcuSolve results along the centerline of the pipe and along the pipe wall. The AcuSolve results show good agreement with the experimental results for the temperature, indicating that the two-phase nucleate boiling is properly captured.

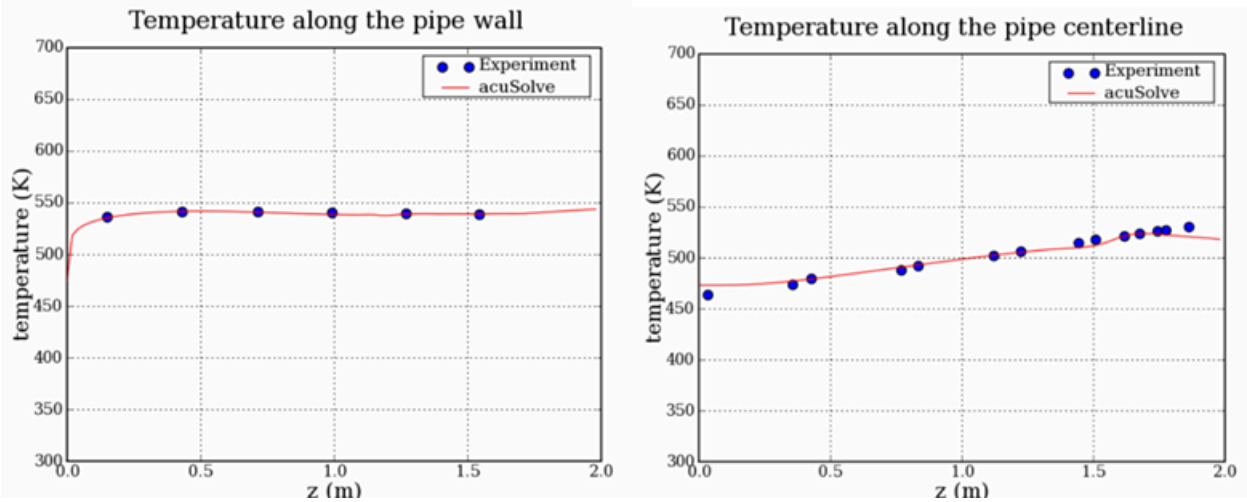


Figure 600: Temperature Values for Varying Streamwise Distance Compared to Experimental Data

Summary

The AcuSolve solution compares well with experimental results for two-phase nucleate boiling simulations. In this application, the temperature of the wall as the onset of boiling approaches are simulated with AcuSolve using the nucleate boiling feature and the SA turbulence model. The experimental values of temperature are presented with the corresponding AcuSolve results. A good agreement of simulation results with the experiment validates the ability to solve two-phase nucleate boiling using the nucleate boiling capabilities of AcuSolve.

Simulation Settings for Two-Phase Nucleate Boiling in a Cylindrical Pipe

HyperWorks database file: `<your working directory>\pipe_two_phase_boiling\pipe_two_phase_boiling.hm`.

Global

- Problem Description
  - Analysis type – Transient
  - Turbulence equation – SA
  - Temperature equation – Advective Diffusive
- Auto Solution Strategy
  - Maximum time steps – `500`
  - Initial time increment – `0.003`
  - Convergence Tolerance – `0.001` sec
  - Relaxation factor – `0.3`
- Surface Tension Model (“Water_NB-Vapor_NB”)
  - Type – Constant
  - Surface Tension – `0.02382`
- Material Model
  - Vapor_NB
    - Type – Constant
    - Density – `23.75` kg/m^3
    - Viscosity – `1.79e-05` kg/m-sec
    - Specific Heat – `4225` J/kg-K
    - Latent Heat – `1675570`
    - Latent Heat Temperature – `530.55` K
    - Conductivity – `0.02528` W/m-K
  - Water_NB
    - Type – Constant
    - Density – `800` kg/m3
    - Viscosity – `0.0001339` kg/m-sec
    - Specific Heat – `4500` J/kg-K
    - Conductivity – `0.65` W/m-K
- Multifield parameter (Field interaction model)
  - Type – Algebraic Eulerian
  - Phase change type – Wall Boiling
  - Carrier field - Water
  - Disperse field – Vapor
  - Disperse field diameter type – Boiling kurul exponential
  - Drag model – Ishii zuber
  - Lift Model – Legendre Magnaudet

Model

- Volumes
  - Fluid
    - Material – Vapor_Water
- Surfaces
  - Inflow
    - Simple Boundary Condition – Inflow
    - Inflow type – Mass Flux Rate
    - Mass Flux Rate – `0.167634` kg/sec
    - Temperature – `473` K
  - Outflow
    - Simple Boundary Condition – Outflow
    - Pressure – `4500000` N/m2
  - Wall
    - Simple Boundary Condition – Wall
    - Temperature type – Flux
    - Heat Flux – `570000` W/m2

References

B. Koncar, E. Krapper, Y. Egorov, 2005, "CFD MODELING OF SUBCOOLED FLOW BOILING FOR NUCLEAR ENGINEERING APPLICATIONS", International Conference Nuclear Energy for New Europe 2005, Bled, Slovenia, September 5-8,2005.

Single-Phase Nucleate Boiling in a Rectangular Channel

In this application, AcuSolve is used to simulate the wall heat flux due to nucleate boiling at a heated wall inside a rectangular channel with water flow. Results are compared with experimental heat flux measurements as reported by Steiner, et al. (2005). The close agreement of AcuSolve results with experimental results validates the ability of AcuSolve to model single phase nucleate boiling problems.

Problem Description

The problem consists of a channel with a heated wall at the bottom. The temperature of the wall is selected to onset the nucleate boiling at the heated wall. The dimensions of the inlet are 0.03 x 0.04 m; the inlet velocity (v) is 0.39 m/s and the temperature (T) of the fluid entering the inlets is varied from 373.15 K (100 C) to 406.15 (133 C)), while the atmospheric pressure is specified to be 2 bar. The pre-heated water enters the inlets and heat is transferred into the fluid from the heated walls. The heat causes sub-cooled boiling to occur in the region close to the wall and leads to the formation of bubbles at nucleation sites. The surface tension and vapor phase models are specified to emulate the physical process of water changing state to water vapor.

The heat transfer in this regime is dominated by two effects, the macro convection due to the motion of the bulk liquid and the latent heat transport associated with the evaporation of the liquid micro-layer between the bubble and the heated wall. Each of these effects are modeled with AcuSolve and the prediction of their processes is demonstrated in the following results.

The AcuSolve simulation is prepared as a steady state heat transfer simulation to determine the temperature and heat flux on the heated walls of the model. AcuSolve computes the single-phase nucleate boiling by employing Chen’s model for two-phase boiling flow described in Chen (1966). The heat flux values for different wall temperatures are compared against the experimental measurements, as described in Steiner, et al. (2005).

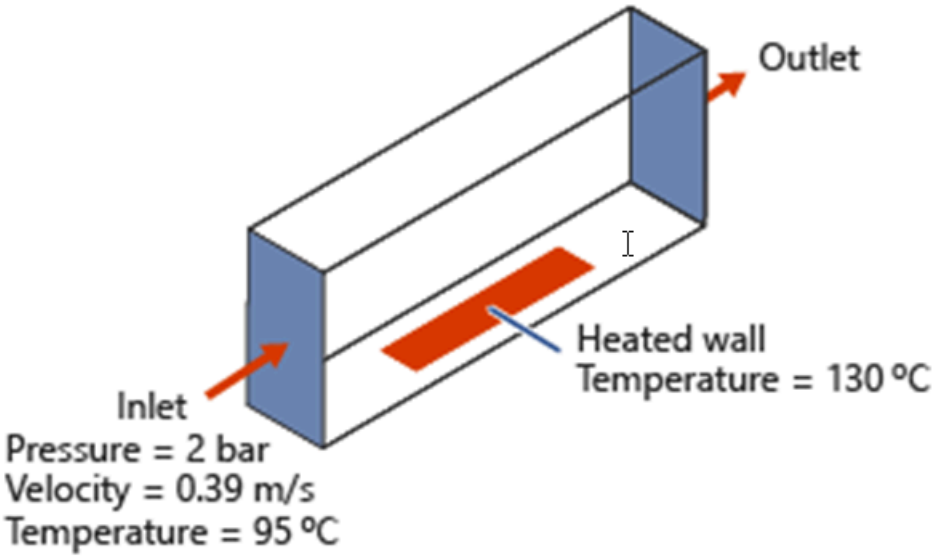


Figure 601: Critical Dimensions and Parameters for Simulating a Single-Phase Nucleate Boiling in a Rectangular Channel

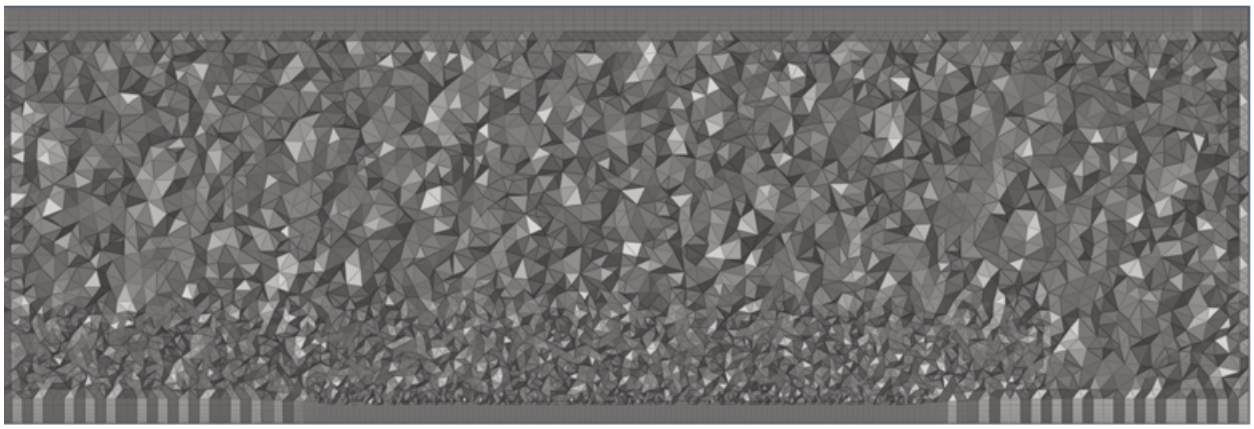


Figure 602: Mesh Used for Simulating a Single-Phase Nucleate Boiling in a Rectangular Channel

AcuSolve Results

The AcuSolve solution is run for heated wall temperature values of 100 C, 105 C, 110 C, 115 C, 120 C, 125 C, 130 C, 133 C and the results presented reflect the heat flux from the wall as the temperature nears the saturation temperature. The experimental values of heat flux (MW/m2) and wall temperature are presented with the corresponding AcuSolve results at seven temperature values. The AcuSolve results show good agreement with the experimental results for the heat flux, indicating that the single-phase nucleate boiling is properly captured.

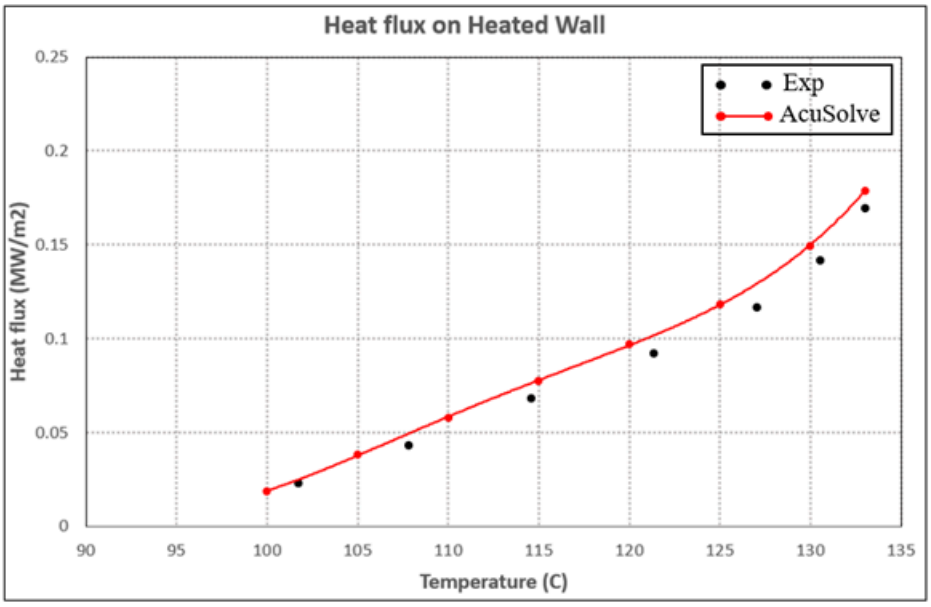


Figure 603: Heat Flux Values for Varying Wall Temperatures Compared to Experimental Data

Summary

The AcuSolve solution compares well with experimental results for single-phase nucleate boiling simulations. In this application, heat flux generated by the wall as the onset of boiling approaches are simulated with AcuSolve using the nucleate boiling feature and the RKE turbulence model. The experimental values of heat flux for the wall temperature range are presented with the corresponding AcuSolve results. A good agreement of simulation results with the experiment validates the ability to solve single-phase nucleate boiling using the nucleate boiling capabilities of AcuSolve.

Simulation Settings for Single-Phase Nucleate Boiling in a Rectangular Channel

HyperWorks CFD database file: `<your working directory>\channel_single_phase_boiling \channel_single_phase_boiling.hm`.

Global

- Problem Description
  - Analysis type – Steady
  - Turbulence equation – RKE
  - Temperature equation – Advective Diffusive
  - Nucleate Boiling Single Phase – On
- Auto Solution Strategy
  - Convergence Tolerance – `0.001` sec
  - Relaxation factor – `0.4`
- Surface Tension Model (“Water-srfTns”)
  - Type – Constant
  - Surface Tension – `0.07`

- Material Model
  - Vapor
    - Type – Constant
    - Density – `1.128` kg/m^3
    - Viscosity – `1.29e-5` kg/m-sec
    - Specific Heat – `2174.59` J/kg-K
    - Latent Heat – `2256000`
    - Latent Heat Temperature – `393.45` K
    - Conductivity – `0.02749` W/m-K
    - Turbulent Prandtl number – `1.0`
  - Water
    - Type – Constant
    - Density – `965.36` kg/m^3
    - Viscosity – `0.000314` kg/m-sec
    - Specific Heat – `4204.8` J/kg-K
    - Conductivity – `0.675` W/m-K
    - Turbulent Prandtl number – `0.91`
    - Vapor phase model – Vapor
    - Surface Tension model – Water-srfTns

Model

- Volumes
  - Fluid
    - Material– Water
- Surfaces
  - Inflow
    - Simple Boundary Condition – Inflow
    - Inflow type – Average Velocity
    - Average Velocity – `0.39` m/sec
    - Temperature – `368.15` K
  - Outflow
    - Simple Boundary Condition – Outflow
    - Back flow condition – On
    - Temperature back flow type – Mass flux average
    - Kinetic energy back flow type – Mass flux average
    - Dissipation rate back flow type – Mass flux average
  - Bottom
    - Simple Boundary Condition – Wall
  - Top

        - Simple Boundary Condition – Wall
    - Side_MinY
        - Simple Boundary Condition – Wall
    - Side_MaxY
        - Simple Boundary Condition – Wall
    - Heated Wall
        - Simple Boundary Condition – Wall
        - Temperature type – Value
        - Temperature – [373.15, 378.15, 383.15, 388.15, 393.15, 398.15, 403.15, 406.15] K

References

Helfried Steiner, Alexander Kobor, Ludwig Gebhard, 2005, "A wall heat transfer model for subcooled boiling flow", International Journal of Heat and Mass Transfer, Vol 48, pp. 4161- 4173.

Chen, J.C., 1966, "Correlation for Boiling Heat Transfer to Saturated Fluids in Convective Flow", United States: N. p., 1962. Web. doi:10.2172/4636495.

Supersonic Flow Through a Converging-Diverging Nozzle

In this application, AcuSolve is used to simulate the high-speed turbulent flow in a converging and then diverging nozzle. The flow within the nozzle enters as subsonic, reaches sonic at the throat and shortly after develops a normal shock. AcuSolve results are compared with experimental results adapted from Bogar and Sajben (1983). The close agreement of AcuSolve results to experimental measurements validates the ability of AcuSolve to simulate internal supersonic flows where normal shocks are present.

Problem Description

The problem consists of a converging and then diverging nozzle represented as an extruded planar surface, as shown in the image below, which is not drawn to scale. The length of the domain is 0.213 m with a throat height of 0.044 m. The stagnation pressure and static temperature are constrained at the inlet to 135,000 Pa and 265.98 K, respectively. The static pressure is defined using the outflow boundary condition, where P_{static}=97216.08 Pa. The flow in the diffuser has an inlet Reynolds number of $6.5x10^5$. The upper and lower walls are set to no-slip and the side walls are set to slip, while the exterior walls are specified to be adiabatic. Images of the numerical mesh are shown below.

The AcuSolve simulation is prepared to model the pseudo-transient state to determine the shock location and corresponding scalar quantities within the diffuser. AcuSolve computes the flow and thermal solution by simulating a planar, two-dimensional flow problem with physical dimensions and input quantities as described in the Sajben Diffuser case presented by Bogar and Sajben (1983). The gas in the simulation domain enters at subsonic conditions and is forced to accelerate beyond Mach=1.0 as it passes through the throat. After reaching supersonic speed a normal shock wave develops causing the flow speed to reduce back below sonic. The pressure along the bottom wall of the diffuser is compared against experimental measurements to demonstrate the solver's capability to solve supersonic cases.

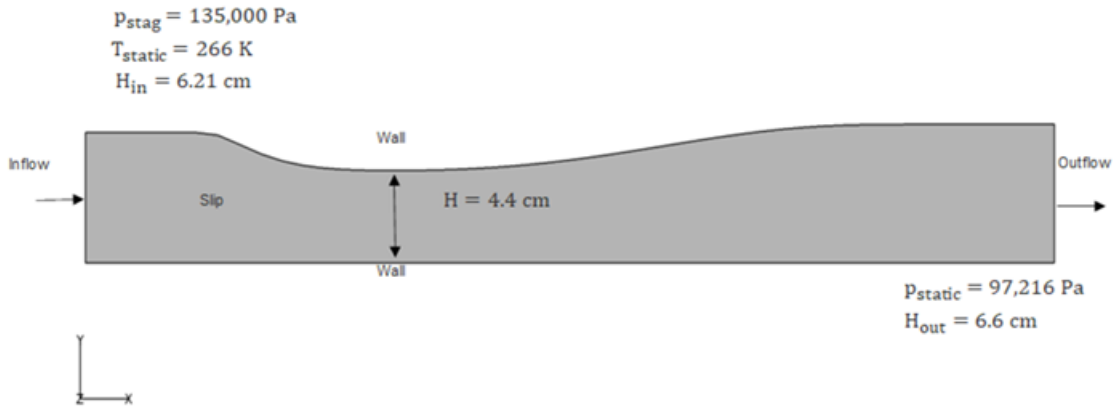


Figure 604: Parameters for Simulating Compressible Flow within a Converging-Diverging Nozzle

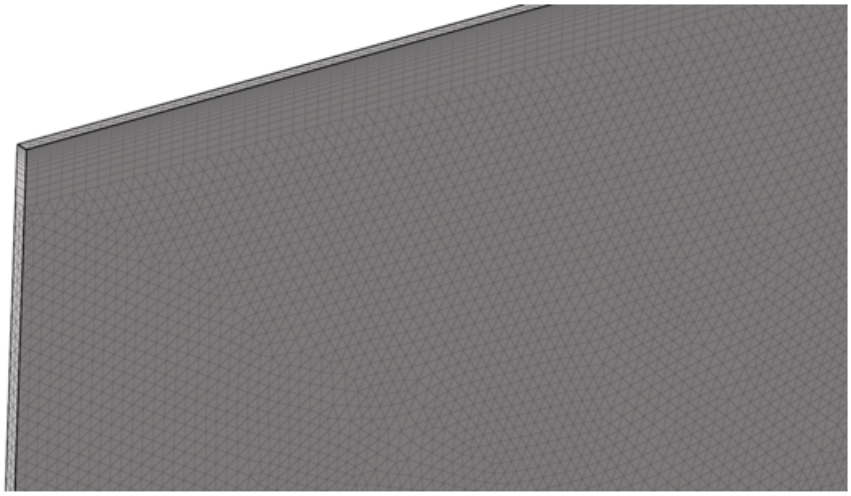


Figure 605: Mesh used for Simulating Compressible Flow in a Converging-Diverging Nozzle

AcuSolve Results

The AcuSolve solution is run for 0.025 seconds (6,250 timesteps with dt=4.0x10^{-6}sec) and converges to a pseudo-steady solution. The change in pressure from the inlet to outlet causes the flow to accelerate within the throat of the diffuser until it reaches approximately Mach=1.35. A normal shock is present just downstream of where the cross-sectional area of the nozzle increases, as shown in the image below. The numerical solution can be compared with the reference after normalizing the pressure along the wall by the inlet stagnation pressure (135 kPa) and the distance along the bottom wall by the nozzle throat height (0.044 m). The image below shows the normalized pressure versus normalized distance in comparison to NASA reference and experimental results. The image shows black circles representing the experimental measurements (Bogar and Sajben 1983), a dashed blue line representing the SA solution as obtained through NASA publication (Mohler 2005) and a solid red line representing the AcuSolve results with the Spalart-Allmaras turbulence model. The non-dimensional pressure within the diffuser agrees well with the reference data, demonstrating the correct physical location of the normal shock and expected moderate flow speed reduction within the constant cross-section diffuser portion of the nozzle.

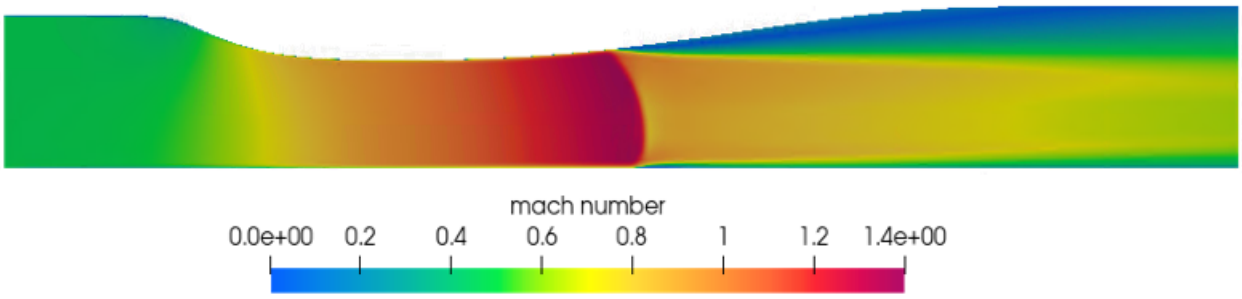


Figure 606: Contours of Mach Number within a Converging-Diverging Nozzle

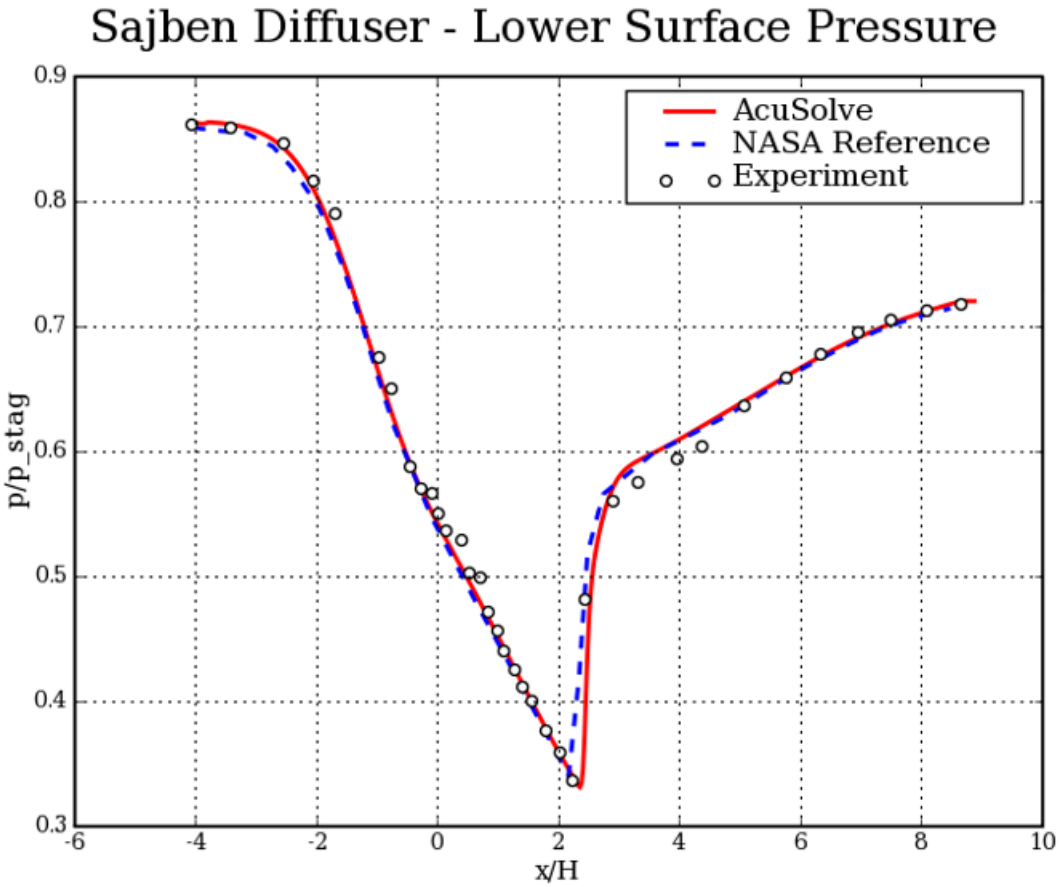


Figure 607: Normalized Pressure Versus Normalized Distance in Comparison to NASA Reference and Experimental Results

Summary

The AcuSolve solution compares well with experimental and numerical results for the described simulation. In this application, compressibility effects are accounted for using the coupled compressible flow solver with the ideal gas material definition. The thermal and momentum exchange within the nozzle is computed with AcuSolve using the compressible Navier-Stokes solver with the Spalart-Allmaras turbulence model. The experimental values of pressure are presented with the corresponding AcuSolve results and show good agreement, validating the ability to solve compressible cases with the presence of normal shocks. The results indicate that AcuSolve is able to properly predict the peak pressure magnitude and location within the diffuser while maintaining the normal shock when the time-step is selected to result in a maximum CFL of approximately 30.

Simulation Settings for Supersonic Flow Through a Converging-Diverging Nozzle

HyperWorks CFD database file: `<your working directory>\diffuser_compressible\diffuser_compressible.hm`

Global

- Problem Description

    - Flow – Compressible Navier Stokes
    - Analysis type – Transient
    - Turbulence equation – SA
    - Temperature equation – Advective Diffusive
- Auto Solution Strategy
    - Initial time increment – `4.0E-6`
    - Final time – `0.025` sec
    - Convergence Tolerance – `0.001` sec
    - Relaxation factor – `0.5`
- Material Model
    - Air-Ideal Gas
        - Type – Ideal_Gas
        - Viscosity – `1.781e-05` kg/m-sec
        - Specific Heat – `1005` J/kg-K
        - Conductivity – `0.02521` W/m-K
        - Gas Constant – `287.058` J/kg-K

Model

- Volumes
    - Fluid
        - Material – Air-Ideal Gas
- Surfaces
    - Inflow
        - Simple Boundary Condition – Inflow
        - Inflow type – Stagnation Pressure
        - Stagnation Pressure – `135000.0` N/m2
        - Turbulence_input_type – Direct
        - Eddy Viscosity – `1e-6` m^2/s
        - Temperature – `265.98` K
    - Outflow
        - Simple Boundary Condition – Outflow
        - Pressure – `97216.08` N/m2
    - Wall_1
        - Simple Boundary Condition – Wall
        - Type – auto_wall
    - Wall_2
        - Simple Boundary Condition – Wall
        - Type – auto_wall
    - Slip_1

        - Simple Boundary Condition – Slip
    - Slip_2
        - Simple Boundary Condition – Slip

References

Bogar, T. J., Sajben, M., and Kroutil, J. C. (1983) "Characteristic Frequencies of Transonic Diffuser Flow Oscillations," AIAA Journal, Vol. 21, No. 9, pp. 1232-1240.

Mohler, S.R., "Wind-US Unstructured Flow Solutions for a Transonic Diffuser," NASA CR-2005-213417, January 2005.

Moving Mesh

10

This section includes validation cases that consider time dependent motion within the domain, requiring that the mesh movement be modeled with a differential equation, a fully defined mesh motion or by interpolated mesh motion.

This chapter covers the following:

- Ideal Gas Compression in an Actuating Piston (p. 832)
- Laminar Free Surface Flow Inside a Rotating Cavity (p. 839)
- Turbulent Flow Over an Oscillating Rigid Body Assembly (p. 845)
- Circumferential Flow in a Cylinder Induced by a Rotating Solid (p. 853)
- Multiphase Flow Within a Sloshing Tank (p. 859)

Ideal Gas Compression in an Actuating Piston

In this application, AcuSolve is used to simulate pressure and temperature inside an actuating piston using the ideal gas relationship and fully defined mesh motion. AcuSolve results are compared with analytical results as described in Moran and Shapiro (2000). The close agreement of AcuSolve results with analytical results validates the ability of AcuSolve to model cases with material properties defined by the ideal gas law subjected to significant mesh distortion.

Problem Description

The problem consists of air compressed by a piston within a cylinder 10 m long with a diameter of π (3.14159) m, as shown in the following image, which is not drawn to scale. The piston is driven by a crankshaft 4 m long attached to a connecting rod 6 m long. The crankshaft rotates at 60o/s around a center point. At time (t) = 0.0 s the crank and piston are at top dead center (TDC) with an initial cylinder volume of 80 m^3. At t = 3.0 s the piston is at bottom dead center (BDC), at which point the volume in the cylinder is reduced to 16 m^3. The piston then moves back to TDC at t = 6.0 s. Air at atmospheric conditions, with material properties of an ideal gas and a dynamic viscosity of 1.781 X 10^5 kg/m-sec is the fluid modeled in the domain.

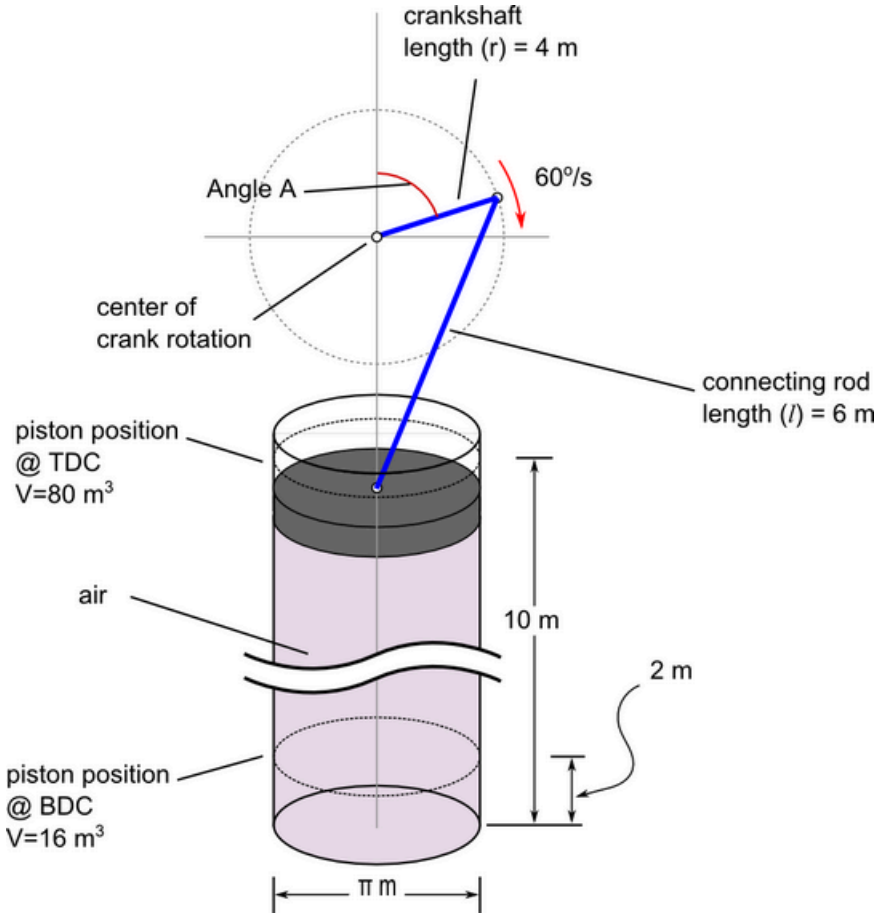


Figure 608: Critical Dimensions and Parameters for Simulating Ideal Gas Compression in an Actuating Piston

The motion of the piston is described by the following equation.

$$x = r*\cos A + \sqrt{l^2 - r^2 \sin^2 A} \quad (27)$$

Where

- x is the distance of the piston from TDC
- r is the length of the connecting rod, 4 m
- A is the crank angle as a function of time (t)
- l is the connecting rod length, 6 m

During the simulation, the top surface of the cylinder, representing the piston, moves with an applied mesh motion that mimics the motion of the reciprocating crank, rod, and piston assembly. The ideal gas is compressed by contracting the mesh according to the motion of that assembly and by allowing the fluid properties to change as a function of time.

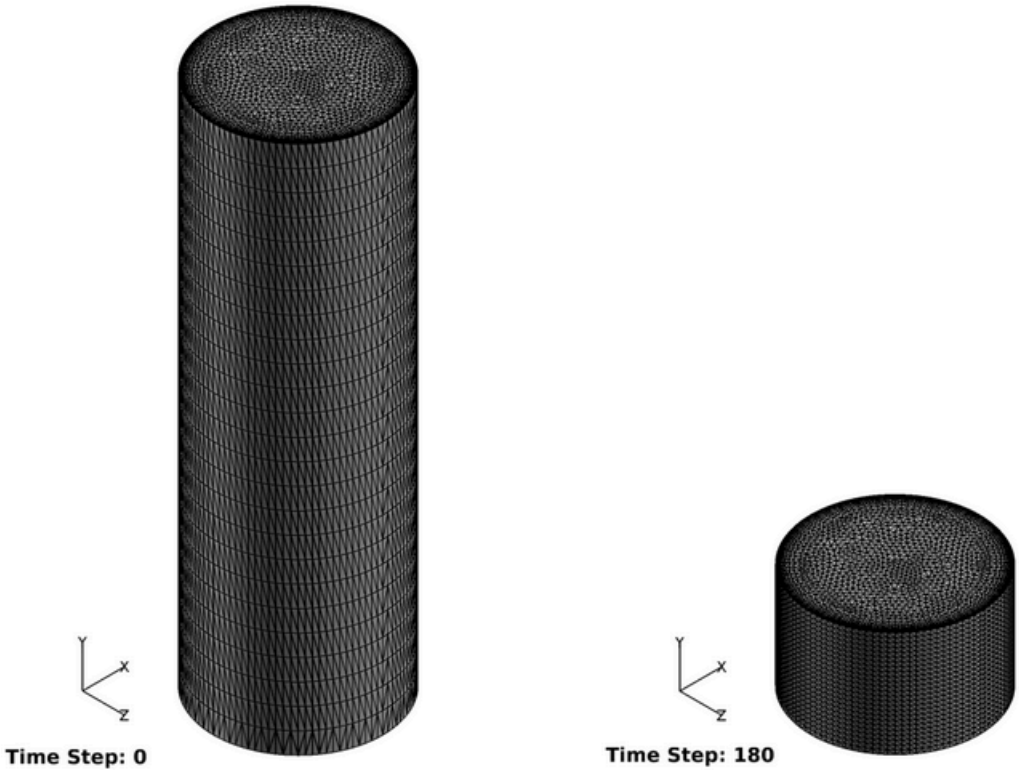


Figure 609: Mesh Used for Simulating Ideal Gas Compression in an Actuating Pistion at Time Step 0 and Time Step 180 (3 s)

AcuSolve Results

The simulation was run as transient for a total of 360 time steps with a duration of 6.0 seconds. The AcuSolve solution shows time dependent pressure and temperature in a cylinder volume that compresses and expands in a 6.0 second cycle. Pressure and temperature increase as the cylinder volume decreases, and returns toward initial conditions as the cylinder volume expands. The contours of pressure and temperature within the cylinder at the initial stage (t = 0.0 s) and the half cycle (t = 3.0 s) are shown in the following images.

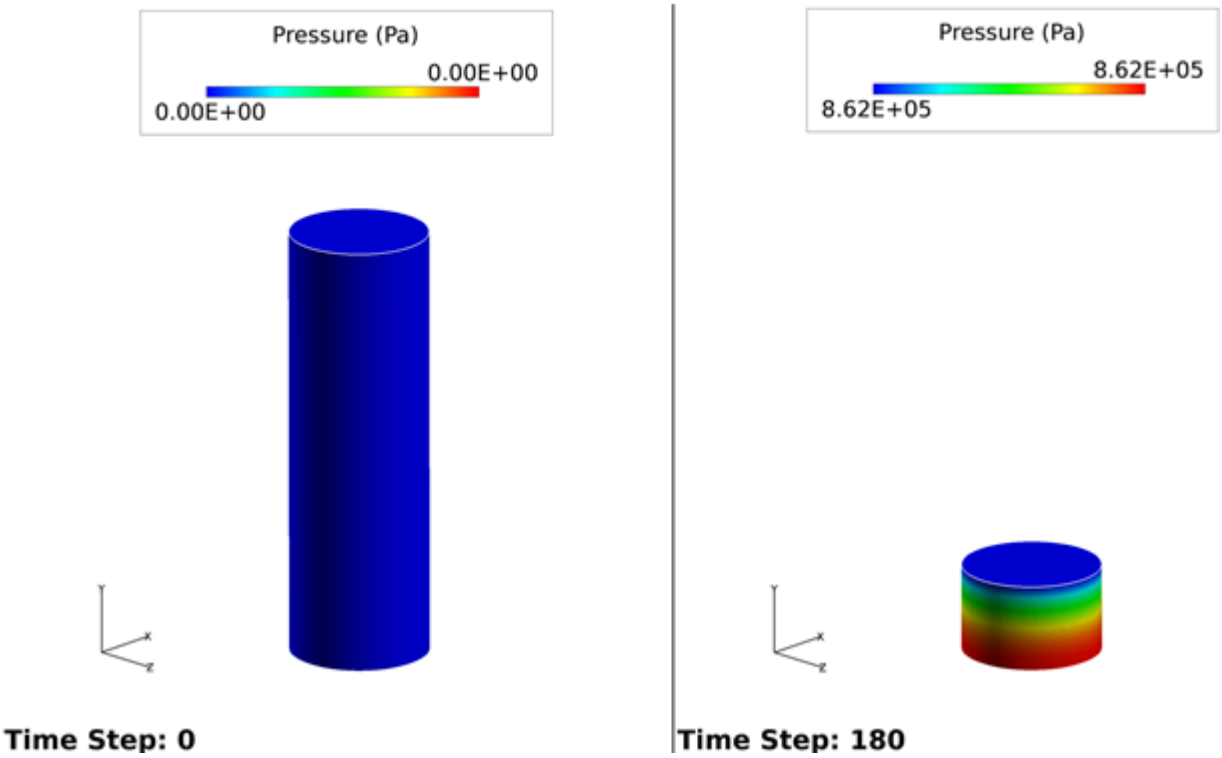


Figure 610: Pressure Distribution Within the Domain with the Piston at TDC and BDC

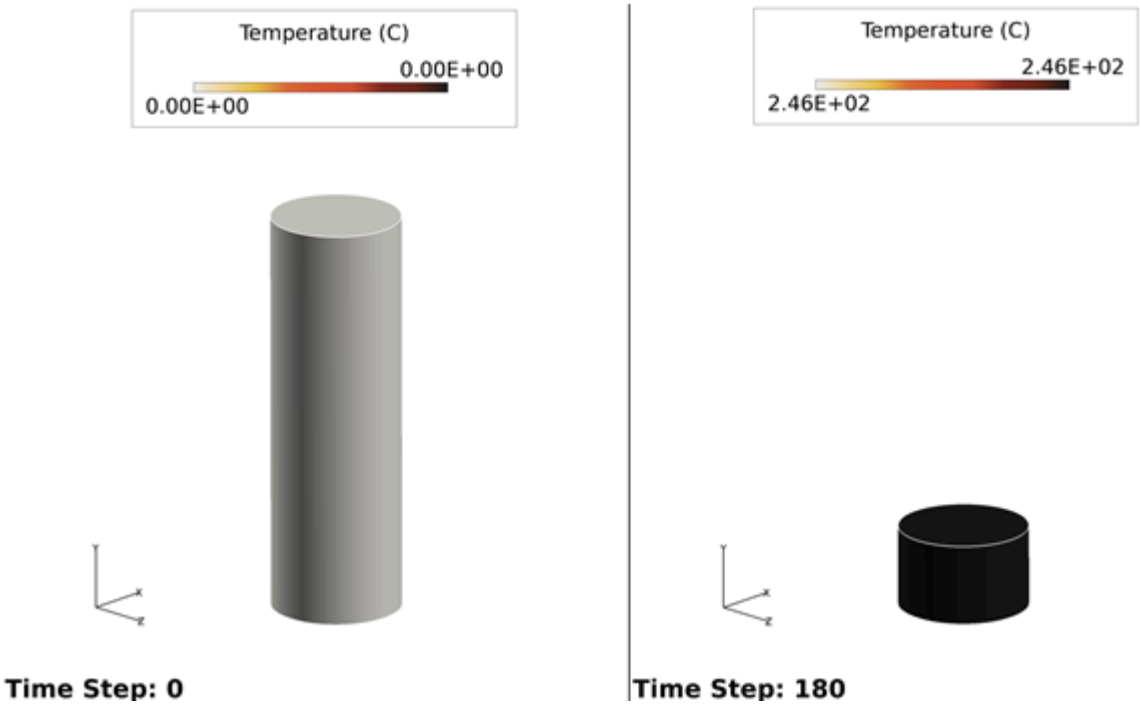


Figure 611: Temperature Distribution Within the Domain with the Piston at TDC and BDC

Comparison of time history plots of the AcuSolve and analytical solutions shows that the AcuSolve solution is nearly identical to the analytical solution. The AcuSolve computed internal pressure reaches a maximum of 8.62 X 105 Pa and the temperature reaches a maximum of 246.45 degrees C.

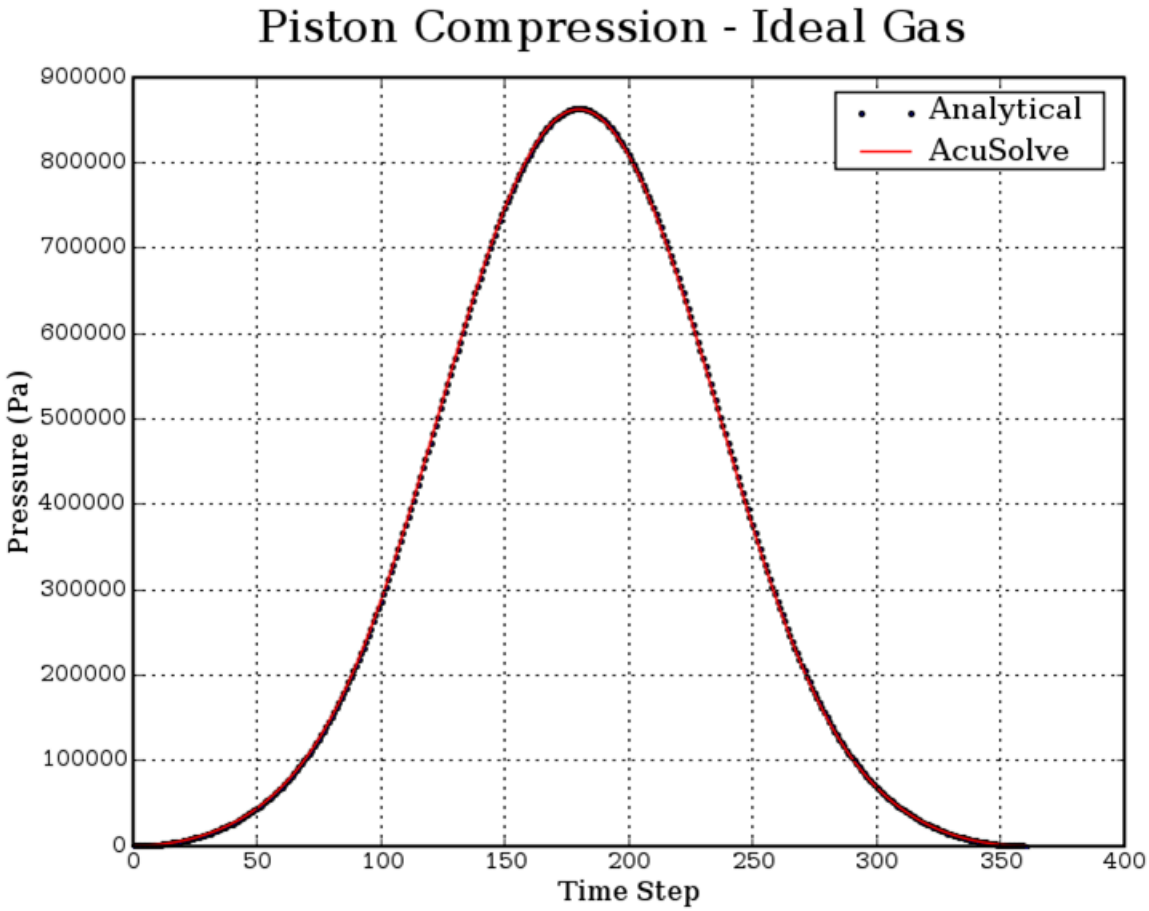


Figure 612: History Plots of Pressure for AcuSolve and Analytical Solutions

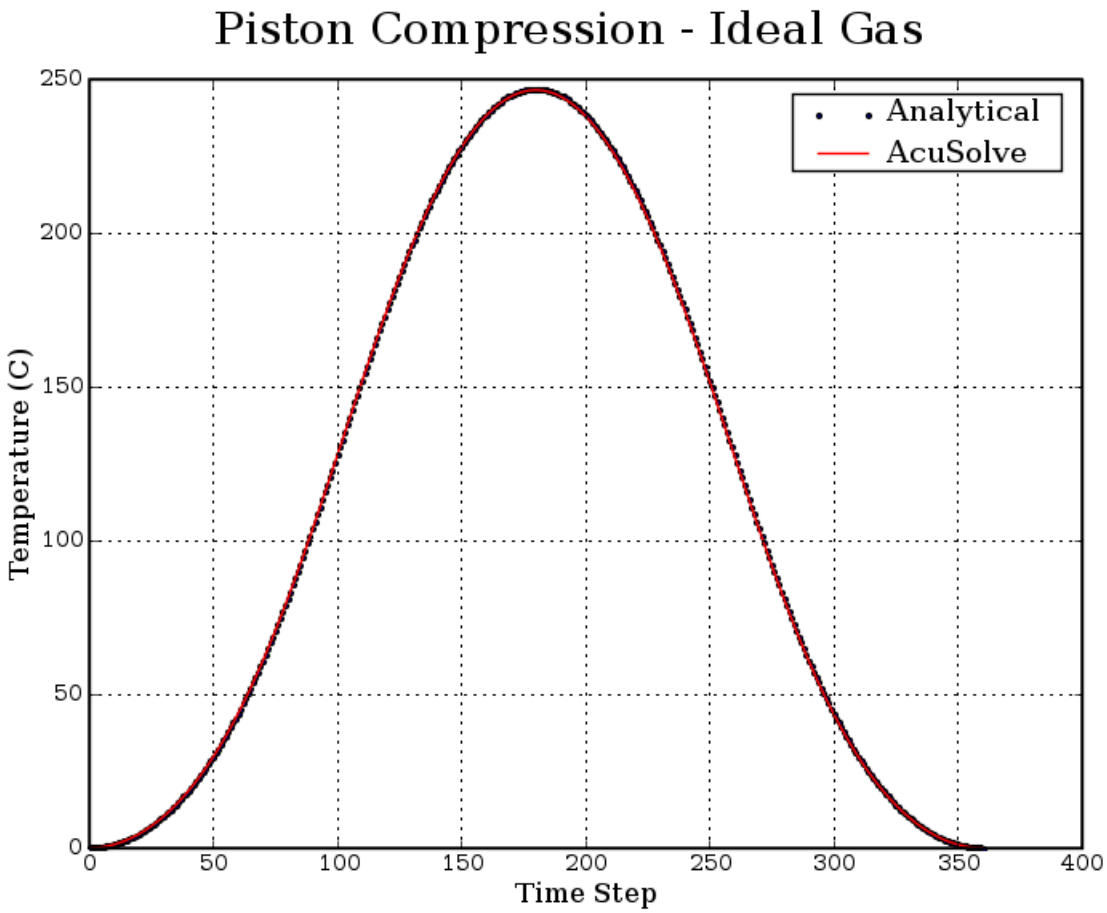


Figure 613: History Plots of Temperature for AcuSolve and Analytical Solutions

Summary

The AcuSolve solution compares well with analytical results for ideal gas compression in an actuating piston. The AcuSolve transient solution compares nearly identically with the analytical solution, with 0.1 percent and 0.16 percent error for the maximum pressure and temperature, respectively. As a result, AcuSolve demonstrates the ability to predict ideal gas compression in an actuating piston.

Simulation Settings for Ideal Gas Compression in an Actuating Piston

AcuConsole database file: `<your working directory>\cylinder_piston_compression\cylinder_piston_compression.acs`

Global

- Problem Description
  - Analysis type - Transient
  - Temperature equation - Advective Diffusive
  - Turbulence equation - Laminar
  - Mesh type - Fully Specified

- Auto Solution Strategy
  - Max time steps - `360`
  - Initial time increment - `0.01667` sec
  - Convergence tolerance - `1.0e-5` sec
  - Max stagger iterations - `10`
- Multiplier Function
  - Piston
    - Type - Piecewise Linear
    - Curve fit variable - Time
    - Curve fit values - (included in `.acs` based on equation discussed in problem description)
- Material Model
  - Air
    - Density
      1. Type - Ideal Gas
      2. Gas constant - `286.9` J/kg-K
      3. Abs. pressure offset - `101325.0` N/m2
      4. Abs. temperature offset - `273.15` K
    - Viscosity - `1.781e-5` kg/m-sec
- Mesh Motion
  - Piston
    - Type - Translation
    - Translation velocity - `0.0`, `-1.0`, `0.0`
    - Velocity variable - Multiplier Function
    - Translation multiplier function - Piston

  Model
- Volumes
  - Fluid
    - Element Set
      1. Material model - Air
      2. Compression heating - On
    - Element Output - on
- Surfaces
  - BDC
    - Simple Boundary Condition
      1. Type - Wall
      2. Wall velocity type - Match Mesh Velocity
      3. Mesh displacement BC type - Fixed
  - SideWall

        - Simple Boundary Condition
            1. Type - Wall
            2. Wall velocity type - Match Mesh Velocity
            3. Mesh displacement BC type - Fixed
    - TDC
        - Simple Boundary Condition
            1. Type - Wall
            2. Mesh displacement BC type - Fixed
            3. Mesh motion - Piston
- Nodes
    - VolumeNodes
        - Mesh X-Displacement
            1. Type - Zero
        - Mesh Y-Displacement
            1. Type - Linear
            2. Mesh motion - Piston
            3. Curve fit variable - Y reference coordinate
                1. X1 - `10.0` m
                2. Y1 - `1.0` m
                3. Y2 - `0.0` m
        - Mesh Z-Displacement
            1. Type - Zero

References

M.J. Moran and H.N Shapiro. "Fundamentals of Engineering Thermodynamics". Wiley. 4th Ed. 2000.

Laminar Free Surface Flow Inside a Rotating Cavity

In this application, AcuSolve is used to solve for the flow field within a rotating cavity with the top of the cavity free to move as if it was exposed to air. The height of the free surface is determined and compared against the analytical solution for the same rotational velocity under the standard gravitational force.

Problem Description

The problem consists of a fluid with arbitrary material properties rotating within an axisymmetric cavity. The cavity is 1.0 m in height with a radius of 0.5 m and is rotating at a constant speed of 3.0 rad/sec, as shown in the following image, which is not drawn to scale. The model is simulated as transient with the fluid initially at rest within the cavity. The radial velocity applied to the cavity walls causes the fluid's free surface to creep up the side wall forming a parabolic shape. The height of this surface is compared against the analytical solution as described in White, 2003.

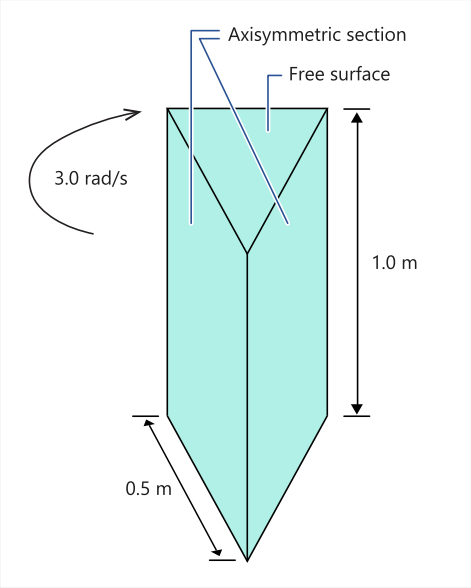


Figure 614: Critical Dimensions and Parameters used for Simulating a Laminar Free Surface Inside a Rotating Cavity

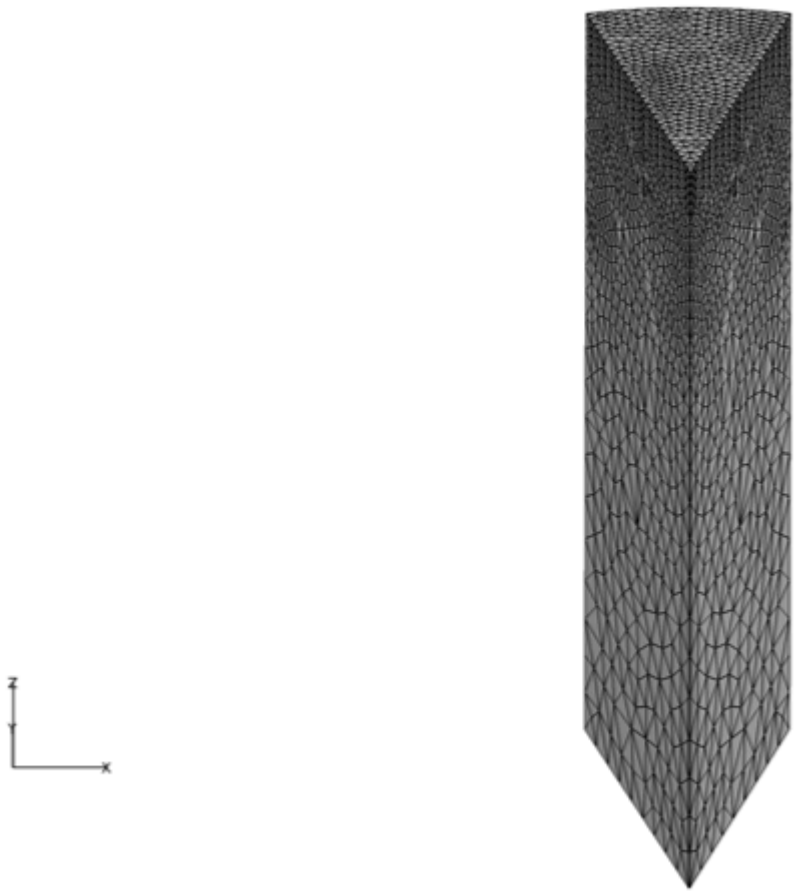


Figure 615: Mesh used for Simulating Laminar Free Surface Flow Inside a Rotating Cavity

The problem is simulated as axisymmetric by considering a 30 degree portion of the cavity with rotationally periodic boundary conditions applied on the planar surfaces representing the cut faces of the cavity.

AcuSolve Results

The AcuSolve solution reaches a quasi-static result with the free surface height stabilizing, demonstrating the final flow conditions of the simulation. As the fluid within the cavity is subjected to the multiple reference frame simulating the rotating boundaries the free surface begins to deform. At the center of the cavity the fluid height decreases and in order to conserve mass the height steadily increases as a function of the radial distance from the center. The surface height takes the form of a parabola as described in White, 2003. The following image demonstrates the shape that the fluid forms within the cavity, showing the vertical displacement of the rotating fluid. The free surface height is compared with the analytical solution where the image shows black circles representing the analytical solution and a solid red line for the AcuSolve results.

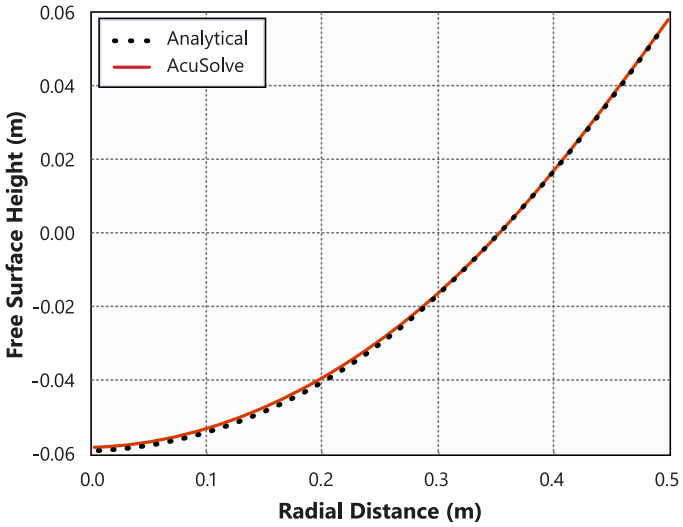


Figure 616: Free Surface Height of the Fluid Within the Cavity as a Function of Distance from the Center of the Domain at the Final Timestep

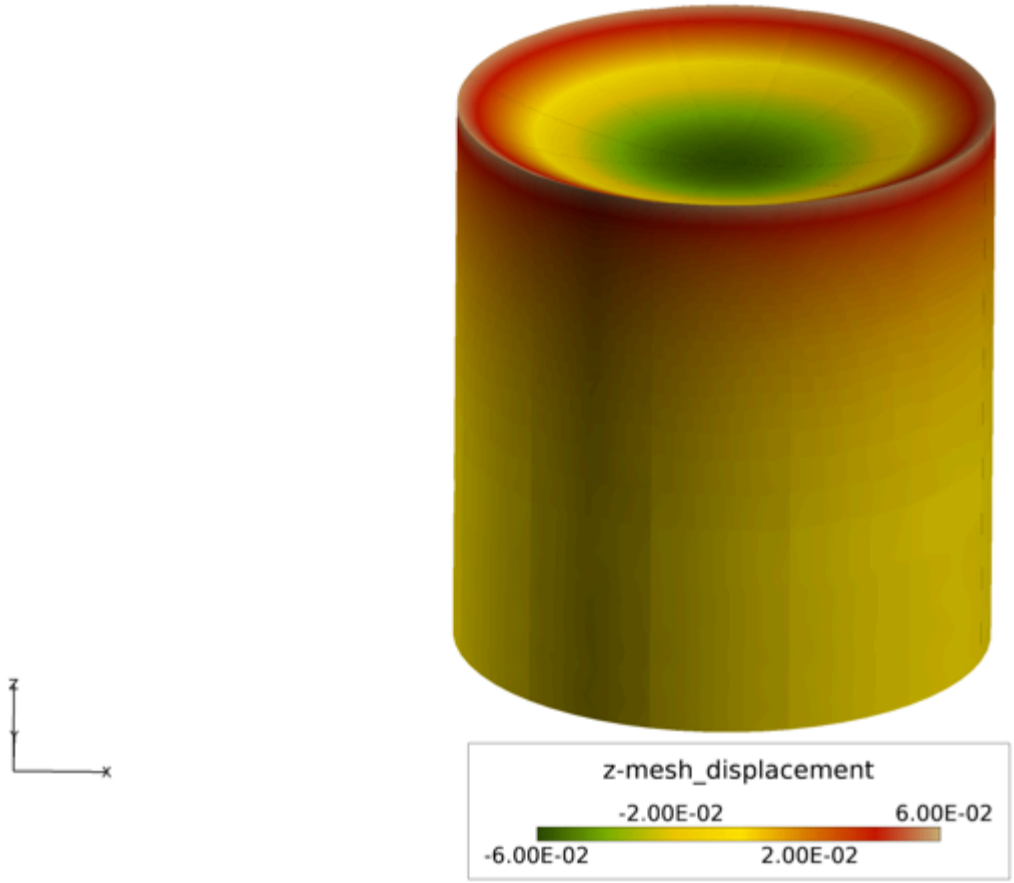


Figure 617: Vertical Mesh Displacement Within the Rotating Cavity at the Final Time Step (Shown as the Complete Cavity, using the Results from the Axisymmetric Section)

Summary

The AcuSolve solution compares well with analytical results for laminar free surface flow inside a rotating cavity. In this application, a fluid initially at rest is subjected to an angular velocity about the center of the cavity. As a result of the prescribed velocity, the fluid is forced to the outer wall of the cavity and develops a free surface profile in the shape of a parabola. The AcuSolve solution for the free surface height matches nearly exactly with the analytical results, with only minor differences based on the convergence criteria that you specified.

Simulation Settings for Laminar Free Surface Flow Inside a Rotating Cavity Fluid

Global

- Problem Description
  - Analysis type - Transient
  - Flow equation - Navier Stokes
  - Turbulence equation - Laminar
  - Mesh type - Arbitrary Mesh Movement (ALE)
- Auto Solution Strategy
  - Final time - `15.0` sec
  - Initial time increment- `0.05` sec
  - Convergence tolerance - `0.001`
  - Min stagger iterations - `0`
  - Max stagger iterations - `4`
- Material Model
  - Fluid
    - Density
      1. Type - Constant
      2. Density - `10` kg/m3
    - Viscosity
      1. Type - Constant
      2. Viscosity - `3.0` kg/m-sec
- Reference Frame
  - Omega
    - Rotation Center
      1. X-coordinate - `0.0` m
      2. Y-coordinate - `0.0` m
      3. Z-coordinate - `0.0` m
    - Angular velocity
      1. X-component - `0.0` rad/sec
      2. Y-component- `0.0` rad/sec
      3. Z-component - `3.0` rad/sec

Model

- Volumes
  - Fluid
    - Element Set
      1. Material model - Fluid
      2. Body force - Gravity
      3. Reference frame - Omega
- Surfaces
  - + Y
    - Simple Boundary Condition - (disabled to allow for nodal boundary conditions)
    - Advanced Options
      1. Nodal Boundary Conditions
         1. X-velocity
            1. Type - Constant
            2. Reference frame - Omega
            3. Constant value - `0.0`
         2. Y-velocity
            1. Type - Constant
            2. Reference frame - Omega
            3. Constant value - `0.0`
         3. Mesh X-Displacement
            1. Type- Zero
         4. Mesh Y-Displacement
            1. Type- Zero
  - -Z
    - Simple Boundary Condition
      1. Type - Wall
      2. Reference frame - Omega
      3. Mesh displacement BC type - Fixed
  - Axisymmetric +X
    - Simple Boundary Condition (disabled to allow for nodal boundary conditions)
  - Axisymmetric -X
    - Simple Boundary Condition (disabled to allow for nodal boundary conditions)
  - Free_Surface
    - Simple Boundary Condition
      1. # Type - Free Surface
- Periodics

- Axisymmetric Condition
- Periodic Boundary Condition
  - Type - Axisymmetric
  - Rotation Axis
    1. Point 1
       1. x-coordinate - 0.0 m
       2. y-coordinate - 0.0m
       3. z-coordinate - 0.0m
    2. Point 2
       1. x-coordinate - 0.0 m
       2. y-coordinate - 0.0m
       3. z-coordinate - 1.0m
- Nodes
  - All
    1. Mesh X-Displacement
       1. Type - Zero
    2. Mesh Y-Displacement
       1. Type - Zero
  - Centerline
    1. X-Velocity
       1. Type - Zero
    2. Y-velocity
       1. Type - Zero
    3. Mesh X-Displacement
       1. Type - Zero
    4. Mesh Y-Displacement
       1. Type - Zero

References

White, F. Fluid Mechanics. New York: McGrawHill. 2003

Turbulent Flow Over an Oscillating Rigid Body Assembly

In this application, AcuSolve is used to simulate the fluid-structure interaction of a fluid moving over a cylinder/plate assembly. AcuSolve results are compared with experimental results as described in Gomes and Lienhart (2009). The close agreement of AcuSolve results with the experimental results validates the ability of AcuSolve to model cases in which the fluid forces lead to structural motions.

Problem Description

The problem consists of a fluid having material properties of standard water with density of 998 kg / m^3 and kinematic viscosity of 0.97e-6 m^2/sec through a two dimensional channel over a cylinder and plate assembly. The diameter of the cylinder is 0.022 m and the plate length is 0.042 m, while the inlet velocity is specified to match experimental conditions with a max velocity of 1.07 m/sec, as is shown in the following image, which is not drawn to scale. The model is simulated as transient with constant inflow conditions, allowing an oscillatory motion of the assembly to develop. The Shear Stress Transport (SST) turbulence model is used to model the turbulent portion of the flow and AcuSolve's internal rigid body motion is used to capture the motion of the oscillating assembly.

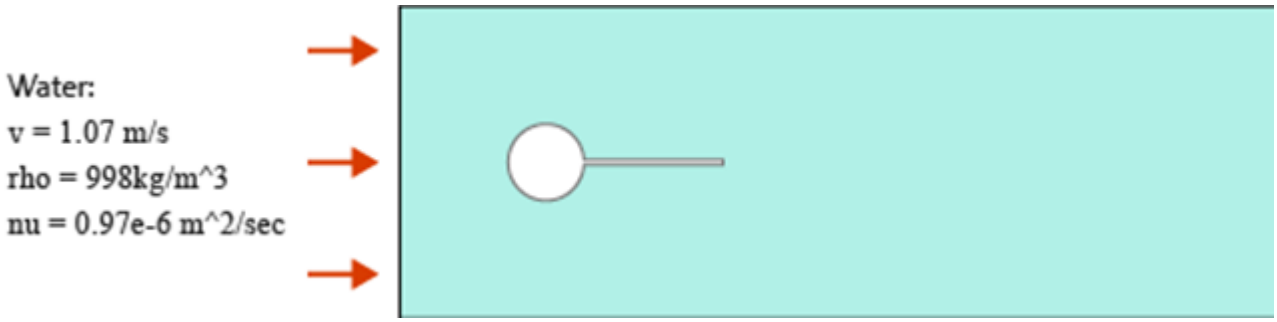


Figure 618: Critical Dimensions and Parameters used for Simulating Rigid Body Motion of Flow Past a Cylinder/Plate Assembly

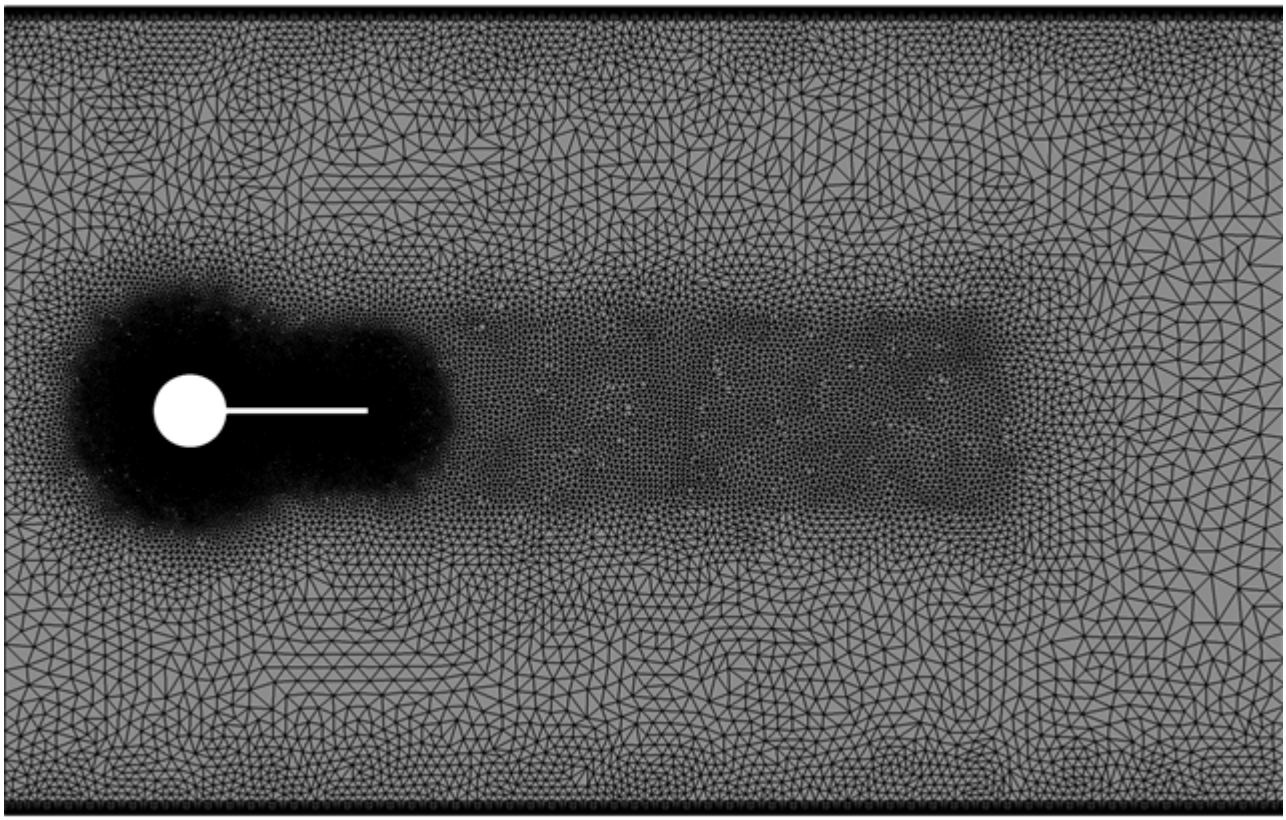


Figure 619: Mesh used for Simulating Rigid Body Motion of Flow Past a Cylinder/Plate Assembly

The simulation was performed as a two dimensional problem by constructing a volume mesh that contains a single layer of elements extruded in the cross stream direction, normal to the flow plane and by imposing symmetry boundary conditions on the extruded planes. The upper and lower walls are specified as no-slip and the inlet velocity is specified to match the conditions of the experiment (Gomes and Lienhart 2009).

AcuSolve Results

The AcuSolve solution reached a regularly repeating oscillatory state and the simulation was allowed to proceed for 10 seconds of physical time to obtain a sufficient number of cycles for statistical analysis. The motion of the cylinder/plate assembly is directly attributed to the vortices shedding in its wake. The fluctuating loads on the assembly that result from the vortex shedding lead to a repeating cycle of structural rotation. The dominant oscillation frequency from the simulation was found to match well with the experimental measurements, within approximately 3.5 percent. The images below show the rigid body displacement of the assembly as it oscillates within the flow. Contours of velocity magnitude demonstrate the forcing on the assembly, while the mesh motion around the structure is captured and plotted for a single time step. Two dimensional plots showing the angular displacement demonstrate the motion, showing a single red line for the AcuSolve results.

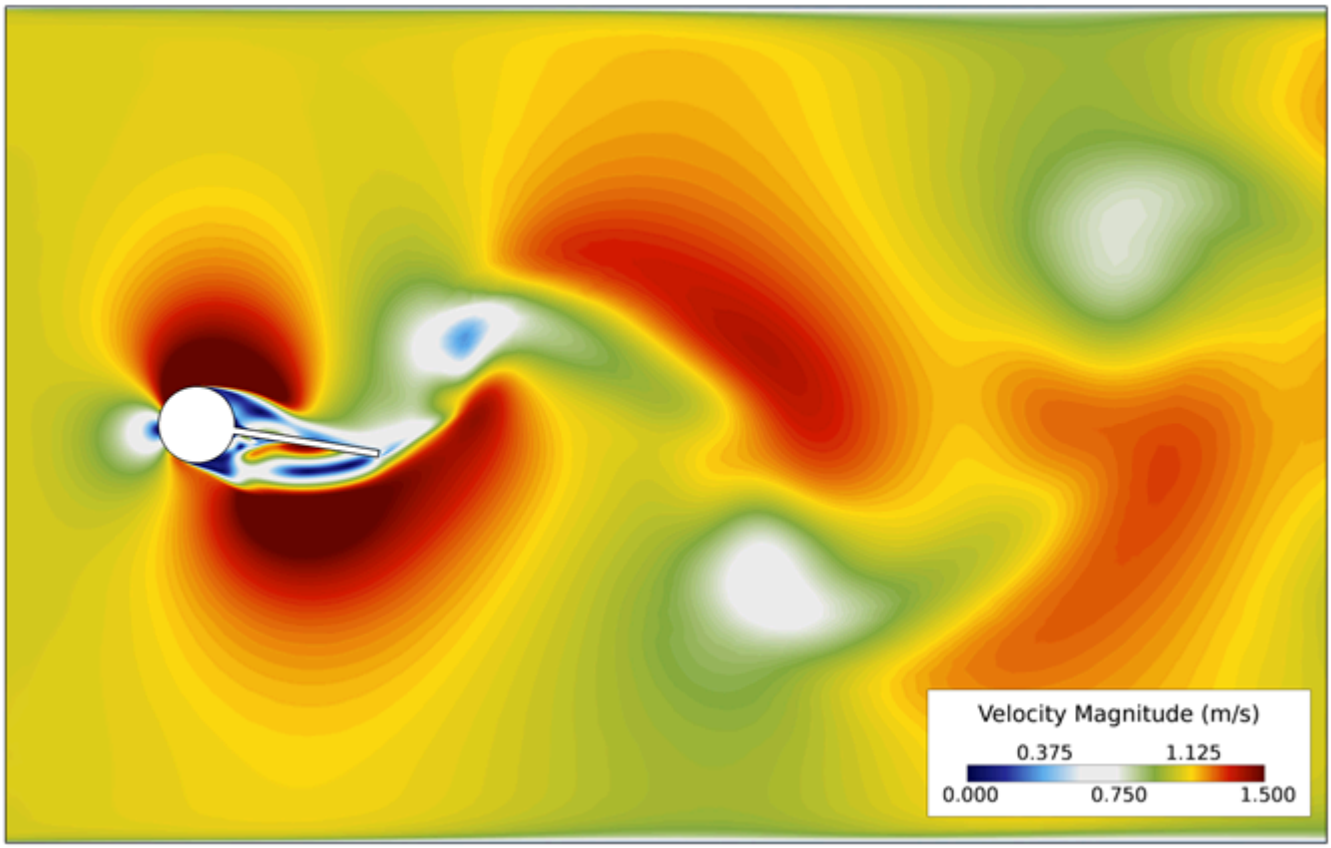


Figure 620: Velocity Contours Near the Assembly for a Single Time Step During the Simulation

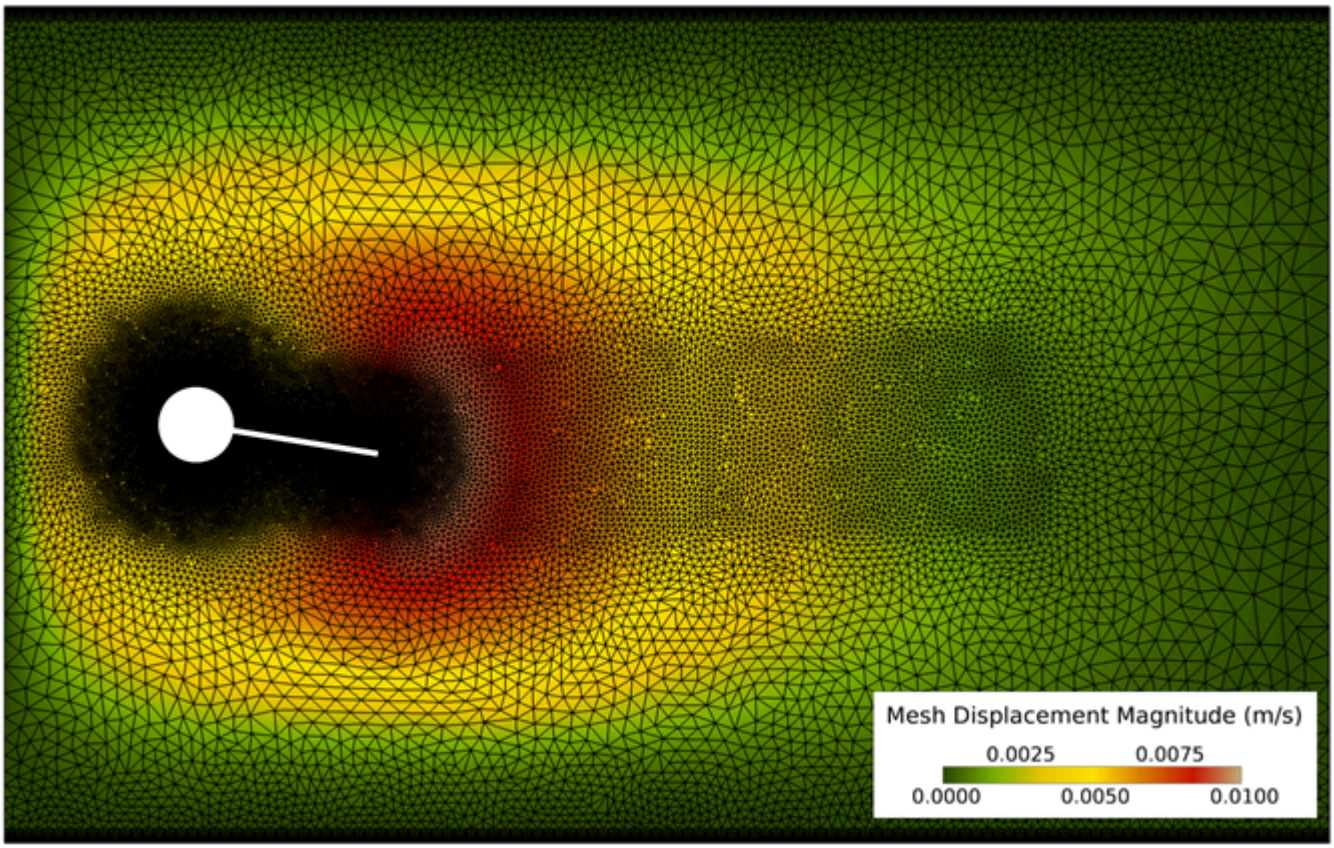


Figure 621: Mesh Displacement Contours Near the Assembly for a Single Time Step During the Simulation

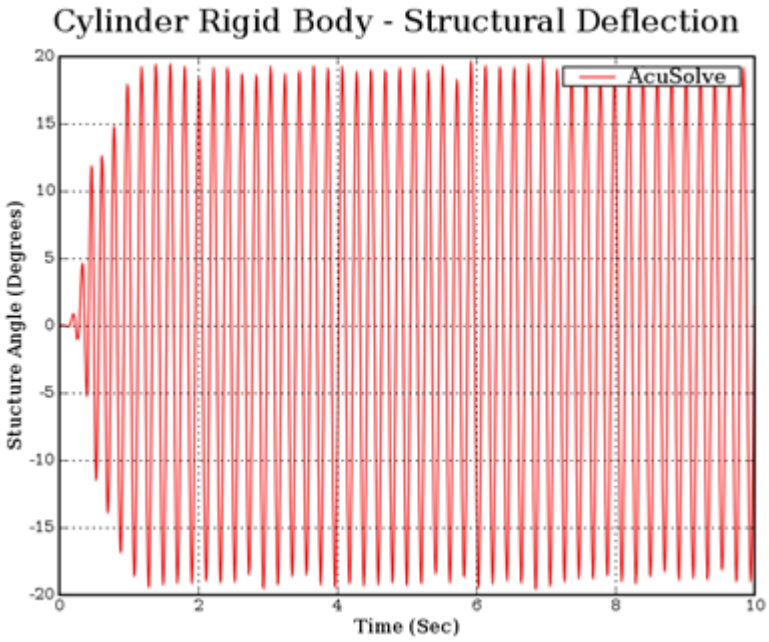


Figure 622: Rigid Body Displacement of the Assembly as a Function of Time, Showing the Oscillation Develop into the Pseudo-Steady Motion

The dominant frequency of the oscillation is easily identified in the Fast Fourier Transform (FFT) of the deflection angle, shown in the plot below.

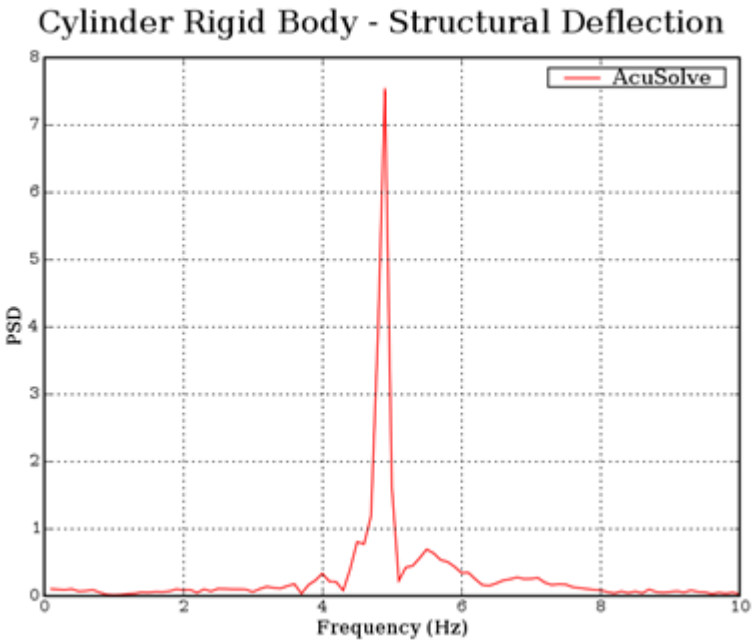


Figure 623: FFT of the Rigid Body Displacement Angle, Showing Power Spectral Density as a Function of Frequency

Summary

The AcuSolve solution compares well with experimental data for flow past an oscillating cylinder/plate assembly. In this application, water moves over the cylinder/plate assembly, giving rise to unsteady loading that causes the body to rotate as a rigid body. The good agreement with the natural frequency of oscillation compared to the experimental data demonstrates that AcuSolve is capable of predicting fluid forced motion with an internal rigid body dynamic solver.

Simulation Settings for Turbulent Flow Over an Oscillating Rigid Body Assembly

AcuConsole database file: `<your working directory>\cylinder_rigidbody_turbulent\cylinder_rigidbody_turbulent.acs`

Global

- Problem Description
  - Analysis type - Transient
  - Turbulence equation - SST
  - Mesh Type- Fully Specified
- Auto Solution Strategy
  - Final Time - `10.0`
  - Initial Time Increment- `0.005`
  - Convergence tolerance- `0.001`
  - Max stagger iterations- `3`
- Material Model
  - Water
    - Type- Constant
    - Density- `998.0` kg/m3
    - Viscosity- `0.00096806` kg/m*sec
- Mesh Motion
  - Interpolated
    - Type- Interpolated Motion
    - Interpolated motion surfaces
      1. Bottom
      2. Top
  - RigidBody
    - Type- Rigid Body Dynamic
      1. Z rotation- Active
      2. Mass- `0.2089` kg
      3. Dyadic
         1. X-X - `3.7 e-5` kg-m2
         2. Y-Y- `3.7 e-5` kg-m2
         3. Z-Z - `3.7 e-5` kg-m2

Model
- Volumes
  - Volume
    - Element Set
      1. Material model- Water
      2. Mesh motion- Interpolated
- Surfaces
  - Body
    - Simple Boundary Condition
      1. Type- Wall
      2. Mesh displacement BC type- Fixed
      3. Mesh motion- RigidBody
    - Interpolated Motion Surface
  - Bottom
    - Simple Boundary Condition
      1. Type- Wall
      2. Mesh displacement BC type- Fixed
    - Interpolated Motion Surface
  - Inflow
    - Simple Boundary Condition
      1. Type- Inflow
      2. Inflow type- Velocity
      3. X Velocity- `1.07` m/sec
      4. Turbulence input type- Auto
      5. Turbulence intensity type- High
    - Advanced Options
      1. Nodal Boundary Conditions
      2. X-velocity
         1. Type- Linear
         2. Precedence- `2`
         3. Curve fit variable- Y coordinate
         4. Curve fit values- Provided
      3. Y-velocity
         1. Type- Zero
      4. Z-velocity
         1. Type- Zero
  - Bottom
    - Simple Boundary Condition

1. Type- Wall
2. Mesh displacement BC type- Fixed
3. Mesh motion- RigidBody

- Interpolated Motion Surface

- Outflow
  - Simple Boundary Condition
    1. Type- Outflow
- Top
  - Simple Boundary Condition
    1. Type- Wall
    2. Mesh displacement BC type- Fixed
  - Interpolated Motion Surface
- maxZ
  - Simple Boundary Condition
    1. Type- Slip
- minZ
  - Simple Boundary Condition
    1. Type- Slip

References

Gomes, J. P. and Lienhart, H. (2009) Experimental Benchmark: Self-excited Fluid-structure Interaction Test Cases, in Fluid-Structure Interaction II: Modeling, Simulation, Optimization, Bungartz, H. J., Mehl, M., Schafer, M. (eds.), 383-412, Springer-Verlag.Ryhming.

Circumferential Flow in a Cylinder Induced by a Rotating Solid

In this application, AcuSolve is used to simulate the flow of air between concentric cylinders that is initiated by the rotation of the solid inner cylinder. The outer cylinder is held stationary while the inner cylinder rotates with a constant speed. AcuSolve results are compared with analytical results as described in White (1991). The close agreement of AcuSolve results with analytical results validates the ability of AcuSolve to maintain a continuous velocity across a non-conformal guide surface interface.

Problem Description

The problem consists of a fluid with material properties of a viscous fluid with the density of air rotating between two infinitely long concentric cylinders, as shown in the following image, which is not drawn to scale. The radius of the outer cylinder is 3.0 m and the radius of the inner cylinder is 1.5 m. The inner cylinder is defined as a solid medium and rotates at 1 rad/sec. The inner cylinder's surface velocity is mapped to the adjacent surface within the fluid medium, while the outer cylinder is fixed. The induced flow is laminar and exhibits a steady state behavior after running for a short period of physical time. The rotation of the inner cylinder causes the fluid to rotate due to viscous shearing near the wall. As the outer cylinder is fixed, a velocity gradient is generated as a function of radius within the flow domain.

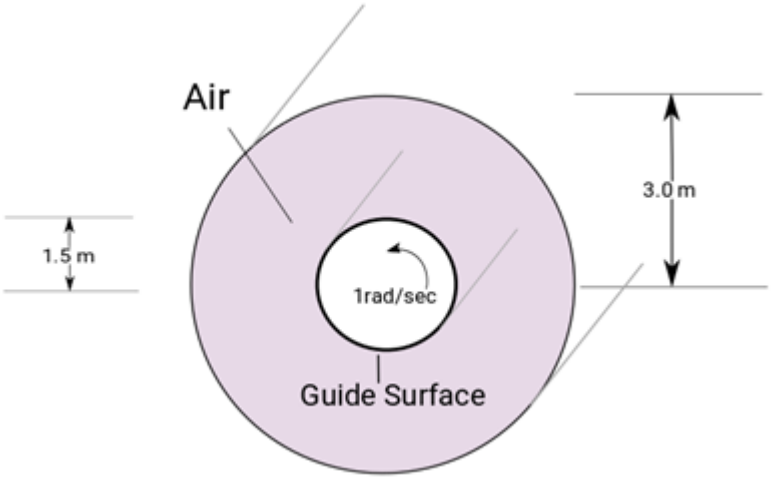


Figure 624: Critical Dimensions and Parameters Used for Simulating Flow Between Two Concentric Cylinders Split with a Guide Surface

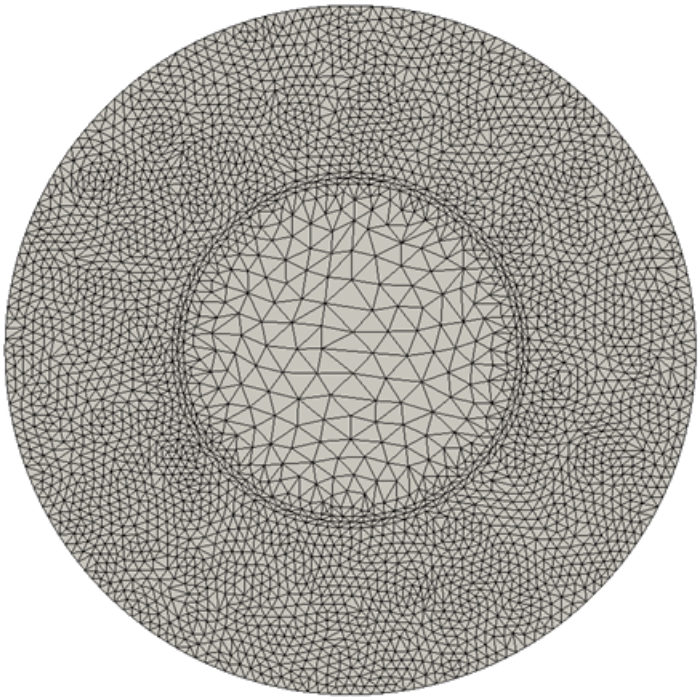


Figure 625: Mesh Used for Simulating Flow Between Two Concentric Cylinders

The simulation was performed as a two dimensional problem by constructing a volume mesh that contains a single layer of elements in the extruded direction, normal to the flow plane and by imposing slip flow and mesh boundary conditions on the extruded planes.

AcuSolve Results

The AcuSolve solution reaches a quasi-static result with the velocity between the two cylinders reaching a steady state at the simulation end time. As the solid inner cylinder rotates, it acts as a guide surface for the fluid elements to track and inherit the two velocity components. The velocity at the edge of the inner cylinder is equal to exactly the rotational speed multiplied by the radius. As the radius increases, the flow velocity reduces until it reaches zero at the outer diameter. The following images show the tangential velocity within the fluid as a function of radius from the center. The tangential velocity is compared with the analytical solution. The image below shows black circles representing the analytical solution and a solid red line for the AcuSolve results.

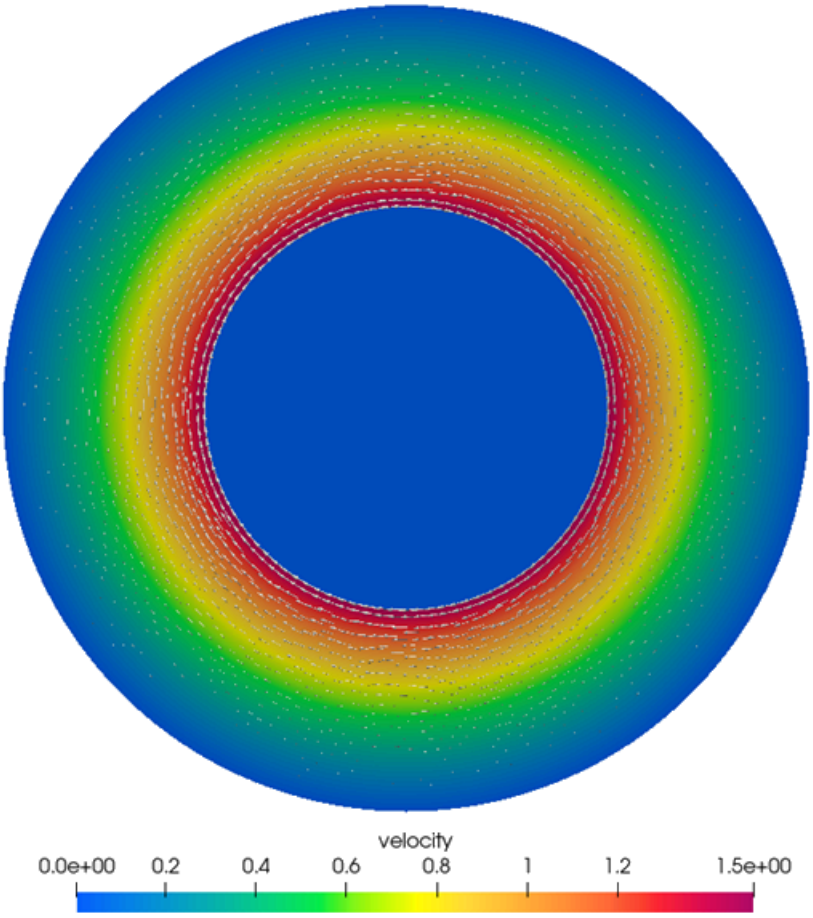


Figure 626: Contours and Vectors of Velocity Between the Concentric Cylinders

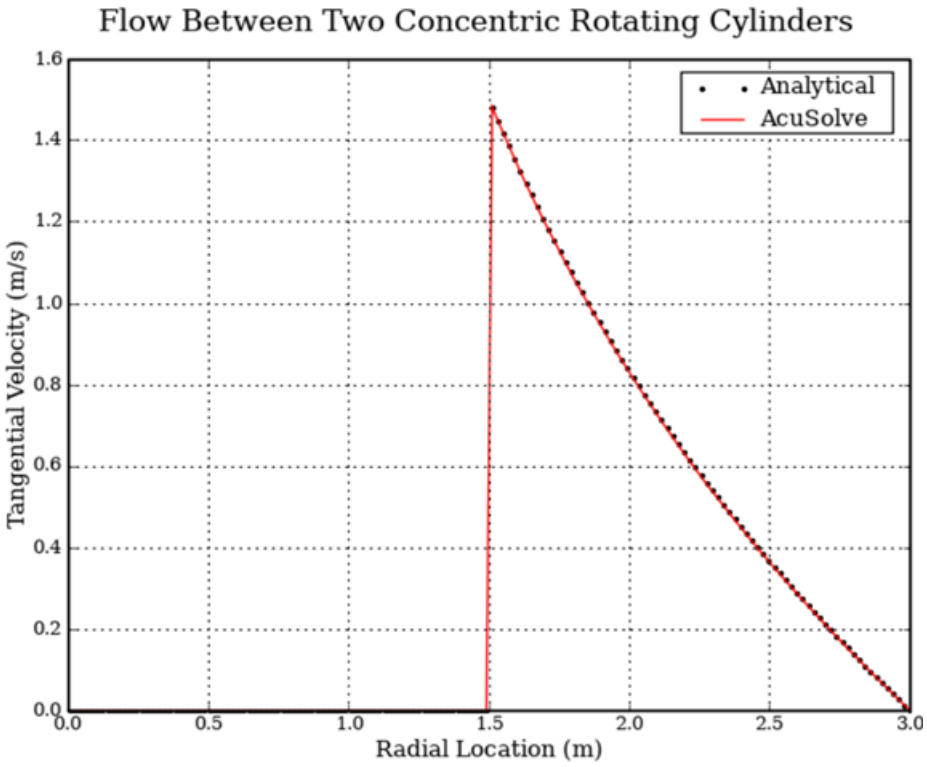


Figure 627: Tangential Velocity Within the Solid and Fluid as a Function of Radial Distance from the Center at the Final Timestep

Summary

The AcuSolve solution compares well with analytical results for laminar flow between concentric cylinders, where the inner cylinder guides the adjacent fluid elements. In this application, a fluid initially at rest inherits the angular velocity from the inner cylinder while the outer cylinder does not rotate. As a result of the inherited velocity and viscosity of the fluid, flow develops between the two cylinders. The AcuSolve solution for the tangential velocity as a function of radius matches exactly with the analytical results.

Simulation Settings for Flow Between Concentric Split Cylinders

HyperWorks CFD database file: `<your working directory>\annulus_split_rotating \annulus_split_rotating.hm`

- Problem Description
  - Analysis type - Transient
  - Flow equation - Navier Stokes
  - Turbulence equation - Laminar
  - Mesh type - Arbitrary Mesh Movement (ALE)
- Auto Solution Strategy
  - Max time steps - `40`
  - Initial time increment- `0.02` sec

- Convergence tolerance - `0.001`
- Min stagger iterations - `2`
- Max stagger iterations - `4`

- Material Model
  - Air
    - Density
      1. Type - Constant
      2. Density - `1.225` kg/m3
    - Viscosity
      1. Type - Constant
      2. Viscosity - `1.781` kg/m-sec
- Mesh Motion
  - Rotation
    - Rotation Center
      1. X-coordinate - `2.0` m
      2. Y-coordinate - `0.0` m
      3. Z-coordinate - `0.0` m
    - Angular velocity
      1. X-component - `1.0` rad/sec
      2. Y-component- `0.0` rad/sec
      3. Z-component - `0.0` rad/sec

  Model
- Volumes
  - CylinderInner
    - Element Set
      1. Medium - Solid
      2. Material model - Aluminum
  - CylinderOuter
    - Element Set
      1. Medium - Fluid
      2. Material model - Air
- Surfaces
  - InBottom
    - Simple Boundary Condition
      1. Type- Slip
      2. Mesh displacement type- Slip
  - InInterf

        - Simple Boundary Condition
            1. Type- Wall
            2. Mesh displacement type- Fixed
            3. Mesh motion- Rotation
        - Guide Surface
            1. Type- Faceted
    - InTop
        - Simple Boundary Condition
            1. Type- Slip
            2. Mesh displacement type- Slip
    - OutBottom
        - Simple Boundary Condition
            1. Type- Slip
            2. Mesh displacement type- Slip
    - OutInterf
        - Simple Boundary Condition
            1. Type- Wall
            2. Wall velocity type- Match Mesh Velocity
            3. Mesh displacement type- Guide surface
            4. Guide surface- InInterf
    - OutTop
        - Simple Boundary Condition
            1. Type- Slip
            2. Mesh displacement type- Slip
    - OutWall
        - Simple Boundary Condition
            1. Type- Wall
            2. Mesh displacement type- Fixed
- Nodes
    - PressurePoint
        - Pressure
            1. Type- Zero

References

F. M. White. "Viscous Fluid Flow". Section 3-2.3. McGraw-Hill Book Co., Inc. New York. 1991.

Multiphase Flow Within a Sloshing Tank

In this application, AcuSolve is used to simulate water and the time-dependent interface of air-water within a tank subject to a prescribed sloshing motion. AcuSolve results are compared with experimental pressure measurements as reported by Tankaka, et al. (2000) and Rhee (2005). The close agreement of AcuSolve results with experimental results validates the ability of AcuSolve to model multiphase flow problems with user-defined motion.

Problem Description

The problem consists of a tank filled to 20 percent capacity with water that is rotated or translated according to a user-defined function, as shown in the following image, which is not drawn to scale, where three monitoring locations, P1, P2 and P3, are denoted. The motion of the tank causes the fluid to begin sloshing rapidly, creating a time-dependent pressure field due to the height of the local water column. Non-slip boundary conditions for the top, bottom, left and right sides are applied with slip boundary conditions on the front and back faces. The SST turbulence model along with a global time-step of 0.001 seconds is used for the simulation. The pressure at each of the monitoring locations is compared against the experimental measurements as described in Tankaka, et al. (2000). It should be noted that the pressure computed and presented in the images represent the time-dependent dynamic pressure, static pressure is subtracted to be consistent with the measurements, at the specified point. Roll-Short is the case provided with the Validation Manual. The results for this case as well as Sway - Short are presented within this overview. In each case, the motion profile is defined with the following function and coefficients as defined in the table below.

$$x = A\sin(\omega t) \tag{28}$$

Where A = amplitude of oscillation, ω = frequency of oscillation = 2 π/T, t = time (sec) and T = Time period of oscillation (sec).

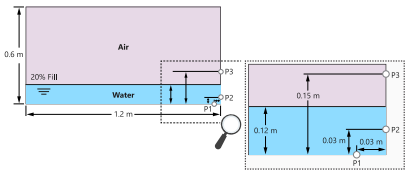


Figure 628: Critical Dimensions and Parameters for Simulating a 2D Tank Slosh with Mesh Motion

Table 39: Sine Function Scaling Parameters for Tank Motion Profile

Cases	Mesh Motion	Amplitude (A)	Time Periods (T)	Tank Filling Level
Sway – Base	Sway motion	0.06 m	1.94 sec	20% height

Cases	Mesh Motion	Amplitude (A)	Time Periods (T)	Tank Filling Level
Sway – Short	Sway motion	0.06 m	1.74 sec	20% height
Roll – Base	Rolling motion	10 degrees	2.25 sec	20% height
Roll – Short	Rolling motion	10 degrees	1.85 sec	20% height

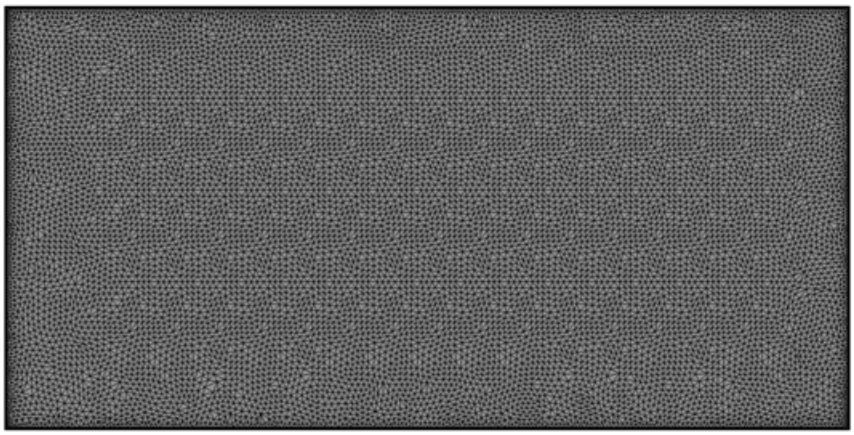


Figure 629: Mesh Used for Simulating Multiphase Sloshing Within a 2D Tank

AcuSolve Results

The AcuSolve solution is run for a time of t/T=5.0, 9.25 sec for Roll - Short, and the results presented reflect the transient motion of the water within the tank. The experimental values of pressure (kPa) and normalized simulation time are presented with the corresponding AcuSolve results at three measurement locations. The AcuSolve results show good agreement with the experimental results for pressure magnitude, the local water column height, as well as accurate timing of the peaks, indicating that the air-water interface is properly captured. Additional motion cases, as well as comparisons between two dimensional versus three dimensional simulations have been simulated with AcuSolve. The accuracy and solution requirements of these simulations are omitted for brevity but are available upon request. It was found that the differences between 2D and 3D simulations may be of interest for engineers, however the 2D results are shown to be adequate and less computationally expensive than 3D in the cases studied.

User-Defined Multiplier Function

This validation case relies on defining the motion of the elements within the tank, leading to the water sloshing in the presence of air. The motion is defined using an AcuSolve User-Defined Function (UDF) to specify the time-dependent multiplier function applied to the mesh motion command. The mesh motion is assigned to the Fluid element set, causing all of the elements to move according to the specified sine function. For the Roll - Short case, the mesh motion command is specified as rotation with the rotation multiplier function specified as rotation. If you are interested in simulating one of the other motion profiles, for example Sway - Base/Short, the type of mesh motion command would be changed to translation with the translation multiplier function assigned with the same UDF. The function name is designated at usrMotion and is contained within the source file `motion.c`. The source file, along with

pre-compiled binaries for Linux64 and Windows64 are provided with the validation case. Depending on your architecture it may be necessary to re-compile the source on the local system. Please refer to the *Programs Reference Manual* for details on using AcuMakeLib or AcuMakeDll for Linux and Windows, respectively.

Summary

The AcuSolve solution compares well with experimental results for tank sloshing simulations. In this application, the time dependent motion of the tank and the multiphase flow solution are simulated with AcuSolve using the level-set formulation and the SST turbulence model. The experimental values for instantaneous pressure at three locations and for two motion profiles are presented with the corresponding AcuSolve results. A good agreement of simulation results with the experiment validates the ability to solve time-dependent/accurate sloshing cases using the multiphase capabilities of AcuSolve.

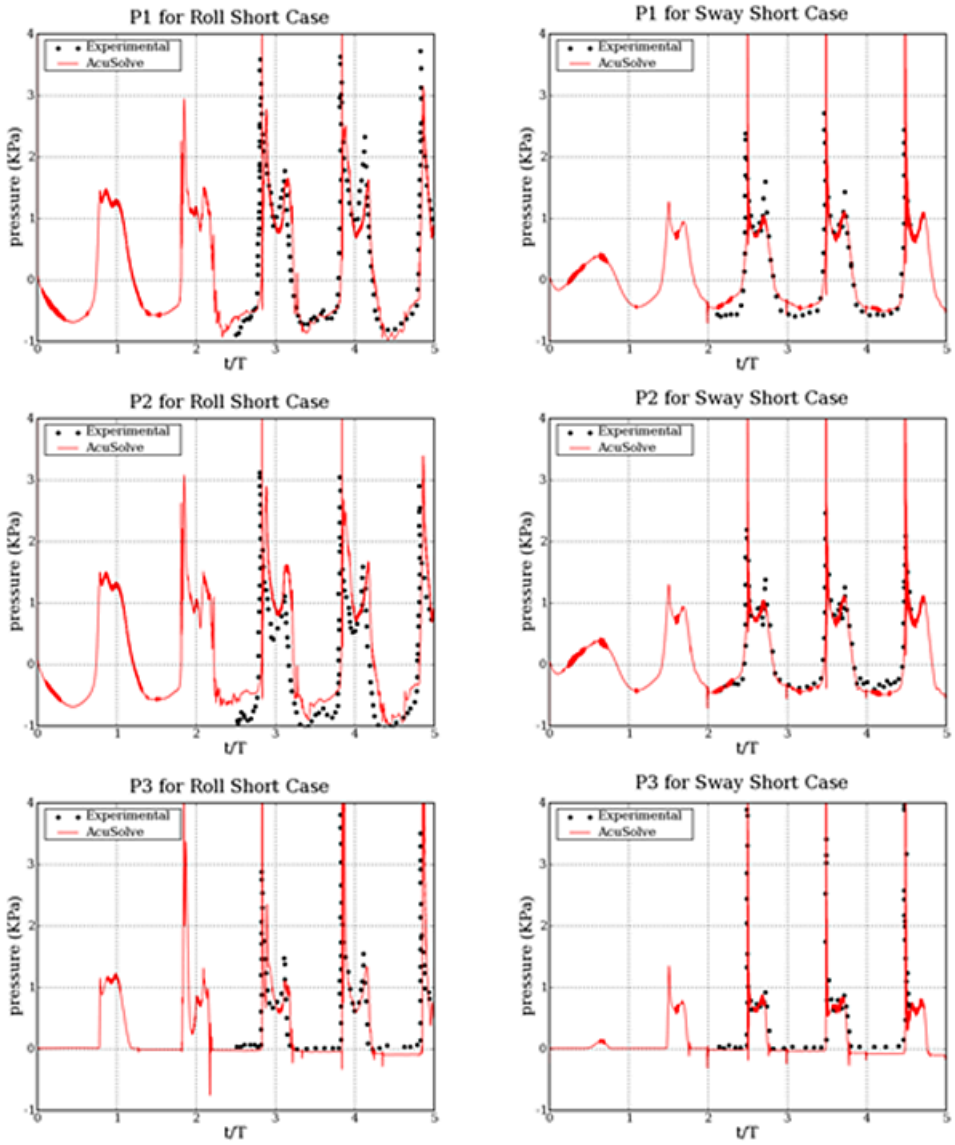


Figure 630: Time Dependent Pressure at Three Monitoring Locations Within the Sloshing Tank for Two Motion Profiles (Roll-Short, Left and Sway-Short, Right)

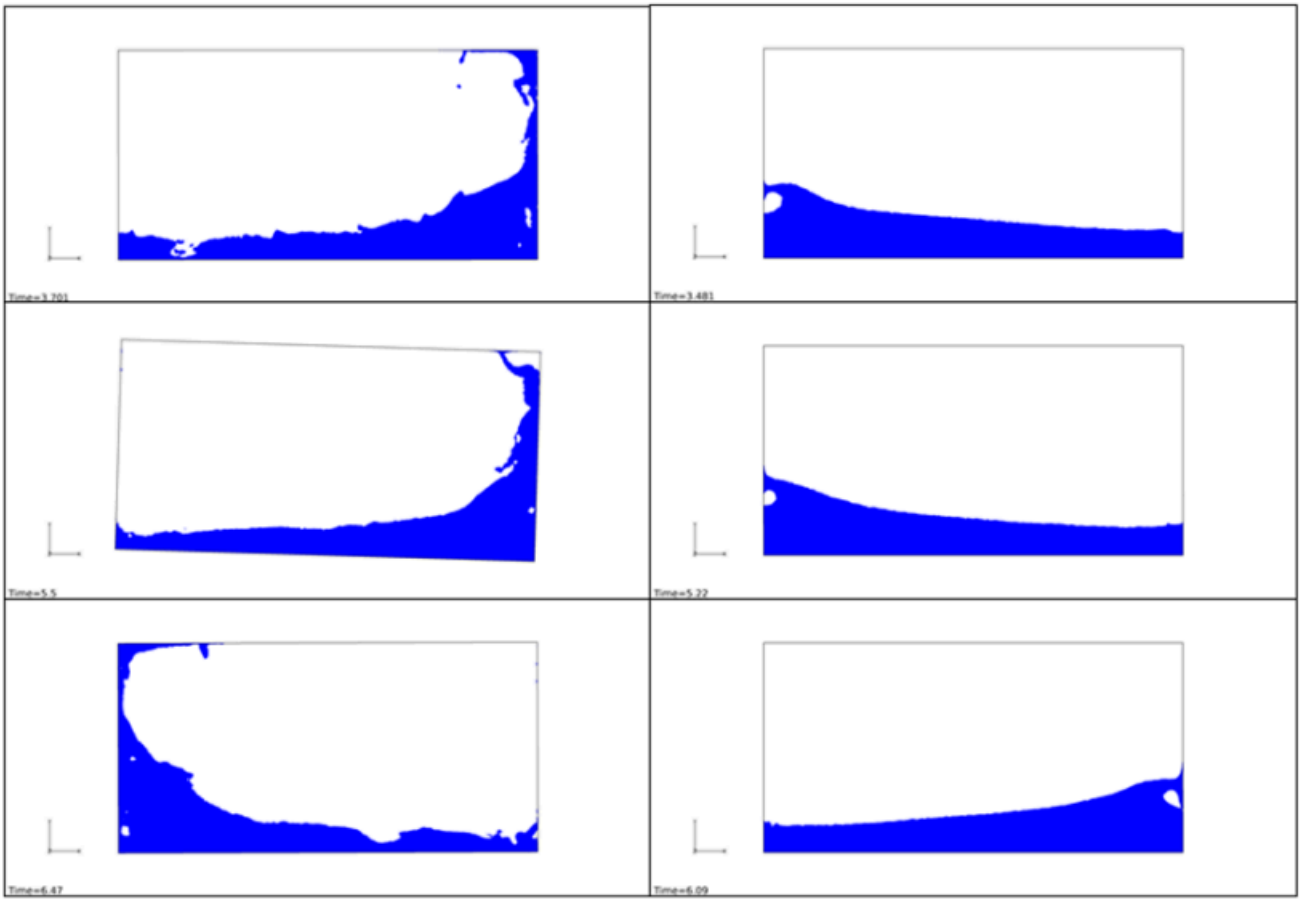


Figure 631: Instantaneous Volume Fraction Contour (Blue Showing Water) at Three Moments in Time (t/T=2.0, 3.0 and 3.5) for Two Motion Profiles (Roll-Short, Left and Sway-Short, Right)

Simulation Settings for Multiphase Flow Within a Sloshing Tank

AcuConsole database file: `<your working directory>\tank_sloshing_multiphase \tank_sloshing.acs`

Global

- Problem Description
  - Analysis type - Transient
  - Turbulence equation - SST
  - Multiphase equation – Level Set
- Auto Solution Strategy
  - Final time - `9.5` sec
  - Initial time increment - `0.001` sec
  - Min stagger iterations - `2`
  - Max stagger iterations - `10`
  - Fluid 1 - Water
  - Fluid 2 - Air

- Multiplier Function
  - rotation
    - Type - User Function
    - User function name - UsrMotion
    - User function values - `10.0`, `1.85`, `0.0`
- Material Model
  - Air
    - Type - Constant
    - Density - `1.225` kg/m^3
    - Velocity - `1.781e-5` kg/m-sec
  - Water
    - Type - Constant
    - Density - `1000` kg/m^3
    - Velocity - `0.001` kg/m-sec
- Mesh motion
  - rotation
    - Type - Rotation
    - Rotation center – `0.0`, `0.0`, `0.0`
    - Angular velocity – `0.0`, `0.0`, `0.0174533` (1.0 deg/sec)
    - Rotation variable – Multiplier Function
    - Rotation multiplier function – rotation

  Model
  - Volumes
    - Fluid
      1. Element Set
         1. Medium – Multiphase
         2. Multi field model – Water-Air
         3. Body force – Gravity
         4. Mesh motion – rotation
- Surfaces
  - x+
    - Simple Boundary Condition – Wall
  - x-
    - Simple Boundary Condition – Wall
  - y+
    - Simple Boundary Condition – Wall
  - y-
    - Simple Boundary Condition – Wall

- z+
  - Simple Boundary Condition – Slip
- z-
  - Simple Boundary Condition – Slip

References

Shin Hyung Rhee, 2005, "Unstructured Grid Based Reynolds-Averaged Navier-Stokes Method for Liquid Tank Sloshing", Journal of Fluids Engineering, Vol 127, pp. 572- 582.

Tanaka, Y., Ando, T., and Miyamoto, T., 2000, "Experimental Study on Sloshing Load Measured by Panel-Type Pressure Gauge," Proc. 74th. General Meeting of Ship Research Institute, Ship Research Institute, Tokyo, Japan, pp. 137-142.

Reference Frame

11

This section includes validation cases that consider multiple reference frame simulations to model the effects of simplified rotational motion.

This chapter covers the following:

- Flow Between Concentric Cylinders (p. 867)
- Flow Inside a Rotating Cavity (p. 873)
- Viscous Heating Inside a Rotating Annulus (p. 881)

Flow Between Concentric Cylinders

In this application, AcuSolve is used to simulate the flow of water between concentric cylinders. The outer cylinder is held stationary while the inner cylinder rotates with a constant speed. AcuSolve results are compared with analytical results as described in White (1991). The close agreement of AcuSolve results with analytical results validates the ability of AcuSolve to model cases containing thin annular gaps with flow induced by rotating walls.

Problem Description

The problem consists of two concentric pipes with water filling the void between them, as shown in the following image, which is not drawn to scale. The radius of the outer pipe is 0.0468 m and the radius of the inner pipe is 0.0178 m. The inner cylinder rotates at 1 rad/sec and the outer cylinder is fixed. The induced flow is laminar and exhibits a steady state behavior. The rotation of the inner cylinder causes the fluid to rotate due to viscous shearing near the wall. As the outer cylinder is fixed, a velocity gradient is generated as a function of radius within the flow domain.

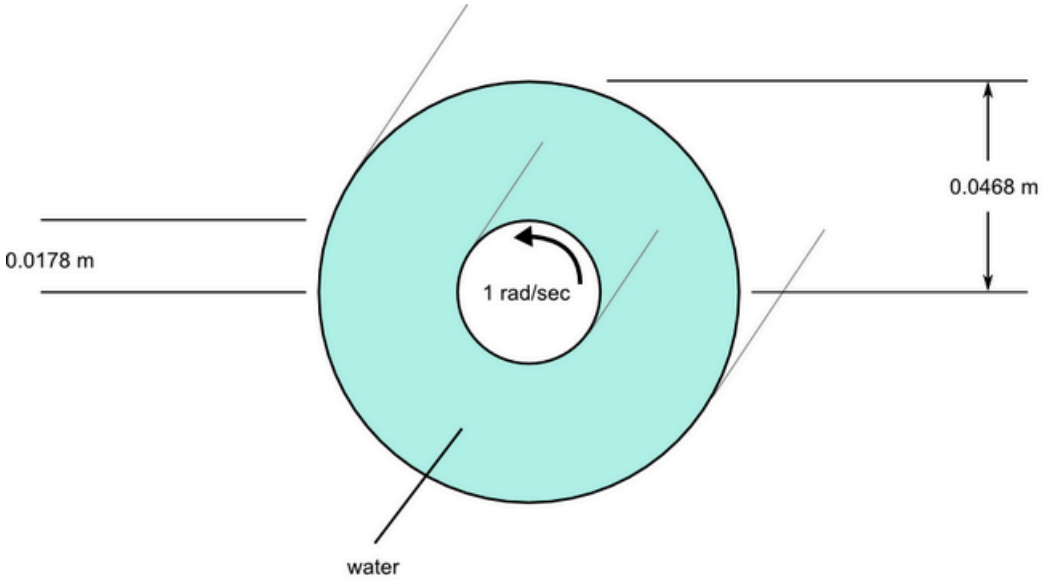


Figure 632: Critical Dimensions and Parameters for Simulating Flow Between Concentric Cylinders

The simulation was performed as a two dimensional problem by restricting flow in the out-of-plane direction through the use of a mesh that is one element thick.

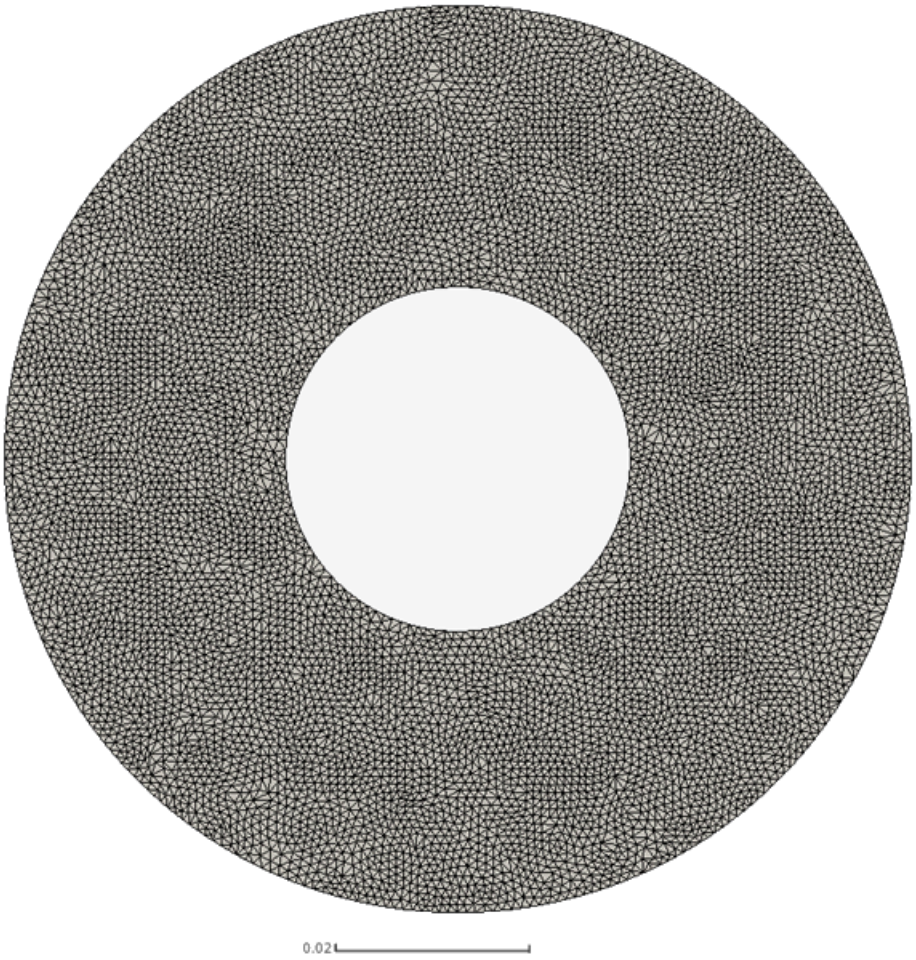


Figure 633: Mesh Used for Simulating Flow Between Concentric Cylinders

AcuSolve Results

The AcuSolve solution converged to a steady state and the results reflect the mean flow conditions. The velocity of the fluid within the cavity is greatest near the rotating inner cylinder. There is a nonlinear decrease in velocity as a function of distance away from the inner cylinder.

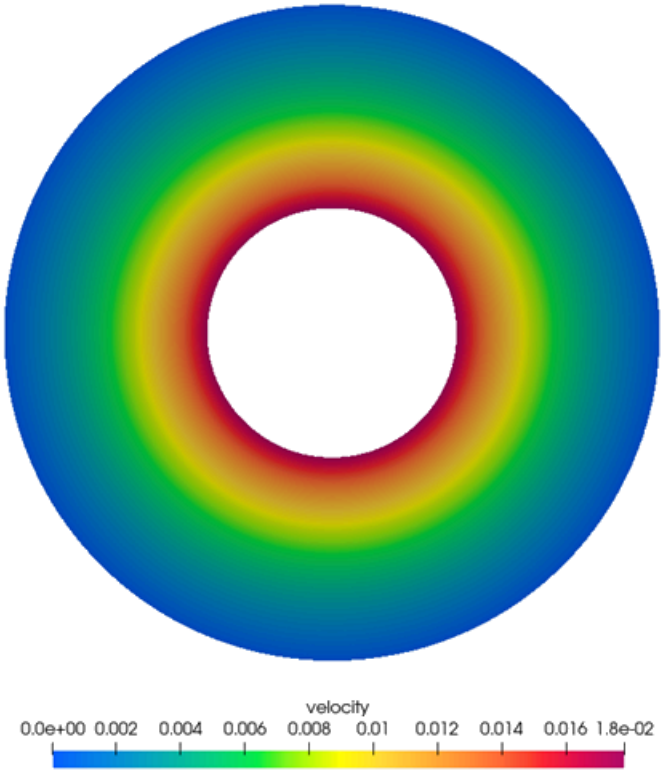


Figure 634: Contours of Tangential Velocity Between the Concentric Cylinders

Analytical tangential velocity at four distances away from the center of the rotating inner cylinder are presented with the corresponding AcuSolve results in the following table.

Table 40:

Distance from the center of rotating cylinder (m)	Analytical tangential velocity (m/s)	AcuSolve tangential velocity (m/s)	Percent deviation from analytical
0.020	0.01514	0.01514	0.04
0.025	0.01059	0.01058	0.10
0.030	0.00727	0.00727	0.06
0.035	0.00466	0.00466	0.10

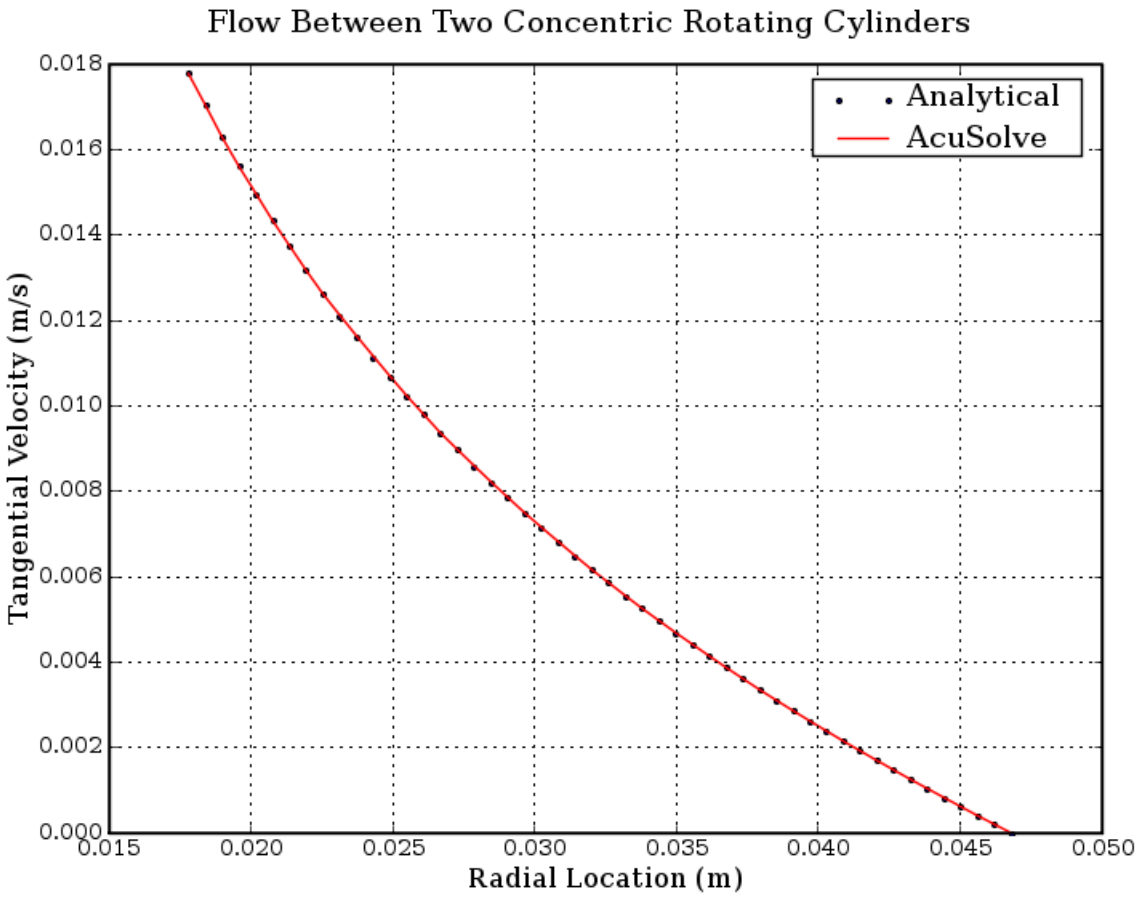


Figure 635: Tangential Velocity Plotted Against Distance from the Center of the Rotating Cylinder

Summary

The AcuSolve solution compares well with analytical results for the flow between concentric cylinders. In this application, the velocity in the annular fluid region is driven by the viscous stresses on the rotating wall. The AcuSolve tangential velocity is within 0.1 percent of the analytical solution at all radial locations.

Simulation Settings for Flow Between Concentric Cylinders

HyperWorks CFD database file: `<your working directory>\annulus_rotating\annulus_rotating.hm`

Global

- Problem Description
  - Analysis type - Steady State
  - Turbulence equation - Laminar
- Auto Solution Strategy
  - Relaxation Factor - `0.2`
- Material Model

- Water
  - Density - `1000.0` kg/m3
  - Viscosity - `0.001` kg/m-sec
- Reference Frame
  - Rotating_Cylinder
    - Rotation center
      1. X-coordinate - `0.0` m
      2. Y-coordinate - `0.0` m
      3. Z-coordinate - `0.0` m
    - Angular velocity
      1. X-component - `0.0` rad/sec
      2. Y-component - `0.0` rad/sec
      3. Z-component - `-1.0` rad/sec

Model

- Volumes
  - Volume
    - Element set
      1. Material model - Water
- Surfaces
  - Boundary1
    - Simple Boundary Condition
      1. Type - Symmetry
  - Boundary2
    - Simple Boundary Condition
      1. Type - Symmetry
  - Inner
    - Simple Boundary Condition
      1. Type - Wall
      2. Reference Frame - Rotating_Cylinder
  - Outer
    - Simple Boundary Condition
      1. Type - Wall
- Nodes
  - Fixed
    - Pressure
      1. Type - Zero

References

F. M. White. "Viscous Fluid Flow". Section 3-2.3. McGraw-Hill Book Co., Inc. New York. 1991.

Flow Inside a Rotating Cavity

In this application, AcuSolve is used to simulate the flow of air in an enclosed cylindrical cavity with a rotating top and a fixed bottom. AcuSolve results are compared with experimental data adapted from Michelsen (1986). The close agreement of AcuSolve results with experimental data validates the ability of AcuSolve to model cases containing enclosed cavities with flow induced by rotating walls.

Problem Description

The problem consists of air in an enclosed cylinder 1.0 m tall with a radius of 1.0 m, as shown in the following image, which is not drawn to scale. The top of the cylinder rotates about its center at 1 rad/s, while the bottom of the cylinder is fixed. As the container top spins, the viscous stresses on the fluid induce a circumferential (swirl) velocity throughout the height of the cylinder. In order to conserve mass and momentum, the fluid generates a radial velocity that changes direction based on distance away from the rotation center of the cylinder.

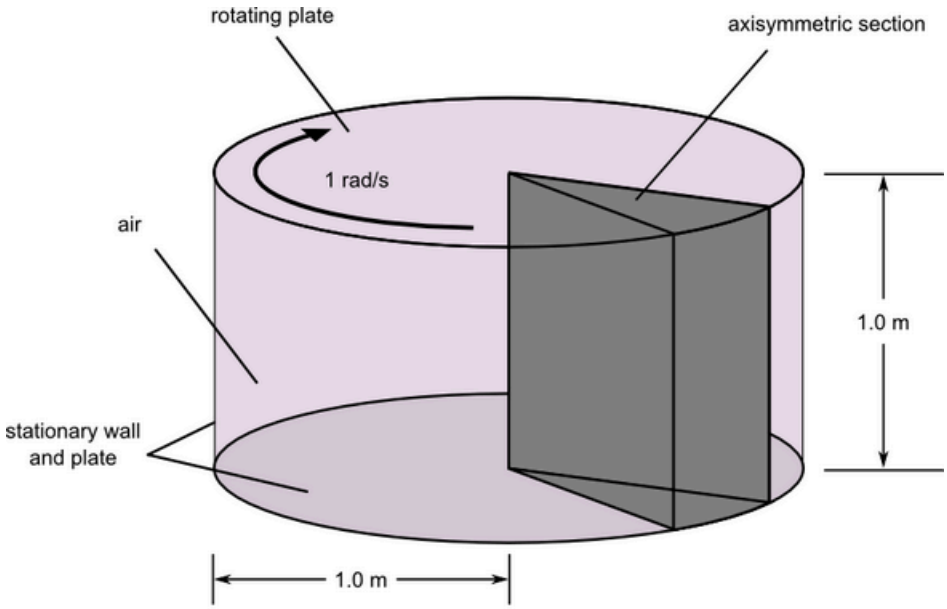


Figure 636: Critical Dimensions and Parameters for Simulating Flow Inside a Rotating Cavity

The flow domain is modeled with axisymmetric periodicity in the circumferential direction, which allows for accurate simulation of the flow while minimizing computational time.

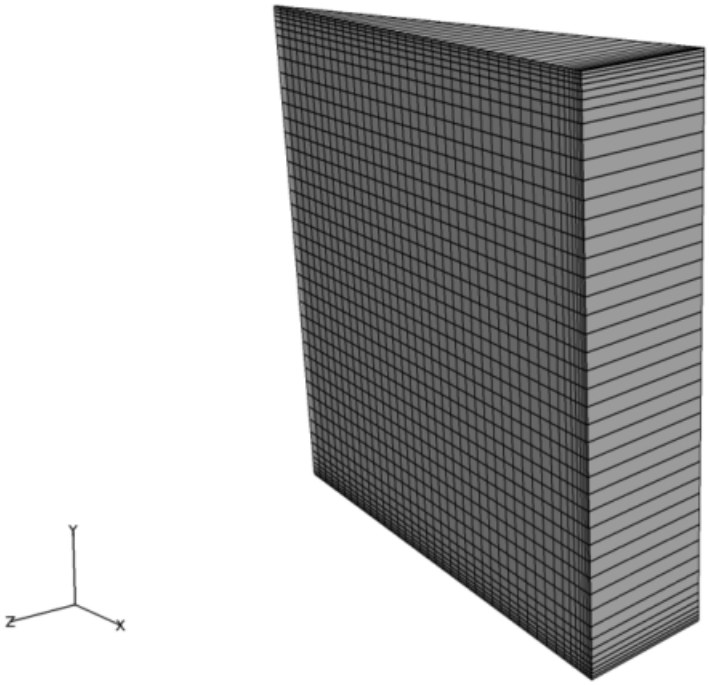


Figure 637: Mesh of Periodic Section Used for Simulating Flow Inside a Rotating Cylinder

AcuSolve Results

The AcuSolve solution converged to a steady state and the results reflect the mean flow conditions. The velocity varies with both vertical location and with distance from the rotation center. The complex flow field develops from a combination of the viscous stresses acting at the rotating cylinder top and at the stationary bottom.

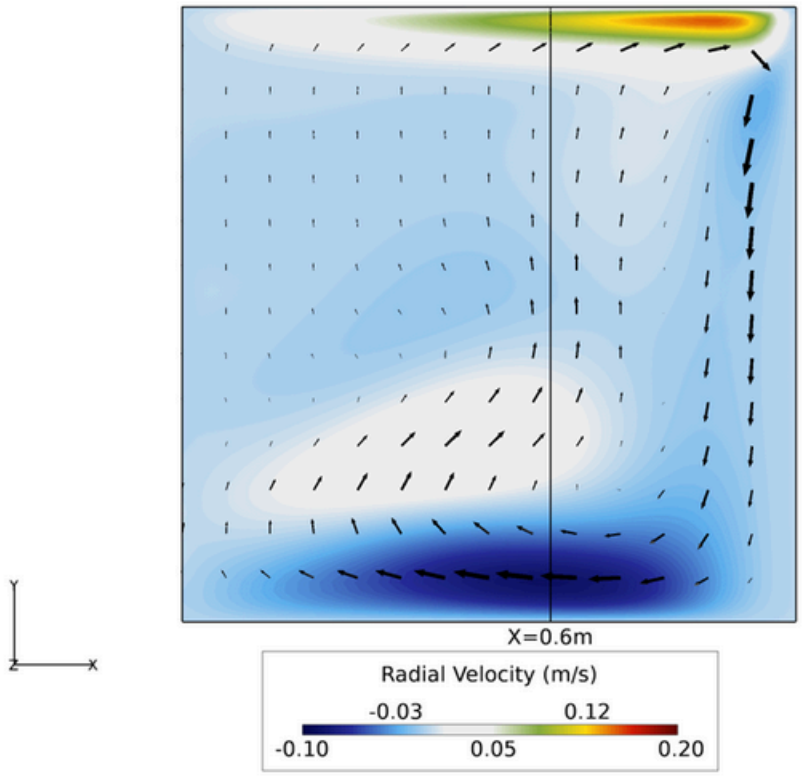


Figure 638: Contours of Radial Velocity with Velocity Vectors. This Image Shows the Front Face of the Modeled Cylinder Wedge, with the Center of Rotation on the Left Edge. The Vertical Line Represents a Radial Location 0.6 m From the Center of Rotation.

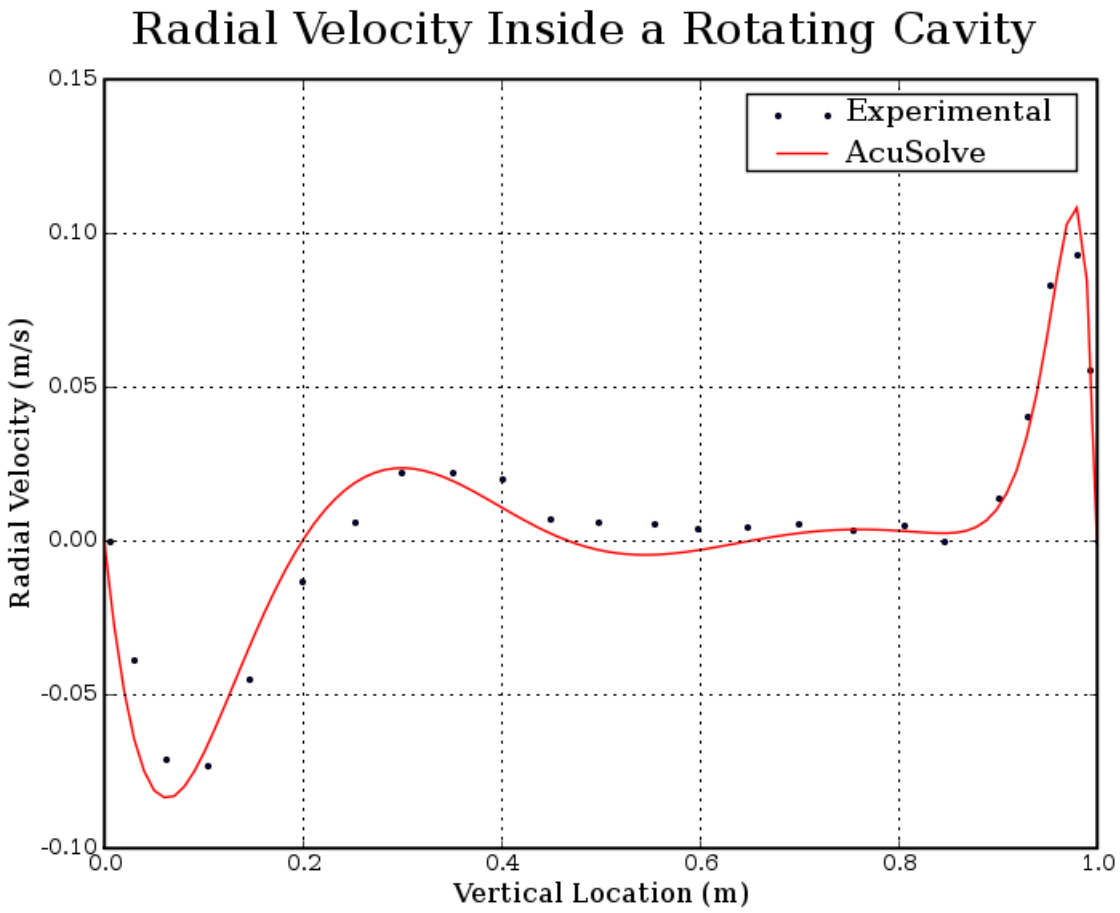


Figure 639: Radial Velocity (at 0.6 m From the Center of Rotation) as a Function of Vertical Location From Cylinder Bottom

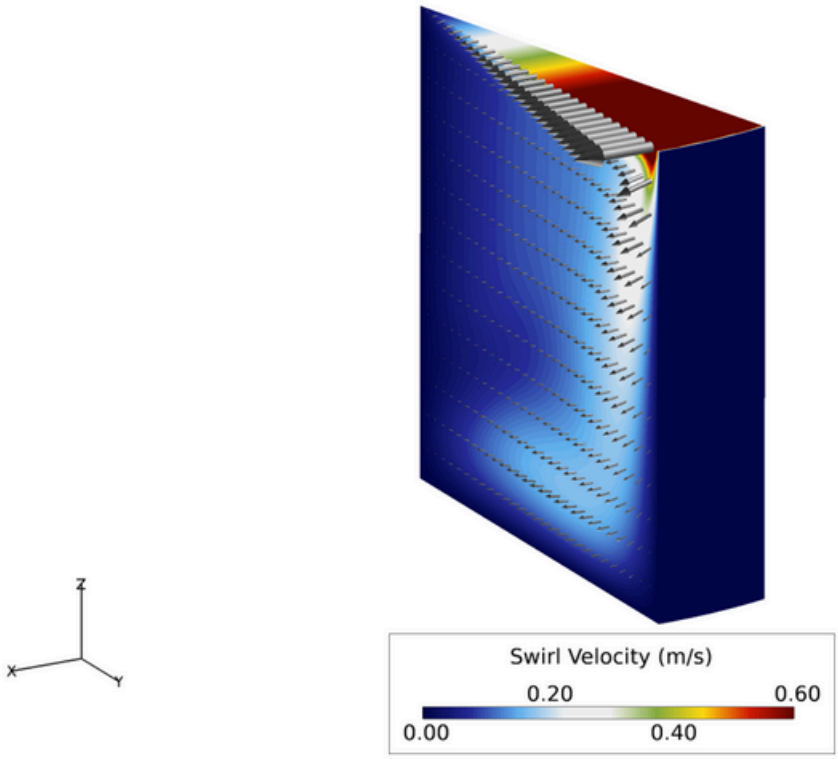


Figure 640: Contours of Swirl Velocity with Velocity Vectors

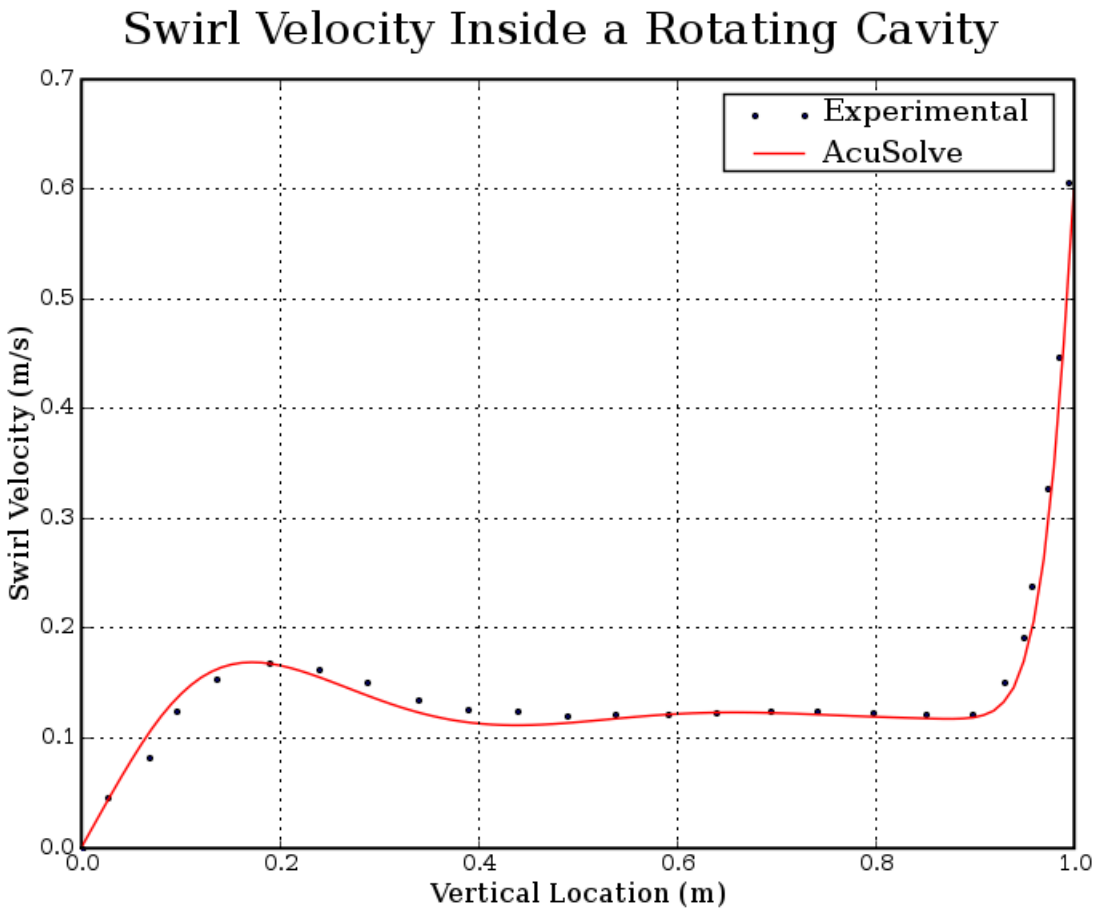


Figure 641: Swirl Velocity (at 0.6 m From Center of Rotation) as a Function of Vertical Location From the Cylinder Bottom

Summary

The AcuSolve solution compares well with the experimental data for flow induced by a rotating top of an enclosed cylinder. In this application, the flow in the fluid region is driven by the viscous stresses near the rotating top. Viscous stresses drag the fluid in a circular direction near the spinning wall. The angular velocity of the fluid decreases as distance from the top wall increases. Radial velocity develops as a result of the migration of the fluid toward the outer wall in regions of high angular velocity. The AcuSolve radial and swirl velocities compare very closely with the experimental data.

Simulation Settings for Flow Inside a Rotating Cavity

AcuConsole database file: `<your working directory>\cavity_rotating\cavity_rotating.acs`

Global

- Problem Description
  - Analysis type - Steady State
  - Turbulence Equation - Laminar
- Auto Solution Strategy

- Relaxation Factor - 0.4

- Material Model
  - Air
    - Density - 1.0 kg/m3
    - Viscosity - 0.000556 kg/m-sec
- Reference Frame
  - Cavity Rotation
    - Rotation center
      1. X-coordinate - 0.0
      2. Y-coordinate - 0.0
      3. Z-coordinate - 0.0
    - Angular velocity
      1. X-component - 0.0
      2. Y-component - -1.0 rad/sec
      3. Z-component - 0.0

Model

- Volumes
  - Fluid
    - Element Set
      1. Material model - Air
- Surfaces
  - Bottom
    - Simple Boundary Condition
      1. Type - Wall
  - Max_X
    - Simple Boundary Condition
      1. Type - Wall
  - Max_Z
    - Simple Boundary Condition - (disabled to allow for periodic conditions to be set)
  - Min_Z
    - Simple Boundary Condition - (disabled to allow for periodic conditions to be set)
  - Top
    - Simple Boundary Condition
      1. Type - Wall
      2. Reference frame - Cavity Rotation
- Periodics
  - Periodic 1

- Periodic Boundary Condition
  1. Type - Axisymmetric
  2. Rotation axis
     1. point 1
        1. X-coordinate - `0.0` m
        2. Y-coordinate - `0.0` m
        3. Z-coordinate - `0.0` m
     2. point 2
        1. X-coordinate - `0.0` m
        2. Y-coordinate - `1.0` m
        3. Z-coordinate - `0.0` m

References

J. A. Michelsen. "Modeling of Laminar Incompressible Rotating Fluid Flow". AFM 86-05. Ph.D. thesis, Department of Fluid Mechanics, Technical University of Denmark. 1986.

Viscous Heating Inside a Rotating Annulus

In this application, AcuSolve is used to simulate fluid flow and viscous heating in an annulus formed by concentric cylinders. AcuSolve results are compared with analytical results adapted from Bird and others (1960). The close agreement of AcuSolve results with analytical results validates the ability of AcuSolve to model cases with viscous heating.

Problem Description

The problem consists of a viscous fluid filling the annulus between two concentric cylinders, as shown in the following image, which is not drawn to scale. The inner cylinder has a radius of 1.0 m and is fixed in place. The outer cylinder has a radius of 2.0 m and rotates with a constant angular velocity of 0.5 rad/s. The inner cylinder is held at a constant temperature of 273 K and the outer cylinder is held at 274 K.

The rotation of the outer cylinder causes the fluid to rotate due to the viscous shearing near the wall. As the inner cylinder is fixed, a velocity gradient is generated as a function of distance from the inner cylinder center. Viscous stresses within the domain generate significant amounts of heat, leading to a substantial increase in the fluid temperature in regions of high shear.

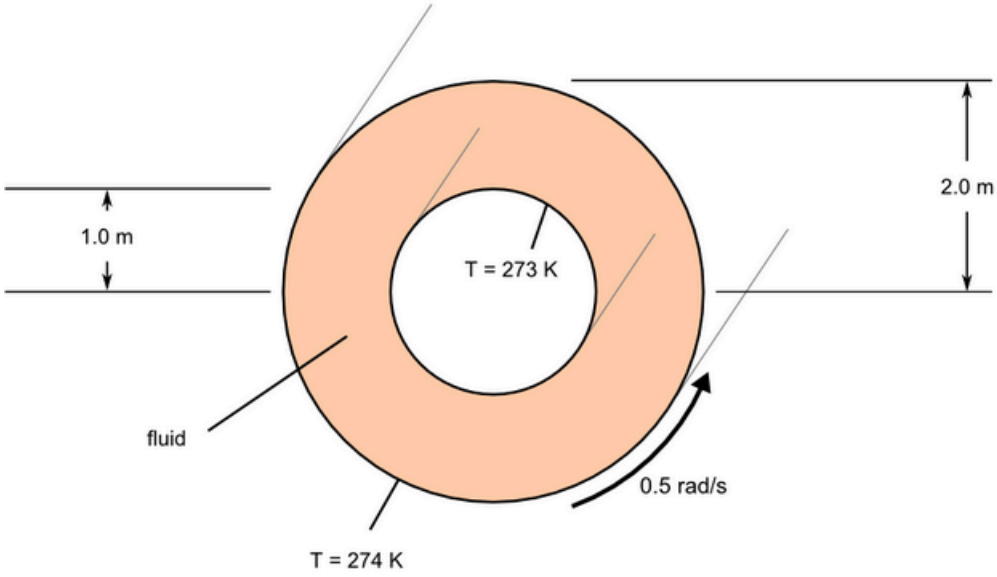


Figure 642: Critical Dimensions and Parameters for Simulating Viscous Heating Inside a Rotating Annulus

The simulation was performed as a two dimensional problem by constructing a volume mesh that contains a single layer of elements in the extruded direction, normal to the flow plane, and by imposing symmetry boundary conditions on the extruded planes.

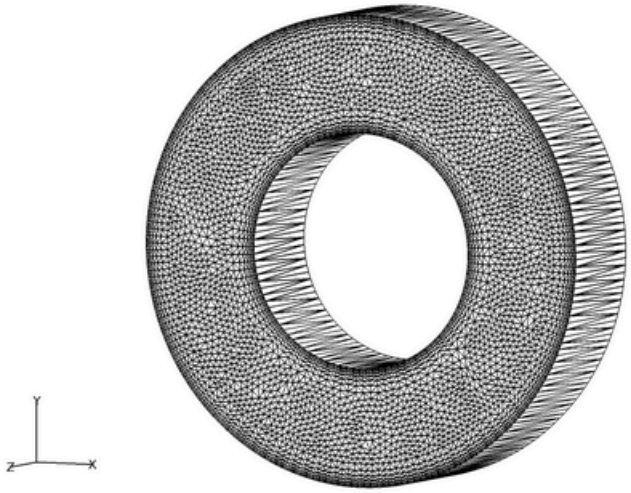


Figure 643: Mesh used for Simulating Viscous Heating Inside a Rotating Annulus

AcuSolve Results

The AcuSolve solution converged to a steady state and the results reflect the mean flow conditions. Flow is induced by the viscous shearing near the outer wall, creating a velocity gradient with the highest velocity near the moving wall.

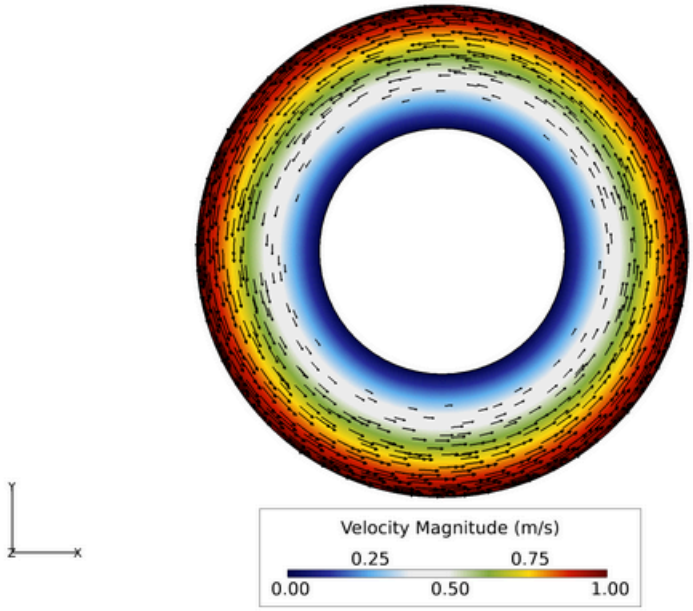


Figure 644: Contours of Velocity Magnitude and Velocity Vectors

The velocity gradient causes viscous heating, causing the fluid temperature to increase. The resulting temperature profile is nonlinear with the highest temperatures occurring in the space between the cylinders.

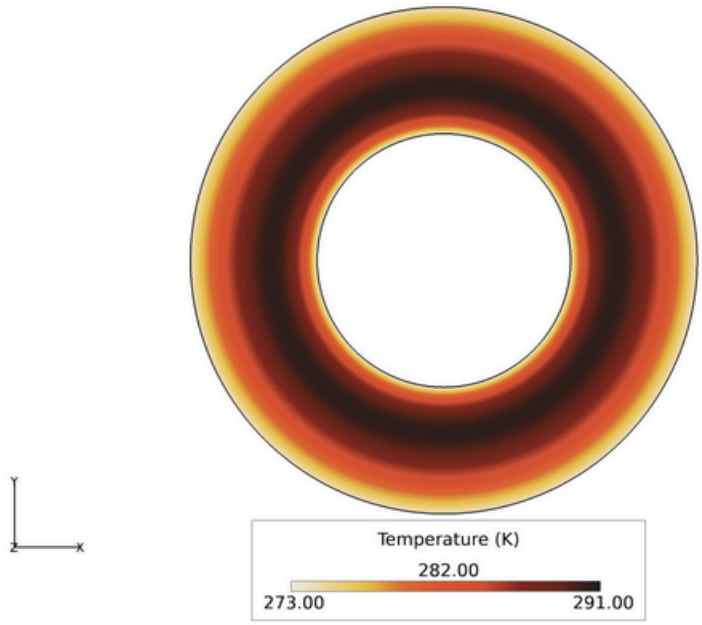


Figure 645: Contours of Temperature

AcuSolve results were compared to analytical results for velocity and for temperature across a range of radial locations.

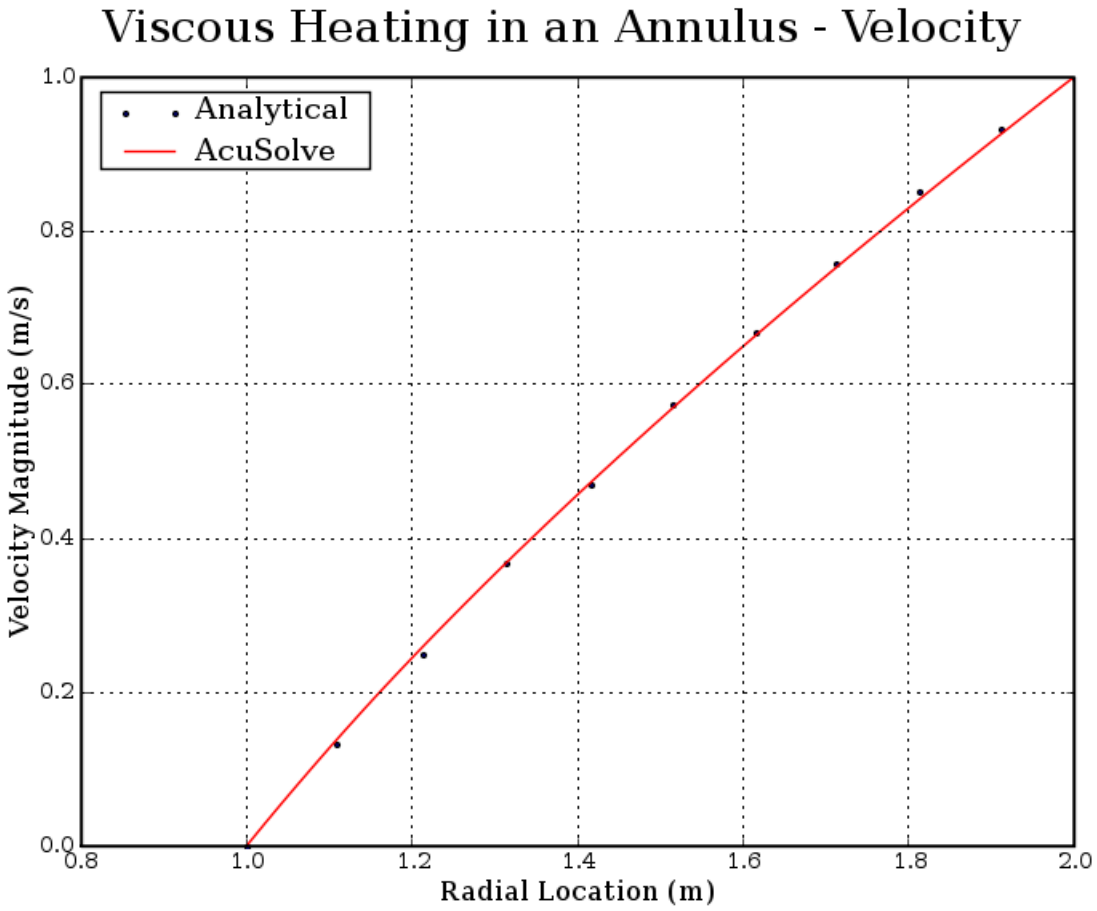


Figure 646: Velocity Magnitude Plotted Against Radial Location from the Center of the Inner Cylinder

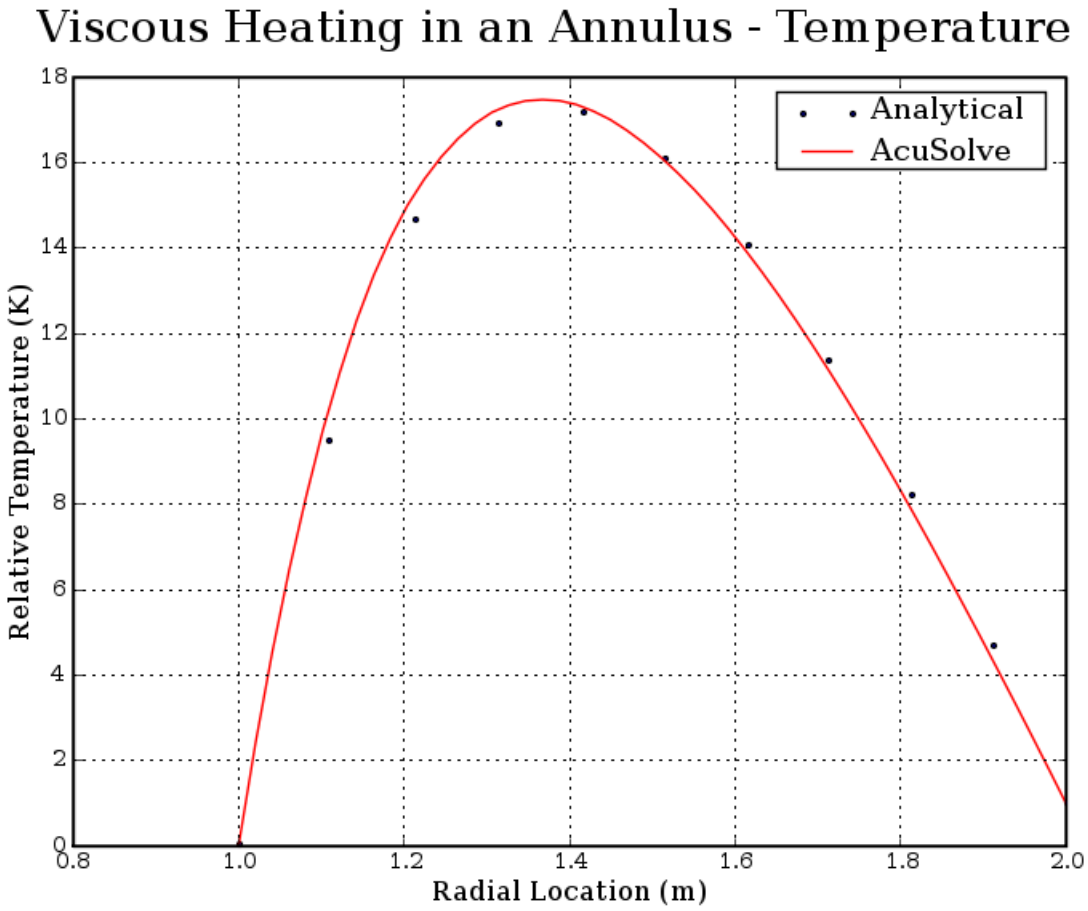


Figure 647: Temperature (Relative to the Inner Cylinder Wall Temperature) Plotted Against Radial Location from the Center of the Inner Pipe

Summary

The AcuSolve results compare well with the analytical results for both the flow field and the temperature across the annulus. In this application, flow is induced due to the viscous stresses generated by the rotation of the exterior cylinder. Velocity gradients between the cylinders give rise to shear stresses that induce frictional heating of the fluid. Due to the high viscosity of the fluid, the viscous heating is significant and leads to large increases in the temperature between the cylinders. This application validates the ability of AcuSolve to simulate flows where the viscous heating contribution is significant.

Simulation Settings for Viscous Heating Inside a Rotating Annulus

AcuConsole database file: `<your working directory>\annulus_rotating_heat\annulus_rotating_heat.acs`

Global

- Problem Description
  - Analysis type - Steady State
  - Temperature equation - Advective Diffusive

- Turbulence equation - Laminar
- Auto Solution Strategy
  - Relaxation factor - `0.2`
- Material Model
  - Fluid
    - Density - `1.0` kg/m3
    - Viscosity - `300` kg/m-sec
    - Conductivity - `1.0` W/m-K
- Reference Frame
  - Outer_Rotation
    - Angular Velocity
      1. X-component - `0.0` rad/sec
      2. Y-component - `0.0` rad/sec
      3. Z-component - `0.5` rad/sec

Model

- Volumes
  - Fluid
    - Element Set
      1. Material model - Fluid
      2. Viscous heating - On
- Surfaces
  - Inner_Cylinder
    - Simple Boundary Condition
      1. Type - Wall
      2. Temperature BC type - Value
      3. Temperature - `273.0` K
  - Outer_Cylinder
    - Simple Boundary Condition
      1. Type - Wall
      2. Reference frame - Outer_Rotation
      3. Temperature BC type - Value
      4. Temperature - `274.0` K
  - Symm_MaxZ
    - Simple Boundary Condition
      1. Type - Symmetry
  - Symm_MinZ
    - Simple Boundary Condition

1 Type - Symmetry

- Nodes
  - Node 1
    - Pressure
      1 Type - Zero

References

R. B. Bird, W. E. Stewart, and E. N. Lightfoot. "Transport phenomena". New York, John Wiley and Sons, 1960

Species Transport

12

This section includes validation cases that consider the mixing of multiple species by modeling the species advection/diffusion equation.

This chapter covers the following:

- Laminar Flow Through a Pipe with Species Transport (p. 889)

Laminar Flow Through a Pipe with Species Transport

In this application, AcuSolve is used to simulate the transport of a passive scalar species in a fully developed laminar flow. AcuSolve results are compared with analytical results as described in Kays and Crawford (1993). The close agreement of AcuSolve results with analytical results validates the ability of AcuSolve to model cases with species transport.

Problem Description

The problem consists of species transport in a pipe 0.005 m in diameter and 0.1 m long, as shown in the following image, which is not drawn to scale. The species transport equation is bounded at the inlet with a value of 1.0, while the boundary condition at the wall is 0.0. These constraints impose a concentration gradient within the fluid. The concentration gradient causes the fraction of species 1 to decrease near the pipe wall due to diffusion. The reduced concentration of the species is transported downstream in the pipe via advection, and leads to a continued decrease in the concentration as flow propagates through the pipe.

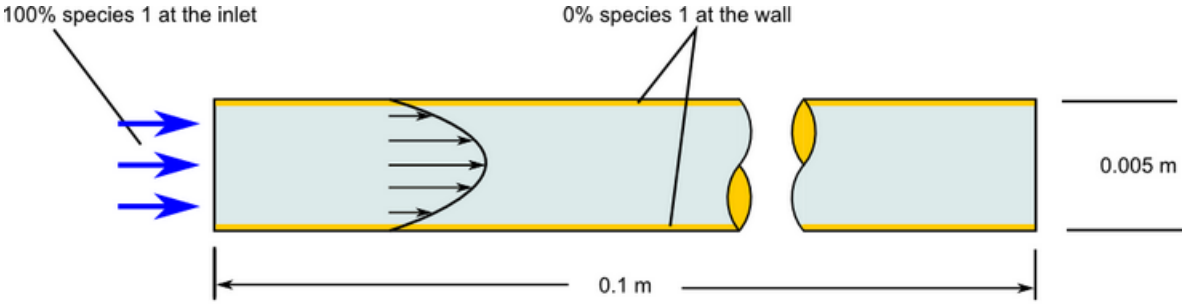


Figure 648: Critical Dimensions and Parameters for Simulating Laminar Flow Through a Pipe with Species Transport

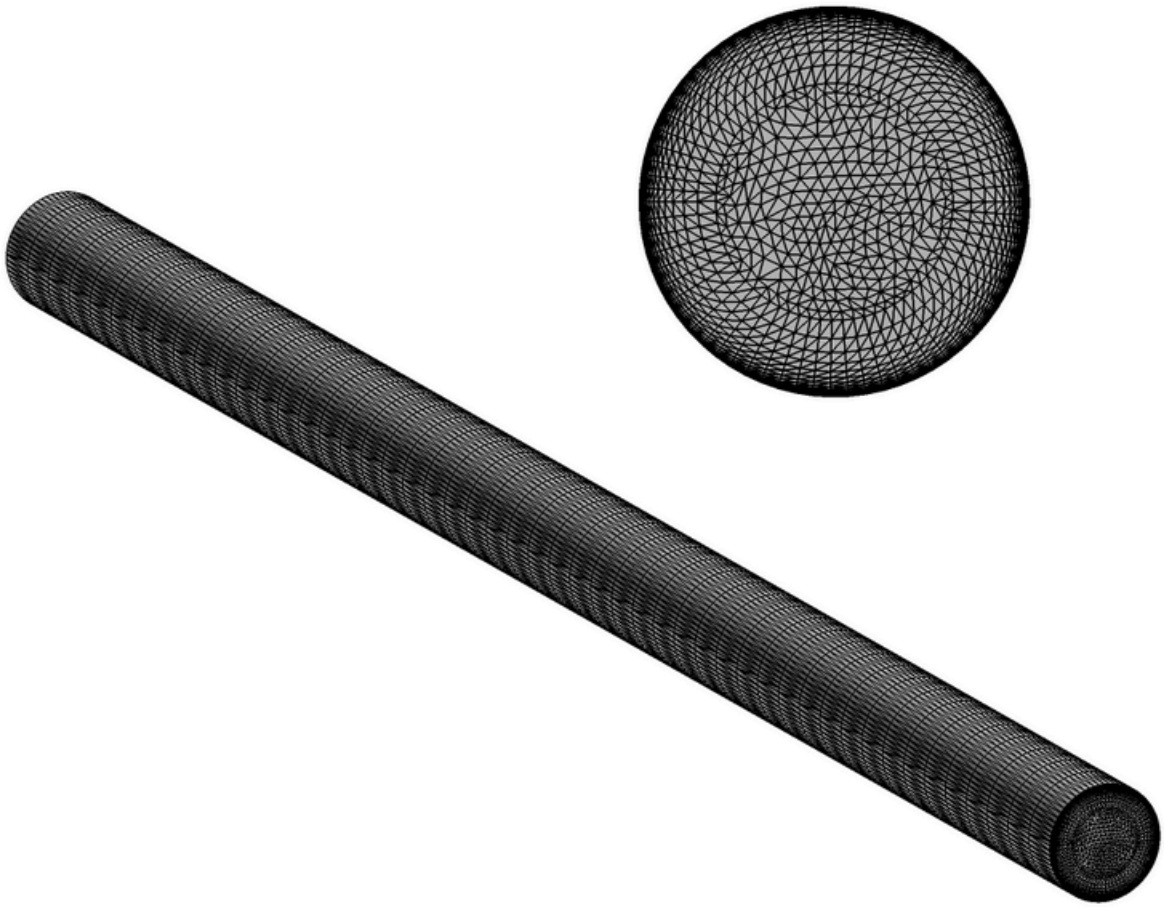


Figure 649: Mesh used for Simulating Laminar Flow Through a Pipe with Species Transport

AcuSolve Results

The AcuSolve solution converged to a steady state and the results reflect the mean flow conditions with the species fraction changing along the length of the pipe. At the inlet, the concentration of species 1 is 100 percent. The fraction of species 1 decreases along the length of the pipe, developing a parabolic concentration profile due to the no-slip walls and the specified concentration at the wall.

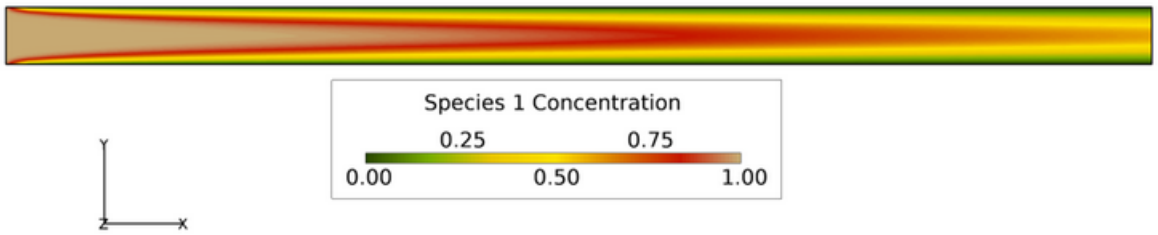


Figure 650: Contours of Concentration for Species 1

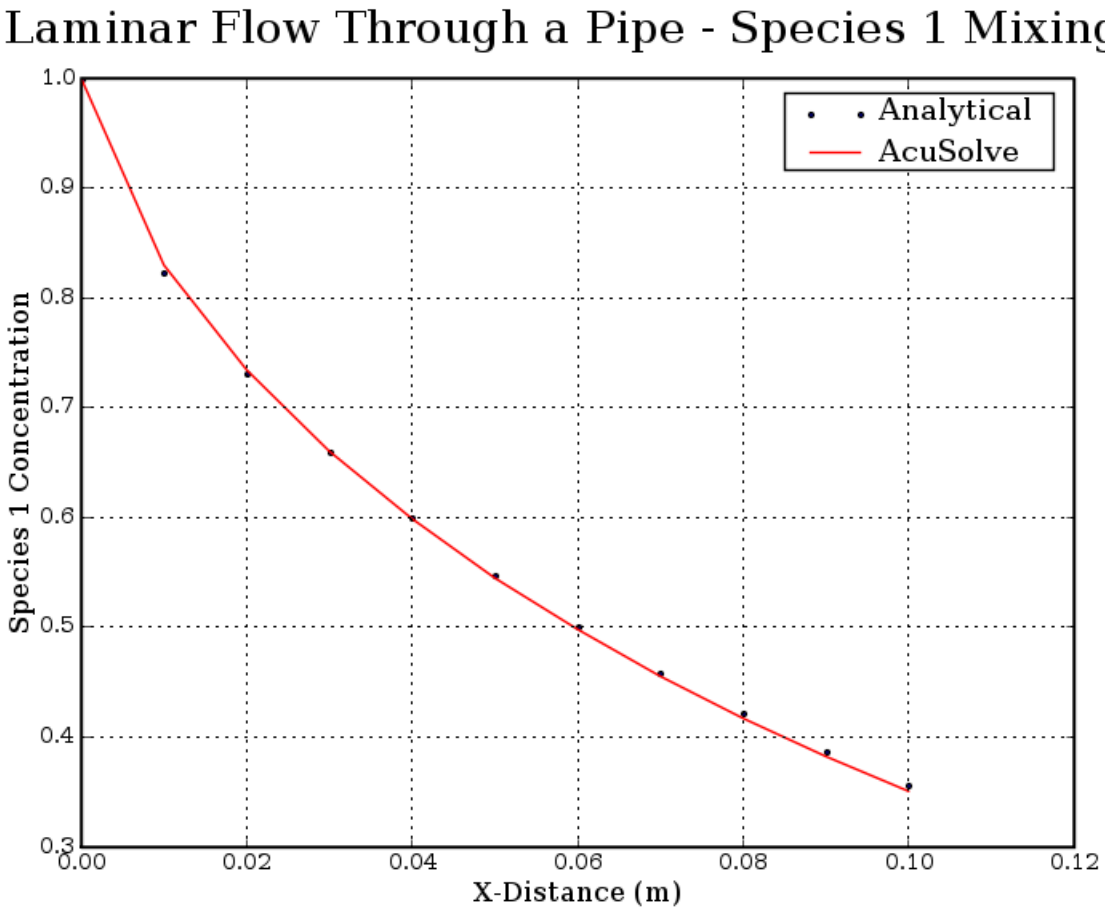


Figure 651: Species 1 Concentration Plotted Against Distance from the Pipe Inlet

Analytical values of the species fraction at different distances along the pipe are presented with the corresponding AcuSolve results in the following table. The analytical solution contains a series of five terms that are summed to yield the values shown in the table.

Table 41:

Distance along pipe (m)	Analytical species 1 fraction	AcuSolve species 1 fraction	Percent deviation from analytical
0	1.0000*	1.0000	0.00
0.01	0.8225	0.8298	0.90
0.02	0.7308	0.7344	0.49
0.03	0.6593	0.6603	0.15
0.04	0.5992	0.5988	0.06
0.05	0.5469	0.5448	0.38
0.06	0.5006	0.4981	0.49
0.07	0.4589	0.4554	0.78
0.08	0.4212	0.4171	0.98
0.09	0.3869	0.3824	1.15
0.1	0.3555	0.3507	1.35

* The theoretical species fraction at the inlet is shown rather than the analytical. In order for the analytical solution to correspond exactly with the theoretical results, additional terms in the series summation would need to be evaluated.

Summary

The AcuSolve solution compares well with analytical results for flow through a pipe with species transport. In this application, a fully developed laminar profile is achieved by enforcing periodic constraints on the pressure and velocity fields. The spatially developing species field is achieved by not enforcing periodicity and allowing the concentration to evolve along the full length of the model. The change in concentration along the pipe length is due to advection in the streamwise direction and diffusion of the species to the outer walls where the concentration is zero. The AcuSolve solution for fraction of species 1 is within 1.35 percent of analytical results.

Simulation Settings for Laminar Flow Through a Pipe with Species Mixing

AcuConsole database file: `<your working directory>\pipe_laminar_species\pipe_laminar_species.acs`.

Global

- Problem Description
  - Analysis type - Steady State

- Species equation - Advective Diffusive
- Num. species - `1`
- Turbulence equation - Laminar

- Auto Solution Strategy
  - Relaxation factor - `0.2`
- Material Model
  - Species1
    - Density - `1.0` kg/m3
    - Viscosity - `1.0e-5` kg/m-sec
    - Diffusivity
      1. 1
         1. Diffusivity - `1.43e-5` kg/m-sec

  Model
- Volumes
  - Fluid
    - Element Set
      1. Material model - Species1
- Surfaces
  - Inflow
    - Simple Boundary Condition - (disabled to allow for periodic conditions to be set)
    - Advanced Options
      1. Nodal Boundary Conditions
         1. Species 1
            1. Type - Constant
            2. Constant value - `1.0`
      2. Integrated Boundary Conditions
         1. Mass Flux
            1. Type - Constant
            2. Constant value - `1.96e-05` kg/sec
  - Outflow
    - Simple Boundary Condition - (disabled to allow for periodic conditions to be set)
  - Wall
    - Simple Boundary Condition
      1. Type - Wall
      2. Species 1 BC type - Value
      3. Species 1 - `0.0`
- Periodics

- Periodic 1
  - Individual Periodic BCs
    1. Velocity
       1. Type - Periodic
    2. Pressure
    3. Type - Single Unknown Offset

References

W. M. Kays and M. E. Crawford. "Convective Heat and Mass Transfer", 3rd Edition. pp. 126-134. McGraw-Hill Book Co., Inc. New York. 1993.

Multiphase

13

This section includes validation cases that consider the immiscible multiphase interaction of two fluids.

This chapter covers the following:

- Multiphase Flow of a 2D Dam Break (p. 896)
- Multiphase Flow Within a Sloshing Tank (p. 900)
- Two-Phase Nucleate Boiling in a Cylindrical Pipe (p. 907)

Multiphase Flow of a 2D Dam Break

In this application, AcuSolve is used to simulate the collapse of a water column surrounded by air. AcuSolve results are compared with experimental results adapted from Rodriguez and others (2013). The close agreement of AcuSolve results with experimental results validates the ability of AcuSolve to model multiphase flow problems.

Problem Description

The problem consists of a column of water being held in place by a membrane in a box of air, as shown in the following image, which is not drawn to scale, where a = 0.05715 m. At t = 0, the membrane is broken, allowing the water column to collapse.

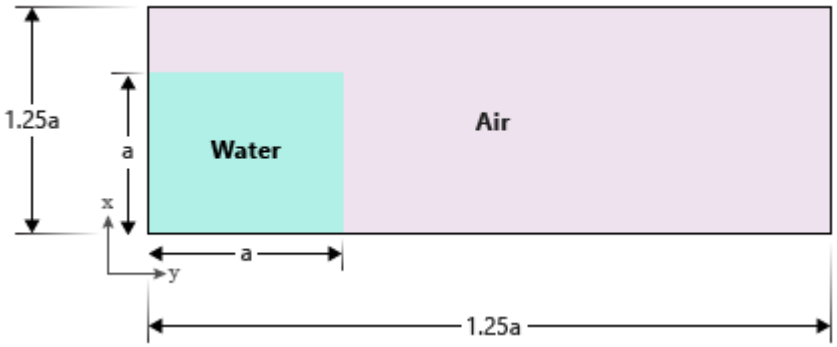


Figure 652: Critical Dimensions and Parameters for Simulating a 2D Dam Break Problem

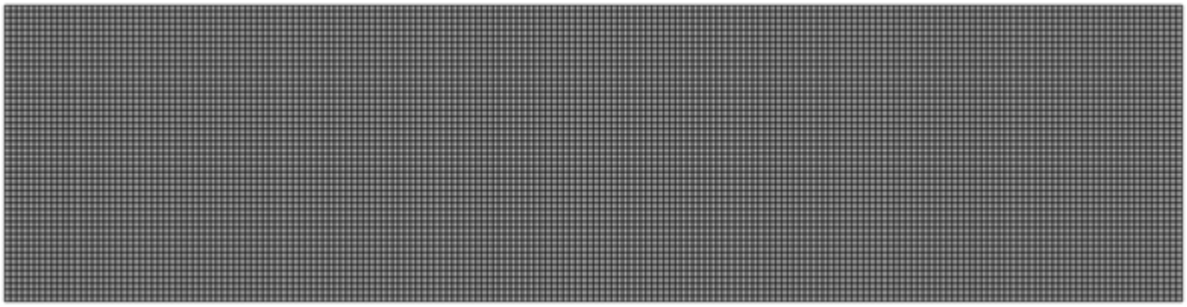


Figure 653: Mesh used for Simulating Multiphase Flow of a 2D Dam Break Problem

AcuSolve Results

The AcuSolve solution is run for a time t = 0.4 sec and the results reflect the transient motion of water column.

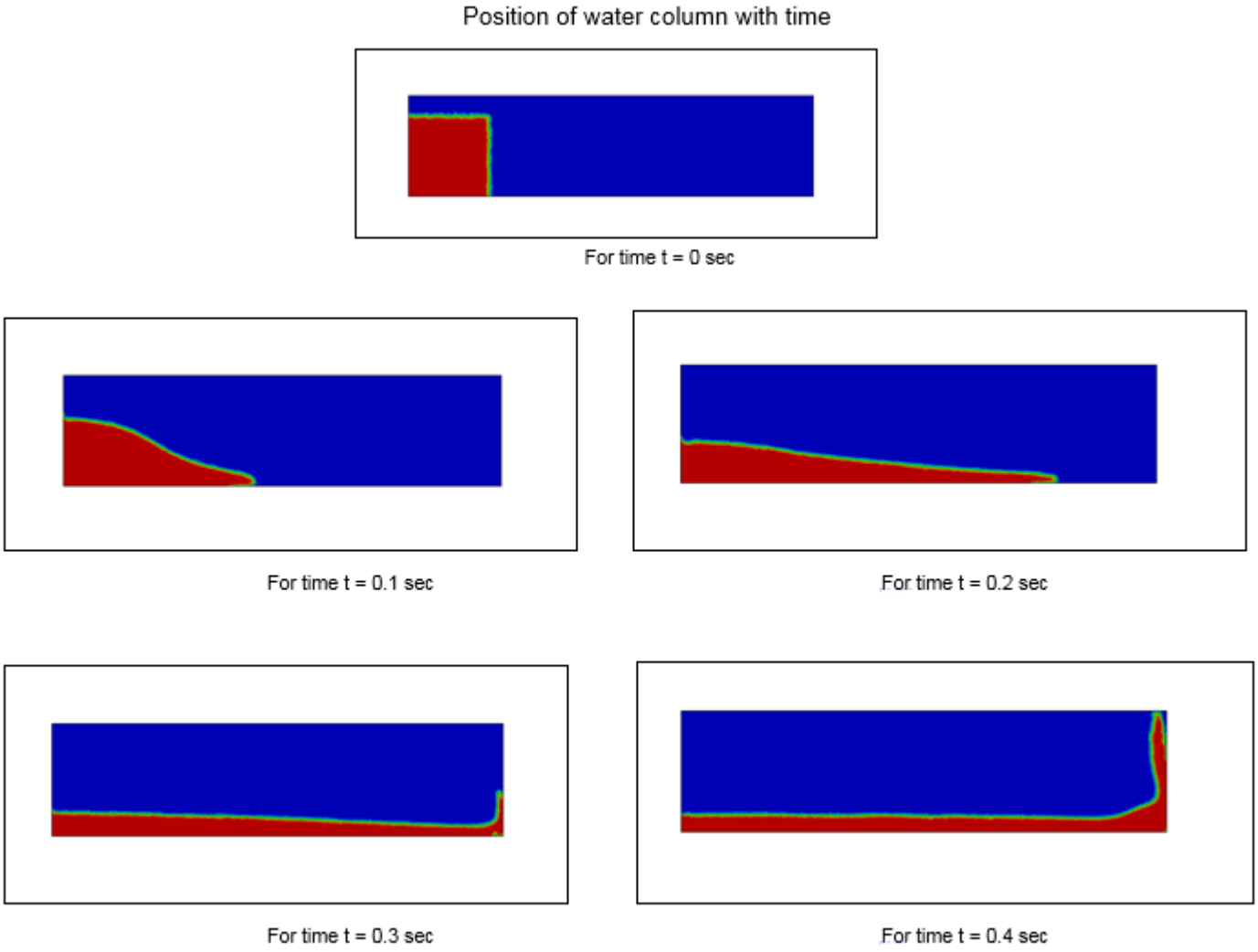


Figure 654:

The experimental values of normalized surge front positions (x/a) and normalized column height (y/a) is presented below with the corresponding AcuSolve results. The AcuSolve results show good agreement with the experimental results.

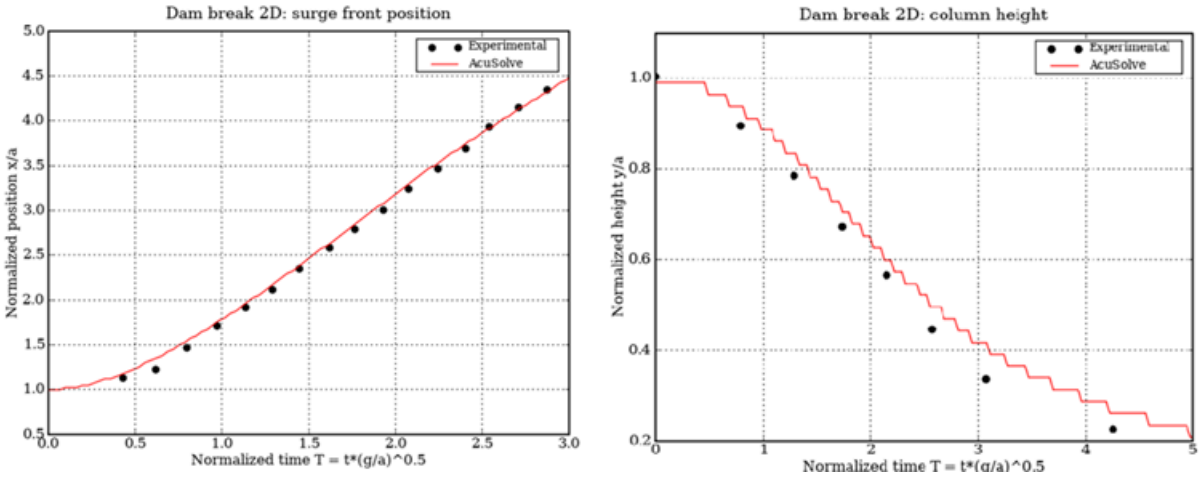


Figure 655: Surge Front Position and Column Height Compared to Experimental Results for Simulating Multiphase Flow of a 2D Dam Break

Summary

The AcuSolve solution compares well with experimental results for a dam break problem. In this application, multiphase flow simulation of the collapse of a water column is performed. The experimental value for the normalized column height and normalized surge front positions is presented with the corresponding AcuSolve results. A good agreement of simulation results with the experiment validates the multiphase capability of AcuSolve.

Simulation Settings for Multiphase Flow of a 2D Dam Break

HyperWorks CFD database file: `<your working directory>\dambreak_multiphase \damnbreak_multiphase.hm`

Global

- Problem Description
  - Analysis type - Transient
  - Multifluid - Level Set
  - Gravitational acceleration - { 0, -9.81, 0 }
- Auto Solution Strategy
  - Final Time - `0.4` sec
  - Initial time increment - `0.0005` sec
  - Fluid 1 - Water
  - Fluid 2 - Air
- Time Integration
  - Time integration order – “second”
- Material Model
  - Air
    - Type - Constant

        - Density - `1.2` kg/m3
        - Viscosity - `1.1818e-006` kg/m-sec
    - Water
        - Type - Constant
        - Density - `1000` kg/m3
        - Viscosity - `0.001` kg/m-sec
- Multifield Parameters → Field Interaction Model
    - Field 1 - Water
    - Field 2 - Air
    - Thickness type - Number of elements
    - Number of elements - `3`
    - Fluid 2 - Air

  Model
- Volumes
    - Fluid
        - Element Set
            1. Medium - Multi Field
            2. Multi field model - Water-Air
- Surfaces
    - +Z
        - Simple Boundary Condition - Slip
    - -Z
        - Simple Boundary Condition - Slip
    - Bottom wall
        - Simple Boundary Condition - Wall
    - Left wall
        - Simple Boundary Condition - Wall
    - Right wall
        - Simple Boundary Condition - Wall
    - Top wall
        - Simple Boundary Condition - Wall

References

Joseph M. Rodriguez, Onkar Sahni, Richard T. Lahey Jr., Kenneth E. Jansen. "A parallel adaptive mesh method for the numerical simulation of multiphase flows", Computers and Fluids, Vol. 87, 2013, pp. 115-131.

Multiphase Flow Within a Sloshing Tank

In this application, AcuSolve is used to simulate water and the time-dependent interface of air-water within a tank subject to a prescribed sloshing motion. AcuSolve results are compared with experimental pressure measurements as reported by Tankaka, et al. (2000) and Rhee (2005). The close agreement of AcuSolve results with experimental results validates the ability of AcuSolve to model multiphase flow problems with user-defined motion.

Problem Description

The problem consists of a tank filled to 20 percent capacity with water that is rotated or translated according to a user-defined function, as shown in the following image, which is not drawn to scale, where three monitoring locations, P1, P2 and P3, are denoted. The motion of the tank causes the fluid to begin sloshing rapidly, creating a time-dependent pressure field due to the height of the local water column. Non-slip boundary conditions for the top, bottom, left and right sides are applied with slip boundary conditions on the front and back faces. The SST turbulence model along with a global time-step of 0.001 seconds is used for the simulation. The pressure at each of the monitoring locations is compared against the experimental measurements as described in Tankaka, et al. (2000). It should be noted that the pressure computed and presented in the images represent the time-dependent dynamic pressure, static pressure is subtracted to be consistent with the measurements, at the specified point. Roll-Short is the case provided with the Validation Manual. The results for this case as well as Sway - Short are presented within this overview. In each case, the motion profile is defined with the following function and coefficients as defined in the table below.

$$x = A\sin(\omega t) \tag{29}$$

Where A = amplitude of oscillation, ω = frequency of oscillation = 2 π/T, t = time (sec) and T = Time period of oscillation (sec).

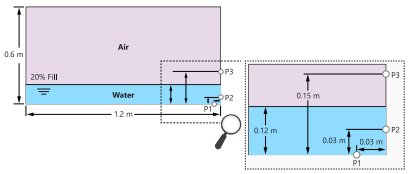


Figure 656: Critical Dimensions and Parameters for Simulating a 2D Tank Slosh with Mesh Motion

Table 42: Sine Function Scaling Parameters for Tank Motion Profile

Cases	Mesh Motion	Amplitude (A)	Time Periods (T)	Tank Filling Level
Sway – Base	Sway motion	0.06 m	1.94 sec	20% height

Cases	Mesh Motion	Amplitude (A)	Time Periods (T)	Tank Filling Level
Sway – Short	Sway motion	0.06 m	1.74 sec	20% height
Roll – Base	Rolling motion	10 degrees	2.25 sec	20% height
Roll – Short	Rolling motion	10 degrees	1.85 sec	20% height

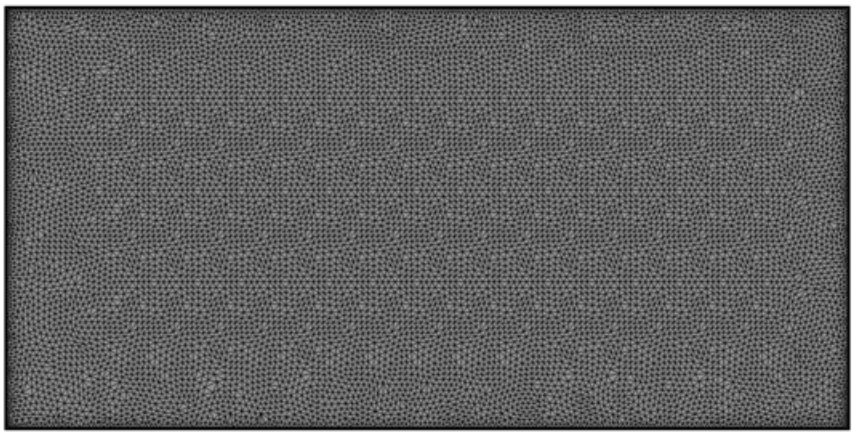


Figure 657: Mesh Used for Simulating Multiphase Sloshing Within a 2D Tank

AcuSolve Results

The AcuSolve solution is run for a time of t/T=5.0, 9.25 sec for Roll - Short, and the results presented reflect the transient motion of the water within the tank. The experimental values of pressure (kPa) and normalized simulation time are presented with the corresponding AcuSolve results at three measurement locations. The AcuSolve results show good agreement with the experimental results for pressure magnitude, the local water column height, as well as accurate timing of the peaks, indicating that the air-water interface is properly captured. Additional motion cases, as well as comparisons between two dimensional versus three dimensional simulations have been simulated with AcuSolve. The accuracy and solution requirements of these simulations are omitted for brevity but are available upon request. It was found that the differences between 2D and 3D simulations may be of interest for engineers, however the 2D results are shown to be adequate and less computationally expensive than 3D in the cases studied.

User-Defined Multiplier Function

This validation case relies on defining the motion of the elements within the tank, leading to the water sloshing in the presence of air. The motion is defined using an AcuSolve User-Defined Function (UDF) to specify the time-dependent multiplier function applied to the mesh motion command. The mesh motion is assigned to the Fluid element set, causing all of the elements to move according to the specified sine function. For the Roll - Short case, the mesh motion command is specified as rotation with the rotation multiplier function specified as rotation. If you are interested in simulating one of the other motion profiles, for example Sway - Base/Short, the type of mesh motion command would be changed to translation with the translation multiplier function assigned with the same UDF. The function name is designated at usrMotion and is contained within the source file `motion.c`. The source file, along with

pre-compiled binaries for Linux64 and Windows64 are provided with the validation case. Depending on your architecture it may be necessary to re-compile the source on the local system. Please refer to the *Programs Reference Manual* for details on using AcuMakeLib or AcuMakeDll for Linux and Windows, respectively.

Summary

The AcuSolve solution compares well with experimental results for tank sloshing simulations. In this application, the time dependent motion of the tank and the multiphase flow solution are simulated with AcuSolve using the level-set formulation and the SST turbulence model. The experimental values for instantaneous pressure at three locations and for two motion profiles are presented with the corresponding AcuSolve results. A good agreement of simulation results with the experiment validates the ability to solve time-dependent/accurate sloshing cases using the multiphase capabilities of AcuSolve.

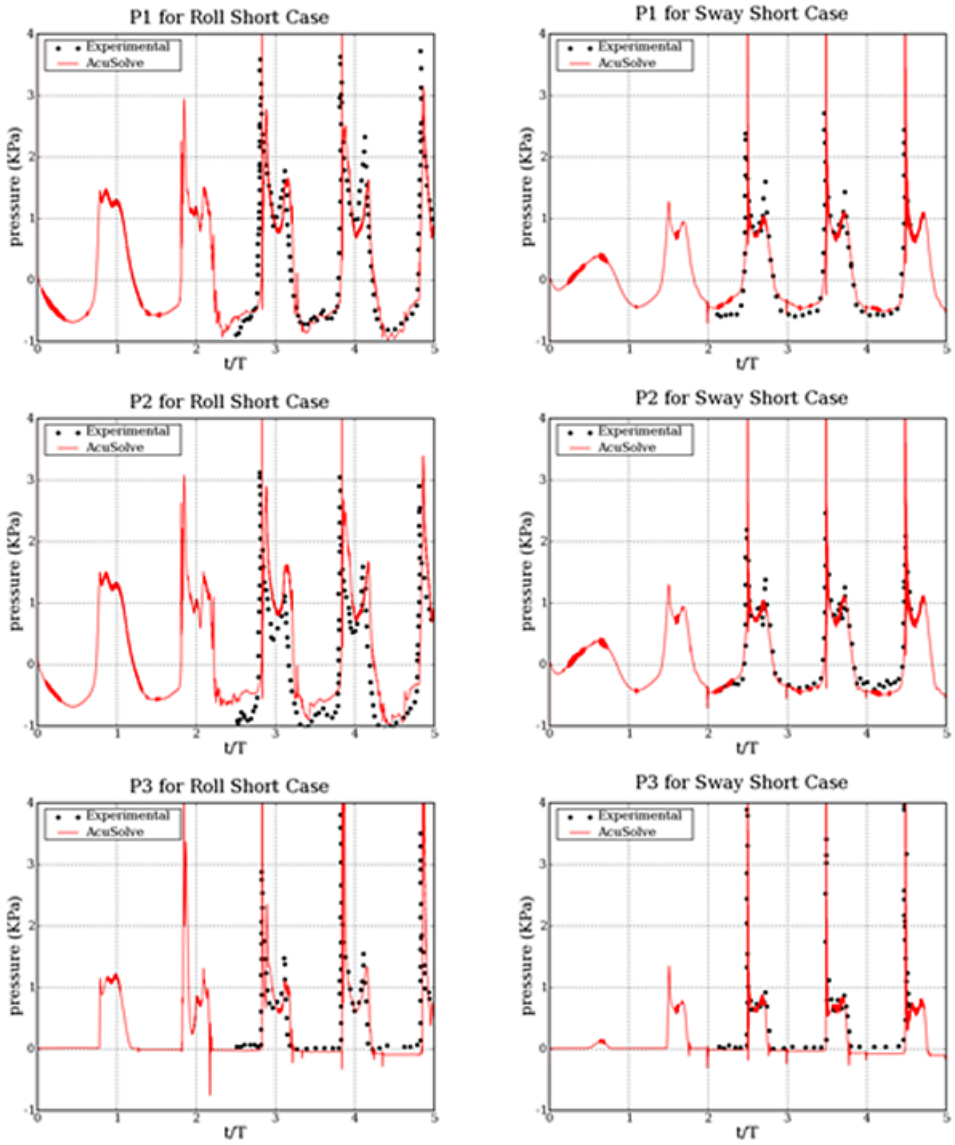


Figure 658: Time Dependent Pressure at Three Monitoring Locations Within the Sloshing Tank for Two Motion Profiles (Roll-Short, Left and Sway-Short, Right)

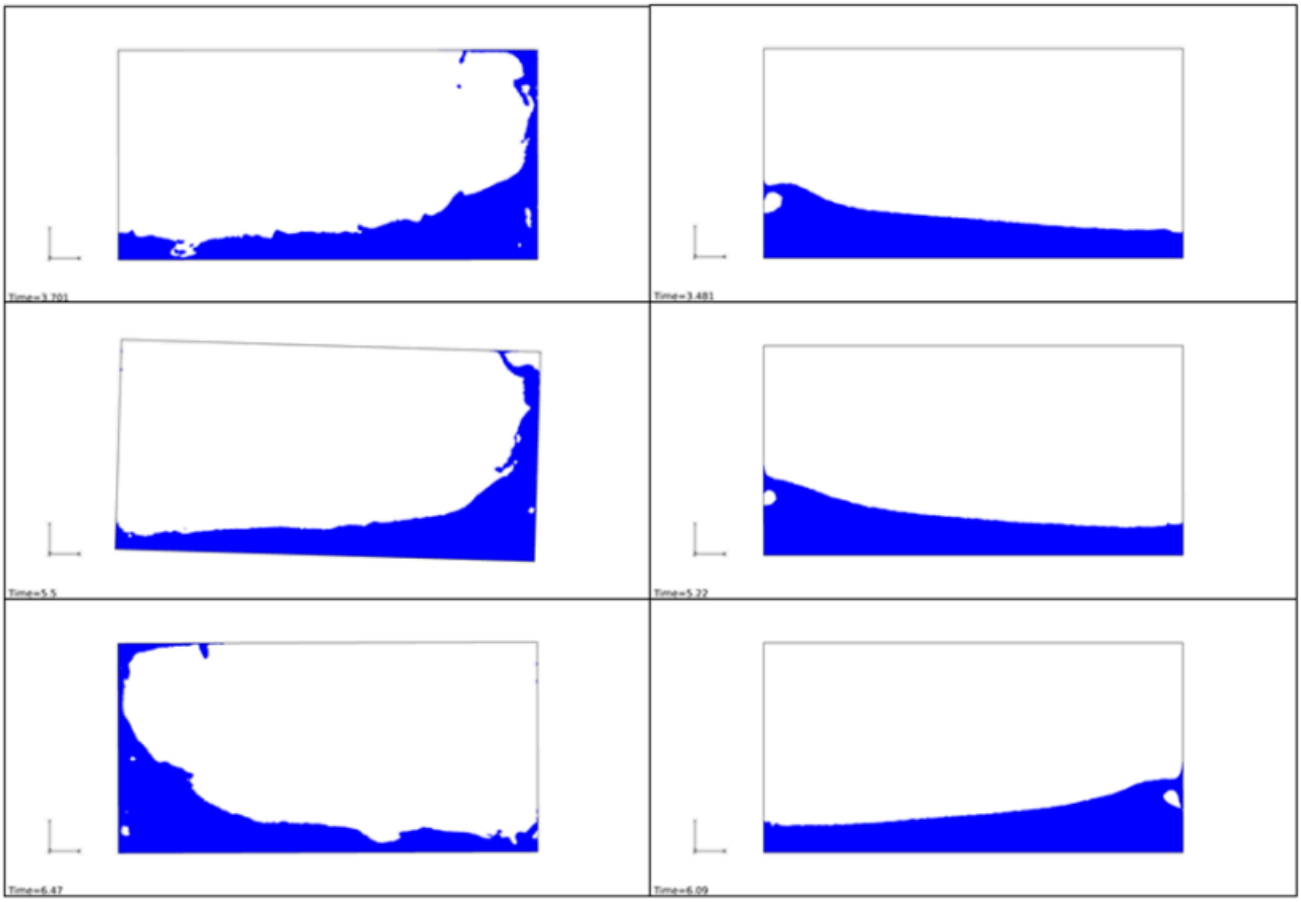


Figure 659: Instantaneous Volume Fraction Contour (Blue Showing Water) at Three Moments in Time (t/T=2.0, 3.0 and 3.5) for Two Motion Profiles (Roll-Short, Left and Sway-Short, Right)

Simulation Settings for Multiphase Flow Within a Sloshing Tank

AcuConsole database file: `<your working directory>\tank_sloshing_multiphase \tank_sloshing.acs`

Global

- Problem Description
  - Analysis type - Transient
  - Turbulence equation - SST
  - Multiphase equation – Level Set
- Auto Solution Strategy
  - Final time - `9.5` sec
  - Initial time increment - `0.001` sec
  - Min stagger iterations - `2`
  - Max stagger iterations - `10`
  - Fluid 1 - Water
  - Fluid 2 - Air

- Multiplier Function
  - rotation
    - Type - User Function
    - User function name - UsrMotion
    - User function values - `10.0`, `1.85`, `0.0`
- Material Model
  - Air
    - Type - Constant
    - Density - `1.225` kg/m^3
    - Velocity - `1.781e-5` kg/m-sec
  - Water
    - Type - Constant
    - Density - `1000` kg/m^3
    - Velocity - `0.001` kg/m-sec
- Mesh motion
  - rotation
    - Type - Rotation
    - Rotation center – `0.0`, `0.0`, `0.0`
    - Angular velocity – `0.0`, `0.0`, `0.0174533` (1.0 deg/sec)
    - Rotation variable – Multiplier Function
    - Rotation multiplier function – rotation

  Model
  - Volumes
    - Fluid
      1. Element Set
         1. Medium – Multiphase
         2. Multi field model – Water-Air
         3. Body force – Gravity
         4. Mesh motion – rotation
- Surfaces
  - x+
    - Simple Boundary Condition – Wall
  - x-
    - Simple Boundary Condition – Wall
  - y+
    - Simple Boundary Condition – Wall
  - y-
    - Simple Boundary Condition – Wall

- z+
  - Simple Boundary Condition – Slip
- z-
  - Simple Boundary Condition – Slip

References

Shin Hyung Rhee, 2005, "Unstructured Grid Based Reynolds-Averaged Navier-Stokes Method for Liquid Tank Sloshing", Journal of Fluids Engineering, Vol 127, pp. 572- 582.

Tanaka, Y., Ando, T., and Miyamoto, T., 2000, "Experimental Study on Sloshing Load Measured by Panel-Type Pressure Gauge," Proc. 74th. General Meeting of Ship Research Institute, Ship Research Institute, Tokyo, Japan, pp. 137-142.

Two-Phase Nucleate Boiling in a Cylindrical Pipe

In this application, AcuSolve is used to simulate the changes in wall temperature due to two-phase nucleate boiling at the heated walls of a pipe with water flowing through it. AcuSolve results are compared with experimental results adapted from Koncar and others (2015). The close agreement of AcuSolve results with experimental results validates the ability of AcuSolve to model two-phase nucleate boiling problems.

Problem Description

The problem consists of a pipe with heated surrounding walls, as shown in the following image, which is not drawn to scale. The length of the pipe is 2 m and the radius is 0.0017 m. Mass flux at the inlet is 900 kg/m^2 and the temperature of the fluid entering the pipe is 473 K. A heat flux of 570,000 W/m^2 is applied on the walls. The preheated water enters the inlet and heat is transferred to the fluid from the walls. The heat causes sub-cooled boiling to occur in the region close to the wall and leads to the formation of bubbles at nucleation sites.

During sub-cooled boiling flow, heat and mass exchange between the phases takes place on the heated wall and in sub-cooled liquid flow. On the heated surface the vapor bubbles are generated and as they move through the sub-cooled liquid they condense and release the latent heat.

The AcuSolve simulation is set up to model transient state heat transfer to determine the temperature along the centerline of the pipe and along the heated pipe walls of the model. AcuSolve computes the two-phase nucleate boiling by simulating the three-dimensional flow in a heated pipe for two-phase boiling flow, as described in Koncar (2005). The temperatures along the centerline of the pipe and along the pipe walls are compared against the experimental measurements, as described in Koncar, et al. (2005).

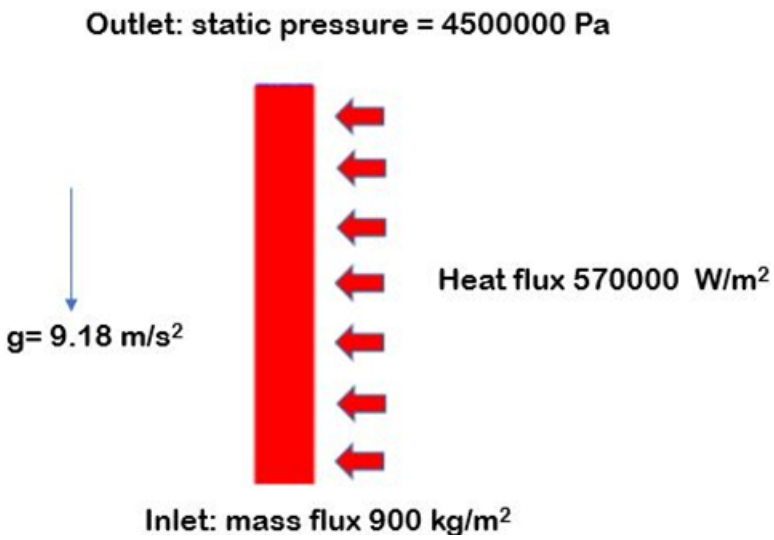


Figure 660: Parameters for Simulating a Two-Phase Nucleate Boiling Problem of a Pipe

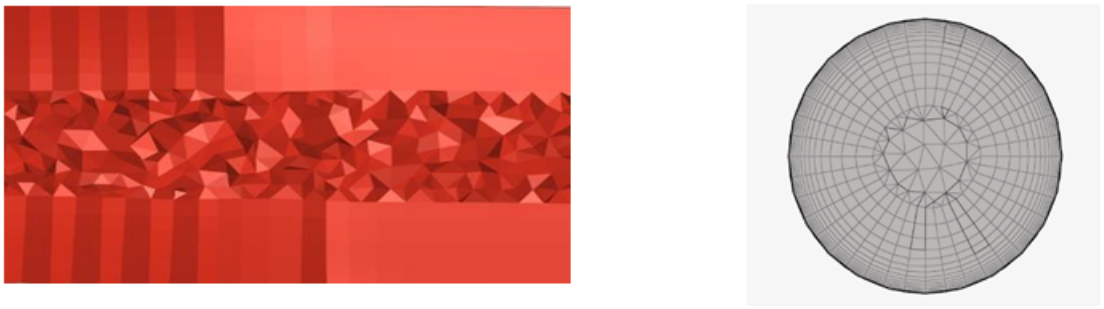


Figure 661: Mesh used for Simulating Two-Phase Flow in a Pipe

AcuSolve Results

The AcuSolve solution is run for a heat flux of 570,000 W/m^2 and the results are presented in the following image. The experimental values of wall temperature are presented with the corresponding AcuSolve results along the centerline of the pipe and along the pipe wall. The AcuSolve results show good agreement with the experimental results for the temperature, indicating that the two-phase nucleate boiling is properly captured.

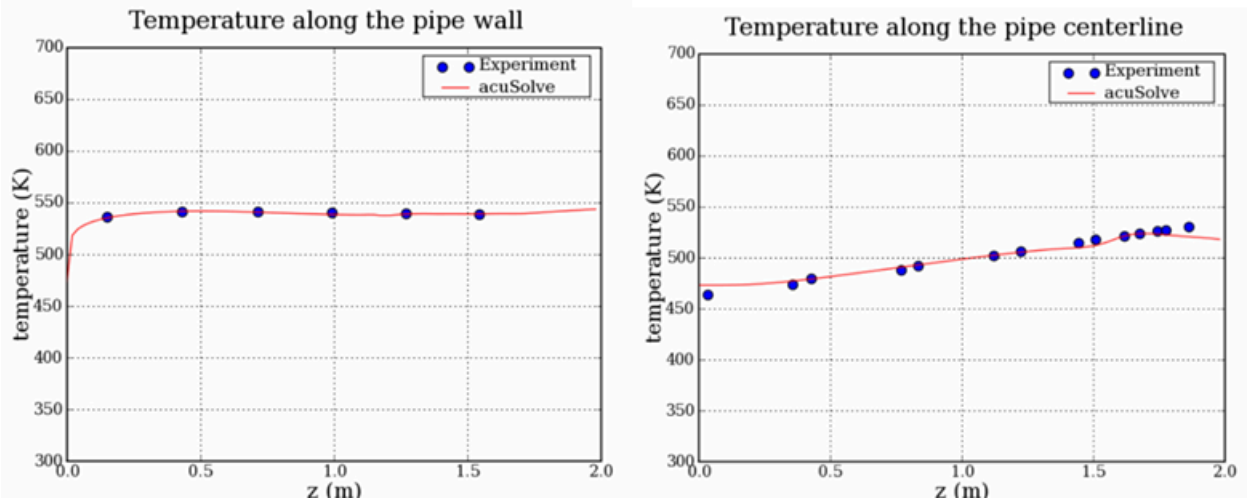


Figure 662: Temperature Values for Varying Streamwise Distance Compared to Experimental Data

Summary

The AcuSolve solution compares well with experimental results for two-phase nucleate boiling simulations. In this application, the temperature of the wall as the onset of boiling approaches are simulated with AcuSolve using the nucleate boiling feature and the SA turbulence model. The experimental values of temperature are presented with the corresponding AcuSolve results. A good agreement of simulation results with the experiment validates the ability to solve two-phase nucleate boiling using the nucleate boiling capabilities of AcuSolve.

Simulation Settings for Two-Phase Nucleate Boiling in a Cylindrical Pipe

HyperWorks database file: `<your working directory>\pipe_two_phase_boiling\pipe_two_phase_boiling.hm`.

Global

- Problem Description
  - Analysis type – Transient
  - Turbulence equation – SA
  - Temperature equation – Advective Diffusive
- Auto Solution Strategy
  - Maximum time steps – `500`
  - Initial time increment – `0.003`
  - Convergence Tolerance – `0.001` sec
  - Relaxation factor – `0.3`
- Surface Tension Model (“Water_NB-Vapor_NB”)
  - Type – Constant
  - Surface Tension – `0.02382`
- Material Model
  - Vapor_NB
    - Type – Constant
    - Density – `23.75` kg/m^3
    - Viscosity – `1.79e-05` kg/m-sec
    - Specific Heat – `4225` J/kg-K
    - Latent Heat – `1675570`
    - Latent Heat Temperature – `530.55` K
    - Conductivity – `0.02528` W/m-K
  - Water_NB
    - Type – Constant
    - Density – `800` kg/m3
    - Viscosity – `0.0001339` kg/m-sec
    - Specific Heat – `4500` J/kg-K
    - Conductivity – `0.65` W/m-K
- Multifield parameter (Field interaction model)
  - Type – Algebraic Eulerian
  - Phase change type – Wall Boiling
  - Carrier field - Water
  - Disperse field – Vapor
  - Disperse field diameter type – Boiling kurul exponential
  - Drag model – Ishii zuber
  - Lift Model – Legendre Magnaudet

Model

- Volumes
  - Fluid
    - Material – Vapor_Water
- Surfaces
  - Inflow
    - Simple Boundary Condition – Inflow
    - Inflow type – Mass Flux Rate
    - Mass Flux Rate – `0.167634` kg/sec
    - Temperature – `473` K
  - Outflow
    - Simple Boundary Condition – Outflow
    - Pressure – `4500000` N/m2
  - Wall
    - Simple Boundary Condition – Wall
    - Temperature type – Flux
    - Heat Flux – `570000` W/m2

References

B. Koncar, E. Krapper, Y. Egorov, 2005, "CFD MODELING OF SUBCOOLED FLOW BOILING FOR NUCLEAR ENGINEERING APPLICATIONS", International Conference Nuclear Energy for New Europe 2005, Bled, Slovenia, September 5-8,2005.

Compressible

14

This section includes validation cases that consider the compressibility of the fluid using a variable material model.

This chapter covers the following:

- Supersonic Flow Through a Converging-Diverging Nozzle (p. 912)
- Ideal Gas Compression in an Actuating Piston (p. 917)

Supersonic Flow Through a Converging-Diverging Nozzle

In this application, AcuSolve is used to simulate the high-speed turbulent flow in a converging and then diverging nozzle. The flow within the nozzle enters as subsonic, reaches sonic at the throat and shortly after develops a normal shock. AcuSolve results are compared with experimental results adapted from Bogar and Sajben (1983). The close agreement of AcuSolve results to experimental measurements validates the ability of AcuSolve to simulate internal supersonic flows where normal shocks are present.

Problem Description

The problem consists of a converging and then diverging nozzle represented as an extruded planar surface, as shown in the image below, which is not drawn to scale. The length of the domain is 0.213 m with a throat height of 0.044 m. The stagnation pressure and static temperature are constrained at the inlet to 135,000 Pa and 265.98 K, respectively. The static pressure is defined using the outflow boundary condition, where P_{static}=97216.08 Pa. The flow in the diffuser has an inlet Reynolds number of $6.5x10^5$. The upper and lower walls are set to no-slip and the side walls are set to slip, while the exterior walls are specified to be adiabatic. Images of the numerical mesh are shown below.

The AcuSolve simulation is prepared to model the pseudo-transient state to determine the shock location and corresponding scalar quantities within the diffuser. AcuSolve computes the flow and thermal solution by simulating a planar, two-dimensional flow problem with physical dimensions and input quantities as described in the Sajben Diffuser case presented by Bogar and Sajben (1983). The gas in the simulation domain enters at subsonic conditions and is forced to accelerate beyond Mach=1.0 as it passes through the throat. After reaching supersonic speed a normal shock wave develops causing the flow speed to reduce back below sonic. The pressure along the bottom wall of the diffuser is compared against experimental measurements to demonstrate the solver's capability to solve supersonic cases.

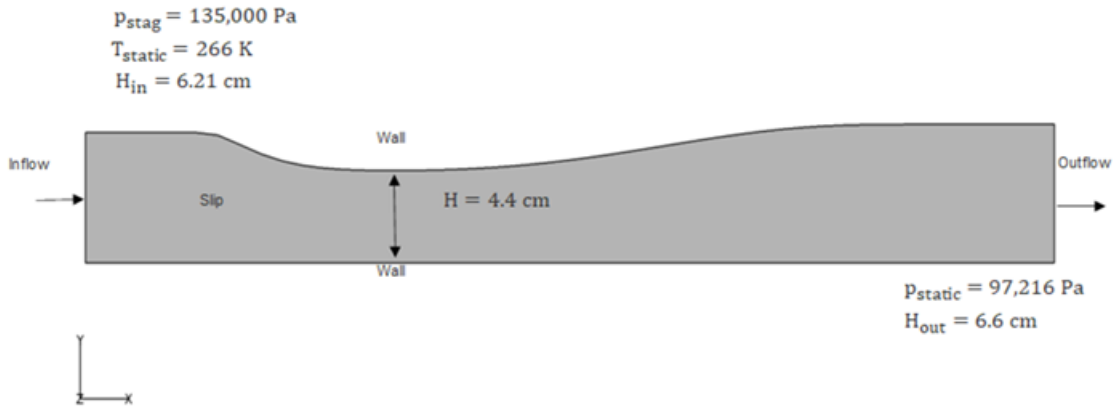


Figure 663: Parameters for Simulating Compressible Flow within a Converging-Diverging Nozzle

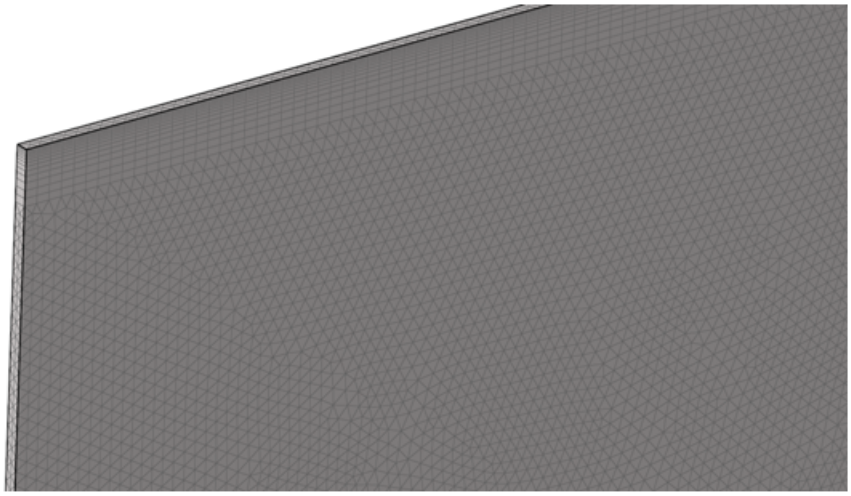


Figure 664: Mesh used for Simulating Compressible Flow in a Converging-Diverging Nozzle

AcuSolve Results

The AcuSolve solution is run for 0.025 seconds (6,250 timesteps with dt=4.0x10^{-6}sec) and converges to a pseudo-steady solution. The change in pressure from the inlet to outlet causes the flow to accelerate within the throat of the diffuser until it reaches approximately Mach=1.35. A normal shock is present just downstream of where the cross-sectional area of the nozzle increases, as shown in the image below. The numerical solution can be compared with the reference after normalizing the pressure along the wall by the inlet stagnation pressure (135 kPa) and the distance along the bottom wall by the nozzle throat height (0.044 m). The image below shows the normalized pressure versus normalized distance in comparison to NASA reference and experimental results. The image shows black circles representing the experimental measurements (Bogar and Sajben 1983), a dashed blue line representing the SA solution as obtained through NASA publication (Mohler 2005) and a solid red line representing the AcuSolve results with the Spalart-Allmaras turbulence model. The non-dimensional pressure within the diffuser agrees well with the reference data, demonstrating the correct physical location of the normal shock and expected moderate flow speed reduction within the constant cross-section diffuser portion of the nozzle.

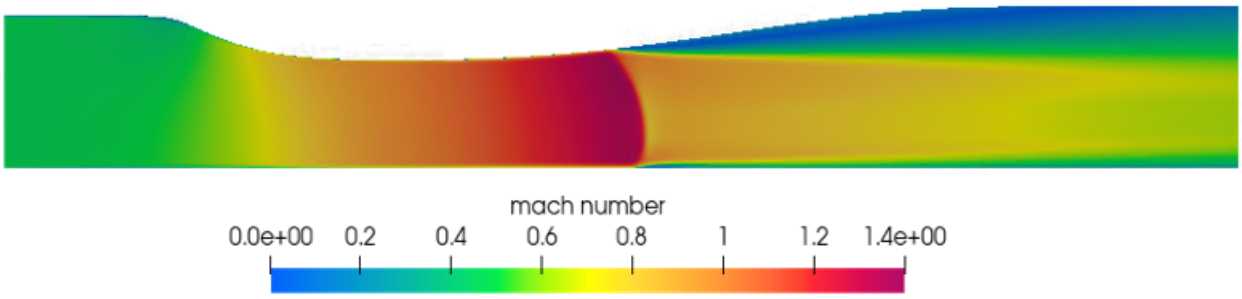


Figure 665: Contours of Mach Number within a Converging-Diverging Nozzle

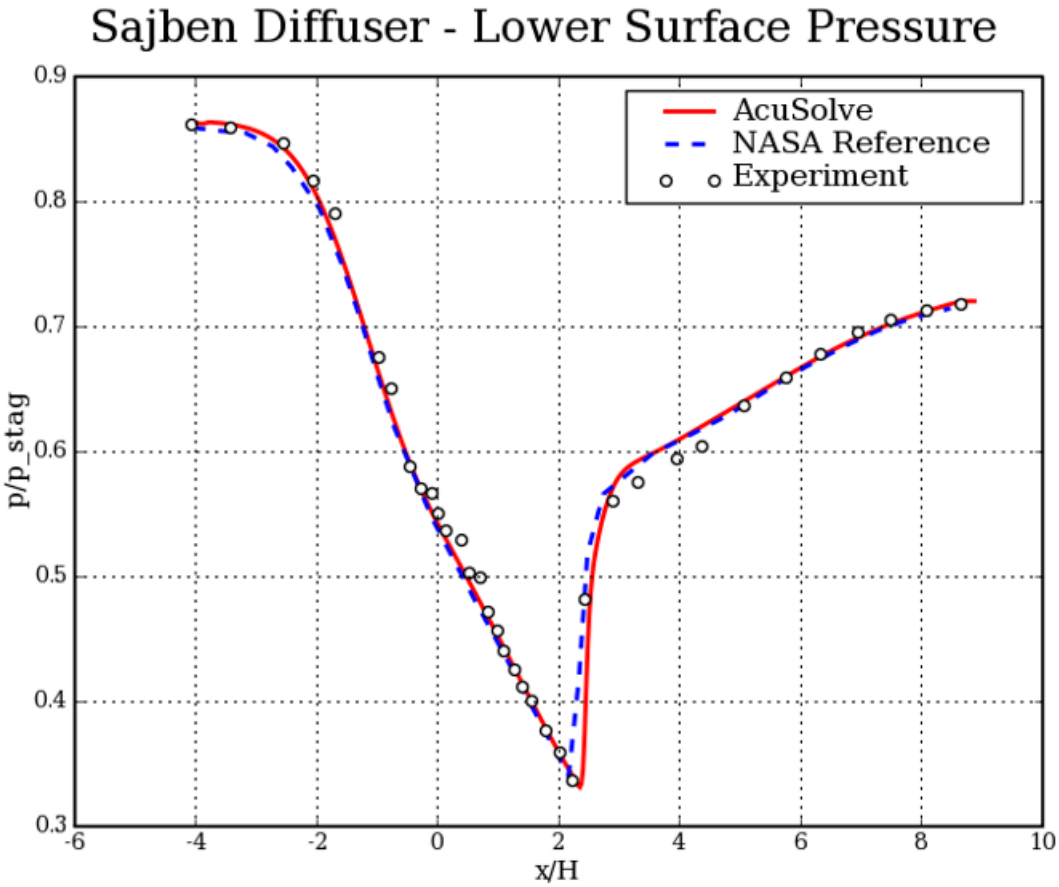


Figure 666: Normalized Pressure Versus Normalized Distance in Comparison to NASA Reference and Experimental Results

Summary

The AcuSolve solution compares well with experimental and numerical results for the described simulation. In this application, compressibility effects are accounted for using the coupled compressible flow solver with the ideal gas material definition. The thermal and momentum exchange within the nozzle is computed with AcuSolve using the compressible Navier-Stokes solver with the Spalart-Allmaras turbulence model. The experimental values of pressure are presented with the corresponding AcuSolve results and show good agreement, validating the ability to solve compressible cases with the presence of normal shocks. The results indicate that AcuSolve is able to properly predict the peak pressure magnitude and location within the diffuser while maintaining the normal shock when the time-step is selected to result in a maximum CFL of approximately 30.

Simulation Settings for Supersonic Flow Through a Converging-Diverging Nozzle

HyperWorks CFD database file: `<your working directory>\diffuser_compressible\diffuser_compressible.hm`

Global

- Problem Description

    - Flow – Compressible Navier Stokes
    - Analysis type – Transient
    - Turbulence equation – SA
    - Temperature equation – Advective Diffusive
- Auto Solution Strategy
    - Initial time increment – `4.0E-6`
    - Final time – `0.025` sec
    - Convergence Tolerance – `0.001` sec
    - Relaxation factor – `0.5`
- Material Model
    - Air-Ideal Gas
        - Type – Ideal_Gas
        - Viscosity – `1.781e-05` kg/m-sec
        - Specific Heat – `1005` J/kg-K
        - Conductivity – `0.02521` W/m-K
        - Gas Constant – `287.058` J/kg-K

Model

- Volumes
    - Fluid
        - Material – Air-Ideal Gas
- Surfaces
    - Inflow
        - Simple Boundary Condition – Inflow
        - Inflow type – Stagnation Pressure
        - Stagnation Pressure – `135000.0` N/m2
        - Turbulence_input_type – Direct
        - Eddy Viscosity – `1e-6` m^2/s
        - Temperature – `265.98` K
    - Outflow
        - Simple Boundary Condition – Outflow
        - Pressure – `97216.08` N/m2
    - Wall_1
        - Simple Boundary Condition – Wall
        - Type – auto_wall
    - Wall_2
        - Simple Boundary Condition – Wall
        - Type – auto_wall
    - Slip_1

        - Simple Boundary Condition – Slip
    - Slip_2
        - Simple Boundary Condition – Slip

References

Bogar, T. J., Sajben, M., and Kroutil, J. C. (1983) "Characteristic Frequencies of Transonic Diffuser Flow Oscillations," AIAA Journal, Vol. 21, No. 9, pp. 1232-1240.

Mohler, S.R., "Wind-US Unstructured Flow Solutions for a Transonic Diffuser," NASA CR-2005-213417, January 2005.

Ideal Gas Compression in an Actuating Piston

In this application, AcuSolve is used to simulate pressure and temperature inside an actuating piston using the ideal gas relationship and fully defined mesh motion. AcuSolve results are compared with analytical results as described in Moran and Shapiro (2000). The close agreement of AcuSolve results with analytical results validates the ability of AcuSolve to model cases with material properties defined by the ideal gas law subjected to significant mesh distortion.

Problem Description

The problem consists of air compressed by a piston within a cylinder 10 m long with a diameter of π (3.14159) m, as shown in the following image, which is not drawn to scale. The piston is driven by a crankshaft 4 m long attached to a connecting rod 6 m long. The crankshaft rotates at 60o/s around a center point. At time (t) = 0.0 s the crank and piston are at top dead center (TDC) with an initial cylinder volume of 80 m^3. At t = 3.0 s the piston is at bottom dead center (BDC), at which point the volume in the cylinder is reduced to 16 m^3. The piston then moves back to TDC at t = 6.0 s. Air at atmospheric conditions, with material properties of an ideal gas and a dynamic viscosity of 1.781 X 10^5 kg/m-sec is the fluid modeled in the domain.

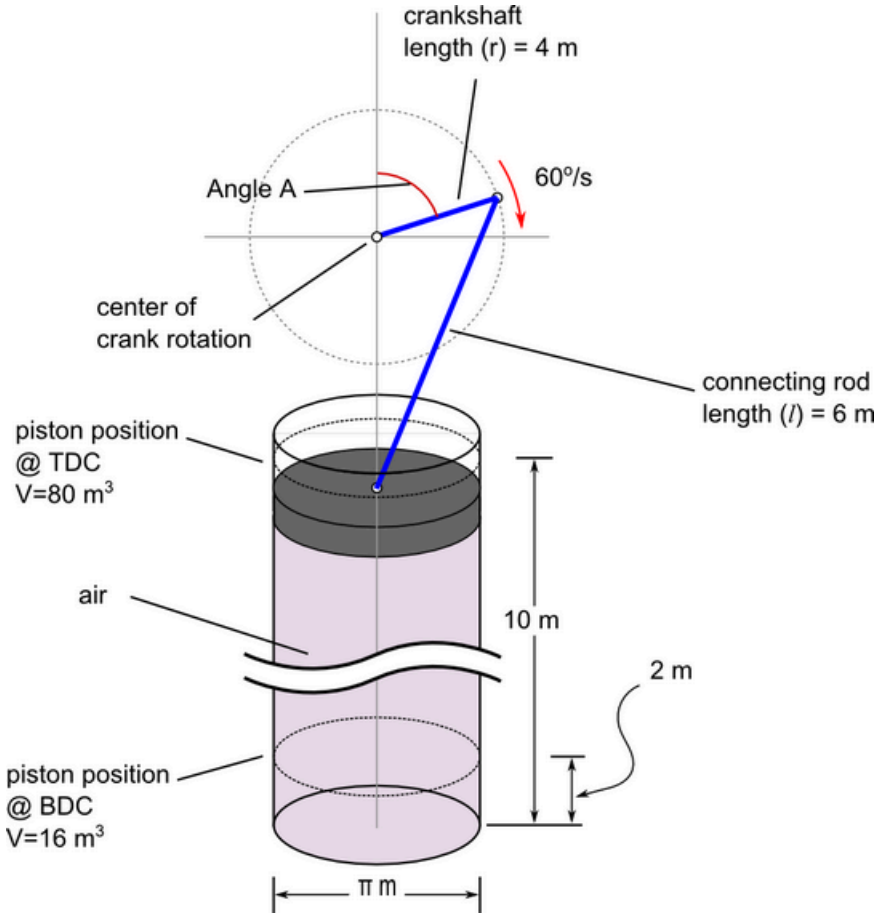


Figure 667: Critical Dimensions and Parameters for Simulating Ideal Gas Compression in an Actuating Piston

The motion of the piston is described by the following equation.

$$x = r*\cos A + \sqrt{l^2 - r^2 \sin^2 A} \quad (30)$$

Where

- x is the distance of the piston from TDC
- r is the length of the connecting rod, 4 m
- A is the crank angle as a function of time (t)
- l is the connecting rod length, 6 m

During the simulation, the top surface of the cylinder, representing the piston, moves with an applied mesh motion that mimics the motion of the reciprocating crank, rod, and piston assembly. The ideal gas is compressed by contracting the mesh according to the motion of that assembly and by allowing the fluid properties to change as a function of time.

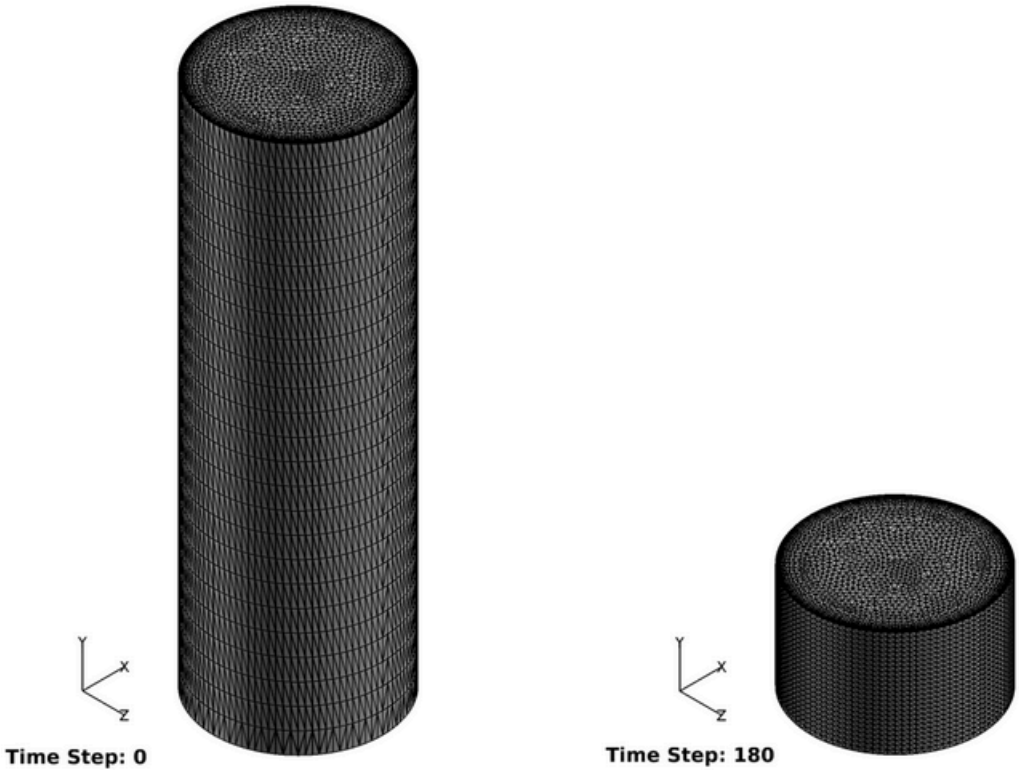


Figure 668: Mesh Used for Simulating Ideal Gas Compression in an Actuating Pistion at Time Step 0 and Time Step 180 (3 s)

AcuSolve Results

The simulation was run as transient for a total of 360 time steps with a duration of 6.0 seconds. The AcuSolve solution shows time dependent pressure and temperature in a cylinder volume that compresses and expands in a 6.0 second cycle. Pressure and temperature increase as the cylinder volume decreases, and returns toward initial conditions as the cylinder volume expands. The contours of pressure and temperature within the cylinder at the initial stage (t = 0.0 s) and the half cycle (t = 3.0 s) are shown in the following images.

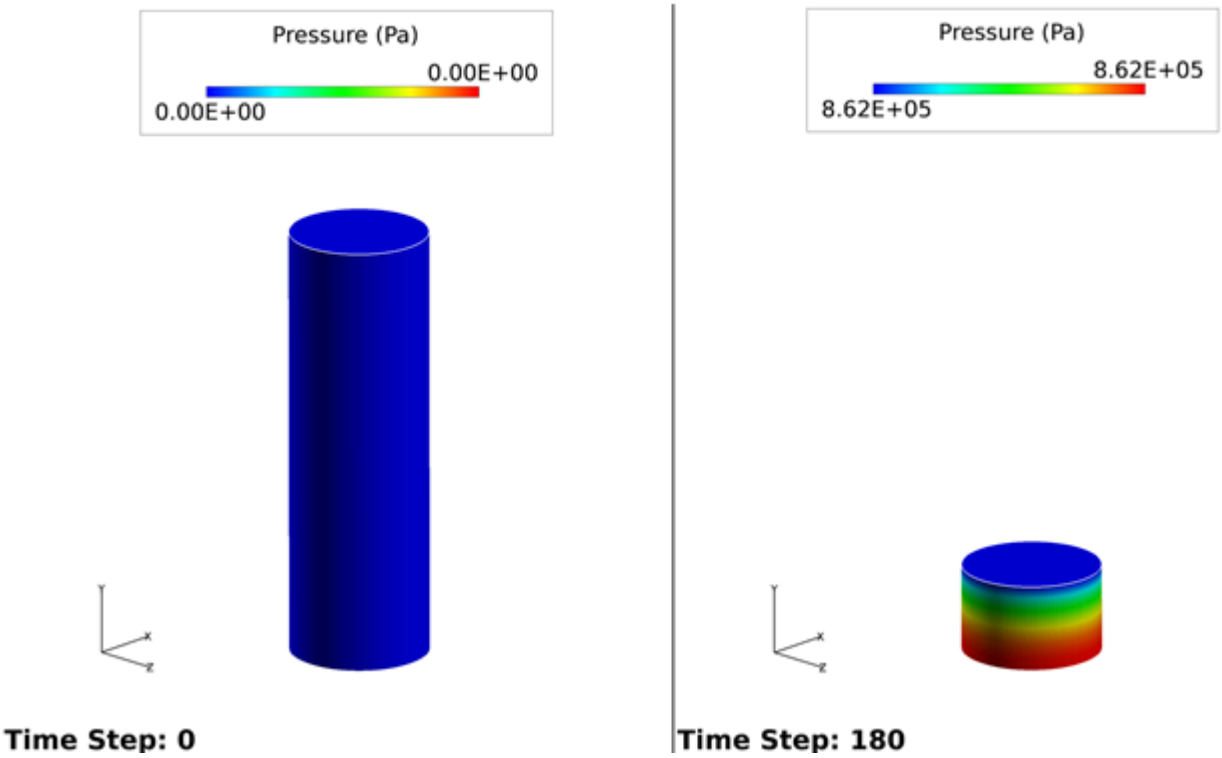


Figure 669: Pressure Distribution Within the Domain with the Piston at TDC and BDC

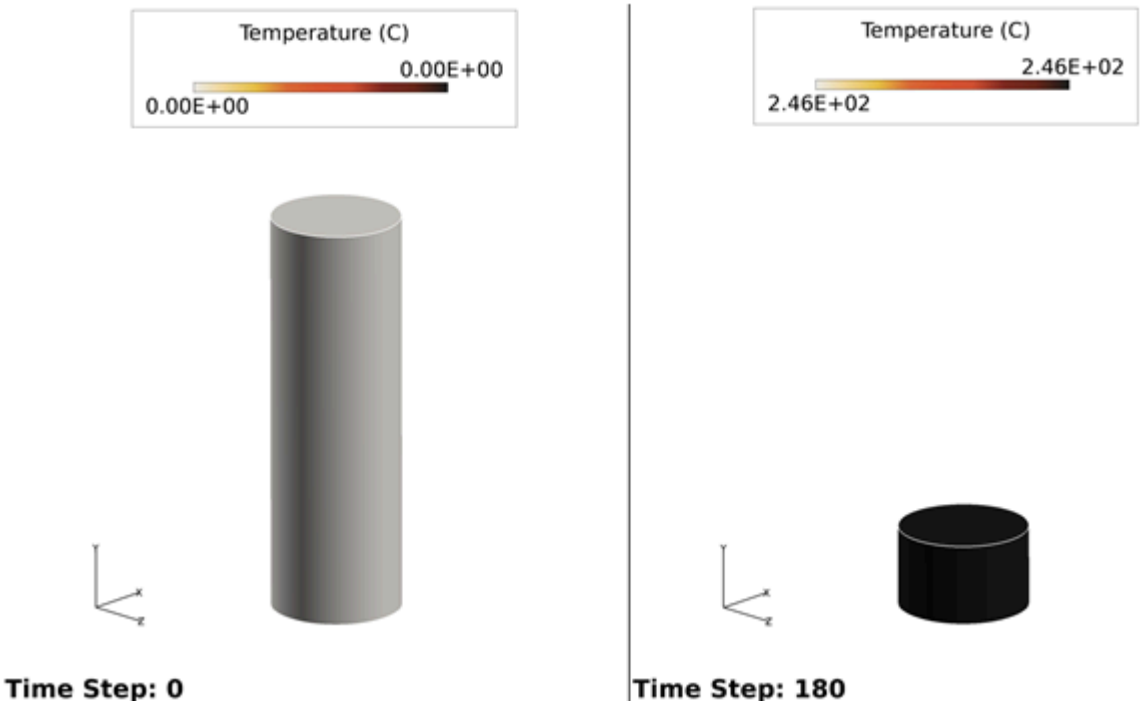


Figure 670: Temperature Distribution Within the Domain with the Piston at TDC and BDC

Comparison of time history plots of the AcuSolve and analytical solutions shows that the AcuSolve solution is nearly identical to the analytical solution. The AcuSolve computed internal pressure reaches a maximum of 8.62 X 105 Pa and the temperature reaches a maximum of 246.45 degrees C.

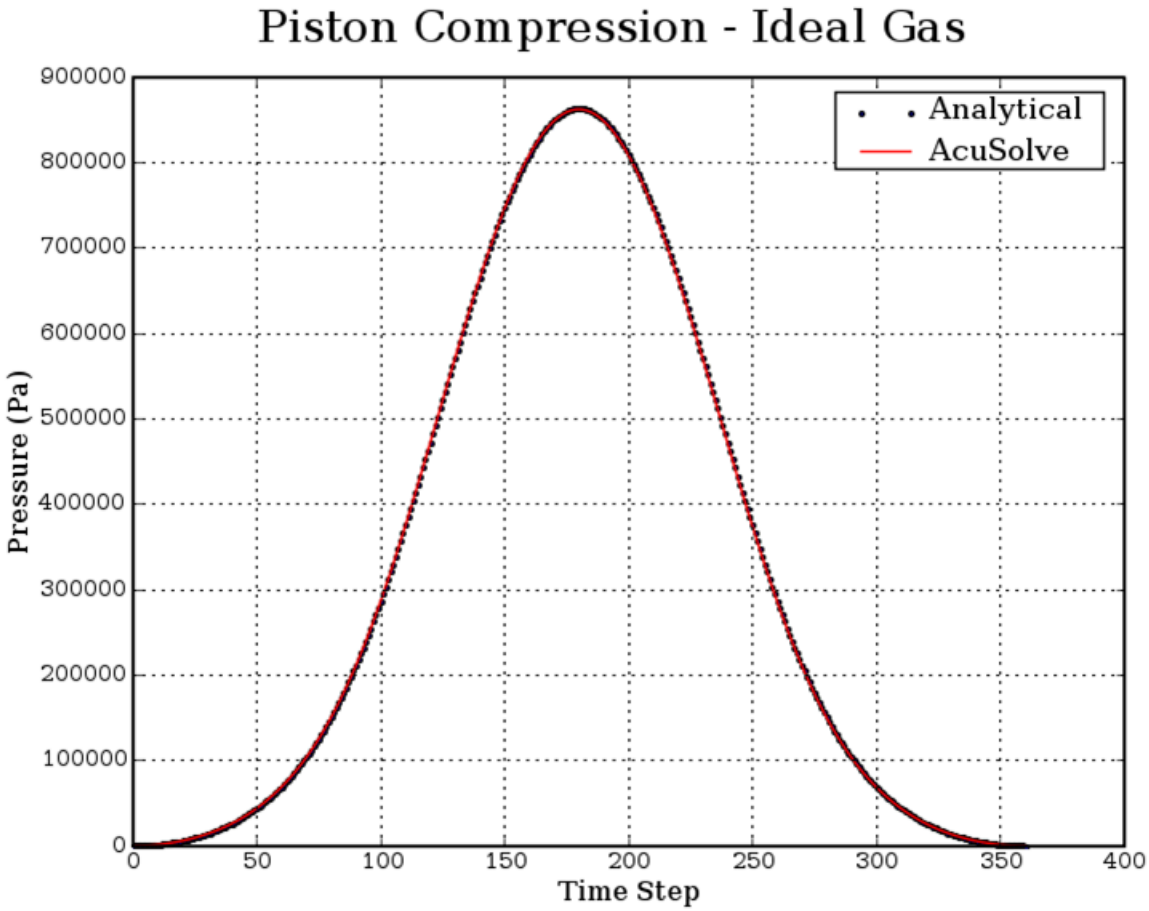


Figure 671: History Plots of Pressure for AcuSolve and Analytical Solutions

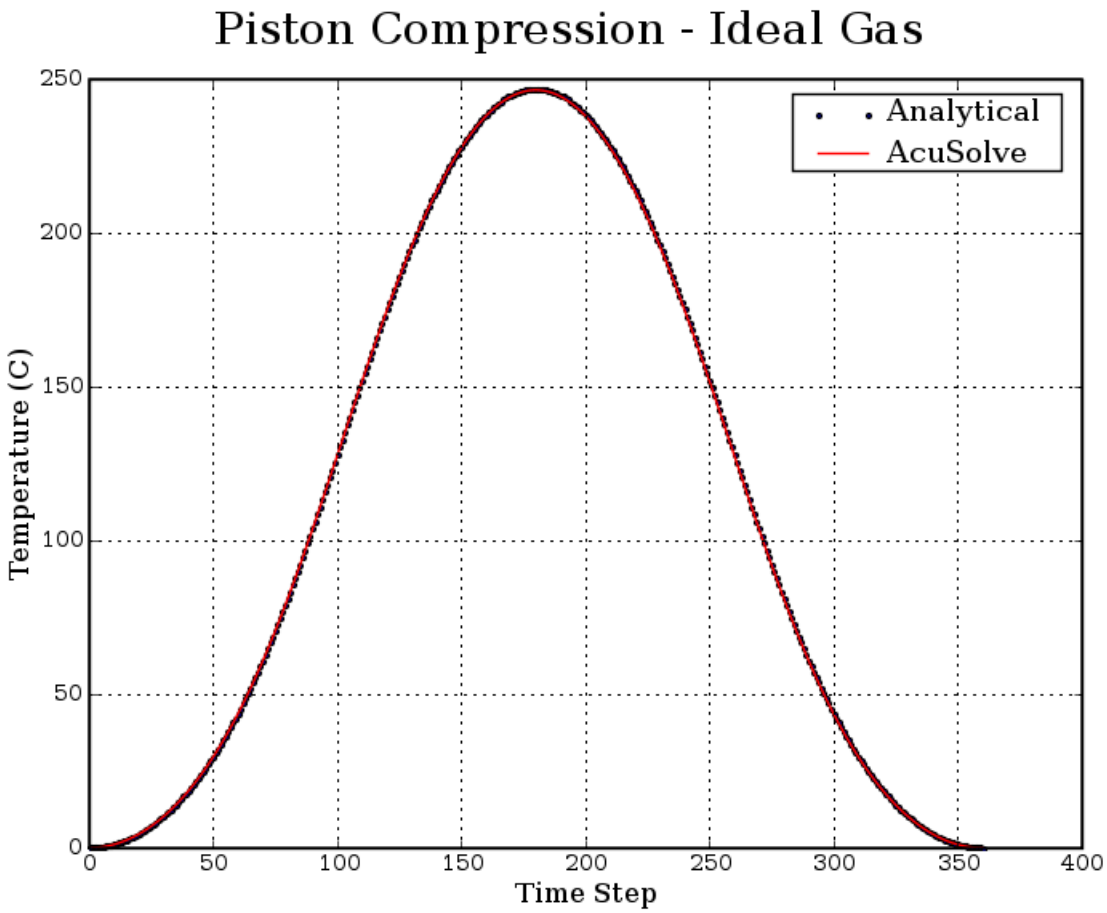


Figure 672: History Plots of Temperature for AcuSolve and Analytical Solutions

Summary

The AcuSolve solution compares well with analytical results for ideal gas compression in an actuating piston. The AcuSolve transient solution compares nearly identically with the analytical solution, with 0.1 percent and 0.16 percent error for the maximum pressure and temperature, respectively. As a result, AcuSolve demonstrates the ability to predict ideal gas compression in an actuating piston.

Simulation Settings for Ideal Gas Compression in an Actuating Piston

AcuConsole database file: `<your working directory>\cylinder_piston_compression\cylinder_piston_compression.acs`

Global

- Problem Description
  - Analysis type - Transient
  - Temperature equation - Advective Diffusive
  - Turbulence equation - Laminar
  - Mesh type - Fully Specified

- Auto Solution Strategy
  - Max time steps - `360`
  - Initial time increment - `0.01667` sec
  - Convergence tolerance - `1.0e-5` sec
  - Max stagger iterations - `10`
- Multiplier Function
  - Piston
    - Type - Piecewise Linear
    - Curve fit variable - Time
    - Curve fit values - (included in `.acs` based on equation discussed in problem description)
- Material Model
  - Air
    - Density
      1. Type - Ideal Gas
      2. Gas constant - `286.9` J/kg-K
      3. Abs. pressure offset - `101325.0` N/m2
      4. Abs. temperature offset - `273.15` K
    - Viscosity - `1.781e-5` kg/m-sec
- Mesh Motion
  - Piston
    - Type - Translation
    - Translation velocity - `0.0`, `-1.0`, `0.0`
    - Velocity variable - Multiplier Function
    - Translation multiplier function - Piston

  Model
- Volumes
  - Fluid
    - Element Set
      1. Material model - Air
      2. Compression heating - On
    - Element Output - on
- Surfaces
  - BDC
    - Simple Boundary Condition
      1. Type - Wall
      2. Wall velocity type - Match Mesh Velocity
      3. Mesh displacement BC type - Fixed
  - SideWall

        - Simple Boundary Condition
            1. Type - Wall
            2. Wall velocity type - Match Mesh Velocity
            3. Mesh displacement BC type - Fixed
    - TDC
        - Simple Boundary Condition
            1. Type - Wall
            2. Mesh displacement BC type - Fixed
            3. Mesh motion - Piston
- Nodes
    - VolumeNodes
        - Mesh X-Displacement
            1. Type - Zero
        - Mesh Y-Displacement
            1. Type - Linear
            2. Mesh motion - Piston
            3. Curve fit variable - Y reference coordinate
                1. X1 - `10.0` m
                2. Y1 - `1.0` m
                3. Y2 - `0.0` m
        - Mesh Z-Displacement
            1. Type - Zero

References

M.J. Moran and H.N Shapiro. "Fundamentals of Engineering Thermodynamics". Wiley. 4th Ed. 2000.

Index

A

AcuSolve validation manual introduction *13*

C

circumferential flow in a cylinder induced by a rotating solid *332*, *592*, *716*, *853*
compressible *911*

E

external flow *637*

F

flow between concentric cylinders *137*, *422*, *440*, *867*
flow inside a rotating cavity *174*, *361*, *477*, *873*

H

heat transfer between concentric cylinders with heat source *800*
heat transfer between radiating concentric cylinders *286*, *432*, *580*, *788*
heat transfer between radiating concentric spheres *314*, *611*, *805*
heat transfer/radiation *738*

I

ideal gas compression in an actuating piston *391*, *524*, *695*, *776*, *832*, *917*
internal flow *438*

L

laminar couette flow with imposed pressure gradient *152*, *343*, *455*
laminar couette flow with imposed pressure gradient and heated walls *158*, *349*, *461*, *744*
laminar flow *331*
laminar flow past a 90 degree t-junction *188*, *369*, *491*
laminar flow past a 90° t-junction *188*, *369*, *491*
laminar flow through a channel with heated walls *201*, *374*, *504*, *756*
laminar flow through a pipe with constant wall temperature *243*, *405*, *531*, *783*
laminar flow through a pipe with species transport *168*, *355*, *471*, *889*
laminar flow through pipe, imposed heat flux *143*, *338*, *446*, *739*
laminar free surface flow inside a rotating cavity *410*, *574*, *702*, *839*
laminar poiseuille flow through a pipe *164*, *428*, *467*
laminar to turbulent transition over an airfoil *297*, *678*, *684*

M

moving mesh *831*
multiphase *895*

multiphase flow of a 2d dam break *896*
multiphase flow within sloshing tank *17*, *604*, *722*, *859*, *900*

N

natural convection in a concentric annulus *182*, *416*, *485*, *750*

O

oscillating laminar flow around a circular cylinder *386*, *653*, *690*

R

radiation heat transfer through a cube with a specular interface *319*, *616*, *810*
reference frame *866*

S

separated laminar flow over a blunt plate *236*, *398*, *658*
single-phase nucleate boiling in rectangular channel *24*, *326*, *627*, *821*
species transport *888*
steady flow *136*
supersonic flow through converging-diverging nozzle *131*, *632*, *733*, *826*, *912*

T

transient flow *689*
transitional flow *683*
turbulent flow *16*
turbulent flow behind open-slit v *33*, *206*, *638*
turbulent flow over backward-facing step *64*, *264*, *552*
turbulent flow over naca 0012 airfoil *94*, *213*, *645*
turbulent flow over oscillating rigid body assembly *102*, *670*, *708*, *845*
turbulent flow past convex curve in channel *79*, *271*, *559*
turbulent flow past wall-mounted hump *56*, *278*, *566*
turbulent flow separation axisymmetric diffuser *71*, *256*, *544*
turbulent flow through 180 degree curved channel *110*, *302*, *586*
turbulent flow through heated periodic channel *121*, *308*, *598*, *794*
turbulent flow through pipe *29*, *148*, *451*
turbulent flow through wavy channel *40*, *193*, *496*
turbulent flow with separation in an asymmetric diffuser *48*, *248*, *536*
turbulent mixing layers in open channel *116*, *292*, *665*
turbulent natural convection inside tall cavity *86*, *221*, *509*, *761*
two-phase nucleate boiling in cylindrical pipe *127*, *623*, *729*, *817*, *907*

V

viscous heating inside a rotating annulus *229*, *379*, *517*, *769*, *881*